

Lalit M. Pandey
Abshar Hasan *Editors*

Nanoscale Engineering of Biomaterials: Properties and Applications

 Springer

Nanoscale Engineering of Biomaterials: Properties and Applications

Lalit M. Pandey • Abshar Hasan
Editors

Nanoscale Engineering of Biomaterials: Properties and Applications

 Springer

Editors

Lalit M. Pandey
Department of Biosciences and
Bioengineering
Indian Institute of Technology Guwahati
Guwahati, Assam, India

Abshar Hasan
School of Pharmacy
University of Nottingham
Nottingham, Nottinghamshire, UK

ISBN 978-981-16-3666-0

ISBN 978-981-16-3667-7 (eBook)

<https://doi.org/10.1007/978-981-16-3667-7>

© The Editor(s) (if applicable) and The Author(s), under exclusive license to Springer Nature Singapore Pte Ltd. 2022

This work is subject to copyright. All rights are solely and exclusively licensed by the Publisher, whether the whole or part of the material is concerned, specifically the rights of translation, reprinting, reuse of illustrations, recitation, broadcasting, reproduction on microfilms or in any other physical way, and transmission or information storage and retrieval, electronic adaptation, computer software, or by similar or dissimilar methodology now known or hereafter developed.

The use of general descriptive names, registered names, trademarks, service marks, etc. in this publication does not imply, even in the absence of a specific statement, that such names are exempt from the relevant protective laws and regulations and therefore free for general use.

The publisher, the authors, and the editors are safe to assume that the advice and information in this book are believed to be true and accurate at the date of publication. Neither the publisher nor the authors or the editors give a warranty, expressed or implied, with respect to the material contained herein or for any errors or omissions that may have been made. The publisher remains neutral with regard to jurisdictional claims in published maps and institutional affiliations.

This Springer imprint is published by the registered company Springer Nature Singapore Pte Ltd. The registered company address is: 152 Beach Road, #21-01/04 Gateway East, Singapore 189721, Singapore

Contents

Part I Introduction to Biomaterials

- 1 Interactions Between the Physiological Environment and Titanium-Based Implant Materials: From Understanding to Control** 3
Sara Ferraris, Yolanda S. Hedberg, James J. Noël, and Silvia Spriano
- 2 Nanoscale Surface Engineering and Characterization of Biomaterials** 27
Abshar Hasan and Lalit M. Pandey
- 3 Progress of Nanotechnology-Based Detection and Treatment of Alzheimer’s Disease Biomarkers** 47
Yashwant Rao Singh, Anupam Shukla, and Sudip Kumar Pattanayek
- 4 Biomaterials: Types and Applications** 89
Aman Bhardwaj and Lalit M. Pandey

Part II Surface Engineering of Metallic Biomaterials

- 5 Overview of Current Additive Manufacturing Technologies for Titanium Bioimplants** 117
Vicky Subhash Telang, Rakesh Pemmada, Seeram Ramakrishna, Puneet Tandon, and Himansu Sekhar Nanda
- 6 Physico-chemical Modifications of Magnesium and Alloys for Biomedical Applications** 131
Satish Jaiswal, Anshu Dubey, and Debrupa Lahiri
- 7 Metallic Foams in Bone Tissue Engineering** 181
Somasundaram Prasad, Sreenivas Raguraman, Raymond Wong, and Manoj Gupta
- 8 Surface Modification of Metallic Biomaterials for Cardiovascular Cells Regulation and Biocompatibility Improvement** 207
Jingan Li and Yachen Hou

- 9 Advancement of Spinel Ferrites for Biomedical Application 227**
Molonnenla Jamir, Aszad Alam, and J. P. Borah

Part III Surface Engineering of Polymeric Biomaterials

- 10 Functionalized 3D Bioactive Polymeric Materials in Tissue Engineering and Regenerative Medicine 257**
Anushree Pandey, Asif Ali, Nikhil Ram Patra, and Yuvraj Singh Negi
- 11 Polymer Matrixes Used in Wound Healing Applications 279**
Md. Sazedul Islam, Md. Ashiqur Rahman, Shafiul Hossain, Papia Haque, Md. Shahruzzaman, and Mohammed Mizanur Rahman
- 12 Conductive Polymers for Cardiovascular Applications 319**
Azka Arshad, Hafsa Irfan, Sunniya Iftikhar, and Basit Yameen
- 13 Engineered Polymeric Materials/Nanomaterials for Growth Factor/Drug Delivery in Bone Tissue Engineering Applications . . . 349**
Neelam Chauhan and Yashveer Singh
- 14 Surface Engineering of Polymeric Materials for Bone Tissue Engineering 397**
Asif Ali, Nikhil Ram Patra, Anushree Pandey, and Yuvraj Singh Negi
- 15 Antibacterial Surface Modification to Prevent Biofilm Formation on Polymeric Biomaterials 425**
Abul K. Mallik, Adib H. Chisty, M. Nuruzzaman Khan, Sumaya F. Kabir, Md. Shahruzzaman, and Mohammed Mizanur Rahman
- 16 Polymer Surface Engineering in the Food Packaging Industry 457**
Iqra Azeem, Binish Ashfaq, Muhammad Sohail, and Basit Yameen
- 17 Polymeric Membranes in Wastewater Treatment 487**
Adil Majeed Rather, Yang Xu, Robert Lewis Dupont, and Xiaoguang Wang
- 18 Functionalized Fluoropolymer Membrane for Fuel Cell Applications 517**
Om Prakash, Ashok K. Pandey, and Pralay Maiti

Part IV Surface Engineering of Ceramic and Composite Biomaterials

- 19 Bioceramics for Biomedical Applications 543**
Rushikesh Fopase and Lalit M. Pandey
- 20 Applications of Nanomaterials in the Textile Industry 567**
Satadru Chakrabarty and Kabeer Jasuja

21 Properties and Characterization of Advanced Composite Materials	589
Md. Shahruzzaman, Shafiu Hossain, Sumaya F. Kabir, Tanvir Ahmed, Md. Minhajul Islam, Sabrina Sultana, Abul K. Mallik, and Mohammed Mizanur Rahman	
22 Insight of Iron Oxide-Chitosan Nanocomposites for Drug Delivery	619
Adib H. Chisty and Mohammed Mizanur Rahman	
23 Nanocomposites Application in Sewage Treatment and Degradation of Persistent Pesticides Used in Agriculture	649
Nusrat Iqbal, Saurabh Dubey, Manmeet Kaur, Samsul Alam, Amrisha Agrawal, Irani Mukherjee, and Jitendra Kumar	
24 Biomimetic Mineralization of Electrospun PCL-Based Composite Nanofibrous Scaffold for Hard Tissue Engineering	683
Arjun Prasad Tiwari, Shiva Pandeya, Deval Prasad Bhattarai, and Mahesh Kumar Joshi	

About the Editors

Lalit M. Pandey is an Associate Professor at the Department of Biosciences and Bioengineering, IIT Guwahati. He received his Ph.D. in Chemical Engineering from the Indian Institute of Technology, Delhi. He was awarded an Erasmus Mundus India4EU fellowship to pursue research at the Laboratoire des Matériaux et du Génie Physique (LMGP), Grenoble-INP, France, from 2010 to 2012. Before joining the IIT Guwahati, he worked as a Scientist with the Central Pollution Control Board, Ministry of Environment & Forests, Government of India from 2009 to 2014, and researched on water and air pollution in agro-based industries. He has received several awards, including the Shastri Covid-19 Pandemic Response Grant (SCPRG) 2020, the DST-UKIERI Award (2018), the IEI (The Institution of Engineers [India]) Young Engineers Award (2017), Innovation in Science Pursuit for Inspired Research (INSPIRE) Faculty Award (2014), and an Early Career Research Award from the Science and Engineering Research Board (SERB), Department of Science & Technology, Government of India. His main research interests include biointerfaces and biomaterials, biochemical engineering, and environmental biotechnology. He has published over seventy research articles in international journals and serves on the editorial board of five international journals. He is serving as Associate Editor in *Frontiers in Bioengineering and Biotechnology* and *Frontiers in Materials*. He has co-edited one book titled *Biointerface Engineering: Prospects in Medical Diagnostics and Drug Delivery* published by Springer Nature in 2020. He is a life member of the International Association of Engineers (IAENG), the Indian Institute of Chemical Engineers (IChE), and Nano and Molecular Society (India), and serves as a reviewer for several peer-reviewed journals.

Abshar Hasan received his Ph.D. in Biosciences and Bioengineering from the Indian Institute of Technology Guwahati, India, in 2018 and began working as a Research Fellow at the School of Engineering and Materials Science, Queen Mary University of London, UK. In 2019, he moved to the University of Nottingham, UK, where he is currently working as a Research Associate at the School of Pharmacy. His research interests lie in engineering metallic and polymeric surfaces to develop functional materials, gain mechanistic insights into protein and cell behavior on surfaces, and develop functional materials for tissue engineering and environmental applications. He is a recipient of a prestigious Commonwealth Split-Site Scholarship

in 2017 and has published more than 25 research articles in peer-reviewed international journals and book chapters. He currently serves as a reviewer for various international journals, including *Pharmaceutics*, *Applied Sciences*, *Materials*, *Coatings*, and *Surfaces*. He is a research member of international scientific societies, e.g., the Royal Society of Chemistry (RSC), UK, and the Tissue and Cell Engineering Society (TCES), UK.

Part I

Introduction to Biomaterials



Interactions Between the Physiological Environment and Titanium-Based Implant Materials: From Understanding to Control

1

Sara Ferraris, Yolanda S. Hedberg, James J. Noël, and Silvia Spriano

Abstract

Titanium and titanium alloys are widely used in different biomedical applications owing to their high biocompatibility, high corrosion resistance, good mechanical properties, and good osseointegration ability. Titanium and its alloys rapidly form a surface oxide layer in air and aqueous environments. This passive and thin (a few nanometers) surface oxide hinders active corrosion and ensures a low metal ion release, enhancing biocompatibility. Compared to that of other biomedical alloys, this surface oxide is exceptionally resistant to chemical attack by halides, primarily chlorides; the presence of fluorides can, in some cases, result in localized corrosion of titanium and its alloys. However, the combination of proteins, inflammatory conditions and bacteria, which for instance generate hydrogen peroxide, can result in a reduction of the corrosion resistance of titanium-based materials. Titanium and its alloying elements, such as aluminum and vanadium, can then be released as ions, which might trigger an immune system response and reduce biocompatibility. Several surface modifications have

S. Ferraris (✉) · S. Spriano

Department of Applied Science and Technology, Politecnico di Torino, Torino, Italy
e-mail: sara.ferraris@polito.it; silvia.spriano@polito.it

Y. S. Hedberg

Department of Chemistry, Division of Surface and Corrosion Science, KTH Royal Institute of Technology, Stockholm, Sweden

Department of Chemistry, Surface Science Western, The University of Western Ontario, London, ON, Canada

e-mail: yhedberg@uwo.ca

J. J. Noël

Department of Chemistry, Surface Science Western, The University of Western Ontario, London, ON, Canada

e-mail: jjnoel@uwo.ca

© The Author(s), under exclusive license to Springer Nature Singapore Pte Ltd. 2022

L. M. Pandey, A. Hasan (eds.), *Nanoscale Engineering of Biomaterials: Properties and Applications*, https://doi.org/10.1007/978-981-16-3667-7_1

been proposed in order to improve the bone-bonding ability of titanium and its alloys, facilitate the healing process, and enhance the success of the implant with a decreased risk of micromotions. Moreover, antimicrobial ions/nanoparticles can be added to the surface to reduce the infection risk. Surface modification of titanium (e.g., with artificially grown, micrometer-thick, titanium oxide layers) can significantly increase the corrosion resistance under critical conditions (e.g., inflammatory response and infection); however, the surfaces are not completely inert and the effect of metal ion/nanoparticle release should be carefully taken into account.

This chapter reviews and discusses the current strategies for modifying and controlling the surface of titanium-based implant materials, with particular focus on corrosion resistance, bone integration, inflammatory and infection control, and interactions with the physiological environment.

Keywords

Titanium · Corrosion resistance · Inflammatory · Bone integration · Infection control

1.1 Introduction

Titanium (Ti) and Ti alloy implant materials can release metal ions and particles into the physiological environment. These can be simple metal ions, aqueous complexes, ions bound to proteins or metal (oxide) particles. Their form (chemical speciation) is decisive for any biological response and might be changed with time or upon a changed environment.

While direct immune response to Ti species has been debated for a long time, newer research shows clear evidence that T-cell-mediated hypersensitivity specific to Ti(IV) exists (Chan et al. 2011; Hamann 2018; Evrard et al. 2010; Hosoki et al. 2016). Hypersensitivity reactions to Ti have traditionally been overshadowed by those to other metals (Evrard et al. 2010; Hosoki et al. 2016) and are—due to chemical limitations—difficult to diagnose by patch testing (Hamann 2018). While Ti and its oxides, such as Ti dioxide (TiO₂), have long been considered nontoxic and biocompatible, newer studies show that this is not always true (Jin and Berlin 2015). Small (<4 μm) released Ti oxide particles can be taken up in cells (Kumazawa et al. 2002), be enriched into the implant-adjacent tissue or distal organs (Swiatkowska et al. 2018; Olmedo et al. 2008; Sarmiento-González et al. 2008), and cause different immunological responses (Thewes et al. 2001). Due to the low solubility of TiO₂, TiO₂ particles, comprising 80% of the total detected Ti, have been found in human post-mortem studies in different organs, such as spleen, liver, and kidney (Peters et al. 2020). TiO₂ nanoparticles are of relatively low toxicity as compared to other metal oxides or metal nanoparticles; however, it is now evident that they can cause the generation of reactive oxygen species, inflammatory response, genotoxicity,

metabolic changes, and potentially carcinogenesis (Grande and Tucci 2016; Shakeel et al. 2016).

The alloying elements in Ti alloys, such as aluminum (Al), niobium (Nb), tin (Sn), vanadium (V), nickel (Ni), or palladium (Pd), are often of greater short-term health concern than Ti (Chen and Thyssen 2018). Other common alloying elements of similar or lower health concern, as compared to Ti, are tantalum (Ta), zirconium (Zr), iron (Fe), and molybdenum (Mo). Chromium (Cr), which is a common metal allergen, can also be an alloying element for titanium alloys (Hamann 2018). These and other alloying elements stabilize different phases of titanium, resulting in different, or a mixture of, crystal structures with unique mechanical, machinability, and corrosion properties (Noël et al. 2018). Commercially pure (cp) Ti is used as coating material or for some dental applications (Gilbert 2017). For many biomedical applications, the use of Ti alloys is necessary, as the mechanical properties of pure Ti are insufficient. The Ti alloy containing 6 wt% Al and 4 wt% V (Ti6Al4V) is commonly used for parts of artificial joints (such as the stem of an artificial hip joint prosthesis), which require high corrosion resistance and high fatigue strength, but not necessarily high wear resistance (Gilbert 2017); titanium and its alloys have very poor wear and fretting resistance. Ti and its alloys possess a comparably high osseointegration (tight integration of the implant with the bone), relatively low density (closer to that of natural bone), and relatively high biocompatibility compared with alternative alloys.

The interface between the Ti (alloy) surface and the physiological environment is dynamic and both sides are influenced by each other. For example, released metals can cause immunological reactions, which in turn can cause a more corrosive environment, triggering more metal release. Infections, specific diseases, and other factors (such as implant design) can also cause aggressive environments leading to corrosion and ultimately health effects or implant failure. This chapter will discuss these corrosion processes, how they are affected by the physiological environment, and how metal release, corrosion, and infections could be minimized by means of surface engineering. A specific focus is on the complex physiological environment in which corrosion resistance, modulation of the inflammatory response, bioactivity, and ability of infection control play interconnected roles. The recent strategies of surface modification of Ti in order to obtain a multifunctional action, which takes all the above-cited parameters into account, are discussed.

1.2 Corrosion Resistance of Ti and Its Alloys in the Biological Environment

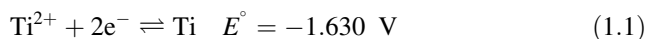
1.2.1 Principles of Corrosion of Ti and Its Alloys

A metal is a conductive material, and as such, electrons can freely move within it. Corrosion of metals occurs via the oxidation of the metal and the reduction of an oxidant, most often oxygen, water, or protons. These two half-cell reactions are balanced such that the number of electrons produced by metal oxidation is equal to

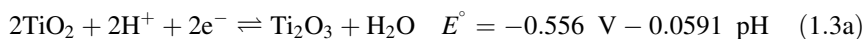
the number consumed in the reduction of oxidants. Due to the electron conductivity of the metal, the reduction half-cell reaction can occur at a very different location and over a differently sized surface area than the oxidation half-cell reaction; these differences are critical for a number of localized corrosion types of Ti metal and its alloys.

Ti metal is thermodynamically unstable in water or air. It is rapidly oxidized and reacts even with hydrogen, nitrogen, and many other elements. Its high affinity for oxygen is key to its ability to form a protective surface oxide that hinders further Ti metal oxidation and ensures Ti and its alloys can withstand the relatively corrosive physiological environment to a large extent. In order to understand the corrosion of Ti and Ti alloys, we need to understand the conditions under which the Ti surface oxide can form and reform.

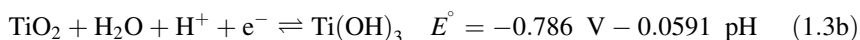
At physiologically relevant pH values, Ti metal is oxidized to TiO_2 in several steps (McCafferty 2010; Schmets et al. 1974), with the following reactions showing the equilibrium states under standard conditions:



or



or



where E° denotes the standard electrode potential in V vs. the standard hydrogen electrode (SHE) and under standard conditions (25 °C, activity of 1, 1 atmosphere gas pressure). For other solute concentrations, the reader is referred to the equations given in Schmets et al. (1974).

All of these reactions occur at potentials far more negative than the stability range of water, which means that the thermodynamic driving force for Ti oxidation to the Ti^{IV} valence state is very high, compared to that of most other metals (Pourbaix 1974). This driving force ensures that a damaged surface oxide is rapidly repaired under benign conditions. This further ensures a very low corrosion rate, under so-called passive conditions, under which subsequent Ti oxidation is limited by restricted mass transport through the formed Ti surface oxide. Under more aggressive, nonpassive conditions, this high thermodynamic driving force toward Ti oxidation can cause a high corrosion rate and large potential differences when coupled with other metals, phases, or intermetallic precipitates, even within the same alloy.

Alloying elements can either improve or degrade the corrosion resistance compared to commercially pure Ti metal.

The Ti-Ni alloy (commercial name “nitinol”), which is used for its shape memory effect in cardiovascular stents and orthodontic appliances, is an example of a Ti alloy with significantly lower corrosion resistance than Ti metal (Ding et al. 2018; Noguchi et al. 2008), accompanied with some Ni release (Saylor et al. 2016; Sullivan et al. 2015), approximately in the same range as, or lower than, austenitic Ni-containing stainless steel (Hedberg and Odnevall Wallinder 2016; Eliades et al. 2004; Suárez et al. 2010). This Ni release can cause a number of clinical adverse effects (Faccioni et al. 2003; Mani et al. 2007; Gong et al. 2013).

Ti alloys containing Al and either V or Nb are widely used for different biomedical applications, especially in orthopedic artificial joint prostheses (Gilbert 2017; Milošev 2017). The Ti alloy containing 6 wt% Al and 4 wt% V (Ti6Al4V) has been reported to have a slightly less protective passive layer than does commercially pure Ti (Shukla et al. 2005). In the same study (Shukla et al. 2005), a higher alloyed Ti alloy with 13.4 wt% Al and 29 wt% Nb (Ti13.4Al29Nb) showed improved corrosion resistance compared with Ti metal over 1 week of exposure in Hank’s solution, a simple physiological simulant containing a number of salts and glucose at a pH value of about 7.4. A detailed X-ray photoelectron spectroscopy study of specimens exposed to Hank’s solution revealed a spontaneous formation of primarily TiO₂ in the surface oxide of Ti6Al4V and small amounts of Al₂O₃ on its outermost surface at the interface with the solution (Milošev et al. 2000). A similar study on Ti6Al7Nb showed that the surface oxide on this alloy formed less sub-oxides of TiO and Ti₂O₃ as compared to Ti6Al4V and possessed a higher corrosion resistance (Milošev et al. 2008).

The formation of the passive surface oxide on Ti and Ti alloys is required for high corrosion resistance. Its formation is, however, strongly dependent on environmental conditions, as discussed in the following section.

1.2.2 Physiological Environments from a Corrosion Perspective

The physiological environment is highly complex, locally different, and dynamic over time. Only recently, it has been acknowledged that simple salt-based solutions, such as 0.9% sodium chloride, Hank’s solution, Ringer’s solution, and phosphate-buffered saline, cannot simulate the physiological environment in a relevant and sufficient way for Ti alloys (Gilbert 2017; Zhang et al. 2018a; Hedberg et al. 2019b).

Halides are important to many localized types of corrosion of passive metals. Ti has been considered to have low susceptibility to chloride-induced corrosion; however, in combination with fluorides and other factors, the chlorides contribute to the corrosion process in a synergistic manner (Li et al. 2007). Fluoride is actively used in the cleaning and protection of natural teeth; therefore, especially Ti-based dental implants and orthodontic Ni-Ti wires are regularly exposed to fluorides. The TiO₂-containing passive film of Ti and its alloys is susceptible to fluoride attack. It was found that fluorides increase the corrosion rates of Ti and its alloys under conditions

of relevance for dental environments (Li et al. 2007; Mirjalili et al. 2013; Noguchi et al. 2008; Reclaru and Meyer 1998).

The physiological environment also contains a high number of complexing agents and proteins. The high ionic strength of the physiological environment ensures their rapid adsorption even on similarly charged surfaces (Fukuzaki et al. 1995; Hedberg et al. 2014; Claesson et al. 1995). Proteins and other complexing agents, such as peptides, amino acids, organic acids, or different anions, can form a complex either directly with Ti or with any of its alloying elements. This can occur either directly with the metal, with a metal ion in solution, or—most relevant for passive conditions—directly with the surface oxide. It has been suggested that this process plays an important role for the depletion of Al_2O_3 from the surface oxide of Ti6Al4V, and that it is accelerated in the presence of hydrogen peroxide (Hedberg et al. 2019b).

Inflammatory and immunological reactions can result in a chemical attack and a very high redox potential in the *in vivo* environment or locally on the implant surface. Most importantly, there is increasing evidence that the surface reactions and corrosion trigger the biological response, which in turn increases the corrosion rate (Hedberg 2018; Gilbert 2017; Milošev 2017). For example, immune and inflammatory cells can produce a range of highly oxidizing species, including hydrogen peroxide, hydroxyl radical, and hypochlorous acid, resulting in an extremely oxidative environment (Gilbert and Kubacki 2016).

1.2.3 Pitting and Crevice Corrosion

Pitting and crevice corrosion are localized corrosion types that are important to most passive metals and alloys. For Ti alloys, most pitting or crevice corrosion cases have been found in conjunction with the crevice induced in modular tapered junctions (Gilbert 2017), schematically illustrated in Fig. 1.1. The difference between pitting and crevice corrosion is its initiation: pitting corrosion requires the damage of the surface oxide, which is often unlikely to occur for Ti alloys, while the crevice already provides the optimal conditions for initiation of this localized corrosion process. Once initiated, the propagation and failure or repassivation steps of pitting and crevice corrosion are similar and involve a large passive area providing the necessary reaction surface area for the cathodic reaction and a very small confined space for the anodic reaction (metal oxidation), which is also driven by significant amounts of proton reduction within its interior (Noël 1999; He et al. 2009). If pitting corrosion occurs, it is often located in the vicinity of a crevice (Gilbert 2017), as the local chemical environment there is far more anaerobic, acidic and enriched in chlorides, fluorides, or other anions able to attack the Ti surface oxide. The anodic half-cell reactions inside the crevice or pit require cathodic half-cell reactions. These cathodic half-cell reactions can involve the reduction of oxygen on passive surfaces of the Ti metal or alloy—far away from the crevice or pit. Another even more important cathodic reaction is the reduction of protons resulting in the formation of hydrogen gas or absorbed hydrogen in the metal (Noël 1999; He et al. 2009), which embrittles

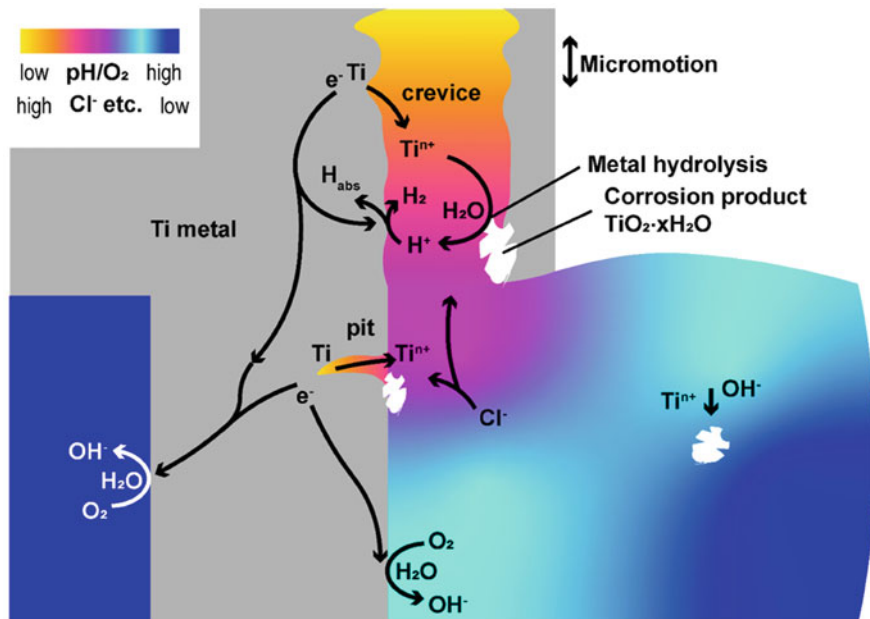


Fig. 1.1 Schematic illustration of the local chemical environment during pitting and crevice corrosion of Ti or its alloys. Inside the confined space of the crevice or pit, the solution chemistry is characterized by a very low pH, an anaerobic environment, and a very high concentration of ions. Charge neutrality is ensured by the free movement of electrons inside the metal and the migration of ions in and out of the confined spaces. The corrosion reactions result in the buildup of corrosion products on the surface of the confined spaces and as particles. Micromotion is often present for crevices of orthopedic and dental implants

the metal and can cause cracking, Fig. 1.1. Protons inside the confined space originate from hydrolysis of the released metal ions. These positively charged protons and metal ions also attract negatively charged counterions, such as chlorides, fluorides, or sulfates, to maintain charge neutrality inside the crevice or pit. This results in an extremely concentrated and aggressive solution chemistry. Although crevice corrosion of CP Ti requires temperatures above $\sim 60^\circ\text{C}$ (Noël 1999), it may proceed at lower temperatures on more susceptible alloys. Crevice and pitting corrosion are often combined with mechanically assisted corrosion types, which then can result in cracking or faster propagation. A change in the geometry, replenishing of the solution inside the confined space, and/or a shift in potential due to oxidants may result in repassivation of the surface. Although crevice and pitting corrosion are rarely observed directly from retrieved Ti alloy implant materials, they are suspected to be part of the overall corrosion mechanism (Hall et al. 2018; Gilbert 2017).

1.2.4 Mechanically Assisted Corrosion Types

Ti and its alloys are usually not intended for wear-exposed parts of biomedical implants due to their relatively low wear resistance, compared to cobalt-chromium (Co-Cr) alloys or ceramic materials. Nevertheless, mechanically induced corrosion types are still of high importance for biomedical Ti (alloys) and therefore an important target for surface engineering.

An important type of corrosion of Ti alloys as biomedical materials is mechanically assisted crevice corrosion (MACC) (Hall et al. 2018; Gilbert 2017), which is the combination of fretting corrosion and crevice corrosion. Fretting corrosion requires micromotion between the Ti (alloy) surface and a hard countersurface able to damage the surface oxide (Swaminathan and Gilbert 2012). In implant materials, such as dental implants (screws) or modular taper junctions of joint prostheses, cyclic micromotions are common. The hard countersurface can, for instance, be an oxide-coated metal, a ceramic material, or particles deriving from the corrosion process (Fig. 1.1) or wear. This oxide damage then initiates or accelerates localized corrosion, most often crevice corrosion.

Stress corrosion cracking can be a result of hydrogen embrittlement (“hydrogen-induced cracking (HIC)” (Clarke et al. 1997; Tal-Gutelmacher and Eliezer 2005)) due to absorbed hydrogen (Fig. 1.1) or be related to the stresses that occur during oxide growth (“oxide-induced stress corrosion cracking”—OISCC) (Gilbert 2017). MACC and OISCC can ultimately result in the buildup of a relatively thick (several hundreds of micrometers) Ti oxide layer, termed “direct conversion to oxide” (Gilbert 2017; Gilbert et al. 2012). These thick Ti oxide layers have been found *in vivo* (Gilbert et al. 2012), especially in modular taper junctions providing the optimal geometry of a crevice in combination with micromotions. The combination of OISCC and direct conversion to oxide can result in rapidly growing pits filled with oxide. As these oxides have a higher volume than the metal (Pilling-Bedworth ratio = 1.73 (Nelson and Oriani 1993)), the material cracks, and the pit can propagate further. This can result in millimeter-long oxide-filled pits and cracks (Gilbert et al. 2012), Fig. 1.2.

1.2.5 Selective, Galvanic, and Intergranular Corrosion

Ti6Al4V contains both alpha (hexagonal closed-packed structure) and beta (body-centered cubic structure) Ti phases. It has been shown for retrieved implants that pits and directly converted oxide propagate along the beta phases and then convert the alpha phases into oxide (Gilbert et al. 2012). This selective corrosion is due to a lower corrosion resistance of the beta phase as compared to the alpha phase (Noël et al. 2018). It has been hypothesized that the combination of hydrogen peroxide (from inflammatory reactions) and active potentials, for example, due to crevice corrosion, can provide conditions that selectively dissolve the beta phase of Ti6Al4V alloys (Gilbert et al. 2012).

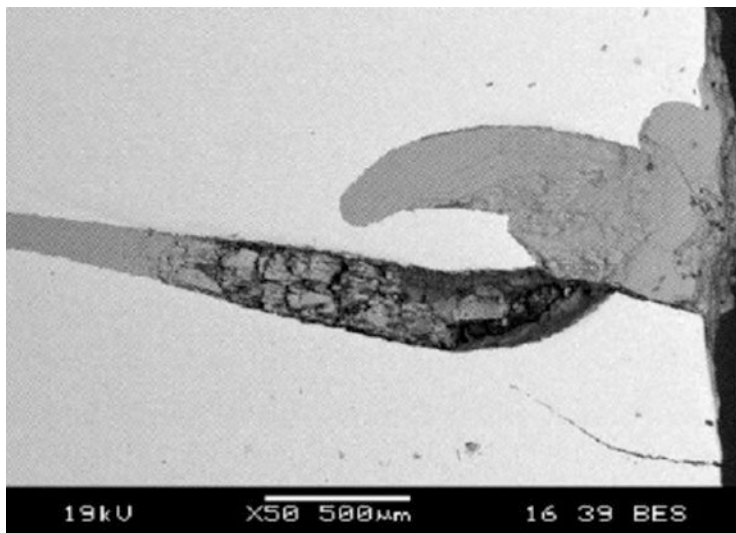


Fig. 1.2 Example of OISCC: oxide-filled deep-plunging pit resulting in cracking in a Ti6Al4V/Ti6Al4V taper region. (Reprinted with permission from John Wiley and Sons (Gilbert et al. 2012))

Intergranular corrosion, for which the corrosion occurs preferentially along grain boundaries, is relatively rare for Ti and its alloys in biomedical applications, but has been observed as a consecutive corrosion mechanism following other corrosion types such as MACC (Gilbert 2017).

Due to the very negative standard potential of Ti and its alloys (see Sect. 1.2.1), this metal can be susceptible to galvanic corrosion when coupled with other metals and when the oxide is damaged. Also, due to its high corrosion resistance in aqueous environments, the surface of Ti and its alloys could act as the cathodic site when coupled to another, less corrosion-resistant alloy. This could result in hydrogen absorption. Coupling to other metals is common in most orthopedic and dental implants (Cortada et al. 2000; Lucas et al. 1981). Galvanic corrosion has, however, not been found to be a dominating corrosion type for biomedical Ti alloys (Cortada et al. 2000; Lucas et al. 1981; Gilbert 2017). Any galvanic effects of incorporated noble metal nanoparticles in the oxide of Ti alloys have recently been studied and are discussed in Sect. 1.4.3.

1.2.6 The Role of Cells, Proteins, and Reactive Oxygen Species

The Ti (alloy) material is not only influenced by the physiological environment but does also change the physiological environment by triggering different cell and immune responses, which in turn influence corrosion mechanisms. This two-way response is a relatively new paradigm within corrosion science and has been supported and proposed by a number of recent scientific studies and discussions

(Gilbert 2017; Hedberg 2018; Hedberg et al. 2019a, b; Gilbert and Kubacki 2016; Gilbert et al. 2015; Milošev 2017; Yu et al. 2015; Zhang et al. 2018a). There is a large arsenal of chemical species and cells in the response of the human body to the metal or alloy. Each of them alone is often not of great concern, but combined with other factors, their action can be devastating to the corrosion process.

A recent study demonstrated a combined effect of mechanical stress and proteins on the corrosion resistance of, and metal release from, Nitinol (Ni-Ti) alloys (Zhang et al. 2020a).

Several studies have shown the combined action of proteins, such as serum albumin, and hydrogen peroxide, which is one of the chemical species produced under inflammatory conditions, on the corrosion resistance of, and metal release from, Ti6Al4V (Yu et al. 2015; Zhang et al. 2018a; Hedberg et al. 2020, 2019b). It has been hypothesized that hydrogen peroxide primarily forms a complex with TiO₂, weakening its bonds and chemical stability, while serum albumin primarily complexes aluminum from the surface oxide (Hedberg et al. 2019b). These complexation processes result first in the enrichment and then the depletion of aluminum in the surface oxide and in the growth of a relatively thick oxide (Hedberg et al. 2019b), similar to those found in vivo. These complexation and metal complex detachment processes take time and are not necessarily possible to detect in short-term accelerated corrosion tests (Zhang et al. 2018a; Hedberg 2018).

It should be emphasized that proteins are not necessarily detrimental to the corrosion process but can also be neutral or beneficial—this depends on the circumstances (Hedberg 2018). In addition to their complexation abilities, they can also have shielding effects, reducing the access to an oxidant, and they can also act as biomarkers, attracting certain cells (both beneficial and detrimental to the corrosion process).

As outlined in Sect. 1.2.2, inflammatory and infection conditions can be considered a worst-case environment. Direct etching tracks related to immune cells have been observed on Co-Cr alloys (Hall et al. 2017), but would most probably result in a thicker oxide, instead of etching, in the case of Ti alloys. The immune system also reacts to protein aggregates, which can be induced by metal ions or nanoparticles (Hedberg et al. 2019a), and wear particles (Sundfeldt et al. 2006). The immune system also reacts to relatively low amounts of released metal ions in the case of sensitization (allergy) to one or several of the metals in the alloys (Chen and Thyssen 2018).

From an engineering perspective, it is, hence, interesting to target the avoidance of infections, the decreased release of metal ions and the increased wear resistance of biomedical Ti alloys.

1.3 Ti Surfaces and Inflammatory Reaction

1.3.1 Host Response to Ti Surfaces

The host response to an implanted biomaterial depends on the material characteristics (e.g., composition, surface texture, degradability, mechanical properties) and host-specific features (such as age, anatomic factors, comorbidities, immune response). This response begins at implantation time and lasts for the whole duration of the material's presence in the human body (Londono and Badylak 2015). The host response is of particular importance because it can affect the implant properties (e.g., degradation, surface alteration) and its functional outcome (e.g., fibrous encapsulation vs. physiological integration).

Upon implantation, the biomaterial surface comes in contact with the physiological fluids and water; ions and proteins sequentially interact within a few seconds. The protein layer, which covers the surface, depends on the material surface properties and affects the cellular/bacterial adhesion to it (Kasemo 2002). The first cells to approach the protein-covered surfaces are neutrophils, with the aim of removing bacteria and debris or damaged tissues in analogy to the conventional wound-healing process in the absence of an implant (Ratner 2001; Londono and Badylak 2015). In 1 day, macrophages reach the surface. As in wound-healing without an implant, the macrophages modulate inflammation (inevitably associated with wounds) to achieve tissue repair. In the presence of a foreign material, the surface properties and host characteristics affect the macrophage response (Ratner 2001, Londono and Badylak 2015). Typically, macrophages can show a pro-inflammatory polarization (M1 state) related to rapid immune activation or an anti-inflammatory polarization (M2) related to wound healing and tissue remodeling. A proper balance between these two states can guarantee a physiological healing, assuring the removal of damaged tissues without the development of chronic inflammatory response (Hotchkiss et al. 2016). In the presence of nondegradable implants (e.g., Ti implants), the macrophages identify the implant as a possible foreign body and try to engulf and digest it: a process often called "frustrated phagocytosis," which ultimately results in the fibrous encapsulation of the implant (Ratner 2001, Londono and Badylak 2015). Metal ions and nanoparticles significantly affect the host response to implants. For example, metal ions can bind host proteins and cause an immunological response resulting in hypersensitivity (Yao et al. 2015). These phenomena are particularly evident for toxic metals such as Ni, Co, and Cr ions released from Co-Cr alloys, or their micro or nanosized particles produced in metal-on-metal joint replacement (recently highly debated). Hypersensitivity and excessive immune response are rarely reported for Ti alloys (Yao et al. 2015). In the case of Ti implants, it has been supposed that the collagenous capsule can evolve into bone mineralization, due to the presence of ions and bone stem cells at the implant site (Ratner 2001). Ti-bone bonding ability has been widely studied, and several surface modifications have been proposed in order to improve it, such as nano/micro textures, bioactive surface layers (obtained by chemical or electrochemical treatments), bioactive coatings (e.g., bioactive glasses or hydroxyapatite), and

surface grafting of bioactive molecules (Souza et al. 2019; Oliver et al. 2019; Spriano et al. 2018, 2010; Kokubo and Yamaguchi 2016; Lugovskoy and Lugovskoy 2014; Chen et al. 2013). The cited surface treatments can induce a significant improvement in the biological response to Ti in terms of osteoblast adhesion, proliferation, and differentiation (in vitro) and of bone formation (in vivo). However, it has been reported that in certain cases a too rapid and conspicuous bone apposition can be associated with an excessive inflammatory response, which can even lead to late implant failure (Stanford 2010). Considering these aspects, the development of Ti surfaces able to improve bone bonding and healing in a physiological manner with strict control of the inflammatory host response is of great interest in the biomaterials field. The strategies currently under investigation for the modulation of inflammatory response to Ti surfaces are discussed in the following section.

Finally, prosthetic infections are always coupled with a strong inflammatory reaction, which can exacerbate the situation and lead to implant failure. The strategies for the preparation of antibacterial surfaces are discussed in Sect. 1.4.

1.3.2 Surface Modifications for Inflammatory Control

The meaning of biocompatibility evolved away from the original concept of an inert, mechanically resistant implant to the concept of a bioactive implant able to improve and fasten tissue integration (especially in the bone contact field) and is today mainly focused on the modulation of the host response to the implant: the goal is a physiological healing, which arises from the modulation of the inflammatory response.

As opposed to bioactivity, bone integration, and even antibacterial activity (see Sect. 1.4), the immunomodulation is still less explored and is actually highly debated in the scientific literature.

Some strategies for the control of the inflammatory response and foreign body reaction have, however, been proposed, such as the tailoring of protein adsorption, the modulation of macrophage polarization, the use of topographical patterns able to modulate macrophage response, the use of biomimetic coatings, the local delivery of anti-inflammatory drugs, the regulation of nitrogen monoxide (NO), and the induction of macrophage apoptosis (Spriano et al. 2018).

Some interesting strategies applied to Ti surfaces are briefly summarized below.

At first, an effect of surface topography on the host immunoresponse has been widely documented in the literature. A reduced attachment of macrophages and the production of anti-inflammatory factors (M2 polarization) have been documented on sandblasted and acid etched surfaces (SLA type) plasma treated to be super-hydrophilic (Hotchkiss et al. 2016) compared to standard tissue culture polystyrene. A combined effect of roughness and wettability has been noticed for these materials. Similarly, it has been observed that a nanotextured Ti oxide layer rich in OH groups (hydrophilic, but not super hydrophilic) on the surface of Ti microbeads implants can significantly reduce macrophage adhesion and increase the production of

anti-inflammatory mediators (Barthes et al. 2020). An anti-inflammatory response of macrophages, mediated by an enhancement of the endothelial cells response and by the reduction of monocytes adhesion, has also been observed on nano- and sub-micrometer-sized rough Ti coatings, intended for cardiovascular applications (Lu and Webster 2015).

On the other hand, M1 macrophage polarization has been observed on TiO₂ nanotubes with a diameter around 100 nm (He et al. 2020, Shen et al. 2019a). However, under oxidative stress, a shift to M2 polarization has been observed in coculture with mesenchymal stem cells (MSc) (Shen et al. 2019b), upon higher MSc recruitment followed by osteogenic differentiation. Moreover, it has been observed that different nanotextures, produced on commercially pure Ti by anodization, able to give an analogous osteogenic activity in vitro, promote different osteointegration in vivo. This effect has been explained by different macrophage polarization mediated by surface roughness.

Ti surfaces have been enriched with various ions, for example, copper (Cu), silver (Ag), and zinc (Zn), in order to promote a multifunctional response (e.g., addition of antibacterial activity) to the implant. Cu²⁺ ions have been introduced on micro-arc oxidized (MAO) Ti by hydrothermal treatment (Huang et al. 2019), by addition of Cu²⁺ ions into the anodization electrolyte (Huang et al. 2018), by selective laser melting of pure Cu (Xu et al. 2018), or by plasma immersion ion implantation (PIII) (Chen et al. 2021). The effect of Cu on the inflammatory response is controversial. Cu addition onto MAO Ti surfaces (Huang et al. 2018, 2019) induced macrophage polarization to the non-favorable inflammatory M1 state, however, a favorable microenvironment for osteogenesis, has been reported due to the release of the pro-osteogenic factor by macrophages cultured on these surfaces. Moreover, an antibacterial activity mediated by macrophages has been observed on these materials. On the other hand, an anti-inflammatory effect has been observed on Ti6Al4V alloy enriched with Cu by selective laser melting (Xu et al. 2018) and on PIII Ti (Chen et al. 2021). It has been observed that the addition of magnesium (Mg) to MAO Ti surfaces is able to promote M2 macrophage polarization (Li et al. 2018a).

An anti-inflammatory effect modulated by calcium (Ca) ions can be cited, considering the reduction of pro-inflammatory factors produced by macrophages on acid etched Ti, enriched with nanoscaled Ca phosphates (Nanotite, Biomet 3i) (Hamlet and Ivanovski 2011). A particular hybrid M1-M2 polarization of macrophages has been observed on hydroxyapatite-coated rough Ti surfaces (Zhang et al. 2019). Finally, ceria (CeO₂) coatings on Ti substrates showed the ability to affect fibronectin orientation and macrophage polarization (M2 state) mediated by the valence state of the Ce ions (Shao et al. 2020).

At last, the strategy of grafting specific organic molecules on Ti surfaces can be reported. The effect of some coupling agents, often used for grafting of biomolecules, on the inflammatory response has been tested. It has been observed that (3-glycidoxypentyl)trimethoxy silane (GPTMS) increases the adsorption of complement proteins and the pro-inflammatory polarization (M1) of macrophages and reduces osteointegration of sandblasted, acid etched Ti, in a dose-dependent

manner (Araújo-Gomes et al. 2019). On the other hand, amino propyl triethoxy silane (APTES) induced M2 macrophage polarization on NaOH treated Ti (Zhang et al. 2018b). A reduction of the inflammatory response has been observed on TiO₂ nanotubes loaded with anti-inflammatory agents such as dexamethasone (Shen et al. 2020) or Interleukin 4(IL4) (Yin et al. 2019). Different peptides, such as a mussel-inspired peptide (Bai et al. 2020) or the cationic peptide cecropin B (Xu et al. 2013), have been coupled with Ti by coordination chemistry or polydopamine-mediated grafting, respectively. Both peptides enabled anti-inflammatory macrophage activity, improvement of osteoblast adhesion and activity, and antibacterial action. A macrophage recruitment agent (SEW2871), intercalated in layer-by-layer chitosan-gelatin coatings on dual acid-etched Ti (He et al. 2020), promoted rapid macrophage recruitment, anti-inflammatory activity, and osteogenesis in in vivo tests. Finally, a multifunctional response (anti-inflammatory, antibacterial, and pro-osteogenic) has been observed after surface grafting of two antibiotics: bacitracin (polydopamine-mediated covalent grafting to Ti6Al4V; Nie et al. 2016) or minocycline (introduced in layer-by-layer chitosan/gelatin coating onto Ti substrates; Shen et al. 2019b).

All these strategies are interesting and promising, but they are often difficult to implement due to the complexity of the biological system to be controlled. In fact, it should be remembered that inflammatory response should be controlled, but not completely suppressed, because it is necessary for tissue healing. Proteins (such as fibronectin), which act as pro-inflammatory agents, can also act as tissue repairing agents and their adsorption must not be completely avoided. The in vivo protein adsorption conditions and cross-talk among different cell types are complex mechanisms, usually different from the ones reproduced in conventional simple in vitro experiments. Moreover, it should be considered that surface modifications, which involve the use of active molecules, can significantly increase the complexity of the regulatory processes of the medical devices.

1.3.3 Inflammatory Response and Corrosion Resistance

As outlined in Sect. 1.2, there is increasing evidence that inflammatory response, which results in high redox potentials and the presence of hydrogen peroxide, has a considerable role in the degradation of Ti (alloys) and the release of metal ions. This is also true for Ti alloys that were optimized for osseointegration, although their corrosion resistance is higher and their metal release is lower, than that of Ti alloys with a thin, native, passive surface oxide (Hedberg et al. 2020).

1.4 Ti Surfaces for Bone Integration and Infection Control

1.4.1 Recent Strategies to Combine Bioactivity and Antibacterial Activity

Prosthetic infections concern 1–2% of hip and knee replacements, and the percentage increases in the case of revision surgery or fixation of open fractures (up to 30–40%) (Trampuz and Widmer 2006). Moreover, prosthetic infections are among the most critical complications in orthopedic surgery because they are associated with both high morbidity and high hospital costs (Trampuz and Widmer 2006; Zimmerli et al. 2004). Even if a strict antibiotic and antibacterial perioperative prophylaxis is currently applied, which can significantly reduce the risk of infection, both orthopedic and dental implant-associated infections are mainly related to bacterial contamination of the implanted surfaces by the formation of a bacterial biofilm (Zimmerli et al. 2004; Subramani et al. 2009). The biofilm is a polysaccharidic structure, in which bacteria can grow and remain mostly unreachable by systemic antibiotics and antimicrobial treatments. In this context, the development of antibacterial surfaces able to limit bacterial adhesion and proliferation is particularly promising.

A first strategy can be the reduction of bacterial adhesion to Ti surfaces without the introduction of any active antibacterial agent. This solution has the advantage that it is not time-limited (no consumption of antibacterial agent due to release), it does not involve potentially toxic substances, and does not require complex certification procedures associated with the release of active agents. On the other hand, it hardly fights infections in cases of severe bacterial contamination (e.g., septic situations). In this scenario, nanotextures have been proposed as potential anti-adhesive Ti surfaces. Nanopatterns, 10–100 nm in depth, have been reported to reduce bacterial adhesion and to impart mechanical stresses to bacterial cell walls, reducing bacterial viability (Linklater et al. 2020). The flexibility and the geometric features (e.g., sharp edges) of these nanotextures can further improve their effectiveness against bacteria. Mammalian cells, in contrast, can better accommodate stresses on nanotextured surfaces due to the higher deformability of their membrane, with resulting high biocompatibility and even cell stimulation ability (focal contact formation) for the host cells. Similarly, a reduced bacterial adhesion has been documented on bioactive nanotextured Ti oxide layers, even in the absence of any antibacterial agent (Ferraris et al. 2019). Recently, the role of surface microstructure of metal surfaces (induced by electron beam or thermal treatments) in reducing bacterial adhesion has also been reported (Ferraris et al. 2019b, 2020).

Several strategies have also been proposed for the realization of bactericidal Ti surfaces. The introduction of inorganic antibacterial agents (e.g., Ag, Cu, and Zn) by means of surface doping (e.g., ion implantation, in situ reduction, or alloys), growth and doping of TiO₂ layers (e.g., anodization), or deposition of doped coatings (e.g., plasma spray, sputtering, or sol-gel), grafting of antimicrobial polymers, antimicrobial peptides, biomolecules, or antibiotics (by direct grafting, covalent grafting mediated by silanes, catechol or phosphates, or entrapment into coatings) can be

cited among the most popular ones (Ferraris and Spriano 2016; Chouirfa et al. 2019; Hickok and Shapiro 2012).

There is a bacterial competition with host cells for surface colonization of implanted biomaterials, as reported in the well-known “race for the surface” (Gristina 1987). Therefore, implant surfaces able to reduce bacterial contamination and at the same time improve tissue adhesion (bioactive and antibacterial) can be of particular interest.

In this view, inorganic antibacterial agents, as well as antibiotics, have been coupled to bioactive Ti surfaces, such as Ca phosphates, hydroxyapatite, or bioactive glass coatings, bioactive TiO₂ layers (obtained in the form of thick coatings, chemically modified thin layers, or nanotubes), porous coatings intended for bone ingrowth, or complex multilayer coatings (Ferraris and Spriano 2016; Chouirfa et al. 2019; Spriano et al. 2018; Raphael et al. 2016).

The above-cited solutions can simultaneously counteract bacterial infection and promote bone regeneration; however, it has been pointed out that in some cases infections can activate macrophages (lipopolysaccharide (LPS) stimulation) to recruit osteoclasts and induce infection-mediated osteolysis (Raphael et al. 2016). In these cases, the immunomodulation strategies discussed in Sect. 1.3 can be of interest to overcome the problem.

All the solutions discussed above are generally tested on bulk plane Ti (alloy) samples or model implants. Currently, additive manufacturing (AM) is becoming popular for the realization of customized Ti implants and the transfer of the developed technologies for generating bioactive and antibacterial surfaces on AM implants is under investigation (Li et al. 2020). Strategies able to modify both the inner and outer surfaces of pores are advantageous for this purpose.

1.4.2 Mechanical Stability

In order to be suitable for clinical applications, innovative antibacterial and bioactive surfaces should be able to sustain implantation loads and friction, as well as mechanical stresses, for the whole implant life. Otherwise, the effective surface exposed to the biological environment will not be the designed one (with antibacterial and bioactive functionalities) and the formation of wear debris can stimulate inflammatory reactions.

Adhesion and mechanical stability have been pointed out as critical issues in the application of anti-adhesive polymers (Raphael et al. 2016); however, they are not always well described for innovative multifunctional surfaces.

Coating adhesion is one of the key factors for the applicability of a coating to implantable medical devices. It can be measured *in vitro* by means of tensile tests, as suggested by ISO standard 13779-4, indentation, scratch, tape, pull-out or bending tests, as reported in the scientific literature for various antibacterial and bioactive coatings (Verné et al. 2008; Utku et al. 2015; Onoki et al. 2008; Ferraris et al. 2020b; Stan et al. 2013; Surmeneva et al. 2017). Moreover, the realization of customized implant simulation tests in non-vital animal bone has been reported as a successful

strategy to test the resistance of new surfaces to implantation friction and loads (Ferraris et al. 2015; Li et al. 2018b).

The adhesion strength of coatings and modified surface layers is strongly affected by the surface pretreatment before coating deposition (e.g., realization of intermediate layers, chemical and electrochemical pretreatments aimed at improving the coating-substrate affinity, and mechanical interlocking), as well as by the process parameters (e.g., in the preparation of TiO₂ nanotubes) or by post-treatments (such as thermal treatments or sterilization processes) and by coating thickness (Stan et al. 2013; Onoki et al. 2008; Utku et al. 2015; Li et al. 2018b; Surmeneva et al. 2017). Recently, it has been evidenced that the addition of graphene oxide to vancomycin-loaded strontium (Sr)doped hydroxyapatite electrodeposited on Ti surfaces can significantly improve the coating's mechanical properties, such as hardness, elastic modulus, and adhesion (Zhang et al. 2020b). Considering bioactive and antibacterial surfaces, the reactivity in physiological environment is another critical factor to be considered, because it can affect their mechanical and chemical stability (Ferraris et al. 2020c).

1.4.3 Chemical Stability and Corrosion Resistance

For surface oxides incorporated with antimicrobial metal nanoparticles, such as Ag (Hedberg et al. 2020) and Cu (Bernstein et al. 2017) nanoparticles, galvanic effects could occur under certain circumstances. While only a slight effect was found in a study on Ti6Al4V with an artificially grown oxide with embedded Ag nanoparticles (Hedberg et al. 2020), a more pronounced galvanic effect was found for Ti6Al4V without such a thick oxide and coated with silver (Furko et al. 2016).

All in all, it is more likely that such surface engineering efforts would benefit the overall corrosion performance by reducing the extent of infection/inflammation; however, under certain circumstances, this galvanic couple could be a triggering factor for other corrosion types.

1.4.4 Ion/Nanoparticles Release

Infection control requires a certain release of antibacterial metal ions, such as Ag and Cu (Spriano et al. 2018). Ideally, this release is limited to ions, and does not include the metal nanoparticles themselves. However, some release of metal nanoparticles can be expected. Indeed, an increased release of particles was observed in vitro for Ti6Al4V with embedded Ag nanoparticles as compared to a Ag-free counterpart; however, it was unclear if this was due to released Ag nanoparticles or due to Ag-ion-induced protein aggregation (Hedberg et al. 2020). The actual measurable and stable ion release is strongly influenced by the solution chemistry of the metal. Ti ions are very unstable in most aqueous and physiologically relevant solutions, while the stability of Al, Ag, and V ions is strongly influenced by the presence of complexing agents such as proteins (Hedberg et al. 2020) and that of Cr ions can

be influenced by the redox potential. This may result in the underestimation of Ti ion release and be a main explanation for the primarily TiO₂-rich oxide growth and the frequently observed presence of TiO₂ particles in vivo.

1.5 Conclusions

Even if Ti and Ti alloys are well-known for their high corrosion resistance and biocompatibility because they are usually greater than those of other metals used for biomedical implants, environmental conditions, especially infections and inflammatory conditions, can strongly affect their surface condition and corrosion. Relevant corrosion types are often caused by a combination of geometrical factors (i.e., crevices), mechanical factors, such as micromotions and fretting, physiological factors, such as inflammation and the presence of complexing proteins, and/or the coupling to other metals. Considering the importance of the physiological environment, the development of new Ti surfaces able to improve tissue bonding and physiological healing with a modulation of the inflammatory host response and control of infection development is of great interest.

Bioactive and antibacterial titanium surfaces have been widely explored in the scientific literature and some surface treatments are already on the market and there is clinical application with encouraging results. However, some concerns related to excessive inflammatory response and possibly infection-mediated osteolysis still exist. In this scenario, surfaces able to promote physiological healing, and also taking the inflammatory response to the implant into account, seem to be very promising. This topic is less explored and its clinical application is not yet ready. For this reason, it is worthy to be investigated in further scientific research.

References

- Araújo-Gomes N, Romero-Gavilán F, Zhang Y, Martínez-Ramos C, Elortza F, Azkargorta M, Martín de Llano JJ, Gurruchaga M, Goñi I, van den Beucken JJJP, Suay J (2019) Complement proteins regulating macrophage polarisation on biomaterials. *Colloids Surf B: Biointerfaces* 181:125–133
- Bai J, Wang H, Chen H, Ge G, Wang M, Gao A, Tong L, Xu Y, Yang H, Pan G, Chu PK, Geng D (2020) Biomimetic osteogenic peptide with mussel adhesion and osteoimmunomodulatory functions to ameliorate interfacial osseointegration under chronic inflammation. *Biomaterials* 255:120197
- Barthes J, Cazzola M, Muller C, Dollinger C, Debry C, Ferraris S, Spriano S, Vrana NE (2020) Controlling porous titanium/soft tissue interactions with an innovative surface chemical treatment: responses of macrophages and fibroblasts. *Mater Sci Eng C* 112:110845
- Bernstein A, Suedkamp N, Mayr HO, Gadow R, Burtscher S, Arhire I, Killinger A, Krieg P (2017) Chapter 5 - thin degradable coatings for optimization of osseointegration associated with simultaneous infection prophylaxis. In: Ficaí A, Grumezescu AM (eds) *Nanostructures for antimicrobial therapy*. Elsevier, Amsterdam, pp 117–137. <https://doi.org/10.1016/B978-0-323-46152-8.00005-6>

- Chan E, Cadosch D, Gautschi OP, Sprengel K, Filgueira L (2011) Influence of metal ions on human lymphocytes and the generation of titanium-specific T-lymphocytes. *J Appl Biomater Biomech* 9(2):137–143. <https://doi.org/10.5301/jabb.2011.8567>
- Chen JK, Thyssen JP (eds) (2018) *Metal allergy - from dermatitis to implant and device failure*, 1st edn. Springer, Cham. <https://doi.org/10.1007/978-3-319-58503-1>
- Chen C, Zhang S-M, Lee I-S (2013) Immobilizing bioactive molecules onto titanium implants to improve osseointegration. *Surf Coat Technol* 228:S312–S317
- Chen L, Wang D, Qiu J, Zhang X, Liu X, Qiao Y, Liu X (2021) Synergistic effects of immunoregulation and osteoinduction of ds-block elements on titanium surface. *Bioact Mater* 6:191–207
- Chouirfa H, Bouloussa H, Mignonney V, Falentin-Daudré C (2019) Review of titanium surface modification techniques and coatings for antibacterial applications. *Acta Biomater* 83:37–54
- Claesson PM, Blomberg E, Fröberg JC, Nylander T, Arnebrant T (1995) Protein interactions at solid surfaces. *Adv Colloid Interface Sci* 57:161–227
- Clarke CF, Hardie D, Ikeda BM (1997) Hydrogen-induced cracking of commercial purity titanium. *Corros Sci* 39(9):1545–1559
- Cortada M, Giner L, Costa S, Gil FJ, Rodríguez D, Planell JA (2000) Galvanic corrosion behavior of titanium implants coupled to dental alloys. *J Mater Sci Mater Med* 11(5):287–293. <https://doi.org/10.1023/a:1008905229522>
- Ding R, Shang J-X, Wang F-H, Chen Y (2018) Electrochemical Pourbaix diagrams of NiTi alloys from first-principles calculations and experimental aqueous states. *Comput Mater Sci* 143:431–438. <https://doi.org/10.1016/j.commatsci.2017.11.033>
- Eliades T, Pratsinis H, Kletsas D, Eliades G, Makou M (2004) Characterization and cytotoxicity of ions released from stainless steel and nickel-titanium orthodontic alloys. *Am J Orthod Dentofacial Orthop* 125(1):24–29
- Evrard L, Waroquier D, Parent D (2010) Allergies to dental metals. Titanium: a new allergen. *Revue médicale de Bruxelles* 31(1):44
- Faccioni F, Franceschetti P, Cerpelloni M, Fracasso ME (2003) In vivo study on metal release from fixed orthodontic appliances and DNA damage in oral mucosa cells. *Am J Orthod Dentofacial Orthop* 124(6):687–693
- Ferraris S, Spriano S (2016) Antibacterial titanium surfaces for medical implants. *Mater Sci Eng C* 61:965–978
- Ferraris S, Bobbio A, Miola M, Spriano S (2015) Micro- and nano-textured, hydrophilic and bioactive titanium dental implants. *Surf Coat Technol* 276:374–383
- Ferraris S, Cochis A, Cazzola M, Tortello M, Scalia A, Spriano S, Rimondini L (2019) Cytocompatible and anti-bacterial adhesion Nanotextured titanium oxide layer on titanium surfaces for dental and orthopedic implants. *Front Bioeng Biotechnol* 7:103. <https://doi.org/10.3389/fbioe.2019.00103>
- Ferraris S, Warchomicka F, Ramskogler C, Tortello M, Cochis A, Scalia A, Gautier di Confienigo G, Keckes J, Rimondini L, Spriano S (2019b) Surface structuring by electron beam for improved soft tissues adhesion and reduced bacterial contamination on Ti-grade 2. *J Mater Process Technol* 266:518–529
- Ferraris S, Warchomicka F, Iranshahi F, Rimondini L, Cochis A, Spriano S (2020) Electron beam structuring of Ti6Al4V: new insights on the metal surface properties influencing the bacterial adhesion. *Materials* 2020(13):409. <https://doi.org/10.3390/ma13020409>
- Ferraris S, Perero S, Costa P, Gautier di Confienigo G, Cochis A, Rimondini L, Renaux F, Vernè E, Ferraris M, Spriano S (2020b) Antibacterial inorganic coatings on metallic surfaces for temporary fixation devices. *Appl Surf Sci* 508:144707
- Ferraris S, Yamaguchi S, Barbani N, Cristallini C, Gautier di Confienigo G, Barberi J, Cazzola M, Miola M, Vernè E, Spriano S (2020c) The mechanical and chemical stability of the interfaces in bioactive materials: the substrate-bioactive surface layer and hydroxyapatitebioactive surface layer interfaces. *Mater Sci Eng C* 116:111238
- Fukuzaki S, Urano H, Nagata K (1995) Adsorption of protein onto stainless-steel surfaces. *J Ferment Bioeng* 80(1):6–11. [https://doi.org/10.1016/0922-338X\(95\)98168-K](https://doi.org/10.1016/0922-338X(95)98168-K)

- Furko M, Lakatos-Varsányi M, Balázi C (2016) Complex electrochemical studies on silver-coated metallic implants for orthopaedic application. *J Solid State Electrochem* 20(1):263–271. <https://doi.org/10.1007/s10008-015-3026-1>
- Gilbert J (2017) Corrosion in the human body: metallic implants in the complex body environment. *Corrosion* 73(12):1478–1495. <https://doi.org/10.5006/2563>
- Gilbert JL, Kubacki GW (2016) Chapter three - oxidative stress, inflammation, and the corrosion of metallic biomaterials: corrosion causes biology and biology causes corrosion A2 - Dziubla, Thomas. In: Butterfield DA (ed) *Oxidative stress and biomaterials*. Academic, Boston, pp 59–88. <https://doi.org/10.1016/B978-0-12-803269-5.00003-6>
- Gilbert JL, Mali S, Urban RM, Silverton CD, Jacobs JJ (2012) In vivo oxide-induced stress corrosion cracking of Ti-6Al-4V in a neck–stem modular taper: emergent behavior in a new mechanism of in vivo corrosion. *J Biomed Mater Res B* 100(2):584–594
- Gilbert JL, Sivan S, Liu Y, Kocagöz SB, Arnholt CM, Kurtz SM (2015) Direct in vivo inflammatory cell-induced corrosion of CoCrMo alloy orthopedic implant surfaces. *J Biomed Mater Res A* 103(1):211–223. <https://doi.org/10.1002/jbm.a.35165>
- Gong Z, Li M, Guo X, Ma Z, Shi J (2013) Stent implantation in patients with metal allergy: a systemic review and meta-analysis. *Coron Artery Dis* 24(8):684–689
- Grande F, Tucci P (2016) Titanium dioxide nanoparticles: a risk for human health? *Mini Rev Med Chem* 16(9):762–769
- Gristina AG (1987) Biomaterial-centered infection: microbial adhesion versus tissue integration. *Science* 237:1588–1595
- Hall DJ, Pourzal R, Lundberg HJ, Mathew MT, Jacobs JJ, Urban RM (2017) Mechanical, chemical and biological damage modes within head-neck tapers of CoCrMo and Ti6Al4V contemporary hip replacements. *J Biomed Mater Res B*. <https://doi.org/10.1002/jbm.b.33972>
- Hall DJ, Pourzal R, Lundberg HJ, Mathew MT, Jacobs JJ, Urban RM (2018) Mechanical, chemical and biological damage modes within head-neck tapers of CoCrMo and Ti6Al4V contemporary hip replacements. *J Biomed Mater Res B* 106(5):1672–1685. <https://doi.org/10.1002/jbm.b.33972>
- Hamann C (2018) Metal allergy: titanium. In: Chen J, Thyssen JP (eds) *Metal allergy*. Springer, Cham, pp 443–466
- Hamlet S, Ivanovski S (2011) Inflammatory cytokine response to titanium chemical composition and nanoscale calcium phosphate surface modification. *Acta Biomater* 7:2345–2353
- He X, Noël JJ, Shoesmith DW (2009) Crevice corrosion of grade-12 titanium. In: Papavinasam S, Berke N, Brossia S (eds) *Advances in electrochemical techniques for corrosion monitoring and measurement*. ASTM International, West Conshohocken, pp 281–299. <https://doi.org/10.1520/STP48753S>
- He Y, Xu K, Li K, Yuan Z, Ding Y, Chen M, Lin C, Tao B, Li X, Zhang G, Liu P, Cai K (2020) Improved osteointegration by SEW2871-encapsulated multilayers on micro-structured titanium via macrophages recruitment and immunomodulation. *Appl Mater Today* 20:100673
- Hedberg YS (2018) Role of proteins in the degradation of relatively inert alloys in the human body. *NPJ Materials Degrad* 2:26. <https://doi.org/10.1038/s41529-018-0049-y>
- Hedberg YS, Odnevall Wallinder I (2016) Metal release from stainless steel in biological environments: a review. *Biointerphases* 11(1):018901–018901–018901–018917. <https://doi.org/10.1116/1.4934628>
- Hedberg Y, Karlsson M-E, Blomberg E, Odnevall Wallinder I, Hedberg J (2014) Correlation between surface physicochemical properties and the release of iron from stainless steel AISI 304 in biological media. *Colloid Surface B* 122:216–222. <https://doi.org/10.1016/j.colsurfb.2014.06.066>
- Hedberg YS, Dobryden I, Chaudhary H, Wei Z, Claesson P, Lendel C (2019a) Synergistic effects of metal-induced aggregation of human serum albumin. *Colloid Surf B* 173:751–758. <https://doi.org/10.1016/j.colsurfb.2018.10.061>
- Hedberg YS, Žnidaršič M, Herting G, Milošev I, Odnevall Wallinder I (2019b) Mechanistic insight on the combined effect of albumin and hydrogen peroxide on surface oxide composition and

- extent of metal release from Ti6Al4V. *J Biomed Mater Res B* 107(3):858–867. <https://doi.org/10.1002/jbm.b.34182>
- Hedberg YS, Gamna F, Padoan G, Ferraris S, Cazzola M, Herting G, Atapour M, Spriano S, Odenvall Wallinder I (2020) Surface modified Ti6Al4V for enhanced bone bonding ability - effects of silver and corrosivity at simulated physiological conditions from a corrosion and metal release perspective. *Corros Sci* 168:108566. <https://doi.org/10.1016/j.corsci.2020.108566>
- Hickok NJ, Shapiro IM (2012) Immobilized antibiotics to prevent orthopaedic implant infections. *Adv Drug Deliv Rev* 64:1165–1176
- Hosoki M, Nishigawa K, Miyamoto Y, Ohe G, Matsuka Y (2016) Allergic contact dermatitis caused by titanium screws and dental implants. *J Prosthodont Res* 60(3):213–219
- Hotchkiss KM, Reddy GB, Hyzy SL, Schwartz Z, Boyan BD, Olivares-Navarrete R (2016) Titanium surface characteristics, including topography and wettability, alter macrophage activation. *Acta Biomater* 31:425–434
- Huang Q, Li X, Elkhooly TA, Liu X, Zhang R, Wu H, Feng Q, Liu Y (2018) The Cu-containing TiO₂ coatings with modulatory effects on macrophage polarization and bactericidal capacity prepared by micro-arc oxidation on titanium substrates. *Colloids Surf B Biointerfaces* 170:242–250
- Huang Q, Ouyang Z, Tan Y, Wu H, Liu Y (2019) Activating macrophages for enhanced osteogenic and bactericidal performance by Cu ion release from micro/nano-topographical coating on a titanium substrate. *Acta Biomater* 100:415–426
- Jin T, Berlin M (2015) Titanium. In: Nordberg GF, Fowler BA, Nordberg M (eds) *Handbook on the toxicology of metals*, vol 2, 4th edn. Elsevier, Amsterdam, pp 1287–1296
- Kasemo B (2002) Biological surface science surface. *Science* 500:656–677
- Kokubo T, Yamaguchi S (2016) Novel bioactive materials developed by simulated body fluid evaluation: surface-modified Ti metal and its alloys. *Acta Biomater* 44:16–30
- Kumazawa R, Watari F, Takashi N, Tanimura Y, Uo M, Totsuka Y (2002) Effects of Ti ions and particles on neutrophil function and morphology. *Biomaterials* 23(17):3757–3764
- Li X, Wang J, E-h H, Ke W (2007) Influence of fluoride and chloride on corrosion behavior of NiTi orthodontic wires. *Acta Biomater* 3(5):807–815. <https://doi.org/10.1016/j.actbio.2007.02.002>
- Li X, Huang Q, Liu L, Zhu W, Elkhooly TA, Liu Y, Feng Q, Li Q, Zhou S, Liu Y, Wu H (2018a) Reduced inflammatory response by incorporating magnesium into porous TiO₂ coating on titanium substrate. *Colloids Surf B Biointerfaces* 171:276–284
- Li T, Gulati K, Wang N, Zhang Z, Ivanovski S (2018b) Understanding and augmenting the stability of therapeutic nanotubes on anodized titanium implants. *Mater Sci Eng C* 88:182–195
- Li J, Cui X, Hooper GJ, Lim KS, Woodfield TBF (2020) Rational design, bio-functionalization and biological performance of hybrid additive manufactured titanium implants for orthopaedic applications: a review. *J Mech Behav Biomed Mater* 105:103671
- Linklater DP, Baulin VA, Juodkazis S, Crawford RJ, Stoodley P, Ivanova EP (2020) Mechano-bactericidal actions of nanostructured surfaces. *Nat Rev Microbiol*. <https://doi.org/10.1038/s41579-020-0414-z>
- Londono R, Badylak SF (2015) Factors which affects the host response to biomaterials. In: Badylak SF (ed) *Host response to biomaterials*. Elsevier, Amsterdam
- Lu J, Webster TJ (2015) Reduced immune cell responses on nano and submicron rough titanium. *Acta Biomater* 16:223–231
- Lucas LC, Buchanan RA, Lemons JE (1981) Investigations on the galvanic corrosion of multialloy total hip prostheses. *J Biomed Mater Res* 15(5):731–747. <https://doi.org/10.1002/jbm.820150509>
- Lugovskoy A, Lugovskoy S (2014) Production of hydroxyapatite layers on the plasma electrolytically oxidized surface of titanium alloys. *Mater Sci Eng C* 43:527–532
- Mani G, Feldman MD, Patel D, Agrawal CM (2007) Coronary stents: a materials perspective. *Biomaterials* 28(9):1689–1710

- McCafferty E (2010) Thermodynamics of corrosion: Pourbaix diagrams. In: Introduction to corrosion science. Springer, New York, pp 95–117. https://doi.org/10.1007/978-1-4419-0455-3_6
- Milošev I (2017) From in vitro to retrieval studies of orthopaedic implants. *Corrosion* 73 (12):1496–1509
- Milošev I, Metikos-Hukovic M, Strehblow HH (2000) Passive film on orthopaedic TiAlV alloy formed in physiological solution investigated by X-ray photoelectron spectroscopy. *Biomaterials* 21(20):2103–2113
- Milošev I, Kosec T, Strehblow HH (2008) XPS and EIS study of the passive film formed on orthopaedic Ti–6Al–7Nb alloy in Hank's physiological solution. *Electrochim Acta* 53 (9):3547–3558. <https://doi.org/10.1016/j.electacta.2007.12.041>
- Mirjalili M, Momeni M, Ebrahimi N, Moayed MH (2013) Comparative study on corrosion behaviour of nitinol and stainless steel orthodontic wires in simulated saliva solution in presence of fluoride ions. *Mater Sci Eng C* 33(4):2084–2093. <https://doi.org/10.1016/j.msec.2013.01.026>
- Nelson JC, Oriani RA (1993) Stress generation during anodic oxidation of titanium and aluminum. *Corros Sci* 34(2):307–326
- Nie B, Ao H, Zhou J, Tang T, Yue B (2016) Biofunctionalization of titanium with bacitracin immobilization shows potential for anti-bacteria, osteogenesis and reduction of macrophage inflammation. *Colloids Surf B Biointerfaces* 145:728–739
- Noël JJ (1999) The electrochemistry of titanium corrosion. PhD Thesis, The University of Manitoba, Manitoba
- Noël J, Ebrahimi N, Shoesmith D (2018) Corrosion of titanium and titanium alloys. In: Wandelt K (ed) *Encyclopedia of interfacial chemistry: surface science and electrochemistry*, vol 6. Elsevier, Amsterdam, pp 192–200
- Noguchi T, Takemoto S, Hattori M, Yoshinari M, Kawada E, Oda Y (2008) Discoloration and dissolution of titanium and titanium alloys with immersion in peroxide- or fluoride-containing solutions. *Dent Mater J* 27(1):117–123
- Oliver JN, Su Y, Lu X, Kuo P-H, Du J, Zhu D (2019) Bioactive glass coatings on metallic implants for biomedical applications. *Bioact. Mater* 4:261–270
- Olmedo DG, Tasat DR, Guglielmotti MB, Cabrini RL (2008) Biodistribution of titanium dioxide from biologic compartments. *J Mater Sci Mater Med* 19(9):3049–3056. <https://doi.org/10.1007/s10856-008-3438-x>
- Onoki T, Hosoi K, Hashida T, Tanabe Y, Watanabe T, Yasuda E, Yoshimura M (2008) Effects of titanium surface modifications on bonding behavior of hydroxyapatite ceramics and titanium by hydrothermal hot-pressing. *Mater Sci Eng C* 28:207–212
- Peters RJ, Oomen AG, van Bommel G, van Vliet L, Undas AK, Munniks S, Bleys RL, Tromp PC, Brand W, van der Lee M (2020) Silicon dioxide and titanium dioxide particles found in human tissues. *Nanotoxicology* 14(3):420–432
- Pourbaix M (1974) *Atlas of electrochemical equilibria in aqueous solution*. NACE, Houston
- Raphel J, Holodny M, Goodman SB, Heilshorn SC (2016) Multifunctional coatings to simultaneously promote osseointegration and prevent infection of orthopaedic implants. *Biomaterials* 84:301e314
- Ratner BD (2001) Replacing and renewing: synthetic materials, biomimetics, and tissue engineering in implant dentistry. *J Dent Educ* 65:1340–1347
- Reclaru L, Meyer JM (1998) Effects of fluorides on titanium and other dental alloys in dentistry. *Biomaterials* 19(1):85–92. [https://doi.org/10.1016/S0142-9612\(97\)00179-8](https://doi.org/10.1016/S0142-9612(97)00179-8)
- Sarmiento-González A, Encinar JR, Marchante-Gayón JM, Sanz-Medel A (2008) Titanium levels in the organs and blood of rats with a titanium implant, in the absence of wear, as determined by double-focusing ICP-MS. *Anal Bioanal Chem* 393(1):335. <https://doi.org/10.1007/s00216-008-2449-2>
- Saylor DM, Adidharma L, Fisher JW, Brown RP (2016) A biokinetic model for nickel released from cardiovascular devices. *Regul Toxicol Pharmacol* 80:1–8. <https://doi.org/10.1016/j.yrtph.2016.05.019>

- Schmets J, van Muylder J, Pourbaix M (1974) Titanium. In: Pourbaix M (ed) Atlas of electrochemical equilibria in - aqueous solutions. NACE, Houston, pp 213–222
- Shakeel M, Jabeen F, Shabbir S, Asghar MS, Khan MS, Chaudhry AS (2016) Toxicity of Nano-titanium dioxide (TiO₂-NP) through various routes of exposure: a review. *Biol Trace Elem Res* 172(1):1–36. <https://doi.org/10.1007/s12011-015-0550-x>
- Shao D, Li K, You M, Liu S, Hu T, Huang L, Xie Y, Zheng X (2020) Macrophage polarization by plasma sprayed ceria coatings on titanium-based implants: cerium valence state matters. *Appl Surf Sci* 504:144070
- Shen X, Yu Y, Ma P, Luo Z, Hu Y, Li M, He Y, Zhang Y, Peng Z, Song G, Cai K (2019a) Titania nanotubes promote osteogenesis via mediating crosstalk between macrophages and MSCs under oxidative stress. *Colloids Surf B Biointerfaces* 180:39–48
- Shen X, Gu H, Ma P, Luo Z, Li M, Hu Y, Cai K (2019b) Minocycline-incorporated multilayers on titanium substrates for simultaneous regulation of MSCs and macrophages. *Mater Sci Eng C* 102:696–707
- Shen K, Tang Q, Fang X, Zhang C, Zhu Z, Hou Y, Lai M (2020) The sustained release of dexamethasone from TiO₂ nanotubes reinforced by chitosan to enhance osteoblast function and anti-inflammation activity. *Mater Sci Eng C* 116:111241
- Shukla AK, Balasubramaniam R, Bhargava S (2005) Properties of passive film formed on CP titanium, Ti–6Al–4V and Ti–13.4Al–29Nb alloys in simulated human body conditions. *Intermetallics* 13(6):631–637. <https://doi.org/10.1016/j.intermet.2004.10.001>
- Souza JCM, Sordi MB, Kanazawa M, Ravindran S, Henriques B, Silva FS, Aparicio C, Cooper LF (2019) Nano-scale modification of titanium implant surfaces to enhance osseointegration. *Acta Biomater* 94:112–131
- Spriano S, Ferraris S, Bianchi CL, Cassinelli C, Torricelli P, Fini M, Rimondini L, Giardino R (2010) Bioactive titanium surfaces. In: Sanchez PN (ed) Titanium alloys: preparation, properties and applications. Nova Science, New York. ISBN: 978-1-60876-151-7
- Spriano S, Yamaguchi S, Bairo F, Ferraris S (2018) A critical review of multifunctional titanium surfaces: new frontiers for improving osseointegration and host response, avoiding bacteria contamination. *Acta Biomater* 79:1–22
- Stan GE, Popa AC, Galca AC, Aldica G, Ferreira JMF (2013) Strong bonding between sputtered bioglass–ceramic films and Ti-substrate implants induced by atomic inter-diffusion post-deposition heat-treatments. *Appl Surf Sci* 280:530–538
- Stanford CM (2010) Surface modification of biomedical and dental implants and the processes of inflammation, wound healing and bone formation *Int. J Mol Sci* 11(1):354–369. <https://doi.org/10.3390/ijms11010354>
- Suárez C, Vilar T, Gil J, Sevilla P (2010) In vitro evaluation of surface topographic changes and nickel release of lingual orthodontic archwires. *J Mater Sci Mater Med* 21(2):675–683. <https://doi.org/10.1007/s10856-009-3898-7>
- Subramani K, Jung RE, Molenberg A, Hämmerle CHF (2009) Biofilm on dental implants: a review of the literature. *Int J Oral Maxillofac Implants* 24(4):616–626
- Sullivan SJL, Dreher ML, Zheng J, Chen L, Madamba D, Miyashiro K, Trépanier C, Nagaraja S (2015) Effects of oxide layer composition and radial compression on nickel release in nitinol stents. *Shape Memory Superelasticity* 1(3):319–327. <https://doi.org/10.1007/s40830-015-0028-x>
- Sundfeldt M, Carlsson LV, Johansson CB, Thomsen P, Gretzer C (2006) Aseptic loosening, not only a question of wear: a review of different theories. *Acta Orthop* 77(2):177–197
- Surmeneva MA, Sharonova AA, Chernousova S, Prymak O, Loza K, Tkachev MS, Shulepov IA, Epple M, Surmenev RA (2017) Incorporation of silver nanoparticles into magnetron-sputteredcalcium phosphate layers on titanium as an antibacterial coating. *Colloids Surf B Biointerfaces* 156:104–113
- Swaminathan V, Gilbert JL (2012) Fretting corrosion of CoCrMo and Ti6Al4V interfaces. *Biomaterials* 33(22):5487–5503

- Swiatkowska I, Mosselmans JFW, Geraki T, Wyles CC, Maleszewski JJ, Henckel J, Sampson B, Potter DB, Osman I, Trousdale RT, Hart AJ (2018) Synchrotron analysis of human organ tissue exposed to implant material. *J Trace Element Med Biol* 46:128–137. <https://doi.org/10.1016/j.jtemb.2017.12.007>
- Tal-Gutelmacher E, Eliezer D (2005) Hydrogen cracking in titanium-based alloys. *J Alloys Compd* 404:621–625
- Thewes M, Kretschmer R, Gfesser M, Rakoski J, Nerlich M, Borelli S, Ring J (2001) Immunohistochemical characterization of the perivascular infiltrate cells in tissues adjacent to stainless steel implants compared with titanium implants. *Arch Orthop Trauma Surg* 121(4):223–226
- Trampuz A, Widmer AS (2006) Infections associated with orthopedic implants. *Curr Opin Infect Dis* 19:349–356
- Utku FS, Seckin E, Goller G, Tamerler C, Urgan M (2015) Electrochemically designed interfaces: hydroxyapatite coated macro-mesoporous titania surfaces. *Appl Surf Sci* 350:62–68
- Verné E, Ferraris S, Miola M, Fucale G, Maina G, Robotti P, Bianchi G, Martinasso G, Canuto RA, Vitale-Brovarone C (2008) Synthesis and characterisation of bioactive and antibacterial glass-ceramic part 2 – plasma spray coatings on metallic substrates. *Adv Appl Ceram* 107:245–253
- Xu D, Yang W, Hu Y, Luo Z, Li J, Hou Y, Liu Y, Cai K (2013) Surface functionalization of titanium substrates with cecropin B to improve their cytocompatibility and reduce inflammation responses. *Colloids Surf B Biointerfaces* 110:225–235
- Xu Z, Lu Y, Li S, Guo S, He M, Luo K, Lin J (2018) Copper-modified Ti6Al4V alloy fabricated by selective laser melting with pro-angiogenic and anti-inflammatory properties for potential guided bone regeneration applications. *Mater Sci Eng C* 90:198–210
- Yao Z, Lin TH, Pajarinen J, Sato T, Goodman S (2015) Host response to orthopedic implants (metals and plastics). In: Badylak SF (ed) *Host response to biomaterials*. Elsevier, Amsterdam
- Yin X, Li Y, Yang C, Weng J, Wang J, Zhou J, Feng B (2019) Alginate/chitosan multilayer films coated on IL-4-loaded TiO₂ nanotubes for modulation of macrophage phenotype. *Int J Biol Macromol* 133:503–513
- Yu F, Addison O, Davenport AJ (2015) A synergistic effect of albumin and H₂O₂ accelerates corrosion of Ti6Al4V. *Acta Biomater* 26:355–365
- Zhang Y, Addison O, Yu F, Troconis BCR, Scully JR, Davenport AJ (2018a) Time-dependent enhanced corrosion of Ti6Al4V in the presence of H₂O₂ and albumin. *Sci Rep* 8(1):3185
- Zhang H, Wu X, Wang G, Liu P, Qin S, Xu K, Tong D, Ding H, Tang H, Ji F (2018b) Macrophage polarization, inflammatory signaling, and NF- κ B activation in response to chemically modified titanium surfaces. *Colloids Surf B Biointerfaces* 166:269–276
- Zhang Y, Cheng X, Jansen JA, Yang F, van den Beucken JJJP (2019) Titanium surfaces characteristics modulate macrophage polarization. *Mater Sci Eng C* 95:143–151
- Zhang C, He L, Chen Y, Dai D, Su Y, Shao L (2020a) Corrosion behavior and in vitro cytotoxicity of Ni–Ti and stainless steel arch wires exposed to lysozyme, ovalbumin, and bovine serum albumin. *ACS Omega*. <https://doi.org/10.1021/acsomega.0c02312>
- Zhang X, Song G, Qiao H, Lan J, Wang B, Yang H, Ma L, Wang S, Wang Z, Lin H, Han S, Kang S, Chang X, Huang Y (2020b) Novel ternary vancomycin/strontium doped hydroxyapatite/graphene oxide bioactive composite coatings electrodeposited on titanium substrate for orthopedic applications. *Colloids Surf A Physicochem Eng Asp* 603:125223
- Zimmerli WJ, Trampuz A, Ochsner PE (2004) Prosthetic-joint infections. *N Engl J Med* 351:16. www.nejm.org. Accessed 14 Oct 2004



Nanoscale Surface Engineering and Characterization of Biomaterials

2

Abshar Hasan and Lalit M. Pandey

Abstract

Natural or synthetic materials that interact with biological environments for medical applications such as to support, enhance, repair, and regulate biological functions are termed as biomaterials. The functionality and applicability of these materials depend on both bulk and the surface properties. While bulk properties are the intrinsic properties of the material, surface properties can be tailored to enhance material performances and functions. Surface properties highly regulate initial processes (i.e., protein adsorption and cell adhesion) taking place on material's surface as soon as they come in contact with biological systems. Thus, surface properties play crucial role in regulating biomolecular and cellular responses. In this chapter, we highlight different approaches such as physical, chemical, and biological methods employed to modify surface properties. State-of-the-art techniques employed for characterizing surfaces after modifications have also been detailed. Finally, we discuss the effect of self assembled monolayers (SAMs) on protein adsorption and cell behavior to provide mechanistic insights to the readers on these phenomenon.

A. Hasan

Bio-Interface and Environmental Engineering Lab, Department of Biosciences and Bioengineering, Indian Institute of Technology Guwahati, Guwahati, Assam, India

School of Pharmacy, University of Nottingham, Nottingham, UK

L. M. Pandey (✉)

Bio-Interface and Environmental Engineering Lab, Department of Biosciences and Bioengineering, Indian Institute of Technology Guwahati, Guwahati, Assam, India

e-mail: lalitpandey@iitg.ac.in

© The Author(s), under exclusive license to Springer Nature Singapore Pte Ltd. 2022

L. M. Pandey, A. Hasan (eds.), *Nanoscale Engineering of Biomaterials: Properties and Applications*, https://doi.org/10.1007/978-981-16-3667-7_2

27

Keywords

Surface functionalization · Protein adsorption · Cell adhesion · Self-assembled monolayers · Silanization · Surface characterization

2.1 Introduction

Progress in material science over the past few decades have offered a plethora of advanced materials with improved functionalities particularly in the biomedical field. Biomaterials, in particular, are widely explored for various applications such as tissue repair and regeneration, regenerative medicine, drug delivery, antifouling applications, environmental applications, wound healing, and diagnostic applications (Fenton et al. 2018; Langer and Peppas 2003; Hasan et al. 2017, 2018d, 2020a, b; Sharma et al. 2018; Tiwari et al. 2017; Saxena et al. 2018a, b; Deka et al. 2018; Kaur et al. 2014; Nair et al. 2015; Balde et al. 2020). “Biomaterials” are defined as a class of synthetic or natural materials that comes in contact with biological fluids for the course of any therapeutic or diagnostic procedure (Ratner et al. 2004). However, a material that fulfills all the requirements for a given specific application is rare. For instance, materials required for load bearing applications such as bone replacement or prosthetic components for total hip replacement are primarily of good mechanical strength but may suffer from poor biocompatibility and vice versa (Kurella and Dahotre 2005). Thus, a material that strikes a balance with bulk and surface properties are desirable. Varying the bulk properties may not be a viable option given the economic and technological limitations and can severely affect the performance of the material.

Despite several decades of research in tissue replacement and biomedical devices, many implanted biomaterials suffer from poor biocompatibility and thus fail to elicit the desired responses in vivo (Chen and Liu 2016). Biomolecular interactions at the interface between surfaces and the biological environment mainly rely on the physicochemical properties of the surfaces which in turn define the biocompatibility and finally decide the fate of the biomaterial. Protein adsorption followed by cell adhesion is the initial most phenomenon that occurs at the interface as soon as any material encounters the biological environment. Nonspecific protein adsorption is deleterious as it may initiate cascades of immunological responses that lead to the failure of the material and implant rejection. However, modulating surface properties can overcome such issues by offering application-specific possibilities with improved functionalities in terms of biocompatibility, shelf life, and overall performance of the materials. Furthermore, surface modifications are desirable in applications wherein polymeric and metallic biomaterials particularly in bone tissue engineering undergo unexpected degradation resulting in the leaching of metal ions and other particulate debris from bulk materials (Eliaz 2019). Such implanted materials can be detrimental to human health. Thus, much emphasis has been given to surface modification techniques in order to shield such unwanted and deleterious process taking place in vitro and in vivo. Various techniques such as

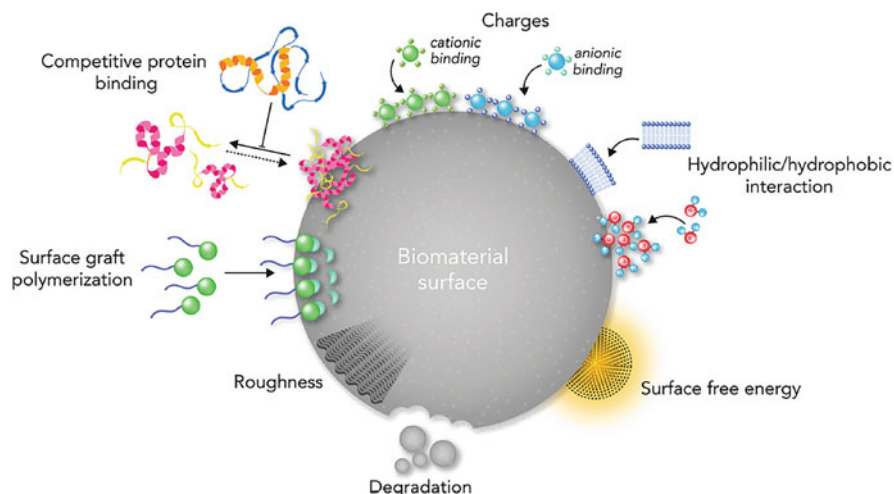


Fig. 2.1 Illustration showing various forms of surface modification and physicochemical properties to regulate surface properties. (Adapted with permission from Rahmati et al. (2020) Copyright 2020 Royal Society of Chemistry)

physical, chemical functionalization, biological, physicochemical, and biochemical (biomolecule immobilization) methods (Fig. 2.1) have been reported in the recent past to address the blood-compatibility, osseointegration, and toxicity-related issues (Hasan and Pandey 2015; Rahmati et al. 2020).

2.1.1 Scope of This Chapter

This chapter aims to provide insights on the effect of surface properties of the biomaterials on biomolecular and cellular responses. Various modification techniques for modulating physicochemical properties of the surface to elicit a desirable biological response are detailed with minimal technical jargon for better understanding of the readers, especially beginners in the field of surface science and material engineering.

2.2 Surface Modification

Bulk properties of the materials decide their suitability for an application while the physicochemical properties of these surfaces define their functional properties and behavior under biological microenvironment to elicit an appropriate and desirable host response. Thus, it is crucial to have materials that offer advanced surface properties such as biocompatibility to successfully deliver their application. Various modification techniques have been developed in the past few decades to regulate surface properties such as topographical features like roughness and patterns, surface

stiffness, surface wettability, surface potential, and energy and nanoscale surface chemistry (Hasan and Pandey 2015; Rahmati et al. 2020). These surface properties regulate and affect biophysical and biochemical signals during host-material interactions. Different modification techniques are discussed in detail below.

2.2.1 Physical Modification

Physical modifications are carried out to mainly control macro- and microscopic surface features such as surface topology, roughness, and surface patterns with negligible or no effect on surface chemistry (Bose et al. 2018). Various physical techniques have been developed for modifying metallic surfaces such as etching (Ban et al. 2006), grid-blasting (Citeau et al. 2005), micromachining (Cei et al. 2011), sputtering (Behera et al. 2018, 2020a, b), and their subsequent combinations. Surface etching involves rigorous treatment with various concentrated acids such as hydrofluoric acid, hydrochloric acid, nitric acid, sulfuric acid, and phosphoric acid to induce metallic hydride and nano- and micro-surface roughness. This collectively alters the surface energy which in turn tunes cell adhesion, proliferation, and tissue integration (Conforto et al. 2002; Ban et al. 2006). Grid-blasting involves blasting the implant surfaces with Al_2O_3 , SiC, hydroxyapatite, and β -tricalcium phosphate particles to induce uniform and submicron surface roughness over large and uneven implant area to facilitate osseointegration during orthopedic and dental applications (Citeau et al. 2005). Laser micromachining is of great interest to attain non-stochastic surfaces using a laser such as Q-switched diode-pumped solid-state Nd-YAG laser (DPSS). This generates a pulse laser beam, which attains controlled and regular size pores on implant surfaces (Cei et al. 2011). Several techniques are used to produce uniform coating thickness such as electrophoretic deposition, laser cladding, ion-beam and magnetron sputtering, and plasma spraying. A detailed explanation of the abovementioned techniques is out of the scope of this chapter but can be found elsewhere (Su et al. 2019; Surmenev and Surmeneva 2019; Narayanan et al. 2008). Calcium-phosphate based coatings on implant surfaces using these techniques are of great interest as they exhibit similar mineral composition found in teeth and bones and thus ease the coated surfaces to integrate with underline native tissues and also prevent corrosion (Behera et al. 2018).

2.2.2 Chemical Modification

2.2.2.1 Plasma Treatment

Plasma is a widely used and preferred choice of the treatment process for modifying polymeric and metallic surfaces due to its attractive features such as: (1) nanoscale modification without altering bulk properties, (2) faster surface modification, (3) cost effective, (4) nonspecific surface activator, and (5) sterile preparation (Yoshida et al. 2013; Richbourg et al. 2019). Choice of plasma source gases such as CO_2 , O_2 , Ar, N_2 , NH_3 , and H_2 and treatment methods such as plasma sputtering, plasma etching,

ion beam, plasma polymerization, and spraying vary from application to application (Hasan and Pandey 2015). While plasma alone enhances cell adhesion due to improved surface wettability, fibronectin-rich serum coating was found to enhance cell adhesion, proliferation, and cell differentiation (Yildirim et al. 2010). NH_3 plasma-treated polylactic acid surface exhibited lesser protein adsorption during *in vitro* studies (Sarapirom et al. 2014) which could be due to reduced surface energy in the presence of amine groups.

2.2.2.2 Chemical Vapor Deposition (CVD)

This approach involves simultaneous deposition and polymerization of reactive monomeric molecules on surfaces. CVD offers advantages over solvent-based methods by directly forming thin mono- or multilayers on surfaces, thereby eliminating surface defects such as surface dewetting, aggregate formation, surface nonuniformity, and risks of toxicity toward cells and tissues due to leftover solvents (Khlyustova et al. 2020). Advancements in CVD techniques such as initiated CVD (iCVD), plasma-enhanced CVD, and oxidative CVD have been widely used to deposit thin films via the chain-growth or the step-growth polymerization mechanisms using ionized gas particles.

2.2.2.3 Atomic Layer Deposition (ALD)

This technique is similar to CVD in depositing a thin film on surfaces but uses a different approach. ALD involves the layer-by-layer deposition of two precursor gases on a substrate surface. The monolayer of the first precursor gas (such as metal halide) adsorbed via chemisorption is followed by the second precursor gas (such as oxygen or nitrogen source) in the presence of an inert atmosphere. The interaction between these two precursor gases results in the formation of a thin layer on the surface. Because of its uniform surface functionalization capabilities, this technique has been widely used for bioelectronic devices, implant devices for tissue engineering and drug delivery, and biosensors applications (Skoog et al. 2013).

2.2.2.4 Electrochemical Deposition (ECD)

ECD or electroplating is a liquid-based technique for depositing conductive materials based on electrochemical properties using an electrode cell apparatus in the presence of electric current. In polymer chemistry, ECD is categorized into electro-polymerization and electrophoretic deposition. In electro-polymerization, monomer deposition and subsequent polymerization occur on the surface of a metal electrode from an electrolyte solution whereas in electrophoretic deposition polymers are directly deposited on a metallic electrode from the electrolyte under the effect of electric charge (Milan and Mordechay 2006).

2.2.2.5 Self-Assembled Monolayers (SAMs)

SAMs are highly organized 2D molecular structures formed on the surfaces in the form of thin films as a result of spontaneous adsorption of monomers (Hasan and Pandey 2018). Most of the SAMs formed on the surfaces are derived from silane- or thiol-based monomers which were first introduced by Sagiv (1980) and Nuzzo and

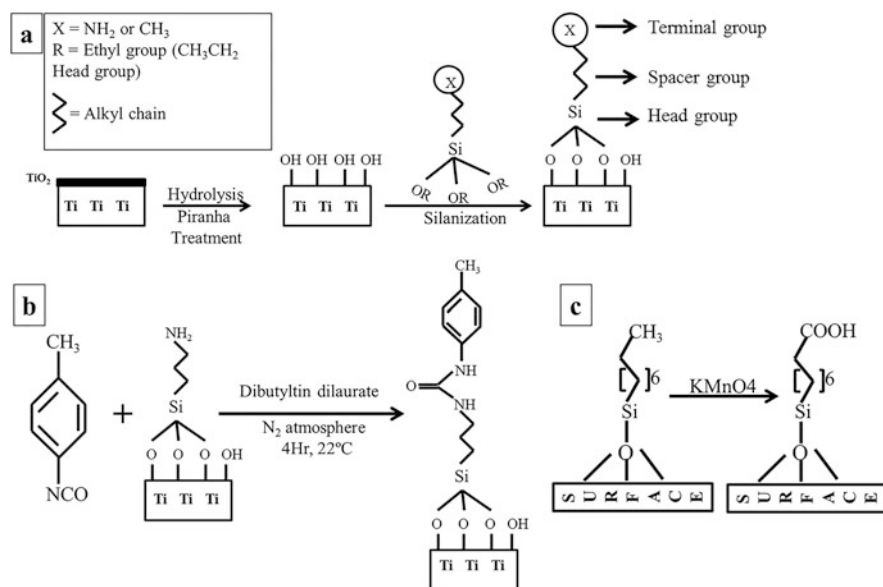


Fig. 2.2 (a) Schematic illustration demonstrating the silanization process and composition of silane molecule, (b, c) show further modification to preformed SAM surface. (Adapted with permission from Hasan et al. (2018b). Copyright 2018 American Chemical Society)

Allara (1983), respectively. Thiols are mainly limited to modify gold surfaces whereas organosilanes can be used to modify metal and ceramic substrates. In this section, we will mainly focus on SAMs of organosilanes, the kinetics of formation and their subsequent effect on protein adsorption and cell adhesion.

SAMs of organosilanes have been widely used for modifying surface properties of various substrates such as metallic, ceramic, and polymeric materials at the nanoscale level for various applications such as bioelectronics, implants surfaces, biosensor, and diagnostic devices. The salient features offered by this versatile system have widened their scope in nanoscience and nanotechnology with the molecular level precision which has now been used to understand macroscopic phenomenon on these surfaces (Park et al. 2010; Pandey et al. 2013). SAM formation primarily involves the use of amphiphilic monomers that comprise of three parts: (1) head group, (2) spacer chain, and (3) free terminal group (Fig. 2.2a). While the head group attaches and helps in packing onto the substrate due to their affinity, the terminal group helps in further functionalization based on the required application (Fig. 2.2b, c). The length of the spacer chain can vary from 1 nm up to several nanometers (Hasan and Pandey 2018).

2.2.2.6 Effect of Self-Assembled Monolayers on Protein Adsorption and Cell Adhesion

Organosilane SAMs Formation and Characterization Tools

SAM formation on substrates is a two-stage process. The first stage of SAM formation is fast and takes only a few minutes to adsorb monomers to form a monolayer from the bulk solution on the surface. The second stage is slower and takes a few hours to complete the rearrangement and reorientation of the attached molecules to form a uniform and defect free monolayer. The rate and quality of SAM formation depend on several factors such as type of solvent, monomer concentration, temperature, size of spacer group (carbon chain), and humidity (Yang et al. 2008; Rozlosnik et al. 2003; Desbief et al. 2011; Hasan and Pandey 2016; Pasternack et al. 2008). Various techniques such as attenuated total reflection-Fourier transform infrared spectroscopy (ATR-FTIR), goniometer, ellipsometer, atomic force microscopy (AFM), quartz crystal microbalance (QCM), and X-ray photoelectron spectroscopy (XPS) have been used in the recent past to characterize SAM quality and the kinetics of formation (Pasternack et al. 2008; Hasan and Pandey 2016; Pandey and Pattanayek 2011, 2013). Estimation of surface charge using zeta-potential is an alternative way of quantifying and confirming the surface modification, as highlighted in the work by Lee and colleagues (Lee et al. 2011).

Effect on Protein Adsorption

SAMs formed on the surfaces regulate physiochemical properties such as surface wettability, roughness, surface potential, and energy, which are known to play a crucial role in controlling biological behavior on modified surfaces. These properties are mainly controlled by the functional terminal groups and spacer length of SAMs (as shown in Fig. 2.2a). By varying the type of functional groups, Hasan et al. showed how pronounced effects can be imparted to surface properties which in turn control protein and cell behavior (Hasan et al. 2018a, b, c; Hasan and Pandey 2020). Water contact angle analysis of carboxy ($-\text{COOH}$) silane, amino ($-\text{NH}_2$) silane, and octyl ($-\text{CH}_3$) silane modified surfaces revealed the formation of hydrophilic (water contact angle, θ of 40°), moderately hydrophilic (θ of 60°), and hydrophobic (θ of 103°) surfaces, respectively. Mixed and hybrid SAMs of amino and octyl SAMs were also prepared that produced moderately hydrophobic (θ of 82° – 86°) surfaces. These surfaces were tested for adsorption behavior of bovine serum albumin (BSA), fibrinogen (FB), immunoglobulin G (IgG) proteins, and their binary mixed protein solutions. It was found that the adsorbed mass increased with the increase in the surface hydrophobicity (Hasan et al. 2018c) (Fig. 2.3a, b). However, the amount of adsorbed protein may vary from protein to protein based on their intrinsic properties like charge and hydrophobicity.

Apart from the amount of adsorbed protein, the secondary structure conformation of adsorbed protein is directly related to its function. Significant changes in the conformation may lead to complete loss of function of a protein. Secondary structures of proteins such as α -helix, β -sheet, β -turn, random, and side chain after adsorption on modified surfaces were analyzed in the amide I region, that is, between

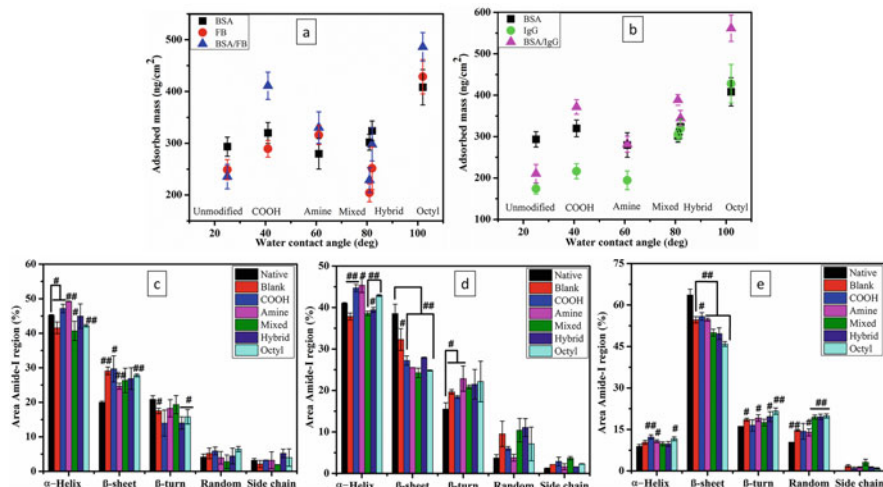


Fig. 2.3 (a, b) show the adsorbed mass of BSA, FB, IgG, from single and their mixed solutions on different modified surfaces. Secondary structure analysis of (c) BSA, (d) FB, and (e) IgG proteins on modified surfaces. (Adapted with permission from Hasan et al. (2018c). Copyright 2018 American Chemical Society)

1600 and 1700 cm^{-1} wavenumber using ATR-FTIR (Fig. 2.3c–e). The percentage content of α -helix for BSA on NH_2 - and $-\text{COOH}$ modified surfaces increased due to enhanced hydrogen bonding with carboxyl and amino groups, respectively, of amino acids present in BSA (Fig. 2.3c). The amount of the β -sheet increased significantly while β -turn content reduced on all the surfaces for BSA. However, the opposite behavior of β -sheet, β -turn content was observed for adsorbed FB and IgG as compared to BSA. β -sheet content reduced while β -turn content increased significantly for FB and IgG on all the surfaces (Fig. 2.3d, e). These observations highlight the role of surface properties in protein-surface interactions.

Effect on Cell Behavior

Cell behavior (i.e., cell adhesion, spreading, proliferation, and differentiation) depends on properties such as surface hydrophilicity, stiffness, potential, roughness, charge, and type of cells used (Arima and Iwata 2007). The general consensus among the scientific community for cell behavior on the surface is that surfaces with wettability range 40° – 60° exhibit the best cell response; however, it does not hold true for all surface types. Surface potential along with surface wettability are known to play a cumulative effect that decides the cell behavior (Hasan et al. 2018b). Hasan et al. demonstrated the role of surface chemistry on the adsorption of the extracellular matrix and cell adhesive protein fibronectin (FN) on different modified surfaces and their subsequent effect on cell adhesion and spreading. FN upon adsorption resulted in the exposure of the RGD loops which is located in the β -turn and known to adhere to cells via integrin interactions. It was found that the content of β -turn in FN increased as the surface hydrophobicity increased (Hasan

et al. 2018b). Among all the modified surfaces (carboxyl, amine, octyl, mixed, and hybrid) reported above, it was observed that hybrid surface is the best modifier due to the increased number of adhered cells and higher proliferation rate. Cells also exhibit higher nuclei area on hybrid surfaces as compared to other surfaces which also indicates their tendency toward cell proliferation (Fig. 2.4).

The cell adhesion is mediated by various proteins. Among them, integrins play critical roles. Integrins are heterodimeric protein ligands (comprises of two subunits: α and β) found across the cell membrane. Integrin ligands recognize and interact with other cells (i.e., cell-cell) and extracellular matrix (ECM, i.e., cell-matrix) proteins and cellular receptors to initiate a cascade of intracellular reactions. They interact to perform various cellular functions such as the assembly of actin filaments for signal transduction, cell morphology, migration, and differentiation (Plow et al. 2000; Hynes 2002). Various ECM proteins for example albumins, vitronectin, fibronectin, laminins, and fibronectin play a central role in the integrin-mediated binding for cellular communication via intracellular cell-responsive signaling. These ECM proteins are folded and held by disulfide bonds and interact with surface topologies via hydrophobic interactions (Jin and Yuan 2011). Different surface chemistries have been reported to exhibit different integrin expression. For instance, Shen et al. reported the higher expression of $\alpha 2$, αV , and $\alpha 5$ subunits on surfaces with higher wettability as compared to hydrophobic surfaces (Shen et al. 2015).

2.2.3 Biological Modification: Protein Immobilization

Material scientists have employed various biological routes to modify surfaces so as to mimic ECM microenvironment to the adhering cells. Various molecules and macromolecules such as ECM, cell adhesion molecules (CAMs), and growth factors have been immobilized to achieve desired cellular functions by regulating cell-surface interactions. These cell adhesion molecules are classified into four types, that is, integrins, cadherins, selectins, and immunoglobulin superfamily molecules. They are found on the cell membranes and interact with the surfaces or with other adjacent cells. These CAMs are known to interact and recognize surfaces and ECM molecules/matrix that trigger intracellular signaling and thus regulate cellular responses such as cell adhesion, spreading, differentiation, migration, and cell-cell communication (Schwartz et al. 1995).

ECM, ECM-mimetic peptides, growth factors, and enzymes have been immobilized on a wide range of surfaces by modifying them chemically using self-assembled monolayers (SAMs) (Wilkinson et al. 2014; Hoarau et al. 2017; Mansur et al. 2005). Protein molecules can be immobilized via several interactive ways such as physical adsorption, covalent bonding, coordination complexes, and charge-charge interactions as shown in Fig. 2.5. Types of protein immobilization change with the change in the application as each method offers its own advantages/disadvantages. The effect of surface properties greatly affects the conformation and orientation of the protein adsorbed or immobilized on it. The conformation and orientation of a protein also depend upon its properties such as charge, size,

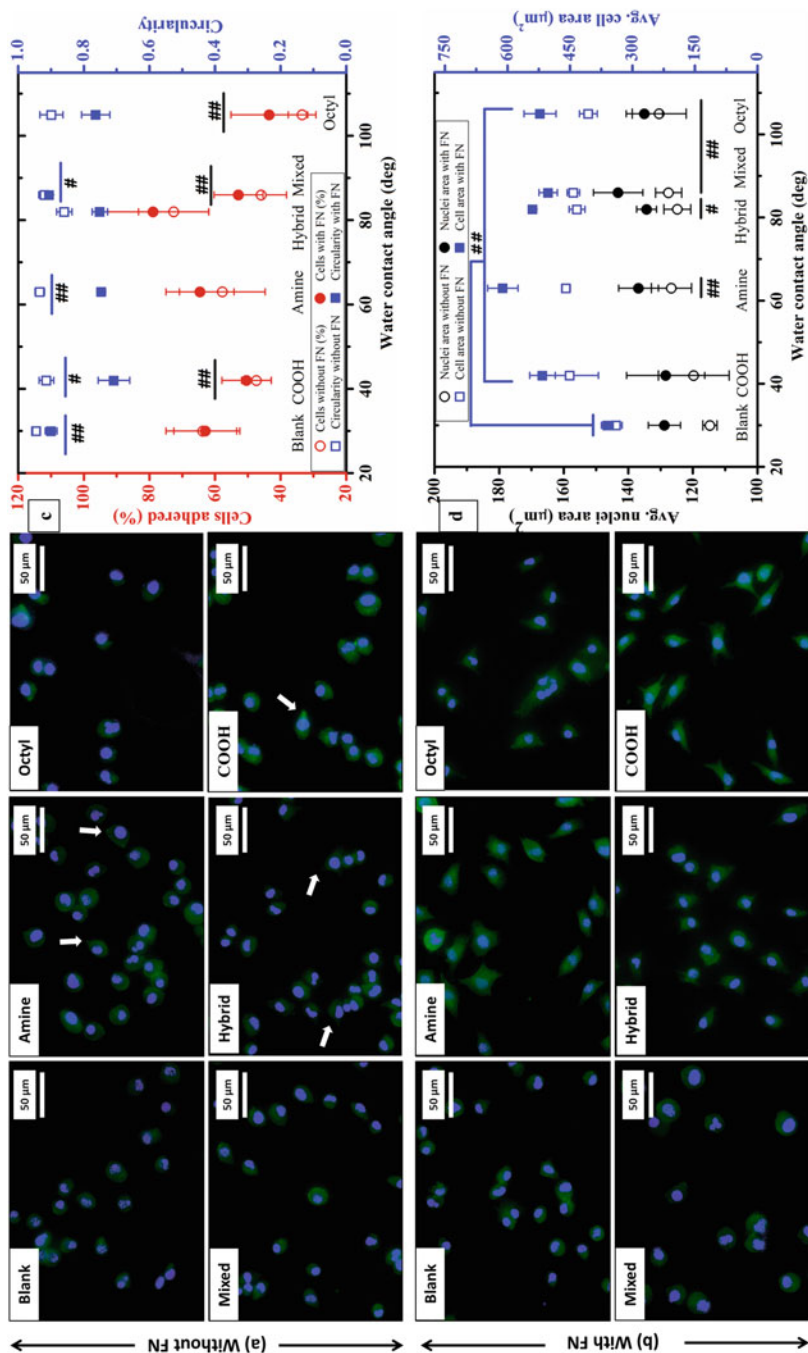


Fig. 2.4 Fluorescent images (actin filaments with green and nucleus with blue) of L929 cells on (a) surfaces without FN and (b) with FN on blank and modified surfaces after 6 h of culture. The scale bar is 50 µm. Analysis of (c) % cells adhered, cell circularity, (d) avg. nuclei, and avg. cell area post 6 h of cell seeding. (Adapted with permission from Hasan et al. (2018b)). Copyright 2018 American Chemical Society

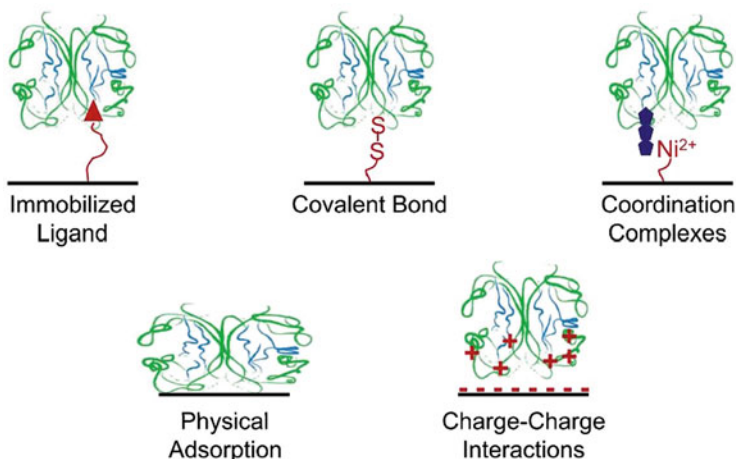


Fig. 2.5 Different methods employed in the immobilization of proteins to the surface. (Reprinted with permission from Castner (2017). Copyright 2017, American Vacuum Society)

hydrophobicity, and rigidity. Other experimental conditions that play role in protein-surface interactions are protein concentration, solution pH, and temperature. Protein-adsorbed mass on the surface varies with initial time points, however, becomes stationary at later time points. This change in protein-adsorbed mass is accompanied by changes in conformation and orientation of the adsorbed protein to attain a stable state and minimum energy.

2.3 Techniques to Characterize Surface Modifications

Advancement in surface science and engineering has resulted in the development of state-of-the-art techniques (Table 2.1) to characterize and confirm successful surface modifications.

2.3.1 X-Ray Photoelectron Spectroscopy (XPS)

XPS, also referred as electron spectroscopy for chemical analysis (ESCA), is a widely used surface analytical technique in material science. It is based on the principle of photoelectric effect and measures the elemental identity, empirical formula, chemical, and electronic state of the elements present in the underlying surface of the materials. Samples are irradiated with X-ray radiation which results in the ejection of photoelectrons, and core electron vacancies are created. These emitted photoelectrons with kinetic energies typically below 2000 keV are measured or detected. The kinetic energies (KE) of these ejected photoelectrons are measured based on the incident X-ray photon, $h\nu$ (using Mg or Al K α radiations) using a

Table 2.1 Summary of techniques used for surface characterization, their working principle, advantages, disadvantages, and applications

Techniques	Principle	Advantages	Disadvantages	Applications
X-ray photoelectron spectroscopy	Based on photoemission/ photoelectric principle	Nondestructive; surface sensitive; elemental mapping	Expensive; high vacuum is required; processing time and data collection are very slow	To analyze the elemental composition of materials
Ellipsometry	Relies on the measurement of the change in polarization of light reflected or transmitted by a material's surface	Noncontact and nondestructive; information on film thickness and refractive index; simple hardware; no coherent source needed	Difficult and time expensive data analysis; low spatial resolution of the measurement	Surface properties such as chemical composition, surface thickness, roughness, conductivity
Fourier transform infrared spectroscopy	Detects the absorption of light by a specimen in the infrared region of electromagnetic spectrum	Sensitive, fast, and easy; relatively inexpensive; high wavenumber accuracy; better sensitivity; high resolution spectra	CO ₂ and H ₂ O sensitive; complex spectra for complex mixtures; cannot detect atoms and monoatomic ions	Analysis of thin films and coatings; to identify contaminants; pharmaceutical research; forensic investigation
Raman spectrometer	Relies upon inelastic scattering of photons, known as Raman scattering	Less sensitive to H ₂ O and temperature change; high specificity	Low sensitivity for samples with weak Raman scattering; cannot be used for alloys; expensive, time-consuming analysis	Material science; forensic science; nanotechnology; mineralogy; detecting polymorphism; analysis of crystalline structure
Atomic force microscopy	Based on piezoelectric effect, a laser beam is focused at back of cantilever that moves up and down on the surface of specimen and the deflection of beam are captured by diode	Sample preparation is easy; nondestructive; accurate height information; works in air, vacuum, and liquids	Limited magnification range; limited scanning speed; high risks of damaging tip and samples	To characterize surface modifications; surface topography and stiffness; protein adsorption and conformation; cell morphology

(continued)

Table 2.1 (continued)

Techniques	Principle	Advantages	Disadvantages	Applications
Contact angle measurement	Based on Young's equation; examine surface's wettability by measuring contact angle at the interface of solid-liquid-vapor	Fast analysis; relatively straightforward technique; inexpensive; provide information on surface energies; hydrated samples can be observed	Dry samples can damage; swelling of samples may give incorrect results; artifact prone; liquid purity is important	Surface wettability; surface energies
Secondary ion mass spectrometry	Bombardment of surface by ion beam and followed by mass spectrometry	Highly sensitive; little or no sample preparation; rapid ionization	Destructive; very expensive; mass interferences; needs highly skilled operator	To characterize surface and subsurface region of materials
Zeta potential/surface charge	Measurement of the concentration of ions of opposite charge bound to the surface of the sample	Cheap, wide time range, simple to perform	Very clean and transparent samples are needed; sensitive to mechanical disturbances	To determine surface charge

binding energy (BE) relationship as $KE = h\nu - BE$. The advantage of XPS is that photoelectrons do not suffer from inelastic scattering and energy loss due to the short-ranged. This makes XPS a highly precise surface technique. Each element on the surface has characteristic binding energy associated with its core electron levels, thus making this technique highly specific for elemental detection. Moreover, XPS is a user-friendly technique as it does not involve any sophisticated sample preparation and can directly use as-synthesized materials for analysis.

2.3.2 Ellipsometry

Ellipsometry is a highly sensitive and nondestructive surface characterization technique to measure optical reflectance of thin films providing information about their optical constants, chemical composition, surface thickness, roughness, doping concentration, surface porosity, conductivity, and other various surface properties. The working principle of ellipsometry relies on the measurement of the change in polarization of light (represented by amplitude ratio and the phase difference) reflected or transmitted by a material's surface depending upon the surface thickness and optical properties. Since the first report on this technique in the 1960s, it has been widely used by material scientists owing to its versatile surface characterization

properties even for nano-thick films. Currently, it is being widely exploited in various fields such as electronic devices (semi- and super-conductors), surface coatings (such as silanization and thiolization), and biological coatings (such as physical and chemical immobilization of biomolecules).

2.3.3 Fourier Transform Infrared Spectroscopy (FTIR)

FTIR is a qualitative analytical tool to analyze surface modification such as functionalization by providing fingerprints of the samples. It measures the infrared spectrum of absorption or emission peaks corresponding to the frequencies of vibrations between the bonds of the atoms making up the material. Its spectrum is recorded between 400 and 4000 cm^{-1} wavenumber based on the molecular fingerprint of the samples. Based on the required applications, FTIR technique had been advanced by coupling with other techniques such as attenuated total reflectance (ATR) (called as FTIR-ATR). It measures absorption or emission spectra up to few microns (0.5–3 μm) on surfaces based on the distance travelled by the effervescent wave generated by an Internal Reflection element. Likewise, other advanced techniques such as FTIR-microscopy, FTIR-photo acoustic spectroscopy (FTIR-PAS), FTIR-polarized optical microscopy, and nano-FTIR spectroscopy have been widely used for material characterization.

2.3.4 Raman Spectrometer

Raman spectroscopy is a nondestructive molecular spectroscopic technique named after Indian physicist C. V. Raman. It is based on the principle that when light interacts with the sample molecules, the majority of the photons scatter at the same energy as that of incident photons while a small number of incident photons scatter at a different frequency. This is called the Raman effect. It investigates the chemical or molecular fingerprints of the samples and relies on the interaction of light with the chemical bonds of the molecules comprising the material. It provides information from the vibrational and rotational states of the molecules to provide details on chemical structure, phase, crystallinity, polymerization, polymorphism, and molecular interactions. Due to its versatile properties, Raman spectroscopy has been widely exploited for characterization in various applications such as food processing, material science, surface modifications, energy storage, and medical diagnostics.

2.3.5 Atomic Force Microscopy (AFM)

Atomic force microscopy (AFM) is a powerful surface analytical technique that enables the imaging of micro- and nanostructured surfaces/coatings of any type of materials such as polymers, ceramics, metallic, composites, glass, and even

biological samples. AFM is based on the interactions of the piezoelectric cantilever fitted with the tip with the sample. The interaction results in the up-down and side-to-side movement of the tip as it scans through the surface. AFM tips are about 10–20 nm in diameter and are micro-fabricated from silicon or silicon nitride. The surface topology is generated through a laser beam reflected off the cantilever which is monitored by a position-sensitive photodetector (PSPD) that detects the motion of the probe. AFM is nowadays widely used to study protein-protein and protein-surface interactions particularly for determining protein distribution, aggregation, and orientation (Hasan et al. 2018c; Migliorini et al. 2018).

2.3.6 Contact Angle Measurement

Contact angle measurements are commonly carried out to analyze surface properties such as wettability (i.e., hydrophilicity and hydrophobicity). A contact angle refers to the angle measured at the interface where a liquid-vapor meets a solid surface. This technique provides information about the surface hydrophobicity, morphology, roughness, and surface potential/energy at a given temperature and pressure. Contact angle (θ) mainly depends on interfacial tensions at the liquid-vapor (LV), solid–liquid (SL), and solid-vapor (SV) interfaces and is related by Young's equation (2.1):

$$\gamma_{SV} - \gamma_{SL} = \gamma_{LV} \cos \theta \quad (2.1)$$

These three phases can be simply created by adding a liquid droplet on a solid surface in the air. The angle produced as a function of surface property can be easily recorded and measured using a contact angle goniometer.

2.3.7 Secondary Ion Mass Spectrometry (SIMS)

SIMS is a destructive but highly sensitive surface analysis technique used to analyze the chemical composition of the surfaces to a depth of 10 nm, with the detection limits ranging from parts per million (ppm) to parts per billion (ppb). Analysis of the surfaces of the samples require sputtering with a highly focused beam of ions (primary) and collecting and analyzing the ejected secondary ions using sensitive detectors under high vacuum such as 10^{-4} Pa. A high vacuum is required to ensure that the secondary electrons do not collide with the background gases while reaching to the detector. It also helps in preventing surface contamination due to the adsorption of gas particles during detection. The m/z (mass per charge ratio) ratios of the ejected secondary ions are analyzed using a mass spectrometer and compared against established standards in order to provide accurate quantitative results on the chemical (elemental and molecular) composition of the surface of the solid samples or thin films.

2.3.8 Zeta Potential/Surface Charge

Role of surface charge in regulating surface processes at the interface is crucial in several scientific and biomedical applications such as biosensors and other diagnostic tools. Techniques to measure this surface property have gained significant advancement over last few decades. Zeta potential is used to measure the effective electric charge on the surface of the material. The basic principle relies on the measurement of the concentration of ions of opposite charge which are in close proximity of the sample's surface bearing net surface charge. For instance, a layer of opposite charged ions binds strongly to the surface when charged particles are suspended in aqueous medium. The thin layer of ions that forms around the particle is called a "Stern layer." This layer further forms a second layer of ions which are loosely associated with the first layer and is referred as "diffusive ion layer." These two layers are collectively called as EDL, or electrical double layer, which regulates and determines the physical-chemical behavior of the particles in aqueous medium such as stability, aggregation, interaction with proteins, cells, and other biological systems. Zeta potential is measured by applying an electric field which results in the random movement of the particles. The ratio of the velocity of the particles and the applied electric field is referred as electrophoretic mobility (μ_e) is measured and used to calculate zeta potential using the Henry's equation (2.2) shown below:

$$\mu_e = \frac{2 \cdot \epsilon \cdot z \cdot f \cdot (k \cdot \alpha)}{3 \cdot \eta} \quad (2.2)$$

where z is zeta potential, and ϵ and η are the dielectric constant and the absolute zero shear viscosity of the medium, respectively.

2.4 Conclusions

Surface properties such as wettability, nano- and micro-topographical features (roughness and topological patterns), surface energy, surface charge, and surface potential mainly regulate protein adsorption, cell behavior, and tissue formation. Various surface modification techniques such as physical, chemical, and biological methods have been employed to modify all types of materials (ceramic, polymeric, and metallic) irrespective of their nature. The type of surface modification varies from application-to-application. For instance, certain applications require no protein adsorption (anti-fouling surfaces), while some applications such as biosensors require specific conformation of adsorbed proteins for optimum sensing and recognition for integrin mediated cell adhesion. However, while scientists have been successful in tailoring surface properties, there still exist the knowledge gap to understand the fundamental mechanisms that control the protein and cell behavior and opens scope for further investigations. Development of the surface modification processes that offer biocompatibility, tissue integration, and antimicrobial properties in a single modified surface are highly desirable for the advancement of the

functional materials particularly in bone tissue engineering. Furthermore, surface modification processes are restricted to the small-scale synthesis in the laboratory. Development and scaling-up of such processes with low capital investment will boost the material science market and will provide better outreach to the consumers.

References

- Arima Y, Iwata H (2007) Effect of wettability and surface functional groups on protein adsorption and cell adhesion using well-defined mixed self-assembled monolayers. *Biomaterials* 28 (20):3074–3082
- Balde A, Hasan A, Joshi I, Nazeer R (2020) Preparation and optimization of chitosan nanoparticles from discarded squilla (*Carinosquilla multicaudinata*) shells for the delivery of anti-inflammatory drug: diclofenac. *J Air Waste Manage Assoc* 70(12):1227–1235
- Ban S, Iwaya Y, Kono H, Sato H (2006) Surface modification of titanium by etching in concentrated sulfuric acid. *Dent Mater* 22(12):1115–1120
- Behera RR, Hasan A, Sankar MR, Pandey LM (2018) Laser cladding with HA and functionally graded TiO₂-HA precursors on Ti-6Al-4V alloy for enhancing bioactivity and cytocompatibility. *Surf Coat Technol* 352:420–436. <https://doi.org/10.1016/j.surfcoat.2018.08.044>
- Behera R, Das A, Hasan A, Pamu D, Pandey L, Sankar M (2020a) Deposition of biphasic calcium phosphate film on laser surface textured Ti-6Al-4V and its effect on different biological properties for orthopedic applications. *J Alloys Compounds* 842:155683
- Behera R, Das A, Hasan A, Pamu D, Pandey L, Sankar M (2020b) Effect of TiO₂ addition on adhesion and biological behavior of BCP-TiO₂ composite films deposited by magnetron sputtering. *Mater Sci Eng C* 114:111033
- Bose S, Robertson SF, Bandyopadhyay A (2018) Surface modification of biomaterials and biomedical devices using additive manufacturing. *Acta Biomater* 66:6–22
- Castner DG (2017) Biomedical surface analysis: evolution and future directions. *Biointerphases* 12 (2):02C301
- Cei S, Legitimo A, Barachini S, Consolini R, Sammartino G, Mattii L, Gabriele M, Graziani F (2011) Effect of laser micromachining of titanium on viability and responsiveness of osteoblast-like cells. *Implant Dent* 20(4):285–291
- Chen F-M, Liu X (2016) Advancing biomaterials of human origin for tissue engineering. *Prog Polym Sci* 53:86–168
- Citeau A, Guicheux J, Vinatier C, Layrolle P, Nguyen TP, Pilet P, Daculsi G (2005) In vitro biological effects of titanium rough surface obtained by calcium phosphate grid blasting. *Biomaterials* 26(2):157–165
- Conforto E, Caillard D, Aronsson B, Descouts P (2002) Electron microscopy on titanium implants for bone replacement after “SLA” surface treatment. *Eur Cells Mater* 3(suppl 1):9–10
- Deka S, Saxena V, Hasan A, Chandra P, Pandey LM (2018) Synthesis, characterization and in vitro analysis of α -Fe₂O₃-GdFeO₃ biphasic materials as therapeutic agent for magnetic hyperthermia applications. *Mater Sci Eng C* 92:932–941. <https://doi.org/10.1016/j.msec.2018.07.042>
- Desbief S, Patrone L, Goguenheim D, Guérin D, Vuillaume D (2011) Impact of chain length, temperature, and humidity on the growth of long alkyltrichlorosilane self-assembled monolayers. *Phys Chem Chem Phys* 13(7):2870–2879
- Eliaz N (2019) Corrosion of metallic biomaterials: a review. *Materials* 12(3):407
- Fenton OS, Olafson KN, Pillai PS, Mitchell MJ, Langer R (2018) Advances in biomaterials for drug delivery. *Adv Mater* 30(29):1705328
- Hasan A, Pandey LM (2015) Polymers, surface-modified polymers, and self assembled monolayers as surface-modifying agents for biomaterials. *Polym-Plast Technol Eng* 54(13):1358–1378

- Hasan A, Pandey LM (2016) Kinetic studies of attachment and re-orientation of octyltriethoxysilane for formation of self-assembled monolayer on a silica substrate. *Mater Sci Eng C* 68:423–429
- Hasan A, Pandey L (2018) Self-assembled monolayers in biomaterials. In: *Nanobiomaterials*. Elsevier, Amsterdam, pp 137–178
- Hasan A, Pandey LM (2020) Surface modification of Ti6Al4V by forming hybrid self-assembled monolayers and its effect on collagen-I adsorption, osteoblast adhesion and integrin expression. *Appl Surf Sci* 505:144611
- Hasan A, Waibhaw G, Tiwari S, Dharmalingam K, Shukla I, Pandey LM (2017) Fabrication and characterization of chitosan, polyvinylpyrrolidone, and cellulose nanowhiskers nanocomposite films for wound healing drug delivery application. *J Biomed Mater Res A* 105(9):2391–2404
- Hasan A, Pattanayek SK, Pandey LM (2018a) Effect of functional groups of self-assembled monolayers on protein adsorption and initial cell adhesion. *ACS Biomater Sci Eng* 4(9):3224–3233
- Hasan A, Saxena V, Pandey LM (2018b) Surface functionalization of Ti6Al4V via self-assembled monolayers for improved protein adsorption and fibroblast adhesion. *Langmuir* 34(11):3494–3506
- Hasan A, Waibhaw G, Pandey LM (2018c) Conformational and organizational insights into serum proteins during competitive adsorption on self-assembled monolayers. *Langmuir* 34(28):8178–8194
- Hasan A, Waibhaw G, Saxena V, Pandey LM (2018d) Nano-biocomposite scaffolds of chitosan, carboxymethyl cellulose and silver nanoparticle modified cellulose nanowhiskers for bone tissue engineering applications. *Int J Biol Macromol* 111:923–934
- Hasan A, Lee K, Tewari K, Pandey LM, Messersmith PB, Faulds K, Maclean M, Lau KHA (2020a) Surface design for immobilization of an antimicrobial peptide mimic for efficient anti-biofouling. *Chem Eur J* 26(26):5789–5793
- Hasan A, Saxena V, Castelletto V, Zimbitas G, Seitsonen J, Ruokolainen J, Pandey LM, Sefcik J, Hamley IW, Lau KHA (2020b) Chain-end modifications and sequence arrangements of antimicrobial Peptoids for mediating activity and Nano-assembly. *Front Chem* 8:416
- Hoarau M, Badieyan S, Marsh ENG (2017) Immobilized enzymes: understanding enzyme–surface interactions at the molecular level. *Org Biomol Chem* 15(45):9539–9551
- Hynes RO (2002) Integrins: bidirectional, allosteric signaling machines. *Cell* 110(6):673–687
- Jin R, Yuan J (2011) Advances in biomimetics. InTech, Rijeka
- Kaur R, Hasan A, Iqbal N, Alam S, Saini MK, Raza SK (2014) Synthesis and surface engineering of magnetic nanoparticles for environmental cleanup and pesticide residue analysis: a review. *J Sep Sci* 37(14):1805–1825
- Khlyustova A, Cheng Y, Yang R (2020) Vapor-deposited functional polymer thin films in biological applications. *J Mater Chem B* 8(31):6588–6609
- Kurella A, Dahotre NB (2005) Surface modification for bioimplants: the role of laser surface engineering. *J Biomater Appl* 20(1):5–50
- Langer R, Peppas NA (2003) Advances in biomaterials, drug delivery, and bionanotechnology. *AIChE J* 49(12):2990–3006
- Lee CH, Park SH, Chung W, Kim JY, Kim SH (2011) Preparation and characterization of surface modified silica nanoparticles with organo-silane compounds. *Colloids Surf A Physicochem Eng Asp* 384(1–3):318–322
- Mansur H, Oréface R, Vasconcelos W, Lobato Z, Machado L (2005) Biomaterial with chemically engineered surface for protein immobilization. *J Mater Sci Mater Med* 16(4):333–340
- Migliorini E, Weidenhaupt M, Picart C (2018) Practical guide to characterize biomolecule adsorption on solid surfaces. *Biointerphases* 13(6):06D303
- Milan P, Mordechay S (2006) *Fundamentals of electrochemical deposition*. Wiley, Chichester
- Nair KK, Kaur R, Iqbal N, Hasan A, Alam S, Raza S (2015) High yield, facile aqueous synthesis and characterization of C18 functionalized iron oxide nanoparticles. *Mater Res Exp* 2(4):045014

- Narayanan R, Seshadri S, Kwon T, Kim K (2008) Calcium phosphate-based coatings on titanium and its alloys. *J Biomed Mater Res B Appl Biomater* 85(1):279–299
- Nuzzo RG, Allara DL (1983) Adsorption of bifunctional organic disulfides on gold surfaces. *J Am Chem Soc* 105(13):4481–4483
- Pandey LM, Pattanayek SK (2011) Hybrid surface from self-assembled layer and its effect on protein adsorption. *Appl Surf Sci* 257(10):4731–4737
- Pandey LM, Pattanayek SK (2013) Properties of competitively adsorbed BSA and fibrinogen from their mixture on mixed and hybrid surfaces. *Appl Surf Sci* 264:832–837
- Pandey LM, Pattanayek SK, Delabouglise D (2013) Properties of adsorbed bovine serum albumin and fibrinogen on self-assembled monolayers. *J Phys Chem C* 117(12):6151–6160
- Park J-W, Kim H, Han M (2010) Polymeric self-assembled monolayers derived from surface-active copolymers: a modular approach to functionalized surfaces. *Chem Soc Rev* 39(8):2935–2947
- Pasternack RM, Rivillon Amy S, Chabal YJ (2008) Attachment of 3-(aminopropyl) triethoxysilane on silicon oxide surfaces: dependence on solution temperature. *Langmuir* 24(22):12963–12971
- Plow EF, Haas TA, Zhang L, Loftus J, Smith JW (2000) Ligand binding to integrins. *J Biol Chem* 275(29):21785–21788
- Rahmati M, Silva EA, Reseland JE, Heyward CA, Haugen HJ (2020) Biological responses to physicochemical properties of biomaterial surface. *Chem Soc Rev* 49(15):5178–5224
- Ratner BD, Hoffman AS, Schoen FJ, Lemons JE (2004) *Biomaterials science: an introduction to materials in medicine*. Elsevier, Amsterdam
- Richbourg NR, Peppas NA, Sikavitsas VI (2019) Tuning the biomimetic behavior of scaffolds for regenerative medicine through surface modifications. *J Tissue Eng Regen Med* 13(8):1275–1293
- Rozlosnik N, Gerstenberg MC, Larsen NB (2003) Effect of solvents and concentration on the formation of a self-assembled monolayer of octadecylsiloxane on silicon (001). *Langmuir* 19(4):1182–1188
- Sagiv J (1980) Organized monolayers by adsorption. 1. Formation and structure of oleophobic mixed monolayers on solid surfaces. *J Am Chem Soc* 102(1):92–98
- Sarapirom S, Yu L, Boonyawan D, Chaiwong C (2014) Effect of surface modification of poly (lactic acid) by low-pressure ammonia plasma on adsorption of human serum albumin. *Appl Surf Sci* 310:42–50
- Saxena V, Hasan A, Pandey LM (2018a) Effect of Zn/ZnO integration with hydroxyapatite: a review. *Mater Technol* 33(2):79–92. <https://doi.org/10.1080/10667857.2017.1377972>
- Saxena V, Hasan A, Sharma S, Pandey LM (2018b) Edible oil nanoemulsion: an organic nanoantibiotic as a potential biomolecule delivery vehicle. *Int J Polym Mater Polym Biomater* 67(7):410–419
- Schwartz MA, Schaller MD, Ginsberg MH (1995) Integrins: emerging paradigms of signal transduction. *Annu Rev Cell Dev Biol* 11(1):549–599
- Sharma S, Hasan A, Kumar N, Pandey LM (2018) Removal of methylene blue dye from aqueous solution using immobilized *Agrobacterium fabrum* biomass along with iron oxide nanoparticles as biosorbent. *Environ Sci Pollut Res* 25(22):21605–21615. <https://doi.org/10.1007/s11356-018-2280-z>
- Shen Y, Gao M, Ma Y, Yu H, F-z C, Gregersen H, Yu Q, Wang G, Liu X (2015) Effect of surface chemistry on the integrin induced pathway in regulating vascular endothelial cells migration. *Colloids Surf B: Biointerfaces* 126:188–197
- Skoog S, Elam J, Narayan R (2013) Atomic layer deposition: medical and biological applications. *Int Mater Rev* 58(2):113–129
- Su Y, Cockerill I, Zheng Y, Tang L, Qin Y-X, Zhu D (2019) Biofunctionalization of metallic implants by calcium phosphate coatings. *Bioact Mater* 4:196–206
- Surmenev RA, Surmeneva MA (2019) A critical review of decades of research on calcium phosphate-based coatings: how far are we from their widespread clinical application? *Curr Opin Biomed Eng* 10:35–44

- Tiwari S, Hasan A, Pandey LM (2017) A novel bio-sorbent comprising encapsulated *Agrobacterium fabrum* (SLAJ731) and iron oxide nanoparticles for removal of crude oil co-contaminant, lead Pb (II). *J Environ Chem Eng* 5(1):442–452
- Wilkinson AE, Kobelt LJ, Leipzig ND (2014) Immobilized ECM molecules and the effects of concentration and surface type on the control of NSC differentiation. *J Biomed Mater Res A* 102(10):3419–3428
- Yang Y, Bittner AM, Baldelli S, Kern K (2008) Study of self-assembled triethoxysilane thin films made by casting neat reagents in ambient atmosphere. *Thin Solid Films* 516(12):3948–3956
- Yildirim ED, Besunder R, Pappas D, Allen F, Güçeri S, Sun W (2010) Accelerated differentiation of osteoblast cells on polycaprolactone scaffolds driven by a combined effect of protein coating and plasma modification. *Biofabrication* 2(1):014109
- Yoshida S, Hagiwara K, Hasebe T, Hotta A (2013) Surface modification of polymers by plasma treatments for the enhancement of biocompatibility and controlled drug release. *Surf Coat Technol* 233:99–107



Progress of Nanotechnology-Based Detection and Treatment of Alzheimer's Disease Biomarkers

3

Yashwant Rao Singh, Anupam Shukla, and Sudip Kumar Pattanayek

Abstract

Alzheimer's disease (AD), responsible for memory loss, language, and learning problems, may lead to a patient's death. Many biomarkers have been identified for disease progressions, such as amyloid-beta, tau proteins, hyperphosphorylated tau protein, oxidative stress, reactive oxygen species, inflammatory cytokines, and some neurotransmitter. Existing expensive techniques like enzyme-linked immunosorbent assay (ELISA), flexible multi-analyte profiling (xMAP), mass spectrometry, single-photon emission computed tomography (SPECT), positron emission tomography (PET), and magnetic resonance imaging (MRI) are being used for the diagnosis of AD. Nanotechnology-based techniques like bio-barcode assay, fluorescence resonance energy transfer microscopy, scanning tunneling microscopy, NanoSIMS microscopy, and iron oxide nanoparticles as a contrast agent in MRI can be used for early diagnosis and detection of AD biomarkers. Various nanoparticles with a biorecognition element are used in sensors such as electrochemical, localized surface plasmon resonance, or molecularly imprinted polymer sensors. These methods can detect AD biomarkers' concentration in real biological fluid samples such as blood, plasma, serum, and cerebrospinal fluid. In addition, nanocarriers (carbon-based nanocarrier, nanoparticles, dendrimers, liposomes, solid lipid nanoparticles, and nanogels) conjugated with drugs are developed for drug delivery to the targeted biomarkers in both in vivo and in vitro models to treat AD.

Y. R. Singh · A. Shukla · S. K. Pattanayek (✉)

Department of Chemical Engineering, Indian Institute of Technology Delhi, New Delhi, India
e-mail: sudip@chemical.iitd.ac.in

© The Author(s), under exclusive license to Springer Nature Singapore Pte Ltd. 2022

L. M. Pandey, A. Hasan (eds.), *Nanoscale Engineering of Biomaterials: Properties and Applications*, https://doi.org/10.1007/978-981-16-3667-7_3

47

Keywords

Alzheimer's disease · Diagnosis · Detection · Nanocarrier · Nanoparticle · Treatment

3.1 Introduction

The advancement of molecular detection, drug delivery, and drug discoveries require an appropriate combination of nanotechnology and biology. The effective binding between appropriately modified nanoparticles (NPs) and biomolecules such as proteins, nucleic acids, or biomarkers offers promises in advancing molecular diagnosis and treatment through molecular targets (Cheng et al. 2006). Biomarkers can be any substance, structure, or process that can be measured in the body and predict the occurrence of disease and affect the treatment of disease (Strimbu and Tavel 2010). In particular, the diagnosis and detection of Alzheimer's disease (AD) are based on the variation of various biomarkers connected to it. Identification of the AD responsible biomarkers (Nazem and Mansoori 2011) is essential.

AD is a progressive neurodegenerative disorder with various symptoms, such as memory loss, poor judgment, difficulties in remembering names, and other mental abilities (Raskin et al. 2015). AD begins many years before the manifestation of clinical symptoms. Early detection of AD helps in presymptomatic disease recognition and improves the diagnostic accuracy in the progress of mild cognitive impairment to the diagnosis of dementia (Small 2000). More than 50 million people have dementia worldwide, and in the age of the increasing population, it is expected to affect 152 million people by 2050 (Patterson 2018). Depending on the AD patients' family history, AD is classified into two groups: familial AD (FAD) and sporadic AD (SAD), as shown in Fig. 3.1. The e4 allele of apolipoprotein E (APOE) is the most vital genetic risk factor and associated with late-onset FAD. FAD accounts for 1–5% of cases, and SAD accounts for about 95% of all AD cases (Reitz and Mayeux 2014). FAD may be found to appear in the age of 40s or 50s, while SAD appears at the age of more than 65 years (Yuan et al. 2013).

Based on the present understanding of AD's mechanism, a large number of biomarkers have been identified. We have looked into various biomarkers' concentrations in various biological fluids to optimize the target biomarker and biological fluid. The detection of AD-related biomarkers using conventional methods and nanotechnology-based methods has been reviewed. This review also covered the possible treatment with nanomaterials' help (liposomes, dendrimers, nanoparticles, etc.) used with drugs to treat AD. A few crucial reviews (Fonseca-Santos et al. 2015; Hettiarachchi et al. 2019; Nazem and Mansoori 2011; Sangubotla and Kim 2018; Scarano et al. 2016; Shui et al. 2018b) have targeted a specific issue in this area. A considerable number of combinations of biomarkers, biological fluids,

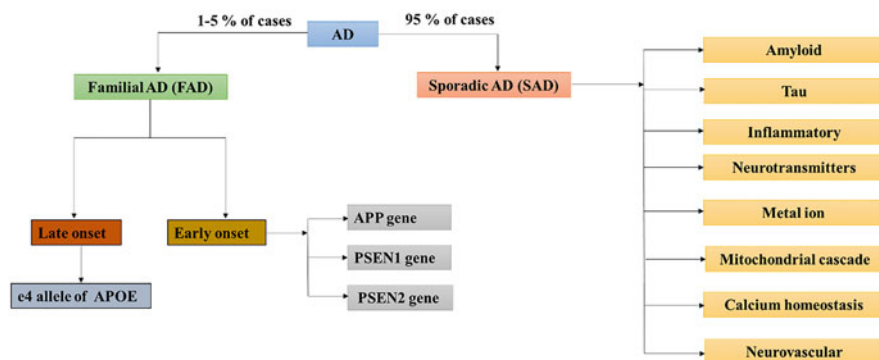


Fig. 3.1 Classification of AD into various types

cost of methods, and ease of doing detection have encouraged us to do this review work.

3.2 Biomarkers in AD

This section provides various biomarkers of AD present in various biological fluids and their detection using conventional methods. This section also elaborates on the problems of various detection methods, cost of detection.

Various hypotheses proposed for the appearance of sporadic AD are as follows: (1) neurotransmitters hypothesis (acetylcholine, glutamate, GABA, 5-HT, and DA), (2) mitochondrial cascade hypothesis (oxidative stress), (3) metal ion hypothesis (increase in iron, copper, and zinc levels which increase the $A\beta$ and toxicity), (4) amyloid hypothesis ($A\beta$ 40, $A\beta$ 42), (5) tau hypothesis (tau, p-tau), (6) inflammatory hypothesis (TNF- α , (IL)-1 β , IL-6, IL-12, IL-13), (7) calcium homeostasis hypothesis ($A\beta$ increases Ca^{+2} levels), and (8) neurovascular hypothesis (inappropriate $A\beta$ clearance across blood-brain barrier (BBB) (Liu et al. 2019). Schematics of the interrelations of a few hypotheses are shown in Fig. 3.2. The different colors correspond to the hypotheses in the production of $A\beta$, which is the cause of neuronal death (N_d) and subsequent reduction in synaptic plasticity. The associated biomarkers to the proposed hypotheses are described in Table 3.1.

The AD biomarkers can be found in various biological fluids such as cerebrospinal fluid (CSF), blood, salivary, and urinary, as listed in Table 3.2. It also lists biomarkers' approximate molecular weight, concentration in a healthy person, the effect of AD on the concentration in the affected person, and the techniques used to detect the effect. The detection of the main three biomarkers, namely, $A\beta$ 42, total tau (Tau), and p-tau 181, present in CSF, is well developed by using the ELISA technique. Early detections were based on the biomarkers present in CSF. Various other methods such as molecular imaging have been developed.

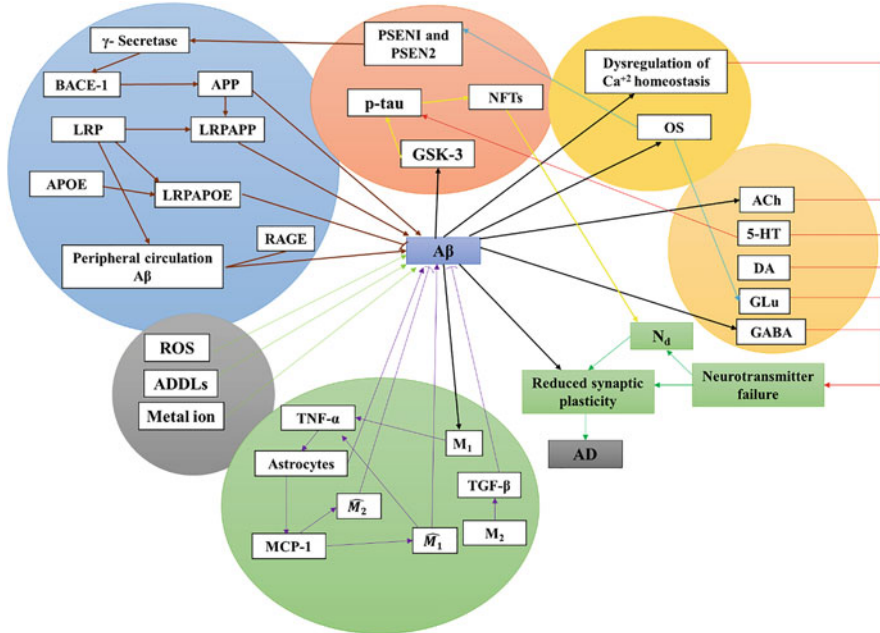


Fig. 3.2 A schematic of the hypotheses of the cause of AD and neuronal death. Neurotransmitters hypothesis: gold color circle; mitochondrial cascade hypothesis and calcium homeostasis hypothesis: yellow; metal ion hypothesis: gray; amyloid hypothesis and neurovascular hypothesis: blue; tau hypothesis: orange; inflammatory hypothesis: green (see also Table 3.1)

In molecular imaging, the images of the specific tracer bound to the targeted biomarkers are taken. Three basic molecular imaging techniques are in use: single-photon emission computed tomography (SPECT), positron emission tomography (PET), and magnetic resonance imaging (MRI). SPECT measures the tau accumulation with reduced regional cerebral blood flow (rCBF). Amyloid PET imaging with specific ligands F florbetapir, F florbetaben, and F flutemetamol for amyloid deposition shows good correlations with autopsy measurements. The PET imaging of the specific biomarkers in the neuroinflammatory process like activated microglia, reactive astrocytes is possible. The PET tracers 18 fluorodeoxyglucose is used to measure the acetylcholine synaptic density. PET (FDG PET) and MRI are more accurate than amyloid PET imaging in predicting dementia (Narayanan and Murray 2016). Diffusion MRI investigates the microstructure of white matter and its loss of integrity with aging due to myelinated fiber degeneration throughout the brain, with most changes occurred for the temporal lobe region in MCI. Structural MRI studies show the decrease in the brain's total volume resulting from cortical thinning and gyral atrophy such that both the entorhinal cortex and the hippocampus show the loss of volume in MCI and AD (Márquez and Yassa 2019). In the imaging technique, one cannot get a correct idea of the concentration of biomarkers.

Table 3.1 Function of biomarkers in AD

Biomarker	Role in AD	Refs.
A β	A β 40 or A β 42 are formed due to proteolytic cleavage of APP by β and γ secretase. This insoluble A β forms extracellular amyloid plaques. The soluble amyloid- β -derived diffusible ligands (ADDLs) are the precursors of the formed A β and can be considered a biomarker	Georganopoulou et al. (2005), Szemraj (2014)
ACh	Acetylcholine (ACh) has a role in attention, learning, memory, stress response, wakefulness and sleep, and sensory information. It has two receptors: Nicotinic and muscarinic. The concentration levels of ACh decrease due to AD, and synaptic loss is found for disease onset	Ferreira-Vieira et al. (2016)
APOE	The e4 allele of apolipoprotein E (APOE) accelerates the A β aggregation at the early onset of AD. The e4 allele of APOE also presents in the form of the APOE-A β complex in the periphery and transports the A β into brain capillaries for more accumulation of A β through the blood. It also has other mechanisms on synaptic plasticity, inflammatory, tau phosphorylation, and neurotoxicity	Kim et al. (2009)
APP	Amyloid precursor protein (APP) is present such that one end is outside the cell and has a β secretase cleavage while the other end is inside a transmembrane and has a γ secretase cleavage and releases insoluble monomer A β	Thinakaran and Koo (2008)
Astrocytes	Activated astrocytes produce A β , and they are involved in the neuroinflammatory component of AD through the release of cytokines and ROS (nitric oxide)	Verkhatsky et al. (2010)
BACE1	β site APP cleaving enzyme 1 (BACE1) is a membrane-bound protein. The sequence preference of β secretase depends upon the mutation in amino acids surrounding the cleavage site of APP such that the substitution of more hydrophobic amino acids improves the efficiency of β secretase cleavage	Cole and Vassar (2007)
DA	Low concentration level of dopamine (DA) found in the striatum, amygdala, substantia nigra, cingulate gyrus, and raphe nucleus of postmortem AD brain in comparison to normal. Dopaminergic neurons have five receptors D ₁ , D ₂ , D ₃ , D ₄ , D ₅ . The density distribution of D ₂ , D ₃ , D ₄ receptors is decreased and that of D ₁ and D ₅ receptors is increased in the striatum and frontal cortex	Mitchell et al. (2011)
GABA	γ -Aminobutyric acid (GABA) has two receptors: Inotropic (GABA _A and GABA _C) and metabotropic (GABA _B) receptors. GABA _B R is present in presynaptic and postsynaptic hippocampal neurons. AD activation of GABA _B R in presynaptic neurons inhibits the neurotransmitter release, and in the	Prakash et al. (2015)

(continued)

Table 3.1 (continued)

Biomarker	Role in AD	Refs.
	postsynaptic neurons, it inhibits the postsynaptic potential	
GSK-3	Glycogen synthase kinase 3 is activated by A β and causes hyperphosphorylation of tau proteins	Llorens-Martín et al. (2014)
GLu	It has two receptors: Iontropic and metabotropic. Alteration in the glutamate receptor signaling causes neurodegeneration like AD such that alteration in metabotropic receptors group I mGluR signaling regulates A β 42 toxicity	(Ribeiro et al. 2017)
5-HT	Serotonin (5-HT) concentration level decreases in the AD brain and decreases memory storage and learning processes. It has specific receptors (5-HTRs) such that 5-HT4R receptor activation helps in non-amyloidogenic cleavage of APP and slows down the production of A β plaques, and 5-HT6R activation can be responsible for the tau phosphorylation	Butzlaff and Ponimaskin (2016)
LRP and RAGE	Lipoprotein receptor-related protein (LRP) is involved in several ways; firstly, it binds with APP to regulate A β . Secondly, LRP binds with APOE to degrade the A β . Lastly, LRP has another role; it binds with A β at BBB and transfers it to the peripheral circulation. The receptor for advanced glycation end products (RAGE) imports A β from the peripheral circulation into the brain	Anastasio (2011)
MCP-1 and macrophage	Monocyte chemoattractant/chemotactic protein (MCP)-1 is activated by the astrocytes and attracts the monocytes from the blood to the brain. It activates the macrophages into two phenotypes: Pro-inflammatory \widehat{M}_1 and anti-inflammatory \widehat{M}_2 . \widehat{M}_1 helps in A β aggregation, while \widehat{M}_2 macrophage supports A β clearance	Hao and Friedman (2016)
Microglia	The amyloid-beta activates the microglia. Activated microglia release cytokines and phagocytosis. Microglia have two phenotypes such that M_1 is involved in pro-inflammatory action while M_2 is involved in anti-inflammatory and tissue repair	Thériault et al. (2015)
OS	Iron accumulation in the AD brain generates hydroxyl radical by Fenton reaction, and A β binds with iron increases oxidative stress (OS). Poor antioxidants, mitochondrial dysfunction, microglial activation, and ROS also increase the OS and cause memory loss	Manoharan et al. (2016)
PSEN1 and PSEN2	PSEN1 and PSEN2 mutation changes the processing of APP and favors more production of long-tailed A β 40 or A β 42	Fraser et al. (2000)
ROS	Reactive oxygen species (ROS) like superoxide anion (O $_2^-$), hydroxyl radical (OH), and H $_2$ O $_2$ have a role in DNA mutations, lipid peroxidation, protein oxidation, microglial proteasome malfunction, astrocyte	Mohsenzadegan and Mirshafiey (2012)

(continued)

Table 3.1 (continued)

Biomarker	Role in AD	Refs.
	activation, inflammation, and cell death. A β induces the ROS in the presence of Fe or Cu	
Tau	The hyperphosphorylation of tau proteins, which have six different isoforms (Tau-441, Tau-412, Tau-410, Tau-383, Tau-381, Tau-353) leads to the formation of NFTs (neurofibrillary tangle) in the human brain	Andreadis (2012)
TGF- β	Transforming growth factor (TGF- β) is an anti-inflammatory cytokine activated by M2 phenotype microglia and helps in the protection of neurons against damage, and overexpression of it reduces the formation of the plaques and A β	Chen et al. (2015)
TNF- α	The pro-inflammatory cytokines such as tumor necrosis factor (TNF- α) and interleukin (IL-1 β , IL-6, IL-12, IL-13) are activated by microglia (M ₁ phenotype) and cause the loss of neurons. M ₂ phenotype microglia activates the anti-inflammatory cytokines (IL-10, IL-4, IL-13) that help in tissue repair and angiogenesis	Wang et al. (2015)

The detection of biomarkers present in the blood is aimed to determine its concentration. The immunoprecipitation method detects the conformation and immunomagnetic reduction (IMR) used to quantify A β , while MS methods measure some sorts of aggregation of A β in AD plasma. The single-molecule array (SIMOA) is an ultrasensitive technique that measures the tau in the blood (Zetterberg 2019). A β is also recognized in the platelets using immunoprecipitation (IP) combined with MS. A β is degraded with time in plasma since hydrophobic A β concentration is ten times lower than CSF due to the formation of a complex with other proteins. MALDI-TOF/TOF mass spectra differentiate the A β 38, A β 40, and A β 42 peptides, quantified using selected reaction monitoring (SRM) (Pannee et al. 2014). The methods used to measure all proteome-based biomarkers (α -2-macroglobulin, monoamine oxidase B, isoprostane 8,12-iso-iPF₂ α -VI, hemopexin, CCL-1, complement C3, plasminogen, folic acid, fibrinogen gamma chain, etc.) of AD in plasma and serum are antibodies array, radioimmunoassay (RIA), two-dimensional polyacrylamide gel electrophoresis (2D-PAGE), GC/MS, LC/MS/MS, MALDI-TOF/MS, multiplex fluorescent immunoassay, etc. (Altuna-Azkargorta and Mendioroz-Iriarte 2020; Lista et al. 2013).

Various methods used to detect biomarkers present in both CSF and blood are based on the measurement of their concentration. Using the ELISA technique, it was reported (Mulder et al. 2010) that there is a fall in the concentration of A β and a rise in the concentration of tau and p-tau in cerebrospinal fluid of AD patients. xMAP measures the binding of specific capture mAbs 4D7A3 (A β 42), AT120 (Tau), or

Table 3.2 Properties of various biomarkers related to AD in different fluids

Biomarker	Molecular Wt. (kDa)	Biological fluid	Typical concentration of the biomarker in fluid (ng/ml) in healthy persons	Effect of AD in its concentration	Techniques used to detect the effect (Refs.)
A β 42		CSF	>0.550	Decreased	ELISA (Mulder et al. 2010)
			0.752 \pm 0.253	Decreased	PEA (Whelan et al. 2019)
			0.750 (0.260–0.960)	Decreased	Luminex xMAP (Zetterberg et al. 2008)
A β 40		Plasma	19.6 $\times 10^{-3} \pm 5.2 \times 10^{-3}$	Decreased	SIMOA and IMR (Lue et al. 2017)
		Saliva	20.82 $\times 10^{-3} \pm 5.55 \times 10^{-3}$	Increased	ELISA (Bermejo-Pareja et al. 2010)
		CSF	5.847 \pm 2.042	Decreased	PEA (Whelan et al. 2019)
		Plasma	5.300 (3.200–7.700)	Decreased	Human A β 40—kit (Zetterberg et al. 2008)
ACh			0.2767 \pm 0.0661	Decreased	SIMOA and IMR (Lue et al. 2017)
		Saliva	2.89 $\times 10^{-3} \pm 4.96 \times 10^{-3}$	Increased	ELISA (Bermejo-Pareja et al. 2010)
	0.14621	CSF	5.04 \pm 1.31	Decreased	HPLC-ECD (Jia et al. 2004)
		Blood	29.24–191.53	Decreased	Pyrolysis-GC-MS (Watanabe et al. 1986)
		Plasma	0.45 \pm 0.05	Decreased	RIA (Fujii et al. 1995)
AD7cNTP		Blood	1.26 \pm 0.15	Decreased	RIA
	41	CSF	1.56 \pm 0.86	Increased	ELISA (Monte et al. 1997)
		Urine	0.5 \pm 0.3	Increased	ELISA AD7c-NTP kit (Zhang et al. 2018)
		CSF	517 (49.5–999.9)	Increased	MSD sAPP ω /sAPP β (Zetterberg et al. 2008)
sAPP- α	110		Increased		
sAPP- β	130		Increased	Multiplex assay	
BACE 1	60	CSF	360.1 (130–590.2)	Increased	WB and ELISA (Zhong et al. 2007)
			0.94 \pm 0.86	Increased	NR (Zetterberg et al. 2008)
			1.38 (0.48–2.58)	Increased	WB and ELISA (Zuliani et al. 2020)
		Blood	36 (28.8–43.2)	Increased	

		Serum	44.4 (36.48–53.52)	Increased	WB and ELISA (Cervellati et al. 2020)
GABA	0.1031	CSF	44.3 ± 10.0	Decreased	HPLC-MS/MS (Song et al. 2005)
		Plasma	8.5 ± 1.6	Decreased	GC/MS (Lancôt et al. 2007)
			98.6 ± 33.9	Decreased	HPLC-MS/MS (Song et al. 2005)
		Saliva	8.94 (4.91) ng/mg of protein	Increased	
GLu	0.14713	CSF	0.87 × 10 ³ (0.47 × 10 ³)	Increased	HPLC (Madeira et al. 2018)
		Plasma	4.07 × 10 ³ ± 0.31 × 10 ³	Increased	Spectrophotometry (Miulli et al. 1993)
p-tau 181		CSF	<0.052	Increased	ELISA (Mulder et al. 2010)
			0.037 ± 0.013	Increased	PEA (Whelan et al. 2019)
			0.350 ± 0.256	Increased	MS (Barthélemy et al. 2020)
			0.057 ± 0.1121	Increased	IMR (Yang et al. 2018)
p-tau 217			2.46 × 10 ⁻³ ± 1.09 × 10 ⁻³	Increased	SIMOA (Tatebe et al. 2017)
			0.0405 × 10 ⁻³ ± 0.0756 × 10 ⁻³	Increased	SPR (Shekhar et al. 2016)
Tau		Serum	124 ± 5.0	Increased	Luminex assays (Shi et al. 2011)
		Saliva	0.090 ± 0.015	Increased	
		CSF	<0.375	Increased	ELISA (Mulder et al. 2010)
		Plasma	0.292 ± 0.089	Increased	PEA (Whelan et al. 2019)
Aβ			18.85 × 10 ⁻³ ± 10.16 × 10 ⁻³	Increased	IMR (Yang et al. 2018)
		Serum	35.02 × 10 ³ ± 1.31 × 10 ³	Increased	SPR (Shekhar et al. 2016)
		Saliva	15.18 × 10 ⁻³ ± 1.4 × 10 ⁻³	Decreased	Luminex assays (Shi et al. 2011)
		Blood	6.79 × 10 ⁴ (3.79 × 10 ⁴ to 10.19 × 10 ⁴)	Decreased	ELISA (Dieplinger and Dieplinger 2015)
Apolipoprotein A1	28	Blood	11.28 × 10 ⁵ ± 4.26 × 10 ⁵	Decreased	ELISA
Apolipoprotein A4	46		27.64 × 10 ⁴ ± 6.58 × 10 ⁴	Increased	ELISA
			40.58 × 10 ³ ± 4.06 × 10 ³	Decreased	ELISA (Lin et al. 1995)

(continued)

Table 3.2 (continued)

Biomarker	Molecular Wt. (kDa)	Biological fluid	Typical concentration of the biomarker in fluid (ng/ml) in healthy persons	Effect of AD in its concentration	Techniques used to detect the effect (Refs.)
APOE	34	Plasma	$74.46 \times 10^3 \pm 25.5 \times 10^3$ 45.9×10^3	Decreased	Luminex xMAP (Teng et al. 2015)
α -1-antitrypsin	52	Blood	$1.259 \times 10^6 \pm 0.139 \times 10^6$	Increased	LC/SRM/MS (Simon et al. 2012) Turbidometric assay (Maes et al. 2006)
BDNF	27	Blood	1.25 ± 0.49	Decreased	ELISA (Gezen-Ak et al. 2013)
Clusterin	60	Blood	82.2 ± 23.4	Increased	ELISA and LC-MS-MS (Killick et al. 2020)
CFH	155	Blood	700 ± 400 AU/ml	Decreased	ELISA (Gezen-Ak et al. 2013)
Cystatin C	13.351	Blood	1099.45 ± 49.66	Decreased	ELISA (Chuo et al. 2007)
DYRK1A	55–95 WB	Blood	100 ± 8 a.u	Decreased	WB (Janel et al. 2011)
DA	0.15318	Serum	$15.318\text{--}15.3180 \times 10^4$	Decreased	HPLC-MS and GC-MS (Zaidi 2018)
5-HT	0.17621	CSF	349.95 ± 29.95	Decreased	HPLC (Tohgi et al. 1992)
Homocysteine	0.13518	Platelet	0.81 ± 0.34 nmol/mg of protein	Decreased	HPLC (Muck-Seler et al. 2009)
		Blood	1.66×10^6 (0.46×10^6)	Increased	Colorimetric activity method (Davidson et al. 2012)
α -2-HS-glycoprotein	50	Blood	298.95×10^3 (53×10^3)	Decreased	ELISA (Smith et al. 2011)
IL-10	18	Blood	$4.86 \times 10^{-3} \pm 2.34 \times 10^{-3}$	Increased	ELISA (Gezen-Ak et al. 2013)
(metal ions)—	0.0558	Serum	1149.48 ± 122.76	Increased	ELISA (Manolov 2017)
Iron	0.0635		1212.85 ± 57.15	Increased	ELISA
copper	0.0654		967.92 ± 52.32	Increased	ELISA
zinc	68	Blood	3.47×10^4 (2.14×10^4)	Increased	NFL kit (Mattison et al. 2017)
NF-L	0.07206	Plasma	383.35 ± 108.09	Increased	LPO-586 kit (McGrath et al. 2001)
OS (MDA)	0.15622	Plasma	1.22×10^3 (0.52×10^3 to 2.26×10^3)	Increased	LPO-586 kit

Phospholipase A2	45	Blood	0.387 ± 0.02 (nmol/mg/min) of protein	Increased	Radio-enzymatic assay (Krzyszczak et al. 2007)
TNF- α	17.3	Blood	$15.98 \times 10^{-3} \pm 6.98 \times 10^{-3}$	Increased	ELISA (Gezen-Ak et al. 2013)
		Serum	$2.42 \times 10^{-3} \pm 1.21 \times 10^{-3}$	Increased	ELISA (Alvarez et al. 2007)
		Saliva	66.259×10^{-3} (591.66×10^{-3})	Increased	Luminex assay (Singhal and Anand 2013)
Transferrin	80	Blood	24×10^5	Increased	Vitros 5.1 from Ortho-Clinical Diagnostics (Torsdottir et al. 2011)
Creatinine	0.11312	Serum	$8.55 \times 10^3 \pm 0.59 \times 10^3$	Decreased	ELISA (Manolov 2017)
		Urine	$7.76 \times 10^3 \pm 1.04 \times 10^3$	Increased	SPOTCHEM D-01 analyzer (Watanabe et al. 2019)
Human urinary albumin	66.5	Urine	$18.59 \times 10^3 \pm 4.69 \times 10^3$	Increased	SPOTCHEM D-01 analyzer (Watanabe et al. 2019)
IL-1 β	30.9318	Saliva	44.54×10^{-3} (32.17×10^{-3})	Increased	Luminex assay (Singhal and Anand 2013)
Lactoferrin	78	Saliva	>7.34	Decreased	ELISA (Ashton et al. 2019)

BDNF brain-derived neurotrophic factor, (*2D-DIGE*) two-dimensional differential gel electrophoresis, *CFH* complement factor H, (*DYRK1A*) dual specificity tyrosine-phosphorylation regulated kinase A, *ECD* electrochemical detector, (*4-HNE*) 4-hydroxynonenal, (*HILIC-UHPLC-QTRAP[®]/MS2*) ultra-performance liquid chromatography coupled with triple-quadrupole linear ion-trap tandem mass spectrometry, *IHC* immunohistochemical, *IMR* immunomagnetic reduction, *LPO* lipid peroxide, *MCI* mild cognitive impairment, *MDA* malondialdehyde, *mean* \pm *SD* or mean \pm SEM or median (interquartile range), or mean (*SD*), median (interquartile ranges) (all nonparametric variables), or median (*IQR*), *MSD* Meso Scale Discovery, (*NF-L*) neurofilament light polypeptide, *NR* not reported, *n* number of subjects, *OD* optical density, *PEA* proximity extension assay, (*Pyrolysis-GC-MS*) pyrolysis-gas chromatography-mass fragmentography, *R/A* radioimmunoassay, (*sAPP- α*) α -cleaved soluble amyloid precursor protein, (*sAPP- β*) β -cleaved soluble amyloid precursor protein, *SIMOA* single molecular array (digital form of ELISA), (*UPLC-Q-ToF MS*) ultra-performance liquid chromatography coupled to time-of-flight mass spectrometry

AT270 (p-tau 181) with epitope region of antigen in cerebrospinal fluid for A β , Tau, and p-tau 181. Electrochemiluminescence (ECL) detection method also measures the concentration of A β 42 and tau protein in CSF (Kang et al. 2013). Western blot analysis (WB) technique in platelets with a monoclonal antibody (mAb) for APP got three molecular weight forms: 130, 110, and 106 kDa. WB with polyclonal antibody (pAb) for BACE 1 forms (BACE 36 kDa/ BACE 57 kDa) (Di Luca et al. 2005). The developed semi-sensitive electrochemiluminescence based assay of p-tau 181 in the CSF fluid has been used for the assay of the p-tau in the plasma fluid. A slightly increased concentration of p-tau 181 in the plasma of AD subjects is reported. The enzymatic degradation of tau protein in plasma, its half-life is shorter (about 10 h) in plasma than in CSF (a few weeks) (Zetterberg 2019).

The studies of biological and pathological changes in AD-related proteins in the urine are limited. A higher concentration in human urinary albumin and urinary creatinine in AD than control subjects are reported using SPOTCHEM D-01 analyzer ((Watanabe et al. 2019). Alzheimer-associated neural thread protein (AD7c-NTP), a potential biomarker for AD in urine, was detected using the ELISA AD7c-NTP kit. Due to AD in subjects, the biomarkers' concentration level decreases (Zhang et al. 2018). Ultra-performance liquid chromatography coupled with triple-quadrupole linear ion-trap tandem mass spectrometry (HILIC-UHPLC-QTRAP[®]/MS2) technique is developed for detection of stages of dementia, such as mild cognitive impairment (MCI), mild dementia, and moderate dementia from the data of neurotransmitter concentration in urine samples. The concentrations of ACh, 5-HT, and GABA in subjects with MCI were two times higher than moderate dementia. The GLu concentration in moderate dementia was approximately two times higher than that in MCI patients (Zhou et al. 2020).

It is expected that any effect in CSF can change the level of AD biomarkers in saliva. A β shows an increment in levels as compared to healthy controls measured by ELISA and nanoparticle immunoassay. The concentration of p-tau in the saliva increases as detected by WB or ultrasensitive single-molecule array techniques. However, tau's concentration decreases in saliva. The effect of AD on the concentration level of AChE in the saliva is controversial: some researchers reported no statistical difference, while some researchers reported an increase in its value. Inflammatory factors like TNF- α and IL-1 β in the salivary were increased in AD as measured by the Luminex assay method (Liang and Lu 2019). Lactoferrin is an antimicrobial peptide with A β binding properties, and concentration level decreased for AD compared to age-matched control as measured by sandwich ELISA (Ashton et al. 2019).

Collection of CSF by a lumbar puncture is an invasive process with side effects and difficulty in screening, so detection of AD biomarkers in blood can be helpful in following and screening of patients for many years (Humpel 2011). The collection of blood-based AD biomarker samples is time- and cost-efficient, which a patient can easily accept. Its poor reproducibility due to differences in sample concentrations limits clinical utilization (O'Bryant et al. 2017).

The detection techniques are expected to be reproducible, inexpensive, and reliable with sensitivity and specificity greater than 80% (Hrubešová et al. 2019). The biomarker should differentiate with other types of dementia like vascular

dementia, mild cognitive impairment, frontotemporal lobe dementia, and Lewy body dementia to identify the required treatments. Some techniques are available to detect at early stages and during AD, but these detection techniques have some advantages and limitations as listed in Table 3.3. The available techniques, such as ELISA, xMAP, and ECL, have the advantage of measuring a concentration of AD biomarkers in biological fluid over other fluid-based techniques owing to the requirement of less sample volume and short processing time.

The cost of conventional methods of detection techniques is described in Table 3.4. Here, we have listed various targeted biomarkers, the instruments used, manufactures of the instruments, and a typical measurement cost. The cost varies with time and process of manufacturing. In general, the imaging-based methods are costlier than the concentration-based methods.

3.3 Nanotechnology in Early Detection of AD

There are two broad classifications of nanotechnology-based approaches; namely, molecular imaging probes-based approach and protein binding-based approach.

The techniques used or tested in the molecular imaging probes-based approach are bio-barcode assay, single-molecule fluorescence microscopy, fluorescence resonance energy transfer (FRET), scanning tunneling microscopy, atomic force microscopy, and NanoSIMS microscopy. Nanotechnology in imaging and detection depends on the designed nanoparticles' electrical, optical, chemical, and biological quality. An early diagnosis is based on the development of nanoparticles for imaging and molecular detection of AD biomarkers. Early detection may help stop the progression because conventional techniques like ELISA or western blot do not precisely measure the concentration. The concentration is quite low in CSF or blood at early stages and can overlap between control and AD subjects (Ahmad et al. 2017).

In the protein binding-based approach using the principle of protein binding, the techniques being developed are two-photon Rayleigh scattering assay, localized surface plasmon resonance, and nanocomposite-based biosensors. The various nanocomposites used in the electrochemical detection are listed in Table 3.5. Nanotechnology has a vital role in the development of biosensors in terms of sensitivity and performance. The use of nanomaterials has improved signal transducer technologies owing to the submicron level, nanosensor, nanoprobe, and other nanosystems that have allowed the rapid multiple analysis of substances *in vivo* (Jianrong et al. 2004). Gold nanoparticles (AuNPs), magnetic nanoparticles (Fe_3O_4), polymers, CNT, graphene, dendrimers, quantum dots, and others are commonly used in the development of a biosensor for the detection of biomolecules owing to exhibit unique and specific properties (Carneiro et al. 2019).

Table 3.3 Techniques available to detect AD and its limitations

Techniques	Target	Matrix	Advantages	Limitations	Refs.
PET	A β	CSF/ brain	It shows amyloid imaging by using a specific tracer like Pittsburgh compound B (PIB). Ligands that bind with A β have high affinity and can be retained for several days	High cost; low availability; requirement for radioactive tracers; half-life of ^{11}C compounds is 20 min; requirement of on-site cyclotron for synthesis; spatial resolution (1 μm)	Skoch et al. (2005)
SPECT	Imaging-based biomarker	rCBF	More clinically available, high sensitivity (10^{-10} to 10^{-11} mol/L), multiplexing capability, unlimited depth penetration	Low spatial resolution (8–10 nm); imaging time in min; minimal 3D anatomical information; ionizing radiation	Zhao et al. (2018)
Surface plasmon resonance	A β , tau	CSF	Monitors molecular interactions in real time; needs small reagents for low-affinity binding interaction compared to equilibrium assays; differentiates dementia with an accumulation of proteins like A β , tau, and α synuclein TAR DNA-binding protein (TDP-43), frontotemporal dementia with parkinsonism-17 (FTDP-17), etc. in neurons	It contains few channels and limited receptors that can be tested per chip; difficult to detect small molecules owing to smaller changes in interfacial refractive index	Wittenberg et al. (2014)
xMAP	A β 42, tau, p-tau 181	CSF	Early detection of A β 42, tau, p-tau 181; wide dynamic range and can be used as calibrators; less sample volume is required in comparison to ELISA; analyzes three biomarkers at a time	Less used as compared to ELISA; optimal concentration detection of three biomarkers is still a challenge; a need to understand the heterogeneous components that may interfere in the affinity or selectivity of antibodies	Kang et al. (2012)
Colorimetric methods	A β	CSF/ serum	High sensitivity and selectivity of A β toward Cu^{+2} and conjugation on AuNPs surface; color change is easily observed; assay time is a few minutes	pH control is required for the dispersion, and aggregation of AuNPs for A β levels of A β in serum is low as compared to LOD of calorimetric methods	Zhou et al. (2015)
MS methods	A β	CSF/ plasma	Robust and accurate; MRM/MS can enhance the LOD of peptides owing to rapidly and continuously monitoring specific ions. MS studies the 26 unique C- and N-terminal truncated proteoforms of A β in the human AD brain; MALDI-TOF/TOF/MS	Less commercially available antibodies are validated by MS methods; LC/MS has a lesser sensitivity as compared to ELISA, WB, and radioimmunoassay; need high-resolution MS instrument to accurately identify large sequences of A β peptides; samples prepared by immunoprecipitation	Liu et al. (2014), Zakharova et al. (2018)

ELISA	A β , tau, p-tau 181	Plasma	differentiates molecular weight of different forms of A β Mostly accepted in clinical practice; standard for quantitative analysis for cytokines, A β , tau, p-tau 181; applied in both CSF and plasma biomarkers	puts a limitation on the extraction of different A β species One analyte at a time; depends upon flat surface 96-well plate, the same antibody to capture subsequent ligand, capture antibodies recognized only N-terminal A β peptide-like 6E10 and interfere inability to detect A β in plasma	Eishal and Mccooy (2006), Oh et al. (2010)
ECL	A β 40 and A β 42	Plasma	Short processing time; small sample volume (50 μ l/well); large dynamic range in the detection of A β 40 and A β 42	Simultaneous detection of multiple biomarkers; mean levels of plasma A β 40, and A β 42 do not differentiate between the diagnostic group; capture antibodies recognized only C-terminal and not N-terminal of A β ; absolute concentration of A β varies	Oh et al. (2010)
MRI	A β , NFTs, tau	Brain	AD pathology is detectable owing to different signals in brain tissues; determines mild cognitive impairment (MCI); differentiates normal cognitive aging from MCI and progressive MCI with an accuracy of 96.5% and 91.74%	Structural MRI lacks molecular specificity and cannot access function; does not detect histopathological hallmarks of AD (A β NFTs, tau); atrophy pattern of AD can overlap with another disease, while measuring a progression change in volume may depend upon on other factors, not on the neuronal loss	Johnson et al. (2012), Rallabandi et al. (2020)
IHC	A β , p-tau	Brain	Identifies the insoluble aggregates of misfolded proteins using antibodies; IHC test for A β and p-tau is easier and reproducible; it also tells the neurons can survive in the presence of tau hyperphosphorylation	False-positive results are common in the IHC technique; the problem in masking of antigens by aldehyde fixatives or paraffin embedding procedures; obtained morphology of tangles and plaques are poor	Kai et al. (2012), Nuovo et al. (2017)

(continued)

Table 3.3 (continued)

Techniques	Target	Source	Advantages	Limitations	Refs.
WB	Tau	Brain	Semi-quantification of protein levels; ability to detect picogram levels of proteins in a sample; separation of protein by gel electrophoresis; determines the molecular weight of proteins using standards; specific antibody finds its target protein in lakhs of different proteins in a sample	Many antibodies show off-target effects after interaction with other proteins; denatured state of primary antibodies does not recognize the immobilized antigens; small proteins (<10 kDa) are not retained while large proteins (>140 kDa) not transferred by the membrane	Ghosh et al. (2014)
Microdialysis	Ach, GLu, GABA, 5-HT, DA	Brain fluid	Coupled with LC; capillary electrophoresis allowed detection of compounds involved in complex biological process; it also detects the neurotransmitters (Ach, GLu, GABA, 5-HT, DA); required small sample volume; measures the concentration levels in picomolar	Poor temporal resolution; the probe of microdialysis can damage the surrounding tissues when applied in a particular part of the brain. The actual concentration of neurochemical present in extracellular brain fluid does not match with microdialysis	Bongaerts et al. (2018)
Fluorescent probes	A β	Brain	Probe with flexible π -conjugated backbone detects very low levels of A β with compressed background and offers strong fluorescent enhancement. Selectivity is high for biomarkers; sufficient cell permeability and toxicity is low; photostability is sufficient	Iminopyridyl chelates bound with Cu or Zn have poor fluorescent properties; the sensing strategy is not suitable for NFTs in comparison to A β owing to less binding modes. In detecting reactive astrocytes, high dose is required and low BBB permeability owing to the negatively charged character. This technique is still away from a clinical trial	Jun et al. (2019)

Table 3.4 Typical cost of detection of various AD biomarkers

Technique	Biomarker	Source	Description	Cost/X	Manufacturer/clinic	Refs.
ELISA	A β 42, tau, p-tau	CSF	NR	€22.08	ELISA kits distributor	Valcarcel-Nazco et al. (2014)
ELISA ECL	A β , tau, p-tau 181 Tau, p-tau 231	CSF	96-well plate Multiplex assay	€68 \$23	Innogenetics, gent, Belgium MSD, Gaithersburg, MD, USA	Regeniter et al. (2012)
Lumbar puncture PET	A β 42 Amyloid PET	CSF Brain	NR ¹¹ C PiB	€150 €2000–2500 \$3000–4500	NR NR	Blennow et al. (2015)
ELISA multiplex ECL assay	A β 40, 42 A β 38, 40, 42	Plasma	NR Multi-spot [®] triplex human (6E10)	\$20 \$16	Invitrogen, CA, USA MSD, Gaithersburg, MD	Oh et al. (2010)
MRI, CT, PET, CSF puncture, blood test	NR	Brain	NR $n = 30$, dementia	€649	German memory clinic	Michalowsky et al. (2017)
MRI MRI + CLP	A β	Brain	NR	€250 €500/ 6 month	Guerbet company Paris	Biasutti et al. (2012)
MRI	A β	Brain	NR	\$1000	NR	Sabbagh et al. (2017)
PET	A β	Brain	¹¹ C PiB	\$5000	NR	(Blennow et al. 2010)
MRI xMAP	A β 42, tau, p-tau	CSF	NR	\$500 \$200	NR Luminex, Austin, TX, USA	

ECL-CLP contrastophore-linker-pharmacophore; electrochemiluminescence, € Euro, *MSD* Meso Scale Discovery, *NR* not reported, n no of patients, \$ US dollar, \bar{X} patient, or sample, or scan, or complete diagnostic process (clinical consultation + technical procedure), or clinical biomarker analysis

Table 3.5 Detection of AD biomarkers using different nanotechnology-based sensors

Target	Source	Sensor	Size of NPs	Detection technique	Linear range (ng/ml)	LOD (ng/ml)	Refs.
A β 42	CSF	LSPR-based sensor using monoclonal antibodies (anti-A β 1–42) immobilized on Au NPs-coated PET substrate	AuNPs—9 nm	LSPR	1×10^{-3} to 150×10^{-3}	1×10^{-3}	Ly and Park (2020)
A β 40	Brain tissue lysate	Monoclonal amyloid antibodies (mAb β_{40}) immobilized on disc-shaped platinum/iridium (Pt/Ir) microelectrode surface	NR	EIS	1×10^{-3} to 10	4.81×10^{-3}	Zakaria et al. (2018)
A β 0	Serum	Sandwich assay of MIP/A β 0 and SiO $_2$ @Ag-aptamer was immobilized on Au-GO nanocomposite-modified GCE	SiO $_2$ NPs —200 nm	DPV	5×10^{-3} to 10×10^{-3}	1.22×10^{-3}	You et al. (2020)
AAT	Serum	Sandwich-type assay and the combination of ALP-AAT Ab-Ag NPs and AAT aptamer on SPCE	CNT (dia —20 nm, length 5 μ m)	CV and DPV	2.6×10^{-3} to 1.04	0.52×10^{-3}	Zhu and Lee (2017)
ACh	Plasma	Hybrid enzymatic fuel cell (EFC)-based sensor with AChE immobilized onto a nanostructured electrode coated onto a Pt surface		SWV and CV	1.46×10^{-2} to 1.46×10^6	1.46×10^3	Moreira et al. (2017)
ACh	Serum	AChE and Cho immobilized on palladium nanoparticles (Pd _{nanoc}) adsorbed over molybdenum disulfide	Pd NPS— (20–30 nm)	EIS and CV	0.14 – 1.46×10^6	0.14	Jain et al. (2019)

		(MoS ₂) nanostructures electrodeposited on the surface of the gold electrode (Au-ET)							
ACh	Serum	ACh and ChO immobilized on Fe ₂ O ₃ /PEDOT-rGO composite-modified FTO	NR	EIS and CV	0.58–1.17 × 10 ⁵	0.58	Chauhan et al. (2017)		
ACh	Serum	PANI/MWCNT/MIP/TpCIPB on graphite conductive support at pH 8.5	MWCNT—15 nm	Potentiometric	3.20 × 10 ³ to 1.46 × 10 ⁶	143.28	Sacramento et al. (2017)		
ACh	PBS	MAA/EGDMA/benzoyl peroxide/ACh/MIP were incorporated into the PVC membrane at pH 7	NR	Potentiometric	4.38 × 10 ³ to 14.62 × 10 ³	1.05 × 10 ³	Kamel et al. (2016)		
ACh	Synthetic urine	ACh immobilized poly (neutral red) (PNR) films formed on Fe ₂ O ₃ nanoparticle-modified electrodes	NR	CV and EIS	365.52–11.69 × 10 ³	152.06	da Silva and Brett (2020)		
APOE4 DNA	Plasma	GQDs-curcumin APOE4 DNA sensor	GQDs—8 nm	DPV	0.02–0.4	0.48 × 10 ⁻³	Mars et al. (2018)		
DA	Urine Serum Blood CSF	rGO/Bi ₂ S ₃ /GCE rGO/PU PGr/GCE NiO NP-MWCNT-DHP/GCE	SWNT— (0.5–1 nm)	CV and DPV CV and DPV CV and DPV DPV, SWV	1.53–6.13 × 10 ³ 15.32 × 10 ⁻³ to 0.176 1.53–7.65 × 10 ³ 10.72–0.73 × 10 ³	1.88 1.53 × 10 ⁻⁴ 0.15 7.65	Tavakolian-Ardakani et al. (2019)		
GABA	BSSA	ECR carbon electrode-based GABA sensor	Carbon film—40 nm	CV	1.47 to 1.47 × 10 ³	4.41	Sekioka et al. (2008)		
GLu	Serum	AuNPs—20 nm	AuNPs—20 nm	CV and EIS		0.23 × 10 ³			

(continued)

Table 3.5 (continued)

Target	Source	Sensor	Size of NPs	Detection technique	Linear range (ng/ml)	LOD (ng/ml)	Refs.
		Glutamate oxidase immobilized on carboxylate MWCNT, AuNPs, and chitosan as a hybrid film electrodeposited on au electrode			0.73×10^3 to 88.10×10^3		Batra and Pundir (2013)
L-Glu	Serum	GlUx immobilized on (Pt NPs)/(MWCNTs)/(PPy) composite modified GCE	MWCNT (dia—50–100 nm, length— 10^{-2} μm), Pt NPs—(20–50 nm)	CV and EIS	1.47×10^3 to 14.71×10^3	0.13×10^3	Maity and Kumar (2019)
Glu	PBS pH 7	LSPR-based glutamate sensor using an optical fiber substrate decorated with (AuNPs) upon which the enzyme (L-GDH) and the coenzyme (NAD ⁺) were immobilized	AuNPs—(15–20 nm)	LSPR	$0-1.47 \times 10^6$	5.29×10^4	Sharma et al. (2019)
5-HT	Serum	PEDOTNT/rGO/AgNPs/GCE	NR	CV, DPV and CA	$0.17-8.81 \times 10^4$	0.017	Sadanandhan et al. (2017)
5-HT	Serum	OPPy/au NFs/CFME	Au NFs—(100–500 nm)	CV	$1.76-1.23 \times 10^3$	0.40	Song et al. (2019)
5-HT	Serum	Electrochemical sensor based on rGO-Ag ₂ Se nanocomposite-modified GCE	Ag ₂ Se—(60–70 nm)	CV and EIS	$17.62-26.43 \times 10^2$	5.21	Panneer Selvam and Yun (2020)
5-HT	Urine	Electrochemical sensor based on 3D ITO electrodes	ITO NPs—50 nm	CV and DPV	8.82×10^3 to 176.21×10^3	1.32×10^3	Matuschek et al. (2017)

Tau-381	Serum	Aptamer-antibody sandwich on an electrode	AuNPs—4 nm	EIS, CV, and DPV	0.5×10^{-3} to 0.1	0.42×10^{-3}	Shui et al. (2018a)
Tau-159 to 163	aCSF Buffer and CCM	Whole anti-tau IgG antibodies are coimmobilized on the sensor surface with PEG	NR	FET	10^{-3} – 10	$<10^{-2}$ $<10^{-3}$	García-Chamé et al. (2020)
2N4R tau protein	Serum	Microelectrode array with four gold microband electrodes coated with oriented antibodies	NR	EIS and CV	10^{-5} to 10^2	10^{-5}	Wang et al. (2017)
TNF- α	Saliva and serum	P3-conjugating polymer with carboxyl side groups and TNF- α antibody immobilized on ITO-covered PET films	ITO—4 nm	EIS and CV	0.01×10^{-3} to 2×10^{-3}	0.0037×10^{-3}	Aydin et al. (2017)
TNF- α	Serum	Anti-human TNF- α Affibody [®] immobilized with support of magnetic beads on SPCE	NR	DPV	0.076–5	0.038	Baydemir et al. (2016)

ACHE acetylcholinesterase, *aCSF* artificial cerebrospinal fluid, *Affibody*[®] nonimmunoglobulin protein, (*ALP*-*AAT* *Ab*-*Ag* *NPs*) alkaline phosphatase-labeled *AAT* antibody-functionalized silver nanoparticles, *AAT* α -1 antitrypsin, *BSA* bovine serum albumin, *CA* chronoamperometry, *CCM* neuronal cell culture media, *CFME* carbon fiber microelectrode, *ChO* choline oxide, *DHP* dihexadecylphosphate, *ECR* electron cyclotron resonance, *FET* field-effect transistors, *FTO* fluorine-doped tin oxide, *GCE* glassy carbon electrode, *GLU**Ox* glutamate oxidase, *GQDs* graphene quantum dots, *hPG* highly porous gold, *ITO* indium tin oxide, (*L-GDH*) *L*-glutamate dehydrogenase, (*LSPR*) localized surface plasmon resonance, (*NAD*⁺) nicotinamide adenine dinucleotide, *NR* not reported, *OPPy* overoxidized polypyrrole, *P3* poly (3-thiophene acetic acid), (*PEG*) polyethylene glycol, *PET* polyethylene terephthalate, *PU* polyurethane, *rGO* reduced graphene oxide, *SPCE* screen-printed carbon electrode, *TpCIPB* Tetrakis(4-chlorophenyl)borate

3.3.1 Molecular Imaging Probes-Based Approach

3.3.1.1 Bio-Barcode Assay

Bio-barcode assay (BCA) is a nanogold diagnostic technology that consists of two probes: one has a monoclonal antibody for adsorption of proteins, nucleic acid, or small molecules, while another contains AuNPs coated with anti-target antibody and thiol-modified DNA as the barcode. Bio-barcode assay has a high sensitivity (5–6 times) than conventional ELISA, and the signal can also be amplified using the polymerase chain reaction (PCR) technique (Wang et al. 2019). The concentration levels of ADDLs and other CSF biomarkers are significantly less ($<1 \times 10^{-3}$ nM) at the early AD stages. The known volume of CSF sample from AD subjects was mixed with AuNPs (0.5 nm) modified with double-stranded oligonucleotides and functionalized magnetic microparticles with antigen-specific Ab (M90) in BCA for detection of ADDLs (Georganopoulou et al. 2005).

3.3.1.2 Scanning Tunneling Microscopy

Scanning tunneling microscopy (STM) is used to investigate materials by quantum mechanical tunneling effect, and tunneling current is highly sensitive to the distance between tip and sample. The vertical STM-based electrical detection technique was developed in which AuNPs (5 nm) antibody fragment complex was bound to antibody fragments against A β immobilized on a gold surface, and after that biosurface was monitored by surface plasmon resonance, while STM characterized current profile to know the concentration (10^{-6} ng/ml) of A β 1–40 (Lee et al. 2009). Choi et al. (2011) developed STM-based electrical detection of A β 1–42 using AuNPs (5 nm)-antibody complex immobilized on indium tin oxide glass patterned with Au nanodot array. STM can measure the concentration of A β as low as 10^{-4} ng/ml.

3.3.1.3 NanoSIMS Microscopy

Nano secondary ion mass spectroscopy (SIMS)-50 instrument has high sensitivity and spatial resolution of 50–100 nm with Cs⁺ source and 150–200 nm with O⁻ source at the subcellular level. NanoSIMS gives new information about the tissue alterations and morphological and chemical modification and can simultaneously identify the presence of five elements such as N, S, P, Fe, Ca in amyloid-beta, pyramidal neurons, glial cells, and neuropilin regions in hippocampal regions of human AD brain as well as in APP/PS1 mice brain. NanoSIMS confirms the presence of low iron content in A β and high calcium content in thalamus regions of APP/PS1 mice (Quintana et al. 2007).

3.3.1.4 Fluorescence Resonance Energy Transfer (FRET) Microscopy

FRET depends upon the interaction of two fluorophores, such as donor (fluorescein) and (rhodamine) acceptor, while the distance between them on a spatial scale should be less than 10 nm. Bacskai et al. (2003) analyzed FRET interactions by applying double immunofluorescence and fluorescence lifetime imaging microscopy (FLIM) instrument in conjunction with a commercial laser scanning multiphoton

microscope. One can obtain different morphological conformation of A β forms as β sheet structures within the senile plaques on the spatial scale in the transgenic mouse model of AD. This technique can be used to study the early formation of senile plaques and their variation with time in the transgenic mice using different anti-A β antibodies that can recognize specific epitopes within A β (Bacskaï et al. 2003).

3.3.1.5 MRI and PET

The brain imaging techniques are operated at higher spatiotemporal sensitivity levels than fluid biomarkers and can distinguish different phases of disease from early to late onset. (Márquez and Yassa 2019). A β peptides present in the form of A β 40 and A β 42 are the main components of senile plaques in AD. To image A β in vivo by ^{11}C -based Pittsburgh compound B PET and ^{18}F -based compounds PET techniques have been developed at preclinical stages (Gong et al. 2019). Phosphorylated tau protein aggregation, NFTs in AD, starts from the transentorhinal/entorhinal cortex to the hippocampus region, and after that, it extends to the temporal lobe and neocortical regions while this pattern helps in stages of AD. PET tracers like ^{18}F THK523, ^{18}F THK5117, ^{18}F THK5105, ^{18}F THK5351, ^{18}F AV1451 (T807), and ^{11}C PBB3 have been developed for human tau imaging in recent years for future clinical progression (Sheikh-Bahaei et al. 2017). MRI shows a higher spatial and temporal resolution but lower sensitivity than PET in the detection of amyloid plaques present in different sections of the brain. The sensitivity can be improved by using contrast agents. In the MRI, paramagnetic agent gadolinium complex Gd^{+3} or Mn^{+2} chelates increase the T1 relaxation rate ($1/T1$) and gives a positive contrast image in T1-weighted scans. Superparamagnetic iron oxide NPs (60–150 nm) affect the T2 relaxation rate, giving a negative contrast image in T2- and T2*-weighted scans and can visualize at a lower concentration than Gd^{+3} (Salerno et al. 2016).

3.3.2 Proteins Binding-Based Approach

3.3.2.1 Two-Photon Rayleigh Scattering Assay

Two-photon Rayleigh scattering (TPRS) generates results in less than 35 min, starting from proteins' binding till detection and analysis. The advantage of this assay is that it is three times more sensitive than any colorimetric technique. AuNps (size 4 nm)-based TPRS assay for the detection of tau proteins has been reported. AuNps is conveniently used in biomarker application and biological imaging owing to lack of toxicity, including shape- and size-dependent optical properties (Neely et al. 2009).

3.3.2.2 Localized Surface Plasmon Resonance

The biomarkers A β 40, A β 42, and tau in human plasma have been detected in the presence of gold nanoparticles of different shapes using localized surface plasmon resonance (LSPR). Three different shapes of AuNPs are (1) spherical (dia. of 50 nm) for A β 40, (2) short rods (aspect ratio 1.6) for A β 42, and (3) long rods (aspect ratio 3.6) for tau protein. Each shape code AuNPs give LSPR peak shift after interaction

of their respective biomarkers, and the limit of detection (LOD) has obtained 34.9×10^{-6} nM, 26×10^{-6} nM, and 23.6×10^{-6} nM for a linear range of logarithm concentration 10^{-5} to 10^2 nM in mimicked blood (Kim et al. 2018).

Sandwich assay of the SPR chip was functionalized using a self-assembled monolayer of mixed COOH- and OH-thiols. Primary antibody Ab (Tau) was immobilized on the surface by incorporating functionalized gold nanoparticles (AuNPs) to detect the tau-A β complex in CSF. The sensor response was obtained in terms of the shift in wavelength when an SPR dip occurs and is proportional to a change in refractive index caused by the binding of proteins to the sensor surface. The limit of detection (LOD) for the tau-A β complex was obtained 1×10^{-3} nM for linear concentration up to $\sim 5 \times 10^{-3}$ nM (Špringer et al. 2020).

3.3.2.3 Electrochemical Sensor

Electroanalytical techniques like electrochemical impedance spectroscopy (EIS), voltammetry, potentiometry, field-effect transistor (FET), and conductometric biosensors are being used to measure the electric signals. EIS can give the information of change in charging capacity, conductivity, or resistivity of an electrochemical interface. The potentiometric biosensor is based on the ion-selective electrode and the reference electrode to measure the charge accumulation on the electrode such that ISE is a membrane-based electrode and potential response according to the concentration of ions (Luo and Davis 2013). The various elements in voltammetric techniques are (1) an electrochemical cell consisting of working, counter, and reference electrodes and (2) potentiostat. Various variants of the techniques are cyclic voltammetry (CV), differential pulse voltammetry (DPV), and square wave voltammetry (SWV). The techniques for sensing an analyte in a linear concentration range (10^{-3} to 10^8 nM). CV is widely used to study the redox process, reaction intermediates, and product stability. The important part is peak potential (E_{pc} , E_{pa}) and peak current (i_{pc} and i_{pa}) of cathodic and anodic peaks. This technique is based on variation in potential applied to both forward and reverse direction with some scan rate to monitor the current. DPV is based on a series of fixed pulse potentials of small amplitude (10–100 mV). The potentials are superimposed on slowly changing base potential. A graph is plotted between the current difference obtained through pulse and base potential. SWV consists of a square wave pulse superimposed on the staircase waveform of ΔE step height, and the net current (i_{net}) is obtained from the difference between forward and reverse current ($i_{for} - i_{rev}$). SWV has several advantages like high sensitivity, repeatability, high signal-to-noise ratio, and rejection of background currents (Kounaves 2007). The electrochemical biosensor produces an electric signal with the interaction of the target analyte and biorecognition element. The electrochemical sensors are of low cost with high sensitivity. It can provide better target analyte information. Electrochemical biosensors can be biocatalytic and affinity-based. In biocatalytic, an enzyme is a sensing element with a catalytic reaction that produces an electric signal. In affinity-based, a selective binding interaction takes place between the analyte and the sensing element such as an antibodies, aptamer, or nucleic acid (Ameri et al. 2020).

3.3.2.4 Molecularly Imprinted Polymer-Based Sensor

The electrochemical sensor is developed for the determination of analyte with ion-exchange membrane, and polymer-modified electrodes with further modification in molecularly imprinted polymer-based sensors (MIPs) are now largely used by the researchers. MIP sensor has high selectivity for a particular analyte that can easily differentiate between analyte and interfering species, a biomolecule present, and the target molecule even at its highest concentration. In MIPs, the monomer interacts with the template, and the initiator is added to start the polymerization process. After polymerization, the template removal takes place, leaving behind the recognition sites (Li et al. 2009). The high stability and reusability of MIPs are the alternatives to biomolecule recognition of elements such as enzymes, antibodies, cell receptor, nucleic acid, and natural receptors. The lifetime of antibodies is 6–12 months and cannot be regenerated after ten cycles and may require refrigeration. MIPs can be stored at ambient temperature for years without a loss in affinity toward proteins and regenerated. MIPs can sustain a high temperature (up to 180 °C), while a biomolecule recognition element can sustain low temperature (below 40 °C). In the biochemical recognition, using elements such as antibodies, cell receptors, and nucleic acid have some inherent limitations like poor reproducibility and instability during the manufacturing process (Whitcombe et al. 2011).

3.4 Nanocarriers in Treatment of AD

Several types of nanocarriers like nanotubes, nanoparticles, nanogels, and nanofibers are available, which can enter through BBB owing to a high chemical, biological stability, and feasibility of allowing both hydrophobic and hydrophilic molecules (Re et al. 2012). Figure 3.3 lists a few nanocarriers tested to deliver drugs through BBB as in vivo and in vitro methods for treating AD. Nanoparticles and drugs used for the treatment of AD are listed in Table 3.6.

3.4.1 Carbon-Based Nanocarriers

3.4.1.1 Carbon Nanotubes

Carbon nanotubes (CNT) are hollow cylindrical sheets whose diameter is in the range of 1–10 nm. This is being used for drug delivery, diagnosis, imaging, tissue engineering, and cancer therapy. The MWCNTs have the potential to deliver a drug overcoming the BBB. Researchers have shown promising results for the drug berberine, loaded in MWCNTs and coated with phospholipid and polysorbate (overall particle size 186 nm) for the treatment of AD. The reported drug absorption and release time are 68.6% and 16 h respectively. This functionalized MWCNT also decreases the amyloid plaques accumulation into the brain (Bilal et al. 2020).

3.4.1.2 Carbon Dots

Carbon dots (CDs) are carbon-based nanoparticles whose size is 1–10 nm. CDs are nontoxic, high biocompatibility, and high photoluminescence. Their high surface to

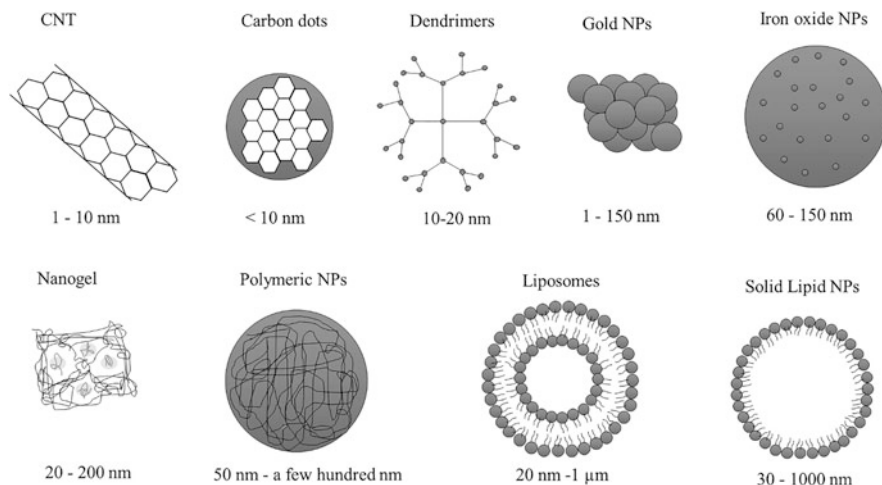


Fig. 3.3 A schematic depiction of the nanocarriers commonly used with drugs for the treatment of AD

volume ratio increases the drug loading capacity. Amphiphilic yellow-emissive CDs (Y-CDs) were developed of size 3 nm, which have hydrophilic and hydrophobic surfaces such that hydrophilic surfaces can inhibit the A β formation, while more hydrophobic functionalities help to cross the BBB through passive diffusion. Y-CDs inhibit APP production and A β fibrillation in the Chinese hamster ovary (CHO) cells (Zhou et al. 2019). CDs were functionalized with transferrin to cross the BBB as confirmed by CNS imaging in a zebrafish. The results were also confirmed by green fluorescent protein-labeled neurons (Ashrafizadeh et al. 2020).

3.4.1.3 Graphene Quantum Dots

Graphene quantum dots (GQD) can be a promising new nanocarrier for drug delivery due to the small size (18 nm), low cost, large specific surface area, high solubility, and nontoxic in both the in vivo and in vitro models. The peptide drug glycine-proline-glutamate conjugated GQD shows inhibition of A β plaques formation and improvement in learning and memory of transgenic mice having APP/PS1. The drug-conjugated GQD helps in the decrease in pro-inflammatory cytokines (IL-1 α , IL-1 β , IL-6, IL-33, IL-17 α , MIP-1 β , and TNF- α). It also helps to increase anti-inflammatory cytokines (IL-4, IL-10). These can stop A β aggregation and protect the synapses as confirmed by the Morris water maze test, immunohistochemical, ELISA, and suspension array (Xiao et al. 2016).

3.4.2 Dendrimers

Dendrimers of size 10–20 nm are highly branched molecules with an initial core, several internal layers, repetitive units, and terminal active surface groups, making

Table 3.6 Drugs delivered using nanocarrier for the treatment of AD

Target	Nanocarrier	Drug	Model	Effect	Refs.
A β	AuNPs	Intrahippocampal (IH) and intraperitoneal (IP) injections	Rat animal model	Improves learning and memory	Sanati et al. (2019)
A β 42	Bifunctionalized liposomes (mApoE-PA-Lipo) with ApoE peptides	Curcumin	APP23 transgenic mice	Decreases in A β 42	Ordóñez-Gutiérrez and Wandosell (2020)
A β 42	Polymeric NPs Coated with PLGA	Curcumin	Both in vitro and in vivo	Increases memory and learning	Gupta et al. (2019)
A β	MWCNTs with phospholipid and polysorbate	Berberine	In vivo	Decreases the amyloid plaques accumulation	Bilal et al. (2020)
A β	Carbon dots	Transferrin	Zebrafish	Inhibit the A β accumulation.	Ashrafizadeh et al. (2020)
ACh A β	Chitosan NPs	Galantamine hydrobromide (GH)	In vitro 5XFAD mice	Increases the nicotinic receptor sensitivity of ACh Decreases the plaque formation and the behavioral decline.	Hettiarachchi et al. (2019)
ACh	Chitosan NPs	Tacrine	In vitro	Inhibits the AChE levels in the cholinergic system and increase the ACh levels	Hettiarachchi et al. (2019)
ACh	Chitosan NPs	Piperine	In vivo animal model	Decrease the AChE and increase the ACh concentration	
ACh ACh	SLNPs SLNPs with polysorbate 80	Curcumin/donepezil Piperine	Mouse model Ibotenic acid-induced AD in mice	ACh levels were improved ACh levels were improved	Fonseca-Santos et al. (2015)
ACh	PAMAM dendrimers	Tacrine	In vivo	Inhibition of AChE	Igartúa et al. (2020)

(continued)

Table 3.6 (continued)

Target	Nanocarrier	Drug	Model	Effect	Refs.
ACh	Liposomes	Rivastigmine	Animal model	Increases the inhibition of Ache	Hadavi and Poot (2016)
OS	Liposomes	Quercetin	Animal model	Decreases oxidative stress	
OS	SLNPs	Lipoyl-memantine	Mouse N2a neuroblastoma	Decreases oxidative damage	Wen et al. (2017)

dendrimers used for drug delivery systems due to low dispersion, high performance, and hydrophobic core. Poly-amidoamine (PAMAM) and poly-propylene imine (PPI)-based dendrimers can be used for AD diagnosis, specific targets for drug delivery, and gene therapy. The challenges are the existing cytotoxic effect and inadequate BBB permeability. The polyester-copolyether dendrimers' (PEPE) structure and properties can overcome the issue of BBB permeability. PAMAM 3, 4, and 5 have hydrolytic properties, which can remove aggregated proteins on incubation with cells. This in turn can inhibit the A β aggregation. It may be due to dendrimers nanomolecules that may bind with A β or increase dissolution or lock the end of amyloid fibrils. Cationic phosphorus dendrimers (CPDs) also show the disruption in A β fibrils and aggregation of other proteins and inhibit the aggregation of MAP-tau (microtubule-associated protein). CPDs also show some qualities like anti-inflammatory process, stop hydrolysis of ACh, and inhibit ROS forming (Aliev et al. 2018).

3.4.3 Nanoparticles

Different nanoparticles have been developed to diagnose and treat AD, which differentiate each other by composition and diagnosis that aim to detect and visualize the pathologies. The fluorescent dye thioflavin-T (ThT) is mostly used in both in vivo and in vitro to detect A β , which emits fluorescence when binds with amyloid fibrils, and mainly Nps are used for therapeutic purposes in the clinics. The disadvantage of ThT is its low permeation through the BBB owing to its hydrophilicity. ThT-loaded nanocapsules containing polybutylcyanoacrylate were introduced in achieving high permeation through BBB. The curcumin-loaded NPs can bind with tau protein and A β in both in vivo and in vitro and inhibit the tau hyperphosphorylation. However, it is easily oxidized, photodegraded, and has poor stability due to hydrolysis in acidic and alkaline medium. New efforts are developed using curcumin-loaded polybutylcyanoacrylate (PBCA). PBCA NPs can increase the half-life of curcumin and concentration in the mice brain as compared to free curcumin. In contrast, curcumin-loaded poly(lactide-*co*-glycolide) (PLGA) NPs may reverse the memory and learning declined by A β . NPs loaded with the iron chelators and copper chelators are applied to remove the brain's metal ions to decrease oxidative stress, but limitations are hepatotoxicity and low transference across the BBB. The development of chelator such as 2-methyl-*N*-(2'-aminoethyl)-3-hydroxyl-4-pyridinone (MAEHP) is conjugated with NPs and have a high affinity toward iron, aluminum, copper, and zinc. In vitro, it inhibits the A β aggregate formation. Clioquinol or 5-chloro-7-iodo-8-hydroxyquinoline (CQ), a metal chelator, can be solubilized and inhibits A β accumulation in vitro, and CQ-loaded PBCA nanoparticles can cross the BBB at a higher threshold and can be used for the treatment of AD (Gupta et al. 2019).

3.4.3.1 Gold Nanoparticles

Gold nanoparticles (AuNPs) are used in drug delivery since their size varies from 1 to 150 nm, which helps control their dispersion and has SPR, optical, and tunable properties. AuNPs can be functionalized using drugs, targeting ligands and genes, because a negative charge on the surface helps in the modification (Singh et al. 2018). The negatively charged AuNPs can adsorb the A β monomers, which inhibit the A β fibrillation process, and dissociates A β formed in vitro. However, in vivo, its effect on progressive cognitive decline and memory is poorly investigated. After intrahippocampal (IH) and intraperitoneal (IP) injections of AuNPs in a rat animal model of AD shows that AuNPs have improved the acquisition and retention of spatial learning and memory in A β (Sanati et al. 2019).

3.4.3.2 Iron Oxide Nanoparticles

Iron oxide nanoparticles (Fe₃O₄ NPs) of size 60–150 nm conjugated with A β oligomer aptamer can measure the A β oligomer in the artificial CSF. Superparamagnetic iron oxide nanoparticles (SPIONs) with 1,1-dicyano-2-[6-(dimethylamino) naphthalene-2-yl] propene (DDNP) have a high binding affinity toward A β 40 aggregates. The amyloid imaging is done through injection of DDNP-SPIONs in the hippocampal area of brain of the tested rat. This leads to the binding of DDNP-SPIONs to the A β plaques. Due to this binding, a significant decrease in the signal intensity was reported in coronal T2*-weighted images in MRI. The amyloid imaging is also reported using natural drug curcumin in conjugation with superparamagnetic iron oxides (SPIOs). γ -Fe₂O₃ NPs can inhibit the microglial cells in rTg4510 tau-mutant mice, and SPIONs coated with poly(ethylene glycol) methyl ether amine (PEG-NH₂) can decrease the A β aggregation (Luo et al. 2020).

3.4.3.3 Nanogels and Polymeric Nanoparticles

Nanogels of size 20–200 nm are the nanosized polymer network. They have both hydrogels and NPs characteristics, which make them useful for specific drug delivery systems. Nanogels have the advantage of having a high loading capacity (40–60%), which is difficult for NPs (Saeedi et al. 2019).

The size range of Polymeric nanoparticles varies from 50 nm to a few hundred nanometers. The loading of drugs can be done through different methods such as surface adsorption, chemical conjugation, and encapsulation. Chitosan NPs loaded with tacrine and galantamine hydrobromide (GH) are mostly used to target the cholinergic system to inhibit the AChE and increase the ACh levels. GH-containing chitosan NPs bind with nicotinic receptors and increase the receptor sensitivity of ACh. Synthetic polymeric NPs are mainly colloidal particles tuned to lipophilicity, charge, and biocompatibility in the synthetic process, and they have low toxicity and high loading drug capacity. Synthetic polymeric NPs coated with polylactide-*co*-glycolide (PLGA), polyethylene glycol (PEG)-phospholipid copolymers, and PEGylated are investigated for AD treatment. PEGylated polymeric NPs can prevent A β aggregation in the brain. polyethylene glycol-polylactic acid (PEG-PLA) NPs can penetrate the BBB. Its efficiency in the clearance of A β peptides was tested in an AD mouse model (Hettiarachchi et al. 2019).

3.4.4 Liposomes and Lipid NPs

Liposomes are vesicles consisting of single or multiple lipid bilayers around the inner aqueous compartment and are categorized as unilamellar and multilamellar, respectively. These are used as carriers of lipophilic or hydrophilic drugs. The size of liposomes is classified based on lamellar sizes. These are as follows: small unilamellar vesicles (20–100 nm), large unilamellar vesicles (>100 nm), giant unilamellar vesicles (~1 μm), oligolamellar vesicles (0.1–1 μm), and multilamellar vesicles (~500 nm) (Fonseca-Santos et al. 2015). Liposomes can carry bioactive molecules inside or outside the particle owing to a highly flexible and biocompatible drug delivery system. The nontargeted liposomes transfer the compounds directly. The targeted liposomes are designed according to interaction with specific targets related to AD's diagnosis and treatment. Liposomes with phosphatidic acid (PA) and cardiolipin can reduce A β levels in APP/PS1 transgenic mice. NPs of poly(lactide-co-glycolide)-poly(ethylene glycol) conjugated with curcumin derivate (PLGA-PEG-B6/Cur) can increase the learning and memory in APP/PS1 transgenic mice. The bifunctionalized liposomes (mApoE-PA-Lipo) with ApoE peptides show a decrease in A β 42 in APP23 transgenic mice confirmed by PET imaging with [^{11}C] Pittsburgh compound B (PIB) (Ordóñez-Gutiérrez and Wandosell 2020).

Lipid NPs of size 30–1000 nm consists of solid lipid NPs (SLNs) and nanostructured lipid carriers (NLCs). Lipid NPs exhibits low toxicity, drug entrapment, prolonged drug release, and high stability. The limitation is that incorporating a drug into SLNs and NLCs depends on lipophilic character, type of lipids, and surfactants. Lipoyl-memantine drug loaded with SLNs shows a decrease in oxidative damage and increases antioxidant capacity in mouse N2a neuroblastoma. Also, ferulic acid was incorporated in SLNs and NLCs, decreasing oxidative stress (Wen et al. 2017).

3.5 Conclusion and Future Strategies

The existing techniques can detect AD biomarkers using brain imaging techniques (MRI, PET, CT, SPECT, IHC, etc.) and fluid-based biomarker techniques (ELISA, xMAP, WB, MS-methods, etc.). These techniques are expensive, tedious, and require highly skilled personnel. Often, the low sensitivity and specificity of methods lead to the scientist finding alternative tools for detection. The concentration level of AD biomarkers is much higher in CSF. The collection of samples from blood, urine, and saliva are noninvasive processes. AD biomarkers detection in the blood is the best alternative to avoid the lumbar puncture process in CSF. There are variations in concentration levels of AD biomarkers in blood since standard calibration methods are still not developed.

The nanomaterials on a surface improve immobilization of biorecognition elements. Further development in MIP-based sensors such as MIP/analyte/nanocomposite-modified GCE can be a promising biosensor in detecting AD biomarkers to detect a low concentration accurately.

Bio-barcode assay, superparamagnetic iron oxide NPs with DDNP as a contrast agent in MRI, AuNPs in (LSPR, TPRS) and carbon NPs (CNT, graphene), and AuNPs in situ polymerization in MIP sensor can be the best alternatives to replace available detection techniques.

Using nanocarriers conjugated with a drug can have a high permeability. Thus the drug can pass through BBB. The bi-functionalized liposomes mApoE-PA-Lipo, liposomes with phosphatidic acid (PA), and cardiolipin can reduce the A β levels. Poly-amidoamine (PAMAM)-based dendrimers can inhibit the A β and remove the toxicity of aggregated proteins. However, it has a poor property to cross BBB. Polyester-copolyether dendrimers (PEPE) were reported to have better BBB permeability. Nanoparticles-based drug delivery using a carrier such as (PEG-PLA) NPs, PBCA NPs, and poly (lactide-*co*-glycolide) (PLGA) NPs can be the best alternatives to cross the BBB and target the specific AD biomarkers for treatment. The nanocarriers' size should be optimized to have high drug loading capacity and sufficiently high diffusion to overcome BBB.

References

- Ahmad J, Akhter S, Rizwanullah M, Khan MA, Pigeon L, Addo RT, Greig NH, Midoux P, Pichon C, Kamal MA (2017) Nanotechnology based theranostic approaches in Alzheimer's disease management: current status and future perspective. *Curr Alzheimer Res* 14:1164–1181. <https://doi.org/10.2174/1567205014666170508121031>
- Aliev G, Ashraf GM, Tarasov VV, Chubarev VN, Leszek J, Gasiorowski K, Makhmutova A, Baeesa SS, Avila-Rodriguez M, Ustyugov AA, Bachurin SO (2018) Alzheimer's disease – future therapy based on dendrimers. *Curr Neuropharmacol* 17:288–294. <https://doi.org/10.2174/1570159x16666180918164623>
- Altuna-Azkargorta M, Mendioroz-Iriarte M (2020) Blood biomarkers in Alzheimer's disease. *Neurology (English Ed.)* 80:578–606. <https://doi.org/10.1016/j.nrleng.2018.03.006>
- Álvarez A, Cacabelos R, Sanpedro C, García-Fantini M, Aleixandre M (2007) Serum TNF-alpha levels are increased and correlate negatively with free IGF-I in Alzheimer disease. *Neurobiol Aging* 28:533–536. <https://doi.org/10.1016/j.neurobiolaging.2006.02.012>
- Ameri M, Shabaninejad Z, Movahedpour A, Sahebkar A, Mohammadi S, Hosseindoost S, Ebrahimi MS, Savardashtaki A, Karimipour M, Mirzaei H (2020) Biosensors for detection of tau protein as an Alzheimer's disease marker. *Int J Biol Macromol* 162:1100–1108. <https://doi.org/10.1016/j.ijbiomac.2020.06.239>
- Anastasio TJ (2011) Data-driven modeling of Alzheimer disease pathogenesis. *J Theor Biol* 290:60–72. <https://doi.org/10.1016/j.jtbi.2011.08.038>
- Andreadis A (2012) Tau splicing and the intricacies of dementia. *J Cell Physiol* 227:1220–1225. <https://doi.org/10.1002/jcp.22842>
- Ashrafizadeh M, Mohammadinejad R, Kailasa SK, Ahmadi Z, Afshar EG, Pardakhty A (2020) Carbon dots as versatile nanoarchitectures for the treatment of neurological disorders and their theranostic applications: a review. *Adv Colloid Interf Sci* 278:1–12. <https://doi.org/10.1016/j.cis.2020.102123>
- Ashton NJ, Ide M, Zetterberg H, Blennow K (2019) Salivary biomarkers for Alzheimer's disease and related disorders. *Neurol Ther* 8:83–94. <https://doi.org/10.1007/s40120-019-00168-1>
- Aydın EB, Aydın M, Sezgintürk MK (2017) A highly sensitive immunosensor based on ITO thin films covered by a new semi-conductive conjugated polymer for the determination of TNF α in human saliva and serum samples. *Biosens Bioelectron* 97:169–176. <https://doi.org/10.1016/j.bios.2017.05.056>

- Bacskaï BJ, Skoch J, Hickey GA, Allen R, Hyman BT (2003) Fluorescence resonance energy transfer determinations using multiphoton fluorescence lifetime imaging microscopy to characterize amyloid-beta plaques. *J Biomed Opt* 8:368. <https://doi.org/10.1117/1.1584442>
- Barthélemy NR, Bateman RJ, Hirtz C, Marin P, Becher F, Sato C, Gabelle A, Lehmann S (2020) Cerebrospinal fluid phospho-tau T217 outperforms T181 as a biomarker for the differential diagnosis of Alzheimer's disease and PET amyloid-positive patient identification. *Alzheimers Res Ther* 12:26. <https://doi.org/10.1186/s13195-020-00596-4>
- Batra B, Pundir CS (2013) An amperometric glutamate biosensor based on immobilization of glutamate oxidase onto carboxylated multiwalled carbon nanotubes/gold nanoparticles/chitosan composite film modified Au electrode. *Sensens Bioelectron* 47:496–501. <https://doi.org/10.1016/j.bios.2013.03.063>
- Baydemir G, Bettazzi F, Palchetti I, Voccia D (2016) Strategies for the development of an electrochemical bioassay for TNF-alpha detection by using a non-immunoglobulin bioreceptor. *Talanta* 151:141–147. <https://doi.org/10.1016/j.talanta.2016.01.021>
- Bermejo-Pareja F, Antequera D, Vargas T, Molina JA, Carro E (2010) Saliva levels of Abeta1-42 as potential biomarker of Alzheimer's disease: a pilot study. *BMC Neurol* 10:108. <https://doi.org/10.1186/1471-2377-10-108>
- Biasutti M, Dufour N, Ferroud C, Dab W, Temime L (2012) Cost-effectiveness of magnetic resonance imaging with a new contrast agent for the early diagnosis of Alzheimer's disease. *PLoS One* 7:e35559. <https://doi.org/10.1371/journal.pone.0035559>
- Bilal M, Barani M, Sabir F, Rahdar A, Kyzas GZ (2020) NanoImpact nanomaterials for the treatment and diagnosis of Alzheimer's disease : an overview. *NanoImpact* 20:100251. <https://doi.org/10.1016/j.impact.2020.100251>
- Blennow K, Hampel H, Weiner M, Zetterberg H (2010) Cerebrospinal fluid and plasma biomarkers in Alzheimer disease. *Nat Rev Neurol* 6:131–144. <https://doi.org/10.1038/nrneurol.2010.4>
- Blennow K, Mattsson N, Schöll M, Hansson O, Zetterberg H (2015) Amyloid biomarkers in Alzheimer's disease. *Trends Pharmacol Sci* 36:297–309. <https://doi.org/10.1016/j.tips.2015.03.002>
- Bongaerts J, De Bundel D, Mangelings D, Smolders I, Vander Heyden Y, Van Eeckhaut A (2018) Sensitive targeted methods for brain metabolomic studies in microdialysis samples. *J Pharm Biomed Anal* 161:192–205. <https://doi.org/10.1016/j.jpba.2018.08.043>
- Butzlaff M, Ponimaskin E (2016) The role of serotonin receptors in Alzheimer's disease. *Opera Medica Physiol* 2:77–86
- Carneiro P, Morais S, Pereira MC (2019) Nanomaterials towards biosensing of Alzheimer's disease biomarkers'. *Nanomaterials* 9(12):1663. <https://doi.org/10.3390/nano9121663>
- Cervellati C, Trentini A, Rosta V, Passaro A, Bosi C, Sanz JM, Bonazzi S, Pacifico S, Seripa D, Valacchi G, Guerini R, Zuliani G (2020) Serum beta-secretase 1 (BACE1) activity as candidate biomarker for late-onset Alzheimer's disease. *GeroScience* 42:159–167. <https://doi.org/10.1007/s11357-019-00127-6>
- Chauhan N, Chawla S, Pundir CS, Jain U (2017) An electrochemical sensor for detection of neurotransmitter-acetylcholine using metal nanoparticles, 2D material and conducting polymer modified electrode. *Sensens Bioelectron* 89:377–383. <https://doi.org/10.1016/j.bios.2016.06.047>
- Chen J-H, Ke K-F, Lu J-H, Qiu Y-H, Peng Y-P (2015) Protection of TGF-β1 against neuroinflammation and neurodegeneration in Aβ1-42-induced Alzheimer's disease model rats. *PLoS One* 10:e0116549. <https://doi.org/10.1371/journal.pone.0116549>
- Cheng M, Cuda G, Bunimovich Y, Gaspari M, Heath J, Hill H, Mirkin C, Nijdam A, Terracciano R, Thundat T (2006) Nanotechnologies for biomolecular detection and medical diagnostics. *Curr Opin Chem Biol* 10:11–19. <https://doi.org/10.1016/j.cbpa.2006.01.006>
- Choi JW, Kamrul Isram ATM, Lee JH, Jung M, Oh BK (2011) Nano-protein array to detect β-amyloid (1-42) using scanning tunneling microscopy. *Sens Lett* 9:828–831. <https://doi.org/10.1166/sl.2011.1624>

- Chuo LJ, Sheu WHH, Pai MC, Kuo YM (2007) Genotype and plasma concentration of cystatin C in patients with late-onset Alzheimer disease. *Dement Geriatr Cogn Disord* 23:251–257. <https://doi.org/10.1159/000100021>
- Cole SL, Vassar R (2007) The Alzheimer's disease Beta-secretase enzyme, BACE1. *Mol Neurodegener* 2:22. <https://doi.org/10.1186/1750-1326-2-22>
- Davidson JE, Lockhart A, Amos L, Stirnadel-Farrant HA, Mooser V, Sollberger M, Regeniter A, Monsch AU, Irizarry MC (2012) Plasma lipoprotein-associated phospholipase A2 activity in Alzheimer's disease, amnesic mild cognitive impairment, and cognitively healthy elderly subjects: a cross-sectional study. *Alzheimers Res Ther* 4:1–3. <https://doi.org/10.1186/alzrt154>
- Di Luca M, Grossi E, Borroni B, Zimmermann M, Marcello E, Colciaghi F, Gardoni F, Intraligi M, Padovani A, Buscema M (2005) Artificial neural networks allow the use of simultaneous measurements of Alzheimer disease markers for early detection of the disease. *J Transl Med* 3:30. <https://doi.org/10.1186/1479-5876-3-30>
- Dieplinger H, Dieplinger B (2015) Afamin - a pleiotropic glycoprotein involved in various disease states. *Clin Chim Acta* 446:105–110. <https://doi.org/10.1016/j.cca.2015.04.010>
- ELSHAL M, MCCOY J (2006) Multiplex bead array assays: performance evaluation and comparison of sensitivity to ELISA. *Methods* 38:317–323. <https://doi.org/10.1016/j.ymeth.2005.11.010>
- Ferreira-Vieira TH, Guimaraes IM, Silva FR, Ribeiro FM (2016) Alzheimer's disease: targeting the cholinergic system. *Curr Neuropharmacol* 14:101–115. <https://doi.org/10.2174/1570159X13666150716165726>
- Fonseca-Santos B, Gremião MPD, Chorilli M (2015) Nanotechnology-based drug delivery systems for the treatment of Alzheimer's disease. *Int J Nanomedicine* 10:4981–5003. <https://doi.org/10.2147/IJN.S87148>
- Fraser PE, Yang D-S, Yu G, Lévesque L, Nishimura M, Arawaka S, Serpell LC, Rogueva E, St George-Hyslop P (2000) Presenilin structure, function and role in Alzheimer disease. *Biochim Biophys Acta Mol basis Dis* 1502:1–15. [https://doi.org/10.1016/S0925-4439\(00\)00028-4](https://doi.org/10.1016/S0925-4439(00)00028-4)
- Fujii T, Yamada S, Yamaguchi N, Fujimoto K, Suzuki T, Kawashima K (1995) Species differences in the concentration of acetylcholine, a neurotransmitter, in whole blood and plasma. *Neurosci Lett* 201:207–210. [https://doi.org/10.1016/0304-3940\(95\)12180-3](https://doi.org/10.1016/0304-3940(95)12180-3)
- García-Chamé M-Á, Gutiérrez-Sanz Ó, Ercan-Herbst E, Hausstein N, Filipiak MS, Ehrnhöfer DE, Tarasov A (2020) A transistor-based label-free immunosensor for rapid detection of tau protein. *Biosens Bioelectron* 159:112129. <https://doi.org/10.1016/j.bios.2020.112129>
- Georganopoulou DG, Chang L, Nam J-M, Thaxton CS, Mufson EJ, Klein WL, Mirkin CA (2005) From the cover: nanoparticle-based detection in cerebral spinal fluid of a soluble pathogenic biomarker for Alzheimer's disease. *Proc Natl Acad Sci* 102:2273–2276. <https://doi.org/10.1073/pnas.0409336102>
- Gezen-Ak D, Dursun E, Hanağasi H, Bilgiç B, Lohman E, Araz ÖS, Atasoy IL, Alaylioğlu M, Önal B, Gürvit H, Yilmazer S (2013) BDNF, TNF α , HSP90, CFH, and IL-10 serum levels in patients with early or late onset Alzheimer's disease or mild cognitive impairment. *J Alzheimers Dis* 37:185–195. <https://doi.org/10.3233/JAD-130497>
- Ghosh R, Gilda JE, Gomes AV (2014) The necessity of and strategies for improving confidence in the accuracy of western blots. *Expert Rev Proteomics* 11:549–560. <https://doi.org/10.1586/14789450.2014.939635>
- Gong N-J, Dibb R, Bulk M, van der Weerd L, Liu C (2019) Imaging beta amyloid aggregation and iron accumulation in Alzheimer's disease using quantitative susceptibility mapping MRI. *NeuroImage* 191:176–185. <https://doi.org/10.1016/j.neuroimage.2019.02.019>
- Gupta J, Fatima MT, Islam Z, Khan RH, Uversky VN, Salahuddin P (2019) Nanoparticle formulations in the diagnosis and therapy of Alzheimer's disease. *Int J Biol Macromol* 130:515–526. <https://doi.org/10.1016/j.ijbiomac.2019.02.156>
- Hadavi D, Poot AA (2016) Biomaterials for the treatment of Alzheimer's disease. *Front Bioeng Biotechnol* 4:49. <https://doi.org/10.3389/fbioe.2016.00049>
- Hao W, Friedman A (2016) Mathematical model on Alzheimer's disease. *BMC Syst Biol* 10:1–18. <https://doi.org/10.1186/s12918-016-0348-2>

- Hettiarachchi SD, Zhou Y, Seven E, Lakshmana MK, Kaushik AK, Chand HS, Leblanc RM (2019) Nanoparticle-mediated approaches for Alzheimer's disease pathogenesis, diagnosis, and therapeutics. *J Control Release* 314:125–140. <https://doi.org/10.1016/j.jconrel.2019.10.034>
- Hrubešová K, Fousková M, Habartová L, Fišar Z, Jiráček R, Raboch J, Setnička V (2019) Search for biomarkers of Alzheimer's disease: recent insights, current challenges and future prospects. *Clin Biochem* 72:39–51. <https://doi.org/10.1016/j.clinbiochem.2019.04.002>
- Humpel C (2011) Identifying and validating biomarkers for Alzheimer's disease. *Trends Biotechnol* 29:26–32. <https://doi.org/10.1016/j.tibtech.2010.09.007>
- Igartúa DE, Martínez CS, del V Alonso S, Prieto MJ (2020) Combined therapy for Alzheimer's disease: tacrine and PAMAM dendrimers co-administration reduces the side effects of the drug without modifying its activity. *AAPS PharmSciTech* 21:1–14. <https://doi.org/10.1208/s12249-020-01652-w>
- Jain U, Khanuja M, Gupta S, Harikumar A, Chauhan N (2019) Pd nanoparticles and molybdenum disulfide (MoS₂) integrated sensing platform for the detection of neuromodulator. *Process Biochem* 81:48–56. <https://doi.org/10.1016/j.procbio.2019.03.019>
- Janel N, Sarazin M, Corlier F, Corne H, De Souza LC, Hamelin L, Aka A, Lagarde J, Blehaut H, Hindié V, Rain JC, Arbones ML, Dubois B, Potier MC, Bottlaender M, Delabar JM (2011) Plasma DYRK1A as a novel risk factor for Alzheimer's disease. *Transl Psychiatry* 4:e425. <https://doi.org/10.1038/tp.2014.61>
- Jia J-P, Jia J-M, Zhou W, Xu M, Chu C, Yan X, Sun Y (2004) Differential acetylcholine and choline concentrations in the cerebrospinal fluid of patients with Alzheimer's disease and vascular dementia. *Chin Med J* 117:1161–1164
- Jianrong C, Yuqing M, Nongyue H, Xiaohua W, Sijiao L (2004) Nanotechnology and biosensors. *Biotechnol Adv* 22:505–518. <https://doi.org/10.1016/j.biotechadv.2004.03.004>
- Johnson KA, Fox NC, Sperling RA, Klunk WE (2012) Brain imaging in Alzheimer disease. *Cold Spring Harb Perspect Med* 2:a006213–a006213. <https://doi.org/10.1101/cshperspect.a006213>
- Jun YW, Cho SW, Jung J, Huh Y, Kim Y, Kim D, Ahn KH (2019) Frontiers in probing Alzheimer's disease biomarkers with fluorescent Small molecules. *ACS Cent Sci* 5:209–217. <https://doi.org/10.1021/acscentsci.8b00951>
- Kai H, Shin R-W, Ogino K, Hatsuta H, Murayama S, Kitamoto T (2012) Enhanced antigen retrieval of amyloid β immunohistochemistry. *J Histochem Cytochem* 60:761–769. <https://doi.org/10.1369/0022155412456379>
- Kamel AH, Al FA, Soror TY, Galal HR (2016) Solid contact biosensor based on man-tailored polymers for acetylcholine detection : application to acetylcholinesterase solid contact biosensor based on man-tailored polymers for acetylcholine detection : application to acetylcholinesterase assay. *Eur Chem Bull* 5(7):266–273. <https://doi.org/10.17628/ecb.2016.5.266>
- Kang J-H, Vanderstichele H, Trojanowski JQ, Shaw LM (2012) Simultaneous analysis of cerebrospinal fluid biomarkers using microsphere-based xMAP multiplex technology for early detection of Alzheimer's disease. *Methods* 56:484–493. <https://doi.org/10.1016/j.ymeth.2012.03.023>
- Kang J-H, Korecka M, Toledo JB, Trojanowski JQ, Shaw LM (2013) Clinical utility and analytical challenges in measurement of cerebrospinal fluid amyloid- β 1–42 and τ proteins as Alzheimer disease biomarkers. *Clin Chem* 59:903–916. <https://doi.org/10.1373/clinchem.2013.202937>
- Killick R, Lunnon K, Lynham S, Broadstock M (2020) Association of plasma clusterin concentration with severity, pathology, and progression in Alzheimer disease. *Arch Gen Psychiatry* 67:739–748
- Kim J, Basak JM, Holtzman DM (2009) The role of apolipoprotein E in Alzheimer's disease. *Neuron* 63:287–303. <https://doi.org/10.1016/j.neuron.2009.06.026>
- Kim H, Lee JU, Song S, Kim S, Sim SJ (2018) A shape-code nanoplasmonic biosensor for multiplex detection of Alzheimer's disease biomarkers. *Biosens Bioelectron* 101:96–102. <https://doi.org/10.1016/j.bios.2017.10.018>
- Kounaves SP (2007) Voltammetric techniques, in: inorganic electrochemistry. Royal Society of Chemistry, Cambridge, pp 49–136. <https://doi.org/10.1039/9781847551146-00049>

- Krzystanek E, Krzystanek M, Opala G, Trzeciak HI, Siuda J, Małeckı A (2007) Platelet phospholipase A2 activity in patients with Alzheimer's disease, vascular dementia and ischemic stroke. *J Neural Transm* 114:1033–1039. <https://doi.org/10.1007/s00702-007-0669-9>
- Lancôt KL, Herrmann N, Rothenburg L, Eryavec G (2007) Behavioral correlates of GABAergic disruption in Alzheimer's disease. *Int Psychogeriatrics* 19:151. <https://doi.org/10.1017/S1041610206003899>
- Lee JH, Kang DY, Kim SU, Yea CH, Oh BK, Choi JW (2009) Electrical detection of β -amyloid (1-40) using scanning tunneling microscopy. *Ultramicroscopy* 109:923–928. <https://doi.org/10.1016/j.ultramicro.2009.03.009>
- Li J, Zhao J, Wei X (2009) A sensitive and selective sensor for dopamine determination based on a molecularly imprinted electropolymer of o-aminophenol. *Sensors Actuators B Chem* 140:663–669. <https://doi.org/10.1016/j.snb.2009.04.067>
- Liang D, Lu H (2019) Salivary biological biomarkers for Alzheimer's disease. *Arch Oral Biol* 105:5–12. <https://doi.org/10.1016/j.archoralbio.2019.06.004>
- Lin RC, Miller BA, Kelly TJ (1995) Concentrations of apolipoprotein AI, AII, and E in plasma and lipoprotein fractions of alcoholic patients: gender differences in the effects of alcohol. *Hepatology* 21:942–949. [https://doi.org/10.1016/0270-9139\(95\)90238-4](https://doi.org/10.1016/0270-9139(95)90238-4)
- Lista S, Faltraco F, Prvulovic D, Hampel H (2013) Blood and plasma-based proteomic biomarker research in Alzheimer's disease. *Prog Neurobiol* 101–102:1–17. <https://doi.org/10.1016/j.pneurobio.2012.06.007>
- Liu Y, Qing H, Deng Y (2014) Biomarkers in Alzheimer's disease analysis by mass spectrometry-based proteomics. *Int J Mol Sci* 15:7865–7882. <https://doi.org/10.3390/ijms15057865>
- Liu P-P, Xie Y, Meng X-Y, Kang J-S (2019) Author correction: history and progress of hypotheses and clinical trials for Alzheimer's disease. *Signal Transduct Target Ther* 4:37. <https://doi.org/10.1038/s41392-019-0071-8>
- Llorens-Martín M, Jurado J, Hernández F, Ávila J (2014) GSK-3 β , a pivotal kinase in Alzheimer disease. *Front Mol Neurosci* 7:1–11. <https://doi.org/10.3389/fnmol.2014.00046>
- Lue LF, Guerra A, Walker DG (2017) Amyloid beta and tau as Alzheimer's disease blood biomarkers: promise from new technologies. *Neurol Ther* 6:25–36. <https://doi.org/10.1007/s40120-017-0074-8>
- Luo X, Davis JJ (2013) Electrical biosensors and the label free detection of protein disease biomarkers. *Chem Soc Rev* 42:5944–5962. <https://doi.org/10.1039/c3cs60077g>
- Luo S, Ma C, Zhu MQ, Ju WN, Yang Y, Wang X (2020) Application of iron oxide nanoparticles in the diagnosis and treatment of neurodegenerative diseases with emphasis on Alzheimer's disease. *Front Cell Neurosci* 14:1–11. <https://doi.org/10.3389/fncel.2020.00021>
- Ly TN, Park S (2020) High performance detection of Alzheimer's disease biomarkers based on localized surface plasmon resonance. *J Ind Eng Chem* 91:182–190. <https://doi.org/10.1016/j.jiec.2020.07.051>
- Madeira C, Vargas-Lopes C, Brandão CO, Reis T, Laks J, Panizzutti R, Ferreira ST (2018) Elevated glutamate and glutamine levels in the cerebrospinal fluid of patients with probable Alzheimer's disease and depression. *Front Psych* 9:1–8. <https://doi.org/10.3389/fpsy.2018.00561>
- Maes OC, Kravitz S, Mawal Y, Su H, Liberman A, Mehindate K, Berlin D, Sahlas DJ, Chertkow HM, Bergman H (2006) Characterization of α 1-antitrypsin as a heme oxygenase-1 suppressor in Alzheimer plasma. *Neurobiol Dis* 24:89–100. <https://doi.org/10.1016/j.nbd.2006.06.009>
- Maity D, Kumar RTR (2019) Highly sensitive amperometric detection of glutamate by glutamic oxidase immobilized Pt nanoparticle decorated multiwalled carbon nanotubes(MWCNTs)/ polypyrrole composite. *Biosens Bioelectron* 130:307–314. <https://doi.org/10.1016/j.bios.2019.02.001>
- Manoharan S, Guillemin GJ, Abiramasundari RS, Essa MM, Akbar M, Akbar MD (2016) The role of reactive oxygen species in the pathogenesis of Alzheimer's disease, Parkinson's disease, and Huntington's disease: a mini review. *Oxidative Med Cell Longev* 2016:1–15. <https://doi.org/10.1155/2016/8590578>

- Manolov V (2017) The role of Iron homeostasis in Alzheimer's disease. *Alzheimer's Neurodegener Dis* 3:1–4. <https://doi.org/10.24966/and-9608/100011>
- Márquez F, Yassa MA (2019) Neuroimaging biomarkers for Alzheimer's disease. *Mol Neurodegener* 14:21. <https://doi.org/10.1186/s13024-019-0325-5>
- Mars A, Hamami M, Bechnak L, Patra D, Raouafi N (2018) Curcumin-graphene quantum dots for dual mode sensing platform: electrochemical and fluorescence detection of APOe4, responsible of Alzheimer's disease. *Anal Chim Acta* 1036:141–146. <https://doi.org/10.1016/j.aca.2018.06.075>
- Mattsson N, Andreasson U, Zetterberg H, Blennow K (2017) Association of plasma neurofilament light with neurodegeneration in patients with Alzheimer disease. *JAMA Neurol* 74:557. <https://doi.org/10.1001/jamaneurol.2016.6117>
- Matuschek L, Göbel G, Lisdat F (2017) Electrochemical detection of serotonin in the presence of 5-hydroxyindoleacetic acid and ascorbic acid by use of 3D ITO electrodes. *Electrochem Commun* 81:145–149. <https://doi.org/10.1016/j.elecom.2017.07.003>
- McGrath LT, McGleenon BM, Brennan S, McColl D, McIlroy S, Passmore AP (2001) Increased oxidative stress in Alzheimer's disease as assessed with 4-hydroxynonenal but not malondialdehyde. *QJM* 94:485–490. <https://doi.org/10.1093/qjmed/94.9.485>
- Michalowsky B, Flessa S, Hertel J, Goetz O, Hoffmann W, Teipel S, Kilimann I (2017) Cost of diagnosing dementia in a German memory clinic. *Alzheimers Res Ther* 9:1–10. <https://doi.org/10.1186/s13195-017-0290-6>
- Mitchell RA, Herrmann N, Lanctôt KL (2011) The role of dopamine in symptoms and treatment of apathy in Alzheimer's disease. *CNS Neurosci Ther* 17:411–427. <https://doi.org/10.1111/j.1755-5949.2010.00161.x>
- Miulli DE, Norwell DY, Schwartz FN (1993) Plasma concentrations of glutamate and its metabolites in patients with Alzheimer's disease. *J Am Osteopath Assoc* 93:670–676. <https://doi.org/10.7556/jaoa.1993.93.6.670>
- Mohsenzadegan M, Mirshafiey A (2012) The immunopathogenic role of reactive oxygen species in Alzheimer disease. *Iran J Allergy Asthma Immunol* 11:203–216. <https://ijaai.tums.ac.ir/index.php/ijaai/article/view/561aai.203216>
- Monte SM, Ghanbari K, Frey WH, Beheshti I, Averbach P, Hauser SL, Ghanbari HA, Wands JR (1997) Characterization of the AD7C-NTP cDNA expression in Alzheimer's disease and measurement of a 41-kD protein in cerebrospinal fluid. *J Clin Invest* 100:3093–3104. <https://doi.org/10.1172/JCI119864>
- Moreira FTC, Sale MGF, Di Lorenzo M (2017) Towards timely Alzheimer diagnosis: a self-powered amperometric biosensor for the neurotransmitter acetylcholine. *Biosens Bioelectron* 87:607–614. <https://doi.org/10.1016/j.bios.2016.08.104>
- Muck-Seler D, Presecki P, Mimica N, Mustapic M, Pivac N, Babic A, Nedic G, Folnegovic-Smalc V (2009) Platelet serotonin concentration and monoamine oxidase type B activity in female patients in early, middle and late phase of Alzheimer's disease. *Prog Neuropsychopharmacol Biol Psychiatry* 33:1226–1231. <https://doi.org/10.1016/j.pnpbp.2009.07.004>
- Mulder C, Verwey NA, van der Flier WM, Bouwman FH, Kok A, van Elk EJ, Scheltens P, Blankenstein MA (2010) Amyloid- β (1–42), total tau, and phosphorylated tau as cerebrospinal fluid biomarkers for the diagnosis of Alzheimer disease. *Clin Chem* 56:248–253. <https://doi.org/10.1373/clinchem.2009.130518>
- Narayanan L, Murray AD (2016) What can imaging tell us about cognitive impairment and dementia? *World J Radiol* 8:240. <https://doi.org/10.4329/wjr.v8.i3.240>
- Nazem A, Mansoori GA (2011) Nanotechnology for Alzheimer's disease detection and treatment. *Insciences J* 1:169–193. <https://doi.org/10.5640/insc.0104169>
- Neely A, Perry C, Varisli B, Singh AK, Arbneshi T, Senapati D, Kalluri JR, Ray PC (2009) Ultrasensitive and highly selective biomarker using two-photon Rayleigh nanoparticle. *ACS Nano* 3:2834–2840
- Nuovo G, Paniccà B, Mezache L, Quiñónez M, Williams J, Vandiver P, Fadda P, Amann V (2017) Diagnostic pathology of Alzheimer's disease from routine microscopy to

- immunohistochemistry and experimental correlations. *Ann Diagn Pathol* 28:24–29. <https://doi.org/10.1016/j.anndiagpath.2017.02.006>
- O'Bryant SE, Mielke MM, Rissman RA, Lista S, Vanderstichele H, Zetterberg H, Lewczuk P, Posner H, Hall J, Johnson L, Fong Y-L, Luthman J, Jeromin A, Batrla-Utermann R, Villarreal A, Britton G, Snyder PJ, Henriksen K, Grammas P, Gupta V, Martins R, Hampel H (2017) Blood-based biomarkers in Alzheimer disease: current state of the science and a novel collaborative paradigm for advancing from discovery to clinic. *Alzheimer's Dement J Alzheimer's Assoc* 13:45–58. <https://doi.org/10.1016/j.jalz.2016.09.014>
- Oh ES, Mielke MM, Rosenberg PB, Jain A, Fedarko NS, Lyketsos CG, Mehta PD (2010) Comparison of conventional ELISA with electrochemiluminescence technology for detection of amyloid- β in plasma. *J Alzheimers Dis* 21:769–773. <https://doi.org/10.3233/JAD-2010-100456>
- Ordóñez-Gutiérrez L, Wandosell F (2020) Nanoliposomes as a therapeutic tool for Alzheimer's disease. *Front Synaptic Neurosci* 12:1–10. <https://doi.org/10.3389/fnsyn.2020.00020>
- Pannee J, Törnqvist U, Westerlund A, Ingelsson M, Lannfelt L, Brinkmalm G, Persson R, Gobom J, Svensson J, Johansson P, Zetterberg H, Blennow K, Portelius E (2014) The amyloid- β degradation pattern in plasma—a possible tool for clinical trials in Alzheimer's disease. *Neurosci Lett* 573:7–12. <https://doi.org/10.1016/j.neulet.2014.04.041>
- Panneer Selvam S, Yun K (2020) A self-assembled silver chalcogenide electrochemical sensor based on rGO-Ag₂Se for highly selective detection of serotonin. *Sensors Actuators B Chem* 302:127161. <https://doi.org/10.1016/j.snb.2019.127161>
- Patterson C (2018) World Alzheimer Report 2018. The state of the art of dementia research: new frontiers. Alzheimer's Disease International, London
- Prakash A, Kalra J, Mani V, Ramasamy K, Majeed ABA (2015) Pharmacological approaches for Alzheimer's disease: neurotransmitter as drug targets. *Expert Rev Neurother* 15:53–71. <https://doi.org/10.1586/14737175.2015.988709>
- Quintana C, Di Wu T, Delatour B, Dhenain M, Guerquin-Kern JL, Croisy A (2007) Morphological and chemical studies of pathological human and mice brain at the subcellular level: correlation between light, electron, and NanoSIMS microscopies. *Microsc Res Tech* 70:281–295. <https://doi.org/10.1002/jemt.20403>
- Rallabandi VPS, Tulpule K, Gattu M (2020) Automatic classification of cognitively normal, mild cognitive impairment, and Alzheimer's disease using structural MRI analysis. *Informatics Med Unlocked* 18:100305. <https://doi.org/10.1016/j.imu.2020.100305>
- Raskin J, Cummings J, Hardy J, Schuh K, Dean R (2015) Neurobiology of Alzheimer's disease: integrated molecular, physiological, anatomical, biomarker, and cognitive dimensions. *Curr Alzheimer Res* 12:712–722. <https://doi.org/10.2174/1567205012666150701103107>
- Re F, Gregori M, Masserini M (2012) Nanotechnology for neurodegenerative disorders. *Maturitas* 73:45–51. <https://doi.org/10.1016/j.maturitas.2011.12.015>
- Regeniter A, Kuhle J, Baumann T, Sollberger M, Herdener M, Kunze U, Camuso MC, Monsch AU (2012) Biomarkers of dementia: comparison of electrochemiluminescence results and reference ranges with conventional ELISA. *Methods* 56:494–499. <https://doi.org/10.1016/j.ymeth.2012.03.019>
- Reitz C, Mayeux R (2014) Alzheimer disease: epidemiology, diagnostic criteria, risk factors, and biomarkers. *Biochem Pharmacol* 88:640–651. <https://doi.org/10.1016/j.bcp.2013.12.024>
- Ribeiro FM, Vieira LB, Pires RGW, Olmo RP, Ferguson SSG (2017) Metabotropic glutamate receptors and neurodegenerative diseases. *Pharmacol Res* 115:179–191. <https://doi.org/10.1016/j.phrs.2016.11.013>
- Sabbagh MN, Lue L-F, Fayard D, Shi J (2017) Increasing precision of clinical diagnosis of Alzheimer's disease using a combined algorithm incorporating clinical and novel biomarker data. *Neurol Ther* 6:83–95. <https://doi.org/10.1007/s40120-017-0069-5>
- Sacramento AS, Moreira FTC, Guerreiro JL, Tavares AP, Sales MGF (2017) Novel biomimetic composite material for potentiometric screening of acetylcholine, a neurotransmitter in Alzheimer's disease. *Mater Sci Eng C* 79:541–549. <https://doi.org/10.1016/j.msec.2017.05.098>

- Sadanandhan NK, Cheriyaathuchenaaramvalli M, Devaki SJ, Ravindranatha Menon AR (2017) PEDOT-reduced graphene oxide-silver hybrid nanocomposite modified transducer for the detection of serotonin. *J Electroanal Chem* 794:244–253. <https://doi.org/10.1016/j.jelechem.2017.04.027>
- Saeedi M, Eslamifard M, Khezri K, Dizaj SM (2019) Applications of nanotechnology in drug delivery to the central nervous system. *Biomed Pharmacother* 111:666–675. <https://doi.org/10.1016/j.biopha.2018.12.133>
- Salerno M, Santo D, Porcheras D (2016) Alzheimer's disease : the use of contrast agents for magnetic resonance imaging to detect amyloid beta peptide inside the brain. *Coord Chem Rev* 327–328:27–34. <https://doi.org/10.1016/j.ccr.2016.04.018>
- Sanati M, Khodaghali F, Aminyavari S, Ghasemi F, Gholami M, Kebriaeezadeh A, Sabzevari O, Hajipour MJ, Imani M, Mahmoudi M, Sharifzadeh M (2019) Impact of gold nanoparticles on amyloid β -induced Alzheimer's disease in a rat animal model: involvement of STIM proteins. *ACS Chem Neurosci* 10:2299–2309. <https://doi.org/10.1021/acschemneuro.8b00622>
- Sangubotla R, Kim J (2018) Recent trends in analytical approaches for detecting neurotransmitters in Alzheimer's disease. *TrAC Trends Anal Chem* 105:240–250. <https://doi.org/10.1016/j.trac.2018.05.014>
- Scarano S, Lisi S, Ravelet C, Peyrin E, Minunni M (2016) Detecting Alzheimer's disease biomarkers: from antibodies to new bio-mimetic receptors and their application to established and emerging bioanalytical platforms – a critical review. *Anal Chim Acta* 940:21–37. <https://doi.org/10.1016/j.aca.2016.08.008>
- Sekioka N, Kato D, Kurita R, Hirono S, Niwa O (2008) Improved detection limit for an electrochemical γ -aminobutyric acid sensor based on stable NADPH detection using an electron cyclotron resonance sputtered carbon film electrode. *Sensors Actuators B Chem* 129:442–449. <https://doi.org/10.1016/j.snb.2007.08.040>
- Sharma P, Semwal V, Gupta BD (2019) Highly sensitive and selective localized surface plasmon resonance biosensor for detecting glutamate realized on optical fiber substrate using gold nanoparticles. *Photonics Nanostructures Fundam Appl* 37:100730. <https://doi.org/10.1016/j.photonics.2019.100730>
- Sheikh-Bahaei N, Sajjadi SA, Manavaki R, Gillard JH (2017) Imaging biomarkers in Alzheimer's disease: a practical guide for clinicians. *J Alzheimers Dis Rep* 1:71–88. <https://doi.org/10.3233/adr-170013>
- Shekhar S, Kumar R, Rai N, Kumar V, Singh K, Upadhyay AD, Tripathi M, Dwivedi S, Dey AB, Dey S (2016) Estimation of tau and phosphorylated Tau181 in serum of Alzheimer's disease and mild cognitive impairment patients. *PLoS One* 11:e0159099. <https://doi.org/10.1371/journal.pone.0159099>
- Shi M, Sui Y-T, Peskind ER, Li G, Hwang H, Devic I, Ghingina C, Edgar JS, Pan C, Goodlett DR, Furay AR, Gonzalez-Cuyar LF, Zhang J (2011) Salivary tau species are potential biomarkers of Alzheimer's disease. *J Alzheimers Dis* 27:299–305. <https://doi.org/10.3233/JAD-2011-110731>
- Shui B, Tao D, Cheng J, Mei Y, Jaffrezic-Renault N, Guo Z (2018a) A novel electrochemical aptamer–antibody sandwich assay for the detection of tau-381 in human serum. *Analyst* 143:3549–3554. <https://doi.org/10.1039/C8AN00527C>
- Shui B, Tao D, Florea A, Cheng J, Zhao Q, Gu Y, Li W, Jaffrezic-Renault N, Mei Y, Guo Z (2018b) Biosensors for Alzheimer's disease biomarker detection: a review. *Biochimie* 147:13–24. <https://doi.org/10.1016/j.biochi.2017.12.015>
- da Silva W, Brett CMA (2020) Novel biosensor for acetylcholine based on acetylcholinesterase/poly(neutral red) – deep eutectic solvent/Fe₂O₃ nanoparticle modified electrode. *J Electroanal Chem* 42:114050. <https://doi.org/10.1016/j.jelechem.2020.114050>
- Simon R, Girod N, Fonbonne C, Salvador A, Clément Y, Lantéri P, Amouyel P, Lambert JC, Lemoine J (2012) Total ApoE and ApoE4 isoform assays in an Alzheimer's disease case-control study by targeted mass spectrometry (n = 669): a pilot assay for methionine-containing proteotypic peptides. *Mol Cell Proteomics* 11:1389–1403. <https://doi.org/10.1074/mcp.M112.018861>

- Singh P, Pandit S, Mokkalapati VRSS, Garg A, Ravikumar V, Mijakovic I (2018) Gold nanoparticles in diagnostics and therapeutics for human cancer. *Int J Mol Sci* 19:1979. <https://doi.org/10.3390/ijms19071979>
- Singhal RK, Anand S (2013) Salivary-42, IGF-I, IGF-II, alpha amylase, IL-1 and TNF-alpha in Alzheimer's disease: a useful diagnostic tool. *Web Med Cent*. 4–9. http://www.webmedcentral.com/article_view/4440
- Skoch J, Dunn A, Hyman BT, Bacskai BJ (2005) Development of an optical approach for noninvasive imaging of Alzheimer's disease pathology. *J Biomed Opt* 10:011007. <https://doi.org/10.1117/1.1846075>
- Small GW (2000) Early diagnosis of Alzheimer's disease: update on combining genetic and brain-imaging measures. *Dialogues Clin Neurosci* 2:241–246
- Smith ER, Nilforooshan R, Weaving G, Tabet N (2011) Plasma fetuin-A is associated with the severity of cognitive impairment in mild-to-moderate alzheimer's disease. *J Alzheimers Dis* 24:327–333. <https://doi.org/10.3233/JAD-2011-101872>
- Song Y, Shenwu M, Dhossche D, Liu Y (2005) A capillary liquid chromatographic/tandem mass spectrometric method for the quantification of γ -aminobutyric acid in human plasma and cerebrospinal fluid. *J Chromatogr B* 814:295–302. <https://doi.org/10.1016/j.jchromb.2004.10.046>
- Song J, Wang L, Hetong Q, Honglan Q, Zhang C (2019) Highly selective electrochemical method for the detection of serotonin at carbon fiber microelectrode modified with gold nanoflowers and overoxidized polypyrrole. *Chin Chem Lett* 30:1643–1646
- Špringer T, Hemmerová E, Finocchiaro G, Křištofiková Z, Vyháněk M, Homola J (2020) Surface plasmon resonance biosensor for the detection of tau-amyloid β complex. *Sensors Actuators B Chem* 316:128146. <https://doi.org/10.1016/j.snb.2020.128146>
- Strimbu K, Tavel JA (2010) What are biomarkers? *Curr Opin HIV AIDS* 5:463–466. <https://doi.org/10.1097/COH.0b013e32833ed177>
- Szemeraj J (2014) New type of BACE1 siRNA delivery to cells. *Med Sci Monit* 20:2598–2606. <https://doi.org/10.12659/MSM.891219>
- Tatebe H, Kasai T, Ohmichi T, Kishi Y, Kakeya T, Waragai M, Kondo M, Allsop D, Tokuda T (2017) Quantification of plasma phosphorylated tau to use as a biomarker for brain Alzheimer pathology: pilot case-control studies including patients with Alzheimer's disease and down syndrome. *Mol Neurodegener* 12:1–11. <https://doi.org/10.1186/s13024-017-0206-8>
- Tavakolian-Ardakani H, Cristea M-A, Marrazza (2019) Latest trends in electrochemical sensors for neurotransmitters: a review. *Sensors* 19:2037. <https://doi.org/10.3390/s19092037>
- Teng E, Chow N, Hwang KS, Thompson PM, Gyls KH, Cole GM, Jack CR Jr, Shaw LM, Trojanowski JQ, Soares HD, Weiner MW, Apostolova LG (2015) Low plasma ApoE levels are associated with smaller hippocampal size in the Alzheimer's Disease Neuroimaging Initiative Cohort. *Dement Geriatr Cogn Disord* 39:154–166. <https://doi.org/10.1159/000368982>
- Thériault P, ElAli A, Rivest S (2015) The dynamics of monocytes and microglia in Alzheimer's disease. *Alzheimers Res Ther* 7:41. <https://doi.org/10.1186/s13195-015-0125-2>
- Thinakaran G, Koo EH (2008) Amyloid precursor protein trafficking, processing, and function. *J Biol Chem* 283:29615–29619. <https://doi.org/10.1074/jbc.R800019200>
- Tohgi H, Abe T, Takahashi S, Kimura M, Takahashi J, Kikuchi T (1992) Concentrations of serotonin and its related substances in the cerebrospinal fluid in patients with Alzheimer type dementia. *Neurosci Lett* 141:9–12. [https://doi.org/10.1016/0304-3940\(92\)90322-X](https://doi.org/10.1016/0304-3940(92)90322-X)
- Torsdottir G, Kristinnsson J, Snaedal J, Jóhannesson T (2011) Ceruloplasmin and Iron proteins in the serum of patients with Alzheimer's disease. *Dement Geriatr Cogn Dis. Extra* 1:366–371. <https://doi.org/10.1159/000330467>
- Valcárcel-Nazco C, Perestelo-Pérez L, Molinuevo JL, Mar J, Castilla I, Serrano-Aguilar P (2014) Cost-effectiveness of the use of biomarkers in cerebrospinal fluid for Alzheimer's disease. *J Alzheimers Dis* 42:777–788. <https://doi.org/10.3233/JAD-132216>
- Verkhatsky A, Olabarria M, Noristani HN, Yeh C, Rodriguez JJ (2010) Astrocytes in Alzheimer's disease. *Neurotherapeutics* 7:399–412. <https://doi.org/10.1016/j.nurt.2010.05.017>

- Wang W-Y, Tan M-S, Yu J-T, Tan L (2015) Role of pro-inflammatory cytokines released from microglia in Alzheimer's disease. *Ann Transl Med* 3:136. <https://doi.org/10.3978/j.issn.2305-5839.2015.03.49>
- Wang SX, Acha D, Shah AJ, Hills F, Roitt I, Demosthenous A, Bayford RH (2017) Detection of the tau protein in human serum by a sensitive four-electrode electrochemical biosensor. *Biosens Bioelectron* 92:482–488. <https://doi.org/10.1016/j.bios.2016.10.077>
- Wang Y, Jin M, Chen G, Cui X, Zhang Y, Li M, Liao Y, Zhang X, Qin G, Yan F, Abd El-Aty AM, Wang J (2019) Bio-barcode detection technology and its research applications: a review. *J Adv Res* 20:23–32. <https://doi.org/10.1016/j.jare.2019.04.009>
- Watanabe M, Kimura A, Akasaka K, Hayashi S (1986) Determination of acetylcholine in human blood. *Biochem Med Metab Biol* 36:355–362. [https://doi.org/10.1016/0885-4505\(86\)90147-7](https://doi.org/10.1016/0885-4505(86)90147-7)
- Watanabe Y, Hirao Y, Kasuga K, Tokutake T, Semizu Y, Kitamura K, Ikeuchi T, Nakamura K, Yamamoto T (2019) Molecular network analysis of the urinary proteome of Alzheimer's disease patients. *Dement Geriatr Cogn Dis Extra* 9:53–65. <https://doi.org/10.1159/000496100>
- Wen MM, El-Salamouni NS, El-Refaie WM, Hazzah HA, Ali MM, Tosi G, Farid RM, Blanco-Prieto MJ, Billa N, Hanafy AS (2017) Nanotechnology-based drug delivery systems for Alzheimer's disease management: technical, industrial, and clinical challenges. *J Control Release* 245:95–107. <https://doi.org/10.1016/j.jconrel.2016.11.025>
- Whelan CD, Mattsson N, Nagle MW, Vijayaraghavan S, Hyde C, Janelidze S, Stomrud E, Lee J, Fitz L, Samad TA, Ramaswamy G, Margolin RA, Malarstig A, Hansson O (2019) Multiplex proteomics identifies novel CSF and plasma biomarkers of early Alzheimer's disease. *Acta Neuropathol Commun* 7:169. <https://doi.org/10.1186/s40478-019-0795-2>
- Whitcombe MJ, Chianella I, Larcombe L, Piletsky SA, Noble J, Porter R, Horgan A (2011) The rational development of molecularly imprinted polymer-based sensors for protein detection. *Chem Soc Rev* 40:1547–1571. <https://doi.org/10.1039/c0cs00049c>
- Wittenberg NJ, Wootla B, Jordan LR, Denic A, Warrington AE, Oh S-H, Rodriguez M (2014) Applications of SPR for the characterization of molecules important in the pathogenesis and treatment of neurodegenerative diseases. *Expert Rev Neurother* 14:449–463. <https://doi.org/10.1586/14737175.2014.896199>
- Xiao S, Zhou D, Luan P, Gu B, Feng L, Fan S, Liao W, Fang W, Yang L, Tao E, Guo R, Liu J (2016) Graphene quantum dots conjugated neuroprotective peptide improve learning and memory capability. *Biomaterials* 106:98–110. <https://doi.org/10.1016/j.biomaterials.2016.08.021>
- Yang C-C, Chiu M-J, Chen T-F, Chang H-L, Liu B-H, Yang S-Y (2018) Assay of plasma phosphorylated tau protein (threonine 181) and total tau protein in early-stage Alzheimer's disease. *J Alzheimers Dis* 61:1323–1332. <https://doi.org/10.3233/JAD-170810>
- You M, Yang S, An Y, Zhang F, He P (2020) A novel electrochemical biosensor with molecularly imprinted polymers and aptamer-based sandwich assay for determining amyloid- β oligomer. *J Electroanal Chem*. <https://doi.org/10.1016/j.jelechem.2020.114017>
- Yuan W, Chen S, Ge X-m, Chen Y, Lu N, Liu Z (2013) Advances with RNA interference in Alzheimer's disease research. *Drug Des Devel Ther* 42:117. <https://doi.org/10.2147/DDDT.S40229>
- Zaidi SA (2018) Development of molecular imprinted polymers based strategies for the determination of dopamine. *Sensors Actuators B Chem* 265:488–497. <https://doi.org/10.1016/j.snb.2018.03.076>
- Zakaria N, Ramli MZ, Ramasamy K, Meng LS, Yean CY, Banga Singh KK, Zain ZM, Low K-F (2018) An impedimetric micro-immunosensing assay to detect Alzheimer's disease biomarker: A β 40. *Anal Biochem* 555:12–21. <https://doi.org/10.1016/j.ab.2018.05.031>
- Zakharova NV, Bugrova AE, Kononikhin AS, Indeykina MI, Popov IA, Nikolaev EN (2018) Mass spectrometry analysis of the diversity of A β peptides: difficulties and future perspectives for AD biomarker discovery. *Expert Rev Proteomics* 15:773–775. <https://doi.org/10.1080/14789450.2018.1525296>

- Zetterberg H (2019) Blood-based biomarkers for Alzheimer's disease—an update. *J Neurosci Methods* 319:2–6. <https://doi.org/10.1016/j.jneumeth.2018.10.025>
- Zetterberg H, Andreasson U, Hansson O, Wu G, Sankaranarayanan S, Andersson ME, Buchhave P, Londos E, Umek RM, Minthon L, Simon AJ, Blennow K (2008) Elevated cerebrospinal fluid BACE1 activity in incipient Alzheimer disease. *Arch Neurol* 65:1102–1107. <https://doi.org/10.1001/archneur.65.8.1102>
- Zhang QE, Ling S, Li P, Zhang S, Ng CH, Ungvari GS, Wang LJ, Lee SY, Wang G, Xiang YT (2018) The association between urinary alzheimer-associated neuronal thread protein and cognitive impairment in late-life depression: a controlled pilot study. *Int J Biol Sci* 14:1497–1502. <https://doi.org/10.7150/ijbs.25000>
- Zhao J, Chen J, Ma S, Liu Q, Huang L, Chen X, Lou K, Wang W (2018) Recent developments in multimodality fluorescence imaging probes. *Acta Pharm Sin B* 8:320–338. <https://doi.org/10.1016/j.apsb.2018.03.010>
- Zhong Z, Ewers M, Teipel S, Bürger K, Wallin A, Blennow K, He P, McAllister C, Hampel H, Shen Y (2007) Levels of β -secretase (BACE1) in cerebrospinal fluid as a predictor of risk in mild cognitive impairment. *Arch Gen Psychiatry* 64:718–726. <https://doi.org/10.1001/archpsyc.64.6.718>
- Zhou Y, Dong H, Liu L, Xu M (2015) Simple colorimetric detection of amyloid β -peptide (1–40) based on aggregation of gold nanoparticles in the presence of copper ions. *Small* 11:2144–2149. <https://doi.org/10.1002/smll.201402593>
- Zhou Y, Liyanage PY, Devadoss D, Rios Guevara LR, Cheng L, Graham RM, Chand HS, Al-Youbi AO, Bashammakh AS, El-Shahawi MS, Leblanc RM (2019) Nontoxic amphiphilic carbon dots as promising drug nanocarriers across the blood-brain barrier and inhibitors of β -amyloid. *Nanoscale* 11:22387–22397. <https://doi.org/10.1039/c9nr08194a>
- Zhou GS, Yuan YC, Yin Y, Tang YP, Xu RJ, Liu Y, Chen PD, Yin L, Duan JA (2020) Hydrophilic interaction chromatography combined with ultrasound-assisted ionic liquid dispersive liquid–liquid microextraction for determination of underivatized neurotransmitters in dementia patients' urine samples. *Anal Chim Acta* 1107:74–84. <https://doi.org/10.1016/j.aca.2020.02.027>
- Zhu G, Lee HJ (2017) Electrochemical sandwich-type biosensors for α -1 antitrypsin with carbon nanotubes and alkaline phosphatase labeled antibody-silver nanoparticles. *Biosens Bioelectron* 89:959–963. <https://doi.org/10.1016/j.bios.2016.09.080>
- Zuliani G, Trentini A, Rosta V, Guerrini R, Pacifico S, Bonazzi S, Guiotto A, Passaro A, Seripa D, Valacchi G, Cervellati C (2020) Increased blood BACE1 activity as a potential common pathogenic factor of vascular dementia and late onset Alzheimer's disease. *Sci Rep* 10:1–8. <https://doi.org/10.1038/s41598-020-72168-3>



Biomaterials: Types and Applications

4

Aman Bhardwaj and Lalit M. Pandey

Abstract

Advancement in the field of biomedicine led to futuristic research in biomaterial fabrication. Biomaterials are the material mediators tackling the issues faced in the field of life science. It comprises materials as varied as metals, polymers, ceramics and composites. This chapter addresses the impact of biomaterials in the field of biomedicine, specifically implants. Implants are designed to aid in the normal functioning of a damaged body part. Under the physiological microenvironment, interfacial interactions are quite complicated at the implant site. Present implants are susceptible to degradation in the body, leading to the generation of the debris that ultimately attracts the site's immunological agents. Micromotion, biocompatibility and bone interlocking are key aspects determining the osseointegration and thus the implant's success in the long run. Biomaterials can be easily engineered to address the biocompatibility, osseointegration, bacterial invasion and biofouling issues currently faced by the various implants. Various biomaterials and their potential applications have been explored in great detail. Current limitations and biomimetic inspired alternate strategies for eradicating the limitations have also been presented in this chapter. Biomaterial fabrication to mimic the natural bone or part thereof, one of the hot topics of the ongoing research, has also been highlighted.

Keywords

Biomaterial · Biocompatibility · Osseointegration · Surface modification · Orthopaedic implants · Tissue engineering

A. Bhardwaj · L. M. Pandey (✉)

Bio-Interface and Environmental Engineering Lab, Department of Biosciences and Bioengineering, Indian Institute of Technology Guwahati, Guwahati, Assam, India

e-mail: lalitpandey@iitg.ac.in

© The Author(s), under exclusive license to Springer Nature Singapore Pte Ltd. 2022

L. M. Pandey, A. Hasan (eds.), *Nanoscale Engineering of Biomaterials: Properties and Applications*, https://doi.org/10.1007/978-981-16-3667-7_4

4.1 Introduction

Biomaterials are synthetic or nature-derived materials that aid in the normal functioning of a diseased or lost body part for enhancing longevity and normal well-being either directly or indirectly (Rahmati et al. 2016). Few applications of biomaterials include orthopaedics, dental implants, soft/hard bone implants, blood vessels, artificial heart valves, stents, pacemakers and hip or knee replacement (Rahmati et al. 2016; Hu et al. 2019; Jemat et al. 2015; Zhao et al. 2015; Dangas et al. 2016; Zhang et al. 2018; Cui et al. 2016; Chen and Thouas 2015). Apart from implant material, biomaterials find applications in other fields of biomedical engineering also such as in surgical instruments, artificial organs, blood storage bags, drug delivery, tissue engineering and others (Tan et al. 2020; Xu et al. 2015; dos Santos et al. 2017; Hadsjesfandiari et al. 2018). At the biomaterial interface in the physiological microenvironment, protein-surface interactions, protein-protein interactions, inflammatory reactions and many other dynamic interactions occur simultaneously (Pacelli et al. 2016). For effectiveness, biomaterials need to be integrated with the surrounding tissues/bones without intervening fibrous tissue material (Augustine et al. 2017). This can be achieved by tuning the bio-interfacial interactions by applying the surface engineering approaches.

Developments of the biomaterials have been divided into four generations, as shown in Fig. 4.1. The first generation of biomaterials was developed in the 1960s–1970s and focused on implant-body integration. The common feature of the first-generation biomaterials was bio-inertness, and they were designed to minimize the immunological response to the foreign material. The first biomaterial developed was vanadium steel that was adapted to manufacture bone fracture plates and screws. Other examples comprise stainless steel, cobalt-chromium alloys, titanium and

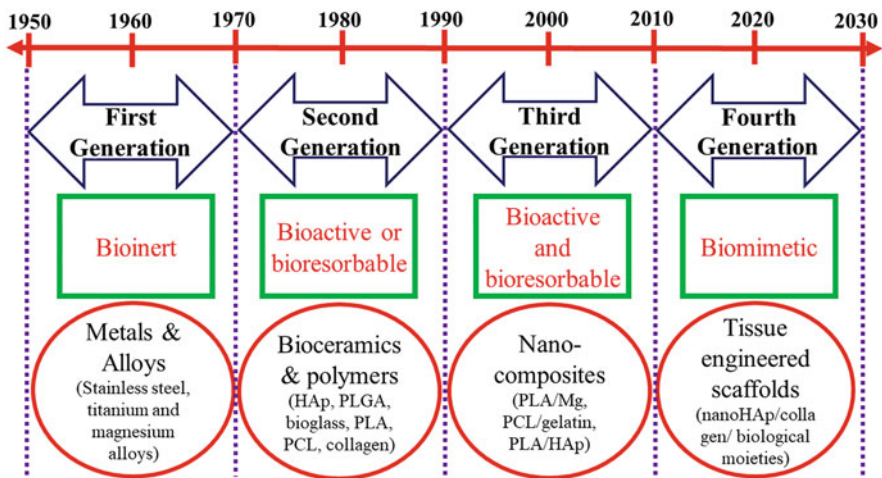


Fig. 4.1 Different generations of the biomaterials based on bioinert, bioactive, bioactive, resorbable and biomimetic properties

alloys. The second-generation biomaterials were developed to enhance the shortcomings of the existing biomaterials and comprised of bioactive or resorbable materials. These biomaterials are readily used for orthopaedic and dental implants. Second-generation biomaterials comprise various ceramic and polymeric biomaterials. Resorption in the physiological microenvironment is not enough for the effective integration of the biomaterials in the body. Biomaterial capable of stimulating specific responses at the molecular level necessitated the development of the third generation of biomaterials. These biomaterials comprise the features of bioactivity and resorption and activate the genes stimulating the tissue regeneration in the host. The fourth generation of biomaterials are referred as ‘biomimetic’ and ‘smart’ materials. These biomaterials interact at molecular, cellular and tissue levels and are used for regenerative medicine, tissue engineering and repair. The fourth generation of biomaterials are hybrid materials designed to monitor extracellular and intracellular responses using bioelectric signals and manipulate these signals for tissue regeneration (Ning et al. 2016).

Metallic biomaterials have excellent mechanical and other surface properties that make them the ideal material for implant fabrication. Stainless steel and cobalt-chromium are used for implant-related applications (Hayes et al. 2018). With the advent of technology, new metallic materials like magnesium alloys and titanium alloys have been developed. Ti6Al4V alloy of titanium is the routinely applied biomaterial for implant-related applications (Hasan and Pandey 2020). However, these metallic biomaterials suffer from certain issues like poor osseointegration, which paved the way for the surface engineering and development of other binary and ternary metallic biomaterials.

Polymer biomaterials are also utilized for various biomedical-related applications. It provides the ease of tunability and manufacturability. They can be cast into any desired shape depending on applications (Guo and Ma 2018). Natural, semisynthetic and synthetic polymeric materials have been developed for different applications. Further, the surface properties of these polymeric biomaterials can be modulated easily by surface modification strategies. Two or more polymers can also be combined in different ratios to fabricate polymer composites with hybrid properties. Polymer behaviour in the physiological environment is quite complicated and undergoes degradation, leading to the polymer constituents’ release; these restrict polymers in the long run (Shen et al. 2015).

Ceramics biomaterials are mostly utilized as surface coatings to enhance the bioactivity of other implant materials. Many ceramics materials such as calcium hydrogen phosphate (CAP) and hydroxyapatite (HAP) resemble the constituents of natural bones (Borkowski et al. 2015). Ceramics are brittle and susceptible to cracks and mostly utilized for biodegradable implant fabrication. Ceramics are known to enhance the implant’s osseointegration, but they suffer from poor mechanical properties and degradation in physiological conditions (Bona et al. 2015; Li and Hastings 2016). Composite materials are fabricated by combining two or more biomaterials keeping their individual properties intact to generate material with enhanced properties (De Santis et al. 2019). Such composites are classified as particulate and fibrous, depending on the constituents.

This chapter highlights the various biomaterials currently applied in the field of biomedical engineering. It briefly focuses on implant development using different biomaterials. Salient features for implants have been outlined. Current progress in tissue engineering and orthopaedic implants development have been highlighted.

4.2 Types of Biomaterials

In this section, different biomaterials utilized for the various biomedical applications have been thoroughly discussed. Key features and the limitations of biomaterials have also been highlighted, along with the mentioned biomaterials' applications. Biomaterials have been discussed with implant development as the prime focus. Table 4.1 summarizes the various biomaterials utilized for biomedical applications. The intent of this section is to introduce the various biomaterials in a simplified manner.

4.2.1 Metallic Biomaterials

Various metals and their alloys have been explored for different biomedical applications based on mechanical, chemical and surface properties. 316L stainless steel exhibits remarkable mechanical and electrochemical properties such as better corrosion resistance, work hardening and formability (Correa et al. 2018; Bagherifard et al. 2016). Stainless steel with Young's modulus of 210 GPa is utilized to develop orthopaedic and dental implants (Nnamchi 2016). CoCrMo alloys' application as the dental material was initially started in the late 1990s and now are used as an orthopaedic implant material. These alloys are widely used for the augmentation, replacement and repair of the damaged bones. For example, CoCrMo wrought grade alloys are frequently used to manufacture the knee and hip joints (Alemón et al. 2015). However, recent concerns regarding corrosion and the generation of toxic wear debris limited their utilization (Gilbert et al. 2015). It has been observed that corrosion is also mediated by the inflammatory agents that are attracted at the implant site (Gilbert et al. 2015). Besides, the lack of interaction between tissue and implants led to exploring other strategies for implant fabrication (Correa et al. 2018). In this regard, various surface modification strategies have been utilized for improving the tribo-corrosion behaviour, such as the multilayer coating of TiAlVCN/CN_x on the CoCrMo alloys. Multilayer coating comprised one layer of TiAlV, nine layers of carbon nitride (CN_x), nine layers of TiAlVCN and a top layer of CN_x on CoCrMo substrate, as visible by the cross-sectional SEM image in Fig. 4.2 (Alemón et al. 2015).

Ti alloys' lower rigidity compared to CoCr alloys and stainless steel makes them a suitable material for implant development, particularly for orthopaedic and dental implants (Nnamchi et al. 2016; Santos et al. 2015). Titanium and alloys display good biocompatibility, corrosion resistance and lower elastic modulus (Xie et al. 2015). Passive TiO₂ layer present on the surface of Ti6Al4V imparts corrosion resistance

Table 4.1 Biomedical applications of the various biomaterials

Biomaterial		Application	References
Type	Name		
Metal	316 L	Orthopaedic implants	Bagherifard et al. (2016)
	CoCr	Hip/knee joints	Alemón et al. (2015)
	CoCrMo	Orthopaedic implants	Gilbert et al. (2015)
	AZ31	Degradable bone implants	Ren et al. (2015)
	Ti6Al4V	Orthopaedic/dental implants	Jain and Bajpai (2019)
Polymer	PVC	Catheters	Lucas et al. (2016)
	UHMWPE	Acetabular cup	Shahemi et al. (2018)
	Polypropylene	Sutures	López-Saucedo et al. (2018)
	PMMA	Ocular lenses	Ko et al. (2017)
	Polyurethanes	Implant coating	Kondyurina et al. (2015)
	Polycaprolactone	Tissue engineering	Mondal et al. (2016)
	Poly(lactic acid)	Orthopaedic regenerative medicine	Narayanan et al. (2016)
	PEKK	Bone tissue engineering	Adamzyk et al. (2016)
Ceramics	Polyester	Cardiac tissue engineering	Davenport Huyer et al. (2016)
	HAp	Bioactivity enhancement	Behera et al. (2018b)
	Calcium phosphate	Bioactivity/tribological features enhancement	Behera et al. (2018a)
	Bioceramic	Bone healing	Ginebra et al. (2018)
	Ceravital	Middle ear surgery	Bose et al. (2017)
Composites	Chitosan/TiO ₂	Wound dressing/skin regeneration	Behera et al. (2017)
	HAp/ β glucan	Bone substitute	Borkowski et al. (2015)
	PMMA/silica	Corrosion resistant coating	Harb et al. (2020)
	Alumina/zirconia	Dental implant	Schierano et al. (2015)
	Zn/HAp	Orthopaedic applications	Yang et al. (2018)

PVC polyvinyl chloride, *UHMWPE* ultra-high molecular weight polyethylene, *PMMA* polymethylmethacrylate, *PEKK* polyetherketone ketone, *HAp* hydroxyapatite

(Costa et al. 2019). β phase titanium alloys are the most promising candidates for implant development due to good biocompatibility and superior mechanical property (Neacsu et al. 2015). Titanium alloys occur in the β phase at a higher temperature, and β phase stabilizers are used to obtain the β phase at a lower temperature (Nnamchi et al. 2016).

The addition of Mo to titanium imparts the low elasticity with superior strength for implant development and is a most efficient β phase stabilizer (Nnamchi 2016). However, Mo addition has ductility and density issues that alloying Zr and Nb can address to Ti-Mo-based binary alloy to form Ti₆Mo₄Nb₄Zr, which resulted in

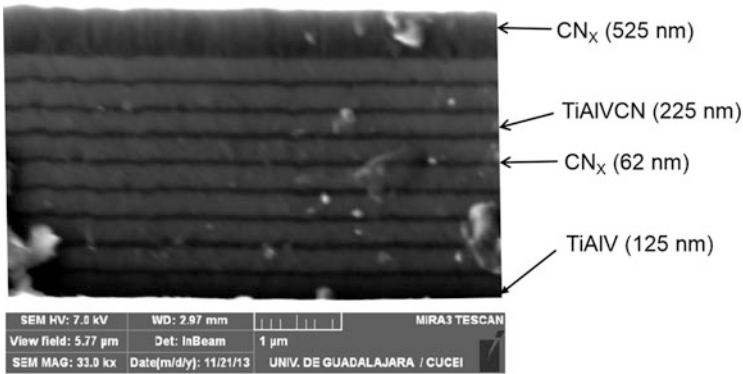


Fig. 4.2 SEM image showing the cross-section of multilayer coating of TiAlVCN/CN_x on the CoCrMo alloys containing the layers from the bottom as one layer of TiAlV, nine layers of carbon nitride, nine layers of TiAlVCN and a top layer of carbon nitride. (Adapted with permission from Tribology International 81 (2015): 159–168 (Alemón et al. 2015))

Young's modulus of 32.3 GPa (Nnamchi 2016). Nb addition improves the hot workability and mechanical performance, while strength is increased by Zr addition (Nnamchi 2016). β alloy Ti-(3–18)Mn, low-cost and biocompatible alloys, exhibit high tensile strength and performance comparable to widely utilized Ti6Al4V alloys (Santos et al. 2015).

However, Ti6Al4V suffers from poor wear resistance, stress shielding and micromotion at the implant site, which causes the detachment of the debris. Cyclic load-bearing areas such as plates and screws lead to the generation of debris (Rahmati et al. 2016). This leads to the release of metal leachate in the vicinity. The release of aluminium and vanadium from the Ti6Al4V is toxic to the human body. Al release results in neurotoxic effects in the body (Santos et al. 2015). Vanadium ions above the concentration of 23 μM become toxic to the physiological microenvironment (Costa et al. 2019). The released metal leachates interact with surrounding tissues, which causes the immunological response and failure of the implant (Toptan et al. 2016). Toxicity issues of Al and V led to the exploration of other non-toxic β phase stabilizers such as tantalum (Ta), zirconium (Zr) and niobium (Nb) for alloy fabrication. Ti₁₃Nb₁₃Zr, Ti-Mo, Ti₁₂Mo₆Zr₂Fe and Ti₂₉Nb₁₃Ta_{4.6}Zr are some of the recently developed biomaterials to address the leaching issues of the titanium alloys (Correa et al. 2018). However, the higher cost of Ta and Nb steered the examination of low-cost candidates such as manganese (Santos et al. 2015; Correa et al. 2018).

Further, mismatch in Young's modulus of cortical bone (10–30 GPa) and the metallic implant such as Ti6Al4V (110 GPa) cause stress shielding effect leading to bone resorption (Santos et al. 2015). This causes weak interfacial interactions between the implant and host bone, bone atrophy, and premature rejection of the implants (Neacsu et al. 2015). The development of alloys with Young's modulus closer to the bone might address the stress shielding issue. Recently binary and

ternary titanium alloys were developed with desirable Young's modulus such as Ti₃₅Nb₄Sn (43 GPa), Ti₁₅Mo (78 GPa) and Ti₁₅Mo₅Zr₃Al (80 GPa) (Santos et al. 2015). Non-toxic β stabilizers-based binary (Ti-Mo, Ti-Nb) and ternary (Ti-Mo-Nb and Ti-Ta-Nb) alloys provide the low modulus (~80 GPa) suitable for implants with low-stress shielding effect (Neacsu et al. 2015). Alloying Mo, Zr and Nb with Ti resulted in Ti₈Mo₄Nb₂Zr with Young's modulus of 35 GPa comparable to that of cortical bone, making it suitable for implant development (Nnamchi et al. 2016).

Besides, Ti6Al4V suffers from fretting wear and poor tribological features. Metal ions released from the surface may infiltrate the intercellular spaces or penetrate the cellular structures leading to metallosis (Jamrozik et al. 2015). This challenge is addressed by applying surface modification strategies such as shot peening, water jet peening, case hardening, low plasticity burnishing, plasma nitriding and LASER peening (Kumar et al. 2015; Samanta et al. 2018). The tribological behaviour of Ti alloys can be addressed by reinforcing with B₄C particles by a hot pressing method (Toptan et al. 2016). Anodization based surface modification strategy can be used to block cellular infiltration. This process involves forming a thin oxide layer onto the outermost surface whose properties are dependent on the production method, time of oxidation, electrolyte and electric parameters used for the process (Jamrozik et al. 2015). Plasma nitriding also improves wear resistance, which in turn prevents inflammation at the site (Samanta et al. 2018). Various other surface modification techniques like thermal oxidation, etching, sputtering, silanization, surface roughening and surface coatings are reported to improve the integration of the implant surface with the host tissues (Wang et al. 2016; Khanlou et al. 2015; Nouri and Wen 2015; Behera et al. 2018a; Hasan et al. 2018a).

To mimic the natural Extracellular Matrix (ECM) in the metallic biomaterials, various porous metallic biomaterials are developed using selective laser melting (SLM) to improve the biological properties of the metallic biomaterials (Van Hooreweder et al. 2017; Xie et al. 2015). Porous metallic biomaterials mimic the natural bones' mechanical and topological properties, making them a suitable candidate for orthopaedic applications (Bobbert et al. 2017). Porous titanium alloys were developed with non-toxic alloying elements to transfer stress from the implant to the host bone (Xie et al. 2015). Porous structure enhances the electrochemical and mechanical properties of the implants (Xie et al. 2015). Ti-(Ta, Nb)-Fe alloys based development of porous Ti with reduced processing can be a promising biomaterial for orthopaedic applications (Biesiekierski et al. 2016).

The promising biodegradable ability of Mg alloys enabled the design of implants with better stiffness and mechanical strength (Cifuentes et al. 2016). Implants fabricated using magnesium and biodegradable alloys possess mechanical properties comparable to the natural bone and high biocompatibility and strength/weight ratio. Magnesium ions in magnesium-based implants stimulate new bone formation and osteogenesis (Ren et al. 2015). However, these biodegradable Mg alloys suffer from drawbacks such as a faster degradation rate due to the elevated pH of the surrounding microenvironment. The formation of hydroxide as the degradation product causes the release of hydrogen from the site leading to irritation to the surrounding tissues. These challenges have compromised the long-term biocompatibility of the Mg

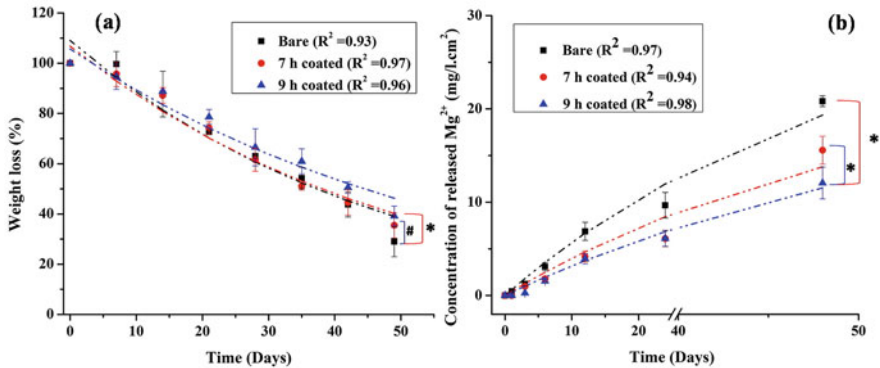


Fig. 4.3 (a) Weight loss of the uncoated and HAp coated AZ31 alloys at different periods, (b) amount of magnesium ions released from the uncoated and HAp coated AZ31 alloys. (Adapted with permission from Materials Letters 270 (2020): 127732 (Yadav et al. 2020))

alloys. Degradation of the alloys depends on the alloying material, grain size and metal purity (Cifuentes et al. 2016). The presence of chloride ions in the physiological microenvironment elevates the corrosion rate of AZ31 Mg alloys. Various strategies like anodization, sputtering, electroplating, thermal spraying, micro-arc oxidation and organic coatings enhance the corrosion resistance of the magnesium and alloys (Ren et al. 2015; Tang and Gao 2016). Yadav et al. studied the degradation behaviour of pristine and coated AZ31 surfaces in simulated body fluid (SBF). They monitored the decrease in the weight and liberation of the magnesium ions from the surface with time as shown in Fig. 4.3. Degradation studies exhibited an exponential loss of the weight for all the surfaces; however, the degradation rate decreased by 20% after coating as compared to the pristine surfaces (Yadav et al. 2020). The corrosion resistance of the magnesium-based biomaterials can also be improved by alloying with zinc or calcium, but the low solubility of other metals in magnesium limits this approach (Tang and Gao 2016). In this direction, alloying magnesium to form binary (Mg-Ca) and ternary (Mg-Zn-Ca) alloys resulted in enhanced corrosion resistance (Bian et al. 2016; Jang et al. 2015).

4.2.2 Polymeric Biomaterials

Polymeric biomaterials exhibit many advantages compared to other biomaterials such as Young's modulus similar to the human bone and radio-transparency (Hasan and Pandey 2015). But they also possess a few drawbacks, such as lack of adequate bone integration and unregulated degradation rates (Vergnol et al. 2016). Both natural and synthetic polymers are utilized as biomaterials for the fabrication of implants. Chitosan is a natural biocompatible and osteoconductive polymer and explored for wound healing applications (Khoshakhlagh et al. 2017). Natural hydrophilic polymer gelatin is a derivative of collagen protein. Thus along with

biocompatibility, gelatin exhibits a tunable degradation rate in the physiological environment (Ren et al. 2017). These polymeric biomaterials such as collagen, polyamide, gelatin, polyester and chitosan also suffer from low physical and mechanical properties compared to natural bones (Barrioni et al. 2015).

Many synthetic polymers are utilized for application in bone tissue engineering like poly(lactic acid) (PLA), poly(caprolactone) (PCL), poly(glycolic acid) (PGA) and copolymers due to better mechanical strength, biocompatibility and bioresorbability (Gao et al. 2016). In the standard design of the artificial hip joint, an acetabular cup is lined with a polymer liner, usually ultra-high molecular weight polyethylene (UHMWPE) (Samanta et al. 2018). Polyetheretherketone (PEEK) and polyetherketoneketone (PEKK) are the members of the high-temperature thermoplastic polyaryletherketone (PAEK) polymers. PEKK is a promising candidate for the fabrication of implants with stiffness and density comparable to the natural bone, good biocompatibility and ease of patient-specific implant fabrication using the 3D laser sintering technique (Adamzyk et al. 2016). However, these PAEK family polymers suffer from poor osseointegration at the bone-implant interface due to the formation of the fibrous tissue layers on the implant surface (Adamzyk et al. 2016).

Polyurethane (PUs) is the widely utilized synthetic polymer for biomedical applications due to its mechanical, biological and physicochemical properties tunability. Biodegradable PU films can be fabricated using PCL triol and poly(ethylene glycol) (PEG) as the soft segment and glycerol and hexamethylene diisocyanate (HDI) as the hard segment (Barrioni et al. 2015). PU polymers display better versatility and mechanical properties due to the presence of both hard and soft segments. The soft segment is usually composed of polycarbonate polyols, polyether or polyester, and add elastomeric features to the PU polymer backbone. Hard segments arise due to reaction between diamine/diol chain extender and diisocyanate and are responsible for the mechanical strength due to urethane linkage mediated hydrogen bonds (Barrioni et al. 2015). Figure 4.4 shows the synthesis of PU from its precursors, including polytetramethylene ether glycol (PTMG 1000), isophorone diisocyanate (IPDI), and 2,2-bis(hydroxymethyl) butyric acid (DMBA) via three steps: pre-polymerization, chain reaction and neutralization (Da et al. 2017). PUs can be easily tuned by varying the hard to soft segment ratio, molecular weight and chemical composition (Barrioni et al. 2015). PUs are effectively processed into fibrous scaffolds and films (Xu et al. 2015).

PCL is a biocompatible hydrolysable hydrophobic polymer with a slower degradation rate in the physiological microenvironment and high tensile strength and releases non-toxic products on degradation (Barrioni et al. 2015; Ren et al. 2017). PCL has a low melting point (55–60 °C) and offers good blend capability with other additives, enabling the fabrication of scaffolds with a specific shape. However, PCL lacks bioactivity that can be addressed by blending with bioactive materials like ceramics (Gao et al. 2016). In contrast, PEG is a hydrophilic polymer soluble in organic solvents and water, non-antigenic and non-immunogenic and releases non-toxic degradation molecules (Barrioni et al. 2015). PEG is widely reported to resist non-specific adsorption via its strong hydration layer and steric repulsion

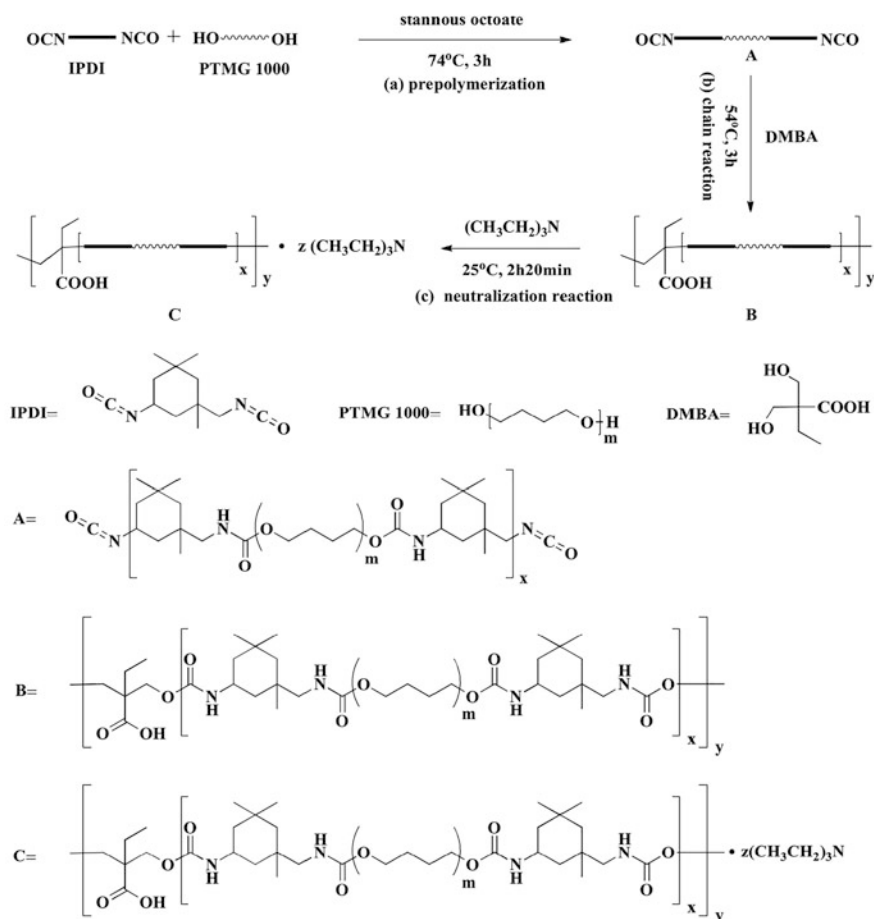


Fig. 4.4 Schematic showing the polyurethane synthesis via bulk polymerization of polytetramethylene ether glycol (PTMG 1000), isophorone diisocyanate (IPDI), and 2,2-bis(hydroxymethyl) butyric acid (DMBA) species. (Adapted with permission from *Acta biomaterials* 59 (2017): 45–57 (Da et al. 2017))

(Hasan and Pandey 2015). However, the poor stability of PEG in physiological environments limits its practical in vivo biomedical applications.

Aliphatic polyester family member PLA contains ester groups that make them vulnerable to hydrolytic degradation in the physiological microenvironment. This degradation leads to a decrease in the molecular weight due to ester bond cleavage in the polymeric chain and secretion of the lactic acid in the tissue vicinity, converted to carbon dioxide and water via the citric acid cycle (Cifuentes et al. 2016). The degradation of polyester polymers releases acidic products that cause tissue necrosis and enhance the immunological response at the site (Manavitehrani et al. 2015). The degradation of polyesters is complex and depends on the size, shape, molecular

weight, crystallinity, chirality and processing conditions (Vergnol et al. 2016). Biodegradable polymers like PLA and PGA hold promise in the field of dental and orthopaedic implants for bone replacement (Vergnol et al. 2016). Bioresorbable polymers exhibit an uncontrolled dissolution rate in the microenvironment, which increases due to a decrease in the pH because of the presence of inflammatory agents at the site. Bio-resorption might cause fibrous capsule formation and inflammation leading to implant failure (Vergnol et al. 2016). These drawbacks of the bioresorbable polymers is addressed by incorporating carbon nanotubes or ceramic materials, which decreases the degradation rate in the physiological environment (Cifuentes et al. 2016).

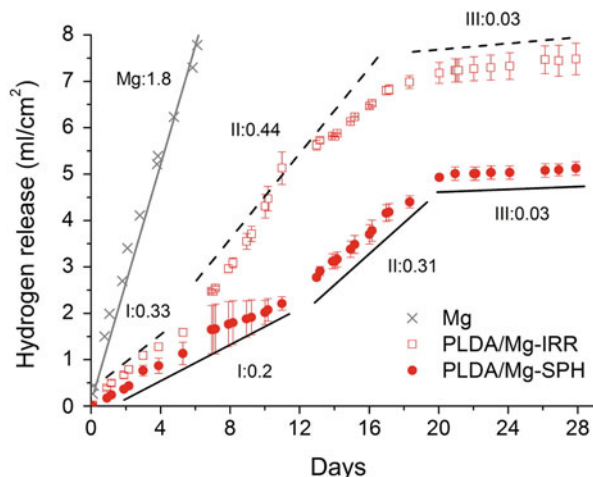
4.2.3 Ceramic Biomaterials

Ceramic biomaterials are composed of metallic/non-metallic elements and are classified based on physiological microenvironment behaviour. Ceramics are classified as bioinert ceramics, biodegradable/bioresorbable ceramics and bioactive ceramics (Hench 2015; Piconi 2017; Vallet-Regí and Salinas 2019; Monsees et al. 2017). The main constituent of the natural bone matrix is nano-hydroxyapatite (nano-HAP) $[(Ca_{10}(PO_4)_6(OH)_2)]$, which is applied extensively for fabricating biomimicking biomaterials for implant-related applications. HAP is also used as a bone substitute as it resembles the nanocrystals present in the natural bone (Gao et al. 2016). Morphology, crystallinity, size and surface properties of the nano-HAP can be easily tailored for the desired applications (Gao et al. 2016). The stronger bond formation capability of bioglass bioceramics makes it ideal for bone grafting applications because of its similarity with the inorganic component of the natural bone (Khoshakhlagh et al. 2017). Bioactive glass interacts with the body fluids and creates an alkaline environment due to salting out of bioactive glass (Vergnol et al. 2016). Bioglass was observed to precipitate the calcium phosphates in the physiological solutions (Khoshakhlagh et al. 2017). This leads to the formation of an apatite layer on the surface. Bio-ceramics based surface coatings are known to enhance the bioactivity of titanium and alloys (Rahmati et al. 2016). Ceramics such as Al_2O_3/Si_3N_4 are used in combination with metallic biomaterials to enhance the wear resistance of the artificial hip joints (Samanta et al. 2018). Ceramics are also widely utilized for the fabrication of orbital and dental implant (Alkharrat et al. 2018; Chen et al. 2016; Elsayed et al. 2017; Schierano et al. 2015; Baino 2018; Kammermeier et al. 2016). However, ceramics suffer from surface cracking under stress conditions, leading to implant failure (Toptan et al. 2016).

4.2.4 Composite Biomaterials

Composite biomaterials are composed of two or more materials to fabricate an implant material with desired/hybrid features (Ünal et al. 2016). This enables the design of biomaterials with combined features originated from the constituents of

Fig. 4.5 The degradation behaviour of the Mg/PLA composites as a function of the hydrogen release after immersion in PBS for a span of time where IRR means irregularly shaped and SPH refers to spherical particle composite. (Adapted with permission from *Acta biomaterialia* 32 (2016): 348–357 (Cifuentes et al. 2016))



composites. In turn, this addresses the limitations of individual materials to quite an extent. The composites are found to offer improved mechanical properties, wear-resistance and degradation behaviour, along with multifunctionality. Various composites are used for load-bearing, dental and orthopaedic implants along with drug delivery applications (Nemati et al. 2019; Yang et al. 2018; Vallittu 2018; Janićević et al. 2019).

The incorporation of hard ceramics particles with metals results in metal matrix composites (MMCs) which improves the wear-resistant and load-bearing properties of the composite; for example, the addition of boron carbide to titanium results in MMCs (Toptan et al. 2016). Cifuentes et al. investigated the degradation behaviour of the fabricated biodegradable composites with magnesium microparticles (10 wt %) reinforced polylactic acid (PLA) matrix. Mg reinforcement regulated the degradation behaviour of the PLA/Mg composites, and the shape of the microparticles controlled the degradation rate of the composite as shown in Fig. 4.5. Hydrogen release was faster for initial 5–6 days and started to stabilize after 20 days of immersion in the PBS solution. The reinforcement of spherical microparticles resulted in a slower degradation rate than the irregular shaped microparticles due to the lower surface area to volume ratio. Irregular microparticles resulted in surface cracks leading to a faster dissolution rate (Cifuentes et al. 2016). Manavitehrani et al. fabricated a composite of poly(propylene carbonate) and starch to eradicate the risk of harmful product leaching in the tissue vicinity. The fabricated composite properties were tuned by varying the concentration of the starch in the composite, as the compression strength varied depending on the starch content (0.2–33.9 MPa) (Manavitehrani et al. 2015).

Tuning the degradation rate of the composites is a prerequisite for the development of composite biomaterials (Cifuentes et al. 2016). The main disadvantage of the conventional bioresorbable material is the lack of bioactivity, low mechanical properties and uncontrolled degradation of the material in the physiological

environment (Yan et al. 2018; Bohnenberger and Schmid 2014). Healing of the bone can be met only when the degradation of the biomaterial and bone healing rate are in synchrony with each other. Further understanding of the degradation kinetics, especially the underlying mechanisms such as corrosion behaviour and matrix hydrolysis, led to tuning the composite properties for better bone healing (Cifuentes et al. 2016; Majoni and Chaparadza 2018). The incorporation of metallic biomaterial with bio-resorbable polymers (poly (α -hydroxy acid)) to form composites enhanced the degradation behaviour (Cifuentes et al. 2016). Besides, polymer properties can be enhanced by incorporating the polymeric matrix with bioactive ceramic fillers such as HAP and tricalcium phosphates. Bioactive ceramic fillers form a calcium phosphate layer on interaction with the body fluids that improve the bone-bonding ability. PLA properties were tuned by the addition of the bioactive mineral to form the organic-inorganic composites. Bioactive ceramic fillers decreased the degradation rate and neutralized the released lactic acid (Vergnol et al. 2016). Composite of bioglass/chitosan has been utilized as injectable bone substituent material due to better biological properties (Khoshakhlagh et al. 2017).

Nowadays, scaffolds with tunable properties based on hybrid composites developed that contains both synthetic and natural polymers. Natural polymers such as gelatin, chitosan and collagen simulate the natural physiological micro-structures, thus stimulating the attachment, proliferation and differentiation of the cells. Synthetic polymers aid the mechanical properties of the composites (Da et al. 2017). These nanofibrous scaffolds can be fabricated using many techniques such as dry spinning, wet spinning, electrospinning, phase separation and self-assembly (Ren et al. 2017). Hart et al. utilized a 3D printing technique to fabricate the composite based on the self-assembled supramolecular polymeric network impregnated with silica nanoparticles that were non-toxic towards the chondrogenic cell line (Hart et al. 2016). Ke et al. fabricated a guided bone regeneration membrane via electrospinning based on the PCL-gelatin hybrid nanofibres using genipin as the crosslinker. Acetic acid was used to make a homogeneous membrane by resolving the phase separation of PCL and gelatin. Nanofibrous membranes mimicked the natural ECM with high surface area and porosity that resulted in better cellular interactions. Surface properties were easily modified by varying the ratio of PCL to gelatin. Electrospun PCL/gelatin nanofibres are shown in Fig. 4.6. Nanofibres exhibited an average diameter of 200–600 nm and were relatively uniform and smooth. The introduction of gelatin resulted in a decrease in the viscosity of the spinning solution, leading to reduced diameters of nanofibres. Samples with 3:7 ratio of PCL to gelatin (P3G7 and cP3G7) resulted in the most densely packed nanofibres (Ren et al. 2017).

The nanocomposite (CCNWs-AgNPs) of silver nanoparticles (AgNPs) decorated on carboxylated CNWs (CCNWs) exhibited dual functions of improved mechanical strength and induced antimicrobial activity (Hasan et al. 2018b). In another study, a composite film of chitosan (CS) and polyvinylpyrrolidone (PVP) with incorporated cellulose nanowhiskers (CNWs) was explored for drug delivery application (Hasan et al. 2017). The integration of CNWs enhanced the thermal and mechanical

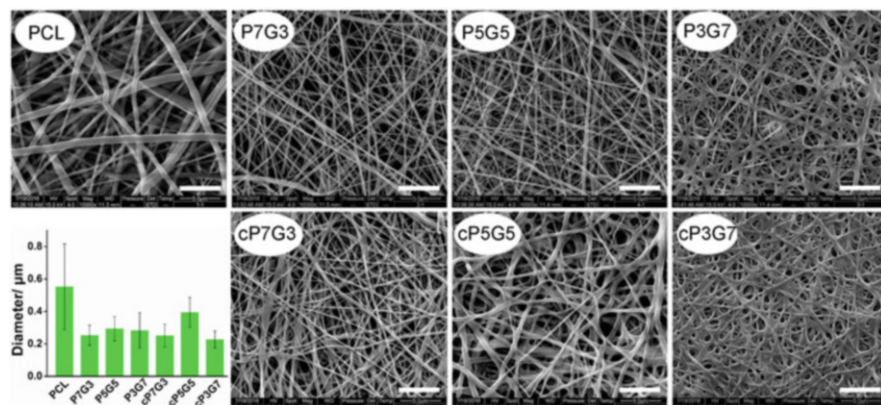


Fig. 4.6 Fabrication of the electrospun PCL/gelatin nanofibers with varying ratio of PCL to gelatin shown in the SEM images; cP7G3, cP5G5 and cP3G7 shows the change in the nanofibers post crosslinking with genipin where c before the name depicts the crosslinked nanofibers. (Adapted with permission from *Materials Science and Engineering: C* 78 (2017): 324–332 nanofibers (Ren et al. 2017))

properties of films. The prepared composite films also resulted in high biocompatibility with excellent antibacterial activities.

4.3 Biomaterials for Implant Fabrication

The implant site undergoes inflammation and migration, and subsequent proliferation of the immunological mediators occurs at the site. The immunological response is quite complex at the implantation site. Post implantation, the interactions of immune cells with the implant surfaces initiate the immunological cascade that ultimately determines the fate of the implant material. The integration and long-term implant survival depend on the immune system's initial response to the implant surface (Hotchkiss et al. 2016; Gilbert et al. 2015). Innate immune response agents, namely platelets, neutrophils and macrophages, migrate to the implant site and attract other immune cells by releasing cytokines and chemokines. This leads to phagocytosis of the damaged cells/tissues. Macrophages are the critical mediator of the initial immune response and inflammation at the site, along with normal tissue homeostasis maintenance (Hotchkiss et al. 2016). The prolonged immune response may damage the proximal healthy tissues due to chronic immune response (Shao et al. 2020). Moreover, collagen network formation and angiogenesis also occur as a part of the healing process. Loading of the inflammatory agents causes the generation of the reactive oxygen species (ROS) that impairs the proper wound healing (Geesala et al. 2016).

Cell response to the implant is determined by the surface properties such as wettability, surface topography and chemistry. Implant surface interactions with

the physiological surrounding further get complicated due to the calcium, phosphate and chloride ions in the microenvironment (Cifuentes et al. 2016). A study on the effect of surface roughness and wettability of implant material concluded that an increase in hydrophilicity and surface roughness resulted in synergism with increased osseointegration and reduced healing times, thus increasing the success rate (Hotchkiss et al. 2016). Thus, osteogenic differentiation is promoted by surface modification strategies, which enhance the wettability and surface roughness. Keeping the complex interfacial phenomenon at the implant surface, various features crucial for implant fabrication are discussed in this section.

4.3.1 Features of Ideal Biomaterials

The biomaterial selection for implant fabrication depends on the volume, size and shape of the affected site and the patient-related ailments for an ideal bone substitute material. Biocompatibility, osseointegration and biomechanics are among the main features of an ideal biomaterial (Adamzyk et al. 2016). Biocompatibility of the implant material determines the success of the material that dependent on the implant-tissue/bone interlocking, lack of micromotion, biofouling and bacterial invasion at the implant site (Kumar et al. 2015; Rahimizadeh et al. 2018; Cai et al. 2016). Few general criteria are listed below.

- (a) As cell-surface interactions are mediated by proteins, mimicking the ECM might enhance bone regeneration at a fast pace. ECM being a complex dynamic structure with various proteins (fibrin, collagen and elastin), hormones, signaling molecules, growth factors and glycosaminoglycans becomes challenging to be mimicked easily (Da et al. 2017). Instead of mimicking the natural ECM, it can be incorporated in biomaterials like an amalgamation of the ECM in synthetic polymers to prepare a scaffold (Da et al. 2017). Surfaces pre-adsorbed with adhesive proteins like fibronectin and collagen exhibit better cell adhesion and spreading (Hasan et al. 2018a; Hasan and Pandey 2020).
- (b) Surface microstructure, chemistry, topography and surface energy of the biomaterials determine the response of the fabricated implant material for response in the biological microenvironment (Bagherifard et al. 2016). Nano-/microscale surface roughness improves the osteoblast adhesion, proliferation and spreading along with deposition of the calcium-containing mineral and alkaline phosphatase production (Bagherifard et al. 2016). Implant surface and biomacromolecule interactions are also modulated by the grain size and crystal structure of the implant materials (Bagherifard et al. 2016).
- (c) Reconstruction and reorganization of functional tissues are required to recover the damaged bone tissue (Gao et al. 2016). Faster growth of cell and tissue on the damaged site is one of the prerequisites for developing the implant materials (Chakraborty et al. 2016). The development of biomaterial with surface properties comparable to the diseased/damaged site's tissues/bone amplifies the healing process. In this direction, selecting a biomaterial for implant

fabrication with no stress shielding prevents bone degradation/resorption at the site due to osteoclast activity (Rahimizadeh et al. 2018).

- (d) Bone-implant direct interactions occur only in the case of an implant without fibrous tissue growth at the site. Direct interaction leads to the spreading, growth and differentiation of the osteoblasts on the implant surface, thus assuring and eliminating the biofouling agents from the site.
- (e) Applications of the antimicrobial agents on the implant surface eliminate the pathogenic contamination at the site, thus contributing to the success of the implant (Parmar et al. 2018).

4.4 Applications

Biomaterials with desirable features are used for a varied number of applications in the biomedical field. This section discusses the applications of different biomaterials in the field of orthopaedic implants and tissue engineering.

4.4.1 Orthopaedic Implants

The advancements in surface engineering have enabled us to tune the physical, chemical, surface and biological properties of implant biomaterials. Bock et al. modified the properties of silicon carbide ceramic for orthopaedic implant application. Silicon carbide is unique as it possesses higher fracture toughness, strength, scratch resistance, biocompatibility and resistance to bacterial adhesion. Changes in the surface composition and properties of silicon carbide were investigated to vary the chemical, thermal and mechanical treatments. Thermal treatment in air/N₂ reduced the contact angle to $9 \pm 1^\circ$, compared to etched in hydrofluoric acid (HF) ($60 \pm 13^\circ$) and control sample ($66 \pm 12^\circ$). Surface roughness enhanced for the HF etched surface (341 nm) compared to control (336 nm) and decreased for air/N₂ thermal treated surfaces (287–296 nm) (Bock et al. 2015). Yazdi et al. investigated the effect of the biodegradable magnesium-based ternary alloy (Mg-Zn-Ca) on the adipose-derived behaviour of mesenchymal stem cells (ASCs) for orthopaedic applications. Alloying of Mg with Zn and Ca improved the corrosion resistance of alloys as compared to pure Mg. The viability and proliferation of the ASCs enhanced with no observed toxic effects of the Zn, Ca and Mg (Fazel Anvari-Yazdi et al. 2016).

To enhance the tissue growth at the implant site, Chakraborty et al. utilized a pulsed electro-deposition method for the coating of HAP and calcium hydrogen phosphate on the SS316 surface at different current densities from the diluted calcium phosphate solution (Chakraborty et al. 2016). A mixture of CAP and HAP were deposited using this method with 70% crystallinity. Lower current density (5 mA/cm^2) produced surfaces with 400–500 nm flakes, whereas the current density of 10 mA/cm^2 produced a highly porous surface with nano-crystallite size. The deposited coating consisted of nano-crystalline HAP, similar to the human bone

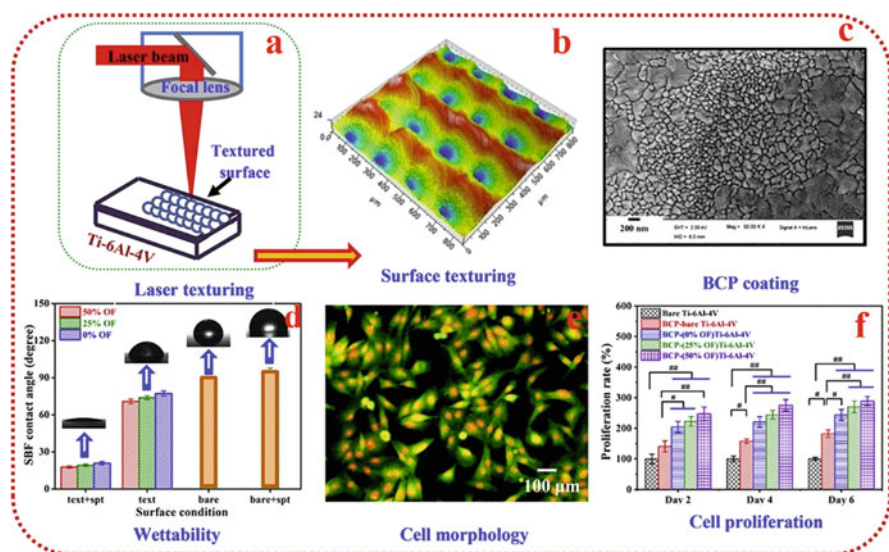


Fig. 4.7 Schematic showing the deposition of the calcium phosphate by laser texturing; (b, c) surface textures as analysed using a 2D profilometer and SEM; (d) contact angle measurement performed to determine the surface wettability; (e, f) cell adhesion and proliferation studies. (Adapted with permission from Journal of Alloys and Compounds 842 (2020): 155683 (Behera et al. 2020a))

(Chakraborty et al. 2016). In a study, biphasic calcium phosphate (BCP) film was deposited on bare as well as textured Ti6Al4V specimens by radio frequency (RF) sputtering (Behera et al. 2020a). The texturing resulted in the enhanced wettability of Ti6Al4V because of increased surface roughness from 94 nm to 1.84 μm. The water contact angle decreased from 89° to 71°. BCP deposited textured surfaces resulted in better adhesion and proliferation of osteoblast cells compared to bare Ti6Al4V and BCP deposited bare Ti6Al4V surfaces. This indicated improved cellular behaviour with increased roughness of surfaces with the same surface chemistry as displayed in Fig. 4.7 (Behera et al. 2020a).

In another study, BCP and titania (TiO₂) composite films were deposited on Ti6Al4V substrates by RF magnetron sputtering (Behera et al. 2020b). The wettability and bonding strength of composite films were improved with an increase in TiO₂ contents. Cell adhesion and proliferation significantly improved on coated Ti6Al4V as compared to the uncoated surface. In a separate investigation, Pradhan et al. investigated the effect of TiO₂ and niobium oxide (Nb₂O₅) on the biocompatibility enhancement of Ti6Al4V alloys for orthopaedic implants. The effect of the crystallinity on the surface bioactivity was evaluated by varying the heating temperature. Both Nb₂O₅ (525 °C) and TiO₂ (500 °C) showed CaP precipitation in the simulated body fluid, which is used as an indicator of bioactivity. Additionally, cell viabilities on both surfaces were above 100% (Pradhan et al. 2016).

4.4.2 Tissue Engineering

Usually, bone reconstruction is preferred using autogenous bone, but it involves increased operative procedures along with the morbidity of the donor. To address this issue, 3D scaffolds have been prepared for tissue engineering applications. Scaffolds with 3D configuration can be fabricated using electrospinning, phase separation, tomography mediated deposition and extrusion (Gao et al. 2016). Scaffold architecture regulates the cellular behaviour of attachment, migration, proliferation and differentiation (Gao et al. 2016).

Adamzyk et al. fabricated biocompatible 3D polyetherketoneketone (PEKK) scaffolds. It was observed that human MSCs were successfully differentiated into different cell lineages such as adipogenic, osteogenic and chondrogenic under suitable stimulations. The fabricated scaffold was conducive to human and ovine MSCs that is supporting attachment, growth and differentiation required for tissue engineering applications (Adamzyk et al. 2016). Goncalves et al. fabricated a 3D scaffold based on PCL and starch incorporated with iron oxide magnetic nanoparticles (MNPs) for tissue engineering applications. The effect of MNPs on the tenogenic differentiation capability of the adipose stem cells was investigated, and magnetic-driven stimulation was found to influence the stem cell response (Goncalves et al. 2016). The hierarchical structure of the aligned fibres was responsible for the functionality and mechanical properties of the tendon (Goncalves et al. 2016). In a separate study, Gao et al. fabricated a novel mussel-inspired nano-HAP using polydopamine as the template and was electrospun with PCL to form a nanofibrous scaffold for bone regeneration applications (Gao et al. 2016). This scaffold enhanced the adhesion, proliferation and spreading of the human mesenchymal stem cells (hMSCs) along with enhancement of the osteogenesis in the hMSCs (Gao et al. 2016). In another investigation, Cheng et al. fabricated a blood vessel mimicking scaffold of PCL and poly(lactide-*co*-glycolide) (PLGA) with a multilayered tubular structure. It contained an outer shrinkable PLGA layer and an inner expandable PCL layer for artificial blood vessels. These fabricated scaffolds retained the size/shape during the degradation over months due to expansion of the inner PCL layer and shrinkage of the outer PLGA layer as illustrated in Fig. 4.8 (Cheng et al. 2017).

Conventional soft tissue replacement suffers from many drawbacks, such as lack of mechanical integrity, fibrous capsular contraction and resilience. Tissue regeneration can be stimulated using resorbable scaffolds. Further, the optimal degradation rate is a crucial asset for scaffold fabrication as a higher degradation rate minimizes the foreign body interactions with the immunological agents. In contrast, a slower degradation rate allows cell infiltration and growth with mechanical support (Xu et al. 2015). In a study, Da et al. fabricated a 3D scaffold using small intestinal submucosa (SIS) containing bioactive ECM with PU for soft tissue engineering purpose. SIS is an acellular matrix with an intact natural composition that enhanced tissue regeneration and differentiation (Da et al. 2017). Geesala et al. fabricated a porous scaffold of PEG-PU with an interpenetrating polymer network for tissue repair enhancement and cell delivery. These fabricated scaffolds prevented the

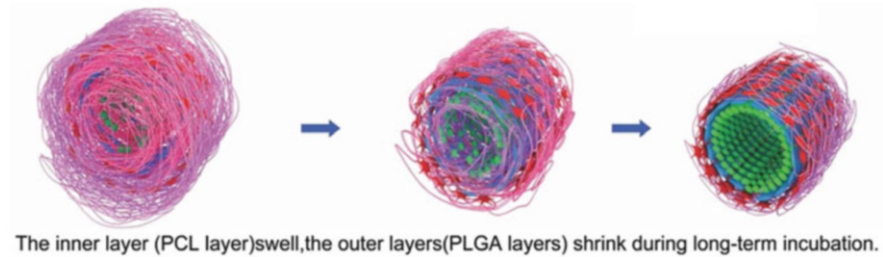


Fig. 4.8 Schematic showing the swelling behaviour of the cell-laden multilayered PCL-PLGA tubes. A long-term culture resulted in the shrinking of the outer PLGA layer and swelling of the inner PCL layer. (Adapted with permission from *Adv Mater*, 29 (2017), 1700171 (Cheng et al. 2017))

cellular oxidative stress at the injured sites and were highly cytocompatible, thermo-stable with better porosity and undergo biodegradation at an acidic pH of 5.8 (Geesala et al. 2016). In another study, Xu et al. fabricated a bioactive/biodegradable scaffold based on reduction sensitive elastomeric PUs to control the scaffold degradation rate according to an application. An antioxidant such as glutathione was incorporated in the scaffold for initializing and controlling the scaffold degradation rate, which was dependent on the disulphide amount in the PUs backbone (Xu et al. 2015).

In a study, Buyuksungur et al. fabricated PCL scaffolds based on fused deposition modelling. They modified them with poly(propylene fumarate) and nano-HAP to control the porosity, mechanical strength, osteoconductivity and surface wettability (Buyuksungur et al. 2017). These scaffolds were implanted in rabbits' femurs with and without seeding with rabbit Bone Marrow Stem Cells (BMSC). BMSC seeded scaffolds exhibited improved tissue regeneration after 4 and 8 weeks (Buyuksungur et al. 2017). In another study, Bassous et al. fabricated 3D printed Ti6Al4V-based Hive™ interbody fusion scaffolds to investigate the osteoblast adhesion and proliferation capability of the 3D scaffold along with the bone mineralization (Bassous et al. 2019). The surface roughness regulated the surface wettability (surface energy), which tuned the adhesion and proliferation of human fetal osteoblasts (hFOBs). The scaffolds also showed substantial deposition of calcium from metabolizing hFOBs, which restricted the attachment of bacteria. Further, pre-adsorption of casein proteins and the Hive™ substrates also restricted the bacterial attachment (Bassous et al. 2019).

4.5 Conclusion and Future Scope

In recent times, biomaterials have been extensively utilized in the field of biomedical engineering like orthopaedic and dental implants, hip and knee joints and many other load-bearing applications. Different metals and alloys, polymers, ceramics and composites are being explored as biomaterials. Various metallic implants such as

stainless steel, cobalt-chromium alloys, magnesium alloys and titanium alloys provide better mechanical and surface properties. However, they suffer from certain limitations, which are addressed by physical and chemical modification techniques. Tuning the surface properties of the implant materials is carried out to a certain degree depending on the desired applications. Polymers, both natural and synthetic, are utilized for a wide range of biomedical applications. Ease of tunability, manufacturability and availability make them the most versatile biomaterials. Polymers easily mimic the natural ECM of the body, thus enhancing the success rate of the fabricated implants. Many ceramic materials mimic the natural bone constituent and appear promising candidates for the fabrication of implants with bone-like surface properties. Composite material combines two or more biomaterials to suit the needs of the desired applications. This enables design of biomaterials with hybrid features.

Satisfactory progress has been made in the field of biomaterials development for different biomedical applications. However, certain issues and scopes need to be resolved for the betterment of implant development, like the fabrication of implants with reduced side effects and immunological responses. Biomaterials with self-antibacterial properties are needed to address the challenges of antimicrobial resistance and hospital-acquired infections. Thus, multifunctional biomaterials need to be designed for a given application. Cost and durability of the implants are a concern that need to be addressed simultaneously. Reducing the need for implant replacement and enhancing the osseointegration of implant with minimized micromotion are the properties that should to be incorporated in future implant materials.

References

- Adamzyk C, Kachel P, Hoss M, Gremse F, Modabber A, Holzle F, Tolba R, Neuss S, Lethaus B (2016) Bone tissue engineering using polyetherketoneketone scaffolds combined with autologous mesenchymal stem cells in a sheep calvarial defect model. *J Craniomaxillofac Surg* 44(8):985–994. <https://doi.org/10.1016/j.jcms.2016.04.012>
- Alemón B, Flores M, Ramírez W, Huegel JC, Broitman E (2015) Tribocorrosion behavior and ions release of CoCrMo alloy coated with a TiAlVCN/CNx multilayer in simulated body fluid plus bovine serum albumin. *Tribol Int* 81:159–168. <https://doi.org/10.1016/j.triboint.2014.08.011>
- Alkharat AR, Schmitter M, Rues S, Rammelsberg PJ (2018) Fracture behavior of all-ceramic, implant-supported, and tooth-implant-supported fixed dental prostheses. *Clin Oral Investig* 22(4):1663–1673
- Augustine R, Dan P, Sosnik A, Kalarikkal N, Tran N, Vincent B, Thomas S, Menu P, Rouxel D (2017) Electrospun poly(vinylidene fluoride-trifluoroethylene)/zinc oxide nanocomposite tissue engineering scaffolds with enhanced cell adhesion and blood vessel formation. *Nano Research* 10(10):3358–3376. <https://doi.org/10.1007/s12274-017-1549-8>
- Bagherifard S, Slawik S, Fernández-Pariente I, Pauly C, Mücklich F, Guagliano M (2016) Nano-scale surface modification of AISI 316 L stainless steel by severe shot peening. *Mater Des* 102: 68–77. <https://doi.org/10.1016/j.matdes.2016.03.162>
- Baino FJML (2018) Porous glass-ceramic orbital implants: a feasibility study. *Mater Lett* 212:12–15

- Barrioni BR, de Carvalho SM, Orefice RL, de Oliveira AA, Pereira Mde M (2015) Synthesis and characterization of biodegradable polyurethane films based on HDI with hydrolyzable crosslinked bonds and a homogeneous structure for biomedical applications. *Korean J Couns Psychother* 52:22–30. <https://doi.org/10.1016/j.msec.2015.03.027>
- Bassous NJ, Jones CL, Webster TJ (2019) 3-D printed Ti-6Al-4V scaffolds for supporting osteoblast and restricting bacterial functions without using drugs: Predictive equations and experiments. *Acta Biomater* 96:662–673. <https://doi.org/10.1016/j.actbio.2019.06.055>
- Behera SS, Das U, Kumar A, Bissoyi A, Singh AK (2017) Chitosan/TiO₂ composite membrane improves proliferation and survival of L929 fibroblast cells: Application in wound dressing and skin regeneration. *Int J Biol Macromol* 98:329–340. <https://doi.org/10.1016/j.ijbiomac.2017.02.017>
- Behera RR, Das A, Pamu D, Pandey LM, Sankar MR (2018a) Mechano-tribological properties and in vitro bioactivity of biphasic calcium phosphate coating on Ti-6Al-4 V. *J Mech Behav Biomed Mater* 86:143–157. <https://doi.org/10.1016/j.jmbbm.2018.06.020>
- Behera RR, Hasan A, Sankar MR, Pandey LM (2018b) Laser cladding with HA and functionally graded TiO₂-HA precursors on Ti-6Al-4 V alloy for enhancing bioactivity and cytocompatibility. *Surf Coat Technol* 352:420–436. <https://doi.org/10.1016/j.surfcoat.2018.08.044>
- Behera RR, Das A, Hasan A, Pamu D, Pandey LM, Sankar MR (2020a) Deposition of biphasic calcium phosphate film on laser surface textured Ti-6Al-4 V and its effect on different biological properties for orthopedic applications. *J Alloys Compd* 842:155683. <https://doi.org/10.1016/j.jallcom.2020.155683>
- Behera RR, Das A, Hasan A, Pamu D, Pandey LM, Sankar MR (2020b) Effect of TiO₂ addition on adhesion and biological behavior of BCP-TiO₂ composite films deposited by magnetron sputtering. *Mater Sci Eng C* 114:111033. <https://doi.org/10.1016/j.msec.2020.111033>
- Bian D, Zhou W, Liu Y, Li N, Zheng Y, Sun Z (2016) Fatigue behaviors of HP-Mg, Mg-Ca and Mg-Zn-Ca biodegradable metals in air and simulated body fluid. *Acta Biomater* 41:351–360. <https://doi.org/10.1016/j.actbio.2016.05.031>
- Biesiekierski A, Lin J, Li Y, Ping D, Yamabe-Mitarai Y, Wen C (2016) Investigations into Ti-(Nb, Ta)-Fe alloys for biomedical applications. *Acta Biomater* 32:336–347. <https://doi.org/10.1016/j.actbio.2015.12.010>
- Bobbert FSL, Lietaert K, Eftekhari AA, Pouran B, Ahmadi SM, Weinans H, Zadpoor AA (2017) Additively manufactured metallic porous biomaterials based on minimal surfaces: a unique combination of topological, mechanical, and mass transport properties. *Acta Biomater* 53:572–584. <https://doi.org/10.1016/j.actbio.2017.02.024>
- Bock RM, McEntire BJ, Bal BS, Rahaman MN, Boffelli M, Pezzotti G (2015) Surface modulation of silicon nitride ceramics for orthopaedic applications. *Acta Biomater* 26:318–330. <https://doi.org/10.1016/j.actbio.2015.08.014>
- Bohnenberger T, Schmid U (2014) Layer-by-layer approach for deposition of pure carbon nanotubes and composite films for use as electrodes in electrochemical devices. *Thin Solid Films* 565:116–121
- Bona AD, Pecho OE, Alessandretti RJM (2015) Zirconia as a dental biomaterial. *Materials* 8(8):4978–4991
- Borkowski L, Pawlowska M, Radzki RP, Bienko M, Polkowska I, Belcarz A, Karpinski M, Slowik T, Matuszewski L, Slosarczyk A, Ginalska G (2015) Effect of a carbonated HAP/beta-glucan composite bone substitute on healing of drilled bone voids in the proximal tibial metaphysis of rabbits. *Korean J Couns Psychother* 53:60–67. <https://doi.org/10.1016/j.msec.2015.04.009>
- Bose S, Banerjee D, Bandyopadhyay A (2017) Introduction to biomaterials and devices for bone disorders. In: *Materials for bone disorders*. Elsevier, Amsterdam, pp 1–27
- Buyuksungur S, Endogan Tanir T, Buyuksungur A, Bektas EI, Torun Kose G, Yucel D, Beyzadeoglu T, Cetinkaya E, Yenigun C, Tonuk E, Hasirci V, Hasirci N (2017) 3D printed poly(epsilon-caprolactone) scaffolds modified with hydroxyapatite and poly(propylene

- fumarate) and their effects on the healing of rabbit femur defects. *Biomater Sci* 5(10):2144–2158. <https://doi.org/10.1039/c7bm00514h>
- Cai XY, Li NN, Chen JC, Kang ET, Xu LQ (2016) Biomimetic anchors applied to the host-guest antifouling functionalization of titanium substrates. *J Colloid Interface Sci* 475:8–16. <https://doi.org/10.1016/j.jcis.2016.04.034>
- Chakraborty R, Sengupta S, Saha P, Das K, Das S (2016) Synthesis of calcium hydrogen phosphate and hydroxyapatite coating on SS316 substrate through pulsed electrodeposition. *Korean J Couns Psychother* 69:875–883. <https://doi.org/10.1016/j.msec.2016.07.044>
- Chen Q, Thouas GA (2015) Metallic implant biomaterials. *Mater Sci Eng R Rep* 87:1–57
- Chen Y-W, Moussi J, Drury JL, Wataha JC (2016) Zirconia in biomedical applications. *Expert Rev Med Devices* 13(10):945–963
- Cheng S, Jin Y, Wang N, Cao F, Zhang W, Bai W, Zheng W, Jiang X (2017) Self-adjusting, polymeric multilayered roll that can keep the shapes of the blood vessel scaffolds during biodegradation. *Adv Mater* 29(28):1700171. <https://doi.org/10.1002/adma.201700171>
- Cifuentes SC, Gavilan R, Lieblich M, Benavente R, Gonzalez-Carrasco JL (2016) In vitro degradation of biodegradable polylactic acid/magnesium composites: relevance of Mg particle shape. *Acta Biomater* 32:348–357. <https://doi.org/10.1016/j.actbio.2015.12.037>
- Correa DRN, Kuroda PAB, Lourenço ML, Fernandes CJC, Buzalaf MAR, Zambuzzi WF, Grandini CR (2018) Development of Ti-15Zr-Mo alloys for applying as implantable biomedical devices. *J Alloys Compd* 749:163–171. <https://doi.org/10.1016/j.jallcom.2018.03.308>
- Costa BC, Tokuhara CK, Rocha LA, Oliveira RC, Lisboa-Filho PN, Costa Pessoa J (2019) Vanadium ionic species from degradation of Ti-6Al-4 V metallic implants: In vitro cytotoxicity and speciation evaluation. *Korean J Couns Psychother* 96:730–739. <https://doi.org/10.1016/j.msec.2018.11.090>
- Cui Z, Yang B, Li R-KJE (2016) Application of biomaterials in cardiac repair and regeneration. *Engineering* 2(1):141–148
- Da L, Gong M, Chen A, Zhang Y, Huang Y, Guo Z, Li S, Li-Ling J, Zhang L, Xie H (2017) Composite elastomeric polyurethane scaffolds incorporating small intestinal submucosa for soft tissue engineering. *Acta Biomater* 59:45–57. <https://doi.org/10.1016/j.actbio.2017.05.041>
- Dangas GD, Weitz JI, Giustino G, Makkar R, Mehran RJ (2016) Prosthetic heart valve thrombosis. *J Am Coll Cardiol* 68(24):2670–2689
- Davenport Huyer L, Zhang B, Korolj A, Montgomery M, Drecun S, Conant G, Zhao Y, Reis L, Radisic M (2016) Highly elastic and moldable polyester biomaterial for cardiac tissue engineering applications. *ACS Biomater Sci Eng* 2(5):780–788
- De Santis R, Guarino V, Ambrosio L (2019) Composite biomaterials for bone repair. In: *Bone repair biomaterials*. Elsevier, Amsterdam, pp 273–299
- dos Santos V, Brandalise RN, Savaris M (2017) Biomaterials: characteristics and properties. In: *Engineering of biomaterials*. Springer, New York, pp 5–15
- Elsayed A, Wille S, Al-Akhali M, Kern M (2017) Comparison of fracture strength and failure mode of different ceramic implant abutments. *J Prosthet Dent* 117(4):499–506
- Fazel Anvari-Yazdi A, Tahermanesh K, Hadavi SM, Talaei-Khozani T, Razmkhah M, Abed SM, Mohtasebi MS (2016) Cytotoxicity assessment of adipose-derived mesenchymal stem cells on synthesized biodegradable Mg-Zn-Ca alloys. *Korean J Couns Psychother* 69:584–597. <https://doi.org/10.1016/j.msec.2016.07.016>
- Gao X, Song J, Ji P, Zhang X, Li X, Xu X, Wang M, Zhang S, Deng Y, Deng F, Wei S (2016) Polydopamine-templated hydroxyapatite reinforced polycaprolactone composite nanofibers with enhanced cytocompatibility and osteogenesis for bone tissue engineering. *ACS Appl Mater Interfaces* 8(5):3499–3515. <https://doi.org/10.1021/acsami.5b12413>
- Geesala R, Bar N, Dhoke NR, Basak P, Das A (2016) Porous polymer scaffold for on-site delivery of stem cells--protects from oxidative stress and potentiates wound tissue repair. *Biomaterials* 77:1–13. <https://doi.org/10.1016/j.biomaterials.2015.11.003>

- Gilbert JL, Sivan S, Liu Y, Kocagoz SB, Arnholt CM, Kurtz SM (2015) Direct in vivo inflammatory cell-induced corrosion of CoCrMo alloy orthopedic implant surfaces. *J Biomed Mater Res A* 103(1):211–223. <https://doi.org/10.1002/jbm.a.35165>
- Ginebra M-P, Espanol M, Maazouz Y, Bergez V, Pastorino D (2018) Bioceramics and bone healing. *EFORT Open Rev* 3(5):173–183
- Goncalves AI, Rodrigues MT, Carvalho PP, Banobre-Lopez M, Paz E, Freitas P, Gomes ME (2016) Exploring the potential of starch/polycaprolactone aligned magnetic responsive scaffolds for tendon regeneration. *Adv Healthc Mater* 5(2):213–222. <https://doi.org/10.1002/adhm.201500623>
- Guo B, Ma PX (2018) Conducting polymers for tissue engineering. *Biomacromolecules* 19(6):1764–1782. <https://doi.org/10.1021/acs.biomac.8b00276>
- Hadjesfandiari N, Weinhart M, Kizhakkedathu JN, Haag R, Brooks DE (2018) Development of antifouling and bactericidal coatings for platelet storage bags using dopamine chemistry. *Adv Healthc Mater* 7(5):1700839
- Harb SV, Uvida MC, Trentin A, Oliveira Lobo A, Webster TJ, Pulcinelli SH, Santilli CV, Hammer P (2020) PMMA-silica nanocomposite coating: effective corrosion protection and biocompatibility for a Ti6Al4V alloy. *Korean J Couns Psychother* 110:110713. <https://doi.org/10.1016/j.msec.2020.110713>
- Hart LR, Li S, Sturgess C, Wildman R, Jones JR, Hayes W (2016) 3D printing of biocompatible supramolecular polymers and their composites. *ACS Appl Mater Interfaces* 8(5):3115–3122. <https://doi.org/10.1021/acsami.5b10471>
- Hasan A, Pandey LM (2015) Polymers, surface-modified polymers, and self assembled monolayers as surface-modifying agents for biomaterials. *Polym-Plast Technol Eng* 54(13):1358–1378
- Hasan A, Pandey LM (2020) Surface modification of Ti6Al4V by forming hybrid self-assembled monolayers and its effect on collagen-I adsorption, osteoblast adhesion and integrin expression. *Appl Surf Sci* 505:144611. <https://doi.org/10.1016/j.apsusc.2019.144611>
- Hasan A, Waibhaw G, Tiwari S, Dharmalingam K, Shukla I, Pandey LM (2017) Fabrication and characterization of chitosan, polyvinylpyrrolidone, and cellulose nanowhiskers nanocomposite films for wound healing drug delivery application. *J Biomed Mater Res A* 105(9):2391–2404. <https://doi.org/10.1002/jbm.a.36097>
- Hasan A, Saxena V, Pandey LM (2018a) Surface functionalization of Ti6Al4V via self-assembled monolayers for improved protein adsorption and fibroblast adhesion. *Langmuir* 34(11):3494–3506. <https://doi.org/10.1021/acs.langmuir.7b03152>
- Hasan A, Waibhaw G, Saxena V, Pandey LM (2018b) Nano-biocomposite scaffolds of chitosan, carboxymethyl cellulose and silver nanoparticle modified cellulose nanowhiskers for bone tissue engineering applications. *Int J Biol Macromol* 111:923–934. <https://doi.org/10.1016/j.ijbiomac.2018.01.089>
- Hayes JS, Kloppel H, Wieling R, Sprecher CM, Richards RG (2018) Influence of steel implant surface microtopography on soft and hard tissue integration. *J Biomed Mater Res B Appl Biomater* 106(2):705–715. <https://doi.org/10.1002/jbm.b.33878>
- Hench LL (2015) The future of bioactive ceramics. *J Mater Sci Mater Med* 26(2):86
- Hotchkiss KM, Reddy GB, Hyzy SL, Schwartz Z, Boyan BD, Olivares-Navarrete R (2016) Titanium surface characteristics, including topography and wettability, alter macrophage activation. *Acta Biomater* 31:425–434. <https://doi.org/10.1016/j.actbio.2015.12.003>
- Hu C, Ashok D, Nisbet DR, Gautam VJB (2019) Bioinspired surface modification of orthopedic implants for bone tissue engineering. *Biomaterials* 219:119366
- Jain A, Bajpai V (2019) Mechanical micro-texturing and characterization on Ti6Al4V for the improvement of surface properties. *Surf Coat Technol* 380:125087. <https://doi.org/10.1016/j.surfcoat.2019.125087>
- Jamrozik MK, Szweczenko J, Basłaga M, Nowinska K (2015) Technological capabilities of surface layers formation on implant made of Ti-6Al-4V ELI alloy. *Acta Bioeng Biomech* 17(1):31–37. <https://doi.org/10.5277/ABB-00065-2014-03>

- Jang Y, Tan Z, Jurey C, Xu Z, Dong Z, Collins B, Yun Y, Sankar J (2015) Understanding corrosion behavior of Mg-Zn-Ca alloys from subcutaneous mouse model: effect of Zn element concentration and plasma electrolytic oxidation. *Korean J Couns Psychother* 48:28–40. <https://doi.org/10.1016/j.msec.2014.11.029>
- Janićijević Ž, Ninkov M, Kataranovski M, Radovanović F (2019) Poly (DL-lactide-co-ε-caprolactone)/poly (acrylic acid) composite implant for controlled delivery of cationic drugs. *Macromol Biosci* 19(2):1800322
- Jemat A, Ghazali MJ, Razali M, Otsuka Y (2015) Surface modifications and their effects on titanium dental implants. *Biomed Res Int* 2015:791725
- Kammermeier A, Rosentritt M, Behr M, Schneider-Feyrer S, Preis V (2016) In vitro performance of one-and two-piece zirconia implant systems for anterior application. *J Dent* 53:94–101
- Khanlou HM, Ang BC, Barzani MM, Silakhori M, Talebian S (2015) Prediction and characterization of surface roughness using sandblasting and acid etching process on new non-toxic titanium biomaterial: adaptive-network-based fuzzy inference system. *Neural Comput Appl* 26(7):1751–1761
- Khoshakhlagh P, Rabiee SM, Kiaee G, Heidari P, Miri AK, Moradi R, Moztaaradeh F, Ravarian R (2017) Development and characterization of a bioglass/chitosan composite as an injectable bone substitute. *Carbohydr Polym* 157:1261–1271. <https://doi.org/10.1016/j.carbpol.2016.11.003>
- Ko J, Cho K, Han SW, Sung HK, Baek SW, Koh W-G, Yoon JSJC, Biointerfaces SB (2017) Hydrophilic surface modification of poly (methyl methacrylate)-based ocular prostheses using poly (ethylene glycol) grafting. *Colloids Surf B Biointerfaces* 158:287–294
- Kondyurina I, Nechitailo G, Svistkov A, Kondyurin A, Bilek M (2015) Urinary catheter with polyurethane coating modified by ion implantation. *Nucl Instrum Methods B* 342:39–46
- Kumar D, Nadeem Akhtar S, Kumar Patel A, Ramkumar J, Balani K (2015) Tribological performance of laser peened Ti-6Al-4 V. *Wear* 322–323:203–217. <https://doi.org/10.1016/j.wear.2014.11.016>
- Li J, Hastings G (2016) Oxide bioceramics: inert ceramic materials in medicine and dentistry. In: *Handbook of biomaterial properties*. Springer, New York, pp 339–352
- López-Saucedo F, Flores-Rojas GG, López-Saucedo J, Magariños B, Alvarez-Lorenzo C, Concheiro A, E B (2018) Antimicrobial silver-loaded polypropylene sutures modified by radiation-grafting. *Eur Polym J* 100:290–297
- Lucas EJ, Baxter C, Singh C, Mohamed AZ, Li B, Zhang J, Jayanthi VR, Koff SA, VanderBrink B, Justice SS (2016) Comparison of the microbiological milieu of patients randomized to either hydrophilic or conventional PVC catheters for clean intermittent catheterization. *J Pediatr Urol* 12(3):172.e171–172.e178
- Majoni S, Chaparadza A (2018) Thermal degradation kinetic study of polystyrene/organophosphate composite. *Thermochim Acta* 662:8–15
- Manavitehrani I, Fathi A, Wang Y, Maitz PK, Dehghani F (2015) Reinforced poly(propylene carbonate) composite with enhanced and tunable characteristics, an alternative for poly(lactic Acid). *ACS Appl Mater Interfaces* 7(40):22421–22430. <https://doi.org/10.1021/acsami.5b06407>
- Mondal D, Griffith M, Venkatraman SS (2016) Polycaprolactone-based biomaterials for tissue engineering and drug delivery: current scenario and challenges. *Int J Polym Mater Polym Biomaterials* 65(5):255–265
- Monsees TK, Ak Azem F, Cotrut CM, Braic M, Abdulgader R, Pana I, Birlik I, Kiss A, Booyesen R, Vladescu A (2017) Biodegradable ceramics consisting of hydroxyapatite for orthopaedic implants. *Coatings* 7(11):184
- Narayanan G, Vernekar VN, Kuyinu EL, Laurencin CT (2016) Poly (lactic acid)-based biomaterials for orthopaedic regenerative engineering. *Adv Drug Deliv Rev* 107:247–276
- Neacsu P, Gordin DM, Mitran V, Gloriant T, Costache M, Cimpean A (2015) In vitro performance assessment of new beta Ti-Mo-Nb alloy compositions. *Korean J Couns Psychother* 47:105–113. <https://doi.org/10.1016/j.msec.2014.11.023>

- Nemati S, Hosseini HA, Hashemzadeh A, Mohajeri M, Sabouri Z, Darroudi M, Oskuee RK (2019) Cytotoxicity and photocatalytic applications of biosynthesized ZnO nanoparticles by Rheum turketicum rhizome extract. *Mater Res Express* 6(12):125016
- Ning C, Zhou L, Tan G (2016) Fourth-generation biomedical materials. *Mater Today* 19(1):2–3. <https://doi.org/10.1016/j.mattod.2015.11.005>
- Nnamchi PS (2016) First principles studies on structural, elastic and electronic properties of new Ti Mo Nb Zr alloys for biomedical applications. *Mater Des* 108:60–67. <https://doi.org/10.1016/j.matdes.2016.06.066>
- Nnamchi PS, Obayi CS, Todd I, Rainforth MW (2016) Mechanical and electrochemical characterisation of new Ti-Mo-Nb-Zr alloys for biomedical applications. *J Mech Behav Biomed Mater* 60:68–77. <https://doi.org/10.1016/j.jmbbm.2015.12.023>
- Nouri A, Wen C (2015) Introduction to surface coating and modification for metallic biomaterials. In: *Surface coating and modification of metallic biomaterials*. Elsevier, Amsterdam, pp 3–60
- Pacelli S, Manoharan V, Desalvo A, Lomis N, Jodha KS, Prakash S, Paul AJ (2016) Tailoring biomaterial surface properties to modulate host-implant interactions: implication in cardiovascular and bone therapy. *J Mater Chem B* 4(9):1586–1599
- Parmar V, Kumar A, Mani Sankar M, Datta S, Vijaya Prakash G, Mohanty S, Kalyanasundaram D (2018) Oxidation facilitated antimicrobial ability of laser micro-textured titanium alloy against gram-positive *Staphylococcus aureus* for biomedical applications. *J Laser Appl* 30(3):032001. <https://doi.org/10.2351/1.5039860>
- Piconi C (2017) Bioinert ceramics: state-of-the-art. In: *Key engineering materials*. Trans Tech Publications, Stafa-Zurich, pp 3–13
- Pradhan D, Wren AW, Mixture ST, Mellott NP (2016) Investigating the structure and biocompatibility of niobium and titanium oxides as coatings for orthopedic metallic implants. *Korean J Couns Psychother* 58:918–926. <https://doi.org/10.1016/j.msec.2015.09.059>
- Rahimizadeh A, Nourmohammadi Z, Arabnejad S, Tanzer M, Pasini D (2018) Porous architected biomaterial for a tibial-knee implant with minimum bone resorption and bone-implant interface micromotion. *J Mech Behav Biomed Mater* 78:465–479
- Rahmati B, Sarhan AAD, Zalnezhad E, Kamiab Z, Dabbagh A, Choudhury D, Abas WABW (2016) Development of tantalum oxide (Ta-O) thin film coating on biomedical Ti-6Al-4V alloy to enhance mechanical properties and biocompatibility. *Ceram Int* 42(1):466–480. <https://doi.org/10.1016/j.ceramint.2015.08.133>
- Ren Y, Zhou H, Nabiyouni M, Bhaduri SB (2015) Rapid coating of AZ31 magnesium alloy with calcium deficient hydroxyapatite using microwave energy. *Korean J Couns Psychother* 49:364–372. <https://doi.org/10.1016/j.msec.2015.01.046>
- Ren K, Wang Y, Sun T, Yue W, Zhang H (2017) Electrospun PCL/gelatin composite nanofiber structures for effective guided bone regeneration membranes. *Korean J Couns Psychother* 78: 324–332. <https://doi.org/10.1016/j.msec.2017.04.084>
- Samanta A, Bhattacharya M, Ratha I, Chakraborty H, Datta S, Ghosh J, Bysakh S, Sreemany M, Rane R, Joseph A, Mukherjee S, Kundu B, Das M, Mukhopadhyay AK (2018) Nano- and micro-tribological behaviours of plasma nitrided Ti6Al4V alloys. *J Mech Behav Biomed Mater* 77:267–294. <https://doi.org/10.1016/j.jmbbm.2017.09.013>
- Santos PF, Ninomi M, Cho K, Nakai M, Liu H, Ohtsu N, Hirano M, Ikeda M, Narushima T (2015) Microstructures, mechanical properties and cytotoxicity of low cost beta Ti-Mn alloys for biomedical applications. *Acta Biomater* 26:366–376. <https://doi.org/10.1016/j.actbio.2015.08.015>
- Schierano G, Mussano F, Faga MG, Menicucci G, Manzella C, Sabione C, Genova T, MMV D, Peirone B, Cassenti A (2015) An alumina toughened zirconia composite for dental implant application: in vivo animal results. *Biomed Res Int* 2015:157360
- Shahemi N, Liza S, Abbas A, Merican AM (2018) Long-term wear failure analysis of uhmwpe acetabular cup in total hip replacement. *J Mech Behav Biomed Mater* 87:1–9

- Shao D, Li K, You M, Liu S, Hu T, Huang L, Xie Y, Zheng X (2020) Macrophage polarization by plasma sprayed ceria coatings on titanium-based implants: cerium valence state matters. *Appl Surf Sci* 504:144070. <https://doi.org/10.1016/j.apsusc.2019.144070>
- Shen X, Su F, Dong J, Fan Z, Duan Y, Li S (2015) In vitro biocompatibility evaluation of bioresorbable copolymers prepared from L-lactide, 1, 3-trimethylene carbonate, and glycolide for cardiovascular applications. *J Biomater Sci Polym Ed* 26(8):497–514. <https://doi.org/10.1080/09205063.2015.1030992>
- Tan F, Zhu Y, Ma Z, Al-Rubeai M (2020) Recent advances in the implant-based drug delivery in otorhinolaryngology. *Acta Biomater* 108:46–55. <https://doi.org/10.1016/j.actbio.2020.04.012>
- Tang H, Gao Y (2016) Preparation and characterization of hydroxyapatite containing coating on AZ31 magnesium alloy by micro-arc oxidation. *J Alloys Compd* 688:699–708. <https://doi.org/10.1016/j.jallcom.2016.07.079>
- Toptan F, Rego A, Alves AC, Guedes A (2016) Corrosion and tribocorrosion behavior of Ti-B4C composite intended for orthopaedic implants. *J Mech Behav Biomed Mater* 61:152–163. <https://doi.org/10.1016/j.jmbbm.2016.01.024>
- Ünal M, Akkuş O, Marcus RE (2016) Fundamentals of musculoskeletal biomechanics. In: *Musculoskeletal research and basic science*. Springer, New York, pp 15–36
- Vallet-Regí M, Salinas AJ (2019) Ceramics as bone repair materials. In: *Bone repair biomaterials*. Elsevier, Amsterdam, pp 141–178
- Vallittu PK (2018) Fiber-reinforced composites for implant applications. *J Prosthet Dent* 5(3):194–201
- Van Hooreweder B, Apers Y, Lietaert K, Kruth JP (2017) Improving the fatigue performance of porous metallic biomaterials produced by selective laser melting. *Acta Biomater* 47:193–202. <https://doi.org/10.1016/j.actbio.2016.10.005>
- Vergnol G, Ginsac N, Rivory P, Meille S, Chenal JM, Balvay S, Chevalier J, Hartmann DJ (2016) In vitro and in vivo evaluation of a polylactic acid-bioactive glass composite for bone fixation devices. *J Biomed Mater Res B Appl Biomater* 104(1):180–191. <https://doi.org/10.1002/jbm.b.33364>
- Wang G, Li J, Lv K, Zhang W, Ding X, Yang G, Liu X, Jiang X (2016) Surface thermal oxidation on titanium implants to enhance osteogenic activity and in vivo osseointegration. *Sci Rep* 6: 31769
- Xie F, He X, Lv Y, Wu M, He X, Qu X (2015) Selective laser sintered porous Ti–(4–10)Mo alloys for biomedical applications: Structural characteristics, mechanical properties and corrosion behaviour. *Corros Sci* 95:117–124. <https://doi.org/10.1016/j.corsci.2015.03.005>
- Xu C, Huang Y, Wu J, Tang L, Hong Y (2015) Triggerable degradation of polyurethanes for tissue engineering applications. *ACS Appl Mater Interfaces* 7(36):20377–20388. <https://doi.org/10.1021/acsami.5b06242>
- Yadav VS, Kumar A, Das A, Pamu D, Pandey LM, Sankar MR (2020) Degradation kinetics and surface properties of bioceramic hydroxyapatite coated AZ31 magnesium alloys for biomedical applications. *Mater Lett* 270:127732. <https://doi.org/10.1016/j.matlet.2020.127732>
- Yan H, Huang D, Chen X, Liu H, Feng Y, Zhao Z, Dai Z, Zhang X, Lin QJPB (2018) A novel and homogeneous scaffold material: preparation and evaluation of alginate/bacterial cellulose nanocrystals/collagen composite hydrogel for tissue engineering. *Polym Bull* 75(3):985–1000
- Yang H, Qu X, Lin W, Wang C, Zhu D, Dai K, Zheng Y (2018) In vitro and in vivo studies on zinc-hydroxyapatite composites as novel biodegradable metal matrix composite for orthopedic applications. *Acta Biomater* 71:200–214
- Zhang J, Gao X, Kan J, Ge Z, Han L, Lu S, Tian N, Lin S, Lu Q, Wu X (2018) Intravascular ultrasound versus angiography-guided drug-eluting stent implantation: the ULTIMATE trial. *J Am Coll Cardiol* 72(24):3126–3137
- Zhao X, Irvine SA, Agrawal A, Cao Y, Lim PQ, Tan SY, Venkatraman SS (2015) 3D patterned substrates for bioartificial blood vessels—the effect of hydrogels on aligned cells on a biomaterial surface. *Acta Biomater* 26:159–168

Part II

Surface Engineering of Metallic Biomaterials



Overview of Current Additive Manufacturing Technologies for Titanium Bioimplants

5

Vicky Subhash Telang, Rakesh Pemmada, Seeram Ramakrishna, Puneet Tandon, and Himansu Sekhar Nanda

Abstract

Titanium (Ti) and its alloys are the common biometals used for the manufacturing of various bioimplants for orthopedic and dental applications. These biometals are having fascinating physical and biological properties, such as high mechanical strength, high corrosion resistance and excellent biocompatibility. Commercially available pure titanium (CP-Ti) and $(\alpha + \beta)$ Ti-6Al-4 V are few typical Ti-commercially available biometals used for manufacturing of Ti-bioimplants. Recently, β -titanium with low modulus and innocuous elemental composition has been evolved as a new group of Ti for manufacturing bioimplants for specific orthopedic applications. Ti-bioimplants are manufactured via non-economic and

V. S. Telang

Biomedical Engineering and Technology Laboratory, Discipline of Mechanical Engineering, PDPM Indian Institute of Information Technology, Design and Manufacturing, Jabalpur, Madhya Pradesh, India

deLOGIC Laboratory, Discipline of Mechanical Engineering, PDPM Indian Institute of Information Technology, Design and Manufacturing, Jabalpur, Madhya Pradesh, India

R. Pemmada · H. S. Nanda (✉)

Biomedical Engineering and Technology Laboratory, Discipline of Mechanical Engineering, PDPM Indian Institute of Information Technology, Design and Manufacturing, Jabalpur, Madhya Pradesh, India

e-mail: himansu@iiitdmj.ac.in

S. Ramakrishna

Centre for Nanofibers and Nanotechnology, Department of Mechanical Engineering, National University of Singapore, Singapore, Singapore

P. Tandon

deLOGIC Laboratory, Discipline of Mechanical Engineering, PDPM Indian Institute of Information Technology, Design and Manufacturing, Jabalpur, Madhya Pradesh, India

e-mail: ptandon@iiitdmj.ac.in

conventional subtractive machining processes. Advanced manufacturing techniques, such as additive manufacturing (AM) provides an ideal platform to investigate and create more customized and complex bioimplant with porous structures. In addition, AM manufactured bioimplants have shown enhanced osseointegration over the preceding generation Ti-bioimplants. This chapter reviews the current AM-technologies for manufacturing of Ti-bioimplants with an emphasis on processing parameters, developed microstructure and associated mechanical properties of the final product. The chapter also highlights the effect of porous structure on the mechanical performances of the manufactured Ti-bioimplants.

Keywords

Additive manufacturing · Bioimplants · Ti and Ti-alloys · Mechanical properties · Porous structure · Orthopedic

5.1 Introduction

Biomedical materials are amalgamated products of natural or artificial materials. These materials are mostly used as the support structures, for example, bioimplants for orthopedic fractures and resorbable materials or porous scaffolds for regenerative therapies (Liu et al. 2015). Mechanical stability of the bioimplants is very crucial for their specific application, for example, orthopedic fractures and dental implants. In some cases, bioimplants need to be flexible, with high plasticity and adequate rigidity to allow the necessary expansion like cardiac stents and breast implants. Orthopedic bioimplants are having high mechanical strength and meant to withstand continuous loading. Therefore, materials involved should be either metallic (biometals) or any other material with similar materials and mechanical properties. In this context, biometals have high corrosion resistance and excellent mechanical properties, exhibit biocompatible characteristics such as non-toxicity, non-immunogenicity and non-allergic properties (Hermawan et al. 2011). In some cases, biometals are prone to corrosion due to the presence of various types of proteins, amino acids and inorganic ions in the blood. The released metal ions from the implanted materials may combine with the other biologically available molecules to form metal oxides, metal hydroxides and other chemical compounds to cause further cytotoxicity, allergic reactions, cancer and so on (Hanawa 2004).

The commonly used biometals are usually Ti and Ti-alloys, stainless steel (SS) and cobalt-chromium (Co-Cr) alloys. Table 5.1 summarizes the properties and application of these common biometals in bioimplant manufacturing. In the past few years, 316 L type of SS and Ti as well as Ti-alloys are used for manufacturing bioimplants for orthopedic applications. The application of the common biometals ranges from cardiovascular (stents) to orthopedic (in the form of screws, plates, rods, pins, etc.) (Taljanovic et al. 2003; Mantripragada et al. 2013; Bordji et al. 1996). Due to the poor fatigue strength, SS is commonly used as

Table 5.1 Comparison of mechanical properties and applications of Ti-biometal with other biomaterials (Trevisan et al. 2018)

Properties and applications	Material			
	Pure Ti	Ti-alloy (Ti-6Al-4 V)	Stainless steel 316 L	Co-Cr alloys
Elastic modulus (Gpa)	110	116	193	232
Yield strength (Mpa)	485	795	190	190
Ultimate tensile strength (Mpa)	550	860	490	490
Cardiovascular	Yes	Yes	Yes	Yes
Orthopaedic	Yes	Yes	Yes	Yes
Craniofacial	Yes	Yes	Yes	Yes

non-permanent bioimplants. Earlier, Co-Cr alloys were preferred over SS for permanent bioimplants due to their high corrosion resistance properties. However, Co-Cr alloys are known to release the ions in vivo, leading to carcinogenic consequences. The potential limitation of Co-Cr bioimplants elicits the use of Ti as an alternative and better substitute.

Ti and Ti-alloys have emerged as an ideal choice for the manufacturing of bioimplants because of their high biocompatibility and excellent corrosion-resistant properties (Shi et al. 2017). Ti-alloys are generally preferred for manufacturing cardiovascular stents and other bioimplants such as dental, craniomaxillofacial and orthopaedic domains as shown in Fig. 5.1. The surface of the Ti-based bioimplants is usually covered with a non-stoichiometric layer of titanium oxide (TiO_{2-x}). The oxide layer is generally formed by the reaction of atmospheric O_2 with pure Ti at the surface of the bioimplants (Kumar et al. 2015). This passive oxide layer usually protects the Ti-bioimplants from surface-induced corrosion.

This book chapter summarizes the development and manufacturing of Ti-based bioimplants fabricated by advanced AM technique. Ti and Ti- alloy bioimplants produced by AM technology were comparatively studied with consideration of various fabrication processing parameters.

5.2 Additive Manufacturing of Ti Bioimplants

In the recent decade, AM has emerged as a promising technology to stimulate and improve the development of biomedical products (Das 2003). AM technology aids the fabrication of the patient-specific bioimplants in a relatively shorter duration. In accordance with the ASTM F42 technical committee, AM is the process of consolidation of materials to form a three-dimensional (3D) object from 3D model data. It is achieved by a layer-upon-layer approach (Gong et al. 2014). AM technology provides the flexibility to manufacture complex geometries which usually cannot be achieved by a traditional machining process, such as casting, forging and subtractive machining (Telang et al. 2021). Porous bioimplants fabricated using AM technology are light weighted products having lower Young's modulus, which

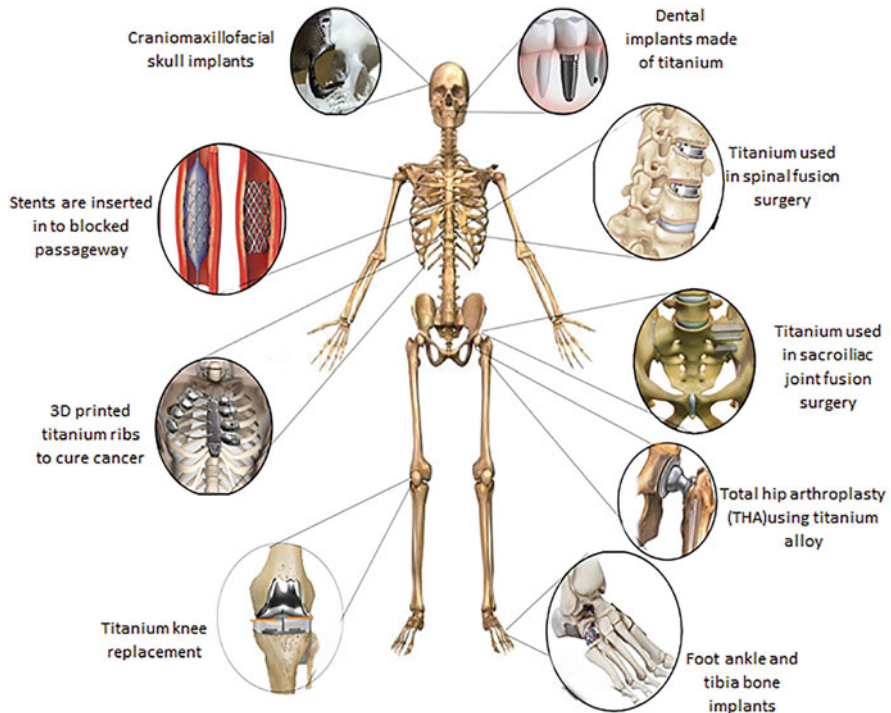


Fig. 5.1 A schematic representation illustrating the various application of titanium and its alloys in biomedical applications

supports the ingrowth of bone tissue. AM technology also offers structural accuracy, superior strength and geometrical flexibility, better integrity along with the ease of multi-material fabrication.

Until now most of the Ti-bioimplants are manufactured using conventional manufacturing techniques such as investment casting, forging, hot rolling and subtractive machining. In recent decades, AM of Ti-bioimplants has received greater attention due to its wide range of applications start from orthopaedic to dental. The most common AM processes used for the metals are direct energy deposition (DED) and powder bed fusion (PBF). These processes are based on technologies such as laser metal deposition (LMD), selective laser melting (SLM) and electron beam melting (EBM).

5.2.1 Laser Metal Deposition

The laser metal deposition technique is a form of direct energy deposition process that injects the metal powder into the focused high power laser beam in a controlled atmosphere (Stavropoulos and Foteinopoulos 2018). The high power beam is guided

through a narrow-focused region, where the metal deposition and melting occur simultaneously as shown in Fig. 5.2. The focused laser beam melts the feed metal powder and produces a molten pool. In this process, the laser beam nozzle moves along the Z-axis, whereas the workpiece moves in the XY direction to form the desired geometry (Ryu et al. 2020). After completion of all tracks in the XY plane, the nozzle is further elevated along Z-axis to deposit the subsequent layer. The process is repeated till the component with desired geometry is achieved. Laser power, powder flow rate, shielding gas flow rate and scanning speed are the processing parameters that affect the quality, surface finish, metallurgical and mechanical properties of the fabricated bioimplant. The laser energy density is usually calculated from the following equation.

$$\text{Energy density} = \frac{\text{Laser power}}{\text{Scan speed laser} \times \text{spot diameter}}$$

This process has been used to process different biometal-based bioimplants such as SS and Ti. The components produced are having graded compositions and good porosity (Ahsan et al. 2011). This process can also be used to build a new structure over an existing component (Gao et al. 2007). Woo et al. fabricated a 3D structure of Ti-6Al-4 V by laser-assisted melting (LAM) technique (Woo et al. 2020). The Ti-6Al-4 V powder of particle size 150–200 μm was transported continuously through a three-way coaxial nozzle with argon (Ar) gas shielding. Nitrogen (N_2)

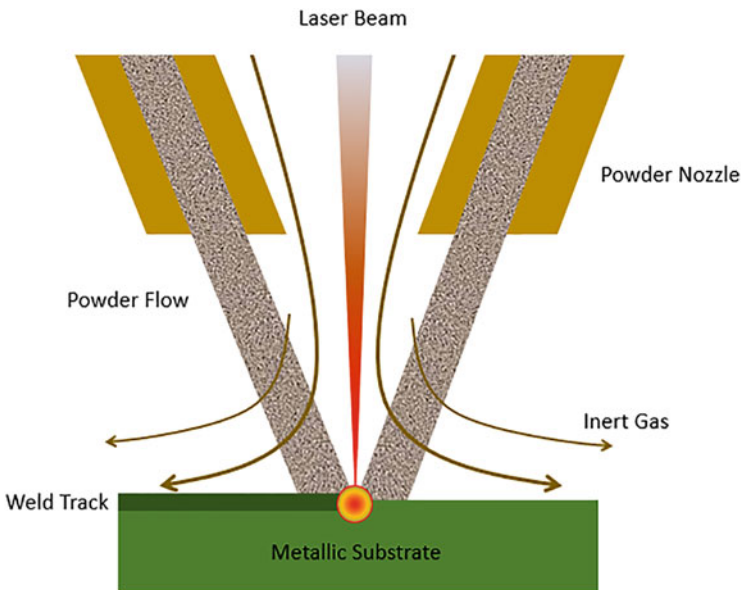


Fig. 5.2 Schematic showing a typical LMD process for fabrication of Ti-Bioimplants. (Figure adapted with permission from Junker et al. (2018))

and Ar can be used as shielding gases during the fabrication of these components. The LMD fabricated components usually have certain surface roughness, but they can be further reduced by preheating the feed material. The components fabricated by this process has improved mechanical strength over ASTM specification standards. It was also observed that the component had a uniform and similar grain structure beneath the machined surface. Microstructure does not only influence the material hardness but also significantly affect the mechanical strength and ductility (Junker et al. 2018).

One of the major challenges in LMD-based AM of Ti is to develop strategies or methods for the successful deposition of the metal powder on the substrate. Bhardwaj et al. studied the DED-laser AM technique, which is also considered as a modified LMD (Bhardwaj et al. 2019). A 3D component was manufactured using Ti and molybdenum (Mo) powder mixture. The size and shape of the feedstock powder affect the behaviour of the fabricated component. In order to get better flowability, the spherical-shaped powder was used as a feedstock. Spherical shaped powder enables the facile flow of the particles across the nozzle orifice. It was also observed that a high feed rate could cause an increase in track width and decreasing in the laser energy per unit mass of the powder and also the fusion rate. The porosity of the manufactured bioimplant was also increased due to the availability of a surplus amount of feed material. The components fabricated using this process demonstrated small and uniform grains with columnar dendritic structure. The microvoids were generated due to the entrapment of gas in the melt pool during the fabrication process. Further, these microvoids could be reduced with the application of various scan strategies. The mechanical strength of the component was lower than that of casting components, which could reduce the stress shielding effect.

Further, the effective development of various types of Ti alloys creates futuristic opportunities in the improvement and advancement of the LMD technique to fabricate innovative Ti-bioimplants. The future work should be concentrated on the implementation of various scan strategies and build orientation of the microstructure without affecting the mechanical behaviour of Ti-bioimplants.

5.2.2 Selective Laser Melting

Selective laser melting (SLM) works on the phenomenon closer to that of selective laser sintering (SLS). It is based on the powder melting and fusion with a very high energy power source (Spears and Gold 2016). In a controlled inert environment, a high energy laser beam is directed towards the uppermost layer of a powder bed, thus concealing the selective cross-sectional geometry of the component. After melting of the first layer, the built platform is lowered along the Z-axis by a certain distance equal to the layer thickness of the print. A fresh layer of powder is dispersed over the past layer. The process is rehased until the ideal and desired geometry is achieved.

Figure 5.3 represents a schematic of the process flow of a typical SLM technique. In this process, the motion of the laser beam is governed by an F-theta lens, and the

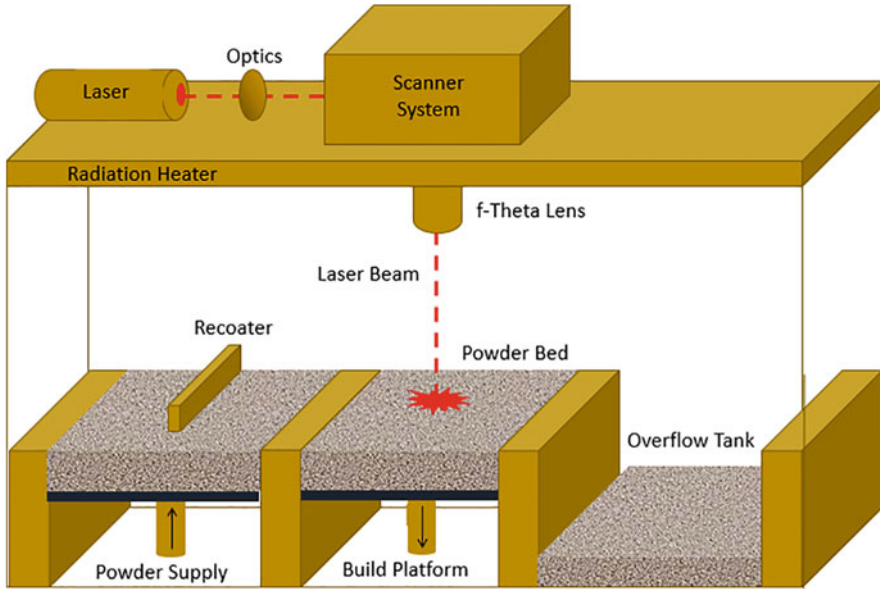


Fig. 5.3 Schematic showing the process flow diagram of typical SLM process for fabrication of Ti-Bioimplants. (Figure adapted with permission from Reiff et al. (2018))

focus is controlled by a galvanometer (Reiff et al. 2018). The whole solid part is obtained with the help of gravity, capillary forces and thermal effect (Zhang and Attar 2016). The laser power, scanning speed, scan strategy, layer thickness and hatching distance are the major printing parameters that influence the build quality and mechanical behaviour of the fabricated component. Since numerous processing parameters are involved in this process, an appropriate control over certain parameters can result in the fabrication of a high-quality component. Hence by determining the laser energy density, it is possible to predict the dimensional accuracy of the bioimplant or bioimplant component. The laser energy density in SLM can be determined by the following equation (Wu et al. 2017).

$$\text{Energy density} = \frac{\text{Laser power}}{\text{Scan speed} \times \text{Layer thickness} \times \text{Scan spacing}}$$

SLM technique has already been successfully employed to process and fabricate a variety of Ti-bioimplants such as Ti-6Al-4 V, Ti-24Nb-4Zr-8Sn and CP-Ti (Hao et al. 2016). Zhen Wang et al. built a 3D component by SLM technique using spherical sized gas-atomized Ti-6Al-4 V powder (Wang et al. 2019). The powder bed was preheated and Ar gas was used for shielding. It was observed that the surface roughness was dependent on the laser scanning speed. The increase in scanning speed could result in the reduction of surface roughness. The components fabricated at low scan speed showed coarsened and near-equiaxial grain microstructures, while a high scan speed could result in the formation of columnar

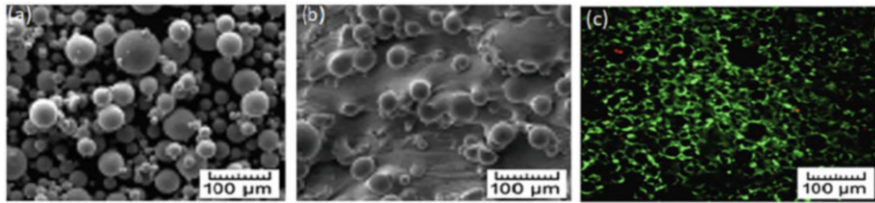


Fig. 5.4 (a) SEM image of spherical shaped gas atomized particles of Ti-6Al-4 V, (b) SLM product surface in semi melted powder form, (c) SLM specimen after 24 h of cell culture (green = live cell, red = dead cell). (Figure adapted with permission from Fousová et al. (2017) from Elsevier)

and epitaxial grains. It is evident that the microstructure of the fabricated component is directly influenced by the processing parameters. It was also found that the components fabricated by the SLM process were having improved mechanical strength than those of the forged samples.

Fousová et al. fabricated a fully dense porous bioimplant using Ti-6Al-4 V (Fousová et al. 2017). The gas atomized particles of the metal alloy are shown in (Fig. 5.4a). The product surface of semi-melted metal powder is demonstrated in (Fig. 5.4b). The rapid cooling of the metal melt pool forms acicular grains in the martensitic phase. The acicular grains in the martensitic phase could be transformed into a mixture of α and β phase after treated with heat. During this solidification process, small pores were also observed making the bioimplant surface porous. The gradient porosity of the bioimplant significantly reduces the mechanical strength of the fabricated components. In vitro cell culture experiments demonstrated most of the cells over the bioimplant are living cells (green fluorescent) with few dead cells (red fluorescent) indicating an improved biocompatibility of the fabricated bioimplants (Fig. 5.4c).

Zhou et al. used the gas atomized Ti6Al4V powder to fabricate a 3D component by the SLM technique (Zhou et al. 2018). In order to enhance the product quality, the whole fabrication process was conducted under the vacuum condition followed by the post-processing steps such as hot isostatic pressing. It was observed that the bulk energy density could significantly influence the grain structure. As the bulk energy density was increased, heat energy supplied to the melt pool was also increased leading to the formation of a deeper melt pool. The uniform grain structure was achieved at low energy density. However, the coarse grain structure was observed at a higher energy density. The porosity of the sample was reduced significantly compared to conventional SLM specimens. Schulze et al. additively manufactured Ti-alloy specimen using the SLM technique (Schulze et al. 2018). The pre-alloyed powder of β -phase Ti-42Nb was used as feed material to form a 3D structure and subsequent post-processing was followed. It was observed that the post-processing thermal treatment could result in the formation of coarse grain microstructure. The tensile strength of the fabricated component was significantly improved compared to commercially pure Ti or Ti-6Al-4 V.

Although the SLM has a high potential to produce Ti- bioimplants, further experimentation is still required to ensure the authenticity of the components for practical applications. Further by optimizing the processing parameters, there is a greater probability to enhance the residual stress, thermal gradient, surface roughness and molten liquid behaviour of Ti and Ti-alloys.

5.2.3 Electron Beam Melting

Electron beam melting (EBM) or electron powder bed fusion melting is an AM process in which the electron beam energy is utilized to melt the metal powder (Trevisan et al. 2018). It can be used to fabricate nearly full density parts in a vacuum environment as shown in Fig. 5.5. The metal or metal alloy -powder bed is preheated and sintered using the defocused electron beam, offering electrical conductivity to the powder layer. After sintering the layer, the build platform is lowered by a certain distance equal to the layer thickness of the component. A fresh layer of powder is dispersed over the previous layer. This whole procedure is repeated until the desired geometry is achieved. The EBM provides an ideal contamination-free environment

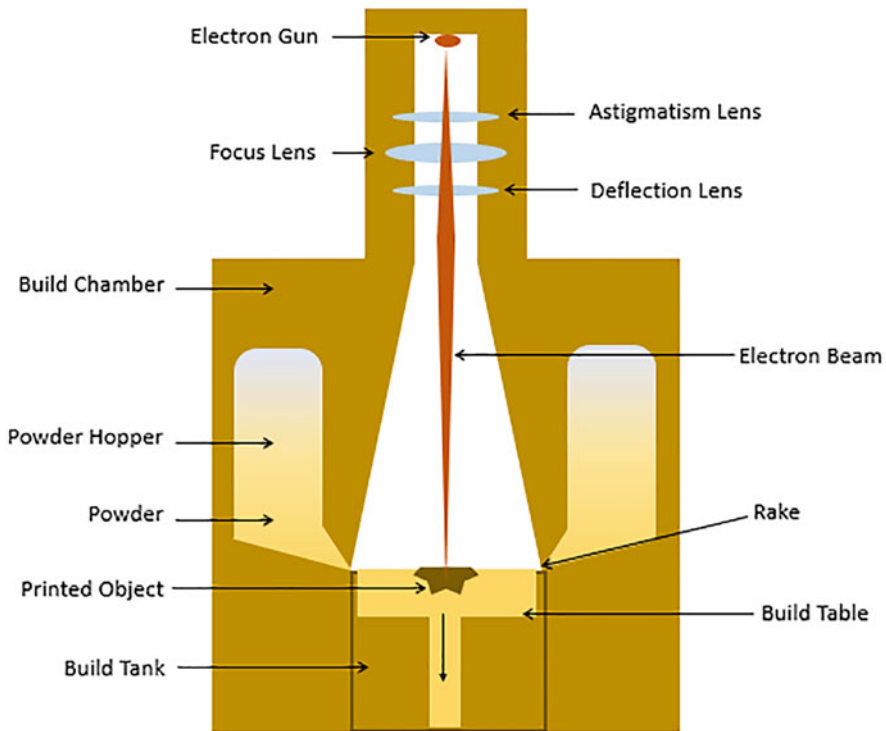


Fig. 5.5 Schematic of a typical EBM process for fabrication of Ti-Bioimplants. (Figure adapted with permission from ISAAC ANDERSON (n.d.))

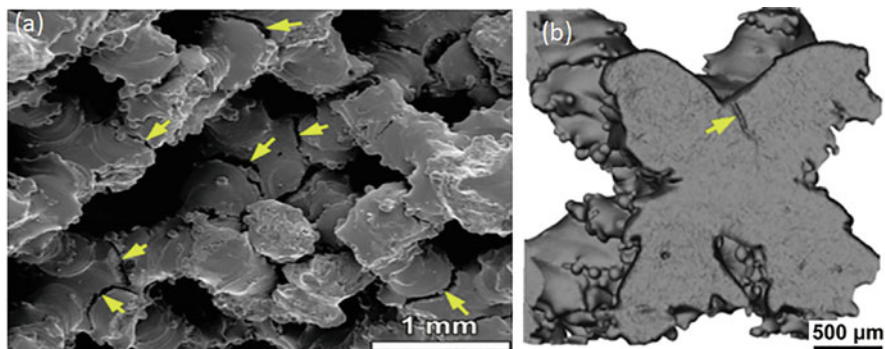


Fig. 5.6 SEM images of 3D printed (a, b) rhombic dodecahedron structured Ti2448 surface after fatigue test. (Yellow arrows indicate the position of fatigue cracks.) (Figure adapted with permission from Liu et al. (2017) from Elsevier)

for the fabrication of highly reactive materials. These reactive materials (biometal or biometal-alloys) have an affinity for oxygen, such as Ti-6Al-4 V (Liu et al. 2019). The EBM has a faster-built rate compared to DED and SLM because of its high scanning speed and superior energy input.

Li et al. used the EBM method to manufacture an orthogonal structured 3D porous bioimplant of Ti-6Al-4 V (Li et al. 2010). Ti and Ti-alloys are bioinert in nature, and these materials are generally encapsulated by fibrous tissue after being implanted inside the body. The bioactivity of the preheated component was evaluated by means of apatite-forming ability after soaking the sample in simulated body fluid (SBF) solution up to a certain period under static conditions. It was observed that the mechanical properties of orthogonal structured components produced by EBM are similar to a cortical bone. The resulted specimen further demonstrated enhanced biocompatibility after the surface treatment.

The other biocompatible Ti-alloy such as Ti-24Nb-4Zr-8Sn (Ti2448) exhibiting a low uniaxial tensile elastic modulus of approximately 45 GPa is being used for the fabrication of bone bioimplants and some of them have shown future clinical prospects (Liu et al, 2018). β -Ti alloys are non-toxic and bio-corrosion resistant. Liu et al. fabricated a dodecahedron structured porous bioimplant by EBM using β -type Ti2448 alloy (Liu et al. 2017). The powder used was having the composition of Ti-23.9Nb-3.9Zr-8.2Sn-0.190 in weight percentage. The samples fabricated exhibited an excellent elasticity and porosity with a decrease in yield strength. It was observed that due to a decrease in the yield strength, most of the cracks could appear at the nod of the component (Fig. 5.6a, b).

The mechanical strength of the bioimplants is also influenced by their design pattern. In order to withstand different loading conditions, the trabecular pattern is preferred. Marin et al. used the EBM technique to fabricate a 3D porous structure of Ti-6Al-4 V (Marin et al. 2010). The trabecular porous components were produced to maximize the osseointegration of the bioimplant.

EBM technology has significant potential to revolutionize the biomedical industry. EBM relies on electric charge and hence non-conducting material cannot be used with this technique (ISAAC ANDERSON n.d.). The complex structure generated by EBM offers improved bone ingrowth and excellent mechanical properties. Future work should be focused on enhancing the surface morphology of the Ti bioimplants by reducing the defects in fabricated products. Additional efforts are also required on the creation of reliable bioimplants and novel designs to get better outcomes in terms of their performances.

5.3 Challenges in AM of Ti Bioimplants

The recent development in AM techniques has empowered us to explore the modern manufacturing concepts to fabricate the dense metallic complex structure. Despite the progress, there are still several challenges associated with the manufacturing of Ti bioimplants. Ti has poor thermal conductivity, making itself difficult to process under the high heat source fabrication methods. These fabrication processes also affect the dimensional accuracy and topological resolution of the fabricated components. Further, it also causes the formation of air pockets due to the entrapment of the gases inside the melt pool. In addition, these air pockets tend to develop cracks during post-processing heat treatment. The spherically shaped powder is always a better choice as the flowability of the feed material affects the bioimplant behaviour. However, the use of Ti and Ti-alloy spherical shape powder is limited (Attar et al. 2020). Generally, the Ti-metal matrix upon alloying has different melting temperature, viscosities and solidification behaviour, making them complicated to process inside the laser-based AM process.

5.4 Methods to Control Ti Bioimplant Failure

Ti and Ti-alloys have exceptional biocompatibility and mechanical properties. However, the exposure of Ti bioimplants surface to the body fluids may lead to various complications in the long-term. Therefore, it is important to enhance the consistency of the bioimplants to reduce biological and biomechanical failure (Chakraborty et al. 2019; Bosco et al. 2012). There are various methods to overcome the uncontrolled ion release from Ti bioimplants. These include alloying, purification, surface treatment and protective film coating. The pure Ti can be prone to severe plastic deformation at room temperature, leading to a thickness reduction up to 90% without cracking (Elias et al. 2019). The bioimplants should possess sufficient stiffness to reduce bone stress shielding which is crucial for orthopedic applications. The stress shielding can be reduced up to a certain extent by the usage of bioimplants with mechanical strength similar to that of a natural bone. Alloying the biomaterials with other metal impurities could allow to achieve an adequate mechanical strength similar to that of a natural bone. Alloying the Ti bioimplants with the elements such as niobium (Koike et al. 2007), manganese (Zhang et al.

2009), zirconium (Cremasco et al. 2011), magnesium (Gu et al. 2017), aluminium (Bărbîntă et al. 2014) and vanadium (Costa et al. 2019) in a considerable amount has reported to improve the biocompatibility via biochemical and biomechanical effects. Experimental studies have demonstrated that the Ti-biometal surfaces coated with the bioactive glass and the bioceramic has shown an improved bonding strength, corrosion and wear resistance (Zafar et al. 2019).

5.5 Conclusion

Ti and Ti-alloys have excellent biocompatibility, corrosion resistance and mechanical properties, making it an interesting biometal for orthopedic applications. AM techniques such as LMD, SLM and EBM are gaining popularity in the biomedical field due to their flexibility to build patient-specific bioimplants and customized porous structures or components that enable bone ingrowth with sufficient cell proliferation and differentiation. The porous structure can enhance the biocompatibility of the Ti bioimplants by reducing the Young's modulus of the components. The fabricated bioimplants are also known for their lower stress shielding effect. Ti-6Al-4V, Ti2448 and other Ti-alloys with high bioactivity, low cytotoxicity and high corrosion resistance would be promising materials for the next generation of biomedical applications. Besides, the complex structures generated by the AM techniques deliver an improved mechanical behaviour. However, extensive *in vitro* and *in vivo* examinations are still in progress to analyse the accurate material behaviour of the additively manufactured bioimplants throughout their service.

References

- Ahsan MN, Paul CP, Kukreja LM, Pinkerton AJ (2011) Porous structures fabrication by continuous and pulsed laser metal deposition for biomedical applications; modelling and experimental investigation. *J Mater Process Technol* 211(4):602–609
- Attar H, Ehtemam-Haghighi S, Soro N, Kent D, Dargusch MS (2020) Additive manufacturing of low-cost porous titanium-based composites for biomedical applications: Advantages, challenges and opinion for future development. *J Alloys Compd* 827:154263
- Bărbîntă AC, Earar K, Crimu CI, Drăgan LA, Munteanu C (2014) *In vitro* evaluation of the cytotoxicity of some new titanium alloys. *Key Eng Mater* 587:303–308
- Bhardwaj T, Shukla M, Paul CP, Bindra KS (2019) Direct energy deposition - laser additive manufacturing of titanium-molybdenum alloy: parametric studies, microstructure and mechanical properties. *J Alloys Compd* 787:1238–1248
- Bordji K, Jouzeau JY, Mainard D, Payan E, Delagoutte JP, Netter P (1996) Evaluation of the effect of three surface treatments on the biocompatibility of 316L stainless steel using human differentiated cells. *Biomaterials* 17(5):491–500
- Bosco R, Van Den Beucken JV, Leeuwenburgh S, Jansen J (2012) Surface engineering for bone implants: a trend from passive to active surfaces. *Coatings* 2(3):95–119
- Chakraborty R, Raza MS, Datta S, Saha P (2019) Synthesis and characterization of nickel free titanium-hydroxyapatite composite coating over Nitinol surface through *in-situ* laser cladding and alloying. *Surf Coatings Technol* 358:539–550

- Costa BC, Tokuhara CK, Rocha LA, Oliveira RC, Lisboa-Filho PN, Costa Pessoa J (2019) Vanadium ionic species from degradation of Ti-6Al-4V metallic implants: In vitro cytotoxicity and speciation evaluation. *Mater Sci Eng C* 96:730–739
- CreMASCO A, Messias AD, Esposito AR, Duek EADR, Caram R (2011) Effects of alloying elements on the cytotoxic response of titanium alloys. *Mater Sci Eng C* 31(5):833–839
- Das S (2003) Physical aspects of process control in selective laser sintering of metals. *Adv Eng Mater* 5(10):701–711
- Elias CN, Fernandes DJ, De Souza FM, Monteiro EDS, De Biasi RS (2019) Mechanical and clinical properties of titanium and titanium-based alloys (Ti G2, Ti G4 cold worked nanostructured and Ti G5) for biomedical applications. *J Mater Res Technol* 8(1):1060–1069
- Fousová M, Vojtěch D, Kubásek J, Jablonská E, Fojt J (2017) Promising characteristics of gradient porosity Ti-6Al-4V alloy prepared by SLM process. *J Mech Behav Biomed Mater* 69:368–376
- Gao SY, Zhang YZ, Shi LK, Du BL, Xi MZ, Ji HZ (2007) Research on laser direct deposition process of Ti-6Al-4V alloy. *Acta Metallurgica Sinica (English Letters)* 20(3):171–180
- Gong H, Rafi K, Gu H, Starr T, Stucker B (2014) Analysis of defect generation in Ti-6Al-4V parts made using powder bed fusion additive manufacturing processes. *Addit Manuf* 1:87–98
- Gu XN et al (2017) Degradation, hemolysis, and cytotoxicity of silane coatings on biodegradable magnesium alloy. *Mater Lett* 193:266–269
- Hanawa T (2004) Metal ion release from metal implants. *Mater Sci Eng C* 24(6–8 Spec. Iss.):745–752
- Hao YL, Li SJ, Yang R (2016) Biomedical titanium alloys and their additive manufacturing. *Rare Met* 35(9):661–671
- Hermawan H, Ramdan D, Djuansjah JR (2011) Metals for biomedical applications. In: *Biomedical engineering from theory to applications*, vol 1, pp 411–430
- ISAAC ANDERSON. Electron beam melting. <https://www.isaacanderson.co.uk/portfolio/electron-beam-melting>
- Junker D, Hentschel O, Schmidt M, Merklein M (2018) Investigation of heat treatment strategies for additively-manufactured tools of X37CrMoV5-1. *Metals (Basel)* 8(10):1–13
- Koike M, Lockwood PE, Wataha JC, Okabe T (2007) Initial cytotoxicity of novel titanium alloys. *J Biomed Mater Res B Appl Biomater* 83(2):327–331
- Kumar A, Biswas K, Basu B (2015) Hydroxyapatite-titanium bulk composites for bone tissue engineering applications. *J Biomed Mater Res A* 103(2):791–806
- Li X, Wang C, Wang L, Zhang W, Li Y (2010) Fabrication of bioactive titanium with controlled porous structure and cell culture in vitro. *Xiyou Jinshu Cailiao Yu Gongcheng/Rare Met Mater Eng* 39(10):1697–1701
- Liu CF, Lee TH, Liu JF et al (2018) A unique hybrid-structured surface produced by rapid electrochemical anodization enhances bio-corrosion resistance and bone cell responses of β -type Ti-24Nb-4Zr-8Sn alloy. *Sci Rep* 8:6623. <https://doi.org/10.1038/s41598-018-24590-x>
- Liu LH et al (2015) Ultrafine grained Ti-based composites with ultrahigh strength and ductility achieved by equiaxed microstructure. *Mater Des* 79:1–5
- Liu YJ et al (2017) Compressive and fatigue behavior of beta-type titanium porous structures fabricated by electron beam melting. *Acta Mater* 126:58–66
- Liu W et al (2019) Surface modification of biomedical titanium alloy: micromorphology, microstructure evolution and biomedical applications. *Adv Eng Mater* 9(4):249
- Mantripragada VP, Lecka-Czernik B, Ebraheim NA, Jayasuriya AC (2013) An overview of recent advances in designing orthopedic and craniofacial implants. *J Biomed Mater Res A* 101(11):3349–3364
- Marin E, Fusi S, Pressacco M, Paussa L, Fedrizzi L (2010) Characterization of cellular solids in Ti6Al4V for orthopaedic implant applications: Trabecular titanium. *J Mech Behav Biomed Mater* 3(5):373–381
- Reiff, C, Wulle, F, Riedel, O, Epple, S, Onuseit, V (2018) On inline process control for selective laser sintering. In: *Eighth international conference on mass customization and personalisation – community of Europe (MCP-CE 2018)*, vol 141, pp 230–239

- Ryu DJ et al (2020) Titanium porous coating using 3D direct energy deposition (DED) printing for cementless TKA implants: does it induce chronic inflammation? *Materials (Basel)* 13(2):1–13
- Schulze C, Weinmann M, Schweigel C, Keßler O, Bader R (2018) Mechanical properties of a newly additive manufactured implant material based on Ti-42Nb. *Materials (Basel)* 11(1):13–16
- Shi Q, Qian Z, Liu D, Liu H (2017) Surface modification of dental titanium implant by layer-by-layer electrostatic self-assembly. *Front Physiol* 8:1–7
- Spears TG, Gold SA (2016) In-process sensing in selective laser melting (SLM) additive manufacturing. *Integr Mater Manuf Innov* 5(1):16–40
- Stavropoulos P, Foteinopoulos P (2018) Modelling of additive manufacturing processes: a review and classification. *Manuf Rev* 5:2
- Taljanovic MS et al (2003) Joint arthroplasties and prostheses. *Radiographics* 23(5):1295–1314
- Telang VS, Pemmada R, Thomas V, Ramakrishna S, Tandon P, Nanda HS (2021) Harnessing additive manufacturing for magnesium based metallic bioimplants: recent advances and future perspectives. *Curr Opin Biomed Eng* 17:100264
- Trevisan F et al (2018) Additive manufacturing of titanium alloys in the biomedical field: processes, properties and applications. *J Appl Biomater Funct Mater* 16(2):57–67
- Wang Z, Xiao Z, Tse Y, Huang C, Zhang W (2019) Optimization of processing parameters and establishment of a relationship between microstructure and mechanical properties of SLM titanium alloy. *Opt Laser Technol* 112:159–167
- Woo WS, Kim EJ, Jeong HI, Lee CM (2020) Laser-assisted machining of Ti-6Al-4V fabricated by DED additive manufacturing. *Int J Precis Eng Manuf Green Technol* 7(3):559–572
- Wu Z et al (2017) Preparation and application of starch/polyvinyl alcohol/citric acid ternary blend antimicrobial functional food packaging films. *Polymers (Basel)* 9(3):1–19
- Zafar MS, Farooq I, Awais M, Najeeb S, Khurshid Z, Zohaib S (2019) Bioactive surface coatings for enhancing osseointegration of dental implants. Elsevier, Amsterdam
- Zhang LC, Attar H (2016) Selective laser melting of titanium alloys and titanium matrix composites for biomedical applications: a review. *Adv Eng Mater* 18(4):463–475
- Zhang F, Weidmann A, Nebe BJ, Burkel E (2009) Preparation of TiMn alloy by mechanical alloying and spark plasma sintering for biomedical applications. *J Phys Conf Ser* 144:012007
- Zhou B, Zhou J, Li H, Lin F (2018) A study of the microstructures and mechanical properties of Ti6Al4V fabricated by SLM under vacuum. *Mater Sci Eng A* 724:1–10



Physico-chemical Modifications of Magnesium and Alloys for Biomedical Applications

6

Satish Jaiswal, Anshu Dubey, and Debrupa Lahiri

Abstract

A unique combination of impressive biodegradability and biocompatibility makes magnesium (Mg) and its alloys a promising candidate in biomedical applications, considering the issue of resurgery associated with the conventional metallic implants. Unfortunately, due to high electrochemical potential (-2.37 V), Mg shows limited corrosion resistance in the physiological environment. Surface properties, such as reactivity (inert or active), surface free energy and surface roughness, play a significant role in the corrosion behaviour of Mg-based alloys. Additionally, cellular interaction, such as protein adsorption, cell adhesion, proliferation and tissue formation, primarily depends on the surface characteristics of the Mg-based implants. Thus, it is vital to engineer the surfaces of the implants, while preserving the bulk properties, in order to control the biodegradation and simultaneously enhancing the subsequent interaction of implants surfaces with the host tissues. Engineered surfaces of the Mg implants, with appropriate corrosion resistance, surface chemistry and topography, might improve the response of the host organism at macroscopic, cellular and protein level at the tissue-implant interface. Various surface modification approaches like physico-chemical, mechanical and biological techniques have been invented to enhance the degradation resistance and bioactivity of Mg-based materials. Physico-chemical modifications such as surface coating, heat treatment, micro-arc oxidation, plasma surface modification, laser surface modification and electrode deposition have been explored to alter the surface characteristics of Mg and its alloys for biomedical applications. In this chapter, efforts have been taken to present a critical status of contemporary research and development on

S. Jaiswal · A. Dubey · D. Lahiri (✉)

Biomaterials and Multiscale Mechanics Laboratory, Department of Metallurgical and Materials Engineering, Indian Institute of Technology, Roorkee, Uttarakhand, India

© The Author(s), under exclusive license to Springer Nature Singapore Pte Ltd. 2022

131

L. M. Pandey, A. Hasan (eds.), *Nanoscale Engineering of Biomaterials: Properties and Applications*, https://doi.org/10.1007/978-981-16-3667-7_6

physico-chemical surface modification methods of the Mg-based material system for biomedical applications.

Keywords

Magnesium · Physico-chemical surface modification · Biodegradation · Biocompatibility

6.1 Introduction

In biomedical research, the development of biomaterials represents a fast-growing domain and is a cornerstone of modern medical practise, saving millions of lives every year. As per the report of Grand View Research, Inc., the worldwide biomaterials market size is anticipated to grow up to approximately USD 348 billion by 2027, with a compound annual growth rate (CAGR) of 15.9% (Grand View Research 2020). The recent advancement in the biomaterials field show significant promise to provide implants for better treatment/replacement of damaged and diseased tissues with improved functionalities. As per the type of materials used, biomaterials can be classified into three different types, namely metallic, polymeric and ceramic-based biomaterials. Due to the limited mechanical attributes of polymeric and ceramic biomaterials, especially early in the tissue development process, the use of these biomaterials is not suitable for load-bearing implants (Love 2017). Metallic biomaterials are primarily used in a situation where significant mechanical integrity is required (Prasad et al. 2017). Given the current problems such as higher rejection of implants from the host tissues, high demand is placed on the surface engineering of biomedical implants (Nouri and Wen 2015). Apart from the bulk properties of metallic biomaterials, the surface characteristics of materials are crucial to clinical success. Recent advances in the surface modification to improve bioactivity, biocompatibility and mechanical integrity of biomedical materials have established a new opportunity for their use in tissue engineering. In order to cater to the specific need and application, the surface modification of existing biomaterials to tailor the physical and biological properties are more economical and less time consuming, as compared to the development of new biomaterials (Nouri and Wen 2015).

Surface chemistry and surface morphology of the biomaterials play a critical role in maximising the biocompatibility and service reliability during contact with the body fluids (Tang et al. 2008). Specifically, in the case of load-bearing application, besides the mechanical properties, the biomaterials must also be non-toxic to cells and living tissues in the human body (Kasuga 2010; Niinomi 2019). So, the surface of biomaterials should be designed in such a way that it would encourage the attachment and growth of bone cells and newly formed bone during service condition (Gobbi et al. 2019). Surface modification of the implants has become an increasingly popular method to enhance the implant's multifunctionality, tribological behaviour, topography and biocompatibility.

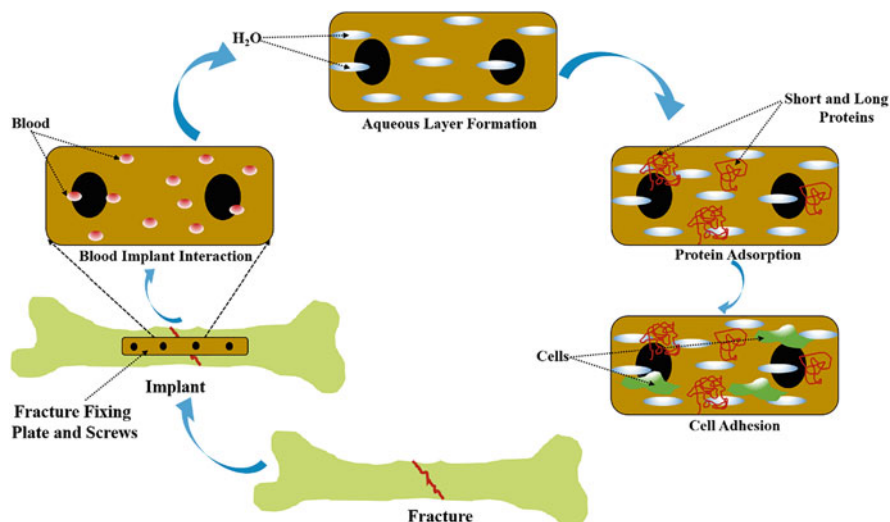


Fig. 6.1 Schematic showing the sequence of events occurring at the biomaterials surfaces during immediate contact with the body fluid

Once a biomaterial is implanted in the human body, there is a series of events that take place between the host tissue and implanted materials. This series of events in sequential order is shown on the fracture fixing accessories for a fractured bone in the schematic diagram (Fig. 6.1). Surface modification methods of biomaterials facilitate stabilising the bioactivity of implants at the tissue-implant interface, while simultaneously maintaining sufficient mechanical properties.

6.1.1 Metallic Biomaterials, Surfaces and Biocompatibility

Nowadays, significant emphasis has been given to the multifunctionality of the adopted biomaterials. For example, a load-bearing implant is designed to provide mechanical support for bone regeneration along with the capability to stimulate cell attachment and tissue formation. Current commercially available metallic implants, such as stainless steel (SS), titanium (Ti) alloys and cobalt-chromium (Co-Cr) alloys, fall under the bio-inert category (Poinern et al. 2012). These metallic implants are used for several load-bearing orthopaedic applications owing to their significant corrosion resistance, which offers excellent long-term mechanical stability (Poinern et al. 2012). Such characteristics of materials allow for selection to meet the specific objective for permanent replacement of the tissue, which has lost the function. However, the reports are also available that the long duration exposure of these materials (SS, Co-Cr and Ti-based alloys) inside the body may increase the possibility of cutaneous and systemic hypersensitivity reactions (Jaiswal et al. 2019a, b). Further, the lack of osseointegration on the surface of material systems leads to the

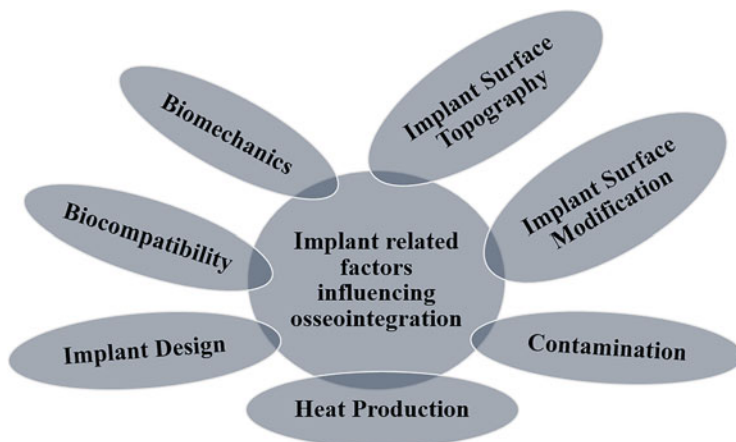


Fig. 6.2 The features of implant materials influencing the loosening

loosening of the implants. Osseointegration generally depends on factors such as surgical-, patient- and implant-related factors (Vootla and Reddy 2017). The features of the implant material influence the loosening, as shown in Fig. 6.2. Implant surface design and topography play a significant role in controlling the loosening of the implants (Vootla and Reddy 2017). For instance, moderately rough implant surfaces develop the best bone fixation. Therefore, the surface modification of biomedical implants is necessary to:

- Increase surface area.
- Remove surface contaminants.
- Offer better bonding.
- Increase surface roughness.
- Increase corrosion resistance.
- Make surface more bioactive.

So, the problem of implant loosening can be minimised with proper effort in place. Several methods are being examined for enhancing and maintaining the fixation. Surface engineering is one of the well-known techniques to stabilise bone-implant interface, and simultaneously retain the adequate mechanical properties for load-bearing implants (Kasemo and Lausmaa 1994; Hornberger et al. 2012; Qiu et al. 2014).

Besides the application in bone implants, metallic cardiovascular stents are also preferred over polymeric counterparts due to the superior mechanical properties and radiopacity. However, the metallic stents are lacking the ideal clinical needs due to the late restenosis, thrombosis and other clinical limitations (Fu et al. 2020). Biocompatibility represents the predominant factor in the development of metallic implants. It is imperative to understand the mechanism through which the implant materials transform their structural configuration to tailor the response of proteins,

cells and organisms. In general practise, the implant materials are considered to be compatible with the body for specific biomedical applications when they do not release toxic materials in significant amounts to affect tissues and cells (Niinomi 2019). Leaching of undesirable substances may occur via the surface morphology of implants. Further, the body fluids read the surface morphology and respond. Thus, the understanding of biomaterials surfaces is a prerequisite for the development of implants (Sodhi 1996).

6.1.2 Surface Properties and Analysis

Atoms residing at the outermost surfaces of the biomaterials have unique organisation and reactivity. This unique arrangement of the atoms at the biomaterial surfaces drives most of the biological reactions that occur, namely, cell adhesion, blood compatibility, cell growth and protein adsorption. There are various parameters listed in Fig. 6.3 for describing the surface of the biomaterials. A complete description of the surfaces can be provided by measuring more of these parameters.

In general, the surface properties of biomedical materials are critical at governing biological interactions. Several studies have been performed to show the importance of roughness, wettability, chemical composition, crystallinity, electrical charge, surface mobility and inhomogeneity to real body environment (Elias et al. 2008, Rosales-Leal et al. 2010, Deng et al. 2015). In general, bulk properties of implants tailor mechanical integrity. However, the surface characteristics play a significant

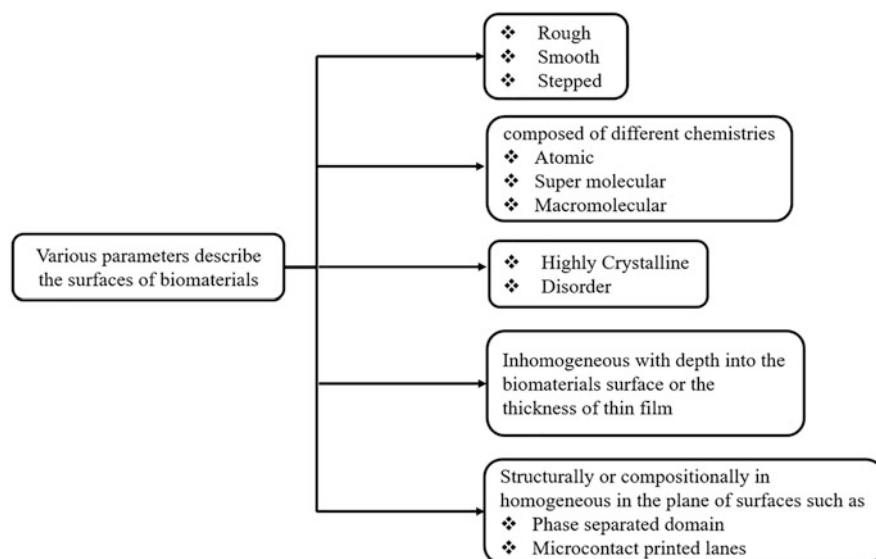


Fig. 6.3 A list of parameters defining the surfaces of a biomaterials

role in many physico-chemical processes, such as the interaction of body fluids and adhesion of cells and biomolecules to implants, which initiate degradation of implants and release of foreign ions in the body fluids. So, in-depth analysis of the surface properties is a prerequisite for the development of biomedical implants.

Modern surface science presents several surface analysis methods for assessing the surface characteristics of the biomaterials. However, the major techniques like contact angle measurements (to find out the wettability and surface energy), X-ray photoelectron spectroscopy (XPS, X-ray induced emission of electrons of characteristic energy), secondary ion mass spectroscopy (SIMS, secondary ions are sputtered on solid films), Fourier-transform infrared spectroscopy (FTIR, IR radiation is adsorbed and excites molecular vibrations), scanning tunnelling microscopy (STM, use of electrical voltage to tip/sample), scanning electron microscopy (SEM, sample surface is scanned with the focused beam of electrons) and atomic force microscopy (AFM, measures the force between the sample and probe) are utilised to examine the surface properties of the biomaterials.

6.1.3 Insight into the Biological Activity of the Surfaces of the Implant

The major limitation in the design and development of superior implants is the lack of insights into the primary interaction between tissue and implant surfaces. An implant surface meets tissues after implantation inside the human body. These surfaces are highly perturbed by the preceding handling of the materials and surgical procedure. So, the immediate focus of scientific curiosity would be the interface between the artificial implant and human tissue. The initial interaction between implant and tissue surfaces occurs at the molecular level. The adsorption of proteins, reactions of biomolecules, inorganic ions, water from the dissolution of ionic, atomic or molecular chunks from implant surfaces are the initial reactions occur between implants and tissue surfaces (Bruinink et al. 2014). Schematic representation of primary interactions of implant and tissue is depicted in Fig. 6.4.

The tissue-implant interface is a dynamic, non-reversible system. It is due to the continuous healing process, where the condition of bone tissue and surface characteristics of the implants frequently changes in the body fluid (Kasemo and Lausmaa 1986, 1988). The surface of implants, stabilised in the ambient condition, is prone to react in the physiological environment to lower the energy of the system further (Kasemo and Lausmaa 1994). Thus, there is a built-in thermodynamic drive in implants to react at the tissue-implants interface in the body fluid environment.

6.1.4 Magnesium and Its Alloys as Biomedical Materials

Bone tissue is continuously experiencing remodelling in response to the imposed stresses generated by daily human activities (Grand View Research 2020). Metallic biomaterials, like Ti6Al4V, Co-Cr alloys and stainless steel (SS), are currently used

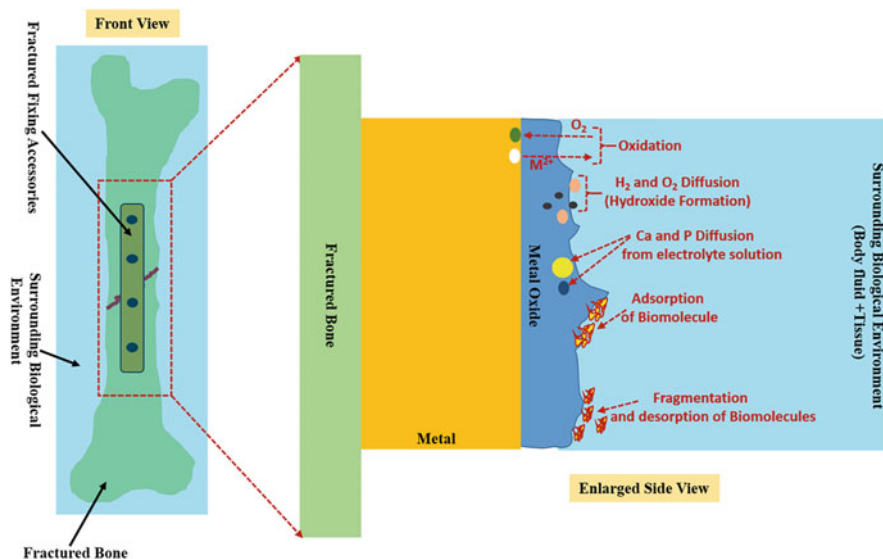


Fig. 6.4 The schematic illustration of the insight of the tissue-implant interface in the body fluid environment

as temporary implants (Nayak et al. 2016; Jaiswal et al. 2018, 2019a, b). These materials do not degrade in the body environment and often result in stress-shielding phenomenon due to the mismatch of elastic modulus with the natural human bone (Jaiswal et al. 2018; Dubey et al. 2019a, b, c). The stress-shielding effect can be observed under the non-uniform loading condition. The bulk of the mechanical loading is bear by metallic implants, whereas the surrounding tissues undergo comparatively minimum loading stress. This reduced stress loading condition leads to bone resorption (Rashmir-Raven et al. 1995; Nagels et al. 2003). The mechanical wear and degradation of the metallic implants release toxic metal ions (e.g. cobalt (Co), chromium (Cr) and nickel (Ni)) into the human body (Poinern et al. 2012; Jacobs et al. 1991). These toxic metallic ions deteriorate the biocompatibility of implants (Poinern et al. 2012; Lhotka et al. 2003; Woodman et al. 1983). Consequently, the implant loosening occurs after some time of implantation. Besides, following the complete healing of the fractured bone or allergic response due to the released metallic ions, revision surgery is needed to take out these implant materials (Jaiswal et al. 2018).

In contrast to this, biodegradable implants are considered revolutionary biomedical materials due to their bioactive and multi-biofunctional characteristics. Recently, Mg-based materials are emerging as new potential biodegradable temporary orthopaedic implants. While comparing with the traditional biodegradable implants, such as polymers and bioglass, Mg-based materials possess unique properties like light-weight, density similar to human bone and significant mechanical strength. In addition to this, the degradation products of Mg-based implants are physiologically

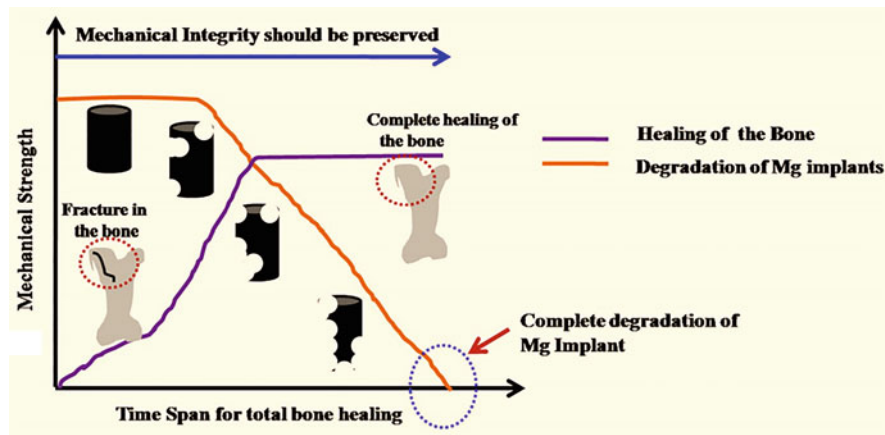


Fig. 6.5 Schematic illustration of the kinetics desired for Mg-based biodegradable implants. (Reprinted by permission from Springer Nature (Jaiswal et al. 2019a, b))

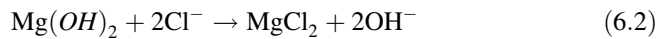
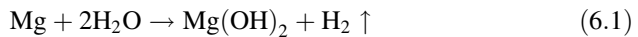
beneficial, considering the fact that a healthy adult human body stores ~30 g of Mg ions in both bone tissue and muscle (Saris et al. 2000). In addition, the bivalent ion characteristic of Mg ions helps in apatite formation in the bone matrix and is also beneficial in several metabolic reactions within the human body (Kim et al. 2003). In addition, one of the recent studies showed the novel antibacterial behaviour of Mg-based implant against *Pseudomonas aeruginosa*, *Escherichia coli* and *Staphylococcus aureus* (Robinson et al. 2010).

Keeping the above-mentioned comparatively favourable properties of Mg metals, the biomedical community has lately explored the Mg-based implants as potential biodegradable implants for temporary biomedical application. The development of biodegradable Mg-based stents has shown the potential to reduce long-term issues like late restenosis, thrombosis and mechanical instability (Fu et al. 2020). However, the Mg-based implants, proposed for biomedical applications, should meet a number of strict requirements. Figure 6.5 shows a schematic representation of the desirable kinetics required for the combination of properties for Mg-based biodegradable implants until the total healing of the fractured bone tissue takes place.

6.1.5 Limitations with Mg-Based Implants

The biodegradable nature of Mg-based materials in the physiological environment is the major advantage over permanent conventional metallic implants, which originates due to the high standard electrode potential of Mg (-2.37 V) (Jaiswal et al. 2018; Dubey et al. 2019a, b, c). Unfortunately, the major limitation with the Mg-based implants is the severe degradation rate in the physiological environment (Dubey et al. 2019a, b, c). Rapid degradation of the Mg-based implants generates significant hydrogen gas (H_2), which accumulates in the form of gas bubbles

surrounding the implant sites. Additionally, due to the severe degradation, a sudden localised increase in the pH is also observed. In general, it corrodes relatively faster in the *in vivo* environment. An electrochemical reaction occurs at the surfaces of Mg-based implants in the aqueous environment, which yields the magnesium hydroxide $\text{Mg}(\text{OH})_2$ and H_2 gas as the degradation product (Dubey et al. 2019a, b, c). $\text{Mg}(\text{OH})_2$ gets deposited as a thin protective layer on the exposed surface of Mg-based implants. In the presence of a high concentration (>30 mM) of chloride ions (Cl^-) in the physiological environment, $\text{Mg}(\text{OH})_2$ gets converted into highly soluble magnesium chloride (MgCl_2). Thus, continuous corrosion of Mg-based implants could be observed in the *in vivo* environment (Cl^- content in body fluid is ~ 150 mM). The following electrochemical reactions elucidate the degradation mechanism of the Mg metals (Virtanen 2011; Jaiswal et al. 2019a, b; Xin 2011).



The schematic representation of the degradation mechanism of Mg-based implants is depicted in Fig. 6.6.

It has been observed that Mg-based implants degrade faster at the early stage of the implantation, due to the absence of a protective layer, leading to the continuous reduction of mechanical integrity and, finally, the implant failure. Several efforts such as alloying (with aluminium (Al), zinc (Zn), calcium (Ca), zirconium (Zr) and rare-earth), surface modification and fabrication of composites have been tried to tailor the degradation rate of Mg implants (Virtanen 2011; Xin et al. 2011; Kania et al. 2020; Willumeit et al. 2011; Sezer et al. 2018; Rahim et al. 2018; Jaiswal et al. 2019a, b). Several promising techniques related to each field have been explored in the recent years. However, a further in-depth organised study is still required before using these material systems *in vivo* (Guo 2010).

It has been observed that the alloying of Mg is quite challenging because of low solubility of many alloying elements in Mg. In contrast to this, surface modification is of high importance and an appropriate way to enhance the degradation resistance (Hornberger et al. 2012). In surface modification techniques, the substrate is modified without any changes in the chemical composition of the substrate. Surface modification of Mg-based implants has been extensively studied as one of the major strategies to prevent severe corrosion. It also offers to tailor the mechanical properties and biocompatibility of Mg-based materials focusing to obtain a temporospatial complementary relationship between the degradation of implant and bone regeneration. Several surface modification techniques have been explored, till date, to prevent degradation and enhance the biocompatibility of Mg-based materials.

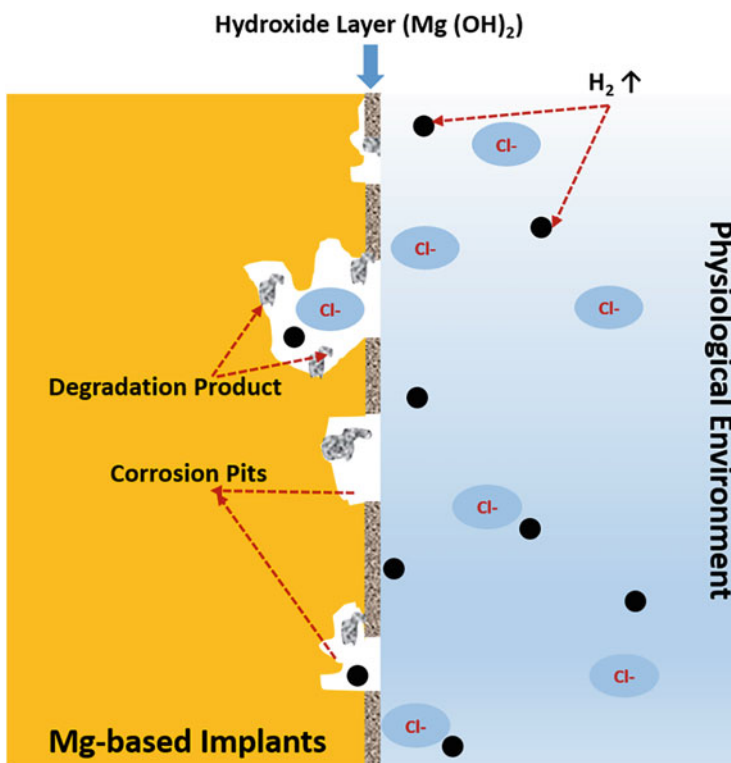


Fig. 6.6 Schematic representation of corrosion mechanism at the Mg implant surfaces in the physiological environment

6.2 Surface Modification Techniques of Mg-Based Implants

The fabrication of Mg-based implants necessitates amalgamation of a multitude of attributes, including desirable surface properties, to encourage significant biocompatibility. These implant materials are intended to interact with the biological environment to augment, treat or replace any tissue, organ or function of human body (John et al. 2015). The primary concern with Mg-based implants is the severe corrosion rate (Jaiswal et al. 2019a, b). A controlled and uniform corrosion rate needs to be maintained before using in the real body environment. Besides, significant mechanical integrity, biocompatibility and bioactivity are needed until the affected part of the body is fully healed to ensure the durability, functionality and biological response of biomedical implants. These issues need to be addressed before proceeding the Mg-based implants to market or implanting in the human body. The ability to alter the surface properties to maintain the significant degradation resistance and biocompatibility, while maintaining the bulk properties of implants, is the unique advantage of surface modification methods.

In general, the surface modification of implants can be classified into three exclusively different categories:

- Physically or chemically tailoring the surface atoms, molecules or compounds (e.g. mechanical roughening, etching, chemical modification).
- Surface coating with materials having a different composition (e.g. thin film deposition, grafting coating).
- Generating surface texture or pattern.

The biological response to Mg-based implants can be altered due to the changes in the surface chemistry and physical structure, after surface modification (Qiu et al. 2014). To enhance the degradation resistance and biocompatibility of Mg-based implants, a multitude of elaborate surface modification strategies like physico-chemical, mechanical and biological modification techniques are being exercised nowadays to generate desired surface characteristics. These are intuitive and straightforward approaches to obtain modified implant surfaces. Physico-chemical modification of Mg-based implants is widely researched throughout the globe. In this chapter, the major focus is on the physico-chemical modification of Mg-based implants for temporary orthopaedic applications. The details about the physico-chemical modification techniques are presented in the following section.

6.2.1 Physico-chemical Modification of Mg and Its Alloys

Physico-chemical modification is a versatile technology in surface engineering to enhance the surface properties and biocompatibility of biomedical implants. Biomedical implant surfaces are modified by physico-chemical methods to:

- Modulate cell adhesion and proliferation.
- Control protein adsorption.
- Modify blood compatibility.
- Improve wear and corrosion resistance.
- Improve lubricity.
- Alter transport properties.
- Modify electrical characteristics.

Based on the modification's reinforcement, surface alteration of biomedical implants by physico-chemical methods can be classified into two different heads: surface coating/film deposition and coating-free methods. Figure 6.7 shows the chart for different types of physico-chemical surface modification techniques categorised in both heads.

Detailed strategies behind the different types of physico-chemical surface modification are presented in Table 6.1. Detailed elaboration of each physico-chemical surface modification technique on Mg-based implants is discussed in the following subheadings.

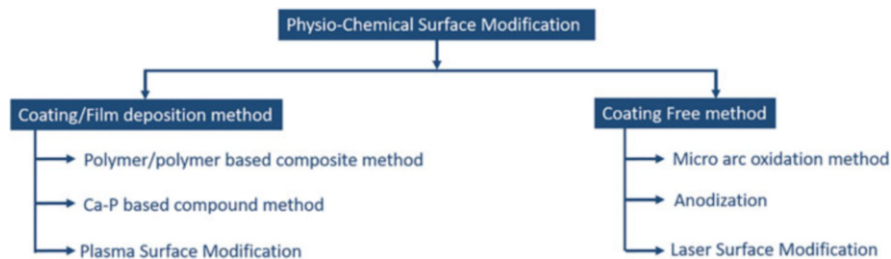


Fig. 6.7 Different types of physico-chemical techniques available for surface modification of implants

Table 6.1 Strategies behind the different types of physico-chemical surface modification techniques

Serial no.	Surface modification technique	Strategies
1.	Surface coating	The implant surface is coated to avoid the direct exposure to the physiological environment
2.	Surface grafting	The polymer chains are added to the substrate surfaces
3.	Abrasive blasting and surface etching	Surfaces are deformed plastically, removing particles from the surfaces and etching with acid
4.	High-temperature treatment	The substrate surfaces are converted into the oxide layers via vapour or steam treatments

6.2.1.1 Coating/Film Deposition Techniques

A plausible approach to improve the degradation resistance and biocompatibility of Mg-based materials is to cover the exposed surfaces via surface coating techniques (John et al. 2015). The coating technique is used to tailor the surface characteristics of implants without changing the bulk properties of the implants (Matthews and Holmberg et al. 1994). The schematic representation of the concept of surface coating on the Mg-based orthopaedic implants is shown in Fig. 6.8.

Coating acts as an effective barrier to impede the penetration of vicious ions (e.g. Cl^-), which attribute severe corrosion in Mg-based materials (Antunes and De Oliveira 2009; Wood 2007). Numerous methods have been developed to coat the surfaces of the biomedical implant (orthopaedic and cardiovascular stent) with various types of coating materials. Coating methods, such as plasma spraying, sol-gel coating, sputter deposition, electrophoretic deposition and dip coating, are widely used to modify the surfaces of Mg-based implants. A detailed elaboration of the different types of coating materials and their method on Mg-based implants surfaces is mentioned in the following section.

Polymer/Polymer-Based Composite Coatings

Based on the intended application of the Mg-based temporary implants, the prerequisite of the polymer-based coatings is biodegradability in the physiological environment (Lenz 1993). In addition to this, the polymer coatings should have

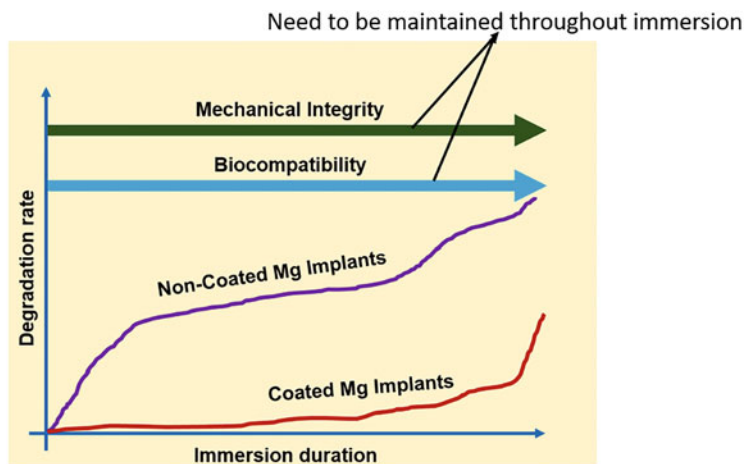


Fig. 6.8 Schematic showing the concept of surface coating on the Mg-based implants

significant mechanical strength and corrosion resistance during the essential time to adapt and complete the implant performance in the human body. In general, the biodegradable polymer with the corrosion rate lower than the Mg-based implants is used as the best way to impede severe corrosion in the body fluid (Lenz 1993). Several biodegradable polymers such as polycaprolactone (PCL), polylactic acid (PLA), polyglycolide (PGA), polylactic-*co*-glycolic acid (PLGA), poly(lactic acid) (PLLA), polyethylenimine (PEI) and the combination of the polymers like PLA-PCL and PCL-PLLA have been used as the coating polymers for Mg-based implants (Hornberger et al. 2012). Polymers such as PLA, PGA and chitosan have shown significant biocompatibility and biodegradability in the physiological environment (Li et al. 2016). In addition, these polymers have been used as suitable carriers for controlled drug release (Li et al. 2016). The use of biodegradable polymer coatings on cardiovascular stents facilitates the complete elution of drugs, reduces inflammatory response and decreases risk of endothelial dysfunction and thrombosis (Amruthaluri 2014). Rahimi-Roshan et al. (2020) coated AZ31 Mg alloys with biodegradable PLA-cellulose nanoparticles (CNs) composite via dip immersion method with a withdrawal speed of 80 mm/min. Different composition of CNs (1, 5 and 10 wt.%) was used to make different coating solutions. Polymer composite solution was thoroughly homogenised via ultrasonic homogeniser, prior to coating on the Mg alloy. The coating of 10 wt.% CNs polymer composite solution reduced the adhesion to the Mg substrate due to the agglomeration of CNs (Fig. 6.9). In another study, PEI was applied to the AZ31 Mg alloy sheet via the spin coating technique (Conceicao et al. 2010). The coating solution was prepared using two different solvents (Dimethylacetamide (DMAc) and *N*-methyl-2-pyrrolidone (NMP)). The effect of various parameters (solvent type and spin speed) on the efficacy of coating was evaluated in terms of corrosion protection. The maximum coating thickness of $\sim 3.2 \mu\text{m}$ was obtained at the spin speed of 1000 rpm (produced

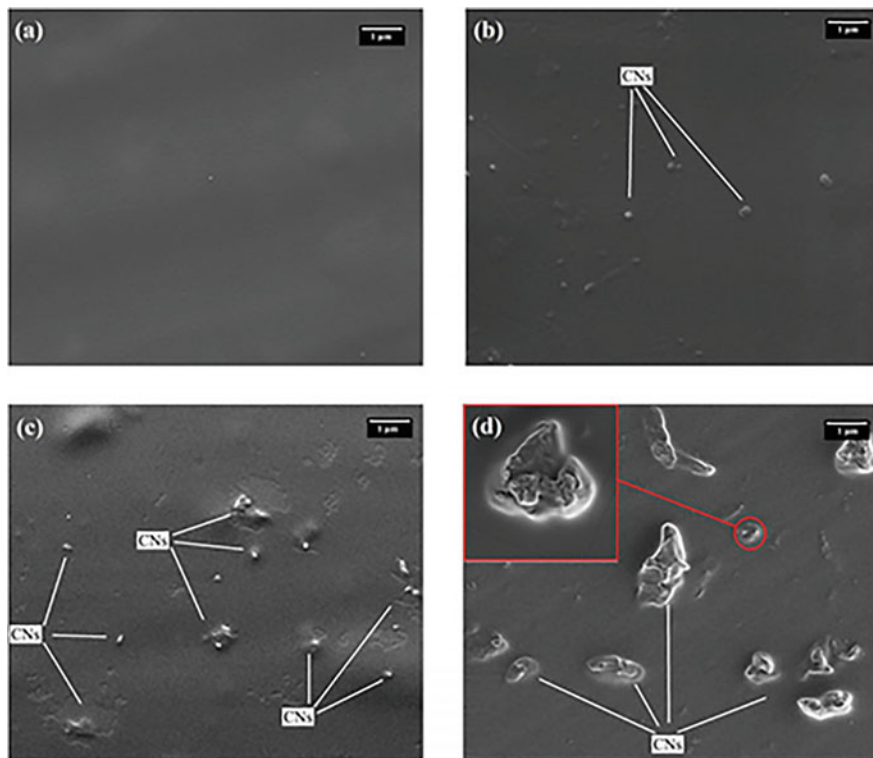


Fig. 6.9 SEM micrographs of the coatings on AZ31 Mg alloy: (a) PLA, (b) PLA-1 wt.% CNs, (c) PLA-5 wt.% CNs and (d) PLA-10 wt.% CNs. (Reprinted by permission from Taylor and Francis Ltd. (Rahimi-Roshan et al. 2020))

by the solution PEI/DMAc (15/85)) (Fig. 6.10b). The hydroxide produced by the chemical reaction of Mg surfaces and water reacts with the PEI and forms a protective layer of Mg polyamate and polyamic acid. PEI coating prepared using DMAc solvent showed comparatively better corrosion resistance due to the lower diffusion.

Wong et al. (2010) coated AZ91 Mg alloy with two different concentrations of PCL (3.33 and 2.5% w/v) in dichloromethane (DCM) solution. The two different solvents were chosen to fabricate various porous sizes and porosities. The coating was deposited layer by layer on the alloy surfaces via a custom-designed spraying device. The low porosity membrane (LPM) and high porosity membrane (HPM) were deposited on the alloy surfaces. The pores formed on the LPM and HPM surfaces of the alloy are shown in Fig. 6.11. Gu et al. (2016) performed elastomeric coating on AZ31 Mg stent with poly (carbonate urethane) urea (PCUU) for possible application in the cardiovascular stent. The efficacy of these coatings was compared with the PLGA coating on the AZ31 Mg stent. The PCUU- and PLGA-coated AZ31 Mg stents were expanded from 4 to 6 mm using the balloon catheter

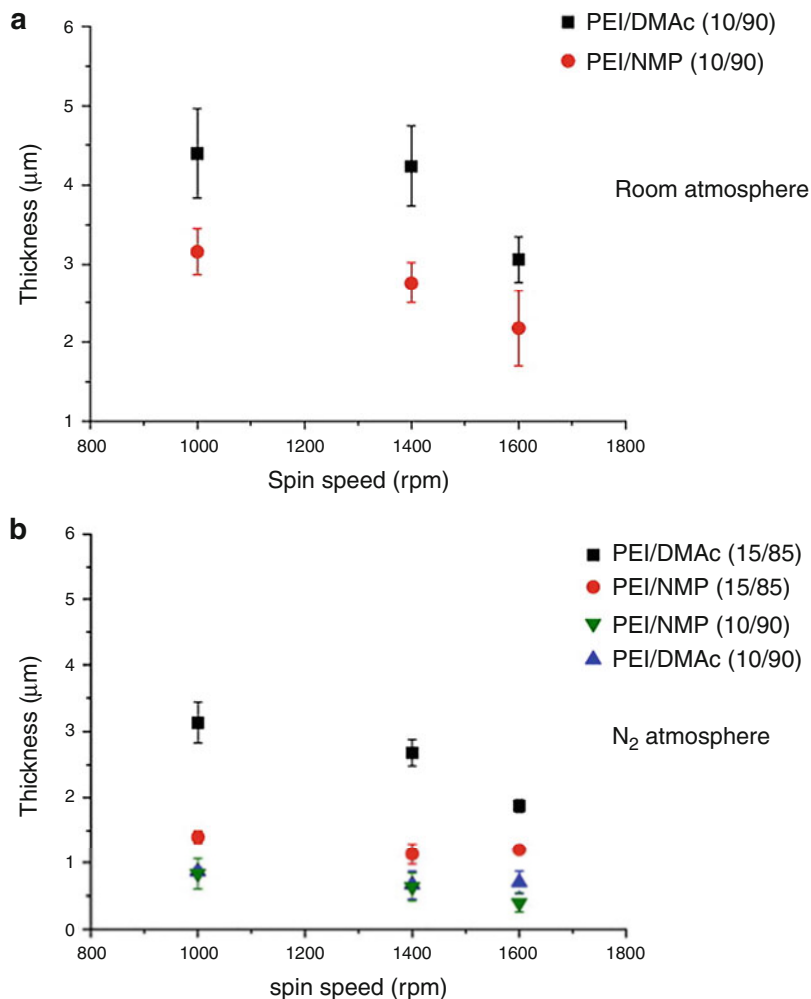


Fig. 6.10 The thickness of the PEI coating for different spin speed and solvent medium in (a) room and (b) nitrogen (N_2) atmosphere. (Reprinted from Conceicao et al. (2010) with permission from Elsevier)

(expansion ratio 50%). PCUU coating on AZ31 Mg stent maintained the coating integrity, while PLGA coating delaminated at the same expansion ratio (Fig. 6.12).

Li et al. (2010) have coated Mg-6Zn alloys surfaces with PLGA to enhance the degradation resistance and cell attachment in the physiological environment. The dip-coating techniques were used to coat alloy surfaces with two different concentrations (2 and 4 wt.%) of the PLGA in chloroform solvent. The mass gain of the samples was considered to evaluate the coating thickness of the samples. In another study on ZM21 Mg alloy, a phosphate-doped polyaniline (PANI) coating was employed to enhance the degradation resistance (Sathiyarayanan et al. 2006).

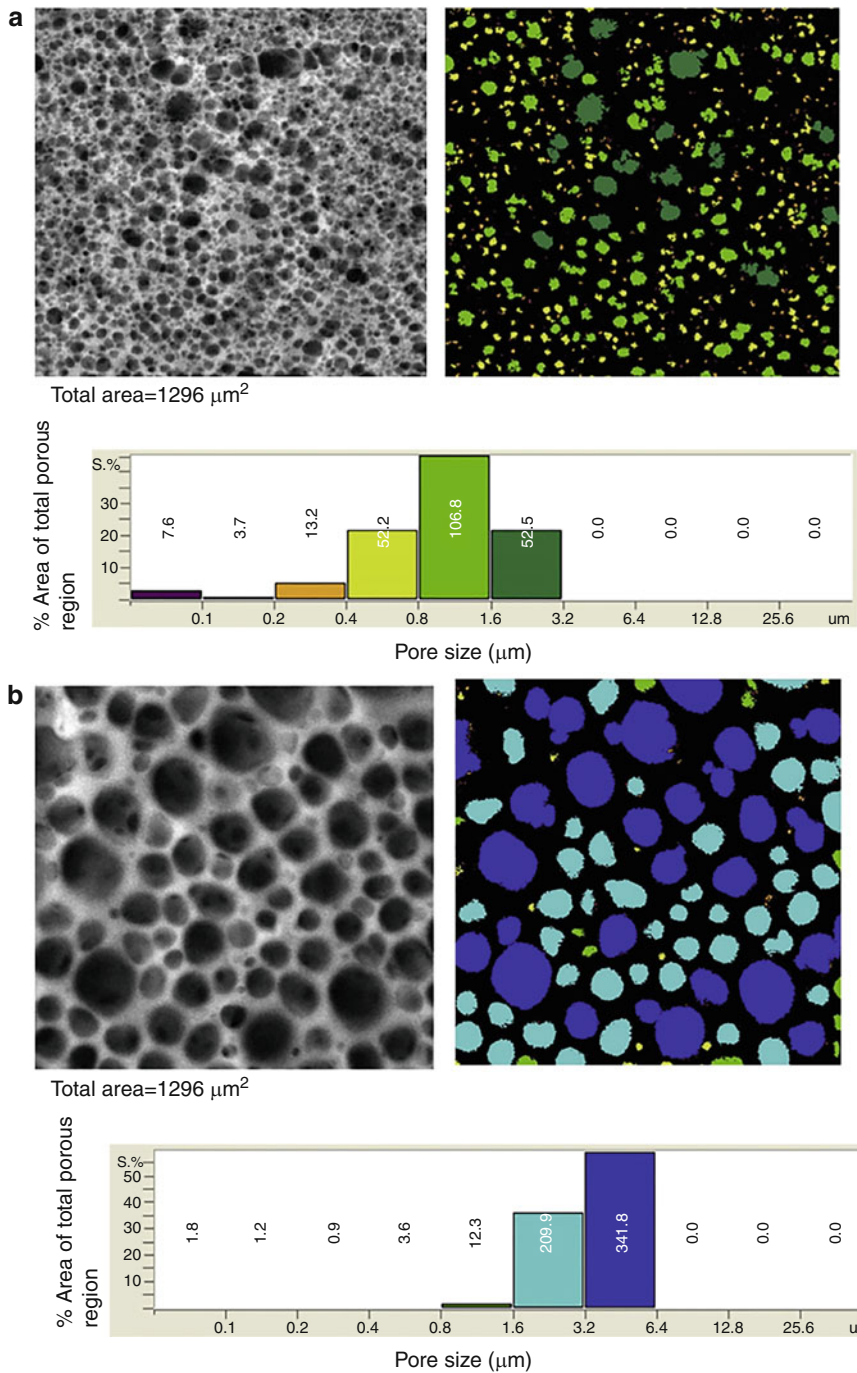


Fig. 6.11 Pore morphology and size distribution for LPM and HPM coating on AZ91 Mg alloy. (Reprinted from Wong et al. (2010) with permission from Elsevier)

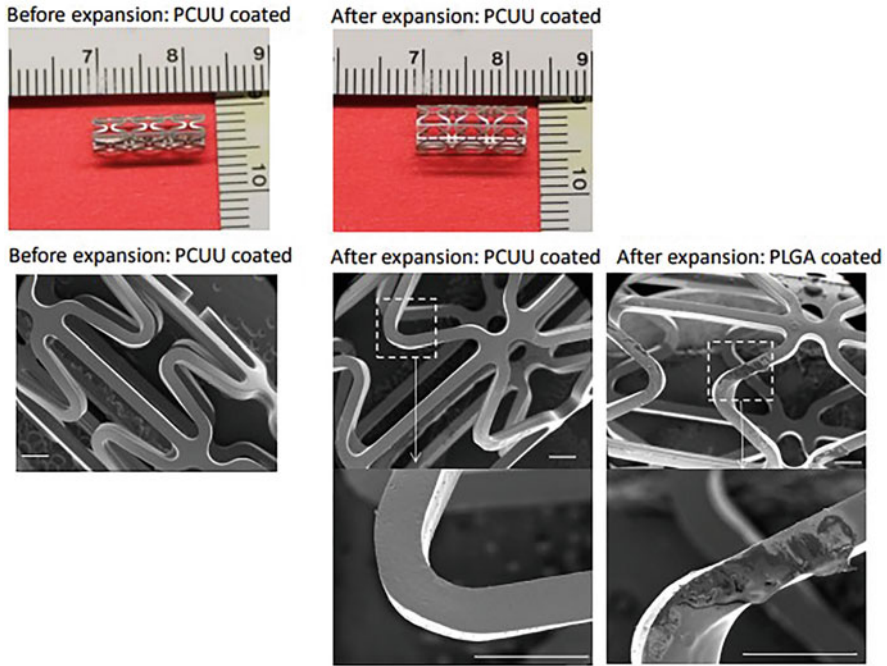


Fig. 6.12 The expansion of AZ31 Mg alloy stent coated with PCUU and PLGA polymer (SEM image have a scale bar of 500 μm). (Reprinted from Gu et al. (2016) with permission from Elsevier)

The chemical oxidative technique was followed to get aniline's reaction with ammonium per sulphate in a phosphoric acid solution, resulting in the polyaniline coating on the alloy.

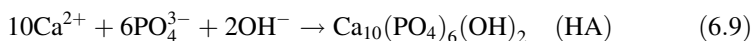
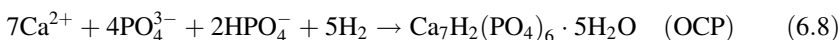
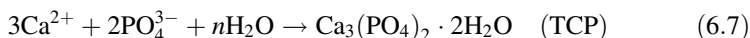
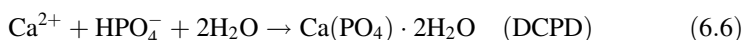
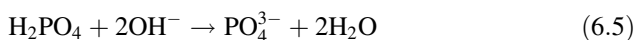
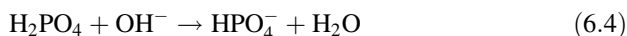
Calcium–Phosphate (Ca-P)-Based Compound Coatings

The Ca-P-based compounds belong to the orthophosphate family and naturally found in many biological structures. Ca-P-based minerals are the main inorganic substances in the human bone tissue and widespread coating materials for the Mg-based materials system for the orthopaedic application. It has shown significant biocompatibility, bone inductivity, bioactivity and non-toxicity in the in vivo application (Shadanbaz and Dias 2012; Xu et al. 2009; Liu et al. 2011). Additionally, Ca-P-based coatings improve the corrosion and wear resistance properties of the Mg-based implants (Dinu et al. 2017; Bala Srinivasan et al. 2010; Ali et al. 2020). There are several types of Ca-P-based compounds coatings, such as:

1. Hydroxyapatite (HA) $\rightarrow \text{Ca}_{10}(\text{PO}_4)_6(\text{OH})_2$.
2. Dicalcium phosphate dehydrate (Brushite, DCPD) $\rightarrow \text{CaHPO}_4 \cdot 2\text{H}_2\text{O}$.
3. Amorphous calcium phosphate (ACP) $\rightarrow \text{Ca}_8(\text{PO}_4)_6 \cdot n\text{H}_2\text{O}$.
4. Tricalcium phosphate (TCP)

- α -TCP (α -whitlockite) $\rightarrow \alpha\text{-Ca}_3(\text{PO}_4)_2$,
 - β -TCP (β -whitlockite) $\rightarrow \beta\text{-Ca}_3(\text{PO}_4)_2$.
5. Octacalcium phosphate (OCP) $\rightarrow \text{Ca}_8\text{H}_2(\text{PO}_4)_6$.
 6. Fluorapatite (FHA) $\rightarrow \text{Ca}_{10}(\text{PO}_4)_6\text{F}_2$.
 7. Anhydrous calcium phosphate (monetite) $\rightarrow \text{CaHPO}_4$.

They are being deposited on the Mg-based materials system for the orthopaedic application. Formation of Ca-P-based compound coating on Mg-based implants proceeds by the following chemical reactions:



Several coating techniques, such as biomimetic, sol-gel, electrodeposition and hydrothermal treatment, have been extensively used for the surface coating of Mg-based materials via Ca-P compound coatings.

HA is a naturally found mineral form of Ca apatites and is found in a significant amount in the human bone and teeth. The biological and synthetic stoichiometric structure of HA has shown hexagonal symmetry, as proven via X-ray structural analysis (De Leeuw 2001; McLean and Nelson 1982). HA is thermally stable up to 1300 °C, and no phase change was observed below this temperature (Rapacz-Kmita et al. 2005). The hydroxyl group of HA structure is generally substituted by fluoride, chloride and carbonate to produce non-stoichiometric HA (Shadanbaz and Dias 2012). Singh et al. (2015) coated the Mg-3Zn alloy substrate with HA via sol-gel coating techniques to enhance the mechanical integrity, corrosion resistance and bioactivity of the Mg-3Zn alloy. The effect of various surface roughness of substrate and sintering temperature of HA coatings on the mechanical properties of synthesised coatings has been established. SEM images of the cross-section of coatings on the substrate at different surface roughness and sintering temperatures are shown in Fig. 6.13. Figure 6.13b, d shows comparatively higher coating thickness than Fig. 6.13 a and c due to the high surface roughness of the samples. A very robust interface without delamination can be observed in Fig. 6.13c. A clear sign of delamination was observed in Fig. 6.13a due to low surface roughness and comparatively lower sintering temperature (i.e. 300 °C). It was observed that the surface

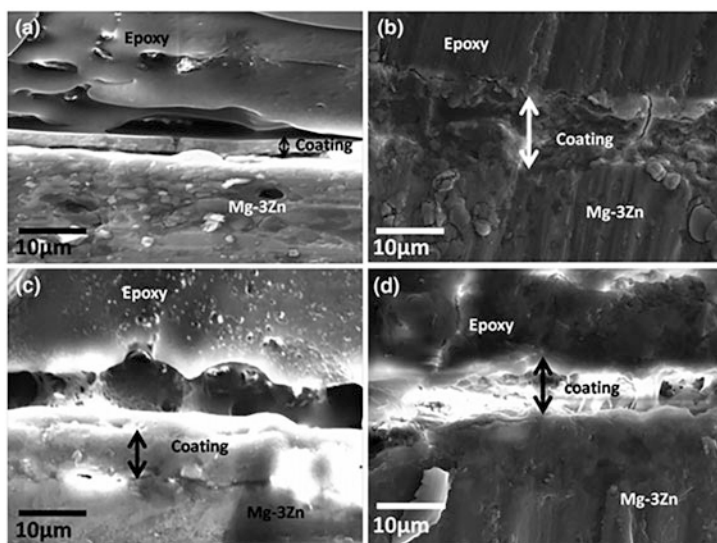


Fig. 6.13 The cross-sectional SEM images of the coating at 300 °C and surface roughness (a) 15–20 nm, (b) 130–150 nm, and sintering at 400 °C and surface roughness (c) 15–20 nm, (d) 130–150 nm. (Reprinted by permission from Springer Nature, (Singh et al. 2015))

roughness of the Mg-3Zn alloy substrate and the sintering temperature of the HA coating played a major role in deciding the coating thickness and integrity.

In another coating fabrication method, Kumar et al. (2016) have electrophoretically deposited HA on the Mg-3Zn alloy substrate. The coatings with the lower surface roughness (i.e. 15–20 nm) of the substrate have shown a uniform coating layers with very few minor cracks. This study has demonstrated the potential of electrophoretic deposition technique on the Mg-based alloy to enhance the mechanical and corrosion resistance. The morphology of the coating surfaces at various surface roughness and sintering temperatures is shown in Fig. 6.14. It can be seen that the coating at comparatively higher surface roughness and lower annealing temperature resulted into the improper integrity and inhomogeneous shrinkage (Fig. 6.14a, a'). Pores and micro-cracks were also seen in these micrographs. However, increasing the annealing temperature and lowering the surface roughness of substrate resulted in to the better coating integration due to the higher diffusion of HA particles into the substrate at interface (Fig. 6.14d, d').

In another study, tin dioxide (SnO₂)-doped Ca-P coating was fabricated on Mg-1Li-1Ca alloy using hydrothermal process (Cui et al. 2019). Doping of SnO₂ nanoparticles in Ca-P coating enhanced the compactness and crystallinity of the coatings. In addition to this, the crystallinity and morphology of the coatings can be varied by tailoring the hydrothermal processing parameters. In vitro corrosion and antibacterial efficacy of the coatings were evaluated. A three-layered structure, which consists of Ca₃(PO₄)₂, (Ca, Mg)₃(PO₄)₂, SnO₂ and MgHPO₄·3H₂O, led to the formation of Ca₁₀(PO₄)₆(OH)₂ in Hank's solution. The cross-section images of

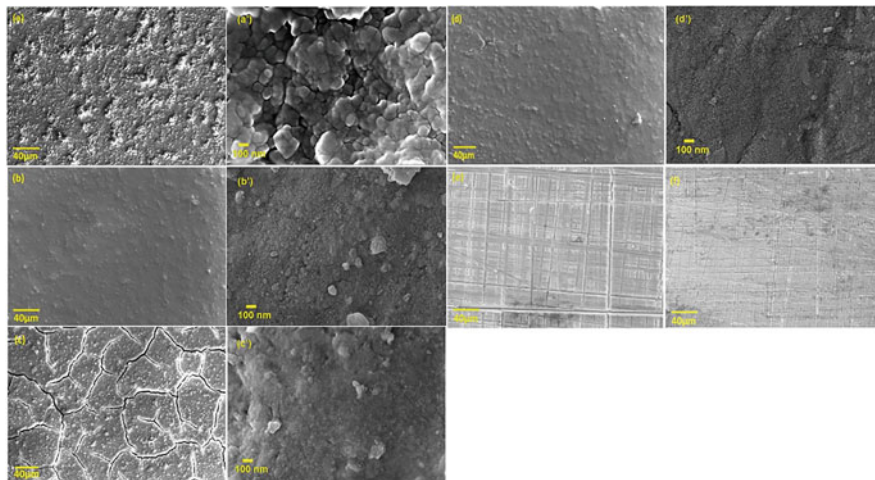


Fig. 6.14 SEM images showing the morphology of the HA coating (electrophoretically deposited) on Mg substrate, sintered at 300 °C and surface roughness of (a and a') 130–150 nm and (b and b') 15–20 nm. HA-coated Mg substrate sintered at 400 °C and surface roughness of (c and c') 130–150 nm and (d and d') 15–20 nm. SEM micrograph of the bare substrates showing surface roughness of (e) 130–150 nm and (f) 15–20 nm. (Reprinted from Kumar et al. (2016) with permission from Elsevier)

the coating and energy-dispersive X-ray spectroscopy (EDS) line scanning data are shown in Fig. 6.15.

Plasma Surface Modification

Several factors would be involved in choosing the suitable coating methods for Mg-based alloy. The factors such as geometry, substrate material, product design, cost and the intended applications are taken into consideration for choosing the best suitable coating for Mg-based implants. The process parameter and coating thickness are two critical factors frequently highlighted for designing the useful coatings on the Mg-based alloys. Depending on the substrate materials, feedstock form (powder, precursor) and deposition method, the coating thickness can be varied. The typical thickness range obtained in the various surface modification techniques is presented in Fig. 6.16.

The synergistic effect of the ion beam technology and conventional plasma is obtained in the plasma surface modification technique and has significant medical implants with intricate shapes. The thermal spraying coating/plasma spraying process involves the spraying of melted (or heated) materials onto the surface of the substrate. The coating precursor is heated by high-temperature and high-energy electrical source (plasma or arc) followed by the spraying of high-velocity precursor particles on a substrate in an inert atmosphere (such as argon). A coating is deposited onto the substrate by the accumulation of sprayed particles. The types of different plasma surface modification techniques are presented in Fig. 6.17.

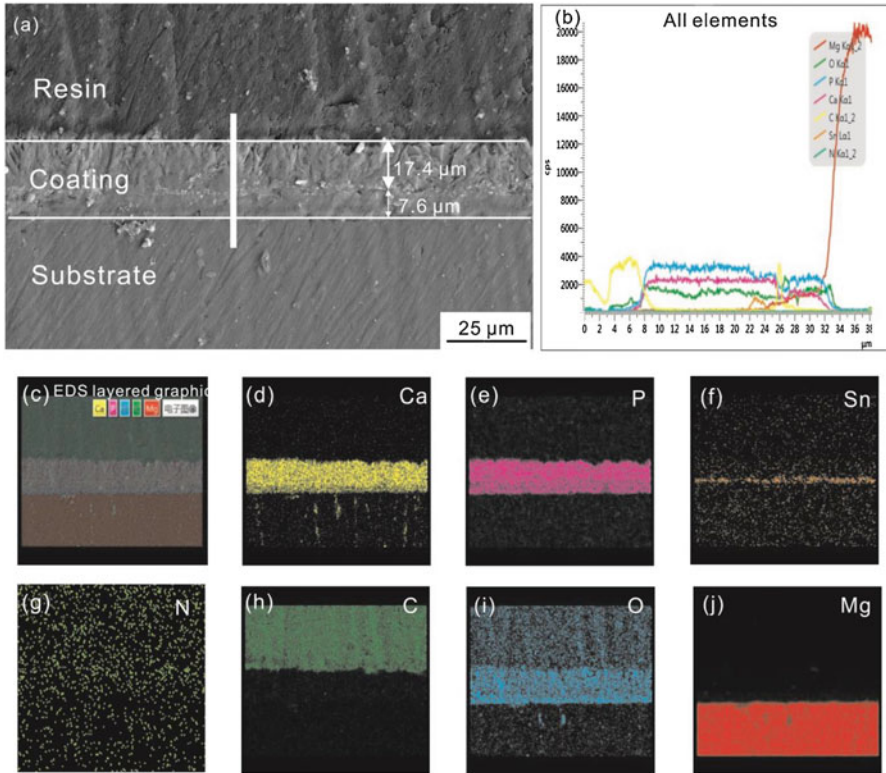


Fig. 6.15 The cross-section image of the coatings (a) and EDS line scanning analysis of the coatings (b–j). (Reprinted from Cui et al. (2019) with permission from Elsevier)

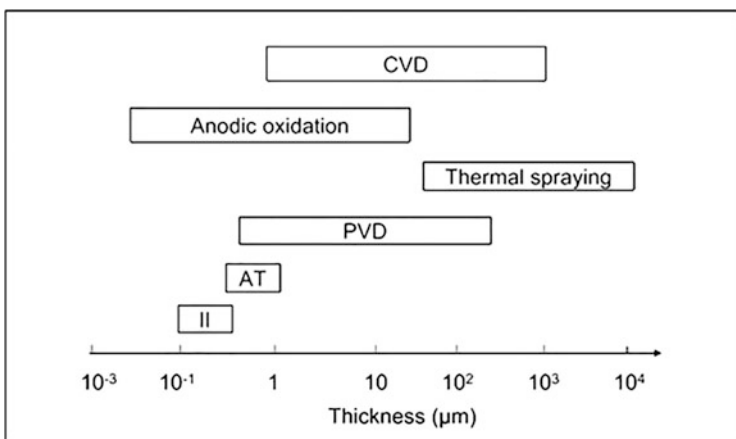


Fig. 6.16 Typical thickness range of the various surface coating technique. (Reprinted from Yang et al. (2010) with permission from Elsevier)

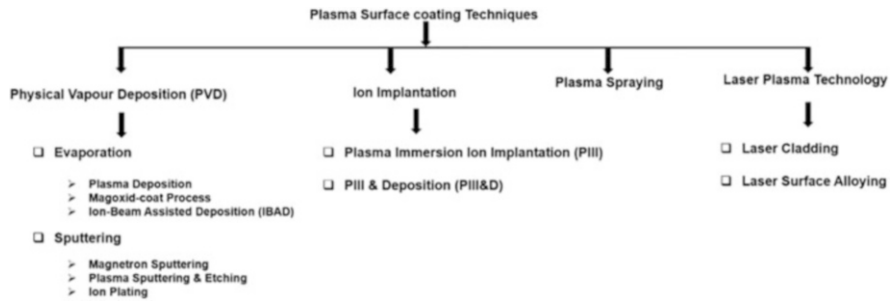


Fig. 6.17 Types of novel plasma surface modification techniques

With regards to the Mg and its alloy for medical implants, plasma surface modifications methods offer several benefits as follows (Sodhi 1996):

- Simple fabrication technique.
- Unique film chemistry.
- The better adhesion strength between coatings and substrate.
- Conformal and pinhole-free coatings.
- Excellent permeation barrier with low levels of leachable.
- Sterile upon preparation.

In the case of PVD coatings, atoms, ions and molecules of the intended coating materials are physically deposited onto the substrate in a chamber containing a controlled atmosphere at reduced pressure. It has been observed that controlling the deposition temperature in Mg-based implants is quite challenging. Besides, the adhesion strength of the coating is significantly dependent on the deposition temperature of the PVD coatings (Yang et al. 2010). In one of the previous studies, significant adhesion of titanium nitride (TiN) coating was achieved on AZ91 Mg alloy, using a pulsed bias voltage during deposition (Yang et al. 2010). The Ca-P coating was also achieved via the IBAD coating method on AZ31 Mg alloy, and a post-treatment annealing (250 °C for 2 h and deionised water immersion for the next 30 min at 100 °C) was also employed for tailoring the crystallinity of the coatings (Yang et al. 2008). The width of the interface region is evaluated via the composition depth profile using auger electron spectroscopy (AES) as shown in Fig. 6.18. The broad interface region was chosen due to the ability of IBAD, which can provide bombardment with energetic ions during deposition. Thus, the IBAD offers fabrication of biocompatible coatings that adhered strongly to Mg substrates.

Sputtering processes involve the electrical generation of a plasma between the coating materials and the substrate. It offers relatively high deposition rates with large deposition areas on complicated shapes and even allows to deposit coating at lower temperatures. The additional gas ionisation or plasma confinement is a strategy to enhance plasma ionisation. The Al and Al/Ti multilayer coating was deployed on AZ31 Mg alloy, and a compact columnar microstructure was obtained

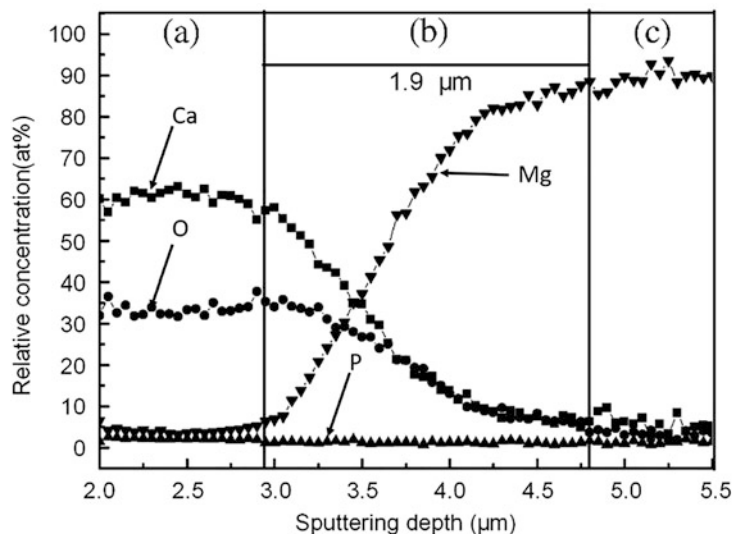


Fig. 6.18 The compositional depth profile measured via AES at different regions: (a) film, (b) interfacial and (c) substrate. (Reprinted from Yang et al. (2008) with permission from Elsevier)

(Wu 2007). The morphology of the top surface of Al-coated Mg alloy had a pyramid-like morphology with fully grown facets. However, the multilayer coating was quite smoother and showed a similar round roof-like morphology. In recent days, plasma spraying of the Mg-based alloys has gained significant interest due to the ability to treat the substrate with complex geometries and covers a broad spectrum of the materials for coatings. In one of the plasma spraying modification techniques, the cathodic arc process was employed to fabricate a double layer coating of alumina (Al_2O_3)/Al (1 μm) and zirconia (ZrO_2)/Zr (1.5 μm) on AZ91 Mg alloy (Xin et al. 2009). The bonding characteristic of the coating (O_2) and substrate materials (Mg) was enhanced by applying an intermediate layer of Al or Zr to form a direct link. In addition to this, laser surface alloying methods have also been employed to enhance corrosion properties selectively. A single and multiple layers of coatings were successfully synthesised via laser cladding and alloying of Al powder on Mg alloys (Kutschera and Galun 2000). The deposited layers showed significant bond properties, and microstructure presented very few or no porosities and cracks on coatings.

6.2.1.2 Coating-Free Techniques

Micro-Arc Oxidation method (MAO)

MAO, an electrochemical oxidation process, is generally applied to the Mg-based materials to convert its substrate to oxide. Due to the application of higher potentials, discharge occurs and resulting plasma oxidises the substrate surfaces. It has the ability to fabricate porous ceramic coating with high adhesion to the substrate

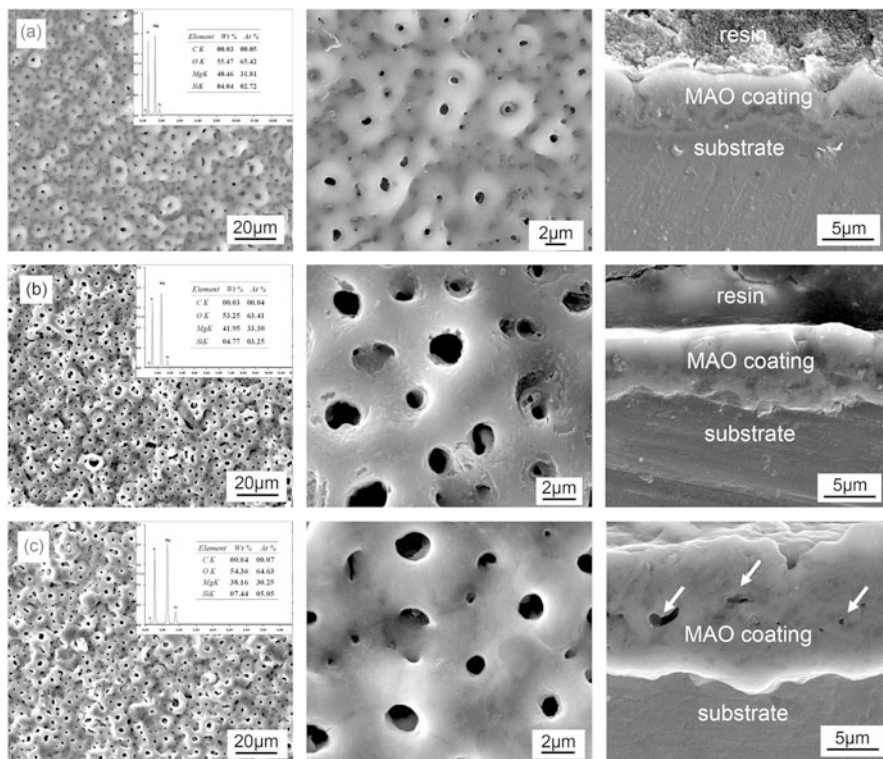


Fig. 6.19 SEM images of the surface and cross-section morphology of MAO coating on Mg-Ca alloy at (a) 300 V, (b) 360 V and (c) 400 V. (Reprinted from Gu et al. (2011) with permission from Elsevier)

(Nassif and Ghayad 2013). Dense MAO coatings on Mg-based alloys are being developed using high voltage. In many studies, the porous coatings are used as the intermediate layer for depositing Ca-P-based compounds (i.e. HA) (Duan et al. 2006). It has been observed that porous morphology can generate a pinning force, when HA is deposited in the pores. In one of the previous studies of MAO coating on Mg-Ca alloy (Gu et al. 2011), the effect of various voltages (range 360–400 V for 10 min) on the coating characteristics in terms of surface morphology and phase constitution were extensively evaluated. The Mg-Ca alloy was employed as the working electrode and stainless steel as a counter electrode. The solution of 10 g/L Na_2SiO_3 with 3.5 g/L NaOH was used as the aqueous electrolyte. The morphology of the surfaces and cross-section at different voltages is shown in Fig. 6.19.

Micropores and micro-cracks have also been seen in the MAO coatings, which might be detrimental from the degradation perspective in the electrolyte solution. Significant corrosion protection of MAO-coated Mg alloys can only be achieved by tailoring the surface defects of the coatings. The sol-gel and organic polymer material composite techniques have been applied to seal the pores of the MAO

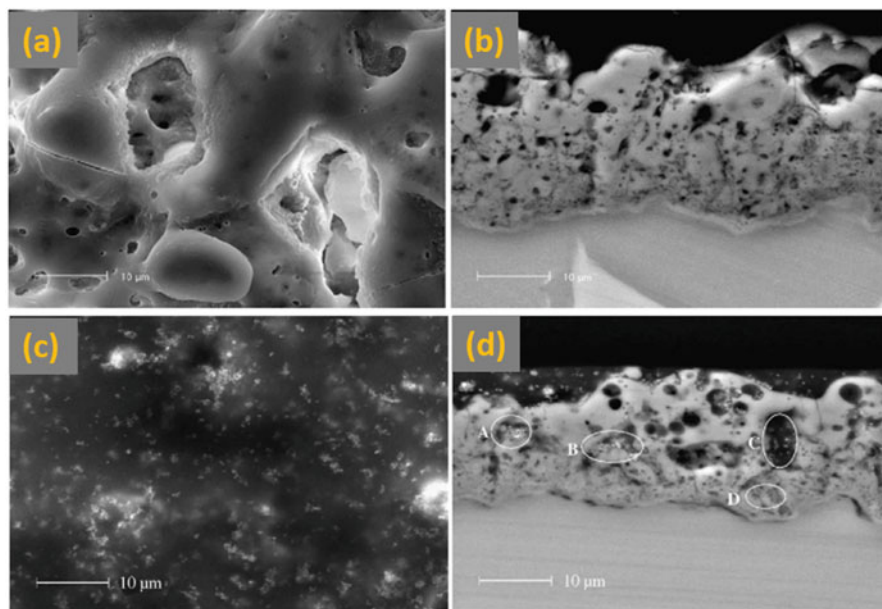


Fig. 6.20 SEM micrograph of the MAO-coated (a) surface and (b) cross-section. Sealing of the MAO coatings: (c) surface and (d) cross-section. (Reprinted from Duan et al. (2006) with permission from Elsevier)

coating, deposited on Mg-based alloys. Duan et al. (2006) fabricated MAO coating on the AZ91 Mg alloy, followed by top coating sealing via multi-immersion technique under low-pressure conditions. A physical interlocking between the MAO layers and the sealing agent was observed in the SEM examination. Besides, the sealing agents covered the surface uniformly and penetrated the pores and microcracks present in the MAO layers. SEM micrographs of the surface and cross-section, before and after the sealing process, are shown in Fig. 6.20.

Researchers have also explored the copper (Cu) element doping in MAO coating on Mg-2Zn-1Gd-0.5Zr, to enhance antibacterial characteristics as well as degradation resistance of the Mg alloy (Chen et al. 2019). To fabricate Cu-added MAO coating on Mg alloys, 1 g/L nano-CuO was mixed with the electrolyte ingredients (1 g/L Nano-HA, 8 g/L KF and 3 g/L $(\text{NaPO}_3)_6$).

The coating parameters were as follows: working voltage—360 V, working duty cycle—40%, working frequency—1000 Hz and preparation time—5 min. SEM micrographs and XRD patterns of the coating is shown in Fig. 6.21. Micropores sizes increase after the addition of Cu elements in MAO coatings (Fig. 6.21b). The presence of Cu in the MAO coating was confirmed via XRD phase analysis.

Anodisation

Anodisation is another nanostructure coating technique on Mg-based materials. In this technique, the surface of the working electrode (Mg metals) converts to oxide

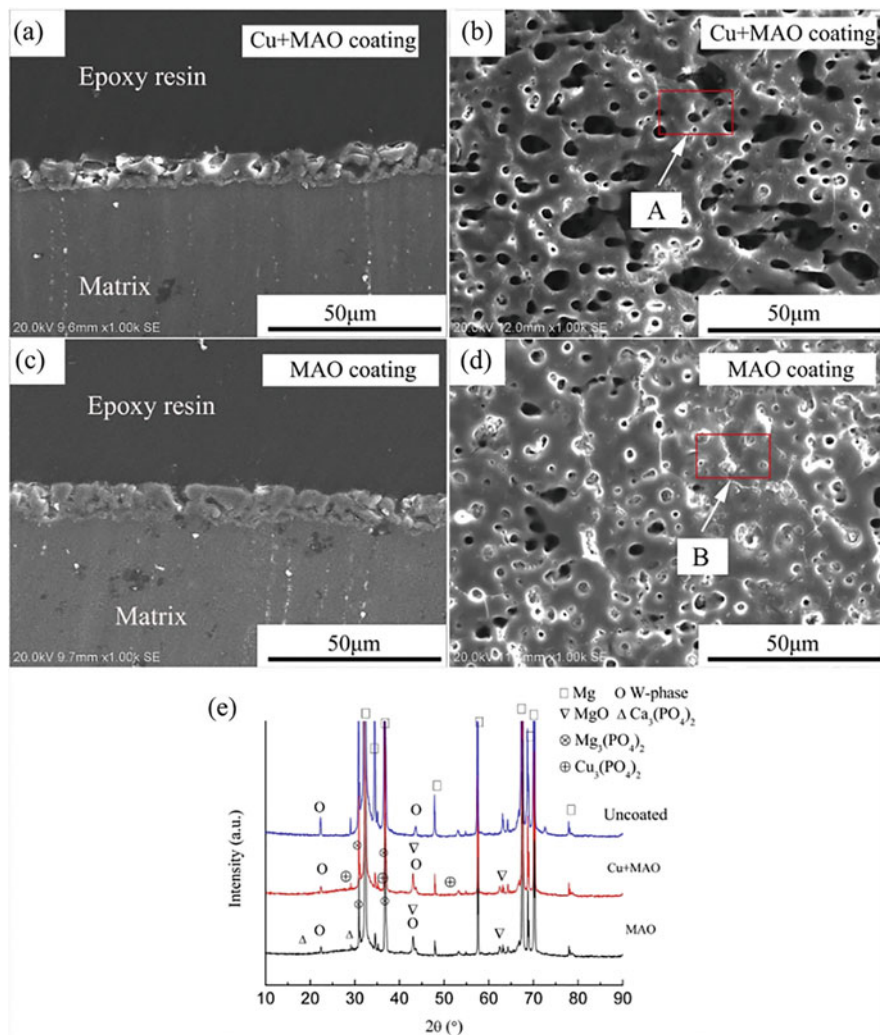


Fig. 6.21 SEM micrographs and XRD pattern of the Cu-added MAO coating on Mg-2Zn-1Gd-0.5Zr alloy. (Reprinted from Chen et al. (2019) with permission from Elsevier)

film via an electrolytic oxidation process (Xue et al. 2011; Zhang et al. 2002). The applied voltage or current significantly influences the anodising behaviour (film thickness) of Mg-based alloys. Besides, various passive and active states can be obtained by varying the applied voltage, current, time, substrate and electrolyte (Yerokhin et al. 1999). Several aspects of anodisation that influence the coating on Mg-based materials are shown in the schematic in Fig. 6.22. The selection of electrolyte should be carefully designed to obtain thick, durable and non-toxic coatings on Mg-based substrates. Xue et al. (2011) have synthesised coating via

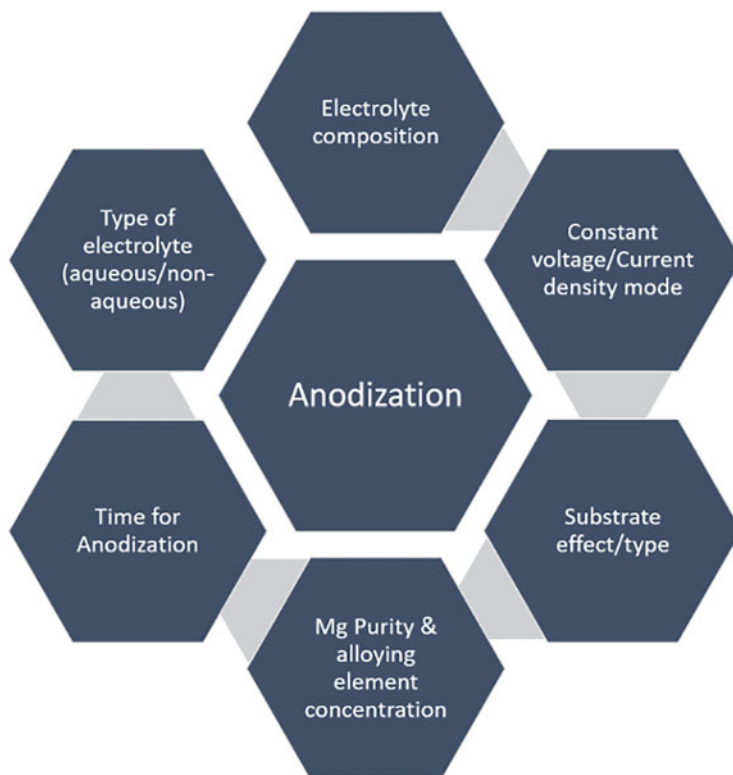


Fig. 6.22 Factors influencing the anodising behaviour of Mg-based alloys

the anodising process on the AZ91D Mg alloy. The potential of anodising on these alloys was evaluated in terms of degradation resistance, by varying the applied voltage, current and different anodising time (Xue et al. 2011). Increasing the time of anodisation has changed the morphology of the surfaces and the size of the pores. After 3 h of anodisation, the morphology of surfaces was smooth, but the pore size was larger (Fig. 6.23).

In another study (Zhang et al. 2002), the effect of treatment time and the temperature of electrolyte solution on anodising behaviour (film thickness) of AZ91D Mg alloy was studied, as shown in Fig. 6.24. To some extent, the growth of film depends on the applied voltage. Higher voltage is associated with the increased film thickness, while anodising under constant current condition.

Laser Surface Modification

Laser surface modification of Mg-based alloy is attracting significant attention from researchers for biomedical applications. It has the potential to offer a broad range of possibilities in obtaining the required composition and microstructural modification

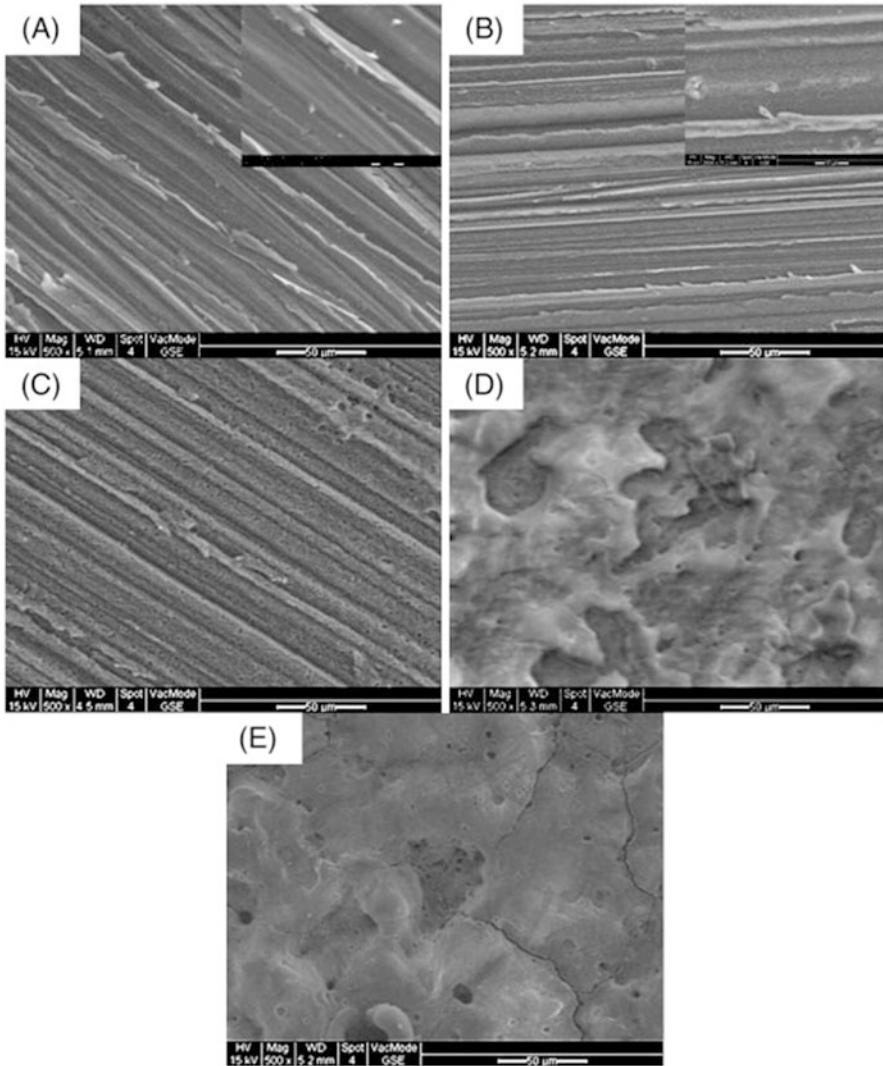


Fig. 6.23 The effect of anodising time variation on the surface morphology and pore size of AZ91D Mg alloy. (Reprinted from Xue et al. (2011) with permission from Elsevier)

on the Mg-based surfaces via a range of laser and materials surfaces interaction. Various laser surface modification approaches for Mg-based alloys are as follows:

- Laser surface melting (LSM).
- Laser surface alloying (LSA).
- Laser surface cladding (LSC).

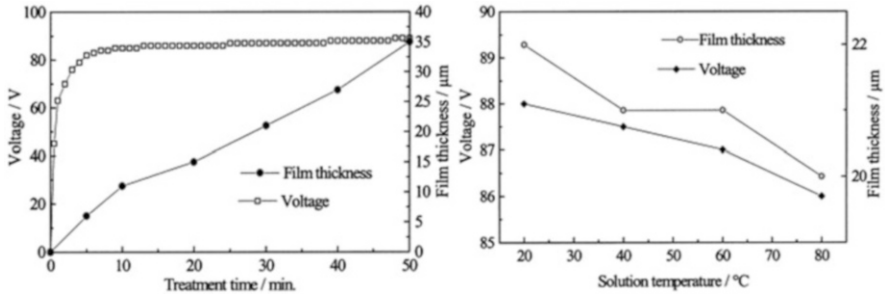


Fig. 6.24 The variation of film thickness to treatment time for anodising and solution temperature of the electrolyte. (Reprinted from Zhang et al. (2002) with permission from Elsevier)

- Laser composite surface (LCS).
- Laser shock peening (LSP).

The Nd:YAG, CO₂ and excimer lasers have been predominantly utilised to modify the metallic surfaces (Singh and Harimkar 2012). Some of the significant advantages of laser surface modification include noncontact processing, rapid processing and the ability to produce novel and refined grain structure of Mg alloys. The final microstructure, phase and composition of the coatings depend on several factors like cooling rate, solidification rate, temperature gradient, interfacial effects and elemental evaporation during the laser-surface interaction (Singh and Harimkar 2012). In the surface modification of Mg-based materials, the use of protective gases during laser application becomes very important to shield the surfaces from oxidation.

Ho et al. (2015) have performed the laser surface treatment using a 3-kW diode-pumped ytterbium fibre laser system in continuous-wave delivery mode on AZ31 Mg alloys at different laser processing parameters (energy density of 1.06, 2.12, 3.18, 4.24 and 5.31 J/m² × 10⁶). The grain size of the alloy decreased as the energy density of the laser is increased (Fig. 6.25). Grain refinement of AZ31B Mg alloy can be clearly observed with the increment of laser energy density (Fig. 6.25a, f). Also, the effect of cooling rate on grain size variation is shown in Fig. 6.25. Increasing the cooling rate resulted in the decrement in the grain size of alloy (Fig. 6.25).

Coy et al. (2010) modified the AZ91D Mg alloy surface via excimer laser surface melting, and a significant dissolution of the second phase of Mg₁₇Al₁₂ in AZ91D was observed during laser surface processing. The number of pulses was varied (10, 25 and 50) to get different sizes of the melted surfaces. SEM micrograph of the cross-section is shown in Fig. 6.26. Similar results were also reported for WE43 and ZE41 Mg alloys, using the laser processing technique (Guo et al. 2005; Khalfaoui et al. 2010).

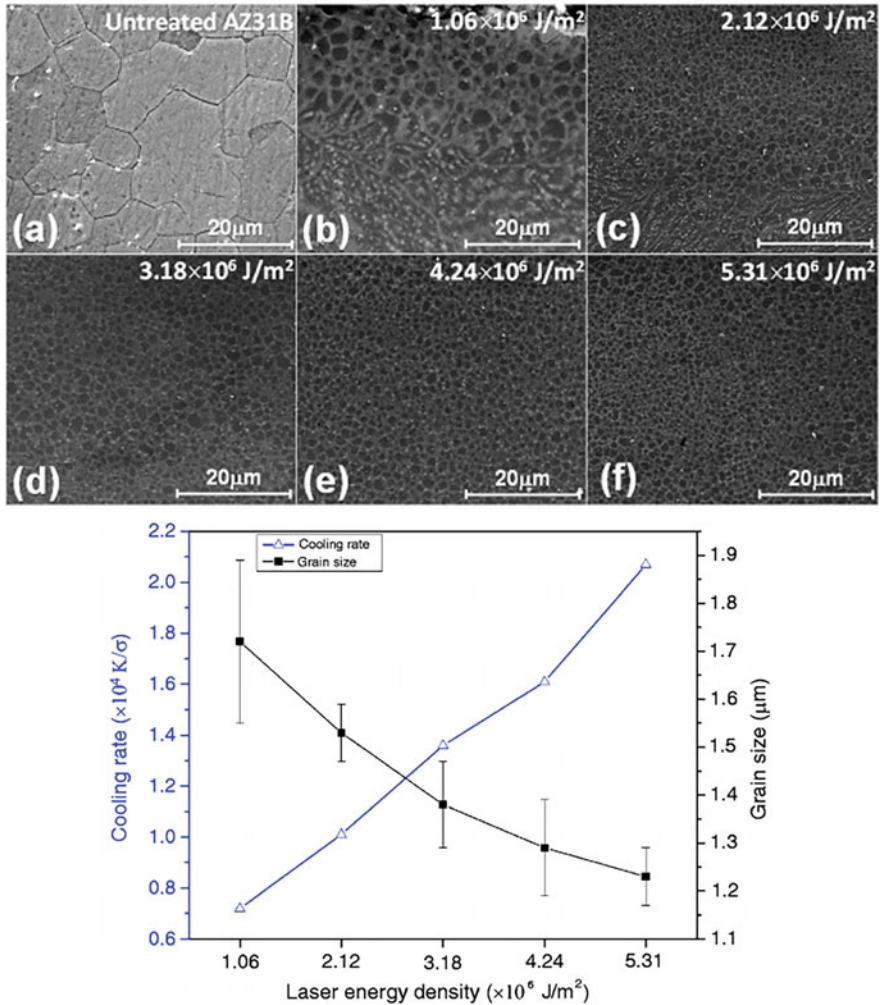


Fig. 6.25 The effect of processing parameters of laser surface treatment on the grain size of AZ31 Mg alloy. (Reprinted from Ho et al. (2015) with permission from SAGE publications)

6.3 Effect of Physico-chemical Modifications on Implant Performance

In order to fabricate the ideal Mg-based implants, several efforts have been made by the researchers with the different combinations of the properties. The strategies such as alloying, surface treatment/coating and mechanical processing have been studied. Different types of coatings have been used for enhancing the surface properties of the Mg-based implants without compromising the bulk attributes. The primary list of

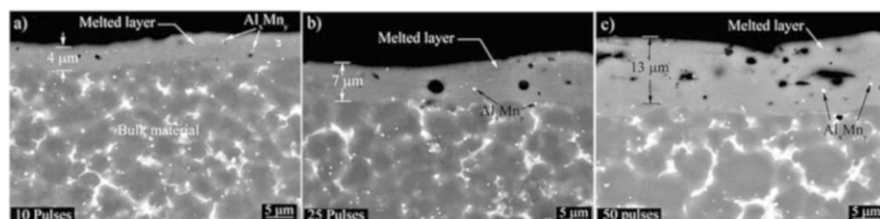


Fig. 6.26 The cross-section image of the laser modified AZ91D Mg alloy at different pulse (a) 10, (b) 25 and (c) 50 pulse. (Reprinted from Coy et al. (2010) with permission from Elsevier)

properties for the design and development of Mg-based biodegradable implants are as follows (Narayanan et al. 2014):

- Significant mechanical strength and integrity should be maintained until the damaged tissue is healed correctly.
- The excellent corrosion resistance in the physiological environment during the initial periods of implantation followed by the uniform degradation fashion.
- The excellent biocompatibility and bioactivity behaviour within the real body environment.
- The protein adhesion and wettability are essential criteria to be focussed.

This section elaborates the effect of different physico-chemical surface modification methods on corrosion, mechanical, protein adsorption wettability and biocompatibility behaviour of Mg-based alloys and their potential use in biomedical applications.

6.3.1 Degradation Behaviour

The major challenge with the Mg-based implants is the high degradation rate when it comes in contact with the physiological environment (standard electrode potential = -2.37 V). The severe corrosion rate led to a rapid drop in the mechanical integrity of Mg implants during the in-service condition. The interaction of Mg metals with an aqueous environment involves the release of H_2 gas as the by-products and the formation of $Mg(OH)_2$ layer. The strengthening and dissolution of the $Mg(OH)_2$ layer depend further on the elements present in the electrolyte and immersion duration. The Cl^- ions in the physiological solutions convert $Mg(OH)_2$ layer into the $MgCl_2$ (highly soluble chloride). Thus, hydroxide layers lose their function when the concentration of Cl^- ions in the body-fluid is above 30 mmol/L. Hence, to design and develop the Mg-based implants for biomedical applications, it is also necessary to understand the effect of physiological solutions on the degradation performance of the implants. The previous studies on the physico-chemical modification of Mg-based alloy surfaces have shown significant control on the degradation rate (Kumar et al. 2016; Li et al. 2010). The comparative efficacy of

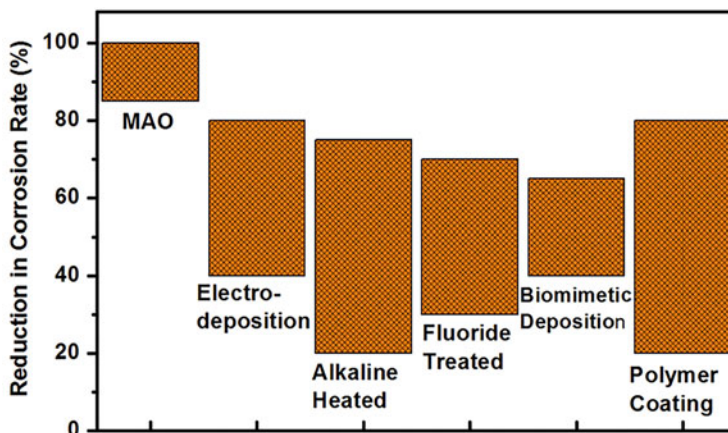


Fig. 6.27 The efficacy of the different physico-chemical surface modification methods to tailor the degradation rate

the different physico-chemical surface modification methods on the Mg-based implants has been presented in Fig. 6.27. A range of ~20–90% reduction in the degradation rate was observed after the deployment of different physico-chemical methods on Mg-based alloys.

Hypothetically, a thick compacted coating is assumed to be a better solution to resist corrosion behaviour of the Mg-based biomaterials. But the generation of hydrogen bubbles at the coating interface limits the complete compact coating through chemical methods. Hence, in several approaches, the researchers have tried to apply a pre-treatment on Mg surfaces, which could improve the quality of the coating adhesions. In one of the coatings (double-layer of HA and PLA) on Mg metal (Oosterbeek et al. 2013), the researchers have shown the correlation of the adhesion strength of coatings and degradation resistance. As per the outcomes, the adhesion strength of the coating should be higher to get significant corrosion resistance for a suitable immersion period. A detailed corrosion mechanism of bioceramic polymer coating in the physiological environment is schematically shown in Fig. 6.28. MAO coatings have received considerable attention amongst other physico-chemical methods (Narayanan et al. 2014). The porous nature of the coating improves the adhesion strength and better stress distribution over the Mg substrate resulting in higher bonding strength. Besides, in the initial periods of implantation, MAO coatings show a slow degradation rate, while accelerated degradation is seen in later stages. The surface modification via different Ca-P compound on Mg-Zn alloy was fabricated, and their corrosion resistance was evaluated in terms of hydrogen evaluation. Fluoride-doped HA (FHA)-treated alloy showed lower degradation resistance as compared to other coating materials (Fig. 6.29).

Besides, the surface modification via fluoride coatings on Mg-Ca and AZ31 Mg alloy also significantly reduced the corrosion rate when compared to the base metal

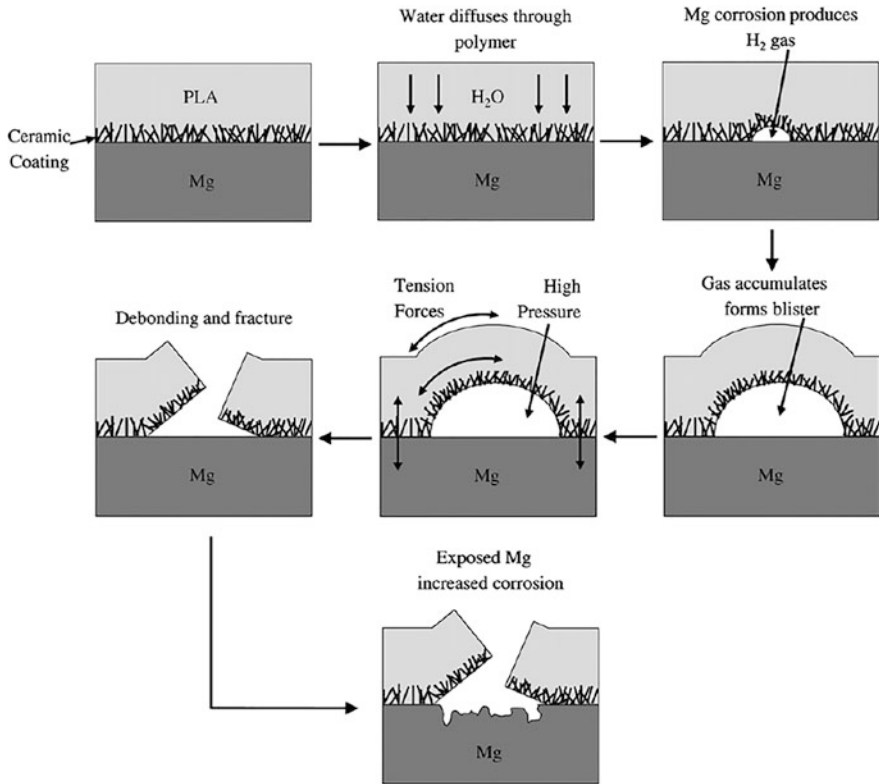


Fig. 6.28 The schematic representation of the corrosion mechanism of coatings in the physiological environment. (Reprinted from Oosterbeek et al. (2013) with permission from Elsevier)

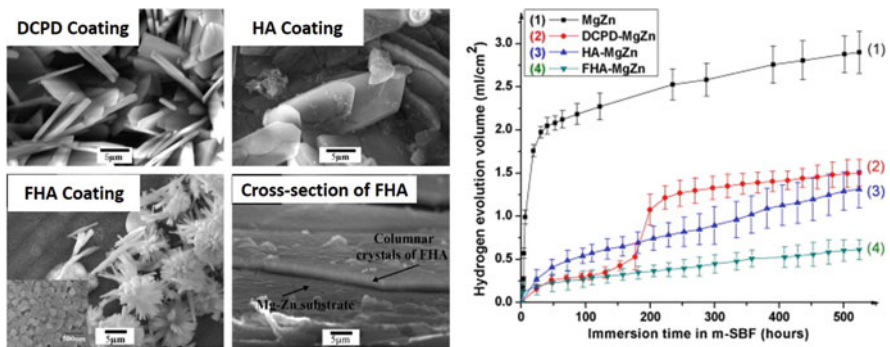


Fig. 6.29 SEM micrograph of the coating and hydrogen evaluation tests for all the coatings. (Reprinted from Song et al. (2010) with permission from Elsevier)

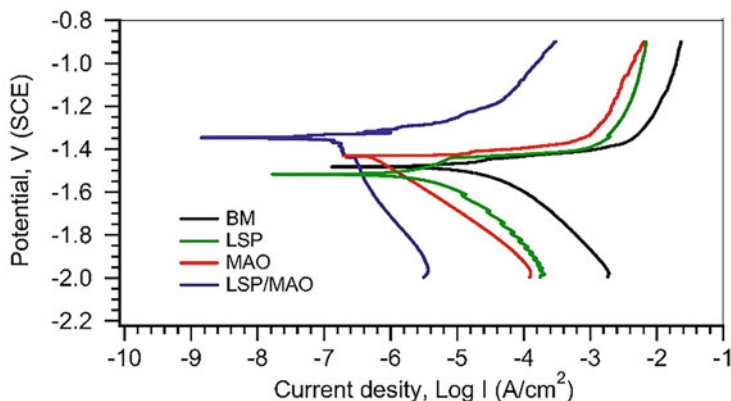


Fig. 6.30 The potentiodynamic polarisation curves for different coating technique. (Reprinted from Xiong et al. (2017) with permission from Elsevier)

(Drynda et al. 2010). However, the use of hydrofluoric acid for MgF_2 coating generation might be harmful to the operators as well as body environments.

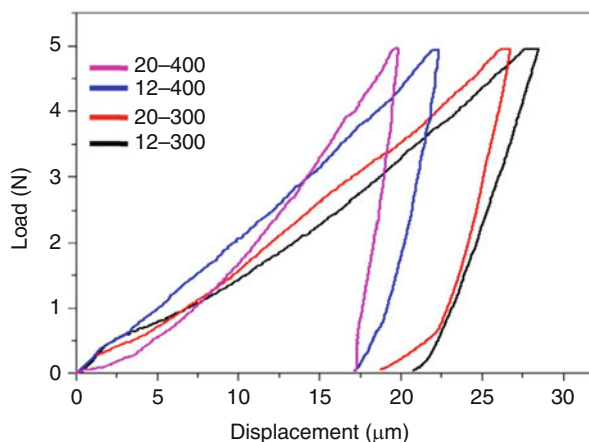
The Ca-P-based compound coatings are getting significant interest in reducing the corrosion rate of Mg-based implants. HA being bioactive, and having properties such as osteoinductivity and osteoconductivity, makes it a better coating substance to tune the corrosion behaviour of Mg-based materials (Jaiswal et al. 2020). Kannan and Orr (2011) coated AZ91 Mg alloy with HA at different cathodic voltages to improve the mechanical integrity by tailoring the degradation resistance in the SBF solution. The uncoated AZ91 Mg alloy exhibited $\sim 40\%$ less mechanical strength after 5 days of immersion. Further, the use of AZ91 alloys in biomedical implants (presence of Al may cause Alzheimer disease), and short duration immersion testing is still a concern for commercial uses.

Xiong et al. (2017) pre-treated AZ80 Mg alloy using laser shock peening (LSP) followed by the fabrication of composite bio coating on it via micro-arc oxidation (MAO) to enhance the mechanical integrity and degradation resistance in SBF solution. The potentiodynamic polarisation curves are shown in Fig. 6.30. LSP-treated samples have shown grain refinement and consequently enhanced corrosion resistance.

6.3.2 Mechanical Integrity of the Coatings

The mismatch of the physical, chemical and mechanical properties of the Mg substrate and coating materials results in stress and strains in the materials system, which can develop the premature crack in the modified Mg surface. The development of any possible micro-cracks in the coating allows the aggressive ions to enter the interface and accelerate the degradation process. Additionally, the reliability and solidity of the surface-modified Mg implant in vivo depend on the localised

Fig. 6.31 The load versus displacement curve for the nanoindentation study of EPD coated HA on Mg-3Zn alloy. (Reprinted from Kumar et al. (2016) with permission from Elsevier)



mechanical properties of the coatings. So, the local mechanical properties of the coatings become necessary for the reliability of implants. Hardness (H) and elastic modulus (E) of the coatings have been extensively studied in the available literature.

In one of the HA coatings, via radio frequency (RF) magnetron sputtering, on AZ91D Mg alloy showed an improvement of ~ 370 and 80% for hardness and elastic modulus, respectively, as compared to uncoated AZ91D Mg alloy (Melnikov et al. 2017). In another study, a thin layer of HA was synthesised on the AZ31 Mg alloy via RF magnetron sputtering at the bias of 50 V. An increment of ~ 82 and 46% in the H and E values of the coated AZ31 alloy was observed, in comparison to bare AZ31 Mg alloy (Surmeneva et al. 2015). It has been seen that the nanoindentation of the thin film is very sensitive towards the surface roughness, elastic anisotropy, grain size and the film thickness on the substrate. The changes in surface roughness and annealing temperature of HA film could change the hardness and elastic modulus values of coatings. Similar behaviour was observed in other studies of HA coating on Mg-3Zn substrate via sol-gel technique (Singh et al. 2015). The characteristics values of hardness and Young's modulus of micro-arc-oxidised (MAO) coating, grown on the AZ31B Mg alloy, were evaluated via Weibull approach and obtained as 3 and 90 GPa, respectively (Dey et al. 2013). Further, sealing of the micropores on MAO coating showed a marginal increment in the E values, while H values remained the same even after sealing.

The EPD of HA coating on Mg-3Zn substrate was evaluated in terms of the biomechanical stability of the coating, which was the function of surface roughness of the substrate and the sintering temperature of the HA coating (Kumar et al. 2016). The load versus displacement plot for the nanoindentation study is shown in Fig. 6.31. At 400°C of annealing, mechanical properties, that is, H, E and fracture toughness, increased by 30% , 26% and 73% , respectively, with the decrease in surface roughness of the coating from $130\text{--}150$ to $15\text{--}20$ nm. While keeping the surface roughness constant (i.e. $15\text{--}20$ nm), changes in temperature of annealing

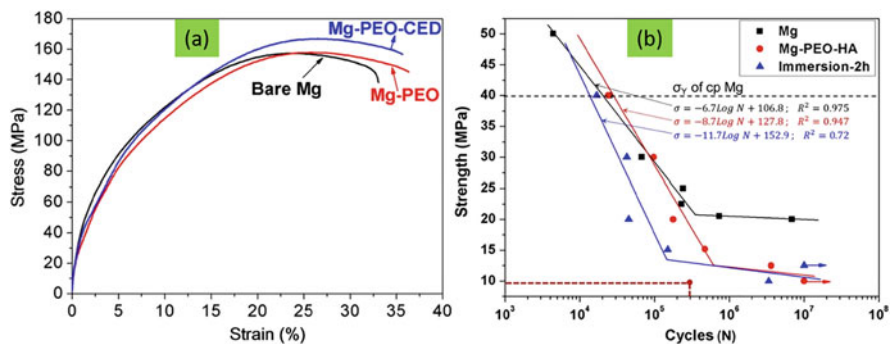


Fig. 6.32 (a) The tensile stress-strain plot and (b) S-N fatigue curve for coated and non-coated Mg samples. Dotted lines show the required values for real service conditions. (Reprinted from Gao et al. (2015) with permission from Elsevier)

(from 300 to 400 °C) caused an increment in H, E and fracture toughness by 37%, 47% and 48%, respectively.

The bredigite ceramic ($\text{Ca}_7\text{MgSi}_4\text{O}_{16}$)/anodic spark deposition (ASD) coating on AZ91 Mg alloy was fabricated via EPD methods (Razavi et al. 2014a, b, c). The compression test of SBF immersed bare AZ91 samples, ASD and bredigite/ASD-coated samples were performed after 4 weeks. Interestingly, only a 5% decrement in the strength of bredigite/ASD-coated samples was observed. The coating of bredigite on the Mg alloy delayed the corrosion and consequently retained the compressive strength. On another effort, plasma electrolytic oxidation (PEO)-coated samples showed minimal effect on the tensile strength (Fig. 6.32a), as compared to bare Mg (Gao et al. 2015). The presence of compressive in-plane residual stress in the coated sample offered comparatively better fatigue performance than the bare Mg in the low-cycle region (Fig. 6.32b). However, a reduced fatigue limit was reported in the high-cycle region due to the increased roughness of the coating/substrate interface. Surface modification of Mg alloys via Ca-P deposition by IBAD method showed an increment in the H and E values by 77.5 and 55.7%, respectively, when compared to the naked substrate sample (Yang et al. 2008).

Further, other available literature have also shown improvement in the mechanical behaviour of the Mg-based materials after surface modifications (Xiong et al. 2017; Wang et al. 2011; Butt et al. 2017; Diez et al. 2016; Bakhsheshi-Rad et al. 2014; Razavi et al. 2014a, b, c; Bakhsheshi-Rad et al. 2016a, b).

6.3.3 Protein Adhesion Study

During implantation in the physiological milieu, protein adsorption is the spontaneous action that occurs on the implant, followed by cell attachment, proliferation and migration. Hence, it becomes necessary to understand the protein adsorption mechanism and factors affecting it in designing the biocompatible material and fracture

fixing accessories. Due to the presence of different sizes of proteins and their affinity towards the implant surface, the mobile and smaller proteins (e.g. albumin) dominate the protein adsorption phenomenon and later replaced by the more abundant proteins (fibrinogen).

The physical and chemical characteristics of implant surfaces tailor the quantity, density, conformations and orientations of the adsorbed proteins. The driving forces such as electrostatic interactions, Van der Waals forces and hydrogen bonding are the primary cause for protein adsorption on metallic surfaces. Besides, the hydrophilic and hydrophobic nature of the implant surfaces also influences the amount of protein adsorption. The protein-surface interactions at the molecular scale are governed by the pH of the media and surface roughness. However, very few studies are available on the protein adhesion of the surface-modified Mg-based implants (Dubey et al. 2019a, b, c; Virtanen 2011; Jaiswal et al. 2019a, b; Silva et al. 2010; Zeng et al. 2014).

Zhang et al. (2020) studied the proteins interaction mechanism of MAO-coated biodegradable AZ31 Mg alloy. A thin protein layer (of albumin) was adsorbed on the MAO-coated surfaces due to the electrostatic interactions. Eventually, the corrosion rate of the MAO-coated Mg alloy decreased by ~25%. Further, the PEO-treated pure Mg alloy (Wan et al. 2013) was immersed in different environments: simulated body fluid (SBF), sodium chloride (NaCl) and phosphate buffer saline (PBS) with the addition of albumin. Figure 6.33 shows a schematic illustration of the degradation mechanism of PEO-coated Mg alloy immersed in two different solutions, that is, PBS and albumin-added PBS solutions. The albumin acted as an inhibitor and enhanced the degradation resistance of PEO-coated Mg alloy surface. The corroded micrographs of the PEO-coated Mg alloy, after 14 days of soaking in the different solutions, are depicted in Fig. 6.34. Protein adsorption on coated Mg impeded coating degradation and enhanced the degradation resistance due to the synergetic effect of protein adsorption and salts.

6.3.4 Wettability Study

The hydrophilic and hydrophobic nature of the implant surface determines the efficacy of the cell adhesion, protein expression and growth of new bone tissue on the Mg-based implants. Hence, surface wettability is another vital parameter for the development of biocompatible surface-modified Mg-based implants.

Most researchers have used water as a medium for contact angle measurement. The study reveals that the Mg-based implants become hydrophilic after coatings (Bakhsheshi-Rad et al. 2017). Figure 6.35 is showing the contact angles of different coated samples in the water medium. The deposition of ZnO on Mg-based alloys increased hydrophobicity. However, the presence of Si-OH functional groups in baghdadite coating (absorbs water molecules by H₂ bonding) increased the wettability. A similar observation was made in other studies (Bakhsheshi-Rad et al. 2016a, b; Amaravathy et al. 2014a, b), and it has been noted that coatings provided increased surface roughness, offering larger contact area.

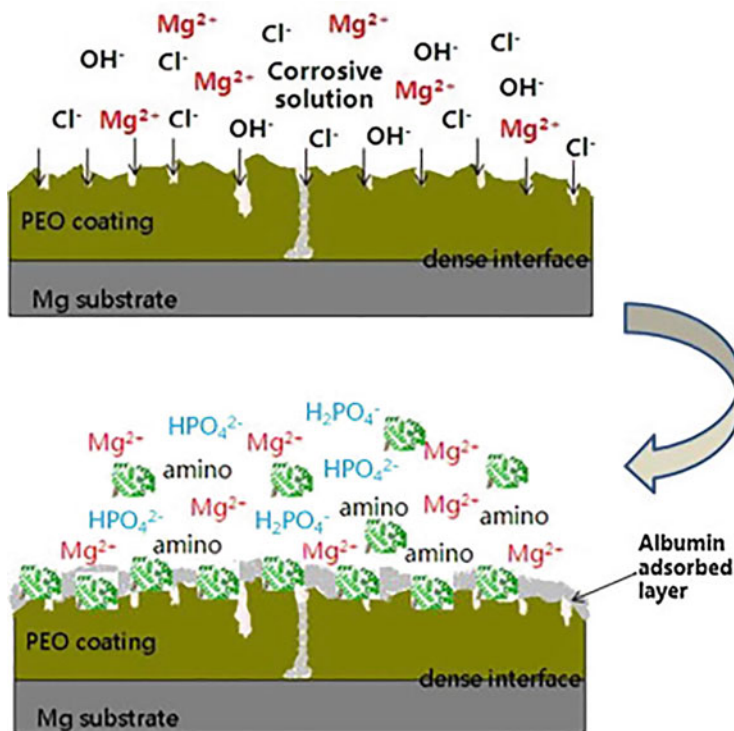


Fig. 6.33 Schematic illustration of the corrosion mechanism of PEO-coated Mg substrate immersed in PBS and albumin-added PBS solutions. (Reprinted from Wan et al. (2013) with permission from Elsevier)

Further, Nb_2O_5 -coated substrate, via the sol-gel process, shows higher surface free energy (66.40 mJ/m^2) than the uncoated surface (30.77 mJ/m^2) (Amaravathy et al. 2014a, b). The presence of a vast amount of hydroxyl groups acted as sites for water adsorption and improved the wettability and surface free energy.

6.3.5 Biocompatibility Study

Biocompatibility is a property of high relevance in the development of biomedical implants. The surface-modified layers should not elicit any toxic effects in the human body. Thus, biocompatibility study becomes an essential criterion while designing the modified surface of Mg-based materials. There are various methods through which the cytotoxic behaviour of surface-modified Mg-based systems can be assessed. These methods typically involve cell viability, MTT assay, DAPI staining and live/dead assay in vitro studies, whereas in vivo studies give histological and X-ray analysis. The surface biocompatibilities of the implants at the initial stages are substantially affected by the chemical composition, microstructure and

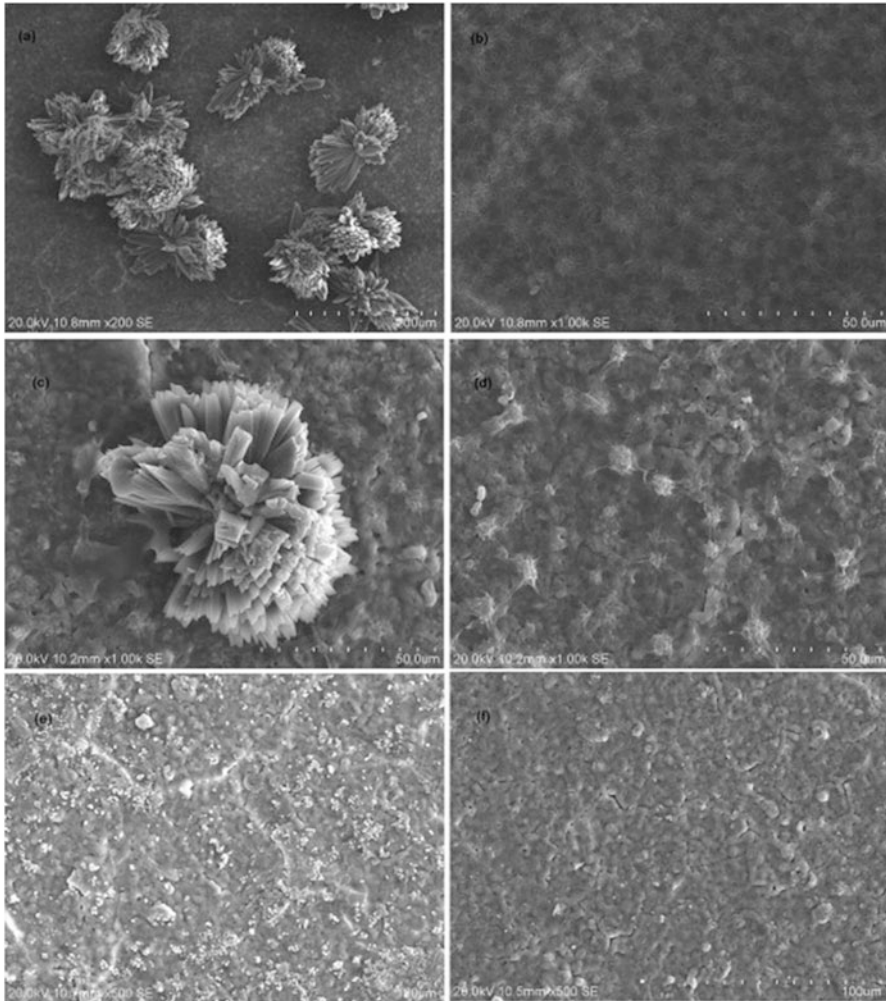


Fig. 6.34 The SEM micrograph of the degraded PEO-coated samples captured after 14 days of immersion in the different solutions (a, b) PBS, (c, d) PBS + albumin, (e) NaCl and (f) NaCl +albumin. (Reprinted from Wan et al. (2013) with permission from Elsevier)

physicochemical properties of the modified coatings. Besides, the biocompatibility of the implants is also tuned by the degradation products, which is directly related to the compositions of the modified coating layers. Figure 6.36 is showing the schematic illustration of surface roughness variations on the biocompatibility of the surfaces.

The surface chemistry (addition of calcium and phosphates) and roughness of the fabricated coatings on the Mg-based materials significantly affect the cell adhesion behaviour (Lorenz et al. 2009). Further, the corrosion product of the surface-modified Mg-based implants also influences the initial biocompatibility (Gu et al.

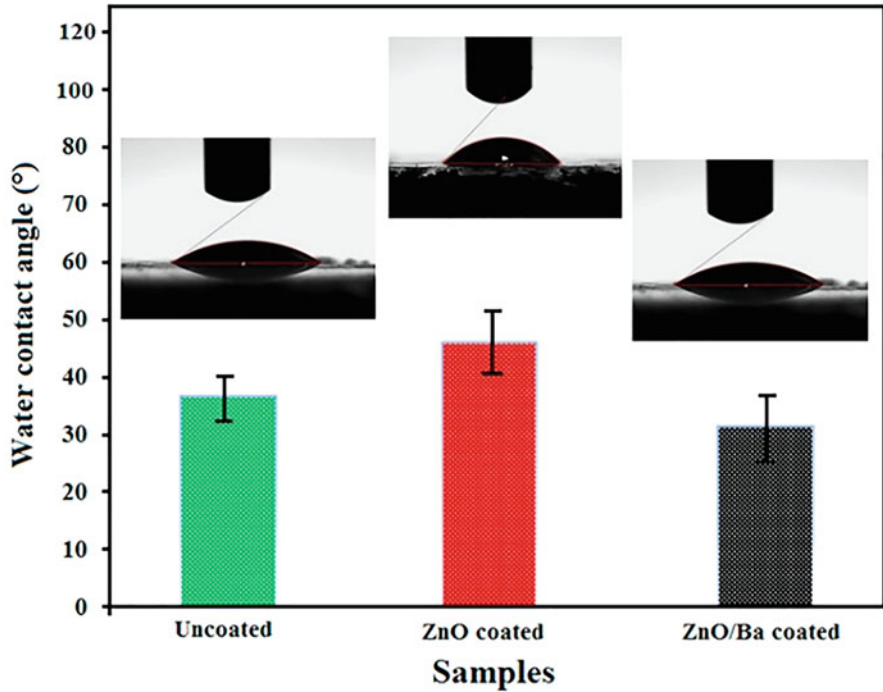


Fig. 6.35 The contact angle measurement of uncoated, ZnO-coated and baghdadite-coated Mg alloy. (Reprinted from Bakhsheshi-Rad et al. (2017) with permission from Elsevier)

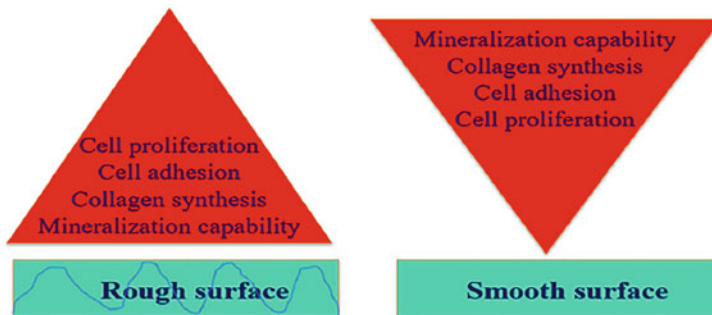


Fig. 6.36 The schematic representation shows the biocompatibility behaviour with the roughness of coating surfaces (Rahman et al. 2020)

2011; Wong et al. 2010; Wang et al. 2013a, b, Keim et al. 2011; Lorenz et al. 2009). In one of the studies, the alkaline treatment (soaking time-24 h and annealing at 500 °C for 12 h) of Mg-1.4Ca alloy fabricated an MgO layer on the Mg alloy. No cell toxicity (L929 cells 7-day culture) was found for the heat-treated Mg alloy (Gu et al. 2011). In another study, pure Mg surface, modified with NaOH solution at room

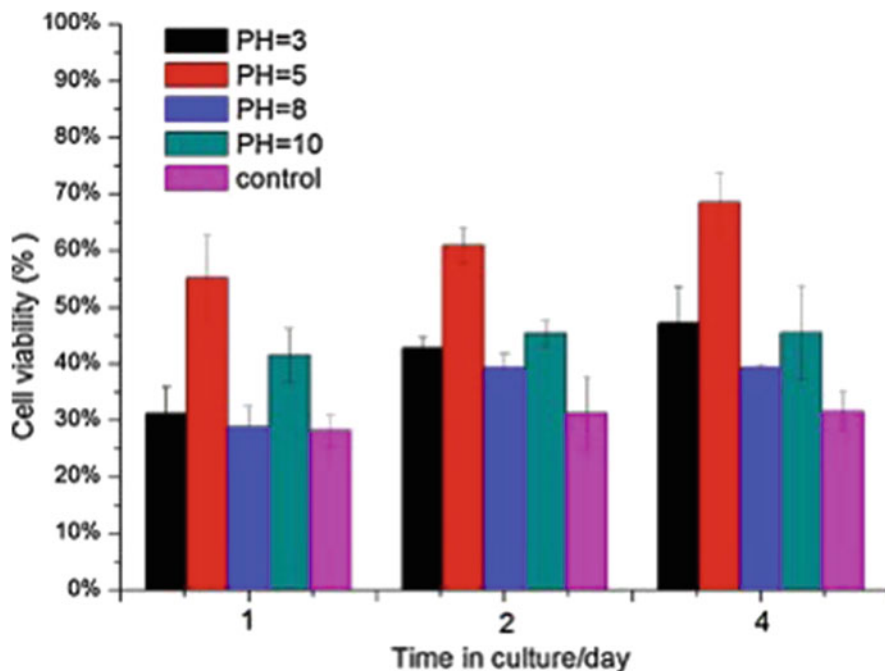


Fig. 6.37 The cell viability behaviour of phytic acid-modified WE43 Mg alloy at various pH scale. (Reprinted from Ye et al. (2012) with permission from Elsevier)

temperature for 24 h, led to reduced cell densities (Keim et al. 2011). The WE43 Mg alloy, modified in phytic acid at different pH values, exhibited better cell viability compared to the non-modified alloys (Ye et al. 2012) (Fig. 6.37). Guan et al. (2012) electrophoretically deposited HA on the Mg-4.0Zn-1.0Ca-0.6Zr alloy. The higher growth rate of L929 fibroblasts was seen on the HA-coated samples in comparison to uncoated Mg alloy.

Micro-arc oxidation coatings have shown tremendous potential in enhancing the cell compatibility of the Mg-based materials (Zeng et al. 2016; Bakhsheshi-Rad et al. 2018; Xu et al. 2020). Strontium (Sr)-doped MAO coating deposited on the ZK60 Mg alloy showed cell viability for MC3T3-E1 cells and alkaline phosphatase (ALP) activity, which significantly improved with Sr-incorporated coating (Lin et al. 2014) (Fig. 6.38).

The composite coating of HA-chitosan on Mg alloy (AZ31) using aerosol deposition technique showed better biocompatibility than the only HA coating. The presence of chitosan in the composite coating enhanced the bioactivity of the surfaces (Hahn et al. 2011). The initial biocompatibility behaviour of the implants is assessed via *in vitro* studies. In contrast, the *in vivo* studies give insight into the tissue response and long-term degradation profile of the surface-modified Mg-based implants. Wang et al. (2013a, b) performed a bioactivity assessment of MgF₂- and Ca-P-coated Mg-3Zn-0.8Zr alloys separately using the *in vivo* implantation in the

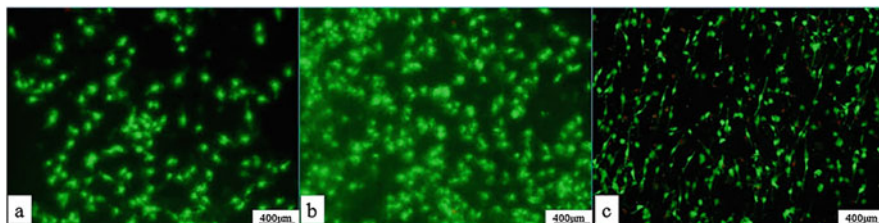


Fig. 6.38 Fluorescence images showing the live/dead dye-stained preosteoblasts captured after 24 h of cultivation on the surfaces of (a, b) P and Sr-P coating and (c) bare ZK60 alloys. (Reprinted from Lin et al. (2014) with permission from Elsevier)

femoral shaft of the rabbits. The new trabecula bone formed was much neat for the MgF_2 sample compared to Ca-P and bare samples (Fig. 6.39). There was no sign of inflammation and gas around the implant/bone interface after 3 months of implantation. Chen et al. (2019) utilised MAO/ED composite coating on Mg-Zn-Ca alloy for possible implantation in the femur shaft of white rabbit (New Zealand). It took 8–18 weeks to form new bone around the MAO/ED-coated sample, which was similar to the original bone tissue. After 50 weeks, the coated sample was degraded completely.

6.4 Summary, Challenges and Future Directions

The most widely used surface-modified coating techniques, particularly for Mg-based materials, have been found to enhance corrosion, mechanical behaviour, wettability, protein adhesion and biocompatibility behaviour, indicating their potential use in biomedical application. An extensive survey of several biocompatible coating techniques and their influence on Mg-based materials, accomplished over the decades, has been summarised in this chapter. The improvements of the primary concern, that is, the high degradation rate of Mg-based materials, have been extensively discussed.

The selection of appropriate coating material, coating technique and factors affecting processing parameters are an essential task to achieve accurate and appropriate degradation rates of the surface-modified Mg-based substrates. The most common coating used is Ca-P-based compounds, but its limitation is instability during more prolonged exposure to the physiological environment due to cracks development in the coatings. Electrophoretic deposition is a predominantly used coating method for the deposition of HA and doped HA (with F, Zn, Si and Sr) on Mg-based substrates. However, in EPD, significant adhesion of the coating to the substrate is a major limitation due to the low melting point of the Mg metal. The dip-coated biodegradable polymer composite on Mg-based materials has not shown significant long-term degradation protection. The anodising method develops passive oxide layers on the surface of Mg-based materials and has shown tremendous potential in corrosion resistance improvement. However, the formation of structural

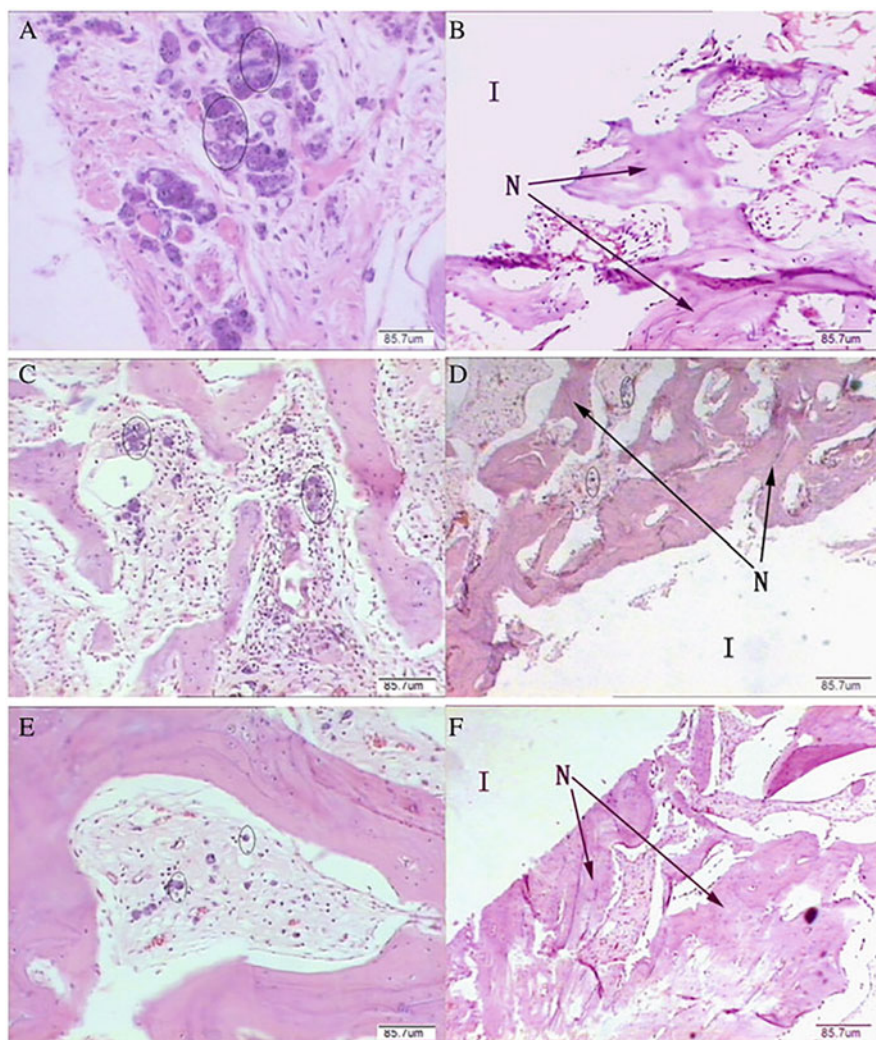


Fig. 6.39 Histological images of (a, b) the interfaces (implant/bone) around uncoated, (c, d) Ca-P-coated and (e, f) MgF₂-coated alloy after 3 months of operation. (In the micrographs, I stands for the implant, N for the newly formed trabecular bone and circle denotes magnesium granules). (Reprinted from Wang et al. (2013a, b) with permission from Elsevier)

defects and substrate “age softening phenomenon” limits their extensive use for the surface modification of Mg-based materials. MAO techniques have also proved their potential in reducing the degradation rate of Mg-based materials. The presence of higher pore density on the MAO-modified Mg-based materials surface restricts their widespread application in a highly corrosive environment (e.g. body fluids). Laser-based surface modification of Mg-based materials has also significantly improved

the degradation resistance in the physiological environment (e.g. SBF). However, the limitations such as the coarse microstructure formation and cracks induced due to laser irradiation by high thermal stress during operations need to be tailored for wide acceptability.

Hence, there is still scope in the design and development of areas, which need attention in engineering the surfaces of the Mg-based biomedical implants. Future studies are recommended to develop defect-free coatings on Mg-based implants. Effective collaboration amongst interdisciplinary fields such as biology, engineering, materials and medical science is imperative to focus on the future significant clinical development of effective coating methods on Mg-based materials. Functionalised processing of the coating is currently developing with great potential in the future. A combination of surface modification method could also assist in achieving the specific surface requirement. The studies like self-healing coatings and functionally gradient coatings can be explored for the potential application in biomedical application. A more extended period (e.g. 6–12 month) of in vitro and in vivo studies is required for developing surface-modified implants to check the efficacy of coatings. Due to the high susceptibility of Mg-based materials to localised corrosion, effective surface modification is required to retain the mechanical integrity of implants for a longer duration into the body fluid. The journey to modify the surfaces of the Mg-based materials to offer both long-term degradation resistance and significant biocompatibility for biomedical application continues.

References

- Ali M, Elsherif M, Salih AE, UI-Hamid A, Hussein MA, Park S, Butt H (2020) Surface modification and cytotoxicity of Mg-based bio-alloys: an overview of recent advances. *J Alloys Compd* 825:154140
- Amaravathy P, Sathyanarayanan S, Sowndarya S, Rajendran N (2014a) Bioactive HA/TiO₂ coating on magnesium alloy for biomedical applications. *Ceram Int* 40:6617–6630
- Amaravathy P, Sowndarya S, Sathyanarayanan S, Rajendran N (2014b) Novel sol gel coating of Nb₂O₅ on magnesium alloy for biomedical applications. *Surf Coat Technol* 244:131–141
- Amruthaluri S (2014) An investigation on biocompatibility of bio-absorbable polymer coated magnesium alloys FIU Electronic Theses and Dissertations 1742
- Antunes RA, De Oliveira MCL (2009) Corrosion processes of physical vapor deposition-coated metallic implants. *Crit Rev Biomed Eng* 37:425–460
- Bakhsheshi-Rad HR, Hamzah E, Daroonparvar M, Ebrahimi-Kahrizangi R, Medraj M (2014) In-vitro corrosion inhibition mechanism of fluorine-doped hydroxyapatite and brushite coated Mg–Ca alloys for biomedical applications. *Ceram Int* 40:7971–7982
- Bakhsheshi-Rad HR, Hamzah E, Kasiri-Asgarani M, Jabbarzare S, Iqbal N, Kadir MA (2016a) Deposition of nanostructured fluorine-doped hydroxyapatite–polycaprolactone duplex coating to enhance the mechanical properties and corrosion resistance of Mg alloy for biomedical applications. *Mater Sci Eng C* 60:526–537
- Bakhsheshi-Rad HR, Hamzah E, Ismail AF, Kasiri-Asgarani M, Daroonparvar M, Parham S, Medraj M (2016b) Novel bi-layered nanostructured SiO₂/Ag-FHAp coating on biodegradable magnesium alloy for biomedical applications. *Ceram Int* 42:11941–11950
- Bakhsheshi-Rad HR, Hamzah E, Ismail AF, Aziz M, Kasiri-Asgarani M, Akbari E, Hadisi Z (2017) Synthesis of a novel nanostructured zinc oxide/baghdadite coating on Mg alloy for biomedical

- application: in-vitro degradation behavior and antibacterial activities. *Ceram Int* 43:14842–14850
- Bakhsheshi-Rad HR, Hamzah E, Ismail AF, Aziz M, Daroonparvar M, Saebnoori E, Chami A (2018) In vitro degradation behavior, antibacterial activity and cytotoxicity of TiO₂-MAO/ZnHA composite coating on Mg alloy for orthopedic implants. *Surf Coat Technol* 334:450–460
- Bala Srinivasan P, Blawert C, Störmer M, Dietzel W (2010) Characterisation of tribological and corrosion behaviour of plasma electrolytic oxidation coated AM50 magnesium alloy. *Surf Eng* 26:340–346
- Bruinink A, Bitar M, Pleskova M, Wick P, Krug HF, Maniura-Weber K (2014) Addition of nanoscaled bioinspired surface features: a revolution for bone related implants and scaffolds? *J Biomed Mater Res A* 102:275–294
- Butt MS, Bai J, Wan X, Chu C, Xue F, Ding H, Zhou G (2017) Mechanical and degradation properties of biodegradable Mg strengthened poly-lactic acid composite through plastic injection molding. *Mater Sci Eng C* 70:141–147
- Chen J, Zhang Y, Ibrahim M, Etim IP, Tan L, Yang K (2019) In vitro degradation and antibacterial property of a copper-containing micro-arc oxidation coating on Mg-2Zn-1Gd-0.5 Zr alloy. *Colloids Surf B* 179:77–86
- Conceicao TF, Scharnagl N, Blawert C, Dietzel W, Kainer KU (2010) Corrosion protection of magnesium alloy AZ31 sheets by spin coating process with poly (ether imide). *Corros Sci* 52:2066–2079
- Coy AE, Viejo F, Garcia-Garcia FJ, Liu Z, Skeldon P, Thompson GE (2010) Effect of excimer laser surface melting on the microstructure and corrosion performance of the die cast AZ91D magnesium alloy. *Corr Sci* 52:387–397
- Cui LY, Wei GB, Han ZZ, Zeng RC, Wang L, Zou YH, Guan SK (2019) In vitro corrosion resistance and antibacterial performance of novel tin dioxide-doped calcium phosphate coating on degradable Mg-1Li-1Ca alloy. *J Mater Sci Technol* 35:254–265
- De Leeuw NH (2001) Local ordering of hydroxy groups in hydroxyapatite. *Chem Commun* 17:1646–1647
- Deng Y, Liu X, Xu A, Wang L, Luo Z, Zheng Y, Deng F, Wei J, Tang Z, Wei S (2015) Effect of surface roughness on osteogenesis in vitro and osseointegration in vivo of carbon fiber-reinforced polyetheretherketone-nanohydroxyapatite composite. *Int J Nanomedicine* 10:1425–1447
- Dey A, Rani RU, Thota HK, Sharma AK, Bandyopadhyay P, Mukhopadhyay AK (2013) Microstructural, corrosion and nanomechanical behaviour of ceramic coatings developed on magnesium AZ31 alloy by micro arc oxidation. *Ceram Int* 39:3313–3320
- Diez M, Kang MH, Kim SM, Kim HE, Song J (2016) Hydroxyapatite (HA)/poly-L-lactic acid (PLLA) dual coating on magnesium alloy under deformation for biomedical applications. *J Mater Sci Mater Med* 27:34
- Dinu M, Ivanova AA, Surmeneva MA, Braic M, Tyurin AI, Braic V, Vladescu A (2017) Tribological behaviour of RF-magnetron sputter deposited hydroxyapatite coatings in physiological solution. *Ceram Int* 43:6858–6867
- Drynda A, Hassel T, Hoehn R, Perz A, Bach FW, Peuster M (2010) Development and biocompatibility of a novel corrodible fluoride-coated magnesium-calcium alloy with improved degradation kinetics and adequate mechanical properties for cardiovascular applications. *J Biomed Mater Res A* 93:763–775
- Duan H, Du K, Yan C, Wang F (2006) Electrochemical corrosion behavior of composite coatings of sealed MAO film on magnesium alloy AZ91D. *Electrochim Acta* 51:2898–2908
- Dubey A, Jaiswal S, Ghosh S, Roy P, Lahiri D (2019a) Protein adsorption and biodegradation behaviour of Mg–3Zn/HA for biomedical application. *Nanomater Energy* 8:23–32
- Dubey A, Jaiswal S, Haldar S, Roy P, Lahiri D (2019b) Mg-3Zn/HA biodegradable composites synthesised via spark plasma sintering for temporary orthopedic implants. *J Mater Eng Perform* 28:5702–5715

- Dubey A, Jaiswal S, Lahiri D (2019c) Mechanical integrity of biodegradable Mg–HA composite during in vitro exposure. *J Mater Eng Perform* 28:800–809
- Elias CN, Oshida Y, Lima JHC, Muller CA (2008) Relationship between surface properties (roughness, wettability and morphology) of titanium and dental implant removal torque. *J Mech Behav Biomed Mater* 1:234–242
- Fu J, Su Y, Qin YX, Zheng Y, Wang Y, Zhu D (2020) Evolution of metallic cardiovascular stent materials: a comparative study among stainless steel, magnesium and zinc. *Biomaterials* 230:119641
- Gao Y, Yerokhin A, Matthews A (2015) Mechanical behaviour of cp-magnesium with duplex hydroxyapatite and PEO coatings. *Mater Sci Eng C* 49:190–200
- Gobbi SJ, Gobbi VJ, Rocha Y (2019) Requirements for selection/development of a biomaterial. *Biomedical J Sci. ISSN-2574-1241*
- Grand View Research (2020) Biomaterials market size worth \$348.4 billion by 2027
- Gu XN, Li N, Zhou WR, Zheng YF, Zhao X, Cai QZ, Ruan L (2011) Corrosion resistance and surface biocompatibility of a microarc oxidation coating on a Mg–Ca alloy. *Acta Biomater* 7:1880–1889
- Gu X, Mao Z, Ye SH, Koo Y, Yun Y, Tiasha TR, Wagner WR (2016) Biodegradable, elastomeric coatings with controlled anti-proliferative agent release for magnesium-based cardiovascular stents. *Colloids Surf B Biointerfaces* 144:170–179
- Guan RG, Johnson I, Cui T, Zhao T, Zhao ZY, Li X, Liu H (2012) Electrodeposition of hydroxyapatite coating on Mg-4.0Zn-1.0Ca-0.6 Zr alloy and in vitro evaluation of degradation, hemolysis, and cytotoxicity. *J Biomed Mater Res A* 100:999–1015
- Guo W (2010) A review of magnesium/magnesium alloys corrosion and its protection. *Recent Patents on Corrosion Science*
- Guo LF, Yue TM, Man HC (2005) Excimer laser surface treatment of magnesium alloy WE43 for corrosion resistance improvement. *J Mater Sci* 40:3531–3533
- Hahn BD, Park DS, Choi JJ, Ryu J, Yoon WH, Choi JH, Kim SG (2011) Aerosol deposition of hydroxyapatite–chitosan composite coatings on biodegradable magnesium alloy. *Surf Coat Technol* 205:3112–3118
- Ho YH, Vora HD, Dahotre NB (2015) Laser surface modification of AZ31B Mg alloy for bio-wettability. *J Biomater Appl* 29:915–928
- Hornberger H, Virtanen S, Boccaccini AR (2012) Biomedical coatings on magnesium alloys—a review. *Acta Biomater* 8:2442–2455
- Jacobs JJ, Skipor AK, Black J, Urban RM, Galante JO (1991) Release and excretion of metal in patients who have a total hip-replacement component made of titanium-base alloy. *J Bone Joint Surg Am* 73:1475–1486
- Jaiswal S, Kumar RM, Gupta P, Kumaraswamy M, Roy P, Lahiri D (2018) Mechanical, corrosion and biocompatibility behaviour of Mg-3Zn-HA biodegradable composites for orthopaedic fixture accessories. *J Mech Behav Biomed* 78:442–454
- Jaiswal S, Dubey A, Lahiri D (2019a) In vitro biodegradation and biocompatibility of Mg–HA-based composites for orthopaedic applications: a review. *J Indian Inst Sci* 99:303–327
- Jaiswal S, Dubey A, Haldar S, Roy P, Lahiri D (2019b) Differential in vitro degradation and protein adhesion behaviour of spark plasma sintering fabricated magnesium-based temporary orthopaedic implant in serum and simulated body fluid. *Biomed Mater* 15:015006
- Jaiswal S, Dubey A, Lahiri D (2020) The influence of bioactive hydroxyapatite shape and size on the mechanical and biodegradation behaviour of magnesium based composite. *Ceram Int* 46:27205–27218
- John AA, Subramanian AP, Vellayappan MV, Balaji A, Jaganathan SK, Mohandas H, Yusof M (2015) Physico-chemical modification as a versatile strategy for the biocompatibility enhancement of biomaterials. *RSC Adv* 5:39232–39244
- Kania A, Pilarczyk W, Szindler MM (2020) Structure and corrosion behavior of TiO₂ thin films deposited onto Mg-based alloy using magnetron sputtering and sol-gel. *Thin Solid Films* 701:137945

- Kannan MB, Orr L (2011) In vitro mechanical integrity of hydroxyapatite coated magnesium alloy. *Biomed Mater* 6:045003
- Kasemo B, Lausmaa J (1986) Surface science aspects on inorganic biomaterials. *CRC Crit Rev Clin Neurobiol* 2:335–380
- Kasemo B, Lausmaa J (1988) Biomaterials and implant surfaces: a surface science approach. *Int J Oral Maxillofac Implants* 3:247–259
- Kasemo B, Lausmaa J (1994) Surface properties and processes of the biomaterial-tissue interface. *Mater Sci Eng C* 1:115–119
- Kasuga T (2010) Coatings for metallic biomaterials. In: *Metals for biomedical devices*. Woodhead Publishing, Sawston
- Keim S, Brunner JG, Fabry B, Virtanen S (2011) Control of magnesium corrosion and biocompatibility with biomimetic coatings. *J Biomed Mater Res B* 96:84–90
- Khalifaoui W, Valerio E, Masse JE, Autric M (2010) Excimer laser treatment of ZE41 magnesium alloy for corrosion resistance and microhardness improvement. *Opt Laser Eng* 48:926–931
- Kim SR, Lee JH, Kim YT, Riu DH, Jung SJ, Lee YJ, Kim YH (2003) Synthesis of Si, Mg substituted hydroxyapatites and their sintering behaviors. *Biomaterials* 24:1389–1398
- Kumar RM, Kuntal KK, Singh S, Gupta P, Bhushan B, Gopinath P, Lahiri D (2016) Electrophoretic deposition of hydroxyapatite coating on Mg–3Zn alloy for orthopaedic application. *Surf Coat Technol* 287:82–92
- Kutschera U, Galun R (2000) Wear behaviour of laser surface treated magnesium alloys. In: *Magnesium alloys and their applications*. Wiley, Weinheim, pp 330–335
- Lenz RW (1993) Biodegradable polymers. In: *Biopolymers I*. Springer, Berlin
- Lhotka C, Szekeres T, Steffan I, Zhuber K, Zweymüller K (2003) Four-year study of cobalt and chromium blood levels in patients managed with two different metal-on-metal total hip replacements. *J Orthop* 21:189–195
- Li JN, Cao P, Zhang XN, Zhang SX, He YH (2010) In vitro degradation and cell attachment of a PLGA coated biodegradable Mg–6Zn based alloy. *J Mater Sci* 45:6038–6045
- Li X, Liu X, Wu S, Yeung KWK, Zheng Y, Chu PK (2016) Design of magnesium alloys with controllable degradation for biomedical implants: from bulk to surface. *Acta Biomater* 45:2–30
- Lin X, Yang X, Tan L, Li M, Wang X, Zhang Y, Qiu J (2014) In vitro degradation and biocompatibility of a strontium-containing micro-arc oxidation coating on the biodegradable ZK60 magnesium alloy. *Appl Surf Sci* 288:718–726
- Liu GY, Hu J, Ding ZK, Wang C (2011) Bioactive calcium phosphate coating formed on micro-arc oxidised magnesium by chemical deposition. *Appl Surf Sci* 257:2051–2057
- Lorenz C, Brunner JG, Kollmannsberger P, Jaafar L, Fabry B, Virtanen S (2009) Effect of surface pre-treatments on biocompatibility of magnesium. *Acta Biomater* 5:2783–2789
- Love BJ (2017) *Biomaterials: a systems approach to engineering concepts*. Academic, Boston
- Matthews A, Holmberg K (1994) *Coatings tribology: properties, techniques and applications in surface engineering*. Elsevier, Amsterdam
- McLean JD, Nelson DGA (1982) High-resolution n-beam lattice images of hydroxyapatite. *Micron* (1969) 13:409–413
- Melnikov ES, Surmeneva MA, Tyurin AI, Pirozhkova TS, Shuvarin IA, Prymak O, Surmenev RA (2017) Improvement of the mechanical properties of AZ91D magnesium alloys by deposition of thin hydroxyapatite film. In: *Nano hybrids and composites, vol 13*. Trans Tech Publications, Stafa-Zurich, pp 355–361
- Nagels J, Stokdijk M, Rozing PM (2003) Stress shielding and bone resorption in shoulder arthroplasty. *J Shoulder Elb Surg* 12:35–39
- Narayanan TS, Park IS, Lee MH (2014) Strategies to improve the corrosion resistance of microarc oxidation (MAO) coated magnesium alloys for degradable implants: prospects and challenges. *Prog Mater Sci* 60:1–71
- Nassif N, Ghayad I (2013) Corrosion protection and surface treatment of magnesium alloys used for orthopaedic applications. *Adv Mater Sci Eng* 532896:1–10

- Nayak S, Bhushan B, Jayaganthan R, Gopinath P, Agarwal RD, Lahiri D (2016) Strengthening of Mg based alloy through grain refinement for orthopaedic application. *J Mech Behav Biomed* 59:57–70
- Niinomi M (2019) Design and development of metallic biomaterials with biological and mechanical biocompatibility. *J Biomed Mater Res Part A* 107:944–954
- Nouri A, Wen C (2015) Introduction to surface coating and modification for metallic biomaterials. In: *Surface coating and modification of metallic biomaterials*. Woodhead Publishing, Sawston
- Oosterbeek RN, Seal CK, Seitz JM, Hyland MM (2013) Polymer–bioceramic composite coatings on magnesium for biomaterial applications. *SurfCoat Tech* 236:420–428
- Poinern GEJ, Brundavanam S, Fawcett D (2012) Biomedical magnesium alloys: a review of material properties, surface modifications and potential as a biodegradable orthopaedic implant. *Am J Biomed Eng* 2:218–240
- Prasad K, Bazaka O, Chua M, Rochford M, Fedrick L, Spoor J, Markwell D (2017) Metallic biomaterials: current challenges and opportunities. *Materials* 10:884
- Qiu ZY, Chen C, Wang XM, Lee IS (2014) Advances in the surface modification techniques of bone-related implants for last 10 years. *Regen Biomater* 1:67–79
- Rahim MI, Ullah S, Mueller PP (2018) Advances and challenges of biodegradable implant materials with a focus on magnesium-alloys and bacterial infections. *Metals* 8:532
- Rahimi-Roshan N, Hassannejad H, Nouri A (2020) Corrosion and mechanical behaviour of biodegradable PLA-cellulose nanocomposite coating on AZ31 magnesium alloy. *Surf Eng* 37:236–245
- Rahman M, Dutta NK, Roy Choudhury N (2020) Magnesium alloys with tunable interfaces as bone implant materials. *Front Bioeng Biotechnol* 8:564
- Rapacz-Kmita A, Paluszkiwicz C, Ślósarczyk A, Paszkiewicz Z (2005) FTIR and XRD investigations on the thermal stability of hydroxyapatite during hot pressing and pressureless sintering processes. *J Mol Struct* 744:653–656
- Rashmir-Raven AM, Richardson DC, Aberman HM, De Young DJ (1995) The response of cancellous and cortical canine bone to hydroxylapatite-coated and uncoated titanium rods. *J Appl Biomater* 6:237–242
- Razavi M, Fathi M, Savabi O, Vashae D, Tayebi L (2014a) Improvement of biodegradability, bioactivity, mechanical integrity and cytocompatibility behavior of biodegradable Mg based orthopedic implants using nanostructured bredigite ($\text{Ca}_7\text{MgSi}_4\text{O}_{16}$) bioceramic coated via ASD/EPD technique. *Ann Biomed Eng* 42:2537–2550
- Razavi M, Fathi M, Savabi O, Beni BH, Vashae D, Tayebi L (2014b) Nanostructured merwinite bioceramic coating on Mg alloy deposited by electrophoretic deposition. *Ceram Int* 40:9473–9484
- Razavi M, Fathi M, Savabi O, Beni BH, Vashae D, Tayebi L (2014c) Surface microstructure and in vitro analysis of nanostructured akermanite ($\text{Ca}_2\text{MgSi}_2\text{O}_7$) coating on biodegradable magnesium alloy for biomedical applications. *Colloids Surf B Biointerfaces* 117:432–440
- Robinson DA, Griffith RW, Shechtman D, Evans RB, Conzemi MG (2010) In vitro antibacterial properties of magnesium metal against *Escherichia coli*, *Pseudomonas aeruginosa* and *Staphylococcus aureus*. *Acta Biomater* 6:1869–1877
- Rosales-Leal JI, Rodríguez-Valverde MA, Mazzaglia G, Ramón-Torregrosa PJ, Díaz-Rodríguez L, García-Martínez O, Vallecillo-Capilla M, Ruíz C, Cabrerizo-Vílchez MA (2010) Effect of roughness, wettability and morphology of engineered titanium surfaces on osteoblast-like cell adhesion. *Colloids Surf A Physicochem Eng Aspects* 365:222–229
- Saris NEL, Mervaala E, Karppanen H, Khawaja JA, Lewenstam A (2000) Magnesium: an update on physiological, clinical and analytical aspects. *Clin Chim Acta* 294:1–26
- Sathiyarayanan S, Azim SS, Venkatachari G (2006) Corrosion resistant properties of polyaniline–acrylic coating on magnesium alloy. *Appl Surf Sci* 253:2113–2117
- Sezer N, Evis Z, Kayhan SM, Tahmasebifar A, Koç M (2018) Review of magnesium-based biomaterials and their applications. *J Magnes Alloy* 6:23–43

- Shadanbaz S, Dias GJ (2012) Calcium phosphate coatings on magnesium alloys for biomedical applications: a review. *Acta Biomater* 8:20–30
- Silva RA, Urzúa MD, Petri DF, Dubin PL (2010) Protein adsorption onto polyelectrolyte layers: effects of protein hydrophobicity and charge anisotropy. *Langmuir* 26:14032–14038
- Singh A, Harimkar SP (2012) Laser surface engineering of magnesium alloys: a review. *JOM* 64:716–733
- Singh S, Kumar RM, Kuntal KK, Gupta P, Das S, Jayaganthan R, Lahiri D (2015) Sol–gel derived hydroxyapatite coating on Mg–3Zn alloy for orthopedic application. *JOM* 67:702–712
- Sodhi RN (1996) Application of surface analytical and modification techniques to biomaterial research. *J Electron Spectrosc* 81:269–284
- Song Y, Zhang S, Li J, Zhao C, Zhang Z (2010) Electrodeposition of Ca–P coatings on biodegradable Mg alloy: in vitro biomineralization behavior. *Acta Biomater* 6:1736–1742
- Surmeneva MA, Tyurin AI, Mukhametkaliyev TM, Pirozhkova TS, Shuvarin IA, Syrtanov MS, Surmenev RA (2015) Enhancement of the mechanical properties of AZ31 magnesium alloy via nanostructured hydroxyapatite thin films fabricated via radio-frequency magnetron sputtering. *J. Mech. Behav. Biomed.* 46:127–136
- Tang L, Thevenot P, Hu W (2008) Surface chemistry influences implant biocompatibility. *Curr Top Med Chem* 8:270–280
- Virtanen S (2011) Biodegradable Mg and Mg alloys: corrosion and biocompatibility. *Mat Sci Eng B Adv* 176:1600–1608
- Vootla N, Reddy K (2017) Osseointegration-key factors affecting its success-an overview. *IOSR J Appl Dent* 16:62–68
- Wan P, Lin X, Tan L, Li L, Li W, Yang K (2013) Influence of albumin and inorganic ions on electrochemical corrosion behavior of plasma electrolytic oxidation coated magnesium for surgical implants. *Appl Surf Sci* 282:186–194
- Wang Q, Tan L, Zhang Q, Qiu J, Yang K (2011) Precipitation control and mechanical property of calcium phosphate-coated AZ31B alloy for biomedical application. *Biomed Eng Appl Bas C* 23:193–203
- Wang J, Jiang H, Chen M, Bi Y, Liu D (2013a) In vivo comparative property study of the bioactivity of coated Mg–3Zn–0.8 Zr alloy. *Mater Sci Eng C* 33:3263–3272
- Wang J, He Y, Maitz MF, Collins B, Xiong K, Guo L, Huang N (2013b) A surface-eroding poly (1, 3-trimethylene carbonate) coating for fully biodegradable magnesium-based stent applications: toward better biofunction, biodegradation and biocompatibility. *Acta Biomater* 9:8678–8689
- Willumeit R, Fischer J, Feyerabend F, Hort N, Bismayer U, Heidrich S, Mihailova B (2011) Chemical surface alteration of biodegradable magnesium exposed to corrosion media. *Acta Biomater* 7:2704–2715
- Wong HM, Yeung KW, Lam KO, Tam V, Chu PK, Luk KD, Cheung KM (2010) A biodegradable polymer-based coating to control the performance of magnesium alloy orthopaedic implants. *Biomaterials* 31:2084–2096
- Wood RJ (2007) Tribo-corrosion of coatings: a review. *J Phys D Appl Phys* 40:5502
- Woodman JL, Jacobs JJ, Galante JO, Urban RM (1983) Metal ion release from titanium-based prosthetic segmental replacements of long bones in baboons: a long-term study. *J Orthop* 1:421–443
- Wu G (2007) Fabrication of Al and Al/Ti coatings on magnesium alloy by sputtering. *Mater Lett* 61:3815–3817
- Xin Y, Huo K, Hu T, Tang G, Chu PK (2009) Mechanical properties of Al₂O₃/Al bi-layer coated AZ91 magnesium alloy. *Thin Solid Films* 517:5357–5360
- Xin Y, Hu T, Chu PK (2011) In vitro studies of biomedical magnesium alloys in a simulated physiological environment: a review. *Acta Biomater* 7:1452–1459
- Xiong Y, Hu Q, Song R, Hu X (2017) LSP/MAO composite bio-coating on AZ80 magnesium alloy for biomedical application. *Mater Sci Eng C* 75:1299–1304

- Xu L, Pan F, Yu G, Yang L, Zhang E, Yang K (2009) In vitro and in vivo evaluation of the surface bioactivity of a calcium phosphate coated magnesium alloy. *Biomaterials* 30:1512–1523
- Xu H, Hu T, Wang M, Zheng Y, Qin H, Cao H, An Z (2020) Degradability and biocompatibility of magnesium-MAO: the consistency and contradiction between in-vitro and in-vivo outcomes. *Arab J Chem* 13:2795–2805
- Xue D, Yun Y, Schulz MJ, Shanov V (2011) Corrosion protection of biodegradable magnesium implants using anodisation. *Mater Sci Eng C* 31:215–223
- Yang JX, Jiao YP, Cui FZ, Lee IS, Yin QS, Zhang Y (2008) Modification of degradation behavior of magnesium alloy by IBAD coating of calcium phosphate. *Surf Coat Technol* 202:5733–5736
- Yang J, Cui FZ, Lee IS, Wang X (2010) Plasma surface modification of magnesium alloy for biomedical application. *Surf Coat Technol* 205:S182–S187
- Ye CH, Zheng YF, Wang SQ, Xi TF, Li YD (2012) In vitro corrosion and biocompatibility study of phytic acid modified WE43 magnesium alloy. *Appl Surf Sci* 25:3420–3427
- Yerokhin AL, Nie X, Leyland A, Matthews A, Dowey SJ (1999) Plasma electrolysis for surface engineering. *Surf Coat Technol* 122:73–93
- Zeng RC, Hu Y, Guan SK, Cui HZ, Han EH (2014) Corrosion of magnesium alloy AZ31: the influence of bicarbonate, sulphate, hydrogen phosphate and dihydrogen phosphate ions in saline solution. *Corros Sci* 86:171–182
- Zeng RC, Cui LY, Jiang K, Liu R, Zhao BD, Zheng YF (2016) In vitro corrosion and cytocompatibility of a microarc oxidation coating and poly (l-lactic acid) composite coating on Mg–1Li–1Ca alloy for orthopedic implants. *ACS Appl Mater Interface* 8:10014–10028
- Zhang Y, Yan C, Wang F, Lou H, Cao C (2002) Study on the environmentally friendly anodising of AZ91D magnesium alloy. *Surf Coat Technol* 161:36–43
- Zhang ZQ, Wang L, Zeng MQ, Zeng RC, Kannan MB, Lin CG, Zheng YF (2020) Biodegradation behavior of micro-arc oxidation coating on magnesium alloy—from a protein perspective. *Bioact Mater* 5:398–409



Metallic Foams in Bone Tissue Engineering

7

Somasundaram Prasad, Sreenivas Raguraman, Raymond Wong, and Manoj Gupta

Abstract

Bone defects occur due to factors such as congenital anomaly, trauma, and osseous deficiency following resection of tumours. Biomaterials are required for bone augmentation of the lost bone architecture. Clinicians attempting to regenerate the tissue and restore its function and aesthetics because of trauma, pathology, or congenital defects face a substantial challenge. The concept of using metallic foam in bone tissue engineering is a key factor in the regeneration of critical size bone defects. Significant research efforts have been dedicated to the development of metallic foams for bone tissue engineering due to their suitable mechanical and biological properties. Although, at present, most of the studies are focused on non-load bearing materials, many materials are also being investigated for hard tissue repair. Several biocompatible metallic foam materials such as titanium alloys, tantalum, iron, zinc, and magnesium alloys have been commonly employed as implants in biomedical applications. They are often used to replace and regenerate the damaged bones or to provide structural support for healing bone defects. The bone cells develop on the porous regions of the implants. These cells develop over the surface of the foam, which imparts the integrity and strength. The scaffolds help in regeneration of the biological structural components of the extracellular matrix. This chapter focuses on the

S. Prasad · R. Wong

NUCOH, Faculty of Dentistry, National University of Singapore, Singapore, Singapore

S. Raguraman

Department of Metallurgical and Materials Engineering, National Institute of Technology, Tiruchirappalli, Tamil Nadu, India

M. Gupta (✉)

Department of Mechanical Engineering, National University of Singapore, Singapore, Singapore
e-mail: mpegm@nus.edu.sg

commonly used metallic foams for bone tissue engineering, their properties, applications, and cellular interactions.

Keywords

Metallic foams · Tissue engineering · Titanium · Magnesium · Scaffolds

7.1 Introduction

Amongst all the tissues, bone is the tissue that is transplanted the most. The autologous bone grafts, which are currently the best standard, have few limitations. These limitations mainly include the requirement of secondary surgery for graft removal, increased morbidity, and lower availability. Besides, the grafts procured from animals may lead to issues such as immune attack and transmission of diseases, making it difficult for graft application Prasadh et al. 2020. To overcome these limitations, in recent days, there have been several studies conducted in the development of synthetic materials for graft applications. Bone grafting is required in situations where clinical treatment becomes a significant difficulty, as in the critical-sized defects in bones, which are the result of pathological fractures and high impact injuries. As mentioned above, autografts are still considered the best despite their significant limitations (Campana et al. 2014; Keating et al. 2005). The major limitations of allografts and xenografts, including disease transmission, poor osteogenic properties resulting in bone absorption and failure, and complications involved in immunity response, lead to their limited usage (Athanasίου et al. 2009; Dimitriou et al. 2011).

Due to their enhanced mechanical properties, metals are the commonly used biomaterials involved in implant applications when compared to their polymeric and ceramic counterparts. Excellent tensile strength, fatigue strength, and fracture toughness deem metals to be amongst the best candidates for medical device fabrication used in the replacement of hard tissues such as hip and dental implants, bone plates, and coronary stents (Niinomi 2008). Porous materials are widely considered for such biomedical applications that require a 3D porous network combined with enhanced mechanical properties, in addition to excellent biocompatibility and regulated degradation. The major applications of these are porous biomedical devices and prostheses, *in vitro* and *in vivo* scaffolds for tissue regenerations, macro-, micro-, and nano-particulate foams for drug delivery, diagnostic and sensing, and 3D culture platforms used for the investigation of cancer development and response to drug. The performance of these biomedical foams—and therefore their field of application—resides in the sapient control over the different features and functionalities of the foams which in turn depends on the appropriate selection of materials and fabrication processes. For example, in designing porous scaffolds for tissue engineering, the porous structure, including surface-to-volume ratio, pore size, and interconnection degree, is a key factor in controlling cell behaviour and new tissue development (Salerno et al. 2009; Hasan et al. 2018b).

The functionality of the foams can be further enhanced by the integration of the control over cell fate through control of morphogen spatially and chronologically, and delivery of growth factor from the scaffold material (Biondi et al. 2008; Chan and Mooney 2008; Sands and Mooney 2007). The fabrication of the biomedical foams can be carried out by using several processing techniques, which have specific control over their morphological, microstructural, and nano-structural characteristics and their degradation properties (Chevalier et al. 2008; Guarino et al. 2008). Moreover, the recent developments in lower temperatures and toxic-free processes had led to controlled sequestration and release of bioactive moieties (Lavan et al. 2003).

In the past decade, the introduction of computer-aided approaches, micro-fabrication technology, and micro-fluidic segregation has led to vast development and enhancement in the architecture and composition of biomedical foams (Choi et al. 2007; Hollister 2005; Melchels et al. 2010; Sands and Mooney 2007). This has further led to the elucidation of many underlying mechanics, thereby leading to the development of foams and scaffolds with multiple functions and enhanced performances. In the present scenario, considerable research is being carried out for designing and fabricating the miniaturized foams that have nanoscale properties, which could be a combination of technological potential with cues from biophysics and biochemistry. These devices can be used for several applications such as building blocks for in vitro cell culture and in vivo regeneration of tissues, in situ therapeutic/prophylactic treatment, sensors and actuators for improving health, and many others.

7.2 Requirements of an Ideal Metallic Foam

7.2.1 Biological and Structural Prerequisites for an Ideal Scaffold for Tissue Engineering

The use of natural macromolecules (collagen, chitosan, silk) for the synthesis of scaffolds, which are meant for the engineering of tissues, has developed significantly (Gao et al. 2015; Malda et al. 2007). The idea is to seed to the patient's cell before implantation into the body within the scaffold (Jonitz et al. 2011). These scaffolds could be directly implanted to support in situ cell growth, proliferation, and regeneration of tissues (Li and Kawashita 2011). However, the approach taken does not have a significant influence as the scaffolds are seldom of immense importance due to their influence in cell growth and promotion of maturation in tissues (Jonitz et al. 2011; Kraus et al. 2012). Over the past few years, many studies have been carried out in this field for the development of suitable scaffolds and their applications (Fig. 7.1) (Chen et al. 2014; Li and Kawashita 2011; Zhang et al. 2014).

Biomaterial scaffolds should meet several requirements for tissue engineering applications (Fig. 7.2). These include:

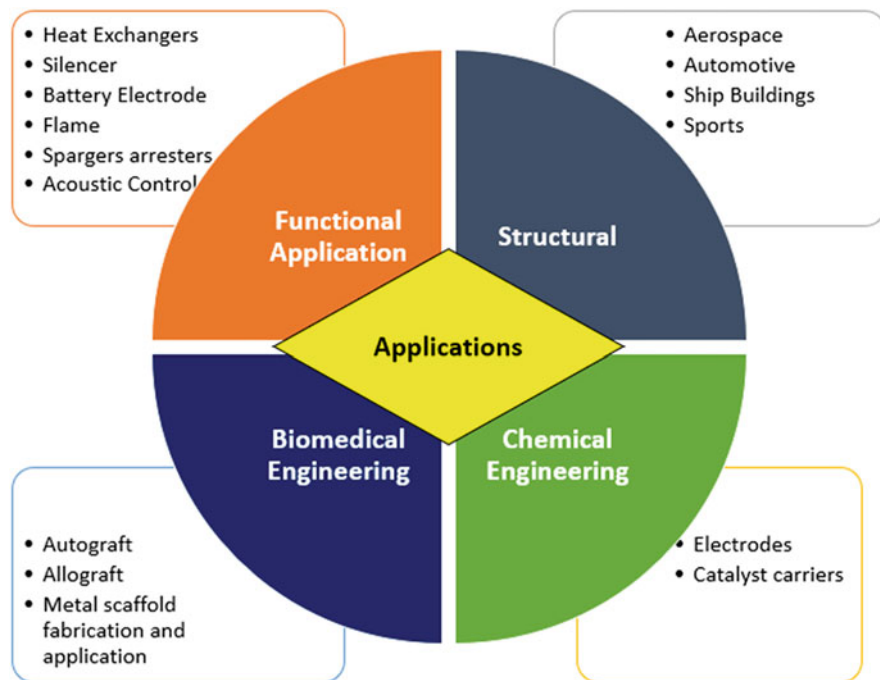


Fig. 7.1 Application of metallic foams

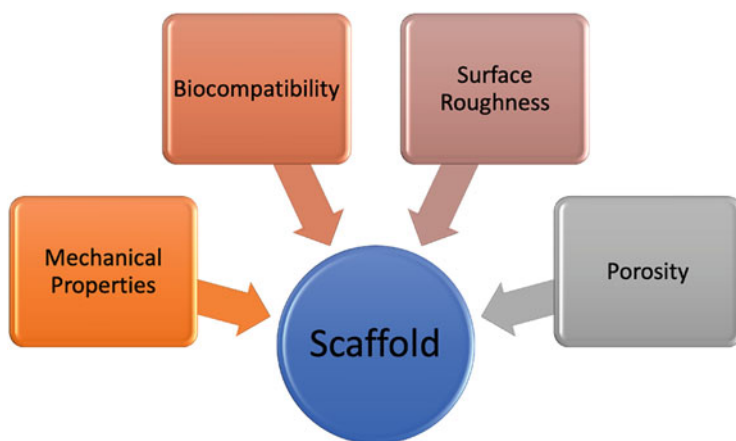


Fig. 7.2 Requirement of metallic foams for bio-applications

1. Biocompatibility (based on the intended use).
2. Biodegradability (based on the clearance through normal pathways).
3. Porosity (based on effective cell/nutrient transport).
4. Equivalent mechanical properties to the intended tissue.

5. Similar structural morphology as of the intended tissue, to have similar conditions as in vivo conditions (Cox et al. 2015; Leukers et al. 2005; Seitz et al. 2005).

Based on the tissue involved, the characteristic requirement varies. These requirements are illustrated in the forthcoming subsections.

7.2.2 Biocompatibility

The biocompatibility of the scaffolds is significant in tissue engineering as it ensures proper functioning and low toxicity (Mandrycky et al. 2016; Qi et al. 2017). There have been several researches (both in vitro and in vivo) conducted, which mentioned low cytotoxicity of nanocellulose-based materials (Eqtesadi et al. 2016; Hench 2006; Ilharborde et al. 2008; Liu and Ma 2004; Mendoza García et al. 2017; Nocera et al. 2018; Ravi and Chaikof 2010; Saranya et al. 2011; Westhauser et al. 2016a; Zhu and Marchant 2011). The route internalization combined with inhalation has a significant influence over the biocompatibility, thereby representing a major issue, which is the higher aspect ratio in the nanocelluloses (Buyuksungur et al. 2017; Goh and Ooi 2008; Teixeira et al. 2019; Wang et al. 2016; Westhauser et al. 2016b). These nanocelluloses are of great promise to tissue engineering as they are usually haemocompatible and biocompatible (Ge et al. 2009c). Due to the absence of a mechanism to explain the breakdown of cellulose by enzymes, there is a requirement of new testing techniques to measure the bio-distribution of nanocellulose and clearance (Mendoza García et al. 2017).

7.2.3 Biodegradability

In tissue engineering, the absence of nanocellulose breakdown by enzymes in almost all species in vivo should be given consideration. Hence, it is important to identify the inflammatory response for prolonged periods through the chronic toxicity studies in vivo (Ge et al. 2009a, b). The degradation of scaffolds must ideally occur in vivo post the regeneration of the newer tissues (Ikeda et al. 2009). This degradation should happen at particular periods alone based on the growth of the interested tissue. Hence, it is imperative to study further the mechanisms of clearance of the nanocellulose that biodegrade partially (Nagura et al. 2007). This clearance depends on a multitude of nanocellulose properties such as type, aspect ratio, surface chemistry, etc. Also, the overall clearance could be influenced by the degradable nanocellulose combined with other polymer matrices, or in vivo-tested cross-linked chemistries (Chia and Wu 2014; 池田里砂 2011).

7.2.4 Porosity

The numerical translation of the quantity of void space associated with the given geometry's volume is referred to as porosity. The porosity is the most exceptional feature that helps in differentiating the scaffolds in the case of tissue engineering. The nanocellulose is very suitable for such applications due to the possibility of maintaining the mechanical strength and ability to customize the porous 3D-based architectures. The interconnectivity of the pores plays a significant role as this leads to the removal of wastes and diffusion of oxygen and nutrients (Lin et al. 2016). The infiltration of cells and blood vessels is also important as they spread through the entire scaffold without compromise on the new tissue formation (Morris et al. 2017; Rajaram et al. 2015).

The scaffolds possessing hierarchical morphologies in combination with increased porosity encourages initial stage of osteoinduction. The pore size also affects behaviour of the cells and the growth of blood vessels. Thus, the pore size needs to be controlled to promote the regeneration of tissues (Liu et al. 2013; Huh et al. 2018; Kim et al. 2017a; Lin et al. 2016; Morris et al. 2017; Mozdzen et al. 2016; Rajaram et al. 2015; Williams et al. 2005). The investigation carried out by Murphy et al. (2010) revealed that cell count was larger in porous scaffolds with 120–325 μm size range. The investigations of Mandal and Kundu (2009) revealed the multiplication and relocation of the human dermal fibroblast cells on 3D scaffolds, having pores in 200–250 μm size range. Oliviero et al. (2012) stated that the pore size should be at least in the range of 30–40 μm to ensure the nutrient diffusion within scaffolds. Artel et al. (2011) demonstrated that the rate of vascularization in scaffolds rises with size of pores increasing from 160 to 270 μm , which augment neovascularization. As mentioned in the earlier paragraphs, cryogels are prioritized over aerogels due to the pore size (micrometric/sub-millimetric range). Thus, scaffold's features such as porosity, pore size, and pore interconnectivity can be tuned by ice-templating. Nevertheless, super-critically dried gels as well as foams are suitable for applications including insulation, cargo delivery, catalysis, and adsorption (Budtova 2019; Kobayashi et al. 2014; Yang et al. 2017b).

7.2.5 Mechanical Performance

From the previous sections, it can be understood that porosity is necessary for several applications, which involve nanocellulose 3D scaffolds. However, the issue is that porosity negatively influences certain important properties such as strength (Hollister 2005). Hence, it is necessary to achieve a balance as the scaffolds should possess sufficient mechanical properties almost equivalent to that of a regular tissue, and should augment the cell migration and regeneration of tissues (Karageorgiou and Kaplan 2005). The mechanical integrity of nanocellulose is not suitable for stiffer tissues, including load-bearing tissues such as bones and cartilages. Therefore, to improve mechanical properties without compromising on porosity, covalent cross-linking of nanocellulose might be required (Tang et al.

2019). Amongst appropriate cross-linkers, tannic acid (Huang et al. 2018), 1,2,3,4-butane tetracarboxylic acid (BTCA) (Hamedi et al. 2013), citric acid (Kim et al. 2017b), sodium (meta)periodate (Cervin et al. 2016), and commercial products including Kymene™ (Zhang et al. 2012) have been reported. Based on the chemical nature, glyoxal, genipin, and glutaraldehyde have been suggested as well (Huang et al. 2018; Kim et al. 2017b; Naseri et al. 2016). Additionally, the creation of reversible, noncovalent cross-links namely hydrazone bonds and supramolecular or supracolloidal interactions, including ionic cross-linking between oppositely charged nanocelluloses, is highly desirable in enhancing the mechanical integrity while concurrently facilitating biodegradation.

The microstructure can also be modified to obtain suitable mechanical behaviour of nanocellulose dried gels and foams. Tripathi et al. (2019) correlated the long-range order of CNC into nematic and chiral nematic phases. This correlation was carried out through non-solvent-induced phase separation, evaporation-induced self-assembly, and supercritical drying post changing the solvents to acetone.

7.2.6 Structural Morphology

The internal and surface structure of a scaffold are very significant and influence several factors affecting the promotion of natural cellular functions such as adsorption of proteins and cell adhesion (Fabbro et al. 2012). Pattison et al. (2005) carried out studies that revealed a positive relation between scaffold roughness and attachment and proliferation of the cell. Moreover, studies revealed that smooth surfaces facilitated the multiplication of multipotent cells into a specialized cell types, such as fibroblasts. In contrast, the rough surfaces promoted the differentiation of other cell types, including the ones implicated in bone formation (Boyan et al. 2017; Schwartz et al. 1999). The cell growth can be influenced by factors including scaffold anisotropy as in myoblast cells, where they preferentially grow towards the direction of nanocellulose alignment (Dugan et al. 2010, 2013). Hence, it is essential to tailor the surface of the scaffolds for each application intricately. In conclusion, these nanocellulose-based scaffolds must attach, provide support to tissues, and offer a structurally coherent environment for regeneration.

7.3 Non-biodegradable Metallic Foams

The most commonly used biomaterials employed for replacing the structural components of the human body are the metals due to their superior mechanical properties compared to polymers and ceramics (Table 7.1) (Rahim et al. 2018). Besides, metals exhibit enhanced tensile and fatigue strength and fracture toughness, thereby making them suitable for the devices used in hard tissue displacements such as artificial hip joints, bone plates, coronary stents, knee implants, and dental implants (Niinomi 2008). In the recent past, magnesium-based alloys have been employed to synthesize biodegradable bone implants. The lower density of the

Table 7.1 Basic properties of implant materials (Rahim et al. 2018)

Implant material	Degradation speed	Physical and corrosion characteristics	Biological effects	Biodynamic effects	References
Organicopolymers	Adjustable	Potentially flexible but mostly too weak for load-bearing applications; implant swelling in moist environments; X-ray transparent	Inflammatory acidic hydrolysis products	Bio-tolerant	Athanasiou et al. (1996) and Ceonzo et al. (2006)
Iron	Very slow; complete degradation may require several years	Sturdy but irregular corrosion characteristics	Accumulation of inflammatory iron hydroxide particles in various tissues	–	Bowen et al. (2012), Hermawan et al. (2010) and Pierson et al. (2012)
Zinc-based	Slow; life-time far exceeds expected healing periods	Suboptimal strength	Non-inflammatory	–	Vojtěch et al. (2011) and Yang et al. (2017a)
Magnesium-based	Rapid; danger of mechanical implant failure before the healing process is completed	Alloys with sufficient strength available; compliance can be adjusted; irregular pitting corrosion; corrosion coat formation due to slowly dissolving solid precipitates resulting in reduction of initial corrosion rates	Non-inflammatory; gas accumulation in the tissue; accumulating solid corrosion products or gaseous hydrogen may exert pressure on non-yielding bony tissue	–	Staiger et al. (2006) and Zhao et al. (2017a, b)
Surgical steel	Inert	Sturdy; suitable for load-bearing applications; allows for ductile thin vascular stent struts	Non-inflammatory, inert	Bio-tolerant	Perren et al. (2017)
Titanium	Inert	Sturdy; highly suitable for load-bearing applications	Non-inflammatory, bone-friendly surface oxide layer	Bio-inert	Perren et al. (2017)

magnesium, its requirement in metabolism, and mechanical properties similar to that of bone tissue assist in enhancing mechanical strength (Niinomi 2008; Staiger et al. 2006). However, the degradation rate of pure magnesium is very high; hence, it is often alloyed with minor additions of calcium, zinc, aluminium, manganese, or rare-earth elements to slow the degradation rate (Staiger et al. 2006).

The commercially used metallic biomaterials used in implant applications are Type 316L stainless steels, cobalt-chromium-molybdenum alloys, commercially pure titanium, and Ti-6Al-4V alloys (Sumita et al. 2004). These materials were initially developed for industrial purposes; however, they have been used in biomaterial applications due to their enhanced corrosion resistance and mechanical properties. The bio-performances of these metals can be modified using techniques such as alloying, annealing, and surface treatment technologies. The 316L austenitic stainless steel is one of the most commonly used bio-metals due to its lower cost compared to other alloys, including cobalt-chromium alloys and titanium alloys (Niinomi 2008; Staiger et al. 2006; Sumita et al. 2004). Nickel-free alloys are also being developed to further enhance corrosion resistance, by replacing the Ni with other austenitic stabilizers such as nitrogen and manganese (Sumita et al. 2004).

7.3.1 Titanium-Based Foams

Titanium-based alloys have several advantages such as enhanced biocompatibility, high specific strength, low Young's modulus, and enhanced resistance to corrosion. Due to these properties, they are used for scaffold applications for bone formation and remodelling in critical defects (Spoerke et al. 2008; Hasan et al. 2018a). The Ti alloys are used as implant materials to augment support for bone healing in various forms, such as plates (Souer et al. 2010), meshes (Sakat et al. 2016), or cages (Siu et al. 2018) in orthopaedic fields (Guo et al. 2013) (Fig. 7.3).

The fabrication of porous Ti-6Al-4V scaffolds via inkjet-based powder-bed printing process was first carried out by Barui et al. (2017), where the total porosity was 57% inhomogeneous porous designs and 45% in gradient porous designs. The interconnectivity was around 99% amongst the micron-sized pores. The compressive yield strength of 47 MPa and elastic modulus of 2 GPa was seen on homogeneous scaffolds upon uniaxial compression, whereas in gradient scaffolds, the yield strength and elastic modulus observed were 90 MPa and 3.3 GPa, respectively (Barui et al. 2017). Cho et al. (2015) illustrated the application of 3D titanium implants for cavalier defects, which were results of traumatic subdural hematoma and meningioma. The tailor-made 3D porous titanium implant had been given to reconstruct the cavalier, which was synthesized per patient-specific 3D-computed tomography data. It was observed that implants fitted accurately without any complications 6 months post implant insertion, thus reported satisfaction (Cho et al. 2015). Park et al. (2016) conducted clinical trial on patients having large skull defects. The treatment was carried out using a custom-made 3D titanium implant. The implant fixation and symmetry of the skull remained good post follow up as well (Park et al. 2016).

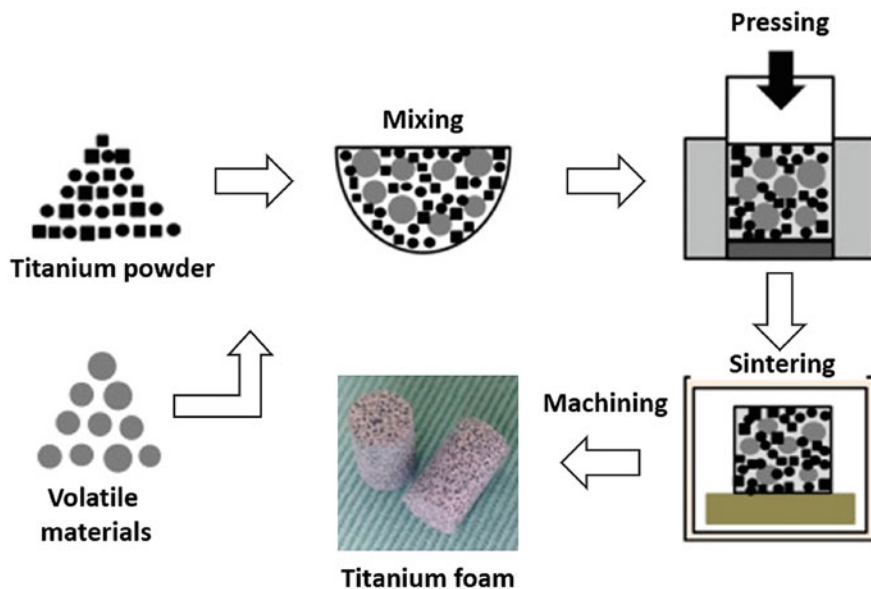


Fig. 7.3 Fabrication of titanium (Ti) foam by the powder sintering method. (Reprinted from (Matsushita et al. 2017) with permission from Elsevier)

In the recent past, multiple research efforts have been made for the application of three-dimensional titanium implants in orthopaedic trauma. Hamid et al. (2016) reported a case of open, comminuted distal tibia and fibula fractures with the segmental bone defect of the distal tibia. 3D-printed titanium scaffold was packed with mounts of autografts and allografts and was used to replace the distal tibia and talus. 13 months follow-up showed successful bone integration, and the patient returned to normalcy without discomfort (Hamid et al. 2016). Non-biodegradable nature of scaffolds composed of Ti-based alloys limits their use in the repair of bone defect, but their usage in treating massive segmental bone defects is still favoured.

Titanium is chemically unreactive in the physiological environment, and it has the ability of osseointegration with bone (Davies 2007; Behera et al. 2020a). Upon oxidation, titanium forms a stable oxide layer, providing enhanced biocompatibility. This passive oxidation layer is self-passivating; in other words, it can regenerate autogenously. The nature of this oxide layer prevents corrosion and a significant influence on physicochemical properties namely crystallinity and segregation of impurity. Enhanced biocompatibility is observed in the titanium alloys compared to other alloys. Titanium-aluminium-vanadium alloys exhibit superior mechanical strength when compared to commercially pure titanium and is thus widely used in total joint implants. The major issue with these Ti-6Al-4 V alloys is the presence of V, which is toxic in elemental form, thus leading to the development of novel beta Ti alloys with elements such as Ta, Nb, and Zr, which are not toxic in nature (Okazaki 2001).

Excellent biocompatibility can be observed in porous Ti-based alloys (Behera et al. 2020b). In recent decades, bioactive meshes composed of Ti have been incorporated in spine fusion surgery (Zdeblick and Phillips 2003). The cylindrical titanium mesh cage is being used for the past 15 years for anterior lumbar interbody fusion (ALIF). The Ti-based mesh cages were utilized for bone grafts in spinal fusion which were limited due to complications and morbidity in the second site [74]. This problem can be rectified by the usage of hydroxyapatite to provide bioactivity and to augment osteoconduction (Thalgott et al. 2002; Niu et al. 2005). Regardless of the development of various alloys for tissue engineering, the titanium-based alloys are the widely used and considered the best. Ti being paramagnetic is harmless to patients undergoing magnetic resonance imaging (MRI). The addition of certain growth factors can enhance osseointegration property. In applications such as mandibular reconstruction or bone augmentation or implant defects, higher bone regeneration has been achieved with the delivery of TGF- β and BMP-2 via Ti-based scaffold (Jansen et al. 2005). The BMP-2 growth factor can deliver specific cellular responses, thus leading to the quicker formation of tissues (Zhang et al. 2006).

7.3.2 Tantalum-Based Foams

The porous tantalum has peculiar properties, with porosity over 80%, where pores are completely interconnected, thus leading to quick and protected bone growth (Bobyne et al. 1999a, b). The stress-shielding effect is lowered significantly as the elastic modulus of these scaffolds is tantamount to that of bone. Ta has sufficient mechanical properties to existing conditions prevailing in the human body. Thus, it can also be used in primary and revision total knee arthroplasty (TKA), which was illustrated by Bobyne et al. (1999a, b). They used a carbon-based trabecular metal, where Ta was deposited on the surface, which was highly biocompatible in many animal models (Bobyne et al. 1999a, b). The trabecular metals exhibited higher stability and osteoconduction compared to other materials. Despite its recent evolution as biomaterial, there have been several clinical data (Zou et al. 2004; Tanzer et al. 2001; Meneghini et al. 2008; Adams et al. 2005) and preclinical studies (Vehof et al. 2000, 2002; Van Den Dolder et al. 2003; Kroese-Deutman et al. 2005; Hartman et al. 2005; Habibovic et al. 2005) augmenting porous tantalum as an effective alternative for orthopaedic applications.

The tantalum-based foams stand out compared to other metals due to their enhanced properties such as homogeneity and structural continuity, strength, lower stiffness, higher levels of porosity, and higher frictional coefficient (Lee et al. 2015). Through additive manufacturing, scaffolds with high levels of porosity having intricate configurations and constant pore shape and size can be synthesized (Liu et al. 2006). In the recent past, much emphasis was placed on the development of 3D tantalum implants for repairing the critical-sized bone defects.

The primary issue in utilizing the macroscopic scaffold is their lower diffusion capacity in the aqueous solutions in large bone defects (Malda et al. 2007). The consumption of oxygen and acidification within tantalum scaffolds, along with the

analysis of the movement of the osteoblasts in the *in vitro* study, was investigated by Jonitz et al. (2011) The concentration of oxygen reduced after a day (24 h) and retained at a lower level in the subsequent week (7 days). During incubation, lower levels of acidification were observed in the core and periphery of the scaffolds. After 8 days of incubation, osteoblasts of humans were yet to be detected on the tantalum scaffold surface until 10 mm distance. Hence, it was assumed that osteoblasts settled at the tantalum-based scaffolds under critical oxygen and nutrient supply in large bone defects (Jonitz et al. 2011). However, as in the case of Ti, Ta scaffolds are also non-biodegradable, thereby restricting their application in many bone defect repairs.

7.3.3 Nickel-Titanium Alloy (Nitinol)

Nitinol is one of the superior titanium-containing alloys, which has several uses due to its excellent characteristics such as shaper memory effect, biocompatibility, and superplasticity even at porous states (Prymaka et al. 2005; Greiner et al. 2005). Their elastic modulus and compressive strengths are 2.3 GPa and 208 MPa, respectively, which are almost equivalent to those of bones. The porous NiTi is extensively used in the synthesis of intramedullary nails and intervertebral spacers employed in treating scoliosis due to their enhanced biocompatibility (Tarniță et al. 2009). NiTi has been proved to be more biocompatible than stainless steels through *in vivo* testing and preclinical experience (Tarniță et al. 2009; Assad et al. 2002a, b). Good biocompatibility on surface-modified NiTi has been reported (Michiardi et al. 2006; Kapanen et al. 2001; Firstov et al. 2002; Armitage et al. 2003). Due to its high biocompatibility, physical properties, and SME, the NiTi can be of significant application in orthopaedic applications, which mainly involves in the creation of scaffold that can change shape post implantation (SME effect) in which the initiation of SME occurs at temperature of physiological environment. The toxicity as in case of Ti and Ta alloys is the major issue with release of Ni ions, which has limited the NiTi application for implant applications in Europe and the USA. This issue can be addressed by performing surface treatment including oxidation treatment of NiTi to obtain a Ni-free surface (Michiardi et al. 2006) and replacing Ni with Nb, which are currently studied, and their performance in biological organisms need to analysed in the future (Suzuki et al. 2006).

7.4 Biodegradable Metallic Foams

The main limitation of metallic scaffolds is their low biodegradation, i.e. osteogenesis rates and degradation rates are not coherent (Li and Kawashita 2011). Iron-based materials show better biodegradability compared to Ti-based alloys. These alloys have been employed in the synthesis of 3D printed scaffolds. This has been illustrated by Chou et al. (2013) where the scaffolds were milled Fe-30Mn (wt %) powder fabricated by an inkjet 3D printing process. The porosity of

the printed scaffold was as high as 36.3% and showed equivalent mechanical properties as that of natural bone. Also, pore infiltration of MC3T3-E1 pre-osteoblast cells exhibited superior cytocompatibility. The high degradation rate of the Fe-30Mn scaffold was a stand-out. Thus, it was reported that 3D-printed Fe-30Mn scaffold was apt for low load-bearing applications, and the fabrication of biodegradable systems was achieved by inkjet printing processes (Prymak et al. 2005; Chou et al. 2013).

In the recent past, magnesium-based alloys are gaining significant traction due to their excellent properties such as completely bioresorbability, mechanical properties equivalent to that of bone, facilitation of bone growth, and their favourable role in the attachment of cells (Staiger et al. 2006). The biodegradability of Mg prevents the secondary surgery required for scaffold removal. Thus, Mg is a potential load-bearing material, including their use in biomedical applications, such as for coronary stents (Heublein et al. 2003; Erbel et al. 2007). Several alloying elements, such as cerium, neodymium, and praseodymium, are being added to pure Mg for bone fixation devices (Witte et al. 2005, 2006) for osteo-applications. The evaluation of Mg-Ca alloys in vitro and in vivo for orthopaedic applications revealed that excess Mg is removed as part of the urine (Saris et al. 2000; Li et al. 2008). There is a concern about the application of pure Mg due to rapid degradation, thus leading to hyper-magnesia. However, there are several routes, such as coating with ceramics (Li et al. 2004), titanium (Zhang et al. 2005), and alloying (Zhang et al. 2009) to alleviate these drawbacks.

Currently, the porous Mg-based alloys are attractive for metallic scaffold applications due to their enhanced biocompatibility, bioactivity, and biodegradability (Kraus et al. 2012). Zhang et al. (2014) revealed the 3D-interconnected pores with a porosity range of 33% to 54% in a novel porous Mg. These Mg scaffolds exhibited lower elastic modulus ranging from 0.10 to 0.37 GPa and compressive strength ranging from 11.1 to 30.3 MPa. Hence, 3D-printed Mg scaffold is considered as a potential implant material (Zhang et al. 2014). In Chen et al.'s (2014) study, β -TCP was coated on Mg scaffolds to control the detrimental osteo-immunomodulatory properties of the Mg-based scaffolds in vitro. The osteogenic mechanism of the scaffolds was shown by macrophage-mediated osteogenic differentiation of bone marrow stromal cells (BMSCs). It inhibited osteoclastogenesis through the downregulation of macrophage colony-stimulating factor (MCSF) and tartrate-resistant acid phosphatase (TRAP) as well as inhibition of the receptor activator of nuclear factor kappa-B ligand (RANKL)/receptor activator of nuclear factor kappa-B (RANK) system (Chen et al. 2014). Liu et al. (2014) implanted the porous Mg and HA scaffolds in the femoral condyle of rabbits. The desired biocompatibility was achieved in both the scaffolds; however, in Mg scaffolds, substantial new bone ingrowth followed by the degradation (outside to inside) was observed, but very few osteoblasts were observed on the surface without degradation of the scaffold in the case of HA scaffold. The magnesium scaffolds are an excellent choice for bone defect repair due to their osteogenesis and degradation properties (Liu et al. 2014). Clinical trials of these scaffolds are yet to be conducted; nevertheless, additive manufacturing of these scaffolds looks promising.

7.5 Metallic Foams for Cell Culture

Engineering of tissues for therapeutic applications utilizing culturing transplanted cells within 3D porous scaffolds is one of the most investigated approaches of tissue engineering research. The *in vitro* synthesis of biological tissues is preferred in necessary biological studies and pharmacological and toxicological screens and as replacement tissues for clinical applications. *In vivo*, cell behaviour is the result of a cascade of events that relies on the interaction between cells and the 3D microenvironment, comprising the ECM surrounding cells and molecular cues. In order to recapitulate the *in vivo* milieu, a vital issue is to understand how cells respond to such micro-environmental stimuli by determining cell–scaffold cross-talk dynamics. This aspect is essential for developing cell-instructive materials able to guide successful tissue regeneration. The features of scaffolds, such as composition, degradation, pore structure, and mechanical properties and their influence, have been analysed as of now for several cell–scaffold combinations. There have been several works (Sung et al. 2004; Lee et al. 2001; Hu et al. 2003) illustrating the optimization of scaffold induced regeneration by a selection of constituent materials, thereby getting the required surface chemistry, degradation rate, and mechanical properties. Moreover, the pore characteristics such as porosity, pore size, shape, and interconnectivity act coherently with the other parameters by regulating cell spatial distribution, infiltration, and the transport of fluids, such as nutrients and oxygen, across the entire cell–scaffold constructs (Salerno et al. 2010; Guarino et al. 2008). Major obstacles to the *in vitro* generation of functional tissues and their widespread clinical use are related to a limited understanding of the regulatory role of specific physicochemical culture parameters on tissue development (Martin et al. 2004). For the *in vitro* culture of 3D tissues having a thickness greater than 200 μm , the oxygen and soluble nutrients content reduces (Salerno et al. 2010). To overcome the cons of static cultures, bioreactors which can regulate and monitor the biological and biochemical processes are developed. In particular, bioreactors have demonstrated outstanding potential for: (1) improving cell seeding uniformity, proliferation, and ECM biosynthesis within the entire scaffold pore structure characterized by different physical and chemical properties, and (2) stimulating mechanically transplanted cells to induce correct cell differentiation and tissue development (Martin et al. 2004).

Achieving *in vivo* tissue-induced regeneration for injured tissues and/or organs by means of porous scaffolds represents the most important goal of tissue engineering. In general, optimal scaffolds for the *in vivo* tissue repair/ regeneration must serve four primary purposes:

1. Define a space that will shape the regenerating tissue.
2. Provide temporary structural function in the implantation site whilst tissue regenerates.
3. Stimulate the progressive formation of a functional new tissue within the pore structure.

4. Degrade progressively, matching the rate of new tissue growth, without releasing toxic by-products.

Since scaffold-based approaches were first proposed in tissue engineering, a massive research effort has been carried out about the effect of scaffold composition, microstructure, and degradation on *in vivo* tissue-induced regeneration. Materials from synthetic or natural resources, as well as multi-phase composites, were implanted in well-established *in vivo* models for the repair/regeneration of tissues such as bone, cartilage, and skin (Staiger et al. 2006; Nair and Laurencin 2007; Mano et al. 2007). The presence of the pore structure and the maintenance of sufficient structural integrity are critical aspects for *in vivo* implantation. Indeed, porosity is necessary for initial cell attachment and migration and for mass transfer of nutrients and metabolites and provides sufficient space for development and later remodelling of the organized tissue (Karageorgiou and Kaplan 2005). Concomitantly, the structural integrity may permit cell and tissue remodelling until achieving stable biomechanical conditions and vascularization at the host site. As the degree of remodelling depends on the tissue itself and its host anatomy and physiology, scaffold degradation and concomitant evolution of structural properties must be accurately controlled for the envisioned application. In general, scaffold implantation triggers a series of body responses which are included in the so-called “foreign-body reaction” characterized by non-specific protein adsorption to the scaffold surface and the adhesion of a number of different cells to the scaffold, such as monocytes/macrophages, leukocytes, and platelets. If the inflammation persists, the macrophages fuse together to form giant cells, finally leading to the formation of a collagenous capsule surrounding the implant. It is therefore clear that to induce successful tissue regeneration *in vivo*, the scaffolds must be able to control the biological response induced by them. One of the most investigated strategies to address this issue has been the modification of the surface properties of porous scaffolds to guide protein adsorption. Initial protein–material interactions are vital as it controls and guides the attachment of cells and adhering process. Cell adhesion to adsorbed proteins is facilitated through integrin and other receptors inside the cell membrane (García 2005). Therefore, it is universally recognized that controlling protein adsorption on the surface of biomaterials may be vital in the control and direction of cell response to biomaterials. A plethora of techniques has been developed in order to modify surface characteristics, including biomaterial chemistry, wettability, and morphology and to improve *in vivo* tissue-induced regeneration. Bioactivation of polymeric scaffolds by means of micro- and nano-metric fillers incorporation represents one of the most used approaches for bone regeneration. Indeed, the inorganic phase may improve the deposition of new bone inside the implant and the consequent integration of the scaffold with the surrounding tissue. A comprehensive account of this topic can be found in the review of Rezwani et al. (2006). Chemical grafting has been also proposed to improve the functionality of implanted scaffolds. This approach involves activating the surface with reactive groups followed by grafting the desired functionality to the surface. Short oligopeptides exhibiting specific binding domains, as well as whole proteins such

as fibronectin, vitronectin, laminin, and collagen, have been attached to the surface of the scaffolds to support cells and present an instructive background to guide their behaviour. Zheng et al. (2012) improved the functionality of polycaprolactone vascular graft by means of RGD coating. The obtained implants showed decreased occlusion, improved haemocompatibility, enhanced cell infiltration, and homogeneous distribution, compared to untreated implants. Although this approach still remains common owing to its comparative minimalism, its efficacy requires tight control over the composition of the adsorbed protein layer to stimulate a constructive cell response, aiding wound repair and integration of tissues. Conversely, proteins in an unrecognizable state may indicate foreign materials to be isolated or removed. Concomitantly, it is worth noting that the *in vivo* efficacy of these approaches has yet to be demonstrated. In particular, further efforts and well-characterized animal implantation models are necessary to provide a correlation between surface functionality and short-term *in vivo* response, as well as to demonstrate that this approach can be also efficacious for the control of long-term *in vivo* cellular responses. Functional porous biomaterials must as well be adept of undertaking an active transformation from one state to another state in the presence of biological systems. For instance, the transformation from an injectable state to a solid state is highly advantageous for usage in minimally invasive surgical procedures to alleviate problems associated with the implantation of prefabricated scaffolds. Injectable materials can also be combined with cells and bioactive molecules to improve regeneration. The injectability of a scaffold is generally related to the rheological properties of the formulations, and the setting time of the precursors is determined by the structure/composition of the formulations and their processing conditions (Hou et al. 2004). Amongst the different biomaterials, calcium phosphate cements are the most investigated injectable foams for minimally invasive bone regeneration. Indeed, these materials offer the possibility of combining bioactivity, injectability, and *in situ* self-setting properties coupled with a macro- and nano-porous structure for bone cell adhesion and tissue ingrowth. CaP cements can endure a self-setting process post injection, based upon the cementing action of acidic and basic CaP compounds once wet by body fluids. The setting time can be also altered by the addition of manipulator compounds to the wetting medium. Kim and co-workers (Kim et al. 2009) developed a novel pH- and thermo-sensitive hydrogel as an injectable scaffold for autologous bone tissue engineering (Kim et al. 2006, 2009; Hou et al. 2004). *In vivo* implantation of cell-seeded porous scaffolds belongs to the so-called “cell therapy” and has been proposed as a suitable approach to improve implant bonding and integration to the surrounding tissue, as well as new tissue vascularization. The positive effect of seeding cells within porous scaffolds before implantation has been reported for different scaffolds and tissues, such as bone (Kim et al. 2006, 2009; Hou et al. 2004).

7.6 Concluding Remarks

Demand for personalized medical treatment has increased significantly especially in the case of patient-specific medical devices. These devices must be designed to accommodate every patient and every disease, in addition to quick and cheap distribution to respond successfully to the demand. Moreover, if devices with complex shapes and structures historically unable to be assembled by traditional manufacturing methods were to be made readily available, a new form of advanced medical care would arise. In this chapter, we explored the future of different types of metallic foams. In terms of the elastic modulus, foam is superior to bulk material, since the modulus of such materials can be effortlessly modified by changing the pore structure. Nevertheless, bulk materials possess superior mechanical strength compared to porous material. Therefore, it is essential to balance the mechanical properties of these devices effectively. A porous material may be used as a substitute for prosthesis in which the deformation is almost similar to that of the surrounding bone. Porous materials that are subjected to bioactivity induction treatments are useful for stable repair of the system and shortening the healing time. Additionally, designing software for the precise design of a system to suit the infected part of the body using computed tomography images of the affected region is also important in medical applications of these materials. When a simple design procedure is made available, it is certain to become a norm for medical devices requiring a porous and rigid structure for large bone defects. Devices made up of bioactive porous and solid materials are expected towards becoming commonly used in orthopaedics and oral maxillofacial surgery.

References

- Adams JE, Zobitz ME, Reach JR, An K-N, Lewallen DG, Steinmann SP (2005) Canine carpal joint fusion: a model for four-corner arthrodesis using a porous tantalum implant. *J Hand Surg Am* 30:1128–1135
- Armitage DA, Parker TL, Grant DM (2003) Biocompatibility and hemocompatibility of surface-modified NiTi alloys. *J Biomed Mater Res A* 66:129–137
- Artel A, Mehdizadeh H, Chiu Y-C, Brey EM, Cinar A (2011) An agent-based model for the investigation of neovascularization within porous scaffolds. *Tissue Eng A* 17:2133–2141
- Assad M, Chernyshov A, Leroux MA, Rivard CH (2002a) A new porous titanium–nickel alloy: part 1. Cytotoxicity and genotoxicity evaluation. *Biomed Mater Eng* 12:225–237
- Assad M, Chernyshov A, Leroux MA, Rivard CH (2002b) A new porous titanium–nickel alloy: part 2. Sensitization, irritation and acute systemic toxicity evaluation. *Biomed Mater Eng* 12:339–346
- Athanasiou KA, Niederauer GG, Agrawal CM (1996) Sterilization, toxicity, biocompatibility and clinical applications of polylactic acid/polyglycolic acid copolymers. *Biomaterials* 17:93–102
- Athanasiou VT, Papachristou DJ, Panagopoulos A, Saridis A, Scopa CD, Megas P (2009) Histological comparison of autograft, allograft-DBM, xenograft, and synthetic grafts in a trabecular bone defect: an experimental study in rabbits. *Med Sci Monit* 16:BR24–BR31
- Barui S, Chatterjee S, Mandal S, Kumar A, Basu B (2017) Microstructure and compression properties of 3D powder printed Ti-6Al-4V scaffolds with designed porosity: experimental and computational analysis. *Mater Sci Eng C* 70:812–823

- Behera R, Das A, Hasan A, Pamu D, Pandey L, Sankar M (2020a) Deposition of biphasic calcium phosphate film on laser surface textured Ti–6Al–4V and its effect on different biological properties for orthopedic applications. *J Alloys Compd* 842:155683
- Behera R, Das A, Hasan A, Pamu D, Pandey L, Sankar M (2020b) Effect of TiO₂ addition on adhesion and biological behavior of BCP-TiO₂ composite films deposited by magnetron sputtering. *Mater Sci Eng C* 114:111033
- Biondi M, Ungaro F, Quaglia F, Netti PA (2008) Controlled drug delivery in tissue engineering. *Adv Drug Deliv Rev* 60:229–242
- Bobyn J, Stackpool G, Hacking S, Tanzer M, Krygier J (1999a) Characteristics of bone ingrowth and interface mechanics of a new porous tantalum biomaterial. *J Bone Joint Surg* 81:907–914
- Bobyn JD, Toh K-K, Hacking SA, Tanzer M, Krygier JJ (1999b) Tissue response to porous tantalum acetabular cups: a canine model. *J Arthroplasty* 14:347–354
- Bowen PK, Drelich J, Buxbaum RE, Rajachar RM, Goldman J (2012) New approaches in evaluating metallic candidates for bioabsorbable stents. *Emerg Mater Res* 1:237–255
- Boyan BD, Lotz EM, Schwartz Z (2017) Roughness and hydrophilicity as osteogenic biomimetic surface properties. *Tissue Eng A* 23:1479–1489
- Budtova T (2019) Cellulose II aerogels: a review. *Cellul* 26:81–121
- Buyuksungur S, Tanir TE, Buyuksungur A, Bektas EI, Kose GT, Yucel D, Beyzadeoglu T, Cetinkaya E, Yenigun C, Tönük E (2017) 3D printed poly (ϵ -caprolactone) scaffolds modified with hydroxyapatite and poly (propylene fumarate) and their effects on the healing of rabbit femur defects. *Biomater Sci* 5:2144–2158
- Campana V, Milano G, Pagano E, Barba M, Cicione C, Salonna G, Lattanzi W, Logroscino G (2014) Bone substitutes in orthopaedic surgery: from basic science to clinical practice. *J Mater Sci Mater Med* 25:2445–2461
- Ceozzo K, Gaynor A, Shaffer L, Kojima K, Vacanti CA, Stahl GL (2006) Polyglycolic acid-induced inflammation: role of hydrolysis and resulting complement activation. *Tissue Eng* 12:301–308
- Cervin NT, Johansson E, Larsson PA, Wågberg L (2016) Strong, water-durable, and wet-resilient cellulose nanofibril-stabilized foams from oven drying. *ACS Appl Mater Interfaces* 8:11682–11689
- Chan G, Mooney DJ (2008) New materials for tissue engineering: towards greater control over the biological response. *Trends Biotechnol* 26:382–392
- Chen Z, Mao X, Tan L, Friis T, Wu C, Crawford R, Xiao Y (2014) Osteoimmunomodulatory properties of magnesium scaffolds coated with β -tricalcium phosphate. *Biomaterials* 35:8553–8565
- Chevalier E, Chulia D, Pouget C, Viana M (2008) Fabrication of porous substrates: a review of processes using pore forming agents in the biomaterial field. *J Pharm Sci* 97:1135–1154
- Chia HN, Wu BM (2014) High-resolution direct 3D printed PLGA scaffolds: print and shrink. *Biofabrication* 7:015002
- Cho HR, Roh TS, Shim KW, Kim YO, Lew DH, Yun IS (2015) Skull reconstruction with custom made three-dimensional titanium implant. *Arch Craniofac Surg* 16:11
- Choi NW, Cabodi M, Held B, Gleghorn JP, Bonassar LJ, Stroock AD (2007) Microfluidic scaffolds for tissue engineering. *Nat Mater* 6:908–915
- Chou D-T, Wells D, Hong D, Lee B, Kuhn H, Kumta PN (2013) Novel processing of iron–manganese alloy-based biomaterials by inkjet 3-D printing. *Acta Biomater* 9:8593–8603
- Cox SC, Thornby JA, Gibbons GJ, Williams MA, Mallick KK (2015) 3D printing of porous hydroxyapatite scaffolds intended for use in bone tissue engineering applications. *Mater Sci Eng C* 47:237–247
- Davies JE (2007) Bone bonding at natural and biomaterial surfaces. *Biomaterials* 28:5058–5067
- Dimitriou R, Jones E, McGonagle D, Giannoudis PV (2011) Bone regeneration: current concepts and future directions. *BMC Med* 9:1–10
- Dugan JM, Gough JE, Eichhorn SJ (2010) Directing the morphology and differentiation of skeletal muscle cells using oriented cellulose nanowhiskers. *Biomacromolecules* 11:2498–2504

- Dugan JM, Collins RF, Gough JE, Eichhorn SJ (2013) Oriented surfaces of adsorbed cellulose nanowhiskers promote skeletal muscle myogenesis. *Acta Biomater* 9:4707–4715
- Eqtesadi S, Motealleh A, Pajares A, Guiberteau F, Miranda P (2016) Improving mechanical properties of 13–93 bioactive glass robocast scaffold by poly (lactic acid) and poly (ϵ -caprolactone) melt infiltration. *J Non Cryst Solids* 432:111–119
- Erbel R, di Mario C, Bartunek J, Bonnier J, de Bruyne B, Eberli FR, Erne P, Haude M, Heublein B, Horrigan M (2007) Temporary scaffolding of coronary arteries with bioabsorbable magnesium stents: a prospective, non-randomised multicentre trial. *Lancet* 369:1869–1875
- Fabbro A, Villari A, Laishram J, Scaini D, Toma FM, Turco A, Prato M, Ballerini L (2012) Spinal cord explants use carbon nanotube interfaces to enhance neurite outgrowth and to fortify synaptic inputs. *ACS Nano* 6:2041–2055
- Firstov G, Vitchev R, Kumar H, Blanpain B, van Humbeeck J (2002) Surface oxidation of NiTi shape memory alloy. *Biomaterials* 23:4863–4871
- Gao G, Yonezawa T, Hubbell K, Dai G, Cui X (2015) Inkjet-bioprinted acrylated peptides and PEG hydrogel with human mesenchymal stem cells promote robust bone and cartilage formation with minimal printhead clogging. *Biotechnol J* 10:1568–1577
- García AJ (2005) Get a grip: integrins in cell–biomaterial interactions. *Biomaterials* 26:7525–7529
- Ge Z, Tian X, Heng BC, Fan V, Yeo JF, Cao T (2009a) COMMUNICATION: histological evaluation of osteogenesis of 3D-printed poly-lactic-co-glycolic acid (PLGA) scaffolds in a rabbit model. *Biomed Mater* 4:021001
- Ge Z, Tian X, Heng BC, Fan V, Yeo JF, Cao T (2009b) Histological evaluation of osteogenesis of 3D-printed poly-lactic-co-glycolic acid (PLGA) scaffolds in a rabbit model. *Biomed Mater* 4: 021001
- Ge Z, Wang L, Heng BC, Tian X-F, Lu K, Tai Weng Fan V, Yeo JF, Cao T, Tan E (2009c) Proliferation and differentiation of human osteoblasts within 3D printed poly-lactic-co-glycolic acid scaffolds. *J Biomater Appl* 23:533–547
- Goh YQ, Ooi CP (2008) Fabrication and characterization of porous poly (l-lactide) scaffolds using solid–liquid phase separation. *J Mater Sci Mater Med* 19:2445–2452
- Greiner C, Oppenheimer SM, Dunand DC (2005) High strength, low stiffness, porous NiTi with superelastic properties. *Acta Biomater* 1:705–716
- Guarino V, Causa F, Salerno A, Ambrosio L, Netti P (2008) Design and manufacture of microporous polymeric materials with hierarchal complex structure for biomedical application. *Mater Sci Technol* 24:1111–1117
- Guo Z, Iku S, Mu L, Wang Y, Shima T, Seki Y, Li Q, Kuboki Y (2013) Implantation with new three-dimensional porous titanium web for treatment of parietal bone defect in rabbit. *Artif Organs* 37:623–628
- Habibovic P, Li J, Van der Valk CM, Meijer G, Layrolle P, Van Blitterswijk CA, de Groot K (2005) Biological performance of uncoated and octacalcium phosphate-coated Ti6Al4V. *Biomaterials* 26:23–36
- Hamed M, Karabulut E, Marais A, Herland A, Nyström G, Wågberg L (2013) Nanocellulose aerogels functionalized by rapid layer-by-layer assembly for high charge storage and beyond. *Angew Chem* 125:12260–12264
- Hamid KS, Parekh SG, Adams SB (2016) Salvage of severe foot and ankle trauma with a 3D printed scaffold. *Foot Ankle Int* 37:433–439
- Hartman EH, Vehof JW, Spauwen PH, Jansen JA (2005) Ectopic bone formation in rats: the importance of the carrier. *Biomaterials* 26:1829–1835
- Hasan A, Saxena V, Pandey LM (2018a) Surface functionalization of Ti6Al4V via self-assembled monolayers for improved protein adsorption and fibroblast adhesion. *Langmuir* 34:3494–3506
- Hasan A, Waibhaw G, Saxena V, Pandey LM (2018b) Nano-biocomposite scaffolds of chitosan, carboxymethyl cellulose and silver nanoparticle modified cellulose nanowhiskers for bone tissue engineering applications. *Int J Biol Macromol* 111:923–934
- Hench LL (2006) The story of bioglass®. *J Mater Sci Mater Med* 17:967–978

- Hermawan H, Purnama A, Dube D, Couet J, Mantovani D (2010) Fe–Mn alloys for metallic biodegradable stents: degradation and cell viability studies. *Acta Biomater* 6:1852–1860
- Heublein B, Rohde R, Kaese V, Niemeyer M, Hartung W, Haverich A (2003) Biocorrosion of magnesium alloys: a new principle in cardiovascular implant technology? *Heart* 89:651–656
- Hollister SJ (2005) Porous scaffold design for tissue engineering. *Nat Mater* 4:518–524
- Hou Q, Paul A, Shakesheff KM (2004) Injectable scaffolds for tissue regeneration. *J Mater Chem* 14:1915–1923
- Hu Y, Winn SR, Krajchich I, Hollinger JO (2003) Porous polymer scaffolds surface-modified with arginine-glycine-aspartic acid enhance bone cell attachment and differentiation in vitro. *J Biomed Mater Res A* 64:583–590
- Huang Y, Zhu Y, Egap E (2018) Semiconductor quantum dots as photocatalysts for controlled light-mediated radical polymerization. *ACS Macro Lett* 7:184–189
- Huh J, Lee J, Kim W, Yeo M, Kim G (2018) Preparation and characterization of gelatin/ α -TCP/SF biocomposite scaffold for bone tissue regeneration. *Int J Biol Macromol* 110:488–496
- Ikeda R, Fujioka H, Nagura I, Kokubu T, Toyokawa N, Inui A, Makino T, Kaneko H, Doita M, Kurosaka M (2009) The effect of porosity and mechanical property of a synthetic polymer scaffold on repair of osteochondral defects. *Int Orthop* 33:821–828
- Ilharborde B, Morel E, Fitoussi F, Presedo A, Souchet P, Penneçot G-F, Mazda K (2008) Bioactive glass as a bone substitute for spinal fusion in adolescent idiopathic scoliosis: a comparative study with iliac crest autograft. *J Pediatr Orthop* 28:347–351
- Jansen J, Vehof J, Ruhe P, Kroeze-Deutman H, Kuboki Y, Takita H, Hedberg E, Mikos A (2005) Growth factor-loaded scaffolds for bone engineering. *J Control Release* 101:127–136
- Jonitz A, Lochner K, Lindner T, Hansmann D, Marrot A, Bader R (2011) Oxygen consumption, acidification and migration capacity of human primary osteoblasts within a three-dimensional tantalum scaffold. *J Mater Sci Mater Med* 22:2089
- Kapanen A, Ryhänen J, Danilov A, Tuukkanen J (2001) Effect of nickel–titanium shape memory metal alloy on bone formation. *Biomaterials* 22:2475–2480
- Karageorgiou V, Kaplan D (2005) Porosity of 3D biomaterial scaffolds and osteogenesis. *Biomaterials* 26:5474–5491
- Keating J, Simpson A, Robinson C (2005) The management of fractures with bone loss. *J Bone Joint Surg* 87:142–150
- Kim TK, Yoon JJ, Lee DS, Park TG (2006) Gas foamed open porous biodegradable polymeric microspheres. *Biomaterials* 27:152–159
- Kim HK, Shim WS, Kim SE, Lee K-H, Kang E, Kim J-H, Kim K, Kwon IC, Lee DS (2009) Injectable in situ-forming pH/thermo-sensitive hydrogel for bone tissue engineering. *Tissue Eng A* 15:923–933
- Kim WJ, Yun H-S, Kim GH (2017a) An innovative cell-laden α -TCP/collagen scaffold fabricated using a two-step printing process for potential application in regenerating hard tissues. *Sci Rep* 7:1–12
- Kim Y, Kim YK, Kim S, Harbottle D, Lee JW (2017b) Nanostructured potassium copper hexacyanoferrate-cellulose hydrogel for selective and rapid cesium adsorption. *Chem Eng J* 313:1042–1050
- Kobayashi Y, Saito T, Isogai A (2014) Aerogels with 3D ordered nanofiber skeletons of liquid-crystalline nanocellulose derivatives as tough and transparent insulators. *Angew Chem Int Ed* 53:10394–10397
- Kraus T, Fischerauer SF, Hänni AC, Uggowitz PJ, Löffler JF, Weinberg AM (2012) Magnesium alloys for temporary implants in osteosynthesis: in vivo studies of their degradation and interaction with bone. *Acta Biomater* 8:1230–1238
- Kroeze-Deutman H, den Dolder JV, Spauwen P, Jansen J (2005) Influence of RGD-loaded titanium implants on bone formation in vivo. *Tissue Eng* 11:1867–1875
- Lavan DA, McGuire T, Langer R (2003) Small-scale systems for in vivo drug delivery. *Nat Biotechnol* 21:1184–1191

- Lee C, Grodzinsky A, Spector M (2001) The effects of cross-linking of collagen-glycosaminoglycan scaffolds on compressive stiffness, chondrocyte-mediated contraction, proliferation and biosynthesis. *Biomaterials* 22:3145–3154
- Lee JW, Wen HB, Battula S, Akella R, Collins M, Romanos GE (2015) Outcome after placement of tantalum porous engineered dental implants in fresh extraction sockets: a canine study. *Int J Oral Maxillofac Implants* 30:134–142
- Leukers B, Gülkan H, Irsen SH, Milz S, Tille C, Schieker M, Seitz H (2005) Hydroxyapatite scaffolds for bone tissue engineering made by 3D printing. *J Mater Sci Mater Med* 16:1121–1124
- Li Z, Kawashita M (2011) Current progress in inorganic artificial biomaterials. *J Artif Organs* 14:163
- Li L, Gao J, Wang Y (2004) Evaluation of cyto-toxicity and corrosion behavior of alkali-heat-treated magnesium in simulated body fluid. *Surf Coat Technol* 185:92–98
- Li Z, Gu X, Lou S, Zheng Y (2008) The development of binary mg–ca alloys for use as biodegradable materials within bone. *Biomaterials* 29:1329–1344
- Lin K-F, He S, Song Y, Wang C-M, Gao Y, Li J-Q, Tang P, Wang Z, Bi L, Pei G-X (2016) Low-temperature additive manufacturing of biomimic three-dimensional hydroxyapatite/collagen scaffolds for bone regeneration. *ACS Appl Mater Interfaces* 8:6905–6916
- Liu X, Ma PX (2004) Polymeric scaffolds for bone tissue engineering. *Ann Biomed Eng* 32:477–486
- Liu H, Lin J, Roy K (2006) Effect of 3D scaffold and dynamic culture condition on the global gene expression profile of mouse embryonic stem cells. *Biomaterials* 27:5978–5989
- Liu M, Chou SM, Chua C, Tay B, Ng B (2013) The development of silk fibroin scaffolds using an indirect rapid prototyping approach: morphological analysis and cell growth monitoring by spectral-domain optical coherence tomography. *Med Eng Phys* 35:253–262
- Liu Y, Yang Z, Tan L, Li H, Zhang Y (2014) An animal experimental study of porous magnesium scaffold degradation and osteogenesis. *Braz J Med Biol Res* 47:715–720
- Malda J, Klein TJ, Upton Z (2007) The roles of hypoxia in the in vitro engineering of tissues. *Tissue Eng* 13:2153–2162
- Mandal BB, Kundu SC (2009) Cell proliferation and migration in silk fibroin 3D scaffolds. *Biomaterials* 30:2956–2965
- Mandrycky C, Wang Z, Kim K, Kim D-H (2016) 3D bioprinting for engineering complex tissues. *Biotechnol Adv* 34:422–434
- Mano J, Silva G, Azevedo HS, Malafaya P, Sousa R, Silva SS, Boesel L, Oliveira JM, Santos T, Marques A (2007) Natural origin biodegradable systems in tissue engineering and regenerative medicine: present status and some moving trends. *J R Soc Interface* 4:999–1030
- Martin I, Wendt D, Heberer M (2004) The role of bioreactors in tissue engineering. *Trends Biotechnol* 22:80–86
- Matsushita T, Fujibayashi S, Kokubo T (2017) Titanium foam for bone tissue engineering. In: *Metallic foam bone*. Elsevier, Amsterdam
- Melchels FP, Feijen J, Grijpma DW (2010) A review on stereolithography and its applications in biomedical engineering. *Biomaterials* 31:6121–6130
- Mendoza García MA, Izadifar M, Chen X (2017) Evaluation of PBS treatment and PEI coating effects on surface morphology and cellular response of 3D-printed algininate scaffolds. *J Funct Biomater* 8:48
- Meneghini RM, Lewallen DG, Hanssen AD (2008) Use of porous tantalum metaphyseal cones for severe tibial bone loss during revision total knee replacement. *JBJS* 90:78–84
- Michiardi A, Aparicio C, Planell J, Gil F (2006) New oxidation treatment of NiTi shape memory alloys to obtain Ni-free surfaces and to improve biocompatibility. *J Biomed Mater Res B Appl Biomater* 77:249–256
- Morris VB, Nimbalkar S, Younesi M, McClellan P, Akkus O (2017) Mechanical properties, cytocompatibility and manufacturability of chitosan: PEGDA hybrid-gel scaffolds by stereolithography. *Ann Biomed Eng* 45:286–296

- Mozden LC, Rodgers R, Banks JM, Bailey RC, Harley BA (2016) Increasing the strength and bioactivity of collagen scaffolds using customizable arrays of 3D-printed polymer fibers. *Acta Biomater* 33:25–33
- Murphy CM, Haugh MG, O'Brien FJ (2010) The effect of mean pore size on cell attachment, proliferation and migration in collagen–glycosaminoglycan scaffolds for bone tissue engineering. *Biomaterials* 31:461–466
- Nagura I, Fujioka H, Kokubu T, Makino T, Sumi Y, Kurosaka M (2007) Repair of osteochondral defects with a new porous synthetic polymer scaffold. *J Bone Joint Surg* 89:258–264
- Nair LS, Laurencin CT (2007) Biodegradable polymers as biomaterials. *Prog Polym Sci* 32:762–798
- Naseri N, Poirier J-M, Girandon L, Fröhlich M, Oksman K, Mathew AP (2016) 3-dimensional porous nanocomposite scaffolds based on cellulose nanofibers for cartilage tissue engineering: tailoring of porosity and mechanical performance. *RSC Adv* 6:5999–6007
- Niinomi M (2008) Metallic biomaterials. *J Artif Organs* 11:105
- Niu C-C, Chen L-H, Lai P-L, Fu T-S, Chen W-J (2005) Trapezoidal titanium cage in anterior cervical interbody fusion: a clinical experience. *Chang Gung Med J* 28:212–221
- Nocera AD, Comín R, Salvatierra NA, Cid MP (2018) Development of 3D printed fibrillar collagen scaffold for tissue engineering. *Biomed Microdevices* 20:26
- Okazaki Y (2001) A new Ti–15Zr–4Nb–4Ta alloy for medical applications. *Curr Opin Solid State Mater Sci* 5:45–53
- Oliviero O, Ventre M, Netti P (2012) Functional porous hydrogels to study angiogenesis under the effect of controlled release of vascular endothelial growth factor. *Acta Biomater* 8:3294–3301
- Park E-K, Lim J-Y, Yun I-S, Kim J-S, Woo S-H, Kim D-S, Shim K-W (2016) Cranioplasty enhanced by three-dimensional printing: custom-made three-dimensional-printed titanium implants for skull defects. *J Craniofac Surg* 27:943–949
- Pattison MA, Wurster S, Webster TJ, Haberstroh KM (2005) Three-dimensional, nano-structured PLGA scaffolds for bladder tissue replacement applications. *Biomaterials* 26:2491–2500
- Perren S, Regazzoni P, Fernandez A (2017) How to choose between the implant materials steel and titanium in orthopedic trauma surgery: part 1–mechanical aspects. *Acta Chir Orthop Traumatol Cech* 84:9–12
- Pierson D, Edick J, Tauscher A, Pokorney E, Bowen P, Gelbaugh J, Stinson J, Getty H, Lee CH, Drelich J (2012) A simplified in vivo approach for evaluating the bioabsorbable behavior of candidate stent materials. *J Biomed Mater Res B Appl Biomater* 100:58–67
- Prasadh S, Manakari V, Parande G, Wong RCW, Gupta M (2020) Hollow silica reinforced magnesium nanocomposites with enhanced mechanical and biological properties with computational modeling analysis for mandibular reconstruction. *Int J Oral Sci* 12(1):1–11
- Prymak O, Bogdanski D, Köller M, Esenwein SA, Muhr G, Beckmann F, Donath T, Assad M, Epple M (2005) Morphological characterization and in vitro biocompatibility of a porous nickel–titanium alloy. *Biomaterials* 26(29):5801–5807
- Qi X, Pei P, Zhu M, Du X, Xin C, Zhao S, Li X, Zhu Y (2017) Three dimensional printing of calcium sulfate and mesoporous bioactive glass scaffolds for improving bone regeneration in vitro and in vivo. *Sci Rep* 7:42556
- Rahim MI, Ullah S, Mueller PP (2018) Advances and challenges of biodegradable implant materials with a focus on magnesium-alloys and bacterial infections. *Metals* 8:532
- Rajaram A, Schreyer DJ, Chen DX (2015) Use of the polycation polyethyleneimine to improve the physical properties of alginate–hyaluronic acid hydrogel during fabrication of tissue repair scaffolds. *J Biomater Sci Polym Ed* 26:433–445
- Ravi S, Chaikof EL (2010) Biomaterials for vascular tissue engineering. *Regen Med* 5:107–120
- Rezwani K, Chen Q, Blaker JJ, Boccaccini AR (2006) Biodegradable and bioactive porous polymer/inorganic composite scaffolds for bone tissue engineering. *Biomaterials* 27:3413–3431

- Sakat MS, Kilic K, Altas E, Gozeler MS, Ucuncu H (2016) Comminuted frontal sinus fracture reconstructed with titanium mesh. *J Craniofac Surg* 27:e207–e208
- Salerno A, Oliviero M, Di Maio E, Iannace S, Netti P (2009) Design of porous polymeric scaffolds by gas foaming of heterogeneous blends. *J Mater Sci Mater Med* 20:2043–2051
- Salerno A, Guarnieri D, Iannone M, Zeppetelli S, Netti PA (2010) Effect of micro- and macroporosity of bone tissue three-dimensional-poly (ϵ -caprolactone) scaffold on human mesenchymal stem cells invasion, proliferation, and differentiation in vitro. *Tissue Eng A* 16:2661–2673
- Sands RW, Mooney DJ (2007) Polymers to direct cell fate by controlling the microenvironment. *Curr Opin Biotechnol* 18:448–453
- Saranya N, Saravanan S, Moorthi A, Ramyakrishna B, Selvamurugan N (2011) Enhanced osteoblast adhesion on polymeric nano-scaffolds for bone tissue engineering. *J Biomed Nanotechnol* 7:238–244
- Saris N-EL, Mervaala E, Karppanen H, Khawaja JA, Lewenstam A (2000) Magnesium: an update on physiological, clinical and analytical aspects. *Clin Chim Acta* 294:1–26
- Schwartz Z, Lohmann C, Oefinger J, Bonewald L, Dean D, Boyan B (1999) Implant surface characteristics modulate differentiation behavior of cells in the osteoblastic lineage. *Adv Dent Res* 13:38–48
- Seitz H, Rieder W, Irsen S, Leukers B, Tille C (2005) Three-dimensional printing of porous ceramic scaffolds for bone tissue engineering. *J Biomed Mater Res B Appl Biomater* 74:782–788
- Siu TL, Rogers JM, Lin K, Thompson R, Owbridge M (2018) Custom-made titanium 3-dimensional printed interbody cages for treatment of osteoporotic fracture-related spinal deformity. *World Neurosurg* 111:1–5
- Souer JS, Ring D, Matschke S, Audige L, Maren-Hubert M, Jupiter J (2010) Comparison of functional outcome after volar plate fixation with 2.4-mm titanium versus 3.5-mm stainless-steel plate for extra-articular fracture of distal radius. *J Hand Surg Am* 35:398–405
- Spoerke ED, Murray NG, Li H, Brinson LC, Dunand DC, Stupp SI (2008) Titanium with aligned, elongated pores for orthopedic tissue engineering applications. *J Biomed Mater Res A* 84:402–412
- Staiger MP, Pietak AM, Huadmai J, Dias G (2006) Magnesium and its alloys as orthopedic biomaterials: a review. *Biomaterials* 27:1728–1734
- Sumita M, Hanawa T, Teoh S (2004) Development of nitrogen-containing nickel-free austenitic stainless steels for metallic biomaterials. *Mater Sci Eng C* 24:753–760
- Sung H-J, Meredith C, Johnson C, Galis ZS (2004) The effect of scaffold degradation rate on three-dimensional cell growth and angiogenesis. *Biomaterials* 25:5735–5742
- Suzuki A, Kanetaka H, Shimizu Y, Tomizuka R, Hosoda H, Miyazaki S, Okuno O, Igarashi K, Mitani H (2006) Orthodontic buccal tooth movement by nickel-free titanium-based shape memory and superelastic alloy wire. *Angle Orthod* 76:1041–1046
- Tang J, Song Y, Zhao F, Spinney S, Da Silva Bernardes J, Tam KC (2019) Compressible cellulose nanofibril (CNF) based aerogels produced via a bio-inspired strategy for heavy metal ion and dye removal. *Carbohydr Polym* 208:404–412
- Tanzer M, Kantor S, Bobyn J (2001) Enhancement of bone growth into porous intramedullary implants using non-invasive low intensity ultrasound. *J Orthop Res* 19:195–199
- Tarniță D, Tarniță D, Bizdoacă N, Mîndrilă I, Vasilescu M (2009) Properties and medical applications of shape memory alloys. *Rom J Morphol Embryol* 50:15–21
- Teixeira BN, Aprile P, Mendonça RH, Kelly DJ, Thiré RMDSM (2019) Evaluation of bone marrow stem cell response to PLA scaffolds manufactured by 3D printing and coated with polydopamine and type I collagen. *J Biomed Mater Res B Appl Biomater* 107:37–49
- Thalgott JS, Giuffrè JM, Klezl Z, Timlin M (2002) Anterior lumbar interbody fusion with titanium mesh cages, coralline hydroxyapatite, and demineralized bone matrix as part of a circumferential fusion. *Spine J* 2:63–69

- Tripathi A, Tardy BL, Khan SA, Liebner F, Rojas OJ (2019) Expanding the upper limits of robustness of cellulose nanocrystal aerogels: outstanding mechanical performance and associated pore compression response of chiral-nematic architectures. *J Mater Chem A* 7: 15309–15319
- Van Den Dolder J, Farber E, Spauwen PH, Jansen JA (2003) Bone tissue reconstruction using titanium fiber mesh combined with rat bone marrow stromal cells. *Biomaterials* 24:1745–1750
- Vehof JW, Spauwen PH, Jansen JA (2000) Bone formation in calcium-phosphate-coated titanium mesh. *Biomaterials* 21:2003–2009
- Vehof JW, Haus MT, de Ruijter AE, Jansen JA, Spauwen PH (2002) Bone formation in transforming growth factor beta-1-loaded titanium fiber mesh implants. *Clin Oral Implants Res* 13:94–102
- Vojtěch D, Kubásek J, Šerák J, Novák P (2011) Mechanical and corrosion properties of newly developed biodegradable Zn-based alloys for bone fixation. *Acta Biomater* 7:3515–3522
- Wang M, Favi P, Cheng X, Golshan NH, Ziemer KS, Keidar M, Webster TJ (2016) Cold atmospheric plasma (CAP) surface nanomodified 3D printed polylactic acid (PLA) scaffolds for bone regeneration. *Acta Biomater* 46:256–265
- Westhauser F, Prokscha M, Weis C, Li W, Kneser U, Kauczor H-U, Schmidmaier G, Boccaccini A, Moghaddam A (2016a) P21 three-dimensional polymer coated 45S5-type bioactive glass scaffolds seeded with human mesenchymal stem cells show bone formation in-vivo. *Injury* 47:S32
- Westhauser F, Weis C, Prokscha M, Bittrich LA, Li W, Xiao K, Kneser U, Kauczor H-U, Schmidmaier G, Boccaccini AR (2016b) Three-dimensional polymer coated 45S5-type bioactive glass scaffolds seeded with human mesenchymal stem cells show bone formation in vivo. *J Mater Sci Mater Med* 27:119
- Williams JM, Adewunmi A, Schek RM, Flanagan CL, Krebsbach PH, Feinberg SE, Hollister SJ, Das S (2005) Bone tissue engineering using polycaprolactone scaffolds fabricated via selective laser sintering. *Biomaterials* 26:4817–4827
- Witte F, Kaese V, Haferkamp H, Switzer E, Meyer-Lindenberg A, Wirth C, Windhagen H (2005) In vivo corrosion of four magnesium alloys and the associated bone response. *Biomaterials* 26: 3557–3563
- Witte F, Fischer J, Nellesen J, Crostack H-A, Kaese V, Pisch A, Beckmann F, Windhagen H (2006) In vitro and in vivo corrosion measurements of magnesium alloys. *Biomaterials* 27:1013–1018
- Yang H, Wang C, Liu C, Chen H, Wu Y, Han J, Jia Z, Lin W, Zhang D, Li W (2017a) Evolution of the degradation mechanism of pure zinc stent in the one-year study of rabbit abdominal aorta model. *Biomaterials* 145:92–105
- Yang X-Y, Chen L-H, Li Y, Rooke JC, Sanchez C, Su B-L (2017b) Hierarchically porous materials: synthesis strategies and structure design. *Chem Soc Rev* 46:481–558
- Zdeblick TA, Phillips FM (2003) Interbody cage devices. *Spine* 28:S2–S7
- Zhang E, Xu L, Yang K (2005) Formation by ion plating of Ti-coating on pure mg for biomedical applications. *Scr Mater* 53:523–527
- Zhang W, Walboomers XF, Van Kuppevelt TH, Daamen WF, Bian Z, Jansen JA (2006) The performance of human dental pulp stem cells on different three-dimensional scaffold materials. *Biomaterials* 27:5658–5668
- Zhang E, Xu L, Yu G, Pan F, Yang K (2009) In vivo evaluation of biodegradable magnesium alloy bone implant in the first 6 months implantation. *J Biomed Mater Res A* 90:882–893
- Zhang W, Zhang Y, Lu C, Deng Y (2012) Aerogels from crosslinked cellulose nano/micro-fibrils and their fast shape recovery property in water. *J Mater Chem* 22:11642–11650
- Zhang X, Li X-W, Li J-G, Sun X-D (2014) Preparation and mechanical property of a novel 3D porous magnesium scaffold for bone tissue engineering. *Mater Sci Eng C* 42:362–367
- Zhao D, Wang T, Nahan K, Guo X, Zhang Z, Dong Z, Chen S, Chou D-T, Hong D, Kumta PN (2017a) In vivo characterization of magnesium alloy biodegradation using electrochemical H₂ monitoring, ICP-MS, and XPS. *Acta Biomater* 50:556–565

- Zhao D, Witte F, Lu F, Wang J, Li J, Qin L (2017b) Current status on clinical applications of magnesium-based orthopaedic implants: a review from clinical translational perspective. *Biomaterials* 112:287–302
- Zheng W, Wang Z, Song L, Zhao Q, Zhang J, Li D, Wang S, Han J, Zheng X-L, Yang Z (2012) Endothelialization and patency of RGD-functionalized vascular grafts in a rabbit carotid artery model. *Biomaterials* 33:2880–2891
- Zhu J, Marchant RE (2011) Design properties of hydrogel tissue-engineering scaffolds. *Expert Rev Med Devices* 8:607–626
- Zou X, Li H, Büniger M, Egund N, Lind M, Büniger C (2004) Bone ingrowth characteristics of porous tantalum and carbon fiber interbody devices: an experimental study in pigs. *Spine J* 4: 99–105
- 池田里砂 (2011) The effect of porosity and mechanical property of a synthetic polymer scaffold on repair of osteochondral defects. 神戸大学



Surface Modification of Metallic Biomaterials for Cardiovascular Cells Regulation and Biocompatibility Improvement

Jingan Li and Yachen Hou

Abstract

Interaction of cells and the metallic biomaterials usually happened at the materials' surface and interface, which often decides the biocompatibility and further application of the medical devices. Clinically, severe cardiovascular diseases are often treated by the method of long-term interventional therapy using stents, and wherein the stents made of metallic biomaterials possess a large proportion. Although the existing metallic biomaterials have played excellent roles for stents intervention, which are the benefits from their adaptive mechanical property and some degree of biocompatibility, the complex cellular microenvironment in the focus caused by the development of the disease after intervention has put forward higher requirements for the biocompatibility of the material surface and interface from the simple noncytotoxic to the multi-function of anticoagulation, inhibition of smooth muscle cell proliferation, promotion of endothelial cell growth, and further to the sequential release of these functions, etc. Our latest research also indicated that the endothelial layer on the materials' surface should be built space orderly by endothelial cells, smooth muscle cells, and macrophages. Surface modification is generally accepted as an effective method to endow the metallic biomaterials better biocompatibility wherein, the multifunctional coatings with micro and/or nanoscales play crucial roles in coordinating the interaction between cells and materials and cells and cells, for their size advantage. In this chapter, we introduced the advanced technologies and ideas of surface modification which were systematically studied and widely applied on the cardiovascular metallic biomaterials in recent years.

J. Li (✉) · Y. Hou

Henan Key Laboratory of Advanced Magnesium Alloy, School of Materials Science and Engineering, Zhengzhou University, Zhengzhou, People's Republic of China
e-mail: lijingan@zzu.edu.cn

© The Author(s), under exclusive license to Springer Nature Singapore Pte Ltd. 2022

L. M. Pandey, A. Hasan (eds.), *Nanoscale Engineering of Biomaterials: Properties and Applications*, https://doi.org/10.1007/978-981-16-3667-7_8

207

Keywords

Metallic biomaterials · Surface modification · Biocompatibility · Cardiovascular cells · Spatiotemporal orderliness of function

8.1 Introduction

Cardiovascular disease (CVD) is a class of major healthcare risks that usually result from malfunction in coronary arteries and continues to be the leading reason of morbidity and mortality globally for decades (Hyman 2014). Percutaneous coronary intervention (PCI) using stent has emerged as the typical clinical method of CVD for its advantages of low surgical risk and short recovery time (Fuster 2014). Metallic biomaterials, such as 316L stainless steel (316L SS) and cobalt–chromium (Co–Cr) alloy, are often used as the materials of cardiovascular stents for their excellent mechanical properties and biocompatibility to some extent (Patel et al. 2012). As the statement, their biocompatibility is limited, and so part bare metallic stents may lead to restenosis in a short time after intervention due to poor interaction of the blood, pathological smooth muscle cells (SMC), and the metals (Zago et al. 2012). To solve this problem, the drug-eluting stent (DES) was developed and applied widely; temporarily, the thrombosis and hyperplasia were suppressed. However, stent restenosis caused by late thrombosis and hyperplasia has become a new problem in DES, and it was attributed to the delay of endothelialization caused by drugs' (rapamycin and paclitaxel, etc.) nondifferential killing on SMC and vascular endothelial cells (EC) (Otsuka et al. 2012; Torii et al. 2019). In other words, when the DES-loaded drug is released clearly, the stent surface is not completely covered by the endothelial layer. There is no doubt that surface endothelialization has been identified as the main strategy to solve late stent restenosis.

Surface endothelialization is the process of inducing EC to gather on the stent surface and form a monolayer (Li et al. 2015a, b, c, d; Quan et al. 2020; Kianpour et al. 2020). Initially, a method called “in vitro endothelialization” was used, in which EC were seeded on the implants' surfaces in vitro and set to the focus in vivo (Van der Giessen et al. 1988; Dichek et al. 1989; Flugelman et al. 1992). This method of “in vitro endothelialization” was effective in the first few to dozens of hours, but soon the seeded EC fell off, and exposed proteins secreted by the peeled EC left on the surface, leading to serious thrombosis. Scientists began to realize that the EC cultured in vitro are different from the EC in situ on the blood vessel wall in vivo (Malek and Izumo 1996; Vartanian et al. 2008; Anderson and Hinds 2012). How to induce EC in vivo to participate in the endothelialization of stent surface became a new topic then. Of course, the simplest way is to improve EC aggregation and proliferation by surface modification. However, a large number of studies soon found that the surface modified with proteins that promote EC adhesion also promotes platelet adhesion, which may cause thrombosis; EC grew so slowly that SMC and inflammatory cells would also gather on the surface in front of them (Underwood et al. 1998; Nelson et al. 2000; Yu et al. 2020). And then, tailoring

multifunctional surfaces to mediate anticoagulation, anti-hyperplasia, anti-inflammation, and pro-endothelialization attracted more attention.

Nevertheless, simultaneously endowing the stents surface all these functions with strong effects is difficult. Prof. Nan Huang from Southwest Jiaotong University in China proposed a concept of the “functional sequential coatings on the stents surface” (Qi et al. 2013) and developed a series of such coatings (Qiu et al. 2019; Yang et al. 2015, 2018a, b, 2020a, b; Li et al. 2020a, b; Gao et al. 2020; Tu et al. 2020; Zhang et al. 2019; Xiao et al. 2020). The concept revealed the different interaction of the *in vivo* microenvironment and the stents surface in each time quantum after stent intervention. Blood is the first contact after stent intervention, so anticoagulation is the first function to be released on the stent surface; then the stents will confront macrophage aggregation and pathological SMC migration in the focus, so anti-inflammation and anti-hyperplasia are the necessary functions at the second stage. For maintaining the long-term physiological function, endothelial layer plays crucial roles on the stents surface, and therefore surface endothelialization should be completed at the right time. This theory has been widely recognized, and it still guides the design and development of stents’ surface modification even to this day.

Obviously, since the concept of endothelialization was put forward, EC and their precursors (endothelial progenitor cells, EPC) have been identified as the positive protagonists of stents’ surface modification, which was encouraged to improve, while SMC and macrophages were regarded as the objects of inhibition (Li et al. 2011a, b, c; Chen et al. 2012). However, this standardized endothelialization, that is, the EC directly covering the stents surface without SMC, has never been achieved as an ideal goal. On the basis of the concept of the “functional sequential coatings,” our group further discovered an objective phenomenon, which we think is very important: the EC do not directly contact the stents’ surface including the coatings *in vivo* at any condition; various cells arranged orderly on the stents’ surface, and we named this phenomenon as the “spatio-temporal orderliness of function” (The phenomenon was discovered in 2017, and it was later named in the book by Li et al. (2020c)). There is no doubt that the “spatio-temporal orderliness of function” is a natural phenomenon of interaction between surface and cells. However, by revealing the key node of this phenomenon and combining with surface modification technology such as adjusting nanoscale it can be developed in the direction beneficial to surface endothelialization. For this chapter, the story may begin from DES about something has never been thought deeply.

8.2 What Really Happened for DES in the Cardiovascular Microenvironment?

As known to all, DES is the most widely used cardiovascular interventional therapy medical device in clinic for its strong effects in inhibiting acute and subacute thrombus, and hyperplasia caused by excessive proliferation of SMC in the early stage. As the mainstream stent, it has many advantages, and thus it is expected to have a longer service life, but the restenosis limits its further application and

introduces more complication. It is reported that the incidence of late thrombosis in patients receiving DES treatment is very low, but once it happens, the patient's life is very dangerous, and there is little time for rescue (Omar et al. 2014; Lemesle et al. 2010). At present, most experts believe that the drugs (Rapamycin and paclitaxel, etc.) loaded in DES killed both SMC and EC, which greatly delay the process of endothelialization (Butzal et al. 2004; Gholizadeh et al. 2018; Kim et al. 2008). When the drugs are released clearly, the pathological SMC can proliferate rapidly again under the effect of cascade effect, which leads to hyperplasia. Most people attribute the delay in endothelialization to the fact that the drug killed the EC by mistake (Wang et al. 2017; Miura et al. 2015). However, are only EC mistakenly killed by drugs?

In order to further understand the truth, taking a look at the normal vascular structure is necessary. In human vascular wall, the EC and the contractile SMC are the main components, and the ordered distribution of EC and contractile SMC guarantee the normal physiological functions of the vascular environment (Li et al. 2013a, b, c). EC in a native vessel environment exhibit an elongated, cobblestone, and aligned morphology and growth followed the blood flow direction (Jana 2019). Each EC is attached to several surrounding EC to continuously create an endothelial monolayer as a barrier between the blood flow and the SMC beneath (Morgan et al. 2012). Healthy EC also suppress the adhesion and activation of platelets and macrophages as well as the excessive proliferation of SMC by releasing functional factors, such as nitric oxide (NO), prostacyclin (PGI₂), tissue pathway factor inhibitor (TPFI), and thrombomodulin (TM), etc. (Li et al. 2017a, b, c). Between the EC and SMC, there is a functional layer so-called "basement membrane," which is composed of extracellular matrix (ECM) secreted by the EC and contractile SMC (Li et al. 2017a, b, c). Exosome, a natural nanoparticle (40–200 nm) containing RNA and other factors from the EC, SMC or blood distributes in the basement membrane and transmits signals between cells (Hou et al. 2020). As reported, SMC has two different phenotypes: contractile phenotype and synthetic phenotype (Yoshiyama et al. 2014). Wherein, contractile SMC is the physiological phenotype, which is generally believed that it contributes to vasoconstriction and provides mechanical support for EC (Yoshiyama et al. 2014); synthetic SMC is the pathological phenotype which participates in hyperplasia and interferes with the repair and regeneration of vascular intima (Yoshiyama et al. 2014). From long time ago, many EC/SMC co-culture models have been established in vitro to study the interaction between the two cells (Orlidge and D'Amore 1987; Davies and Kerr 1982; Lavender et al. 2005), but it has been limited by how to regulate the phenotype contraction of SMC. Subsequently, the microstripe pattern was found to regulate SMC from synthetic to contractile phenotype (Li et al. 2013a, b, c). Then, series of EC/SMC co-culture models based on hyaluronic acid (HA) micropatterns were established from our laboratory (Li et al. 2014a, b, 2015a, b, c, d; Li 2018). From these co-culture models, it was discovered that the contractile SMC contributed to the morphology change (to the in vivo phenotype), proliferation, monolayer formation, and functional factors release [NO, PGI₂, TM, TPFI, fibronectin (Fn), etc.].

Review previous description, is only EC that are mistakenly killed by the DES? The answer is clear and absolutely no. Drugs such as rapamycin and paclitaxel have fundamentally damaged the microenvironment which EC depends on for living. The microenvironment includes ECM secreted by the physiological cells and the physiological cells themselves.

8.3 Strategies of Surface Modification with ECM

8.3.1 Surface Modification Aiming at EC

In fact, the researchers first realized the importance of ECM surface modification, because it is simple and direct to select an ECM component for biomaterial surface modification (Li et al. 2008). The modification methods are easy to obtain, such as physical adsorption, electrostatic assembly, chemical grafting, etc. The major proteins in ECM, such as fibronectin (Fn), laminin (Ln), and type I collagen, are used for the surface modification of cardiovascular materials (Fujiwara et al. 2004; Meerovitch et al. 2003). However, it was soon found that these proteins not only promote EC adhesion, but also promote thrombosis and SMC adhesion, and the formation speed of thrombosis and hyperplasia is faster than that of endothelial cell adhesion. Therefore, more methods have been developed to modify the surface with two or more molecules to obtain multiple functions, including anti-coagulation, anti-hyperplasia, anti-inflammation, and improving EC adhesion. Heparin was the most common anticoagulant grafted to the surface with other adhesion promoting molecules at that time. For example, the heparin has been prepared to the titanium (Ti) or 316L SS surface with Fn, Ln or collagens by the methods of layer-by-layer self-assembly, self-assembly after blending, or graft polymerization after group activation (Li et al. 2011a, b, c; Wang et al. 2014; Meslmani et al. 2014). The experimental conditions, such as molecule concentration, pH value, reaction temperature, reaction time, reactive activators, solution ratios, and the numbers of assembly layers, were also adjusted as needed. Despite the use of such advanced and effective methods and the optimization of many parameters, the coordination of surface multi-functions of cardiovascular materials still can't meet the needs of stent, because there are still technical challenges to make it have multiple functions simultaneously. Generally, the function of promoting EC adhesion is limited or not strong enough on the better surface of anticoagulant, anti-hyperplasia, and anti-inflammatory and vice versa.

As mentioned previously, Prof. Nan Huang from Southwest Jiaotong University in China proposed the concept of the “functional sequential coatings on the stents surface” to explain the requirement of biological function after stent intervention (Fig. 8.1). To be specific, in the first stage of stent intervention, anticoagulation is the most important aim, because the stent first contacts the blood, and thus it needs enough anticoagulants such as heparin; after reaching the focus, inhibiting the surrounding inflammatory environment and pathological SMC excessive proliferation becomes another important task, and this task is heparin and some other ECM

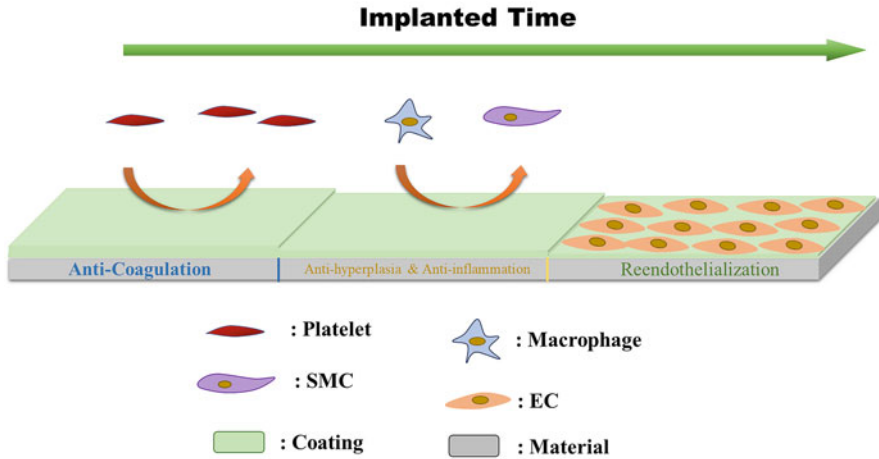


Fig. 8.1 The diagram of the concept “functional sequential coatings on the stents surface”

components can bear, and the copper ions found in later studies (Li et al. 2015a, b, c, d) or the catalytic release of NO by conjugated precursor molecules (Xu et al. 2015) are also very effective. Finally, endothelialization is needed before all the drugs are released clearly or the above functions are weakened. At this time, proteins or EC-specific molecules (such as RGD peptide, REDV peptide or VEGF) fixed to the surface by layered assembly or chemical grafting technology will play a role (Devalliere et al. 2018; Zheng et al. 2012; Noel et al. 2016), while heparin and other drugs released in the first two stages will not interfere with the EC adhesion.

Another risk of heparin use is hemolysis, so a large number of ECM components and their characteristics have been fully explored to replace heparin. Hyaluronic acid (HA), the skeleton component of ECM, has been found to inhibit platelet adhesion and aggregation (Chuang and Masters 2009). Through further study, HA has been proved to have molecular weight (MW)-dependent biological function, that is, high molecular weight (HMW) HA can inhibit the adhesion of EC and the aggregation of inflammatory macrophages, while low molecular weight (LMW) HA can promote the adhesion of EC and inflammatory macrophages (Rayahin et al. 2015). Type IV collagen, the specific component of cardiovascular ECM, is reused for its function of promoting EC adhesion and alleviating pathological SMC microenvironment (Li et al. 2014a, b). Its specific combination with HA makes them popular in the process of coating (Li et al. 2014a, b, 2016a, b). However, no matter how the ECM components are used to modify the surface of cardiovascular materials, the ECM in the natural vascular wall is still considered to be the most ideal surface modification layer. The reason is that the *in vitro* process can't meet the standards of natural ECM in many aspects, such as composition, quantitative ratio, binding mode, and functional release. Therefore, the application of full component ECM in surface modification of cardiovascular biomaterials has entered the field of vision of researchers.

It has been suggested that the acellular vessels should be used for the surface modification of biomaterials. However, at that time, this method had some insuperable defects: firstly, it took too long (more than a week) to treat the tissue with acellular method, which increased the difficulty of subsequent surface modification and reduced its significance in clinical application; secondly, the acellular vascular tissue was not the soluble substance we expected, but a tissue worker with certain hardness and toughness, and this phenomenon further limits its application in the field of surface modification. Problems that can't be solved at the tissue level may be solved at the cellular level. Tu et al. reported that ECM can be enriched by seeding and culturing EC on the metal biomaterials Ti surface. After treated with special acellular reagent and cleaned the cells, EC-ECM-modified Ti surface can be obtained within 20 min. Most of the proteins in the natural EC-ECM, such as Fn, Ln, and collagens, can be detected on the surface modified by EC-ECM. Moreover, the EC-ECM-modified layer can promote the adhesion of EC on Ti surface and inhibit the adhesion of platelets (Tu et al. 2010). After successful preparation of EC-ECM on the Ti surface, the SMC-ECM which secreted from the contractile SMC was also prepared onto Ti surface by the same method. Compared with SMC-ECM and EC-ECM, SMC-ECM was more conducive to the adhesion and proliferation of EC while EC-ECM induced the adherent EC to release more NO (Tu et al. 2013). However, as mentioned above, EC cultured *in vitro* and *in vivo* are quite different, and some scholars have found that the ECM secreted by them is also different (Vartanian et al. 2009). The biggest difference between the two is that EC *in vivo* are affected by blood flow shear stress (BFSS), while EC *in vitro* receive no BFSS action. In our study of 2013, it was found that HA microstripes with a width of 25 μm can simulate the effect of 15 dyn/cm^2 BFSS on the materials surface to regulate the behavior and morphology of EC (Li et al. 2013a, b, c). Our further study in 2015 demonstrated that the ECM secreted by the HA-patterned EC (labeled as ECM/HAP) possessed better hemocompatibility, anti-hyperplasia, anti-inflammation, and pro-EPC-adhesion ability than the EC-ECM (Li et al. 2015a, b, c, d). Yet, compared with the natural basement membrane, the function of ECM/HAP is still deficient due to no ECM secreted by contractile SMC. Incidentally, HA microstripes can also regulate the SMC to contractile phenotype (Li et al. 2013a, b, c). In 2019, our research presented breakthrough on HA micropattern: The HA microstripes were found to bear acellular operations for three times without degradation (Zou et al. 2019), which means the SMC ECM and ECM/HAP can be prepared onto the HA micropatterned surface by successive SMC/EC culturing and decellularization to form a modified layer (labeled as $\text{ECM}_{\text{SMC}/\text{EC}}/\text{HAP}$) like the natural basement membrane (Fig. 8.2). Generous *in vitro* and *in vivo* evaluations verified that $\text{ECM}_{\text{SMC}/\text{EC}}/\text{HAP}$ had better multi-function than ECM/HAP (Han et al. 2019).

Although the ECM-modified layer obtained by the combination of cell culture and decellularization plays an important role in promoting the adhesion, proliferation and function of EC on the surface of cardiovascular biomaterials, the development of this technology still encounters bottlenecks. On the one hand, HA micropattern is suitable for preparation on a wide continuous surface, and it is difficult to be prepared on the stent surface. Meanwhile, the difficulty of cell

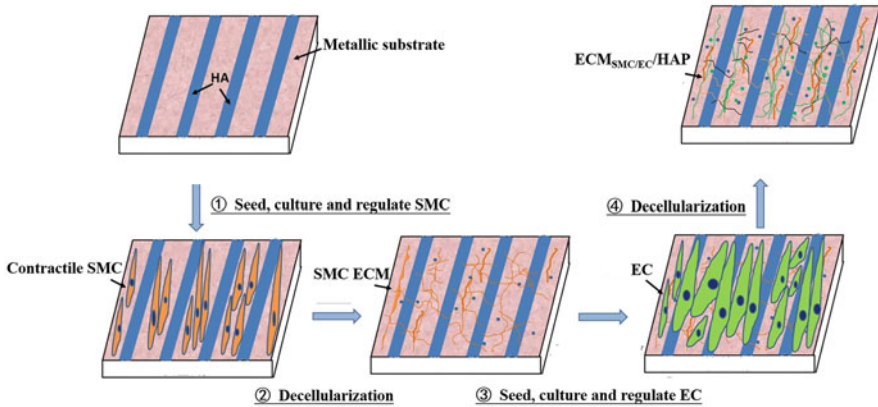


Fig. 8.2 The process diagram of the ECM secreted by the HA micropatterned SMC and EC on the metallic biomaterials

adhesion on curved surface is much greater than that on plane adhesion. Therefore, it greatly limits the application of HA micropattern to regulate cell and decellularization on surface modification of cardiovascular biomaterials. On the other hand, EC reaches the biomaterials surface by migration *in vivo*, and the migration speed of EC is much slower than that of EPC adhesion and proliferation. Therefore, it is generally believed that EPC capture plays a more important role in the process of endothelial repair and regeneration on the surface of cardiovascular materials as a cell source, while the migrated EC plays a more important role in promoting the maturation and differentiation of EPC.

8.3.2 Surface Modification Aiming at EPC

EPC is the precursor of vascular EC mainly derived from bone marrow, which was firstly isolated by Asahara in 1997 (Asahara et al. 2011). In addition to bone marrow, EPC is also found in cord blood, circulating blood, and arterial wall, wherein there is only about 0.01% EPC in human circulating blood (Zammaretti and Zisch 2005). Circulating EPC mainly come from nonhematopoietic tissues such as vascular wall and tend to enter the damaged endothelium to participate in the repairment and regeneration (Fu et al. 2016). EPC can be divided into early EPC (eEPC) and late EPC (lEPC), wherein eEPC have weak proliferative ability and are difficult to be passaged, while lEPC have high proliferative potential, which is similar to microvascular EC (Patel et al. 2016). Several specific antibodies, such as anti-CD34, anti-CD133, and anti-CD146 have been used to capture EPC in the field of surface modification of cardiovascular biomaterials due to their special functions in cell recognition (Su et al. 2017; Takahashi et al. 2014; Chen et al. 2015). Among these specific antibodies, anti-CD34 is the most studied in the field of surface modification of cardiovascular biomaterials benefit from its advantage in capturing massive EPC.

Even an anti-CD34-coated stent (Genous™ stent) has been developed and tested in vivo. Nevertheless, the Genous™ (OrbusNeich Medical Technologies Inc., FL, USA) stent was soon proved to have no significant advances compared to the bare metal stents in suppressing late thrombosis and hyperplasia (Klomp et al. 2014). The clinical failure of this stent was attributed to the poor specificity of anti-CD34 on EPC (Klomp et al. 2014). Thus, the scientists focused on anti-CD133, which is considered to be more specific for EPC, but sooner in vivo experiments showed that there were too few EPC that could be captured by anti-CD133, so that it can't meet the requirement of rapid endothelialization (Wawrzynska et al. 2019). Recent researches indicated that more antibodies, aptamers, and specific peptides had been developed and/or applied for capturing the circulating EPC (Tan et al. 2018; Blindt et al. 2006).

However, as we all know, EPC is only the cell source of endothelial repair, and we value its rapid homing ability and strong proliferation potential. EPC is not a mature EC, so its proliferation is multilayered, and it does not have the ability to form endothelial monolayer. Therefore, inducing EPC to differentiate into mature EC needs specific microenvironment, including normal blood flow, good ECM environment, and pericellular environment. Blood flow should be laminar flow, pericytes should be physiological EC and SMC, ECM should be secreted by physiological cells. Obviously, the microenvironment factors of these requirements are difficult to obtain at the lesion site, so there is a lot of work that needs to be done on the implant and its surface design.

8.4 A Novel Discovery and the Concept "Spatio-temporal Orderliness of Function"

In our published work in 2017, a new discovery overturned our recognition of the mainstream ideas in the field of surface modification of cardiovascular biomaterials (Li et al. 2017a, b, c). Through the specific staining of new regenerated tissue on the surface of vascular implants, we found that EC with specific expression of CD31 would not directly contact with the biomaterials surface (Li et al. 2017a, b, c). Between EC and biomaterials, the contractile SMC covers the surface of biomaterials, while the endothelial monolayer covers the surface of contractile SMC (Li et al. 2017a, b, c). M2 macrophages that specifically express CD206 were also detected in the new regenerated tissue which belong to the cardiovascular biomaterials with excellent endothelialization and lumen patency (Li et al. 2017a, b, c). It is certain that M2 macrophages are the first cells to reach the surface of biomaterials. However, more systematic research is needed to determine whether the role of M2 macrophages is to regulate contractile SMC or to accelerate endothelial monolayer regeneration or both. On the contrary, in the new tissues with incomplete endothelialization or without endothelial monolayer formation, contractile SMC (physiological SMC) and synthetic SMC (pathological SMC) were disorderly distributed, and M1 macrophages (inflammatory macrophages) accumulated in the whole tissue (Li et al. 2017a, b, c). Therefore, synthetic SMC and M1

macrophages are the main culprits of delaying the surface endothelialization of cardiovascular biomaterials.

This new finding provides a new theoretical support to explain the delayed endothelialization of DES. Prior to this, most studies believed that drugs such as paclitaxel and rapamycin loaded with DES also killed EC as endothelialized cell source when killing SMC. However, the fact may be that the whole lesion has been lacking contractile SMC for formation of endothelial monolayer. The novel finding also offers a feasible explanation to the hyperplasia of anti-CD34-coated stents Genous™. The lack of inhibiting synthetic SMC and supporting contractile SMC is an important reason for its rapid endothelialization but insufficient anti-hyperplasia function. Not only the migrated EC can induce the EPC to differentiate, but the contractile SMC may also be an important pericyte microenvironment for EPC to differentiate into EC.

In addition, it was reported that the synthetic SMC could be converted to contractile SMC by changing the microenvironment (Li et al. 2013a, b, c); the M1 macrophages could also be converted to M2 macrophages (Rayahin et al. 2015). This means that we can design the coating of cardiovascular biomaterials not in order to kill or inhibit these pathological cells, but to regulate the transformation of pathological cells into physiological cells so as to facilitate endothelialization. Based on the above understanding, we propose and improve the concept of “spatio-temporal orderliness of function.” This concept reveals that the surface of cardiovascular biomaterials may not regulate EC to participate in endothelialization through direct contact, but provide the necessary benign pericyte microenvironment for EC and EPC by mobilizing and regulating M2 macrophages and contractile SMC, thus promoting endothelialization (Fig. 8.3). In other words, EC and EPC are not the direct targets of biomaterials surface regulation, while contractile SMC and M2 macrophages are the primary and key targets in the conceptual design.

8.5 Surface Modification of Cardiovascular Metallic Biomaterials with Nanoscale Structures

Before the discovery and proposal of the concept “spatio-temporal orderliness of function,” our team prepared a series of nanoscale structures on the surface of cardiovascular biomaterials to regulate the interaction between the microenvironment and the material at the lesion site (He et al. 2018; Han et al. 2017). Titanium-dioxide (TiO₂) film has been widely studied and now applied for the surface modification of cardiovascular stents, but its anti-hyperplasia function is insufficient, so still need to load drugs. In 2014, our team found that the TiO₂ nanotubes (diameters 80–100 nm) prepared by anodic oxidation presented better ability in inhibiting SMC adhesion and proliferation compared with the flat TiO₂ film, but the TiO₂ nanotubes also lead to more platelet adhesion and poor EC growth (Xiang et al. 2014). To solve this problem, the micropatterned TiO₂ nanotubes surface was designed by photolithography combined with anodic oxidation (Xiang et al. 2014). This micropatterned TiO₂ nanotubes surface showed stronger function than pure

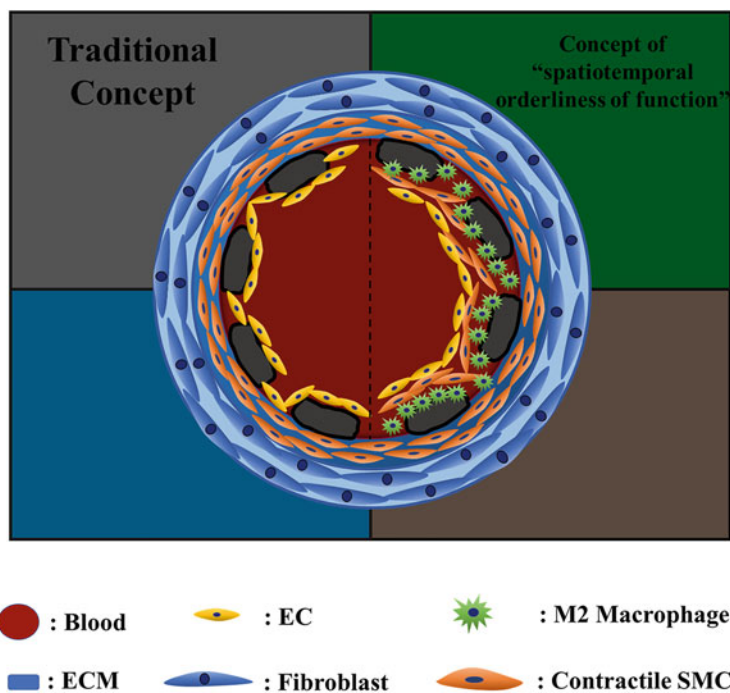


Fig. 8.3 Comparison diagram of traditional concept and the concept of “spatio-temporal orderliness of function” for the endothelialization on the cardiovascular metallic biomaterials

TiO₂ nanotubes in inhibiting SMC adhesion and proliferation, and also better ability in inhibiting platelet adhesion and improving EC growth (Xiang et al. 2014). The further research indicated that the micropatterned TiO₂ nanotubes surface promoted more EC-released NO, TM, and TPF1, suggesting better physiological function of the cells (Xiang et al. 2015).

Due to the excellent biocompatibility of the micropatterned TiO₂ nanotubes surface, it was anticipated to make contribution to inducing various precursor cells, for example, mesenchyma stem cell (MSC) to directionally differentiate into EC (Li et al. 2016a, b). The preliminary results indicated that MSC proliferated rapidly on the micropatterned TiO₂ nanotubes surface, but quite a lot of the proliferative MSC can't touch the micropatterned TiO₂ nanotubes directly. Thus, a method defined as “frequent medium change” (FMC) was used while the cells grew to confluence to avoid contact inhibition on the micropatterned TiO₂ nanotubes surface. However, 6 weeks later, the MSC differentiate into contractile SMC, not the expected EC. In fact, this result has inspired us at the natural level: precursor cells first differentiate into physiological SMC on the surface of micro/nano structures. Without realizing it at the time, we continued fabricating the EC-ECM on the micropatterned TiO₂ nanotubes surface by EC culture and decellularization, and finally induced the MSC to differentiate into EC, 4 weeks later (Wu et al. 2015). Till

2017, when HA coating with different molecular weight was evaluated *in vivo*, we realized the importance of contractile SMC (Li et al. 2017a, b, c), and with the gradual confirmation of follow-up research (Li et al. 2017a, b, c), we put forward the concept “spatio-temporal orderliness of function” in this book.

Since 2018, a kind of natural nano biomaterial has come into our view: Exosomes are natural nanoparticles (40–100 nm) containing complex RNA and proteins, which are involved in the expression of CD31 in artificial cells under blood flow acting (Hou et al. 2020). It has also been reported that exosomes are involved in the exchange of genetic information, resulting in a large number of neovascularization (Valadi et al. 2007). The exosomes mainly come from the multivesicles formed by the invagination of lysosomal particles, and are released into the ECM after fusion with the cell membrane (Mathivanan et al. 2010). When passing through the receptor cells, exosomes can regulate the biological activity of receptor cells through the carrier factors (protein, nucleic acid, and lipid), and then participate in immune response, cell migration, and cell differentiation (Taylor and Gercel-Taylor 2008). The existing researches on exosomes mainly focus on the extraction, composition analysis, and function as injectable drugs. Few people pay attention to the potential application prospects of exosomes in the surface modification of cardiovascular stent materials. In 2019, we obtained a kind of exosomes from the human blood and applied them on surface modification of the commercial cardiovascular stent material 316L SS (Hou et al. 2020). Our data indicated that the exosome-modified surfaces significantly controlled the synthetic SMC into contractile SMC, and the M1 macrophages into M2 macrophages, as well as improving EC proliferation, migration, and NO release. However, the disadvantage of exosome-modified surface is also obvious: the bio-effective time of exosomes is very short, which is only ten to dozens of hours.

Inspired from the exosomes, we attempted to design a novel particle for controlling the behaviors of macrophages, SMC, and EC. In 2020, the HA/polyethyleneimine (PEI) nanoparticles with different diameters were prepared to simulate the exosomes on the nanoscales and bio-function (Wang et al. 2019). These HA/PEI nanoparticles could load the magnesium (Mg) ions, wherein the big Mg-doped HA/PEI nanoparticles (diameter > 150 nm) cannot enter into EC, and thus displayed lower EC number, while the small Mg-doped HA/PEI nanoparticles (diameter < 150 nm) can enter into EC in short time, hence presenting higher EC number. The doped Mg also improved NO release and CD31 expression of the EC by rapid transmembrane absorption. We also investigated the influence of particle sizes of degradation products from Mg alloy on the EC and SMC growth (Wang et al. 2019). Degradation products with smaller particle size and higher Mg ion content were proved to enhance the vital ratio and NO release of EC. These smaller Mg particles cooperated with NO released by EC to inhibit synthetic SMC and M1 macrophages more effectively. All these results mean that controlling the particle size and Mg ion content of the degradation products of Mg alloy, or controlling the degradation behavior of Mg alloy, will contribute to realize the “spatio-temporal orderliness of function” on the Mg alloy stent, which may be conducive to solve the problem of delayed endothelialization on the surface of biodegradable Mg alloy

stents. Based on the above understanding, we prepared a kind of poly-dopamine (PDA)/HA coating to regulate the degradation of Mg alloy (Li et al. 2020a, b). The PDA/HA coating can not only prolong the degradation time of Mg alloy in blood vessels, but also significantly improve the blood compatibility of Mg alloy, promote the formation of contractile SMC, and the growth of EC.

8.6 A Viewpoint and Perspectives

It is really very lucky to discover the distribution and interaction of biomaterials, M2 macrophages, and contractile SMC and EC/EPC in the process of physiological repair and regeneration of endothelial monolayer after cardiovascular devices implantation, and propose the concept or viewpoint of “spatio-temporal orderliness of function.” Further efforts make the scientific community more sure that the key technology during endothelialization should be regulating the phenotypes of SMC and macrophages, instead of killing them. Natural or biomimetic ECM and nanoparticles play crucial roles on the intercellular communication and interaction between biomaterials and cells (Fig. 8.4). Biodegradable absorbable stent is the inevitable trend of cardiovascular interventional therapy. The scale and effective component content of the degradation products are the key factors to determine the repair and regeneration of the physiological tissue at the lesion site. Surface modification is an important guarantee to control the degradation behavior of biodegradable stents. The now available coatings of biodegradable stents are obtained from the coatings from traditional non-degradable metal stents, which have great functional

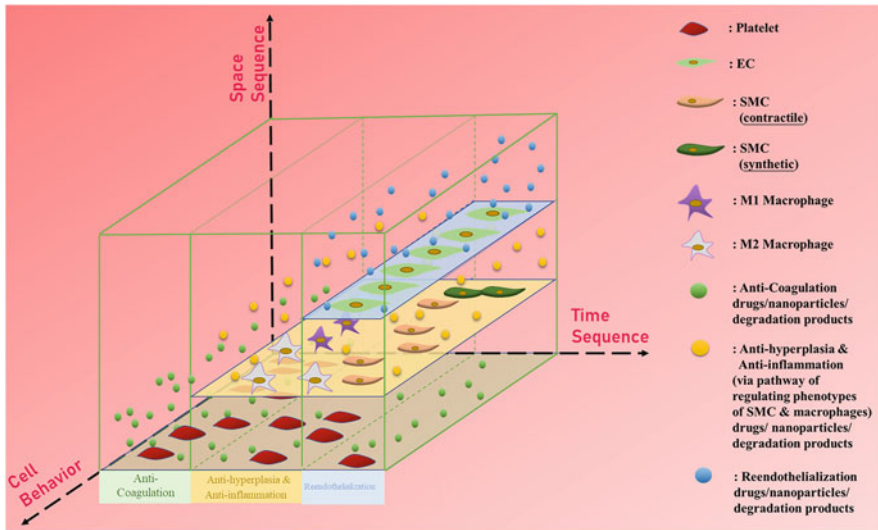


Fig. 8.4 Roles of drugs, nanoparticles, and degradation products for the “spatio-temporal orderliness of function” of the cardiovascular biomaterials

limitations. Therefore, the perspectives of surface modification of cardiovascular metallic biomaterials should focus on the development of special coatings for biodegradable metallic stents.

Acknowledgments We would like to thank Dr. Lalit Pandey and Dr. Abshar Hasan for making our views published in this chapter, especially thank Dr. Lalit Pandey for his invitation. Taking this opportunity, we would like to express our thanks to Prof. N. Huang, Prof. P. Yang, Prof. J.Y. Chen, Prof. J. Wang, Prof. Y.X. Leng, Prof. G.J. Wan, Assoc. Prof. A.S. Zhao, Assoc. Prof. Y.C. Zhao, Assoc. Prof. Y.J. Weng, Assoc. Prof. Q.F. Tu, Assoc. Prof. X.S. Jiang, Assoc. Prof. F.J. Jing, and Assoc. Prof. D. Xie of Southwest Jiaotong University in China for their guidance and instruction during our doctoral degree and post-doctoral research. Without their guidance and help, we would not have obtained today's understanding of cardiovascular metallic biomaterials and the coatings. Prof. N. Huang's concept of the "functional sequential coatings on the legs surface" is the basis and premise of the concept "spatial temporal order of function" we proposed in this chapter. In addition, we would like to express our heartfelt thanks and respect to Prof. S.K. Guan of Zhengzhou University in China for his support and guidance during our study in Zhengzhou University. It was Prof. S.K. Guan who led us into the field of biodegradable metallic stents. Finally, we would like to thank everyone who has helped us in the scientific study and academic research.

References

- Anderson DEJ, Hinds MT (2012) Extracellular matrix production and regulation in micropatterned endothelial cells. *Biochem Biophys Res Commun* 427(1):159–164
- Asahara T, Kawamoto A, Masuda H (2011) Concise review: circulating endothelial progenitor cells for vascular medicine. *Stem Cells* 29:1650–1655
- Blindt R, Vogt F, Astafieva I, Fach C, Hristov M, Krott N, Seitz B, Kapurniotu A, Kwok C, Dewor M, Bosserhoff AK, Bernhagen J, Hanrath P, Hoffmann R, Weber C (2006) A novel drug-eluting stent coated with an integrin-binding cyclic Arg-Gly-asp peptide inhibits neointimal hyperplasia by recruiting endothelial progenitor cells. *J Am Coll Cardiol* 47:1786–1795
- Butzal M, Loges S, Schweizer M, Fischer U, Gehling UM, Hossfeld DK, Fiedler W (2004) Rapamycin inhibits proliferation and differentiation of human endothelial progenitor cells in vitro. *Exp Cell Res* 300(1):65–71
- Chen J, Cao J, Wang J, Maitz MF, Guo L, Zhao Y, Li Q, Xiong K, Huang N (2012) Biofunctionalization of titanium with PEG and anti-CD34 for hemocompatibility and stimulated endothelialization. *J Colloid Interface Sci* 368(1):636–647
- Chen JL, Li QL, Xu JG, Zhang L, Maitz MF, Li J (2015) Thromboresistant and rapid-endothelialization effects of dopamine and staphylococcal protein A mediated anti-CD34 coating on 316L stainless steel for cardiovascular devices. *J Mater Chem B* 3:2615–2623
- Chuang TW, Masters KS (2009) Regulation of polyurethane hemocompatibility and endothelialization by tethered hyaluronic acid oligosaccharides. *Biomaterials* 30(29):5341–5351
- Davies PF, Kerr C (1982) Co-cultivation of vascular endothelial and smooth muscle cells using microcarrier techniques. *Exp Cell Res* 141(2):455–459
- Devalliere J, Chen Y, Dooley K, Yarmush ML, Uygun BE (2018) Improving functional re-endothelialization of acellular liver scaffold using REDV cell-binding domain. *Acta Biomater* 78:151–164
- Dichek DA, Neville RF, Zwiebel JA, Freeman SM, Leon MB, Anderson WF (1989) Seeding of intravascular stents with genetically engineered endothelial cells. *Circulation* 80:1347–1353

- Flugelman MY, Virmani R, Leon MB, Bowman RL, Dichek DA (1992) Genetically engineered endothelial cells remain adherent and viable after stent deployment and exposure to flow *in vitro*. *Circ Res* 70(2):348–354
- Fu GW, Yu ZJ, Chen YQ, Chen YD, Tian F, Yang XD (2016) Direct adsorption of anti-CD34 antibodies on the nano-porous stent surface to enhance endothelialization. *Acta Cardiol Sin* 32:273–280
- Fujiwara H, Gu J, Sekiguchi K (2004) Rac regulates integrin-mediated endothelial cell adhesion and migration on laminin-8. *Exp Cell Res* 292(1):67–77
- Fuster V (2014) Top 10 cardiovascular therapies and interventions for the next decade. *Nat Rev Cardiol* 11:671–683
- Gao P, Qiu H, Xiong K, Li X, Tu Q, Wang H, Lyu N, Chen X, Huang N, Yang Z (2020) Metal-catechol-(amine) networks for surface synergistic catalytic modification: therapeutic gas generation and biomolecule grafting. *Biomaterials* 248:119981
- Gholizadeh S, Visweswaran GRR, Storm G, Hennink WE, Kamps JAAM, Kok RJ (2018) E-selectin targeted immunoliposomes for rapamycin delivery to activated endothelial cells. *Int J Pharm* 548(2):759–770
- Han C, Li J, Zou D, Luo X, Yang P, Zhao A, Huang N (2017) Mechanical property of TiO₂ micro/nano surfaces based on the investigation of residual stress, tensile force and fluid flow shear stress: for potential application of cardiovascular devices. *J Nano Res* 49:190–201
- Han C, Luo X, Zou D, Li J, Zhang K, Yang P, Huang N (2019) Nature-inspired extracellular matrix coating produced by micro-patterned smooth muscle and endothelial cells endows cardiovascular materials better biocompatibility. *Biomater Sci* 7:2686–2701
- He Z, Li J, Luo X, Zou D, Yang P, Zhao A, Huang N (2018) Mechanical property of TiO₂ Nanotubes surface based on the investigation of residual stress, tensile force and fluid flow shear stress: for potential application of cardiovascular devices. *J Nanosci Nanotechnol* 18:798–804
- Hou YC, Li JA, Zhu SJ, Cao C, Tang JN, Zhang JY, Guan SK (2020) Tailoring of cardiovascular stent material surface by immobilizing exosomes for better pro-endothelialization function. *Colloids Surf B Biointerfaces* 189:110831
- Hyman SE (2014) The unconscionable gap between what we know and what we do? *Sci Transl Med* 6:253cm9
- Jana S (2019) Endothelialization of cardiovascular devices. *Acta Biomater* 99:53–71
- Kianpour G, Bagheri R, Pourjavadi A, Ghanbari H (2020) *In situ* synthesized TiO₂-polyurethane nanocomposite for bypass graft application: *in vitro* endothelialization and degradation. *Mater Sci Eng C* 114:111043
- Kim JW, Suh SY, Choi CU, Na JO, Kim EJ, Rha SW, Park CG, Seo HS, Oh DJ (2008) Six-month comparison of coronary endothelial dysfunction associated with Sirolimus-eluting stent versus paclitaxel-eluting stent. *J Am Coll Cardiol Intv* 1(1):65–71
- Klomp M, Beijik MAM, Winter RJ (2014) Genous™ endothelial progenitor cell-capturing stent system: a novel stent technology. *Expert Rev Med Devices* 11(2):365–375
- Lavender MD, Pang Z, Wallace CS, Niklason LE, Truskey GA (2005) A system for the direct co-culture of endothelium on smooth muscle cells. *Biomaterials* 26(22):4642–4653
- Lemesle G, Maluenda G, Collins SD, Waksman R (2010) Drug-eluting stents: issues of late stent thrombosis. *Cardiol Clin* 28(1):97–105
- Li JA (2018) Constructing a spatially ordered composite system on cardiovascular biomaterials surface to create preferable endothelial microenvironment. *Basic Clin Pharmacol Toxicol* 123 (supplement 3):18–19
- Li G, Shi X, Yang P, Zhao A, Huang N (2008) Investigation of fibrinogen adsorption on solid surface by quartz crystal microbalance with dissipation(QCM-D) and ELISA. *Solid State Ion* 179(21–26):932–935
- Li G, Yang P, Guo X, Huang N, Shen R (2011a) An *in vitro* evaluation of inflammation response of titanium functionalized with heparin/fibronectin complex. *Cytokine* 56(2):208–217
- Li G, Yang P, Huang N (2011b) Layer-by-layer construction of the heparin/fibronectin coatings on titanium surface: stability and functionality. *Phys Proc* 18:112–121

- Li G, Yang P, Qin W, Maitz MF, Zhou S, Huang N (2011c) The effect of coimmobilizing heparin and fibronectin on titanium on hemocompatibility and endothelialization. *Biomaterials* 32 (21):4691–4703
- Li J, Zhang K, Liao Y, Yang P, Maitz MF, Huang N (2013a) Co-culture of vascular endothelial cells and smooth muscle cells by hyaluronic acid micro-pattern on titanium surface. *Appl Surf Sci* 273:24–31
- Li J, Zhang K, Yang P, Qin W, Li G, Zhao A, Huang N (2013b) Human vascular endothelial cell morphology and functional cytokine secretion influenced by different size of HA micro-pattern on titanium substrate. *Colloids Surf B Biointerfaces* 110:199–207
- Li J, Zhang K, Yang P, Wu L, Chen J, Zhao A, Li G, Huang N (2013c) Research of smooth muscle cells response to fluid flow shear stress by hyaluronic acid micro-pattern on a titanium surface. *Exp Cell Res* 319(17):2663–2672
- Li J, Zhang K, Chen H, Liu T, Yang P, Zhao Y, Huang N (2014a) A novel coating of type IV collagen and hyaluronic acid on stent material-titanium for promoting smooth muscle cells contractile phenotype. *Mater Sci Eng C* 38:235–243
- Li J, Zhang K, Xu Y, Chen J, Yang P, Zhao Y, Zhao A, Huang N (2014b) A novel co-culture models of human vascular endothelial cells and smooth muscle cells by hyaluronic acid micro-pattern on titanium surface. *J Biomed Mater Res A* 102A:1950–1960
- Li L, Xu Y, Zhou Z, Chen J, Yang P, Yang Y, Li J, Huang N (2015a) The effects of cu-doped TiO₂ thin films on hyperplasia, inflammation and bacteria infection. *Appl Sci* 5(4):1016–1032
- Li J, Zhang K, Wu F, He Z, Yang P, Huang N (2015b) Constructing bio-functional layers of hyaluronan and type IV collagen on titanium surface for improving endothelialization. *J Mater Sci* 50:3226–3236
- Li J, Zhang K, Wu J, Liao Y, Yang P, Huang N (2015c) Co-culture of endothelial cells and patterned smooth muscle cells on titanium: construction with high density of endothelial cells and low density of smooth muscle cells. *Biochem Biophys Res Commun* 456:555–561
- Li J, Zhang K, Wu J, Zhang L, Yang P, Tu Q, Huang N (2015d) Tailoring of the titanium surface by preparing cardiovascular endothelial extracellular matrix layer on the hyaluronic acid micro-pattern for improving biocompatibility. *Colloids Surf B Biointerfaces* 128:201–210
- Li J, Qin W, Zhang K, Wu F, Yang P, He Z, Zhao A, Huang N (2016a) Controlling mesenchymal stem cells differentiate into contractile smooth muscle cells on a TiO₂ micro/nano interface: towards benign pericytes environment for endothelialization. *Colloids Surf B Biointerfaces* 145:410–419
- Li J, Zhang K, Ma W, Wu F, Yang P, He Z, Huang N (2016b) Investigation of enhanced hemocompatibility and tissue compatibility associated with multi-functional coating based on hyaluronic acid and type IV collagen. *Regener Biomater* 3(3):149–157
- Li J, Wu F, Zhang K, He Z, Zou D, Luo X, Fan Y, Yang P, Zhao A, Huang N (2017a) Controlling molecular weight of hyaluronic acid conjugated on amine-rich surface: towards better multi-functional biomaterials for cardiovascular implants. *ACS Appl Mater Interfaces* 9:30343–30358
- Li J, Zhang K, Huang N (2017b) Engineering cardiovascular implant surfaces to create a vascular endothelial growth microenvironment. *Biotechnol J* 12(12):1600401
- Li J, Zou D, Zhang K, Luo X, Yang P, Jing Y, Zhang Y, Cui G, Huang N (2017c) Strong multi-functions based on conjugating chondroitin sulfate on amine-rich surface direct vascular cells fate for cardiovascular implanted devices. *J Mater Chem B* 5:8299–8313
- Li J, Chen L, Zhang X, Guan S (2020a) Enhancing biocompatibility and corrosion resistance of biodegradable mg-Zn-Y-Nd alloy by preparing PDA/HA coating for potential application of cardiovascular biomaterials. *Mater Sci Eng C* 109:110607
- Li X, Liu J, Yang T, Qiu H, Lu L, Tu Q, Xiong K, Huang N, Yang Z (2020b) Mussel-inspired “built-up” surface chemistry for combining nitric oxide catalytic and vascular cell selective properties. *Biomaterials* 241:119904
- Li J, Zhang K, Hou Y (2020c) Chapter: from selective cardiovascular cells adhesion to regulating “spatiotemporal orderliness of function”: understanding based on biomaterials surface

- modification with functional molecules. In: *Current topics in medicine and medical research 2020/BP/5767D*
- Malek AM, Izumo S (1996) Mechanism of endothelial cell shape change and cytoskeletal remodeling in response to fluid shear stress. *J Cell Sci* 109:713–726
- Mathivanan S, Ji H, Simpson RJ (2010) Exosomes: extracellular organelles important in intercellular communication. *J Proteomics* 73(10):1907–1920
- Meerovitch K, Bergeron F, Leblond L, Grouix B, Poirier C, Bubenik M, Chan L, Gourdeau H, Bowlin T, Attardo G (2003) A novel RGD antagonist that targets both $\alpha v\beta 3$ and $\alpha 5\beta 1$ induces apoptosis of angiogenic endothelial cells on type I collagen. *Vascul Pharmacol* 40(2):77–89
- Meslmani BA, Mahmoud G, Strehlow B, Mohr E, Leichtweiß T, Bakowsky U (2014) Development of thrombus-resistant and cell compatible crimped polyethylene terephthalate cardiovascular grafts using surface co-immobilized heparin and collagen. *Mater Sci Eng C* 43:538–546
- Miura K, Nakaya H, Kobayashi Y (2015) Experimental assessment of effects of antiproliferative drugs of drug-eluting stents on endothelial cells. *Cardiovasc Revasc Med* 16(6):344–347
- Morgan JT, Wood JA, Shah NM, Hughbanks ML, Russell P, Barakat AI, Murphy CJJB (2012) Integration of basal topographic cues and apical shear stress in vascular endothelial cells. *Biomaterials* 33(16):4126–4135
- Nelson PR, Kehas AJ, Wagner RJ, Proia RR, Cronenwett JL, Powell RJ (2000) Smooth muscle cells alter endothelial cell regulation of smooth muscle cell migration. *J Am Coll Surg* 191 (4 supplement 1):s3
- Noel S, Fortier C, Murschel F, Belzil A, Gaudet G, Jolicoeur M, Crescenzo GD (2016) Co-immobilization of adhesive peptides and VEGF within a dextran-based coating for vascular applications. *Acta Biomater* 37:69–82
- Omar HR, Mangar D, Sullebarger JT, Sprenger C, Camporesi EM (2014) Post-operative simultaneous very late two-vessel drug eluting stent thrombosis with sparing of bare metal stent in a Jehovah's witness after clopidogrel withdrawal. *J Cardiol Cases* 9(2):57–60
- Orlidge A, D'Amore PA (1987) Inhibition of capillary endothelial cell growth by pericytes and smooth muscle cells. *J Cell Biol* 105(3):1455–1462
- Otsuka F, Finn AV, Yazdani SK, Nakano M, Kolodgie FD, Virmani R (2012) The importance of the endothelium in atherothrombosis and coronary stenting. *Nat Rev Cardiol* 9:439–453
- Patel MR, Marso SP, Dai D, Anstrom KJ, Shunk KA, Curtus JP, Brennan JM, Messenge JC, Douglas PS (2012) Comparative effectiveness of drug-eluting versus bare-metal stents in elderly patients undergoing revascularization of chronic Total coronary occlusions: results from the National Cardiovascular Data Registry, 2005–2008. *J Am Coll Cardiol Intv* 5(10):1054–1061
- Patel J, Donovan P, Khosrotehrani K (2016) Concise review: functional definition of endothelial progenitor cells: a molecular perspective. *Stem Cells Transl Med* 5:1302–1306
- Qi P, Maitz MF, Huang N (2013) Surface modification of cardiovascular materials and implants. *Surf Coat Technol* 233:80–90
- Qiu H, Qi P, Liu J, Yang Y, Tan X, Xiao Y, Maitz MF, Huang N, Yang Z (2019) Biomimetic engineering endothelium-like coating on cardiovascular stent through heparin and nitric oxide-generating compound synergistic modification strategy. *Biomaterials* 207:10–22
- Quan L, Ge S, Liu C, Jia D, Wang G, Yin T (2020) Impact of a bioactive drug coating on the biocompatibility of magnesium alloys. *J Mater Sci* 55:6051–6064
- Rayahin JE, Buhman JS, Zhang Y, Koh TJ, Gemeinhart RA (2015) High and low molecular weight hyaluronic acid differentially influence macrophage activation. *ACS Biomater Sci Eng* 1 (7):481–493
- Su H, Xue G, Ye C, Wang Y, Zhao A, Huang N, Li J (2017) The effect of anti-CD133/fucoidan bio-coatings on hemocompatibility and EPC capture. *J Biomater Sci Polym Ed* 28 (17):2066–2081
- Takahashi M, Matsuoka Y, Sumide K, Nakatsuka R, Fujioka T, Kohno H, Sasaki Y, Matsui K, Asano H, Kaneko K, Sonoda Y (2014) CD133 is a positive marker for a distinct class of primitive human cord blood-derived CD34-negative hematopoietic stem cells. *Leukemia* 28:1308–1315

- Tan KX, Danquah MK, Sidhu A, Yon LS, Ongkudon CM (2018) Aptamer-mediated polymeric vehicles for enhanced cell-targeted drug delivery. *Curr Drug Targets* 19:248–258
- Taylor DD, Gercel-Taylor C (2008) MicroRNA signatures of tumor-derived exosomes as diagnostic biomarkers of ovarian cancer. *Gynecol Oncol* 110(1):13–21
- Torii S, Jinnouchi H, Sakamoto A, Kutyna M, Cornelissen A, Kuntz S, Guo L, Mori H, Harari E, Paek KH, Fernandez R, Chahal D, Romero ME, Kolodgie FD, Gupta A, Virmani R, Finn AV (2019) Drug-eluting coronary stents: insights from preclinical and pathology studies. *Nat Rev Cardiol* 17:37–51
- Tu Q, Zhao Y, Xue X, Wang J, Huang N (2010) Improved Endothelialization of titanium vascular implants by extracellular matrix secreted from endothelial cells. *Tissue Eng A* 16(12):3635–3645
- Tu Q, Yang Z, Zhu Y, Xiong K, Maitz MF, Wang J, Zhao Y, Huang N, Jin J, Lei Y (2013) Effect of tissue specificity on the performance of extracellular matrix in improving endothelialization of cardiovascular implants. *Tissue Eng A* 19:91–102
- Tu Q, Zhao X, Liu S, Li X, Zhang Q, Yu H, Xiong K, Huang N, Yang Z (2020) Spatiotemporal dual-delivery of therapeutic gas and growth factor for prevention of vascular stent thrombosis and restenosis. *Appl Mater Today* 19:100546
- Underwood PA, Bean PA, Whitelock JM (1998) Inhibition of endothelial cell adhesion and proliferation by extracellular matrix from vascular smooth muscle cells: role of type V collagen. *Atherosclerosis* 141(1):141–152
- Valadi H, Ekstrom K, Bossios A, Sjostrand M, Lee JJ, Lotvall JO (2007) Exosome-mediated transfer of mRNAs and microRNAs is a novel mechanism of genetic exchange between cells. *Nat Cell Biol* 9(6):654–U72
- Van der Giessen WJ, Sorruys PW, Visser WJ, Verdouw PD, Van Schalkwijk WP, Jongkind JF (1988) Endothelialization of intravascular stents. *J Interv Cardiol* 1:109–120
- Vartanian KB, Kirkpatrick SJ, Hanson SR, Hinds MT (2008) Endothelial cell cytoskeletal alignment independent of fluid shear stress on micropatterned surfaces. *Biochem Biophys Res Commun* 371(4):787–792
- Vartanian KB, Kirkpatrick SJ, Mccarty OJT, Vu TQ, Hanson SR, Hinds MT (2009) Distinct extracellular matrix microenvironments of progenitor and carotid endothelial cells. *J Biomed Mater Res A* 91(2):528–539
- Wang J, Chen Y, Liu T, Wang X, Liu Y, Wang Y, Chen J, Huang N (2014) Covalent co-immobilization of heparin/laminin complex that with different concentration ratio on titanium surface for selectively direction of platelets and vascular cells behavior. *Appl Surf Sci* 317:776–786
- Wang Y, Chen J, Tang W, Zhang Y, Li X (2017) Rapamycin inhibits the proliferation of endothelial cells in hemangioma by blocking the mTOR-FABP4 pathway. *Biomed Pharmacother* 85:272–279
- Wang S, Zhu S, Zhang X, Li J, Guan S (2019) Effects of degradation products of biomedical magnesium alloys on nitric oxide release from vascular endothelial cells. *Med Gas Res* 9(3):153–159
- Wang Z, Zhu S, Wang L, Chang L, Wang J, Li J, Guan S (2020) Preparing a novel magnesium-doped hyaluronan/polyethyleneimine nanoparticle to improve endothelial functionalization. *IET Nanobiotechnol* 14(2):142–147
- Wawrzynska M, Duda M, Wysokinska E, Strzadala L, Bialy D, Ulatowska-Jarza A, Kalas W, Kraszewski S, Paslawski R, Biernat P, Pastawska U, Zielonka A, Podbielska H, Kopaczyńska M (2019) Functionalized CD133 antibody coated stent surface simultaneously promotes EPCs adhesion and inhibits smooth muscle cell proliferation—a novel approach to prevent in-stent restenosis. *Colloid Surf B Biointerfaces* 174:587–597
- Wu J, Li J, Wu F, He Z, Yang P, Huang N (2015) Effect of micropatterned TiO₂ nanotubes thin film on the deposition of endothelial extracellular matrix: for the purpose of enhancing surface biocompatibility. *Biointerphases* 10:04A302

- Xiang L, Li C, Yang P, Li J, Huang N (2014) Fabrication of micro-patterned titanium dioxide nanotubes thin film and its biocompatibility. *J Eng* 12:665–671
- Xiang L, Li J, He Z, Wu J, Yang P, Huang N (2015) Design and construction of TiO₂ nanotubes in microarray using two-step anodic oxidation for application of cardiovascular implanted devices. *Micro Nano Lett* 10(6):287–291
- Xiao Y, Wang W, Tian X, Tan X, Yang T, Gao P, Xiong K, Tu Q, Wang M, Maitz MF, Huang N, Pan G, Yang Z (2020) A versatile surface bioengineering strategy based on mussel-inspired and bioclickable peptide mimic. *Research* 2020:7236946. <https://doi.org/10.34133/2020/7236946>
- Xu Y, Li J, Yao L, Li L, Yang P, Huang N (2015) Preparation and characterization of cu-doped TiO₂ thin films and effects on platelet adhesion. *Surf Coat Technol* 261:436–441
- Yang Z, Yang Y, Xiong K, Li X, Qi P, Tu Q, Jing F, Weng Y, Wang J, Huang N (2015) Nitric oxide producing coating mimicking endothelium function for multifunctional vascular stents. *Biomaterials* 63:80–92
- Yang Z, Qiu H, Li X, Gao P, Huang N (2018a) Plant-inspired gallolamine catalytic surface chemistry for engineering an efficient nitric oxide generating coating. *Acta Biomater* 76:89–98
- Yang Z, Yang Y, Zhang L, Xiong K, Li X, Zhang F, Wang J, Zhao X, Huang N (2018b) Mussel-inspired catalytic selenocystamine-dopamine coatings for long-term generation of therapeutic gas on cardiovascular stents. *Biomaterials* 178:1–10
- Yang T, Du Z, Qiu H, Gao P, Zhao X, Wang H, Tu Q, Xiong K, Huang N, Yang Z (2020a) From surface to bulk modification: plasma polymerization of amine-bearing coating by synergic strategy of biomolecule grafting and nitric oxide loading. *Bioact Mater* 5(1):17–25
- Yang Z, Zhao X, Hao R, Tu Q, Tian X, Xiao Y, Xiong K, Wang M, Feng Y, Huang N, Pan G (2020b) Bioclickable and mussel adhesive peptide mimics for engineering vascular stent surfaces. *Proc Natl Acad Sci* 117(28):16127–16137. <https://doi.org/10.1073/pnas.2003732117>
- Yoshiyama S, Chen Z, Okagaki T, Kohama K, Nasu-Kawaharada R, Izumi T, Ohshima N, Nagai T, Nakamura A (2014) Nicotine exposure alters human vascular smooth muscle cell phenotype from a contractile to a synthetic type. *Atherosclerosis* 237(2):464–470
- Yu S, Cheng Y, Li B, Xue J, Yin Y, Gao J, Gong Z, Wang J, Mu Y (2020) M1 macrophages accelerate renal glomerular endothelial cell senescence through reactive oxygen species accumulation in streptozotocin-induced diabetic mice. *Int Immunopharmacol* 81:106294
- Zago AC, Costa MA, Zago AJ, Rossato JS, Matte BS, Iturry-Yamamoto G, Mossmann M, Savaris R, Albertal M, Rochal CS, Healy AM, Walker R, Tahara S, Simon DI (2012) Identification of genes involved in smooth muscle cell protein synthesis with increased expression in atheromatous plaques associated with Neointimal hyperplasia after bare-metal stenting: a GENESIS-R study. *Rev Bras Cardiol Inv (English Ed)* 20(2):140–145
- Zammaretti P, Zisch AH (2005) Adult “endothelial progenitor cells”—renewing vasculature. *Int J Biochem Cell Biol* 37:493–503
- Zhang F, Zhang Q, Li X, Huang N, Zhao X, Yang Z (2019) Mussel-inspired dopamine-CuII coatings for sustained in situ generation of nitric oxide for prevention of stent thrombosis and restenosis. *Biomaterials* 194:117–129
- Zheng W, Wang Z, Song L, Zhao Q, Zhang J, Li D, Wang S, Han J, Zheng XL, Yang Z, Kong D (2012) Endothelialization and patency of RGD-functionalized vascular grafts in a rabbit carotid artery model. *Biomaterials* 33(10):2880–2891
- Zou D, Luo X, Han C, Li J, Yang P, Li Q, Huang N (2019) Preparation of a biomimetic ECM surface on cardiovascular biomaterials via a novel layer-by-layer decellularization for better biocompatibility. *Mater Sci Eng C* 96:509–521



Advancement of Spinel Ferrites for Biomedical Application

9

Molongnenla Jamir, Aszad Alam, and J. P. Borah

Abstract

Magnetic nanoparticles (MNPs) specially ferrites have attracted increased attention over the past decades as a potential candidate in the field of biomedical applications (e.g. magnetic hyperthermia, drug delivery, magnetic resonance imaging (MRI), etc.) due to their controllable and enhanced magnetic properties. Among the numerous MNPs, spinel ferrites have gained significant attention due to their inherent characteristics like tunable magnetic properties, non-toxicity, and biocompatibility as well as highly efficient and tissue-specific MNP aggregation in the cancer cells. Owing to the superparamagnetic nature of ferrites, several properties of spinel ferrite MNPs and their nanocomposites are substantially dependent on the size, shape, and the distribution of the MNPs. These MNPs show instability over longer periods due to the agglomeration caused by their higher surface energies. Therefore, strategies like grafting and functionalizing with polymers have demonstrated to stabilize the MNPs chemically. The polymeric platform provides higher synthetic freedom allowing the MNPs to be customized for our specific needs. Modification of spinel ferrites by alloying or coating for tuning its properties as per the requirements in the field of nanomedicine have instigated new therapeutic treatment to replace the previous traditional one.

Keywords

Magnetic nanoparticle · Magnetic hyperthermia · Superparamagnetism · Magnetic anisotropy · Spinel ferrite

M. Jamir · A. Alam · J. P. Borah (✉)

Department of Physics, National Institute of Technology Nagaland, Dimapur, Nagaland, India

© The Author(s), under exclusive license to Springer Nature Singapore Pte Ltd. 2022

227

L. M. Pandey, A. Hasan (eds.), *Nanoscale Engineering of Biomaterials: Properties and Applications*, https://doi.org/10.1007/978-981-16-3667-7_9

9.1 Introduction

Many attempts are being made to surmount the inadequacies of conventional treatment and diagnosis. The use of biocompatible magnetic nanoparticles (MNPs) are rapidly increasing in the field of nanomedicine. The rising interest in MNPs stems from their ability to induce motion and rotation to the particle when exposed to external magnetic field. Consequently, this widens many applications for transporting and immobilizing the MNPs and can be used to deliver magnetically tagged entities, like anticancer drug, to the affected cell region. Moreover, for their controllable sizes ranging from few nanometers to hundreds of nanometers, which puts them at dimensions smaller than or equivalent to those of a gene (2 nm wide and 10–100 nm long), a protein (5–50 nm), a virus (20–450 nm) and (10–100 μm), and makes it possible for the MNPs to get closer to a biological entity of interest (Pankhurst et al. 2003). Additionally, the MNPs can be made to respond to time varying magnetic fields, which results in heating up the MNPs, and can be used as potential hyperthermia agents. Especially, spinel ferrite MNPs that show numerous properties, in particular high magnetization, high anisotropy contributions and superparamagnetism, are increasingly being used in many biomedical applications, like hyperthermia, targeted drug delivery as well as magnetic resonance imaging (MRI) (Ravichandran and Velumani 2020; Alghamdi et al. 2020; Nigam and Pawar 2020; Somvanshi et al. 2020; Wang et al. 2020; Zhang et al. 2020). Aside from the aforementioned applications, spinel ferrite MNPs are further useful in the development of modern sensors and biosensors, applicable both in the industrial as well as biomedical fields (Beveridge et al. 2011; Carregal-Romero et al. 2013; Lee et al. 2014; Rocha-Santos 2014). Furthermore, spinel ferrite MNPs are robust toward some pathogenic microorganisms owing to their strong antimicrobial activity (Abdel Maksoud et al. 2018). The spinel ferrites are potentially suitable for biomedical applications based on the fact that these MNPs do not retain residual magnetization upon removal of external applied magnetic field, and also because of the low toxicity and biocompatibility as well as for possessing tunable magnetic properties. Over and above, the meticulous crystal chemistry of spinel ferrites have spectacular execution in acclimation of magnetic nature as chemical composition regulates the crystal structure and cationic distribution, which in turn come up with a mean to administer the physical properties, by the selection of copacetic chemical entity, synthesis strategy, and circumstances (Mathew and Juang 2007; Tatarchuk et al. 2017). The quoted relation interdependence becomes pronounced at the nanoscale range (Carta et al. 2009). However, the large-scale synthesis of spinel ferrites is still a growing area of research. There are a handful of recent works suggesting few feasible approaches, like microwave-assisted combustion method, conventional ceramic method, sol–gel approach, etc., for the large-scale synthesis of spinel ferrite (Dippong et al. 2019; Cobos et al. 2020; Han et al. 2020; Karakas 2020). Owing to these unique characteristics, spinel ferrites are the extensively studied compounds with the aim of solving the existing issues in the field of nanomedicine.

9.2 Prelude to Magnetism

A magnetic field (H) is produced whenever there is an electrical charge in motion, or by a permanent magnet and this magnetic field exerts a force on the source in either of the cases. In response to which the medium shows some magnetic induction (B), which is linked to the magnetic field via permeability of the medium. There is a linear relation, $B = \mu_0 H$, for most of the materials. Nonetheless, for materials of our importance, different relation is pronounced, manifesting two contributors in the induction, one is due to the magnetic field (H) and another on the part of magnetization (M) of the material, collectively written as $B = \mu_0(H + M)$ (Jiles 1991). Magnetic induction aligns the dipoles to make the parallel assembly of moments with respect to itself. These magnetic moments are referred to as the ratio of the highest value of torque on a magnetic dipole and induction. The magnetization is a material-dependent property, influenced by the magnetic moment of the particular constituent as well as their synergy with each other, quantified as the magnetic moment in a unit volume. Along with magnetization and induction, material properties can be illustrated through its response in terms of how magnetizable is the aforementioned specimen in the applied field, described as susceptibility (χ), is the ratio of M and H , consequently becomes significant in the magnetic materials categorization (Spaldin 2010).

9.2.1 Classification of Magnetic Materials

Diamagnetic materials have zero effective magnetic moments and they show negative susceptibility which has its origin in the precession of the electronic orbit around the applied magnetic field direction. Paramagnetic materials have permanent magnetic dipoles, and subsequently small net magnetization with a small positive susceptibility in the response of an external magnetic field. Furthermore, the Curie law of paramagnetism tells about the inversely proportional nature of susceptibility toward the temperature, which can be seen in Fig. 9.1. Figure 9.1 also shows that materials of antiferromagnetic nature have maximum susceptibility at Néel temperature (T_N) and displays paramagnetic behavior above (T_N). Moreover, antiparallel arrangement due to negative interaction between permanent magnetic moments is present. Linear $M-H$ curves will be facilitated for magnetizations of dia-, para- and antiferromagnetic materials. In contrary to other magnetic materials, ferromagnets and ferrimagnets have a completely different nature. In ferromagnetic materials, neighboring atoms experience a strong but short-range interaction, termed as exchange interactions, accompanying their positive parallel alignment, which can be magnetized into regions of uniform magnetization in a spontaneous manner, exhibiting a nonlinear response to the applied external field. This behavior is characteristic of both ferromagnetic and ferrimagnetic materials, termed “hysteresis,” where demagnetization would not recall the original path, hence magnetization is no longer a single-valued function of field. The field reversal magnitude required to achieve initial zero induction corresponds to the coercivity (H_c). The

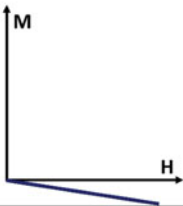
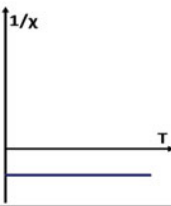
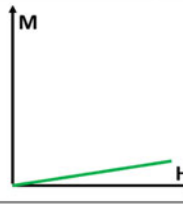
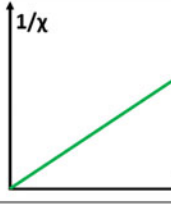
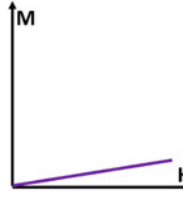
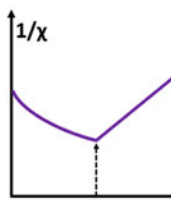
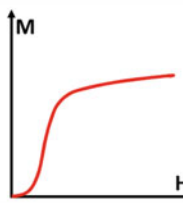
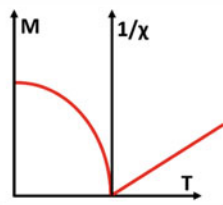
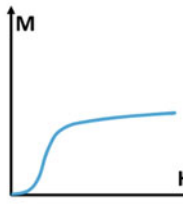
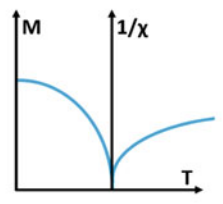
Material Type	Magnetization Vs Field behavior	The inverse of susceptibility Vs Temperature variation
Dia-magnetic		
Para-magnetic		
Antiferro-magnetic		
Ferro-magnetic		
Ferri-magnetic		

Fig. 9.1 Magnetic behavior of different materials with field and temperature, respectively

magnetization value when a material is fully magnetized by the alignment of all the domains along the direction of applied field direction, especially for larger fields is called the saturation magnetization, M_s , which becomes zero at Curie temperature (T_c), in consistency with the divergence of susceptibility, χ at that point. Above T_c , material exhibits paramagnetic nature according to the Curie–Weiss law of

ferromagnetism. Ferrimagnetic material faces a strong, negative interaction between the two sublattices which are occupied by two or more magnetic species, possessing different magnetic moments, resulting into antiparallel spin-lattice arrangement giving rise to a spontaneous magnetic moment below T_c (Krishnan 2016).

9.2.2 Magnetic Domains and Superparamagnetism

9.2.2.1 Magnetic Domain and Domain Walls

A cluster of aligned spins having unidirectional magnetic moments, considered as magnetic domains, are teamed up during magnetization. This parallel alignment of magnetic dipole moments is attributed to a potent driving force, exchange energy in the case of ferromagnetic materials. Domain walls are the boundaries, having a specific width and a particular amount of energy associated with it, separating adjacent domains. Figure 9.2 displays the schematic diagram of multidomain particle, where at first, favorably aligned domains will grow on the expanse of subsequent reduction in domains that are oppositely aligned to the field, followed by magnetic moment rotation of unfavorably aligned domains. Furthermore, coherent rotations are performed at high fields involving the gradual rotation of closely oriented magnetic moments, leading to a uniformly magnetized specimen (Jiles 1991).

9.2.2.2 Superparamagnetism

With decreasing size of the particle to a critical size limit that it becomes close to Bloch wall size, domain walls energy can be made comparable to magnetic anisotropy, making domain walls motion unpropitious and turns out to be single-domain particles. At this size, magnetization is through coherent rotation of spins and their behavior was first described by the Stoner-Wohlfarth model (Stoner and Wohlfarth 1948), neglecting the effect of thermal relaxations. But then again, particles of much smaller size are influenced by thermal fluctuations, regarded as superparamagnetic, are described by the combination of theories involving thermal relaxation. Figure 9.3 shows the variation of coercivity in terms of magnetic particle with respect to its diameter. Néel in 1949 explained the absence of their stable magnetization by virtue of thermal fluctuations, become significant at this size (Hergt et al. 2010). The behavior of these kinds of materials is restricted by Bean and Jacobs (1956) and

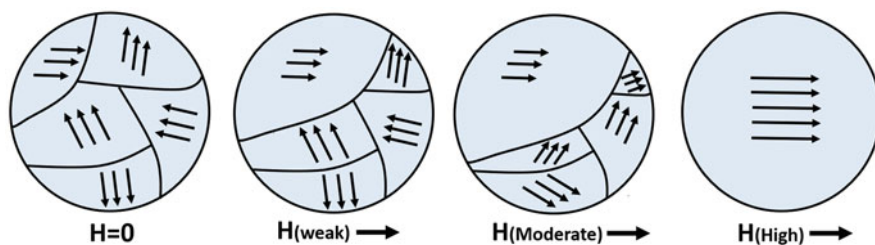


Fig. 9.2 Magnetic domains in the absence and presence of an external magnetic field (H)

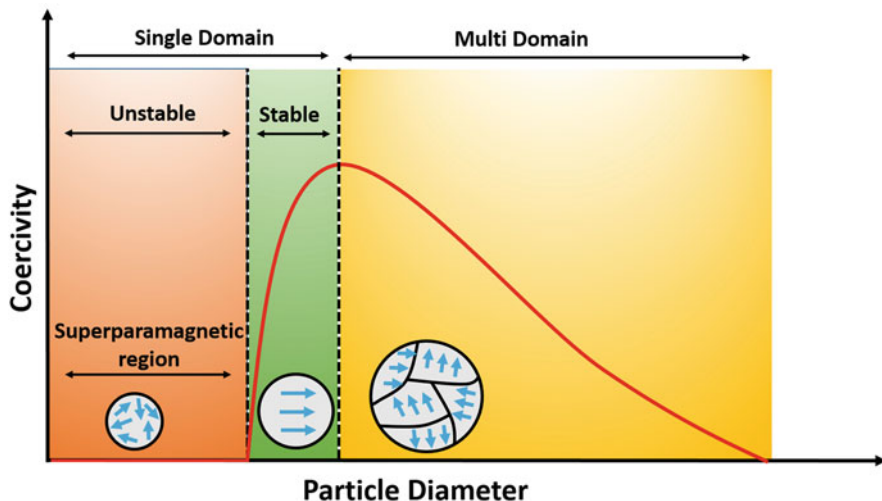


Fig. 9.3 Coercivity variation of magnetic particle with respect to its diameter

later by Bean and Livingston (1959), as the exposition of no hysteresis display during magnetization together with the superposition of the curve in M versus H/T plots conducted at different temperatures. In order to explain superparamagnetism, Brown (1963), defines the relaxation time τ for the net magnetization of such particles, $\tau = \tau_0 \exp^{\Delta E/k_B T}$, which is the time required for spontaneous switching of the magnetization of an ideal particle by crossing the barrier of anisotropy energy. The measurement time frame τ_m has a strong dominance on the magnetic behavior, such that $\tau_m \gg \tau$, referring to quick thermal relaxation, easily overcoming the energy barrier (ΔE) and finally exhibiting superparamagnetic behavior. Slower relaxation time can be understood for $\tau_m \ll \tau$, confirming a blocked state having quasi-static properties. Blocking temperature T_B is determined at $\tau_m = \tau$ (Dobson 2012).

9.2.3 Anisotropy in Magnetic Materials

The above-mentioned energy barrier is originated from intrinsic and extrinsic factors, such as magnetocrystalline and shape anisotropies. Anisotropy, whether it is inherent of the material or induced, impels critically during magnetization, and in resulting hysteresis curve, therefore called into play in predicting and controlling the magnetic properties for specific applications. It either depends on the bulk of the material like magnetocrystalline anisotropy, shape anisotropy, stress anisotropy, exchange anisotropy, or related to the surface.

9.2.3.1 Magnetocrystalline Anisotropy

Magnetocrystalline anisotropy is a material inherent ability in the preference of magnetization along with certain crystallographic directions, leading to saturation

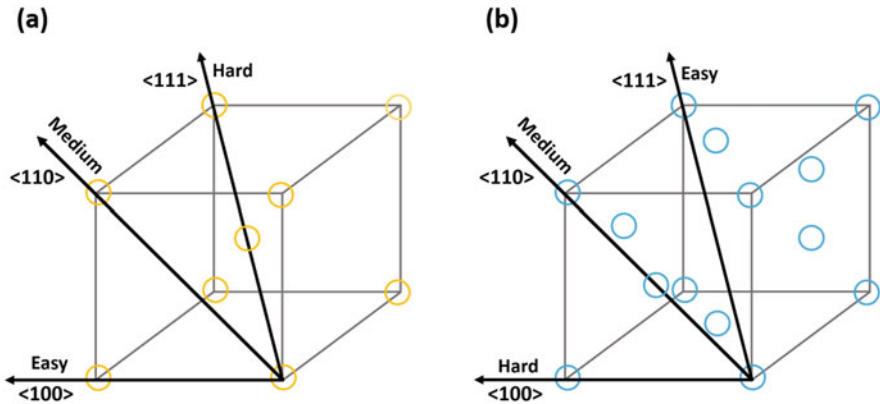


Fig. 9.4 Easy, medium, and hard magnetization directions of (a) bcc-Fe, (b) fcc-Ni

of magnetization at smaller field values in those directions, thence called easy axis. Forenamed is equitable of the total area under the $M-H$ curve for a field in a particular crystallographic direction, or citing the difference in energy for easy and hard directional magnetization over a unit volume. That being the case, anisotropy energy is associated with a crystal having magnetization in a hard direction as a result of already applied force that diverted the magnetization. The magnetically anisotropic quintessence in ferromagnetic materials of cubic symmetry is a typical case of magnetocrystalline anisotropy. Under uniform field, the energy essential for magnetization of a unit volume in a cubic crystal is determined with the help of direction cosines α_1 , α_2 , and α_3 of angles a , b , and c that magnetization forms with all the three-axis of crystals respectively. The cubic anisotropy in the form of their series expansion is given as (Bozorth 1936):

$$E = K_0 + K_1(\alpha_1^2\alpha_2^2 + \alpha_2^2\alpha_3^2 + \alpha_3^2\alpha_1^2) + K_2(\alpha_1^2\alpha_2^2\alpha_3^2) + \dots$$

The values of K_0 , K_1 , K_2 are fixed for a certain material at a specific temperature.

After avoiding K_2 ascribed to its minute quantity and K_0 for the sake of its unallied nature with angle, the sign of K_1 functions substantially and undertakes the easy axis determination. Showing compliance with heretofore, bcc-Fe and cubic ferrite with cobalt content hold positive K_1 and follow the order of $E_{100} < E_{110} < E_{111}$, whereas a contrary sequence is noticed for a negative K_1 in fcc-Ni and ferrites hardly having cobalt content (shown in Fig. 9.4). For this reason, iron shows spontaneous magnetization of demagnetized domains to saturation in $\langle 100 \rangle$ direction. Aforeknown magnetization can be attained with shallow fields, as per the fact that domain growth will lead to the saturation magnetization upon applying a field in easy $\langle 100 \rangle$ direction, providing a low field is obligatory for domain wall motion. On the flip side, a reasonably high field is a requisite for saturation in $\langle 110 \rangle$ direction, eventuates through domain rotation involving the forceful rotation of magnetic moments subduing the above-mentioned crystal anisotropy. The easy magnetization

for all the ferrites except those containing cobalt is in $\langle 111 \rangle$ directions (Cullity and Graham 2009). Uniaxial anisotropy present in a crystal that has a single easy axis exclusively. The angle θ between z -axis as the easy axis and magnetization is used to quantify uniaxial axis anisotropy as (Laurent et al. 2011),

$$E = KV \sin^2\theta$$

where, K and V are anisotropy and volume respectively.

Magnetocrystalline energy emerges from the spin–orbit interaction, and ultimately a demonstration of favoring decisive crystallographic directional orientation, since spin reorientation requires orbital reorientation, providing orbits are already coupled and have a preference for those specific directions (Coey 2010). This anisotropy is observed as conducting to the null result near Curie temperature in as much as the absence of preference in the orientation of the paramagnetic case (Spaldin 2010).

Additionally, the polycrystalline materials having asymmetric shapes exhibit a kind of anisotropy as a result of their shape, even though there is no liking in grain orientation, ensuing a shape anisotropy regardless of no allowance of crystalline anisotropy, as magnetization is untroublesome along their long axis. Stress development in the course of abrupt cooling or annealing effectuates stress anisotropy. A set of ferromagnetic and antiferromagnetic material account for exchange anisotropy owing to their interfacial magnetic coupling. Materials surfaces have the broken symmetry and atomic disorder, culminating into the induction of local crystal field pertaining easy axis or easy plane anisotropy, esteemed as surface anisotropy, and effectuate magnetically harder nature of the surface, attaining an efficacious axial characteristic at the right angle to the surface. Taking all into consideration, a concluding parameter is effective anisotropy energy, and the aforesaid incorporates bulk anisotropy in the conjugation of its surface counterpart.

9.3 Theory of Ferrites

Magnetic moments are in an ordered arrangement in ferrimagnetic and antiferromagnetic materials possessing an exchange coupling among them, foster an antiparallel configuration of sublattices of the crystal structure. Thereupon identical response from the sublattices, counterbalance each other and give rise to antiferromagnetism below Néel temperature. While in ferrimagnets consideration, below Curie temperature, these sublattices have incommensurate responses, bring on an overall magnetization (Krishnan 2016). Aforestated materials are predominantly inorganic oxides featuring in any of the two spinel or non-spinel structures covering garnet, hexagonal, and orthoferrite structures. Ferrites belong to iron oxides incorporating other transition metal or lanthanides, and possess sizable magnetic saturation values, sight far-flung effectiveness in biomedical applications.

9.3.1 Non-spinel Ferrites

The garnet ferrites appear as $M_3Fe_5O_{12}$ formula, containing a trivalent ion M of transition metal or lanthanides, while the iron is in the trivalent state as shown in Fig. 9.5 (left panel). The unit cell consists of 160 atoms in the form of eight formula units, having 24 dodecahedral sites occupied by M ions, whose magnetization utterly disagrees with those at the tetrahedral sites. Secondly, 16 octahedral and 24 tetrahedral sites are engaged in keeping ferric ions in contrastingly magnetized states relative to one another (Valenzuela 2012; Uchida et al. 2013). However, both sites are weakly coupled with dodecahedral sites, begetting a feeble ferrimagnetic nature.

Hexagonal ferrites offer hard magnetic character abiding the chemical formula of $MFe_{12}O_{19}$, M is a bulkier divalent ion. This structure has octahedral and tetrahedral sites captured by trivalent iron ions and can be viewed in Fig. 9.5 (middle panel). Conjointly, ferric ions elicit a trigonal bipyramid geometry with five oxygen ions (Kojima 1982; Trukhanov et al. 2018).

Figure 9.5 (right panel) shows orthoferrite which ideally has a cubic structure alongside general formula $MFeO_3$, M referring to a large trivalent ion chiefly of rare earth elements positioned on corners in cuboctahedral coordination, together with ferric ion of body center domicile; additionally, the face center positions belong to oxygen ions (Tokunaga et al. 2009).

9.3.2 Spinel Ferrites

Spinel ferrites are in most cases magnetically soft materials, with minimal losses through eddy current. They have a typical representation of MFe_2O_4 , taking in trivalent ferric ion together with divalent metal ion M. A total of eight formula units construct one unit cell, each formula unit is composed of Face centred cubic (FCC) lattice arrangement of oxygen atoms, being the origin of tetrahedrally coordinated A site and octahedrally coordinated B site giving rise to 32 octahedral plus 64 tetrahedral sites (Andersen et al. 2018). Howbeit, only 16 octahedral and 8 tetrahedral sites are filled, citing their 1/2 and 1/8 cation occupancy respectively as displayed in Fig. 9.6. These cations are said to be assigned in cubic crystal symmetry

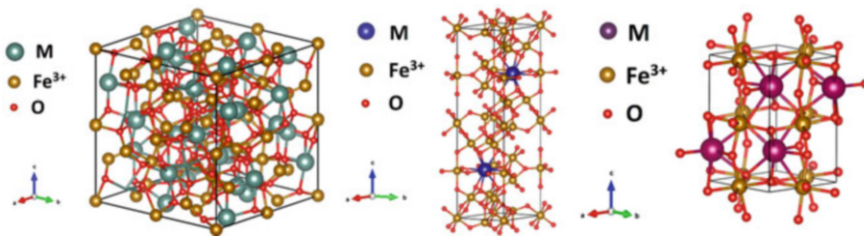


Fig. 9.5 Left panel figure denotes garnet ferrite, middle panel is hexagonal ferrite, and the right panel represents orthoferrite structure

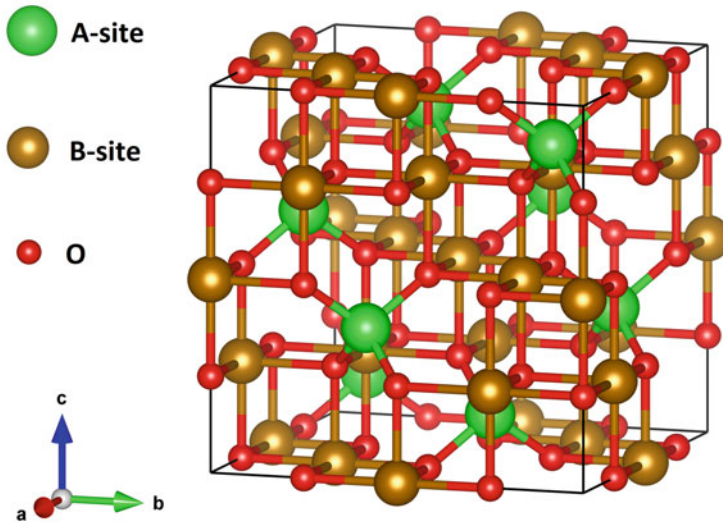


Fig. 9.6 Structure of cubic spinel ferrites (*A* – tetrahedral site, *B* – octahedral site)

in such a manner that switching their location maneuvers the magnetic feature, therefore categorized as normal, inverse, and mixed spinel ferrites. Bearing in mind that magnetic moments of species at tetrahedral and octahedral positions are counseled in the conflicting state, administrating antiferromagnetic synergy (da Silva et al. 2019).

Normal spinels carry divalent metal and trivalent ferric ions on tetrahedrally and octahedrally coordinated locations respectively, as $(M^{2+})_A(Fe^{3+})_2B O_4$ representation. Nonmagnetic cations ordinarily sit on tetrahedral sites, in particular, zinc ferrite and cadmium ferrite are evident (Amiri et al. 2019).

For spinel to be called inverse, half of the trivalent ferric ion fills all the tetrahedral spots, and the remaining other half shares octahedral sites with divalent metal ion *M*. This case is represented as $(Fe^{3+})_A(M^{2+}Fe^{3+})_B O_4$, where the magnetization is governed by moments of divalent ions only, in consideration of net null magnetic moment for ferric ions attributed to abolition in its oppositely oriented moments of tetrahedral and octahedral sites (Adeela et al. 2018). Cobalt ferrite, nickel ferrite, and magnetite as well belong to the mentioned inverse spinel structure. Yet, when the two kinds of metal ions do not have a definite share of these sites, rather having random distribution, then designated as mixed spinels and can be represented by the formula $[(M^{2+})_x(Fe^{3+})_y]_A[(M^{2+})_{1-x}(Fe^{3+})_{2-y}]_B O_4$ (Hernández-Gómez et al. 2018).

9.3.2.1 Cationic Distribution in Spinel Ferrite

The distribution of cations over the *A* and *B* sites categorically influence the magnetic properties of spinel. This distribution is governed by several aspects of these ions, like radius, electronic configuration, and electrostatic energy. Since trivalent ions generally have smaller ionic radii than divalent ones, hence they prefer

tetrahedral occupancy, as tetrahedral sites have lesser volume than octahedral sites. An inverse spinel structure is preferred in this scenario. Sometimes, a cation shows affinity toward one of the two possible sites, owing to the fact that its electronic configuration is best suited for the coordination associated with that specific site. Ions whose d -orbitals are completely filled will have a tendency to form sp^3 hybrid orbital; that is why ions sit on the tetrahedral sites (Cotton and Wilkinson 1974). Electrostatic or Madelung energy plays a vital role in the distribution of formation of metal ions in spinel ferrites. It is the energy acquired during the formation of spinel lattice when faraway ions are coming close to each other in this process (Smit and Winj 1959). Often, this cationic distribution is in the intermediate range having mixed or random spinel structure, which is characterized by a parameter called the degree of inversion (Harris and Šepelák 2018). Basically, the fraction of trivalent ferric ions that are present on tetrahedral sites is termed as the degree of inversion (δ) (Concas et al. 2009).

$$\delta = \frac{\text{Fe}^{3+} \text{ A - site}}{\text{Fe}^{3+} \text{ B - site}}$$

The value of δ ranges from zero for normal spinel to one for inverse spinel, whereas $\delta = 1/3$ represents a completely random distribution (Lazarević et al. 2015).

9.3.3 Magnetic Ordering

Ferrites generally have negative exchange energies, based on three feasible classes of magnetic interaction between the metallic ions. The extent of this interaction energy reckons with the separation of two ions from an intermediate oxygen ion via which this superexchange mechanism occurs, in an inversely proportional manner. The metal ion–oxygen–metal ion angle is also a decisive factor, which gives maximum exchange energy at 180° .

9.3.3.1 Néel Theory of Ferrimagnetism

Néel considered tetrahedral and octahedral sublattices, A and B in a ferrimagnetic material of spinel structure in such a manner that inter sublattice interaction A–B dominates over intra sublattice interaction A–A and B–B, creating a collinear structure of spins. In this circumstance, the A and B sites will have antiparallel magnetic moments, and the difference between these two will bring on the overall magnetic moment. As a result, saturation magnetization (M_s) is determined from the difference of total octahedral site magnetization (M_B) and total tetrahedral site magnetization (M_A). Furthermore, cationic distribution can be estimated on the grounds of M_s . This theory shows the hyperbolic nature of the curve above Curie temperature when plotted between the inverse of susceptibility and temperature. Additionally, below Curie temperature, there are multiple possible forms of magnetization behavior with respect to temperature, subjected to the distribution of cations in the sublattices (Smart 1955).

According to Weiss molecular field theory, where he assumed an internal molecular field (H_M) having a proportional relationship with magnetization, supplementary to an externally applied field (H_0),

$$H = H_0 + H_M$$

Néel extended this theory for ferrimagnets involving two different sublattices, then the overall magnetic force acting on each sublattice can be written as:

$$H = H_0 + H_A \quad \text{or} \quad H = H_0 + H_B$$

where H_A and H_B are internal molecular field acting on A and B sites respectively.

Considering, H_{AA} and H_{AB} are the fields experienced by ions on-site A due to adjacent A and B site ions respectively. Similarly, the field acting on B site due to nearby B and A site ions are H_{BB} and H_{BA} .

$$H = H_0 + H_{AA} + H_{AB} \quad \text{or} \quad H = H_0 + H_{BB} + H_{BA}$$

Subsequently, the total magnetic force acting on sublattices is expressed in terms of magnetic moments of sublattice A (M_A) and sublattice B (M_B), γ being the molecular coefficients associated with sublattices.

$$H = H_0 + \gamma_{AA}M_A + \gamma_{BA}M_B \quad \text{or} \quad H = H_0 + \gamma_{BB}M_B + \gamma_{BA}M_A$$

Néel theory is a molecular field theory associated with magnetic ordering by superexchange interaction, which is a function of p -orbital orientation of oxygen with adjacent metal cations. It involves the hopping mechanism of electrons between the magnetic metal ions and intermediate oxygen anion, where an excited oxygen electron transferred to transition metal ion will have the opposite spin with respect to remaining unpaired electrons that oxygen has. This phenomenon introduces a negative exchange integral having a much larger value for cation pair which makes 180° angle with adjacent oxygen ion. The angle between A-site cation and B-site cation through oxygen ion (A-O-B angle) is almost 180° , which is in accordance with Néel's consideration of A-B interaction dominating over A-A and B-B interactions. However, Néel's theory fits for the explanation of numerous inverse spinels but then gives up in case of mixed ferrites due to a puzzling scenario (Willard et al. 1999).

9.3.3.2 Yafet-Kittel Theory

When magnetic ions are replaced by nonmagnetic ions in ferrimagnetic materials, especially in mixed ferrites, the intra sublattice interaction starts challenging inter sublattice interaction, leading to frustration of several moments. Atomic dipole moments will no longer be collinear, rather locally canted around the magnetic interaction. Mixed ferrites like $Zn_xNi_{1-x}Fe_2O_4$, $Zn_xMn_{1-x}Fe_2O_4$, and $Zn_xCo_{1-x}Fe_2O_4$ show a linear increase in saturation magnetization with early increment in zinc content. But at large concentration, there is a deviation from linearity

which is the failure of Néel's theory (Topkaya et al. 2013). Yafet and Kittel described this exchange coupling phenomenon by considering the noncollinear structuring of spin arrangement resulting in magnetization vectors exhibiting triangular spin structures (Yafet and Kittel 1952). In the above-mentioned case with the increasing composition of nonmagnetic Zn^{+2} ion on A site, a small number of remaining ferric ion are incompetent for the alignment of all the B site moments antiparallel to them. Here, A–B exchange interaction decreases and becomes inferior to B–B exchange interaction, resulting in an imperfect alignment, called spin canting. This occurred by splitting of B sublattice into two parts B' and B'' at Yafet angle (θ_{YK}) with the net magnetization direction of the sublattice. Both parts may have moments antiparallel to each other, giving rise to a ferrimagnetic arrangement. On the other hand, it can also be ferromagnetically saturated. Another possible configuration is the antiferromagnetic coupling of both parts. Mean-field approximation is utilized to each sublattice in the Yafet-Kittel model, involving interaction from the ions on the same sublattice as well as on other sublattices.

Later, several other theories were proposed to illustrate the ferromagnetic compartment, starting from statistical model by Gilleo (1960) to random canting model of Rosencwaig (1970).

9.4 Applications

9.4.1 Magnetic Hyperthermia

Therapeutically, hyperthermia focuses mainly on heating the cancer cells up to a temperature range of 41–46 °C to elevate the therapeutic efficiency for cancer therapy. Magnetic hyperthermia treatment requires heat to improvise the temperature which is generated by MNPs that are finely dispersed in a physiological solution exposed to an alternating magnetic field (AMF) (Habib et al. 2008). The process where magnetic energy is transformed by MNPs to heat energy is observed by different magnetic class of nanoparticles like ferrimagnetic, ferromagnetic, and superparamagnetic states; however, heating efficiency can be tuned by various parameters like magnetic anisotropy, saturation magnetization apart from tailoring the size of MNPs, and magnetic field characteristics (Hervault and Thanh 2014; Obaidat et al. 2014; Deka et al. 2018). Therefore, the main concern regarding this treatment is the use of suitable nanoparticles. Forthwith several types of studies based on magnetic hyperthermia treatment have been carried out. The condition for successful implementation of hyperthermia as an alternate cancer treatment lies in the appropriate design of the MNPs with tunable properties for a safer and better efficient cancer therapy. For hyperthermia treatment, MNPs must be biocompatible, nonimmunogenic, cell acceptance, and in particular, having the ability to produce effective heating profiles after being exposed to AMF. In this regard, iron oxide-based spinel ferrites and their nanocomposites are a group of promising materials that are being commonly used for magnetic hyperthermia treatment (Kozissnik et al. 2013; Gutiérrez and Alvarez 2018).

9.4.1.1 Mechanisms for Heat Generations

When MNPs are placed under AMF, magnetic energy is dissipated in the form of thermal energy. The loss of thermal energy in MNPs caused by the AMF can occur by means of several mechanisms, like eddy current, hysteresis, and relaxation. A reasonable bit of each mechanism is mostly associated with the size, and magnetic anisotropy of the MNPs, along with the fluid viscosity, used for the measurement of heat being released (Shaterabadi et al. 2018).

(a) Eddy Current Loss

Following the law of induction, when an AMF is applied on the MNPs, the time varying magnetic flux will induce circular currents called Eddy currents and heating occurs due to these induced currents which flow opposing the applied magnetic field H . This results in a loss of magnetic energy as heat. The power density due to Eddy current loss formulated by Goldman (2006),

$$P_e = KB_m^2 f^2 d^2 / \rho$$

where K is a sample geometry-dependent factor, B_m denotes the maximum magnetic induction, f denotes the frequency, d denotes the smallest dimension transverse to the magnetic flux and ρ denotes the resistivity.

For nanomaterials, the eddy current loss is extremely small as MNPs have significantly poor electrical conductivity to generate a sizeable induction heating (Suriyanto and Kumar 2017).

(b) Hysteresis Loss

Hysteresis losses mainly occur in large-sized multidomain MNPs (ferrimagnetic/ferromagnetic materials). When the MNPs are subjected to an external magnetic field, the domains with magnetic moments parallel to magnetic field will grow, while the domains with moments aligned opposite will shrink. Such domain wall displacement will continue till the moments of each domains are aligned along the applied magnetic field and saturation magnetization is reached. When the AMF is removed, the magnetization does not vanish completely, and this is called remanent magnetization or remanence (M_r). The magnetization, M of a ferrimagnet/ferromagnet plotted against the applied magnetic field, H traces out a loop, called hysteresis loop, characterized by the coercivity (H_c) and remanence (M_r) of the material is displayed in Fig. 9.7. An amount of energy is required to rotate the magnetic moments from one favorable direction to another unfavorable direction, and this energy is released as heat when the magnetic moment reverts back to a low energy state. The area of the hysteresis loop is directly proportional to the energy released as heat during one complete cycle of the applied magnetic field. The power dissipated per hysteresis cycle can be described by the equation

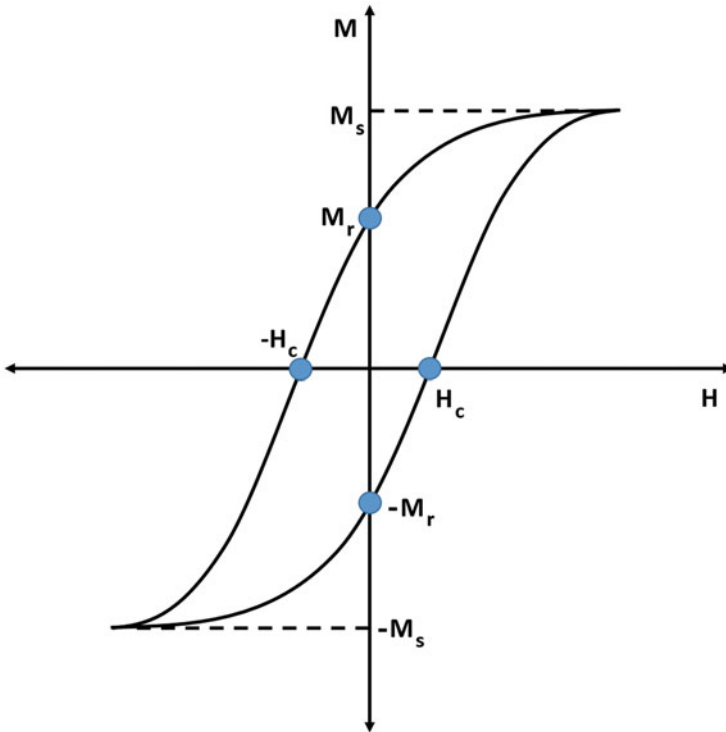


Fig. 9.7 Hysteresis loop of ferri/ferromagnetic materials

$$P_H = \mu_0 f \oint H dM$$

where μ_0 is the magnetic permeability of free space and f is the frequency of applied magnetic field. The loop integral is over the hysteresis loop.

(c) Relaxation Loss

When the size of the MNPs is smaller than the superparamagnetic limit, the anisotropy energy of the MNPs might become smaller than the thermal energy, $k_B T$. At this stage, the particle moment starts rotating freely along all directions which leads to zero net magnetization without an externally applied magnetic field. Consequently, heat dissipation from the MNPs is mainly caused by the delay in the relaxation process of the magnetic moments either through the rotation of the moments within the MNPs, surmounting the magnetic anisotropy barrier (Néel relaxation) or through the rotation of the MNPs itself that creates frictional losses within the system (Brownian relaxation), when the MNPs are exposed to an external AMF with different magnetic field reversal times. The schematic representations of these relaxation processes are displayed in Fig. 9.8. The Néel (τ_N) and Brownian (τ_B) relaxation times of the MNPs are given by the following equations (Shaterabadi et al. 2018).

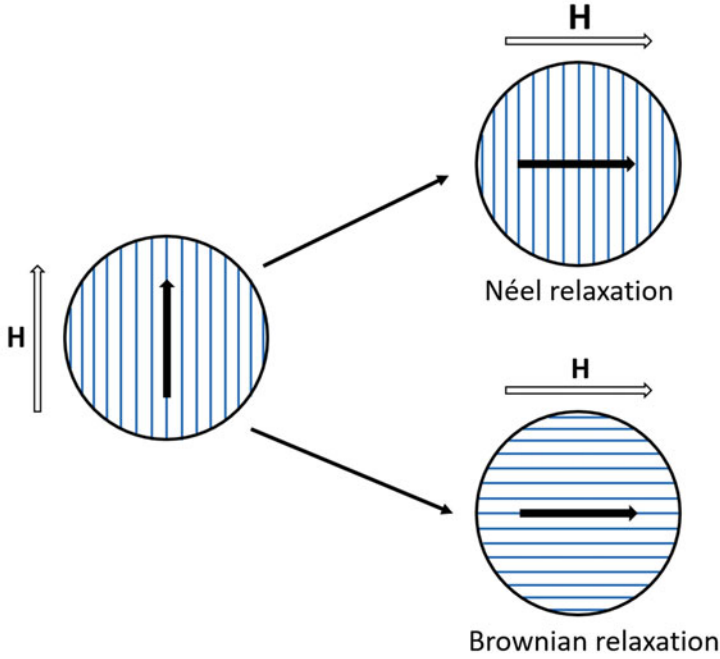


Fig. 9.8 Schematic representation of relaxation process in MNPs

$$\tau_N = \frac{\tau_0}{2} \sqrt{\frac{\pi k_B T}{K_{\text{eff}} V}} \exp\left(\frac{K_{\text{eff}} V}{k_B T}\right)$$

$$\tau_B = \frac{3\eta V_H}{k_B T}$$

where the factor $\tau_0 \approx 10^{-9}$ s, K_{eff} is the effective anisotropy, V is the volume of the MNPs, k_B is the Boltzmann constant, T is the temperature, η is the coefficient of viscosity of the liquid containing the MNPs and V_H is the hydrodynamic volume of the MNPs.

From the above-mentioned equations, it is obvious that the magnetic relaxation time depends on the particle diameters. For smaller particle, the predominant mechanism is the Néel relaxation process, whereas beyond a specific critical size limit, the dominant mechanism is the Brownian relaxation process (Ludwig et al. 2013). When both Néel and Brownian relaxations are assumed to occur simultaneously for the sizes close to the critical size range, the characteristic relaxation or effective relaxation time τ_{eff} can be expressed by the following relation

$$\frac{1}{\tau_{\text{eff}}} = \frac{1}{\tau_{\text{N}}} + \frac{1}{\tau_{\text{B}}}$$

Nonetheless, the τ_{eff} is predominated by the shorter relaxation time (τ_{N} or τ_{B}).

(d) Specific Absorption Rate (SAR)

During the hyperthermia treatment, the affected cell is heated from inside and out. To enhance the heat generation from the MNPs, it requires a high concentration of the MNPs at the affected cell site, and at present, it is only attainable by direct infusion of the MNPs into the affected cell. The power of heat dissipation by the MNPs under the influence of external AMF with field strength H and frequency f is formulated by Rosensweig (2002) and is given by

$$P = \mu_0 \pi \chi'' f H^2$$

where μ_0 denotes the magnetic permeability of free space and χ'' denotes the imaginary part of magnetic susceptibility $\chi = \chi' - i\chi''$ and can be expressed as the following

$$\chi'' = \left[\frac{\omega \tau}{1 + (\omega \tau)^2} \right] \chi_0$$

where χ_0 denotes the equilibrium susceptibility and $\omega = 2\pi f$ and τ denotes the effective relaxation time.

The heating efficiency of the MNPs is typically represented by the specific power loss (SLP), also known as specific absorption rate (SAR), measured in watts per gram, and is expressed as

$$\text{SLP}(f, H) = \frac{P}{\rho} = \frac{\mu_0 \pi \chi'' f H^2}{\rho}$$

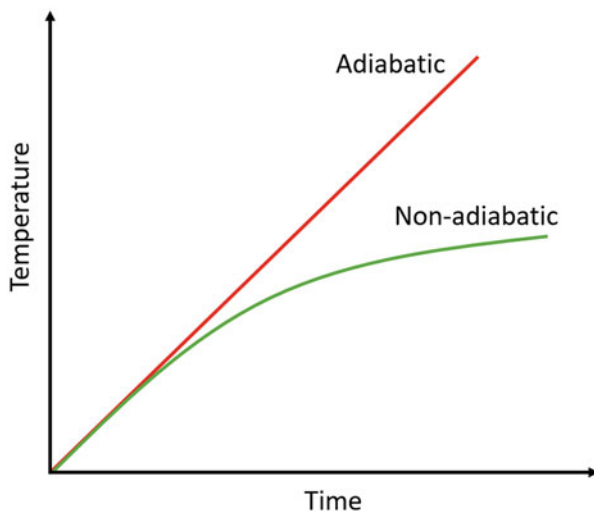
where ρ denotes the mass density of the MNPs.

Despite the fact, the used field parameters play a pivotal role for the outcome in SLP. It is difficult to directly compare the SLP values measured with different groups of varying field parameters. Therefore, in order to have a good comparison, Kallumadil et al. (2009) proposed a scheme to measure intrinsic loss power (ILP), which is defined as the normalized SLP to the f and H^2 dependence, and can be expressed as,

$$\text{ILP} = \frac{\text{SLP}(f, H)}{f H^2}$$

Estimating SLP values under adiabatic condition through calorimetry gives the best definite values even though it demands highly sophisticated instruments compared to different methods. Adiabatic magnetothermal arrangement to determine the SLP values was only reported by Natividad et al. 2011. To

Fig. 9.9 Temperature versus time graph for adiabatic and nonadiabatic setup



perform such experiment, it requires a vacuum proof defenders for the samples to be kept. These kinds of setups give a better temperature control because of the metallic shielding, but on the other hand, large dimensional adiabatic system is required where the samples are kept which may limit the generation of alternating magnetic field. Therefore, this high-tech sophisticated setup confines the approach for SLP measurement under adiabatic calorimetry conditions. In adiabatic conditions, setup prohibits the heat to be transferred between the MNPs and their surrounding environments. Therefore, the total heat generated by the MNPs is contributed to the rise in temperature. In this model, the sample temperature T depends on the power P and the heat capacity C contributed by the MNPs.

$$P = C \frac{dT(t)}{dt}$$

Figure 9.9 shows the temperature versus time graph of adiabatic setup. In adiabatic condition, there is increase in temperature with the applied alternating magnetic field producing a linear heating curve. However, unlike in adiabatic setups, in nonadiabatic systems, the samples start to lose their heat energy to their surrounding environment immediately when the temperature of the sample rises beyond the temperature of the surrounding, and thus produces a nonlinear heating curve, as displayed in Fig. 9.9. Huang et al. (2012) and Wang et al. (2013) addressed the potential sources of errors with the nonadiabatic arrangements during the SLP measurements. Furthermore, Wildeboer et al. (2014) reported the significance of precise SLP measurements and reassessed few potential errors of measurements. They proposed a slope corrected rate determination method which provides more accurate SLP values using nonadiabatic setups than the most widely employed initial slope method.

9.4.1.2 Properties Influencing the Heat Generation

(a) Particle Size Effect

In determining the heat generation and the relaxation times by the MNPs, the particles are assumed to be of the same sizes. Heat dissipation in MNPs is mainly generated through the basic mechanisms like hysteresis loss, Néel, and Brownian relaxations. But, the dominance of these mechanisms depends greatly on the size of MNPs. In actual practice, the size distribution of MNPs is broad and usually extends from single domain to multidomain and synthesizing of MNPs with adequately narrow size distribution, exhibiting only one distinct reversal mechanism, is not an easy task to achieve. There are only few studies to precisely grasp the particle size distribution effect on MNPs heating efficiency. Hergt et al. (2008) demonstrated that the field amplitude and frequency strongly depend on the mean size as well as on the variance of the MNPs. They proposed that MNPs with narrow size distribution and having mean size corresponding to the maximum H_c within the range of single domain could produce optimum heating efficiency. Therefore, in order to achieve optimum heating efficiency, narrow size distribution as well as the mean particle size should be optimized concerning the field amplitude and frequency. In their recent work, Gupta and Sharma (2019) have reported the possibility of tuning the magnetic properties of Fe_3O_4 MNPs by manipulating the size using a biosurfactant agent as stevioside (a natural plant-based glycoside). These biosurfactant enhanced the hyperthermic efficiency by reducing the particle size which is essential for hyperthermia cancer treatment. Further, this study was carried out in vitro on rat C6 glioma cells which showed the efficiency of cell death at 43 °C after 30 min.

(b) Anisotropy Effect

It is well established that the various forms of anisotropy like magnetocrystalline anisotropy, surface anisotropy, shape anisotropy, and exchange anisotropy influence the magnetic properties of the materials. Numerous studies revealed that magnetic anisotropy is the key factor controlling the heating of the MNPs (Kolhatkar et al. 2013; Mehdaoui et al. 2013; Obaidat et al. 2015). Through theoretical modeling, it was revealed that the magnetic anisotropy varies inversely with the MNPs sizes (Habib et al. 2008). Hence, the size at which the MNPs generate maximum heating power decreases as the magnetic anisotropy constant increases. Carrey et al. (2011) approximated the optimum anisotropy to generate maximum heating that can be analytically calculated using their proposed model. They proposed that the magnetic anisotropy should become the central parameter in the experimental investigations for magnetic hyperthermia. However, it is also crucial to mention that depending on several other factors, the magnetic anisotropy can lead to increased or decreased heating efficiencies of MNPs (Verde et al. 2012; Obaidat et al. 2015). Researchers reported that the heating efficiency depends on morphology (shape anisotropy) of the nanoparticles. Simeonidis et al. (2013) found out that similar size, cubic iron oxide particles have superior magnetic heating efficiency compared to spherical nanoparticles. Again, Lee et al. (2011) reported that the anisotropy of the exchange coupled core-shell nanoparticle can be tuned for efficient

self-heating response. Recently, Darwish et al. (2020) synthesized eight different types of bi-magnetic core shell of ferrite MNPs. They explained that synthesized core-shell MNP structures improved the properties of heating efficiency with applied field. Especially, tuning the properties of synthesized core-shell MNPs, the SLP at specific diameter can be improved and used for hyperthermia treatment.

(c) Dipolar Interactions Effect

Ferrofluids are frequently described as coated single-core magnetic particles, homogeneously dispersed in a medium and exhibiting uniform distances between the single cores. However, in reality, particularly when the MNPs are injected into the body, agglomeration takes place due to the interparticle or dipolar interactions between the single cores. As the interparticle distance decreases with agglomeration or increased particle concentration, the dipolar interaction increases, and hence, increasing dipolar interactions are likely to influence the magnetic relaxations and thus affecting the heating response of the MNPs. The Néel relaxation process are directly affected by these interactions, which is the principal heat generation mechanism in hyperthermia studies (Piñeiro-Redondo et al. 2011). However, there have been numerous conflicting experimental and theoretical studies describing how increased dipolar interactions influence the relaxation time. Mørup and Tronc (1994) proposed a model predicting the influence of dipolar interactions on the relaxation times of superparamagnetic MNPs. They showed that with decrease in dipolar interactions, the relaxation time decreases. Furthermore, Mehdaoui et al. (2013) investigated the effect of magnetic interactions on the heating efficiency with same size MNPs but with varying anisotropy. The authors reported that strong dipolar interactions can arrange the MNPs in the form of chains with uniaxial anisotropy leading to maximum SAR value. Piñeiro-Redondo et al. (2011) revealed that with increased dipolar interactions, the Néel relaxation time increases resulting in decreased SAR values for coated magnetite samples; however, the authors also showed enhanced heating efficiency for the bare magnetite samples with increase in particle concentration, consequently increasing dipolar interactions. They suggested that the coated samples can alter hydrodynamic size modifying the Brownian relaxation time. In case of the bare MNPs, the dipolar interactions are strong even when the concentrations were low, while MNPs tend to aggregate at higher concentrations. Their work summarizes conflicting role of dipolar interactions on the heating efficiency of MNPs. The role of interparticle interactions on the heating efficiency were also investigated recently in core-shell iron-iron oxide MNPs by manipulating the dipolar interactions between the core and shell of the MNPs (Simeonidis et al. 2020). Their study revealed that samples having noncoherent reversal are more adequate to generate large SAR values because nontrivial magnetization reversal reduces the dipolar interactions which eventually diminish the possibility of agglomeration. In a recent study, it has been reported that dipolar interaction plays a significant role in self-heating behavior of the MNPs for hyperthermia study (Jamir et al. 2020). They showed that surface functionalization of

magnetite with organic polymers leads to reduced dipolar interaction which significantly enhances the heating ability of the MNPs.

9.4.2 Drug Delivery

Traditional cancer therapy approaches show various limitations which include small and unspecified outcomes and hence low efficiency individualizing between good and affected cancer cells. Current developments for nanotechnology have introduced innovative therapeutic nanomaterials that avail to benefit various targeting approaches. Utilizing nanotechnology in medicine, particularly drug delivery have advanced promptly over the past few years. Presently, myriad MNPs are under research for drug delivery systems, which involve study in cancer treatment. Functionalized MNPs used in drug delivery system might include drugs anticipated to be delivered into infectious cells involving sensors and actuators that manipulate and control the drug delivery system. The external magnetic force can influence the magnetic properties of MNPs. Therefore, during the drug delivery mechanism, the MNPs are coerced to magnetic carriers in which the drug localized is based on the conflict among the force implemented on the charge carriers by blood cells and generated magnetic forces from the magnet.

Ferrites-based MNPs with a surrounding layer of polymers have been comprehensively used in treatments due to their high tolerance in regards with organic solvents, low toxicity and better bioavailability as compared with free drugs (Subramani and Ahmed 2018). The PVP-coated MnFe_2O_4 MNPs was studied by Wang et al. (2018). These MNPs have high drug-loading capacity of doxorubicin hydrochloride (DOX) and the loaded drug exhibited remarkable release character with pH sensitivity, favorable for the prevention of quick release of anticancer drug. Again, chitosan-cross-linked carboxymethyl- β -cyclodextrin-modified magnetite (Fe_3O_4) displayed a promising approach for high efficiency of inclusion capacity for antitumor drug delivery in cancer treatment (Liu et al. 2012). Jose et al. (2020) studied a novel application of ZnFe_2O_4 and Ag-substituted ZnFe_2O_4 on drug delivery. They loaded the MNPs with an anticancer drug, Curcumin coated with casein micelle to make the compounds less toxic allowing the MNPs to flow freely in the blood cells. They developed an efficient pH-sensitive drug delivery mechanism for higher drug concentration for targeting the malignant cells.

9.4.3 Magnetic Resonance Imaging

Among the various techniques, magnetic resonance imaging (MRI) is a predominant technique in detecting the location and allocating cells in noninvasive way. Advantages of using MRI is that it has higher spatial resolution and finer tissue contrast. The mechanism of MRI is set on minimizing the longitudinal/transverse relaxations times T_1 and T_2 respectively based on H_2O protons. Therefore, when a steady magnetic field is applied to the affected cells, these H_2O protons are aligned

along the direction of the applied field and using computer software, the resulting images of internal structures are depicted under resonance effect. The contrast agents, T_1 is used in blood pool imaging and T_2 in extracellular agents for biomedical treatment. Many studies have been performed in order to enhance resolution and contrast of MRI, therefore, MNPs are used to improve the contrast agents.

The drawback of MRI technique is that it gives sensitive low signals; however, it can be prevented by using MNPs to improve the signals. Fe_3O_4 MNPs has been studied as the signal enhancer in MRI (Jun et al. 2005). In this work, they have reported that the magnetism and induced MRI signals correlates with the size of nanocrystals and showed excellent MRI contrast agents for cancer diagnosis. Furthermore, many researchers have explored several ferrites with modulated properties for MRI applications. Vecchione et al. (2017) studied using lecithin stabilized nanoemulsions packed with $\text{Co}_{0.5}\text{Fe}_{2.5}\text{O}_4$ nanocubes and they observed that contrast agents were found to be based on the nanoemulsions concentrations. In vivo study was also carried out in Melanoma-bearing C57BL/6 male which was injected with MNPs where a time-dependent accumulation was established in the affected parenchyma. A similar study on TAMRA-coated $\text{CoFe}_2\text{O}_4/\text{MnFe}_2\text{O}_4$ MNPs by Zhang et al. (2017) proposed that MNPs ultimately enhances the contrast agents in MRI at the side of affected tumor so that the maximum variation in T_2 weighted value was detected at 12 h postinjection of MNPs. They also did a combined study for MRI and fluorescent labeling in vivo using tumor-bearing female BALB/c mice as well as in vitro using MGC-803 human gastric cell line. Faraji et al. (2019) reported that highly stable PEG-coated manganese ferrite (MnFe_2O_4) at pH near the physiological pH range showed enhanced MRI contrast effect as well as good biocompatible behavior.

9.5 Conclusions

In this chapter, we have gone through the basic properties related to the spinel ferrite MNPs along with some milestones achieved by these MNPs in the field of biomedical applications. Over the past few years, numerous physical, chemical and preclinical research strategies have been proposed by the researchers and pharma industries into the development of high-quality spinel ferrite-based MNPs, which can be tailored for magnetic hyperthermia treatments, MRI and targeted drug delivery in the field of nanomedicine. However, cost-effective synthesis of sizable amount of ferrite MNPs for biomedical applications requires additional research. Moreover, applications of spinel ferrites in different biomedical fields are prominent, although the toxicity of some spinel ferrites should be carefully weighed well before commercialization or usage on a larger extent. In reality, synthesizing large amount of spinel ferrites with all the optimal properties remains an active area of research. Lastly, some challenges still need to be considered regarding the use of spinel ferrites as an alternative cancer treatment. One of the most important challenges is the lack of human trials in these fields. Researchers and pharmaceutical industries are still reliant on animal trials concerning the risks involved in the human trials.

References

- Abdel Maksoud MIA, El-Sayyad GS, Ashour AH et al (2018) Synthesis and characterization of metals-substituted cobalt ferrite [$M_xCo_{(1-x)}Fe_2O_4$; ($M = Zn, Cu$ and Mn ; $x = 0$ and 0.5)] nanoparticles as antimicrobial agents and sensors for Anagrelide determination in biological samples. *Mater Sci Eng C* 92:644–656. <https://doi.org/10.1016/j.msec.2018.07.007>
- Adeela N, Khan U, Naz S et al (2018) Role of Ni concentration on structural and magnetic properties of inverse spinel ferrite. *Mater Res Bull* 107:60–65. <https://doi.org/10.1016/j.materresbull.2018.06.032>
- Alghamdi N, Stroud J, Przybylski M et al (2020) Structural, magnetic and toxicity studies of ferrite particles employed as contrast agents for magnetic resonance imaging thermometry. *J Magn Magn Mater* 497:165981. <https://doi.org/10.1016/j.jmmm.2019.165981>
- Amiri M, Salavati-Niasari M, Akbari A (2019) Magnetic nanocarriers: evolution of spinel ferrites for medical applications. *Adv Colloid Interf Sci* 265:29–44. <https://doi.org/10.1016/j.cis.2019.01.003>
- Andersen HL, Saura-Múzquiz M, Granados-Miralles C et al (2018) Crystalline and magnetic structure–property relationship in spinel ferrite nanoparticles. *Nanoscale* 10:14902–14914. <https://doi.org/10.1039/C8NR01534A>
- Bean CP, Jacobs IS (1956) Magnetic granulometry and super-paramagnetism. *J Appl Phys* 27:1448–1452. <https://doi.org/10.1063/1.1722287>
- Bean CP, Livingston JD (1959) Superparamagnetism. *J Appl Phys* 30:S120–S129. <https://doi.org/10.1063/1.2185850>
- Beveridge JS, Stephens JR, Williams ME (2011) The use of magnetic nanoparticles in analytical chemistry. *Annu Rev Anal Chem* 4:251–273. <https://doi.org/10.1146/annurev-anchem-061010-114041>
- Bozorth RM (1936) Determination of ferromagnetic anisotropy in single crystals and in polycrystalline sheets. *Phys Rev* 50:1076–1081. <https://doi.org/10.1103/PhysRev.50.1076>
- Brown WF (1963) Thermal fluctuations of a single-domain particle. *Phys Rev* 130:1677–1686. <https://doi.org/10.1103/PhysRev.130.1677>
- Carregal-Romero S, Caballero-Díaz E, Beqa L et al (2013) Multiplexed sensing and imaging with colloidal nano- and microparticles. *Annu Rev Anal Chem* 6:53–81. <https://doi.org/10.1146/annurev-anchem-062012-092621>
- Carrey J, Mehdaoui B, Respaud M (2011) Simple models for dynamic hysteresis loop calculations of magnetic single-domain nanoparticles: application to magnetic hyperthermia optimization. *J Appl Phys* 109:083921. <https://doi.org/10.1063/1.3551582>
- Carta D, Casula MF, Falqui A et al (2009) A structural and magnetic investigation of the inversion degree in ferrite nanocrystals MFe_2O_4 ($M = Mn, Co, Ni$). *J Phys Chem C* 113:8606–8615. <https://doi.org/10.1021/jp901077c>
- Cobos MA, de la Presa P, Llorente I et al (2020) Effect of preparation methods on magnetic properties of stoichiometric zinc ferrite. *J Alloys Compd* 849:156353. <https://doi.org/10.1016/j.jallcom.2020.156353>
- Coe JMD (2010) Magnetism and magnetic materials, 1st edn. Cambridge University Press, Delhi
- Concas G, Spano G, Cannas C et al (2009) Inversion degree and saturation magnetization of different nanocrystalline cobalt ferrites. *J Magn Magn Mater* 321:1893–1897. <https://doi.org/10.1016/j.jmmm.2008.12.001>
- Cotton FA, Wilkinson G (1974) Advanced inorganic chemistry, 1st edn. Wiley, New York
- Cullity BD, Graham CD (2009) Introduction to magnetic materials, 2nd edn. Wiley, New York
- Darwish MSA, Kim H, Lee H et al (2020) Engineering core-shell structures of magnetic ferrite nanoparticles for high hyperthermia performance. *Nano* 10:1–16. <https://doi.org/10.3390/nano10050991>
- Deka S, Saxena V, Hasan A et al (2018) Synthesis, characterization and in vitro analysis of $\alpha-Fe_2O_3-GdFeO_3$ biphasic materials as therapeutic agent for magnetic hyperthermia applications. *Mater Sci Eng C* 92:932–941. <https://doi.org/10.1016/j.msec.2018.07.042>

- Dippong T, Goga F, Levei EA, Cadar O (2019) Influence of zinc substitution with cobalt on thermal behaviour, structure and morphology of zinc ferrite embedded in silica matrix. *J Solid State Chem* 275:159–166. <https://doi.org/10.1016/j.jssc.2019.04.011>
- Dobson P (2012) Nanomedicine: design and applications of magnetic nanomaterials, nanosensors and Nanosystems, by Vijay K. Varadan, Linfeng Chen and Jining Xie. *Contemp Phys* 53:1. <https://doi.org/10.1080/00107514.2012.686521>
- Faraji S, Dini G, Zahraei M (2019) Polyethylene glycol-coated manganese-ferrite nanoparticles as contrast agents for magnetic resonance imaging. *J Magn Magn Mater* 475:137–145. <https://doi.org/10.1016/j.jmmm.2018.11.097>
- Gilleo MA (1960) Superexchange interaction in ferrimagnetic garnets and spinels which contain randomly incomplete linkages. *J Phys Chem Solids* 13:33–39. [https://doi.org/10.1016/0022-3697\(60\)90124-4](https://doi.org/10.1016/0022-3697(60)90124-4)
- Goldman A (2006) *Modern ferrite technology*. Springer, New York
- Gupta R, Sharma D (2019) Biofunctionalization of magnetite nanoparticles with stevioside: effect on the size and thermal behaviour for use in hyperthermia applications. *Int J Hyperth* 36:302–312. <https://doi.org/10.1080/02656736.2019.1565787>
- Gutiérrez TJ, Alvarez VA (2018) Nanoparticles for hyperthermia applications. In: *Handbook of nanomaterials for industrial applications*. Elsevier, Amsterdam, pp 563–576. <https://doi.org/10.1016/B978-0-12-813351-4.00032-8>
- Habib AH, Ondeck CL, Chaudhary P et al (2008) Evaluation of iron-cobalt/ferrite core-shell nanoparticles for cancer thermotherapy. *J Appl Phys* 103:1–4. <https://doi.org/10.1063/1.2830975>
- Han X, Liu S, Huo X et al (2020) Facile and large-scale fabrication of (Mg,Ni)(Fe,Al)₂O₄ heterogeneous photo-Fenton-like catalyst from saprolite laterite ore for effective removal of organic contaminants. Elsevier B.V., Amsterdam
- Harris VG, Šepelák V (2018) Mechanochemically processed zinc ferrite nanoparticles: evolution of structure and impact of induced cation inversion. *J Magn Magn Mater* 465:603–610. <https://doi.org/10.1016/j.jmmm.2018.05.100>
- Hergt R, Dutz S, Röder M (2008) Effects of size distribution on hysteresis losses of magnetic nanoparticles for hyperthermia. *J Phys Condens Matter* 20:385214. <https://doi.org/10.1088/0953-8984/20/38/385214>
- Hergt R, Dutz S, Zeisberger M (2010) Validity limits of the Néel relaxation model of magnetic nanoparticles for hyperthermia. *Nanotechnology* 21:015706. <https://doi.org/10.1088/0957-4484/21/1/015706>
- Hernández-Gómez P, Valente MA, Graça MPF, Muñoz JM (2018) Synthesis, structural characterization and broadband ferromagnetic resonance in Li ferrite nanoparticles. *J Alloys Compd* 765:186–192. <https://doi.org/10.1016/j.jallcom.2018.06.172>
- Hervault A, Thanh NTK (2014) Magnetic nanoparticle-based therapeutic agents for thermochemotherapy treatment of cancer. *Nanoscale* 6:11553–11573. <https://doi.org/10.1039/c4nr03482a>
- Huang S, Wang S-Y, Gupta A et al (2012) On the measurement technique for specific absorption rate of nanoparticles in an alternating electromagnetic field. *Meas Sci Technol* 23:035701. <https://doi.org/10.1088/0957-0233/23/3/035701>
- Jamir M, Islam R, Pandey LM, Borah JP (2020) Effect of surface functionalization on the heating efficiency of magnetite nanoclusters for hyperthermia application. *J Alloys Compd* 854:157248. <https://doi.org/10.1016/j.jallcom.2020.157248>
- Jiles D (1991) *Introduction of magnetism and magnetic materials*, 1st edn. Springer, New Delhi
- Jose R, Rinita J, Jothi NSN (2020) Synthesis and characterisation of stimuli-responsive drug delivery system using ZnFe₂O₄ and Ag_{1-x}Zn_xFe₂O₄ nanoparticles. *Mater Technol* 36:1–9. <https://doi.org/10.1080/10667857.2020.1758481>
- Jun YW, Huh YM, Choi JS et al (2005) Nanoscale size effect of magnetic nanocrystals and their utilization for cancer diagnosis via magnetic resonance imaging. *J Am Chem Soc* 127:5732–5733. <https://doi.org/10.1021/ja0422155>

- Kallumadil M, Tada M, Nakagawa T et al (2009) Suitability of commercial colloids for magnetic hyperthermia. *J Magn Magn Mater* 321:1509–1513. <https://doi.org/10.1016/j.jmmm.2009.02.075>
- Karakas İH (2020) The effects of fuel type onto the structural, morphological, magnetic and photocatalytic properties of nanoparticles in the synthesis of cobalt ferrite nanoparticles with microwave assisted combustion method. *Ceram Int*. <https://doi.org/10.1016/j.ceramint.2020.10.144>
- Kojima H (1982) *Handbook of Ferromagnetic Materials*, vol 3, pp 305–391. [https://doi.org/10.1016/S1574-9304\(05\)80091-4](https://doi.org/10.1016/S1574-9304(05)80091-4)
- Kolhatkar AG, Jamison AC, Litvinov D, Willson RC, Lee TR (2013) Tuning the magnetic properties of nanoparticles. *Int J Mol Sci* 14:15977–16009. <https://doi.org/10.3390/ijms140815977>
- Kozissnik B, Bohorquez AC, Dobson J, Rinaldi C (2013) Magnetic fluid hyperthermia: advances, challenges, and opportunity. *Int J Hyperth* 29:706–714. <https://doi.org/10.3109/02656736.2013.837200>
- Krishnan KM (2016) *Fundamentals and applications of magnetic materials*, 1st edn. Oxford University Press, New York
- Laurent S, Dutz S, Häfeli UO, Mahmoudi M (2011) Magnetic fluid hyperthermia : focus on superparamagnetic iron oxide nanoparticles. *Adv Colloid Interf Sci* 166:8–23. <https://doi.org/10.1016/j.cis.2011.04.003>
- Lazarević ZŽ, Sekulić DL, Ivanovski VN, Romčević NŽ (2015) A structural and magnetic investigation of the inversion degree in spinel NiFe_2O_4 , ZnFe_2O_4 and $\text{Ni}_{0.5}\text{Zn}_{0.5}\text{Fe}_2\text{O}_4$ ferrites prepared by soft mechanochemical synthesis. *Int J Mater Metall Eng* 9:1014–1018
- Lee JH, Jang JT, Choi JS et al (2011) Exchange-coupled magnetic nanoparticles for efficient heat induction. *Nat Nanotechnol* 6:418–422. <https://doi.org/10.1038/nnano.2011.95>
- Lee J-H, Kim J, Levy M et al (2014) Magnetic nanoparticles for ultrafast mechanical control of inner ear hair cells. *ACS Nano* 8:6590–6598. <https://doi.org/10.1021/nn5020616>
- Liu XL, Fan HM, Yi JB et al (2012) Optimization of surface coating on Fe₃O₄ nanoparticles for high performance magnetic hyperthermia agents. *J Mater Chem* 22:8235–8244. <https://doi.org/10.1039/c2jm30472d>
- Ludwig F, Eberbeck D, Löwa N et al (2013) Characterization of magnetic nanoparticle systems with respect to their magnetic particle imaging performance. *Biomed Tech Eng* 58:535. <https://doi.org/10.1515/bmt-2013-0013>
- Mathew DS, Juang RS (2007) An overview of the structure and magnetism of spinel ferrite nanoparticles and their synthesis in microemulsions. *Chem Eng J* 129:51–65. <https://doi.org/10.1016/j.cej.2006.11.001>
- Mehdaoui B, Tan RP, Meffre A et al (2013) Increase of magnetic hyperthermia efficiency due to dipolar interactions in low-anisotropy magnetic nanoparticles: theoretical and experimental results. *Phys Rev B* 87:174419. <https://doi.org/10.1103/PhysRevB.87.174419>
- Mørup S, Tronc E (1994) Superparamagnetic relaxation of weakly interacting particles. *Phys Rev Lett* 72:3278–3281. <https://doi.org/10.1103/PhysRevLett.72.3278>
- Natividad E, Castro M, Mediano A (2011) Adiabatic magnetothermia makes possible the study of the temperature dependence of the heat dissipated by magnetic nanoparticles under alternating magnetic fields. *Appl Phys Lett* 98:1–4. <https://doi.org/10.1063/1.3600633>
- Nigam A, Pawar SJ (2020) Structural, magnetic, and antimicrobial properties of zinc doped magnesium ferrite for drug delivery applications. *Ceram Int* 46:4058–4064. <https://doi.org/10.1016/j.ceramint.2019.10.243>
- Obaidat IM, Issa B, Haik Y (2014) Magnetic properties of magnetic nanoparticles for efficient hyperthermia. *Nano* 5:63–89. <https://doi.org/10.3390/nano5010063>
- Obaidat I, Issa B, Haik Y (2015) Magnetic properties of magnetic nanoparticles for efficient hyperthermia. *Nano* 5:63–89. <https://doi.org/10.3390/nano5010063>

- Pankhurst QA, Connolly J, Jones SK, Dobson J (2003) Applications of magnetic nanoparticles in biomedicine. *J Phys D Appl Phys* 36:R167–R181. <https://doi.org/10.1088/0022-3727/36/13/201>
- Piñero-Redondo Y, Bañobre-López M, Pardiñas-Blanco I et al (2011) The influence of colloidal parameters on the specific power absorption of PAA-coated magnetite nanoparticles. *Nanoscale Res Lett* 6:383. <https://doi.org/10.1186/1556-276X-6-383>
- Ravichandran M, Velumani S (2020) Manganese ferrite nanocubes as an MRI contrast agent. *Mater Res Exp* 7:016107. <https://doi.org/10.1088/2053-1591/ab66a4>
- Rocha-Santos TAP (2014) Sensors and biosensors based on magnetic nanoparticles. *TrAC Trends Anal Chem* 62:28–36. <https://doi.org/10.1016/j.trac.2014.06.016>
- Rosenzweig A (1970) Localized canting model for substituted ferrimagnets. I. Singly substituted YIG systems. *Can J Phys* 48:2857–2867. <https://doi.org/10.1139/p70-356>
- Rosensweig RE (2002) Heating magnetic fluid with alternating magnetic field. *J Magn Magn Mater* 252:370–374. [https://doi.org/10.1016/S0304-8853\(02\)00706-0](https://doi.org/10.1016/S0304-8853(02)00706-0)
- Shaterabadi Z, Nabiyouni G, Soleymani M (2018) Physics responsible for heating efficiency and self-controlled temperature rise of magnetic nanoparticles in magnetic hyperthermia therapy. *Prog Biophys Mol Biol* 133:9–19. <https://doi.org/10.1016/j.pbiomolbio.2017.10.001>
- da Silva FG, Depuyrot J, Campos AFC et al (2019) Structural and magnetic properties of spinel ferrite nanoparticles. *J Nanosci Nanotechnol* 19:4888–4902. <https://doi.org/10.1166/jnn.2019.16877>
- Simeonidis K, Martinez-Boubeta C, Balcells L et al (2013) Fe-based nanoparticles as tunable magnetic particle hyperthermia agents. *J Appl Phys* 114:103904. <https://doi.org/10.1063/1.4821020>
- Simeonidis K, Martinez-Boubeta C, Serantes D et al (2020) Controlling magnetization reversal and hyperthermia efficiency in core–shell iron–iron oxide magnetic nanoparticles by tuning the interphase coupling. *ACS Appl Nano Mater* 3:4465–4476. <https://doi.org/10.1021/acsnm.0c00568>
- Smart JS (1955) The Néel theory of ferrimagnetism. *Am J Phys* 23:356–370. <https://doi.org/10.1119/1.1934006>
- Smit J, Winj HP (1959) *Ferrites*, 1st edn. Cleaver-Hume Press, London
- Somvanshi SB, Kharat PB, Khedkar MV, Jadhav KM (2020) Hydrophobic to hydrophilic surface transformation of nano-scale zinc ferrite via oleic acid coating: magnetic hyperthermia study towards biomedical applications. *Ceram Int* 46:7642–7653. <https://doi.org/10.1016/j.ceramint.2019.11.265>
- Spaldin NA (2010) *Magnetic materials fundamentals and applications*, 2nd edn. Cambridge University Press, New York
- Stoner EC, Wohlfarth EP (1948) A mechanism of magnetic hysteresis in heterogeneous alloys. *Phil Trans R Soc Lond Ser A Math Phys Sci* 240:599–642. <https://doi.org/10.1098/rsta.1948.0007>
- Subramani K, Ahmed W (2018) Chapter 17 - Nanoparticulate drug-delivery systems for oral cancer treatment. In: Subramani K, Ahmed W (eds) *Emerging nanotechnologies in dentistry*, 2nd edn. William Andrew Publishing, New York, pp 355–370
- Suriyanto NEYK, Kumar SD (2017) Physical mechanism and modeling of heat generation and transfer in magnetic fluid hyperthermia through Néelian and Brownian relaxation: a review. *Biomed Eng Online* 16:36. <https://doi.org/10.1186/s12938-017-0327-x>
- Tatarchuk T, Bououdina M, Judith Vijaya J, John Kennedy L (2017) Spinel ferrite nanoparticles: synthesis, crystal structure, properties, and perspective applications. *Springer Proc Phys* 195:305–325. https://doi.org/10.1007/978-3-319-56422-7_22
- Tokunaga Y, Furukawa N, Sakai H et al (2009) Composite domain walls in a multiferroic perovskite ferrite. *Nat Mater* 8:558–562. <https://doi.org/10.1038/nmat2469>
- Topkaya R, Baykal A, Demir A (2013) Yafet-Kittel-type magnetic order in Zn-substituted cobalt ferrite nanoparticles with uniaxial anisotropy. *J Nanoparticle Res* 15:1359. <https://doi.org/10.1007/s11051-012-1359-6>

- Trukhanov AV, Trukhanov SV, Kostishyn VG et al (2018) Correlation of the atomic structure, magnetic properties and microwave characteristics in substituted hexagonal ferrites. *J Magn Magn Mater* 462:127–135. <https://doi.org/10.1016/j.jmmm.2018.05.006>
- Uchida K, Nonaka T, Kikkawa T et al (2013) Longitudinal spin Seebeck effect in various garnet ferrites. *Phys Rev B* 87:104412. <https://doi.org/10.1103/PhysRevB.87.104412>
- Valenzuela R (2012) Novel applications of ferrites. *Phys Res Int* 2012:591839. <https://doi.org/10.1155/2012/591839>
- Vecchione R, Quagliariello V, Giustetto P et al (2017) Oil/water nano-emulsion loaded with cobalt ferrite oxide nanocubes for photo-acoustic and magnetic resonance dual imaging in cancer: in vitro and preclinical studies. *Nanomed Nanotechnol Biol Med* 13:275–286. <https://doi.org/10.1016/j.nano.2016.08.022>
- Verde EL, Landi GT, Carrião MS et al (2012) Field dependent transition to the non-linear regime in magnetic hyperthermia experiments: comparison between maghemite, copper, zinc, nickel and cobalt ferrite nanoparticles of similar sizes. *AIP Adv* 2:032120. <https://doi.org/10.1063/1.4739533>
- Wang S-Y, Huang S, Borca-Tasciuc D-A (2013) Potential sources of errors in measuring and evaluating the specific loss power of magnetic nanoparticles in an alternating magnetic field. *IEEE Trans Magn* 49:255–262. <https://doi.org/10.1109/TMAG.2012.2224648>
- Wang G, Zhao D, Ma Y et al (2018) Synthesis and characterization of polymer-coated manganese ferrite nanoparticles as controlled drug delivery. *Appl Surf Sci* 428:258–263. <https://doi.org/10.1016/j.apsusc.2017.09.096>
- Wang Y, Zou L, Qiang Z et al (2020) Enhancing targeted cancer treatment by combining hyperthermia and radiotherapy using Mn–Zn ferrite magnetic nanoparticles. *ACS Biomater Sci Eng* 6:3550–3562. <https://doi.org/10.1021/acsbiomaterials.0c00287>
- Wildeboer RR, Southern P, Pankhurst QA (2014) On the reliable measurement of specific absorption rates and intrinsic loss parameters in magnetic hyperthermia materials. *J Phys D Appl Phys* 47:495003. <https://doi.org/10.1088/0022-3727/47/49/495003>
- Willard MA, Nakamura Y, Laughlin DE, Mchenry ME (1999) Magnetic properties of ordered and disordered spinel-phase ferrimagnets. *J Am Ceram Soc* 46:3342–3346
- Yafet Y, Kittel C (1952) Antiferromagnetic arrangements in ferrites. *Phys Rev* 87:290–294. <https://doi.org/10.1103/PhysRev.87.290>
- Zhang Q, Yin T, Gao G et al (2017) Multifunctional Core@Shell magnetic nanoprobe for enhancing targeted magnetic resonance imaging and fluorescent labeling in vitro and in vivo. *ACS Appl Mater Interfaces* 9:17777–17785. <https://doi.org/10.1021/acsmi.7b04288>
- Zhang H, Wang J, Zeng Y et al (2020) Leucine-coated cobalt ferrite nanoparticles: synthesis, characterization and potential biomedical applications for drug delivery. *Phys Lett A* 384:126600. <https://doi.org/10.1016/j.physleta.2020.126600>

Part III

Surface Engineering of Polymeric Biomaterials



Functionalized 3D Bioactive Polymeric Materials in Tissue Engineering and Regenerative Medicine

10

Anushree Pandey, Asif Ali, Nikhil Ram Patra, and Yuvraj Singh Negi

Abstract

The three-dimensional (3D) analogs of the extracellular matrix (ECM) have gained noteworthy attention in current years, owing to their promising tissue regeneration tendency and cell proliferative ability. The three-dimensional scaffolds perform an essential role of basic skeleton in regenerative medicine. They provide mechanical integrity and support to the regenerating tissue to help with cell adhesion, cell proliferation, and cell differentiation. A scaffold is needed to regain functionality or regenerate the tissue, which acts as a substitute matrix for cell proliferation as well as the extracellular deposition of the matrix, with subsequent growth till the time the tissues have fully regained and/or regenerated. Conducting substrates of polymer render the potential to electrically stimulate the scaffolds and also augment the regeneration of electroactive tissue like nerve and muscle significantly. Electrically conductive scaffolds are fabricated using solvent casting, particle leaching process, electrospinning of polymer-conductive mixtures with extra polymers, and performing polymer deposition on template scaffolds. On conducting scaffolds, bioactive molecules are also immobilized, which allows the scaffolds multifunctional tissue engineering clues. In addition, the relations between the neural and cardiac cells and the conducting scaffolds were also analyzed in this chapter. Consequently, processing and tissue engineering technologies of conducting scaffolds can significantly affect tissue engineering and other bio-related fields.

A. Pandey · A. Ali · N. R. Patra · Y. S. Negi (✉)

Department of Polymer and Process Engineering, Indian Institute of Technology, Roorkee, Uttarakhand, India

© The Author(s), under exclusive license to Springer Nature Singapore Pte Ltd. 2022

L. M. Pandey, A. Hasan (eds.), *Nanoscale Engineering of Biomaterials: Properties and Applications*, https://doi.org/10.1007/978-981-16-3667-7_10

257

Keywords

Functionalized 3D bioactive polymeric materials · Biomaterials for tissue engineering · Conducting polymers · Poly(lactic-*co*-glycolic) acid · Poly (L-lactic acid) · Nerve regeneration

10.1 Introduction

Implantable 3D scaffolds are employed to repair and reconstruct diverse structural disorders in large and functioning organs. The scaffolds include a structure to repair defects, while encouraging cell connection, extracellular matrix (ECM) proliferation vessel development, regeneration, nerves, joints, bones, etc. Scaffolds are elastic, fibrous, or permeable biomaterials in three dimensions (3D), intended to enable the transportation of liquids and gases from the body, fostering cell deposition of relationships, viability, and extracellular matrix of low inflammation and toxicity, though at some stage with controlled biodegradation. The artificial substance covered with various tissue grafts is called alloplasty. The biologically active alloplasty scaffolds guarantee the tissue help, which often act as a transport mechanism for bioactive compounds (cytokines, medicines, toxins, enzymes) and provide templates for the attachment of genetically transduced cells to build fresh regeneration and morphogenesis centers for tissues.

Three-dimensional (3D) biomaterial scaffolds used for tissue engineering can be chemically composed of natural ceramics, metals, and glass-ceramics and organic, hybrid polymers. More recently, the emphasis has been on biodegradable biomaterials, which should not be explanted in an individual. Every biomaterial has its own unique chemical, physical, and technical properties, while the transmission and control power form 3D, including geometry. The preference of production methods depends on the unique scaffolding criteria, anything of concern, and limits on machines (Chia and Wu 2015). Computer-aided concept development (computer-aided design, CAD) tools and rapid prototyping enable for the development of objects with a macro- (size and form overall), micro- (size of the pores, form, interconnection, and distribution), and nanoarchitecture at times. The configuration of the scaffold should be individualized for the patient data preparing specific 3D model of some porosity or vasculature systems, consistent with various biomaterials and those molecules. The use of 3D printers has revolutionized the regenerative approach for treatment.

Most of the works have recently been undertaken to establish a collection of novel biomaterials and composites with improved viability of the cells, cell proliferation, and printability, exhibiting several important characteristics. For example, biomimicry approach provides organization of numerous cellular components (such as growth factors, ECM proteins, hormones, etc.) to imitate a living tissue to enhance cell signaling or ECM creation (Jammalamadaka and Tappa 2018). Biomimetic scaffolds are also used to supply medicinal substances, such as enzymes, growth factors, drugs, and so forth, and the anchoring of these items onto the

scaffold is critically important. It is noteworthy that interactions between biomaterial and cells are important to cell viability, proliferation, and differentiation, and for the overall tissue growth. Thus, biomaterial characteristics, for example, surface chemistry, charge, ruggedness, reactivity, and hydrophilicity, have to be carefully tailored, based on specific application (Hasan and Pandey 2015). The aim here through this review is to provide in-depth insights into implantable scaffolds for both in vitro and in vivo performances.

10.1.1 Requirements for a 3D Scaffold

A scaffold architecture requires physicochemical (surface composition, biodegradation, porosity, etc.), mechanical (elastic modulus, stiffness, etc.), and synthetic (vascularization, cell adhesion, etc.) properties, specifications for biocompatibility, etc. and issues related to sterilization and viability of commercialization. Enhancing the 3D scaffolding bioactivity and features serving as engineered structures or the form, height, power, porosity, and degradation of matrix rate is easily regulated. Those regeneration models have been planned in the past few years, it has evolved. The affected tissue required to fix the scaffold will be built and produced in a manner close to that of an anatomical framework and physical and biomechanical emulation of initial clothing. It is the 3D scaffold which can withstand the external pressures and loads induced by the creation of fresh tissues preserving technical assets similar to those of the local landscape material (Engler et al. 2006). Biomaterials may be degraded on the surface or bulk. Unlike the bulk degeneration which breaks the internal structure, the bulk structure of the material is maintained by surface degradation. Degradation rate should match the growth of the tissue without separating toxic by-products. The basic geometry of the scaffold shall retain a porous or fibrous design and further provides a high ratio of surface area to volume for cell attachment and the development of materials. Nerve fibers are closely related spatially to cells expressing the receptor for neuropeptides and shall be developed simultaneously with a new fabric, to control homeostasis. The peripheral distribution is typically in the human body, the nerves and blood vessels follow one another's development, since they are anatomically linked and affect the growth and evolution of each other (Feng et al. 2015). As the production of multitissue is still difficult to control, autologous neurovascular forms of microsurgical bundles combined during scaffold implantation are possible concepts for improving the scaffolding efficiency (Marrella et al. 2018).

A cascade of biological events, following the injury migration of stem cells, chemokine, and the secretion of the growth factor, is used to repair the tissue destroyed. Scaffolds could mimic those processes, stimulated and organized by the addition of diverse bioactive products' mobility like genes, peptides, aptamers (single oligonucleotide resistance), growth factors, antibodies, drugs, or even ECM.

10.2 Functionalized 3D Bioactive Polymeric Materials

Bioactivity refers to a material's potential to affect its biological environs. The concept was first described by Langer and Vacanti in the 1990s, as three-dimensional "tissue engineering." Ever since (3D) has been historically organized, biomaterial-based scaffolds were employed to create a bioactive environment where the cells adhere to as well as proliferate (Langer and Vacanti 1993). At the time, 3D scaffolds were tested for a broad spectrum of applications from nerve regeneration, bone regeneration, regeneration of the ligament/tendon, muscle regeneration, to even extra (Lee et al. 2015a, b, 2014).

In the direction of creating these polymer scaffolds, natural and synthetic biomaterials have become well known, due in major part to their vastness of bioactivity and property diversity (Pişkin 1995; "Natural and Synthetic Biomedical Polymers - 1st Edition n.d.; Shelke et al. 2014). Indigenous natural polymers are the first biodegradable materials used for scaffolding clinically, since they have stronger average experiences with different cell types and inadequate immune response. Yet industrial synthetic polymers, they were later made cheaper and allowed a better functionality in view of the need for industrial polymers in specific, immune reaction or injuriousness with the usage of polymer combinations (Dhandayuthapani et al. 2011). Among the synthetic polymers, poly(glycolic acid) (PGA), poly(L-lactic acid) (PLLA), poly(lactic-co-glycolic) acid (PLGA), and poly(caprolactone) (PCL) are presently the utmost prevalent for the establishment of 3D macromolecular structures in the custom of making biodegradable scaffolds (Müller et al. 2006; Narayanan et al. 2014; Shelke et al. 2014). Such polymers are also used along with the carbon polymers to improve hydrophilicity-based unfavorable problems, attachment of cells, and biodegradability. What's more, the scaffolding surfaces are regulated with different ligands like protein molecules which assist to improve cellular response.

A three-dimensional scaffold is currently anticipated to show a least of the subsequent three design features for cell room and the transfer and linkage of minerals, mechanical properties appropriate for the envisioned use, and in the directive for biocompatibility preventing an inappropriate immune response (Holzwarth and Ma 2011). A big benefit of using 3D tissue engineering scaffolds is the mechanical power capacity to work, speed of degradation, and cellular adhesion. There is a wide selection of various methods for keeping the scaffold usable, the maximum of which hinge on the content query. External surface alteration to enhance appropriate cell proliferation molecules has remained to be used with numerous versatile polymeric materials. Such as, copolymerization using the similar monomers was employed to render polymeric functional scaffolds for the promotion of cell adhesion to resolve restrictions of the parent polymer (Liu et al. 2012). Additional benefit about the functionality stays in the manufacturing technology, like three-dimensional printing, microparticles' electro-spinning, and hydrogel, can cause a lot of dissimilar things such as the cell adhesion, rate of degradation, and mechanical properties.

3D structures produced in the system of nanofibers by electrospinning are one of the most commonly used styles of scaffolds and were proved to be particularly useful in imitating the extracellular climate, excellently because of their larger surface area-to-volume ratios, mechanical properties, great porosity, and a distribution of size of the pores present (Lee et al. 2015b). Within such scaffolds, both the alignment and diameter of the fabricated fibers are exploited to get dissimilar responses at the cellular level relying on the application (Lee et al. 2007). Scaffolds made from 3D hydrogel are often commonly used because of its distinctive, stimuli properties, and its remarkable aptitude to preserve the innovative structure well. In addition, dynamic representatives like growth, using hydrogel scaffold features, may be unconfined at a specific required rate, because of their forces of encapsulation of bioactive agents (Zhu and Marchant 2011; Shelke et al. 2016). Besides those approaches, scaffolds made using PLLA, PLGA micro-particles, and their mixtures with natural polymers are widespread because of their ability to lessen the ruin of numerous compressed biological macromolecules with the capacity to release molecules for drawn-out time limits (Chau et al. 2008; Sahoo et al. 2005; García Cruz et al. 2008; Lasprilla et al. 2012).

10.3 Synthetic/Natural Biomaterials Actively Assisting in Tissue Engineering

10.3.1 Poly(L-Lactic Acid)

Poly(L-lactic acid) is a biologically degradable, organic polyester derived from poly-L-lactide polymerization, produced from green energy materials like starch, and has a broad range of uses, including as sutures, medication distribution tubes, prosthetics, skin, arterial grafts, bone, screws' scaffold reconstruction, and fastening pins (Kronenthal et al. 1975). Another instance of a Food and Drug Administration (FDA)-approved PLLA drug is Sculptra™, which is a commonly used injectable for treating facial atrophy (Narins et al. 2009). Poly(L-lactic acid) often degrades to nontoxic by-products and can be blended easily with other materials, making their use common (Hule and Pochan 2007). Although PLLA has a faster degradation rate, it is still considered to be relatively slow compared to PCL via bulk degradation, compared to other polymeric biomaterials employed in tissue scaffolding (Shasteen and Choy 2011). PLLA also has a large degree of crystallinity in its fragments, which may result in the deterioration of redness in the physique and often combined with additional polymers to create three-dimensional scaffolds (Lasprilla et al. 2012). Fukushima and Kimura, whose PLLA is developed as a result of the intermingling of L-lactic acid and D,L-lactic acid as D, L-lactic acid more swiftly and without high crystallinity and inflammation, have proven to solve the dilemma and enable greater bioactivity (Fukushima and Kimura 2008).

One example of an inflammatory scaffold composite PLLA requirement for reductions is illustrated in Fig. 10.2, demonstrating the surface morphology of poly(L-lactic acid)—Rg3 nanofiber matrix utilizing the surface electron microscopy

(SEM) technique. Thus, synthesized fibers displayed pure poly(L-lactic acid) (a), poly(L-lactic acid) with 2% of Rg3 (b), 6% Rg3 (c) poly(L-lactic acid), and 10% Rg3 (d) poly(L-lactic acid) respectively. Rg3, a renowned blemish reduction compound, has the function of all PLLA-linked inflammation counteractors and requires a quicker regeneration of the skin (Cui et al. 2013). It can be observed that in nature the fibers are fairly even and infiltrate the scaffold pores for cell use. Including electrospinning, other approaches include three-dimensional printing, and the solvent print casting may be employed to achieve nontoxic bioactivity of blended PLLA enhanced scaffolds.

10.3.2 Poly(Lactic-co-Glycolic) Acid

Poly(lactic-co-glycolic) acid (PLGA) is a mixture of PLLA and PGA polymers and is among one of the most ordinarily produced tissue engineering synthetic biodegradable polymers. The higher the PGA ratio inside a PLGA scaffold the more it is required to degrade rapidly. Its degradation by-products, glycolic and lactic acid, are nontoxic (Göpferich 1996). The use of PLGA has been popular for a number of causes: being adaptable, biological degradability, and configuration of a dissimilar variety of formulation, and the surface alteration for anticipated targeted drug delivery (Danhier et al. 2012). One case approved by the FDA is Osteofoam™ scaffold for bone tissue engineering, which shows a close 3D morphology to the trabecular bone in humans and cell colonization was seen to enable (Holy et al. 1997; Ishaug et al. 1997).

Sadly, PLGA, being a very widely used polymer, has one major drawback that restricts its use. Its biodegradation by-products are predicted to be highly acidic, thus, in larger quantities, can rapidly be precisely problematic for their metabolization in the human body (Kerimoğlu and Alarcin n.d.). It may be a concern particularly for medicine delivery systems, in the presence of active acids. Many studies have attempted to mitigate the consequences of PLGA depletion by-products of the core drawback. One conventionally prevalent solution is to adjust the proportion specifically for PGA:PLLA, in such a way that there is a higher amount for PGA resulting in a higher rate of degradation, and less acidic by-products all emitted at once. Recently, however, it has been shown that the pH of PLGA by-products may increase in the presence of particular salts, principally to a greater overall bioactivity, especially in relations of applications for distribution filing (Houchin and Topp 2008).

PLGA has been used for the development of nanoparticles and microparticles; 3D drug delivery scaffolds and tissue engineering applications (Locatelli and Franchini 2012; Faisant et al. 2002; Shelke et al. 2016, 2010; Ren et al. 2005; Pavia et al. 2001; Thomson et al. 1995).

10.3.3 Polycaprolactone

The first synthesized, well-recognized polyester material in the 1930s, polycaprolactone (PCL), was extensively used to make 3D scaffolds to be used in tissue engineering. In fact, the nature of PCL is elastic and also possesses the nonpolar methylene group and an ester bond which is semipolar. It is employed differently, including in film, fiber, and as microparticulate. This is used in the production of its bioactive materials' composite material form with other polymers, for example, chitosan and gelatin, for different tissue regeneration applications (Zhang et al. 2005; Gerçek et al. 2008; Kazimoğlu et al. 2003; Alves Da Silva et al. 2010; Yoshimoto et al. 2003; Narayanan et al. 2015). To count its uses in the field of tissue engineering, polycaprolactone is commonly relevant to numerous drug delivery systems and it is approved by the FDA for a lot of diverse pharmaceuticals (Woodruff and Hutmacher 2010). The mechanical use of polyesters has been popularized, since PCL is comparatively more elastic than others (Lowry et al. 1997). Its benefits include good drug permeability across biological membranes, relatively leisurely degradation rate, and lesser by-products of other polyesters that make it useful for drug production in field applications, and tissue engineering in recent years (Ulery et al. 2011).

Polycaprolactone has been observed to be strongly soluble and merge consistently with additional biomaterials (Chandra and Rustgi 1998; Okada n.d.; Arof et al. 1995). Nevertheless, its fairly unhasty degradation cycle (2–4 years) acts as a drawback, rendering it a good short-term market for product scaffolding and growth factor distribution. However, PCL lacks the cellular adhesive properties alone, without any kind of functionality (Cipitria et al. 2011). Numerous methods of enhancing its bioactivity include copolymerization, surface flexibility, and mixing forms to overcome the drawback (Cheng and Teoh 2004). Chang et al. have proved poly(epsilon-caprolactone)/graft/type II collagen/grafted/chondroitin sulfate scaffolds made from the leaching of particulates and PCL topographic alteration which were filled in with collagen type II and chondroitin sulfate used in aiding chondrocyte proliferation (Chang et al. 2010). Proliferation was observed at large cellular intervals throughout the 4-week culture span. Histological staining has identified a large secreted amount of collagen, an essential marker for cellular viability. It has been shown that cells will bear exactly the same phenotype within a porous PCL scaffold as chondrocytes which demonstrate the feasibility of porous PCL scaffolds within native cartilage tissue for its application in tissue engineering and their aptitude to simulate the environment of native tissues (Izquierdo et al. 2007). It is a significant observation to show the tremendous functional ability of PCL scaffolds and the absence of unmodified PCL bioactivity.

10.3.4 Collagen

There are about 29 recognized collagen types that all have different properties and can be extracted for almost all animals on earth like humans. Collagen is embedded in the extracellular matrix and shape in bones with gels or fibers to help tissues

(Parenteau-Bareil et al. 2010). Thanks to the variety of collagens we have designed, and their function in organ growth and help employed as three-dimensional scaffoldings for a number of tissue engineering uses, from rough material similar to the bone to the regeneration of soft tissues, for example, vasculature, cartilage, and nerves (Oliveira et al. 2010; Pang and Greisler 2010; Vickers et al. 2006; Barnes et al. 2007; Ceballos et al. 1999; Aravamudhan et al. 2013). Numerous forms of collagens, namely I, II, III, V, and XI, were verified for application in tissue engineering and regenerative medicine. Form I, by several of these scholars, has been identified by way of “gold standard” of collagen, due to the reduced immune hyperreactivity correlated herewith (Parenteau-Bareil et al. 2010). Furthermore, the collagen gap is a very small characteristic through different host populations, which may contribute to potentially undesired variations within certain engineered scaffolds (Lin and Liu 2006). Additionally, collagen scaffolds may be very challenging to synthesize, but show no major improvements in the credibility of the planned form, as is often sadly the case of fat and nutrition (Parenteau-Bareil et al. 2010). Collagen scaffolds normally display a fairly large number of morphologies of rough soil, due to its fibrous nature and sample structural porosity. Fibrous collagen is compatible as far as the processing methods go, while scaffolding is rendered using the regular electrospinning technique and its rabbit conjunctival fibroblast cells have been shown to proliferate speedier on matched fibrous collagen scaffolds than on random fibrous collagen scaffolds, stressing the manufacturing function system used (Zhong et al. 2006; Aravamudhan et al. 2018). Figure 10.1 illustrates porous scaffolds which are often based on collagen, produced by the solvent casting/particle leaching process, separation of phases, foaming of fuel, melting frozen emulsion, with clusters of fibers. A number of such methods do not require properties of cell-based adhesion, due to the shift of morphology on the earth. The good free form manufacturing has been used and is proven to show more effective cellular adherence (Sachlos et al. 2003). Because the cell attachment over collagen scaffolds is extremely contingent over the biomaterial surface morphology, it is necessary to analyze carefully the manufacturing methodology employed and its optimization.

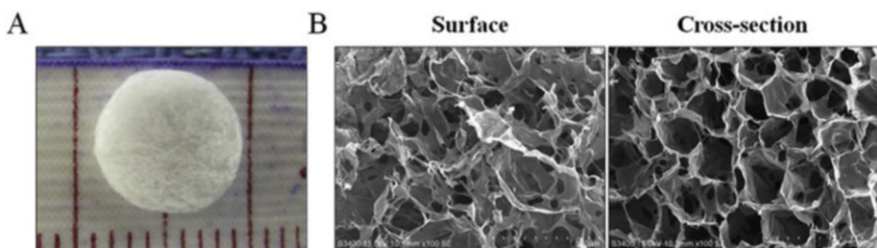


Fig. 10.1 A standard scaffold made from collagen is seen in the above figure, where (a) is a scaffold with a diameter of 8 mm along with a thickness of 2 mm and (b) is an image taken from above the surface (left) from scanning electron microscopy technology and a cross-sectional view of the section in the right. The scaffolds in this image have a pore dimension of around 80 μm approximately and were produced using a lyophilization technique to process the shown highly porous structures. The displayed rough surface morphology is found to be consistent with various type II collagen scaffolds. (Reprinted from Stratton et al. (2016) with permission from Elsevier)

10.3.5 Chitosan Polymer

The chitosan is a biologically degradable linear polysaccharide produced from fractional chitin deacetylation with chemical hydrolysis (Pandey et al. 2021). Chitosan 3D scaffolds showed practical properties and structural characteristics close to those of glycosaminoglycans (GAGs), going on normally as a lubricant inside the human body. It is a real bearing witness to its bioactivity and that it actually encourages except a couple, cellular adhesion without more functionality biomaterials discussed earlier (Chandy and Sharma 1990; Laurencin et al. 2008). Thus, 3D chitosan scaffolds unaided or in blend with other natural polymers are employed in various tissue processing formulations of oil, sponge, or fiber submissions (Croisier and Jérôme 2013). Chitosan has limited its use as a biomaterial with physiological solubility at equilibrium that is beneficial for its application's extended time period (Albanna et al. 2013; Chopra et al. 2006). Therefore, chitosan is considered as a feasible biomaterial for its use in the tissue engineering field in 3D scaffold form (Hasan et al. 2017). In addition, thanks to its multifunctional property chitosan is often blended with structure and ability to crosslink other biomaterials for modifying scaffold properties (Hasan et al. 2018). Chitosan with hyaluronic acid has been observed to have excellent structural efficiency, with collagen type II and GAG positive cartilage staining (Muzzarelli et al. 2012). Likewise, chitosan-polycaprolactone scaffolds employed in tissue engineering display that the bovine chondrocytes adhere to and multiply after 21 days on these three-dimensional scaffolds in vitro (Neves et al. 2011). Nervous regeneration procedures, where collagen chitosan has been proved in arginine-glycine-aspartic acid (RGD)-bearing scaffolds, accelerated a continuous axonal development in 15-mm long rats with nerve defects since 4 months (Xiao et al. 2013).

10.4 Applications of Functionalized 3D Bioactive Polymeric Materials

10.4.1 Neuron Regeneration

While dividing the nervous network into the central nervous system (CNS) and the sympathetic neural network, it is significant to distinguish the differences between them. The former is composed of brain & spinal cord and the latter of ganglia & neurons within the CNS. Tissue research technologies for nerve regeneration have dealt with both systems traditionally (Horner and Gage 2000; Davies et al. 1997; Scheib and Höke 2013). There are a variety of specific problems waiting to be found. But when approached in such a way that in vivo versions will not hold up well, since mice have nerve axons that are narrower and shorter than most functional regeneration in organisms, including the atrophy of target tissues it is hard to accomplish. Because of this cause, more in vivo research of wide animal models close to humans is expected to connect the distance between the abstract and the displayed. The Schwann cells are at the core of peripheral nervous system (PNS) examinations'

rejuvenation processes, regardless of the institutional assistance, and contribute to axonal myelination. So, the three-dimensional scaffolds often employed for applications in nerve rejuvenation must be biologically active, since they have to foster myelination, axonal extension, and systemic reinforcement through Schwann cells. Electrical behavior of polymers has tremendous potential for tissue engineering uses and has been attracting a lot of coverage lately (Guimard et al. 2007). It has been revealed that these electrical stimulations will enhance muscle recovery and nerve, since they are responsive to stimulation from electricity.

Conducting polymers (CPs) have identical electric and optical properties of metal and inorganic semiconductors and reveal the striking properties related to traditional polymers, like synthesis easiness and recovery. This special mix of such polymers has provided such properties a broad variety of microelectronic systems that include battery and photovoltaic power supplies, diode-emitting light and electrochrome screens, and most recently in biotechnology. CPs modulate cellular functions by means of electrical stimulation activities, including adhesion to cells, movement, DNA synthesis, and production of proteins (Foulds and Lowe 1986; Umaña and Waller 1986; Wong et al. 1994; Shi et al. 2004). In fact, some of these experiments included tissues, nerves, bones, and heart cells that respond to electrical interference drives. Most CPs provide significantly numerous benefits for use of biomedicine, which include biocompatibility, locking potential, and controllability of organic molecules' (i.e., reversible doping) escape, power to shift biochemical charge reactions, and the capacity to change electrical, biological, physical, and other properties quickly for the CPs best suited to the complexity of the unique user. Figure 10.2. provides an insight into the use of conductive polymers in various areas of research.

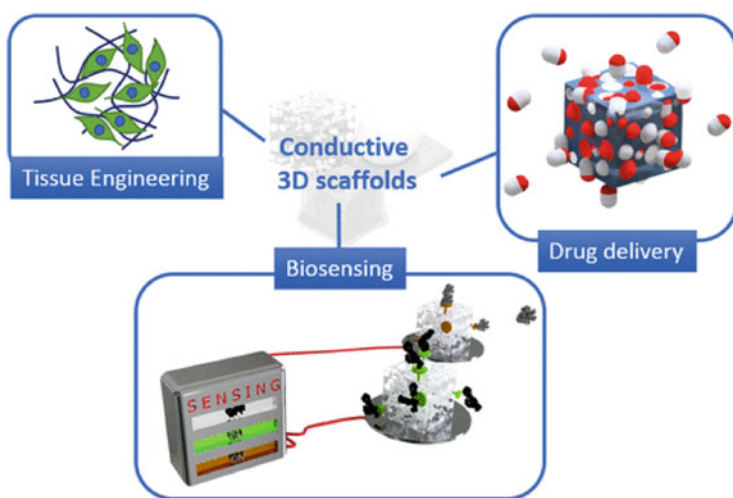


Fig. 10.2 The conductive polymers have a promising role to play in tissue engineering, drug delivery, and biosensing research areas. (Adapted with permission from Alegret et al. (2019). Copyright 2019 American Chemical Society)

Among the previously described 3D structures, nanofibers appear to play a major role in regenerating the nerves, particularly when it comes to nerve guide conduits (NGCs), designed to guide axonal neurite outgrowths. NGCs have several uses which have been documented, for example, the ability to present multifunctional properties aimed at steering axonal development to secrete growth factors from one proximal nerve end tissue repair, and removal of the inhibitory scar tissue to the accident source. Xie et al. reported combining the two in a novel electrospun nanofiber aligned and randomly oriented in a double layer that allows to direct neurite outgrowth *in vitro* when planted earlier with the Schwann cells and also permitted medium to reasonable functional regeneration in a sciatic nerve damage study of 14-mm rats *in vitro*.

10.4.1.1 Functionalization Strategies for the Development of Conducting Polymers

CPs give plenty of benefits, including electrical operation, over other products being the most enchanting land. Yet, there is also the need to refine the content more upon choosing a specific demand. The same specific properties needed for biomedical applications, apart from the conductivity, are biocompatibility and redox stability but further than that require CP amendment that appears to be unique to software. CP for network technology properties, including functionalization of the biomolecule, rugged, hydrophobic, three-dimensional coating geometry, redox stabilization, and abrasion, is perilous. The neural testing implementations for surface fabrics, hydrophobicity, and cell specificities are to boost and hold a strong signal-to-noise level for the neuronal signal identification.

A widespread biological optimization strategy, the features of a CP include the bioactive good molecules. It can be accomplished with numerous techniques that include actual adsorption, clogging, doping, and the covalent fixing of biomolecules' available adsorption body making it simple, but the molecule can be adsorbed, dissociate, and make "inactive" content. One form not covalent is entrapment, which can be done with the molecule you want, the monomer or electrolyte solution, currently throughout summary. The CP doping process, essential to induce conductivity, may be used to alter CPs' noncovalent and the novel properties' introduced application chosen. The possible application of the dopants is in comprehensively providing that the dopant chosen is charged. Additionally, the techniques may be covalently used to allow CPs to function more permanently. It is necessary to synthesize monomer with anticipated functional groups, then polymerization. Covalent alteration too is necessary for postpolymerizing, but further with insoluble polymers challenging. It is really necessary to remember that the steric results of every built-in functional community can interfere with the planarity of the conjugated systems that can sequentially diminish conductivity. CPs are functionalized by various biomolecules that have made engineers in biomedicine change CPs with biological sensor elements, and switch on & off various signaling pathways to build CPs that augment adherence and proliferation among the different types of cells and boost their cells to be biocompatible.

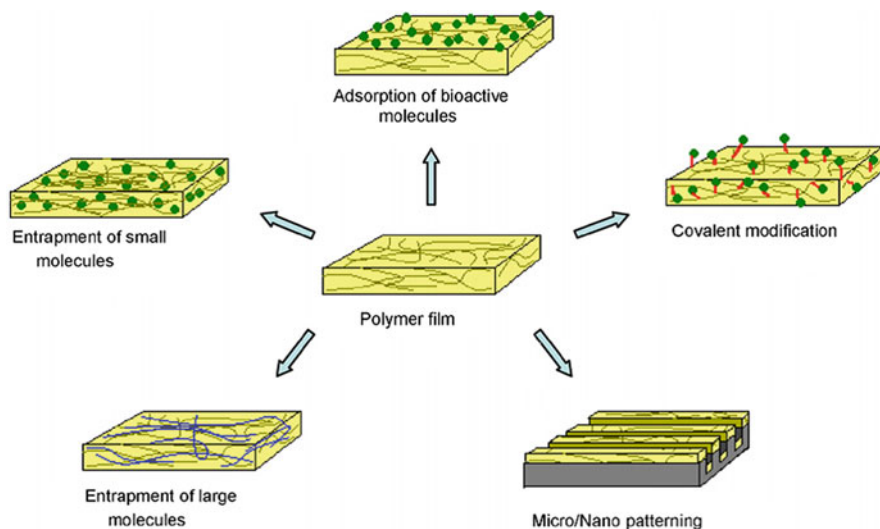


Fig. 10.3 Examples of alteration techniques used in polymer conductions. Chemically and physically, CPs were adjusted using an amount of method as a way of improving bioactivity, conductivity, and topography/spatial geometry. Little typical changes in approaches are seen, including the noncovalent chemical approaches which are trapping and adsorption of molecules, chemical conjugation through covalent bond, and micropatterning by normal lithography methods. (Reprinted from Guimard et al. (2007) with permission from Elsevier)

Equally essential is the understanding of the physical properties of CPs as their chemical electrical properties' composition. Most CPs, for starters, are crystalline and have the porosity reduced. Overcoming weaknesses like crystalline product efforts were made to paint certain CPs with or tie CPs covalently to a more malleable material, For example, polyester (for example, poly(lactic-*co*-glycolic acid)). Figure 10.3. illustrates the guidance of CP properties in general (roughness in topography, porosity, hydrophobicity, mechanical strength, grip, degradability, redox stabilization, conductivity) may be accomplished by the chemical means already described, such as molecules being incorporated as or via dopants' containment or by covalent insertion of highly functional classes within a backbone, can improve conductivity, for example, or make degrading (Guimard et al. 2007). The micropatterning and modification of parameters of synthesis, such as the use of surfactants, temperature, and deposition charges, regulated for CP electrochemical synthesis, where methods were also used to manipulate successfully many physical characteristics.

Needless to mention, the nanofibers continue to be extremely common among NGCs. It was lately revealed that the protein layers composed of silk fibroin and human protein treated with tropoelastin blend display a noteworthy sum of neuritis growth and Schwann cell expansion in vitro region development (White et al. 2015). This latest biodegradable scaffold received both a strong biomaterial portion of silk and a 2.4-fold upsurge in the ability for neurite extension by tropoelastin, relative to

normal poly-D-lysine. NGCs are repeatedly sometimes usable with other proteins like laminin or collagen, which activates the growth of nerve axons and enhances the effective regeneration of nerves (Cao et al. 2013).

Only recently, hydrogels were used as scaffolds for regeneration of the nervous system when studies indicate that scaffolds of this existence can also play a part in assisting axonally dependent Schwann cell restoration. Recently, Tseng et al. 2015 showed that the hydrogels based on chitosan (1.5 kPa rigidity) with proliferating ability and differentiating properties in vitro neuroprogenitors are used for rejuvenation of the central nervous system consuming a model of zebrafish lesion (Tseng et al. 2015).

10.4.2 Bone Regeneration

The artificial polymer frameworks for the purpose of tissue engineering began with the need for bone grafts used historically for treating osteogenic defects (Bose et al. 2012). Already, a move toward nanostructured materials has also been made for bone recovery because of its capacity to trigger changes in the body cells (Li et al. 2013). Among the scaffolding materials, the most famous for hydroxyapatite and β -tricalcium phosphate (β -TCP) is bone regeneration. Thanks to dimensional similarity (β -TCP) and bioactive glass (Damien and Parsons 1991). The benefits of inorganic products, such as these, seem to be big ones dealing with compressive power and possible osteoconductivity (Schmitz et al. 1999).

These compounds are also combined with other biodegradable products and bioactivity polymers. A novel kind of amalgamated framework was introduced by Zhang et al. (2005), who showed that the spongy spiral-structured nanohydroxyapatite/polycaprolactone scaffolds (1:4) created use the adjusted salt leaching and seeding technique for human fetal osteoblasts (hFOBs) for a span of 14 days, when the volume of mineralized extracellular significantly decreased the material matrix. Markers of bone mineralization like bone-sialoprotein, osteonectin, and a type I collagen are tested with reverse polymerase transcriptase, analyzing the moving sequence reaction (Zhang et al. 2014). Figure 10.4. here depicts the bone remodeling using macroporous scaffolds.

10.4.3 Muscular Regeneration

Regeneration of muscle tissues posed some very challenging difficulties, maybe more than both nerves and regeneration of the bone tissue. Such problems are attributed in large part to the reality that scaffolding will all have structural stability which can also cause heavy contraction as well as regeneration of energy. There are three categories of muscles known as cardiac, smooth, and soft. Above everything, the heart muscle tissue is a nonstriated muscle tissue, which is found in the chamber partitions of the heart, mostly in several other organ walls, and in the skeletal muscles the fibers share a distinct skeletal attachment (Kikuchi and Poss 2012).

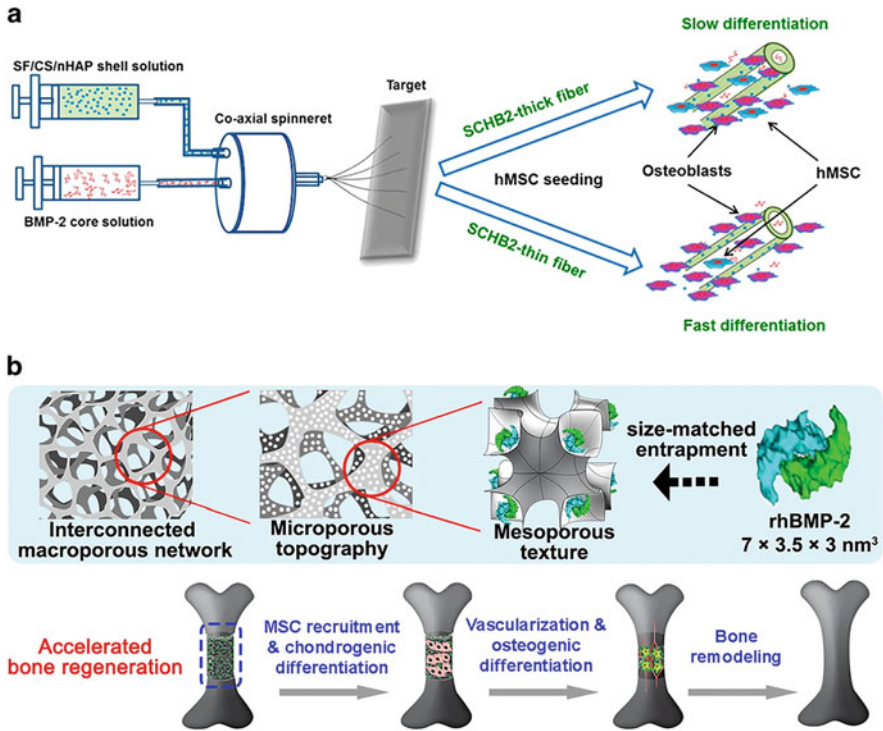


Fig. 10.4 (a) Preparation of SCHB2-thick and SCHB2-thin NFMs through coaxial electrospinning and their influence on hMSCs. (b) Trimodal macro/micro/nanoporous scaffold for accelerated bone regeneration (Yi et al. 2016)

The cardiomyocytes are at the center of heart muscle regeneration, capable of identifying the most essential shapes in cardiac muscle tissues. Cardiomyocytes are normally seeded on scaffolds of gelatin, collagen, alginate, or PGA, though the layering of cell panes in 3D assembly was suggested without synthetic scaffolding, the bioactivity can increase (Shimizu et al. 2003). Peptides such as RGD connection to the scaffold augment cellular activity functions. Neonatal rats have been seen to be cardiac, since the cells seeded on macroporous alginate immobilized in RGD scaffolds facilitated stronger cellular level linkage and acceleration of cardiac tissue regeneration in vitro than unmodified on core patchy scaffolds to alginate (Shachar et al. 2011). Western blotting proved the protein production to be important for the health of cells, like *N*-cadherin, α -actinin, and relaxin-43. Cellular apoptosis, in turn, in RGD-immobilized macropores substantially decreased the alginate scaffolds with respect to the control group. Even support overall is given for the scaffold functionality, especially when it arises to cellular level linking molecules, for instance, vitronectin and fibronectin, which play functions close to RGD (Nikolovski and Mooney 2000).

10.4.4 Tendon/Ligament Regeneration

The tendon refers to the striated muscle tissue mentioned formerly which will not heal really quickly after death, yet sometimes after recovery during the final recovery cycle small accidents will pose difficulties. Therefore, 3D scaffolding is of vital significance for a strengthening of tendons. Traditional methods, like grafts, do not work to bring back the original's technical and technological properties like how the tendon promotes cell proliferation, as well as a variety of through-the-years' alternatives to this problem have been suggested. The tendon extracellular matrix includes primarily type I collagen and is currently the framework itself is fluid and interwoven, rendering it a 3D, biomimetic relatively difficult setting to re-create.

Polymeric materials, including all uses as in tendon regeneration which display extraordinarily powerful mechanical properties, are sometimes used as scaffolds for examples silk and PLGA. It has been stated that when PLGA-silk fibrous scaffolds are employed as basic fibroblast growth factor (bFGF)-releasing structures, it stimulates differentiation of the mesenchymal progenitor cells (MPCs) and in vitro attachment (Sahoo et al. 2010). The bFGF was encapsulated and published with PLGA fibers, while the microfibrillar silk was used for reinforcement. Results displayed a surge in common gene expression in ECM proteins between ligament and tendon, and augmented production of collagen. Many past reports, such as of Ouyang et al. have stated that PLGA trim filled with stromal cells of the bone marrow (bMSCs) stimulates the construction of type I collagen in 10-mm long rabbits' Achilles tendon (AT) in vivo defects which help to restore the innate tendon environment (Ouyang et al. 2003).

Ligaments, mainly consisting of fibroblasts along with collagen types I and III, have attracted interest in thick matrix in tissue engineering because of their perilous duty as the anterior cruciate ligament (ACL) functions in the stabilization of the knees. Since ACL's low healing ability needs outstanding mechanical properties such as stability, polymeric scaffolds include PLLA or silk fibers they were employed to produce various growth factors and impersonate the mechanical ones in the natural tissue condition properties (C. T. Laurencin and Freeman 2005).

10.5 A Viewpoint

Although a variety of problems remain, 3D as organized biomaterial-based scaffolds hold promising future proposals in tissue engineering. When tissue technology appeared, it was previously called science fiction in the 1990s, which has now become truth. Scaffolds are produced using a variety of biomimetic, plastic, and industrial products. The process known as 3D printing provides expectations for potential large manufacturing capacities, perhaps more so than other forms of 3D scaffolding specified. Scaffolding is also quite at the front of growth factors, as the differentiation and cellular proliferation may be brought over at a quicker pace, predominantly where vascularization concerned is hurdle away. Apparently, there are a variety of common approaches to choose between. Ultimately, it would most

definitely be a combination of dissimilar varieties of manufacturing, different development drivers, and specific biomaterials that render the scaffold superior for a really successful user unique, while nerve repair NGCs are, of definition, one of the most common scaffolding systems.

References

- Albanna MZ, Bou-Akl TH, Blowytsky O, Walters HL, Matthew HWT (2013) Chitosan fibers with improved biological and mechanical properties for tissue engineering applications. *J Mech Behav Biomed Mater* 20:217–226. <https://doi.org/10.1016/j.jmbbm.2012.09.012>
- Alegret N, Dominguez-Alfaro A, Mecerreyes D (2019) 3D scaffolds based on conductive polymers for biomedical applications. *Biomacromolecules*. <https://doi.org/10.1021/acs.biomac.8b01382>
- Alves Da Silva ML, Martins A, Costa-Pinto AR, Costa P, Faria S, Gomes M et al (2010) Cartilage tissue engineering using electrospun PCL nanofiber meshes and MSCs. *Biomacromolecules* 11 (12):3228–3236. <https://doi.org/10.1021/bm100476r>
- Aravamudhan A, Ramos DM, Nip J, Harmon MD, James R, Deng M et al (2013) Cellulose and collagen derived micro-nano structured scaffolds for bone tissue engineering. *J Biomed Nanotechnol* 9(4):719–731. <https://doi.org/10.1166/jbn.2013.1574>
- Aravamudhan A, Ramos DM, Nip J, Kalajzic I, Kumbhar SG (2018) Micro-nanostructures of cellulose-collagen for critical sized bone defect healing. *Macromol Biosci* 18(2). <https://doi.org/10.1002/mabi.201700263>
- Arof AK, Subban RHY, Radhakrishna S (1995) Solid state batteries from chitosan based biopolymers. In: *Polymers and other advanced materials*. Springer, New York, pp 539–544. https://doi.org/10.1007/978-1-4899-0502-4_54
- Barnes CP, Pemble CW IV, Brand DD, Simpson DG, Bowlin GL (2007) Cross-linking electrospun type II collagen tissue engineering scaffolds with carbodiimide in ethanol. *Tissue Eng* 13 (7):1593–1605. <https://doi.org/10.1089/ten.2006.0292>
- Bose S, Roy M, Bandyopadhyay A (2012) Recent advances in bone tissue engineering scaffolds. *Trends Biotechnol* 30:546–554. <https://doi.org/10.1016/j.tibtech.2012.07.005>
- Cao J, Xiao Z, Jin W, Chen B, Meng D, Ding W et al (2013) Induction of rat facial nerve regeneration by functional collagen scaffolds. *Biomaterials* 34(4):1302–1310. <https://doi.org/10.1016/j.biomaterials.2012.10.031>
- Ceballos D, Navarro X, Dubey N, Wendelschafer-Crabb G, Kennedy WR, Tranquillo RT (1999) Magnetically aligned collagen gel filling a collagen nerve guide improves peripheral nerve regeneration. *Exp Neurol* 158(2):290–300. <https://doi.org/10.1006/exnr.1999.7111>
- Chandra R, Rustgi R (1998) Biodegradable polymers. *Prog Polym Sci* 23(7):1273–1335. [https://doi.org/10.1016/S0079-6700\(97\)00039-7](https://doi.org/10.1016/S0079-6700(97)00039-7)
- Chandy T, Sharma CP (1990) Chitosan - as a biomaterial. *Biomater Artif Cells Artif Organs* 18 (1):1–24. <https://doi.org/10.3109/10731199009117286>
- Chang KY, Hung LH, Chu IM, Ko CS, Der Lee Y (2010) The application of type II collagen and chondroitin sulfate grafted PCL porous scaffold in cartilage tissue engineering. *J Biomed Mater Res A* 92(2):712–723. <https://doi.org/10.1002/jbm.a.32198>
- Chau DYS, Agashi K, Shakesheff KM (2008) Microparticles as tissue engineering scaffolds: manufacture, modification and manipulation. *Mater Sci Technol* 24(9):1031–1044. <https://doi.org/10.1179/174328408X341726>
- Cheng Z, Teoh SH (2004) Surface modification of ultra thin poly (*ε*-caprolactone) films using acrylic acid and collagen. *Biomaterials* 25(11):1991–2001. <https://doi.org/10.1016/j.biomaterials.2003.08.038>
- Chia HN, Wu BM (2015) Recent advances in 3D printing of biomaterials. *J Biol Eng* 9(1):1–14. <https://doi.org/10.1186/s13036-015-0001-4>

- Chopra S, Mahdi S, Kaur J, Iqbal Z, Talegaonkar S, Ahmad FJ (2006) Advances and potential applications of chitosan derivatives as mucoadhesive biomaterials in modern drug delivery. *J Pharm Pharmacol* 58(8):1021–1032. <https://doi.org/10.1211/jpp.58.8.0002>
- Cipitria A, Skelton A, Dargaville TR, Dalton PD, Huttmacher DW (2011) Design, fabrication and characterization of PCL electrospun scaffolds - a review. *J Mater Chem* 21:9419–9453. <https://doi.org/10.1039/c0jm04502k>
- Croisier F, Jérôme C (2013) Chitosan-based biomaterials for tissue engineering. *Eur Polym J* 49:780–792. <https://doi.org/10.1016/j.eurpolymj.2012.12.009>
- Cui W, Cheng L, Hu C, Li H, Zhang Y, Chang J (2013) Electrospun poly(L-lactide) fiber with ginsenoside Rg3 for inhibiting scar hyperplasia of skin. *PLoS One* 8(7):e68771. <https://doi.org/10.1371/journal.pone.0068771>
- Damien CJ, Parsons JR (1991) Bone graft and bone graft substitutes: a review of current technology and applications. *J Appl Biomater* 2:187–208. <https://doi.org/10.1002/jab.770020307>
- Danhier F, Ansorena E, Silva JM, Coco R, Le Breton A, Pr at V (2012) PLGA-based nanoparticles: an overview of biomedical applications. *J Control Release* 161:505–522. <https://doi.org/10.1016/j.jconrel.2012.01.043>
- Davies SJA, Fitch MT, Memberg SP, Hall AK, Raisman G, Silver J (1997) Regeneration of adult axons in white matter tracts of the central nervous system. *Nature* 390(6661):680–683. <https://doi.org/10.1038/37776>
- Dhandayuthapani B, Yoshida Y, Maekawa T, Kumar DS (2011) Polymeric scaffolds in tissue engineering application: a review. *Int J Polym Sci* 2011:290602. <https://doi.org/10.1155/2011/290602>
- Engler AJ, Sen S, Sweeney HL, Discher DE (2006) Matrix elasticity directs stem cell lineage specification. *Cell* 126(4):677–689. <https://doi.org/10.1016/j.cell.2006.06.044>
- Faisant N, Siepmann J, Benoit JP (2002) PLGA-based microparticles: elucidation of mechanisms and a new, simple mathematical model quantifying drug release. *Eur J Pharm Sci* 15(4):355–366. [https://doi.org/10.1016/S0928-0987\(02\)00023-4](https://doi.org/10.1016/S0928-0987(02)00023-4)
- Feng L, Lingling E, Liu H (2015) The effects of separating inferior alveolar neurovascular bundles on osteogenesis of tissue-engineered bone and vascularization. *Biomed Pap* 159(4):637–641. <https://doi.org/10.5507/bp.2014.050>
- Foulds NC, Lowe CR (1986) Enzyme entrapment in electrically conducting polymers. Immobilisation of glucose oxidase in polypyrrole and its application in amperometric glucose sensors. *J Chem Soc* 82(4):1259–1264. <https://doi.org/10.1039/F19868201259>
- Fukushima K, Kimura Y (2008) An efficient solid-state polycondensation method for synthesizing stereocomplexed poly(lactic acid)s with high molecular weight. *J Polym Sci A Polym Chem* 46(11):3714–3722. <https://doi.org/10.1002/pola.22712>
- García Cruz DM, Escobar Ivirico JL, Gomes MM, G omez Ribelles JL, S anchez MS, Reis RL, Mano JF (2008) Chitosan microparticles as injectable scaffolds for tissue engineering. *J Tissue Eng Regen Med* 2(6):378–380. <https://doi.org/10.1002/term.106>
- Ger ek I, Tiđlı RS, G m şdereliođlu M (2008) A novel scaffold based on formation and agglomeration of PCL microbeads by freeze-drying. *J Biomed Mater Res A* 86A(4):1012–1022. <https://doi.org/10.1002/jbm.a.31723>
- G pferich A (1996) Mechanisms of polymer degradation and erosion. *Biomaterials* 17(2):103–114. [https://doi.org/10.1016/0142-9612\(96\)85755-3](https://doi.org/10.1016/0142-9612(96)85755-3)
- Guimard NK, Gomez N, Schmidt CE (2007) Conducting polymers in biomedical engineering. *Prog Polym Sci* 32:876–921. <https://doi.org/10.1016/j.progpolymsci.2007.05.012>
- Hasan A, Pandey LM (2015) Review: polymers, surface-modified polymers, and self assembled monolayers as surface-modifying agents for biomaterials. *Polym Plast Technol Eng* 54(13):1358–1378. <https://doi.org/10.1080/03602559.2015.1021488>
- Hasan A, Waibhaw G, Tiwari S, Dharmalingam K, Shukla I, Pandey LM (2017) Fabrication and characterization of chitosan, polyvinylpyrrolidone, and cellulose nanowhiskers nanocomposite films for wound healing drug delivery application. *J Biomed Mater Res A* 105(9):2391–2404. <https://doi.org/10.1002/jbm.a.36097>

- Hasan A, Waibhaw G, Saxena V, Pandey LM (2018) Nano-biocomposite scaffolds of chitosan, carboxymethyl cellulose and silver nanoparticle modified cellulose nanowhiskers for bone tissue engineering applications. *Int J Biol Macromol* 111:923–934. <https://doi.org/10.1016/j.ijbiomac.2018.01.089>
- Holy C, Shoichet M, Davies J (1997) Bone marrow cell colonization of, and extracellular matrix expression on, biodegradable polymers. *Cells Mater* 7(3). <https://digitalcommons.usu.edu/cellsandmaterials/vol7/iss3/7>
- Holzwarth JM, Ma PX (2011) 3D nanofibrous scaffolds for tissue engineering. *J Mater Chem* 21:10243–10251. <https://doi.org/10.1039/c1jm10522a>
- Horner PJ, Gage FH (2000) Regenerating the damaged central nervous system. *Nature* 407:963–970. <https://doi.org/10.1038/35039559>
- Houchin ML, Topp EM (2008) Chemical degradation of peptides and proteins in PLGA: a review of reactions and mechanisms. *J Pharm Sci* 97:2395–2404. <https://doi.org/10.1002/jps.21176>
- Hule RA, Pochan DJ (2007) Polymer nanocomposites for biomedical applications. *MRS Bull* 32(4):354–358. <https://doi.org/10.1557/mrs2007.235>
- Ishaug SL, Crane GM, Miller MJ, Yasko AW, Yaszemski MJ, Mikos AG (1997) Bone formation by three-dimensional stromal osteoblast culture in biodegradable polymer scaffolds. *J Biomed Mater Res* 36(1):17–28. [https://doi.org/10.1002/\(SICI\)1097-4636\(199707\)36:1<17::AID-JBM3>3.0.CO;2-O](https://doi.org/10.1002/(SICI)1097-4636(199707)36:1<17::AID-JBM3>3.0.CO;2-O)
- Izquierdo R, Garcia-Giralto N, Rodriguez MT, Cáceres E, García SJ, Gó Mez Ribelles JL et al (2007) Biodegradable PCL scaffolds with an interconnected spherical pore network for tissue engineering. *J Biomed Mater Res* 85:25–35. <https://doi.org/10.1002/jbm.a.31396>
- Jammalamadaka U, Tappa K (2018) Recent advances in biomaterials for 3D printing and tissue engineering. *Journal of Functional Biomaterials* 9(1):22. <https://doi.org/10.3390/jfb9010022>
- Kazimoğlu C, Bölükbaşı S, Kanatlı U, Şenköylü A, Altun NŞ, Babacı C et al (2003) A novel biodegradable PCL film for tendon reconstruction: archilles tendon defect model in rats. *Int J Artif Organs* 26(9):804–812. <https://doi.org/10.5301/IJAO.2008.3035>
- Kerimoğlu O, Alarcin E (n.d.) Poly(lactic-co-glycolic acid) based drug delivery devices for tissue engineering and regenerative medicine. <https://doi.org/10.5222/ankem.2012.086>
- Kikuchi K, Poss KD (2012) Cardiac regenerative capacity and mechanisms. *Annu Rev Cell Dev Biol* 28:719–741. <https://doi.org/10.1146/annurev-cellbio-101011-155739>
- Kronenthal RL, Oser Z, Martin E (eds) (1975) *Polymers in medicine and surgery*. Springer, Boston. <https://doi.org/10.1007/978-1-4684-7744-3>
- Langer R, Vacanti JP (1993) Tissue engineering. *Science* 260(5110):920–926. <https://doi.org/10.1126/science.8493529>
- Lasprilla AJR, Martinez GAR, Lunelli BH, Jardini AL, Filho RM (2012) Poly-lactic acid synthesis for application in biomedical devices - a review. *Biotechnol Adv* 30:321–328. <https://doi.org/10.1016/j.biotechadv.2011.06.019>
- Laurencin CT, Freeman JW (2005) Ligament tissue engineering: an evolutionary materials science approach. *Biomaterials* 26(36):7530–7536. <https://doi.org/10.1016/j.biomaterials.2005.05.073>
- Laurencin C, Jiang T, Kumbar S, Nair L (2008) Biologically active chitosan systems for tissue engineering and regenerative medicine. *Curr Top Med Chem* 8(4):354–364. <https://doi.org/10.2174/156802608783790974>
- Lee SJ, Yoo JJ, Lim GJ, Atala A, Stitzel J (2007) In vitro evaluation of electrospun nanofiber scaffolds for vascular graft application. *J Biomed Mater Res A* 83(4):999–1008. <https://doi.org/10.1002/jbm.a.31287>
- Lee P, Tran K, Chang W, Shelke NB, Kumbar SG, Yu X (2014) Influence of chondroitin sulfate and hyaluronic acid presence in nanofibers and its alignment on the bone marrow stromal cells: cartilage regeneration. *J Biomed Nanotechnol* 10(8):1469–1479. <https://doi.org/10.1166/jbn.2014.1831>
- Lee P, Tran K, Chang W, Fang Y-L, Zhou G, Junka R et al (2015a) Bioactive polymeric scaffolds for osteochondral tissue engineering: *in vitro* evaluation of the effect of culture media on bone marrow stromal cells. *Polym Adv Technol* 26(12):1476–1485. <https://doi.org/10.1002/pat.3680>

- Lee P, Tran K, Zhou G, Bedi A, Shelke NB, Yu X, Kumbar SG (2015b) Guided differentiation of bone marrow stromal cells on co-cultured cartilage and bone scaffolds. *Soft Matter* 11 (38):7648–7655. <https://doi.org/10.1039/c5sm01909e>
- Li X, Wang L, Fan Y, Feng Q, Cui FZ, Watari F (2013) Nanostructured scaffolds for bone tissue engineering. *J Biomed Mater Res A* 101:2424–2435. <https://doi.org/10.1002/jbm.a.34539>
- Lin YK, Liu DC (2006) Comparison of physical-chemical properties of type I collagen from different species. *Food Chem* 99(2):244–251. <https://doi.org/10.1016/j.foodchem.2005.06.053>
- Liu X, Holzwarth JM, Ma PX (2012) Functionalized synthetic biodegradable polymer scaffolds for tissue engineering. *Macromol Biosci* 12:911–919. <https://doi.org/10.1002/mabi.201100466>
- Locatelli E, Franchini MC (2012) Biodegradable PLGA-b-PEG polymeric nanoparticles: synthesis, properties, and nanomedical applications as drug delivery system. *J Nanopart Res* 14:1316. <https://doi.org/10.1007/s11051-012-1316-4>
- Lowry KJ, Hamson KR, Bear L, Peng YB, Calaluce R, Evans ML et al (1997) Polycaprolactone/glass bioabsorbable implant in a rabbit humerus fracture model. *J Biomed Mater Res* 36 (4):536–541. [https://doi.org/10.1002/\(SICI\)1097-4636\(19970915\)36:4<536::AID-JBM12>3.0.CO;2-8](https://doi.org/10.1002/(SICI)1097-4636(19970915)36:4<536::AID-JBM12>3.0.CO;2-8)
- Marrella A, Lee TY, Lee DH, Karuthedom S, Syla D, Chawla A et al (2018) Engineering vascularized and innervated bone biomaterials for improved skeletal tissue regeneration. *Mater Today* 21(4):362–376. <https://doi.org/10.1016/j.mattod.2017.10.005>
- Müller FA, Müller L, Hofmann I, Greil P, Wenzel MM, Staudenmaier R (2006) Cellulose-based scaffold materials for cartilage tissue engineering. *Biomaterials* 27(21):3955–3963. <https://doi.org/10.1016/j.biomaterials.2006.02.031>
- Muzzarelli RAA, Greco F, Busilacchi A, Sollazzo V, Gigante A (2012) Chitosan, hyaluronan and chondroitin sulfate in tissue engineering for cartilage regeneration: a review. *Carbohydr Polym* 89:723–739. <https://doi.org/10.1016/j.carbpol.2012.04.057>
- Narayanan G, Gupta BS, Tonelli AE (2014) Poly(ϵ -caprolactone) nanowebs functionalized with α - and γ -cyclodextrins. *Biomacromolecules* 15(11):4122–4133. <https://doi.org/10.1021/bm501158w>
- Narayanan G, Gupta BS, Tonelli AE (2015) Estimation of the poly (ϵ -caprolactone) [PCL] and α -cyclodextrin [α -CD] stoichiometric ratios in their inclusion complexes [ICs], and evaluation of porosity and fiber alignment in PCL nanofibers containing these ICs. *Data Brief* 5:1048–1055. <https://doi.org/10.1016/j.dib.2015.11.009>
- Narins RS, Coleman WP, Glogau RG (2009) Recommendations and treatment options for nodules and other filler complications. *Dermatol Surg* 35(suppl 2):1667–1671. <https://doi.org/10.1111/j.1524-4725.2009.01335.x>
- Natural and Synthetic Biomedical Polymers - 1st Edition (n.d.). <https://www.elsevier.com/books/natural-and-synthetic-biomedical-polymers/kum-bar/978-0-12-396983-5>. Accessed 1 Aug 2020
- Neves SC, Moreira Teixeira LS, Moroni L, Reis RL, Van Blitterswijk CA, Alves NM et al (2011) Chitosan/poly(ϵ -caprolactone) blend scaffolds for cartilage repair. *Biomaterials* 32 (4):1068–1079. <https://doi.org/10.1016/j.biomaterials.2010.09.073>
- Nikolovski J, Mooney DJ (2000) Smooth muscle cell adhesion to tissue engineering scaffolds. *Biomaterials* 21(20):2025–2032. [https://doi.org/10.1016/S0142-9612\(00\)00079-X](https://doi.org/10.1016/S0142-9612(00)00079-X)
- Okada M (n.d.) Chemical syntheses of biodegradable polymers. www.elsevier.com/locate/ppolysci
- Oliveira SM, Ringshia RA, Legeros RZ, Clark E, Yost MJ, Terracio L, Teixeira CC (2010) An improved collagen scaffold for skeletal regeneration. *J Biomed Mater Res A* 94(2):371–379. <https://doi.org/10.1002/jbm.a.32694>
- Ouyang HW, Goh JCH, Thambyah A, Teoh SH, Lee EH (2003) Knitted poly-lactide-co-glycolide scaffold loaded with bone marrow stromal cells in repair and regeneration of rabbit achilles tendon. *Tissue Eng* 9(3):431–439. <https://doi.org/10.1089/107632703322066615>
- Pandey A, Sauraj A, Negi Y (2021) Synthesis of polygonal chitosan microcapsules for the delivery of amygdalin loaded silver nanoparticles in breast cancer therapy. *Mater Today Proc* 43:3744–3748. <https://doi.org/10.1016/j.matpr.2020.10.988>

- Pang Y, Greisler HP (2010) Using a type I collagen based system to understand cell-scaffold interactions and to deliver chimeric collagen binding growth factors for vascular tissue engineering. *J Investig Med* 58:845. <https://doi.org/10.231/JIM.0b013e3181ee8177>
- Parenteau-Bareil R, Gauvin R, Berthod F (2010) Collagen-based biomaterials for tissue engineering applications. *Materials* 3(3):1863–1887. <https://doi.org/10.3390/ma3031863>
- Pavia DL, Lampman GM, Kriz GS (2001) Introduction to spectroscopy, 3rd edn. Thomson Learning, Boston
- Pişkin E (1995) Review biodegradable polymers as biomaterials. *J Biomater Sci Polym Ed* 6 (9):775–795. <https://doi.org/10.1163/156856295X00175>
- Ren T, Ren J, Jia X, Pan K (2005) The bone formation in vitro and mandibular defect repair using PLGA porous scaffolds. *J Biomed Mater Res A* 74(4):562–569. <https://doi.org/10.1002/jbm.a.30324>
- Sachlos E, Reis N, Ainsley C, Derby B, Czernuszka JT (2003) Novel collagen scaffolds with predefined internal morphology made by solid freeform fabrication. *Biomaterials* 24 (8):1487–1497. [https://doi.org/10.1016/S0142-9612\(02\)00528-8](https://doi.org/10.1016/S0142-9612(02)00528-8)
- Sahoo SK, Panda AK, Labhasetwar V (2005) Characterization of porous PLGA/PLA microparticles as a scaffold for three dimensional growth of breast cancer cells. *Biomacromolecules* 6(2):1132–1139. <https://doi.org/10.1021/bm0492632>
- Sahoo S, Toh SL, Goh JCH (2010) A bFGF-releasing silk/PLGA-based biohybrid scaffold for ligament/tendon tissue engineering using mesenchymal progenitor cells. *Biomaterials* 31 (11):2990–2998. <https://doi.org/10.1016/j.biomaterials.2010.01.004>
- Scheib J, Höke A (2013) Advances in peripheral nerve regeneration. *Nat Rev Neurol* 9:668–676. <https://doi.org/10.1038/nrneurol.2013.227>
- Schmitz JP, Hollinger JO, Milam SB (1999) Reconstruction of bone using calcium phosphate bone cements: a critical review. *J Oral Maxillofac Surg* 57(9):1122–1126. [https://doi.org/10.1016/S0278-2391\(99\)90338-5](https://doi.org/10.1016/S0278-2391(99)90338-5)
- Shachar M, Tsur-Gang O, Dvir T, Leor J, Cohen S (2011) The effect of immobilized RGD peptide in alginate scaffolds on cardiac tissue engineering. *Acta Biomater* 7(1):152–162. <https://doi.org/10.1016/j.actbio.2010.07.034>
- Shasteen C, Choy YB (2011) Controlling degradation rate of poly(lactic acid) for its biomedical applications. *Biomed Eng Lett* 1:163–167. <https://doi.org/10.1007/s13534-011-0025-8>
- Shelke NB, Rokhade AP, Aminabhavi TM (2010) Preparation and evaluation of novel blend microspheres of poly(lactic- co -glycolic)acid and pluronic F68/127 for controlled release of repaglinide. *J Appl Polym Sci* 116(1):366–372. <https://doi.org/10.1002/app.30173>
- Shelke NB, James R, Laurencin CT, Kumbar SG (2014) Polysaccharide biomaterials for drug delivery and regenerative engineering. *Polym Adv Technol*. <https://doi.org/10.1002/pat.3266>
- Shelke NB, Lee P, Anderson M, Mistry N, Nagarale RK, Ma X-M et al (2016) Neural tissue engineering: nanofiber-hydrogel based composite scaffolds. *Polym Adv Technol* 27(1):42–51. <https://doi.org/10.1002/pat.3594>
- Shi G, Rouabhia M, Wang Z, Dao LH, Zhang Z (2004) A novel electrically conductive and biodegradable composite made of polypyrrole nanoparticles and polylactide. *Biomaterials* 25 (13):2477–2488. <https://doi.org/10.1016/j.biomaterials.2003.09.032>
- Shimizu T, Yamato M, Kikuchi A, Okano T (2003) Cell sheet engineering for myocardial tissue reconstruction. *Biomaterials* 24(13):2309–2316. [https://doi.org/10.1016/S0142-9612\(03\)00110-8](https://doi.org/10.1016/S0142-9612(03)00110-8)
- Stratton S, Shelke NB, Hoshino K, Rudraiah S, Kumbar SG (2016) Bioactive materials bioactive polymeric scaffolds for tissue engineering. *Bioact Mater* 1(2):93–108. <https://doi.org/10.1016/j.bioactmat.2016.11.001>
- Thomson RC, Yaszemski MJ, Powers JM, Mikos AG (1995) Fabrication of biodegradable polymer scaffolds to engineer trabecular bone. *J Biomater Sci Polym Ed* 7(1):23–38. <https://doi.org/10.1163/156856295X00805>

- Tseng TC, Tao L, Hsieh FY, Wei Y, Chiu IM, Hsu SH (2015) An injectable, self-healing hydrogel to repair the central nervous system. *Adv Mater* 27(23):3518–3524. <https://doi.org/10.1002/adma.201500762>
- Ulery BD, Nair LS, Laurencin CT (2011) Biomedical applications of biodegradable polymers. *J Polym Sci B Polym Phys* 49:832–864. <https://doi.org/10.1002/polb.22259>
- Umaña M, Waller J (1986) Protein-modified electrodes. The glucose oxidase/polypyrrole system. *Anal Chem* 58(14):2979–2983. <https://doi.org/10.1021/ac00127a018>
- Vickers SM, Squitieri LS, Spector M (2006) Effects of cross-linking type II collagen-GAG scaffolds on chondrogenesis in vitro: dynamic pore reduction promotes cartilage formation. *Tissue Eng* 12(5):1345–1355. <https://doi.org/10.1089/ten.2006.12.1345>
- White JD, Wang S, Weiss AS, Kaplan DL (2015) Silk-tropoelastin protein films for nerve guidance. *Acta Biomater* 14:1–10. <https://doi.org/10.1016/j.actbio.2014.11.045>
- Wong JY, Langer R, Ingber DE (1994) Electrically conducting polymers can noninvasively control the shape and growth of mammalian cells. *Proc Natl Acad Sci U S A* 91(8):3201–3204. <https://doi.org/10.1073/pnas.91.8.3201>
- Woodruff MA, Huttmacher DW (2010) The return of a forgotten polymer - polycaprolactone in the 21st century. *Prog Polym Sci* 35:1217. <https://doi.org/10.1016/j.progpolymsci.2010.04.002>
- Xiao W, Hu XY, Zeng W, Huang JH, Zhang YG, Luo ZJ (2013) Rapid sciatic nerve regeneration of rats by a surface modified collagen-chitosan scaffold. *Injury* 44(7):941–946. <https://doi.org/10.1016/j.injury.2013.03.029>
- Yi H, Ur Rehman F, Zhao C, Liu B, He N (2016) Recent advances in nano scaffolds for bone repair. *Bone Res* 4(1):16050. <https://doi.org/10.1038/boneres.2016.50>
- Yoshimoto H, Shin YM, Terai H, Vacanti JP (2003) A biodegradable nanofiber scaffold by electrospinning and its potential for bone tissue engineering. *Biomaterials* 24(12):2077–2082. [https://doi.org/10.1016/S0142-9612\(02\)00635-X](https://doi.org/10.1016/S0142-9612(02)00635-X)
- Zhang Y, Ouyang H, Chwee TL, Ramakrishna S, Huang ZM (2005) Electrospinning of gelatin fibers and gelatin/PCL composite fibrous scaffolds. *J Biomed Mater Res B Appl Biomater* 72(1):156–165. <https://doi.org/10.1002/jbm.b.30128>
- Zhang W, Zhu C, Ye D, Xu L, Zhang X, Wu Q et al (2014) Porous silk scaffolds for delivery of growth factors and stem cells to enhance bone regeneration. *PLoS One* 9(7):1–9. <https://doi.org/10.1371/journal.pone.0102371>
- Zhong S, Teo WE, Zhu X, Beuerman RW, Ramakrishna S, Yung LYL (2006) An aligned nanofibrous collagen scaffold by electrospinning and its effects on in vitro fibroblast culture. *J Biomed Mater Res A* 79(3):456–463. <https://doi.org/10.1002/jbm.a.30870>
- Zhu J, Marchant RE (2011) Design properties of hydrogel tissue-engineering scaffolds. *Expert Rev Med Devices* 8:607–626. <https://doi.org/10.1586/erd.11.27>



Polymer Matrixes Used in Wound Healing Applications

11

Md. Sazedul Islam, Md. Ashiqur Rahman, Shafiu Hossain, Papia Haque, Md. Shahrzaman, and Mohammed Mizanur Rahman

Abstract

Wound healing is a complex physiological process that involves a continuous sequence of inflammation, cell proliferation, matrix deposition, and tissue remodeling, and is regulated by cytokines, chemokines, and growth factors. Different approaches have been made to accelerate wound healing because the consequence becomes worse if it takes too long to heal the wound. Polymer matrixes in the form of hydrogel, film, foam, sponge, nanofibrous membrane, or scaffold have been subjected to research for years in wound healing applications because of their ability to inhibit bleeding, remove excess exudates, maintain a moist environment, and protect the wound from infection and sepsis caused by microorganisms. Moreover, these matrixes can carry and deliver drugs, growth factors, and promoters which enhance cell growth and proliferation, resulting in an acceleration in wound healing. These polymers can be natural, synthetic, or their blends that possess the properties like biodegradability, biocompatibility, non-toxicity, hemostasis, antimicrobial, antioxidant, and anti-inflammatory properties which are particularly effective in the treatment of wounds. The main objective of this chapter is to give recent information about different types of polymer matrixes fabricated from natural polymers (cellulose, chitosan, alginate,

M. S. Islam · M. A. Rahman · P. Haque · M. Shahrzaman · M. M. Rahman (✉)
Faculty of Engineering and Technology, Department of Applied Chemistry and Chemical Engineering, University of Dhaka, Dhaka, Bangladesh
e-mail: mizanur.rahman@du.ac.bd

S. Hossain

Faculty of Engineering and Technology, Department of Applied Chemistry and Chemical Engineering, University of Dhaka, Dhaka, Bangladesh

Department of Chemical Engineering and Polymer Science, Shahjalal University of Science and Technology, Sylhet, Bangladesh

gelatin, collagen, fibrin, etc.), synthetic polymers (polyglycolic acid, polylactic acid, polyacrylic acid, poly- ϵ -caprolactone, polyvinylpyrrolidone, polyvinyl alcohol, polyethylene glycol, etc.), and their blends used in wound healing applications. Future aspects of these types of matrixes in wound management are also discussed.

Keywords

Wound healing · Bioactive substances · Polymer matrix · Natural polymers · Synthetic polymers

11.1 Introduction

Wounds can be of various types but effective healing of wounds requires a suitable material that can cover the wound to prevent bacterial infection, protect it from further physical damage, and help in faster reconstruction of dermal and epidermal tissues. Plasters, cotton, wool, lint, gauzes, and other conventional wound dressing materials are usually passive products which do not encourage the healing process of wounds. These materials often suffer from disadvantages like susceptibility toward microbial attack, risk of infection, frequent change of dressing, moisture-absorbing tendency, impermeability to water vapor and oxygen, and adhering nature which make them painful to remove from the wounded place (Mayet et al. 2014). As a result, efforts have been made to prepare advanced dressing materials that possess properties like biocompatibility and biodegradability, non-antigenicity, ability to maintain a moist wound environment, antimicrobial activity to suppress microbial growth, sufficient water vapor and oxygen permeability, non-adherence, and ease of removal after healing (Dhivya et al. 2015; Naseri-Nosar and Ziora 2018).

Wound healing is a multistage process that progresses through a series of inter-reliant and corresponding stages including homeostasis, inflammation, proliferation (increase in the number of cells), and tissue remodeling to restore the integrity of damaged tissues. Different growth factors, growth promoters, cytokines, macrophages, fibroblasts, and extracellular matrixes are also involved in this healing process (Dhivya et al. 2015). With better understanding of the healing process, it is now obvious to develop dressing materials that not only protect the wound but also ensure a suitable environment and pharmacological support to promote the healing process. This includes the development of materials able to deliver drugs, growth factors, and promoters to the site of wound to stimulate or promote events in wound healing, from cellular migration to the production of extracellular matrix (ECM) components (Murray et al. 2019).

Considering these requirements, recent researches are focused on the development of polymer matrix-based dressing materials which are able to enhance the healing process. Both natural and synthetic polymers as well as their combinations have been employed for this purpose. Natural polymers possess some intrinsic properties like biocompatibility, biodegradability, non-irritant, easy resorption,

similarity to the extracellular matrix, etc. (Mallik et al. 2019), which are particularly useful in wound healing applications. Being similar to macromolecules recognized by the human body, natural polymers prevent the adverse immunological reactions and are safe to use (Naseri-Nosar and Ziora 2018).

Natural polymers like cellulose, alginates, chitin, chitosan, heparin, chondroitin, agar, carrageenan, collagen, gelatin, fibrin, keratin, silk fibroin, fucoidan, and their derivatives are extensively used in wound healing and tissue engineering applications (Mogoşanu and Grumezescu 2014). Chemical similarities of polysaccharides with heparin make them more hemocompatible than other biopolymers (Malafaya et al. 2007). Chitosan, a polysaccharide, has hemostatic, analgesic, anti-inflammatory, and antimicrobial properties, and its monomeric unit, *N*-acetylglucosamine, occurs in hyaluronic acid, an extracellular macromolecule that performs important function in wound healing (Islam et al. 2020). Collagen possesses good hemostatic properties, low antigenicity, and appropriate mechanical properties, and it promotes the migration, attachment, and growth of cells and tissues to facilitate wound healing (Ansari et al. 2018). Although natural polymers have good biocompatibility and biodegradability, most of them suffer from poor mechanical properties and often prone to microbial contamination (Gaspar-Pintilieşcu et al. 2019).

Synthetic polymers like polyglycolic acid, polylactic acid, polyacrylic acid, poly- ϵ -caprolactone, polyvinylpyrrolidone, polyvinyl alcohol, polyethylene glycol, etc. as well as their derivatives have been investigated extensively to prepare wound dressing materials (Mogoşanu and Grumezescu 2014). Control over synthesis and modification of synthetic polymers make them advantageous where stable dressing materials of specific physicochemical and mechanical properties are to be produced. However, most synthetic polymers are biologically inert and thus do not offer therapeutic advantages and suffer from limited cellular recognition, poor biocompatibility, and biodegradability.

The problems exhibited by natural and synthetic polymers separately can be solved by combining both polymers to form a blend matrix. The combination of polymers allows for the integration of useful properties of both polymers, and thus the physicochemical, biological, and mechanical properties are improved due to synergistic effect. As a result, the biocompatibility and biodegradability problems of synthetic polymers can be solved by combining them with natural polymers. In the same way, poor mechanical properties of natural polymers can be improved by blending them with synthetic polymers. Moreover, the blend matrix can be fabricated in the form of hydrogel, film, foam, sponge, nanofibrous membrane, or scaffold which make them suitable for application on various types of wounds (Mayet et al. 2014).

This chapter provides the recent information regarding different types of polymer matrixes used in wound management and their effect on healing process. Different forms of these polymer matrix-based dressing materials and their advantages and disadvantages are also discussed here.

11.2 Forms of Polymer Matrixes Used in Wound Healing Applications

Shape, size, porosity, mechanical strength, and stiffness of polymer matrix invariably matter its performance to wound healing applications. Polymer materials used in wound healing purposes can be classified as follows: (a) zero dimensional such as nanoparticles, polymer micelle, and dendrimers; (b) one dimensional (1D) such as nanofiber, nanowhiskers, nanorods, and nanowires; (c) two dimensional (2D) such as films, sheets, and membrane; and (d) three dimensional (3D) which is scaffold.

11.2.1 Zero-Dimensional Polymer Matrix

Polymeric nanoparticles have all dimensions in nanoscale, and therefore they are termed zero-dimensional materials. They can adhere to the cell surface and subsequently release the loaded drug to the cell. These particles can also enter the cell by endocytosis. In this process, they first bind with the cell surface receptor, and the formation of endosome takes place. Endosome may be lysed with the help of lysosomal enzymes and the nanoparticles release in the cytoplasm (Mukherjee et al. 2014; Islam et al. 2017).

11.2.2 1D Polymer Matrix

Polymer materials in the form of 1D are less likely to be used alone in wound healing action. Different shapes of nano-sized 1D polymer matrix being incorporated into other forms of matrices (2D or 3D) are used in wound management. Polymeric 1D structures like nanofibers of chitin, chitosan, poly(lactic-co-glycolic acid), polylactic acid, poly(vinyl alcohol), and polycaprolactone (Bayat et al. 2019; Liu et al. 2017; Jung et al. 2018), and nanowhiskers of cellulose and chitin (Hasan et al. 2017; Izumi et al. 2015) have been extensively investigated for their potential to be used in wound healing applications. Most of these 1D structures have antimicrobial properties and rapid hemostasis functions which make them suitable for the preparation of wound dressing material (Liu et al. 2017).

11.2.3 2D Polymer Matrix

All the 2D polymer matrices are geometrically planar surfaces with varying thicknesses. Polymer sheets have thickness greater than 0.5 mm, whereas their films have thickness less than 0.5 mm. Membrane presents thickness similar to the films but they have the capacity to stand alone or freestanding without any support where films need some substrate over which it can stand. 2D materials are fabricated by several techniques such as vapor deposition, molding, solvent casting, and melt

diffusion method. These materials are very useful for introducing surface effects on the wounded area. They can provide fast biosorption and covering protection for bacteria to come in contact with the injured place. However, films or sheets create a barrier for oxygen to reach the wounded area which can delay the healing process.

11.2.4 3D Polymer Matrix

11.2.4.1 Scaffold

Porosity in scaffold is the key point to target during its fabrication although the effects of surface chemistry, cell culture conditions, mechanical properties, and [degradation rate](#) play a large role in tissue formation in wound healing process (Eltom et al. 2019). Pores can be classified into micropores (0.1–2 nm), mesopores (2–50 nm), and macropores (>50 nm) according to their dimension. The pore size of 20 μm is required for fibroblast growth. Porosity in scaffolds can vary from 40 to 90% of the total size of the material. Pore size in scaffold should be large enough to allow cells to penetrate and migrate within the scaffold structure, as well as small enough to allow the binding of a critical number of cells at the same (Loh and Choong 2013). Scaffold can be fabricated using different techniques, that is, electrospinning, copolymerization/crosslinking, salt leaching, microfluidics, gas foaming, freeze-drying, solvent casting, etc.

Scaffolds usually provide a provisional support to body structures to allow the stress transfer over-time to wounded area along with cell regeneration there. In cell regeneration process, they include retention and deliverance of cells and other growth factors for cell attachment and migration. It helps to prevent potential development of necrotic center by limiting the cell cluster size to the pore size of the material (Tran et al. 2011). However, they have poor biodegradability and biocompatibility accompanied by potential toxic degradation of by-products.

Biomaterial scaffolds can also be classified into several groups such as sponge, foam, composite, fibrous scaffold, and hydrogel based on very minute differences to each other.

- (a) **Sponges**—They have open pores like a mesh. They facilitate proper chemical leaching, thorough interconnectivity, and high moisture absorption through the material. However, the structure is mechanically weaker than foam and tends to break down quickly.
- (b) **Foam**—This 3D structure poses closed pores. They provide higher cushioning in the structure; however, movement of cell materials is restrained there from one pore to other. There is a chance of remaining artifacts in the pores which may cause undesirable interactions with the cell materials.
- (c) **Hydrogel**—They are highly crosslinked polymers with high water retention capacity. They are typically biocompatible. They give similar characteristics to native tissues. Hydrogels can even be used as injectable scaffolds to fill irregularly shaped defects (Alaribe et al. 2016). They can incorporate with cells and bioactive agents which ultimately help in cell growth in wounds. In

some cases, uncontrolled dissolution of them may happen. They are mechanically not very strong, and during preparation their pore size is difficult to control.

- (d) **Composite scaffold**—This scaffold carries a multiphase system within its structure. They have the advantages of good biodegradation, biocompatibility, high toughness, and absorbability. Unfortunately, they sometimes produce toxic and acidic degradation products in wound site and cause inflammation. They have poor cell affinity and cell–matrix interaction (Ge et al. 2008).

11.2.4.2 Fibrous Scaffold

They are basically nanofibrous mats and currently fabricated by several techniques such as electrospinning, self-assembly, and phase separation (Bhattarai et al. 2004). Nanofibers have high surface area to volume, and in the fibrous mat structure they provide micron-level space of channeling between fiber orientations. This channeling helps in cell proliferation process. However, they are comparatively weak in mechanical strength.

11.2.4.3 Microspheres Scaffold

They are generally a polymer matrix used for drug encapsulation for the release of drugs at a moderately slow rate over an extended period of time (Liechty et al. 2010). Microspheres have several advantages, such as ease of controlling morphological aspects and flexible nature to control the release kinetics of encapsulated factors (Jaklenec et al. 2008) They are usually fabricated by solvent vapor treatment, heat sintering, non-solvent sintering, particle aggregation methods, etc.

11.2.4.4 Hydrocolloids

They are composed of a compounded mixture of natural polymer particles dispersed in a matrix of a hydrophobic pressure-sensitive polymer, such as elastomers and adhesives. Hydrocolloids are impermeable to water vapor but absorb wound exudate.

In future, hierarchical porous polymeric scaffold will probably be used more in wound management due to its high capacity in cell regeneration process. Rapid prototyping process can fabricate this type of scaffold. A computer-aided system will develop scaffold mimicking the microstructure of living tissues by creating libraries of unit cells based on mathematical models aided by software. Selective laser sintering, wax printing, stereolithography, fused deposition modeling, bio-plotter, and 3D printing are already in use to fabricate this type of scaffolds (Do et al. 2015).

11.3 Natural Polymer-Based Matrixes

11.3.1 Polysaccharide-Based Matrixes

Polysaccharides are complex bio-macromolecules that are naturally abundant and possess excellent physical and biochemical characteristics. They are extensively utilized in wound healing applications due to their unique characteristics like

biodegradability, biocompatibility, non-toxicity, and poly-functionality (Aduba and Yang 2017). They are also capable of enzyme immobilization (Sharmeen et al. 2019) and can be utilized to load and deliver suitable enzymes involved in wound healing process. Various polysaccharides like cellulose, alginate, chitin, chitosan, chondroitin, and hyaluronic acid are commonly used for the development of biomaterials.

11.3.1.1 Cellulose

Cellulose is the most abundant polysaccharide which is renewable and readily available natural polymer in the biosphere. It is mainly extracted from plant cell wall and partially synthesized from microbes, for example, bacteria, algae, and molds. Cellulose and its derivatives show several excellent features which make them attractive for wound dressing applications (Kabir et al. 2018). In a research, three-dimensional web-like bacterial cellulose gel network loaded with silver nanoparticles was developed and evaluated for its potential to be exploited as an antimicrobial membrane for wound healing application (Pal et al. 2017). The addition of silver nanoparticles imparted antimicrobial property to the membrane, and it showed strong killing rate of bacteria for long term. Moreover, the controlled release of silver from the membrane reduced the risk of toxicity when applied to wound healing. In addition, this biocomposite membrane was stable in moist environment which indicated its applicability in healing of exudate surrounding wounds. Nuutila et al. prepared a nanofibrillar cellulose hydrogel for inhibition of skin wound contraction during the healing period (Nuutila et al. 2018). The study demonstrated that the hydrogel had a very pleasant feeling when applied onto wounded skin due to its exceptionally low tackiness. About 70% wound contraction was achieved with the hydrogel within 14 days of healing. In addition, it increased the amount of alfa-smooth muscle cells and promoted the migration of keratinocytes and desired re-epithelialization of the wounds.

In addition, cellulose-based matrixes like quaternized hydroxyethyl cellulose–mesocellular silica foam (Wang et al. 2019), bacterial cellulose–zinc oxide (ZnO) nanocomposites (Khalid et al. 2017), cellulose–nanosilver sponge (Ye et al. 2016), nanofibrillated cellulose hydrogels (Basu et al. 2018), silver nanoparticles incorporated bamboo cellulose nanocrystals (Singla et al. 2017), and bacterial cellulose sponge (Ye et al. 2018) are also reported as potential polymer matrixes that can be used in wound healing purposes.

11.3.1.2 Alginate

Alginate is a naturally available anionic biopolymer which is mainly extracted from brown algae. The easy availability, biocompatibility, non-toxicity, and cost-effectiveness of alginate have increased its utilization in wound dressing application (Aderibigbe and Buyana 2018). Alginate-based hydrogel can be prepared using different crosslinking agents, and it facilitates wound healing by maintaining moist environment and minimizing bacterial infection. In a study, alginate hydrogel was prepared to incorporate the antibacterial agent naringenin (4,5,7-trihydroxyflavanone) and to evaluate its ability to be utilized as skin wound dressing material (Salehi et al. 2020). The wound treatment performed with hydrogel made

from alginate loaded with 20% naringenin exhibited excellent anti-infective and anti-inflammatory characteristics. It healed the skin wound with closure rate of about 68% and 95% after 7 and 14 days of initial wounding, respectively. Interestingly, it recuperated the natural beauty of the skin and rejuvenated the hair follicles. Babavalian et al. developed a hydrogel of alginate incorporated with an antimicrobial agent (CM11 peptide) and evaluated its wound healing capacity against methicillin-resistant *Staphylococcus aureus* (MRSA) bacteria (Babavalian et al. 2015). CM11-loaded alginate sulfate hydrogel was applied on a mice model, and complete healing was observed after 12 days of initial wounding. More than 99% of the bacterial killing rate was obtained by increasing the peptide concentration in alginate sulfate hydrogel.

11.3.1.3 Chitin and Chitosan

Chitin is recognized as the highest naturally available polysaccharide after cellulose. It is extracted from exoskeletons of crustaceans and cell walls of microbes. Chitosan, which is obtained by the deacetylation of chitin, performs better solubility properties compared to chitin. Both chitin and chitosan as well as their derivatives show outstanding features that are beneficial for wound healing like biocompatibility, biodegradability, non-toxicity, non-allergic activity, hemostatic activity, mucoadhesive, and antimicrobial properties (Ahmed and Ikram 2016a; Biswas et al. 2020).

Guo et al. prepared aerogel from nanoparticles of chitin for wound healing application (Guo et al. 2019). It showed excellent performance to accelerate the healing of wound because of its high swelling property, adequate biocompatibility, and excellent porous structure. The aerogel expedited the early stage of healing by the inhibition of inflammation and the formation of granulation tissues. In addition, it accelerated the fibroblast proliferation and macrophage migration as well as promoted the vascularization during the healing process. Colobatiu et al. developed a chitosan film and evaluated its potential as a diabetic wound dressing material (Colobatiu et al. 2019). The film kept the epidermal surface wet and accelerated the wound healing process. Moreover, the film made the surface suitable for the growth, propagation, and division of fibroblast cells which indicated its excellent biocompatibility. It performed unique hemostatic features and promoted the penetration and the relocation of neutrophils and macrophages in the initial stage of healing. The film inserted on the diabetic wounds healed almost 90% after 14 days of initial wounding. The improved healing condition was indicated by the intact skin layer of collagen fiber and fibroblasts. In addition, chitosan-based matrixes such as chitosan sponge (Xia et al. 2020), chitosan membrane (Ma et al. 2017), and chitosan aerogel (López-Iglesias et al. 2019) were prepared for the treatment of wounded tissues.

11.3.1.4 Chondroitin

Chondroitin is a natural polysaccharide which is found in connective tissues, synovial fluid, and bones (Pal and Saha 2019). This linear polymer molecule consists of glucuronic acid and sulfated *N*-acetylglucosamine. The excellent biological

properties such as anti-inflammatory and immune-modulatory of chondroitin have made it promising for wound healing application. Gilbert et al. prepared a biocompatible, non-immunogenic, and pliable hydrogel based on chondroitin for skin wound healing (Gilbert et al. 2004). The hydrogel enhanced the re-epithelialization and increased the dermal collagen reproduction in the wounded area. The improved wound healing is due to the angiogenesis and osteoblastic activity of the hydrogel. It was proposed that by acting as a surrogate extracellular matrix, the chondroitin sulfate hydrogel served as a repository for cytokines and growth factors produced by the regenerating mucosa.

11.3.1.5 Hyaluronic Acid

Hyaluronic acid is a natural polysaccharide and the member of the glycosaminoglycan group that is composed of repeated disaccharide unit of two sugars, glucuronic acid, and *N*-acetyl-glucosamine. The hyaluronic acid having high molecular mass is found in the synovial fluid of bone and cartilage and also in the ocular and dermal tissues (Gupta et al. 2019). The wide availability, biocompatibility, and non-toxicity properties of this naturally occurring polymer have made it a perfect wound healing material. Hu et al. proposed a hyaluronic acid graft that promoted healing and reduced scar formation in wounded area of the skin (Hu et al. 2003). The three-dimensional graft was prepared by crosslinking hyaluronic acid with glutaraldehyde. The hyaluronic acid graft performed excellent wound healing property with faster wound closure (15.85 ± 4.77 h) compared to non-treated samples. Furthermore, it also regenerated the natural appearance of the skin by reducing the scar formation. This graft improved the clinical healing process by preventing the continuous bleeding with the early occlusion of the blood vessel.

11.3.2 Protein-Based Matrixes

Proteins are natural macromolecules that are biologically important because of their unique structure. These polypeptides consist of repeated unit of amino acids which contain both the acidic carboxylic group and basic amino group. Different types of proteins like collagen, gelatin, soy protein, keratin, and silk fibroin are used for the development of natural biomaterials that can repair wounded tissues.

11.3.2.1 Collagen

Collagen is a well-known fibrous and structural protein that is the most abundant in animals. This fibrillar structure is very important to keep the actual arrangement and integrity of the tissues. The biodegradable and non-toxic collagen material can be formulated into differently structured biomaterials that are suitable for wound dressing purposes. Helary et al. prepared a concentrated collagen hydrogel for repairing severe skin wounds like venous leg ulcers or diabetic foot ulcers (Helary et al. 2012). The result showed that the re-epithelialization and neovascularization of cell were started on the seventh day of healing. It allowed the persistence of fibroblasts within the material by favoring proliferation and inhibiting apoptosis.

In addition, the cell number assessed in the hydrogel was surprisingly increased at 21 days of observation. The cell proliferation activity and enhanced cell viability of this biomaterial have made it a new approach for wound dressing application. Collagen-based matrixes such as Triphala incorporated collagen sponge (Kumar et al. 2010), collagen scaffold (Natarajan et al. 2013), and collagen film (Subagio et al. 2020) were developed and utilized as a wound healing material.

11.3.2.2 Gelatin

Gelatin is a biopolymer which can be obtained from the hydrolysis treatment of collagen. It is suitable for the development of wound dressing matrices or membranes because of its low immunogenicity, cell proliferation, and adhesion properties (Cai et al. 2016; Khan et al. 2017). It is extensively used for the preparation of hydrogel and film-type materials. In a research, gel and film were prepared from cuttlefish skin gelatin and evaluated their potentiality as wound healing materials (Jridi et al. 2017). The result demonstrated that the gelatin film and gel were able to accelerate wound healing with wound closure rate of 82.10% and 85.88%, respectively, after 12 days of application. These materials promoted the healing process by maintaining adequate moisture in the wounded area. Furthermore, these gels and films prevented inflammation and oxidative damage as well as acted as a carrier for antioxidant and antimicrobial substances.

11.3.2.3 Keratin

Keratin is a naturally abundant animal protein which is found in skin and hair of mammals and feather of birds. The cysteine-rich structure of keratin increases its mechanical strength. It can be used as a potential biomaterial due to its intrinsic characteristics like biodegradability, biocompatibility, mechanical durability, and easy availability (Feroz et al. 2020). The fast re-epithelialization ability has increased its suitability for wound healing, but poor solubility has limited its application. Wang et al. fabricated a hydrogel from feather keratin and evaluated its efficacy as a wound healing material (Wang et al. 2017). The result showed that approximately 90% wound closure was obtained after 10 days of application (Fig. 11.1). In addition, the complete re-epithelialization was achieved after 21 days of initial wounding. It accelerated the formation of thin epidermal layer and facilitated tissue regeneration by rejuvenating hair follicles. This hydrogel showed excellent wound healing properties due to the ability of rapid hemostasis and maintaining sealed moisture environment at the wounded area.

11.3.2.4 Silk Fibroin

Silk fibroin is a naturally available protein that is collected from *Bombyx mori*. It is a potential biomaterial for wound dressing application as it can promote the attachment and proliferation of cells. Ju et al. fabricated a silk fibroin nanomatrix using modified electrospinning method for wound healing application (Ju et al. 2016). The treatment of skin wounds using silk fibroin nanomatrix was decreased to 4% after 28 days of initial wounding. It inhibited the formation of edema or granulation tissues and exhibited all the histological characteristics of normal skin. This

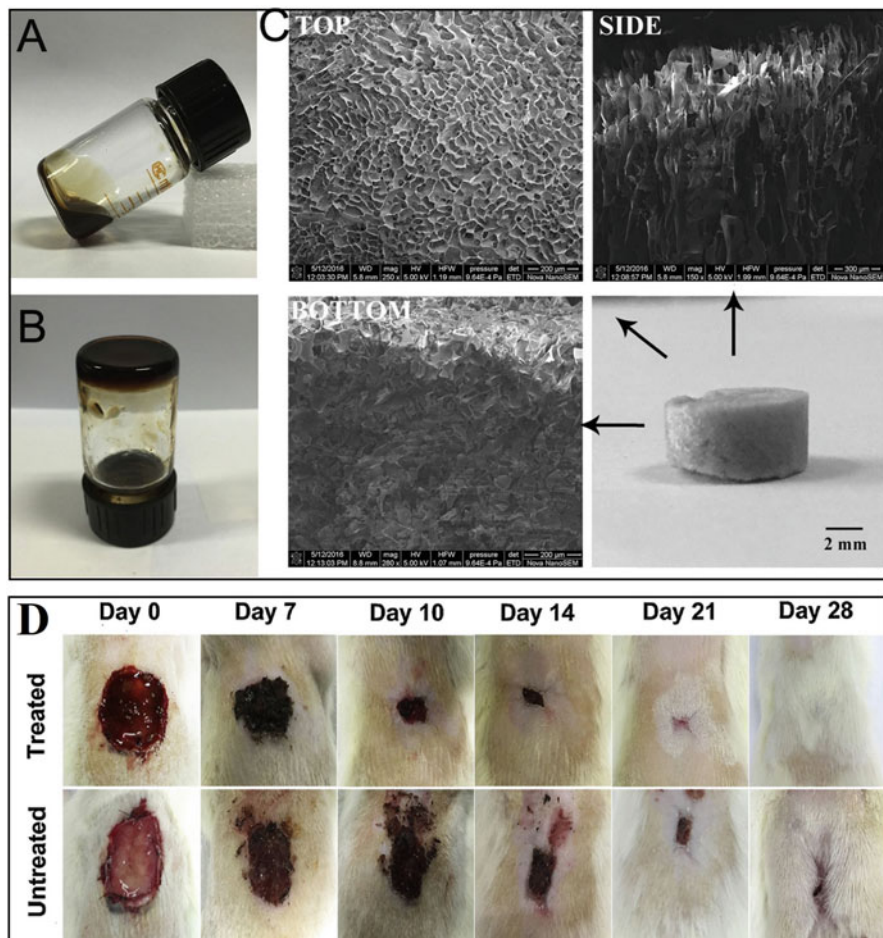


Fig. 11.1 Optical images of the vial inversion tests of the keratin solution before (a) and after (b) gel formation. (c) A cylindrical-shaped lyophilized keratin hydrogel is illustrated from multiple views from different profiles of scanning electron micrographs containing the highly porous structure and (d) photographs of wound healing process untreated or treated with keratin hydrogel on days 0, 7, 10, 14, 21, and 28 of post-wounding (Scale bar = 1 cm). (Figure is adapted with permission from the original article of Wang et al. (2017) (Copyright 2016 Elsevier B.V.))

nanomatrix can be used as an excellent wound dressing material due to its anti-inflammatory, quick re-epithelialization, low scar formation, and rapid healing properties. Honey-loaded 3D silk fibroin porous scaffolds were found to be effective skin substitutes for scarless regenerative wound healing (Rajput et al. 2020). The scaffold was biocompatible with desired swelling and degradation properties and showed improved attachment, proliferation, and uniform distribution of fibroblasts throughout the matrix. With this scaffold, normal homeostasis with proper re-epithelialization was attained which revealed the potential of this scaffold to be utilized as epidermal and dermal substitute for wound repairing purposes.

11.3.2.5 Soy Protein

Soy protein is a naturally abundant substance which is emerging as a new material for application in biomedical field. It can easily be extracted from widely available legume crop, soybean. The intrinsic properties of soy protein such as ability to accelerate cell adhesion and cell growth have made it suitable for wound dressing. Goder et al. prepared a novel soy protein film and assessed its ability to be a wound healing material (Goder et al. 2020). The film was obtained by the solvent casting method using glyoxal as crosslinker. The cell viability of the film was found to be around 76% after 24 h of observation. Moreover, it kept the wound surface wet at a desired level during the healing period by maintaining a fixed water vapor transmission rate.

Special features of some recently developed natural polymer-based matrixes investigated in wound healing application are summarized in Table 11.1.

11.4 Synthetic Polymer-Based Matrixes

In recent years, wound healing has been streamlined and consists of synthetic polymers for wound management. This section explains the details about the matrixes prepared from synthetic polymers including polylactic acid, polyvinyl alcohol, polyacrylic acid, polyethylene glycol, polyglycolic acid, polycaprolactone, polyvinylpyrrolidone, etc. These synthetic polymer matrixes are clinically used in wound healing management nowadays. Synthetic polymer matrixes used for wound healing purposes are developed by different methods like chemical and physical crosslinking, irradiation, electrospinning, etc.

11.4.1 Polylactic Acid (PLA)

PLA displays high biodegradability, biocompatibility as well as it can assist the growth and propagation of dermal cells (Foldberg et al. 2012). PLA gains high interest due to its cost-effective production from sugar beets and corn. Erika Adomavičiūtė and his coworkers reported the preparation of non-woven material using electrospun PLA and silver nanoparticles for wound healing application (Adomavičiūtė et al. 2017). The antimicrobial test assured its ability of inhibiting the growth of microorganisms. Moreover, Nguyen et al. developed curcumin-loaded PLA nanofibers mat by electrospinning method for the curing of wounded skin (Nguyen et al. 2013). They examined the bioactivity of the electrospun mat by following the *in vitro* testing method using the C2C12 myoblast cells in order to evaluate its cytotoxicity and ability related to the growth, addition, and proliferation of the cells. Prepared mat effectively reduced the wound closure time which was confirmed by *in vivo* testing method. In addition, a wet-electrospun PLA 3D nanofibrous scaffolds (PLA-S) were prepared by Ghorbani et al. (2018) using wet-electrospinning method. They applied the PLA-S in mouse model to evaluate the biocompatibility and healing ability of these fibers to treat skin wounds. The

Table 11.1 Some recently developed natural polymer-based matrixes investigated in wound healing application

Sl. No.	Name of the polymer matrix	Form of the matrix	Loaded drug/species	Special features	Mode of investigation	Time to heal wound (days)	References
01.	Bacterial cellulose—Silver montmorillonite nanocomposites	Scaffold	–	<ul style="list-style-type: none"> • Incorporation of silver and montmorillonite increases water content and scaffold stability • Good biocompatibility and high antimicrobial activity 	In vitro	–	Horue et al. (2020)
02.	Annatto-loaded cellulose acetate nanofiber	Scaffold	Annatto extract	<ul style="list-style-type: none"> • Ideal physicochemical, and thermal properties for potential wound healing applications • Promotes fibroblast cellular proliferation 	In vitro and in vivo	15	dos Santos et al. (2020)
03.	Naringenin incorporated alginate hydrogel	Hydrogel	Naringenin	<ul style="list-style-type: none"> • Significantly higher cell viabilities • Biodegradable and non-toxic 	In vitro and in vivo	14	Salehi et al. (2020)
04.	Honey coupled 3D alginate hydrogel	Hydrogel	Honey	<ul style="list-style-type: none"> • Good mechanical strength, degradability, and swelling • Minimal fibroblast migration to the granulation tissue after matrix remodeling with negligible scar formation 	In vitro and in vivo	12	Mukhopadhyay et al. (2020)
05.	Genipin-crosslinked carboxymethyl chitosan hydrogel	Hydrogel	Aloe vera	<ul style="list-style-type: none"> • Ability to prevent hypertrophic scar formation during wound healing 	In vitro and in vivo	14	Zhang et al. (2020a)
06.	Quercetin-loaded chitosan triphosphate nanoparticles	Nanoparticles	Quercetin	<ul style="list-style-type: none"> • Reduce tumor necrosis factor alpha • Significantly increased endothelial growth factor as well 	In vitro and in vivo	21	Choudhary et al. (2020)

(continued)

Table 11.1 (continued)

Sl. No.	Name of the polymer matrix	Form of the matrix	Loaded drug/species	Special features	Mode of investigation	Time to heal wound (days)	References
07.	Growth factor loaded methacrylated hyaluronic acid hydrogel	Hydrogel	Basic fibroblast growth factor (bFGF)	<p>as transforming growth factor beta1</p> <ul style="list-style-type: none"> • Ability to release bFGF in a controlled and sustained manner • Considerably improved wound healing with accelerated re-epithelialization, granulation formation, collagen, deposition, and skin appendage regeneration 	In vitro and in vivo	17	Chen et al. (2020)
08.	Self-expandable collagen sponge	Sponge	S-nitrosoglutathione	<ul style="list-style-type: none"> • Ability to release nitric oxide topically • Enhances relocation and infiltration of leucocytes, macrophages, and keratinocytes to the affected tissues of wound • Accelerates wound closure by increasing neovascularization and collagen deposition 	In vitro and in vivo	12	Póvoa et al. (2020)
09.	Degradable gelatin-dopamine interpenetrating polymer network cryogel	Cryogel	-	<ul style="list-style-type: none"> • Excellent blood clotting ability and increased number of blood cells and platelet attachment and activation • Ability to stop deep massive noncompressible hemorrhage • Possesses high antioxidant activity and NIR irradiation 	In vitro and in vivo	14	Huang et al. (2020)

10.	Keratin-coated silver nanoparticles	Powder	Silver nanoparticles	aided photothermal antibacterial ability <ul style="list-style-type: none"> • Biocompatible and significantly accelerates wound closure and epithelization • Inhibits the growth of <i>Escherichia coli</i> and <i>Staphylococcus aureus</i> 	In vitro and in vivo	15	Konop et al. (2020)
11.	Chromenopyrazole antioxidant-loaded silk fibroin nanofibers scaffold	Nanofibrous scaffold	Chromenopyrazole	<ul style="list-style-type: none"> • Excellent cell viability and superior antioxidant efficacy • Enhances the adhesion and proliferation of fibroblast cells 	In vitro	-	Kandhasamy et al. (2019)
12.	Bupivacaine-loaded soy protein films	Film	Bupivacaine	<ul style="list-style-type: none"> • Tailorable mechanical and physical characteristics • Good biocompatibility with desired drug release profile 	In vitro	-	Goder et al. (2020)

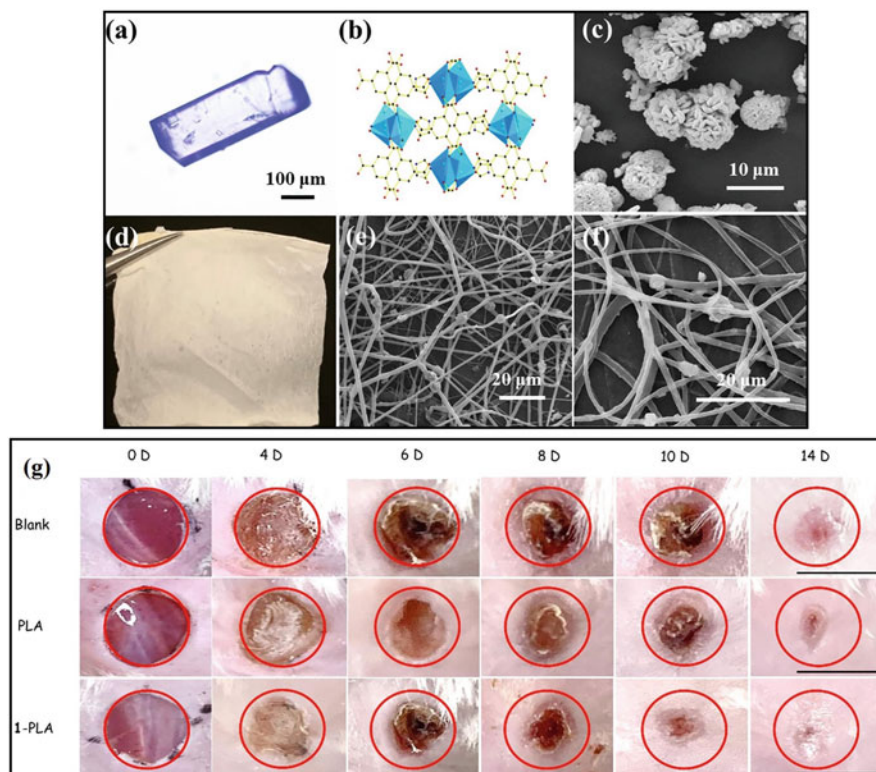


Fig. 11.2 (a) Optical image of bulk crystal of MOF synthesized from Ag (I) ions, 1,3,5-benzenetricarboxylate and imidazole, (b) monoclinic crystal structure of MOF, (c) SEM image of MOF particles, (d) optical photograph, and (e, f) SEM images of MOF-PLA composite fibrous mat. (g) Optical photographs of wounds healing process covered with blank PLA and 1-PLA. Complete healing is observed with wounds covered by MOF-PLA composite by day 14, whereas wounds treated with pure PLA or left untreated are yet to be healed completely. Scale bar: 10 mm. (The figure is adapted with permission from the original article of Zhang et al. (2020b) (Copyright 2020 Elsevier B.V.))

results of their in vivo and in vitro studies revealed that the 3D fibrous PLA-S could be a prospective material for wound repair.

Zhang et al. prepared electrospun fibrous mat from PLA and silver (I) metal-organic framework (MOF) to investigate its potential as an active antibacterial wound dressing material (Zhang et al. 2020b). The prepared MOF-PLA showed exceptional antibiosis strength against several bacteria like *Escherichia coli*, *Pseudomonas aeruginosa*, *Staphylococcus aureus*, and *Mycobacterium smegmatis*. The composite mat was applied on a dermal infection of Kunming female mice to observe its actual anti-infection healing result (Fig. 11.2). The results indicated that the mat was more effective in wound healing with a healing ratio of 99.9% compared to PLA (86.7%) and untreated group (80.1%).

11.4.2 Polyvinyl Alcohol (PVA)

PVA, which is a synthetic polymer and soluble in hydrophilic solvent, has been prevalently utilized in biomedical field, for example, wound healing. This biocompatible polymer has numerous advantages including non-toxicity, high hydrophilicity, biodegradability, excellent processability, chemical resistance, water absorbency as well as swelling properties suitable for wound dressing. PVA nanofibers show anti-inflammatory properties by absorbing wound exudate and assist in tissue redevelopment due to their non-toxicity, biocompatibility, and oxygen accessibility. Jatoi et al. developed an antimicrobial wound repairing material composed of carbon nanotubes, silver nanoparticles, and PVA nanofibers (Jatoi et al. 2019). This nanocomposite biomaterial performed excellent antibacterial properties showing high killing rate of bacteria and long-term inhibition of bacterial growth. Furthermore, Sharon L. Bourke and his coworkers developed a photo-crosslinked poly(vinyl alcohol) hydrogel for sustained release of growth factors for repairing skin wound (Bourke et al. 2003). The hydrogel was fabricated by ultraviolet photo-crosslinking of acrylamide functionalized PVA. They conducted the release studies by means of growth factor in vehicles with hydrophilic filler exhibited prolonged release of platelet-derived growth factor (PDGF- β).

11.4.3 Polyethylene Glycol (PEG)

PEG is amphiphilic in nature and soluble in polar solvents like water. It is widely acceptable to biomedical researchers due to its excellent wound healing characteristics like biocompatibility, biodegradability, non-toxicity, transparency, and cost-effectiveness. Recently, Chen et al. prepared a hydrogel sealant made of PEG material for effective wound repairing (Chen et al. 2018). They assessed the properties of hydrogel related to cell and tissue regeneration like cytotoxicity, irritation, sensitization, pyrogen, and systemic toxicity, by following the *in vitro* testing method. Moreover, Anumolu et al. developed doxycycline-loaded PEG hydrogels (Anumolu et al. 2010) and confirmed their wound repairing ability in half mustard and nitrogen mustard-exposed rabbit corneas in culture medium. In their study, they assured the healing capacity of the prepared hydrogel by assessing its ability of repairing the wounded area of ocular mustard injuries and found it to be 2.5- to 3.4-fold higher effective compared to the non-wounded corneas. Also, Chen prepared a hydrogel composed of thiolated PEG (SH-PEG) and silver nitrate (AgNO_3) through crosslinking method for wound repairing in diabetic affected living organism (Chen et al. 2019a) which showed great promise in healing of wounds.

11.4.4 Polyacrylic Acid (PAA)

PAA, also known as Carbopol, is a synthetic biocompatible polymer utilized in biomedical fields such as wound healing application and transdermal drug delivery. Recently, J. Kim and his teammates prepared a hydrogel made of PAA containing propolis for the repairing of skin wound in mouse (Kim and Lee 2018). The term propolis (CHP) can be defined as the resinous mixture collected by honeybees from several sources like tree buds, sap flows, and exudates. The examination of histological tissue showed that CHP encouraged new tissue development and re-epithelialization in the wounded area that may be supportive for the advancement of wound repairing. Furthermore, Choi et al. prepared PAA nanogel (Ag-PAAC) incorporated with silver particle using electron beam irradiation method (Choi et al. 2013). The Ag-PAAC hydrogels showed good antibacterial effect against *Escherichia coli* and *Staphylococcus aureus*. In vivo studies indicated that the Ag-PAAC nanogels perform an excellent wound repairing ability.

11.4.5 Polyglycolic Acid (PGA)

PGA is a biocompatible and thermoplastic polymer used for different biomedical purposes, especially for wound dressing. Murata et al. also described the application of Neoveil which is a mesh sheet composed of PGA for open wounds in oral surgery. Moreover, Miyaguchi et al. reported the effects of covering surgical wounds by PGA sheet for post-tonsillectomy pain (Miyaguchi et al. 2016). In addition, Shinozaki reported the repairing of wounds resultant from the resection of oral or oropharyngeal squamous cell carcinoma using the grafted polyglycolic acid sheet patches (Shinozaki et al. 2013).

11.4.6 Polycaprolactone (PCL)

PCL is a hydrophobic synthetic polymer which contains semi-crystalline structure. It is used for the development of wound healing materials due to its excellent mechanical properties as well as for its biocompatibility, non-immunogenicity, and slow biodegradability. Recently, Simões et al. developed MRPs (Maillard reaction products)-modified PCL membranes by electrospinning method for wound repairing purposes (Simões et al. 2018). The prepared membranes have successfully inhibited the growth of *Staphylococcus aureus* and *Pseudomonas aeruginosa* without causing any toxicity to human fibroblasts. Furthermore, a nanocomposite scaffold was fabricated from PCL and quaternary ammonium salt-modified montmorillonite (MMT) by Sadeghianmaryan et al. (2020) using electrospinning technique for wound dressing applications. The low toxicity resulting from the cytotoxicity test of PCL-MMT nanocomposite scaffolds has assured its suitability as wound repairing materials. Gamez and his coworkers prepared efficient antibacterial carvacrol (CAR) and thymol (THY)-loaded electrospun PCL mats using electrospinning technique for

wound dressings (Gamez et al. 2019). The prepared CAR- and THY-loaded mats were capable to entirely destroy both gram-positive (*Staphylococcus aureus* ATCC 25923) and gram-negative (*Escherichia coli* S17 strain) bacteria. Also, A.P. Rameshbabu reported a method for the development of PCL nanofiber mats mixed with placental-derived bioactive molecules (PCL-sPEM) having growth factors for cutaneous wound repairing (Rameshbabu et al. 2018). The result showed that the PCL-sPEM nanofiber mats are capable of healing critical skin wounds with faster wound closure of dermal tissues.

11.4.7 Polyvinylpyrrolidone (PVP)

PVP is a hydrophilic synthetic polymer and able to be used as a skin substitute, due to its biocompatibility, biodegradability, low toxicity, and good water vapor transmission property. Very recently, Chinatankul et al. developed monolaurin-loaded shellac-PVP (SHL-PVP) nanofibers for application in wound healing (Chinatankul et al. 2019). The fabricated SHL-PVP fibers added with monolaurin performed an outstanding action against *Staphylococcus aureus* and *Candida albicans* bacterial strain which suggests that SHL-PVP fibers might be successfully utilized for wound repairing purposes. Moreover, Dai et al. developed a novel medicated electrospun emodin-PVP blended nanofibrous membrane for faster wound repairing (Dai et al. 2012). The in vitro dissolution tests confirmed the better release kinetics of the blended nanofibrous membrane of the entrapped drug (emodin) as compared to the pure drug. All the tests related to the repairing of skin wound reveal that the emodin-loaded nanofibrous membrane is suitable to be used as a healing material.

11.5 Polymer Blend Matrixes

11.5.1 Natural-Natural Polymer Blend Matrixes

11.5.1.1 Chitosan-Starch

Starch is a biocompatible, biodegradable, and low-cost natural polymer. It is a promising biopolymer in the field of tissue engineering, wound dressing, and many other medical applications (Chen et al. 2019b). Cornstarch-dextran and chitosan-based composite were found useful in wound healing application (Wittaya-arekul and Prahsarn 2006). The presence of cornstarch and dextran with chitosan increased the water uptake capacity and oxygen penetration at the wound. The film showed better antibacterial resistance. In another study, chitosan-sago starch matrix loaded with gentamycin which was fabricated by the solvent casting method, and it heals wound (16 days) faster than the untreated control (24 days) (Arockianathan et al. 2012).

11.5.1.2 Collagen–Chitosan

Collagen–chitosan blend matrix has been widely used nowadays for wound management. Collagen and chitosan can be blended together to produce a film that can accelerate wound healing by fibroblastic cell migration as well as with collagen deposition (Ahmed and Ikram 2016b). Fan et al. prepared a scaffold from collagen, chitosan, and TiO₂ nanoparticles (Fan et al. 2016). Cytotoxicity, water absorption capacity, red blood cell aggregation, porosity, and antibacterial activity investigation proved good permeability, non-toxicity, and cell proliferation capacity of the scaffold. In a study, silver nanoparticle-loaded collagen–chitosan scaffold was found to accelerate the healing process by regulating the migration of fibroblastic cell and macrophage activation (You et al. 2017). Nanosilver accelerated the fibroblastic migration at 10 ppm concentration. The results revealed that nanosilver-loaded collagen–chitosan was bactericidal, anti-inflammatory, and promotes wound healing. Cell-penetrating peptide (oligoarginine, R8)-loaded collagen–chitosan gel was found effective for wound management (Li et al. 2019). The gel was prepared by physical crosslinking method as shown in Fig. 11.3a. The gel was applied in vivo on wound created in mice and after 14 days, wound treated with the gel showed 98% of new skin generation (Fig. 11.3b). From the histopathological studies, it was found that that the gel enhanced granulation tissue formation and collagen deposition.

11.5.1.3 Chitosan–Gelatin

Chitosan–gelatin nanofiber membrane incorporated with Fe₃O₄ nanoparticles has been found to be a recent advancement in wound dressing application (Cai et al. 2016). Chitosan–gelatin nanofiber membrane containing 1% (by weight) iron oxide nanoparticles showed optimum mechanical properties. Increase in the concentration of iron oxide nanoparticles results in expanded inhibition zone for *Escherichia coli* and *Staphylococcus aureus*. The enhancement in the mechanical and antimicrobial properties makes Fe₃O₄–chitosan–gelatin nanofibrous membrane an efficient material for wound management. Patel et al. prepared a chitosan–gelatin film for sustained release of lupeol in wounds (Patel et al. 2018). Solvent casting method was utilized to prepare lupeol-incorporated chitosan–gelatin film, while glutaraldehyde and glycerol were used as a crosslinker and plasticizer, respectively. Antioxidant assay, cell viability (90%) by MTT (3-(4, 5-dimethylthiazolyl-2)-2, 5-diphenyltetrazolium bromide) assay, and antibacterial activity (23 mm inhibition zone) of lupeol-entrapped chitosan–gelatin hydrogel film showed that the hydrogel film was a potential carrier of lupeol for its sustained release in the wounded area. 3D scaffolds of photo-crosslinked chitosan–gelatin hydrogel is another biomaterial that can be used in chronic wound healing. The hydrogel matrix was prepared by methacrylated chitosan and gelatin with a photo-crosslinker. Depending on the concentration of polymer and irradiation time with the photo-crosslinker, the degrees of the hydrogel vary from 500 to 2000%. The hydrogel showed more than 95% viability toward human embryonic kidney cells (HEK293T) that proved its biocompatibility (Carvalho and Mansur 2017).

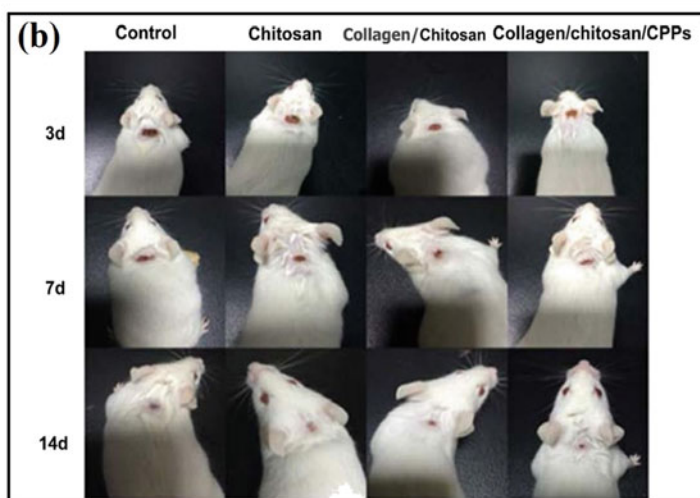
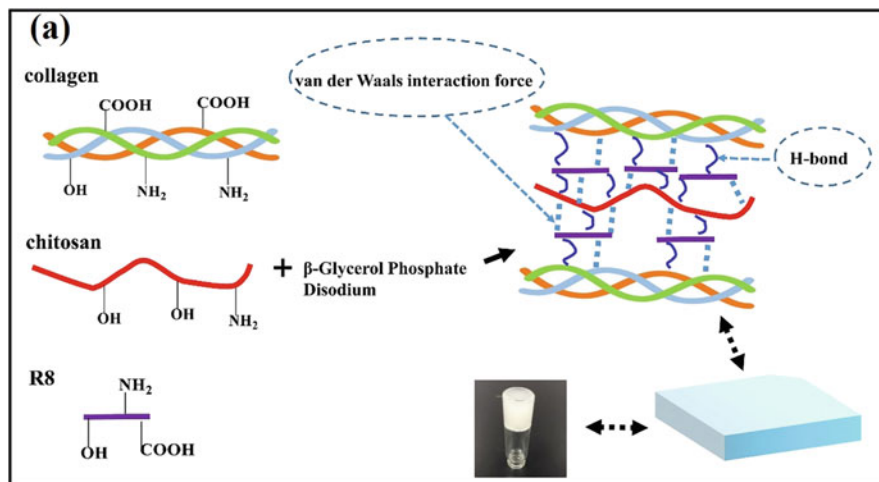


Fig. 11.3 (a) Schematic illustrations showing the preparation of gel from collagen, chitosan, and CPP (Oligoarginine, R8). (b) Images of wounds healing process in mice, untreated (control) and treated with chitosan, collagen–chitosan, and collagen–chitosan–CPP at 3, 7, and 14 days (scale bar $1.0 \times 1.0 \text{ cm}^2$). (The figure is adapted with permission from the original article of Li et al. (2019) (Copyright 2018 Elsevier B.V.))

11.5.1.4 Alginate–Chitosan

Hydrogel prepared from alginate and other polymers like chitosan have become popular in wound management, drug delivery, and tissue engineering (Lee and Mooney 2012). In a study, hesperidin-loaded alginate–chitosan hydrogel was prepared which showed highly porous structure with high water uptake, antibacterial

activity, and non-toxicity against fibroblast cell. In vivo studies suggested that the hydrogel with hesperidin is a better bandage material than normal gauze bandage (Bagher et al. 2020). Rahman et al. prepared a nanocomposite dressing material from the chitosan and alginate by crosslinking them with sodium tripolyphosphate and loaded ZnO and calcium phosphate nanoparticles in it (Rahman et al. 2020). The composite was efficient to inhibit the growth of *Escherichia coli* and *Salmonella enterica*. From in vivo study, it was found that the composite healed faster than normal gauze bandage due to the release of calcium ion (61% at pH 5.00) from the matrix in an acidic condition of the wound. However, ciprofloxacin hydrochloride-doped bilayer biocomposite membrane of alginate and chitosan is another remarkable work in the field of wound dressing (Han et al. 2014). The membrane was biocompatible and inhibited the growth of microorganisms within 7 days. Pharmacodynamic studies revealed the sustained release nature of the drug, which improved the effectiveness of the membrane in wound healing process.

11.5.1.5 Cellulose–Alginate

Blend matrixes prepared from cellulose and alginate have properties like biocompatibility, adhesiveness, hydrophilicity, and non-antigenicity which can help tissue repair and regeneration. A three-dimensional porous scaffold was fabricated from bacterial cellulose and alginate to treat chronic wounds and tissue regeneration (Alexis et al. 2017). MTT assay with bovine cells showed non-toxic nature for the scaffold. Composite dressing material prepared from bacterial cellulose, alginate, and gelatin was found effective in wound healing application (Chiaoprakobkij et al. 2019). Glycerol, a plasticizer, was used to improve the water uptake capability of the composite. From cytotoxicity test and cell culture of human keratinocyte cells with prepared biocomposite film, enhanced cell proliferation and keratinocyte migration were observed. Incorporation of chitosan and copper sulfate increases the antimicrobial property of bacterial cellulose and alginate composite, and the composite showed excellent resistance toward the growth of *Escherichia coli* and *Staphylococcus aureus* (Wichai et al. 2019). Silver sulfadiazine (AgSD)-loaded cellulose–alginate (BC-SA) composite was prepared by Shao et al. to investigate and evaluate its performance as wound dressing material (Shao et al. 2015). The drug-loaded composite was cytocompatible and showed enhanced antimicrobial activity against *Escherichia coli*, *Staphylococcus aureus*, and *Candida albicans*.

Besides, silver nanoparticle-doped collagen–alginate biocomposite (Zhang et al. 2018), biomimetic nanofibrous matrices of chitosan–collagen (Huang et al. 2015), cellulose–alginate sponges (Pei et al. 2015), silver nanoparticle-incorporated gelatin–cellulose hydrogel (Gou et al. 2020), etc. are also found to be effective in wound healing application. *A nanocomposite fabricated from carboxylated cellulose nanowhiskers and silver nanoparticles exhibited excellent mechanical and antimicrobial activity. Chitosan and carboxymethyl cellulose-based nanocomposite showed porous scaffold with high swelling capacity. The properties of the scaffold were directly connected to the concentration of the components. This scaffold was an excellent material to prevent infections in bone* (Hasan et al. 2018).

11.5.2 Synthetic–Synthetic Polymer Blend Matrixes

11.5.2.1 PLA–Synthetic Polymer Blend

Curcumin-loaded polylactic acid (PLA) and hyperbranched polyglycerol (HPG) blend matrix were found to be efficient in rapid wound healing owing to its swelling and moisture retention capacity (Perumal et al. 2017). This biodegradable matrix with curcumin helped to complete migration of the cells across the artificial wound within 36 h. The degradation behavior of the matrix was dependent on HPG content, and the release of curcumin could thus be controlled. PLA–HPG–curcumin blend showed better cell viability, curcumin release, and finally healing property than PLA–curcumin scaffold. On the other hand, thermoquinone (TQ)-incorporated PLA–cellulose acetate scaffold was found to mimic extracellular matrix because of its 3D nanofibrous structure (Gomaa et al. 2017). TQ prevented the growth of bacteria in the early stage (up to 9 days) due to its sustained release. TQ-incorporated PLA–cellulose acetate scaffold significantly promoted the healing process by controlling the formation of granular tissue and re-epithelialization. Bonan et al. fabricated a fibrous membrane from PLA, PVP, and copaiba oil by the solution blowing method and evaluated its performance as wound dressing material (Bonan et al. 2017). The presence of copaiba oil in the membrane worked as a barrier for bacteria, and PVP favored the degradation of the membrane. The above properties make this membrane a potential candidate for wound dressing applications.

11.5.2.2 PVA–Synthetic Polymer Blend

Electrospun nanofibrous mats prepared from PVA and polyvinyl acetate (PVAc) and loaded with drug ciprofloxacin could be an effective wound dressing material (Jannesari et al. 2011). Swelling ratio and drug release behavior of the nanofibrous mat are dependent on the amount of polymer and loaded drug in the composite. However, PVA–polyvinyl pyrrolidone–PEG-blended electrospun nanofiber with aloe vera gel is also a potential dressing material (Uslu and Aytimur 2012). Crystallinity and crosslinking of the hybrid polymer are directly related to the concentration of aloe vera gel in the matrix. Furthermore, the introduction of hydroxypropyl methylcellulose with aloe vera increased the water retention capacity of the hybrid nanofibers. A highly porous structure of the nanofibers facilitated oxygen penetration and prevented the infiltration of bacteria in a wounded place. In a study, it was found that composite nanofibers prepared from PVA, PVP, pectin, mafenide acetate, and silver (Ag) nanoparticles had the ability to accelerate skin wound healing (Alipour et al. 2019). Electrospinning technique was used to obtain the composite nanofibers. Ag nanoparticle-loaded nanofibers showed better healing properties as compared to composite without Ag nanoparticles. It was concluded that the healing rate was dependent on the amount of Ag loaded to the nanofibers as it inhibits the growth of both gram-positive and gram-negative bacteria.

11.5.2.3 PCL–PVP

PVP is renowned for its excellent solubility in water, and when it is mixed with another biocompatible synthetic polymer PCL, the resulting blend matrix becomes competent for wound healing applications. A composite was obtained from PCL, PVP, and silver nanoparticles to investigate its possibility to use as wound dressing material (Jia et al. 2016). Swelling behavior and antimicrobial and mechanical properties exhibited its capability to create a moist environment and inhibit bacteria growth which is required for effective healing of wound.

11.5.2.4 PCL–PLA

PCL and PLA are both renowned for their biodegradability, biocompatibility, and wide applications in biomedical field. The demand for PCL and PLA to fabricate dressing materials for wound healing applications is increasing day by day. In a study, wound dressing mats were prepared from tetracycline antibiotic-incorporated PCL–PLA mixture applying electrospinning (Zahedi et al. 2012). The performance studies of the composite were investigated by studying the release behavior of the drug from the composite, water retention and uptake capability, and antimicrobial resistance against bacterial growth to compare with commercially available dressing materials. The prepared composite showed improved performance than traditional dressing material due to the presence of hydrophilic PCL and PLA in the blended composite. Karami et al. developed PCL–PLA hybrid nanofiber mats loaded with a herbal drug named thymol (1.2% v/v) (Karami et al. 2013). The release behaviors of the drug from PCL, PLA, and the nanohybrid mats were investigated, and a maximum of 72% release of drug was observed from the nanohybrid mats. In vivo rat model and histopathological analysis showed 92.5% of healing after 14 days which was much better than commercially available wound dressing materials like comfeel plus and gauze bandage.

Some synthetic–synthetic polymer blend matrixes investigated in wound healing application are listed in Table 11.2.

Besides, synthetic–synthetic polymer blend matrixes like silver nanoparticle-loaded PLA–PEG film (Bardania et al. 2020), micro-nanostructured poly(butylene-succinate-co-adipate) (PBSA)-PVP and PEG film (Haidar et al. 2020), and PVA–PVP nanofibrous membranes (Shankhwar et al. 2016) are also found effective in wound management.

11.5.3 Natural–Synthetic Polymer Blend Matrixes

11.5.3.1 Chitosan–PVA

Chitosan–PVA blend matrix is widely used in wound dressing applications because of its biocompatibility, biodegradability, and improved mechanical characteristics (Gutha et al. 2017). Chitosan–PVA matrix loaded with ZnO nanoparticles shows potential antimicrobial and wound healing activities. Gutha et al. prepared chitosan–PVA–ZnO beads by the solvent casting method (Gutha et al. 2017). The beads showed enhanced zone of inhibition than chitosan and chitosan–PVA matrix in case

Table 11.2 Some synthetic–synthetic polymer blend matrixes investigated in wound healing application

Sl. No.	Name of the polymer matrix	Form of the matrix	Loaded drug/species	Special features	Mode of investigation	Time to heal wound (days)	References
01.	Curcumin-loaded PCL–PVA	Multilayered nanofibrous mat	Curcumin	<ul style="list-style-type: none"> • Excellent biocompatibility, water absorbability, and antibacterial property 	In vitro	–	Saeed et al. (2017)
02.	PVA–PCL hybrid nanofibrous mat	Nanofibrous mat	Phenytoln sodium	<ul style="list-style-type: none"> • Enhances the formation of epidermis and collagen deposition 	In vitro and in vivo	14	Zahedi et al. (2013)
03.	Silver nanoparticle-incorporated PCL–PVA	Nanofibers	Silver nanoparticles	<ul style="list-style-type: none"> • High swelling property • Good antibacterial activity 	In vitro	–	Du et al. (2016)
04.	Curcumin-loaded PCL–PEG nanofibers	Nanofibrous mat	Curcumin	<ul style="list-style-type: none"> • Good fibroblastic cell viability and antimicrobial property • Accelerates the healing of wound 	In vitro and in vivo	10	Bui et al. (2014)
05.	Curcumin-loaded PCL–PEG–PCL	Fibrous mats	Curcumin	<ul style="list-style-type: none"> • Good antioxidant efficacy, low cytotoxicity, and promotes dermal wound healing 	In vitro and in vivo	21	Fu et al. (2014)
06.	Nitrofurazone-loaded PVA–PEG semi-IPN hydrogel	Semi-IPN hydrogels	Nitrofurazone	<ul style="list-style-type: none"> • Reduces vapor transmission rate, sustained release of drug • Accelerates burn and acute wound contraction 	In vitro and in vivo	7	Gupta et al. (2013)
07.	PVA–PEG hydrogel film	Hydrogel film	Asiaticoside	<ul style="list-style-type: none"> • Good biocompatibility, swelling ability, elastic property, and antimicrobial activity 	In vitro	–	Ahmed et al. (2018)
08.	Porous PLA–PEG film	Film	Gentamicin sulfate	<ul style="list-style-type: none"> • Inhibits bacterial growth • Enhanced water vapor transmission and oxygen permeability 	In vitro	–	Chitrattha and Phaechamud (2016)

of gram-positive as well as gram-negative bacteria. Similarly, ZnO nanoparticles incorporated chitosan–PVA–starch hydrogel membrane is another potential biomaterial for wound management (Baghaie et al. 2017). It was found better to apply the material at the early stage of wound healing and was resistant toward a wide range of bacteria. This hydrogel membrane was also found to be non-toxic for fibroblastic cells.

11.5.3.2 Chitosan–PEG

Sufficient antimicrobial activity, accelerated wound healing property, and non-cytotoxicity are the prime factors for a wound dressing matrix. In recent times, chitosan–PEG blend matrix has become popular for wound dressing applications. PEG is a synthetic polymer which is used in several biomedical fields like wound dressing, drug delivery, and tissue engineering (Chandy 2020). Blending of PEG with chitosan enhances the ductility and the flexibility of the matrix (Zarrintaj et al. 2020). Silver nanoparticle-incorporated chitosan–PEG matrix was found effective in healing chronic wound in diabetic patients (Masood et al. 2019). The nanocomposites had antibacterial and antioxidant properties with excellent water uptake ability. Ag nanoparticle-incorporated chitosan–PEG hydrogel showed better healing capacity as compared to chitosan–PEG hydrogel in diabetes-induced rabbits. In a research, genipin-crosslinked chitosan (GC)–PEG matrix incorporated with silver and ZnO nanoparticles showed better antibacterial and wound healing capacity than GC–PEG hydrogels and GC–PEG–ZnO nanocomposites (Liu and Kim 2012). Masud et al. prepared a biocomposite from chitosan, PEG, and ZnO nanoparticles by solvent casting method and loaded it with an antibiotic drug, Gentamicin sulfate (Masud et al. 2020). The prepared nanocomposite was non-toxic and biocompatible and showed rapid wound healing property (complete healing within 10 days) than the commercially available bandages.

11.5.3.3 Alginate–PVA

The use of sodium alginate in biomedical applications is increasing not only for its biocompatibility or non-toxicity but also for its outstanding capability to enhance the healing rate of acute wound (Kamoun et al. 2015). A nanobiocomposite sponge was prepared from sodium alginate, graphene oxide, and PVA applying freeze–thawing cyclic process by Ma et al. (2019). Graphene oxide was used to intensify the mechanical properties, chemical properties, and biological activity. The prepared nanocomposite sponge showed suitable water uptake ability, breathability, and mechanical properties and excellent resistance toward the growth of both *Escherichia coli* and *Staphylococcus aureus*. CCK-8 assay analysis shows the enhanced cell proliferation capacity of the composite which is very crucial for wound management. Commercially available essential oils (cinnamon, clove, and lavender) show antimicrobial properties and contain cinnamaldehyde, cinnamyl acetate, linalool, eugenol, and so on. Incorporation of essential oils into electrospun nanofibers is very efficient in wound management (Okamoto and John 2013). Essential oils incorporated electrospun nanofibers of sodium alginate, and PVA was investigated to evaluate the antibacterial activity against bacteria (Rafiq et al.

2018). The nanofibers with cinnamon oil showed a maximum of 2.7 cm zone of inhibition against *Staphylococcus aureus*. Nanoclay has been found potential in drug delivery and wound management in recent times (Roozbahani et al. 2017). A study showed the potentiality of hybrid hydrogel made from laponite–alginate–PVA for wound management with excellent mechanical properties, degradation rate, and biocompatibility (Golafshan et al. 2017). The effectiveness was investigated with a rat model and cell culture of fibroblasts. Results showed that laponite (0.5%) increases blood coagulation and swelling activity more than alginate–PVA hydrogels.

11.5.3.4 Silk–PVA

To improve the fragile property of silk sericin, a research was carried out to blend it with PVA to prepare a film (He et al. 2017). The film was found to have good mechanical properties and high water retention ability. Incorporation of silver nanoparticles in the film can resist the growth of *Escherichia coli* and *Salmonella aureus*. Electrospun nanofiber made from non-mulberry and mulberry silk fibroin (SF) with PVA was applied to the wound of alloxan-induced diabetic rabbits (Chouhan et al. 2018). Non-mulberry SF (NMSF) was found to be more effective for tissue granulation, angiogenesis, and re-epithelialization. Gene expression of NMSF-treated diabetic wound results in accelerated ECM deposition and higher wound breaking strength than the control group and Mulberry SF group.

11.5.3.5 Gelatin–PEG

Nowadays, gelatin–PEG blend matrix, especially hydrogel, has found applications in biomedical field, especially in wound dressing due to its biodegradability, high moisture content, and excellent penetrability of nutrients and metabolites. Hydrogels synthesized by enzymatic crosslinking of silver nanoparticle-incorporated gelatin–PEG–dopamine matrix is an excellent material in wound dressing as it showed resistance against the growth of both gram-positive and gram-negative bacteria (Pham et al. 2020).

Table 11.3 summarizes some special features of natural–synthetic polymer blend matrixes investigated in wound management.

In addition, chitosan–PVP–nanocellulose composite (Poonguzhali et al. 2017), nanostarch-reinforced chitosan–PVP blend (Poonguzhali et al. 2018), nitrofurazone containing PVA–sodium alginate gel (Kim et al. 2008), carboxymethyl cellulose–PEG hydrogels (Capanema et al. 2018), and bacterial cellulose–PEG (Cai and Kim 2010) are some propitious materials for wound healing. Chitosan–PVP doped with cellulose nanowhiskers is a potential drug delivery material in wound dressing management. The addition of cellulose nanowhiskers in the polymer blend increases the mechanical and thermal properties of the composite. The sustained release nature of drug, biocompatibility, and antimicrobial property of the nanobiocomposite showed its efficiency as a wound dressing material (Hasan et al. 2017).

Table 11.3 Some natural–synthetic polymer blend matrixes investigated in wound healing application

Sl. No.	The name of the polymer matrix	Form of the matrix	Drug loaded/ species	Special features	Mode of investigation	Time to heal wound (days)	References
01	Silver oxide nanoparticle-loaded chitosan–PVP film	Film	Silver oxide nanoparticles	<ul style="list-style-type: none"> • Excellent antimicrobial and wound healing property 	In vitro and in vivo	14	Archana et al. (2015)
02	Titanium dioxide nanoparticle-loaded chitosan–PVP nanocomposite	Sheet	Titanium dioxide nanoparticles	<ul style="list-style-type: none"> • Good antibacterial activity, mechanical property, and biocompatibility. • Hydrophilic in nature 	In vitro and in vivo	16	Archana et al. (2013)
03	ZnO nanoparticle-incorporated chitosan–PVA–starch hydrogel	Hydrogel membrane	ZnO nanoparticles	<ul style="list-style-type: none"> • Non-toxic toward fibroblastic cell, wide range antibacterial activity 	In vitro and in vivo	7	Baghaie et al. (2017)
04	Silk fibroin–PEG semi-IPN network	Sponge	–	<ul style="list-style-type: none"> • Enhances cell proliferation and collagen deposition 	In vitro and in vivo	12	Kweon et al. (2008)
05	Silk sericin–PEG diacrylate	Hydrogel	–	<ul style="list-style-type: none"> • Excellent mechanical properties • Non-cytotoxic to human fibroblastic cells 	In vitro	–	Punyamoonwongsa et al. (2019)
06	PCL–gelatin–nanochitosan–curcumin	Scaffold	Curcumin	<ul style="list-style-type: none"> • Good mechanical and structural properties including porosity, uniformity, and pore size • Higher cell proliferation capacity 	In vitro and in vivo	14	Zahiri et al. (2020)
07	Spirulina extract impregnated alginate–PCL nanofibers	Nanofibers	Spirulina extract	<ul style="list-style-type: none"> • Improves cell adhesion • High water uptake ability 	In vitro and in vivo	9	Choi et al. (2017)
08	PCL–gelatin–clove essential oil	Nanofiber mats	Clove oil	<ul style="list-style-type: none"> • Good antibacterial property • Non-toxic against human fibroblastic cell. 	In vitro	–	Unalan et al. (2019)

09	Silver nanoparticle-loaded PVP-alginate	Hydrogel	Silver nanoparticles	<ul style="list-style-type: none"> • Efficient fluid handling capacity • Excellent antimicrobial property 	In vitro	–	Singh and Singh (2012)
10	PVA-cellulose nanowhiskers nanocomposite	Hydrogel	–	<ul style="list-style-type: none"> • Outstanding mechanical characteristic swelling ability • Strong activity against microorganisms 	In vitro	–	Gonzalez et al. (2014)

11.6 Future Aspects

Wound healing involves some closely connected consecutive stages with different kinds of ions, enzymes, cytokines, hormones, and growth factors. Providing these elements to the site of wound externally can be helpful for faster healing of wound. However, the localized delivery of cell growth factors, ions, enzymes, or even antibiotic drugs to wounded area is yet to be explored completely. Polymer matrixes in the form of dressing materials are well capable of loading and delivering these elements to the site of wound and accelerate the healing process. Polymers or blend of polymers (both natural and synthetic) is biocompatible, biodegradable, non-toxic, and can deliver bioactive substances that can promote cell proliferation and collagen deposition. But most of these wound dressing materials fail to reduce scar formation and promote the growth of hair follicles, glands, nerves, etc. So, advancement in polymer matrixes for wound healing to overcome these shortcomings is a need in near future. Moreover, bacteria are becoming resistant to antibiotics nowadays. Delivery of nanoparticles that possess antimicrobial properties through polymer matrixes can be explored to avoid the use of antibiotic drugs. Future research should be focused on developing polymer matrixes integrated with sensors to monitor pH, moisture, and oxygen level, and having stimuli-responsive release characteristics of bioactive substances.

11.7 Conclusion

Because of heterogeneous nature of wounds, selection of proper dressing material is a vital step in wound management. For a successful wound management, dressing materials are required to support the wound beds, to protect them from the factors that may hinder healing such as contamination, bacterial attack, or loss of moisture and to accelerate various stages of wound healing. An extraordinary advancement in science and technology has taken place over the past decades which leads to a better understanding of wound management like different stages of wound healing, effect of local wound factors, and interaction between wound and extracellular matrix. From that point of view, different polymeric matrices have been clinically used in wound dressings because of their inherent properties like biocompatibility, biodegradability, hemostatic property, and ability to promote tissue regeneration. Moreover, different drugs, growth factors, enzymes, growth promoters, and other bioactive substances can be loaded in these matrixes to support and accelerate the healing process. Alginate, collagen, hyaluronic acid, poly(lactic-co-glycolic acid)-based bio-engineered skin substitutes, composite skin grafts, epidermal autografts, and dermal substitutes have been in clinical trials, and some of them have already been approved by FDA and available in market [Orcel (Forticell Bioscience, Inc., New York, NY, USA), Apligraf (Organogenesis, Inc., Canton, MA, USA)] (Mir et al. 2018). Overall, polymer matrix-based systems have all the potential to fulfill the requirements of advanced wound dressing materials.

References

- Aderibigbe BA, Buyana B (2018) Alginate in wound dressings. *Pharmaceutics* 10(2):42
- Adomavičiūtė E, Pupkevičiūtė S, Juškaitė V, Žilius M, Stanys S, Pavilonis A, Briedis V (2017) Formation and investigation of electrospun PLA materials with propolis extracts and silver nanoparticles for biomedical applications. *J Nanomater* 2017:8612819
- Aduba DC, Yang H (2017) Polysaccharide fabrication platforms and biocompatibility assessment as candidate wound dressing materials. *Bioengineering* 4(1):1
- Ahmed S, Ikram S (2016a) Chitosan based scaffolds and their applications in wound healing. *Achiev Life Sci* 10(1):27–37
- Ahmed S, Ikram S (2016b) Chitosan based scaffolds and their applications in wound healing. *Achiev in the life sciences* 10(1):27–37
- Ahmed AS, Mandal UK, Taher M, Susanti D, Jaffri JM (2018) PVA-PEG physically cross-linked hydrogel film as a wound dressing: experimental design and optimization. *Pharm Dev Technol* 23(8):751–760
- Alaribe FN, Manoto SL, Motaung SC (2016) Scaffolds from biomaterials: advantages and limitations in bone and tissue engineering. *Biologia* 71(4):353–366
- Alexis O, Guang Y, Guiaro M (2017) New approach for skin repair by using bacterial cellulose altered with paraffin and porous bacterial cellulose based scaffold with alginate. *J Anal Pharm Res* 5(3):00141
- Alipour R, Khorshidi A, Shojaei AF, Mashayekhi F, Moghaddam MJM (2019) Skin wound healing acceleration by Ag nanoparticles embedded in PVA/PVP/pectin/mafenide acetate composite nanofibers. *Polym Test* 79:106022
- Ansari M, Kordestani SS, Nazralizadeh S, Eslami H (2018) Biodegradable cell-seeded collagen based polymer scaffolds for wound healing and skin reconstruction. *J Macromol Sci B* 57(2):100–109
- Anumolu SS, DeSantis AS, Menjoge AR, Hahn RA, Beloni JA, Gordon MK, Sinko PJ (2010) Doxycycline loaded poly (ethylene glycol) hydrogels for healing vesicant-induced ocular wounds. *Biomaterials* 31(5):964–974
- Archana D, Singh BK, Dutta J, Dutta P (2013) In vivo evaluation of chitosan–PVP–titanium dioxide nanocomposite as wound dressing material. *Carbohydr Polym* 95(1):530–539
- Archana D, Singh BK, Dutta J, Dutta P (2015) Chitosan-PVP-nano silver oxide wound dressing: in vitro and in vivo evaluation. *Int J Biol Macromol* 73:49–57
- Arockianathan PM, Sekar S, Kumaran B, Sastry T (2012) Preparation, characterization and evaluation of biocomposite films containing chitosan and sago starch impregnated with silver nanoparticles. *Int J Biol Macromol* 50(4):939–946
- Babavalian H, Latifi AM, Shokrgozar MA, Bonakdar S, Mohammadi S, Moghaddam MM (2015) Analysis of healing effect of alginate sulfate hydrogel dressing containing antimicrobial peptide on wound infection caused by methicillin-resistant *Staphylococcus aureus*. *Jundishapur J Microbiol* 8(9):e28320
- Baghaie S, Khorasani MT, Zarrabi A, Moshtaghian J (2017) Wound healing properties of PVA/starch/chitosan hydrogel membranes with nano zinc oxide as antibacterial wound dressing material. *J Biomater Sci Polym Ed* 28(18):2220–2241
- Bagher Z, Ehterami A, Safdel MH, Khastar H, Semiari H, Asefnejad A, Davachi SM, Mirzaii M, Salehi M (2020) Wound healing with alginate/chitosan hydrogel containing hesperidin in rat model. *J Drug Deliv Sci Technol* 55:101379
- Bardania H, Mahmoudi R, Bagheri H, Salehpour Z, Fouani MH, Darabian B, Khoramrooz SS, Mousavizadeh A, Kowsari M, Moosavifard SE (2020) Facile preparation of a novel biogenic silver-loaded Nanofilm with intrinsic anti-bacterial and oxidant scavenging activities for wound healing. *Sci Rep* 10(1):1–14
- Basu A, Celma G, Strømme M, Ferraz N (2018) In vitro and in vivo evaluation of the wound healing properties of nanofibrillated cellulose hydrogels. *ACS Appl Bio Mater* 1(6):1853–1863

- Bayat S, Amiri N, Pishavar E, Kalalinia F, Movaffagh J, Hashemi M (2019) Bromelain-loaded chitosan nanofibers prepared by electrospinning method for burn wound healing in animal models. *Life Sci* 229:57–66
- Bhattarai SR, Bhattarai N, Yi HK, Hwang PH, Cha DI, Kim HY (2004) Novel biodegradable electrospun membrane: scaffold for tissue engineering. *Biomaterials* 25(13):2595–2602
- Biswas S, Ahmed T, Islam MM, Islam MS, Rahman MM (2020) Biomedical applications carboxymethyl chitosans. In: Gopi S, Thomas S, Pius A (eds) *Handbook of chitin and chitosan*, vol 3. Woodhead Publishing, Elsevier, Swaston, pp 433–470
- Bonan RF, Bonan PR, Batista AU, Perez DE, Castellano LR, Oliveira JE, Medeiros ES (2017) Poly (lactic acid)/poly (vinyl pyrrolidone) membranes produced by solution blow spinning: structure, thermal, spectroscopic, and microbial barrier properties. *J Appl Polym Sci* 134(19):44802
- Bourke SL, Al-Khalili M, Briggs T, Michniak BB, Kohn J, Poole-Warren LA (2003) A photo-crosslinked poly (vinyl alcohol) hydrogel growth factor release vehicle for wound healing applications. *AAPS PharmSci* 5(4):101–111
- Bui HT, Chung OH, Cruz JD, Park JS (2014) Fabrication and characterization of electrospun curcumin-loaded polycaprolactone-polyethylene glycol nanofibers for enhanced wound healing. *Macromol Res* 22(12):1288–1296
- Cai Z, Kim J (2010) Bacterial cellulose/poly (ethylene glycol) composite: characterization and first evaluation of biocompatibility. *Cellulose* 17(1):83–91
- Cai N, Li C, Han C, Luo X, Shen L, Xue Y, Yu F (2016) Tailoring mechanical and antibacterial properties of chitosan/gelatin nanofiber membranes with Fe₃O₄ nanoparticles for potential wound dressing application. *Appl Surf Sci* 369:492–500
- Capanema NS, Mansur AA, de Jesus AC, Carvalho SM, de Oliveira LC, Mansur HS (2018) Superabsorbent crosslinked carboxymethyl cellulose-PEG hydrogels for potential wound dressing applications. *Int J Biol Macromol* 106:1218–1234
- Carvalho IC, Mansur HS (2017) Engineered 3D-scaffolds of photocrosslinked chitosan-gelatin hydrogel hybrids for chronic wound dressings and regeneration. *Mater Sci Eng C* 78:690–705
- Chandy T (2020) Biocompatibility of materials and its relevance to drug delivery and tissue engineering. In: *Biointegration of medical implant materials*. Elsevier, Amsterdam, pp 297–331
- Chen S-L, Fu R-H, Liao S-F, Liu S-P, Lin S-Z, Wang Y-C (2018) A PEG-based hydrogel for effective wound care management. *Cell Transplant* 27(2):275–284
- Chen H, Cheng R, Zhao X, Zhang Y, Tam A, Yan Y, Shen H, Zhang YS, Qi J, Feng Y (2019a) An injectable self-healing coordinative hydrogel with antibacterial and angiogenic properties for diabetic skin wound repair. *NPG Asia Mater* 11(1):1–12
- Chen J, Chen L, Xie F, Li X (2019b) Toxicology of starch-based DDSs. In: *Drug delivery applications of starch biopolymer derivatives*. Springer, New York, pp 133–137
- Chen A, Huang W, Wu L, An Y, Xuan T, He H, Ye M, Qi L, Wu J (2020) Bioactive ECM mimic hyaluronic acid dressing via sustained releasing of bFGF for enhancing skin wound healing. *ACS Appl Biol Mater* 3(5):3039–3048
- Chiaoprakobkij N, Seetabhawang S, Sanchavanakit N, Phisalaphong M (2019) Fabrication and characterization of novel bacterial cellulose/alginate/gelatin biocomposite film. *J Biomater Sci Polym Ed* 30(11):961–982
- Chinatangkul N, Tubtimsri S, Panchapornpon D, Akkaramongkolporn P, Limmatvapirat C, Limmatvapirat S (2019) Design and characterisation of electrospun shellac-polyvinylpyrrolidone blended micro/nanofibres loaded with monolaurin for application in wound healing. *Int J Pharm* 562:258–270
- Chitraththa S, Phaechamud T (2016) Porous poly (DL-lactic acid) matrix film with antimicrobial activities for wound dressing application. *Mater Sci Eng C* 58:1122–1130
- Choi J-B, Park J-S, Khil M-S, Gwon H-J, Lim Y-M, Jeong S-I, Shin Y-M, Nho Y-C (2013) Characterization and antimicrobial property of poly (acrylic acid) nanogel containing silver particle prepared by electron beam. *Int J Mol Sci* 14(6):11011–11023
- Choi JI, Kim MS, Chung GY, Shin HS (2017) Spirulina extract-impregnated alginate-PCL nanofiber wound dressing for skin regeneration. *Biotechnol Bioprocess Eng* 22(6):679–685

- Choudhary A, Kant V, Jangir BL, Joshi V (2020) Quercetin loaded chitosan tripolyphosphate nanoparticles accelerated cutaneous wound healing in Wistar rats. *Eur J Pharmacol* 880:173172
- Chouhan D, Janani G, Chakraborty B, Nandi SK, Mandal BB (2018) Functionalized PVA–silk blended nanofibrous mats promote diabetic wound healing via regulation of extracellular matrix and tissue remodelling. *J Tissue Eng Regen Med* 12(3):e1559–e1570
- Colobatiu L, Gavan A, Potarniche A-V, Rus V, Diaconeasa Z, Mocan A, Tomuta I, Mirel S, Mihaiu M (2019) Evaluation of bioactive compounds-loaded chitosan films as a novel and potential diabetic wound dressing material. *React Funct Polym* 145:104369
- Dai X-Y, Nie W, Wang Y-C, Shen Y, Li Y, Gan S-J (2012) Electrospun emodin polyvinylpyrrolidone blended nanofibrous membrane: a novel medicated biomaterial for drug delivery and accelerated wound healing. *J Mater Sci Mater Med* 23(11):2709–2716
- Dhivya S, Padma VV, Santhini E (2015) Wound dressings—a review. *Biomedicine* 5(4):22
- Do AV, Khorsand B, Geary SM, Salem AK (2015) 3D printing of scaffolds for tissue regeneration applications. *Adv Healthc Mater* 4(12):1742–1762
- dos Santos AEA, dos Santos FV, Freitas KM, Pimenta LPS, de Oliveira AL, Marinho TA, de Avelar GF, da Silva AB, Ferreira RV (2020) Cellulose acetate nanofibers loaded with crude annatto extract: preparation, characterization, and in vivo evaluation for potential wound healing applications. *Mater Sci Eng C Mater Biol Appl* 118:111322
- Du L, Xu H, Li T, Zhang Y, Zou F (2016) Fabrication of silver nanoparticle/polyvinyl alcohol/polycaprolactone hybrid nanofibers nonwovens by two-nozzle electrospinning for wound dressing. *Fibers Polym* 17(12):1995–2005
- Eltom A, Zhong G, Muhammad A (2019) Scaffold techniques and designs in tissue engineering functions and purposes: a review. *Adv Mater Sci Eng* 2019:3429527
- Fan X, Chen K, He X, Li N, Huang J, Tang K, Li Y, Wang F (2016) Nano-TiO₂/collagen-chitosan porous scaffold for wound repairing. *Int J Biol Macromol* 91:15–22
- Feroz S, Muhammad N, Ranayake J, Dias G (2020) Keratin-based materials for biomedical applications. *Bioact Mater* 5(3):496–509
- Foldberg S, Petersen M, Fojan P, Gurevich L, Fink T, Pennisi CP, Zachar V (2012) Patterned poly (lactic acid) films support growth and spontaneous multilineage gene expression of adipose-derived stem cells. *Colloids Surf B Biointerfaces* 93:92–99
- Fu SZ, Meng XH, Fan J, Yang LL, Wen QL, Ye SJ, Lin S, Wang BQ, Chen LL, Wu JB (2014) Acceleration of dermal wound healing by using electrospun curcumin-loaded poly (ϵ -caprolactone)-poly (ethylene glycol)-poly (ϵ -caprolactone) fibrous mats. *J Biomed Mater Res B Appl Biomater* 102(3):533–542
- Gamez E, Mendoza G, Salido S, Arruebo M, Irusta S (2019) Antimicrobial electrospun polycaprolactone-based wound dressings: an in vitro study about the importance of the direct contact to elicit bactericidal activity. *Adv Wound Care* 8(9):438–451
- Gaspar-Pintiliescu A, Stanciuc A-M, Craciunescu O (2019) Natural composite dressings based on collagen, gelatin and plant bioactive compounds for wound healing: a review. *Int J Biol Macromol* 138:854–865
- Ge Z, Jin Z, Cao T (2008) Manufacture of degradable polymeric scaffolds for bone regeneration. *Biomed Mater* 3(2):022001
- Ghorbani S, Eyni H, Tiraihi T, Salari Asl L, Soleimani M, Atashi A, Pour Beiranvand S, Ebrahimi Warkiani M (2018) Combined effects of 3D bone marrow stem cell-seeded wet-electrospun poly lactic acid scaffolds on full-thickness skin wound healing. *Int J Polym Mater* 67(15):905–912
- Gilbert ME, Kirker KR, Gray SD, Ward PD, Szakacs JG, Prestwich GD, Orlandi RR (2004) Chondroitin sulfate hydrogel and wound healing in rabbit maxillary sinus mucosa. *Laryngoscope* 114(8):1406–1409
- Goder D, Matsliah L, Giladi S, Reshef-Steinberger L, Zin I, Shaul A, Zilberman M (2020) Mechanical, physical and biological characterization of soy protein films loaded with bupivacaine for wound healing applications. *Int J Polym Mater* 70:345–355

- Golafshan N, Rezahasani R, Esfahani MT, Kharaziha M, Khorasani S (2017) Nanohybrid hydrogels of laponite: PVA-alginate as a potential wound healing material. *Carbohydr Polym* 176:392–401
- Gomaa SF, Madkour TM, Moghannem S, El-Sherbiny IM (2017) New polylactic acid/cellulose acetate-based antimicrobial interactive single dose nanofibrous wound dressing mats. *Int J Biol Macromol* 105:1148–1160
- Gonzalez JS, Ludueña LN, Ponce A, Alvarez VA (2014) Poly (vinyl alcohol)/cellulose nanowhiskers nanocomposite hydrogels for potential wound dressings. *Mater Sci Eng C* 34:54–61
- Gou L, Xiang M, Ni X (2020) Development of wound therapy in nursing care of infants by using injectable gelatin-cellulose composite hydrogel incorporated with silver nanoparticles. *Mater Lett* 277:128340
- Guo X, Xu D, Zhao Y, Gao H, Shi X, Cai J, Deng H, Chen Y, Du Y (2019) Electroassembly of chitin nanoparticles to construct freestanding hydrogels and high porous aerogels for wound healing. *ACS Appl Mater Interfaces* 11(38):34766–34776
- Gupta A, Upadhyay NK, Parthasarathy S, Rajagopal C, Roy PK (2013) Nitrofurazone-loaded PVA-PEG semi-IPN for application as hydrogel dressing for normal and burn wounds. *J Appl Polym Sci* 128(6):4031–4039
- Gupta RC, Lall R, Srivastava A, Sinha A (2019) Hyaluronic acid: molecular mechanisms and therapeutic trajectory. *Front Vet Sci* 6:192
- Gutha Y, Pathak JL, Zhang W, Zhang Y, Jiao X (2017) Antibacterial and wound healing properties of chitosan/poly (vinyl alcohol)/zinc oxide beads (CS/PVA/ZnO). *Int J Biol Macromol* 103:234–241
- Haidar NB, Marais S, Dé E, Schaumann A, Barreau M, Feuilloley MG, Duncan AC (2020) Chronic wound healing: a specific antibiofilm protein-asymmetric release system. *Mater Sci Eng C* 106:110130
- Han F, Dong Y, Song A, Yin R, Li S (2014) Alginate/chitosan based bi-layer composite membrane as potential sustained-release wound dressing containing ciprofloxacin hydrochloride. *Appl Surf Sci* 311:626–634
- Hasan A, Waibhaw G, Tiwari S, Dharmalingam K, Shukla I, Pandey LM (2017) Fabrication and characterization of chitosan, polyvinylpyrrolidone, and cellulose nanowhiskers nanocomposite films for wound healing drug delivery application. *J Biomed Mater Res A* 105(9):2391–2404
- Hasan A, Waibhaw G, Saxena V, Pandey LM (2018) Nano-biocomposite scaffolds of chitosan, carboxymethyl cellulose and silver nanoparticle modified cellulose nanowhiskers for bone tissue engineering applications. *Int J Biol Macromol* 111:923–934
- He H, Cai R, Wang Y, Tao G, Guo P, Zuo H, Chen L, Liu X, Zhao P, Xia Q (2017) Preparation and characterization of silk sericin/PVA blend film with silver nanoparticles for potential antimicrobial application. *Int J Biol Macromol* 104:457–464
- Helary C, Zarka M, Giraud-Guille MM (2012) Fibroblasts within concentrated collagen hydrogels favour chronic skin wound healing. *J Tissue Eng Regen Med* 6(3):225–237
- Horue M, Cacicedo ML, Fernandez MA, Rodenak-Kladniew B, Sánchez RMT, Castro GR (2020) Antimicrobial activities of bacterial cellulose-silver montmorillonite nanocomposites for wound healing. *Mater Sci Eng C* 116:111152
- Hu M, Sabelman EE, Cao Y, Chang J, Hentz VR (2003) Three-dimensional hyaluronic acid grafts promote healing and reduce scar formation in skin incision wounds. *J Biomed Mater Res B Appl Biomater* 67(1):586–592
- Huang R, Li W, Lv X, Lei Z, Bian Y, Deng H, Wang H, Li J, Li X (2015) Biomimetic LBL structured nanofibrous matrices assembled by chitosan/collagen for promoting wound healing. *Biomaterials* 53:58–75
- Huang Y, Zhao X, Zhang Z, Liang Y, Yin Z, Chen B, Bai L, Han Y, Guo B (2020) Degradable gelatin-based IPN Cryogel hemostat for rapidly stopping deep noncompressible hemorrhage and simultaneously improving wound healing. *Chem Mater* 32(15):6595–6610

- Islam MS, Haque P, Rashid TU, Khan MN, Mallik AK, Khan MNI, Khan M, Rahman MM (2017) Core-shell drug carrier from folate conjugated chitosan obtained from prawn shell for targeted doxorubicin delivery. *J Mater Sci Mater Med* 28(4):55
- Islam MS, Rahman MS, Ahmed T, Biswas S, Haque P, Rahman MM (2020) Chitosan and chitosan-based biomaterials for wound management. In: Gopi S, Thomas S, Pius A (eds) *Handbook of chitin and chitosan*, vol 3. Woodhead Publishing, Elsevier, Swaston, pp 721–759
- Izumi R, Komada S, Ochi K, Karasawa L, Osaki T, Murahata Y, Tsuka T, Imagawa T, Itoh N, Okamoto Y (2015) Favorable effects of superficially deacetylated chitin nanofibrils on the wound healing process. *Carbohydr Polym* 123:461–467
- Jaklenc A, Hinckfuss A, Bilgen B, Ciombor DM, Aaron R, Mathiowitz E (2008) Sequential release of bioactive IGF-I and TGF- β 1 from PLGA microsphere-based scaffolds. *Biomaterials* 29(10):1518–1525
- Jannesari M, Varshosaz J, Morshed M, Zamani M (2011) Composite poly (vinyl alcohol)/poly (vinyl acetate) electrospun nanofibrous mats as a novel wound dressing matrix for controlled release of drugs. *Int J Nanomedicine* 6:993
- Jatoi AW, Ogasawara H, Kim IS, Ni Q-Q (2019) Polyvinyl alcohol nanofiber based three phase wound dressings for sustained wound healing applications. *Mater Lett* 241:168–171
- Jia Y, Huang G, Dong F, Liu Q, Nie W (2016) Preparation and characterization of electrospun poly (ϵ -caprolactone)/poly (vinyl pyrrolidone) nanofiber composites containing silver particles. *Polym Compos* 37(9):2847–2854
- Jridi M, Sellimi S, Lassoued KB, Beltaief S, Souissi N, Mora L, Toldra F, Elfeki A, Nasri M, Nasri R (2017) Wound healing activity of cuttlefish gelatin gels and films enriched by henna (*Lawsonia inermis*) extract. *Colloids Surf Physicochem Eng Aspects* 512:71–79
- Ju HW, Lee OJ, Lee JM, Moon BM, Park HJ, Park YR, Lee MC, Kim SH, Chao JR, Ki CS (2016) Wound healing effect of electrospun silk fibroin nanomatrix in burn-model. *Int J Biol Macromol* 85:29–39
- Jung H-S, Kim MH, Shin JY, Park SR, Jung J-Y, Park WH (2018) Electrospinning and wound healing activity of β -chitin extracted from cuttlefish bone. *Carbohydr Polym* 193:205–211
- Kabir SF, Sikdar PP, Haque B, Bhuiyan MR, Ali A, Islam M (2018) Cellulose-based hydrogel materials: chemistry, properties and their prospective applications. *Prog Biomater* 7(3):153–174
- Kamoun EA, Kenawy E-RS, Tamer TM, El-Meligy MA, Eldin MSM (2015) Poly (vinyl alcohol)-alginate physically crosslinked hydrogel membranes for wound dressing applications: characterization and bio-evaluation. *Arab J Chem* 8(1):38–47
- Kandhasamy S, Arthi N, Arun RP, Verma RS (2019) Synthesis and fabrication of novel quinone-based chromenopyrazole antioxidant-laden silk fibroin nanofibers scaffold for tissue engineering applications. *Mater Sci Eng C* 102:773–787
- Karami Z, Rezaeian I, Zahedi P, Abdollahi M (2013) Preparation and performance evaluations of electrospun poly (ϵ -caprolactone), poly (lactic acid), and their hybrid (50/50) nanofibrous mats containing thymol as an herbal drug for effective wound healing. *J Appl Polym Sci* 129 (2):756–766
- Khalid A, Khan R, Ul-Islam M, Khan T, Wahid F (2017) Bacterial cellulose-zinc oxide nanocomposites as a novel dressing system for burn wounds. *Carbohydr Polym* 164:214–221
- Khan MN, Hasan MM, Islam MS, Biswas S, Rashid TU, Mallik AK, Zaman A, Sharmeen S, Haque P, Rahman MM (2017) Biomimetic gelatin nanocomposite as a scaffold for bone tissue repair. In: *Handbook of composites from renewable materials*. Scrivener Publishing, Austin, pp 487–525
- Kim J, Lee C-M (2018) Transdermal hydrogel composed of polyacrylic acid containing Propolis for wound healing in a rat model. *Macromol Res* 26(13):1219–1224
- Kim JO, Park JK, Kim JH, Jin SG, Yong CS, Li DX, Choi JY, Woo JS, Yoo BK, Lyoo WS (2008) Development of polyvinyl alcohol-sodium alginate gel-matrix-based wound dressing system containing nitrofurazone. *Int J Pharm* 359(1–2):79–86
- Konop M, Czuwara J, Kłodzińska E, Laskowska AK, Sulejczak D, Damps T, Zielenkiewicz U, Brzozowska I, Sureda A, Kowalkowski T (2020) Evaluation of keratin biomaterial containing

- silver nanoparticles as a potential wound dressing in full-thickness skin wound model in diabetic mice. *J Tissue Eng Regen Med* 14(2):334–346
- Kumar MS, Kirubanandan S, Sripriya R, Sehgal PK (2010) Triphala incorporated collagen sponge—a smart biomaterial for infected dermal wound healing. *J Surg Res* 158(1):162–170
- Kweon H, Yeo J-H, Lee K-G, Lee HC, Na HS, Won YH, Cho CS (2008) Semi-interpenetrating polymer networks composed of silk fibroin and poly (ethylene glycol) for wound dressing. *Biomed Mater* 3(3):034115
- Lee KY, Mooney DJ (2012) Alginate: properties and biomedical applications. *Prog Polym Sci* 37(1):106–126
- Li M, Han M, Sun Y, Hua Y, Chen G, Zhang L (2019) Oligoarginine mediated collagen/chitosan gel composite for cutaneous wound healing. *Int J Biol Macromol* 122:1120–1127
- Liechty WB, Kryscio DR, Slaughter BV, Peppas NA (2010) Polymers for drug delivery systems. *Annu Rev Chem Biomol Eng* 1:149–173
- Liu Y, Kim H-I (2012) Characterization and antibacterial properties of genipin-crosslinked chitosan/poly (ethylene glycol)/ZnO/Ag nanocomposites. *Carbohydr Polym* 89(1):111–116
- Liu M, Duan X-P, Li Y-M, Yang D-P, Long Y-Z (2017) Electrospun nanofibers for wound healing. *Mater Sci Eng C* 76:1413–1423
- Loh QL, Choong C (2013) Three-dimensional scaffolds for tissue engineering applications: role of porosity and pore size. *Tissue Eng Part B Rev* 19(6):485–502
- López-Iglesias C, Barros J, Ardao I, Monteiro FJ, Alvarez-Lorenzo C, Gómez-Amoza JL, García-González CA (2019) Vancomycin-loaded chitosan aerogel particles for chronic wound applications. *Carbohydr Polym* 204:223–231
- Ma Y, Xin L, Tan H, Fan M, Li J, Jia Y, Ling Z, Chen Y, Hu X (2017) Chitosan membrane dressings toughened by glycerol to load antibacterial drugs for wound healing. *Mater Sci Eng C* 81:522–531
- Ma R, Wang Y, Qi H, Shi C, Wei G, Xiao L, Huang Z, Liu S, Yu H, Teng C (2019) Nanocomposite sponges of sodium alginate/graphene oxide/polyvinyl alcohol as potential wound dressing: in vitro and in vivo evaluation. *Compos Part B Eng* 167:396–405
- Malafaya PB, Silva GA, Reis RL (2007) Natural–origin polymers as carriers and scaffolds for biomolecules and cell delivery in tissue engineering applications. *Adv Drug Deliv Rev* 59(4–5):207–233
- Mallik AK, Shahruzzaman M, Islam MS, Haque P, Rahman MM (2019) Biodegradability and biocompatibility of natural polymers. In: *Natural polymers for pharmaceutical applications*. Apple Academic Press, Boca Raton, pp 133–168
- Masood N, Ahmed R, Tariq M, Ahmed Z, Masoud MS, Ali I, Asghar R, Andleeb A, Hasan A (2019) Silver nanoparticle impregnated chitosan-PEG hydrogel enhances wound healing in diabetes induced rabbits. *Int J Pharm* 559:23–36
- Masad RA, Islam MS, Haque P, Khan MNI, Shahruzzaman M, Khan M, Takafuji M, Rahman MM (2020) Preparation of novel chitosan/poly (ethylene glycol)/ZnO bionanocomposite for wound healing application: effect of gentamicin loading. *Materialia* 12:100785
- Mayet N, Choonara YE, Kumar P, Tomar LK, Tyagi C, Du Toit LC, Pillay V (2014) A comprehensive review of advanced biopolymeric wound healing systems. *J Pharm Sci* 103(8):2211–2230
- Mir M, Ali MN, Barakullah A, Gulzar A, Arshad M, Fatima S, Asad M (2018) Synthetic polymeric biomaterials for wound healing: a review. *Prog Biomater* 7(1):1–21
- Miyaguchi S-I, Horii A, Kambara R, Takemoto N, Akazawa H, Takahashi N, Baba H, Inohara H (2016) Effects of covering surgical wounds with polyglycolic acid sheets for posttonsillectomy pain. *Otolaryngol Head Neck Surg* 155(5):876–878
- Mogoşanu GD, Grumezescu AM (2014) Natural and synthetic polymers for wounds and burns dressing. *Int J Pharm* 463(2):127–136
- Mukherjee B, Dey NS, Maji R, Bhowmik P, Das PJ, Paul P (2014) Current status and future scope for nanomaterials in drug delivery. In: *Application of nanotechnology in drug delivery*. IntechOpen, London

- Mukhopadhyay A, Rajput M, Barui A, Chatterjee SS, Pal NK, Chatterjee J, Mukherjee R (2020) Dual cross-linked honey coupled 3D antimicrobial alginate hydrogels for cutaneous wound healing. *Mater Sci Eng C* 116:111218
- Murray RZ, West ZE, Cowin AJ, Farrugia BL (2019) Development and use of biomaterials as wound healing therapies. *Burns Trauma* 7:s41038–41018–s40139–41037
- Naseri-Nosar M, Ziora ZM (2018) Wound dressings from naturally-occurring polymers: a review on homopolysaccharide-based composites. *Carbohydr Polym* 189:379–398
- Natarajan V, Krithica N, Madhan B, Sehgal PK (2013) Preparation and properties of tannic acid cross-linked collagen scaffold and its application in wound healing. *J Biomed Mater Res B Appl Biomater* 101(4):560–567
- Nguyen TTT, Ghosh C, Hwang S-G, Dai Tran L, Park JS (2013) Characteristics of curcumin-loaded poly (lactic acid) nanofibers for wound healing. *J Mater Sci* 48(20):7125–7133
- Nuutila K, Laukkanen A, Lindford A, Juteau S, Nuopponen M, Vuola J, Kankuri E (2018) Inhibition of skin wound contraction by nanofibrillar cellulose hydrogel. *Plast Reconstr Surg* 141(3):357e–366e
- Okamoto M, John B (2013) Synthetic biopolymer nanocomposites for tissue engineering scaffolds. *Prog Polym Sci* 38(10–11):1487–1503
- Pal D, Saha S (2019) Chondroitin: a natural biomarker with immense biomedical applications. *RSC Adv* 9(48):28061–28077
- Pal S, Nisi R, Stoppa M, Licciulli A (2017) Silver-functionalized bacterial cellulose as antibacterial membrane for wound-healing applications. *ACS omega* 2(7):3632–3639
- Patel S, Srivastava S, Singh MR, Singh D (2018) Preparation and optimization of chitosan-gelatin films for sustained delivery of lupeol for wound healing. *Int J Biol Macromol* 107:1888–1897
- Pei Y, Ye D, Zhao Q, Wang X, Zhang C, Huang W, Zhang N, Liu S, Zhang L (2015) Effectively promoting wound healing with cellulose/gelatin sponges constructed directly from a cellulose solution. *J Mater Chem B* 3(38):7518–7528
- Perumal G, Pappuru S, Chakraborty D, Nandkumar AM, Chand DK, Doble M (2017) Synthesis and characterization of curcumin loaded PLA—Hyperbranched polyglycerol electrospun blend for wound dressing applications. *Mater Sci Eng C* 76:1196–1204
- Pham T-N, Jiang Y-S, Su C-F, Jan J-S (2020) In situ formation of silver nanoparticles-contained gelatin-PEG-dopamine hydrogels via enzymatic cross-linking reaction for improved antibacterial activities. *Int J Biol Macromol* 146:1050–1059
- Poonguzhali R, Basha SK, Kumari VS (2017) Synthesis and characterization of chitosan-PVP-nanocellulose composites for in-vitro wound dressing application. *Int J Biol Macromol* 105:111–120
- Poonguzhali R, Basha SK, Kumari VS (2018) Nanostarch reinforced with chitosan/poly (vinyl pyrrolidone) blend for in vitro wound healing application. *Polym Plast Technol Eng* 57(14):1400–1410
- Póvoa VC, dos Santos GJ, Picheth GF, Jara CP, da Silva LC, de Araújo EP, de Oliveira MG (2020) Wound healing action of nitric oxide-releasing self-expandable collagen sponge. *J Tissue Eng Regen Med* 14(6):807–818
- Punyamoonwongsa P, Klayya S, Sajomsang W, Kunyane C, Aueviriyavit S (2019) Silk sericin semi-interpenetrating network hydrogels based on PEG-Diacrylate for wound healing treatment. *Int J Polym Sci* 2019:4740765
- Rafiq M, Hussain T, Abid S, Nazir A, Masood R (2018) Development of sodium alginate/PVA antibacterial nanofibers by the incorporation of essential oils. *Mater Res Express* 5(3):035007
- Rahman MA, Islam MS, Haque P, Khan MN, Takafuji M, Begum M, Chowdhury GW, Khan M, Rahman MM (2020) Calcium ion mediated rapid wound healing by nano-ZnO doped calcium phosphate-chitosan-alginate biocomposites. *Materialia* 13:100839
- Rajput M, Mandal M, Anura A, Mukhopadhyay A, Subramanian B, Paul RR, Chatterjee J (2020) Honey loaded silk fibroin 3D porous scaffold facilitates homeostatic full-thickness wound healing. *Materialia* 12:100703

- Rameshbabu AP, Datta S, Bankoti K, Subramani E, Chaudhury K, Lalzawmliana V, Nandi SK, Dhara S (2018) Polycaprolactone nanofibers functionalized with placental derived extracellular matrix for stimulating wound healing activity. *J Mater Chem B* 6(42):6767–6780
- Roobahani M, Kharaziha M, Emadi R (2017) pH sensitive dexamethasone encapsulated laponite nanoplatelets: release mechanism and cytotoxicity. *Int J Pharm* 518(1–2):312–319
- Sadeghianmaryan A, Yazdanpanah Z, Soltani YA, Sardroud HA, Nasirtabrizi MH, Chen X (2020) Curcumin-loaded electrospun polycaprolactone/montmorillonite nanocomposite: wound dressing application with anti-bacterial and low cell toxicity properties. *J Biomater Sci Polym Ed* 31(2):169–187
- Saeed SM, Mirzadeh H, Zandi M, Barzin J (2017) Designing and fabrication of curcumin loaded PCL/PVA multi-layer nanofibrous electrospun structures as active wound dressing. *Prog Biomater* 6(1–2):39–48
- Salehi M, Ehterami A, Farzamfar S, Vaez A, Ebrahimi-Barough S (2020) Accelerating healing of excisional wound with alginate hydrogel containing naringenin in rat model. *Drug Deliv Transl Res* 11:142–153
- Shankhwar N, Kumar M, Mandal BB, Robi P, Srinivasan A (2016) Electrospun polyvinyl alcohol-polyvinyl pyrrolidone nanofibrous membranes for interactive wound dressing application. *J Biomater Sci Polym Ed* 27(3):247–262
- Shao W, Liu H, Liu X, Wang S, Wu J, Zhang R, Min H, Huang M (2015) Development of silver sulfadiazine loaded bacterial cellulose/sodium alginate composite films with enhanced antibacterial property. *Carbohydr Polym* 132:351–358
- Sharmeen S, Rahman MS, Islam MM, Islam MS, Shahruzzaman M, Mallik AK, Haque P, Rahman MM (2019) Application of polysaccharides in enzyme immobilization. In: *Functional polysaccharides for biomedical applications*. Elsevier, Amsterdam, pp 357–395
- Shinozaki T, Hayashi R, Ebihara M, Miyazaki M, Tomioka T (2013) Mucosal defect repair with a polyglycolic acid sheet. *Jpn J Clin Oncol* 43(1):33–36
- Simões D, Miguel SP, Correia IJ (2018) Biofunctionalization of electrospun poly (caprolactone) fibers with Maillard reaction products for wound dressing applications. *React Funct Polym* 131:191–202
- Singh R, Singh D (2012) Radiation synthesis of PVP/alginate hydrogel containing nanosilver as wound dressing. *J Mater Sci Mater Med* 23(11):2649–2658
- Singla R, Soni S, Kulurkar PM, Kumari A, Mahesh S, Patil V, Padwad YS, Yadav SK (2017) In situ functionalized nanobiocomposites dressings of bamboo cellulose nanocrystals and silver nanoparticles for accelerated wound healing. *Carbohydr Polym* 155:152–162
- Subagio A, Umiati N, Gunawan V (2020) Growth of collagen-nanosilver (Co-AgNP) biocomposite film with electrospinning method for wound healing applications. In: *Journal of Physics: conference series*, vol 1, p 012032. IOP Publishing
- Tran RT, Naseri E, Kolasnikov A, Bai X, Yang J (2011) A new generation of sodium chloride porogen for tissue engineering. *Biotechnol Appl Biochem* 58(5):335–344
- Unalan I, Endlein SJ, Slavik B, Buettner A, Goldmann WH, Detsch R, Boccaccini AR (2019) Evaluation of electrospun poly (ϵ -caprolactone)/gelatin nanofiber mats containing clove essential oil for antibacterial wound dressing. *Pharmaceutics* 11(11):570
- Uslu I, Aytimur A (2012) Production and characterization of poly (vinyl alcohol)/poly (vinylpyrrolidone) iodine/poly (ethylene glycol) electrospun fibers with (hydroxypropyl) methyl cellulose and aloe vera as promising material for wound dressing. *J Appl Polym Sci* 124(4):3520–3524
- Wang J, Hao S, Luo T, Cheng Z, Li W, Gao F, Guo T, Gong Y, Wang B (2017) Feather keratin hydrogel for wound repair: preparation, healing effect and biocompatibility evaluation. *Colloids Surf B Biointerfaces* 149:341–350
- Wang C, Niu H, Ma X, Hong H, Yuan Y, Liu C (2019) Bioinspired, injectable, quaternized hydroxyethyl cellulose composite hydrogel coordinated by Mesocellular silica foam for rapid, noncompressible hemostasis and wound healing. *ACS Appl Mater Interfaces* 11(38):34595–34608

- Wichai S, Chuysinuan P, Chairwut S, Ekabutr P, Supaphol P (2019) Development of bacterial cellulose/alginate/chitosan composites incorporating copper (II) sulfate as an antibacterial wound dressing. *J Drug Deliv Sci Technol* 51:662–671
- Wittaya-areekul S, Prahsarn C (2006) Development and in vitro evaluation of chitosan-polysaccharides composite wound dressings. *Int J Pharm* 313(1–2):123–128
- Xia G, Zhai D, Sun Y, Hou L, Guo X, Wang L, Li Z, Wang F (2020) Preparation of a novel asymmetric wettable chitosan-based sponge and its role in promoting chronic wound healing. *Carbohydr Polym* 227:115296
- Ye D, Zhong Z, Xu H, Chang C, Yang Z, Wang Y, Ye Q, Zhang L (2016) Construction of cellulose/nanosilver sponge materials and their antibacterial activities for infected wounds healing. *Cellulose* 23(1):749–763
- Ye S, Jiang L, Wu J, Su C, Huang C, Liu X, Shao W (2018) Flexible amoxicillin-grafted bacterial cellulose sponges for wound dressing: in vitro and in vivo evaluation. *ACS Appl Mater Interfaces* 10(6):5862–5870
- You C, Li Q, Wang X, Wu P, Ho JK, Jin R, Zhang L, Shao H, Han C (2017) Silver nanoparticle loaded collagen/chitosan scaffolds promote wound healing via regulating fibroblast migration and macrophage activation. *Sci Rep* 7(1):1–11
- Zahedi P, Karami Z, Rezaeian I, Jafari SH, Mahdavi P, Abdolghaffari AH, Abdollahi M (2012) Preparation and performance evaluation of tetracycline hydrochloride loaded wound dressing mats based on electrospun nanofibrous poly (lactic acid)/poly (ϵ -caprolactone) blends. *J Appl Polym Sci* 124(5):4174–4183
- Zahedi P, Rezaeian I, Jafari SH (2013) In vitro and in vivo evaluations of phenytoin sodium-loaded electrospun PVA, PCL, and their hybrid nanofibrous mats for use as active wound dressings. *J Mater Sci* 48(8):3147–3159
- Zahiri M, Khanmohammadi M, Goodarzi A, Ababzadeh S, Farahani MS, Mohandesnezhad S, Bahrami N, Nabipour I, Ai J (2020) Encapsulation of curcumin loaded chitosan nanoparticle within poly (ϵ -caprolactone) and gelatin fiber mat for wound healing and layered dermal reconstitution. *Int J Biol Macromol* 153:1241–1250
- Zarrintaj P, Saeb MR, Jafari SH, Mozafari M (2020) Application of compatibilized polymer blends in biomedical fields. In: *Compatibilization of polymer blends*. Elsevier, Amsterdam, pp 511–537
- Zhang H, Peng M, Cheng T, Zhao P, Qiu L, Zhou J, Lu G, Chen J (2018) Silver nanoparticles-doped collagen–alginate antimicrobial biocomposite as potential wound dressing. *J Mater Sci* 53(21):14944–14952
- Zhang N, Gao T, Wang Y, Liu J, Zhang J, Yao R, Wu F (2020a) Modulating cationicity of chitosan hydrogel to prevent hypertrophic scar formation during wound healing. *Int J Biol Macromol* 154:835–843
- Zhang S, Ye J, Sun Y, Kang J, Liu J, Wang Y, Li Y, Zhang L, Ning G (2020b) Electrospun fibrous mat based on silver (I) metal-organic frameworks-poly(lactic acid) for bacterial killing and antibiotic-free wound dressing. *Chem Eng J* 390:124523



Conductive Polymers for Cardiovascular Applications

12

Azka Arshad, Hafsa Irfan, Sunniya Iftikhar, and Basit Yameen

Abstract

The prevalence of cardiovascular diseases (CVDs) has taken a sharp rise, accounting for almost 25% of the total fatalities globally. Fortunately, the advances in therapeutic and diagnostic technologies have also been keeping up to tackle this rising challenge. The technologies based on biocompatible conductive polymers, which can be processed as composite films, nanofibers, hydrogels, and composite scaffolds, are attracting increasing interest. This chapter is focused on evaluating the role of biocompatible conductive polymers in addressing CVDs from diagnostic and therapeutic perspectives. Depending on their chemical nature, polymers can exhibit both electronic (π -conjugated polymers) and ionic conductivities (ion conductive polymers). Materials, based either entirely on conductive polymers or on their combination with other nanomaterials, are being engineered for application in addressing various CVDs. These applications include cardiac tissue engineering for treating myocardial infarction, improving the human cardiac myocyte attachment, proliferation, interaction, expression of cardiac-specific proteins, and developing conductive cardiac patches. In addition, conductive polymers based technologies are being developed for microenvironment regulation to enhance the action potential in the cardiac cells and cell-to-cell communication, nerve regeneration and repair via prosthesis electrode-tissue interface, wound healing by inducing angiogenesis, sensing of biomarkers related to cardiac failure, and monitoring and augmenting heart activity by supplying electrical signals via implantable devices. Despite significant progress, there remain challenges blocking the way for the clinical translation of these

A. Arshad · H. Irfan · S. Iftikhar · B. Yameen (✉)

Department of Chemistry and Chemical Engineering, Syed Babar Ali School of Science and Engineering (SBASSE), Lahore University of Management Sciences (LUMS), Lahore, Pakistan
e-mail: basit.yameen@lums.edu.pk

© The Author(s), under exclusive license to Springer Nature Singapore Pte Ltd. 2022

319

L. M. Pandey, A. Hasan (eds.), *Nanoscale Engineering of Biomaterials: Properties and Applications*, https://doi.org/10.1007/978-981-16-3667-7_12

conductive polymer based technologies. In this chapter, we have reviewed some state-of-the-art developments providing a structure and property relationship that makes this particular class of polymers especially suitable for addressing CVDs.

Keywords

Conductive polymers · Cardiovascular diseases · Diagnosis and prognosis · Therapeutics · Biodegradability and biocompatibility · Conductivity

12.1 Introduction

For decades, conductivity was a property ascribed only to inorganic materials, whereas insulation was in the organic materials domain. In 1954, the discovery of perylene-bromine complex—a purely organic species exhibiting high electrical conductivity—changed the way scientists looked at the organic materials forever (Jonas and Heywang 1994). It had opened another dimension with the promising potential of organic materials to supplant metals. One such class of organic materials is polymers. It is noteworthy that the recent developments in polymer science and technology have brought us face to face with many inorganic-based polymers as well. Polymers are a class of synthetic or natural macromolecules that are composed of small repeating units, known as monomers. Some common examples of polymers are polyethylene, polyvinyl chloride (PVC), polyvinyl alcohol (PVA), and nylon. From textiles to pharmaceuticals, these macromolecules have a wide range of applications.

Polymers were imagined to be insulators until the advent of a new class. In 1976, Hideki Shirakawa accidentally discovered polyacetylene as a lustrous black solid. Owing to its conjugated *p*-orbitals, polyacetylene gave more room for the electrons to move and thus exhibited properties that are akin to semiconductors. Hideki then collaborated with Alan MacDiarmid and Alan Heeger to study the properties of polyacetylene in more detail at the University of Pennsylvania. They discovered that upon oxidation of polyacetylene with a halogen vapor (iodine/bromine), the electrical conductivity of this material could be enhanced up to a level comparable with that of copper. Shirakawa, MacDiarmid, and Heeger received the Nobel Prize in chemistry in the year 2000 for their discovery and subsequent work in the development of these conductive polymers. Since then, this class of polymers has attracted the focus of some of the most exceptional researchers of our time. Conductive polymers (CPs) have taken the world by storm with their exceptional ability to mimic the electrical and optical properties of metal and semiconductors while retaining the mechanical properties and characteristics specific to the polymers. The smooth, versatile, and creative ways to manufacture them have given CPs the main spotlight. The CPs have got particular limelight for their potential usage in biomedical applications because of the intelligent ways with which they can be made to interact with and respond to various tissues (muscle, epithelium, and nerve). The biocompatibility of these materials remains intact while they electrically

communicate with the electroactive tissues. This has enabled scientists to employ the use of CPs to develop medical devices with increased electrical conductivity, stability, and sensitivity. Beside electrical conductivity, polymers can also be made to conduct ions by functionalizing them with ionic functionalities. In this chapter, we will be looking more closely at the special classes of electrically and ionically conductive polymers that are being applied for addressing CVDs. In the first half of the chapter, we will zoom into their classifications, their synthetic techniques, their physicochemical properties which make them suitable for biomedical applications, and the different ways to enhance these properties. In the latter half of the chapter, we zoom in on the CVDs and how the CPs are proving themselves useful in their diagnosis, prognosis, and therapeutic applications.

12.2 Types of Conductive Polymers

As introduced earlier, there are two broad categories of conductive polymers: electrically conductive π -conjugated polymers (PCPs) and ion-conductive polymers (ICPs). In this section, we take a closer look at these types.

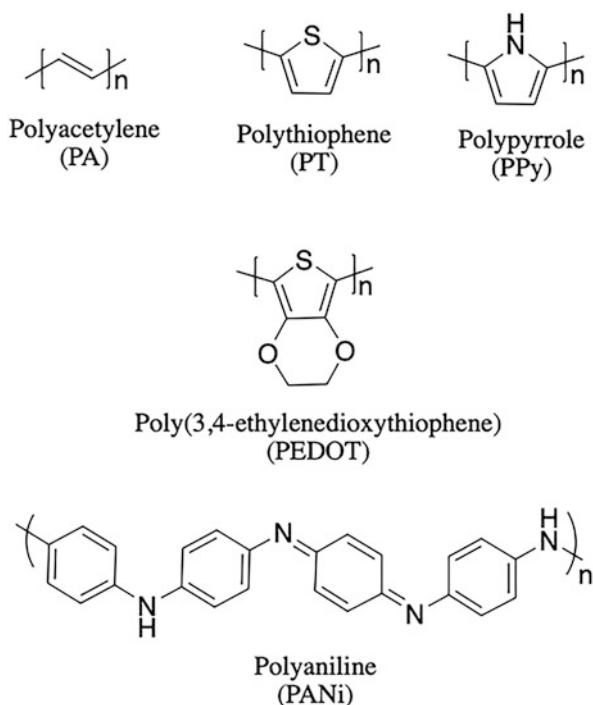
12.2.1 π -Conjugated Polymers

For the longest time, metals held hegemony over the conductivity, primarily owing it to the free electrons in their valence band. These valence band electrons could very quickly be mobilized, therefore, carrying current. Now, this feature was inherently absent in the covalent compounds, especially the polymers with their outermost electrons mostly engaging in sigma bonding because of the sp^3 hybridization. However, conjugated backbones, such as those of polyacetylene, have a π -electron cloud that is delocalized over the entire polymer molecule. It should be noted that conjugation alone cannot account for significant conductivity. The chain must be either doped (by either oxidative or reductive measures) or perturbed using other techniques, enhancing the conductivity of the organic polymers. Perturbation through oxidation is much more prevalent for the transition of these otherwise semiconducting polymers into their conductive forms. This way, the polymer chain is left electron deficient, requiring anions from an oxidizing medium for charge compensation (Walton 1991). The common types of these polymers (Fig. 12.1) include polyacetylenes, polypyrroles, polyanilines, and their derivatives.

12.2.2 Ion-Conductive Polymers

The polymers that exhibit conductivity based on ionic groups present in the polymer molecule (in the backbone or as pendant groups) or in the surrounding medium (electrolyte) are called the ionic conductive polymers (ICPs) (Gupta et al. 2020). The

Fig. 12.1 Structures of some π -conjugated polymers



concept of ICPs was introduced in 1951 (Doscher et al. 1951) when certain salts were observed to interact with the poly(ethylene oxide) chains, following which it was one of the hottest areas for research throughout the 1960s (Blumberg et al. 1964; Mocanin and Cuddihy 1966; Lundberg et al. 1966; Iwamoto et al. 1968; Binks and Sharples 1968; Yokoyama et al. 1969). Studies showed that this polymer-salt interaction was similar to that of the alkali-crown ether complexes—the ether oxygen of the polymer chains was interacting with the cations. Other examples of polymer electrolyte systems include heteropolymer systems like that of poly(ethylene oxide)/poly(methylene oxide) (PEO/PMO) and poly(ethylene oxide)/poly(methyl methacrylate) (PEO/PMMA) along with monovalent cations to trivalent cations (Na^+ , K^+ , Co^{2+} , Ni^{2+} , Cd^{2+} , Eu^{3+} , and La^{3+}) (Linford 1993). Beside, polymers functionalized with cationic, anionic, or zwitterionic functional groups are extensively studied and are generally referred to as polyelectrolytes.

12.3 Synthesis Techniques for the CPs

Now that we have established some understanding of how these CPs (both PCPs and ICPs) are categorized, we now move on to studying some of the ways to synthesize them. The PCPs can be synthesized via different electrochemical and chemical methods and so we will briefly overview them in this section. The discussion on

synthetic techniques for PCPs will be followed by a brief description of the ways in which ICPs can be synthesized.

12.3.1 Electrochemical Methods for the Synthesis of PCPs

Electrochemical polymerization (EP) has emerged as a useful technique for the PCP synthesis. The electrochemical system comprises three electrodes (working, counter, and reference electrodes) together with electrolyte and monomer solution in a suitable solvent (Fig. 12.2). In this process, nickel-, chromium-, gold-, titanium-, palladium-, and platinum-based electrodes are widely used as anodes. Moreover, the monomers utilized in this process may have low anodic potential and are more susceptible to electrophilic substitution. Oxidation of monomers at the surface of working electrodes leads to the generation of radical cations that can further react with other monomers to form insoluble chains of polymer. In the case of aniline and pyrrole, monomers undergo electrochemical oxidation at high positive electrode potential and yield radicals or other species that react to give the final polymer. By this method, oligomers or polymers can be conveniently synthesized from their

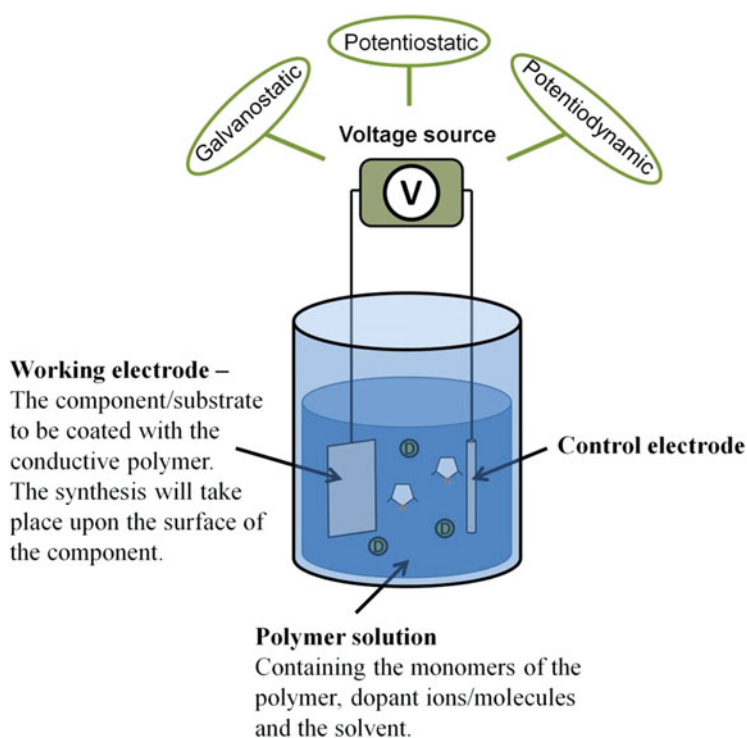


Fig. 12.2 Electrochemical polymerization process by employing a reference, working, and the counter electrode system (Balint et al. 2014)

corresponding monomers. Different experimental conditions such as monomer concentration, type of electrolyte, and applied electrode potential can be tuned to synthesize various PCP structures including micrometer-sized particles as well as the thick and compact polymer layers on the surface of the electrode. PCPs such as polypyrrole (PPy), polyaniline (PANI), and poly(3,4-ethylenedioxythiophene) (PEDOT) are frequently synthesized through electrochemical methods (Sadki et al. 2000; Itoi et al. 2017; Musumeci et al. 2013). Potentiostatic, galvanostatic, and potentiodynamic techniques are the three main methodologies followed for the electrochemical polymerization (Gupta et al. 2016). The electrochemical synthesis offers a convenient in situ deposition of polymers; however, the quantity and nature of the bioactive materials that can be incorporated in the electroactive platforms are limited. Besides, the given method needs an electrode for the deposition of the polymer, and so the amount of polymer deposited and the range of morphologies that can be achieved are restricted by the surface area and geometry of the electrode. These conditions make it difficult to control the physicochemical properties of the resulting polymers.

12.3.2 Chemical Methods for the Synthesis of PCPs

With the rising interest in applications of the PCPs in diverse areas, there is a dire need to develop novel synthetic routes to access these materials with a better control over their chemical and physical properties. For instance, many PCPs such as poly(phenylene), poly(phenylenevinylene), and polythiophene exhibit poor solubility and are difficult to process. The solubility issue could be overcome by incorporating suitable side chains into the monomer. Chemical methods developed for the synthesis of PCPs are important not only for the synthesis of bulk quantities of such polymers, but also for controlling their physicochemical nature by tuning their molecular design. To develop better understanding, different chemical methods employed for the PCP synthesis are described next.

12.3.2.1 Chemical Oxidative Polymerization

In this polymerization method, oxidation of monomers is achieved by using an oxidizing agent (ferric chloride, ammonium persulfate) as shown in Fig. 12.3, followed by the generation of a radical ion that initiates the polymerization. The chemical oxidative polymerization can be used to create a diverse range of novel

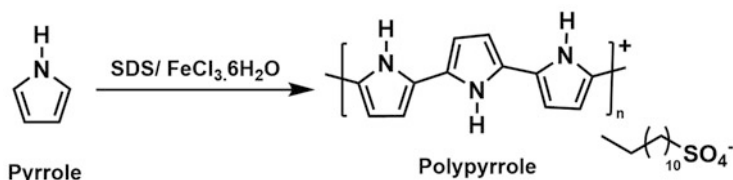


Fig. 12.3 Synthesis of polypyrroles by chemical oxidative polymerization

PCPs that cannot be easily synthesized by the electrochemical methods (Šišáková et al. 2020; Sapurina and Stejskal 2008; Kumar et al. 2012). Unfortunately, the polymers synthesized by chemical methods have lower conductivity than the electrochemically synthesized counterparts. One of the greatest limitations of oxidative coupling methods is its restricted control over molar mass and regioselectivity of the synthesized polymer.

12.3.2.2 Cross-Coupling Polymerization

Cross-coupling polymerization reactions are catalyzed by transition metals and offer a particularly powerful and multipurpose method for the C–C bond formation and also enable the development of a sophisticated and extensive library of the PCPs (Fig. 12.4). The general mechanism of coupling reactions involves the oxidative addition of transition metal-based catalysts across the carbon-halogen bond, followed by the transmetalation, which is concluded with a reductive elimination through the formation of the C–C bond with the renewal of catalysts (García-Melchor et al. 2013). Since the advent of the PCPs, many research groups have synthesized different conductive polymers by utilizing the cross-coupling reactions. Various transition metal catalyzed cross-coupling reactions include the Suzuki–Miyaura coupling (Lennox and Lloyd-Jones 2014), Sonogashira coupling (Wang and Gao 2014), and Stille coupling (Amatore et al. 2003).

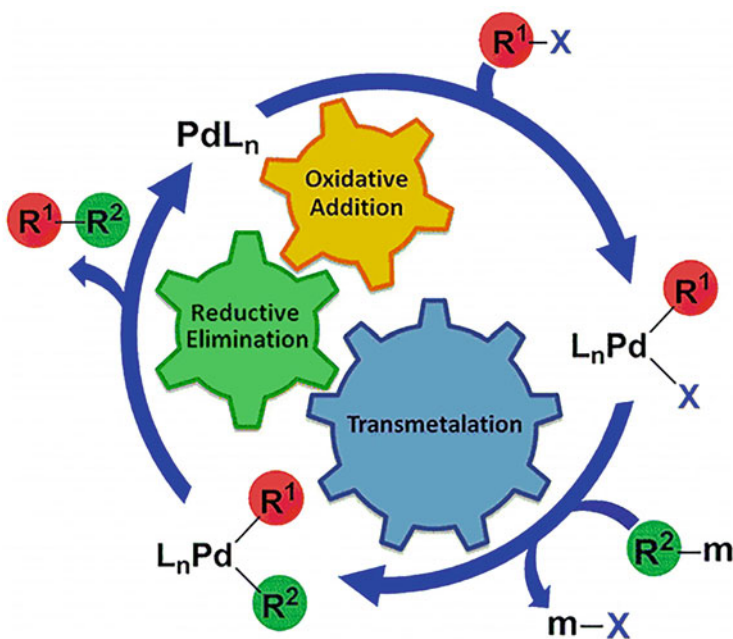


Fig. 12.4 General scheme of cross-coupling reaction catalyzed by transition metal catalyst. (Reprinted with permission from García-Melchor et al. (2013). Copyright (2013) American Chemical Society)

12.3.2.3 Grignard Metathesis (GRIM) Polymerization

The so far described methods involve random couplings that lead to the loss of *regioregularity*. It must be understood that in the backbone of a conjugated polymer, steric twisting can arise due to various random couplings, and that can reduce the electrical conductivity and other desirable properties of the PCPs (Stefan et al. 2012). The problem was solved when the highly regioregular poly(3-alkylthiophene) (rrP3AT) was first synthesized, by the group of Richard McCullough, through a method famously known as the McCullough method and the Grignard metathesis (GRIM) polymerization (Loewe et al. 2001). The synthesis of rrP3ATs via GRIM method not only expanded the library of novel functional polythiophenes, but also improved their electrical conductivity, primarily owing to their planar backbone and organized three-dimensional polycrystalline structures (Amna et al. 2020). One significant benefit of the GRIM polymerization is that it renders the utilization of both the reactive transition metals and cryogenic temperatures unnecessary. Therefore, it offers an efficient and convenient method to synthesize regioregular polythiophenes and enables the bulk scale production of high-molecular-weight polymers with a precise control over the molecular weight, side chain functionalities, and end groups. The synthesis of highly regioregular polythiophenes is basically a transition metal-catalyzed cross-coupling polymerization reaction that comprises a catalytic cycle based on three consecutive steps (oxidative addition, transmetalation, and reductive elimination). Yokoyama et al. (2004) has proposed that the GRIM polymerization developed by McCullough proceeds through a chain-growth mechanism and also has a living system. In GRIM polymerization, the molecular weight of the PCP can be controlled as a function of the reaction time and the amount of nickel catalyst (Iovu et al. 2005). The basic mechanism involved for the synthesis of highly regioregular polythiophene via GRIM polymerization is depicted in Fig. 12.5. The catalytic cycle involves the monomer reaction with Ni(dppp)Cl₂ to give the organonickel intermediate that immediately undergoes reductive elimination to generate the dimer and a Ni(0)-based associated pair. The oxidative addition of the dimer to the nickel center gives new organonickel compounds that are followed by transmetalation and reductive elimination to give another associated pair. In this way, the polythiophene chain grows by inserting single monomer units in the catalytic cycle, whereas the Ni(dppp) moiety is always incorporated as an end group into the polymer chain (Iovu et al. 2005). It is believed that Ni(dppp)Cl₂ is more likely to act as an initiator instead of a catalyst that can limit the polymerization process to one end of the growing chain of polymers. The living nature of the polymerization can be validated by experimental analysis; first, higher monomer conversion gives higher degree of polymerization; second, at the end of polymerization the addition of different Grignard reagents result in the endcapping of polythiophenes (Bahri-Laleh et al. 2014).

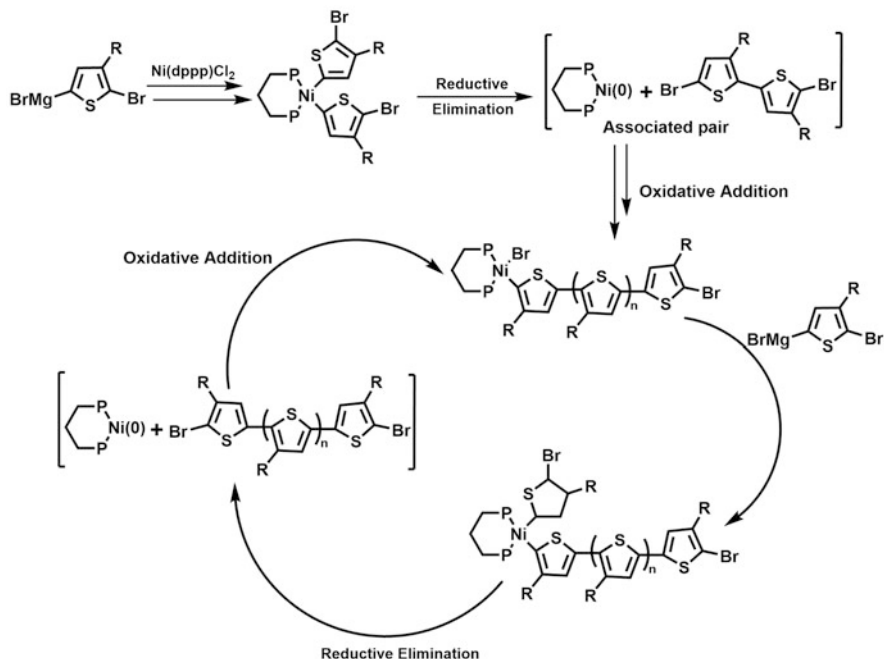


Fig. 12.5 Mechanism of Grignard metathesis (GRIM) polymerization. (Reprinted with permission from Iovu et al. (2005). Copyright (2005) American Chemical Society)

12.3.3 Synthesis Techniques for the ICPs

We can employ the well-known polymerization techniques such as radical polymerization including atom transfer radical polymerization (ATRP) (Kato et al. 1995; Wang Wang and Matyjaszewski 1995), reversible addition-fragmentation chain transfer (RAFT) polymerization (Yeole 2010), condensation polymerization, and ring opening polymerization for the synthesis of ion-conductive polymers. These methods can produce polymers with cationic, anionic, or zwitterionic pendant groups and exhibit intrinsic ion conductivity. Alternatively the synthesized polymers such as PEO or PMO can be mixed with the suitable salts to form the required ICP systems.

12.4 Physicochemical Properties of Conductive Polymers for Biomedical Applications

Now that we have familiarized ourselves with the categorization and synthetic techniques used to manufacture the CPs, we are now prepared enough to indulge in their properties. In this section, we look at the properties that have enabled the CPs to have such a massive impact, especially in the biomedical sector. We also discuss

how these properties can be further manipulated and enhanced to achieve the desired results.

12.4.1 Some Properties Common to All CPs

The CPs because of their unique structure and properties such as excellent biocompatibility (both in vivo and in vitro), stable conductivity under physiological conditions, excellent chemical stability (e.g., in air and water), and excellent redox properties have opened a new doorway to endless possibilities (Nezakati et al. 2018; Balint et al. 2014). In addition, the provision of side chain engineering offers installation of a wide variety of pendant groups as per the requirement of the target application (Lam and Tang 2005). Most of the conductive polymers are hydrophobic and exhibit poor solubility; however, their hydrophilicity can be increased in many ways, including copolymerization with monomers having hydrophilic substituents to produce hydrophilic polymers (Balint et al. 2014). Studies have also been carried out to understand how the chain length (conjugation length) affects the conductivity and other physical properties of these polymers. It has been demonstrated that short oligomers of polythiophene (up to 11 thiophene units) exhibit conductive and polymeric properties similar to that of a high-molecular-weight polythiophene polymer (Ten Hoeve et al. 1991). Another study has found that the conductive properties of oligomers and their carrier mobility increase as a function of the conjugation length (Garnier et al. 1993). Films fabricated from π -conjugated polymers are generally not transparent. Achieving good optical transparency and conductivity is a challenging task. Attempts to achieve transparency can affect the conductivity of the material. The transparency of the conductive polymer films can be increased by using dilute solutions during film fabrication (Nezakati et al. 2018). Alternately, block copolymerization with optically transparent blocks (Yin et al. 1997), grafting transparency imparting alkyl side chains (Glenis et al. 1995; Zotti et al. 1997), blending with a transparent polymer (Laakso et al. 1989; Isotalo et al. 1993), and forming composites with optically transparent additives can be explored (Meador et al. 1997). The CPs, particularly the heteroaromatic class of the PCPs, offer another unique property of electrochromism. This primarily results from the visible color changes that result as a consequence of the conversion of oxidized forms to neutral forms (Walton 1991).

12.4.2 Enhancing the Properties of the CPs

There are numerous ways in which the properties of these conductive polymers can be enhanced. Some of these ways are discussed here. It is also noteworthy to highlight how easy it is to manipulate these properties; for example, PANi's electrical properties can be manipulated simply by protonation or charge transfer doping, giving greater control over the electrical, magnetic, mechanical, and thermal properties of the resulting material (Nezakati et al. 2018; Balint et al. 2014).

CPs hold a special position when it comes to biomedical applications, primarily because these macromolecules can be modified via chemical or physical methods. Deciphering the structure and property relationship is important for further advancement and development of novel and efficient smart materials. Therefore, different methods are being employed to optimize the physicochemical properties of the CPs and to improve their integration with the biological systems. The physical adsorption method exploits the physical interactions between the surfaces derived from the CPs and biomolecules. As the CPs carry significant charges (e.g., chemically doped π -conjugated polymers), the electrostatic forces between the cationic part of the polymer and anionic biomolecules can be exploited to enhance the interactions between the CPs and the biomolecules. However, other interactions such as hydrophobic and Van der Waals interactions also contribute toward these interactions, especially for the adsorption of antibodies and other proteins (Ahuja et al. 2007). To increase the binding efficiency of the PCPs and biomolecules in particular, the entrapment method has been employed. This technique provides straightforward and prolonged immobilization compared to the simple physical adsorption. It is the most widely used method when PCP-based materials with extracellular matrix (ECM) mimetic properties are being required. It is likely to noncovalently integrate with both low- and high-molecular-weight components of the ECM (Cosnier 1999). Moreover, the doping method can be employed to bind various bioactive molecules to PCPs. This process can be carried out chemically, electrochemically, or by a photodoping method (Kim et al. 2007). To improve the long-term stability and to enhance polymer integration with a biological system, PCPs can also be conjugated to the bioactive species via covalent methods. In this case, the functionalization can be achieved either by using functional monomers during polymer synthesis or via postsynthetic modification protocols (Handa et al. 2015; Lee et al. 2009). Thus, these methods are efficient tools to improve the properties of CPs making them suitable for biomedical-related applications.

12.5 Cardiovascular Diseases (CVDs)

According to the World Health Organization (WHO), CVDs are the leading cause of deaths around the globe. An estimated 17.9 million deaths occurred in 2016 from CVDs, which represent 31% of the total deaths, and of those, 85% were from stroke and heart attack. In the United States, every one in four people die from a cardiac disease. Thus, the graveness of these diseases has prompted medical and healthcare professionals to devise and advance the cardiac therapeutics. CVDs are generally a set of maladies of the heart and the blood vessels. WHO has categorized the CVDs into following main subsets: coronary heart diseases (the coronary vessels are damaged), cerebrovascular diseases (blood vessels supplying blood to the brain are damaged), peripheral arterial diseases (blood vessels supplying blood to the limbs are damaged), rheumatic heart diseases (the coronary vessels and valves are damaged due to the rheumatic fever), congenital heart diseases (deformity in the

heart structure at birth), and deep vein thrombosis and pulmonary embolism—thromboembolism (blood clot in veins of legs which travels to the heart and lungs).

Coronary heart disease (CHD) is the most dangerous type of CVD. CHD develops when coronary arteries grow narrower, thus preventing the blood and oxygen supply to the heart. Cholesterol and waste products from the cells build up on the arterial walls (atherosclerosis) creating plaques. When these plaques rupture, platelets cluster around the area to repair the damage in the arteries forming a clot. These plaques, along with the clots, constrict the arteries and obstruct blood flow to the heart, which can be lethal, leading to a heart attack. The coronary arteries form a mesh on the heart's surface, and if they are blocked, the heart cannot receive oxygenated blood. Thus, physical activities, even the light ones, become painful. This can induce angina, marked by heaviness, pain, and burning in the chest area. Following techniques are employed for CHD diagnosis: electrocardiogram, Holter monitor, echocardiogram, computed tomography (CT) scans, coronary characterization via X-rays, nuclear ventriculography, and stress test.

Cerebrovascular disease is a set of disorders where blood vessels and blood supply to the brain are compromised. If there is a blockage in the blood vessels, the blood supply to the brain is hampered; thus, neurons do not get enough oxygen, and as a result, brain damage can occur. In cerebrovascular disease conditions, just like CHD, the arteries can become narrow due to the atherosclerosis and form a clot in the vessels inside the brain, arteries, and veins. This can lead to stroke, transient ischemic attack, aneurysm, subarachnoid hemorrhage, and vascular malformation, which is why the cerebrovascular disease is the fifth highest cause of deaths in the United States, with an average of 795,000 strokes reported every year. The diagnosis of cerebrovascular disease is carried out through angiography, CT or magnetic resonance imaging (MRI) scans, and electrocardiogram (ECG). The treatment includes medication that breaks up the blood clots (tPA), carotid endarterectomy, carotid angioplasty, and stenting (Pappachan and Kirkham 2008).

Peripheral arterial disease (PAD) occurs when the vessels (both arteries and veins) supplying blood to the limbs, kidneys, and stomach are shrunk due to the atherosclerosis, an injury to the limbs, or a genetic ailment in the muscles and ligaments. It accounts for 8.5 million patients in the United States, making up 12–20% of the people over 60 years affected by this disease. PAD's common fatalities are due to heart attack and stroke, and it can make physical activities such as walking an insufferable act. The diagnosis includes an ankle-brachial index, ultrasound scans, angiography, Doppler and duplex imaging, CT scans, and magnetic resonance angiography (MRA). The medicated treatment includes antihypertensive drugs and statins and angiotensin-converting enzyme (ACE) inhibitors (Olin and Sealove 2010).

Worldwide, rheumatic heart disease (RHD) accounts for 230,000–500,000 deaths per year. RHD involves the heart valves becoming permanently damaged. The heart valve damage usually happens when the condition is left untreated or undertreated. An immune response causes an inflammatory condition, which can result in valve damage. The diagnosis includes EKG, ECG, and blood tests. The medicines used for treatment include antibiotics, anti-inflammatory drugs, corticosteroids, and

anticonvulsant medications. A more invasive way is to surgically replace the mitral valve with either a mechanical or tissue valve (Watkins et al. 2018).

Congenital heart disease is marked by defects in the structure of heart or a greater number of blood vessels present at the time of birth. Almost 1% of the babies in the United States are subject to this disease at birth. The diagnosis includes echocardiography, ECG, X-ray, and pulse oximetry. The treatment involves a heart transplant, valve replacement, or angioplasty, all of which are carried out through either an open heart surgery or a catheter (Hoffman 2013).

Thromboembolism is a cardiac disease in which a blood clot (thrombus) forms inside the deep veins in a person's limbs. This disease accounts for 900,000 patients every year and takes 60,000–100,000 lives annually. The diagnosis requires a CT scan, blood test, and ultrasounds. Anticoagulant drugs are mostly used to treat this disease (Moheimani and Jackson 2011).

In the past few decades, we have seen a dramatic improvement in the treatment and prevention of CVDs, yet it tolls the most significant number of deaths every year. CVD drug innovation, quality of care, and affordability still pose severe challenges to the biomedical community and the public. While the patients appreciate the ongoing treatments in this field, they often complain about the expense, the subpar quality, and complexities. As mentioned earlier, in the diagnosis and treatments of each CVD, it is essential to take drugs. However, not many of these drugs are efficient. They do not fully get absorbed by the body, or are released too fast or do not reach the target organ/tissue or pose serious side effects. Thus, there is a need for an efficacious and advanced drug delivery system that differentially targets the diseased area in the body. This may also help in minimizing the side effects of any treatment regimen, thus providing a protection for the organs where the drug is not supposed to act. The diagnostic and surgical equipment are sometimes too bulky, so their miniaturization is essential, for example, through stronger, smaller, more flexible leads and body of the equipment(s). Further challenges in currently used conventional CVD therapeutics are discussed under the applications of conductive polymers (McClellan et al. 2019).

12.6 Conductive Polymers in Action

Until this point, we have attained a fair grasp on the identity, synthetic techniques, and properties of the CPs. We have developed some understanding of why these materials are so sought after for the biomedical applications in general and CVDs specifically. In this section, we go on and finally examine various studies illuminating how the biocompatible and conductive polymers have helped advance technologies aiding the diagnosis, prognosis, and therapy of the CVDs.

12.6.1 Diagnosis and Prognosis

Did you know that the CPs are helping the development of sensors doing exactly what our noses and tongues do? These are quite literally called electronic noses (used in gas analysis) and electronic tongues (used in fluid analysis) and these electronic noses and tongues have found uses in detecting fire, smokes, and analyzing the tastes and composition of different wines and other edible items, going up to understanding the ionic content in various fluids. Conductive polymers have not only significantly improved medical diagnostics, but have pretty much revolutionized the very concept of sensors across all industries; from becoming pioneer materials in active packaging in the food industry to carefully monitoring the pollution in the environment sector. Based on their molecular and macroscopic structures, these polymers can interact with a wide variety of materials and translate this interaction into a detectable and readable electrical signal. This feature makes them stand out among “smart” materials. For a material to be called smart, it is not enough for it to merely show a change in one of its properties upon interaction with another medium, it must be able to respond to that medium and the changes in that medium in a way that is specific, quantifiable, and also reproducible. These materials give the sensors more control over the range of selectivity, design, and more flexibility. Unlocking the current and future potential of these materials in the field of sensors is beyond the scope of this chapter. In this section, we are attempting to examine how these materials are being utilized in the medical diagnosis and prognosis of CVDs (Cichosz et al. 2018). The applications discussed here include the monitoring of the electrocardiogram (ECG), blood pressure, and heartbeat rate as well as for the detection of biomarkers related to cardiac failures.

12.6.1.1 ECG Monitoring

Electrocardiography is a very reliable method of diagnosis, especially for CVDs, and has a substantial presence in clinical practice. Monitoring the ECG signals has proven to be extremely helpful in detecting a CVD well before its onset and manifestation in the structural form of diseased tissue. This helps in managing the diseases and delaying the onset (at times altogether preventing the disease because of the timely intervention) and is very cost-effective for the patients. For the longest time, Ag/AgCl disposable electrodes have been used to perform electrocardiography, and they have provided excellent results; however, there are specific challenges and limitations to their use, which probed the scientific community to find a better substitute. Some of these limitations arise from the fact that these silver-based electrodes require a gel electrolyte for proper function, and this gel has been shown to cause skin irritation and rashes when used for a prolonged time. It also gives high impedance on drying, thus creating more noise and signal distortion, which compromises the device fidelity. Scientists have been working to come up with an alternate method in which this gel electrolyte can be removed altogether, and the answer was hidden in the textile-based wearable electrodes. Wearable health-monitoring devices and sensors based on textiles have got much traction in the last decade; however, they have faced challenges of their own. For example, the irregular

surface of the electrodes and the increased and prolonged skin contact increases impedance, thus compromising signal reliability. Many scientists are skeptical about their use as sensors for signals which are really weak or even relying on the accuracy of their measurement in the first place (Pani et al. 2016, 2018).

CPs have brought in the solution for tweaking these problems faced by the wearable textile-based electrodes. CPs have enabled scientists to transform nonconductive textile fibers into more stable and reliable conductive forms. CPs, in general, exhibit *field emission effect*, helping in the development of noncontact sensing strategies; *percolation*, increasing the applied current can induce charge percolation; and *tunneling effect*, used to induce electron flows for distances smaller than 10 nm. These properties have resulted in an influx of researchers trying to explore these polymers as more efficient and reliable electrode materials with increased signal fidelity. Most have chosen poly-3,4-ethylene dioxythiophene doped with poly(styrene sulfonate) (PEDOT:PSS) as the go-to polymer for such applications. This conductive polymer offers excellent biocompatibility, increased electrochemical and thermal stability, and a much lower bandgap, hence making it an excellent electrode material for the detection and recording of the extracellular potential in vitro and in vivo. The ability of PEDOT:PSS to conduct both ionically and electronically and to possess ionic mobility accounts for the decreased difference between tissue and electrode's electrochemical impedance, thus very tactfully eliminating the need for the use of an electrolyte gel. Conductive polymers have played an enormous role in the miniaturization of the devices and their long-term recording of the ECG. They have also made these devices much more user-friendly and comfortable for use in the day-to-day lives. CPs offer a variety of ways to construct textile ECG electrodes with higher surface conductivity. Studies have been conducted in which such electrodes have been made out of finished textiles; these textile fibers (in their nonconductive forms) are treated with a CP based solution (e.g., PEDOT:PSS) and after drying are made to pass through several roles to remove the excess polymer. In another process (mimicking the Japanese kimono dyeing method), a polyimide master was covered with polydimethylsiloxane (PDMS) to define the pattern, thus allowing the treatment of only the specific areas of the finished garment. The whole process is followed by applying the CP onto the untreated patches with a brush and left to dry. Screen printing and inkjet printing have also been employed to produce CP-based electrochemical biosensors offering excellent stability and reproducibility with the advantage of a lower production cost. Flexography and 3D printing can also be employed, and as every technique has its own merits and demerits, the final verdict lies with the scientist and depends on the textile substrate and the required electrical properties needed (Pani et al. 2016, 2018).

Studies have also shown the development of polypyrrole (PPy)-based textile electrodes used to monitor ECG signals by employing an in situ polymerized PPy-coated Lycra fabrics (Zhou et al. 2014). Using PPy has certain advantages. PPy allows for in situ fabric coating through chemical or electrochemical polymerization. Electrochemical polymerization results in thicker and evenly coated layers on the fabrics, thus imparting superior electrical conductivity. In a study by Zhou et al.,

the cotton-based fabric was coated with PPy through in situ chemical and electrochemical polymerization. The samples were analyzed post coating via SEM, EIS, and ECG signal monitoring.

12.6.1.2 Blood Pressure and Heartbeat Rate Monitoring

Wearable health monitoring systems stand on the foundations of the revolution leading to the widespread research in smart and flexible sensing devices. These devices obtain information on wrist pulse, heart rate, and blood and intraocular pressure employing various mechanisms, such as piezoresistive, piezoelectric, capacitive, and field-effect transistor (FET)-based devices. There are already numerous health and fitness applications accessible on these smart devices, which compare the person's data to the standard set in the reference and report to the doctors when there is an anomaly. Monitoring heartbeat and the blood pressure during strenuous exercise and sports is extremely crucial for people who are at a higher risk or are already suffering from cardiovascular disease. They also prove especially helpful when the CVDs onset is particularly asymptomatic. For example, in atherosclerosis, the patient does not show any symptoms; however, it does affect the arterial blood pressure, thus changing the wrist pulse waveform and hence is detectable by such wearable devices. The conventional methods to measure all these vitals are uncomfortable, rigid, and costly compared to the user-friendly flexible electronics, which have in the first place opened the door to the world of wearable devices for long-term monitoring without any discomfort. As mentioned in the earlier section of ECG monitoring, CPs have helped develop numerous such sensing devices for early diagnosis. CPs such as PANi, PPy, P3HT, and PEDOT:PSS have been effectively used for the fabrication of FET-based flexible electronics. Polymeric materials are desirable for such applications because of their tunable chemical and mechanical properties. Their value for the Young's modulus is comparable to human skin, making them more suitable compared to the inorganic-based nanowires. Researchers have often relied on the piezoresistive sensors because of their low cost and user-friendly nature. These devices sense pressure and translate those pressure changes into a resistance signal. CP films show great piezoresistive properties and thus have been extensively exploited for such applications. However, the sensors based on CPs are relatively insensitive, less reproducible in low pressure regimes, and unstable. This problem has also been addressed by developing nanomaterial forms of the CPs. In conductive nanomaterials, piezoresistive sensing depends on the conductors' contact area when subjected to the deformation by compression. Research has highlighted the use of highly conductive 3D electrospun mats derived from poly(vinylidene fluoride-*co*-hexafluoropropene) (PVDF-HFP)/PEDOT. These mats have shown to have superior mechanical properties and display much more sensitivity to pressure, detecting even slight changes in the pressure. This sensor is also based on the piezoresistive nature of the nanomaterial (Wang et al. 2017; Kweon et al. 2018).

12.6.1.3 Detection of Biomarkers Related to Cardiac Failure

Biomarkers are naturally occurring molecules that can act as indicators of the presence or the severity of a sickness. Biosensors that can sense and recognize the

biomarkers related to CVDs can help in the timely diagnosis and treatment of these diseases and reduce the overall cost of the patient's treatment. The main challenges faced in this domain are that the currently available techniques are very costly and time-consuming. Hence, scientists worldwide are working to find alternatives that are cheap, reliable, precise, rapid, and accurate in their analysis and are also biologically compatible. For CVDs in specific, numerous biomarkers can be studied. Some of the most important ones are creatine kinase MB (CK-MB), creatine kinase MM (CK-MM), C-reactive protein (CRP), interleukins (IL-1 β , IL-6, IL-8), myoglobin (MYO), cardiac troponins (cTnI and cTnT), tumor necrosis factor alpha (TNF- α), heart-type fatty-acid-binding protein (H-FABP), and NT-proBNP (Bakirhan et al. 2018).

One study has made quite an effective use of polyaniline (PANI)-based nanowires in developing highly specific biosensors particularly for cardiac biomarkers such as cTnI, Myo, BNP, and CK-MB (indicators for myocardial infarction). Although Myo is perhaps the most important biomarker for detecting and diagnosing myocardial infarction, studies have shown that it is cross-linked with skeletal muscle pain. Thus, it is necessary to keep a check on the rest of the biomarkers as well. While cTnI is specific to the myocytes and is not found in the healthy cardiac tissues, the others (CK-MB and BNP) are directly related to the recurrence of cardiac abnormalities leading to myocardial infarction and other CVDs. CPs like PANI and PPy are exceptionally suitable for developing biosensors for these biomarkers because they impart properties like controllable conductivity, mechanical flexibility, and exceptional bioaffinity, which are severely lacking in the inorganic materials. The nanomaterial (made from the CP) surface is functionalized by attaching an antibody that can bind to the target proteins and the CP's ability to efficiently translate this binding through changes in conductance, capacitance, and impedance is what makes them especially suitable for this purpose. In this particular study, a single PANI-based nanowire was fabricated (using the electrochemical deposition method), and then functionalized using the mAbs (myocardial antibodies) via covalent linkage to the nanowire using the surface immobilization method. The mAbs target these biomarkers as mentioned earlier, and the detection is achieved through analyzing the change in the wire conductance upon interaction with the biomarkers. The nanowires were tested with phosphate-buffered saline (PBS), bovine serum albumin (BSA), and other nontarget biomarkers, and owing to the specificity of the mAbs, this PANI-based nanowire showed no change in conductance. In this study, PANI-based nanowires in combination with microfluidic channels detected these biomarkers even at extremely low concentrations, thus proving an ultrahigh sensitivity, cTnI (250 fg/mL), Myo (100 pg/mL), BNP (50 fg/mL), and CK-MB (150 fg/mL). It is also worthy to note that this mode of detection gives diagnosis within minutes, while conventional methods like that of the immunoassay require several hours before a result can be seen. The integration of microfluidic channels with the nanowires accounts for increased accuracy and ensures that the sample solution is slowly flowing through only the active part of the nanowires (Lee et al. 2012).

12.6.2 Therapeutics

Having discussed the diagnosis and prognosis applications of the CPs, we now move on to their therapeutic applications. Researchers are working tirelessly to come up with novel strategies that are not only efficient but also cost-effective and readily available. The significant development in polymer science and technology has given us multiple polymeric materials that meet the criteria mentioned earlier. Biocompatible and conductive polymers are promising materials for the treatment of the CVDs primarily owing to their ease of synthesis, flexibility, molecular imprint ability, abundant availability, sensitivity and precision, less/nontoxicity, reduced chances of immune rejection, cost-effectiveness, high shelf-life, and excellent reproducibility (Gupta et al. 2020). This section looks at how the CPs help the advancement of treatments on various fronts such as cardiac action potential and ion transport, stem cell studies, pacemaker, cardiac implants, cardiac tissue engineering, and conductive cardiac patches for use in the CVD therapy.

12.6.2.1 Cardiac Action Potential and Ion Transport

Cardiac action potential refers to a brief potential difference across the cell membrane of cardiomyocytes. This potential difference exists due to the movement of ions in and out of the cells. This mechanism regulates the contraction and relaxation of cardiac muscles. However, in some cardiovascular diseases, the propagation of this electrical impulse gets disrupted, leading to asynchronous heartbeats. For example, in post-myocardial infarction, the cardiomyocytes are replaced with fibrous tissues, which causes abnormal electrical impulses. CPs have been under several investigations to mitigate such problems. Polypyrrole (PPy) and chitosan hydrogels made via chemical oxidative polymerization have been reported to show positive improvements in synchronizing cardiac electrical signals and improving conduction velocity. This hybrid is also biocompatible, injectable, and shows excellent mechanical strength (Mihic et al. 2015). Moreover, another CP, poly-3-amino-4-methoxy benzoic acid (PAMB), was synthesized and grafted onto nonconductive gelatin. PAMB is effective in self-doping capacity at physiological pH values, which helps sustain its conductivity in biological tissues. PAMB was employed in the development of conductive hydrogel that exhibited improved conductivity compared to the regular gelatin hydrogel. Microelectrode array analysis showed higher field potential amplitude while improved electrical impulse propagation and synchronized heart contraction was demonstrated (Zhang et al. 2019). Additionally, poly(3,4-ethylenedioxythiophene) polystyrene sulfonate (PEDOT:PSS) biocompatible conductive polymer microwires were used to modulate action potential in cardiac cells. These wires are conductive (~ 30 S/cm), small and have a diameter in the range of 860 nm to 4.5 μm . When tested, these microwires successfully regulated the action potentials of cardiac cells by showing the cellular contractions that coincide with the applied voltage frequency. Moreover, the membrane integrity assays confirmed that the wires' voltage did not harm the cardiomyocytes.

12.6.2.2 Stem Cell Studies

Cardiac stem cells can form heart structures and, upon activation, can generate parenchymal cells and coronary vessels, preventing potential heart failure. Myocardial infarction obstructs a coronary artery by a blood clot that causes death of the cardiomyocytes going downstream. Cardiac tissue engineering via stem cell therapy has been remedial for myocardial infarction. Smart materials such as the CPs can open new vistas in this research regarding supporting and stimulating stem cells. Stem cell therapy is an emerging avenue to repair heart tissue that is dysfunctional. It accomplishes myocardial regeneration, and stem cells *in vivo* can be supported via scaffold materials. 3D scaffolds, that are made to be electromechanically active by using CPs, can provide an optimal microenvironment in various ways. Examples include electromechanically stimulating cardiac stem cells providing an environment that imitates the heart's structural architecture (Gelmi et al. 2016). The scaffold's mechanical actuation pioneered discrete microfiber actuation within a scaffold structure. It enabled it to provide circumscribing and coherent physiological strain to each cell, mimicking the cyclic mechanical flow and force within the heart. The electromechanically active fiber (EMAF) scaffold, made from poly(lactic-co-glycolic acid) and coated with PPy, can support and stimulate pluripotent stem cells (iPS) directly. The cells exhibited remarkable cell viability after stimulation and a strong implication for the iPS could undergo differentiation. EMAF scaffold can be put in any standard Petri dish or well plate with a standard cell culture media. The EMAF provides mechanical stimulation and electrical stimulation, which makes it the first fibrous material that can deliver both types of stimulation to seeded cells. The electroactive scaffolds did not show any cytotoxic effects on the iPS, and instead elicited an improved expression of cardiac markers in stimulated and unstimulated protocols (Gelmi et al. 2016). In another study, a string of conductive hydrogels derived from chitosan-grafted-aniline tetramer (CS-AT) were synthesized. The hydrogels can be easily injected, exhibit self-healing properties, and showed promising results as cell delivery vehicles for cardiac cell therapy. CS-AT and benzaldehyde groups capped poly(ethylene glycol) were first made into separate solutions and then mixed under physiological conditions to synthesize the hydrogels. These hydrogels showed a conductivity of 2×10^{-3} S/cm, comparable to that of cardiac tissues found within the human body (Dong et al. 2016). These hydrogels displayed substantial lethality against bacteria, adhesiveness, and degradation inside the human body. Additionally, they proved to be biocompatible so they could enhance the multiplication of the C2C12 cells and avert injury when cells are injected into the body. C2C12 cells and H9c2 cells were entrapped in the hydrogel and showed a linear trend of controlled release, which was favorable. Another study demonstrated the use of chitosan-based hydrogel as an injectable cell delivery vehicle to improve cell retention and advance the cardiac differentiation of the brown stem cells, which are derived from adipose (Dong et al. 2016). Furthermore, myocardial infarction can be ameliorated by loading the conductive hydrogels with plasmid DNA encoding endothelial NOs (eNOs) nanocomplexes and stem cells. After a hydrogel-based comprehensive complex is administered into the damaged myocytes of rats, eNOs in myocardial tissue showed an improved expression, which

can be seen along with an enhanced response to proangiogenic stimuli growth factors and myocardium-related mRNA (Guo and Ma 2018). The ECG and histological analysis can confirm a prominent improvement in the ejection fraction, decreased QRS interval, and shrunk infarction size, all of which showcase that the conductive hydrogel entrapped with stem cells and gene-encoding eNOs nanoparticles is a promising remedial approach for the curing of myocardial infarction (Guo and Ma 2018). For fine-tuning of cardiac patches using stem cells, PPy polymer surfaces, using an extensive range of dopants, for example, polystyrene sulfonate (PSS), bibenzylidene-D-sorbitol (DBS), and polythiophenes (pTS), were studied to evaluate how properties of the surface are subject to the proliferation of the stem cells. For the compatibility of the PPy films synthesized from different dopants, DBS was produced from PPy films with good biocompatibility and cell viability for cardiac progenitor cells (CPCs) (Puckert et al. 2016). It is thus implied that the PPy materials offer a befitting surface for the proliferation of CPCs. Additionally, the CPCs are not affected by small-scale variations in the material properties, for example, roughness, surface energy, and morphology. This is propitious for the future of PPy as a material for cardiac patch applications. The gross biocompatibility of the material is not sensitive to manipulating the polymer to optimize other properties, such as conductivity or flexibility (Puckert et al. 2016).

12.6.2.3 Pacemaker

The pacemaker is a cardiac implantable device used to regulate abnormal heart rhythms. Conventionally, metals are used for pacemaker electrodes, but they are susceptible to corrosion due to harsh *in vivo* environments. On the other hand, ceramics are highly stable implantable materials, especially the polymer-derived ceramics (PDC). PDCs are an attractive alternative due to their hardness, electrical conductivity, tribological activities, and the ease with which their shapes can be altered post formation (Grossenbacher et al. 2015). These can be fabricated via microneedling. The mold can be fabricated on a silicon wafer, coated with a silane monolayer and carbon layer (to improve electrical conductivity), then a ceramic precursor polymer can fill the mold subject to high pressure. The cross-linked polymer can then be removed from the mold, and sintered. Moreover, when investigated on three different *in vivo* assays, these PDCs proved to be biocompatible, with efficacy just as high as a standard implantable pacemaker (Grossenbacher et al. 2015). Another method of making an implantable electrode of a pacemaker is to form a polymer layer on a conductive (metal) electrode surface and then etching the CP layer to remove it in the form of a micropattern in a way that it exposes a portion of the conductive electrode surface. This is done to improve the biocompatibility of the pacemaker as it exposes an organic interface to the biological tissues instead of a metal surface (Jiang et al. 2012). A new approach is being taken to structure 3D, tissue-like electrode scaffolds to replace the planar metal electrodes. Their fabrication is based on the electrospinning process and treating them at a high temperature to form a porous fiber scaffold. In comparison to a metal electrode, for example, 2D Tin electrode, the new electrode showed enhanced electrical performance due to its increased surface area, in addition to subsiding the cytotoxicity of

metal electrodes. After embedding the 3D fiber scaffold in human cardiomyocytes, a tissue-electrode hybrid was made coupled with a cardiac patch resulting in increased electrical excitation and mechanical stability (Weigel et al. 2018).

12.6.2.4 Cardiac Implant

Cardiac implantable devices (CIDs) can be categorized as passive or active. Passive CIDs are not powered, for example, coronary stents. In contrast, active CIDs harness electrical energy because they are used to monitor physiological or pathological signals in the body or induce therapeutic effects by transmitting impulses to organs and tissues, for example, cardioverter-defibrillator (Bussoo et al. 2018). Coronary stents are implanted to improve blood and oxygen perfusion to the heart and provide mechanical support to the coronary arteries, which prevent restenosis (artery recoiling) after balloon angioplasty. For the latter purpose, drug-eluting stents (DES) are employed, which release bioactive molecules over sometime, interfering with the process of restenosis (Bussoo et al. 2018). PPy can be electrosynthesized on a metal substrate to form a film which can incorporate antirestenosis bioactive drugs (these make up the electrolyte for polymerization which are entrapped inside the polymer once it is discharged to its neutral form) whose amount can be controlled by the charge involved during the electropolymerization process. This method is safe, fast, cheap, and efficient in the sense that it can release the drugs up to 7–30 days, which is an ideal time range for DES application (Arbizzani et al. 2007). Electrochemically polymerized poly(3,4-ethylenedioxythiophene) (PEDOT) nanohybrid films on stainless steel surfaces can improve the hemocompatibility of cardiovascular stents. In this, PEDOT is doped with graphene oxide (GO), PSS, or heparin (HEP). As compared to the bare surface of the substrate, the coated surface shows improvement in wettability, hence less adsorption of human serum albumin (HSA) and reduced platelet adhesion because the negative charge of GO produces an expelling force against negatively charged proteins and platelets (Yang et al. 2019). In general, there are several techniques for coating stents with CPs, for example, dipping stents in polymer drug solution and drying the deposited film on the stent or chemical vapor deposition. However, the former yields nonuniform coating, and the latter requires high pressure and temperature. Conversely, the CP films can ensure uniform coating with controlled thickness and can be produced in milder conditions (Okner et al. 2007). CVDs like arrhythmias (unrhythmic heartbeat) require cardiac resynchronization therapy, which involves implants such as implantable cardioverter-defibrillator (ICD). ICD can monitor the rhythm of the heart and can be therapeutic by sending electrical shocks when the heart rate is above a preset number (Bardy et al. 2005). It requires electrodes, which can be coated with CPs. In a study, an ICP was used for coating a “hot can” defibrillator electrode. This polymeric coating (e.g., polyethylene oxide containing NaCl or alike) can coat and fill the pores of the electrode with a high surface area to provide a smooth and continuous ionic network from the “can” to the adjacent body tissue. A noble metal or its oxide (e.g., platinum black or iridium oxide) is applied over titanium housing, yielding a porous electrode with a high surface area. A conductive polymeric layer is then applied over the metal/oxide layer. The CP is biocompatible and both

chemically and mechanically stable. It does not leach out over the time of the defibrillator usage since the polymeric molecular weight is relatively high. The “hot can” defibrillator with polymeric coating disables the development of high polarization at the can-tissue interface. It maintains a continuous and uniform defibrillation threshold than previously used ICDs, hence improved the viability of pectoral implantation, especially in a “dry pocket” environment (Munshi 2001).

12.6.2.5 Cardiac Tissue Engineering

CVDs, particularly myocardial infarction, are associated with electrical disturbances due to vital cardiomyocyte failure. Unlike other tissues, the cardiac muscle has limited regenerative capacity. Once damaged, myocardial infarction usually causes permanent cell loss and fibrous scar tissue. Many researchers have been exploring the applications of cardiac tissue engineering in recent years, including the biomimetic scaffolding. Adding to the tissue-engineered method, including nanopatterned superficial surfaces, degradable polymer-based drug release, and electroactive polymers for integrated biodetection may provide new solutions for different material properties, both bulk and surface. Conventional polymers, such as PANi, and PPy-based conductive electroactive surfaces promote cell growth and proliferation by electrical stimulation, through their ability to electronically regulate the various physical and chemical properties. Specific cell reactions depend on surface characteristics of the polymer, such as ruggedness, surface free energy, topography, chemical charging, electronic conductivity, and mechanical properties. Thus, on electrical stimulation, conductive polymer-based materials will significantly enhance the biological functions of the cells (Ravichandran et al. 2010; Guo and Ma 2018). Cardiomyocytes and associated cell populations of the progenitor have been found to proliferate and migrate by electrophysiological stimulation. Electrically conductive materials have been successfully used to replicate the inherent property of cardiac cells. The stability, controllable electrical conductivity, and unusual redox properties have made the polyanilines (PANi) stand out among various CPs. Depending on its proton doping state, PANi can be transformed from conductive to an electrically isolated form in an emeraldine oxidation state. Therefore, PANi was investigated as a cardiovascular engineering scaffold. Generally, composite materials can be used in various heart tissue engineering applications as a temporary substratum to facilitate tissue formation under sufficient electrochemical and mechanical stimulation (Gajendiran et al. 2017). Therefore, biological tissues having mechanical features, and several mechanisms, commonly called mechanotransduction mechanisms, have been described to understand how the cellular activity is affected by the mechanical stimuli (Hardy et al. 2013).

12.6.2.6 Conductive Cardiac Patches

Myocardial infarction (MI) results in the development of nonconductive fibrous cavity tissues at a multiphase heart injury site. The electrical biomaterial is widely used to increase biogenerated cardiac tissue’s physiological relevance *in vitro*. The engineering of scaffolds that are biocompatible with adequate mechanical strength and electrical conductivity for cardiac tissue regeneration still has many limitations.

Currently the therapy for these conditions is limited to the lifestyle modification, medications, and potential heart transplants when the disease is too extreme. Limited regenerative cardiac capacities restrict the effectiveness of the therapy and contribute to potential health concerns. While therapeutic technologies for treating heart tissue dysfunction are increasingly needed, cardiac patches are currently a primary focus (Horbett 2020). These patches are constructed for incorporation into the natural tissue of the patients to provide medical support and cure to the affected areas. A promising solution is to modify synthetic biodegradable biomaterials to personalize material characteristics and provide other desired features for the fabrication of cardiac patches. Thus, cardiac patches are a promising new tool for treating and restoring both diseased and affected myocardium. Using a relatively simple idea, scientists have designed a scaffold that serves as a heart bandage to the native heart tissue. The development of a patch is subject to three essential conditions: (a) a physiologically exact microstructure for the scaffold, (b) a mechanical structure which supports heartbeat dynamics, and (c) biocompatible and degradable (conductive polymer-based patches should be compatible with living cells and also degradable once living cells regenerate). Such patches are intended to be applied to the heart surface and are designed to “cover” the dying area of the heart. The patch microstructure, porosity, and mechanical properties, along with biocompatibility and biodegradability, should all reflect the physiological requirements of the heart if they are to be incorporated as a functional therapeutic portion. The patch will contain many cells and biological components that remain in the tissue after the insertion (Xu et al. 2020). The scaffold will also ensure its inclusion in the native tissue, due to its biodegradable and biocompatible characteristics.

Synthetic polymeric scaffolds such as PANi are excellent candidates for producing cardiac tissue patches since they can be easily modified to match different tissue needs. These polymers have the mechanical strength and high biocompatibility, which can be easily manipulated. Besides, synthetic polymers may be engineered to meet natural cardiac tissue requirements such as durability, porosity, and microstructure. While polymers can reduce cell adhesion and integration as a biomaterial themselves, some improvements like adding stimuli and growth factors can sustain their popularity in tissue scaffolding. Cardiac scaffolds need a certain amount of mechanical resistance and elasticity to withstand the dynamic nature of the heart. Many heart scaffolds contain a combination of polymers to achieve these qualities. Blending polymers are used for integrating the mechanical characteristics of different polymers into a scaffold, containing several desirable characteristics. The production methods for such products differ significantly due to various material properties and physiological specifications.

12.7 Current Challenges in the Field

Owing to their conductivity, mechanical properties, and biocompatibility of the CPs, significant progress has been achieved in the biomedical field. Nevertheless, some challenges still limit the utilization of these polymer materials, and in this section, we explore and analyze some of the significant limitations faced by the CPs.

12.7.1 Biodegradability

One of the significant challenges is the intrinsic nonbiodegradable nature of PCPs. To overcome this limitation, one could look more into expanding the macromolecular design and synthesize the degradable linkers that can be assembled into degradable PCPs with optimal conductivity and biodegradability. This limitation is more critical in the tissue engineering-based treatments for the CVDs, where PCP-based scaffolds are being employed to improve cell growth while retaining their integrity for a specific period during that cell growth. It cannot be ignored that these materials must be broken down into small units that can be easily discharged from the body without producing any harmful effects. The *in vivo* and *in vitro* roles of degradable PCPs in the proliferation and differentiation process of electrically responsive cells and tissues are still relatively unknown. In treating the CVDs, it is crucial to understand how well the PCP-based scaffolds are degraded, regenerated, and/or repaired. We must also gain clarity over how well the cells and tissues can be integrated with the surrounding environment when the PCP-based scaffolds are decomposed. Interestingly, all these directions have not been understood yet, and these aspects are certainly worth the explorations. Therefore, the current PCP library requires significant expansion and modifications to cater to particular bioengineering applications (Park et al. 2019).

12.7.2 Conductivity

The optimization of electrical conductivity in the PCPs is another big challenge in this field. For conduction, the PCPs need to be in an oxidized or reduced state. The backbone of the conjugated polymers ionized via the redox process entails the availability of oppositely charged ions (dopant ions), which optimizes conduction. In the backbone of the PCPs, the dopant ions can be introduced either by simple mixing or via the chemical immobilization method. When dopant ions bind with the conjugated polymers via noncovalent interaction, there is a possibility that dopant ions having low molecular weight may percolate from the conjugated polymer matrix into the biological milieu, ultimately reducing the electrical conductance of the conjugated polymer. This phenomenon is particularly significant in the PCP-based biosensing devices. The devices can be made functional by removing the biologically active dopant ions on electrical stimulation. In the treatment of myocardial infarction, the PCPs such as PPy were integrated into the system to

enhance the electrical conductance and induce cell signaling. By coupling the biocompatibility with electrical conductivity, the developed system was well structured with cardiac treatment requirements. Although these were a few ways in which the scientists tried to address the issue of conductivity, the engineering of biocompatible scaffolds with adequate and stable electrical conductivity for cardiac tissue regeneration still has many limitations (Le et al. 2017).

12.7.3 Biocompatibility

The third major challenge that limits the complete utilization of CPs in the biomedical applications is their biocompatibility. The materials needed to integrate with cells or tissues require long-term stability during storage and resistance to chemical and biological fluids. In cardiovascular regeneration, biomaterials scaffolds are significantly involved in the repair and regeneration of tissues and organ defects. Different biocompatible polymeric materials are being designed to be employed at the infarction site to develop new tissues and stimulate new blood vessels. A major limitation of the cardiovascular bioengineering is the limited biocompatibility of biomaterials with the recipient's blood. Although significant advancement has been made by developing various biocompatible and useful materials, including polymers, metals, and natural biological materials, some deficiencies need to be addressed. A biomaterial utilized in cardiovascular regenerative technology can be achieved either from a natural source or via the synthetic process, ideally mimicking cardiac tissue properties. Although synthetic materials are easy to develop, they have lesser biocompatibility with the counter biological part that ultimately limits the application (Tomczykowa and Plonska-Brzezinska 2019).

12.8 Future Perspective

The applications of CPs for addressing various CVDs in either diagnostic or therapeutic settings are fast growing. It must, however, be acknowledged that more clinical phase studies are required. We also must make it a point to develop advanced synthetic strategies for the manufacturing of both the ion-conductive and π -conjugated polymers with a precise molecular design as per the requirement of the target biomedical application. The development of CPs that impersonates the characteristics of normal cardiovascular tissues would help in advancing this field. Besides, a range of novel surface modification techniques must be designed to develop materials with high biocompatibility with the cardiovascular tissues. Nanotechnology has introduced new advancements in the field of cardiology. The unique physicochemical properties of nanomaterials can help create unprecedented conductive materials to fight the CVDs. However, we need to first address the safety-related concerns associated with nondegradable nanomaterials before advancing their widespread use of in vivo applications. Even though the PCPs have been demonstrated to be biocompatible in vitro, detailed investigations of their in vivo biocompatibility

and biodegradability remain wanting. Nonetheless, keeping in view the current status of the developments, as highlighted in this chapter, exciting technologies employing CPs in combating the CVDs are expected to emerge in the near future.

Acknowledgment B.Y. acknowledges support from HFSP (RGY0074/2016), HEC for NRPU (Project No. 20-1740/R&D/10/3368, 20-1799/R&D/10-5302, and 5922), TDF-033 grants, and LUMS for start-up fund and FIF grants.

References

- Ahuja T, Mir IA, Kumar D (2007) Biomolecular immobilization on conducting polymers for biosensing applications. *Biomaterials* 28(5):791–805
- Amatore C, Bahsoun AA, Jutand A, Meyer G, Ndedi Ntepe A, Ricard L (2003) Mechanism of the Stille reaction catalyzed by palladium ligated to arsine ligand: PhPdI (AsPh₃)(DMF) is the species reacting with vinylstannane in DMF. *J Am Chem Soc* 125(14):4212–4222
- Amna B, Siddiqi HM, Hassan A, Ozturk T (2020) Recent developments in the synthesis of regioregular thiophene-based conjugated polymers for electronic and optoelectronic applications using nickel and palladium-based catalytic systems. *RSC Adv* 10(8):4322–4396
- Arbizzani C, Mastragostino M, Nevi L, Rambelli L (2007) Polypyrrole: a drug-eluting membrane for coronary stents. *Electrochim Acta* 52(9):3274–3279
- Bahri-Laleh N, Poater A, Cavallo L, Mirmohammadi SA (2014) Exploring the mechanism of Grignard metathesis polymerization of 3-alkylthiophenes. *Dalton Trans* 43(40):15143–15150
- Bakirhan NK, Ozcelikay G, Ozkan SA (2018) Recent progress on the sensitive detection of cardiovascular disease markers by electrochemical-based biosensors. *J Pharm Biomed Anal* 159:406–424
- Balint R, Cassidy NJ, Cartmell SH (2014) Conductive polymers: towards a smart biomaterial for tissue engineering. *Acta Biomater* 10(6):2341–2353
- Bardy GH, Lee KL, Mark DB, Poole JE, Packer DL, Boineau R, Ip JH (2005) Amiodarone or an implantable cardioverter–defibrillator for congestive heart failure. *N Engl J Med* 352(3):225–237
- Binks AE, Sharples A (1968) Electrical conduction in olefin oxide polymers. *J Polym Sci* 6(A2):407
- Blumberg AA, Pollack SS, Hoeve CA (1964) A Poly (ethylene Oxide)-Mercuric Chloride Complex. *J Polym Sci* 2(A2):2499
- Bussooa A, Neale S, Mercer J (2018) Future of smart cardiovascular implants. *Sensors* 18(7):2008
- Cichosz S, Masek A, Zaborski M (2018) Polymer-based sensors: a review. *Polym Test* 67:342
- Cosnier S (1999) Biomolecule immobilization on electrode surfaces by entrapment or attachment to electrochemically polymerized films. A review. *Biosens Bioelectron* 14(5):443–456
- Dong R, Zhao X, Guo B, Ma PX (2016) Self-healing conductive injectable hydrogels with antibacterial activity as cell delivery carrier for cardiac cell therapy. *ACS Appl Mater Interfaces* 8(27):17138–17150
- Doscher TM, Myers GC, Atkins DC Jr (1951) The behavior of nonionic surface active agents in salt solutions *J Colloid Sci* 6:223
- Gajendiran M, Choi J, Kim SJ, Kim K, Shin H, Koo HJ, Kim K (2017) Conductive biomaterials for tissue engineering applications. *J Ind Eng Chem* 51:12–26
- García-Melchor M, Braga AA, Lledós A, Ujaque G, Maseras F (2013) Computational perspective on Pd-catalyzed C–C cross-coupling reaction mechanisms. *Acc Chem Res* 46(11):2626–2634
- Garnier F, Deloffre F, Horowitz G, Hajlaoui R (1993) Structure effect on transport of charge carriers in conjugated oligomers. *Synth Metals* 57(2–3):4747–4754

- Gelmi A, Cieslar-Pobuda A, de Muinck E, Los M, Rafat M, Jager EWH (2016) Direct mechanical stimulation of stem cells: a beating electromechanically active scaffold for cardiac tissue engineering. *Adv Healthc Mater* 5(12):1471–1480
- Glenis S, Benz M, LeGoff E, Kanatzidis MG, DeGroot DC, Schindler JL, Kannewurf CR (1995) Electrochemical synthesis and electronic properties of poly (3, 4-dibutyl- α -terthiophene). *Synth Met* 75(3):213–221
- Grossenbacher J, Gullo MR, Dalcanale F, Blugan G, Kuebler J, Lecaudé S et al (2015) Cytotoxicity evaluation of polymer-derived ceramics for pacemaker electrode applications. *J Biomed Mater Res A* 103(11):3625–3632
- Guo B, Ma PX (2018) Conducting polymers for tissue engineering. *Biomacromolecules* 19(6):1764–1782
- Gupta R, Singhal M, Nataraj SK, Srivastava DN (2016) A potentiostatic approach of growing polyaniline nanofibers in fractal morphology by interfacial electropolymerization. *RSC Adv* 6(111):110416–110421
- Gupta S, Sharma A, Verma RS (2020) Polymers in biosensor devices for cardiovascular applications. *Curr Opin Biomed Eng* 13:69–75
- Handa NV, Serrano AV, Robb MJ, Hawker CJ (2015) Exploring the synthesis and impact of end-functional poly(3-hexylthiophene). *J Polym Sci A* 53(7):831–841
- Hardy JG, Lee JY, Schmidt CE (2013) Biomimetic conducting polymer-based tissue scaffolds. *Curr Opin Biotechnol* 24(5):847–854
- Hoffman JIE (2013) The global burden of congenital heart disease : review article. *Cardiovasc J Afr* 24(4):141–145
- Horbett TA (2020) Selected aspects of the state of the art in biomaterials for cardiovascular applications. *Colloids Surf B Biointerfaces* 191:110986
- Iovu MC, Sheina EE, Gil RR, McCullough RD (2005) Experimental evidence for the quasi-“living” nature of the Grignard metathesis method for the synthesis of regioregular poly (3-alkylthiophenes). *Macromolecules* 38(21):8649–8656
- Isotalo H, Ahlskog M, Stubb H, Laakso J, Kärnä T, Jussila M, Österholm JE (1993) Stability of processed poly (3-octylthiophene) and its blends. *Synth Metals* 57(1):3581–3586
- Itoi H, Hayashi S, Matsufusa H, Ohzawa Y (2017) Electrochemical synthesis of polyaniline in the micropores of activated carbon for high-performance electrochemical capacitors. *Chem Commun* 53(22):3201–3204
- Iwamoto R, Saito Y, Ishihara H, Tadokoro H (1968) Structure of poly (ethylene oxide) complexes. II. Poly (ethylene oxide)–mercuric chloride complex. *J Polym Sci* 6(A2):1509
- Jiang et al (2012) Conductive polymer patterned electrode for pacing. *Cardiac Pacemakers Inc.* <https://patents.google.com/patent/US8311606>
- Jonas F, Heywang G (1994) Technical applications for conductive polymers. *Electrochim Acta* 39(8–9):1345–1347
- Kato M, Kamigaito M, Sawamoto M, Higashimura T (1995) Polymerization of methyl methacrylate with the carbon tetrachloride/dichlorotris-(triphenylphosphine)ruthenium(II)/methylaluminum bis(2,6-di-tert-butylphenoxide) initiating system: possibility of living radical polymerization. *Macromolecules* 28(5):1721–1723
- Kim DH, Richardson-Burns SM, Hendricks JL, Sequera C, Martin DC (2007) Effect of immobilized nerve growth factor on conductive polymers: electrical properties and cellular response. *Adv Funct Mater* 17(1):79–86
- Kumar A, Singh R, Gopinathan SP, Kumar A (2012) Solvent free chemical oxidative polymerization as a universal method for the synthesis of ultra high molecular weight conjugated polymers based on 3, 4-propylenedioxythiophenes. *Chem Commun* 48(40):4905–4907
- Kweon OY, Lee SJ, Oh JH (2018) Wearable high-performance pressure sensors based on three-dimensional electrospun conductive nanofibers. *NPG Asia Mater* 10(6):540–551
- Laakso J, Österholm JE, Nyholm P (1989) Conducting polymer blends. *Synth Met* 28(1–2):467–471
- Lam JW, Tang BZ (2005) Functional polyacetylenes. *Acc Chem Res* 38(9):745–754

- Le TH, Kim Y, Yoon H (2017) Electrical and electrochemical properties of conducting polymers. *Polymers* 9(4):150
- Lee JY, Lee JW, Schmidt CE (2009) Neuroactive conducting scaffolds: nerve growth factor conjugation on active ester-functionalized polypyrrole. *J R Soc Interface* 6(38):801–810
- Lee I, Luo X, Huang J, Cui XT, Yun M (2012) Detection of cardiac biomarkers using single polyaniline nanowire-based conductometric biosensors. *Biosensors* 2(2):205–220
- Lennox AJ, Lloyd-Jones GC (2014) Selection of boron reagents for Suzuki–Miyaura coupling. *Chem Soc Rev* 43(1):412–443
- Linford RG (1993) Electrical and electrochemical properties of ion conducting polymers. In: *Applications of electroactive polymers*. Springer, Dordrecht, pp 1–28
- Loewe RS, Ewbank PC, Liu J, Zhai L, McCullough RD (2001) Regioregular, head-to-tail coupled poly(3-alkylthiophenes) made easy by the GRIM method: investigation of the reaction and the origin of Regioselectivity. *Macromolecules* 34(13):4324–4333
- Lundberg RD, Bailey FE, Callard RW (1966) Interactions of inorganic salts with poly(ethylene oxide) *J Polym Sci* 4(A1):1563
- McClellan M, Brown N, Califf RM, Warner JJ (2019) Call to action: urgent challenges in cardiovascular disease: a presidential advisory from the American Heart Association. *Circulation* 139:e44–e54
- Meador MAB, Hardy-Green D, Auping JV, Gaier JR, Ferrara LA, Papadopoulos DS et al (1997) Optimization of electrically conductive films: poly (3-methylthiophene) or polypyrrole in Kapton. *J Appl Polym Sci* 63(7):821–834
- Mihic A, Cui Z, Wu J, Vlacic G, Miyagi Y, Li S, Li R (2015) A conductive polymer hydrogel supports cell electrical signaling and improves cardiac function after implantation into myocardial infarct. *Circulation* 132(8):772–784
- Mocanin J, Cuddihy EF (1966) *J Polym Sci* 14(C):311
- Moheimani F, Jackson DE (2011) Venous thromboembolism: classification, risk factors, diagnosis, and management. *ISRN Hematology* 2011:1–7
- Munshi Z (2001) Defibrillator housing with conductive polymer coating. Intermedics Inc. <https://patents.google.com/patent/US6295474>
- Musumeci C, Hutchison JA, Samorì P (2013) Controlling the morphology of conductive PEDOT by in situ electropolymerization: from thin films to nanowires with variable electrical properties. *Nanoscale* 5(17):7756–7761
- Nezakati T, Seifalian A, Tan A, Seifalian AM (2018) Conductive polymers: opportunities and challenges in biomedical applications. *Chem Rev* 118(14):6766–6843
- Okner R, Oron M, Tal N, Mandler D, Domb AJ (2007) Electrocoating of stainless steel coronary stents for extended release of paclitaxel. *Mater Sci Eng C* 27(3):510–513
- Olin JW, Sealove BA (2010) Peripheral artery disease: current insight into the disease and its diagnosis and management. *Mayo Clin Proc* 85(7):678–692
- Pani D, Dessi A, Saenz-Cogollo JF, Barabino G, Fraboni B, Bonfiglio A (2016) Fully textile, PEDOT:PSS based electrodes for wearable ECG monitoring systems. *IEEE Trans Biomed Eng* 63(3):540–549
- Pani D, Achilli A, Bonfiglio A (2018) Survey on textile electrode technologies for electrocardiographic (ECG) monitoring, from metal wires to polymers. *Adv Mater Technol* 3(10):1800008
- Pappachan J, Kirkham FJ (2008) Cerebrovascular disease and stroke. *Arch Dis Child* 93(10):890–898
- Park Y, Jung J, Chang M (2019) Research progress on conducting polymer-based biomedical applications. *Appl Sci* 9(6):1070
- Puckert C, Gelmi A, Ljunggren MK, Rafat M, Jager EWH (2016) Optimisation of conductive polymer biomaterials for cardiac progenitor cells. *RSC Adv* 6(67):62270–62277
- Ravichandran R, Sundarajan S, Venugopal JR, Mukherjee S, Ramakrishna S (2010) Applications of conducting polymers and their issues in biomedical engineering. *J R Soc Interface* 7 (suppl_5):S559–S579



Engineered Polymeric Materials/Nanomaterials for Growth Factor/Drug Delivery in Bone Tissue Engineering Applications

13

Neelam Chauhan and Yashveer Singh

Abstract

Accelerating number of bone fractures/disorders, increased global burden, high demand, and limited availability of traditional bone grafts have shifted the research interest toward development of alternatives strategies, including the development of growth factor/drug delivery systems. The conventional delivery methods are limited in application due to the poor local retention, half-life, stability, requirement of high dosage, and inactivation of growth factor and drugs in biological systems. Polymeric materials/nanomaterials have emerged as promising candidates for therapeutic delivery of growth factors and drugs in tissue engineering applications due to their functionality and highly porous structure, which is suitable for high drug loading and extracellular-mimicking properties that promote cell attachment and proliferation for tissue repair. Engineering of polymeric materials has resulted in advancement of polymer chemistry in drug delivery applications by providing stimuli-sensitive polymeric systems, which can respond to pH, temperatures, and the presence of biomolecules. Different polymeric structures, such as nanofibers, nanoparticles, hydrogels, and 3D-printed scaffolds, have been investigated to overcome the problem of low drug efficacy and burst release. The polymeric materials maximize the effectiveness of growth factors/drugs by providing sustained, controlled, and localized release. However, the selection of polymers and growth factors/drugs is significantly important for the optimization and development of drug release systems similar to the release of growth/osteogenic factors in natural bone healing. This chapter focuses on the design strategies being employed for the next-generation engineered polymeric material/nanomaterial-based advanced

N. Chauhan · Y. Singh (✉)

Department of Chemistry, Indian Institute of Technology Ropar, Rupnagar, Punjab, India
e-mail: yash@iitr.ac.in

© The Author(s), under exclusive license to Springer Nature Singapore Pte Ltd. 2022

L. M. Pandey, A. Hasan (eds.), *Nanoscale Engineering of Biomaterials: Properties and Applications*, https://doi.org/10.1007/978-981-16-3667-7_13

349

delivery systems for enhancing the bone repair and regeneration as well as their potential application in regenerative medicine.

Keywords

Bone · Drugs · Growth factors · Engineered polymeric structures · Smart polymeric systems · Growth factor/drug release · Polymeric nanomaterials

13.1 Introduction

Bone fractures/injuries affect millions of people worldwide, posing a heavy global economic burden (Meling et al. 2009; Bonafede et al. 2013). Bone tissue forms an essential part of the body and serves as a structural scaffold and supports kinematic motion while protecting our vital organs. Skeletal injuries due to falls, accidents, trauma, infections, tumors, or other bone-related disorders are very common and often require surgical interventions (Meling et al. 2009; Einhorn and Gerstenfeld 2015; Amir et al. 2019). Musculoskeletal injuries are predicted to be one of the major causes of morbidity and mortality worldwide (Agarwal-Harding et al. 2016; Mattson et al. 2019). The bone is a complex tissue and it consists of about 30% organic (collagen and proteoglycans) and 70% inorganic components (hydroxyapatite and amorphous calcium phosphate) having inherent ability to remodel and heal to maintain the tissue integrity (Salgado et al. 2004). The natural fracture/bone healing is a slow and time taking process that relies on the biological responses. Several conditions, such as osteoporosis, diabetes, autoimmune disorders, trauma, infections, and fixation stability, may significantly affect the biological responses during the fracture or bone injury; thus, compromising the healing and leading to the poor clinical outcomes. These conditions may result in about 10% delayed union or nonunion cases requiring additional surgical procedures (Einhorn and Gerstenfeld 2015). The rapid acceleration in bone-related disorders, fractures, and heavy economic burden posed due to the high demand of bone substitutes/grafts has motivated researchers to work on the advancement in bone tissue engineering. Currently, natural grafts including autograft and allografts are considered as the gold standard for the bone substitute, but the limited supply, risks of infection, disease transmission, and host responses have limited their use; thus, generating the demand for novel treatment strategies (Einhorn and Gerstenfeld 2015; Lee et al. 2015; Wang and Yeung 2017). These current strategies generally include systemic administration of bone-forming drugs, hormones, or other biomolecules, the development of synthetic grafts, onsite delivery of drugs, growth factors, and cells from the graft to address the limitations associated with the current approaches of bone regeneration (Shi et al. 2019). The local delivery of drugs and growth factors from the biomaterials has shown promising results and several polymeric systems are being explored to enhance the bone tissue regeneration by on-site delivery of drugs and biomolecules along with providing the matrix/scaffold for the cell attachment and tissue integration (Luginbuehl et al. 2004; Kempen et al. 2009b; de Guzman et al. 2013, p. 2;

Peterson et al. 2014; Martino et al. 2015). Bone tissue possess unique material and biological properties and, therefore, designing an effective bone regeneration solution requires a greater understanding of the natural healing process, biomolecules, and molecular mechanisms involved in the healing process.

13.1.1 Fracture Healing

The fracture healing comprises of mainly three phases: inflammation, repair, and remodeling (Fig. 13.1). These phases of healing overlap and can be distinguished by cellular and molecular factors (Kolar et al. 2010; Einhorn and Gerstenfeld 2015). The role and timing of these factors in the bone-healing process may provide important insights in designing the new delivery strategies to enhance bone regeneration. Bone fracture results in the disruption of the blood supply, leading to the

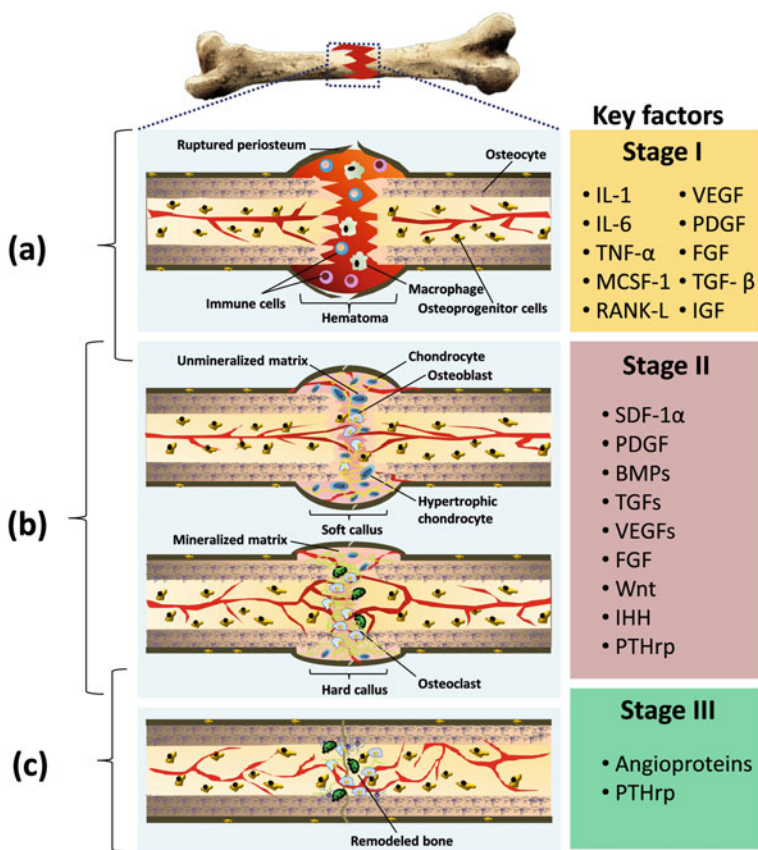


Fig. 13.1 Fracture healing phases and key factors involved at different stages of healing. (a) Inflammation, (b) repair, and (c) remodeling

formation of hematoma at the injury site. Initially, acute inflammatory responses can be seen within 24 h at the injury site with the expression of inflammatory markers initiating the repair process by stimulating angiogenesis process and recruiting mesenchymal stem cells at the site for the deposition of extracellular matrix (Kolar et al. 2010; Claes et al. 2012). Various proinflammatory cytokines, including interleukins (IL-1 and IL-6), tumor necrosis factor- α (TNF- α), macrophage colony-stimulating factor 1 (M-CSF-1), receptor activator of nuclear factor kappa-B ligand (RANKL), and transforming growth factor- β (TGF- β) can be seen in the early phases (Fig. 13.1a) (Marsell and Einhorn 2011; Claes et al. 2012; Einhorn and Gerstenfeld 2015). TNF- α and IL-6 play a very important role in tissue regeneration and their complete absence has shown to delay the mesenchymal stem cell differentiation (Gerstenfeld et al. 2003; Yang et al. 2007). However, prolonged inflammation period or chronic inflammation due to the conditions, such as infection and autoimmune diseases, may lead to the failed or impaired healing (Claes et al. 2012; Einhorn and Gerstenfeld 2015). In normal conditions, the inflammation phase is succeeded by the repair phase (Fig. 13.1b). The damage and rupture of blood vessels create the hypoxic environment triggering the release of proangiogenic factors, such as vascular endothelial growth factor (VEGF), angiopoietin-1, and platelet-derived growth factor (PDGF), promoting the vascularization of the newly formed bone tissues at the injury site (Grundnes and Reikerås 1992; Mayr-wohlfart et al. 2002; Hankenson et al. 2011).

The breakdown products are removed and the hematoma is replaced in a stepwise manner with the dense granulation tissues. Depending on the mechanical stability of the fracture site, the healing may take place directly or indirectly (Yu et al. 2010; Foster et al. 2020). In the direct healing, stability of the fracture site allows bridging of Haversian canals and results in osteoclasts infiltration, followed by the vascularization and recruitment of fibroblasts, MSCs, and osteoprogenitor cells by macrophages. The mineralization of long bones follows endochondral ossification route (Marsell and Einhorn 2011; Claes et al. 2012; Ghiasi et al. 2017). The mechanically unstable fractures lead to the indirect bone healing, both intramembranous and endochondral ossification (Claes et al. 2012; Ghiasi et al. 2017). The high mechanical strain in this case results in lesser new vessel formation, and the low oxygen level shifts the equilibrium of progenitor cells toward chondrogenic differentiation. The cartilaginous tissue formation takes place within 7–10 days of the injury (Grundnes and Reikerås 1992; Marsell and Einhorn 2011). SDF-1 α is released from the periosteum and induces the phase of bone healing by inducing cell migration toward the bone formation site (Kitaori et al. 2009). Bone morphogenetic protein (BMP) and TGF- β help in bone regeneration by triggering the differentiation of chondrocytes (Benazet et al. 2009; Einhorn and Gerstenfeld 2015). BMP along with the Indian hedgehog (IHH) and parathyroid hormone-related protein (PTHrP) pathways stimulate the hypertrophy of chondrocytes toward bone, resulting in the formation of the mineralized bone matrix (Mak et al. 2008; Benazet et al. 2009; Haumer et al. 2018).

The final phase of fracture healing involves remodeling of the bone that may take place up to years to maintain the structural and mechanical integrity of the bones

(Fig. 13.1c). The hypertrophic chondrocytes become apoptotic and start releasing calcium after 2 weeks of bone fracture (Einhorn 1998, 2005; Thompson et al. 2015). The increase in the mechanical strength of the calcified callus reduces the tissue strain; thus, favoring the vessel formation and recruitment of MSCs and monocytes (Melnyk et al. 2008; Haumer et al. 2018). These differentiate into the osteoblasts and osteoclasts and the remodeling of bone starts (Einhorn 1998; Einhorn and Gerstenfeld 2015). This leads to the transformation of woven bone to the lamellar bone (Schindeler et al. 2008). These events are regulated by osteoblast-secreted cytokines MCSF and RANKL (Schindeler et al. 2008). The decrease in most inflammatory cytokines, except IL-1, TNF- α , and BMP-2, can be seen in this phase (Claes et al. 2012). As the gap is filled, the low tissue strain allows the intramembranous ossification after 4–6 weeks of bone fracture (Claes 2011).

13.1.2 Role of Growth Factors, Drugs, and Other Biomolecules in Bone Regeneration

Bone healing is a complex process that is accomplished by coordinated involvement of cells, bioactive molecules, and extracellular matrix. Cells release several growth factors at the injury site to induce and promote the bone regeneration and remodeling process. Growth factors are signaling molecules that induce and control various cell responses. Several inflammatory, angiogenic, osteogenic, and systematic factors are involved in bone repair and remodeling (Einhorn 1998; Einhorn and Gerstenfeld 2015). The inflammatory factors, including TNF- α , ILs, and prostaglandins, are responsible for the stimulation and differentiation of osteoblast and osteoclast cells and their release also activates the secondary signal cascade, resulting in enhanced angiogenesis (Kanzaki et al. 2002; Gerstenfeld et al. 2003; Ponte et al. 2007). Several anti-inflammatory and immunomodulatory factors, corticosteroids, and anti-inflammatory drugs have been reported to show the proregenerative or proresorptive effects. Angiogenesis factors, such as vascular endothelial growth factor (VEGF), platelet-derived growth factor (PDGF), fibroblast growth factor (FGF), and insulin-like growth factor (IGF), have been explored in the bone regeneration as they promote the development of vascular network at the injury site; thus, supporting the osteogenic, chondrogenic, and mesenchymal stem cells (Schmidmaier et al. 2001; Keramaris et al. 2008; Wu et al. 2020). Among them VEGF has been extensively investigated and have been found to increase the vascularization and bone regeneration (Keramaris et al. 2008). However, the delivery of VEGF along with other osteogenic factors have shown more promising results in bone regeneration (Peng et al. 2002; Patel et al. 2008; Kempen et al. 2009b; Lee et al. 2020). Osteogenic growth factors, such TGF- β , BMPs, growth differentiation factor (GDF), and stromal-derived growth factor-1 (SDF1), have been also explored (Lieberman et al. 2002; Park et al. 2005; Kitaori et al. 2009; Kempen et al. 2009b; Yamano et al. 2014). TGF- β have shown bone induction but only up to endochondral bone formation (Ramoshebi et al. 2002; Ripamonti 2006). List of factors and drugs explored in bone regeneration applications is provided in Table 13.1.

Table 13.1 List of commonly used growth factors and drugs and their outcomes in bone regeneration (Aronin et al. 2010, p. 7; Donneys et al. 2012; Cattalini et al. 2012; Ibrahim et al. 2014; Einhorn and Gerstenfeld 2015; Yuasa et al. 2015; Shah et al. 2015; Gupta et al. 2019; Kuroda et al. 2019)

Growth factors/drugs		Effects/outcomes
Growth factors	TGF- β	Induce bone formation
	FGF-2	Induce angiogenesis and promote bone regeneration
	BMP-2 and BMP-7	Increase de novo bone formation
	VEGF	Increase angiogenesis and bone regeneration
	GDF	Enhance bone repair
	IGF	Enhance tissue regrowth
	PDGF	Support bone regeneration by enhancing angiogenesis
Hormones	PTH	Promote bone formation or resorption depending on the dose
Drugs and other molecules	Alendronate Ibandronate Pamidronate Zoledronate Clodronate	Reduce bone resorption and increase mineralization
	Dexamethasone	Inhibit osteoclastogenesis and promote osteoblastogenesis (dose dependent)
	FTY720	Promote angiogenesis and osteogenesis
	Deferoxamine (DFO)	Vascular response on bone regeneration
	Simvastatin Lovastatin	Anti-inflammatory and proangiogenic activities, promote osteogenesis

BMP isoforms, such as BMP-2, BMP-4, and BMP-7, have shown more promising results in de novo bone formation in ectopic and orthotopic sites (Kirker-Head 2000; Seeherman and Wozney 2005). Some systematic factors, such as parathyroid hormone (PTH), growth hormone, steroids, calcitonin, and Vitamin D, have also been investigated in bone tissue engineering and reported to promote bone formation (Weiss et al. 1981; Kempen et al. 2010; Hankenson et al. 2011; Abbassy et al. 2016). The growth factors may provide specific control over regeneration by manipulating the signaling processes. Although these molecules have shown good results in bone healing alone or in combination with other growth factors or drugs, the selection of growth factor is critical to maximizing the bone repair. Several drugs have also been explored in this field due to the high cost and low stability of growth factors. Bisphosphonates, such as alendronate, ibandronate, pamidronate, and zoledronate, have been explored in bone tissue regeneration and showed improved bone formation and prevention of bone resorption. Dexamethasone and FTY720 have shown increased osteogenesis.

13.1.3 General Requirements of Matrix/Scaffolds for Growth Factor/Drug Delivery

Bone is a very complex tissue and, therefore, designing the scaffolds require several considerations, including the choice of material, biocompatibility, biodegradation, osteoinductive/osteogenic nature, mechanical strength, porosity, and growth factor/drug release, to support the cell adhesion, proliferation, nutrient exchange, diffusion of biomolecules, and integration of scaffold. Several efforts have been made to incorporate growth factors/drugs within the matrix/scaffolds to provide their local release at the injury site to improve bone-healing outcomes. Among them, the extracellular matrix (ECM)-mimicking scaffolds provide the native-like environment to the cells for attachment and proliferation along with the release of growth factors/drugs to induce osteogenesis and enhance bone healing (Hudalla and Murphy 2011; Martino et al. 2015). The scaffolds working as a delivery carrier must fulfill some additional criteria, like high loading capacity, uniform distribution, targeted delivery, controlled/sustained release, and physical and chemical stability, and must protect the host molecules from losing their activity (Fig. 13.2). The optimization of drug loading and release from a scaffold requires certain considerations such as composition of scaffold, morphology, porosity, cross-linking, loading capacity, nature of interactions between the drug and the scaffold, binding affinities, stability of loaded molecule, and degradation of the matrix.

13.2 Challenges

Systemic delivery of growth factors and drugs is limited due to their short half-life, instability, and undesirable toxicity (Xinluan et al. 2015; Kuroda et al. 2019). Targeted delivery approaches are helpful in overcoming these limitations. There is a critical need to design bone substitutes providing local delivery of osteogenic agents. The drug delivery approaches have significantly advanced in the last few

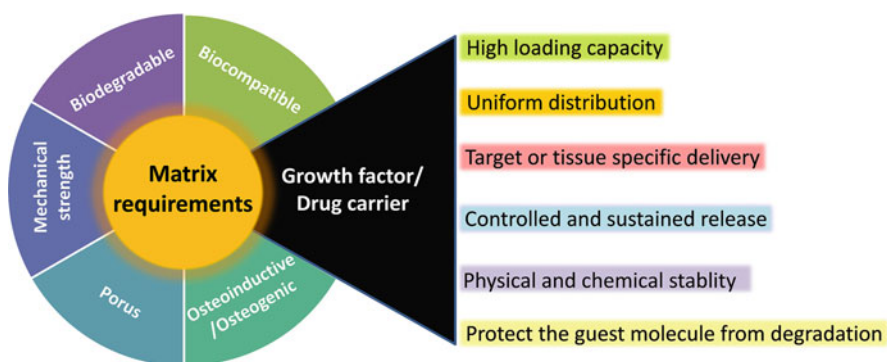


Fig. 13.2 General requirements of matrices/scaffolds for local delivery of growth factors/drugs for bone tissue engineering applications

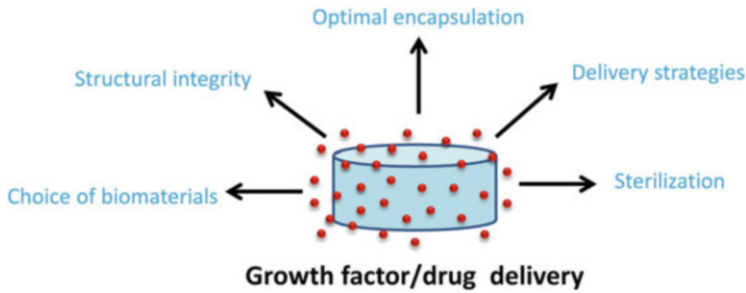


Fig. 13.3 Challenges in growth factor/drug delivery

years but designing an ideal delivery system suitable for all applications remains challenging as different shape, size, and structure of bone defects require different mode of delivery, mechanical, and degradation properties. Earlier permanent implants were employed for drug delivery but due to their poor integration and other limitations, degradable implants are now preferred (Vo et al. 2012). It is also challenging to design a scaffold releasing the growth factor/drug to restore to tissue at the same rate as that of implant degradation. The delivery systems for bone tissue engineering require long-term controlled release of growth factors/drugs and it is challenging to maintain its bioactivity throughout the course. Major challenges in growth factor delivery are listed in Fig. 13.3.

The optimization of drug loading also varies from one case to other and the interaction of different materials with the encapsulated growth factor/drug may lead to the loss of their integrity, thus resulting in low bioactivity. The modifications of growth factors and drugs for incorporation in the scaffolds and controlled release may also reduce their functionalities. Therefore, it is not easy to develop a single delivery strategy that can overcome all drawbacks of the carrier. It is also difficult to select a material having interconnected porous network required for cellular ingrowth along with providing the adequate mechanical support throughout the healing phase. Besides, the sterilization of growth factors encapsulated grafts also remains a major drawback.

13.3 Materials for Growth Factor/Drug Delivery

A wide range of materials have been explored as delivery systems for temporal and spatial control of growth factors/drugs/other bioactive molecules. Various metal, ceramic, and polymer-based implants have been evaluated as drug delivery carriers by physically or chemically loading the growth factor/drug molecules. A list of growth factor/drug-loaded biomaterials and polymeric systems available in market and undergoing clinical trials is provided in Tables 13.2 and 13.3.

Table 13.2 Growth factor/drug-loaded biomaterials for bone regeneration in market

Product	Composition	Application	Company	References
INFUSE [®] Bone graft	Collagen sponge loaded with BMP-2 titanium/PEEK cage	Replacement of autograft, degenerative disc diseases, anterior lumbar interbodyfusion (ALIF), spinal fusion, and open tibial shaft fractures	Medtronic, Inc.	https://global.medtronic.com/xg-en/e/response/infuse-bone-graft.html
Osigraft (OP-1 [®]) Implant & Putty)	BMP-7 containing type 1 bovine bone collagen matrix mixed with the putty additive carboxymethylcellulose sodium	Fracture healing of the long bones, and treating lumbar spine pseudoarthrosis	Olympus Biotech	https://www.strykemed.com/media/1976/op-1-implant-msds.pdf (withdrawn)
Augment [®]	PDGF loaded in tricalcium phosphate matrix	Hindfoot and ankle fusion procedures	Wright Medical Group	https://www.wright.com/biologics_self/augment-injectable
GEM 21S [®]	PDGF with an osteoconductive matrix, β -TCP	Dental problems such as intrabony, periodontal defects, furcation periodontal defects, and gingival recession associated with periodontal defects	Lynch Biologics	https://www.lynchbiologics.com/products/gem-21s/

13.3.1 Metals and Ceramics-Based Materials

Metal-based implants (mainly titanium and stainless steel) are highly used in orthopedic applications due to their high mechanical properties (Peterson et al. 2014; Prasad et al. 2017). These implants result in poor integration due to their inert nature and lack of osteoprogenitor function, which may lead to the formation of fibrous capsules around the implant, resulting in the loosening of implants and compromise in the long-term activity (Prasad et al. 2017; Kämmerer et al. 2020). Physical loading and chemical conjugation of growth factors, drugs, or other bioactive molecules have been explored on these implants to improve the bone-healing outcomes. BMP-2, FGF, VEGF, *N*-bisphosphonate, and dexamethasone incorporation into metallic implants have been carried out to improve the osseointegration (Kim et al. 2011; Peterson et al. 2014; Al-Jarsha et al. 2018; Kämmerer et al. 2020). Kim et al. immobilized the BMP-2 and heparin on titanium (Ti) surfaces and reported increased ALP activities, calcium deposition, and osteoblast function and decreased

Table 13.3 Growth factor/drug-loaded biomaterials for bone regeneration in clinical trials

Product	Composition	Phase	Application	Organization	References
KUR-111 KUR-112	Fibrin matrix+ HA/TCP loaded with PTH	2	Tibial plateau fractures Tibial shaft fractures	Kuros Biosurgery AG	NCT00533793 https://kurosbio.com/fibrin-ptb/tibial-plateau-fractures/ NCT04294004
KUR-113 bone graft	TGp PTH1-34 in fibrin	2	Degenerative disc disease, spinal fusion	Kuros Biosurgery AG	NCT04294004
FGF-2 gelatin hydrogels	rhFGF-2 in gelatin hydrogels	Preparatory	Tibial shaft fractures	–	Kawaguchi et al. (2010)
Rosuvastatin gel with 1:1 mixture of PRF and bone graft	Combination of rosuvastatin (RSV) in situ gel with the mixture of autologous platelet-rich fibrin (PRF) and HA bone graft	4	Mandibular degree II furcation defects	Government Dental College and Research Institute, Bangalore	NCT02369250
Simvastatin-methylcellulose gel	Simvastatin-methylcellulose	4	Alveolar bone in periodontitis	University of Nebraska	NCT03452891
rhFGF-2/HA	rhFGF-2 in sodium hyaluronate	1, 2	Human intrabony defects	Universidade Federal Fluminense	NCT02337166

inflammatory responses (Kim et al. 2011). Peterson et al. developed multilayer coatings of poly(methacrylic acid) and poly-L-histidine on anodized Ti surfaces immobilized with BMP-2 or FGF that provided sustained release of growth factors over 25 days with BMP-2 release being more effective than FGF for bone growth (Peterson et al. 2014). Poly(ethyl acrylate) (PEA) and fibronectin (FN)-coated Ti discs loaded with BMP-7 were developed and reported to promote potential osteodifferentiation of human mesenchymal stem cells (HMSCs) (Al-Jarsha et al. 2018). Although these efforts improved implants' interaction with cells, the surface adsorption of drugs or growth factors on metallic implants resulted in an initial burst release, resulting in adverse effects in several cases.

Kämmerer et al. chemically modified the titanium (TiO₂) surface with BMP-2, BMP-7, and an anti-osteoclastic drug (alendronic acid) and it showed significant improvement in cell growth and alkaline phosphatase (ALP) expressions at third and seventh day of bone-marrow-derived stem cell (BMSC) culture (Kämmerer et al. 2020). In order to improve the osteogenic potential and growth factor loading of bone implants, ceramics such as bone-derived minerals, tricalcium phosphates (TCP), hydroxyapatite (HA), and bioglass (BG) have also been used alone or in combination as osteoinductive coatings on metallic implants or scaffold carriers for growth factors and drugs. Teotia et al. reported that the nanohydroxyapatite and calcium sulfate bone substitutes functionalized with BMP-2 and zoledronic acid in low doses resulted in highest mineralization and neo-bone formation compared to ceramics loaded with zoledronic acid alone and without BMP-2 or zoledronic acid, when implanted in 8.5-mm critical size defect in calvarium of male Wistar rats for 8 weeks (Teotia et al. 2017). Calcium phosphates (CaP) have also been explored for FGF, hepatocyte growth factor (HGF), rhBMP-2, endothelial growth factor (EGF), FGF-2, and dexamethasone release and shown improvement in bone regeneration. Mesoporous bioactive glasses (MBG) are considered as osteoconductive and osteoinductive, and possess high specific surface area that makes them suitable for growth factor delivery applications. Different growth factors (BMP and VEGF) and drugs (dexamethasone, gentamicin, and ibuprofen) can be easily loaded and released from MBG particles, fibers, scaffolds, and composites (Wu et al. 2009, 2013; Dai et al. 2011; Wu and Chang 2012; Kim et al. 2016). Although the highly porous and osteoinductive nature of ceramics make them a suitable candidate for drug loading and cell activities, the burst release of growth factor/drug due to the electrostatic interactions or dissolution or degradation of ceramics limits their use as drug carriers, and usually polymer coating is employed to attain sustained release.

13.3.2 Polymeric Materials

Polymeric materials have been explored as drug carriers in bone tissue regeneration due to their versatile and tunable properties. Most polymeric materials closely mimic the extracellular matrix and, thus, provide the surface for cell attachment and growth. Biodegradable polymers can be tuned to resorb by the body after bone healing. The polymers contain variety of functional groups and can be functionalized easily as per

the requirement to load drugs physically or chemically. Polymers used in bone regeneration are classified as natural and synthetic polymers.

13.3.2.1 Natural Polymers

Proteins and polysaccharides extracted from plants, algae, animal, or human sources are considered as natural polymers. They have been proven to be useful material for tissue engineering due to their high biocompatibility, ECM-mimicking nature, and favorable degradation products (Mano et al. 2007). Collagen is a protein and most extensively used natural polymer, which forms a major organic component of the bones. Fibrinogen/fibrin is a fibrous protein, which forms a temporary matrix at the wound and have several binding sites for cells, growth factors, and ECM (Martino et al. 2014). These proteins have been used for biomolecule delivery but their proteolytic stability remains a major concern (Rajangam and An 2013). Other common natural polymers used for growth factor/drug delivery in bone tissue engineering are gelatin, keratin, silk fibroin (SF), alginate, chitosan, hyaluronic acid, heparin sulfate, pullulan, and dextran as they possess excellent biocompatibility and low immunogenicity (de Guzman et al. 2013). These polymers also possess functional groups that can be utilized for physical cross-linking and chemical modifications. The 3D networks formed by natural polymers can retain high water contents, are highly porous, and mimic ECM. Collagen-based scaffolds have been shown to promote osteogenic gene expression of MSCs and mineralization and, therefore, explored for the release of exogenous growth factors, such as FGF, PDGF, VEGF, IGF-1, HGF, BMP-2, TGF- β , and GDF-5 (Kanematsu et al. 2004; Yamano et al. 2014). Yamano et al. reported that the collagen membranes (CM) loaded with PDGF and GDF-5 showed significant bone regeneration compared to the control and CM alone, with more effectiveness in case of collagen membranes loaded with GDF-5 (Fig. 13.4) (Yamano et al. 2014).

Gelatin and silk fibroin have emerged as alternatives of collagen. Silk fibroin is biocompatible, osteoconductive, and possesses excellent mechanical properties (Meinel et al. 2005). The scaffold developed using silk fibroin has been investigated as the carrier of BMP-2 and showed good osteogenic outcomes (Ma et al. 2016). Gelatin-based materials have also shown improvement in cell attachment (Chen et al. 2007). Chitosan is among the commonly used natural polymer derived from chitin. It is reported to promote cell adhesion and proliferation as well as osteoblast differentiation along with antibacterial and mucoadhesive properties (Levengood and Zhang 2014; Tao et al. 2020). Hyaluronic acid and pullulan have been reported to support attachment and proliferation of mesenchymal stem cells (Singh et al. 2016; Zhai et al. 2020). Different polymeric structures fabricated using these polymers have been utilized in growth factor/drug delivery. Several growth factors including BMPs, VEGF, FGF, PDGF, TGF- β , and drugs have been tested using natural polymers. Generally, these polymers are found to show burst release due to the rapid degradation in biological environment but modification in their physical or chemical structure or processing usually improves the control release kinetics. Although natural polymers show excellent biocompatibility and bioactivity, their rapid degradation and poor mechanical strength limit their use in bone regeneration.

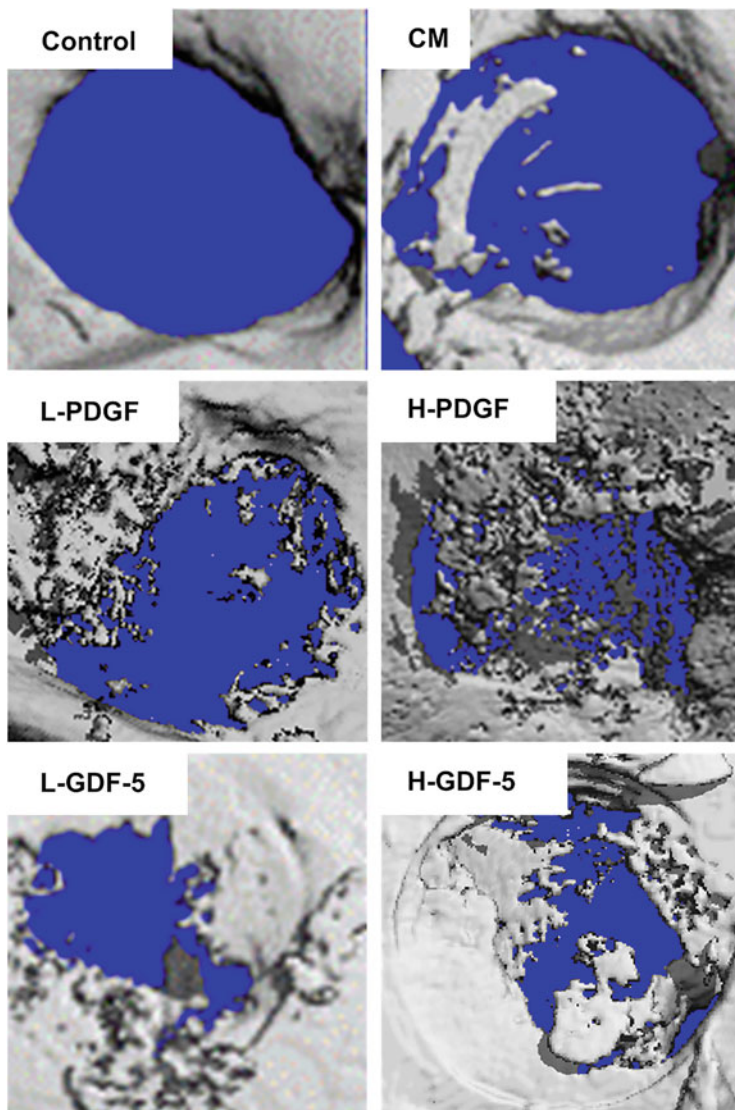


Fig. 13.4 Micro-CT images of new bone formation in rat mandible defects treated with collagen membrane (CM), and collagen membranes containing 0.5 μg PDGF (L-PDGF), 1 μg PDGF (H-PDGF), 20 μg GDF (L-GDF5), and 60 μg GDF-5 (H-GDF5) after 4 weeks of surgery. The blue color represents nonmineralized defect. (Reproduced with permission from Yamano et al. 2014)

13.3.2.2 Synthetic Polymers

Synthetic polymers have been extensively explored in growth factor/drug delivery in bone tissue engineering. They can be designed to overcome the limitations

associated with natural polymers. These polymers can be easily processed and tuned physically, chemically, and mechanically for delivery applications even though they are associated with disadvantages, such as acute or chronic immune response, bulk degradation, low clearance rate, and limited biological activities (Gunatillake and Adhikari 2003; Puppi et al. 2010). Poly(methyl methacrylate) (PMMA) polymers have been used as bone filler and cement (Freeman et al. 1982). It is a nondegradable polymer and impedes bone remodeling (Freeman et al. 1982; Maloney et al. 1990). Several polymers, such as poly(ethylene glycol) (PEG), polyurethanes (PU), poly(ϵ -caprolactone) (PCL), poly(anhydrides), poly(α -hydroxy acids), poly(propylene fumarate) (PPF), poloxamers, polyphosphates, and poly(phosphagens), have been explored in bone tissue engineering till date (Kempen et al. 2009a; Hudalla and Murphy 2011; Yu et al. 2015). Polyesters, such as polylactic acid (PLA), poly(glycolic acid), and poly(lactic-*co*-glycolic acid) (PLGA), have been used as growth factor carriers in bone regeneration. PLA nanosheets loaded with BMP-2 are reported to show constant and sustained release of BMP-2 for more than 2 months in vitro and induce bone regeneration in critical-sized mouse calvaria defects (Fig. 13.5) (Huang et al. 2017).

Different polymeric structures have been used to successfully encapsulate and retain the bioactivities of TGF- β 1, BMP, and IGF. PLA, PGA, and PLGA showed limitations associated with acidic degradation products, resulting in tissue damage (Gunatillake and Adhikari 2003). PPF- and PCL-based scaffolds have shown high mechanical properties suitable for bone tissue engineering applications. PPF-based scaffolds have been explored to release BMP-2 (Kempen et al. 2009a). PCL nanofibers have been explored for the sustained release of dexamethasone for bone regeneration applications (Martins et al. 2010). Most synthetic polymers discussed here are hydrophobic, lack cell binding properties, and do not support cell attachment (Pierschbacher and Ruoslahti 1984; Lieb et al. 2003). PEG is a hydrophilic and biocompatible polymer widely used for the controlled and sustained release of growth factors, as it is known to increase the half-life and retain the bioactivity of growth factors. Its poor mechanical strength limits its use. Synthetic polymers can be mixed with natural polymer to improve their bioactivity.

13.3.3 Polymer Composites

Composite materials are formed by combining two or more different materials with different composition in such a way that the combinations result in specific biological, physical, chemical, and mechanical properties. Composites contain a continuous matrix and a dispersed phase. The choice of matrix and dispersed phase is critical to determining the properties of composite. Composites are made by different combinations of natural polymers with synthetic polymers and polymers with ceramics (Poh et al. 2020). As bone is made-up of organic and inorganic components, the composite materials fabricated using a combination of polymers/proteins and ceramics are best suited for bone regeneration applications because their mechanical and biological properties can be modulated. Incorporation of ceramics,

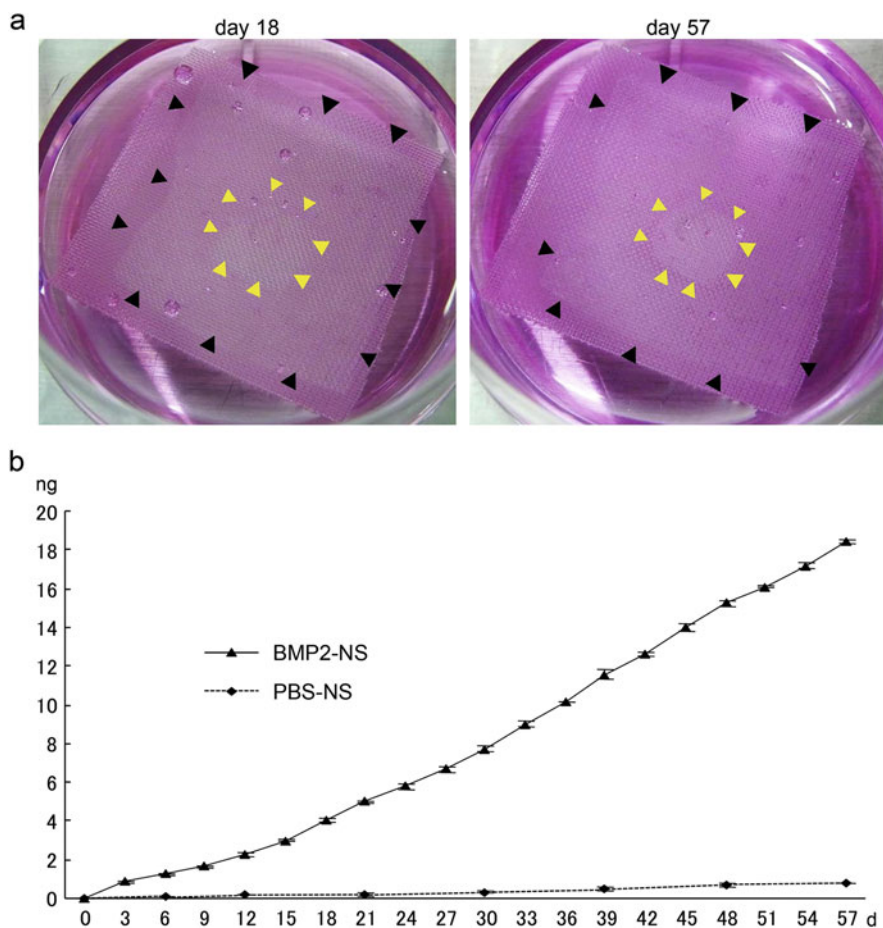


Fig. 13.5 In vitro release of BMP-2 from PLA nanosheets (reproduced with permission from Huang et al. 2017). (a) Sandwich-type PLA nanosheet soaked in DMEM at 37 °C at 18 and 57 days of incubation. Black arrows represent edges of large nanosheet and yellow arrows represent small nanosheet edges. (b) Cumulative release profiles of BMP-2 released from PLA nanosheets loaded with BMP-2 (BMP2-NS) or PBS (PBS-NS)

such as HA, bioglass, and β -TCP, to the polymer matrix, such as PLLA, PLGA, PEG, collagen, silk fibroin, dextran, pullulan, and chitosan, has shown enhanced mechanical strength (Barone et al. 2011; Poh et al. 2020). Ceramic materials impart the polymer composites with load bearing, retarded delivery, and osteoinductive properties. Several composite biomaterials have been investigated for growth factor/drug delivery and showed promising outcomes in bone regeneration. Electrospun fibrous scaffolds of PCL-gelatin incorporated with bioactive glass nanoparticles (mBGn) loaded with dexamethasone showed almost linear release kinetics for up to 28 days and substantial osteogenic effects (El-Fiqi et al. 2015). PCL/nHA/BG

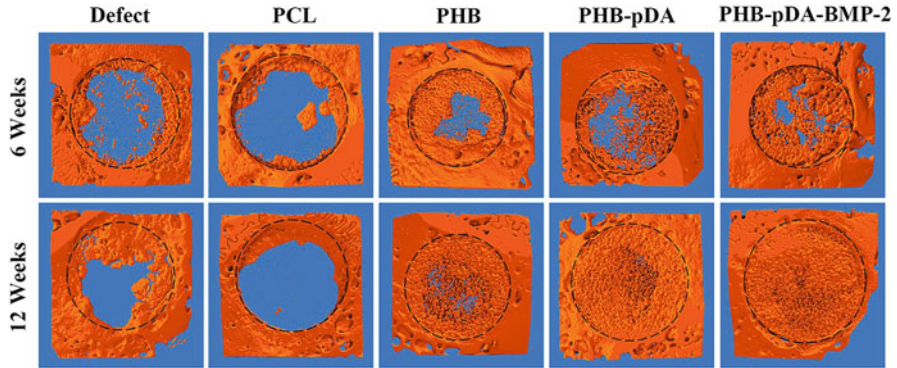


Fig. 13.6 Micro-CT images of calvaria bone defects showing new bone formation in control, PCL-, PHB-, PHB-pDA-, and PHB-pDA-BMP-2-treated groups after 6 and 12 weeks of implantation. (Reproduced with permission from Li et al. 2019)

(PHB) incorporated with polydopamine (pDA) and BMP-2 has shown long-term sustained release of BMP-2 and complete healing of calvaria bone defects in rabbits in 12 weeks (Fig. 13.6) (Li et al. 2019).

13.4 Encapsulation of Growth Factors/Drugs in Polymeric Materials and Nanomaterials

A wide range of delivery systems have been developed for local release of bioactive molecules. The growth factor/drug can be encapsulated in the polymeric matrix either physically or chemically. The encapsulation of growth factor prevents the loss of its bioactivity. Both physical and chemical strategies of loading growth factors/drugs are discussed in this section.

13.4.1 Physical Immobilization

Growth factors/drugs can be physically encapsulated in polymeric carrier systems, such as microspheres, hydrogels, liposomes, and micelles, and the loading is governed by electrostatic interactions, hydrophobic interactions, and hydrogen bonding (Park et al. 2005; Mao et al. 2014; Li et al. 2015; Juhl et al. 2019). These molecules are physically adsorbed on the matrix and their encapsulation to the matrix prevents their denaturation. The polyionic complexes formed by the electrostatic interactions between the polymers and drugs have been explored for the drug delivery applications in bone regeneration (Kim et al. 2011; Ao et al. 2020). In physical loading, the release of growth factor/drug is driven by passive diffusion or material degradation. The quantity and degradation rate of material can be controlled to tune the release rate. The surface area and porosity of scaffolds also influence the

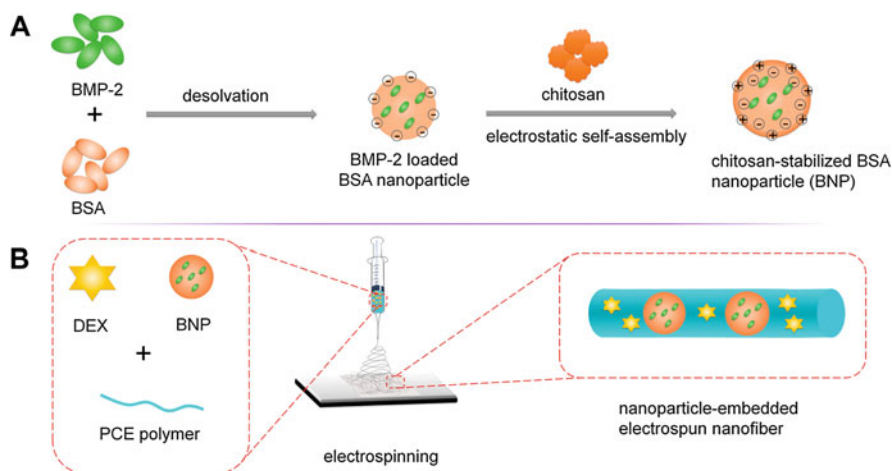


Fig. 13.7 Dual loading of BMP-2 and dexamethasone in BSA nanoparticle-embedded electrospun nanofibers. (Reproduced with permission from Li et al. 2015.) (a) Physical loading of BMP-2 in BSA nanoparticles stabilized with chitosan. (b) Electrospinning of dexamethasone and BNP-embedded PCE copolymer nanofibers

loading of growth factors/drugs. Collagen sponges have been extensively explored to deliver BMP-2 in bone fusion and fracture repair applications (Kanematsu et al. 2004). The materials showing high-affinity noncovalent interactions with the growth factor/drug have been shown to attain high encapsulation efficiency. Heparin-based scaffolds have been found to interact with BMP-2 through its N-terminal heparin-binding region, resulting in high adsorption (Kim et al. 2011; Gandhi and Mancera 2012; Ao et al. 2020). Physical encapsulation of drugs along with the growth factors has been used to enhance the osteogenic outcomes. Li et al. developed a nanoparticle-embedded electrospun nanofiber scaffold for physical encapsulation and dual release of BMP-2 and dexamethasone (Li et al. 2015). The encapsulation of BMP-2 in BSA nanoparticles was carried out to prevent BMP-2 from losing its bioactivity, and these BMP-2-loaded BSA nanoparticles were then blended with dexamethasone and poly(ϵ -caprolactone)-*co*-poly(ethylene glycol) (PCE) copolymer for coelectrospinning (Fig. 13.7). It preserved the bioactivity of BMP-2 along with a patterned release of dexamethasone within first 8 days and BMP-2 release lasting up to 35 days, resulting in significant repair of rat calvaria defects than that of the nanofiber scaffold without BMP-2 and dexamethasone. A nucleotide aptamer-functionalized fibrin hydrogel had been reported to improve the retention and release kinetics of the growth factor (Juhl et al. 2019). The fibrinogen (F) was functionalized with anti-VEGF aptamer using the thiol-acrylate chemistry, followed by VEGF addition and hydrogel fabrication. It provided the improved VEGF release, enhanced angiogenesis, and osteogenesis *in vivo* (Fig. 13.8).

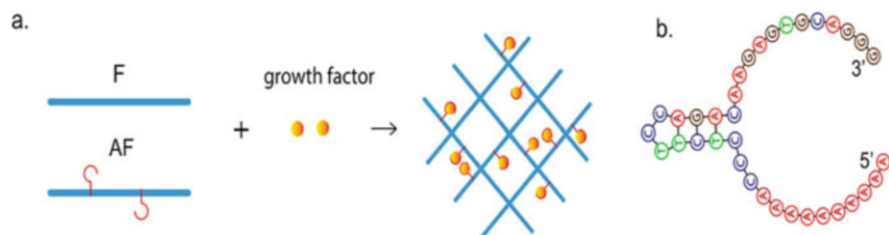


Fig. 13.8 Aptamer-functionalized fibrinogen hydrogel loaded with a growth factor. (Reproduced with permission from Juhl et al. 2019.) (a) Growth factor (VEGF) loading in hydrogels fabricated using native fibrinogen (F) and aptamer-functionalized fibrinogen (AF). (b) Secondary structure of anti-VEGF aptamer

13.4.2 Chemical Conjugation/Tethering

Covalent attachment of growth factors/drugs provide a better control over loading and release profiles and helps in designing stimuli-responsive delivery systems. Growth factors and polymers are chemically modified to obtain functional groups, such as amines, thiols, acrylates, hydrazides, aldehydes, and azides, to conjugate the growth factors/drugs to the polymeric materials (Bentz et al. 1998; DeLong et al. 2005; He et al. 2008; Chen et al. 2012; Koehler et al. 2013; Vogus et al. 2017). Initially, succinimidyl groups containing homobifunctional PEG linkers were employed to conjugate growth factors to the collagen-based biomaterials. The modified TGF- β and other growth factors resulted in improved outcomes compared to the unmodified growth factors (Bentz et al. 1998). NHS coupling is used to conjugate the growth factors with PEG and other polymers. In some studies, acrylated growth factors conjugated with PEG diacrylate through photopolymerization were also reported (DeLong et al. 2005). Click chemistry has emerged as a promising technique to conjugate bioactive molecules due to its high specificity and low toxicity (He et al. 2008). Click chemistry provides simultaneous tethering of growth factors/drugs and hydrogel fabrication. These strategies employing the use of amine group present in the lysine or at the N-terminal of growth factors were promising but may interfere with their bioactivity (Veronese 2001).

Thiol coupling strategies were used to conjugate bioactive molecules using the cysteines present in their backbone or by functionalization using additional cysteines. The C-terminus of VEGF was functionalized with cysteine and linked to vinyl sulfone groups on PEG linkers, using Michael-type addition (Zisch et al. 2003). Diels-Alder approach had been used for conjugating bioactive molecules with promising results (Koehler et al. 2013). In a study, tetrafunctional maleimide PEGs were cross-linked with tetrafunctional thiols through Michael addition and the furan-functionalized dexamethasone was conjugated in the polymeric matrix through Diels-Alder reaction between furan-functionalized dexamethasone and PEG maleimide (Fig. 13.9). It provided the long-term controlled release of drug, leading to an improved osteogenic differentiation and mineralization. Another study

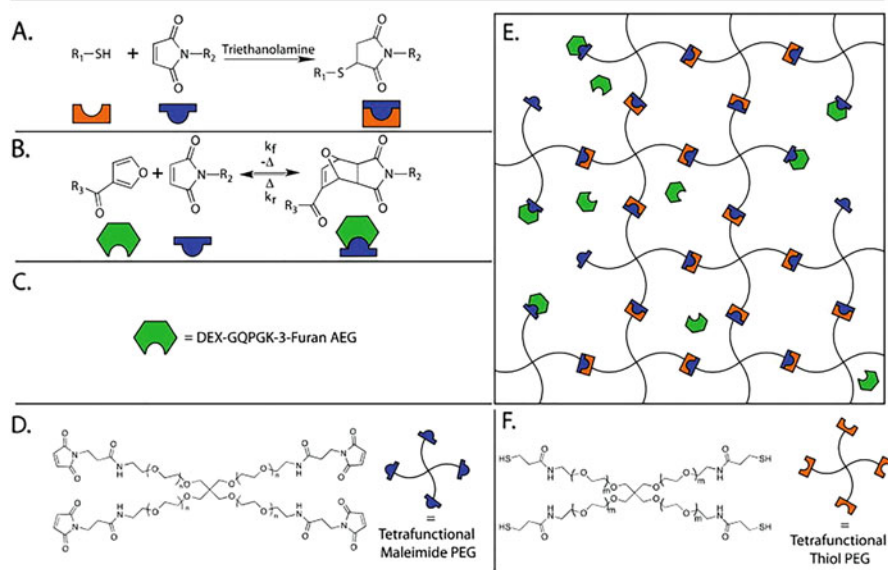


Fig. 13.9 Hydrogels with Diels-Alder modulated release of dexamethasone. (Reproduced with permission from Koehler et al. 2013.) (a) Michael addition reaction between thiol and maleimide groups of PEGs. (b) Diels-Alder reaction between furan on dexamethasone and maleimide groups on PEG. (c) Dexamethasone-labeled peptide with furan functionality. (d, f) Tetrafunctional maleimide and thiol PEG linkers. (e) Hydrogel network having Diels-Alder conjugated dexamethasone

reported that the bioactivity of the growth factors is influenced by the cross-linking chemistry. The activity of BMP-2 was higher in hydrazone cross-linked hyaluronic acid hydrogels than those with thiol-maleimide cross-links. Thiol-functionalized hyaluronic acid hydrogels incubated with BMP-2 showed diminished phosphorylation of Smad 1/5/8 (signal transducer of osteogenic differentiation), whereas no effect was seen in case of aldehyde-functionalized hyaluronic acid. Higher bone formation was observed in case of hyaluronic acid hydrogels with hydrazone cross-links ($18 \pm 4.25 \text{ mm}^3$) than with thiol-maleimide cross-links ($1.25 \pm 0.52 \text{ mm}^3$), after 8 weeks of implantation (Fig. 13.10).

13.5 Engineered Polymeric Materials/Nanomaterials for Growth Factor/Drug Delivery

Polymeric materials/nanomaterials have been investigated for growth factor/drug delivery. The conventional delivery methods, such as intravenous infusion, were employed for the delivery of bioactive molecules but they were associated with shortcomings, such as poor local retention and stability, high dosage requirements, low efficiency, and loss in their bioactivities. Engineered polymers are being used to

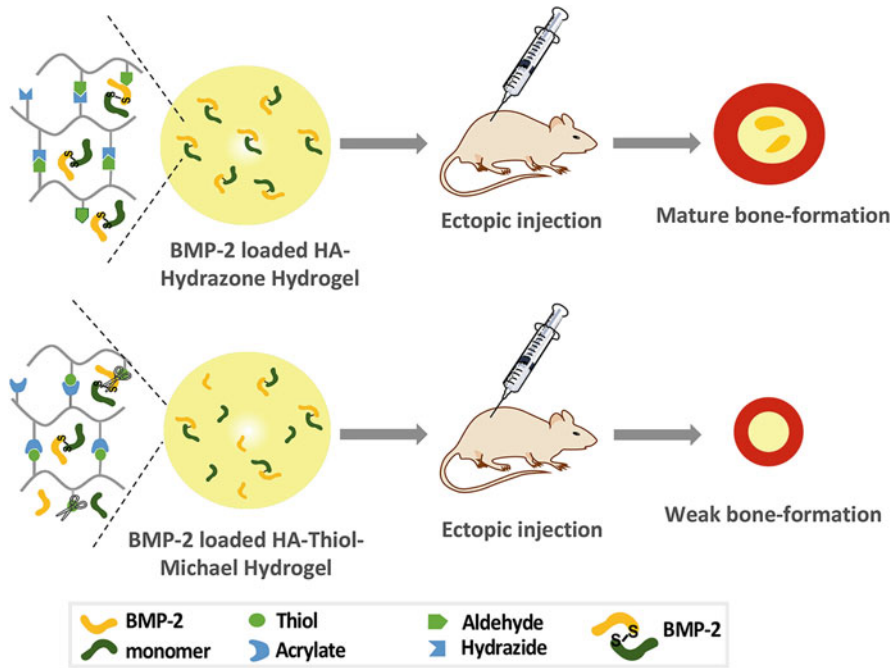


Fig. 13.10 BMP-2-loaded hyaluronic acid-hydrazone (HA-hydrazone) and HA-thiol-Michael hydrogel showing the difference in bone formation after ectopic implantation of hydrogels. (Reproduced with permission from Paidikondala et al. 2019)

tune the loading and release of bioactive molecules and it has resulted in the advancement in polymeric structures and development of smart delivery systems. Various engineered polymeric structures and stimuli-sensitive smart delivery systems will be discussed in this section.

13.5.1 Structure-Based Delivery Systems

Efforts have been made to develop different polymeric structures, such as nanofibers, nanoparticles, microparticles, films, hydrogels, and 3D-printed scaffolds, based on the requirements in order to overcome the limitations associated with the conventional delivery systems (Fig. 13.11).

13.5.1.1 Polymer-Growth Factor/Drug Conjugates and Nano/Microparticles

Polymeric macromolecules are conjugated with drugs and other bioactive molecules for the development of systematic or local delivery vehicles for bone tissue engineering applications. Conjugation of bioactive therapeutics to polymers improves the drug's solubility in water, increases their half-life, stability, and retention time in

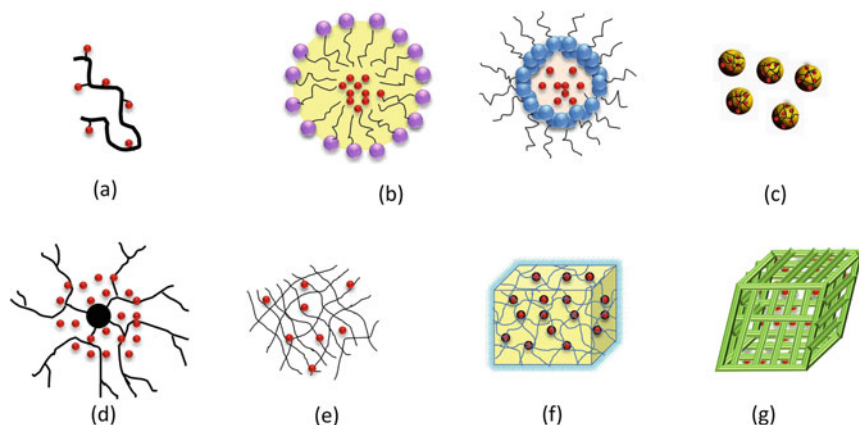


Fig. 13.11 Engineered polymeric structures for growth factor/drug delivery. (a) Polymer-drug/growth factor conjugates, (b) micelles and reverse micelles, (c) nanoparticles, (d) dendrimers, (e) nanofibers, (f) hydrogels, (g) 3D printed scaffolds

systemic circulation, and allows control over the release (Vogus et al. 2017). The delivery to the disease/injury site involves either noncovalent encapsulation of drugs or covalent conjugation to the polymer (Kaminskas et al. 2012). The noncovalent encapsulation of drugs is carried out in polymer assemblies, such as micelles or nano/microparticles, allow the utilization of unmodified drug/growth factor. The covalent conjugation of growth factors/drugs to polymers requires modification using specific linkers and it allows a preferential release in the presence of biological cues. PDCs have shown promising outcomes. Polyglutamates, bisphosphonates, and polyaspartates have been used as synthetic ligands to target bone tissues (Culpepper et al. 2013; Jiang et al. 2014; Cole et al. 2016). The conjugation of alendronate (a bisphosphonate drug used to treat osteoporosis) to poly(*N*-(2-hydroxypropyl) methacrylamide (HPMA) or poly(ethylene glycol) (PEG) or their combination with other polymers resulted in high accumulation in bone tissues (Wang et al. 2003; Chen et al. 2012; Karacivi et al. 2017). Dendrimers are branched polymers that have been conjugated to drugs and other bioactive molecules for delivery applications. One important aspect of growth factor or protein delivery is to protect its structure and bioactivity.

Polymeric micro- and nanoparticles, including micelles and liposomes (Park et al. 2007), have been successful in the growth factor/drug delivery, as they can encapsulate them within their core shell while protecting it from degradation. Amphiphilic block copolymers have been used to encapsulate drugs because they form micelles due to self-aggregation in aqueous medium. Micelles and reverse micelles are employed in drug delivery applications due to their biocompatible nature and capability to protect encapsulated agent (Aliabadi and Lavasanifar 2006). Polymeric micelles have been employed for simvastatin, dexamethasone, and methotrexate delivery to the bone and have shown great potential in this field (Liu et al. 2013; Wang et al. 2016; Xu et al. 2018b). Wang et al. reported that a micelle system

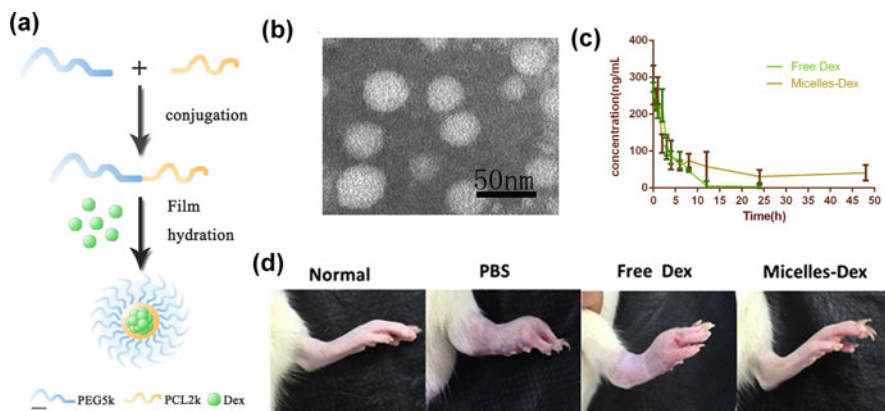


Fig. 13.12 Fabrication and characterization of dexamethasone-loaded micelles. (a) Schematic representation of drug-loaded micelle formation. (Reproduced with permission from Wang et al. 2016.) (b) TEM images of drug-loaded micelles. (c) Pharmacokinetics of free drug and drug-loaded micelles. (d) Photographs of hind legs from different treatment groups for swelling observations

fabricated from amphipathic poly(ethylene glycol)-block-poly(ϵ -caprolactone) (PCL-PEG) polymer by film dispersion for dexamethasone loading and release showed relatively long, persistence present in the circulation and preferential accumulation in inflamed joints (Wang et al. 2016). The expression of TNF- α and IL-1 β was significantly reduced in the groups treated with the drug-loaded micelles compared to the free drug, and the swelling in hind limbs of groups treated with the drug-loaded micelles was significantly reduced (Fig. 13.12). Micelles have been decorated with bisphosphonates for the targeted delivery of antibiotics to the bone (Cong et al. 2015; Kamble et al. 2020). Liposomes have been investigated for the growth factor/drug delivery to the bone (Metselaar et al. 2003; Park et al. 2007; Mao et al. 2014; Kroon et al. 2015; Crasto et al. 2016). The introduction of polymers, such as PEG, to liposomal formulations has provided the strategy to design biologically inert and safe platform for drug delivery by incorporating characteristics like reduced interactions with serum proteins, longer blood circulation time, and low immunogenicity. Mao et al. have developed a liposomal formulation showing enhanced targeted delivery of FTY720, with entrapment efficiency of $\sim 85\%$ (Mao et al. 2014, p. 720).

13.5.1.2 Polymeric Nanofibers

Polymeric nanofiber-based scaffolds have been found to be interesting candidates for bone repair as they possess ECM-mimicking structure, morphology, and superior ability to promote osteogenesis (Carbone et al. 2014; Chen et al. 2017). The 3D network of nanofibers resemble the extracellular matrix and provides a high surface area for drug loading. Electrospinning technique is a simple and most widely used technique for the preparation of nano- to microsized fibers. The therapeutic agents

can be incorporated into the interior or the surface of single nanofiber to obtain sustained drug delivery. Polymeric materials like silk fibroin (Li et al. 2006), PCL (Martins et al. 2010), chitosan-based (Tao et al. 2020), collagen/PCL, poly(DL-lactide-*co*-glycolide) (PLGA) (Lee et al. 2013), PLA (Ding et al. 2013; Cho et al. 2014; Madhurakkat Perikamana et al. 2015), hyaluronan/PLA (Wu et al. 2020), polycaprolactone (PCL)/gelatin (Wang et al. 2019), PCL/PVA (Mickova et al. 2012), SF/PCL/PVA (Cheng et al. 2019), and poly(L-lactide-*co*-caprolactone)/collagen/gelatin (Su et al. 2012) have been explored for the delivery of dexamethasone, BMP-2, BMP-7, VEGF, FGF, alendronate, and other therapeutics in bone regeneration. PLGA/PCL nanofibers were used to deliver FTY720, a targeted agonist of sphingosine-1-phosphate receptors 1 and 3, and reported to enhance vascularization and osseous tissue growth in critical-sized bone defects (Das et al. 2013). PEG/PCL-based nanofibers with core-shell structures have proved to be promising for the redox-sensitive delivery of BMP-2 to the bone (Gong et al. 2018). In a study, polydopamine (pDA)-mediated BMP-2 immobilization was carried out on PLA nanofibers for the guided bone regeneration (GTR) (Cho et al. 2014). The BMP-2 retained their activity on the nanofibers for up to 28 days and showed significant enhancement in ALP activities and calcium mineralization after 14 days of culture. These nanofibers showed good osteogenic outcomes at low dose of BMP-2. Another study reported that the incorporation of alendronate- and BMP-2-mimicking peptide-conjugated heptaglutamate moiety into mineralized nanofiber fragments of PLGA/collagen/gelatin nanofibers via calcium chelation resulted in significant enhancement in new bone formation compared to the unfilled defect control (Boda et al. 2020). The difference was not significant (alendronate) for single and coloaded (alendronate and BMP-2-mimicking peptide) bone grafts.

Coaxial electrospinning technique and layer-by-layer (LBL) assembly techniques have been used to incorporate growth factors/drugs into polymeric nanofibers having core-shell structure. Core-shell structure of nanofibers provides protection to growth factors and allows their sustained release. A core-shell SF/PCL/PVA nanofibrous mat was prepared by coaxial electrospinning, and LBL techniques were used to incorporate BMP-2 in the core along with the connective tissue growth factor (CTGF) on the surface of nanofibers (Cheng et al. 2019). These nanofibers provided coordinated temporal release of BMP-2 and CTGF, and showed increased vessel formation and improved bone tissue recovery. The transient release of CTGF resulted in proangiogenic effects on the bone healing, and sustained release of BMP-2 from these nanofibers showed 43% improvement in bone regeneration than the only BMP-2 release systems. Although these electrospun nanofibers mimic of ECM resulted in improved osteogenic outcomes, the smooth surface of these nanofibers did not mimic the nanotopography of collagen surface found in ECM, which is important to determine cell responses. Huang et al. investigated the natural collagen fibers mimicking drug-loaded core-shell nanofibers with hierarchical nanostructures in bone regeneration (Huang et al. 2020). The BMP-2-loaded PCL/PVA nanofibers were fabricated by coaxial electrospinning and their surface was decorated with nanoshish-kebab (SK) structures (Fig. 13.13), which were made up of nanofiber (shish) and disc-shaped lamellae (kebabs). These structures resulted

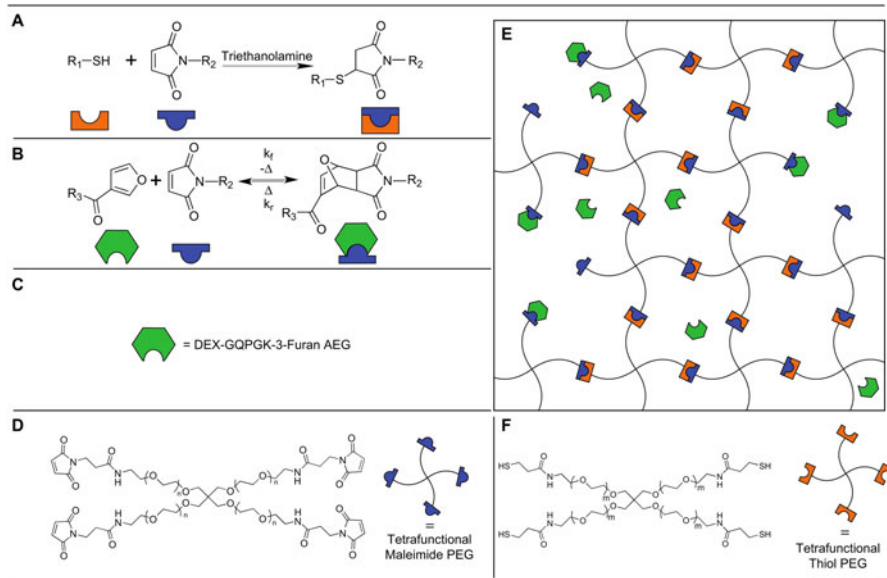


Fig. 13.13 Nanoshish-kebab (SK)-decorated BMP-2-loaded core-shell nanofibers and their role in bone regeneration. NB represents new bone. (Reproduced with permission from Huang et al. 2020)

in increased proliferation, attachment, and osteogenic activities of cells. The BMP-2 release from the nanofibers (SK-PCL/PVA-BMP-2) exhibited release kinetics similar to zero order. The SK-PCL/PVA group resulted in more bone formation ($24.57 \pm 3.81\%$) compared to the control group ($1.21 \pm 0.23\%$). The best results were obtained in case of SK-PCL/PVA-BMP-2 group ($76.38 \pm 4.13\%$), which showed more bone formation compared to PCL/PVA-BMP-2 group ($39.86 \pm 5.74\%$), suggesting that the hierarchical nanostructured surfaces on BMP-2-loaded core-shell nanofibers promoted osteointegration. In another study, collagen nanofibers were assembled in the pores of electrospun membranes of VEGF-loaded hyaluronan-PLA to obtain hierarchical micro/nanofibrous membranes providing the sustained release of VEGF for periosteal regeneration (Wu et al. 2020).

13.5.1.3 Gels/Hydrogels

Hydrogels are interesting candidates as carriers for growth factor/drug delivery in bone regeneration as they possess ECM-mimicking structure with 3D-interconnected porous networks and provide suitable environment for cell growth and sustained release of biomolecules/drugs (Bai et al. 2018). Both natural and synthetic polymers have been investigated as hydrogels or polymeric scaffolds for bone regeneration applications. Growth factors/drugs can be incorporated into hydrogels either by noncovalent interactions or covalent bonds to control the release kinetics. The hydrogel-based scaffolds can be tailored to improve and control various properties, like porosity, stiffness, drug encapsulation efficiency,

injectability, biodegradation, and stimuli-responsive nature (Bentz et al. 1998; Ham et al. 2016; Bai et al. 2018; Kim et al. 2020).

Glycosaminoglycans (GAGs) were modified with the pendent aldehyde groups to tune the degradation of hydrogels and release of growth factors from the matrix (Wang et al. 2013). The physical properties and release of BMP-2 from pegylated fibrinogen (PF) hydrogels containing encapsulated BMP-2 protein were controlled by varying the size and amount of PEG-diacrylate linker (Ben-David et al. 2013). Comparable PEG/albumin hydrogels were also investigated for BMP-2 release in bone defects (Kossovser et al. 2020) and PVA/heparin-based hydrogels were prepared with hydrazone linkages for the pH-controlled release of VEGF (Roberts et al. 2015). Keratin hydrogels were tuned for erosion and controlled delivery of insulin-like growth factor- α . Mixtures of keratases and keratin were cross-linked using disulfide chemistry to control the erosion of hydrogels and control the growth factor release (Ham et al. 2016). Injectable hydrogels have been explored as minimum-invasive drug delivery carriers in bone regeneration. Injectable CaSO_4 /FGF-18 incorporated within chitin-PLGA hydrogels have been reported for the sustained release of FGF-18 and almost-complete bone healing of cranial bone defect (Sivashanmugam et al. 2017). Hydroxypropyl guar-graft-poly(*N*-vinylcaprolactam) copolymer was synthesized by graft polymerization to impart thermoresponsive properties in the hydrogels to control the drug delivery (Parameswaran-Thankam et al. 2018). Interpenetrating thiolated PEG-diacrylate hydrogel networks (IPN) incorporated with either polycation-based coacervates or gelatin microparticles were explored for maintaining the bioactivity and sustained release of BMP-2 to achieve enhanced skull bone regeneration (Kim et al. 2018c).

Impact of cross-linking chemistry was observed on bone formation and BMP-2 release, and hydrazone cross-linked hydrogels showed higher bone formation than thiol-Michael cross-linked hydrogels (Paidikondala et al. 2019). Ao et al. reported a fibrin glue/fibronectin/heparin-based hydrogel as a promising delivery system for BMP-2 to induce bone formation in calvaria critical-sized defects. The release of BMP-2 from these hydrogels was largely dependent on degradation (Ao et al. 2020). Several complex hydrogel-based scaffolds fabricated by incorporating nanoparticles or nanofibers have been investigated for the growth factor/drug delivery in bone regeneration. Lee et al. fabricated a patterned scaffold system containing PCL/gelatin fibers and PEG hydrogel micropatterns using a combination of electrospinning and photolithography techniques for the controlled and sequential release of multiple growth factors (Lee and Koh 2014). Firstly, glutaraldehyde-cross-linked PCL/gelatin nanofibers were fabricated to form electrospun scaffold, followed by drop casting of PEG-diacrylate and 2-hydroxy-2-methylpropiophenone (HOMPP) precursors, and placing a photomask array of microwells over them (Fig. 13.14). The scaffolds were exposed to UV light and unreacted precursors were removed by washing with water to obtain hydrogel-incorporated patterned nanofibrous scaffolds. FGF was adsorbed on fibers, while BMP-2 was entrapped in the hydrogel matrix for the sequential delivery of low doses of FGF initially and long-time sustained release of BMP-2 to promote osteogenic differentiation of hMSCs. Injectable hydrogel scaffolds fabricated by encapsulating chitosan

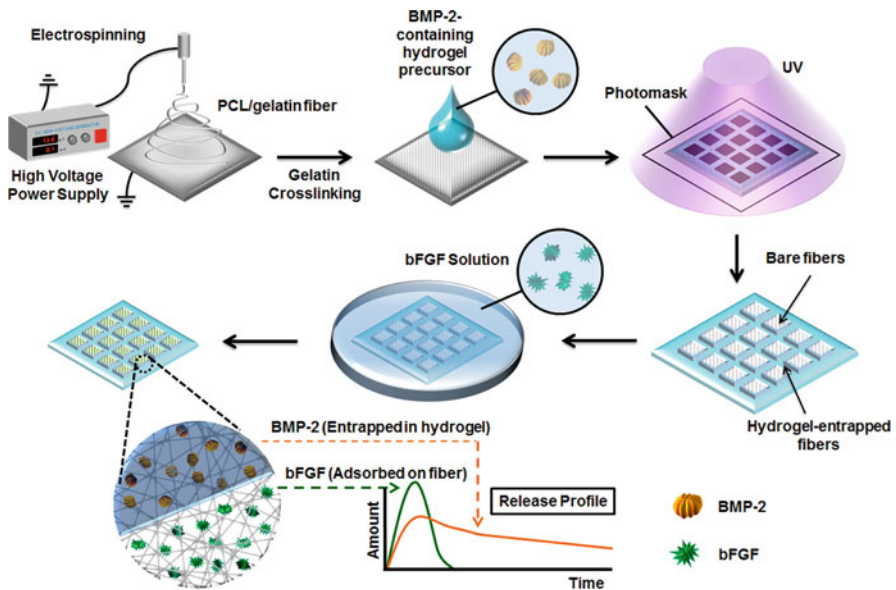


Fig. 13.14 Micropatterned hydrogel-nanofiber scaffolds for growth factor delivery in bone regeneration. (Reproduced with permission from Lee and Koh 2014)

microparticles as carriers of BMP-9 in VEGF-loaded thermosensitive hydrogels have also been explored for bone regeneration (Gaihre et al. 2019). The complex hydrogel system containing methylcellulose and alginate cross-linked with calcium and loaded with chitosan microparticles showed increased efficiency of loaded growth factors at the target site and resulted in enhanced osteogenic activities of hMSCs.

Subbiah et al. developed an injectable microparticle-incorporated hydrogel system for VEGF and BMP-2 delivery in a composite injury model (Subbiah et al. 2020). BMP-2-loaded heparin methacrylamide microparticles (HMP) were incorporated in VEGF-encapsulated Ca-alginate gels. This system containing VEGF encapsulated in alginate resulted in an early release by day 7, while maintaining the controlled release of BMP-2 from the HMPs. Although the system was capable to provide the tunable release of growth factors, the results showed that VEGF alone was not significant to enhance the bone-healing effects of low-dose BMP-2 irrespective of simultaneous or tunable release kinetics in a critical composite injury. Hydrogels hold a great promise so far as the encapsulation and sustained delivery of growth factors/proteins are concerned but their brittle structure and low cell infiltration capabilities have created a need to investigate other systems such as cryogels to overcome these challenges, as they possess highly interconnected macroporous structures (Kim et al. 2018b; Lee et al. 2020). Polymeric cryogels are formed at a subzero temperature by lyophilizing the ice crystals during cryogelation process. Lee et al. developed a double cryogel (DC) system for the dual delivery of growth factors with different release kinetics. The DC system was fabricated by

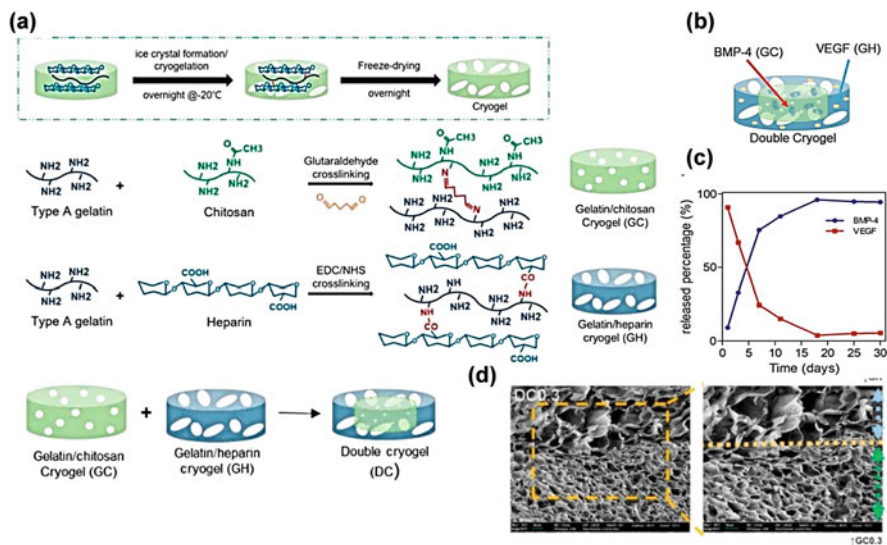


Fig. 13.15 Dual crygel (DC) system for the sequential release of growth factors. (Reproduced with permission from Lee et al. 2020.) (a) Fabrication of gelatin/chitosan (GC) crygel, gelatin/heparin (GH) crygel, and double crygel (DC). (b) Double crygel (DC) incorporated with BMP-2 and VEGF. (c) Percent release from DC (fabricated using 0.3% w/v chitosan) for 30 days. (d) FESEM images of DC

surrounding BMP-2-loaded gelatin/chitosan (GC) cryogels with VEGF-loaded gelatin/heparin (GH) crygel (Lee et al. 2020). The DC cryogels exhibited a highly porous network and the outer layer of DC resulted in the initial release of VEGF to stimulate angiogenesis and vascularization in the defect, whereas the inner GC layer led to sustained release of BMP-2 to induce osteogenesis (Fig. 13.15). The sequential and sustained release of growth factors from the DC gels showed good outcomes in bone regeneration in critical-sized cranial defect models.

13.5.1.4 3D-Printed Scaffolds

Three-dimensional (3D) printing is currently the most explored technique for the development of advanced scaffolds with appropriate functions to treat bone fractures or defects (Wang et al. 2020). The printed scaffolds provide several advantages over conventional scaffolds, such as customization of shape, pore size, and tunability of mechanically properties (Kim et al. 2010; Schüller-Ravoo et al. 2011; Bose et al. 2013). The scaffolds closely mimic the multiscale structure of tissues and provide the local and sustained release of growth factors/drugs. Various additive manufacturing approaches (AM) including 3D printing, rapid prototyping, solid freeform fabrication, direct digital manufacturing, selective laser sintering, stereolithography, and 3D plotting are used to fabricate such scaffolds (Bose et al. 2003, 2018; Chia and Wu 2015; Guvendiren et al. 2016). The advancement in 3D printing techniques has provided versatile scaffolds with new functions. These

techniques provide precise control over complex pore geometries, size, and interconnectivity of pores, thereby providing control over overall mechanical strength of scaffold and cell infiltration (Bose et al. 2013; Wang et al. 2020). They also provide flexibility to prepare patient-specific predesigned scaffolds that can match the bone defect size and geometry (Bonda et al. 2015; Geven et al. 2015). The surface of scaffolds can be modified and growth factors/drugs can be incorporated by physical or chemical cross-linking.

Several 3D-printed polymeric scaffolds have been investigated. PCL-based 3D architectures were prepared through 3D plotting and wet spinning, and loaded with BMP-2/9 to investigate the effect of scaffold architecture on growth factor delivery and bone regeneration. The result indicated that the architecture did not affect the release kinetics (BSA) but the proliferation and osteogenic differentiation of MSCs (Yilgor et al. 2010). The 3D-printed alginate scaffolds cross-linked using CaCl_2 and incorporating BMP-2-loaded gelatin microspheres were investigated and these tissue-engineered bioprinted constructs were found effective in promoting osteogenic differentiation *in vitro* and *in vivo* through controlled release of BMP-2 (Poldervaart et al. 2013). The internal vascularization of scaffolds with high osteoinductive properties closely mimicked the bone developmental stage. Using this approach, Yan et al. investigated a 3D-printed biodegradable scaffold fabricated using layer-by-layer assembly technique for the control release of deferoxamine (DFO) (Yan et al. 2019), which is an iron chelator and used as a hypoxia mimic to induce vascularization of scaffolds and activate HIF1- α , resulting in the activation of proangiogenic gene cascades. It may also induce osteogenic differentiation of preosteoblast cells. The 3D-printed PCL scaffolds were modified with amine groups followed by carboxymethyl chitosan (CCS) and loaded with DFO, as shown in Fig. 13.16. These scaffolds showed high biocompatibility and mechanical properties matching the cancellous bone, promoted vascularization, and enhanced bone formation at the defect site. Several other 3D-printed PEG, PCL, and PLA scaffolds have been developed for the controlled/sustained release of growth factors and drugs and showed promising outcomes in bone regeneration (Li et al. 2018; Kim et al. 2018a; Kondiah et al. 2020; Yao et al. 2020).

The 3D-printed scaffolds have been employed for the dual delivery of growth factors and/or drugs. Teotia et al. fabricated alendronate (ZA) and BMP-loaded 3D scaffolds using layer-by-layer solidification of photo-cross-linkable poly(trimethylene carbonate) resin containing high ratio of ceramics. Next, the scaffolds were filled with microporous cryogels to enhance the overall surface area that resulted in the enhancement in overall surface area for cell infiltration. Their studies indicated the potential application of BMP and ZA-loaded 3D-printed scaffolds in critical-sized long bone and cranial defect healing (Teotia et al. 2020). Wang et al. have investigated the dual delivery of angiogenic and osteogenic peptides using cryogenic 3D printing of scaffolds (Wang et al. 2021). The scaffolds were fabricated by cryogenic 3D printing of osteogenic peptide containing water/PLGA/emulsion and β -tricalcium phosphate, followed by surface coating of angiogenic peptides. They showed hierarchical porous structure that was mechanically comparable to cancellous bone. Improved angiogenesis and osteogenic effects were obtained due to the quick release of angiogenic peptide and sustained release of osteogenic peptide.

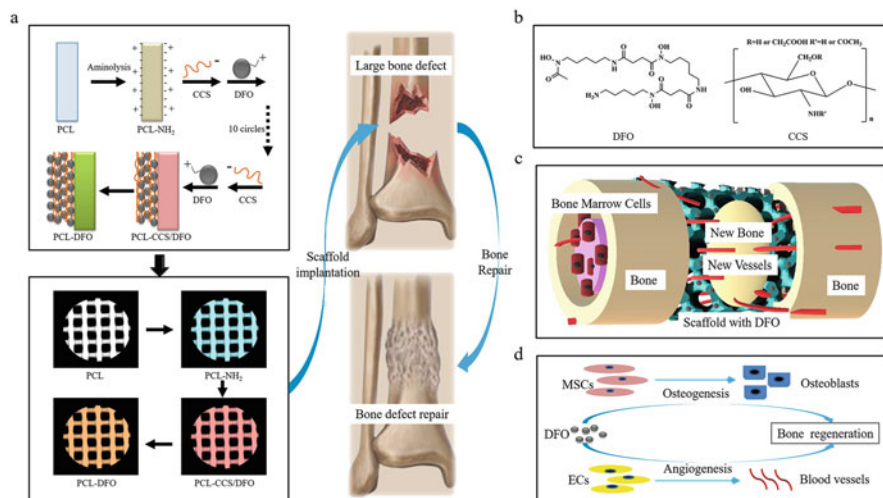


Fig. 13.16 Deferoxamine (DFO) loading on the surface of 3D-printed PCL scaffold and its effect on bone regeneration (reproduced with permission from Yan et al. 2019). (a) Fabrication of DFO-loaded PCL scaffolds by surface aminolysis and layer-by-layer assembly of carboxymethyl chitosan (CCS). (b) Chemical structure of DFO and CCS. (c) The angiogenic and osteogenic effects of PCL-DFO scaffold. (d) The mechanism of bone regeneration promoted by DFO in mesenchymal cells (MSCs) and vascular endothelial cells (ECs)

13.5.2 Stimuli-Responsive Delivery Systems

Polymer science and engineering has enabled scientists to overcome challenges associated with the polymeric biomaterials in biomedical applications. Advancement in this field has led to the design and development of a new class of polymers that changes their physical and/or chemical properties when exposed to an external stimuli (Hoffman 1995; Wei et al. 2017). These smart/intelligent/stimuli-responsive polymers have been explored for on-demand growth factor/drug in bone regeneration. Such polymers respond to change in pH (Kocak et al. 2017), temperature (Doberenz et al. 2020), magnetic field (Manouras and Vamvakaki 2017), and the presence of specific biomolecules (Xu et al. 2018a). The stimuli-responsive elements included in the delivery systems often mimic natural conditions (Korde and Kandasubramanian 2019). Various polymeric materials in combination with other materials have been engineered to provide smart drug delivery systems as per the requirements. Usually a sensitive/stimuli-responsive moiety is incorporated in polymeric backbones. Different types of smart polymeric systems under investigation for growth factor/drug delivery in bone tissue engineering will be discussed in this section.

13.5.2.1 pH Responsive

The polymers containing acidic or basic moieties are capable of accepting or releasing protons in response to the change in pH and, therefore, considered as

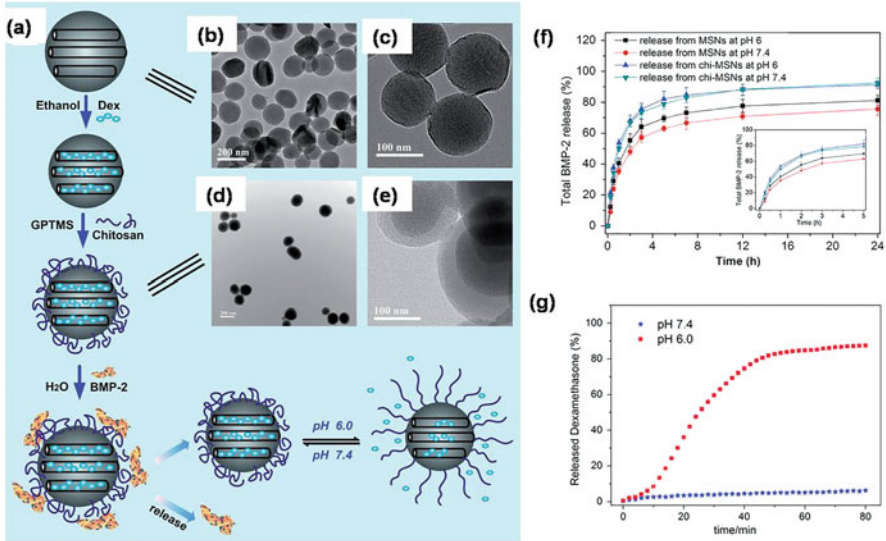


Fig. 13.17 (a) Dexamethasone/BMP-2@chi-MSNs synthesis for the controlled release of BMP-2 and pH-sensitive drug release. (b, c) TEM and HRTEM images of MSNs. (d, e) TEM and HRTEM images of chi-MSNs. (f) In vitro release profiles of BMP-2. (g) In vitro release profiles of drug. (Reproduced with permission from Gan et al. 2015a)

pH-responsive polymers (Kocak et al. 2017). Such materials are used in drug delivery applications. The accumulation of lactic acid at the fracture site due to interrupted blood supply may result in low pH (Zhang et al. 2017) and prolonged inflammatory responses due to the bone diseases, such as rheumatoid arthritis and infection, may also alter the pH of bone tissue. The resorption by osteoclasts also creates an acidic microenvironment (Arnett and Dempster 1986). Consequently, pH-responsive growth factor/drug delivery can be employed in such conditions. Various polymers, gels/hydrogels, microparticles, and polymeric coatings with pH-responsive functional groups and/or linkages have been investigated. Chitosan is among the most extensively investigated polymer because chitosan-based materials show pH-responsive properties due to the presence of free amine groups in the polymer structure. The noncovalent interactions with the functional groups of chitosan facilitate the loading of growth factors and drugs.

Mesocellular foam-based nanocarriers were fabricated by cross-linking glycidoxypropyltrimethoxysilane (GPTMS) with *N*-carboxymethyl chitosan for the pH-sensitive release of BMP-2, while maintaining its bioactivity (Gan et al. 2015b). Chitosan (Chi)-coated mesoporous silica nanoparticles (MSNs) were developed for the dual delivery of BMP-2 and dexamethasone and it resulted in significantly increased osteoblastic differentiation in vitro and in vivo (Gan et al. 2015a). The drug was loaded into the hydrophobic nanochannels of MSNs, which were coated with chitosan and cross-linked using GPTMS, followed by the physical coating of BMP-2 on chitosan surface (Fig. 13.17). BMP-2 was released immediately from the

surface of chitosan-MSNs (Chi-MSNs), whereas the drug was released after the endocytosis in cells. The low pH value resulted in change in the dispersing states of chitosan due to the protonation of amino groups; thus, resulting in the drug release into the cytosol. Luca et al. investigated the chitosan and hyaluronic acid-based hydrogels for BMP-2 delivery and observed that the nature of carrier and formulation pH influences the formation of bone volume and quality (Luca et al. 2010). Polyelectrolyte multilayer (PEM) systems have been explored as pH-responsive systems. PEM systems fabricated using layer-by-layer deposited poly(β -aminoester) (PBAE) and chondroitin sulfate (CS) for BMP-2 release resulted in enhanced preosteoblast differentiation than free BMP (Macdonald et al. 2011). In another study, combined VEGF and BMP-2 release resulted in 33% higher bone density in the de novo bone compared to BMP-2 alone (Shah et al. 2011). Poly-L-lysine (PLL)/hyaluronic acid (HA) PEMs also released BMP-2 (Crouzier et al. 2011) while preserving its secondary structure in films (Gilde et al. 2012), and hydrated and dry coatings on Ti surfaces (Guillot et al. 2013). The BMP-2 adsorbed on anodized Ti surface followed by poly-L-histidine and poly(methacrylic acid) coatings on it showed high levels of protein release over several months while preserving its bioactivity (Salvi et al. 2016). The protection of growth factors and maintaining the concentrations in therapeutic window are critical to obtaining the desired outcomes. Polymeric nanocapsules protecting internally loaded growth factors for pH-sensitive release have been reported (Yan et al. 2010; Tian et al. 2016).

Deng et al. reported 3D-printed polyetheretherketone (PEEK) scaffolds for pH-responsive delivery of Ag^+ for in vivo antibacterial activity and Ca^{2+} release for bone in growth and osseointegration in infective bone defects (Deng et al. 2020). The Ag/apatite-integrated PEEK scaffolds were prepared by multilayer coatings of polydopamine (pDA), silver nanoparticles (AgNP), and apatite. In presence of acidic conditions, the solubility of apatite increased; thus, enhancing the delivery of Ca^{2+} and PO_4^{3-} ions, resulting in osteoinduction. The calibrated release of Ag^+ with these ions provided a synergistic antibacterial and osteogenic local environment and the attachment of bacteria to the implant surface resulted in the production of lactic or acetic acid, leading to a pH reduction; thus, providing the stimulus for ion release.

13.5.2.2 Temperature Sensitive

Thermoresponsive polymeric materials modulate their properties in response to change in temperature. Such hydrogels are promising in tissue engineering applications as they can show sol-to-gel conversion and change in their swelling and degradation behavior when subjected to a temperature change. Thermoresponsive polymers and cross-linkers allow injectability and in situ gelation of hydrogels. Most thermoresponsive polymers used in tissue engineering applications have lower critical solution temperature (LCST) (Schild and Tirrell 1990; Klouda 2015) and form hydrogels on increasing the temperature. Polymers like chitosan, poly(polyethylene glycol citrate-*co*-*N*-isopropylacrylamide) (PPCN), hydroxypropyl guar-graft-poly(*N*-vinyl caprolactam) (HPG-gPNVCL), PCL, poly(*e*-caprolactone-*co*-1,4,8-trioxa-[4.6]spiro-9-undecanone)-poly(ethyleneglycol)-poly(*e*-aprolactone-*co*-1,4,8-trioxa[4.6]spiro-9-undecanone)(PECT), poly

(ϵ -caprolactone-co-lactide)-*b*-poly(ethyleneglycol)-*b*-poly(ϵ -caprolactone-co-lactide), poly(NIPAM-co-DMAEMA), and cellulose have been investigated as thermoresponsive systems for growth factor and drug delivery in bone regeneration (Liu et al. 2014; Morochnik et al. 2018; Müller et al. 2018; Parameswaran-Thankam et al. 2018; Chen et al. 2019; Gaihre et al. 2019; Maturavongsadit et al. 2020).

The macroporous hydrogels show good cell penetration but often lead to rapid burst release of drugs. Dexamethasone-glycidyl methacrylated dextran (Dex-GMA)/gelatin scaffolds containing microspheres loaded with BMP have been used for temperature-sensitive release (Chen et al. 2007). The incorporation of microspheres into hydrogels resulted in the sustained release. The thermoresponsive properties of matrix provided control over the growth factor/drug release. Besides growth factor delivery, the most challenging task in this field is to design and develop smart and minimally invasive scaffolds for irregular bone defects. Stimuli-responsive shape memory scaffolds/hydrogels have provided a solution to this problem. Liu et al. developed a PCL and hydroxyapatite-based porous scaffold loaded with BMP-2 that can be compressed to a small volume using hot compression, which can subsequently regain its original shape at body temperature. These scaffolds showed controlled release of BMP-2 and promoted new bone formation on implantation in rabbit mandibular bone defects (Liu et al. 2014). Gaihre et al. developed an injectable scaffold by using the combination of chitosan microparticles (MPs) with thermoresponsive methylcellulose (MC) gels loaded with BMP-2 and VEGF. MPs were loaded with BMP-9 and incorporated in the gel, whereas VEGF was introduced within the gel matrix (Fig. 13.18). The temperature-sensitive gelation at physiological temperature resulted in an injectable growth factor delivery system. The release of VEGF from these scaffolds was higher compared to BMP-9. The BMP-9-VEGF-loaded MP gels significantly enhanced the subcutaneous and cranial bone formation as observed from the micro-CT images at 6 and 12 weeks of implantation (Gaihre et al. 2019).

Kim et al. developed poly(ϵ -caprolactone-co-lactide)-*b*-poly(ethylene glycol)-*b*-poly(ϵ -caprolactone-co-lactide)- and *O*-phosphorylethanolamine-conjugated alginate hydrogels that can transform to hydrogels at physiological temperature (37 °C) (Kim et al. 2020). The thermoresponsive property of these bioconjugates enabled their subcutaneous administration as sols at lower temperature into the dorsal region of Sprague-Dawley rats and in situ hydrogel formation at 37 °C. These in situ hydrogels demonstrated the sustained release of BMP-2 and biomineralization in in vitro and in vivo. Thus, thermoresponsive hydrogels hold potential as injectable drug delivery carriers in bone regeneration.

13.5.2.3 Biomolecule Sensitive

Biomolecules, such as enzymes, play important roles in the biological activities of bone and other tissues with injury or disorders. Matrix metalloproteinases (MMPs) are found at the injury site and play a crucial role in ECM remodeling. A provisional fibrin-rich matrix containing growth factors is formed by platelets, neutrophils, and macrophages after the injury. It is degraded by MMPs and growth factors regulate vascularization and tissue regeneration in that region (Ravanti and Kähäri 2000).

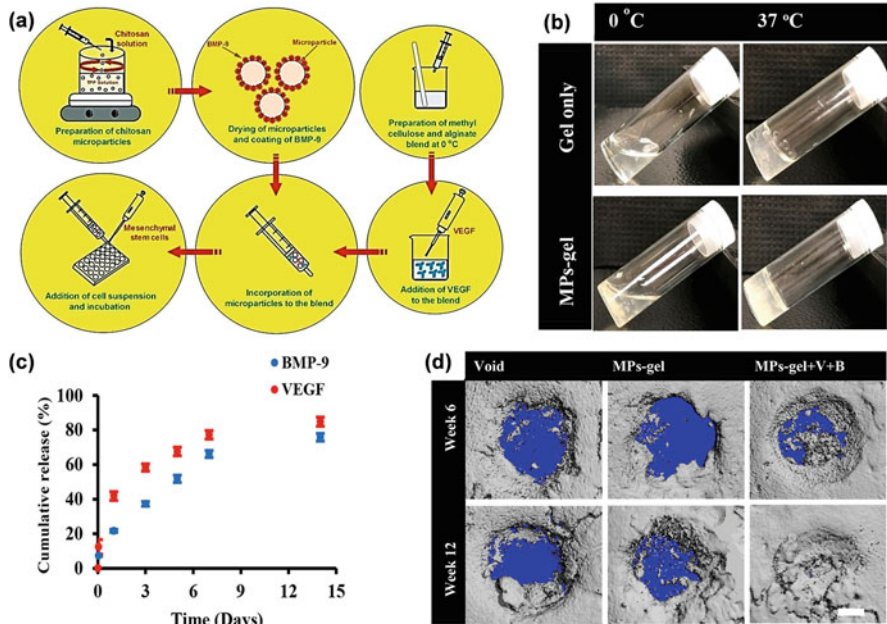


Fig. 13.18 Thermoresponsive MP gels for BMP-2 and VEGF delivery (reproduced with permission from Gaihre et al. 2019). (a) Fabrication of MP gels. (b) Thermoresponsive sol-to-gel conversion. (c) BMP-2 and VEGF release from MP-gel scaffolds. (d) Micro-CT analysis of cranial defects of rats after 6 and 12 weeks

MMP expressions are found to be high in bone and cartilage under several pathological conditions, like rheumatoid arthritis, osteoporosis, infection, and osteoarthritis. Enzyme-sensitive biomaterial matrix has been developed for the on-demand release of growth factors and drugs. Lutolf et al. synthesized a MMP-sensitive BMP-2-loaded PEG-based hydrogel to regenerate bone within an orthotopic model (Lutolf et al. 2003). The proteolytic degradation of gels by MMP-2 resulted in 100% BMP-2 release, which was only 10% in saline, demonstrating that the release kinetics was degradation dependent. These BMP-2-loaded MMP-sensitive hydrogels improved the bone-healing outcomes in comparison to hydrogels without MMP-sensitive activities or without BMP-2.

MMP-sensitive BMP-2-loaded polymeric delivery vehicles were fabricated using thiol-ene chemistry and showed improved bone formation in critical-sized bone defects in comparison to adsorbable collagen sponge (Mariner et al. 2013). In another approach, MMP-sensitive difunctional peptides were used for cross-linking maleimide-modified hyaluronic acid polymers to fabricate hydrogels capable of protease-mediated degradation and BMP-2 release (Holloway et al. 2014). BMP-2 release from these hydrogels increased with a decrease in cross-linking density of polymers or an increase in collagenase concentration. BMP-2-loaded hyaluronan

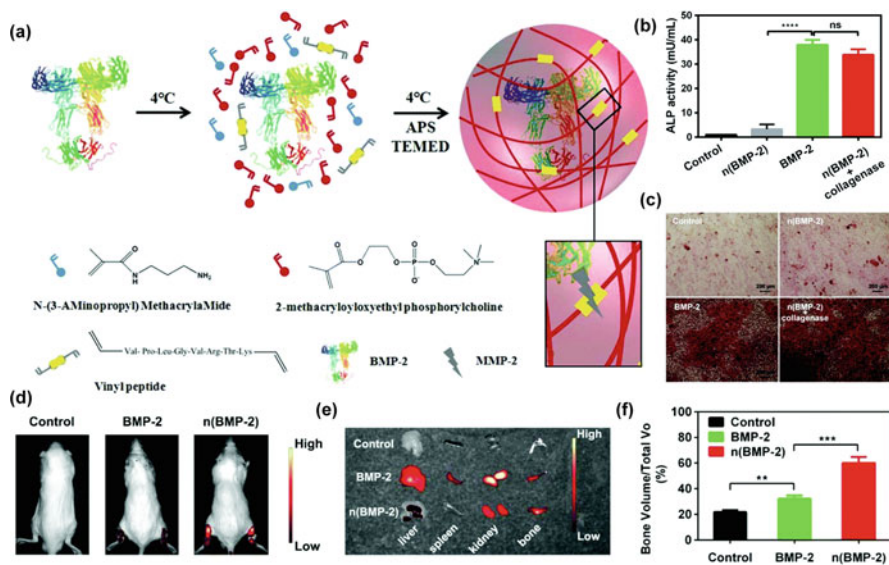


Fig. 13.19 MMP-sensitive polymeric nanocapsules for BMP-2 delivery at the fracture site. (Reproduced with permission from Qi et al. 2019.) (a) BMP-2-loaded nanocapsule formation and cleavage of MMP-sensitive peptide linker by MMPs. (b) ALP activities of MSCs incubated with native BMP-2 and n(BMP-2) ($****P < 0.0001$). (c) Alizarin red staining to visualize calcium nodule accumulation in MSCs at 21 days. (d) In vivo fluorescence images of tibial injury. (e) BMP-2 and n(BMP-2) distribution in main tissues and the tibial injury site after intravenous injection of native BMP-2 and n(BMP-2). (f) Semi-quantitative analysis of the bone tissue volume per total tissue volume (BV/TV) after 2 weeks of therapy ($**P < 0.01$, $***P < 0.001$)

hydrogels covalently linked with bisphosphonate (BP) ligands have been investigated for proteolytic degradation-mediated enzyme-responsive release of BMP-2 (Hulsart-Billström et al. 2013). These hydrogels exhibited less than 10% BMP-2 release over 2 weeks and preserved its bioactivity, resulting in the induction of osteogenic differentiation. Chondroitin sulfate and PEG-based hybrid hydrogel system were incorporated with MMP-sensitive lysine peptides for MMP-sensitive degradation leading to tunable BMP-2 release and increased osteogenic activities (Anjum et al. 2016).

Polymeric nanocapsules have emerged as another interesting candidate for enzyme-sensitive release of growth factors. BSA-based nanocapsules have been reported for the enzyme-responsive release of VEGF (Wen et al. 2011; Qi et al. 2019). Qi et al. reported the effectiveness of enzyme-responsive release of BMP-2 from systemically administered polymeric nanocapsules for promoting bone regeneration (Qi et al. 2019). The monomer 2-(methacryloyloxy)ethyl phosphorylcholine (MPC) and the MMP-sensitive bisacryloylated VPLGVRTK peptide along with BSA were used for the fabrication of these capsules by in situ free radical polymerization method in presence of ammonium persulfate (APS) and 10% *N,N,N',N'*-tetramethylethylenediamine (TEMED) (Fig. 13.19). These nano-

BMP capsules (n(BMP)) retained the structure and function of BMP-2 during the circulation time (~48 h) and accumulated at the fracture site through malformed blood vessels. The accumulation of native BMP-2 was very less, as they were rapidly eliminated (~30 min) from the circulation. It was due to the reduced adsorption of serum proteins on nanocapsules that the uptake by macrophages decreased in comparison to native BMPs. At the fracture site, the degradation of n(BMPs) by MMPs led to the release of BMP-2, resulting in efficient repair of bone. The *in vitro* studies showed increased ALP activities and calcium deposition at 21 days suggesting the efficiency of these nanocapsules in growth factor release. The biodistribution of native BMP and n(BMP) showed that the nanocapsules reduced the elimination of BMP-2 by liver, spleen, and kidney and *in vivo* studies showed significantly increased bone formation by n(BMP). Overall, these nanocapsules provide a promising approach for the systemic delivery of growth factors for fracture healing.

Beside enzymes, glucose has been used as a stimulus for the growth factor delivery. Xiao et al. developed glucose-sensitive core cell nanofibers for BMP-2 release to treat mandible defects in diabetic rats (Xiao et al. 2019). The inner core layer of fibers was formed using BMP-2-loaded polyethylene oxide, whereas the outer shell layer comprised of polyvinyl alcohol (PVA) cross-linked *N*-(2-hydroxyl) propyl-3-trimethylammonium chitosan chloride (HTCC). The immobilization of glucose oxidase on these nanofibers imparted glucose sensitivity to the material. It reacts with glucose and converts it into gluconic acid resulting in a decreased pH. HTCC can sense the pH, leading to swelling or shrinkage of the matrix for growth factor release.

13.5.2.4 Redox Responsive

Reactive oxygen species (ROS) are generally produced during inflammation in response to the immune system against the pathogenic microbes and foreign agents (Kim and Wong 2013). Elevated levels of ROS have been detected in bone-related disorders, leading to tissue damage and impaired healing (Porto et al. 2015).

Redox-responsive systems have been investigated for the growth factor/drug release in bone tissue engineering. A study reported that injectable hydrogels fabricated from thiolated PEG precursors via disulfide bond were able to release the bioactive molecules upon encountering a reductant, such as glutathione (GSH). GSH is commonly present in the ECM and secreted in excess, when the level of ROS becomes high at the injury microenvironment. These hydrogels were able to provide sustained release of BMP-2, resulting in an increased ectopic bone formation (Yang et al. 2014). Gong et al. fabricated redox-sensitive poly(ethylene oxide) (PEO)-PCL nanofibers with a core-shell structure for BMP-2 delivery in the bone defect (Gong et al. 2018). PEO loaded with BMP-2 forms the inner core region of the nanofiber, whereas 6-arm PEG-PCL/6-arm PEG-PCL-sulphydryl nanogels (c-6A PEG-PCL/6A PEG-PCL-SH NGs) containing disulfide linkages form the outer shell of the nanofibers. The outer shell of nanofibers responds to GSH concentration leading to nanogel degradation and increased permeability of shell, resulting in the release of BMP-2 from the inner core region *in vitro* and *in vivo* (Fig. 13.20). BMP-2 release

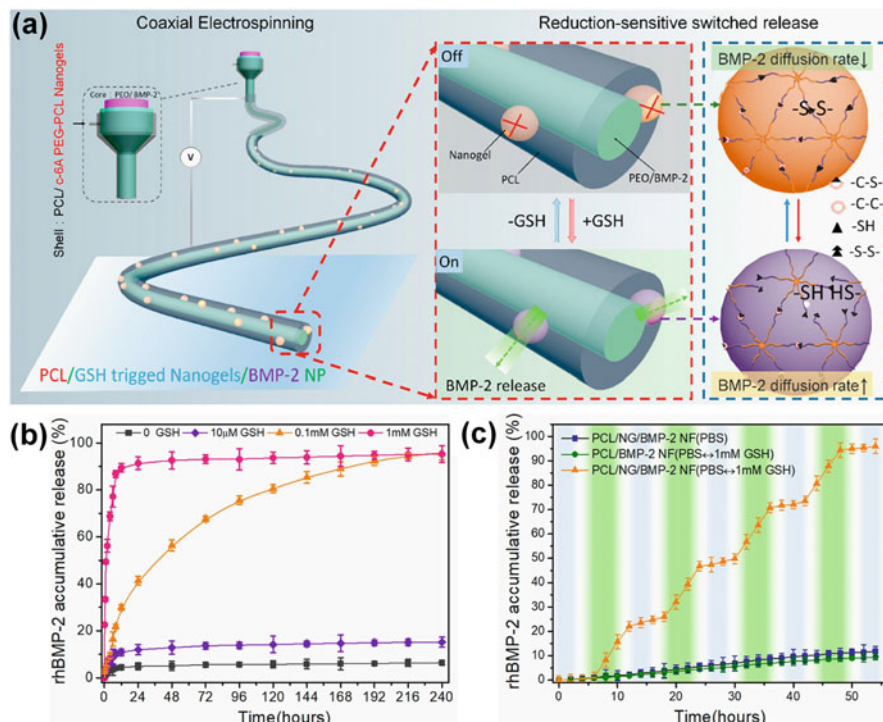


Fig. 13.20 Redox-sensitive BMP-2 release from nanofibers with core-shell nanostructure. (Reproduced with permission from Gong et al. 2018.) (a) Fabrication of nanogel-in-nanofiber device via coaxial electrospinning and redox-responsive release of BMP-2 mediated via outer shell degradation. (b) Release profiles of BMP-2 from the nanofibers at different concentrations of GSH. (c) BMP-2 release from nanofibers on increasing GSH at fixed intervals

from the inner core of nanofibers increased with an increase in GSH concentration—10 μM , 0.1 mM, and 1 mM GSH, which resulted in 13 ± 1.5 , 55 ± 2.5 , and $90 \pm 2.9\%$ of BMP-2 release after 48 h of incubation. The redox switched behavior of nanofibers was monitored by incubating in GSH for 8 h, PBS for 8 h, and GSH for four cycle tests, and resulted in a sharp increase in BMP-2 concentration in GSH and slight increase in PBS for all cycles. The nanogels released $10\% \pm 3.2\%$ BMP-2 after four cycles, whereas the cumulative release from the PCL/NG/BMP-2 NF was observed to be $94.5 \pm 2.19\%$.

13.5.2.5 Magnetic/Electromechanical/Light Responsive

The polymeric biomaterials have been incorporated with external physical stimuli, like magnetic field, electric field, light, mechanical strain, and ultrasound, to remotely trigger the release of therapeutic payloads (Bansal and Zhang 2014; Linsley et al. 2015; Manouras and Vamvakaki 2017; Wang et al. 2018; Madani et al. 2020; Lanier et al. 2020). A study reported near-infrared (NIR) light-triggered release of Sr^{2+} ions from PLGA loaded with SrCl_2 and black phosphorous

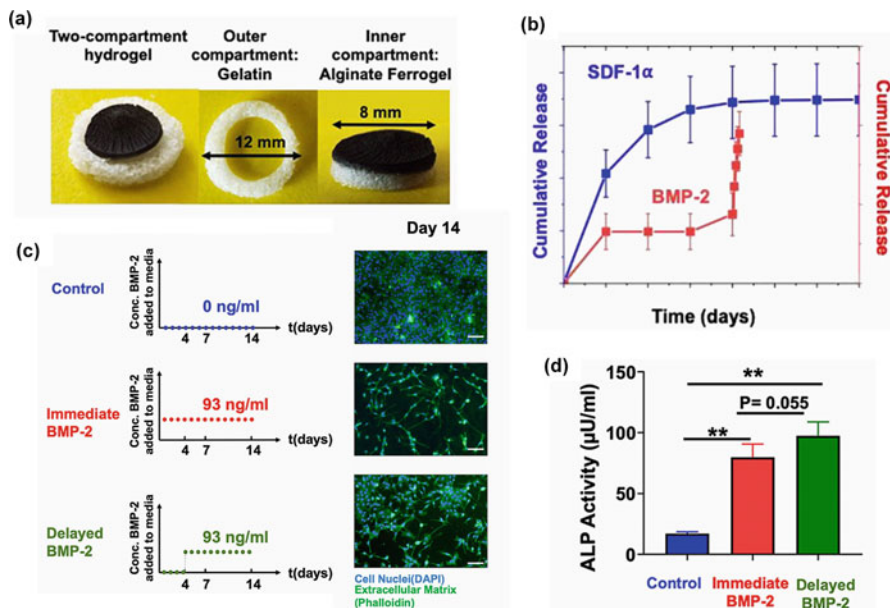


Fig. 13.21 Magnetic stimuli-responsive delivery of BMP-2 and SDF-1 α from two compartment hydrogel system to recruit mouse mesenchymal stem cells (mMSCs). (Reproduced with permission from Madani et al. 2020.) (a) Images of two compartment magnetic-responsive gels. (b) Cumulative SDF-1 α release from outer compartment of gel. (c) Magnetically triggered delayed delivery of BMP-2 from inner compartment of gels and its effect on 2D cell culture at 14 days. (d) ALP activities at 14 days. **Indicates statistically significant difference ($p < 0.01$)

(BP) nanosheets for excellent bone regeneration capabilities (Wang et al. 2018). BP was incorporated in BP-SrCl₂/PLGA microspheres for the NIR-responsive behavior. The rapid increase in local temperature by NIR radiation leads to an increase in glass transition temperature (T_g) of PLGA, causing the collapse and cracks in microspheres, resulting in Sr²⁺ release. Magnetically responsive two-compartment biomaterial systems were investigated for on-demand control over sequential delivery of BMP-2 and SDF-1 α to optimize the bone regenerative outcomes (Madani et al. 2020). The two-compartment biomaterial consisted of an outer compartment made-up of hollow cylindrical gelatin gels (outer diameter of scaffold: 12 mm) and inner compartment made-up of 8 mm alginate ferrogels (Fig. 13.21). The outer compartment was loaded with SDF-1 α and inner compartment with BMP-2. The release of SDF-1 α from outer compartment resulted in the recruitment of cells, whereas the release of BMP-2 from inner compartment was magnetically controlled. This system was capable of releasing BMP-2 in a delayed manner in response to magnetic field applied; thus, providing a control over the timing between bone progenitor recruitment by SDF-1 α and release of BMP-2 for osteodifferentiation. The ALP activities of cells provided with delayed release of BMP-2 at 14th day were significantly higher than that of cells with immediate release of BMP-2 and control, suggesting the potential of this system in bone regeneration.

13.6 Conclusions

Polymeric materials and nanomaterials fabricated from both natural and synthetic polymers have been employed as drug delivery carriers to enhance bone regeneration. Advancement in polymer engineering has resulted in the development of diverse polymeric structures and smart drug delivery systems capable of tunable local delivery of growth factors/drugs to the defect site along with providing an ECM-mimicking structure to support cell growth and infiltration to enhance the osteogenic outcomes. Growth factor/drug-loaded polymeric systems, like polymer-drug bioconjugates, nanoparticles, microparticles, micelles, nanofibers, hydrogels, polymeric scaffolds, multicomponent polymeric systems, and 3D-printed scaffolds, have shown promising results both *in vitro* and *in vivo*. The smart polymeric systems have been also used for the on-demand release of growth factors/drugs upon exposure to a stimulus. Advanced drug-loading techniques, like core-shell nanofibers, microparticles in hydrogel systems, and layer-by-layer loading, have been employed using different polymer-based systems to control the drug concentration and release kinetics. Dual/multiple bioactive factors and their sequential release have been investigated in order to mimic the natural microenvironment and phases of bone healing. Although multifunctional growth factor/drug carriers have been developed to overcome the challenges associated with bone regeneration, the design and development of a carrier mimicking the natural bone healing remains a challenge. Bone healing is a complex process that requires the involvement of multiple bioactive molecules at various phases of healing and, therefore, it is highly desirable to investigate multifunctional and multiresponsive hybrid materials mimicking the bone-healing process to overcome the challenges of bone regeneration. The stability and cost of growth factors also remains another major concern and, therefore, several combinations of angiogenic and osteogenic factors/drugs should be investigated using the biomaterials that can enhance the osteogenic outcomes while reducing the side effects of drugs by providing the controlled/sequential and sustained release. Difference in size and structure of grafts required for different patients or fracture sites require patient-specific customized grafts. Multifunctional and multiresponsive 3D-printed scaffolds must be investigated further for desired outcomes in bone regeneration.

Acknowledgments YS gratefully acknowledges financial assistance from the SERB, New Delhi (EMR/2017/000045), and NC is thankful to the Indian Institute of Technology Ropar, Rupnagar, for the institute fellowship.

References

- Abbassy MA, Watari I, Bakry AS et al (2016) Calcitonin and vitamin D3 have high therapeutic potential for improving diabetic mandibular growth. *Int J Oral Sci* 8:39–44
- Agarwal-Harding KJ, von Keudell A, Zirkle LG et al (2016) Understanding and addressing the global need for orthopaedic trauma care. *J Bone Joint Surg* 98:1844–1853

- Aliabadi HM, Lavasanifar A (2006) Polymeric micelles for drug delivery. *Expert Opin Drug Deliv* 3:139–162
- Al-Jarsha M, Moulisova V, Leal-Egana A et al (2018) Engineered coatings for titanium implants to present ultra-low doses of BMP-7. *ACS Biomater Sci Eng* 4:1812–1819
- Amir O, Berry SD, Zullo AR et al (2019) Incidence of hip fracture in native American residents of U.S. nursing homes. *Bone* 123:204–210
- Anjum F, Lienemann PS, Metzger S et al (2016) Enzyme responsive GAG-based natural-synthetic hybrid hydrogel for tunable growth factor delivery and stem cell differentiation. *Biomaterials* 87:104–117
- Ao Q, Wang S, He Q et al (2020) Fibrin glue/fibronectin/heparin-based delivery system of BMP2 induces osteogenesis in MC3T3-E1 cells and bone formation in rat Calvarial critical-sized defects. *ACS Appl Mater Interfaces* 12:13400–13410
- Arnett TR, Dempster DW (1986) Effect of pH on bone resorption by rat osteoclasts *in vitro*. *Endocrinology* 119:119–124
- Aronin CEP, Sefcik LS, Tholpady SS et al (2010) FTY720 promotes local microvascular network formation and regeneration of cranial bone defects. *Tissue Eng A* 16:1801–1809
- Bai X, Gao M, Syed S et al (2018) Bioactive hydrogels for bone regeneration. *Bioactive Mater* 3:401–417
- Bansal A, Zhang Y (2014) Photocontrolled nanoparticle delivery systems for biomedical applications. *Acc Chem Res* 47:3052–3060
- Barone DT-J, Raquez J-M, Dubois P (2011) Bone-guided regeneration: from inert biomaterials to bioactive polymer (nano)composites: bone-guided regeneration. *Polym Adv Technol* 22:463–475
- Benazet J-D, Bischofberger M, Tiecke E et al (2009) A self-regulatory system of interlinked signaling feedback loops controls mouse limb patterning. *Science* 323:1050–1053
- Ben-David D, Srouji S, Shapira-Schweitzer K et al (2013) Low dose BMP-2 treatment for bone repair using a PEGylated fibrinogen hydrogel matrix. *Biomaterials* 34:2902–2910
- Bentz H, Schroeder JA, Estridge TD (1998) Improved local delivery of TGF-beta2 by binding to injectable fibrillar collagen via difunctional polyethylene glycol. *J Biomed Mater Res* 39:539–548
- Boda SK, Wang H, John JV et al (2020) Dual delivery of alendronate and E7-BMP-2 peptide via calcium chelation to mineralized nanofiber fragments for alveolar bone regeneration. *ACS Biomater Sci Eng* 6:2368–2375
- Bonafede M, Espindle D, Bower AG (2013) The direct and indirect costs of long bone fractures in a working age US population. *J Med Econ* 16:169–178
- Bonda DJ, Manjila S, Selman WR, Dean D (2015) The recent revolution in the design and manufacture of cranial implants. *Neurosurgery* 77:814–824
- Bose S, Darsell J, Kintner M et al (2003) Pore size and pore volume effects on alumina and TCP ceramic scaffolds. *Mater Sci Eng C* 23:479–486
- Bose S, Vahabzadeh S, Bandyopadhyay A (2013) Bone tissue engineering using 3D printing. *Mater Today* 16:496–504
- Bose S, Ke D, Sahasrabudhe H, Bandyopadhyay A (2018) Additive manufacturing of biomaterials. *Prog Mater Sci* 93:45–111
- Carbone EJ, Jiang T, Nelson C et al (2014) Small molecule delivery through nanofibrous scaffolds for musculoskeletal regenerative engineering. *Nanomedicine* 10:1691–1699
- Cattalini JP, Boccaccini AR, Lucangioli S, Mouriño V (2012) Bisphosphonate-based strategies for bone tissue engineering and orthopedic implants. *Tissue Eng Part B Rev* 18:323–340
- Chen F-M, Zhao Y-M, Sun H-H et al (2007) Novel glycidyl methacrylated dextran (Dex-GMA)/gelatin hydrogel scaffolds containing microspheres loaded with bone morphogenetic proteins: formulation and characteristics. *J Control Release* 118:65–77
- Chen H, Li G, Chi H et al (2012) Alendronate-conjugated amphiphilic hyperbranched polymer based on Boltorn H40 and poly(ethylene glycol) for bone-targeted drug delivery. *Bioconjug Chem* 23:1915–1924

- Chen Z, Bachhuka A, Wei F et al (2017) Nanotopography-based strategy for the precise manipulation of osteoimmunomodulation in bone regeneration. *Nanoscale* 9:18129–18152
- Chen W, Zhi M, Feng Z et al (2019) Sustained co-delivery of ibuprofen and basic fibroblast growth factor by thermosensitive nanoparticle hydrogel as early local treatment of peri-implantitis. *Int J Nanomed* 14:1347–1358
- Cheng G, Yin C, Tu H et al (2019) Controlled co-delivery of growth factors through layer-by-layer assembly of core–shell nanofibers for improving bone regeneration. *ACS Nano* 13:6372–6382
- Chia HN, Wu BM (2015) Recent advances in 3D printing of biomaterials. *J Biol Eng* 9:4
- Cho H, Madhurakkat Perikamana SK, Lee J et al (2014) Effective immobilization of BMP-2 mediated by polydopamine coating on biodegradable nanofibers for enhanced in vivo bone formation. *ACS Appl Mater Interfaces* 6:11225–11235
- Claes L (2011) Biomechanical principles and mechanobiologic aspects of flexible and locked plating. *J Orthop Trauma* 25:S4–S7
- Claes L, Recknagel S, Ignatius A (2012) Fracture healing under healthy and inflammatory conditions. *Nat Rev Rheumatol* 8:133–143
- Cole LE, Vargo-Gogola T, Roeder RK (2016) Targeted delivery to bone and mineral deposits using bisphosphonate ligands. *Adv Drug Deliv Rev* 99:12–27
- Cong Y, Quan C, Liu M et al (2015) Alendronate-decorated biodegradable polymeric micelles for potential bone-targeted delivery of vancomycin. *J Biomater Sci Polym Ed* 26:629–643
- Craστο GJ, Kartner N, Reznik N et al (2016) Controlled bone formation using ultrasound-triggered release of BMP-2 from liposomes. *J Control Release* 243:99–108
- Crouzier T, Sailhan F, Becquart P et al (2011) The performance of BMP-2 loaded TCP/HAP porous ceramics with a polyelectrolyte multilayer film coating. *Biomaterials* 32:7543–7554
- Culpepper BK, Morris DS, Prevelige PE, Bellis SL (2013) Engineering nanocages with polyglutamate domains for coupling to hydroxyapatite biomaterials and allograft bone. *Biomaterials* 34:2455–2462
- Dai C, Guo H, Lu J et al (2011) Osteogenic evaluation of calcium/magnesium-doped mesoporous silica scaffold with incorporation of rhBMP-2 by synchrotron radiation-based μ CT. *Biomaterials* 32:8506–8517
- Das A, Segar CE, Hughley BB et al (2013) The promotion of mandibular defect healing by the targeting of S1P receptors and the recruitment of alternatively activated macrophages. *Biomaterials* 34:9853–9862
- DeLong SA, Moon JJ, West JL (2005) Covalently immobilized gradients of bFGF on hydrogel scaffolds for directed cell migration. *Biomaterials* 26:3227–3234
- Deng Y, Shi X, Chen Y et al (2020) Bacteria-triggered pH-responsive osteopotentiating coating on 3D-printed Polyetheretherketone scaffolds for infective bone defect repair. *Ind Eng Chem Res* 59:12123–12135
- Ding S, Li J, Luo C et al (2013) Synergistic effect of released dexamethasone and surface nanoroughness on mesenchymal stem cell differentiation. *Biomater Sci* 1:1091
- Doberenz F, Zeng K, Willems C et al (2020) Thermoresponsive polymers and their biomedical application in tissue engineering – a review. *J Mater Chem B* 8:607–628
- Donneys A, Farberg AS, Tchanque-Fossuo CN et al (2012) Deferoxamine enhances the vascular response of bone regeneration in mandibular distraction osteogenesis. *Plast Reconstr Surg* 129:850–856
- Einhorn TA (1998) The cell and molecular biology of fracture healing. *Clin Orthop Relat Res* 355S: S7–S21
- Einhorn TA (2005) The science of fracture healing. *J Orthop Trauma* 19:S4–S6
- Einhorn TA, Gerstenfeld LC (2015) Fracture healing: mechanisms and interventions. *Nat Rev Rheumatol* 11:45–54
- El-Fiqi A, Kim J-H, Kim H-W (2015) Osteoinductive fibrous scaffolds of biopolymer/mesoporous bioactive glass nanocarriers with excellent bioactivity and long-term delivery of osteogenic drug. *ACS Appl Mater Interfaces* 7:1140–1152

- Foster AL, Moriarty TF, Zalavras C et al (2020) The influence of biomechanical stability on bone healing and fracture-related infection: the legacy of Stephan Perren. *Injury* 52:43–52. S0020138320305519
- Freeman M, Bradley G, Revell P (1982) Observations upon the interface between bone and polymethylmethacrylate cement. *J Bone Joint Surg* 64-B:489–493
- Gaihre B, Unagolla JM, Liu J et al (2019) Thermoresponsive injectable microparticle–gel composites with recombinant BMP-9 and VEGF enhance bone formation in rats. *ACS Biomater Sci Eng* 5:4587–4600
- Gan Q, Zhu J, Yuan Y et al (2015a) A dual-delivery system of pH-responsive chitosan-functionalized mesoporous silica nanoparticles bearing BMP-2 and dexamethasone for enhanced bone regeneration. *J Mater Chem B* 3:2056–2066
- Gan Q, Zhu J, Yuan Y et al (2015b) A proton-responsive ensemble using mesocellular foam supports capped with N,O-carboxymethyl chitosan for controlled release of bioactive proteins. *J Mater Chem B* 3:2281–2285
- Gandhi NS, Mancera RL (2012) Prediction of heparin binding sites in bone morphogenetic proteins (BMPs). *Biochim Biophys Acta* 1824:1374–1381
- Gerstenfeld L, Cho T-J, Kon T et al (2003) Impaired fracture healing in the absence of TNF- α signaling: the role of TNF- α in endochondral cartilage resorption. *J Bone Miner Res* 18:1584–1592
- Geven MA, Varjas V, Kamer L et al (2015) Fabrication of patient specific composite orbital floor implants by stereolithography: patient specific composite orbital floor implants. *Polym Adv Technol* 26:1433–1438
- Ghiasi MS, Chen J, Vaziri A et al (2017) Bone fracture healing in mechanobiological modeling: a review of principles and methods. *Bone Rep* 6:87–100
- Gilde F, Maniti O, Guillot R et al (2012) Secondary structure of rhBMP-2 in a protective biopolymeric carrier material. *Biomacromolecules* 13:3620–3626
- Gong T, Liu T, Zhang L et al (2018) Design redox-sensitive drug-loaded nanofibers for bone reconstruction. *ACS Biomater Sci Eng* 4:240–247
- Grundnes O, Reikerås O (1992) Blood flow and mechanical properties of healing bone: femoral osteotomies studied in rats. *Acta Orthop Scand* 63:487–491
- Guillot R, Gilde F, Becquart P et al (2013) The stability of BMP loaded polyelectrolyte multilayer coatings on titanium. *Biomaterials* 34:5737–5746
- Gunatillake P, Adhikari R (2003) Biodegradable synthetic polymers for tissue engineering. *eCM* 5:1–16
- Gupta S, Del Fabbro M, Chang J (2019) The impact of simvastatin intervention on the healing of bone, soft tissue, and TMJ cartilage in dentistry: a systematic review and meta-analysis. *Int J Implant Dent* 5:17
- Guvendiren M, Molde J, Soares RMD, Kohn J (2016) Designing biomaterials for 3D printing. *ACS Biomater Sci Eng* 2:1679–1693
- de Guzman RC, Saul JM, Ellenburg MD et al (2013) Bone regeneration with BMP-2 delivered from keratose scaffolds. *Biomaterials* 34:1644–1656
- Ham TR, Lee RT, Han S et al (2016) Tunable keratin hydrogels for controlled erosion and growth factor delivery. *Biomacromolecules* 17:225–236
- Hankenson KD, Dishowitz M, Gray C, Schenker M (2011) Angiogenesis in bone regeneration. *Injury* 42:556–561
- Haumer A, Bourguine PE, Occhetta P et al (2018) Delivery of cellular factors to regulate bone healing. *Adv Drug Deliv Rev* 129:285–294
- He X, Ma J, Jabbari E (2008) Effect of grafting RGD and BMP-2 protein-derived peptides to a hydrogel substrate on osteogenic differentiation of marrow stromal cells. *Langmuir* 24:12508–12516
- Hoffman AS (1995) “Intelligent” polymers in medicine and biotechnology. *Macromol Symp* 98:645–664

- Holloway JL, Ma H, Rai R, Burdick JA (2014) Modulating hydrogel crosslink density and degradation to control bone morphogenetic protein delivery and in vivo bone formation. *J Control Release* 191:63–70
- Huang K-C, Yano F, Murahashi Y et al (2017) Sandwich-type PLLA-nanosheets loaded with BMP-2 induce bone regeneration in critical-sized mouse calvarial defects. *Acta Biomater* 59:12–20
- Huang C, Yang G, Zhou S et al (2020) Controlled delivery of growth factor by hierarchical nanostructured core-shell nanofibers for the efficient repair of critical-sized rat calvarial defect. *ACS Biomater Sci Eng* 6:5758–5770
- Hudalla GA, Murphy WL (2011) Biomaterials that regulate growth factor activity via bioinspired interactions. *Adv Funct Mater* 21:1754–1768
- Hulsart-Billström G, Yuen PK, Marsell R et al (2013) Bisphosphonate-linked hyaluronic acid hydrogel sequesters and enzymatically releases active bone morphogenetic protein-2 for induction of osteogenic differentiation. *Biomacromolecules* 14:3055–3063
- Ibrahim N'I, Khamis MF, Mod Yunoh MF et al (2014) Targeted delivery of lovastatin and tocotrienol to fracture site promotes fracture healing in osteoporosis model: micro-computed tomography and biomechanical evaluation. *PLoS One* 9:e115595
- Jiang T, Yu X, Carbone EJ et al (2014) Poly aspartic acid peptide-linked PLGA based nanoscale particles: potential for bone-targeting drug delivery applications. *Int J Pharm* 475:547–557
- Juhl O, Zhao N, Merife A-B et al (2019) Aptamer-functionalized fibrin hydrogel improves vascular endothelial growth factor release kinetics and enhances angiogenesis and osteogenesis in critically sized cranial defects. *ACS Biomater Sci Eng* 5:6152–6160
- Kamble S, Varamini P, Müllner M et al (2020) Bisphosphonate-functionalized micelles for targeted delivery of curcumin to metastatic bone cancer. *Pharm Dev Technol* 25:1118–1126
- Kaminskas LM, McLeod VM, Porter CJH, Boyd BJ (2012) Association of chemotherapeutic drugs with dendrimer nanocarriers: an assessment of the merits of covalent conjugation compared to noncovalent encapsulation. *Mol Pharm* 9:355–373
- Kämmerer PW, Pabst AM, Dau M et al (2020) Immobilization of BMP-2, BMP-7 and alendronic acid on titanium surfaces: adhesion, proliferation and differentiation of bone marrow-derived stem cells. *J Biomed Mater Res* 108:212–220
- Kanematsu A, Yamamoto S, Ozeki M et al (2004) Collagenous matrices as release carriers of exogenous growth factors. *Biomaterials* 25:4513–4520
- Kanzaki H, Chiba M, Shimizu Y, Mitani H (2002) Periodontal ligament cells under mechanical stress induce osteoclastogenesis by receptor activator of nuclear factor κ B ligand up-regulation via prostaglandin E2 synthesis. *J Bone Miner Res* 17:210–220
- Karacivi M, Sumer Bolu B, Sanyal R (2017) Targeting to the bone: alendronate-directed combretastatin A-4 bearing antiangiogenic polymer-drug conjugates. *Mol Pharm* 14:1373–1383
- Kawaguchi H, Oka H, Jingushi S et al (2010) A local application of recombinant human fibroblast growth factor 2 for tibial shaft fractures: a randomized, placebo-controlled trial. *J Bone Miner Res* 25:2735–2743
- Kempen DHR, Kruyt MC, Lu L et al (2009a) Effect of autologous bone marrow stromal cell seeding and bone morphogenetic protein-2 delivery on ectopic bone formation in a microsphere/poly(propylene fumarate) composite. *Tissue Eng A* 15:587–594
- Kempen DHR, Lu L, Heijink A et al (2009b) Effect of local sequential VEGF and BMP-2 delivery on ectopic and orthotopic bone regeneration. *Biomaterials* 30:2816–2825
- Kempen DHR, Lu L, Hefferan TE et al (2010) Enhanced bone morphogenetic protein-2-induced ectopic and orthotopic bone formation by intermittent parathyroid hormone (1–34) administration. *Tissue Eng A* 16:3769–3777
- Keramaris NC, Calori GM, Nikolauou VS et al (2008) Fracture vascularity and bone healing: a systematic review of the role of VEGF. *Injury* 39:S45–S57
- Kim SJ, Wong PKY (2013) ROS upregulation during the early phase of retroviral infection plays an important role in viral establishment in the host cell. *J Gen Virol* 94:2309–2317

- Kim K, Yeatts A, Dean D, Fisher JP (2010) Stereolithographic bone scaffold design parameters: osteogenic differentiation and signal expression. *Tissue Eng Part B Rev* 16:523–539
- Kim SE, Song S-H, Yun YP et al (2011) The effect of immobilization of heparin and bone morphogenic protein-2 (BMP-2) to titanium surfaces on inflammation and osteoblast function. *Biomaterials* 32:366–373
- Kim E-C, Lim H-C, Nam OH et al (2016) Delivery of dexamethasone from bioactive nanofiber matrices stimulates odontogenesis of human dental pulp cells through integrin/BMP/mTOR signaling pathways. *Int J Nanomed* 11:2557
- Kim B-S, Yang S-S, Kim CS (2018a) Incorporation of BMP-2 nanoparticles on the surface of a 3D-printed hydroxyapatite scaffold using an ϵ -polycaprolactone polymer emulsion coating method for bone tissue engineering. *Colloids Surf B: Biointerfaces* 170:421–429
- Kim I, Lee SS, Bae S et al (2018b) Heparin functionalized injectable cryogel with rapid shape-recovery property for neovascularization. *Biomacromolecules* 19:2257–2269
- Kim S, Kim J, Gajendiran M et al (2018c) Enhanced skull bone regeneration by sustained release of BMP-2 in interpenetrating composite hydrogels. *Biomacromolecules* 19:4239–4249
- Kim SH, Thambi T, Giang Phan VH, Lee DS (2020) Modularly engineered alginate bioconjugate hydrogel as biocompatible injectable scaffold for in situ biomineralization. *Carbohydr Polym* 233:115832
- Kirker-Head C (2000) Potential applications and delivery strategies for bone morphogenetic proteins. *Adv Drug Deliv Rev* 43:65–92
- Kitaori T, Ito H, Schwarz EM et al (2009) Stromal cell-derived factor 1/CXCR4 signaling is critical for the recruitment of mesenchymal stem cells to the fracture site during skeletal repair in a mouse model. *Arthritis Rheum* 60:813–823
- Klouda L (2015) Thermoresponsive hydrogels in biomedical applications. *Eur J Pharm Biopharm* 97:338–349
- Kocak G, Tuncer C, Büttin V (2017) pH-responsive polymers. *Polym Chem* 8:144–176
- Koehler KC, Alge DL, Anseth KS, Bowman CN (2013) A Diels–Alder modulated approach to control and sustain the release of dexamethasone and induce osteogenic differentiation of human mesenchymal stem cells. *Biomaterials* 34:4150–4158
- Kolar P, Schmidt-Bleek K, Schell H et al (2010) The early fracture hematoma and its potential role in fracture healing. *Tissue Eng Part B Rev* 16:427–434
- Kondiah PJ, Kondiah PPD, Choonara YE et al (2020) A 3D bioprinted pseudo-bone drug delivery scaffold for bone tissue engineering. *Pharmaceutics* 12:166
- Korde JM, Kandasubramanian B (2019) Fundamentals and effects of biomimicking stimuli-responsive polymers for engineering functions. *Ind Eng Chem Res* 58:9709–9757
- Kossov O, Cohen N, Lewis JA et al (2020) Growth factor delivery for the repair of a critical size tibia defect using an acellular, biodegradable polyethylene glycol–albumin hydrogel implant. *ACS Biomater Sci Eng* 6:100–111
- Kroon J, Buijs JT, van der Horst G et al (2015) Liposomal delivery of dexamethasone attenuates prostate cancer bone metastatic tumor growth in vivo. *Prostate* 75:815–824
- Kuroda Y, Kawai T, Goto K, Matsuda S (2019) Clinical application of injectable growth factor for bone regeneration: a systematic review. *Inflamm Regen* 39:20
- Lanier OL, Ficarrotta JM, Adjei I et al (2020) Magnetically responsive polymeric microparticles for the triggered delivery of a complex mixture of human placental proteins. *Macromol Biosci* 21:e2000249
- Lee HJ, Koh W-G (2014) Hydrogel micropattern-incorporated fibrous scaffolds capable of sequential growth factor delivery for enhanced osteogenesis of hMSCs. *ACS Appl Mater Interfaces* 6:9338–9348
- Lee YJ, Lee J-H, Cho H-J et al (2013) Electrospun fibers immobilized with bone forming peptide-1 derived from BMP7 for guided bone regeneration. *Biomaterials* 34:5059–5069
- Lee F-H, Shen P-C, Jou I-M et al (2015) A population-based 16-year study on the risk factors of surgical site infection in patients after bone grafting: a cross-sectional study in Taiwan. *Medicine* 94:e2034

- Lee SS, Kim JH, Jeong J et al (2020) Sequential growth factor releasing double cryogel system for enhanced bone regeneration. *Biomaterials* 257:120223
- Levengood SKL, Zhang M (2014) Chitosan-based scaffolds for bone tissue engineering. *J Mater Chem B* 2:3161
- Li C, Vepari C, Jin H-J et al (2006) Electrospun silk-BMP-2 scaffolds for bone tissue engineering. *Biomaterials* 27:3115–3124
- Li L, Zhou G, Wang Y et al (2015) Controlled dual delivery of BMP-2 and dexamethasone by nanoparticle-embedded electrospun nanofibers for the efficient repair of critical-sized rat calvarial defect. *Biomaterials* 37:218–229
- Li X, Wang Y, Wang Z et al (2018) Composite PLA/PEG/nHA/dexamethasone scaffold prepared by 3D printing for bone regeneration. *Macromol Biosci* 18:1800068
- Li X, Yin H-M, Luo E et al (2019) Accelerating bone healing by decorating BMP-2 on porous composite scaffolds. *ACS Appl Bio Mater* 2:5717–5726
- Lieb E, Tessmar J, Hacker M et al (2003) Poly(D,L-lactic acid)-poly(ethylene glycol)-monomethyl ether diblock copolymers control adhesion and osteoblastic differentiation of marrow stromal cells. *Tissue Eng* 9:71–84
- Lieberman JR, Daluiski A, Einhorn TA (2002) The role of growth factors in the repair of bone: biology and clinical applications. *J Bone Joint Surg Am* 84:1032–1044
- Linsley CS, Quach VY, Agrawal G et al (2015) Visible light and near-infrared-responsive chromophores for drug delivery-on-demand applications. *Drug Deliv Transl Res* 5:611–624
- Liu X, Li X, Zhou L et al (2013) Effects of simvastatin-loaded polymeric micelles on human osteoblast-like MG-63 cells. *Colloids Surf B: Biointerfaces* 102:420–427
- Liu X, Zhao K, Gong T et al (2014) Delivery of growth factors using a smart porous nanocomposite scaffold to repair a mandibular bone defect. *Biomacromolecules* 15:1019–1030
- Luca L, Rougemont A-L, Walpoh BH et al (2010) The effects of carrier nature and pH on rhBMP-2-induced ectopic bone formation. *J Control Release* 147:38–44
- Luginbuehl V, Meinel L, Merkle HP, Gander B (2004) Localized delivery of growth factors for bone repair. *Eur J Pharm Biopharm* 58:197–208
- Lutolf MP, Weber FE, Schmoekel HG et al (2003) Repair of bone defects using synthetic mimetics of collagenous extracellular matrices. *Nat Biotechnol* 21:513–518
- Ma D, An G, Liang M et al (2016) A composited PEG-silk hydrogel combining with polymeric particles delivering rhBMP-2 for bone regeneration. *Mater Sci Eng C* 65:221–231
- Macdonald ML, Samuel RE, Shah NJ et al (2011) Tissue integration of growth factor-eluting layer-by-layer polyelectrolyte multilayer coated implants. *Biomaterials* 32:1446–1453
- Madani SZM, Reisch A, Roxbury D, Kennedy SM (2020) A magnetically responsive hydrogel system for controlling the timing of bone progenitor recruitment and differentiation factor deliveries. *ACS Biomater Sci Eng* 6:1522–1534
- Madhurakkat Perikamana SK, Lee J, Ahmad T et al (2015) Effects of immobilized BMP-2 and nanofiber morphology on in vitro osteogenic differentiation of hMSCs and in vivo collagen assembly of regenerated bone. *ACS Appl Mater Interfaces* 7:8798–8808
- Mak KK, Kronenberg HM, Chuang P-T et al (2008) Indian hedgehog signals independently of PTHrP to promote chondrocyte hypertrophy. *Development* 135:1947–1956
- Maloney W, Jasty M, Rosenberg A, Harris W (1990) Bone lysis in well-fixed cemented femoral components. *J Bone Joint Surg* 72-B:966–970
- Mano JF, Silva GA, Azevedo HS et al (2007) Natural origin biodegradable systems in tissue engineering and regenerative medicine: present status and some moving trends. *J R Soc Interface* 4:999–1030
- Manouras T, Vamvakaki M (2017) Field responsive materials: photo-, electro-, magnetic- and ultrasound-sensitive polymers. *Polym Chem* 8:74–96
- Mao Y, Wang J, Zhao Y et al (2014) A novel liposomal formulation of FTY720 (Fingolimod) for promising enhanced targeted delivery. *Nanomedicine* 10:393–400

- Mariner PD, Wudel JM, Miller DE et al (2013) Synthetic hydrogel scaffold is an effective vehicle for delivery of INFUSE (rhBMP2) to critical-sized calvaria bone defects in rats. *J Orthop Res* 31:401–406
- Marsell R, Einhorn TA (2011) The biology of fracture healing. *Injury* 42:551–555
- Martino MM, Briquez PS, Guc E et al (2014) Growth factors engineered for super-affinity to the extracellular matrix enhance tissue healing. *Science* 343:885–888
- Martino MM, Briquez PS, Maruyama K, Hubbell JA (2015) Extracellular matrix-inspired growth factor delivery systems for bone regeneration. *Adv Drug Deliv Rev* 94:41–52
- Martins A, Duarte ARC, Faria S et al (2010) Osteogenic induction of hBMSCs by electrospun scaffolds with dexamethasone release functionality. *Biomaterials* 31:5875–5885
- Mattson P, Ntezirayo E, Aluisio A et al (2019) Musculoskeletal injuries and outcomes pre- and post-emergency medicine training program. *West J Emerg Med* 20:857–864
- Maturavongsadit P, Paravyan G, Shrivastava R, Benhabbour SR (2020) Thermo-/pH-responsive chitosan-cellulose nanocrystals based hydrogel with tunable mechanical properties for tissue regeneration applications. *Materialia* 12:100681
- Mayr-wohlfart U, Waltenberger J, Hausser H et al (2002) Vascular endothelial growth factor stimulates chemotactic migration of primary human osteoblasts. *Bone* 30:472–477
- Meinel L, Fajardo R, Hofmann S et al (2005) Silk implants for the healing of critical size bone defects. *Bone* 37:688–698
- Meling T, Harboe K, Sørreide K (2009) Incidence of traumatic long-bone fractures requiring in-hospital management: a prospective age- and gender-specific analysis of 4890 fractures. *Injury* 40:1212–1219
- Melnyk M, Henke T, Claes L, Augat P (2008) Revascularisation during fracture healing with soft tissue injury. *Arch Orthop Trauma Surg* 128:1159–1165
- Metselaer JM, Wauben MHM, Wagenaar-Hilbers JPA et al (2003) Complete remission of experimental arthritis by joint targeting of glucocorticoids with long-circulating liposomes. *Arthritis Rheum* 48:2059–2066
- Mickova A, Buzgo M, Benada O et al (2012) Core/Shell nanofibers with embedded liposomes as a drug delivery system. *Biomacromolecules* 13:952–962
- Morochnik S, Zhu Y, Duan C et al (2018) A thermoresponsive, citrate-based macromolecule for bone regenerative engineering: thermoresponsive macromolecule for bone regenerative engineering. *J Biomed Mater Res* 106:1743–1752
- Müller M, Urban B, Reis B et al (2018) Switchable release of bone morphogenetic protein from thermoresponsive poly(NIPAM-co-DMAEMA)/cellulose sulfate particle coatings. *Polymers* 10:1314
- Paidikondala M, Wang S, Hilborn J et al (2019) Impact of hydrogel cross-linking chemistry on the *in Vitro* and *in Vivo* bioactivity of recombinant human bone morphogenetic protein-2. *ACS Appl Bio Mater* 2:2006–2012
- Parameswaran-Thankam A, Parnell CM, Watanabe F et al (2018) Guar-based injectable thermoresponsive hydrogel as a scaffold for bone cell growth and controlled drug delivery. *ACS Omega* 3:15158–15167
- Park H, Temenoff JS, Holland TA et al (2005) Delivery of TGF- β 1 and chondrocytes via injectable, biodegradable hydrogels for cartilage tissue engineering applications. *Biomaterials* 26:7095–7103
- Park J, Lutz R, Felszeghy E et al (2007) The effect on bone regeneration of a liposomal vector to deliver BMP-2 gene to bone grafts in peri-implant bone defects. *Biomaterials* 28:2772–2782
- Patel ZS, Young S, Tabata Y et al (2008) Dual delivery of an angiogenic and an osteogenic growth factor for bone regeneration in a critical size defect model. *Bone* 43:931–940
- Peng H, Wright V, Usas A et al (2002) Synergistic enhancement of bone formation and healing by stem cell-expressed VEGF and bone morphogenetic protein-4. *J Clin Invest* 110:751–759
- Peterson AM, Pilz-Allen C, Kolesnikova T et al (2014) Growth factor release from polyelectrolyte-coated titanium for implant applications. *ACS Appl Mater Interfaces* 6:1866–1871

- Pierschbacher MD, Ruoslahti E (1984) Cell attachment activity of fibronectin can be duplicated by small synthetic fragments of the molecule. *Nature* 309:30–33
- Poh PSP, Woodruff MA, García-Gareta E (2020) Polymer-based composites for musculoskeletal regenerative medicine. In: *Biomaterials for organ and tissue regeneration*. Elsevier, Amsterdam, pp 33–82
- Poldervaart MT, Wang H, van der Stok J et al (2013) Sustained release of BMP-2 in bioprinted alginate for osteogenicity in mice and rats. *PLoS One* 8:e72610
- Ponte AL, Marais E, Gally N et al (2007) The in vitro migration capacity of human bone marrow mesenchymal stem cells: comparison of chemokine and growth factor chemotactic activities. *Stem Cells* 25:1737–1745
- Porto ML, Rodrigues BP, Menezes TN et al (2015) Reactive oxygen species contribute to dysfunction of bone marrow hematopoietic stem cells in aged C57BL/6 J mice. *J Biomed Sci* 22:97
- Prasad K, Bazaka O, Chua M et al (2017) Metallic biomaterials: current challenges and opportunities. *Materials* 10:884
- Puppi D, Chiellini F, Piras AM, Chiellini E (2010) Polymeric materials for bone and cartilage repair. *Prog Polym Sci* 35:403–440
- Qi H, Yang L, Li X et al (2019) Systemic administration of enzyme-responsive growth factor nanocapsules for promoting bone repair. *Biomater Sci* 7:1675–1685
- Rajangam T, An SSA (2013) Fibrinogen and fibrin based micro and nano scaffolds incorporated with drugs, proteins, cells and genes for therapeutic biomedical applications. *Int J Nanomed* 8:3641
- Ramoshebi LN, Matsaba TN, Teare J et al (2002) Tissue engineering: TGF- β superfamily members and delivery systems in bone regeneration. *Expert Rev Mol Med* 4:1
- Ravanti L, Kähäri VM (2000) Matrix metalloproteinases in wound repair (review). *Int J Mol Med* 6:391–798
- Ripamonti U (2006) Soluble osteogenic molecular signals and the induction of bone formation. *Biomaterials* 27:807–822
- Roberts JJ, Naudiyal P, Jugé L et al (2015) Tailoring stimuli responsiveness using dynamic covalent cross-linking of poly(vinyl alcohol)-heparin hydrogels for controlled cell and growth factor delivery. *ACS Biomater Sci Eng* 1:1267–1277
- Salgado AJ, Coutinho OP, Reis RL (2004) Bone tissue engineering: state of the art and future trends. *Macromol Biosci* 4:743–765
- Salvi C, Lyu X, Peterson AM (2016) Effect of assembly pH on polyelectrolyte multilayer surface properties and BMP-2 release. *Biomacromolecules* 17:1949–1958
- Schild HG, Tirrell DA (1990) Microcalorimetric detection of lower critical solution temperatures in aqueous polymer solutions. *J Phys Chem* 94:4352–4356
- Schindeler A, McDonald MM, Bokko P, Little DG (2008) Bone remodeling during fracture repair: the cellular picture. *Semin Cell Dev Biol* 19:459–466
- Schmidmaier G, Wildemann B, Stemberger A et al (2001) Biodegradable poly(D,L-lactide) coating of implants for continuous release of growth factors. *J Biomed Mater Res* 58:449–455
- Schüller-Ravoo S, Feijen J, Grijpma DW (2011) Preparation of flexible and elastic poly(trimethylene carbonate) structures by stereolithography. *Macromol Biosci* 11:1662–1671
- Seeherman H, Wozney JM (2005) Delivery of bone morphogenetic proteins for orthopedic tissue regeneration. *Cytokine Growth Factor Rev* 16:329–345
- Shah NJ, Macdonald ML, Beben YM et al (2011) Tunable dual growth factor delivery from polyelectrolyte multilayer films. *Biomaterials* 32:6183–6193
- Shah SR, Werlang CA, Kasper FK, Mikos AG (2015) Novel applications of statins for bone regeneration. *Natl Sci Rev* 2:85–99
- Shi R, Huang Y, Ma C et al (2019) Current advances for bone regeneration based on tissue engineering strategies. *Front Med* 13:160–188
- Singh RS, Kaur N, Rana V, Kennedy JF (2016) Recent insights on applications of pullulan in tissue engineering. *Carbohydr Polym* 153:455–462

- Sivashanmugam A, Charoenlarp P, Deepthi S et al (2017) Injectable shear-thinning CaSO₄/FGF-18-incorporated chitin-PLGA hydrogel enhances bone regeneration in mice cranial bone defect model. *ACS Appl Mater Interfaces* 9:42639–42652
- Su Y, Su Q, Liu W et al (2012) Controlled release of bone morphogenetic protein 2 and dexamethasone loaded in core-shell PLLACL-collagen fibers for use in bone tissue engineering. *Acta Biomater* 8:763–771
- Subbiah R, Cheng A, Ruehle MA et al (2020) Effects of controlled dual growth factor delivery on bone regeneration following composite bone-muscle injury. *Acta Biomater* 114:63–75
- Tao F, Cheng Y, Shi X et al (2020) Applications of chitin and chitosan nanofibers in bone regenerative engineering. *Carbohydr Polym* 230:115658
- Teotia AK, Raina DB, Singh C et al (2017) Nano-hydroxyapatite bone substitute functionalized with bone active molecules for enhanced cranial bone regeneration. *ACS Appl Mater Interfaces* 9:6816–6828
- Teotia AK, Diemel K, Qayoom I et al (2020) Improved bone regeneration in rabbit bone defects using 3D printed composite scaffolds functionalized with Osteoinductive factors. *ACS Appl Mater Interfaces* 43:48340–48356
- Thompson EM, Matsiko A, Farrell E et al (2015) Recapitulating endochondral ossification: a promising route to *in vivo* bone regeneration: recapitulating endochondral ossification for bone regeneration. *J Tissue Eng Regen Med* 9:889–902
- Tian H, Du J, Wen J et al (2016) Growth-factor nanocapsules that enable tunable controlled release for bone regeneration. *ACS Nano* 10:7362–7369
- Veronese FM (2001) Peptide and protein PEGylation. *Biomaterials* 22:405–417
- Vo TN, Kasper FK, Mikos AG (2012) Strategies for controlled delivery of growth factors and cells for bone regeneration. *Adv Drug Deliv Rev* 64:1292–1309
- Vogus DR, Krishnan V, Mitragotri S (2017) A review on engineering polymer drug conjugates to improve combination chemotherapy. *Curr Opin Colloid Interface Sci* 31:75–85
- Wang W, Yeung KWK (2017) Bone grafts and biomaterials substitutes for bone defect repair: a review. *Bioactive Mater* 2:224–247
- Wang D, Miller S, Sima M et al (2003) Synthesis and evaluation of water-soluble polymeric bone-targeted drug delivery systems. *Bioconjug Chem* 14:853–859
- Wang S, Oommen OP, Yan H, Varghese OP (2013) Mild and efficient strategy for site-selective aldehyde modification of Glycosaminoglycans: tailoring hydrogels with tunable release of growth factor. *Biomacromolecules* 14:2427–2432
- Wang Q, Jiang J, Chen W et al (2016) Targeted delivery of low-dose dexamethasone using PCL-PEG micelles for effective treatment of rheumatoid arthritis. *J Control Release* 230:64–72
- Wang X, Shao J, Abd El Raouf M et al (2018) Near-infrared light-triggered drug delivery system based on black phosphorus for *in vivo* bone regeneration. *Biomaterials* 179:164–174
- Wang Y, Cui W, Zhao X et al (2019) Bone remodeling-inspired dual delivery electrospun nanofibers for promoting bone regeneration. *Nanoscale* 11:60–71
- Wang C, Huang W, Zhou Y et al (2020) 3D printing of bone tissue engineering scaffolds. *Bioactive Mater* 5:82–91
- Wang C, Lai J, Li K et al (2021) Cryogenic 3D printing of dual-delivery scaffolds for improved bone regeneration with enhanced vascularization. *Bioactive Mater* 6:137–145
- Wei M, Gao Y, Li X, Serpe MJ (2017) Stimuli-responsive polymers and their applications. *Polym Chem* 8:127–143
- Weiss RE, Singer FR, Gorn AH et al (1981) Calcitonin stimulates bone formation when administered prior to initiation of osteogenesis. *J Clin Invest* 68:815–818
- Wen J, Anderson SM, Du J et al (2011) Controlled protein delivery based on enzyme-responsive Nanocapsules. *Adv Mater* 23:4549–4553
- Wu C, Chang J (2012) Mesoporous bioactive glasses: structure characteristics, drug/growth factor delivery and bone regeneration application. *Interface Focus* 2:292–306

- Wu C, Ramaswamy Y, Zhu Y et al (2009) The effect of mesoporous bioactive glass on the physiochemical, biological and drug-release properties of poly(dl-lactide-co-glycolide) films. *Biomaterials* 30:2199–2208
- Wu C, Fan W, Chang J, Xiao Y (2013) Mesoporous bioactive glass scaffolds for efficient delivery of vascular endothelial growth factor. *J Biomater Appl* 28:367–374
- Wu L, Gu Y, Liu L et al (2020) Hierarchical micro/nanofibrous membranes of sustained releasing VEGF for periosteal regeneration. *Biomaterials* 227:119555
- Xiao Y, Gong T, Jiang Y et al (2019) Controlled delivery of recombinant human bone morphogenetic protein-2 by using glucose-sensitive core-shell nanofibers to repair the mandible defects in diabetic rats. *J Mater Chem B* 7:4347–4360
- Xinluan W, Yuxiao L, Helena N et al (2015) Systemic drug delivery systems for bone tissue regeneration—a mini review. *Curr Pharm Des* 21:1575–1583
- Xu M-M, Liu R-J, Yan Q (2018a) Biological stimuli-responsive polymer systems: design, construction and controlled self-assembly. *Chin J Polym Sci* 36:347–365
- Xu X-L, Li W-S, Wang X-J et al (2018b) Endogenous sialic acid-engineered micelles: a multifunctional platform for on-demand methotrexate delivery and bone repair of rheumatoid arthritis. *Nanoscale* 10:2923–2935
- Yamano S, Haku K, Yamanaka T et al (2014) The effect of a bioactive collagen membrane releasing PDGF or GDF-5 on bone regeneration. *Biomaterials* 35:2446–2453
- Yan M, Du J, Gu Z et al (2010) A novel intracellular protein delivery platform based on single-protein nanocapsules. *Nature Nanotechnol* 5:48–53
- Yan Y, Chen H, Zhang H et al (2019) Vascularized 3D printed scaffolds for promoting bone regeneration. *Biomaterials* 190–191:97–110
- Yang X, Ricciardi BF, Hernandez-Soria A et al (2007) Callus mineralization and maturation are delayed during fracture healing in interleukin-6 knockout mice. *Bone* 41:928–936
- Yang F, Wang J, Cao L et al (2014) Injectable and redox-responsive hydrogel with adaptive degradation rate for bone regeneration. *J Mater Chem B* 2:295–304
- Yao C, Lai Y, Chen Y, Cheng C (2020) Bone morphogenetic protein-2-activated 3D-printed Poly(lactic acid) scaffolds to promote bone regrowth and repair. *Macromol Biosci* 20:2000161
- Yilgor P, Sousa RA, Reis RL et al (2010) Effect of scaffold architecture and BMP-2/BMP-7 delivery on in vitro bone regeneration. *J Mater Sci Mater Med* 21:2999–3008
- Yu YY, Lieu S, Lu C et al (2010) Immunolocalization of BMPs, BMP antagonists, receptors, and effectors during fracture repair. *Bone* 46:841–851
- Yu X, Tang X, Gohil SV, Laurencin CT (2015) Biomaterials for bone regenerative engineering. *Adv Healthc Mater* 4:1268–1285
- Yuasa M, Yamada T, Taniyama T et al (2015) Dexamethasone enhances osteogenic differentiation of bone marrow- and muscle-derived stromal cells and augments ectopic bone formation induced by bone morphogenetic protein-2. *PLoS One* 10:e0116462
- Zhai P, Peng X, Li B et al (2020) The application of hyaluronic acid in bone regeneration. *Int J Biol Macromol* 151:1224–1239
- Zhang Z, Lai Q, Li Y et al (2017) Acidic pH environment induces autophagy in osteoblasts. *Sci Rep* 7:46161
- Zisch AH, Lutolf MP, Ehrbar M et al (2003) Cell-demanded release of VEGF from synthetic, biointeractive cell-ingrowth matrices for vascularized tissue growth. *FASEB J* 17:2260–2262



Surface Engineering of Polymeric Materials for Bone Tissue Engineering **14**

Asif Ali, Nikhil Ram Patra, Anushree Pandey, and Yuvraj Singh Negi

Abstract

Bone substitutes are under constant research since decades due to persistent cases of accidental trauma, aging, sports injuries, and surgical interventions affecting quality and length of human life. A bone has a vascular matrix with hard connective tissues and serves as exoskeleton for protecting visceral organs of the body. It possesses regenerating potential throughout the life of an individual and plays a key role in the production of blood cells, locomotion, and providing a posture and aesthetic look to the body. Delay and failure of the self-repair process in large bone defects necessitate the understanding of cell–matrix interactions required for tissue formation. Compliance and health issues associated with autologous bone graftings like pain, shortage of donor site, and limitation of special shape and multiple surgeries have motivated the search for artificial bone substitute. One such attempt being made is the development of artificial extracellular matrix (ECM) for bone growth. These porous matrices act as templates for cell attachment, proliferation, and differentiation of cells, and organize them into functional tissues. The chapter covers the strategies involved in the development and engineering of extracellular matrix which can elicit new bone formation on the target site avoiding unnecessary complications.

Keywords

Surface modification · Bone regeneration · Surface patterning · Chemical treatment · Mechanical cues · Polymeric implants

A. Ali · N. R. Patra · A. Pandey · Y. S. Negi (✉)

Department of Polymer and Process Engineering, Indian Institute of Technology, Roorkee, Uttarakhand, India

e-mail: ynegifpt@iitr.ernet.in

© The Author(s), under exclusive license to Springer Nature Singapore Pte Ltd. 2022

L. M. Pandey, A. Hasan (eds.), *Nanoscale Engineering of Biomaterials: Properties and Applications*, https://doi.org/10.1007/978-981-16-3667-7_14

397

14.1 Introduction

Bone serves as a strong framework of the body that not only assists in locomotion and protection of visceral organs but also produces multiple progenitor blood cells and helps in homeostasis by storing Ca and P ions. Bone diseases account for more than half of the population above 50 years of age (Chahal et al. 2019). Despite the inherent healing tendency of natural bone large segmental bone defects aroused due to bone tumor resection, accidental injuries and aging cannot be accomplished without any assistive therapy, which may involve surgical intervention and implantation. Right from earlier century, materials such as wood, corals, shells, and several metals (gold, silver, and amalgam) were used to correct defects arising from missing human aesthetic and functional parts such as teeth and bones; however, alternative materials of ancient times were mostly bioinert (biologically inert) and interacted less with the surrounding tissues. The materials were even toxic to humans. Complications that arose due to microbial infections or implant failure resulted in compliance issues affecting quality and length of life.

Though autologous grafting is regarded as the gold standard of treatment but morbidity, lack of desirable shape and size of bone is one of the major challenges (Qu et al. 2019). This creates the need for artificial bone substitute which can sustain cyclic load in dynamic conditions without undergoing fatigue failure. Unlike infinite loading cycles exhibited by native tissue, artificial substitutes have limited life and start to deteriorate with respect to environmental changes, time, and repeated stress; hence, a search for a strategy which can fill the gap with the natural counterpart by engineering the extracellular matrix with/without assistance of biochemical and biomechanical signals and harvested cells became a possible hope and a thrust area for research in the field of bone tissue engineering. Degradable polymer matrix with cell proliferation ability can be the best susceptible technique for the growth of natural bone tissue that can restore the lost one by allowing the growth of natural tissue construct. These matrices behave as temporary biological scaffold or growth template which allow the cell to crawl and proliferate through the mechanical framework and integrate into functional tissue (Hasan et al. 2017). Scaffold directs the growth of new bone cells, promotes angiogenesis, and invokes attachment of cells to nearby intrinsic tissues followed by degradation. The main aim behind bone scaffold is to mimic the structural and mechanical properties of cancellous bone as close as possible. An ideal scaffold must be (a) bioresorbable/biodegradable; (b) good mechanical and chemical properties and stability; and (c) good adhesion, migration, and differentiation capability with the cells. It must also possess optimum pore size and interconnected pore morphology to allow proper diffusion of nutrients and metabolites, synchronized degradation with growing tissues, nontoxic degradation product, sterilizable, and good mineralization tendency. Since last decades biodegradable natural-based polymers (collagen, silk, alginate, chitosan, hyaluronic acid) and synthetic polymers (poly(lactic acid): PLA, poly(glycolic acid): PGA, poly(lactic-*co*-glycolide): PLGA, poly(*ε*-caprolactone): PCL, polyhydroxyalkanoates: PHA) are widely been studied for exploring an ideal biomedical substitute. These polymer matrices are modified in various ways to further improve the properties and

overcome the shortcomings to be best suited as a tissue engineering construct. The modification may range from surface functionalization, processing methods to hybridized composites. Some of the recent trends involve the application of conductive polymers (CPs), inducers (signaling molecules), and mechanical signals (elastic polymer networks such as hydrogels) for three-dimensional (3D) bone tissue engineering construct.

A bone structure has a complex hierarchy ranging from components in macro- to nanoscale. It consists mainly of hydroxyapatite (HA) and collagen which accounts for a total of 95% of bone mass in dry conditions. The inorganic minerals present in bone such as calcium, phosphate, carbonate, and hydroxyl salts also increase the mechanical strength and osteoconductivity of the bone. The organic component consists of interwoven collagen fibers within a hydrated network of glycosaminoglycans (GAG) chains. The structure acts as a frame and provides mechanical strength to the network fibrils. The stoichiometric composition of natural biological apatites varies due to the presence of certain amounts of impurities such as Mg^{2+} , Na^+ , Cl^- , K^+ , F^- , and Zn^{2+} in the human body. The human skeleton has HA as its major inorganic component. It has two types of bones: (1) Compact bone and (2) trabecular or spongy bone. Compact bone is densely hard solid with some grooves for Haversian canals, osteons, and lamellae. It accounts for 80% of the total bone mass of human skeleton and provides a smooth, white, and solid look to the bone; on the other hand, trabecular bone has interconnected porous network and possesses a high surface-to-bone ratio. Compact bone is stiffer and more robust in longitudinal than transverse section and has 20% higher compressive strength as compared to cancellous bone. Cancellous bone has a compressive strength in the range of 2–12 MPa and elastic modulus of 0.05–0.5 GPa. The mechanical strength of cancellous bone depends upon the distribution of trabeculae. Mechanical properties of bone vary with respect to age and body part and have anisotropic Young's modulus and yield strength (Fig. 14.1).

14.2 Biological Response to Implanted Biomaterial

The body response to implanted biomaterials starts with a cascade of immunological reactions which begins with initial stage of protein adsorption. Surface properties are one of the factors which govern protein adsorption on the matrix. Modifying the surface chemistry of a material results in different protein expression profiles and cytokine responses. Conformational changes in localized proteins at biomaterial interface result in exposure of some masked domains or epitopes, which can then be recognized by immune cells resulting in variation in immunological responses (Chen et al. 2016). Low molecular proteins are first to get attached to the surface followed by one with high molecular weight. Blood proteins such as fibrinogen, fibronectin, vitronectin, and complement system get adsorbed on surface of biomaterials within few seconds forming a transient surface matrix. Activation of complement system and signaling cascade is followed by thrombus formation and activation of other cell populations (Chen et al. 2016). Factor XII (Hageman Factor)

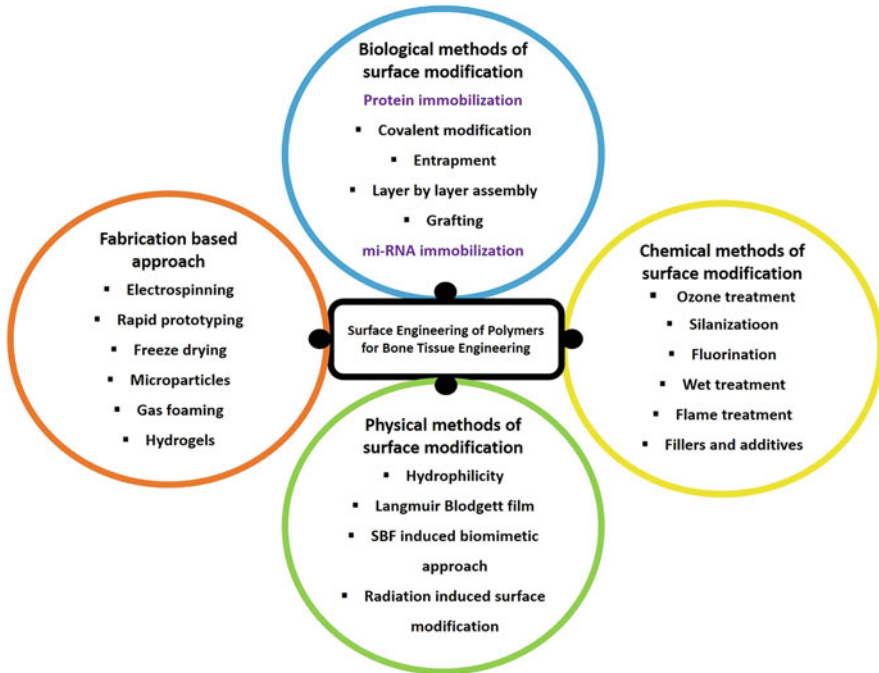


Fig. 14.1 Methodology involved in surface engineering of polymers

and high MW kininogen are the key components triggering thrombus formation. Blood material interaction also triggers inflammatory response with the release and activation of neutrophils or (PMNs). With an effort to degrade the material, polymorphonuclear leucocytes (PMNs) release proteolytic enzymes and reactive oxygen species (ROS) which may corrode or erode a part of material. Though disappearance of PMNs from implantation site within the first 2 days occurs as a result of apoptosis, mast cell degranulation continues to release inflammatory cytokines and histamines which further escalates the immune response (Schindler et al. 2007). Chemokines and chemoattractants recruit the monocytes to implant surfaces where they differentiate themselves into macrophages. These macrophages phagocytize particles released from biomaterial interface; if the particle size is greater than the optimum size for engulfing, the macrophages coalesce to form foreign body giant cells (FBGC) to remove the particulate antigen. These macrophages are classified into M1 and M2 phenotypes based on surface markers. M1 macrophages are known as proinflammatory macrophages that appear during initial response and secrete inflammatory cytokines; however, activated M2 macrophages govern late stages of the tissue repair process, leading to the formation of either new bone or fibrous capsule, by secretion of relevant cytokines (Mills et al. 2000). There is switching between M1 and M2 macrophages during the entire healing process (Mosser and Edwards 2008). The switching pattern decides the acceptance or rejection of implants or suitability of

biomaterial for cellular proliferation or fibrous encapsulation. Excessive switching of M1 leads to prolonged inflammatory response, while excessive switching of M2 leads to a scar or delayed wound healing response. Hence, there exists a balance and synchronized switching pattern between the two phenotypes for proper tissue regeneration.

14.3 Fabrication-Based Surface Engineering

14.3.1 Electrospinning

Electrospinning is a technique of fabricating fibrous nonwoven mat of polymer solution with fiber diameter in the nano range. It is a solution-based approach and relies on the electrostatic repulsion between surface charges to form nanofibers. The technique involves extrusion of viscoelastic polymer through a stainless-steel needle under high voltage. A variety of natural and synthetic biomaterials can be aligned into fibrous architecture resembling natural extracellular matrix (ECM) such as chitosan, collagen, PVA, and PLA. They also mimic the biological function of ECM and acts as template for cell proliferation and differentiation (Bianco et al. 2009). Cell morphology, attachment tendency, function, and physiological response depend on the composition and topology of nanofibers. High aspect ratio nanofillers such as cellulose nanocrystals (CNC), carbon nanotube (CNT), and silver nanorods can easily be aligned during electrospinning giving the product superior mechanical, electrical, and thermal properties. The properties of electrospun composite largely depend upon the nature and concentration of filler used. Electrospun fabrics incorporated with bioresorbable and bioactive fillers account for higher cell proliferation and differentiation (Okamoto and John 2013). The electrospun mat of poly (3-hydroxybutyrate-co-3-hydroxyhexanoate)/silk supported differentiation and proliferation of human umbilical cord-derived mesenchymal stem cells (hUC-MSC) (Ling et al. 2020). Consistent release of vitamin D3 for 30 days was observed from PCL/Gel/nanoHAp/D3 composite electrospun mat and demonstrated synergistic response of nanoHA and D3 in mineralization, osteoconductivity, and differentiation of stem cells (Sattary et al. 2019).

14.3.2 3D Printing

It is a computer-aided fabrication technology, which can make objects achieve rapid and seamless transition between a computer model and the physical product. It is a highly precise way of fabricating scaffolds with controlled pore size and pore wall thickness. Various methods and printing materials are used in conventional AM, such as stereolithography (SLA), fused deposition modeling (FDM), selective laser sintering (SLS), power-based 3D printing, 3D printing, extrusion deposition, and 3D bioprinting. There exists very fewer differences between 3D printed and CT imaged model. It promotes enhanced productivity in a cost-effective way. 3D bioprinting

technology has an edge over other fabrication technologies. It incorporates cells, growth factors, and biomaterials all together as bioink in a printer cartridge and proceeds by layer-by-layer deposition approach to generate tissue-like three-dimensional construct. It uses photopolymerization to crosslink deposited ink layer according to a computer design program. The technique has accuracy in the construction of complex geometries of both hard and soft tissues such as multilayered skin, bone, myocardium, tracheal splint, cartilage, and neuron. Multicomponent composite is also fabricated easily by this technique. PCL/Gel/bacterial cellulose/0.25%HAp were successfully printed with uniform pore dimensions and demonstrated significant osteoconductive potential (Cakmak et al. 2020).

14.3.3 Hydrogels

Hydrogels are three-dimensional network of water-absorbing polymeric material with highly flexible hydrophilic chains. They also can serve as ECM for tissue engineering construct.

They have the potential for delivery of drugs and growth factors in both in vivo and in vitro cases depending upon the nature of molecule and site of action. They can be synthesized from both natural and synthetic polymers. Besides conventional 3D gel structure hydrogel microbeads, nanogel, hydrogel, nanofibers, and injectable hydrogel system are some other physical forms of hydrogel used in bone tissue engineering (Bai et al. 2018). Fabrication involves use of both physical and chemical techniques such as warming, stirring, coacervation, chemical crosslinking, radiation crosslinking, and gelation of polyelectrolyte complex with oppositely charged ions. Encapsulation of cells by hydrogel provides hydrated environment for cellular growth and proliferation. Biological properties of hydrogels can be tuned either by functionalizing the matrix chemically or by biological peptides such as arginine–glycine–aspartic (RGD), incorporating growth factors, drugs, bioactive ceramics, or antimicrobial compounds.

14.3.4 Microparticles

Porous microparticles are usually deployed in biomedical field as drug delivery vehicles or transportation of growth factors in a controlled fashion for site-specific delivery systems. They were initially developed for the delivery of anticancer drugs, but due to advancement in research there was a paradigm shift in their applications and eventually, they made their way for tissue regenerations. They gained importance for their use as an injectable scaffold. Scaffold-based porous microparticles provide a unique overlap between tissue engineering and drug delivery system.

14.3.5 Gas Foaming

This method involves bubbling inert gas into a precursor polymer solution for the transformation of liquid into porous foam. Powder foaming is one of the alternative techniques of foaming within polymer solution, where the dissolved powder chemically reacts with another component of solution to produce foam. This foam gets entrapped by the solution and lyophilized to get well-defined porous morphology. The drawback of gas foaming is lack of precise control over the morphology of the scaffold. Composites of various synthetic polymers such as polyurethane have been fabricated by this process with a library of fillers including bioactive and bioresorbable ceramics to improve properties and make the matrix best susceptible for bone tissue engineering application.

14.3.6 Freeze-Drying

Lyophilization or freeze-drying is a low-temperature dehydration process that involves the removal of ice by freezing the product at low pressure followed by sublimation (Fig. 14.2). It is regarded as standard experimental method for removing solvents or volatile organic residues. It is also considered to be a versatile method to achieve the plasticity of materials. The pores formed in matrix are replica of the ice crystals developed prior to sublimation. The interconnected pore morphology and irreversible change in microstructure of matrix prompt researchers to use the matrix as bone tissue supporting construct. The average size of pores in porous architecture

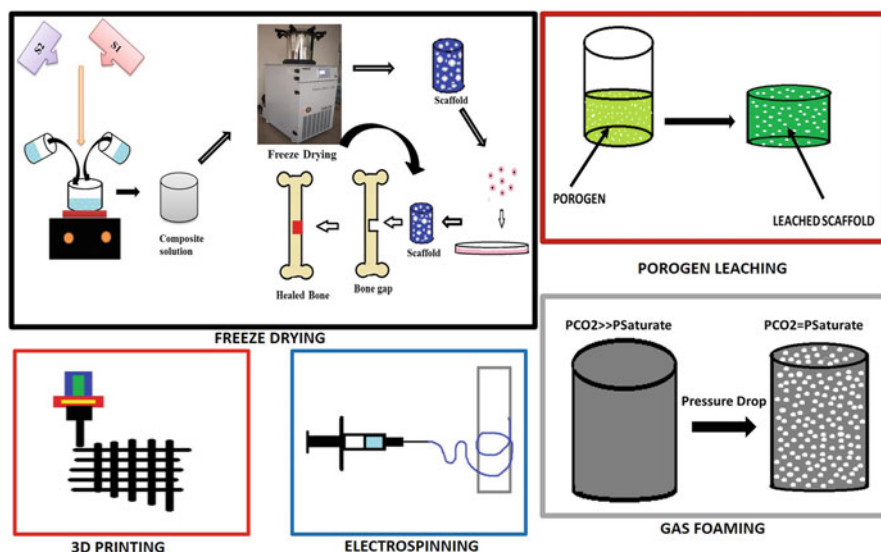


Fig. 14.2 Major processing techniques for fabrication of scaffolds

mostly used for bone tissue engineering range from 100 to 300 μm . The mechanical, biological, and morphological properties of freeze matrix are usually tuned by varying types and concentrations of fillers.

14.4 Response to Mechanical Stimulus

Cells not only adhere to the matrix but actively interact with their mechanical signals and remodel their cytoskeletal network accordingly. Mechanical stimuli exhibited by surface characteristics of biomaterial regulate the cellular behavior through structural ligands, signaling peptides, proteases, and inhibitors. Cell response, according to the contractile force sensed by them, depends upon stiffness and state of polymer in stress and normal condition (Shi et al. 2016). Tuning the mechanical properties and surface characteristics of polymer results in the transduction of different force signals to cells, thus increasing or reducing cellular response. Bone marrow-derived mesenchymal stem cells (BMSC) have been reported to undergo neurogenesis and osteogenesis on soft and stiff substrates, respectively. Elasticity-dependent adhesion eventually leads to changes in cell morphology, migration, gene expression, and subsequent functions (Guilak et al. 2009). It also regulates proliferation and apoptosis. Stiff substrate shows lower apoptosis than soft ones (Kong et al. 2005). Rigid surfaces also provoke strong cell adhesion tendency. In substrates with gradient elasticity, the stronger contraction is generated on a more rigid region, thereby directing the movement of cells toward such region. Differentiation is also tuned by elasticity. It also varies with rigidity of substrate but within defined elastic range. Cells differentiate easily with similar elasticity of substrate as native tissues.

14.5 Surface Topography

Cell polarity is one of the factors which regulates organogenesis, and its disruption leads to pathological conditions including metastatic malignancy (Zhang et al. 2018). It is highly influenced by the surface topography of a material. The nano and microscopic geometry in topography are decisive factors affecting the spreading, shape, spatial arrangement, and functions of cells. Nanotopographical cues impact the most either by elongating or aligning the cells parallel to the pattern or in a favorable direction (Fig. 14.3). Nanogrooves such as nanopits and nanopost affect filopodia formation and spreading of cells depending on the distribution, density, and size of nanogrooves (Zhang et al. 2018). Uniform and well-spread mesenchymal stem cells (MSC) undergo osteogenic differentiation easily than nonuniform growth. Substrates with nanogratings have been reported to accelerate cell adhesion and migration. Rectangular pattern with a higher aspect ratio and pentagonal pattern with subcellular concave regions have been reported to readily promote osteogenic differentiation of MSCs. Polymer scaffolds with microgrooves in radial arrangement were reported to facilitate guided osteoblast recruitment and enhanced bone repair. Surface topography of scaffold is also tuned by nanofiller

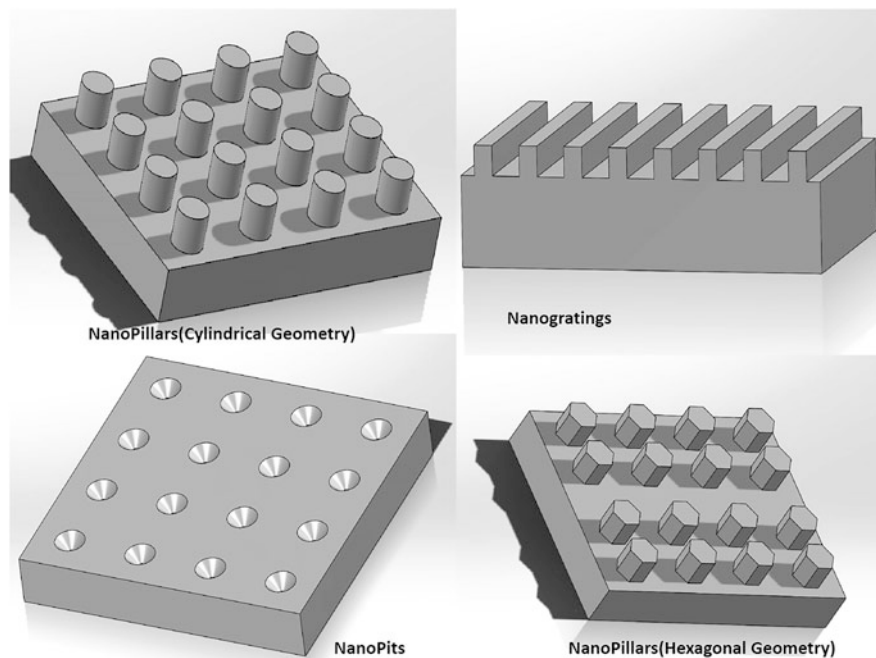


Fig. 14.3 Typical forms of patterned cues

addition. Nanofillers have been reported to alter the surface roughness of pore walls which further regulates the cell adhesion and proliferation process in scaffold matrix (Ali et al. 2019, 2020). Contractile force of cells is one of the essential factors governing migration and proliferation of cells in a three-dimensional porous matrix. Variation in distribution of nanofillers generates patterns of mechanical stimulus which modulates intercellular forces. The upregulation of contractile forces results in an increase in the turnover of focal adhesion proteins such as zyxin, vinculin, talin, and paxillin (Giudicessi et al. 2008).

Nanotopography has been known to affect the proliferation of human embryonic stem cells (hESC). Stem cells growing on nanofibrillar scaffolds have enhanced Nanog expression and activated phosphoinositide 3-kinase which is responsible for higher self-renewal tendency of stem cells. Laser-generated nanopattern on polymer substrate has been reported to activate β -catenin gene responsible for high cell proliferation tendency of endothelial cells (Scherthner et al. 2012). Nanotopographical surfaces are reported to promote differentiation of stem cells, particularly into osteogenic lineage when used in combination with osteogenic medium (Ma et al. 2007; You et al. 2010). Differentiation of cells is not only influenced by the width of the pattern but depth of the pattern too (Zouani et al. 2012). They are also utilized for the formation of multicellular structure with enhanced functionality. Cells cultured on microcantilevers exhibited anisotropic

actin organization and had 65–85% higher contractile force compared with flat surfaces (Patel et al. 2011). Photolithography and electron beam lithography are commonly used techniques in the formation of nanopatterns of polymer surface.

14.6 Hydrophilicity

Hydrophilicity is one of the major factors governing protein adsorption in polymer matrix. Hydrophobic surface favors adsorption of protein on the surface of biomaterial, while hydrophilic surfaces may restrict protein binding. The strong attachment of protein on the surface of hydrophobic materials might denature the protein's native conformation and bioactivity. Water adhesion tension (τ°) of a surface determines the hydrophilicity of a material. Vogler established the relation between aqueous adhesion tension and contact angle of liquid and represented it as $\gamma^\circ = \gamma \cos \theta$, where γ is the surface tension of water. Materials with a contact angle greater than 65 were regarded as hydrophobic and surfaces less than that are considered hydrophilic (Matlaga et al. 1976). So both cases of extreme hydrophilic and hydrophobic are not favorable for cell attachment; instead surfaces with moderate wettability absorb requisite amount of protein and hence elicit cell response avoiding unnecessary risk of conformational changes in adsorbed protein that may trigger immune response. Several methods are employed for improving hydrophilicity of hydrophobic materials to tune their surface in a direction of getting cellular response. One such measure is plasma treatment which can attach hydroxyl, amino, carboxyl, and sulfate groups using various reactive gases. Another method is grafting hydrophilic polymer on polymer substrate via grafting copolymerization. The introduction of peroxide group in polymer matrix can be used to initiate grafting polymerization under UV irradiation. Adjusting photo-oxidation time and grafting time of polymer, density of the attached hydrophilic group can easily be tuned. Usually, hydrophilic polymers such as poly(hydroxyethyl methacrylate) (HEMA) and poly(acrylamide) are grafted over hydrophobic polymers such as polyurethane, polycaprolactone, polymethyl methacrylate, and polylactic acid to introduce hydrophilic nature. Hydrophobic materials have been reported to invoke more monocyte adhesion in respect to hydrophilic materials resulting in a heightened local immune reaction. On the contrary, hydrophilic surfaces have been reported to inhibit macrophage adhesion and fusion into FBGCs (Ma et al. 2007).

14.7 Microcontact Printing

It is a soft lithography technique developed by Whiteside's group which translates topographical pattern into chemical patterns on the biomaterial surface. Substance to be printed (such as proteins) is coated on polydimethylsiloxane (PDMS) stamp with desired pattern. The stability of micropatterned substrate relies on the interaction between adsorbed protein and hydrophobic surfaces or chemical linkages between metallic surface and desired group. It is an effective step in regulating cellular

responses such as cellular orientation, attachment, and proliferation. This technique combines with self-assembly monolayer (SAM) to prepare surfaces with a precise physical or chemical pattern. Rectangular islands of laminin and fibronectin on gold substrate or honeycomb pattern of polylysine on borosilicate glass are some of the examples of this technology (Ma et al. 2007).

14.8 Surface Charge

Charge on the matrix surface is responsible for affinity-based binding approach for biomolecules and proteins. Electrostatic interaction or ligand–receptor pairing is used to immobilize bioactive molecules on the surface of polymer for desirable biomedical applications such as drug delivery and tissue construct. Polymers having cationic nature trigger higher inflammatory response than anionic and neutral ones. Since the majority of body cells are negatively charged, loss of negative surface charge of mammalian body cells by positively charged polymeric surface may induce localization and conformational changes in protein which trigger immunological responses.

- The presence of negatively charged COOH group on the surface of biomaterials enhances fibrinogen and albumin adsorption and increased cell proliferation tendency; however, it exhibits density or concentration-dependent behavior (Vladkova 2010). The presence of extra negatively charged COOH group on surface inhibits cell adhesion.
- OH groups are one of the most abundant functional groups present on surface of biomaterial even on neutral hydrophilic surfaces. Adsorption of fibronectin on surface of polymer containing OH as functional group exhibited increased cell attachment tendency and increased level of vital signaling components responsible for focal adhesion (Abraham et al. 2001).
- Amine (NH₂) group imparts +ve charge to the polymer surface. The presence of amine group resulted in increased proliferation, differentiation, and mineralization of osteoblast cells (Lee et al. 1997). Fibronectin adsorbed on amine-treated surfaces activates target receptors and focal adhesion components.
- Methyl group forms a major component of commonly used biomaterials. The presence of methyl and similar groups makes surface hydrophobic and hence accounts for increased protein adsorption via hydrophobic–hydrophobic interaction between their moieties. However, stronger interaction results in alteration in the conformation of proteins and hence denaturation leading to unfavorable cellular response (Barbosa et al. 2006). Tight binding of proteins of such magnitude also exposes protein sites favorable to immune cells (De Geyter et al. 2013). Surface functionalization by CH₃ has been reported to increase the thickness of fibrous capsule formed on implant surface leading to higher number of inflammatory cells as compared to COOH and OH groups.

14.8.1 Langmuir–Blodgett Film

Langmuir–Blodgett films are formed by depositing organized monolayer of molecules on a solid substrate. Polymer surfaces possess functional groups that help them to be homogeneously and physically coated with amphiphiles using the Langmuir–Blodgett process (De Geyter et al. 2013). Substrate to be coated is dipped into the solution containing coating component and lifted up slowly. Transfer of material from liquid to solid phase is performed by dip and dry technique at the liquid–air interface. Such type of interaction and assembly is achieved by the impact of various forces such as ionic, intermolecular, and capillary action. The amphiphiles used for coating have a surfactant structure with hydrophilic head groups and hydrophobic tails. When a drop of amphiphilic molecule is added in water, the molecules organize themselves at the air–water interface with polar head groups toward the water while hydrophobic tail outside. Due to repulsive effect of hydrophobic groups toward each other, a perfectly ordered deposition of floating liquid monolayer was observed at liquid surface. The organized monolayer adheres to the biomaterial surface depending upon the electrostatic interaction between the molecules and charged substrate. This deposited Langmuir film has opportunities for multilayer structure by successive deposition of a single layer in stacked arrangement of head-to-head and tail-to-tail configuration.

14.9 Biomimetic Approach for Surface Modification

Biomimetic approach of surface modification involves soaking a 3D polymeric construct in simulated body fluid. Mineralizing scaffold before implantation can improve the osteoconductive behavior and alkaline phosphatase (ALP) activity of seeded cells. It also increases the mechanical strength of scaffold; however, the variation in mechanical strength depends upon the rate of mineralization of scaffolds. Several attempts have been made to enhance the mineralization tendency of scaffold (Kretlow and Mikos 2007). Mineralization tendency of a biomaterial is analyzed in *in vitro* conditions using simulated body fluid (SBF). The ionic concentration of SBF is considered similar to that of human blood plasma under mild physiological conditions. The use of more concentrated SBF accelerates the mineralization process (Kretlow and Mikos 2007). Collagen I has been added to 5× SBF to make biomimetic collagen apatite that closely mimics the natural bone surface. Albumin incorporation in SBF also leads to increased calcification due to enhanced nucleation rate. The mineral phase of deposited apatite on the scaffold surface has a tendency to adsorb protein from the surrounding environment and increase the osteoinductive nature of the material. Negatively charged groups like dihydrogen phosphate (PO_4H_2) and carboxylic acid (COOH) that proved to be the most potent inducer of mineralization on the contrary methyl group (CH_3) monolayer have negligible mineralization tendency (Stephansson et al. 2002). Mineralized monolayer exhibits different Ca:P ratios with different crystal morphologies due to variation in the surface charge. *In vivo* mineralization of scaffold is the result of

interaction between fibronectin and charged functional groups, the conformation of which induces integrin binding by osteoblast cells and subsequently mineral deposition.

Chemically incorporating anionic species on the polymeric matrix is one of the strategies to enhance mineralization tendency. Incorporating negatively charged carboxymethyl groups confers higher mineralization in SBF and cell spreading *in vitro* than parent samples (Filmon et al. 2002). Patterning of anionic group on polymer surface accounts for selective orientation and localization of deposited minerals and selective binding of cells. Hydrolysis of scaffold is another strategy to chemically modify surface groups and to introduce anionic entities. Urea and sodium hydroxide-mediated hydrolysis are the most common hydrolysis techniques used for modification. Attaching alkaline phosphatase (ALP) to hydrogels exhibited higher mineralization tendency even that of anionic carboxyl group proving its role in mineralization. One of the biological approaches involves incorporating bone sialoproteins in the matrix (Hunter et al. 2001). Another strategy involves the creation of native or near-native ECM on the scaffold surface by osteoblast under static culture condition in a bioreactor. Culture-generated ECM contains native bone proteins such as BMP-2, VEGF, TGF- β 1, and FGF₂ and promoted cellular proliferation, differentiation, and mineralization, thereby increasing the efficacy of tissue engineering constructs (Gomes et al. 2006; Pham et al. 2006). Phosphate-containing anionic functional groups are the most effective mineral depositing functional groups on polymer surface. They stabilize the interaction of calcium ions over the surface. Even polymer containing pendant phosphorus group or phosphonate side groups mineralize faster than without it (Stancu et al. 2004). Scaffold incorporated with HA or tricalcium phosphate (TCP) as a filler accelerates mineral deposition. Polyethylene glycol (PEG) hydrogels containing phosphodiester backbone show mineralization which is induced in two ways, one of which is over a course of degradation and the other is the release of phosphate by diffusion. It is to be noted that not all the phosphorus-containing polymers show mineralization in comparison to phosphorus-deficient entity. Polymer processing techniques also tune the morphology of the mineral phase and thereby affect the immune response and bone healing capability.

14.10 Effect of Incorporation of Ions

- (a) Calcium (Ca) is an important ingredient of calcium phosphate found in mineralized form or as a bone apatite inside the bone. It is involved in the regulation of signaling pathway associated with the inflammatory response. The noncanonical Wnt5A/Ca²⁺ signal transduction pathway elicits inflammatory response and stimulates macrophage to secrete proinflammatory prostaglandins (De 2011). Extracellular calcium released from bone modulates immune response by regulating hormone-based receptors. It forms an important component of bioactive and bioresorbable ceramics such as HA and β TCP, respectively.

- (b) Silicon (Si) is a trace element essential for bone regeneration. It is found at active calcification sites during early mineralization phase of regenerating bone. Lack of Si supplement leads to bone deformities (Carlisle 1970). Aqueous Si has been studied to enhance osteogenic proliferation, differentiation, and production of collagen. A higher level of Si inhibits osteoclast activity and resorption of excess bone. It also triggers immune reactions; however, nano-sized silica particles induce a milder fibrogenic effect than micro-sized.
- (c) Magnesium (Mg) being biodegradable and biocompatible is currently under research as a dopant and filler in 3D construct because of its mechanical similarity to bone. Hence, incorporation of Mg can reduce chances of stress shielding and improve in vivo degradation properties (Staiger et al. 2006; Wang et al. 2012). Mg^{2+} ions are reported to suppress inflammatory response by inhibiting toll-like receptor (TLR) pathway which otherwise triggers cytokine production. Macrophage's foreign body recognition also occurs by recognizing the TLR pathway which can prolong degradation or may lead to rejection of implants.
- (d) Cobalt (Co) is known to promote angiogenesis by activating HIF (Hypoxia-Inducible Factor) genes which lead to secretion of vascular endothelial growth factor (VEGF). A number of materials modified by introducing cobalt result in increase in vascularization of biomaterials. HIF gene has also been reported to promote proinflammatory effects, and since its toxic effects of Co ions and its implication in the failure of prosthesis cannot be ignored its use in biomaterial is limited and controversial (Shweiki et al. 1992). Incorporation of Co in mesoporous bioactive glass increased VEGF secretion, and the composite increases osteogenesis (Wu et al. 2012a).
- (e) Zinc (Zn) has high mineralization and bone formation tendency, but dietary zinc can retard bone growth. So it is either incorporated as a filler or dopant in 3D polymeric or ceramic biomaterials (Yamaguchi 1998). Besides it also possesses immunomodulatory tendency and has been reported to regulate inflammatory response by stimulating anti-inflammatory and osteogenic cytokines in a concentration-dependent manner. It is involved in collagen production and plays an important role in the mineralization of osteoblast through zinc trafficking that involves zinc transporters and zinc storage proteins (Niranjan et al. 2013).
- (f) Strontium (Sr) has been known to stimulate osteogenesis and inhibit osteoclastogenesis. It has also been used for the treatment of osteoporosis. Sr introduced in CaP ceramics has been reported to inhibit proinflammatory cytokines such as $TNF\alpha$ and IL-6. It has also been known to promote cell proliferation (Wu et al. 2012b; Zhang et al. 2013). Strontium (Sr^{2+}) has synergistic effect on released Calcium (Ca^{2+}) in Sr/HAp/CS scaffold provoking osteogenesis (Lei et al. 2017). Scaffolds with Sr have also been reported to enhance alkaline phosphatase activity indicating high cell differentiation capability.

14.11 Effect of Carbon-Based Fillers for Bone Tissue Engineering

14.11.1 Graphene

Graphene is an allotrope of carbon with sp^2 -hybridized carbon atoms in a hexagonal lattice. It possesses two σ bonds and one π bond linked to a carbon atom. The molecular structure accounts for high thermal and electrical conductivity (Shadjou and Hasanzadeh 2016). The surface area of dispersed Graphene in polymer depends upon how it interacts with the chains. The interaction can be due to π - π stacking, electrostatic interaction or ionic interaction, and Van der Waals forces. Surface functionalization such as amination increases dispersity of sheets in polymer solution. The ability for surface functionalization, tolerable cytotoxicity, and biodegradability has made graphene suitable for tissue engineering application. Entrapment of colloidal HA NPs in 3D graphene network leads to self-assembled graphite-like shell resulting in highly porous, electrically conducting, biocompatible graphene-HA gel for tissue engineering. rGO/HA composite demonstrated spontaneous osteogenic differentiation without inhibition of cell proliferation. They were also found to promote osteogenesis in animal model without evoking inflammatory response (Lee et al. 2015). Graphene at low loading ratios improves mechanical properties due to strong interfacial adhesion between the filler and polymer matrixes which may lead to efficient load transfer; on the contrary, higher concentration lead to agglomeration, resulting in decline in mechanical properties. Graphene oxide (GO) tunes the wettability of scaffolds by adjusting its concentration and imparts hydrophilic characteristics to the matrix. It also enhances the bioactivity of the matrix and stimulates mineralization process. Paramagnetic scaffolds Fe_3O_4 /GO/ β TCP can enhance osteoblast proliferation and differentiation by applying an external magnetic field. rGO/polypyrrole composite demonstrated good ability to stimulate osteoblast proliferation. The scaffolds of such conducting composites are usually prepared by layer-by-layer deposition technique and electrochemical deposition technique (Song et al. 2016). Weak interaction between bioceramics and biopolymer can be resolved by incorporating GO because of its tendency to form electrostatic and π - π stacking linkages. Aspirin-loaded GO-HAp scaffold fabricated by layer-by-layer assembly (LBL) biomineralization technique reduced pain and inflammation at the bone surgical site. Besides imparting mechanical properties incorporation of GO to beta-tricalcium phosphate (β -TCP) activates signaling pathways favorable for osteoblast proliferation (Eivazzadeh-Keihan et al. 2019).

14.11.2 Carbon Nanotubes

CNTs are allotrope of carbon with long thin cylindrical morphology. Due to high agglomeration tendency, they need to be functionalized for effective usage. Functionalization also improves the biocompatibility and cell attachment tendency of carbon nanotubes (CNT). Since the outer wall of CNT is relatively inert as compared to the inner wall, therefore it requires special techniques for modification

in both covalent and noncovalent cases (Liu et al. 2017). In the noncovalent functionalization method, polymer chains are wrapped around CNT and dispersed in the polymer matrix. It involves mild conditions such as sonication and temperature and does not affect the structure of CNT and their properties, unlike covalent modification where direct covalent bonds are formed with carbon atoms. Incorporation of CNT in CS, bioactive glass composite, improved mechanical, chemical, and cell-stimulating properties of scaffold. CNT-coated scaffolds by LBL assembly increased cell differentiation as measured by ALP. CNT possessing neutral electric charge exhibited highest cell growth and produced platelet-like apatite crystals (Zanello et al. 2006). Because of the complicated interaction of CNT with cellular process in bone cells and agglomeration issues, its use as bone filler is still a challenging area of research in bone tissue engineering.

14.11.3 Carbon Dots

Carbon dots (CD) are carbon-based nanomaterial with a negligible dimension of approximately 10 nm (Sun et al. 2006). They are synthesized by laser irradiation on carbon sources and comprise sp^2 - or sp^3 -hybridized carbon atom. They have a broad bandwidth of absorption spectra from 260 to 320 nm. Maintaining efficient mineralization throughout the entire body of scaffold is one of the major challenges which can be solved using appropriate shape and size of dots. CD-peptide composites have been known to possess sufficiently good osteoconductivity, cell adhesion, and mineralization tendency (Gogoi et al. 2016). The uniform distribution of CDs in scaffold improves and stimulates osteogenic activity of cells. Simple fabrication method and low toxicity allow it to be used for bone tissue engineering applications.

14.11.4 Fullerenes

Fullerenes are closed-cage spherical structures of sp^2 -hybridized carbon atoms. C60 and C70 are some common examples of fullerenes. Increased cell adhesion tendency on the surface of fullerene has made it applicable in biomedical field. Nanofibers coated with fullerene exhibited increase in cell proliferation tendency over 4.5 times in 7 days (Bacakova et al. 2007). The material proved to be safe and do not cause DNA damage or altered cell morphology. Regularly aligned fullerene on the material's surface has better cell adhesion and proliferation characteristics than random deposition. They have good stimulation on bone cells and possess high biomineralization tendency on the surface and low cytotoxicity which make them be used for such application.

14.11.5 Nanodiamonds

Nanodiamonds are a form of semiconductor quantum dots. They have high surface areas with tunable mechanical properties (Eivazzadeh-Keihan et al. 2019). They are the only nontoxic carbon nanomaterials that are used in bone tissue engineering applications. They also possess good osteogenetic and mineralization tendency.

14.12 Protein Adsorption

Adsorption of protein on biomaterial surface triggers a cascade of immunological reactions that may lead to acceptance or rejection of implants. Hence, we can say that nonspecific protein adsorption on the surface is one of the reasons for triggering unwanted immune response which may lead to failure of implants. To resolve the issue, the surface must possess antifouling properties and must allow selective adsorption of protein molecules essential for cell bioactivity. Some strategies for optimizing osteoinductive potential involve immobilizing characteristic proteins on the polymer matrix which can trigger desired bioactivity. Proteins immobilized on biomaterials surfaces are generally categorized into two main classes. Cell adhesion proteins such as laminin, Fibronectin, collagen, and vitronectin form the first class. These proteins are derived from ECM and function via ligand–acceptor interaction. Growth factors form the second class of proteins, and these help in tuning cell proliferation and differentiation. Epidermal growth factor (EGF), fibroblast growth factor, vascular endothelial growth factor and, bone morphogenic protein are some of the immobilized proteins on biomaterial surface. Adhesive peptide sequence, that is, RGD, forms an important component of the majority of adhesive protein and serves as a binding domain for integrin receptors present in cells. For controlling protein–surface interaction, hydrophilic groups with neutral charge lacking hydrogen donor groups are also incorporated on polymer surface. PU foam modified with lysine exhibited increased affinity for plasminogen adsorption; however, fluorinated surface has been reported to decrease adsorption of protein from their surface. Change in surface functionalities of biomaterial is reported to alter surface structure of adsorbed proteins. Variation in content of α -helix, β -sheet, or β -coiled conformation in adsorbed protein leads to altered immune response and cellular interactions (Hasan and Pandey 2015; Hasan et al. 2018). Acute inflammatory responses as studied by implanting radiofrequency plasma glow discharge (RFGD) functionalized disk demonstrated a trend in which the cellular response given by the functional groups was arranged in the following order: $-\text{NH}_2 > -\text{CH}_3-\text{CF}_x > -\text{OH} > \text{Siloxy group}$. It has been observed that the fusion of macrophages into granular foreign body giant cells also depends on the functional group and decreases in the following order: $-\text{N}(\text{CH}_3)_2 > -\text{OH} > -\text{CONH} > -\text{SO}_3\text{H} > -\text{COOH}(-\text{COONa})$. Functional groups are also known to tune cell attachment and proliferation and show decrease in attachment tendency in the following hierarchical order of functional groups: $-\text{CH}_2\text{NH}_2 > -\text{CH}_2\text{OH} > -\text{CONH}_2 > -\text{COOH}$. Simply casting proteins on biomaterial surface results in uneven distribution of protein molecules,

so surface treatment is essential for even distribution which may involve few strategies as mentioned below:

- (a) Covalent immobilization of protein molecule on biomaterial surface involves the introduction of reactive functional groups such as carboxylic, amino, or hydroxyl into polymer chains which can serve as coupling sites for protein attachment. Usually, PMMA, polyacrylic acid is grafted on polymer surfaces to introduce carboxylic group. Hydrolysis and aminolysis can introduce reactive groups in polyester. Covalent immobilization of protein can bring a permanent change in a natural conformation of protein.
- (b) Entrapment method involves swelling of polymeric surface insolvent and nonsolvent containing protein molecules followed by immersion of the material in pure nonsolvent solution, resulting in entrapment of protein on the biomaterial surface. Matrix entrapment and membrane entrapment are the two main methods of entrapment. The latter of which involves immobilization of molecules in hollow fiber network or hollow spheres performed by techniques such as microencapsulation.
- (c) Grafting and coating method involves initial covalent attachment of protein on materials followed by physical coating of protein on the attached surface. The density of immobilized biomolecules can easily be controlled by altering the density of attached groups on surface.
- (d) Layer-by-layer assembly is another technique which performs sequential deposition of biomolecules on biomedical surface containing functional groups that derive self-assembly. Most rely on electrostatic interaction between molecules leading to sequential depositions (Ma et al. 2007). It is a delicate process, and the majority of interactions are based on electron transfer.

14.12.1 miRNA Immobilization

miRNA is a short strand of approximately 22-ribonucleotide-long noncoding RNA that regulates functions at posttranscriptional level. miRNA is being used to enhance regeneration of tissues because they regulate the expression of their target genes. miRNA-26a increased osteogenesis by targeting Gsk-3 β in bone repair. miRNA-222-loaded mesoporous silica nanoparticles promoted bone regeneration and neurogenesis in bone marrow (Zhu et al. 2020). It plays role in regulating classical signaling pathways of osteogenic differentiation such as bone morphogenic protein (BMP) and Wnt- β catenin signaling pathway. It can be delivered locally to target cells at the site of implantation by loading it into porous scaffolds and hydrogels which serves as a delivery vector.

14.13 Chemical Modification

Surface chemistry of polymer has been reported to impact protein adsorption on scaffold and interaction between cell and matrix. Chemical grafting of groups on the surface of polymer is another way to enhance osteoconductivity and differentiation of MSC. Chemical modification of polymer surface can be performed by various techniques enlisted below.

14.13.1 Ozone Treatment

Treatment of biomaterials with ozone introduces peroxy groups in polymer for enhancing conjugation capabilities of biomolecules. It is applied along with UV radiations to increase the conjugation rate. Ozone/UV increased hydrophilicity and reduced protein adsorption on grafting polyethylene oxide (PEO), chitosan, and polyvinyl alcohol (PVA) to polyethersulfone membrane (Liu et al. 2008). Monomers can also be grafted on ozone-oxidized surface. Ozone can also be used for sterilization of biomaterials.

14.13.2 Silanization

It is a liquid-phase chemical reaction, especially used in the modification of surfaces with OH functionality. In spite of covalently crosslinked structure between silane and hydroxyl groups, the linkage is readily hydrolyzable. Whitesides group studied the arrangement of silane on polymer surface and dubbed it as self-assembled monolayer (SAM) because it possesses tendency to self-organize on suitably functionalized substrate surface in an ordered monolayer. Molecular vapor deposition is another method used in the process. Organosilanes are used to bind organic polymer to inorganic substrate. Glass-reinforced polymers which employ adhesion between glass and polymer are usually enhanced by the silanization process. Organosilanes with different functional groups like polyethylene glycol (PEG), bromine, and vinyl are commonly being used to tune biological properties. Bromine- and vinyl-terminated silanes are altered by wet chemical methods to generate carboxylic acid, amines, and hydroxyls. Polymers with OH functionality are normally used for such modifications.

14.13.3 Fluorination

Halogenation is performed to tune the surface characteristics of polymer. Fluorination increases the hardness and hydrophobicity of the surface. This also sometimes imparts inertness to the material. Fluorinated RGD sequences were targeted to bioactivate polyurethane surface without altering its characteristic properties (Blit

et al. 2010). The methodology increased cell attachment and proliferation of modified scaffold compared to native scaffold.

14.13.4 Wet Treatment

This method uses the treatment of polymer with liquid reagent to generate reactive functional groups. They have an edge over other techniques as the liquid can penetrate the interconnected three-dimensional porous structure rather than energy involving techniques such as plasma. Alkaline or acid hydrolysis and aminolysis are some examples of the treatment method. Peroxidation of films by treatment with hydrogen peroxide is also done by this method, where the oxidized membrane is placed in monomer solution followed by UV exposure to initiate polymerization on parent polymer substrate. Hydroxyl and carboxyl groups are introduced in polyester by autocatalytic cleavage of ester bonds. Chromic acid is also a potential candidate for introducing carboxyl groups in some polymers. Enhanced surface roughness and hydrophilicity can be achieved using this method. The drawback of such methods includes nonspecific introduction of a range of functional groups in polymer, and the treated liquid may initiate early degradation process resulting in loss in mechanical properties. The process targets side chains of polymer and may depend upon the orientation and arrangement of side chains.

14.13.5 Flame Treatment

Flame treatment is a method of nonspecific surface functionalization that bombards ionized air on a polymer surface creating a variety of oxidation products. It has been reported to impart aldehyde, hydroxyl, and carboxylic acid groups to the surface increasing wettability and cell adhesion (Zhu et al. 2002). Reactive oxygen species produced by the process activates the surface creating further opportunities for grafting by various polymers. The main drawback is that it affects optical property and needs constant monitoring of flame temperature and contact time which is time-consuming and frustrating. The high number of parameters affecting flame treatment and lack of specificity makes the method lag behind in comparison to the latest techniques (Farris et al. 2010).

14.14 Radiation-Induced Surface Modification

Plasma treatment, corona discharge, and UV irradiation also add functional groups such as hydroxyl and amine. Radiation-induced grafting of polymer can be achieved by a broad spectrum of radiations such as gamma, UV, laser, plasma, microwave, infrared, ultrasound, and visible spectrum depending upon time and energy of radiation. They activate the surfaces creating reactive sites and also help to immobilize different molecules on the surface.

14.14.1 Laser

Laser serves as high-energy photon sources with very high intensities. They can induce crosslinking or scission effects. Different types of laser-assisted fabrication technologies are employed which modify biomaterials by making spatial arrangement of patterns at a resolution less than 10 μm . These can be categorized as (1) laser tweezers which use optical forces to trap individual cells and make pattern out of them with high precision; (2) laser-initiated polymerization which generates chemical bonds using laser beam on the precursor; (3) laser-induced forward transfer (LIFT) and matrix-assisted pulsed laser evaporation (MAPLE) to deposit heat-sensitive polymeric material on solid substrate; and (4) laser ablation to selectively remove polymeric biomaterials to create holes, grids, and parallel lines in microscale (Koo et al. 2017). A significant increase in osteogenic expression levels was observed on patterned surface in comparison to the unpatterned surface (Ortiz et al. 2018). Laser treatment of electrospun PCL HA/PVAC surface increased cell viability and cell density of MG63 cell lines (Aragon et al. 2017). Pulsed laser beam was used to control crater size on surface of ultra-high-molecular-weight polyethylene (UHMWPE) with an increment of roughness and wettability (Riveiro et al. 2018). Laser-generated structures provide anchorage and contact guidance to attached cells. Pulsed laser beam produces high-quality patterns on polymer surface especially by reducing pulse length.

14.14.2 Ion Beam

Ion beams are deployed to ionize the surface of biomaterial or implants for improving biological properties. It offers higher resolution patterning than UV, X-ray, etc. This technique is similar to electron beam lithography but uses heavier charged particles in the form of ions. Ion beams of hydrogen, helium, gold, or uranium are usually irradiated on the polymer to alter the surface chemistry of a polymer. The process also depends on the nature of substrate that undergoes recrystallization during annealing. The channeling effect of ions is one of the main unwanted hurdles which create some unevenness in pattern. They are normally observed when the crystallographic axis of grain is aligned in direction of incident radiations (Razali et al. 2019).

14.14.3 Gamma Radiation

The high-energy γ radiation has the potential to trigger polymerization and grafting of monomer on a solid substrate. They have also the tendency to produce peroxides and hydroperoxides on the surface of biomaterial which can serve as initiating site for graft polymerization (Kou et al. 2003). Gamma radiation was used to immobilize sulfonated compound on the surface of the polymer. They were also used to covalently attach albumin to the membrane for increasing hemocompatibility.

Radiation-induced grafting of acrylamide and *N*-vinyl pyrrolidone increased blood compatibility of silicon. Gamma irradiation was also used to synthesize hydrogel for biomedical application. On exposure to radiation in UHMWP, the samples exhibited an increase in modulus and hardness over the untreated ones (Benson 2002).

Following methods are used to induce grafting by gamma-ray irradiation:

1. Free radical assisted irradiation and grafting.
2. Peroxide group mediated grafting.
3. Radiation-induced grafting was initiated by trapped radicals.

14.14.4 UV-Induced Photoactivation

UV irradiation has been widely applied to induce graft polymerization on biomaterial surface using a photoinitiator or photosensitizer (Hoffman 1995). The sample to be grafted is kept under inert atmosphere of argon or nitrogen under vacuum or covered with monomer solution followed by UV irradiation. Benzophenone is the most common photoinitiator used for free radical generation. Irradiation time, monomer concentration, molar ratio, photoinitiator, UV, and solvent type determines the degree of grafting (Xing et al. 2002). Since solvent selection had impact on the degree of grafting and has inconsistency when multiple samples are used, so to minimize the issue solvent-free grafting is performed for biodegradable polymers, where they are subjected to vapor phase of monomers and the grafting reaction is induced by the photoinitiation process.

14.14.5 Electron Beam Lithography

Electron beam lithography is a technique involving focusing of an electron beam on electron-sensitive films for drawing customized shapes and patterns out of it. The process involves selective removal of exposed from non-exposed regions by treatment with solvent. The main advantage of this technique is drawing patterns in the range of 10 nm resolutions. A nanopatterned substrate of particular dimensions and arrangement is a more improved solution for better cell adhesion and proliferation than native and can pave way for better tissue construct.

14.14.6 Plasma Radiation

Plasma is highly energetic radiation comprising of atoms, molecules, charged ions, and electrons created in a medium of certain materials. It is also regarded as the fourth state of matter. Plasma is basically of different forms and those used in industries are cold plasma, low-pressure plasma, nonequilibrium plasma, and glow discharge plasma. The most common glow discharge plasma used for biomaterial surface treatment has radio frequency (RF) discharges in the range of 1 KHz to

1 GHz. RF discharges operate at controllable low pressure, are efficient, and perform spatially uniform coating or create different functionalities on materials surface in the discharge environment. Modification of polyurethane (PU) surface by RF plasma resulted in decreased protein adsorption tendency and increased hemocompatibility. The technique also increased the hydrophilicity and wettability on RF plasma-modified poly(methyl methacrylate) (PMMA) substrate. Vinyl sulfonic acid grafted chitosan by this process exhibited significant cell adhesion tendency. PDMS plate modified with oxygen plasma exhibited increased cell proliferation. Graft polymerization of PEG on PMMA by this technique increased the antistatic property of PMMA.

14.15 Conclusion

Surface engineering of polymers largely depends upon the nature of the polymer (i.e., hydrophilic/hydrophobic or synthetic/natural) and their ability to be processed or modified by particular technique. Using appropriate method for surface modification of substrate results in improved biological, mechanical, and other essential properties which can make the biomaterial suitable as tissue engineering construct. Osteoinduction, differentiation, mineralization, in vivo mechanical stability, and immunomodulation are the major properties that are taken into account when modifying the matrix for bone tissue regeneration.

Acknowledgments The authors would like to acknowledge “The Ministry of Human Resource and Development (MHRD)” for providing financial assistance in the form of stipend.

References

- Abraham GA, De Queiroz AAA, Román JS (2001) Hydrophilic hybrid IPNs of segmented polyurethanes and copolymers of vinylpyrrolidone for applications in medicine. *Biomaterials* 22(14):1971–1985. [https://doi.org/10.1016/S0142-9612\(00\)00381-1](https://doi.org/10.1016/S0142-9612(00)00381-1)
- Ali A et al (2019) Effect of incorporation of montmorillonite on xylan/chitosan conjugate scaffold. *Colloids Surf B Biointerfaces* 180:75–82. <https://doi.org/10.1016/j.colsurfb.2019.04.032>. Elsevier
- Ali A et al (2020) Comparative analysis of TiO₂ and Ag nanoparticles on xylan/chitosan conjugate matrix for wound healing application. *Int J Polym Mater Polym Biomater*:1–10. <https://doi.org/10.1080/00914037.2020.1838519>. Taylor & Francis
- Aragon J et al (2017) Laser-treated electrospun fibers loaded with nano-hydroxyapatite for bone tissue engineering. *Int J Pharm* 525(1):112–122. <https://doi.org/10.1016/j.ijpharm.2017.04.022>. Elsevier BV
- Bacakova L et al (2007) Improved adhesion and growth of human osteoblast-like MG 63 cells on biomaterials modified with carbon nanoparticles. *Diam Relat Mater* 16(12):2133. <https://doi.org/10.1016/j.diamond.2007.07.015>
- Bai X et al (2018) Bioactive hydrogels for bone regeneration. *Bioactive Mater* 3(4):401–417. <https://doi.org/10.1016/j.bioactmat.2018.05.006>. Elsevier

- Barbosa JN et al (2006) The influence of functional groups of self-assembled monolayers on fibrous capsule formation and cell recruitment. *J Biomed Mater Res A* 76(4):737–743. <https://doi.org/10.1002/jbm.a.30602>
- Benson RS (2002) Use of radiation in biomaterials science. *Nucl Instrum Methods Phys Res Sect B Beam Interact Mater Atoms* 191(1–4):752–757. [https://doi.org/10.1016/S0168-583X\(02\)00647-X](https://doi.org/10.1016/S0168-583X(02)00647-X)
- Bianco A et al (2009) Electrospun poly(ϵ -caprolactone)/Ca-deficient hydroxyapatite nanohybrids: microstructure, mechanical properties and cell response by murine embryonic stem cells. *Mater Sci Eng C* 29(6):2063–2071. <https://doi.org/10.1016/j.msec.2009.04.004>. Elsevier BV
- Blit PH et al (2010) Bioactivation of porous polyurethane scaffolds using fluorinated RGD surface modifiers. *J Biomed Mater Res A* 94(4):1226–1235. <https://doi.org/10.1002/jbm.a.32804>
- Cakmak AM et al (2020) 3D printed polycaprolactone/gelatin/bacterial cellulose/hydroxyapatite composite scaffold for bone tissue engineering. *Polymers* 1962. <https://doi.org/10.3390/polym12091962>
- Carlisle EM (1970) Silicon: a possible factor in bone calcification. *Science* 167(3916):279–280. <https://doi.org/10.1126/science.167.3916.279>
- Chahal S, Kumar A, Hussian FSJ (2019) Development of biomimetic electrospun polymeric biomaterials for bone tissue engineering. A review. *J Biomater Sci Polym Ed* 30(14):1308–1355. <https://doi.org/10.1080/09205063.2019.1630699>. Taylor & Francis
- Chen Z et al (2016) Osteoimmunomodulation for the development of advanced bone biomaterials. *Mater Today* 19(6):304–321. <https://doi.org/10.1016/j.mattod.2015.11.004>
- De A (2011) Wnt/Ca 21 signaling pathway : a brief overview the non-canonical Wnt signaling cascade. *Acta Biochim Biophys Hung* 43(10):745–756. <https://doi.org/10.1093/abbs/gmr079>. *Advance*
- De Geyter N et al (2013) Plasma-assisted surface modification of polymeric biomaterials. In: *Low temperature plasma technology: methods and applications*, pp 401–418. <https://doi.org/10.1201/b15153>
- Eivazzadeh-Keihan R et al (2019) Carbon based nanomaterials for tissue engineering of bone: building new bone on small black scaffolds: a review. *J Adv Res* 18:185–201. <https://doi.org/10.1016/j.jare.2019.03.011>
- Farris S et al (2010) The fundamentals of flame treatment for the surface activation of polyolefin polymers - a review. *Polymer* 51(16):3591–3605. <https://doi.org/10.1016/j.polymer.2010.05.036>. Elsevier
- Filmon R et al (2002) Effects of negatively charged groups (carboxymethyl) on the calcification of poly(2-hydroxyethyl methacrylate). *Biomaterials* 23(14):3053–3059. [https://doi.org/10.1016/S0142-9612\(02\)00069-8](https://doi.org/10.1016/S0142-9612(02)00069-8)
- Giudicessi JR, Michael BA, Ackerman J (2008) 纳米形貌作为人间充质干细胞功能的调节剂 Nanotopography as modulator of human mesenchymal stem cell function. *Bone* 23(1):1–7. <https://doi.org/10.1038/jid.2014.371>
- Gogoi S et al (2016) A renewable resource based carbon dot decorated hydroxyapatite nanohybrid and its fabrication with waterborne hyperbranched polyurethane for bone tissue engineering. *RSC Adv* 6(31):26066–26076. <https://doi.org/10.1039/c6ra02341j>
- Gomes ME et al (2006) In vitro localization of bone growth factors in constructs of biodegradable scaffolds seeded with marrow stromal cells and cultured in a flow perfusion bioreactor. *Tissue Eng* 12(1):177–188. <https://doi.org/10.1089/ten.2006.12.177>
- Guilak et al (2009) *Cell Stem Cell* 5(1):17–26. <https://doi.org/10.1016/j.stem.2009.06.016>
- Hasan A, Pandey LM (2015) Review: polymers, surface-modified polymers, and self assembled monolayers as surface-modifying agents for biomaterials. *Polym Plast Technol Eng* 54(13):1358–1378. <https://doi.org/10.1080/03602559.2015.1021488>
- Hasan A et al (2017) Fabrication and characterization of chitosan, polyvinyl pyrrolidone, and cellulose nanowhiskers nanocomposite films for wound healing drug delivery application. *J Biomed Mater Res A* 105(9):2391–2404. <https://doi.org/10.1002/jbm.a.36097>

- Hasan A, Pattanayek SK, Pandey LM (2018) Effect of functional groups of self-assembled monolayers on protein adsorption and initial cell adhesion. *ACS Biomater Sci Eng* 4:3224. <https://doi.org/10.1021/acsbiomaterials.8b00795>
- Hoffman AS (1995) Surface modification of polymers. *Chin J Polym Sci (English Edition)* 13 (3):195–203. <https://doi.org/10.1201/b16347-8>
- Hunter GK et al (2001) Induction of collagen mineralization by a bone sialoprotein-decorin chimeric protein. *J Biomed Mater Res* 55(4):496–502. [https://doi.org/10.1002/1097-4636\(20010615\)55:4<496::AID-JBM1042>3.0.CO;2-2](https://doi.org/10.1002/1097-4636(20010615)55:4<496::AID-JBM1042>3.0.CO;2-2)
- Kong HJ et al (2005) Non-viral gene delivery regulated by stiffness of cell adhesion substrates. *Nat Mater* 4(6):460–464. <https://doi.org/10.1038/nmat1392>
- Koo S et al (2017) Laser-assisted biofabrication in tissue engineering and regenerative medicine. *J Mater Res* 32(1):128–142. <https://doi.org/10.1557/jmr.2016.452>
- Kou RQ et al (2003) Surface modification of microporous polypropylene membranes by plasma-induced graft polymerization of α -allyl glucoside. *Langmuir* 19(17):6869–6875. <https://doi.org/10.1021/la0345486>
- Kretlow JD, Mikos AG (2007) Review: mineralization of synthetic polymer scaffolds for bone tissue engineering. *Tissue Eng* 13(5):927–938. <https://doi.org/10.1089/ten.2006.0394>
- Lee JH et al (1997) Interaction of cells on chargeable functional group gradient surfaces. *Biomaterials* 18(4):351–358. [https://doi.org/10.1016/S0142-9612\(96\)00128-7](https://doi.org/10.1016/S0142-9612(96)00128-7)
- Lee JH et al (2015) Enhanced osteogenesis by reduced graphene oxide/hydroxyapatite nanocomposites. *Sci Rep* 5:18833. <https://doi.org/10.1038/srep18833>
- Lei Y et al (2017) Strontium hydroxyapatite/chitosan nanohybrid scaffolds with enhanced osteoinductivity for bone tissue engineering. *Mater Sci Eng C* 72:134–142. <https://doi.org/10.1016/j.msec.2016.11.063>. Elsevier BV
- Ling S et al (2020) Electrospun poly(3-hydroxybutyrate-co-3-hydroxyhexanoate)/silk fibroin film is a promising scaffold for bone tissue engineering. *Int J Biol Macromol* 145:173–188. <https://doi.org/10.1016/j.ijbiomac.2019.12.149>. Elsevier BV
- Liu SX, Kim JT, Kim S (2008) Effect of polymer surface modification on polymer-protein interaction via hydrophilic polymer grafting. *J Food Sci* 73(3):143–150. <https://doi.org/10.1111/j.1750-3841.2008.00699.x>
- Liu R et al (2017) Noncovalent functionalization of carbon nanotube using poly(vinylcarbazole)-based compatibilizer for reinforcement and conductivity improvement in epoxy composite. *J Appl Polym Sci* 134(26):199–206. <https://doi.org/10.1002/app.45022>
- Ma Z, Mao Z, Gao C (2007) Surface modification and property analysis of biomedical polymers used for tissue engineering. *Colloids Surf B: Biointerfaces* 60(2):137–157. <https://doi.org/10.1016/j.colsurfb.2007.06.019>
- Matlaga BF, Yasenchak LP, Salthouse TN (1976) Tissue response to implanted polymers: the significance of sample shape. *J Biomed Mater Res* 10(3):391–397. <https://doi.org/10.1002/jbm.820100308>
- Mills CD et al (2000) M-1/M-2 macrophages and the Th1/Th2 paradigm. *J Immunol* 164 (12):6166–6173. <https://doi.org/10.4049/jimmunol.164.12.6166>
- Mosser DM, Edwards JP (2008) Exploring the full spectrum of macrophage activation. *Nat Rev Immunol* 8:958–969. <https://doi.org/10.1038/nri2448>
- Niranjana R et al (2013) A novel injectable temperature-sensitive zinc doped chitosan/ β -glycerophosphate hydrogel for bone tissue engineering. *Int J Biol Macromol* 54 (1):24–29. <https://doi.org/10.1016/j.ijbiomac.2012.11.026>. Elsevier BV
- Okamoto M, John B (2013) Synthetic biopolymer nanocomposites for tissue engineering scaffolds. *Prog Polym Sci* 38(10–11):1487–1503. <https://doi.org/10.1016/j.progpolymsci.2013.06.001>. Elsevier
- Ortiz R et al (2018) Laser surface microstructuring of a bio-resorbable polymer to anchor stem cells, control adipocyte morphology, and promote osteogenesis. *Polymers* 10(12):1337. <https://doi.org/10.3390/polym10121337>
- Patel AA, Desai TA, Kumar S (2011) Microtopographical assembly of cardiomyocytes. *Integr Biol* 3(10):1011–1019. <https://doi.org/10.1039/c1ib00024a>

- Pham QP et al (2006) In vitro generated extracellular matrix and fluid shear stress synergistically enhance 3D osteoblastic differentiation. *Proc Natl Acad Sci* 103(8):2488–2493
- Qu H et al (2019) Biomaterials for bone tissue engineering scaffolds: a review. *RSC Adv* 9(45):26252–26262. <https://doi.org/10.1039/c9ra05214c>. Royal Society of Chemistry
- Razali WRW et al (2019) Surface patterning of silicon and germanium using focused ion beam for the development of FinFET structure. In: *Proceedings of the 2019 IEEE regional symposium on micro and nanoelectronics, RSM 2019*. IEEE, pp 116–118. <https://doi.org/10.1109/RSM46715.2019.8943520>
- Riveiro A et al (2018) Laser surface texturing of polymers for biomedical applications. *Front Phys* 6:16. <https://doi.org/10.3389/fphy.2018.00016>
- Sattary M et al (2019) Promoting effect of nano hydroxyapatite and vitamin D3 on the osteogenic differentiation of human adipose-derived stem cells in polycaprolactone/gelatin scaffold for bone tissue engineering. *Mater Sci Eng C* 97(October 2018):141–155. <https://doi.org/10.1016/j.msec.2018.12.030>. Elsevier
- Schernthaner M et al (2012) Nanopatterned polymer substrates promote endothelial proliferation by initiation of β -catenin transcriptional signaling. *Acta Biomater* 8(8):2953–2962. <https://doi.org/10.1016/j.actbio.2012.04.018>. Acta Materialia Inc
- Schindler OS et al (2007) Use of a novel bone graft substitute in peri-articular bone tumours of the knee. *Knee* 14(6):458–464. <https://doi.org/10.1016/j.knee.2007.07.001>
- Shadjou N, Hasanzadeh M (2016) Graphene and its nanostructure derivatives for use in bone tissue engineering: recent advances. *J Biomed Mater Res A* 104(5):1250–1275. <https://doi.org/10.1002/jbm.a.35645>
- Shi C et al (2016) Polymeric biomaterials for bone regeneration. *Ann Joint* 1:27–27. <https://doi.org/10.21037/aoj.2016.11.02>
- Shweiki D et al (1992) Vascular endothelial growth factor induced by hypoxia may mediate hypoxia-initiated angiogenesis. *Nature* 359(6398):843–845. <https://doi.org/10.1038/359843a0>
- Song F et al (2016) Room-temperature fabrication of a three-dimensional reduced-graphene oxide/poly pyrrole/hydroxyapatite composite scaffold for bone tissue engineering. *RSC Adv* 6(95):92804–92812. <https://doi.org/10.1039/c6ra15267h>. Royal Society of Chemistry
- Staiger MP et al (2006) Magnesium and its alloys as orthopedic biomaterials: a review. *Biomaterials* 27:1728–1734. <https://doi.org/10.1016/j.biomaterials.2005.10.003>
- Stancu IC et al (2004) Synthesis of methacryloyloxyethyl phosphate copolymers and in vitro calcification capacity. *Biomaterials* 25(2):205–213. [https://doi.org/10.1016/S0142-9612\(03\)00485-X](https://doi.org/10.1016/S0142-9612(03)00485-X)
- Stephansson SN, Byers BA, García AJ (2002) Enhanced expression of the osteoblastic phenotype on substrates that modulate fibronectin conformation and integrin receptor binding. *Biomaterials* 23(12):2527–2534. [https://doi.org/10.1016/S0142-9612\(01\)00387-8](https://doi.org/10.1016/S0142-9612(01)00387-8)
- Sun YP et al (2006) Quantum-sized carbon dots for bright and colorful photoluminescence. *J Am Chem Soc* 128(24):7756–7757. <https://doi.org/10.1021/ja062677d>
- Vladkova TG (2010) Surface engineered polymeric biomaterials with improved biocontact properties. *Int J Polym Sci* 2010:1–22. <https://doi.org/10.1155/2010/296094>
- Wang J et al (2012) Surface modification of magnesium alloys developed for bioabsorbable orthopedic implants: a general review. *J Biomed Mater Res B Appl Biomater* 100:1691–1701. <https://doi.org/10.1002/jbm.b.32707>
- Wu C, Zhou Y, Fan W et al (2012a) Hypoxia-mimicking mesoporous bioactive glass scaffolds with controllable cobalt ion release for bone tissue engineering. *Biomaterials* 33(7):2076–2085. <https://doi.org/10.1016/j.biomaterials.2011.11.042>. Elsevier
- Wu C, Zhou Y, Lin C et al (2012b) Strontium-containing mesoporous bioactive glass scaffolds with improved osteogenic/cementogenic differentiation of periodontal ligament cells for periodontal tissue engineering. *Acta Biomater* 8(10):3805–3815. <https://doi.org/10.1016/j.actbio.2012.06.023>

- Xing CM, Deng JP, Yang WT (2002) Surface photografting polymerization of binary monomers maleic anhydride and n-butyl vinyl ether on polypropylene film II. Some mechanical aspects. *Polym J* 34(11):809–816. <https://doi.org/10.1295/polymj.34.809>
- Yamaguchi M (1998) Role of zinc in bone formation and bone resorption. *J Trace Elem Exp Med* 11(23):119–135. [https://doi.org/10.1002/\(sici\)1520-670x\(1998\)11:2/3<119::aid-jtra5>3.3.co;2-s](https://doi.org/10.1002/(sici)1520-670x(1998)11:2/3<119::aid-jtra5>3.3.co;2-s)
- You et al (2010) *cBiomacromolecules* 11(7):1856–1862. <https://doi.org/10.1021/bm100374n>
- Zanello LP et al (2006) Bone cell proliferation on carbon nanotubes. *Nano Lett* 6(3):562–567. <https://doi.org/10.1021/nl051861e>
- Zhang Y et al (2013) Strontium-incorporated mesoporous bioactive glass scaffolds stimulating in vitro proliferation and differentiation of bone marrow stromal cells and in vivo regeneration of osteoporotic bone defects. *J Mater Chem B* 1(41):5711–5722. <https://doi.org/10.1039/c3tb21047b>
- Zhang Q et al (2018) Surface engineering of synthetic polymer materials for tissue engineering and regenerative medicine applications. *Biomaterials* 7(2):9622–9629. <https://doi.org/10.1016/j.msec.2018.05.040>. Elsevier
- Zhu Y, Gao C, Shen J (2002) Surface modification of polycaprolactone with poly(methacrylic acid) and gelatin covalent immobilization for promoting its cytocompatibility. *Biomaterials* 23(24):4889–4895. [https://doi.org/10.1016/S0142-9612\(02\)00247-8](https://doi.org/10.1016/S0142-9612(02)00247-8)
- Zhu L, Luo D, Liu Y (2020) Effect of the nano/microscale structure of biomaterial scaffolds on bone regeneration. *Int J Oral Sci* 12(1):1–15. <https://doi.org/10.1038/s41368-020-0073-y>. Springer
- Zouani OF et al (2012) Altered nanofeature size dictates stem cell differentiation. *J Cell Sci* 125(5):1217–1224. <https://doi.org/10.1242/jcs.093229>



Antibacterial Surface Modification to Prevent Biofilm Formation on Polymeric Biomaterials

15

Abul K. Mallik, Adib H. Chisty, M. Nuruzzaman Khan, Sumaya F. Kabir, Md. Shahruzzaman, and Mohammed Mizanur Rahman

Abstract

Antibacterial surface modification of polymeric biomaterials or devices to control diseases is gaining much attention. There are many materials especially polymeric biomaterials used worldwide to improve the health care. However, keeping the surfaces of these biomaterials free from pathogenic microorganisms is a great challenge for their clinical applicability, and these bacterial contaminations could be detrimental to the patient. Another problem of using these biomaterials is the formation of biofilm onto the implant surfaces. Drugs usually cannot penetrate these biofilms formed on the biomaterial surfaces. If infections are treated with common antibiotics, the effectiveness of these antibiotics become very limited as the drug cannot enter inside the biofilm to kill all of the bacteria. Therefore, antibacterial surface modification or surface coatings of biomaterials are thought to be the best technique to avoid biofilm formation to reduce the infection-related problems. Biomolecules such as proteins, carbohydrates, lipids, peptides, etc. are widely used on biomaterial surfaces through various mechanisms to improve biocompatibility and bactericidal effects. In this chapter, we focus on the description of various polymeric biomaterials used and new possibilities in the future in biomedical implants or devices and the biofilm formation mechanism onto their surfaces. Moreover, we also describe how to modify the surfaces of polymeric biomaterials with antibacterial molecules to prevent the biofilm formation. Eventually, the knowledge of common and new methods of surface modification of biomaterials and materials to be used as antibacterial agents will encourage people to use polymeric biomaterials in medical devices or implants.

A. K. Mallik (✉) · A. H. Chisty · M. N. Khan · S. F. Kabir · M. Shahruzzaman · M. M. Rahman
Faculty of Engineering and Technology, Department of Applied Chemistry and Chemical Engineering, University of Dhaka, Dhaka, Bangladesh
e-mail: abulkmallik@du.ac.bd

© The Author(s), under exclusive license to Springer Nature Singapore Pte Ltd. 2022

L. M. Pandey, A. Hasan (eds.), *Nanoscale Engineering of Biomaterials: Properties and Applications*, https://doi.org/10.1007/978-981-16-3667-7_15

425

Keywords

Biomaterial · Biofilm · Polymeric surface · Antimicrobial surface · Implant

15.1 Introduction

A biomaterial can be defined as any material applied for diagnostic, prosthetic, therapeutic, or for storage of blood, and its components come in contact with biological fluids and living tissues without harmfully disturbing the biological constituents of the whole living organism. Various types of biomaterials are available originated from metals, ceramics, and polymers. These materials are used to replace or support the lost, damaged, or malfunctioned body parts by accidents, injury, etc. Biomaterials have been used from the early history of ancient Egyptian, Chinese, Aztec, and Roman cultures for the replacement of damaged tissues of ears, eyes, teeth, nose, etc. For example, gold was used in dentistry to attach or replace the lost teeth and glass in eyes. Day-by-day, material science and medical techniques have been improving and implants becoming sophisticated by fabricating with numerous biomaterials (Hasan et al. 2020b). At the same time, clinical demand of biomaterials to be used as medical devices and implants has been increasing (Yin and Luan 2016). Implants can be described as the objects which do not need any form of power, which may be chemical or electrical, to the formation of a reaction for the correction of certain bodily functions or capturing information from the body (e.g., knee prosthetics, breast implants, etc.). On the other hand, devices are the objects which need any form of power to carry out its expected functions (e.g., pacemakers, defibrillators, etc.) (Teo et al. 2016). Depending on the use and lifetime of the biomedical implants and devices, biomaterials such as polymers, ceramics, and metal and their alloys are applied for the fabrication of them (Xinming et al. 2008; Dormer and Gan 2001; Granchi et al. 2006; Hasan et al. 2020a).

However, main problems of using these materials are their incompatibility and complications with the body tissue would often occur. At the beginning of the twentieth century, materials were anticipated to be inert to be considered as biomaterial. However, inertness is not considered as the main property in the twenty-first century. Inertness of a material indicates its inability to produce immunological or clinically measurable primary or secondary foreign body reactions. This concept has changed in the recent decades, and it is considered that bioactive materials have integrated appropriately with the neighboring tissue (Desmet et al. 2009). Because, if biomaterials as implants have been used for a prolonged period of time in the body, there is a possibility of adhesion and proliferation of bacteria on implant surface. Eventually in some cases, there is a possibility of biofilm formation which originates local infections. In worst cases, these infections causes implant failure and death of the patients (Xu et al. 2017). A lot of implant-associated bacterial infections have been reported. Usually, the tissue contamination by the opportunistic pathogens is protected by the host immune system. Nevertheless, many problems (if this immune response or a local tissue response gets activated owing to implant-associated

infections) like foreign body reaction, acute and chronic inflammation, and granulation of tissue development may occur. Finally, these actions may cause the microbial colonization or biofilm formation as well as implant infections (Andrade Del Olmo et al. 2020). Therefore, the implant infection can be expressed as various interactions between the host immune response and biomaterials (Mariani et al. 2019). On the other hand, microbial contamination through surgery frequently leads to the prosthetic contamination after surgery, and other types of infections like subacute (within 3–24 months) or late infections (more than 24 months) are also reported (Arciola et al. 2018).

Biointegration is necessary which means the actions or processes happen at the implant and host tissues and there will be no toxic effects like inflammation or unusual tissue growth due to the placement of the implant (Ye and Peramo 2014). Optimum surface properties of the implants, devices, and grafts prepared with biomaterials are very important to increase the possibility of biointegration. Moreover, these biomaterials should have other essential bulk properties (particularly mechanical properties) due to their requirement to be compatible with the host bioenvironment. However, obtaining both requirements for designing a biomaterial is not easy. A common way of fabricating biomaterials is taking acceptable bulk properties and enhancing the surface properties by special treatment which is not sufficient to fulfill all of the requirements. Depending on the end uses, both the bulk properties and antibacterial activity of polymer biomaterials can be enhanced by selective surface modification. For example, surface modification of biomaterials can progress the device multifunctionality, tribology, biocompatibility, topography, and especially the antibacterial properties which can reduce the necessity of developing brand new materials with expensive and time-consuming methods. Hence, surface engineering of biomaterials is becoming an emerging area of research to improve human healthcare system. Generally, more than one method is desired to fulfill the demands of biomaterials, and also one should consider the product yield, reproducibility, and reliability before final selection of any one of the methods (Desmet et al. 2009).

In this chapter, we discuss the types and properties of polymeric biomaterials. The limitations of using biomaterials without surface modification and the mechanisms of bacterial adhesion and/or biofilm formation on the implants inside the human body are also discussed. Moreover, biofilm-related infections are discussed. The major part of the chapter focusses on the modification processes of the surfaces of polymeric biomaterials with antibacterial molecules to prevent the biofilm formation. Prevention mechanism of biofilm formation are also discussed.

15.2 Polymeric Biomaterials

15.2.1 Problems of Using Polymeric Biomaterials Without Surface Modification

The single-cell prokaryotic microbes such as bacteria have different forms such as spheres, ellipses, rods, or spirals. These microorganisms having size of a few micrometers live in every portion of the Earth. They have the ability to stick to a surface by being entrenched in ECM-forming biofilms. So, it is expected that the antibacterial polymeric biomaterial substrates should be able to destroy microbes such as bacteria, or hinder or interrupt their growth. Biomaterials used in the manufacture of life-saving medical devices have the risk of infections when applied in the patient's damaged part. The risk of insistent and prolonged contagions will be developed, if the bacteria undergo biofilm formation, and overall transmission to the body circulation system. The medical devices which come in contact with blood display high danger if there are bacteria adhered to the surface of these device materials or exist in the application site of the materials. For example, heart valves, intravenous or dialysis catheters, fluid shunts, cardiac pacemakers, joint prostheses, contact lenses, etc. are the most susceptible to common bacterial infection in body. The most commonly existing microorganisms forming biofilm on prosthesis devices are, namely, *Staphylococcus epidermidis*, *Staphylococcus aureus*, *Pseudomonas aeruginosa*, and *Escherichia coli* (Hall-Stoodley et al. 2004; Stewart and Costerton 2001). Bacteria may be settled on the polymeric prosthesis during surgery, so care must be taken for proper sterilization. However, the expertise of the surgical team, hygiene of the operation area, and all instruments used, as well as the circumstances of the patient and the injured part, are vital issues for the achievement. In the case of the development of biofilm, it is problematic to eradicate all the colonies as they are sheltered by the ECM. In these situations, the first way out is to remove the implant (Baveja et al. 2004). So, it is important to apply antibacterial surface coating on the implant materials.

15.2.2 Polymeric Biomaterials Surface Properties and Morphology

The experimental studies reveal that bacterial adhesion to a material surface is a competing process, where microorganisms contest with host proteins and cells for the colonization on the exterior of transplant materials (Subbiahdoss et al. 2010). Consequently, the perfect surface configuration of the polymer would be one that aggressively endorsed the binding and addition of host cells while stimulating tissue healing. This would inspire the conciliation of host biomolecule addition only to a position that simplifies incorporation of the polymeric biomaterial into the host systems without preventable immune response.

This would concurrently stop bacterial adhesion to surface and biofilm development on it (Liu et al. 2004; Stobie et al. 2008). The surface properties of polymeric biomaterial strongly influence bacterial attachment to its solid surface. The material

surface properties including its physical and chemical properties such as its chemical composition and reactivity, contact angle, polarity, electrostatic interactions, crystallinity, and mobility of the surface functional groups, surface energy and hydrophobicity, surface roughness, porosity, surface structure, depth, density, and grip of the modifying layer. The influences of surface physical and chemical properties on the integration of host cells and bacterial attachment are discussed in the following sections.

15.2.2.1 Surface Free Energy and Hydrophilicity

Surface free energy of solid surface indicates adhesiveness and attraction to other materials. It is due to the active functional groups on the exterior of solid surface and the electrical charges existing on the external surface. The surface energy of a solid become high when energy is increased upon bringing the surface into interaction with other materials. Solid surfaces are wettable by most liquids which possess high surface energy. On the contrary, most liquids do not wet solids having small surface energy. In general, any liquid having surface tension lower than surface free energy of a given solid surface will wet that surface entirely and develop a uniform liquid film on the surface. Surface free energy controls the wettability of the solid surface with water and, consequently, the hydrophilicity. This also influences the sorts and route of the first adsorbed host proteins and cells layer.

The hydrophilic surfaces are categorized with electrical charges and polar functional groups. High surface energy also encourages the addition with host proteins fixed to solid surfaces less strongly due to higher interaction with neighboring water molecules (Ratner et al. 1978; Hasan et al. 2020b; Pandey and Pattanayek 2013). In contrast, protein adsorption in dynamically favorable hydrophobic interactions is supported by hydrophobic solid surfaces. Nevertheless, it may bring powerfully permanent adsorption and denature the protein's natural conformity. Consequently, the protein will denaturate and will lose its bioactivity. The measure of water adhesion tension and degree of contact angle of the liquid drop are defined as the hydrophilicity of materials. Hydrophilic surfaces possess contact angles less than 65° , whereas hydrophobic biomaterial shows contact angles greater than 65° . It was revealed in many studies that solid surfaces that are either very hydrophilic or hydrophobic prevent host proteins and cell attachment. Therefore, for the improvement of proteins attachment and cell proliferation on the solid surfaces, an optimal value of surface hydrophilicity is essential. So, the moderate wettable surface by water is able to adsorb proteins without changing their conformity. They represent optimistic cell adhesion and expansion (Matlaga et al. 1976).

15.2.2.2 Adhesiveness and Functional Groups of Surface

The surface hydration is responsible for the change of the adhesiveness of hydrophilic surfaces. For instance, hydrated PEG/PEO (poly(ethylene glycol)) is provisionally adhesive, while glass is adhesive whether hydrated or not (White et al. 1981). Some polymers used as biomaterials are grouped as adhesive (e.g., poly(methyl methacrylate) (PMMA), tissue culture polystyrene (TCPS), poly(ethylene terephthalate) (PET)), polyurethane (PU), nonadhesive (e.g., polypropylene (PP)),

polytetrafluoroethylene (PTFE), and polyethylene (PE) based on the relationships among cell adhesion and water contact angles. The adhesive and hydrophilic properties of a polymeric biomaterial surfaces also count on the existence or absence of functional groups and their alignment on the surface (Girard-Egrot et al. 2005). The adsorption of proteins also depends on the position of the charged groups whether to the exterior or the interior of the material surface.

The carboxyl ($-\text{COOH}$), hydroxyl ($-\text{OH}$), amino ($-\text{NH}_2$), and methyl ($-\text{CH}_3$) groups are the most common functional groups present on biomaterials. For instance, several studies have been conducted on the occurrence of these groups on the biomaterial surface and their attractions with proteins as these groups are also present in protein structures.

In case of polymeric surfaces, bearing carboxyl ($-\text{COOH}$) groups, have a negative charge functionality on their surfaces with enhanced fibrinogen and albumin adsorption properties. It is also reported that an enlarged functional groups (carboxyl) density contribute an extra negative charges over the surface, which inhibit the cell adhesion and growth (Planell et al. 2010). pHEMA is another common biopolymer containing a hydroxyl ($-\text{OH}$) group. The bendable backbone of the polymer carbon chain can simply revolve and alter the position of the functional groups. pHEMA surface displays a hydroxyl-rich functionality in aqueous media, and in air, a methyl-rich functionality (Girard-Egrot et al. 2005). Hydroxyl ($-\text{OH}$) groups on the surface present an impartial hydrophilic surface. Previous research into surface functionality suggests that cell growth is proportional to the amount of oxygen-containing functionalities (Barbosa et al. 2006). Polymeric biomaterials containing amine ($-\text{NH}_2$) groups display a positive charge on the surface at physiological pH. Studies on the amine-functionalized materials showed appropriate protein conformations after adsorption onto these positively charged surfaces, and these frequently lead to amplified endothelial cell (Lee et al. 1998).

15.2.2.3 Morphology of Polymeric Biomaterials Surface

The primary reasons directly manipulating the cell interaction and tissue inflammatory response are the surface morphology and physical structure. It also responds to biofilm formation on solid surface (Hayward and Chapman 1984). Physical structure such as surface irregularity has a noteworthy consequence on hemocompatibility and biocompatibility of the applied biomaterials. When the number of edges, especially sharp edges, of the applied biomaterials increases, then the intensity of the inflammatory response also increases. Several studies reveal that the inflammatory response against implanted porous materials is more intense than nonporous materials (Bird et al. 1989). For instance, several studies have been performed on the engineered surfaces with micropillars or columns on adhesion of diverse cells. Those studies were designed to know the relation among the stiffness of the surface and cell adhesion. It is assumed from numerous reports that a combination of chemistry, physical forms, and the stiffness of the surfaces is vital in cell adhesion on the polymeric biomaterial exteriors.

15.3 Biofilm

The term “biofilm” was formally introduced in 1978 by Costerton (Costerton et al. 1978). Costerton et al. define biofilm as “a structured community of bacterial cells enclosed in a self-produced polymeric matrix and adherent to an inert or living surface.” Biofilms comprises of two basic substances: bacterial species and extracellular polymeric substances (EPS) (Vasudevan 2014). In short, biofilm can be defined as the communities of microorganisms that are attached on a surface, encased themselves in a self-secreted extracellular polymeric substances (EPS) matrix, and thus resulting in formation of a 3D bacteria community (Narayana and Srihari 2020; Armbruster and Parsek 2018; Rabin et al. 2015).

Bacterial species-produced biofilms are commonly found in the nature called planktonic bacteria (Armbruster and Parsek 2018; Mah and O’toole 2001). On the other hand, bacteria within the biofilm called sessile bacteria, which exist in a dormant growth phase, and their phenotypes are distinct and different from planktonic bacteria (Vilain et al. 2004; Stoodley et al. 2002). Biofilm-associated organisms grow more slowly in comparison to planktonic organisms due to their access to limited nutrient and oxygen (Donlan 2000). In comparison with planktonic counterparts, bacteria within a biofilm are approximately 600 times less susceptible to disinfectants and up to around 1000 times more resistant to antibiotics (Narayana and Srihari 2020; Donlan 2000). This makes biofilms a major public health problem since almost 60–80% of human microbial infections are caused by bacterial growth as a biofilm. Bacterial infections are so sturdy as it results in resistance to therapy and bacterial propagation to the host body as well (Ahmed et al. 2019; Kostakioti et al. 2013). The bacteria known to produce biofilm are *Enterococcus faecium*, *Staphylococcus aureus*, *Klebsiella pneumoniae*, *Acinetobacter baumannii*, *Pseudomonas aeruginosa*, and *Enterobacter* species, collectively known as “ESKAPE” (Rice 2010). They have been nicknamed as “the ESKAPE pathogens,” because of their ability to “escape” from the antibiotic action.

The second component of biofilm is the extracellular polymer matrix (EPS) which provides the matrix or structure for the biofilm. Within the biofilm, the bacteria those attach irreversibly to surfaces (i.e., eradicate by mild rinsing) start cell division, form microcolonies, and then produce the extracellular polymer (Donlan 2001a) matrix which is accounted for approximately 90% of the biomass within the biofilm (Lewandowski and Evans 2000) EPSs are composed of proteins, polysaccharides, lipids, extracellular DNA (3% by weight), and water channels (97% by weight) (Da Cunda et al. 2020). In addition to these substances, EPS also contains carbohydrate-binding proteins, pili, flagella, and other adhesive fibers (Kostakioti et al. 2013). The “water channels” within EPS allow necessary essential nutrients and oxygen to the cells growing during the process of biofilm formation. These extracellular polymeric enclosures not only favor the microorganisms by providing the essential nutrients but also create a favorable environmental condition for their survival and offer architectural integrity (Vasudevan 2014). In the matrix, nutrients, minerals, and various type of host components such as fibrin, RBCs, and platelets are trapped for metabolic consumptions by the resident microorganism, and

water is retained through H-bond formation with hydrophilic polysaccharides (Kostakioti et al. 2013; Donlan 2001a). However, depending on the nutrient availability, enzymes secreted by the bacteria also changes which modifies the EPS composition and thereby tailoring the biofilm architecture in response to the specific environment (Sauer et al. 2004). Thus, a highly hydrated, robust EPS is formed that keeps bacteria in close proximity, enabling intimate cell-to-cell interactions and DNA exchange, while protecting the biomass from desiccation, predation, oxidizing molecules, radiation, and other damaging agents (Flemming and Wingender 2010).

15.3.1 Reason for Biofilm Formation

Microbial biofilms are highly resistant to antibiotics and host immunity system. Formation of biofilms by clinically relevant microbial pathogens is the main cause of many chronic and recurrent infections in the human body (Hall et al. 2014). Biofilms have been accounted for 80% of all microbial infections (Rabin et al. 2015; Sun et al. 2013). These kinds of infections are hard to diagnose and treat (Rabin et al. 2015).

Biofilm-associated infections can be broadly divided into two types: device-associated infections, which are associated with indwelling medical devices; and non-device-associated infections, which contribute about 65% of all bacterial infections (Jamal et al. 2018; Sun et al. 2013).

The former type, device-associated infections, is known as biofilm infections related to implanted external materials and medical devices. Biofilms are formed by single or multiple different species of bacteria (Jamal et al. 2018).

The human body is susceptible to be infected by different microorganisms, such as viruses, fungi, and bacteria. Bacteria can enter human body during surgery or even through a minor injury like a cut finger. Sometimes, people have new implants put into their bodies during surgery, like a new valve in the heart. Bloodstream or urinary tract infections can be caused by biofilms originally formed from different indwelling medical devices including various catheters, mechanical heart valves, sutures, fixation pins and screws, voice prostheses, and dental implants (Unosson 2015; Sun et al. 2013).

Implant-associated infection can commence from many sources. Pathogens may originate from the epithelial flora of patients, hospital personnel, or from any other sources in the environment. These generated microorganism form infectious biofilms on the surfaces of implants and devices, and subsequently get into human organs or tissues (Donlan 2001b). Even after hip or knee implants and heart valve replacements, an infection can arise by hematogenous spread of bacteria which entered into the bloodstream (Unosson 2015). Contamination of implants by bacteria causes the host immune system to react to bacteria and to identify the biomaterial surface as foreign body to cause an inflammatory response.

However, the situation becomes worse when the implant is placed into a fluid, such as bloodstream, or the urinary tract. A conditioning film (comprised of proteinaceous material present in the fluid) is formed on the implant. The surface properties of the implant are then completely masked by the properties of the conditioning film.

Biofilm formation are then significantly impacted by surface topography. Besides, implant surface properties and bacterial cell surface characteristics also play an important for biofilm growth. For example, the presence of flagella, pili, fimbriae, or glycocalyx affects the rate of microbial attachment. To get permanently attached to implant surface, the microbial cells must overcome all repulsive forces. In this regard, during reversible attachment, these appendages allow the cell to remain attached to surface, until the cells get permanently attached. Korber et al. (1989) demonstrated that the flagella facilitated the attachment of Gram-negative bacteria to surfaces. Rosenberg et al. (1982) showed the importance of fimbriae for attachment of bacteria to surface. Microbial cell surface hydrophobicity is also very important for attachment (Unosson 2015). In addition to this, to favor the attachment, bacteria tend to position themselves to maximize their contact area with the surface (Feng et al. 2015). The possible reasons for which bacteria form a biofilm could be as discussed in the next paragraph.

Bacteria form biofilm to enhance their tolerance to harsh environmental conditions. Bacteria in planktonic form are loosely attached to a surface or tissue and thus can be easily washed away by water flow or blood stream. In contrast, bacteria within biofilms can withstand repeated, strong shear forces and are nearly 1000 times more resistant than their planktonic counterpart (Rasmussen and Givskov 2006).

15.3.2 Biofilm Growth

Biofilm formation mainly occurred in four main stages (Crouzet et al. 2014; Jamal et al. 2018):

1. Biofilm adhesion, where planktonic (free floating) bacteria attach to the biomaterial surface.
2. Biofilm formation, where cells aggregate, form microcolonies, and excrete extracellular polymeric substances (EPSs) and become irreversibly attached to the surface.
3. Biofilm maturation, where biofilm matures, cells form multilayered clusters, and three-dimensional growth occurs. After maturation, biofilm causes protection against host defense mechanisms and antibiotics.
4. Detachment/dispersion of biofilm where the biofilm reaches a critical mass disperses planktonic bacteria which may colonize to new surfaces.

15.3.2.1 Biofilm Adhesion

Bacterial adherence to abiotic surfaces is a spontaneous phenomenon. As free-floating bacteria approach a surface, it encounters both attractive and repulsive forces that vary depending on nutrient levels, pH, ionic strength, and temperature (Narayana and Srihari 2020; Kostakioti et al. 2013). This initial attachment is reversible, during which bacteria can detach and reattach the planktonic population if disturbed by repulsive forces, or in the presence of available nutrient. Moreover,

composition of bacterial cell-surface affect the velocity and direction of forces toward or away from the contact surface (Kostakioti et al. 2013). For instance, from a distance of 10–20 nm, the negative charges on the bacterial surface are repelled by the negative charges on contact surfaces (Rabin et al. 2015). This repulsion could, however, be overcome by attractive van der Waals forces, acid base, hydrophobicity, Brownian motion, and gravitational, electrostatic, polar, and ionic interactions between the bacterial cells and the surface (Narayana and Srihari 2020; Ahmed et al. 2019). Along with physical forces, bacterial adhesion to surface occur by bacterial appendages such as pili; flagella act as adhesins and can lead to biofilm formation (Jamal et al. 2018; Ahmed et al. 2019). Adhesion also occurs due to the presence of a thin layer on indwelling medical device or living tissues consisting of proteins such as fibronectin, fibrinogen, vitronectin, thrombospondin, laminin, and collagen (Dunne 2002). This thin layer is called conditioning film on the surface which plays a role in the attachment of bacteria to the abiotic surfaces (Espersen et al. 1990; Ahmed et al. 2019).

Irreversible attachment is attained by those bacteria that can endure shear forces and can maintain a steadfast grip on the surface (Kostakioti et al. 2013). During this stage of attachment, bacteria can also stick to each other (cohesion attachment) or to different surface-bound organisms (adhesion attachment) and thus form aggregates. Interestingly, the presence of one species of microorganism on a surface can enhance the adhesion of other species (Garrett et al. 2008). The hydrophobicity of the surface may also strengthen the attachment of microbes, since it reduces the force of repulsion between the bacteria and the surface (Tribedi and Sil 2014). Microorganisms attach more likely to the hydrophobic and nonpolar surfaces, in comparison to hydrophilic and polar surface (Fletcher and Loeb 1979) (Fig. 15.1).

15.3.2.2 Biofilm Formation

After an attachment of microorganisms to a biotic or an abiotic surface, the bacteria then start to form a monolayer (Da Cunda et al. 2020). Bacteria in monolayer thus form microcolony by producing cellular aggregates through multiplication and division. Several multilayers of bacteria form an organized structure by producing an extracellular polymeric substance (EPS) (Narayana and Srihari 2020). The EPS provides the matrix or structure for the biofilm and consists of polysaccharides, structural proteins, cell debris, nucleic acids, and water channels (Da Cunda et al. 2020; Donlan 2001a). The matrix formation is initially dominated by extracellular DNA (eDNA) whereas later on regulated by polysaccharides and structural proteins (Da Cunda et al. 2020). The attachment is now irreversible and the biofilm starts to grow in a three-dimensional manner (Narayana and Srihari 2020). This three-dimensional (3D) cell mass varies in its bioarchitecture constituting “tower-like” structures (Da Cunda et al. 2020). Bacterial colonies in a biofilm can generally be divided into many microcommunities. These microcommunities coordinate and communicate with each other for exchange of substrate, distribution of important metabolic products, and for secretion of metabolic end-products. For instance, during anaerobic digestion, complex organic matter is converted into CH₄ and CO₂, and requires involvement of a minimum three types of bacteria:

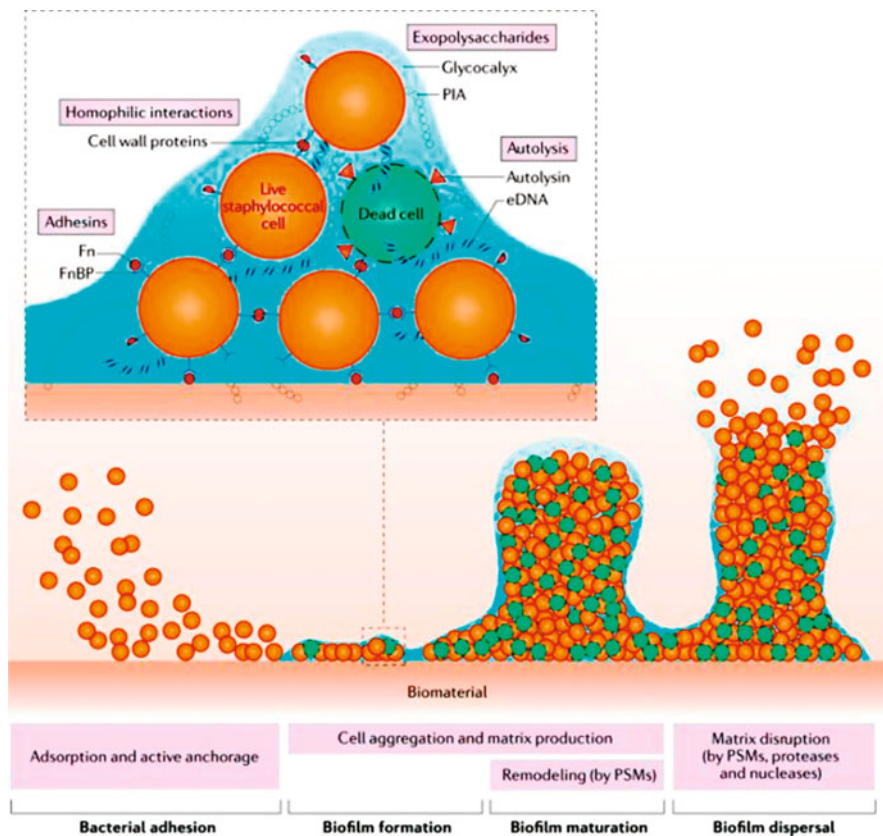


Fig. 15.1 Stages of biofilm formation. After adhesion, bacteria interact with each other to form microcolonies promoting bacterial aggregation. Large bacterial aggregates called towers develop when polymeric matrix in biofilm progresses. PIA and eDNA expression in biofilm also contributes to the biofilm formation. Phenol-soluble modulins form characteristic water channels and are also involved in bacterial dispersal. (Figure adapted from Ahmed et al. (2019) with permission from Elsevier)

(1) fermentative bacteria that start the production of acid and alcohol from organic compounds, (2) acetogenic bacteria that consume the substrates produced, and (3) finally methanogens that convert the acetate, carbon dioxide, and hydrogen into methane and get energy. Thus, it can be said that biofilm provides a perfect environment for the development of syntrophic association, an association of metabolically different bacteria depending on each other for utilization of certain substrates to get energy (Jamal et al. 2018; Davey and O'toole 2000).

15.3.2.3 Biofilm Maturation

Once bacteria have irreversibly attached to a surface, the process of biofilm maturation begins. There are two stages of maturation:

Stage I: Inter-cell communication and the production of autoinducer signal molecules.

Stage II: Increase of the microcolony size and thickness to a value of around 100 μm , forming a macrocolony (Khatoun et al. 2018).

Stage I

In this phase, the adhered cells grow and mature by communicating among themselves through secretion of signaling molecules, known as autoinducers (Davies et al. 1998). Bacteria within biofilm communicate with one another through autoinducer signals (Vasudevan 2014). Cell-to-cell communication is an important process to attain the required microbial cell density. These autoinducers facilitate quorum sensing (Jamal et al. 2018). Maturation stage is regulated by quorum-sensing systems. These factors determine the strength of surface attachment (Narayana and Srihari 2020).

Stage II

Further remodeling, adaptation and development of cells in microcolonies lead to the formation macrocolonies (Ahmed et al. 2019). The growth potential of any bacterial biofilm is regulated by the availability of nutrients, the perfusion of those nutrients to cells within the biofilm, and the removal of waste. The overall density and complexity of the biofilm increase as surface-bound organisms (pili, fimbriae, flagella) begin to actively replicate and the extracellular matrix components start to interact with organic and inorganic molecules of the environment to create the glycocalyx (Dunne 2002). Thus, it can be said that biofilm maturation is achieved by regulation of pili, fimbriae, flagella, exopolysaccharides, and glycocalyx. In addition, there exists an optimum hydrodynamic flow across the biofilm that favors growth and perfusion rather than erosion of the outermost layers. These factors determine the strength of surface attachment. Other factors that control biofilm maturation include internal pH, oxygen perfusion, carbon source, and osmolarity (Dunne 2002; O'toole and Kolter 1998). Biofilm eradication is very hard after maturation.

15.3.2.4 Detachment/Dispersion of Biofilm

Biofilm maturation is followed by the detachment step, which is also crucial for the biofilm life cycle. In this phase, microbial cells within the biofilm undergo quick multiplication and dispersion to convert from sessile into motile form.

Detachment occurs in a spontaneous pattern (Costerton et al. 1999). Many factors are responsible for dispersal of biofilms, such as lack of nutrients, or perfusion, decreased pH, pO_2 , or an accumulation of toxic metabolic by-products, outgrown population, etc. At some point, the biofilm reaches at a critical mass. A dynamic equilibrium is reached at this point where the outermost layer of growth (farthest from the surface) begins to generate planktonic organisms. These organisms are now free to escape the biofilm. Whole or a part of biofilm may disperse. However, release of planktonic bacteria on dispersion of biofilm again promotes the initiation of new biofilms at other sites (Rabin et al. 2015). Some bacteria do not produce extracellular polysaccharide, and the bacterial cells disperse directly into the environment

(Baselga et al. 1994). During the detachment process, microorganism within the biofilm produce different saccharolytic enzymes that help to release the surface of the microbes into a new area for colonization. For instance, *Escherichia coli* produces *N*-acetyl-heparosan lyase, *Pseudomonas aeruginosa* and *Pseudomonas fluorescens* produce alginate lyase, and *Streptococcus equi* produces hyaluronidase for the lysis of the EPS matrix and subsequent detachment (Sutherland 1999). After getting detached from the biofilm, bacteria resume to planktonic mode and float freely in the surrounding body fluids causing spreading of infection. Biofilm dispersion causes the selection of new sites or further local invasion and aid in the spreading of infections (Narayana and Srihari 2020). Proteases and accessory gene regulator (Agr) controls this stage (Jamal et al. 2018).

15.3.3 Infections Due to Biofilm Formation

15.3.3.1 Biofilm-Associated Infections

Microbial biofilms are highly resistant to antibiotics and host immunity system. Formation of biofilms by clinically relevant microbial pathogens is the main cause of many chronic and recurrent infections in the human body (Hall et al. 2014). Biofilms have been accounted for 80% of all microbial infections (Rabin et al. 2015; Sun et al. 2013). These kinds of infections are hard to diagnose and treat (Rabin et al. 2015). Biofilm-associated infections can be broadly divided into two types: device-associated infections, which are associated with indwelling medical devices; and non-device-associated infections, which contribute about 65% of all bacterial infections (Jamal et al. 2018; Sun et al. 2013).

The former type, device-associated infections, is known as biofilm infections related to implanted foreign materials and medical devices. Biofilms are formed by single or multiple different species of bacteria (Jamal et al. 2018).

For instance, bloodstream or urinary tract infections can be caused by biofilms originally formed from different indwelling medical devices including various catheters, mechanical heart valves, sutures, fixation pins and screws, voice prostheses, and dental implants (Unosson 2015; Sun et al. 2013). Implant-associated infection can commence from many sources. Pathogens may originate from the epithelial flora of patients, hospital personnel, or from any other sources in the environment. These generated microorganism form infectious biofilms on the surfaces of implants and devices, and subsequently get into human organs or tissues (Donlan 2001b). Even after hip or knee implants and heart valve replacements, an infection can arise by hematogenous spread of bacteria which entered into the bloodstream (Unosson 2015). Contamination of implants by bacteria causes the host immune system to react to bacteria and to identify the biomaterial surface as foreign body to cause an inflammatory response.

Few Biofilm-associated clinical infections have described below.

Urinary Infection

Biomaterials in the urinary tract, such as catheters, increase the chance of biofilm formation and cause urinary infection (Tenke et al. 2006). Catheters provide surfaces for bacteria to attach. Both the inner and outer surfaces of urinary catheters are infected with bacterial biofilms, for example, *P. mirabilis* biofilms, which can block catheters, and need to be replaced (Jacobsen et al. 2008).

Prosthetic Joint Infection

Gram-positive bacteria, such as *Staphylococci*, usually cause prosthetic joint infection. After surgery, bacteria come from blood or the lymph attached to the surface of prosthetic joints and form biofilms. In contrast to typical bacterial infections, this infection shows other symptoms like pain and emerge (Khardori and Yassien 1995).

Cardiac Valve Infection

Bacterial biofilm on cardiac valve implant causes a disease called prosthetic valve endocarditis. The microorganisms that cause endocarditis are *S. epidermidis*, *S. aureus*, *Streptococcus* spp., *Corynebacterium* spp., *Enterococcus* spp., and *Candida* spp. (Khardori and Yassien 1995). Biofilm formation can disrupt or block the artificial cardiac valve, resulting in diminished flow, turbulence, or even leaking. Detached biofilm cells can transfer along with the blood stream and cause infection in other organs.

Dental Implant Infection

Peri-implantitis is generally caused by biofilm-producing oral pathogens. This infection causes inflammation and a progressive bone loss around the dental implant (Mombelli et al. 2012). Periimplantitis has been reported to affect around 10% of implants and is a major reason of worry for patients and dentists. Species that cause peri-implantitis and other implant-associated infections do not only pose an immediate threat to the implant and the surrounding bone, but may also cause bacteremia. Bacteremia is the presence of bacteria in the bloodstream which can cause infection and biofilm formation even on other sensitive implants such as artificial heart valves (Unosson 2015).

Bone Implant Infections

The microorganisms responsible for orthopedic implant-associated infections have been reported as *Staphylococcus aureus* and *Staphylococcus epidermidis* (Mombelli et al. 2012; Pye et al. 2009). Both of these species are common around the human body. *S. aureus* are available in the nostrils and *S. epidermidis* are found on the skin (Pye et al. 2009). These microorganisms cause harm if the skin barrier is broken, or the immune system is not strong enough. Both of these species are strong biofilm formers and have reported to develop resistance to a range of antibiotics. Unfortunately, the methicillin-resistant strains of *S. aureus* (MRSA) and *S. epidermidis* (MRSE) are often developed at the hospital, which cause worse condition of patient (Unosson 2015).

15.3.3.2 Non-device-Associated Infections

Biofilm-associated clinical infections are often chronic infections and mainly include cystic fibrosis lung infection, recurrent tonsillitis, recurrent urinary tract infection, chronic otitis media, chronic wounds, dental caries, chronic rhinosinusitis, chronic prostatitis, dental caries, and periodontitis (Hall-Stoodley et al. 2012; Del Pozo 2018; Burmølle et al. 2010).

Cystic Fibrosis (CF)

Cystic fibrosis (CF) occurs in the lung and causes formation of thick and sticky mucus. Sticky mucus blocks patient's airway and causes breathing problem (Lyczak et al. 2002). *P. aeruginosa* is mostly responsible for cystic fibrosis (Pedersen et al. 1986). Antibiotic treatment often alleviates *P. aeruginosa* infection; however, it does not necessarily cure the infection. The reason behind incomplete cure is mainly due to *P. aeruginosa* biofilms that cause disease recurrence (Costerton et al. 1999).

Dental Infection

Biofilms play a vital role in dentistry. More than 700 species of bacteria have been reported to cause dental plaque (Overman 2000). Dental plaque is actually composed of mixed biofilms (Overman 2000) and can be divided into healthy and disease-associated dental plaque. The composition of the healthy plaque biofilm is significantly different from disease-associated plaque biofilms.

S. sobrinus and *S. mutans* have been reported to be involved in dental caries, and they have very high acid tolerance (Unosson 2015). *Streptococcus mutans*, which are responsible for both caries and plaque formation, have also been found to colonize on dental implant surfaces (Jamal et al. 2018).

Periodontitis is an infection of the gums. The biofilm formation on gums due to poor oral hygiene also causes tooth loss, soft tissue damage, and damages of the bones supporting the teeth (Kokare et al. 2007). This is caused by *Fusobacterium* and *P. aerobicus* (Narayana and Srihari 2020).

Wounds

Chronic wounds are usually associated with biofilms, whereas acute wounds are not associated with biofilm (James et al. 2008). So, chronic wounds persist and slowly heal. For wound, biofilms are usually formed on the outer layer; however, in few cases, biofilms may also be embedded in the deep layers of a wound, such as *P. aeruginosa* biofilms (Hall et al. 2014).

Bone Infection

Osteomyelitis, a disease of bones, is caused due to the entry of bacteria into bones through the bloodstream or through previous infections (Narayana and Srihari 2020). Bone infection leads to the formation of white blood cells (WBC) which secrete enzymes. These enzymes may lyse the bone and results in the formation of pus which spread through the bone blood vessels and cause tissue damage and deterioration of the function of the affected bone areas (Jamal et al. 2018).

15.4 Improvement of Antibacterial Properties of Polymeric Biomaterials by Surface Modifications

Various surface modification or treatment procedures have been developed for the preparation of antibacterial surfaces over the past decades (Tiller et al. 2001; Bazaka et al. 2011b). The surfaces are usually allowed to undergo either chemical or physical treatments. Such surface modifications include surface functionalization, derivatization, polymerization, or mechanical or surface architecture alteration (Bazaka et al. 2011a; Muñoz-Bonilla and Fernández-García 2012). Among the methods, surface functionalization, derivatization, or polymerization techniques prominently involve the chemical modification of the surface, whereas both the mechanical and surface structuring approaches are considered as the physicochemical alteration of the surfaces (Hochbaum and Aizenberg 2010; Tiller et al. 2001).

15.4.1 Physical Methods

15.4.1.1 Physical Adsorption

By definition, adsorption refers to the linkage of atoms, ions, biomolecules, or molecules of gas, liquid, or dissolved solids onto a different solid state. Adsorption is generally utilized to alter the surfaces of polymeric biomaterials through the successful immobilization of bioactive compounds through ionic attractions or pairing between ligand and receptor (Xia and Whitesides 1998; Takahara et al. 2000). To obtain strong adsorption, substrate materials are required to have certain groups to interrelate the coating materials. As reported, the biotin–avidin correlation is considered as one of the strongest noncovalent bonds with a force up to 250 pN. Adsorption is also promising in case of its application in drug delivery due to its simplicity and reversibility. In various applications, physical adsorption of the molecules that are biocompatible (such as proteins and enzymes) have been found to achieve through dip coating of the substrate materials (Guney et al. 2013).

15.4.1.2 Surface Micro- and Nanopatterning

Biomaterial surface can easily be improved following various techniques to generate both the micro- and nanopatterns. The obtained design can either be arbitrary or well in order (Goddard and Hotchkiss 2007).

Lithography is considered as one of the prominent approaches to pattern biomaterial surface and is normally applied in the microelectronic industries. The topographic pattern, in case of biomaterial applications, is created on the silicon wafer which is simulated on the polymeric surface.

The process is analogous to the photolithography. In this process, a single beam of light (commonly UV) is allowed to cross a film that carries the reverse of the chosen pattern onto the coated silicon surface. After the successful exposure, the substrate undergoes washing and the pattern (which is transferred) gets stable

through etching process with a suitable solvent. Such substrate can also be utilized as a model to produce the reverse copies.

On the other hand, laser machining (a quicker, cleaner, and easier method to adapt) has been demonstrated prominently in various surface modifications (Kurella and Dahotre 2005; Duncan et al. 2002). Complications encountered in photolithographic process was also overcome (difficulties associated with acid etching). Moreover, the expected pattern can easily be organized regarding the height-to-depth ratio and spacing of the surface (Hallgren et al. 2003).

Microcontact printing, considered as another significant surface alteration method, utilizes polydimethylsiloxane (PDMS) stamps having the contrary design shaped on its surface. In this process, a chosen design is produced first on silicon wafer, photoresist in nature, following the regular photolithography as stated earlier. Further, an opposite model can also be attained following thermal curing process (utilizing PDMS) on the surface. Here, PDMS stamp retains as is. In case of printing the biomolecules on the biomaterial surface, the stamp, which is of elastomeric nature, is allowed to dip in a medium containing the particular molecules which is further forced on the directed exterior. Following the same approach, structures including proteins, fluorescent molecules, quantum dots, or even cells can easily be shifted onto a designed surface (Ma et al. 2007; Ozdemir et al. 1999).

15.4.1.3 Langmuir–Blodgett (LB) Film Deposition

Characteristic functionalities present on the surfaces of polymeric biomaterials ensure proper coating, both physically and uniformly with amphiphiles, while implementing the Langmuir–Blodgett (LB) process (Heens et al. 1991). According to this technique, the substrate is allowed to submerge into a solution comprising of the coating materials, which is further removed gradually by taking off. Deposition of the coating materials takes place onto the solid surface while dipping and removing the substrate from solution. However, the presence of surfactant molecules reduces the energy (free energy) while establishing a well-organized single layer on the material surface. Formation of such assembly has been found to be accomplished and controlled by several forces enlisted as intermolecular, capillary, and electrostatic forces or connective motion of solvents (Takahara et al. 2000).

Coating materials usually act like amphiphiles in nature while attaining a surfactant having the structure with both the hydrophilic head and hydrophobic tails. Such molecules are found to get spread rapidly on the surface of the water when a dilute solution of an amphiphile is allowed to add in an aqueous solution. The molecules get rearranged themselves at the interface in a manner whereas the polar head groups remain inside the water and the tail groups remain at the outside. Hydrophobic groups, present on the outside of water, simply deliver a strong repulsive energy to each other resulting in a properly ordered layer that floats at the liquid surface while affecting the surface strain of the liquid (Knobler 1990; Ulman 1991).

The previously arranged layer can further be moved to a biomaterial surface in numerous manners. If a solid material is allowed to get dip in vertical manner and further detached slowly, either the hydrophilic head groups or the hydrophobic tail groups present on the molecules get bonded to the solid surface via ionic attractions

according to the surface charges resulting in a properly ordered monolayer coating known as Langmuir film. Successively, multilayers can also be obtained via continuous deposition of monolayers. Such deposition approach is known as Y-type, involving a stack of head-to-head and tail-to-tail configurations. Nevertheless, the occurrences regarding the transformation of floating monolayer during the immersion (known as X-type deposition) or the emersion (known as Z-type deposition) of the substrate material have also been found in literature (Guney et al. 2013).

15.4.2 Chemical Methods

Surfaces of the polymeric biomaterials can also be modified by numerous methods involving straight chemical reactions with a gaseous medium (for example: ozonization, fluorinization, etc.), reactions with a solution (known as wet treatments), or covalent attachment between the macromolecules to the sample surface (simply known as grafting). The characteristic functionality conveyed to the inactive surface should be well suited with the sensitive sites of the substrate to be covalently bonded to the surface. Covalently bonded molecules usually provide the steadiest bond between the substrate and the molecules. Moreover, such conjugations spread their half-life, retain their activity, and inhibit their metabolism as well when the bonded molecules are bioactive in nature (Kuhl and Griffith-Cima 1996; Zheng et al. 1994).

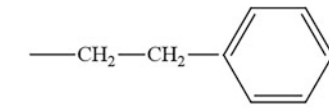
15.4.2.1 Ozone Treatment

Peroxy groups, on which different molecules can get conjugated, in the polymers are attained through the application of ozone. According to various studies, such conjugation can be enhanced with UV irradiation (Gao et al. 2003). In a study, Liu et al. reported the effect of UV irradiation in combination with ozone in case of grafting the polymers that are hydrophilic in nature, for instance, chitosan, poly (vinyl alcohol) (PVA), etc. to a polyethersulfone ultrafiltration membrane (Liu et al. 2008). The alteration process was found successful and the prepared films showed improved hydrophilicity and roughness together with reduced protein adsorption.

15.4.2.2 Silanization

In general, silanization is one of the cheapest and efficient covalent coating method improving materials surface enriched with hydroxyl groups (Hasan et al. 2018a; Hasan and Pandey 2020). Silanized surface can also be altered via further grafting (Hasan et al. 2018b; Hasan and Pandey 2020). In a study, Zhang et al. considered hydroxyapatite (HA) with fluorescein isothiocyanate (FITC) through altering HA by 3-aminopropyltriethoxysilane (AMPTES), and then grafting FITC via successful interaction with the amino group (Zhang et al. 2008; Yuan et al. 2010). Even though the silanization process is very modest and efficient in nature, the reaction conditions (e.g., reaction time and silane concentration) must be cautiously organized to avoid the thick polymerized silane network on the surface. If not, the interaction between silane and the surface can further get hydrolyzed in certain environments

Table 15.1 Silanes used for modifying biomaterials

Silanes	X = Leaving group	R = Functional group
$\begin{array}{c} \text{X} \\ \\ \text{X}-\text{Si}-\text{R} \\ \\ \text{X} \end{array}$	---Cl ---OCH_3 $\text{---OCH}_2\text{CH}_3$	$\text{---(CH}_2\text{)CH}_3$ $\text{---(CH}_2\text{)}_3\text{NH}_2$ $\text{---(CH}_2\text{)}_2\text{(CF}_2\text{)}_5\text{CF}_3$  $\text{---(CH}_2\text{)}_3\text{---O---C(=O)---C(CH}_3\text{)H---CH}_3$

(Wasserman et al. 1989). The chemistry of the distinctive silanes utilized during the modification procedures is shown in Table 15.1.

15.4.2.3 Fluorination

Surface modification of the biomaterials can be achieved through the proper addition of fluorine or other halogens. Among the halogens, fluorine has evoked distinct interests in the recent times as it upsurges both the hardness and hydrophobicity of surfaces. Following the fluorination method, prominently improved hydrophobic surfaces like Teflon (that shows very much nonadhering property) can be produced which further prevents the attachment of protein on the polymeric surfaces (Guney et al. 2013).

15.4.2.4 Wet Treatments

In wet treatments, surface of the materials is generally treated with liquid reagents to produce reactive functional groups (for instance, aminolysis, alkaline, or acidic hydrolysis). In addition, the treatment between the polymeric surface and hydrogen peroxide results in reactive sites for the consecutive attaching of vinyl monomers. On exposure of UV radiation, hydrogen peroxide gets decomposed to yield hydroxyl radicals that exhibit much more sensitivity than that of other oxidative chemicals. This technique is frequently applied to produce hydroperoxide groups on the polymeric surface which is attained by proper dipping of the substrates in hydrogen peroxide solution while irradiating with UV concurrently. The sample is further immersed in a solution of monomer and allowed to expose UV for another session which initiates the polymerization reaction. In alternative study, Goddard et al. reported another promising form of oxidation utilizing low-density polyethylene (LDPE), whereas the samples were endorsed to treat with chromic acid introducing carboxylic groups on the surface (Goddard et al. 2007).

15.4.2.5 Flame Treatment

Flame treatment, usually known as a general surface modification technique, involves bombarding of the polymeric surface with ionized air generating a wide range of oxidation products at the top of various monolayers (Zhu et al. 2002a). In this approach, reactive oxygen is usually produced via successful burning of an oxygen-enriched gas mixture resulting in both the surface wettability and surface energy of the material while increasing the affinity with coatings. Flame treatment has also been reported to provide hydroxyl, aldehyde, and carboxylic acid functionalities to polyethylene and is applied to improve printability, wettability, and adhesion as well (Zhu et al. 2002b). After the complete activation of the surface (by flame treatment), further alteration through grafting of polymeric materials can also be attained.

15.4.3 Biological Methods

Binding between the bioactive molecules and the surface of biomaterials is usually done to modify the compatibility of biomaterials in human body. According to the biological recognition on the cell activities, two main approaches of biomaterials in surface engineering are frequently applied. Primarily, surface properties (such as chemical composition, hydrophilicity/hydrophobicity, surface charge, roughness, etc.) of the materials are modified to a state where the adsorbed proteins can sustain their usual bioactivities though this method cannot prompt specific cell behaviors owing to nonspecific protein adsorption. The second strategy involves direct immobilization of certain biomolecules on the biomaterial surfaces inducing specific cellular responses (Desmet et al. 2009).

Numerous groups of polymers have been found to be used, as shown in Table 15.2, in immobilization process along with a variety of applications. Hence, while binding a bioactive molecule, the surface is allowed to get activated first which further undergoes functionalization through proper binding with a linker (linking can easily be done between the activated surface and bioactive molecule) having different functionalities. Finally, the desired bioactive molecules get bonded covalently to the generated functionalities.

Table 15.2 Varieties of bioactive compounds with their applications

Types	Applications
Enzymes	As biosensors, active packaging, biomaterials, bioreactors, microanalytical devices, etc.
Peptides	In tissue engineering and antimicrobial surfaces
Polysaccharides	In tissue engineering, hemocompatible materials, antimicrobial surfaces, etc.

15.4.4 Radiation Methods

Radiation methods are extremely applied in the field of medical science both in disinfection and stimulation of the surfaces. In medical applications, radiation methods are extensively used for sterilization or surface activation. Generally, certain chemical bonds that are present on the surfaces of biomaterials can easily be broken through irradiation process resulting in free radicals which can further undergo reactions leading to oxygenation or amination. While considering polymers, irradiations with high energy usually provides certain cross-linking and/or degradation on top of activation as well. The produced free radicals can recombine and form cross-linking, or chains can get cleaved resulting in the degradation of polymer matrix (Södergård 2004). Various types of radiations have been found to be successfully applied to biomaterials, and the most common forms are enlisted as plasma, microwave, corona discharge, gamma (γ), and electron (e) beam radiations.

15.5 Mechanism of Preventing Biofilm Formation

The key reason for bacterial infections accompanying polymeric biomaterials is the biofilm. The formation of biofilm starts while the bacterial community sticks to a solid surface. The bacterial inflammation associated with polymeric biomaterials are currently thought to be the most severe and devastating complications for using biofilm as implants and medical devices instead of having some prolific uses. Being indispensable in the healthcare system nowadays, different types of body implants are used every day. These body implants could be affected by the bacterial stream which may cause serious health problems, even death. The death rate of these types of bacterial infections are found more compared with other medical reasons. Thus, the bacterial contamination that developed in implanted devices could be critical as it is reckoned that infections kill more people than other medical causes. Therefore, the ultimate motive is the inhibition of the biofilm genesis or the annihilation of bacterial attachment to the facet of implants. To avoid this bacterial adhesion and subsequent biofilm formation, numerous techniques are studied and most of them are linked with surface design. The approach related to surface design can be classified into two categories (Fig. 15.2): one is bacterial repelling and the other is bacteria-killing surfaces (Vasilev 2019). The former technique acts by prohibiting the development of biofilm, and the latter follows the complete destruction of bacterial cell (Andrade Del Olmo et al. 2020).

15.5.1 Bacteria Repelling Mechanism

This mechanism incorporates several tactics to lessen the bacterial adherence to the surface, for example, preventing the coalition of bacteria, and it is performed by maintaining a certain surface structure that is unfavorable for the growth of

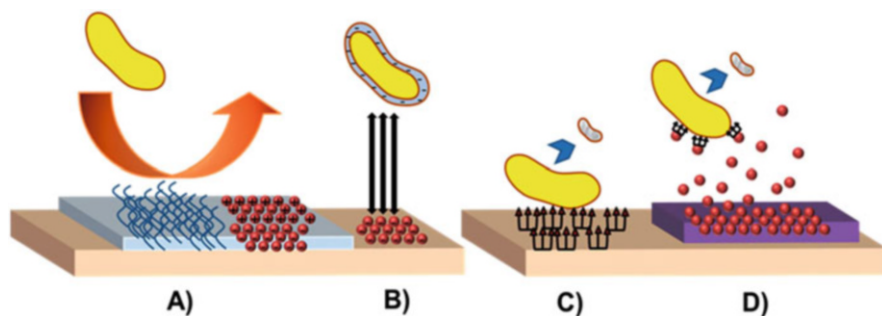


Fig. 15.2 Techniques for the development of antibacterial surfaces based on: (a) steric, (b) electrostatic, (c) contact killing, and (d) biocide release effects (Andrade Del Olmo et al. 2020)

microorganisms. That is why an extremely hydrated surface being able to prevent bacterial adhesion is used to cover the hydrophilic surfaces. Polyethylene glycol (PEG) polymers and zwitterionic elements attached to the surfaces can be treated as good examples of this antibacterial hydrophilic surface. Bacteria repelling action can be illustrated and categorized depending on three effects: (1) steric; (2) electrostatic; and (3) superhydrophobic effects that could be noticed in hydrophilic, charged, and superhydrophobic surfaces, respectively.

15.5.1.1 Hydrophilic Surfaces

It is established that the hydrophilic surfaces avert the adherence of bacteria to the cell wall due to the layer of water molecules acting as a cover. For being adsorbed on the surface, microbes must overcome the obstacle which is created by the hydrogen bond between water layer and hydrophilic material acting as a barrier. This adsorption involves the driving away of water molecules from the surface, particularly a decrease in free energy barrier resulting from the entropic effect produced from the demolition of the hydration layer (Savvides and Bell 1993). Thus, a highly hydrophilic film could act as a repellent for bacterial attachment along with being a simple method. That is why such kinds of coatings have been explored for the last few years. Superhydrophilic zeolites coated on titanium alloy surface showed its potential as body implants without any bacterial infections (Wang et al. 2011). A multi-layer of hydrogen bonding between poly(ethylamine) and poly(urethane acrylate) compounded with silica nanoparticles was reported as a superhydrophilic coating (Lin et al. 2016).

In fact, hydrophilic polymers are able to diminish bacterial adherence to minimum level even so maximum antifouling characteristics are only attained when steric repulsion complements surface hydration (Chen et al. 2010). In this type, some extraordinarily hydrated polymers are given extra emphasis as these have proved the ability to lessen bacterial attachment by steric hindrance. PEG on a surface notably demonstrates a large exclusion volume effect and chain flexibility decreasing protein and bacterial addition. Derivatives of PEG have also been fixed on the surfaces by adsorption or covalent grafting method. The higher duration of bacterial-resisting

activity was confirmed for the covalently linked PEG polymers compared to the physically adsorbed PEG molecules (Kingshott et al. 2003). Moreover, neutral and hydrophilic polymers, such as poly(2-alkyl-2-oxazoline), have also exhibited analogous non-fouling properties to PEG (Hadjesfandiari et al. 2014).

The other type of material termed as polymer brushes are fabricated by grafting high-density polymer molecules on the surface. A clear drop of bacteria adhesion was observed when PEG or PEO (polyethylene oxide) have been grafted to different surfaces. For instance, covalently grafted PEO molecules on the surfaces of glass and silica were responsible for 98% decrease of adhered *Staphylococci* and *Escherichia coli* (Roosjen et al. 2006). Furthermore, equal or even better bacteria-repellent properties homologous to PEG were shown by polyacrylamide (PAAm) brushes that were developed on silicon or golden wafer substrates (Hadjesfandiari et al. 2014).

15.5.1.2 Charged Surfaces

Because of the ionization of carboxyl and phosphate, the cell membrane of microbes produces a negative charge. In consequence, electrostatic repulsion arises during the time negatively charged surfaces and bacteria cells approach together clarifying the general eradication of bacterial attachment (Liu et al. 2014). Surfaces cross-linked with zwitterionic polymers having long chain with containing positively and negatively charged functional groups are intriguingly able to show antifouling properties. In terms of PEG, there acts a physical and energetic barrier originating from the strongly attached aqueous layer at the surface diminishes bacteria adsorption. Compared to hydrophilic polymers, bound water interaction by ionic salvation is stronger than the hydrogen-bonding linkage water, which strengthens the antifouling nature of zwitterionic surfaces (Chen et al. 2010). Apart from the effect of steric hindrance of this hydration layer, the cationic group could kill bacteria on contact.

Preparation of antibacterial coatings for hydrogel, fibers, and membranes requires zwitterionic polymers. It was noticed that formulated poly(sulfobetaine methacrylate) (PSBMA) membranes have strong resistance to Gram-negative *P. aeruginosa* and Gram-positive *P. epidermidis* adhesion (Lalani and Liu 2012). Moreover, a very prospective material for wound healing application from zwitterionic poly(sulfobetaine methacrylate) hydrogel crosslinked with poly(ethylene glycol) dimethacrylate is thought to have enhanced antibacterial and mechanical properties (He et al. 2019).

15.5.1.3 Superhydrophobic Surfaces

Superhydrophobic surfaces are well known and have been investigated for their bacterial antifouling ability. Due to the contact angle of water (>150) of this surface, it is difficult to wet. The superhydrophobicity property of this type surface promotes the elimination of primarily adhered microbes before the biofilm formation by lowering the adhesion force between microbes and the surface. Non-wetting property of hydrophobic surfaces have facilitated numerous characteristics like anti-reflectivity or self-cleaning, thus broadening the utilization of these surfaces (Kang et al. 2010).

From Wenzel theory, it can be depicted that there might be an air layer in between the surface and droplet of water, and this layer allying liquid-solid interfaces approved the capability to minimize bacterial attachment and fostered easy exclusion of bacteria that are attached on the surface area. This superhydrophobicity is the fusion of hierarchical topography in the micrometer or submicrometer scale and a chemical composition that allows a low energy surface (Andrade Del Olmo et al. 2020). This phenomenon is recognized as the effect of lotus leaf where the leaf does not get wet by water droplets, rather droplets roll off very easily (Wu et al. 2018).

15.5.2 Bacterial-Killing Mechanism

This particular mechanism illustrates the application of surfaces having the capability to kill or smash the bacteria or microbes that are attached to them (Tiller et al. 2001). This bacterial-killing activity consists of three effects: (1) nanopatterned; (2) contact-based; and (3) release-based mechanisms which will be discussed briefly.

15.5.2.1 Contact-Based Antibacterial Surfaces

Antibacterial agents or specific biocides that are attached to the surfaces are capable of killing attached bacteria by creating contact-based active materials. These antibacterial agents follow the irreversible bonding when used on the surface of medical accessories (Kaur and Liu 2016). Quaternary ammonium compounds (QACs) and numerous biological macromolecules gained from natural sources including enzymes (AMEs) and peptides (AMPs) having antimicrobial property and chitosan are some examples of such kinds of materials. Thallinger et al. (2013) showed the prevention or destruction of biofilm formation by using the combination of different AMEs (proteases, polysaccharide-degrading enzymes, sensing enzymes, and so on). A recent research showed the inhibition of biofilm construction against monomicrobial polymicrobial biofilms of *Staphylococcus epidermis* using the effectiveness of chitosan-based biomaterial (Tan et al. 2018).

15.5.2.2 Release-Based Antibacterial Surfaces

Release-based antibacterial surfaces have been developed extensively through the last few years. This system destroys bacteria through a controlled release technique to the medium over time with loaded biocides as carriers (Vasilev et al. 2009). The very important time for biofilm genesis is the first 24 h. To attain antibacterial success of an implant, a short-term (24 h) release of biocidal agents is only needed in most of the cases. For instance, ZnO nanoparticle-incorporated medical grade silicone is used as a strategy to diminish the chance of infection (Noimark et al. 2015).

15.5.2.3 Nanopatterned Surfaces with Antibacterial Behavior

Antibacterial surfaces could be derived by fabricating nanopatterns with precise properties. These films should have the parameters of nanoscale as the pattern of the surfaces that demonstrate nonbacterial behavior is microscale sized. Some

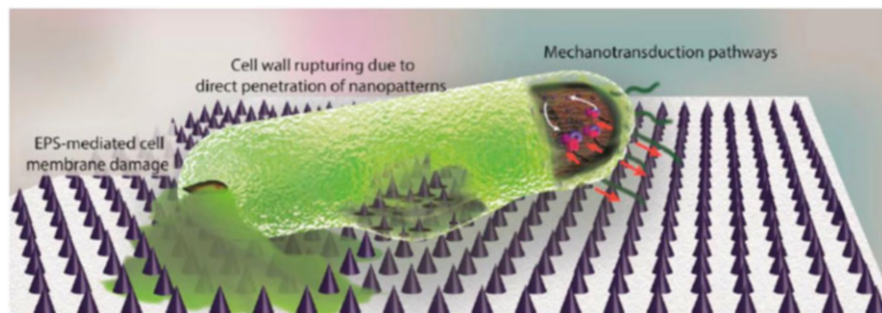


Fig. 15.3 Bacterial-killing mechanism of nanopatterned surfaces (Andrade Del Olmo et al. 2020)

morphological parameters of these nanoshapes, such as height (H), diameter/width (D/W), and interspacing (iS), should be maintained to obtain the bacterial-resistant surface of medical accessories.

It could be concluded that the bactericidal mechanism depends on the destruction of the bacterial cellular membrane as there lies a strong bond between bacteria and patterned surfaces leading to the penetration of high-aspect-ratio nanopatterns (Fig. 15.3) (Modaresifar et al. 2019). The varying values, $100 \text{ nm} < H < 1000 \text{ nm}$, $10 \text{ nm} < D/W < 300 \text{ nm}$, and $iS < 500 \text{ nm}$, are the most studied bactericidal parameters. The inhibition of *E. coli* fabricated by biomimetic nanopillars on poly (methyl methacrylate) after direct contact with nanopillared surfaces was reported (Dickson et al. 2015). Other study presented the antibacterial action against the microbes *Escherichia coli* and *Klebsiella pneumoniae* using nanocone arrays onto polystyrene (Hazell et al. 2018).

15.6 Conclusions and Future Prospects

Biofilm formation on the implant surfaces has been a challenge for the prevention of implant-related infections. Therefore, the demand on research about the fabrication of suitable antibacterial surfaces of biomaterials for the inhibition and reduction of biofilm generation increases day by day. In this chapter, problems of using biomaterials without surface modification, biofilm formation mechanism, and how to improve the antibacterial properties of biomaterials by their surface modifications with various approaches have been discussed. The best surface modification could be achieved by applying combination of more than one surface modification techniques together. Prevention mechanism of biofilm formation by surface modification of substrate surfaces have also been discussed. However, bacterial adhesion is a very complex system and depends on many parameters like used material properties, types of bacteria, and environment. Therefore, further researches are necessary to realize the mechanisms of biofilm formation and implant-related infections in details.

References

- Ahmed W, Zhai Z, Gao C (2019) Adaptive antibacterial biomaterial surfaces and their applications. *Materials Today Bio* 2:100017
- Andrade Del Olmo J, Ruiz Rubio L, Saez Martinez L, Perez-Alvarez V, Vilas Vilela JL (2020) Antibacterial coatings for improving the performance of biomaterials. *Coatings* 10:139
- Arciola CR, Campoccia D, Montanaro L (2018) Implant infections: adhesion, biofilm formation and immune evasion. *Nat Rev Microbiol* 16:397
- Armbruster CR, Parsek MR (2018) New insight into the early stages of biofilm formation. *Proc Natl Acad Sci* 115:4317–4319
- Barbosa JN, Madureira P, Barbosa MA, Aguas AP (2006) The influence of functional groups of self-assembled monolayers on fibrous capsule formation and cell recruitment. *J Biomed Mater Res A* 76:737–743
- Baselga R, Albizu I, Amorena B (1994) Staphylococcus aureus capsule and slime as virulence factors in ruminant mastitis. A review. *Vet Microbiol* 39:195–204
- Baveja J, Willcox M, Hume E, Kumar N, Odell R, Poole-Warren L (2004) Furanones as potential anti-bacterial coatings on biomaterials. *Biomaterials* 25:5003–5012
- Bazaka K, Crawford RJ, Ivanova EP (2011a) Do bacteria differentiate between degrees of nano-scale surface roughness? *Biotechnol J* 6:1103–1114
- Bazaka K, Jacob MV, Crawford RJ, Ivanova EP (2011b) Plasma-assisted surface modification of organic biopolymers to prevent bacterial attachment. *Acta Biomater* 7:2015–2028
- Bird RLR, Hall B, Hobbs K, Chapman D (1989) New haemocompatible polymers assessed by thrombelastography. *J Biomed Eng* 11:231–234
- Burmølle M, Thomsen TR, Fazli M, Dige I, Christensen L, Homøe P, Tvede M, Nyvad B, Tolker-Nielsen T, Givskov M (2010) Biofilms in chronic infections—a matter of opportunity—monospecies biofilms in multispecies infections. *FEMS Immunol Med Microbiol* 59:324–336
- Chen S, Li L, Zhao C, Zheng J (2010) Surface hydration: principles and applications toward low-fouling/nonfouling biomaterials. *Polymer* 51:5283–5293
- Costerton JW, Geesey G, Cheng K-J (1978) How bacteria stick. *Sci Am* 238:86–95
- Costerton JW, Stewart PS, Greenberg EP (1999) Bacterial biofilms: a common cause of persistent infections. *Science* 284:1318–1322
- Crouzet M, Le Senechal C, Brözel VS, Costaglioli P, Barthe C, Bonneau M, Garbay B, Vilain S (2014) Exploring early steps in biofilm formation: set-up of an experimental system for molecular studies. *BMC Microbiol* 14:253
- Da Cunda P, Iribarnegaray V, Papa-Ezdra R, Bado I, González MJ, Zunino P, Vignoli R, Scavone P (2020) Characterization of the different stages of biofilm formation and antibiotic susceptibility in a clinical *Acinetobacter baumannii* strain. *Microb Drug Resist* 26:569–575
- Davey ME, O’toole GA (2000) Microbial biofilms: from ecology to molecular genetics. *Microbiol Mol Biol Rev* 64:847–867
- Davies DG, Parsek MR, Pearson JP, Iglewski BH, Costerton JW, Greenberg EP (1998) The involvement of cell-to-cell signals in the development of a bacterial biofilm. *Science* 280:295–298
- Del Pozo JL (2018) Biofilm-related disease. *Expert Rev Anti-Infect Ther* 16:51–65
- Desmet T, Morent R, De Geyter N, Leys C, Schacht E, Dubrue P (2009) Nonthermal plasma technology as a versatile strategy for polymeric biomaterials surface modification: a review. *Biomacromolecules* 10:2351–2378
- Dickson MN, Liang EI, Rodriguez LA, Vollereaux N, Yee AF (2015) Nanopatterned polymer surfaces with bactericidal properties. *Biointerphases* 10:021010
- Donlan RM (2000) Role of biofilms in antimicrobial resistance. *ASAIO J* 46:S47–S52
- Donlan RM (2001a) Biofilm formation: a clinically relevant microbiological process. *Clin Infect Dis* 33:1387–1392
- Donlan RM (2001b) Biofilms and device-associated infections. *Emerg Infect Dis* 7:277

- Dormer KJ, Gan RZ (2001) Biomaterials for implantable middle ear hearing devices. *Otolaryngol Clin N Am* 34:289–297
- Duncan A, Weisbuch F, Rouais F, Lazare S, Baquey C (2002) Laser microfabricated model surfaces for controlled cell growth. *Biosens Bioelectron* 17:413–426
- Dunne WM (2002) Bacterial adhesion: seen any good biofilms lately? *Clin Microbiol Rev* 15:155–166
- Espersen F, Wilkinson BJ, Gahrn-Hansen B, Rosdahl VT, Clemmensen I (1990) Attachment of staphylococci to silicone catheters in vitro. *APMIS* 98:471–478
- Feng G, Cheng Y, Wang S-Y, Borca-Tasciuc DA, Worobo RW, Moraru CI (2015) Bacterial attachment and biofilm formation on surfaces are reduced by small-diameter nanoscale pores: how small is small enough? *NPJ Biofilms Microbiomes* 1:1–9
- Flemming H, Wingender J (2010) The biofilm matrix. *Nat Rev Microbiol* 8:623–633
- Fletcher M, Loeb G (1979) Influence of substratum characteristics on the attachment of a marine pseudomonad to solid surfaces. *Appl Environ Microbiol* 37:67–72
- Gao C, Guan J, Zhu Y, Shen J (2003) Surface immobilization of bioactive molecules on polyurethane for promotion of cytocompatibility to human endothelial cells. *Macromol Biosci* 3:157–162
- Garrett TR, Bhakoo M, Zhang Z (2008) Bacterial adhesion and biofilms on surfaces. *Prog Nat Sci* 18:1049–1056
- Girard-Egrot AP, Godoy S, Blum LJ (2005) Enzyme association with lipidic Langmuir–Blodgett films: interests and applications in nanobioscience. *Adv Colloid Interf Sci* 116:205–225
- Goddard JM, Hotchkiss J (2007) Polymer surface modification for the attachment of bioactive compounds. *Prog Polym Sci* 32:698–725
- Goddard J, Talbert J, Hotchkiss J (2007) Covalent attachment of lactase to low-density polyethylene films. *J Food Sci* 72:E036–E041
- Granchi D, Cenni E, Trisolino G, Giunti A, Baldini N (2006) Sensitivity to implant materials in patients undergoing total hip replacement. *J Biomed Mater Res B Appl Biomater* 77:257–264
- Guney A, Kara F, Ozgen O, Aksoy EA, Hasirci V, Hasirci N (2013) Surface modification of polymeric biomaterials. Wiley-VCH, Weinheim
- Hadjesfandiari N, Yu K, Mei Y, Kizhakkedathu JN (2014) Polymer brush-based approaches for the development of infection-resistant surfaces. *J Mater Chem B* 2:4968–4978
- Hall MR, Mcgillicuddy E, Kaplan LJ (2014) Biofilm: basic principles, pathophysiology, and implications for clinicians. *Surg Infect* 15:1–7
- Hallgren C, Reimers H, Chakarov D, Gold J, Wennerberg A (2003) An in vivo study of bone response to implants topographically modified by laser micromachining. *Biomaterials* 24:701–710
- Hall-Stoodley L, Costerton JW, Stoodley P (2004) Bacterial biofilms: from the natural environment to infectious diseases. *Nat Rev Microbiol* 2:95–108
- Hall-Stoodley L, Stoodley P, Kathju S, Høiby N, Moser C, William Costerton J, Moter A, Bjarnsholt T (2012) Towards diagnostic guidelines for biofilm-associated infections. *FEMS Immunol Med Microbiol* 65:127–145
- Hasan A, Pandey LM (2020) Surface modification of Ti6Al4V by forming hybrid self-assembled monolayers and its effect on collagen-I adsorption, osteoblast adhesion and integrin expression. *Appl Surf Sci* 505:144611
- Hasan A, Pattanayek SK, Pandey LM (2018a) Effect of functional groups of self-assembled monolayers on protein adsorption and initial cell adhesion. *ACS Biomater Sci Eng* 4:3224–3233
- Hasan A, Waibhaw G, Pandey LM (2018b) Conformational and organizational insights into serum proteins during competitive adsorption on self-assembled monolayers. *Langmuir* 34:8178–8194
- Hasan A, Lee K, Tewari K, Pandey LM, Messersmith PB, Faulds K, Maclean M, Lau KHA (2020a) Surface design for immobilization of an antimicrobial peptide mimic for efficient anti-biofouling. *Chem Eur J* 26:5789–5793

- Hasan A, Saxena V, Castelletto V, Zimbitas G, Seitsonen J, Ruokolainen J, Pandey LM, Sefcik J, Hamley IW, Lau KHA (2020b) Chain-end modifications and sequence arrangements of antimicrobial peptoids for mediating activity and nano-assembly. *Front Chem* 8:416
- Hayward JA, Chapman D (1984) Biomembrane surfaces as models for polymer design: the potential for haemocompatibility. *Biomaterials* 5:135–142
- Hazell G, Fisher LE, Murray WA, Nobbs AH, Su B (2018) Bioinspired bactericidal surfaces with polymer nanocone arrays. *J Colloid Interface Sci* 528:389–399
- He H, Xiao Z, Zhou Y, Chen A, Xuan X, Li Y, Guo X, Zheng J, Xiao J, Wu J (2019) Zwitterionic poly (sulfobetaine methacrylate) hydrogels with optimal mechanical properties for improving wound healing in vivo. *J Mater Chem B* 7:1697–1707
- Heens B, Gregoire C, Pireaux J, Cornelio P, Gardella J Jr (1991) On the stability and homogeneity of Langmuir-Blodgett films as models of polymers and biological materials for surface studies: an XPS study. *Appl Surf Sci* 47:163–172
- Hochbaum AI, Aizenberg J (2010) Bacteria pattern spontaneously on periodic nanostructure arrays. *Nano Lett* 10:3717–3721
- Jacobsen S, Stickler D, Mobley H, Shirliff MJ (2008) Complicated catheter-associated urinary tract infections due to *Escherichia coli* and *Proteus mirabilis*. *Clin Microbiol Rev* 21:26–59
- Jamal M, Ahmad W, Andleeb S, Jalil F, Imran M, Nawaz MA, Hussain T, Ali M, Rafiq M, Kamil MA (2018) Bacterial biofilm and associated infections. *J Chin Med Assoc* 81:7–11
- James GA, Swogger E, Wolcott R, Pulcini ED, Secor P, Sestrich J, Costerton JW, Stewart PS (2008) Biofilms in chronic wounds. *Wound Repair Regen* 16:37–44
- Kang SM, You I, Cho WK, Shon HK, Lee TG, Choi IS, Karp JM, Lee H (2010) One-step modification of superhydrophobic surfaces by a mussel-inspired polymer coating. *Angew Chem Int Ed* 49:9401–9404
- Kaur R, Liu S (2016) Antibacterial surface design—contact kill. *Prog Surf Sci* 91:136–153
- Khardori N, Yassien MJ (1995) Biofilms in device-related infections. *J Ind Microbiol* 15:141–147
- Khatoun Z, Mctiernan CD, Suuronen EJ, Mah T-F, Alarcon EI (2018) Bacterial biofilm formation on implantable devices and approaches to its treatment and prevention. *Heliyon* 4:e01067
- Kingshott P, Wei J, Bagge-Ravn D, Gadegaard N, Gram L (2003) Covalent attachment of poly (ethylene glycol) to surfaces, critical for reducing bacterial adhesion. *Langmuir* 19:6912–6921
- Knobler CM (1990) Recent developments in the study of monolayers at the air-water interface. *Adv Chem Phys* 77:397–449
- Kokare C, Kadam S, Mahadik K, Chopade B (2007) Studies on bioemulsifier production from marine *Streptomyces* sp. S1 6:78–84
- Korber DR, Lawrence JR, Sutton B, Caldwell DE (1989) Effect of laminar flow velocity on the kinetics of surface recolonization by Mot(+) and Mot(-) *Pseudomonas fluorescens*. *Microb Ecol* 18:1–19
- Kostakioti M, Hadjifrangiskou M, Hultgren SJ (2013) Bacterial biofilms: development, dispersal, and therapeutic strategies in the dawn of the postantibiotic era. *Cold Spring Harb Perspect Med* 3:a010306
- Kuhl PR, Griffith-Cima LG (1996) Tethered epidermal growth factor as a paradigm for growth factor-induced stimulation from the solid phase. *Nat Med* 2:1022–1027
- Kurella A, Dahotre NB (2005) Surface modification for bioimplants: the role of laser surface engineering. *J Biomater Appl* 20:5–50
- Lalani R, Liu L (2012) Electrospun zwitterionic poly (sulfobetaine methacrylate) for nonadherent, superabsorbent, and antimicrobial wound dressing applications. *Biomacromolecules* 13:1853–1863
- Lee JH, Khang G, Lee JW, Lee HB (1998) Platelet adhesion onto chargeable functional group gradient surfaces. *J Biomed Mater Res* 40:180–186
- Lewandowski Z, Evans L (2000) Structure and function of biofilms. In: *Biofilms: recent advances in their study and control*, vol 1. Harwood Academics, Amsterdam, p 466
- Lin X, Yang M, Jeong H, Chang M, Hong J (2016) Durable superhydrophilic coatings formed for anti-biofouling and oil–water separation. *J Membr Sci* 506:22–30

- Liu X, Chu PK, Ding C (2004) Surface modification of titanium, titanium alloys, and related materials for biomedical applications. *Mater Sci Eng R Rep* 47:49–121
- Liu S, Kim JT, Kim S (2008) Effect of polymer surface modification on polymer–protein interaction via hydrophilic polymer grafting. *J Food Sci* 73:E143–E150
- Liu C, Su F, Liang J (2014) Facile fabrication of a robust and corrosion resistant superhydrophobic aluminum alloy surface by a novel method. *RSC Adv* 4:55556–55564
- Lyczak JB, Cannon CL, Pier GB (2002) Lung infections associated with cystic fibrosis. *Clin Microbiol Rev* 15:194–222
- Ma Z, Mao Z, Gao C (2007) Surface modification and property analysis of biomedical polymers used for tissue engineering. *Colloids Surf B: Biointerfaces* 60:137–157
- Mah T-FC, O’toole GA (2001) Mechanisms of biofilm resistance to antimicrobial agents. *Trends Microbiol* 9:34–39
- Mariani E, Lisignoli G, Borzi RM, Pulsatelli L (2019) Biomaterials: foreign bodies or tuners for the immune response? *Int J Mol Sci* 20:636
- Matlaga BF, Yasenchak LP, Salthouse TN (1976) Tissue response to implanted polymers: the significance of sample shape. *J Biomed Mater Res* 10:391–397
- Modaresifar K, Azizian S, Ganjian M, Fratila-Apachitei LE, Zadpoor AA (2019) Bactericidal effects of nanopatterns: a systematic review. *Acta Biomater* 83:29–36
- Mombelli A, Müller N, Cionca N (2012) The epidemiology of peri-implantitis. *Clin Oral Implants Res* 23:67–76
- Muñoz-Bonilla A, Fernández-García M (2012) Polymeric materials with antimicrobial activity. *Prog Polym Sci* 37:281–339
- Narayana PSVVS, Srihari PSVV (2020) A review on surface modifications and coatings on implants to prevent biofilm. *Regen Eng Trans Med* 6:330–346. <https://doi.org/10.1007/s40883-019-00116-3>
- Noimark S, Weiner J, Noor N, Allan E, Williams CK, Shaffer MS, Parkin IP (2015) Dual-mechanism antimicrobial polymer–ZnO nanoparticle and crystal violet-encapsulated silicone. *Adv Funct Mater* 25:1367–1373
- O’toole GA, Kolter R (1998) Initiation of biofilm formation in *Pseudomonas fluorescens* WCS365 proceeds via multiple, convergent signalling pathways: a genetic analysis. *Mol Microbiol* 28:449–461
- Overman PR (2000) Biofilm: a new view of plaque. *J Contemp Dent Pract* 1:18–29
- Ozdemir M, Yurteri CU, Sadikoglu H (1999) Physical polymer surface modification methods and applications in food packaging polymers. *Crit Rev Food Sci Nutr* 39:457–477
- Pandey LM, Pattanayek SK (2013) Properties of competitively adsorbed BSA and fibrinogen from their mixture on mixed and hybrid surfaces. *Appl Surf Sci* 264:832–837
- Pedersen SS, Koch C, Heiby N, Rosendal K (1986) An epidemic spread of multiresistant *Pseudomonas aeruginosa* in a cystic fibrosis centre. *J Antimicrob Chemother* 17:505–516
- Planell JA, Navarro M, Altankov G, Aparicio C, Engel E, Gil J, Ginebra MP, Lacroix D (2010) Materials surface effects on biological interactions. In: *Advances in regenerative medicine: role of nanotechnology, and engineering principles*. Springer, Dordrecht
- Pye A, Lockhart D, Dawson M, Murray C, Smith AJ (2009) A review of dental implants and infection. *J Hosp Infect* 72:104–110
- Rabin N, Zheng Y, Opoku-Temeng C, Du Y, Bonsu E, Sintim HO (2015) Biofilm formation mechanisms and targets for developing antibiofilm agents. *Future Med Chem* 7:493–512
- Rasmussen TB, Givskov M (2006) Quorum-sensing inhibitors as anti-pathogenic drugs. *Int J Med Microbiol* 296:149–161
- Ratner BD, Weathersby PK, Hoffman AS, Kelly MA, Scharpen LH (1978) Radiation-grafted hydrogels for biomaterial applications as studied by the ESCA technique. *J Appl Polym Sci* 22:643–664
- Rice LB (2010) Progress and challenges in implementing the research on ESKAPE pathogens. *Infect Control Hosp Epidemiol* 31:S7–S10
- Roosjen A, Busscher HJ, Norde W, Van Der Mei HC (2006) Bacterial factors influencing adhesion of *Pseudomonas aeruginosa* strains to a poly (ethylene oxide) brush. *Microbiology* 152:2673–2682

- Rosenberg M, Bayer EA, Delarea J, Rosenberg E (1982) Role of thin fimbriae in adherence and growth of *Acinetobacter calcoaceticus* RAG-1 on hexadecane. *Appl Environ Microbiol* 44:929–937
- Sauer K, Cullen M, Rickard A, Zeef L, Davies DG, Gilbert P (2004) Characterization of nutrient-induced dispersion in *Pseudomonas aeruginosa* PAO1 biofilm. *J Bacteriol* 186:7312–7326
- Savvides N, Bell T (1993) Hardness and elastic modulus of diamond and diamond-like carbon films. *Thin Solid Films* 228:289–292
- Södergård A (2004) Perspectives on modification of aliphatic polyesters by radiation processing. *J Bioact Compat Polym* 19:511–525
- Stewart PS, Costerton JW (2001) Antibiotic resistance of bacteria in biofilms. *Lancet* 358:135–138
- Stobie N, Duffy B, McCormack DE, Colreavy J, Hidalgo M, Mchale P, Hinder SJ (2008) Prevention of *Staphylococcus epidermidis* biofilm formation using a low-temperature processed silver-doped phenyltriethoxysilane sol–gel coating. *Biomaterials* 29:963–969
- Stoodley P, Sauer K, Davies DG, Costerton JW (2002) Biofilms as complex differentiated communities. *Annu Rev Microbiol* 56:187–209
- Subbiahdoss G, Pidhatika B, Coullerez G, Charnley M, Kuijjer R, Van Der Mei HC, Textor M, Busscher HJ (2010) Bacterial biofilm formation versus mammalian cell growth on titanium-based mono- and bi-functional coating. *Eur Cell Mater* 19:205–213
- Sun F, Qu F, Ling Y, Mao P, Xia P, Chen H, Zhou D (2013) Biofilm-associated infections: antibiotic resistance and novel therapeutic strategies. *Future Microbiol* 8:877–886
- Sutherland IW (1999) Polysaccharases for microbial exopolysaccharides. *Carbohydr Polym* 38:319–328
- Takahara A, Ge S, Kojio K, Kajiyama T (2000) In situ atomic force microscopic observation of albumin adsorption onto phase-separated organosilane monolayer surface. *J Biomater Sci Polym Ed* 11:111–120
- Tan Y, Leonhard M, Ma S, Moser D, Schneider-Stickler B (2018) Efficacy of carboxymethyl chitosan against *Candida tropicalis* and *Staphylococcus epidermidis* monomicrobial and polymicrobial biofilms. *Int J Biol Macromol* 110:150–156
- Tenke P, Kovacs B, Jäckel M, Nagy E (2006) The role of biofilm infection in urology. *World J Urol* 24:13
- Teo AJ, Mishra A, Park I, Kim Y-J, Park W-T, Yoon Y-J (2016) Polymeric biomaterials for medical implants and devices. *ACS Biomater Sci Eng* 2:454–472
- Thallinger B, Prasetyo EN, Nyanhongo GS, Guebitz GM (2013) Antimicrobial enzymes: an emerging strategy to fight microbes and microbial biofilms. *Biotechnol J* 8:97–109
- Tiller JC, Liao C-J, Lewis K, Klibanov AM (2001) Designing surfaces that kill bacteria on contact. *Proc Natl Acad Sci* 98:5981–5985
- Tribedi P, Sil A (2014) Cell surface hydrophobicity: a key component in the degradation of polyethylene succinate by *Pseudomonas* sp. AKS 2. *J Appl Microbiol* 116:295–303
- Ulman A (1991) *Ultrathin organic film*. Academic, New York, p 101
- Unosson E (2015) Antibacterial strategies for titanium biomaterials. *Acta Universitatis Upsaliensis, Uppsala*
- Vasilev K (2019) Nanoengineered antibacterial coatings and materials: a perspective. *Coatings* 9:654
- Vasilev K, Cook J, Griesser HJ (2009) Antibacterial surfaces for biomedical devices. *Expert Rev Med Devices* 6:553–567
- Vasudevan R (2014) Biofilms: microbial cities of scientific significance. *J Microbiol Exp* 1:00014
- Vilain S, Cosette P, Zimmerlin I, Dupont J-P, Junter G-A, Jouenne T (2004) Biofilm proteome: homogeneity or versatility? *J Proteome Res* 3:132–136
- Wang J, Wang Z, Guo S, Zhang J, Song Y, Dong X, Wang X, Yu J (2011) Antibacterial and anti-adhesive zeolite coatings on titanium alloy surface. *Microporous Mesoporous Mater* 146:216–222

- Wasserman SR, Tao YT, Whitesides GM (1989) Structure and reactivity of alkylsiloxane monolayers formed by reaction of alkyltrichlorosilanes on silicon substrates. *Langmuir* 5:1074–1087
- White RA, Hirose FM, Sproat RW, Lawrence RS, Nelson RJ (1981) Histopathologic observations after short-term implantation of two porous elastomers in dogs. *Biomaterials* 2:171–176
- Wu S, Zhang B, Liu Y, Suo X, Li H (2018) Influence of surface topography on bacterial adhesion: a review. *Biointerphases* 13:060801
- Xia Y, Whitesides GM (1998) Soft lithography. *Annu Rev Mater Sci* 28:153–184
- Zinming L, Yingde C, Lloyd AW, Mikhalovsky SV, Sandeman SR, Howel CA, Liewen L (2008) Polymeric hydrogels for novel contact lens-based ophthalmic drug delivery systems: a review. *Cont Lens Anterior Eye* 31:57–64
- Xu Q, Li X, Jin Y, Sun L, Ding X, Liang L, Wang L, Nan K, Ji J, Chen H (2017) Bacterial self-defense antibiotics release from organic–inorganic hybrid multilayer films for long-term anti-adhesion and biofilm inhibition properties. *Nanoscale* 9:19245–19254
- Ye D, Peramo A (2014) Implementing tissue engineering and regenerative medicine solutions in medical implants. *Br Med Bull* 109:3–18
- Yin J, Luan S (2016) Opportunities and challenges for the development of polymer-based biomaterials and medical devices. *Regener Biomater* 3:129–135
- Yuan Y, Liu C, Qian J, Wang J, Zhang Y (2010) Size-mediated cytotoxicity and apoptosis of hydroxyapatite nanoparticles in human hepatoma HepG2 cells. *Biomaterials* 31:730–740
- Zhang Y, Yuan Y, Liu C (2008) Fluorescent labeling of nanometer hydroxyapatite. *J Mater Sci Technol* 24:187–191
- Zheng J, Ito Y, Imanishi Y (1994) Cell growth on immobilized cell-growth factor: 10. Insulin and polyallylamine co-immobilized materials. *Biomaterials* 15:963–968
- Zhu H, Ji J, Lin R, Gao C, Feng L, Shen J (2002a) Surface engineering of poly (DL-lactic acid) by entrapment of alginate-amino acid derivatives for promotion of chondrogenesis. *Biomaterials* 23:3141–3148
- Zhu Y, Gao C, Shen J (2002b) Surface modification of polycaprolactone with poly (methacrylic acid) and gelatin covalent immobilization for promoting its cytocompatibility. *Biomaterials* 23:4889–4895



Polymer Surface Engineering in the Food Packaging Industry

16

Iqra Azeem, Binish Ashfaq, Muhammad Sohail, and Basit Yameen

Abstract

Packaging technologies have gone through a remarkable evolution since their first use in ancient Egypt. Among the diverse variety of materials available, polymers are commonly used to fabricate food packaging. The widespread use of polymers in packaging is due to their availability in large quantities, cost-effectiveness, attractive mechanical performance, and tunable barrier to gases and other volatile odorous compounds. The emerging surface engineering technologies such as mechanical patterning of the polymer surfaces, exposure to high energy radiations, wet chemical and light-induced surface chemical modifications, and nanoparticle application are revolutionizing the polymer-based food packaging industry. Both decorative and functional aspects of packaging encompass these surface engineering technologies, thus preserving the quality and prolonging life span of the packaged food. The polymer-based packaging protects food from spoilage by providing a shield against microbial and chemical toxins, temperature change, oxygen, humidity, light, and external physical forces. Recent innovations in food packaging have introduced new concepts of active, intelligent, and smart packaging. The concomitant developments in stimuli-responsive materials is enabling the advancements in packaging technologies by driving the growth in functional polymeric nanocomposites, nanomaterial-based coatings, electrospun functional material, and nano(bio)sensors. This chapter covers the recent advances in the surface engineering technologies that are at the heart of the development of polymer-based food packaging for the future.

I. Azeem · B. Ashfaq · M. Sohail · B. Yameen (✉)

Department of Chemistry and Chemical Engineering, Syed Babar Ali School of Science and Engineering (SBASSE), Lahore University of Management Sciences (LUMS), Lahore, Pakistan
e-mail: basit.yameen@lums.edu.pk

© The Author(s), under exclusive license to Springer Nature Singapore Pte Ltd. 2022

457

L. M. Pandey, A. Hasan (eds.), *Nanoscale Engineering of Biomaterials: Properties and Applications*, https://doi.org/10.1007/978-981-16-3667-7_16

Keywords

Food packaging · Flexible packaging · Biopolymers and biodegradable polymers · Polymer surface engineering · Active packaging · Smart and intelligent packaging

16.1 Introduction

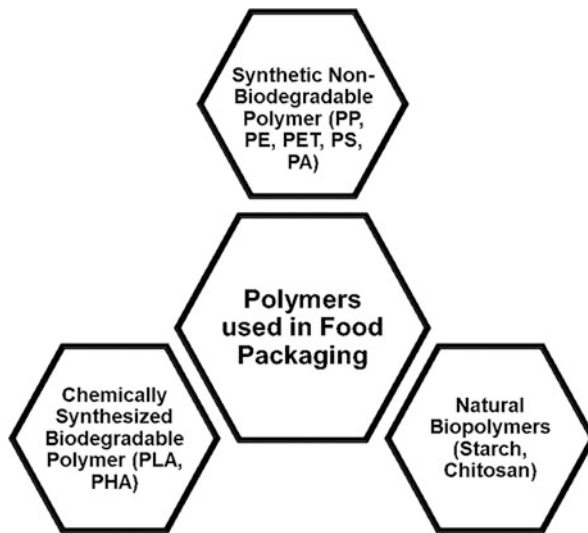
Packaging has become an essential step in food processing. A desirable package is required to preserve the packaged food for a reasonable time at an affordable cost. With the expanding distribution at local and global levels, food packaging is required to play a pivotal role in preserving the nutritional content over the entire supply chain, starting from the farms to the processing facilities and from storage facilities to the end-users. From food safety and quality point of view, packaging helps in protecting food from adverse alterations that may be brought about by the chemical and biological contaminants that can be amplified by environmental factors such as exposure to variations in temperature, oxygen, moisture, and light (Han et al. 2018). Food packaging is being produced from various materials, including glass, tin, paper, and currently, polymers. The widespread use of synthetic polymers for packaging purposes is evident from the fact that about 40% of the total production of synthetic polymers is consumed by the packaging industry (PlasticsEurope 2016). Polymers have emerged as attractive materials for packaging, which is because of their availability in large quantities, attractive mechanical and optical properties, a tunable barrier to gases such as oxygen, carbon dioxide, and volatile odorous compounds, thermal stability over a wide temperature range (from below zero to moderately high temperatures), heat sealability, and recyclability. While bulk properties of the polymers make them suitable for packaging industry, their surface physical and chemical properties are not always appropriate and often require modification for satisfactory decorative and functional performances. The surfaces of polymers can be modified by employing a range of mechanical, physical, and chemical surface engineering methods, which impart desired characteristics to the polymer surfaces. These characteristics include simple properties such as improved adhesiveness, wettability, surface roughness, and barrier properties or more sophisticated characteristics such as reporting counterfeit, detecting and reporting changes in the food quality, altering physical properties of the packaging (e.g., absorbance of barrier), or releasing substances in response to the environmental stimuli (originating from external environment or the packaged food) to protect and enhance the life of the packaged food, are edible, and biodegradable when disposed of. As a result, development of facile and scalable surface modification methods constitutes an active research area in both academic and industrial settings. Various mechanical and physicochemical techniques are being developed to engineer the surface morphology and chemistry of polymers (Siracusa 2019). The choice of surface engineering process depends on the chemical nature of the polymer and the targeted properties that the final packaging is expected to display.

It is worth highlighting here that the evolution in consumer demands due to the ever-evolving lifestyle, retailing practices, and industrial production trends drives the innovation of novel materials for improved, active, and intelligent packaging. The future packaging is expected to display time, temperature, pH, humidity, pathogen threat, and specific food quality indicators on the packaging surface to satisfy end-users. The packaging that can respond to the changes in their environment and make the necessary adjustments in the properties of the packaging materials to enhance or reduce the barrier to light or gases or release active agents to elicit antimicrobial and antifungal activities to protect the packaged food and the concepts of self-cleaning and self-healing surfaces are expected to revolutionize the future landscape of the food packaging. The advancements in the aforementioned technologies are being enabled by the simultaneous developments in designing stimuli-responsive materials, functional polymeric nanocomposites, nanomaterial-based surface coatings, electrospun functional material, and nano(bio)sensors (Youssef and El-Sayed 2018; Silvestre et al. 2011). This chapter provides an insight into the synthetic and natural polymers used for packaging and the recent advances in their surface engineering that are enabling the development of active, smart, and intelligent polymer-based food packaging.

16.2 Polymers for Food Packaging Applications

For over 50 years, the food packaging industries have used a range of synthetic polymers that provide comfort and convenience to mankind. Majority of the currently used synthetic polymers are derived from non-renewable petrochemicals and are non-biodegradable. Polypropylene (PP), polyethylene (PE), polyethylene terephthalate (PET), polybutylene terephthalate (PBT), polyvinyl chloride (PVC), ethylene vinyl alcohol (EVOH), polyamides (PAs), polycarbonate (PC), polymethyl methacrylate (PMMA), polystyrene (PS), acrylonitrile butadiene styrene (ABS), styrene acrylonitrile (SAN) resin, polyarylsulfone (PSU), polyether ether ketone (PEEK), and polyoxymethylene (POM) represent the major classes of synthetic thermoplastic polymers being produced globally. However, polyurethanes (PU), unsaturated polyesters (also known as alkyd resins), melamine resins, vinyl ester resins, acrylic resins, silicon-based polymers, phenol-formaldehyde resins, and urea-formaldehyde resins constitute the major synthetic thermosetting polymers that are being produced across the globe. The total global production of plastics (2018) was estimated to be around 360 million tons. Due to their production and consumption at such a large scale, their petrochemical origin and non-biodegradable nature, genuine concerns related to the sustainable supply of synthetic polymers and the associated environmental impacts are also being recently voiced by the global for-profit and not-for-profit organizations, civil society, governments, and intergovernmental organizations. Therefore, innovative biodegradable polymers synthesized in the laboratories or derived from renewable natural resources have gained much attention as a replacement for non-biodegradable plastics. In addition to looking for more sustainable and environmentally benign alternatives, the development of polymer

Fig. 16.1 Different synthetic and natural polymers used for food packaging



composites (including nanocomposites) to augment various properties of the packaging made from the petrochemical-derived polymers and biopolymer has attracted increasing attention (Balakrishnan et al. 2014).

Polymers used in the food packaging industry can be broadly classified into three categories (1) polymers that are generally non-biodegradable and are derived from the petrochemicals or from the chemicals that are derived from renewable sources (e.g., biomass), (2) biodegradable synthetic polymers that are synthesized either from petrochemicals or from chemicals derived renewable sources (e.g., biomass), and (3) natural biopolymers that are fully derived from the renewable sources (Fig. 16.1).

16.2.1 Synthetic Non-biodegradable Polymers

The most commonly used synthetic non-biodegradable polymers include PE, PP, PET, PS, PVC, and PA, which constitute >80% of all the polymers used to produce films for application in food packaging. Because of its transparent and flexible nature, PE is among the most widely used thermoplastic polymer in food packaging. By varying the polymer chain length and substitution, a variety of PE polymers exhibiting distinct properties can be produced. The commonly used variants of PE include low-density PE (LDPE), linear low-density PE (LLDPE), high-density PE (HDPE), and ultra-high-density PE (UHDPE). Low surface energy and poor PE barrier properties determine their application and treatment processes at the commercial level. PP, another polyolefin, is an attractive packaging material owing to its low density, high melting point, convenient sealability, chemical inertness, and low cost. In contrast to polyolefins, the soft and flexible films can be produced from PVC

by tuning the plasticizer content and stereochemistry. PVC films show lower gas permeability, but higher moisture permeability that limits its application domains. On the other hand, PET, a semi-crystalline polymer with a benzene ring in its chemical structure that provides strength and stiffness to the polymer, is also widely used for packaging various types of foods. PET shows excellent chemical resistance, rigidity, thermal stability, transparency, and barrier properties. It is generally used to make plastic containers and bottles for soft drinks (Shrivastava 2018). PS, produced by free radical polymerization of styrene monomer, is also one of the most consumed polymers in the packaging industry. PS offers high tensile strength, stiffness, and lightweight. Recently, the migration of unreacted monomer styrene from PS derived packaging material into the packaged food was observed. Since styrene has toxic effects on the central nervous system, this migration issue has limited the use of PS in food packaging applications (Abolghasemi-Fakhri et al. 2019). Polymers with amide linkages, known as polyamides, show high mechanical strength. Nylon 6, 6, nylon 6, 10, and nylon 6, 11, are commonly used PAs in food packaging applications. PAs show high permeability to moisture owing to the polar amide groups present in their backbone. This can lead to the plasticizing effects that result in increasing tensile strength, but reducing their tensile strain. Nonetheless, owing to their superior resistance to chemicals, mechanical strength, and barrier properties, PAs have received significant attention for manufacturing flexible films for food products, personal care products, and pharmaceuticals (Bhunia et al. 2013; Robertson 2016). Majority of the synthetic polymers being used for packaging purposes at the commercial scale offer less than optimum surface properties. Therefore, in order to meet the specific characteristics required by the emerging applications, surface engineering of the films derived from these polymers is often required to improve their surface properties such as wettability, printability, and adhesion. The modification of surface properties of packaging material is generally carried out without changing their bulk physiochemical properties. Various surface engineering strategies can be applied for the surface modification of polymer films discussed later in this chapter.

16.2.2 Chemically Synthesized Biodegradable Polymers

Majority of the packaging materials are derived from non-degradable polymers. Besides, many food packaging are multilayered that are difficult to separate. Consequently, polymer packaging derived from the non-degradable polymers are either down cycled or end up in landfills or burnt. Landfilling and burning practices have resulted in the challenge of plastic-related pollution of both land and waters, damaging the different forms of life on earth. To lessen the impact of plastic pollution, eco-friendly biodegradable polymeric materials are being designed for the packaging industry as alternatives to non-degradable plastics. At present, many chemically synthesized biodegradable polymers are commercially available; these include polylactic acid (PLA), polyglycolic acid (PGA), polylactic-*co*-glycolic acid (PLGA), polybutylene succinate (PBS), polycaprolactone (PCL), polyethylene

adipate (PEA), and polydioxanone (PDO) (Siracusa et al. 2008). PLA is a polyester and is the most attractive biodegradable polymers commonly synthesized from the lactic acid derived from the renewable sources (fermented sugar feedstock and corn). It offers attractive physical properties with the added advantage of cost-effectiveness. The performance of the PLA can be controlled by adjusting the ratio of its three stereoisomers L-lactide, D-lactide, and L-D-lactide. PLA is used to manufacture carrier bags, bin bags, and packaging for food. Like PLAs, polyhydroxyalkanoates (PHAs) also belong to the biodegradable polyester family. By varying the polymer chain length and employing combinations of different chain lengths, different types of PHAs have been produced. The crystallinity and polymer chain length determine the rate at which PHAs biodegrade. PHAs are often used to fabricate disposable products, food, and cosmetic containers. Similarly, polymers such as PBS and PCL are biodegradable polymers based on fossil fuel and exhibit mechanical characteristics similar to PE and PP. While we develop a fully biodegradable polymer derived from renewable resources that exhibits a set of properties similar to synthetic plastics, the degradable polymers derived from non-renewable resources may be a transient option to help control the environmental damage associated with plastics. Although biodegradable polymers can degrade in a reasonable time and help reduce environmental pollution, they generally offer less than optimum mechanical strength and thermal stability, limiting their application in the packaging industry on a wider scale (Panchal and Vasava 2020).

16.2.3 Natural Biopolymers

Owing to their (bio)degradability, biocompatibility, eco-friendliness, inherent antibacterial, antioxidant, and anti-inflammatory activities, natural polymers (derived from natural sources) are attractive alternatives to the polymeric materials derived from the non-renewable source. Biopolymers are most suitable for use as edible food packaging (Mustafa and Andreescu 2020). Natural polymers include polysaccharides (starch, cellulose, chitosan, alginate, agar, and carrageenan), and proteins (soy protein, corn zein, wheat gluten, gelatin, collagen, whey protein, and casein). Starch is one of the most abundant biodegradable polymers that offer a moderate oil barrier property. However, its brittleness and hydrophilic nature limit its use for packaging dehydrated food. Similarly, chitosan offers a decent film-forming ability and can be used with other bioactive agents such as high molecular weight carrageenan and alginate that act as a thickener, stabilizing, and gelling agents during the fabrication of edible packaging films (Zhu et al. 2017). Both starch and chitosan exhibit antimicrobial activity that can be employed to fabricate antimicrobial films to enhance the product shelf life by protecting the packaged food from spoilage due to microbial activities. Besides carbohydrates, proteins obtained from plant and animal sources are also attractive materials for packaging applications. Due to the renewable and biodegradable nature, they are used in many industrial applications along with plastics. Proteins are known to be brittle and sensitive to water. Thus, the most efficient ways to use protein-based plastics for industrial

applications are plasticization and mixing with biodegradable polyesters (Mangaraj et al. 2019; Mohamed et al. 2020).

16.2.4 Polymer Nanocomposites

Polymer nanocomposites are multiphase hybrids composed of nanofillers dispersed in a polymer matrix. Besides imparting novel properties to synthetic polymers, nanocomposite can also improve the physicochemical properties of bioderived polymers and enhance their suitability as food packaging materials. The nature of nanofillers plays an important role in designing the nanocomposites and controlling their properties. Nanofillers of appropriate physicochemical properties can enhance mechanical strength, thermal stability, gas and moisture barrier, antioxidant, and antimicrobial properties of the conventional polymer-based packaging materials (Youssef and El-Sayed 2018; Vasile 2018; Arora and Padua 2010). Nanofillers are generally classified into two types:

Inorganic nanofillers include metal or metal oxide nanoparticles (NPs) and clay. Metallic NPs (silver, copper, and zinc NPs) show antimicrobial activity that are recently being applied to fabricate antimicrobial food packaging. Clay NPs such as montmorillonite (MMT), saponite, and hectorite are recognized as promising nanofillers owing to their low cost, ease of availability, considerable improvement in the tensile strength, and comparatively simple process of fabricating nanocomposite (Unalan et al. 2014; Gill et al. 2020).

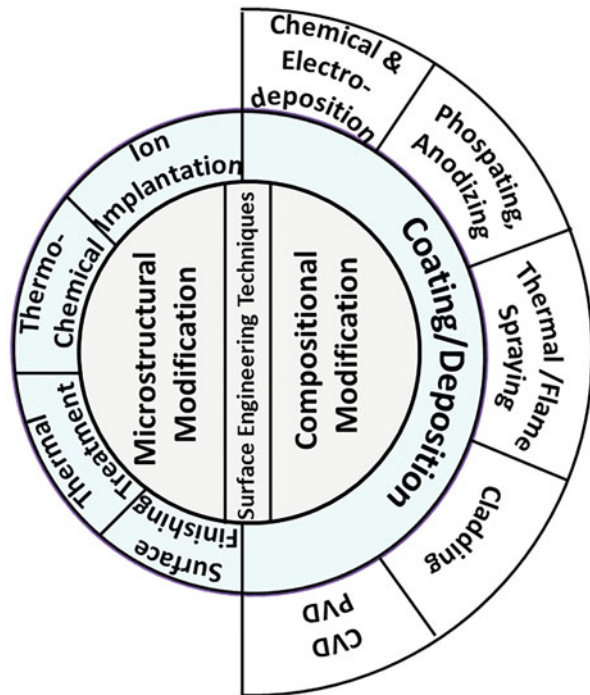
Organic nanofillers include cellulose nanofibrils, chitin nanofibrils, starch nanocrystals, and chitin nanofibrils. As reinforcing agents, cellulose and chitin nanofibrils are used to improve various characteristics of the resulting nanocomposites. They offer optical transparency, non-toxicity, and improved tensile strength when applied as nanofillers to fabricate packaging materials (Valencia et al. 2019; Jeevahan and Chandrasekaran 2019).

Polymer nanocomposites have opened new research avenues for the development of novel packaging materials for the food industry. Employing a very low content of nanofillers, polymer nanocomposites showing improved mechanical and gas barrier properties while retaining the inherent properties of the matrix polymer have been reported. In short, several new research and development avenues to novel packaging technologies have been opened by the developments in the field of polymer nanocomposites. Polymer nanocomposites appear to have a bright future in context of the development of innovative, active, intelligent, and multifunctional food packaging technologies (Shankar and Rhim 2016).

16.3 Surface Engineering Technologies

“Surface,” in its most broad sense, includes the peripheral or the uppermost layer of a physical object. From the materials science perspective, the surface is characterized as the interface between two different phases. In several instances, materials offer attractive bulk properties, while their surface properties are often inadequate for the desired application. Both the surface morphology and surface chemical nature need to be modified to achieve desired surface properties. In this context, many surface engineering strategies are employed as powerful tools for the microstructural and compositional surface modifications to improve the surface morphology or bring suitable chemical functionalities on the surface. The term ‘surface engineering’ covers a wide range of methods that are being employed for research, development and production purposes. During the most recent 20 years, there have been colossal advancements in the field of surface engineering techniques. These techniques are generally categorized into two groups: (1) mechanical surface modification, which encompasses modification of surface physical morphology through surface microstructuring and patterning, (2) physical and chemical surface modification, which brings about change in the surface chemical compositional through a variety of different surface treatment and coating strategies (Mozetič 2019). These two major groups are further classified into various methods that are schematically represented in Fig. 16.2.

Fig. 16.2 Schematic representation of different surface engineering techniques



Ion implantation, thermo-chemical treatments (nitriding, boriding, carburizing, chromizing, and aluminizing), laser and electron beam treatments can be employed to influence the surface properties of the thin layer substrates, whereas, welding and cladding are used to develop thicker coatings on the surface that are mostly employed to impart corrosion resistance to the coated substrates. Some advanced coating technologies such as laser processing, thermal spraying, cold spraying, anodizing, chemical, and physical vapor deposition are also used to impart the desired properties to the substrate surface. These methods can be applied to a range of substrates, including glass, metal, natural and synthetic polymers, irrespective of their physical form and chemical nature (Quintino 2014).

In the context of polymer surface engineering, different mechanical, physical, and chemical methods can be applied to modify surface properties of polymeric substrates. As described earlier, mechanical methods include changing surface roughness and surface physical morphology through surface microstructuring and patterning. The physical methods include treating surfaces with high energy reactive radiations such as plasma, corona, laser, UV, flame, and ion beams. These physical methods can modify the surface roughness as well as modify the surface chemical nature. The chemical modifications imparted through these physical methods are generally confined to the surface polymer molecules and are mostly reported to be short-lived. Chemical surface modification methods result in a permanent change in the surface chemical nature of the polymeric substrates. These methods can be either purely wet chemical or a combination of physical and chemical approaches, leading to a well-defined change in the surface chemical nature. (Nemani et al. 2018). All these methods are briefly discussed in the next section.

16.4 Polymer Surface Engineering Routes

Surface physical and chemical nature of polymer substrates can be modulated to control their surface properties such as hydrophilicity, hydrophobicity, adsorption, desorption, and transportation of materials across polymer membranes, which can greatly influence their performance in a certain application (Hetemi and Pinson 2017). Figure 16.3 demonstrates numerous surface modification methods widely employed to change surface chemistry of polymeric substrates, predominantly in thin-film conformation employed in industrial applications.

16.4.1 Mechanical Routes

Mechanical methods are comparatively simple, economical, and scalable. They are used to modify polymer surface properties by changing their surface roughness at the micro- and nanoscale while maintaining the inherent bulk physical and chemical characteristics of the polymer (Yao et al. 2011). For instance, superhydrophobic PE films were fabricated by using the lamination templating method against woven wire mesh templates. A 3D arrangement of systematic PE micro-posts was formed on the

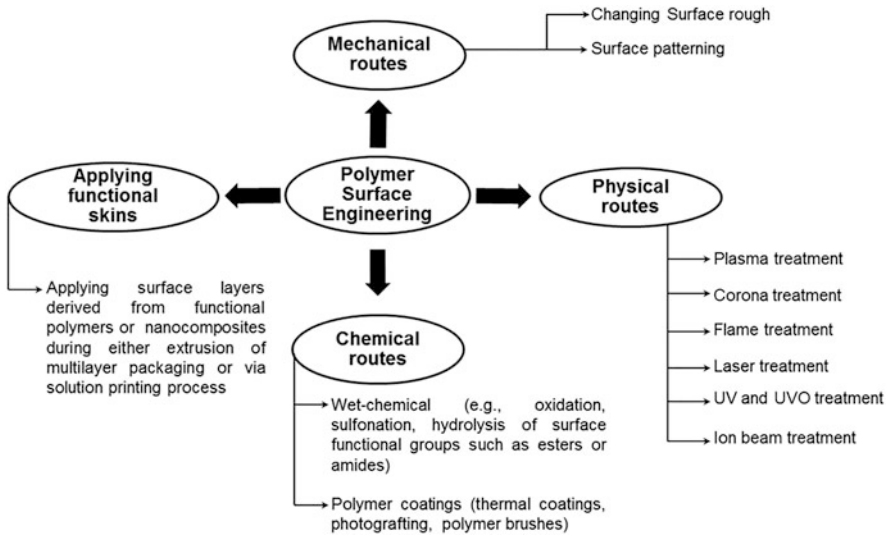
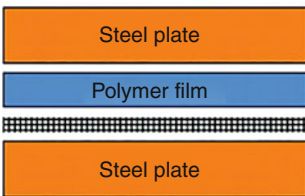


Fig. 16.3 Polymer surface engineering methods

Step 1. Laminate assembly under heat and pressure



Step 2. Cool and peel off mesh

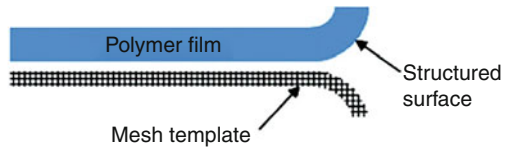


Fig. 16.4 Schematic of the lamination peeling process. (Reprinted with permission of Xu et al. (2011). Copyright (2011) American Chemical Society)

surface of PE films (Xu et al. 2011) (Fig. 16.4). Similarly, an adaptable method has been designed for the successful replication of PP surfaces with T-shaped micropillars using a microinjection compression molding technique. Such methods are excellent candidates for the development of microfluidics (Chen and Huang 2016). Superhydrophobic, anti-fouling, and ice-phobic surfaces useful for industrial applications can also be developed using mechanical methods. The key benefit of mechanical modification is that they do not need chemical treatments that can be difficult to scale during large-scale fabrication. The polymers’ surface engineering by mechanical routes is robust and their impact does not decay over time. They are, however, most suitable for engineering the surfaces of thermoplastics (Xue et al. 2010).

16.4.2 Physical Routes

Plasma Treatment and plasma polymerization: Plasma treatment is a physical treatment that involves exposing the surface of a polymer substrate to partially ionized gas, which is usually obtained when gases are bombarded with either radio or microwaves or electron beam from a hot filament. Typically, cold plasmas having translational energy $\sim 1\text{--}10$ eV that is enough to break chemical bonds to generate reactive species such as ions, radicals, or radical-ions are used. Plasma treatment is certainly the most extensively used method for the surface engineering of polymers (Lieberman and Lichtenberg 2005). Modification through plasma can be categorized into two general categories:

- (a) **Treatment with gas plasma:** Argon (Ar), water (H_2O), oxygen (O_2), and nitrogen (N_2) gas-based plasmas can be applied to produce functionalities that make the surface of polymers hydrophilic, irrespective of the bulk chemical nature of the polymers. For example, PET films treated with O_2 plasma installed hydroxyl ($-\text{OH}$) groups on the surface that helped in binding poly-L-lysine and trichloro(1H,1H,2H,2H-perfluorooctyl) silane via dip-coating and self-assembly methods to fabricate triboelectric generators (TEGs). These generators produce energy using the triboelectric effect, in which when opposite dipole surfaces come in contact with each other, electricity is generated by the charge transfer mechanism (Shin et al. 2015) (Fig. 16.5). Hydrophilic PE, PP, and PET surfaces can also be produced by treating with $\text{H}_2\text{O}/\text{O}_2/\text{NH}_3$ -based plasma (Lee et al. 1991; Kull et al. 2005). Such a plasma setting would install nitrogen- and oxygen-containing functionalities on the surface of polymers. Similarly, the flat surface of PEEK has been treated with air plasma to functionalize their surface with polar groups ($-\text{OH}$, $-\text{CHO}$, and $-\text{COOH}$) (Ellinas et al. 2014). Plasma treatments are offered by many companies such as Dyne Technology, Acxys, Lectrotreat, TriStar Plastics, Keol, Plasma Etch, and Alma Plasma that can be used in textile industry for cleaning, improving surface adhesion, printing, and modifying the surface of the fabric (Zille et al. 2015).
- (b) **Treatment with plasma-containing reactive organic species:** Generally, gas-based plasma modifications are short-lived and lose their effect readily by interacting with molecules in the surroundings. For modification that may last for longer periods, reactive organic molecules (silanes or monomers) are introduced during the plasma treatment at a low vacuum that helps in anchoring organo-silane or polymer coatings on the surface or the treated polymer substrate. For example, PET upon treatment with the plasma containing acrylic acid (AA) led to the PET surface coated with a coating displaying a high density of COOH groups. The surface COOH could be employed in the subsequent conjugation with polyethylene glycol (PEG), and heparin by EDC coupling resulted in antithrombogenic PET surfaces (Pandiyaraj et al. 2009). Other surface functional groups (such as amino, hydroxyl, and carboxylic acid) can be incorporated on the surface for chemical diverse polymers. In the same context, Janus textiles with different wetting properties have been fabricated.

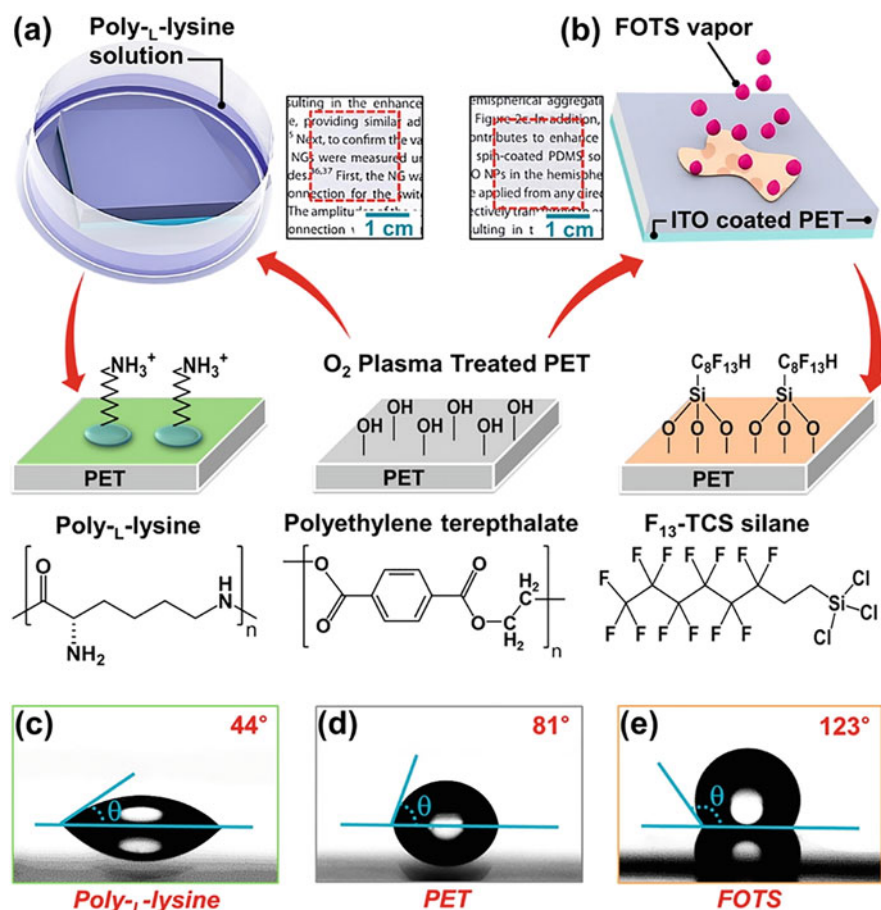


Fig. 16.5 Schematic of plasma-treated PET surface grafted with the poly-L-lysine solution (a) with trichloro(1H,1H,2H,2H-perfluorooctyl) silane (FOTS) (b) Water contact angle measured for functionalized surfaces (c–e). (Reprinted with permission from Shin et al. (2015). Copyright (2015) American Chemical Society)

This simple surface engineering is an innovative method for fabricating durable textiles with waterproof and breathable properties (Airoudj et al. 2016; Sohail et al. 2019; Pegalajar-Jurado et al. 2014; Yameen et al. 2011).

Treatment with corona discharge: Corona discharge, unlike plasma, can be initiated in the air or an inert atmosphere. Since 1960, this physical treatment has been used to modify the polymer surface with the target of increasing surface energy, improving adhesion, improving antifouling properties, and enhancing selective permeability of different gases. This method is also used to sterilize food packaging materials using ozone as a medium (Van Veldhuizen and Rutgers 2001). The reactive species such as ions and radicals strike the polymer surface during corona

discharge and initiate polymerization, surface-confined degradation, and oxidation. The efficacy of corona treatment depends primarily on the energy transmitted by energetic species generated inside the chamber, the thickness of the polymer film under treatment, and humidity. Higher energy is required for thicker films to bring a considerable change in the surface properties (Cáceres et al. 2012). The chemical composition of the film under treatment also plays a role in the effectiveness of corona treatment. For example, PET exhibits more reactive sites than polyolefins after corona treatment (Zenkiewicz 2008). The change in the surface chemical nature of different polymers upon exposure to corona should be carefully studied. For improving surface printability, PET, PE, and PP require lower energy corona to achieve surface with the desired surface energy (Lindner et al. 2018). Corona treatment of various chemically different polymer surfaces can be carried out to effectively improve their wettability that results from the surface oxidation without affecting their bulk properties. It is common to observe that the energy of corona-treated surface decreases with aging (storage time), which happens due to the reorganization of the surface molecules and reaction of the generated groups with the molecules available in their immediate environment. The life of the surface treatment and its decay rate depend on the chemical nature of the polymeric substrate under treatment (Louzi and de Carvalho Campos 2019).

In summary, polymer surface engineering with corona discharge has undergone substantial improvements over the past several years. The most important factor that needs to be considered while performing this treatment is the density of corona discharge. Corona treatment is a short-lived treatment, but the enhancement observed in the surface energy depends on the method variables and the chemical nature of the surface under treatment. In the case of organic solvent-based coatings, the decrease in surface energy overtime is frequently observed. These coatings appear to lose their adhesion property and revert to their original chemical nature, whereas water-based coatings can retain the effect of corona treatment for relatively long periods. The rate of reversion to the original state also varies with the intrinsic surface energies of the treated substrates. To better understand this physical procedure, the association between the corona-treated surface and its impact on other surface properties such as wettability, adhesion, and roughness is subject to detailed analysis.

Ultraviolet (UV) treatment: Another physical method used to modify the surface of polymers is by exposure to UV radiations. For example, direct writing on the thermoplastic polymer bisphenol A polycarbonate (BAPC) surface is made possible by irradiating its surface with high-speed laser light (Jiang et al. 2014). UV radiations are used to develop patterns by placing a mask between the material surface and the source of light (Rajajeyaganthan et al. 2011). UVO method, when UV treatment is performed in the ozone atmosphere, enhances the low surface energy to improve the treated polymer surface adhesion property. For instance, PET and poly(hydroxymethylsiloxane) (PHMS) surfaces were subjected to the UVO treatment to improve adhesion and proliferation of cells (Liu et al. 2016). Compared to the plasma and corona discharge techniques, UV treatment has more control over surface modification with a slower reaction rate. However, the

technique suffers from three major drawbacks, (1) polymers have to be photoactive to respond to the UV radiations, (2) UV treated polymer surfaces gradually revert to their original surface chemical nature, (3) polymers can degrade when subjected to UV radiation for extended periods (Rudko et al. 2015).

Upon UV irradiation, radicals are produced on the surface of polymers bearing photoactive functionalities as part of their chemical structure. PEEK is one such example where benzophenone ring in the main chain of PEEK can act as a photoinitiator when exposed to UV radiations. This characteristic of PEEK can be employed to functionalize PEEK surface via radical reactions such as reactions with vinyl monomers that may result in surface-initiated polymerization (SIP, “grafting-from”) or reactions with any preformed polymers (“grafting-to”) that contain functionalities capable of reacting with the radicals. Similar reactions can be performed by immobilizing photo-reactive functionalities on the surface of polymers that do not intrinsically possess appropriate functionality to participate in photoreactions. In addition to grafting photoinitiator moieties on the polymer surfaces, polymer surfaces have also been functionalized with functionalities that participate in radical reactions such as vinyl-based functionalities. A mixture of a vinyl monomer, vinyl groups containing crosslinker, and an appropriate photoinitiator (UV curable mixture) can be applied to the surface of polymer films functionalized with the vinyl group-containing functionalities. Subsequent exposure to the UV radiations of the appropriate wavelength results in the coating or printing of the polymer films with UV curable coatings. The chemical nature and physical properties and hence the functionality of the coatings can be controlled by adding an appropriate vinyl monomer or a mixture of monomers in the UV curable mixture. Such a UV printing is a cost-effective and efficient polymer surface modification technique that can be applied to a variety of chemically diverse polymer films (Sohail et al. 2019). The effectiveness of UV printing is determined by the required thickness of the coating applied to the surface of the substrate. With the increased required thickness of the coating, the penetration of the UV radiations decreases which reduces the effectiveness of this method (Knaapila et al. 2014). Because of the radical nature of the polymerization, UV printing is sensitive to the presence of O₂ in the atmosphere. The rate of photo-polymerization (photo-curing) decreases as O₂ molecules quickly capture the UV-generated reactive specie to generate peroxy radicals that are least reactive to initiate or continue the process of polymerization. To overcome the oxygen inhibition effect, the inert atmosphere is used during the UV printing of polymer coatings (Studer et al. 2003). Overall, UV printing is a scalable method to graft chemically diverse polymer coatings and fabricate functionalized surfaces as per application needs.

Surface modification by patterning: Polymer surface engineering via patterning develops surfaces that have numerous applications in electronics, optical devices, packaging for food, and biomedicine. For example, inkjet printing technology is used to develop organic electroluminescent displays by deposition of luminescent colloidal quantum dot (QD)-polymer nanocomposites or light-emitting polymers (Wood et al. 2009). Patterning, a cost-effective physical technique, can be applied to a variety of surfaces irrespective of the chemical nature of the substrates. In this

context, a mixture of polymers along with a liquid crystal was exposed to UV light of different wavelengths to initiate polymerization in two directions that led to the formation of micrometer-sized polymer containers filled with a switchable liquid crystal. These designed surfaces were used as displays and can be produced on a variety of substrate (Penterman et al. 2002). Besides fabrication of displays, periodic surface structures were developed on thin films of poly(trimethylene terephthalate) (PTT) when it was exposed to laser light. Such nanostructured substrates were subsequently coated with a gold layer via pulsed laser deposition to effectively use them as substrates for surface-enhanced Raman spectroscopy (SERS) (Rebollar et al. 2012). Similarly, hexagonally ordered metal dot patterns were fabricated by block copolymer nanolithography. Various patterning processes such as instability-induced, evaporation, electric and thermal field gradient, photolithography, block copolymer, microcontact printing, nanoimprinting lithography, laser surface texturing are used to fabricate surfaces with improved surface tension, charge density, and adhesion. Currently, laser surface texturing (LST) is the most studied technique in context of polymeric substrates. The surfaces textured through lasers can be modified at macro, micro, and nano levels with improved resolution and stay sterilized owing to the non-contact design of the technique. LST also has other benefits, including the ability to pattern various surfaces, negligible waste production, precision, high reliability, and reproducibility (Nemani et al. 2018).

16.4.3 Wet-Chemical Routes

Chemical modification is beneficial where conventional physical treatments are inadequate to bring the desired functionalities to the surface of polymer substrates. Chemical methods include wet chemical processes to tune surface properties. For example, the surface energy of nylon can be improved by dipping in an iodine-potassium iodide solution that oxidizes the surface and recorate the surface with reactive functional groups and improves adhesion of the polymer surface toward metals (Abu-Isa 1971). Similarly, PP films treated with chromic acid etching increased the surface oxygen content and improved its adhesion toward epoxy-based adhesives (Regis et al. 2012; Sheng et al. 1995). Similarly, PET surfaces have also been oxidized by the successive treatment with permanganate and sulfuric acid to bring carboxylic groups on the surface. The carboxyl groups could be employed in the subsequent conjugation of the amino group-containing molecules to the surface of PET (Marchand-Brynaert et al. 1995). The use of wet-chemical surface engineering methods is limited because of the corrosive nature of the chemicals (NaOH, permanganate, and sulfuric acid) that are used for surface modifications. In addition to the wet-chemical methods described above, controlled surface chemical modifications can also be employed by performing controlled organic chemistry reactions on the surface of polymers offering functionalities that can be transformed into other functionalities in a controlled manner. For instance, benzophenone groups of PEEK can be reduced to alcohol groups that can be subsequently used in reactions with acid halides. PEEK surface has been modified

with the initiators for the atom transfer radical polymerization (ATRP) and functionalized with the functional polymer brushes via surface-initiated ATRP (SI-ATRP) (Yameen et al. 2009).

16.5 Polymer Surface Engineering for Food Packaging Application

Food packaging is a dynamic industry, which is always in quest of advanced innovation (Siracusa 2019). Polymers indeed show commendable performance when applied in food packaging. Designing new polymer-based materials meeting the emerging needs of next-generation packaging is an active area of research and development in both academic and commercial domains. The need for innovative polymer-based packaged materials is ever expanding with a primary focus on meeting the buyer's requirement of better quality food with an element of traceability. The successful progress in the field of packaging in recent years can be grouped into different categories that are described in the following sections.

16.5.1 Packaging with Improved Mechanical and Barrier Properties

Improved packaging generally refers to the packaging offering enhanced mechanical and barrier properties. Polymer composition and the method used to design the final packaging play a significant role in defining the properties of resulting packaging. The packaging containers commercially used to store food often encounter low temperatures. It is, therefore, necessary to ensure their mechanical performances under these conditions. The values for the tensile strength, tensile strain, and Young's modulus of the food packaging material are important indicators of the mechanical properties of polymers (Siracusa et al. 2008). Among different polymer surface modification methods, cold plasma treatment can be used to improve the mechanical strength, adhesion, sometimes anti-adhesion, printability, and anti-fog properties of packaging materials by carefully tuning their surface energies. It is worth mentioning here that these modifications are short-lived and treated surfaces gradually lose the impact of the surface treatment. To overcome this effect, plasma-assisted deposition of silica nanoparticles after plasma-assisted nano-texturing of surface PC surface led to a long-lasting modification impact that was demonstrated for antifogging surface nature of the treated film (Di Mundo et al. 2014). Besides, a short treatment of gas plasma has been shown to result in efficient inactivation of microorganisms that tend to stick to the polymer surfaces. This method can be employed on plastic bottles, lids, and cling films to quickly sterilize them using cold plasma, without affecting the bulk properties of the polymer film (Thirumdas et al. 2015; Chen et al. 2019). Recently, nanomaterials have been incorporated within the synthetic polymers to improve mechanical strength of the resulting polymer films. Montmorillonite (MMT), the most commonly used cost-effective silicate, incorporated into nylon, LDPE, PS, PLA, EVA copolymer, PET, and

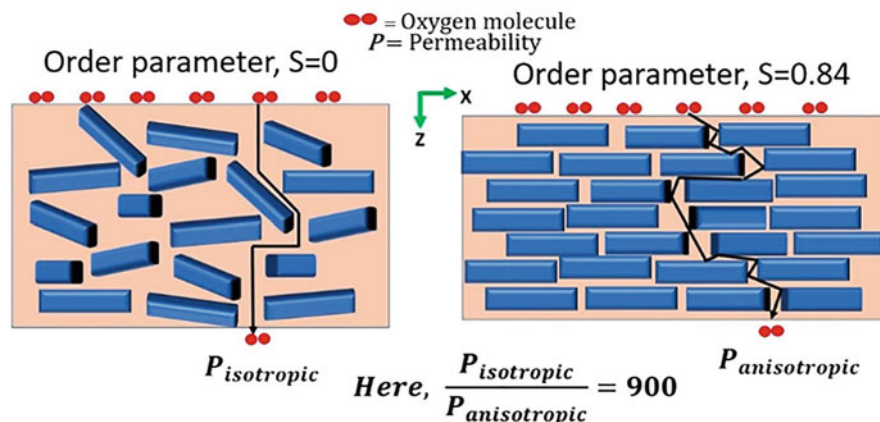


Fig. 16.6 Anisotropic nanocellulose films could be utilized for oxygen-sensitive packaging applications. (Reprinted with permission from Chowdhury et al. (2018). Copyright (2018) American Chemical Society)

chitosan improves the mechanical properties, thermal stability, and water vapor permeability (WVP) of the resulting composite films (Pereira et al. 2009; Molinaro et al. 2013; Parvinzadeh et al. 2010; Abdollahi et al. 2012). Similarly, chitosan films showed an increase in the tensile strength and a decrease in the tensile strain by the addition of 5% (w/w) of nanosilver. PHA films obtained after incorporation of nanosilver and cellulose nanocrystals showed improved mechanical strength compared with the pristine PHA (Rhim et al. 2006; Yu et al. 2014). Other systems such as films produced from microcrystalline cellulose (MCC) and nanosilver containing PLA showed improvement in mechanical properties. In addition to the mechanical property, nanoclay also provides considerable improvements in the gas barrier properties if it is properly distributed in polymer film matrix. This is particularly important for application in packaging for meat, cheese, sweets, cereals, fruit juices, carbonated drinks, and dairy products (Fortunati et al. 2012). Similarly, cellulose-based nanomaterials have been shown to impart improved gas barrier property due to their high crystallinity and polarity. Using a shear-coating technique, low barrier nanocellulose films were converted to superior gas barrier anisotropic films that effectively controls the gas diffusion path and hence tune the barrier properties (Fig. 16.6). Such anisotropic nanocellulose films could be utilized for the fabrication of oxygen-sensitive packaging (Chowdhury et al. 2018).

16.5.2 Active Packaging

Active packaging technologies offer functionalities beyond the regular function expected from the packaging platforms. According to the type of functionality, active packaging technologies are categorized into several groups that are described here (Shankar and Rhim 2016; Yildirim et al. 2018; Vilela et al. 2018).

Antimicrobial packaging: The short shelf-life of fresh foods is due to their high nutrient content and moisture that lead to their rapid decomposition owing to the fast growth of microorganisms. Meat products are particularly susceptible and favor the growth and spread of pathogenic microorganisms. The oxidation of myoglobin, calpains, and fatty acids within the meat causes deterioration of the food quality and safety. Traditionally, refrigeration, as a preservation technique, is used to control microbial growth, but it does not ensure a long shelf-life. Modern packaging technologies have emerged as an effective tool augmenting the effectiveness of the traditional means of food preservation. In this context, antimicrobial packaging technologies are designed to ensure that packaged food is safe against microbial activities and preserve product quality for a more extended period (Fang et al. 2017). In this context, modifying polymer-based packaging material via cold plasma treatment or designing multifunctional composites by adding metal NPs, essential oils, or natural extracts has been explored to fabricate packaging exhibiting antimicrobial properties (Al-Tayyar et al. 2020; Zanetti et al. 2018). For example, chemical resistance, mechanical, thermal, and barrier properties of PET films are suitable for use in different food applications. Cold plasma treatment and surface functionalization of PET surface for immobilization of bioactive molecules have been demonstrated to help in reducing the microbial growth. Similarly, immobilization of antimicrobial peptides on the surface of plasma-treated PET has been shown to reduce the growth of foodborne microorganisms (Gogliettino et al. 2020). In the same context, PET films hydrolyzed through a treatment with NaOH has been demonstrated to adsorb chitosan and hyaluronic acid in a layer-by-layer fashion. Such multilayers adsorbed on the PET surface can be used as potential antibacterial films for packaging food and biomedical devices (Pérez-Álvarez et al. 2016).

Metal and metal oxide NPs, such as silver, copper, titanium, zinc, titanium oxide, zinc oxide, and magnesium oxide NPs, are widely used to impart antimicrobial property to a variety of materials. Polymer nanocomposite containing cellulose acetate, PEG, and cetyltrimethylammonium bromide-modified MMT nanoclay also exhibits appreciable antimicrobial activities (Saha et al. 2016). Similarly, a nanocomposite film based on silver NPs incorporated in the biopolymers such as chitosan, agar, and gelatin showed strong antimicrobial activity against Gram-positive and Gram-negative bacteria (Shankar et al. 2014). Commercially available antimicrobial packaging technologies are primarily based on silver-based additives incorporated into the polymeric materials. Zeomic[®] is among the pioneering technologies and uses inorganic silver-based compounds to inhibit the growth of Gram-positive, Gram-negative bacteria, and fungi. Other systems based on silver in zeolites such as Microban[®], AgIon[®], and Irgaguard[®] work in the same way (Wyrwa and Barska 2017). The successful commercialization of antimicrobial platforms has been obstructed by several distinct hurdles. The major one is the environmental concern throughout the package life cycle starting from the manufacturing to purchase and finally, the disposal. Active packaging technologies that rely on laminated multilayer thermoplastic-based polymeric films to achieve the desired characteristics are difficult to recycle due to their inherent nature. Examining a cradle-to-grave lifecycle throughout the product development process must ensure

that new technologies comply with current environmental regulations (Werner et al. 2017).

Oxygen scavengers: Oxygen scavenging films are designed to better protect oxygen-sensitive foods against bacterial growth, prevent rancidity, avoid yellowing of food, prevent oxidation, and increase life span of food items (Gaikwad et al. 2018). A variety of synthetic polymer-based plastics (PE, LDPE, HDPE, and PET) that are being used for packaging purpose offer less than optimum resistance to permeability to gases across the packaging barrier, which remains a formidable challenge. For many years, significant studies have been done on designing effective oxygen scavenging systems for preserving food. Pyrogallol-coated LDPE films have been shown to exhibit high oxygen scavenging capacity (Gaikwad et al. 2017; Ahn et al. 2016). In addition to coating, an alternative way is to incorporate oxygen scavengers in the packaging film. For example, iron, palladium, and unsaturated hydrocarbon-based scavenging systems have been demonstrate to exhibit high oxygen scavenging rates. Nano iron and palladium-based scavenging systems could be employed in the presence of moisture as well as in inert conditions. They can catalytically form water from O_2 in the presence of H_2 . Another alternative for packing dry foods is unsaturated hydrocarbon-based scavenging systems, but the quality of the packaged food is affected due to the formation of aldehydes, ketones, and organic acids as a by-product. Besides, eco-friendly systems like ascorbic acid, tocopherol, enzyme, and microorganism-based scavenging systems are also designed, but have slower scavenging rates and require light, UV radiation, heat, or transition metal atom as a trigger, which increases the overall cost when compared to the nano iron-based scavenger systems (Dey and Neogi 2019). In the same vein, enzyme-based systems such as hydrophobically modified glucose oxidase mixed with EVA, and such blends when coated on the interior of glass containers act as oxygen scavenging coatings. These coatings effectively reduced the headspace oxygen by 2% and enhanced the protection of oxygen-sensitive food (Wong et al. 2017). In multilayer packaging, polymer incorporated with the oxygen scavenger is generally sandwiched between the two PET films to make a three-layered packaging system. Such a system was tested on freshly cut, untreated apples, and results showed that it has the potential to improve the shelf-life of oxygen-sensitive food items (Shin et al. 2011). Currently, the food packaging industry focuses on designing nanocomposite-based coating like TiO_2 NPs/polymer-based nanocomposites films with methanol as a hole scavenger. Upon UV irradiation, these coatings deoxygenate the surroundings and can be employed as active packaging materials for oxygen-sensitive food items (Xiao-e et al. 2004). Zero valent copper NPs, although have not been much explored in this field, have great potential as oxygen scavenger primarily due to their high tendency to undergo oxidation. In addition to potential use as oxygen scavenger, zero valent copper NPs also exhibit intrinsic antibacterial properties. Such a system can be used to impart both oxygen scavenging and antimicrobial properties to the packaging materials.

Ethylene scavengers: Ethylene (C_2H_4) is a plant hormone responsible for accelerating the respiration rate, resulting in the ripening of fruits and vegetables. Its accumulation during shipping, storage, and handling causes the accelerated

ripening of fruits and vegetables. This needs to be avoided to improve the life of the packaged fruits and vegetables, especially for avoiding food spoilage during shipment via sea (Álvarez-Hernández et al. 2018). The most commonly used ethylene scavengers are silica or alumina-supported potassium permanganate (KMnO_4). KMnO_4 oxidizes ethylene that can be visually detected with a color change from purple to brown. Yet, KMnO_4 cannot be used directly with foodstuffs and mostly placed in the form of sachet within the packaging box due to its high toxicity (Spricigo et al. 2017). Alternative environmentally friendly systems with improved ethylene scavenging ability are required. Different packaging systems are designed including metal oxides, clays, zeolite nanoparticles, and activated carbon. For example, PP films coated with TiO_2 NPs showed higher ethylene scavenging efficacy for packaged horticultural products. This is due to titanium oxide (TiO_2) displaying photocatalytic ability that can photodegrade ethylene and prolong the ripening process (Maneerat and Hayata 2008). Similarly, chitosan films with nanosized TiO_2 showed ethylene absorbance maintaining quality products and extending the shelf life of cherry tomatoes (Kaewklin et al. 2018).

16.5.3 Smart/Intelligent Packaging

Packaging materials are generally applied as passive and inert barriers to avoid humidity, oxygen, and toxins from reaching the food product, thus protecting the quality against chemical and mechanical stresses. The degree of functionality introduced into packaging materials is rapidly increasing, which is supported by the development of innovative systems that can detect and report the food quality change in real time and in some cases even automatically respond to impede the quality of food products from degrading. The objective of intelligent/smart packaging is to monitor the packaged food or its surroundings, by providing the consumers with information about the food quality through a variety of signals. In general, intelligent packaging systems can be comprehended by three main innovations: (1) indicators like chromogenic polymeric materials that can be incorporated within the packaging matrix and help to display quality parameters outside the packaged food (Sadeghi et al. 2020), (2) information carriers, for example, barcodes and radiofrequency identification tags (RFID) that are explicitly specified for storage, distribution, and traceability purposes (Qian et al. 2020), and (3) sensors, which take into consideration a quick and positive evaluation of the analytes in a variety of food items (Ghaani et al. 2016). In order to fabricate sensors within the packaging systems, specific indicators are employed that can respond to the physical or chemical changes happening within the packaged food being monitored. Early detection helps in preventing the intake of hazardous food and thus reduces the chances of food-borne diseases. Intelligent and smart packaging includes gas sensors, chemical sensors, pH indicators, time-temperature indicators, bacterial or fungal growth indicators, and anti-counterfeiting sensors. Nanodevices or nanosensors are being integrated with the modern intelligent packaging. Among nanosensors, optical nanomaterial-based indicators such as metal or metal oxide

NPs, photonic nanocrystals have been extensively applied. Such materials are primarily used owing to their distinctive optical characteristics and high surface reactivity that translate into better performance when compared to the traditional colorimetric indicators (Bumbudsanpharoke and Ko 2019). For instance, chlorogenic acid carbon dots were doped into PVA to fabricate a functional film that also exhibited good physical and mechanical properties. The resulting composite film showed strong antioxidant capacity, resistance against photobleaching, and ability to detect Al^{3+} residues in food, and sense amines produced during spoilage (Zhang et al. 2020). Similarly, colorimetric pH sensors have been integrated with a hybrid food packaging system. For instance, incorporating a dye conjugated cellulose into PVA resulted in a film that exhibited a visible color change from yellow to brick-red and to purple under strong acidic and basic conditions. Such pH sensors were shown to detect spoiled shrimps through change in the color and could be used to visually detect food quality in real time (Ding et al. 2020). These sensors can be fabricated on different substrates such as synthetic polymeric films, paper, glass, and microfluidic devices (Yousefi et al. 2019). Besides, natural food colorant, anthocyanins, incorporated biopolymeric films have been designed that are pH-responsive and have the potential to ensure food safety. Such dyes due to their natural antioxidant property can also help in improving the shelf-life of the packaged food (Roy and Rhim 2021). Poultry industry is one of the largest sectors in the food industries. Poultry industry has adopted the intelligent/smart packaging technologies to improve food safety and maximize customer satisfaction. Indicator devices such as time-temperature indicators, freshness indicators, biosensors, and oxygen sensors are incorporated into the packaging system that monitor temperature, shelf life, and spoilage status. Barcode and identification tags provide detailed information about product starting from the source of production till it reaches to the consumer. Such advanced technology builds trust between the customers and the suppliers that has improved the sales at the domestic and global level (Chowdhury and Morey 2019).

Several gas sensors have been designed that can quantify or identify microorganisms based on their gas emissions. Aerobic microorganisms grow in the presence of oxygen during food storage. This problem has attracted more attention to design harmless and irreversible oxygen sensors. In this context, photoexcitable dyes are usually coated on the inner side of the food packaging, which does not work until exposed to the UV light. The drawback associated with this type of design is that the dye can leach out when in contact with water that not only stains the food but also becomes a potential hazard. Recently, alginate polymer-based oxygen indicator films are designed to prevent dyes from leaching out (Vu and Won 2013). Similarly, the dye leaching was controlled by using furcelleran as the coating polymer, extracted from edible red seaweed (Imran et al. 2016). Besides using dyes, polymer nanocomposites can be employed as monitoring systems for rapid, simple, and cost-effective detection. Such platforms allow monitoring of the quality of packaged foods during transport and storage. To detect specific signal molecules, gold NPs, carbon nanotubes, magnetic NPs, and quantum dots are used as efficient sensing systems due to their unique physicochemical, optical, magnetic, and electrochemical characteristics that show predictive and high sensitivity changes

in response to their interaction with other species of chemical or biological origin. Such sensors are incorporated into packaging materials to detect microbes, toxins, temperature changes, and oxygen (Mustafa and Andreescu 2020).

Electrospinning method has emerged as one of the modern approaches for the production of intelligent packaging. This method is used to produce nanofibers that offer high surface area, and absorbance capacity as well as high porosity. These properties make electrospun nanofibers, along with the active food spoilage indicators, effective in an intelligent packaging. Such novelty, in recent years, is mostly used in designing pH indicators (Aman Mohammadi et al. 2020). Non-destructive colorimetric labels that indicate freshness directly through chemical change within the package or indirectly by a change in storage temperature among wide variety of new technologies are currently being considered for the development of intelligent food packaging systems. Different sensors such as ripeSense, active colorimetric labels developed by Insignia, and Tempix Technologies are commercially available. Temperature-sensitive indicators do not directly provide information; however, they are cost-effective and provide valuable details that help in assessing the shelf-life of the packaged food. Along with commercially available packaging sensors, there are a large number of sensors designed at the lab scale as well where a particular emphasis is on the exclusion of any toxic compounds that may contaminate the packaged food and limit its consumption. Keeping the extensive development in perspective, we are expecting to see continued evolution of the low-cost disposable sensors for monitoring freshness of packaged food all along the supply chain (Dincer et al. 2019).

16.5.4 Packaging Derived from Biopolymers

Biopolymers (carbohydrates, lipids, and proteins) have gained considerable importance in recent years owing to their potential capacities to substitute conventional plastics and are used as edible films/ coatings (Mohamed et al. 2020). These polymers show inherent physicochemical properties that can protect the packaged food. Furthermore, the incorporation of active ingredients such as plasticizers, emulsifiers, antimicrobial agents, and antioxidants in the biopolymer-based packaging materials enhances their mechanical properties and moisture resistance properties, and suitability as packaging materials. Biopolymer-based coatings can also be directly applied as a thin layer on the surface of food by spraying or dipping and can be eaten by the consumer along with the food with zero risks (Janjarasskul and Krochta 2010). Generally, protein-based edible packaging provides mechanical stability and good barrier properties against oxygen, aroma, and oil, whereas lipid-based and carbohydrate-based are used to control moisture permeability and gaseous transmission across the interface, respectively (Wihodo and Moraru 2013). Valencia et al. fabricated a transparent, biodegradable, and flexible film with increased thermal stability from an immersion of oil in water that was stabilized through cellulose nanofibrils by solvent casting method (Valencia et al. 2019). Zhang et al. prepared edible sheets from soya proteins and also observed the effect of plasticizer

and cross-linker (Zhang et al. 2001). In another study, starch-polybutylene adipate-co-terephthalate composite films were prepared by extrusion blowing method, and the effect of starch content on the water barrier and mechanical properties of films was studied (Zhai et al. 2020). In addition to chemical methods, physical methods are also used to design edible packaging. In this context, UV treatment, a low-cost and environment-friendly method, is employed to enhance structural, morphological, barrier, and mechanical properties of the packaging films. Among all other biopolymers, starch has gained considerable attention because of its low cost, biocompatibility, nutritional value, and mechanical properties. To further modify its characteristics, various methods are employed such as physical, enzymatic, chemical, the addition of additives, or a combination of these methods (Souza et al. 2012; Shah et al. 2016). The potential of edible packaging has been well documented by various scientific research groups and by the food industries. A variety of innovative approaches have been designed as substitutes for existing technologies. Nanocomposites are likewise at the front line of biopolymer-based innovative packaging technologies. This allows researchers to engineer nanostructure on the surface of packaging materials to achieve desirable barriers and mechanical properties and to carry bioactive agents. Nevertheless, biopolymer-derived packaging, including edible packaging, needs to overcome several developmental barriers before wide-scale commercial deployment.

16.6 Summary

Polymer surface engineering approaches are being employed to fabricate functional surfaces for the development of innovative packaging technologies. In this chapter, we have discussed mechanical, physical, and chemical routes that are commonly used to achieve the desired surface modifications particular in context of surface engineering of polymer films used in food packaging industry. Food packaging technologies are emerging fast in response to our lifestyle changes and the ever-growing demand for the quality food with a prolonged life span. In this context, we have provided a detailed analysis of the role various emerging technologies, including nanotechnology, are playing in design and development of smart surfaces to develop active and intelligent food packaging technologies. We have particularly provided an overview of the development of packaging platforms exhibiting antimicrobial, oxygen scavenging, improved barrier to gases, and ability to absorb ethylene gas. In addition, we have also described recent advancements in the development of packaging integrated with the sensors for detecting pathogens, allergens, toxins, heavy metals, pH change, temperature change, and ripening indicators such as ethylene and CO₂. In short, this chapter provides a comprehensive guide to different routes that are being employed for polymer surface engineering to develop innovative food packaging technologies.

Acknowledgments B.Y. acknowledges support from HFSP (RGY0074/2016), HEC for NRPU (Project No. 20-1740/R&D/10/3368, 20-1799/R&D/10-5302 and 5922), TDF-033 grants, and LUMS for start-up fund and FIF grants.

References

- Abdollahi M, Rezaei M, Farzi G (2012) A novel active bionanocomposite film incorporating rosemary essential oil and nanoclay into chitosan. *J Food Eng* 111(2):343–350
- Abolghasemi-Fakhri L, Ghanbarzadeh B, Dehghannya J, Abbasi F, Adun P (2019) Styrene monomer migration from polystyrene based food packaging nanocomposite: effect of clay and ZnO nanoparticles. *Food Chem Toxicol* 129:77–86
- Abu-Isa IA (1971) Iodine treatment of nylon: effect on metal plating of the polymer. *J Appl Polym Sci* 15(11):2865–2876
- Ahn BJ, Gaikwad KK, Lee YS (2016) Characterization and properties of LDPE film with gallic-acid-based oxygen scavenging system useful as a functional packaging material. *J Appl Polym Sci* 133(43):44138
- Airoudj A, Bally-Le Gall F, Roucoules V (2016) Textile with durable janus wetting properties produced by plasma polymerization. *J Phys Chem C* 120(51):29162–29172
- Al-Tayyar NA, Youssef AM, Al-Hindi R (2020) Antimicrobial food packaging based on sustainable bio-based materials for reducing foodborne pathogens: a review. *Food Chem* 310:125915
- Álvarez-Hernández MH, Artés-Hernández F, Ávalos-Belmontes F, Castillo-Campohermoso MA, Contreras-Esquivel JC, Ventura-Sobrevilla JM et al (2018) Current scenario of adsorbent materials used in ethylene scavenging systems to extend fruit and vegetable postharvest life. *Food Bioprocess Technol* 11(3):511–525
- Aman Mohammadi M, Hosseini SM, Yousefi M (2020) Application of electrospinning technique in development of intelligent food packaging: a short review of recent trends. *Food Sci Nutr* 8:4656
- Arora A, Padua G (2010) Nanocomposites in food packaging. *J Food Sci* 75(1):R43–R49
- Balakrishnan P, Thomas M, Pothen L, Thomas S, Sreekala M (2014) *Polymer films for packaging*. Springer, Berlin, pp 1–8
- Bhunia K, Sablani SS, Tang J, Rasco B (2013) Migration of chemical compounds from packaging polymers during microwave, conventional heat treatment, and storage. *Compr Rev Food Sci Food Saf* 12(5):523–545
- Bumbudsanpharoke N, Ko S (2019) Nanomaterial-based optical indicators: promise, opportunities, and challenges in the development of colorimetric systems for intelligent packaging. *Nano Res* 12(3):489–500
- Cáceres CA, Mazzola N, França M, Canevarolo SV (2012) Controlling in-line the energy level applied during the corona treatment. *Polym Test* 31(4):505–511
- Chen A-F, Huang H-X (2016) Rapid fabrication of t-shaped micropillars on polypropylene surfaces with robust Cassie–Baxter state for quantitative droplet collection. *J Phys Chem C* 120(3):1556–1561
- Chen Y-Q, Cheng J-H, Sun D-W (2019) Chemical, physical and physiological quality attributes of fruit and vegetables induced by cold plasma treatment: mechanisms and application advances. *Crit Rev Food Sci Nutr* 60:1–15
- Chowdhury E, Morey A (2019) Intelligent packaging for poultry industry. *J Appl Poult Res* 28(4):791–800
- Chowdhury RA, Nuruddin M, Clarkson C, Montes F, Howarter J, Youngblood JP (2018) Cellulose nanocrystal (CNC) coatings with controlled anisotropy as high-performance gas barrier films. *ACS Appl Mater Interfaces* 11(1):1376–1383
- Dey A, Neogi S (2019) Oxygen scavengers for food packaging applications: a review. *Trends Food Sci Technol* 90:26–34

- Di Mundo R, d'Agostino R, Palumbo F (2014) Long-lasting antifog plasma modification of transparent plastics. *ACS Appl Mater Interfaces* 6(19):17059–17066
- Dincer C, Bruch R, Costa-Rama E, Fernández-Abedul MT, Merkoçi A, Manz A et al (2019) Disposable sensors in diagnostics, food, and environmental monitoring. *Adv Mater* 31(30):1806739
- Ding L, Li X, Hu L, Zhang Y, Jiang Y, Mao Z et al (2020) A naked-eye detection polyvinyl alcohol/cellulose-based pH sensor for intelligent packaging. *Carbohydr Polym* 233:115859
- Ellinas K, Pujari SP, Dragatogiannis DA, Charitidis CA, Tserepi A, Zuilhof H et al (2014) Plasma micro-nanotextured, scratch, water and hexadecane resistant, superhydrophobic, and superamphiphobic polymeric surfaces with perfluorinated monolayers. *ACS Appl Mater Interfaces* 6(9):6510–6524
- Fang Z, Zhao Y, Warner RD, Johnson SK (2017) Active and intelligent packaging in meat industry. *Trends Food Sci Technol* 61:60–71
- Fortunati E, Armentano I, Iannoni A, Barbale M, Zaccheo S, Scavone M et al (2012) New multifunctional poly (lactide acid) composites: mechanical, antibacterial, and degradation properties. *J Appl Polym Sci* 124(1):87–98
- Gaikwad KK, Singh S, Lee YS (2017) A pyrogallol-coated modified LDPE film as an oxygen scavenging film for active packaging materials. *Prog Org Coat* 111:186–195
- Gaikwad KK, Singh S, Lee YS (2018) Oxygen scavenging films in food packaging. *Environ Chem Lett* 16(2):523–538
- Ghaani M, Cozzolino CA, Castelli G, Farris S (2016) An overview of the intelligent packaging technologies in the food sector. *Trends Food Sci Technol* 51:1–11
- Gill YQ, Abid U, Song M (2020) High performance Nylon12/clay nanocomposites for potential packaging applications. *J Appl Polym Sci* 137:49247
- Gogliettino M, Balestrieri M, Ambrosio RL, Anastasio A, Smaldone G, Proroga YT et al (2020) Extending the shelf-life of meat and dairy products via PET-modified packaging activated with the antimicrobial peptide MTP1. *Front Microbiol* 10:2963
- Han JW, Ruiz-Garcia L, Qian JP, Yang XT (2018) Food packaging: a comprehensive review and future trends. *Compr Rev Food Sci Food Saf* 17(4):860–877
- Hetemi D, Pinson J (2017) Surface functionalisation of polymers. *Chem Soc Rev* 46(19):5701–5713
- Imran M, Yousaf AB, Zhou X, Liang K, Jiang Y-F, Xu A-W (2016) Oxygen-deficient TiO₂-x/methylene blue colloids: highly efficient photoreversible intelligent ink. *Langmuir* 32(35):8980–8987
- Janjarasskul T, Krochta JM (2010) Edible packaging materials. *Annu Rev Food Sci Technol* 1:415–448
- Jeevahan J, Chandrasekaran M (2019) Nanoedible films for food packaging: a review. *J Mater Sci* 54:12290–12318
- Jiang M, Liu J, Wang S, Lv M, Zeng X (2014) Surface modification of bisphenol a polycarbonate using an ultraviolet laser with high-speed, direct-writing technology. *Surf Coat Technol* 254:423–428
- Kaewklin P, Siripatrawan U, Suwanagul A, Lee YS (2018) Active packaging from chitosan-titanium dioxide nanocomposite film for prolonging storage life of tomato fruit. *Int J Biol Macromol* 112:523–529
- Knaapila M, Høyser H, Kjelstrup-Hansen J, Helgesen G (2014) Transparency enhancement for photoinitiated polymerization (UV curing) through magnetic field alignment in a piezoresistive metal/polymer composite. *ACS Appl Mater Interfaces* 6(5):3469–3476
- Kull KR, Steen ML, Fisher ER (2005) Surface modification with nitrogen-containing plasmas to produce hydrophilic, low-fouling membranes. *J Membr Sci* 246(2):203–215
- Lee JH, Park JW, Lee HB (1991) Cell adhesion and growth on polymer surfaces with hydroxyl groups prepared by water vapour plasma treatment. *Biomaterials* 12(5):443–448
- Lieberman MA, Lichtenberg AJ (2005) Principles of plasma discharges and materials processing. Wiley, Chichester

- Lindner M, Rodler N, Jesdinszki M, Schmid M, Sangerlaub S (2018) Surface energy of corona treated PP, PE and PET films, its alteration as function of storage time and the effect of various corona dosages on their bond strength after lamination. *J Appl Polym Sci* 135(11):45842
- Liu J, He L, Wang L, Man Y, Huang L, Xu Z et al (2016) Significant enhancement of the adhesion between metal films and polymer substrates by UV–ozone surface modification in nanoscale. *ACS Appl Mater Interfaces* 8(44):30576–30582
- Louzi VC, de Carvalho Campos JS (2019) Corona treatment applied to synthetic polymeric monofilaments (PP, PET, and PA-6). *Surf Interfaces* 14:98–107
- Maneerat C, Hayata Y (2008) Gas-phase photocatalytic oxidation of ethylene with TiO₂-coated packaging film for horticultural products. *Trans ASABE* 51(1):163–168
- Mangaraj S, Yadav A, Bal LM, Dash S, Mahanti NK (2019) Application of biodegradable polymers in food packaging industry: a comprehensive review. *J Packag Technol Res* 3(1):77–96
- Marchand-Brynaert J, Deldime M, Dupont I, Dewez J-L, Schneider Y-J (1995) Surface functionalization of poly (ethylene terephthalate) film and membrane by controlled wet chemistry: chemical characterization of carboxylated surfaces. *J Colloid Interface Sci* 173(1):236–244
- Mohamed SA, El-Sakhawy M, El-Sakhawy MA-M (2020) Polysaccharides, protein and lipid-based natural edible films in food packaging: a review. *Carbohydr Polym* 238:116178
- Molinaro S, Romero MC, Boaro M, Sensidoni A, Lagazio C, Morris M et al (2013) Effect of nanoclay-type and PLA optical purity on the characteristics of PLA-based nanocomposite films. *J Food Eng* 117(1):113–123
- Mozetic M (2019) Surface modification to improve properties of materials. Multidisciplinary Digital Publishing Institute, Basel
- Mustafa F, Andreescu S (2020) Nanotechnology-based approaches for food sensing and packaging applications. *RSC Adv* 10(33):19309–19336
- Nemani SK, Annavarapu RK, Mohammadian B, Raiyan A, Heil J, Haque MA et al (2018) Surface modification of polymers: methods and applications. *Adv Mater Interfaces* 5(24):1801247
- Panchal SS, Vasava DV (2020) Biodegradable polymeric materials: synthetic approach. *ACS Omega* 5(9):4370–4379
- Pandiyaraj KN, Selvarajan V, Rhee YH, Kim HW, Shah SI (2009) Glow discharge plasma-induced immobilization of heparin and insulin on polyethylene terephthalate film surfaces enhances anti-thrombogenic properties. *Mater Sci Eng C* 29(3):796–805
- Parvinzadeh M, Moradian S, Rashidi A, Yazdanshenas M-E (2010) Surface characterization of polyethylene terephthalate/silica nanocomposites. *Appl Surf Sci* 256(9):2792–2802
- Pegalajar-Jurado A, Joslin J, Hawker M, Reynolds M, Fisher E (2014) Creation of hydrophilic nitric oxide releasing polymers via plasma surface modification. *ACS Appl Mater Interfaces* 6(15):12307–12320
- Penterman R, Klink SI, De Koning H, Nisato G, Broer DJ (2002) Single-substrate liquid-crystal displays by photo-enforced stratification. *Nature* 417(6884):55–58
- Pereira D, Losada PP, Angulo I, Greaves W, Cruz JM (2009) Development of a polyamide nanocomposite for food industry: morphological structure, processing, and properties. *Polym Compos* 30(4):436–444
- Perez-lvarez L, Lizundia E, del Hoyo S, Sagasti A, Rubio LR, Vilas JL (2016) Polysaccharide polyelectrolyte multilayer coating on poly (ethylene terephthalate). *Polym Int* 65(8):915–920
- PlasticsEurope (2016) *Plastics-the facts 2016*. An analysis of European plastics production, 11
- Qian J, Ruiz-Garcia L, Fan B, Villalba JIR, McCarthy U, Zhang B et al (2020) Food traceability system from governmental, corporate, and consumer perspectives in the European Union and China: a comparative review. *Trends Food Sci Technol* 99:402–412
- Quintino L (2014) Overview of coating technologies. In: *Surface modification by solid state processing*. Elsevier, Amsterdam, pp 1–24
- Rajajeyaganthan R, Kessler F, de Mour Leal PH, Kuhn S, Weibel DE (2011) Surface modification of synthetic polymers using UV photochemistry in the presence of reactive vapours. In: *Macromolecular symposia*. Wiley Online Library, vol 299, pp 175–182

- Rebollar E, Sanz M, Perez S, Hernandez M, Martín-Fabiani I, Rueda DR et al (2012) Gold coatings on polymer laser induced periodic surface structures: assessment as substrates for surface-enhanced Raman scattering. *Phys Chem Chem Phys* 14(45):15699–15705
- Regis S, Jassal M, Mukherjee N, Bayon Y, Scarborough N, Bhowmick S (2012) Altering surface characteristics of polypropylene mesh via sodium hydroxide treatment. *J Biomed Mater Res A* 100(5):1160–1167
- Rhim J-W, Hong S-I, Park H-M, Ng PK (2006) Preparation and characterization of chitosan-based nanocomposite films with antimicrobial activity. *J Agric Food Chem* 54(16):5814–5822
- Robertson GL (2016) Food packaging: principles and practice. CRC Press, Boca Raton
- Roy S, Rhim JW (2021) Anthocyanin food colorant and its application in pH-responsive color change indicator films. *Crit Rev Food Sci Nutr* 61(14):2297–2325
- Rudko G, Kovalchuk A, Fediv V, Chen WM, Buyanova IA (2015) Enhancement of polymer endurance to UV light by incorporation of semiconductor nanoparticles. *Nanoscale Res Lett* 10(1):1–6
- Sadeghi K, Yoon J-Y, Seo J (2020) Chromogenic polymers and their packaging applications: a review. *Polym Rev* 60(3):442–492
- Saha NR, Sarkar G, Roy I, Bhattacharyya A, Rana D, Dhanarajan G et al (2016) Nanocomposite films based on cellulose acetate/polyethylene glycol/modified montmorillonite as nontoxic active packaging material. *RSC Adv* 6(95):92569–92578
- Shah U, Naqash F, Gani A, Masoodi F (2016) Art and science behind modified starch edible films and coatings: a review. *Compr Rev Food Sci Food Saf* 15(3):568–580
- Shankar S, Rhim JW (2016) Polymer nanocomposites for food packaging applications. In: *Functional and physical properties of polymer nanocomposites*, vol 29. Wiley, New York
- Shankar S, Chorachoo J, Jaiswal L, Voravuthikunchai SP (2014) Effect of reducing agent concentrations and temperature on characteristics and antimicrobial activity of silver nanoparticles. *Mater Lett* 137:160–163
- Sheng E, Sutherland I, Brewis D, Heath R (1995) Effects of the chromic acid etching on propylene polymer surfaces. *J Adhes Sci Technol* 9(1):47–60
- Shin Y, Shin J, Lee YS (2011) Preparation and characterization of multilayer film incorporating oxygen scavenger. *Macromol Res* 19(9):869
- Shin S-H, Kwon YH, Kim Y-H, Jung J-Y, Lee MH, Nah J (2015) Triboelectric charging sequence induced by surface functionalization as a method to fabricate high performance triboelectric generators. *ACS Nano* 9(4):4621–4627
- Shrivastava A (2018) Introduction to plastics engineering. William Andrew, Cambridge
- Silvestre C, Duraccio D, Cimmino S (2011) Food packaging based on polymer nanomaterials. *Prog Polym Sci* 36(12):1766–1782
- Siracusa V (2019) Surface modification of polymers for food science. In: *Surface modification of polymers: methods and applications*. Wiley, New York, pp 347–361
- Siracusa V, Rocculi P, Romani S, Dalla Rosa M (2008) Biodegradable polymers for food packaging: a review. *Trends Food Sci Technol* 19(12):634–643
- Sohail M, Ashfaq B, Azeem I, Faisal A, Doğan SY, Wang J et al (2019) A facile and versatile route to functional poly (propylene) surfaces via UV-curable coatings. *React Funct Polym* 144:104366
- Souza A, Benze R, Ferrão E, Ditchfield C, Coelho A, Tadini C (2012) Cassava starch biodegradable films: influence of glycerol and clay nanoparticles content on tensile and barrier properties and glass transition temperature. *LWT Food Sci Technol* 46(1):110–117
- Spricigo PC, Foschini MM, Ribeiro C, Corrêa DS, Ferreira MD (2017) Nanoscaled platforms based on SiO₂ and Al₂O₃ impregnated with potassium permanganate use color changes to indicate ethylene removal. *Food Bioprocess Technol* 10(9):1622–1630
- Studer K, Decker C, Beck E, Schwalm R (2003) Overcoming oxygen inhibition in UV-curing of acrylate coatings by carbon dioxide inerting, part I. *Prog Org Coat* 48(1):92–100
- Thirumdas R, Sarangapani C, Annapure US (2015) Cold plasma: a novel non-thermal technology for food processing. *Food Biophys* 10(1):1–11

- Unalan IU, Cerri G, Marcuzzo E, Cozzolino CA, Farris S (2014) Nanocomposite films and coatings using inorganic nanobuilding blocks (NBB): current applications and future opportunities in the food packaging sector. *RSC Adv* 4(56):29393–29428
- Valencia L, Nomena EM, Mathew AP, Velikov KP (2019) Biobased cellulose nanofibril–oil composite films for active edible barriers. *ACS Appl Mater Interfaces* 11(17):16040–16047
- Van Veldhuizen E, Rutgers W (2001) Corona discharges: fundamentals and diagnostics. In: Invited paper, Proceedings of frontiers in low temperature plasma diagnosis IV, Rolduc, Netherlands, pp 40–49
- Vasile C (2018) Polymeric nanocomposites and nanocoatings for food packaging: a review. *Materials* 11(10):1834
- Vilela C, Kurek M, Hayouka Z, Röcker B, Yildirim S, Antunes MDC et al (2018) A concise guide to active agents for active food packaging. *Trends Food Sci Technol* 80:212–222
- Vu CHT, Won K (2013) Novel water-resistant UV-activated oxygen indicator for intelligent food packaging. *Food Chem* 140(1–2):52–56
- Werner BG, Koontz JL, Goddard JM (2017) Hurdles to commercial translation of next generation active food packaging technologies. *Curr Opin Food Sci* 16:40–48
- Wihodo M, Moraru CI (2013) Physical and chemical methods used to enhance the structure and mechanical properties of protein films: a review. *J Food Eng* 114(3):292–302
- Wong DE, Aandler SM, Lincoln C, Goddard JM, Talbert JN (2017) Oxygen scavenging polymer coating prepared by hydrophobic modification of glucose oxidase. *J Coat Technol Res* 14(2):489–495
- Wood V, Panzer MJ, Chen J, Bradley MS, Halpert JE, Bawendi MG et al (2009) Inkjet-printed quantum dot–polymer composites for full-color ac-driven displays. *Adv Mater* 21(21):2151–2155
- Wyrwa J, Barska A (2017) Innovations in the food packaging market: active packaging. *Eur Food Res Technol* 243(10):1681–1692
- Xiao-e L, Green AN, Haque SA, Mills A, Durrant JR (2004) Light-driven oxygen scavenging by titania/polymer nanocomposite films. *J Photochem Photobiol A Chem* 162(2–3):253–259
- Xu QF, Mondal B, Lyons AM (2011) Fabricating superhydrophobic polymer surfaces with excellent abrasion resistance by a simple lamination templating method. *ACS Appl Mater Interfaces* 3(9):3508–3514
- Xue C-H, Jia S-T, Zhang J, Ma J-Z (2010) Large-area fabrication of superhydrophobic surfaces for practical applications: an overview. *Sci Technol Adv Mater* 11(3):033002
- Yameen B, Alvarez M, Azzaroni O, Jonas U, Knoll W (2009) Tailoring of poly (ether ether ketone) surface properties via surface-initiated atom transfer radical polymerization. *Langmuir* 25(11):6214–6220
- Yameen B, Khan HU, Knoll W, Förch R, Jonas U (2011) Surface initiated polymerization on pulsed plasma deposited Polyallylamine: a polymer substrate-independent strategy to soft surfaces with polymer brushes. *Macromol Rapid Commun* 32(21):1735–1740
- Yao X, Song Y, Jiang L (2011) Applications of bio-inspired special wettable surfaces. *Adv Mater* 23(6):719–734
- Yildirim S, Röcker B, Pettersen MK, Nilsen-Nygaard J, Ayhan Z, Rutkaite R et al (2018) Active packaging applications for food. *Compr Rev Food Sci Food Saf* 17(1):165–199
- Yousefi H, Su H-M, Imani SM, Alkhalidi K, Filipe CDM, Didar TF (2019) Intelligent food packaging: a review of smart sensing technologies for monitoring food quality. *ACS Sens* 4(4):808–821
- Youssef AM, El-Sayed SM (2018) Bionanocomposites materials for food packaging applications: concepts and future outlook. *Carbohydr Polym* 193:19–27
- Yu H, Sun B, Zhang D, Chen G, Yang X, Yao J (2014) Reinforcement of biodegradable poly (3-hydroxybutyrate-co-3-hydroxyvalerate) with cellulose nanocrystal/silver nanohybrids as bifunctional nanofillers. *J Mater Chem B* 2(48):8479–8489

- Zanetti M, Carniel TK, Dalcanton F, dos Anjos RS, Riella HG, de Araujo PH et al (2018) Use of encapsulated natural compounds as antimicrobial additives in food packaging: a brief review. *Trends Food Sci Technol* 81:51–60
- Zenkiewicz M (2008) Corona discharge in an air as a method of modification of polymeric materials' surface layers. *Polimery* 53(1):3–13
- Zhai X, Wang W, Zhang H, Dai Y, Dong H, Hou H (2020) Effects of high starch content on the physicochemical properties of starch/PBAT nanocomposite films prepared by extrusion blowing. *Carbohydr Polym* 239:116231
- Zhang J, Mungara P, Jane, J.-I. (2001) Mechanical and thermal properties of extruded soy protein sheets. *Polymer* 42(6):2569–2578
- Zhang X, Wang H, Niu N, Chen Z, Li S, Liu SX et al (2020) Fluorescent poly (vinyl alcohol) films containing chlorogenic acid carbon nanodots for food monitoring. *ACS Applied Nano Mater* 3(8):7611–7620
- Zhu M, Ge L, Lyu Y, Zi Y, Li X, Li D et al (2017) Preparation, characterization and antibacterial activity of oxidized κ -carrageenan. *Carbohydr Polym* 174:1051–1058
- Zille A, Oliveira FR, Souto AP (2015) Plasma treatment in textile industry. *Plasma Process Polym* 12(2):98–131



Polymeric Membranes in Wastewater Treatment

17

Adil Majeed Rather, Yang Xu, Robert Lewis Dupont, and Xiaoguang Wang

Abstract

Water covers around 71% of the earth's surface; however, only 2.5% is fresh water available for consumption. Rapid industrialization and increasing human activities, such as the use of fertilizers, mining, and pesticides, add many harmful organic and inorganic pollutants into the water, which endangers fresh water resources and the ecological environment. Various conventional methods for wastewater treatment, including chemical precipitation, physical adsorption, ion exchange, and membrane separation have been present since long times. Among these methods, polymeric membrane separation has become the main focus of attention over the past couple of decades for wastewater treatment, owing to an ease of operation, low energy consumption, and their unique and proficient separation of contaminants which yields high-quality treated water. In addition, these membranes can be used at an increased range of temperature conditions and the recyclability of these membranes is also very promising. Polymeric membranes for wastewater treatment are generally separated into four major categories, based on their performance, characteristics, pore size, and specific separation qualities. These four categories are microfiltration (MF), ultrafiltration (UF), nanofiltration (NF), and reverse osmosis (RO). This book chapter will provide a comprehensive summary for readers to understand the progress in the

A. M. Rather · Y. Xu · R. L. Dupont

William G. Lowrie Department of Chemical and Biomolecular Engineering, The Ohio State University, Columbus, OH, USA

X. Wang (✉)

William G. Lowrie Department of Chemical and Biomolecular Engineering, The Ohio State University, Columbus, OH, USA

Sustainability Institute, The Ohio State University, Columbus, OH, USA

e-mail: wang.12206@osu.edu

© The Author(s), under exclusive license to Springer Nature Singapore Pte Ltd. 2022

487

L. M. Pandey, A. Hasan (eds.), *Nanoscale Engineering of Biomaterials: Properties and Applications*, https://doi.org/10.1007/978-981-16-3667-7_17

area of wastewater treatment using polymeric membranes and to highlight the recent advances in polymeric membranes and background study of wastewater treatment. In addition, the potential benefits and challenges of utilizing polymeric membranes for wastewater treatment will be briefly discussed.

Keywords

Polymeric membranes · Porous polymers · Wastewater treatment

17.1 Introduction

The connection between human civilization and water has existed throughout the ages, from the first settlements created in fertile river valleys, to the efforts of the United States Environmental Protection Agency (US EPA), the clean water act, and beyond. Water has been utilized across many eras of human civilization as a source of kinetic energy for mills and other mechanical processes, and as a fuel to keep our biological processes operating, such as crop growth and food digestion (Yevjevich 2009). Thankfully, this invaluable resource makes up approximately 71% of the Earth's surface. However, around 96.5% of the water is found in the oceans and is not safe for drinking. Of the remaining freshwater, almost 69% is found in glaciers and ground ice (Shiklomanov 1993).

The limited sources of freshwater are also in danger from various sources of pollution. For example, the US EPA completed a study on the levels of pollution in the water resources of the United States and found that approximately 55% of the mileage of rivers and streams that were tested were deemed impaired, meaning they were unable to support one or more of their designated uses, such as fishing or swimming. Additionally, 70% of the measured lake acreage, 78% of the measured coastal square mileage, and 98% of the miles of measured Great Lakes coastline were determined to be impaired. On top of this, only 62 total square miles out of the 53,332 square miles that were tested of the Great Lakes open waters were found to be able to support their designated uses as they were not deemed impaired (U.S. Environmental Protection Agency (EPA) 2017). Common sources of pollution were mercury, polychlorinated biphenyls, fertilizers, and pathogens. The sources of these pollutants are commonly storm-water runoff, domestic drainage, and industrial discharges (Virgil 2003).

Storm-water runoff can carry oils, gasoline, and other automotive fluids from roads and other urban areas. It can also carry fertilizers, pesticides, and animal wastes from agricultural fields, with many of these providing sources for nitrogen and phosphorous pollution (Virgil 2003). Domestic drainage includes wastewater produced from domestic sources, including what is flushed down sinks and toilets, and is a common source of pathogens and bacteria. Lastly, industrial discharges come in many forms but are typically larger than domestic sources. For example, pulp and paper mills mix clean water with wood chips and chemicals, such as bleach, during their many processes before eventually removing the water from the finished

products and returning it to the source. In many of these processes, the water must be cleared of pollutants before being returned to nature (Virgil 2003). This can be done through a variety of mechanical or chemical processes, including filtration through a membrane. These pollutants can cause death or outbreaks of diseases like cholera, hepatitis, and typhoid (Khalifa and Bidaisee 2018).

A number of methods have been used to treat the wastewater from urban and industrial sources in an effort to protect and repair the limited supplies of available fresh water. However, many of these methods produce sludge and other by-products that require large amounts of energy to treat. For example, the entire population of 15,014 publicly owned treatment works in the United States and Puerto Rico taken from the 2012 clean watersheds needs survey were found to produce a total of 13.85 million tons of sludge solids per year (Seiple et al. 2017). The sludge that is produced is typically hazardous, containing by-products from reactants or captured pollutants and pathogens, and requires further, energy-intensive treatment. The energy use of wastewater treatment in the United States accounts for around 2% of the total energy use of the country with a third of that being used solely to treat sludge (Pabi et al. 2013). These numbers will increase as the population grows and as more countries begin to develop their own wastewater treatment systems.

To combat the creation of sludge and the high energy usage, polymeric membranes are being implemented to separate solids and sometimes pathogens from wastewater. Polymeric membranes do not require energy to function, and instead depend on the difference in pressure to drive the wastewater through while impeding the flow of pollutants. Additionally, these polymeric membranes do not create sludge that requires further treatment. This chapter will focus on the use of these polymeric membranes for wastewater treatment while providing a brief discussion on other conventional methods.

17.2 Conventional Methods for Wastewater Treatment

This growing problem of water contamination has a significant influence on the economic development of countries, as well as human livelihoods and the quality of the environment, all throughout the globe. Some pollutants, such as heavy metal ions, do not readily biodegrade and, when ingested, can cause a series of irreversible physiological diseases. For instance, mercury (Hg^{2+}) can damage the central nervous system (CNS) and can cause headaches, stomatitis and gastroenteritis (Tchounwou et al. 2003). Similarly, lead (Pb^{2+}) can cause an inadequate stream of oxygen and nutrients throughout the body, resulting in brain and tissue damage (Daniel et al. 2004). Moreover, cadmium ions can replace calcium (Ca^{2+}) ions in the bones and deter the normal deposition of Ca^{2+} resulting in cartilage disease (Miyahara et al. 1984). Excess arsenic can inhibit the normal metabolism of cells in the body, causing cell wounds and eventually leading to organ damage. Additionally, organic pollutants in water, including fertilizers, plasticizers, pesticides, detergents, pharmaceuticals, oils, and other hydrocarbons, are also hazardous and are mainly derived from agricultural runoff, food and paper industries, and domestic sewage. In

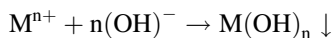
order to metabolize these organic pollutants, a large amount of dissolved oxygen is needed, which in turn jeopardize aquatic organisms and their ecosystem (Goktas and MacLeod 2016). Therefore, the removal of organic and inorganic pollutants and the effective treatment of wastewater are vital for the aquatic ecosystem and for the generally health of humanity. In the past, various conventional methods have been adopted for the treatment of wastewater, including chemical precipitation, ion exchange, adsorption, and biological treatment, which are discussed below.

17.2.1 Chemical Precipitation

Chemical precipitation is a method of wastewater treatment in which the dissolved materials in wastewater are turned into solid, insoluble particles through the addition of various chemicals to the wastewater. Specifically, chemical precipitation is used to remove the ionic constituents from wastewater by reducing their solubility using specific counter ions. Chemical precipitation is mainly utilized in the removal of metal cations but can be used for the removal of anions such as cyanide, phosphates, nitrites, and various organic molecules (Brady 2003; Kwon et al. 2012; Kim et al. 2013). Chemical precipitation is typically followed by a solid separation process such as sedimentation, filtration, and coagulation to remove the precipitates. Most of the metal ions are precipitated through hydroxide precipitation but can also be precipitated through carbonate and sulfide precipitation. In some cases, the chemical constituents to be removed must be oxidized or reduced. Phosphates can be removed by precipitation as iron or alum salts, while fluorine can be eliminated using calcium chloride (CaCl_2). A chemical precipitation method typically includes four major stages including the addition of reagents, flocculation, sedimentation, and solid-liquid separation. Chemical precipitation is performed in various means as described below.

17.2.1.1 Hydroxide Precipitation

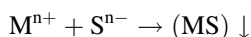
Hydroxide precipitation is a type of chemical precipitation which involves the addition of a suitable hydroxide to the wastewater to form an insoluble metal hydroxide precipitate. The precipitation reaction is illustrated as:



Every metal has a discrete pH value at which the hydroxide precipitation takes place creating the insoluble metal hydroxide. Reagents commonly used for hydroxide precipitation are typically alkaline compounds, such as lime or caustic soda. Although the hydroxide precipitation method has several advantages, including a low cost, simple design, ease of pH control, and an easy removal of the metal hydroxides through flocculation and sedimentation, this method produces a large quantity of relatively low density sludge, which causes dewatering and disposal problems.

17.2.1.2 Sulfide Precipitation

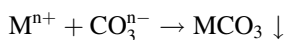
Sulfide precipitation is another chemical precipitation process in which both insoluble sulfides, such as ferrous sulfate, and soluble sulfides, including sodium sulfide and hydrogen sulfide, are used to precipitate the metal ions as insoluble metal sulfides. Sulfide precipitation occurs at neutral pH conditions, as the metal sulfides have a lower solubility than hydroxides below neutral pH and in the alkaline pH range. The basic principle of the sulfide precipitation method is similar to the hydroxide precipitation in which the sulfide is added to the wastewater to precipitate the formed slurry which is subsequently removed through filtration. The formation of metal sulfide is illustrated as:



The benefits of sulfide precipitation over hydroxide precipitation are the reduction in the quantity of sludge generated and the ability to more easily process the sludge to recover the metals which helps offset the cost of treatment. Moreover, the high reactivity of sulfides with metal ions and the insolubility of the metal sulfides are attractive features compared to hydroxide precipitation. However, sulfide precipitation is not viable for all situations because of the toxicity of the sulfide ions and the dangers of hydrogen sulfide (H₂S).

17.2.1.3 Carbonate Precipitation

Carbonate precipitation is generally used to remove metal ions either through converting hydroxides into carbonates using carbon dioxide or direct precipitation using a carbonate reagent like calcium carbonate. The solubility of most carbonates is in between that of hydroxides and sulfides and usually forms easily filtered precipitates. When sodium carbonate is added to water, the basic carbonates are formed as:



The precipitated metal carbonates are generated as a sludge and are removed through filtration.

Chemical precipitation offers many advantages as a treatment alternative for removing many industrial wastewater pollutants. It meets stringent discharge criteria and has been used for many years. Moreover, this method is relatively simple and can be used to remove specific components from wastewater with a high degree of selectivity. However, this technique also possesses several limitations, including a high cost, restrictions to its applications, a high energy input requirement, manual oversight, and the generation of large quantities of sludge.

17.2.2 Ion-Exchange Method

Ion-exchange is a wastewater treatment method in which ions of particular species are replaced with ions of analogous charge but of a different species to generate an insoluble resin. In essence, the ion-exchange method is a sorption process coupled with a reversible chemical reaction. The most common applications of the ion-exchange method are the removal of calcium (Ca^{2+}) and magnesium (Mg^{2+}) through “water softening,” the removal of bicarbonates through de-alkalization, and the removal of all ions through water desalination. Moreover, the ion-exchange method is also very efficient in removing various toxic heavy metal ions including radium (Ra), uranium (U), chromium (Cr), and several charged atoms or ions such as fluorides, nitrates, sulfates, perchlorates, and iron from wastewater (Al-Enezi et al. 2004). The main component of the ion-exchange method is a microporous exchange resin comprising of small, microporous beads that are insoluble in water and organic solvents. The most widely used base materials for ion-exchange resins are polystyrene and polycarbonate with a diameter ranging from 0.3 to 1.3 mm. These beads are composed of around 50% of a water-dispersed gel-structured material. As the water is homogeneously dispersed throughout the beads, the water-soluble materials and particles can freely move in and out of the beads. Each of the monomers in the polymer beads consists of a specific functional group that interacts with various ions through electrostatic interactions. In general, there are two types of ion-exchange resins: cation-exchange resins, which can remove most of the positively charged ions from wastewater including iron, lead, barium, copper, and aluminum, and anionic-exchange resins, which can remove negatively charged ions including nitrates and sulfates.

17.2.3 Adsorption

Adsorption is another wastewater treatment method, where water is passed through a layer of porous and granulated materials like activated charcoal and zeolites. It relies on a surface phenomenon with a common mechanism for the removal of organic and inorganic pollutants. When the wastewater passes through a highly porous surface, the impurities, such as dissolved organic and inorganic molecules, ions, and salts, are removed. Various physical and chemical interactions between the pollutants and the surface drive the adsorption of contaminants onto the surface. The particles retained at the solid surface are known as the adsorbate and the solid surface on which the adsorbate is retained is known as the adsorbent. The adsorption process is one of the most efficient methods of treatment for the removal of organic and inorganic contaminants from wastewater. The adsorption method has several advantages over other techniques because of its simple design and low investment of initial cost and infrastructure while also meeting stringent water quality standards. Adsorption has garnered the attention of many researchers throughout the years.

The adsorbents used during this process are classified as either natural or synthetic. Natural adsorbents include clay, charcoal, zeolites, and ores (Rashed 2013).

These natural adsorbents have several advantages such as being abundant in nature, relatively cheap, and possessing significant potential for modification to enhance their adsorption capabilities. Synthetic adsorbents are developed from household waste, agricultural waste, industrial waste, and polymers.

17.2.4 Biological Treatment

Biological treatment is typically a secondary wastewater treatment that uses bacteria, protozoa, and other specialized microbes to purify wastewater (Jessica et al. 2013; Liu et al. 2013). In this particular treatment, the microorganisms break down the organic pollutants into smaller pieces which stick together creating a flocculation effect allowing the organic contaminants to settle. Subsequently, the produced sludge is dewatered and disposed as a solid waste. Typically, biological wastewater treatment can be classified into three main categories: aerobic, where the microorganism require oxygen to break down organic matter and other contaminants into carbon dioxide (CO₂) and microbial biomass, anaerobic, where microorganisms break down organic pollutants in wastewater without using oxygen, often forming CO₂, methane, and microbial biomass, and anoxic, where microorganisms use other molecules besides oxygen for their growth. Anoxic biological treatments are commonly used for the removal of additional contaminants that are not possible through the other two methods, such as sulfates, nitrites, and selenates. The amount of organic contaminants that can be decomposed through aerobic biological treatment is measured in terms of the biological oxygen demand (BOD) which refers to the amount of dissolved oxygen required by the microorganisms for the breakdown of organic contaminants into smaller molecules (Tripathi and Shukla 1991). In general, biological wastewater treatment optimizes the natural microbial break down of waste and other contaminants into small molecules, which offers a cheap and efficient additional or alternative method for wastewater treatment (Busk et al. 1989).

17.3 Polymeric Membranes

In addition to these methods, another important and widely adopted method for wastewater treatment is the use of polymeric membranes. Polymers are widely used advanced materials and are found in nearly every material used on a daily basis. The significance of polymers has been highlighted in a plethora of applications in different domains of science, technology, and industry, including as biomaterials (Hasan and Pandey 2015; Hasan et al. 2017, 2018), smart materials (Rather and Manna 2016; Parbat et al. 2017; Vanessa et al. 2018), catalytic materials (Xu et al. 2019; Wang et al. 2017), and the removal of oil spills (Rather et al. 2017; Shome et al. 2019). In addition to these applications, polymers have contributed significantly to wastewater treatment.

Membrane separation technologies for wastewater treatment are increasing rapidly because of pressures from environmental protection laws and the strict

regulations on drinking water quality all around the world. Recent advances in membrane-based purification technologies have led to a large utilization of synthetic polymeric membranes for wastewater remediation through the elimination of bacteria, viruses, and other toxic chemicals from the polluted and contaminated water resources. In this regard, the broader applications of synthetic polymeric membranes can be owed to their unique benefits, including the vast number of polymers which allow for the ability to select a specific polymer for the exact separation problem from an existing set of polymers (Visakh and Olga 2016). The removal of selected pollutants and contaminations from the aqueous phase using polymeric membranes can vary significantly and depends on the target pollutants and contaminants as well as several aspects, including the physiochemical properties of the constituents, the condition of operation, and the membrane structure.

To date, a number of polymeric membranes have been developed based on a variety of different components (Anna et al. 2016), such as cellulose acetate (CA), cellulose nitrate, polyethersulfone (PES), polysulfone (PS), polyvinylidene fluoride (PVDF), polypiperazine (PPZ), polypropylene (PP), and polyacrylonitrile (PAN). The first generation of polymeric membrane materials, CA membranes, were produced in 1963 from Loeb and Sourirajan's group and exhibited a high salt rejection with high flux values (Sidney and Srinivasa 1963). They also found applications in a wide range of filtration processes. However, these membranes lacked long-term thermal, biological, and chemical stability, which limits their practical applications in complex conditions including high temperature and extreme pH environments. With the development of other polymeric membranes, PS and PES have emerged among the most common choices for ultrafiltration systems as well as the secondary substrates for nanofiltration and reverse-osmosis processes. These polymeric materials have a high permeability, great selectivity, high mechanical stability, and high chemical resistance. For instance, PES usually has a high glass transition temperature (T_g) at approximately 225 °C and PS shows a high pH stability and oxidation resistance (Souzanchia et al. 2013). However, the main limitation of these polymeric membranes is their intrinsic hydrophobicity, which results in a high biofouling tendency and leads to higher operating costs, shorter lifespans, and irreversible separation performances.

To solve this problem, surface modification tools have been developed to enhance the hydrophilicity of these polymeric materials (Victor et al. 2014). It is generally accepted that increasing the surface hydrophilicity of the polymeric membranes reduces the fouling issues as many foulants, including organic contaminants and proteins, are hydrophobic in nature. There are a lot of methods to develop hydrophilic polymeric membranes, such as the homogeneous physical blending method (Sinha and Purkait 2013; Fan et al. 2014a, b), surface chemical treatment (Xia et al. 2014), and UV irradiation (Vázquez et al. 2005; Gu et al. 2009). Amphiphilic copolymers, like Pluronic F127, can be used as a surfaces modifier and pore-forming agent to prepare antifouling polyethersulfone (PES) ultrafiltration membranes (Zhao et al. 2008). Experimental results have shown that surface modification can be a robust and efficient solution for enhancing the antifouling properties (Rana and Matsuura 2010). Despite various other approaches, including grafting,

hydrophilic modification, and etching, chemical modification is still considered to be the most facile and convenient method for surface modification. In the past, various polymers and surface-modified polymers with tunable surface properties have been explored for various applications, such as antibiofouling, nonspecific protein adsorption, and biocompatibility (Hasan and Pandey 2015). For instance, the amine functionalization of polymeric membranes significantly enhances the hydrophilicity and charge of the membranes. A membrane with more hydrophilicity and charge was found to foul less and better reject salts through increasing the electrostatic interactions (Zinadini et al. 2014).

Similarly, the pH sensitivity of polymeric membranes is another property that can be adjusted through a number of techniques. For example, functional polymers, such as polymethyl methacrylate (PMMA) and polyacrylic acid (PAA), can be mixed with polymeric membranes to enhance their pH sensitivity. Additionally, the shrinking and swelling of the pores of the polymeric membranes can be tuned through the deionization of carboxyl groups ($-\text{COOH}$) around their pK_a which further enhances the permeability of the membranes (Mikaa et al. 1995; Kang and James 2007). The classic method of preparation for these membranes involves the direct blending of PAA with other polymers, so that the elution of PAA is possible even though it is water insoluble. For instance, Wei et al. reported a blending method to prepare tunable polymeric membranes by combining a cross-linked PAA gel with a PES solution by adopting a phase separation technique (Qiang et al. 2009).

Temperature-controlled water filtration is another class of functional polymeric membranes. A commonly used polymer is poly(N-vinylcaprolactam) (PVCL), a thermally responsive polymer with a lower critical solution temperature (LCST) in the physiological range. PVCL-based microgels can be explored to coat the commercially available hollow fiber membranes used for microfiltration and ultrafiltration-based applications (Daniel et al. 2014). The main advantage of these microgel systems is their versatility which allows them to be applied to almost any kind of membrane application by adopting a facile membrane fabrication process. In this instance, the membranes exhibited reversible, thermally responsive permeability and rejection (Young-Hye et al. 2011). The details of various polymeric membranes used for wastewater treatment, their applications, and methods of fabrication are presented in Tables 17.1 and 17.2.

17.3.1 Classification of Polymeric Membranes and Their Applications

The separation performance of porous polymeric membranes usually depends on the effective pore size of the polymeric membrane and the particle size of the constituent particles in the water. As the pore size shrinks, the driving force behind the process, typically the filtration pressure, increases (David et al. 2018). Polymeric membranes are broadly classified into four major categories, based on their pore size, performance, characteristics, and specific separation potentials. These four categories are

Table 17.1 Summary of the fabrication methods of various polymeric membranes used in microfiltration and ultrafiltration and their applications in wastewater treatment

Materials	Pore size	Method of fabrication	Applications	Advantages	Reference
<i>Microfiltration and ultrafiltration</i>	~0.1–1 μm				
Polyvinylidene fluoride (PVDF)	~1 μm	Block copolymer (PEO-b-PA)	Oil-water emulsion filtration	Significantly low-fouling propensity	Freeman and Pinnau ACS Symposium Series 2004 876:1–23
Polyvinylidene fluoride (PVDF)	~0.05–1.5 μm	Cellulose nanofiber (CNF) based PVDF membrane	Eliminate Fe_2O_3 nanoparticles and CV dyes from water	Ecofriendly	Deepu et al. ACS Sustain Chem Eng 2017 5:2026–2033
PVDF	~0.05–1.5 μm	Dimethyl Isosorbide (DMI) as the solvent, PVDF and polyethersulfone-based membranes	UF and MF for water treatment	Tunable pore size in the range of UF and MF	Francesca et al. ACS Sustain Chem Eng 2020 8:659–668
PVDF	~0.1 μm	Hollow-fiber MF/UF membranes	Drinking water production	Fouling mechanisms were investigated	Katsuki et al. J Membr Sci 2020 602:117975–117984
PVDF	~0.22 μm	Biomimetic coated PVDF UF/MF membranes	Underwater anti-oil adhesion behaviors; water remediation of simulated protein waste-water	Greatly enhanced wettability, good harsh condition tolerance, high filtration efficiency, and excellent fouling resistance	Xiaobin et al. J Membr Sci 2020 591:117353–117361
PVDF	~1 μm	Polydopamine (PDA) coated PVDF ultrafiltration membranes	Bovine serum albumin (BSA) and humic acid (HA) separation	Higher hydrophilicity, water permeation and flux recovery ratio (FRR)	Saraswathia et al. J Environ Chem Eng 2017 5:2937–2943
Polypropylene (PP)	~0.2 μm	Sericin-coated PP-based MF membranes	MF water treatment	High fouling resistance performances	Vishal et al. J Chem Tech Biotechnol 2019 94:3637–3649

PP	~0.2 μm	Pre-coagulation/flocculation combined with low pressure membrane filtration through polymer	PP-UF membranes for virus and NOM removal in drinking water production	Without pre-coagulation/flocculation, no (MF) or only minor (UF) virus removal was observed	Fiksdal and Leiknes J Membr Sci 2006 279:364–371
PP	~0.1 μm	Surface deposition of PDA on the membranes	MF membranes for water treatment	Improved fouling resistance performances	McCloskey et al. J Membr Sci 2012 413:82–90
PP	~0.2 μm	Poly[2-(dimethyl amino) ethyl methacrylate] grafted by sequential UV-induced graft polymerization	MF membranes for water treatment	A positively charged membrane surface achieved 100% antibacterial efficiency for tested bacteria	Yang et al. J Membr Sci 2011 376:132–141
Polyethersulfone (PES)	~9.35 μm	Surfactant modification (PSSS)	UF, Flux reduction in PEG and dextran solution	Good fouling resistant properties	Reddy et al. J Membr Sci 2003 214:211–221
PES	~0.5 μm	PDA coated PES UF membranes	UF water treatment	Good anti-fouling ability and enhanced blood compatibility	Chong et al. J Membr Sci 2012 417:228–236
PES	~5–200 nm	PDA coating and PEG grafting	PES-based UF membrane	Good anti-fouling ability	Fang et al. Desalination 2014 344:422–430
PES	~5–200 nm	Poly(ethylenimine) grafting PES-based UF membranes	UF	Good anti-fouling ability and good rejection for proteins	Zhen et al. J Membr Sci 2018 554:125–133
PES/PEG	~30 nm	PEG modified PES-based UF membranes	UF	Enhanced anti-fouling performance	Fan et al. J Membr Sci 2016 499:56–64
Polysulfone (PS)	~10 nm	Polymers, including MC, PVA and PVP	UF	Low deposition of BSA	Kim et al. Desalination 1988 70:229–249
PS	~5–7 nm	Blending with polyamine nanofibers	UF, bovine serum albumin (BSA) and albumin egg (AE) rejection	High mechanical property and thermal stability	Zhifeng et al. J Membr Sci 2008 320:363–371

(continued)

Table 17.1 (continued)

Materials	Pore size	Method of fabrication	Applications	Advantages	Reference
PS	~0.8 μm	Spray coating of PS/PEG block polymer	UF	Pore sizes, hydrophilicity and UF performances are tunable	Wang et al. Chinese J Chem Eng 2020 https://doi.org/10.1016/j.cjche.2020.05.002
PS	~20–26 nm	PEG-b-PSF-b-PEG block copolymer	TFC FO membrane	Improve the water permeability and antifouling property	Seung et al. NPG Asia Mater 2019 11:8–21
PS	~1.9–7.5 μm	Polypyrrole-polysulfone blend UF membranes	UF	pH responsive behavior	Krishmasri et al. Sep Purif Technol 2019 5:115736–115750
Polyacrylonitrile (PAN)	~20 nm	NaOH post-treatment	UF	Good anti-fouling property	Xiangli et al. Sep Purif Technol. 2007 3:265–269
PAN	~1 μm	UV assisted grafting polymers, including AA, HEMA, PEGMA, and POEM with various kDa	UF	Low protein-polymer surface interactions	Mathias et al. J Membr Sci 1996 115:31–47
PAN	~6.5 nm	Hydrolyzed ethanolamine-Polyacrylonitrile UF membrane	Dye-water treatment by UF	Excellent anti-dye fouling and a good rejection property for anionic dyes	Jianhua et al. Chemosphere 2020 3:127390–127400
PAN	~2 μm	Synthesized from polyacrylonitrile (PAN) and hydrophilically modified polyacrylonitrile (HM-PAN)	UF for water treatment	Fouling of protein particles on the blend membranes was able to reduce as the composition of HM-PAN increases	Bumsuk J Membr Sci 2004 229:129–136
Poly(sulfobetaine methacrylate) (PSBMA)	~0.2 μm	PSBMA/PDA co-deposited coating	Application in protein separation	Excellent hydrophilicity, low water flux reduction and high-water flux recovery; good stability in a long-term washing	Rong et al. J Membr Sci 2014 466:18–25

RC-g-PSBMA membrane	~0.2 μm	Atom transfer radical polymerization (ATRP) of a zwitterionic monomer, sulfobetaine methacrylate (SBMA)	Application for protein purification (BSA)	Tunable permeation selectivity	Yong-Hong et al. <i>ACS Appl Mater Interf</i> 2010 2:203–211
Poly (n-isopropylacrylamide) (p(NIPAm))	~20 nm	Co-deposition of stimuli-responsive microgels in the foulant cake layer	Filtrations were done below the lower critical solution temperature (LCST) and temperature was increased to above the LCST for cleaning	Increased fouling reversibility	Canan et al. <i>ACS Appl Mater Interf</i> 2019 11:18711–18719
Poly(ethylene glycol) (PEG)	~12.3 nm	Controlled deposition of zwitterionic polymers and PEG	UF	High-performance, antifouling membranes	Kerianne et al. <i>Langmuir</i> 2019 35:1872–1881
Polyacrylonitrile-block-polyethylene glycol (PAN-b-PEG)	~5 nm	Immersion precipitation phase inversion	UF for water treatment	The antifouling ability of the copolymer membranes increased with increasing PEG content in the copolymer	Xiangrong et al. <i>J Membr Sci</i> 2011 384:44–51
Cellulose-acetate (CA)	–	PEG grafting	UF	Modified surface can decrease the fouling tendency	Morao et al. <i>Environ Prog</i> 2005 24:367–382
CA	–	Zwitterionic brushes-modified cellulose membrane	UF for water treatment	Good anti-biofouling ability and cytocompatibility	Liu et al. <i>J Mater. Chem B</i> 2014 2:7222–7231
Poly(vinyl alcohol) (PVA)	~1 μm	Electro-spinning	Selective and high adsorption of lead (Pb(II)) and cadmium (Cd(II)) ions	High adsorption capacity of Pb(II) and Cd(II)	Karim et al. <i>Ecotoxicol Environ Saf</i> 2019 169:479–486

(continued)

Table 17.1 (continued)

Materials	Pore size	Method of fabrication	Applications	Advantages	Reference
Poly(ether ether ketone) (PEEK)	~20 nm	Photo-induced polymerization	Bovine serum albumin (BSA) separation	Good permeability and antifouling performances	Tingjian et al. <i>Mater Today Commun</i> 2020 23:100945–100952
Poly(phthalazinone ether sulfone ketone) (PPESK)	~10 nm	(Atom transfer radical polymerization) ATRP	UF and BSA filtration	Good anti-fouling property	Li-Ping et al. <i>J Membr Sci</i> 2008 320:407–415

Table 17.2 Summary of the fabrication methods of various polymeric membranes used in nanofiltration and reverse osmosis and their applications in wastewater treatment

Materials	Pore size	Method of fabrication	Applications	Advantages	Reference
<i>Nanofiltration and reverse osmosis</i>	~0.5–10 nm				
Poly(m-phenylene isophthalamide) (PMIA)	2 nm	Phase inversion	Chromium (Cr IV) ion removal from waste-water	Enhanced water permeability	Ren et al. <i>J Environ Sci</i> 2010 22:1335–1341
Piperazine	~5–8 nm	Interfacial polymerization	High salt rejection (98%)	Higher chemical stability	Roy et al. <i>Desalination</i> 2017 :420 241–257
PVA-Al ₂ O ₃	~3–5 nm	Assimilation of PVA/PAA/GA into the microporous ceramic substrate	Dye waste-water treatment, desalination	Performs at higher pH	Wang et al. <i>AIChE J</i> 2013 59:3834–3842
Polyether sulfone (PES)	~4–6 nm	Electron beam irradiation method	Recovery of 1-(5-bromo-fur-2-yl)-2-bromo-2-nitroethane	Above 80% of rejection was observed	Martinez et al. <i>J Ind Eng Chem</i> 2012 18:1635–1641
Polysulfone	~4–10 nm	Interfacial polymerization	Removal of Cr (VI) ions from waste-water	Exceptional chlorine resistance	Hong-mei et al. <i>Desalination</i> 2014 346:122–130
Polymerization of tetraethylenepentamine and 1,3,5-benzenetricarbonyl trichloride with the addition of CaCl ₂	~6 nm	Layer by layer assembly	Inorganic dye removal	Enhanced chlorine resistance, rejection of various inorganic slats	Fan et al. <i>J Membr Sci</i> 2014 452:90–96
Polyelectrolytes Polydiallyldimethylammonium chloride (PDADMAC) and polysodium-4-styrenesulfonate (PSS)	~7–10 nm	Layer by layer assembly	Removal of inorganic salts from aqueous solution	Rejection of bivalent salts including MgSO ₄	Law et al. <i>Desalination</i> 2014 351:19–26

(continued)

Table 17.2 (continued)

Materials	Pore size	Method of fabrication	Applications	Advantages	Reference
Cellulose acetate membranes with surface adsorption of ALG/CHI multilayer	~3–8 nm	Phase inversion	Removal of heavy metal ions	Rejection of bivalent ions and various organic impurities	Ramzi et al. <i>Desalination</i> 2011 266:78–86
Amine-functionalized multiwalled carbon nanotubes (NH ₂ -MWCNTs)/polyethersulfone (PES) nanocomposite	~6–10 nm	Phase inversion	Removal of bivalent inorganic with high water flux	Increase in hydrophilicity, high stability	Vahid et al. <i>J Membr Sci</i> 2014 466:70–81
Blending of O-carboxymethyl chitosan/Fe ₃ O ₄ nanoparticle on Polyethersulfone (PES)	~7.5 nm	Diffusion-induced phase inversion	Inorganic dye removal from water	Enhanced antifouling resistance and water permeation	Zinadinin et al. <i>Desalination</i> 2014 349:145–154
Polyethersulfone membrane blended with ZNO nanoparticles	~7 nm	Immersion precipitation	Inorganic dye removal	Enhanced antibiofouling property	Stefan et al. <i>J Membr Sci</i> 2012 389:155–161
Polysulfone (PSF) membranes blend with IGEPAI	~8–10 nm	Grafting	Removal of Cd from waste-water	Improved hydrophilicity	Saljoughi and Mousavi <i>Sep Purif Technol</i> 2012 90:22–30
Polyamide membranes modified with poly(ethylene glycol) diglycidyl ether	~3–5 nm	Grafting	Removal of salt with high efficiency	Good fouling resistance	Elizabeth et al. <i>J Membr Sci</i> 2011 367:273–287
Grafting poly (amidoamine) dendrimer (PAMAM) on the polyethersulfone (PES) membranes	~5–8 nm	Grafting	Removal of various types of surfactants with high efficiency	Improved water permeability and antibiofouling	Zhu et al. <i>J Membr Sci</i> 2015 487:117–126
Quaternary ammonium compounds (QACs) grafted on PVDF membrane	~6–8 nm	Atom-transfer radical-polymerization (ATRP)	Waste-water treatment	High inhibition rate	Ping et al. <i>J Membr Sci</i> 2019 570:286–293

Chitosan (CS) was blended with PVDF to prepare mixed matrix membrane	~3 nm	Phase inversion	Reduction of fouling	Improved hydrophilicity	Elizalde et al. Sep Purif Technol 2018 190:68–76
<i>Reverse Osmosis</i>	>0.5 nm				
Silver blended asymmetric cellulose acetate (CA) hollow fiber membrane	~0.2–0.5 nm	Jet-wet spinning	Removes dissolved salts and allows water only	Increase in biological stability	Chou et al. Polym Adv Technol 2005 :16 600–607
Coating phospholipid polymer on CA membrane	~0.4 nm	Jet-wet spinning	Rejection of biological pollutants	Increase in fouling resistance	Sang et al. J Membr Sci 2005 249:133–141
Polyamide thin film composite (TFC) with triethanolamine (TEOA)	~0.3 nm	Interfacial polymerization	Treatment of industrial effluents	Antifouling against hydrophobic foulants	Yan et al. J Membr Sci 2016 513:108–116
Polyamide TFC over a microporous PES substrate	~0.2 nm	Interfacial polymerization	Inorganic salt removal	Antifouling against hydrophobic foulants	Khorshidi et al. Sci Rep 2016 6:22069–22078
Hollow fiber membrane from cellulose acetate (CA)	~0.3–0.5 nm	Thermally induced phase separation	Antifouling property for humic acid and BSA	High hydrophilicity and high water-permeability	Shibutani et al. J Membr Sci 2011 376:102–109
Polyamide TFC with carbon nanotubes and graphene oxide	~0.4 nm	Interfacial polymerization	Improved fouling resistance towards various proteins and polysaccharides including BSA, sodium alginate	Good separation performance and chlorine resistance	Simcik et al. Sep Purif Technol 2016 167:163–173
Polyamide TFC with aluminosilicate single-walled nanotubes	~0.6 nm	Interfacial polymerization	Removes salt and allows water	Improved membrane performance, long term durability	Kim et al. J Mater Chem A 2015 3:6798–6809
Polyamide TFC with ordered mesoporous carbons	~0.1–0.4 nm	Interfacial polymerization	Higher permeate flux and high rejection of monovalent and divalent ions	Increase in hydrophilicity	Baroña et al. Desalination 2013 325:138–147
Codeposition of dopamine/PSPE coating on polyamide	~0.2–0.4 nm	Interfacial polymerization	Removal of monovalent and divalent salts	Increase in hydrophilicity and limiting protein adsorption	Kim and Deng J Membr Sci 2011 375:46–54

(continued)

Table 17.2 (continued)

Materials	Pore size	Method of fabrication	Applications	Advantages	Reference
Zeolite nanoparticles dispersed polyamide films	~0.2–0.5 nm	Interfacial polymerization	Water purification	High salt rejection	Jeonga et al. <i>J Membr Sci</i> 2007 294:1–7
Copolymer, poly(vinylpyrrolidone)-co-poly(sulfobetaine methacrylate) (poly(VP-co-SBMA))	~0.1–0.3 nm	Copolymerization	Thermosettable materials in a bioinert interface for medical devices	Thermal-tolerant and fouling-resistant	Chou et al. <i>ACS Appl Mater Interf</i> 2015 7:10096–10107
Nano-NaX zeolite embedded into polyamide films	~0.3–0.4 nm	Interfacial polymerization	Desalination	High thermal stability	Fatizadeh et al. <i>J Membr Sci</i> 2011 375:88–95
TFC of polyamide Aminophend/formaldehyde resin	~0.5 nm	Interfacial polymerization	Desalination above 96%	Excellent anti-chlorine, anti-fouling and reuse performances	Wang et al. <i>J Membr Sci</i> 2020 https://doi.org/10.1016/j.memsci.2020.118496
Crosslinking of amine-functional polyamidoamine (PAMAM)dendrimers and PAMAM–polyethylene glycol (PAMAM–PEG)	~0.2–0.5 nm	In situ crosslinking	Salt removal	Low contact angle and high salt rejection	Sarkar et al. <i>J Membr Sci</i> 2010 349:421–428

microfiltration, ultrafiltration, nanofiltration, and reverse osmosis. The utility and applications of these membranes in various filtration techniques are detailed below.

17.3.1.1 Microfiltration and Ultrafiltration

Microfiltration (MF) is classified as a low-pressure process, with an operating pressure typically below 2 bar. The separations using MF operate through filtering and removing the suspended particles or solids, bacteria, protozoa, and, to a lesser extent, algae, owing to the relatively larger pore size between 100 and 1000 nm (Baker 2012). However, microscopic particles, atomic or ionic species, dissolved particles, natural organic matter, and water can pass through the filter membrane (Crittenden et al. 2012), as depicted in Fig. 17.1. These types of polymeric membranes can generally separate macromolecules of molecular weight less than 100 kDa (Siobhan et al. 2002). The MF membranes are commonly used in the sugar and sweetener industry, dairy industries, and in bioprocessing industries. For example, in the dairy industry, the MF method is mainly used to remove the fat from whey in the production of whey protein isolates, in the purification of cheese brine, and in the separation of casein and serum from skim milk.

Ultrafiltration (UF) membranes also operate mainly through filtering; however, UF membranes possess a wider range than MF membranes with a pore size that is generally between 2 and 100 nm. UF is also considered a low-pressure process and typically operate between 0.1 and 5 bar. Additionally, they are dependent on the transmembrane pressure to drive the separation process. These types of membranes are capable of separating large materials, such as colloids, proteins, enzymes, fats, and bacteria, while allowing sugars, salts, and other low molecular weight solids to pass through, as shown in Fig. 17.1 (El-Dessouky and Ettouney 1999). In this separation process, the separation range is expressed in daltons (Da) or kilodaltons (kDa) and is usually in the range of 1 Da or 100 kDa. For instance, Su et al. used the

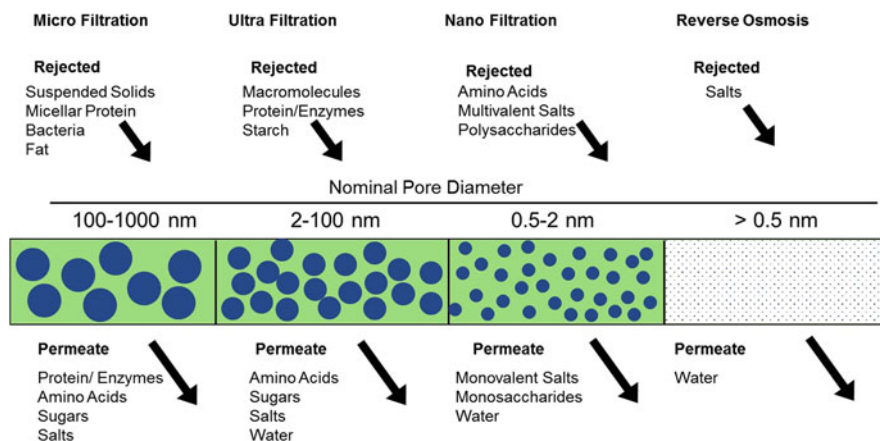


Fig. 17.1 The schematic illustration displays the nominal pore diameter and various pollutants allowed and rejected by various filtration techniques using different polymeric membranes

combination of UF and electro dialysis (ED) for the treatment of a copper slurry (Su et al. 2014). The combined setup of UF and ED removed particles and Cu^{2+} from the slurry through the use of a PVDF flat sheet membrane with a molecular weight cutoff of 30 kDa, corresponding to roughly 4 nm in diameter, while possessing a high mechanical strength.

The elimination rejection achieved by MF and UF polymeric membranes usually depends on the properties of the polymeric membranes and hydrodynamic conditions (Fane et al. 2011). Therefore, interferences in the upstream wastewater treatment process can negatively influence the performance of both MF and UF polymeric membranes.

17.3.1.2 Nanofiltration and Reverse Osmosis

Nanofiltration (NF) refers to the category of polymeric membranes which possess pore sizes in the range of 1 to 10 nm that are operated at high pressure, typically around 3 to 20 bar. The separation range in NF is classified on the basis of rejection of known multivalent cationic solutes including magnesium sulfate (MgSO_4) and by the removal of disinfectant by-products including natural and synthetic organic matter (Raymond 1999; Roy et al. 2017). In general, a typical NF membrane can retain the molecules of varying sizes below and above the pore size of the polymeric membranes (Bruggena et al. 2008). The membranes used for nanofiltration are made of polymer thin films which include PET, PS, PES, or PPZ polymers (Lu et al. 2002; Gopal et al. 2006; Tolba et al. 2015). NF membranes can efficiently remove divalent ions, polysaccharides, and small organic molecules while permitting monovalent ions, water, and monosaccharides, as shown in Fig. 17.1. NF membranes operate at lower pressures and have a higher water permeability than reverse-osmosis systems, thus reducing the specific energy consumption. These properties enable the NF membranes to be applicable in wastewater treatment, biotechnology, pharmaceuticals, and food engineering applications. For instance, Ren et al. demonstrated the sustainability of using poly(m-phenylene isophthalamide) (PMIA) NF membranes for the removal of chromium (Cr) ions from wastewater (Ren et al. 2010). The separation mechanism was mainly based on the interaction of Cr(IV) and the negatively charged NF polymeric membrane. Moreover, NF membranes have also been used to treat seawater, where high recoveries of salt water are possible at reasonable pressures as the membrane allows most of the Na^+ and Cl^- ions to pass through while retaining the unwanted sulfate ions (Davis et al. 1996). It is worth noting that previous research has indicated that NF membrane systems can achieve a higher recovery through nonthermal crystallization (Azadi et al. 2016) and can reduce the second level fouling through pre-ozone treatments (Parka et al. 2017).

Reverse osmosis (RO) is another wastewater treatment process that utilizes a semipermeable membrane to remove various ions, unwanted organic and inorganic molecules, and large particles from drinking water. RO membranes possess pore sizes below 1 nm and operate at high pressures, around 5 to 120 bar. RO is a very versatile method that can remove many types of suspended and dissolved chemical and biological contaminants, including bacteria and salts (David et al. 2016), which

brands it a great source for use in industrial processes and the production of potable water. Interestingly, salts are highly rejected by RO membranes owing to their sub-nanometer scaled pores, commonly used in the removal of salt from seawater (Argyris et al. 2019). For instance, commercial seawater RO membranes can remove 99.5 to 99.8% of NaCl from the seawater. Important polymers that are being used in RO processes include polyamide, cellulose-acetate, cellulose-diacetate, and cellulose-triacetate (Yang et al. 2019). Furthermore, RO is considered as a complete barrier for pathogens, bacteria, and other microorganisms that are harmful to infants and the elderly. For instance, in a previous study of RO based wastewater treatment, it was found that neither *Escherichia coli* nor viruses were detected in the permeate after filtration through the RO polymeric membrane (Tama et al. 2007). Moreover, RO membranes were further found to be beneficial in eliminating high molecular weight organic constituents, such as humic acid and fulvic acid (Rodriguez et al. 2009).

17.3.1.3 Challenges Associated with Polymeric Membranes

Although wastewater treatment using polymeric membranes has shown great potential, there are still several technical challenges that need further investigation and research. Some of the challenges are detailed as below:

1. Polymeric membrane fouling and scaling will lead to the increase of water cost. Fouling and scaling are the accumulation of materials deposited on the polymeric membranes. They usually result in pore clogging and, eventually, decreased flux. Therefore, a regular and periodic cleaning of the polymeric membranes is inevitable, and the expenses associated with filter changes is another hassle that can increase costs.
2. The selectivity of the polymeric membranes to specific waste materials is very important, which is restricted depending on the membrane surface charge and the pore size. However, they require a large amount of energy to maintain high pressure during purification in practical applications. In addition, the fouling-driven decline in polymeric membrane permeability leads to a reduction in the flux. This increases the pressure needed to keep a normal level of flux. Hence, the performance under constant high pressure is a substantial challenge for wastewater treatment using polymeric membranes.
3. Some of the polymeric membrane filtration techniques require some pretreatment methods for some heavily polluted wastewater. These pretreatments include the addition of chemicals or the use of other treatment methods, both of which increase the cost of using polymeric membranes.

17.4 Outlook and Conclusions

Global water scarcity is growing rapidly in many regions of the world due to an increase in human activities and the growth of agricultural and industrial needs. On top of this, unmanaged wastewater streams have caused the pollution of many

existing fresh water sources. Problems with water are expected to grow in the coming decades and water scarcity is expected to appear in many new regions, including those that are currently water rich. Hence, the treatment and reuse of wastewater is a critical issue. In this chapter, we have discussed various conventional methods including chemical precipitation, ion exchange, and adsorption for wastewater treatment. However, these methods have various limitations including a high cost, restrictions to their applications, a high energy input, and the generation of large quantities of sludge during treatment.

In addition to these conventional methods, another class of water treatment using polymeric membranes has been extensively studied and used in a number of applications, including wastewater treatment. Moreover, we have conferred in detail that the separation performance of porous polymeric membranes usually depends on the effective pore size of the polymeric membrane and the size range of contaminants present in water. As the pore size shrinks, the separation process requires a higher driving force, which is typically the filtration pressure. Moreover, we have discussed the four major categories of polymeric membranes of wastewater treatment, including microfiltration, ultrafiltration, nanofiltration, and reverse osmosis, based on their performance, characteristics, pore size, and specific separation qualities. Their applications in wastewater treatment were discussed briefly in this chapter. Additionally, the benefits of polymeric membranes include a series of outstanding properties, such as high flexibility, excellent chemical and mechanical durability, high permeability of water, chemical species selectivity, and efficient removal of waste products. Hence, the development of polymeric membrane technology has allowed for the next generation of water supply systems to advance beyond the conventional and traditional methods with a more affordable price and higher efficiency.

References

- Al-Enezi G, Hamoda MF, Fawzi N (2004) Toxic/hazardous substances & environmental engineering. *J Environ Sci Health* 39(2):455–464
- Anna L, Jeffrey WE, Seth BD (2016) Membrane materials for water purification: design, development and application. *Environ Sci Water Res Technol* 2(1):17–42
- Argyris P, Haralambous KJ, Loizidou M (2019) Desalination brine disposal methods and treatment technologies-a review. *Sci Total Environ* 693(3):133545–133567
- Azadi M, Flavia A, Julien Z, Simon J, James F, Snyder SA (2016) A novel brine precipitation process for higher water recovery. *Desalination* 385(3):69–74
- Baker R (2012) Microfiltration, in membrane technology and applications, vol 5, 3rd edn. Wiley, San Francisco, CA, pp 303–325
- Baroña GNB, Lim J, Choi M, Jung B (2013) Interfacial polymerization of polyamide-aluminosilicate SWNT nanocomposite membranes for reverse osmosis. *Desalination* 325(1):138–147
- Brady RF Jr (2003) Polymer characterisation and analysis, vol 81. American Chemical Society, Oxford University Press, New York, pp 772–773
- Bruggena BV, Mänttäril M, Nyström M (2008) Drawbacks of applying nanofiltration and how to avoid them: a review. *Sep Purif Technol* 63(2):251–263

- Bumsuk J (2004) Preparation of hydrophilic polyacrylonitrile blend membranes for ultrafiltration. *J Membr Sci* 229(2):129–136
- Busk D, Reddy TA, Hayes TD, Schwieger BRJ (1989) Performance of a pilot-scale hyacinth-based secondary treatment system. *J War Poll Cont Fed* 61(7):1217–1223
- Canan A, Papatya K, Ayse A, Çulfaz-Emecen PZ (2019) Co-deposition of stimuli-responsive microgels with foulants during ultrafiltration as a fouling removal strategy. *ACS Appl Mater Interfaces* 11(20):18711–18719
- Chong C, Shuang L, Zhao W, Qiang W, Shengqiang N, Shudong S, Changsheng Z (2012) The hydrodynamic permeability and surface property of polyethersulfone ultrafiltration membranes with mussel-inspired polydopamine coatings. *J Membr Sci* 417(2):228–236
- Chou WL, Yu DG, Yang MC (2005) The preparation and characterization of silver-loading cellulose acetate hollow fiber membrane for water treatment. *Polym Adv Technol* 16(8):600–607
- Chou YN, Chang Y, Wen TC (2015) Applying thermosettable zwitterionic copolymers as general fouling-resistant and thermal-tolerant biomaterial interfaces. *ACS Appl Mater Interfaces* 7(19):10096–10107
- Crittenden J, Trussell R, Hand D, Howe K, Tchobanoglous G (2012) Principles of water treatment, vol 2, 2nd edn. Wiley, Hoboken, NJ, pp 672–698
- Daniel S, Limson JL, Dairam A, Watkins GM, Daya S (2004) Through metal binding, curcumin protects against lead- and cadmium-induced lipid peroxidation in rat brain homogenates and against lead-induced tissue damage in rat brain. *J Inorg Biochem* 98(2):266–275
- Daniel M, Fee P, Wong JE, Andrij P, Matthias W (2014) Temperature-modulated water filtration using microgel-functionalized hollow-fiber membranes. *Angew Chem Int Ed* 53(22):5706–5710
- David MW, Emily WT, Kishor GN, Laith AM, Lienhard V, John H (2016) Energy efficiency of batch and semi-batch (CCRO) reverse osmosis desalination. *Water Res* 106(3):272–282
- David MW, Chakraborty S, Emily WT, Megan HP, Bellona C, Loutatidoud S, Karimigh L, Anne MM, Achillij A, Ghassemig A, Lokesh PP, Snyder SA, Curcioc S, Vecitis CD, Hassan AA, Lienhard VJH (2018) A review of polymeric membranes and processes for potable water reuse. *Prog Polym Sci* 81(2):209–237
- Davis R, Lomax I, Plummer M (1996) Membranes solve north sea water flood sulfate problems. *Oil Gas J* 94(48):59–64
- Deepu A, Gopa K, Daniel P, Mariana AH, Luis Carlos DM, Yves G, Sabu T (2017) Meldrum's acid modified cellulose nanofiber-based polyvinylidene fluoride microfiltration membrane for dye water treatment and nanoparticle removal. *ACS Sustain Chem Eng* 5(2):2026–2033
- Dongwei M, Wang Z, Tao L, Yunxia H, Yong W (2020) Spray coating of polysulfone/poly(ethylene glycol) block polymer on macroporous substrates followed by selective swelling for composite ultrafiltration membranes. *Chin J Chem Eng* 29:85–91. <https://doi.org/10.1016/j.cjche.2020.05.002>
- El-Dessouky HT, Ettouney HM (1999) Plastic/compact heat exchangers for single-effect desalination systems. *Desalination* 122(3):271–277
- Elizabeth MVW, Alyson CS, Mukul MS, Young-Hye L, Benny DF (2011) Surface modification of commercial polyamide desalination membranes using poly(ethylene glycol) diglycidyl ether to enhance membrane fouling resistance. *J Membr Sci* 367(1):273–287
- Elizalde CNB, Al-Gharabli S, Kujawaa J, Mavukkandy M, Hasana SW, Arafat HA (2018) Fabrication of blend polyvinylidene fluoride/chitosan membranes for enhanced flux and fouling resistance. *Sep Purif Technol* 190(9):68–76
- Fan X, Su Y, Zhao X, Li Y, Zhang R, Zhao J, Jiang Z, Zhu J, Ma Y, Liu Y (2014a) Fabrication of polyvinyl chloride ultrafiltration membranes with stable antifouling property by exploring the pore formation and surface modification capabilities of polyvinyl formal. *J Membr Sci* 464(64):100–109

- Fan X, Dong Y, Su Y, Xueting Z, Li Y, Liu J, Jiang Z (2014b) Improved performance of composite nanofiltration membranes by adding calcium chloride in aqueous phase during interfacial polymerization process. *J Membr Sci* 452(2):90–96
- Fan X, Su Y, Zhao X, Li Y, Zhang R, Ma T, Liu Y, Jiang Z (2016) Manipulating the segregation behavior of polyethylene glycol by hydrogen bonding interaction to endow ultrafiltration membranes with enhanced antifouling performance. *J Membr Sci* 499(2):56–64
- Fane AG, Wang R, Jia Y, Wang LK, Chen JP, Hung YT, Shammass NK (2011) Membrane technology: past, present and future. *Memb Desalinat Technol* 13(3):1–45
- Fang L, Jianqiang M, Jianfeng Y, Yanga BO, Qing T, Chunhua D (2014) Surface modification of PES ultrafiltration membrane by polydopamine coating and poly(ethylene glycol) grafting: morphology, stability, and anti-fouling. *Desalination* 344(2):422–430
- Fathizadeh M, Aroujalian A, Raisi AR (2011) Effect of added NaX nano-zeolite into polyamide as a top thin layer of membrane on water flux and salt rejection in a reverse osmosis process. *J Membr Sci* 375(2):88–95
- Fiksdal L, Leiknes TO (2006) The effect of coagulation with MF/UF membrane filtration for the removal of virus in drinking water. *J Membr Sci* 279(2):364–371
- Francesca R, Francesco G, Francesco P, Fabio A, Alberto F (2020) Dimethyl isosorbide as a green solvent for sustainable ultrafiltration and microfiltration membrane preparation. *ACS Sustain Chem Eng* 8(1):659–668
- Freeman BD, Pinnau I (2004) Gas and liquid separations using membranes: an overview. *ACS Symp Ser* 876(1):1–23
- Goktas RK, MacLeod M (2016) Remoteness from sources of persistent organic pollutants in the multi-media global environment. *Environ Pollut* 217(3):33–41
- Gopal R, Kaur S, Ma Z, Chan C, Ramakrishna S, Matsuura T (2006) Electrospun nanofibrous filtration membrane. *J Membr Sci* 281(2):581–586
- Gu JS, Yu HY, Lei H, Tang ZQ, Wei L, Jin Z, Yan MG, Wei XW (2009) Chain-length dependence of the antifouling characteristics of the glycol polymer-modified polypropylene membrane in an SMBR. *J Membr Sci* 326(26):145–152
- Hasan A, Pandey LM (2015) Review: polymers, surface-modified polymers, and self assembled monolayers as surface-modifying agents for biomaterials. *Polym-Plast Technol Eng* 54(13):1358–1378
- Hasan A, Waibhaw G, Tiwari S, Dharmalingam K, Shukla I, Pandey LM (2017) Fabrication and characterization of chitosan, polyvinylpyrrolidone, and cellulose nanowhiskers nanocomposite films for wound healing drug delivery application. *J Biomed Mater Res A* 105(9):2391–2404
- Hasan A, Waibhaw G, Saxena V, Pandey LM (2018) Nano-biocomposite scaffolds of chitosan, carboxymethyl cellulose and silver nanoparticle modified cellulose nanowhiskers for bone tissue engineering applications. *Int J Biol Macromol* 111(3):923–934
- Hong-mei X, Jun-fu W, Xiao-lei W (2014) Nanofiltration hollow fiber membranes with high charge density prepared by simultaneous electron beam radiation-induced graft polymerization for removal of Cr(VI). *Desalination* 346(2):122–130
- Jeonga BH, Hoek EMV, Yan Y, Subramani A, Huang X, Hurwitz G, Ghosh AK, Jawor A (2007) Interfacial polymerization of thin film nanocomposites: a new concept for reverse osmosis membranes. *J Membr Sci* 294(2):1–7
- Jessica B, Damian EH, Hans-Peter EK, Janneke W, Elena K, Carsten P, Thomas AT, Christian NA, Jens A, Benjamin H, Dirk S, Eddy W, Nico B (2013) Is biological treatment a viable alternative for micro pollutant removal in drinking water treatment processes? *Water Res* 47(16):5955–5976
- Jianhua Y, Yixing W, Zhenying L, Yujie L, Yang H, Zhen-liang X (2020) High efficient dye removal with hydrolyzed ethanolamine- polyacrylonitrile UF membrane: rejection of anionic dye and selective adsorption of cationic dye. *Chemosphere* 259(3):127390–127400
- Kang H, James MD (2007) Development and characterization of poly(vinylidene fluoride)-poly(acrylic acid) pore-filled pH-sensitive membranes. *J Membr Sci* 301(2):19–28

- Karima MR, Mohammed OA, Nabeel HA, Hamad FA, Al-Mubaddel FS, Awual MR (2019) Composite nanofibers membranes of poly(vinyl alcohol)/chitosan for selective lead(II) and cadmium(II) ions removal from wastewater. *Ecotoxicol Environ Saf* 169(6):479–486
- Katsuki K, Keita K (2020) Irreversible fouling in hollow-fiber PVDF MF/UF membranes filtering surface water: effects of pre-coagulation and identification of the foulant. *J Membr Sci* 602(1):117975–117984
- Kerianne MD, Christopher A, Kuo-Le B, Todd E, Schiffman JD (2019) Antifouling ultrafiltration membranes with retained pore size by controlled deposition of zwitterionic polymers and poly(ethylene glycol). *Langmuir* 35(5):1872–1881
- Khalifa M, Bidaisee S (2018) The importance of clean water. *Sch J Appl Sci Res* 1(7):17–20
- Khorshidi B, Thundat T, Fleck BA, Sadrzadeh M (2016) A novel approach toward fabrication of high performance thin film composite polyamide membranes. *Sci Rep* 6(6):22069–22078
- Kim ES, Deng B (2011) Fabrication of polyamide thin-film nano-composite (PA-TFN) membrane with hydrophilized ordered mesoporous carbon (H-OMC) for water purifications. *J Membr Sci* 375(2):46–54
- Kim KJ, Fane AG, Fell CJD (1988) The performance of ultrafiltration membranes pretreated by polymers. *Desalination* 70(3):229–249
- Kim IC, Hong S, Tak T, Kwon YN (2013) Interfacially synthesized chlorine-resistant polyimide thin film composite (TFC) reverse osmosis (RO) membranes. *Desalination* 309(2):18–26
- Kim HJ, Lim MY, Jung KH, Kim DG, Lee JC (2015) High-performance reverse osmosis nanocomposite membranes containing the mixture of carbon nanotubes and graphene oxide. *J Mater Chem A* 3(13):6798–6809
- Krishnasri VK, Munmun M, Sirshendu D (2019) Permeability hysteresis of polypyrrole-polysulfone blend ultrafiltration membranes: study of phase separation thermodynamics and pH responsive membrane properties. *Sep Purif Technol* 227(2):115736–115750
- Kwon YN, Shih K, Tang C, Leckie JO (2012) Adsorption of perfluorinated compounds on thin-film composite polyamide membranes. *J Appl Polym Sci* 124(2):1042–1049
- Law YN, Abdul WM, Ching YN, Choe PL, Rosiah R (2014) Development of nanofiltration membrane with high salt selectivity and performance stability using polyelectrolyte multilayers. *Desalination* 351(2):19–26
- Li-Ping Z, Han-Bang D, Xiu-Zhen W, Zhuan Y, Bao-Ku Z, You-Yi X (2008) Tethering hydrophilic polymer brushes onto PPESK membranes via surface-initiated atom transfer radical polymerization. *J Membr Sci* 320(2):407–415
- Liu SJ, Zhao ZY, Li J, Wang J, Qi Y (2013) An anaerobic two-layer permeable reactive bio barrier for the remediation of nitrate-contaminated groundwater. *Water Res* 47(16):5977–5985
- Liu P, Chen Q, Li L, Linb S, Shen J (2014) Anti-biofouling ability and cytocompatibility of the zwitterionic brushes-modified cellulose membrane. *J Mater Chem B* 2(41):7222–7231
- Lu X, Bian X, Shi L (2002) Preparation and characterization of NF composite membrane. *J Membr Sci* 210(1):3–11
- Martinez MB, Vander B, Rodriguez NZ, Alconero PL (2012) Separation of a high-value pharmaceutical compound from waste ethanol by nanofiltration. *J Ind Eng Chem* 18(5):1635–1641
- Mathias U, Matuschewski H, Annett O, Hans-Georg H (1996) Photo-induced graft polymerization surface modifications for the preparation of hydrophilic and low-protein-adsorbing ultrafiltration membranes. *J Membr Sci* 115(1):31–47
- McCloskeya BD, Parkb HB, Hao J, Brandon WR, Millera DJ, Freemana BD (2012) A bioinspired fouling-resistant surface modification for water purification membranes. *J Membr Sci* 413(1):82–90
- Mikaa AM, Childsa RF, Dickson JM, McCarrya BE, Gagnon DR (1995) A new class of polyelectrolyte-filled microfiltration membranes with environmentally controlled porosity. *J Membr Sci* 108(1):37–56
- Miyahara T, Tsukada M, Mori MA, Kozuka H (1984) The effect of cadmium on the collagen solubility of embryonic chick bone in tissue-culture. *Toxicol Lett* 22(1):89–92

- Morao A, Escobar IC, Amorim MTP, Lopes A, Goncalves IC (2005) Post synthesis modification of a cellulose acetate ultrafiltration membrane for applications in water and wastewater treatment. *Environ Prog* 24(4):367–382
- Pabi S, Amarnath A, Goldstein R, Reekie L (2013) Electric Power Research Institute and Water Research Foundation – electricity use and management in the municipal water supply and wastewater industries. Water Research Foundation: Water Research Foundation. Report No.: 3002001433
- Parbat D, Gaffar S, Rather AM, Gupta A, Manna U (2017) A general and facile chemical avenue for controlled and extreme regulation of water-wettability in air and oil-wettability under water. *Chem Sci* 8(9):6542–6554
- Parka M, Anumol T, Simonc J, Zraickc F, Snyder SA (2017) Pre-ozonation for high recovery of nanofiltration (NF) membrane system: membrane fouling reduction and trace organic compound attenuation. *J Membr Sci* 523(1):255–263
- Ping M, Zhang X, Liub M, Wua Z, Wang Z (2019) Surface modification of polyvinylidene fluoride membrane by atom-transfer radical-polymerization of quaternary ammonium compound for mitigating biofouling. *J Membr Sci* 570(2):286–293
- Qiang W, Jie L, Bosi Q, Baohong F, Changsheng Z (2009) Preparation, characterization and application of functional polyethersulfone membranes blended with poly (acrylic acid) gels. *J Membr Sci* 337(2):266–273
- Ramzi HL, Ezdine F, Mohamed SR, André D (2011) Effect of LbL surface modification on characteristics and performances of cellulose acetate nanofiltration membranes. *Desalination* 266(3):78–86
- Rana D, Matsuura T (2010) Surface modifications for antifouling membranes. *Chem Rev* 110(4):2448–2471
- Rashed MN (2013) Adsorption technique for the removal of organic pollutants from water and wastewater. In: *Organic pollutants: monitoring, risk and treatment*, vol 3, pp 165–178
- Rather AM, Manna U (2016) Facile synthesis of tunable and durable bulk superhydrophobic material from amine “reactive” polymeric gel. *Chem Mater* 28(23):8689–8699
- Rather AM, Jana N, Hazarika P, Manna U (2017) Sustainable polymeric material for the facile and repetitive removal of oil-spills through the complementary use of both selective-absorption and active-filtration processes. *J Mater Chem A* 5(44):23339–23348
- Raymond DL (1999) *Water quality and treatment*, vol 5. American Water Works Association and McGraw-Hill, New York, pp 1659–1673
- Reddy AVR, Mohan DJ, Bhattacharya A, Shah VJ, Ghosh PK (2003) Surface modification of ultrafiltration membranes by pre adsorption of a negatively charged polymer: I. permeation of water soluble polymers and inorganic salt solutions and fouling resistance properties. *J Membr Sci* 214(2):211–221
- Ren X, Zhao C, Du S, Wang T, Luan Z, Wang J, Hou D (2010) Fabrication of asymmetric poly (m-phenylene isophthalamide) nanofiltration membrane for chromium (VI) removal. *J Environ Sci* 22(9):1335–1341
- Rodriguez C, Buynder PV, Lugg R, Blair P, Devine B, Cook A, Weinstein P (2009) Indirect potable reuse: a sustainable water supply alternative. *Int J Environ Res Public Health* 6(3):1174–1203
- Rong Z, Peng-Fei R, Hao-Cheng Y, Zhi-Kang X (2014) Fabrication of antifouling membrane surface by poly(sulfobetainemethacrylate)/polydopamine co-deposition. *J Membr Sci* 466(1):18–25
- Roy Y, David MW, Lienhard JH (2017) Effect of temperature on ion transport in nanofiltration membranes: diffusion, convection and electromigration. *Desalination* 420(3):241–257
- Saljoughi E, Mousavi SM (2012) Preparation and characterization of novel polysulfone nanofiltration membranes for removal of cadmium from contaminated water. *Sep Purif Technol* 90(6):22–30
- Sang HY, Junji W, Yasuhiko I, Kazuhiko I (2005) Coupled-diffusion transport of Cr(VI) across anion-exchange membranes prepared by physical and chemical immobilization methods. *J Membr Sci* 249(2):133–141

- Saraswathia MSA, Kausalyaa R, Kaleekkalb NJ, Rana D, Nagendrana A (2017) BSA and humic acid separation from aqueous stream using polydopamine coated PVDF ultrafiltration membranes. *J Environ Chem Eng* 5(3):2937–2943
- Sarkar A, Carver PI, Zhang T, Merrington A, Bruza KJ, Rousseau JL, Keinath SE, Dvornic PR (2010) Dendrimer-based coatings for surface modification of polyamide reverse osmosis membranes. *J Membr Sci* 349(2):421–428
- Seiple TE, Coleman AM, Skaggs RL (2017) Municipal wastewater sludge as a sustainable bioresource in the United States. *J Environ Manage* 197:673–680
- Seung JP, Gouri SD, Schütt F, Rainer A, Yogendra KM, Kumud MT, Tae YK (2019) Visible-light photocatalysis by carbonnano-onion-functionalized ZnO tetrapods: degradation of 2,4-dinitrophenol and a plant-model-based ecological assessment. *NPG Asia Mater* 11(2):8–21
- Shibutani T, Kokitaura T, Ohmukai Y, Maruyama T, Nakatsuka S, Watabe T, Matsuyama H (2011) Membrane fouling properties of hollow fiber membranes prepared from cellulose acetate derivatives. *J Membr Sci* 376(1):102–109
- Shiklomanov IA (1993) *Water in crisis: a guide to the world's fresh water resources*, vol 5. Oxford University Press, New York, pp 13–24
- Shome A, Maji K, Rather AM, Yashwanth A, Patel DK, Manna U (2019) A scalable chemical approach for synthesis of highly tolerant and efficient oil-absorbent. *Chem Asian J* 14(24):4732–4740
- Sidney L, Srinivasa S (1963) Sea water demineralization by means of an osmotic membrane. *Adv Chemother* 38(9):117–132
- Simcik M, Ruzicka MC, Karaszova M, Sedlakova Z, Vejrazka J, Vesely M, Capek P, Friess K, Izak P (2016) Polyamide thin-film composite membranes for potential raw biogas purification: experiments and modeling. *Sep Purif Technol* 167(2):163–173
- Sinha MK, Purkait MK (2013) Increase in hydrophilicity of polysulfone membrane using polyethylene glycol methyl ether. *J Membr Sci* 437(3):7–16
- Siobhan FEB, Maria DK, Melvyn RD, El-Hodalia DEY, Schippers JC (2002) The modified fouling index using ultrafiltration membranes (MFI-UF): characterisation, filtration mechanisms and proposed reference membrane. *J Membr Sci* 197(2):1–21
- Souzanchia S, Vahabzadeha F, Shahrzad F, Seyed NH (2013) Performance of an annular sieve-plate column photoreactor using immobilized TiO₂ on stainless steel support for phenol degradation. *Chem Eng J* 223(23):246–267
- Stefan B, Arcadio S, Patricia L, Lidia B, Bruggena BV, Jeonghwan K (2012) A new outlook on membrane enhancement with nanoparticles: the alternative of ZnO. *J Membr Sci* 389(8):155–161
- Su YN, Lin WS, Hou CH, Den W (2014) Performance of integrated membrane filtration and electro dialysis processes for copper recovery from wafer polishing wastewater. *J Water Process Eng* 4(3):149–158
- Tama LS, Tanga TW, Laub GN, Sharma KR, Chen GH (2007) A pilot study for wastewater reclamation and reuse with MBR/RO and MF/RO systems. *Desalination* 202(3):106–113
- Tchounwou PB, Ayensu WK, Ninashvili N, Sutton D (2003) Environmental exposure to mercury and its toxic opathologic implications for public health. *Environ Toxicol* 18(3):149–175
- Tingjian H, Junfeng L, Yuan C, Tianhaoyue Z, Pengqing L (2020) Improving permeability and antifouling performance of poly (ether ether ketone) membranes by photo-induced graft polymerization. *Mater Today Commun* 23(3):100945–100952
- Tolba OM, Motlak GM, Fadali M, Khalil OA, Almajid KA, Barakat Kim KNA (2015) Effective polysulfone-amorphous SiO₂ NPs electrospun nanofiber membrane for high flux oil/water separation. *Chem Eng J* 279(3):631–638
- Tripathi BD, Shukla SC (1991) Biological treatment of wastewater by selected aquatic plants. *Environ Pollut* 69(1):69–78
- U.S. Environmental Protection Agency (EPA) (2017) *National water quality inventory: report to Congress*, EPA 841-R-16-011

- Vahid V, Majid E, Mohammad HDAF (2014) Fouling reduction and retention increment of polyethersulfone nanofiltration membranes embedded by amine-functionalized multi-walled carbon nanotubes. *J Membr Sci* 466(2):70–81
- Vanessa FC, Daniela MC, Clarisse R, Margarida MF, Senentxu LM (2018) Fluorinated polymers as smart materials for advanced biomedical applications. *Polymers* 10(2):161–187
- Vázquez MI, Lara RDP, Benavente GJ (2005) Modification of cellulosic membranes by γ -radiation: effect on electrochemical parameters and protein adsorption. *Colloids Surf A Physicochem Eng Asp* 270(7):245–251
- Victor K, Daniel JJ, Hilal N (2014) Polymeric membranes: surface modification for minimizing (bio)colloidal fouling. *Adv Colloid Interface Sci* 206(86):116–140
- Virgil K (2003) *Clean water: an introduction to water quality and water pollution control*, 2nd edn. Corvallis, Oregon State University Press
- Visakh PM, Olga N (2016) Nanostructured polymer membranes: applications, state-of-the-art, new challenges and opportunities. In: *Nanostructured polymer membranes: applications*, vol 2, pp 1–25
- Vishal KV, Senthilmurugan S (2019) Fouling resistant sericin-coated polymeric microfiltration membrane. *J Chem Technol Biotechnol* 94(11):3637–3649
- Wang L, Wang N, Zhang G, Shulan J (2013) Covalent crosslinked assembly of tubular ceramic-based multilayer nanofiltration membranes for dye desalination. *AIChE J* 59(10):3834–3842
- Wang D, Duan H, Lü J, Lü C (2017) Fabrication of thermo-responsive polymer functionalized reduced graphene oxide@Fe₃O₄@Au magnetic nanocomposites for enhanced catalytic applications. *J Mater Chem A* 5(10):5088–5097
- Wang Y, Zhang H, Song C, Gao C, Zhu G (2020) Effect of aminophend/formaldehyde resin polymeric nanospheres as nanofiller on polyamide thin film nanocomposite membranes for reverse osmosis application. *J Membr Sci* 614(2):118496–118507
- Xia L, Yiming C, Guodong K, Haijun Y, Xingming J, Quan Y (2014) Surface modification of polyamide nanofiltration membrane by grafting zwitterionic polymers to improve the antifouling property. *J Appl Polym Sci* 131(23):41144–41152
- Xiangli Q, Zhenjia Z, Zhenghua P (2007) Hydrophilic modification of ultrafiltration membranes and their application in salvia Miltiorrhiza decoction. *Sep Purif Technol* 56(3):265–269
- Xiangrong C, Yi S, Fei S, Yinhua W (2011) Antifouling ultrafiltration membranes made from PAN-b-PEG copolymers: effect of copolymer composition and PEG chain length. *J Membr Sci* 384(2):44–51
- Xiaobin Y, Linlin Y, Feitian R, Yifeng H, Duo P, Yongping B, Lu S (2020) Mussel-/diatom-inspired silicified membrane for high-efficiency water remediation. *J Membr Sci* 597(9):117353–117361
- Xu Y, Yao Y, Yu H, Shi B, Gao S, Zhang L, Miller AL, Fang JC, Wang X, Huang K (2019) Nanoparticle-encapsulated hollow porous polymeric nanosphere frameworks as highly active and tunable size-selective catalysts. *ACS Macro Lett* 8(10):1263–1267
- Yan F, Chen H, Lü Y, Lü Z, Yu S, Liu M, Gaoc C (2016) Improving the water permeability and antifouling property of thin-film composite polyamide nanofiltration membrane by modifying the active layer with triethanolamine. *J Membr Sci* 513(2):108–116
- Yang YF, Hu HQ, Yang L, Wan LS, Xu ZK (2011) Membrane surface with antibacterial property by grafting polycation. *J Membr Sci* 376(1):132–141
- Yang Z, Zhou Y, Feng Z, Rui X, Zhang T, Zhang Z (2019) A review on reverse osmosis and nanofiltration membranes for water purification. *Polymers* 11(8):1252–1273
- Yevjevich V (2009) Water and civilization. *Water J* 17(4):163–171
- Yong-Hong Z, Kin-Ho W, Renbi B (2010) A novel electrolyte-responsive membrane with tunable permeation selectivity for protein purification. *ACS Appl Mater Interfaces* 2(1):203–211
- Young-Hye L, Bryan DM, Ratnam S, Ankit V, Benny F, Majed N, James H, Alshakim N, Robert A (2011) Bifunctional hydrogel coatings for water purification membranes: improved fouling resistance and antimicrobial activity. *J Membr Sci* 372(2):285–291

- Zhao W, Yanlei S, Chao L, Qing S, Xue N, Jiang Z (2008) Fabrication of antifouling polyethersulfone ultrafiltration membranes using Pluronic F127 as both surface modifier and pore-forming agent. *J Membr Sci* 318(2):405–412
- Zhen L, Chuan H, Xiaodong W, Zhong W, Mengmeng C, Qiugen Z, Aimei Z, Qinglin L (2018) Towards improved antifouling ability and separation performance of polyethersulfone ultrafiltration membranes through poly(ethylenimine) grafting. *J Membr Sci* 554(2):125–133
- Zhifeng F, Zhi W, Ning S, Jixiao W, Shichang W (2008) Performance improvement of polysulfone ultrafiltration membrane by blending with polyaniline nanofibers. *J Membr Sci* 320(2):363–371
- Zhu WP, Gao J, Sun SP, Zhang S, Chung TS (2015) Poly(amidoamine) dendrimer (PAMAM) grafted on thin film composite (TFC) nanofiltration (NF) hollow fiber membranes for heavy metal removal. *J Membr Sci* 487(2):117–126
- Zinadini S, Zinatizadeh AA, Rahimi M, Vatanpour V, Zangeneh H, Beygzadeh M (2014) Novel high flux antifouling nanofiltration membranes for dye removal containing carboxymethyl chitosan coated Fe_3O_4 nanoparticles. *Desalination* 349(3):145–154



Functionalized Fluoropolymer Membrane for Fuel Cell Applications

18

Om Prakash, Ashok K. Pandey, and Pralay Maiti

Abstract

Polymeric membrane has been the key component of research in view of the fact that previous few decades had newest enhancement in both production and design aspect. Porous and nanochannel developed polymeric membranes have put on much interest in this viewpoint for their consumption in a various sectors such as adhesive, sensor, biotechnology, waste water treatment including separation techniques, and ion exchange membranes (IEMs) for polymer electrolytes membrane fuel cell (PEMFCs), because of their good thermal and outstanding mechanical properties along with electrical properties when properly functionalized with some functional group. This chapter mainly focuses on the research work being conducted on fabricating porous polymeric membranes followed by the functionalization and subsequently their applications in the field of fuel cell technology as electrolyte membranes. In this context, swift heavy ions (SHI) bombardment on the polymeric membrane, design the porous membranes having controlled channel dimension using ions of different size, nanoparticle and fluence variation. The effect of SHI on the polymeric membrane creates reactive sites (free radicals) which are utilized to functionalize the application of fuel cell membrane. However, the aim of this book chapter is to discuss the fabrication of porosity in polymer membrane and subsequent functionalization for energy applications especially in fuel cell technology.

O. Prakash · P. Maiti (✉)

School of the Materials Science and Technology, IIT (BHU), Varanasi, Uttar Pradesh, India
e-mail: pmaiti.mst@itbhu.ac.in

A. K. Pandey

Radiochemistry Division, Bhabha Atomic Research Centre, Trombay, Mumbai, Maharashtra, India

© The Author(s), under exclusive license to Springer Nature Singapore Pte Ltd. 2022

517

L. M. Pandey, A. Hasan (eds.), *Nanoscale Engineering of Biomaterials: Properties and Applications*, https://doi.org/10.1007/978-981-16-3667-7_18

Keywords

Fluoropolymer · Radiation induced grafting · Nanocomposites · MEA stack · Fuel cell · Electrical efficiency

18.1 Introduction

Energy is prime important in all the areas of the modern life including the water, food, and health sectors. Due to increasing world population, the long-term sustainability of the fossil fuel becomes scarce very fast and expensive (Prakash et al. 2020). There is an urgent need to suggest an alternative for fossil fuel energy (Kamcev and Freeman 2016). As a substitute of conversational fuels, clean and environmental friendly biofuels, based on sunlight such as solar cell, based on the chemical reaction like fuel cell, and others like wind, are instantly demanded (Hoogers 2003). As a result, materials that can straightly renovate or store renewable energies are being widely studied, that is, as portable power source is in demand. Developing the new inexpensive technology with better efficiency than existing technology is the real challenge of the day (Javaid Zaidi and Matsuura 2009). Among several emerging technologies, the fuel cell is most promising, greener, and ecofriendly technologies in the field of storage and portable stationary power sources (Wang et al. 2011). The basic parts of the fuel cell are fuel, electrolyte, and electrodes, and the electrolytes are the key component of the technology (Prakash et al. 2020). Porous polymeric membranes put on much awareness in the field of fuel cell technology when functionalized with specific functional group (Thomas et al. 2009). These functional groups are capable of transporting ions and electron and forming complex with the heavy metal ions. Mostly the functional groups are sulfate, phosphate, chlorate, and nitrate for cation exchange membrane and phosphonium, sulfonium and quaternary ammonium (QA) imidazoliums, spiro-ammonium, guanidinium, pyrrolidinium, piperidinium, and metal cations for the anion exchange membranes (AEMs). However, poor acid, base stability, and low ion conductivity of the AEMs remain as challenges in emergent superior performance membrane materials (Liu et al. 2018). Nowadays, non-fluorinated polymer backbones including poly (phenylene oxide), polybenzimidazole, poly (ether sulfone), and poly (ether imide) are used in polymer electrolyte membranes but the major drawbacks of these aromatic-based polymer are thermal stability and flexibility, due to aromatic moieties in the membrane. To overcome the above drawbacks aliphatic fluoropolymers such as poly (vinylidene fluoride) (PVDF) and its copolymers such as (PVdF-HFP), poly (vinylidene fluoride-co-hexafluoropropylene) (PVDF-CTFE), (PVDF-TrFE), poly (vinylidene fluoride-co-chlorotrifluoroethylene), and poly (vinylidene fluoride-co-trifluoroethylene) are being used to make PEMs (Smith et al. 2014). All the above polymer backbones show excellent thermal and mechanical properties because of their nonreactive and insulating behavior which together with their durability and thermal stability convert them for membrane application for fuel cell membranes and other applications

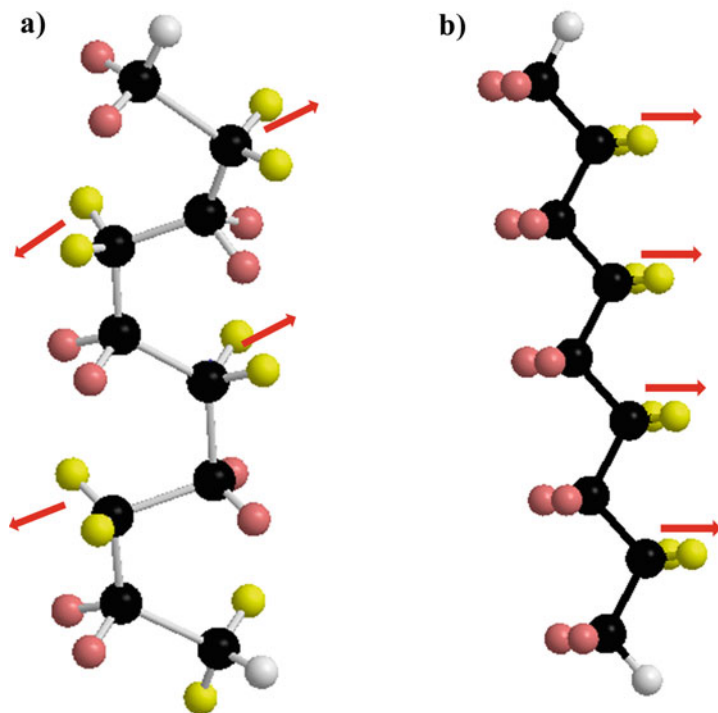


Fig. 18.1 Schematic representation of the (a) α -trans gauche conformation; (b) β -all trans conformation of crystalline PVDF, where black sphere represents the carbon atoms, pink for hydrogen, and yellow for fluorine atoms, and the arrows signify $-\text{CF}_2$ dipole directions

(Prakash et al. 2018). Fluoropolymer like PVDF and its copolymers exhibit different crystalline phases (α , β , γ , δ , and ϵ), some of them are polar/partial phases (β , γ , δ , and ϵ) and others nonpolar (α). The polar phases exhibit the piezoelectric and pyroelectric properties which make them useful for electronic applications. However, conversion is the prime need for electronic applications of the phases, which can also be induced by the addition of some specific fillers, chemical species, and fiber fabrications. The chemical structure of the nonpolar α -phases and polar β -phase with possible configuration is presented in Fig. 18.1 (Jana et al. 2016).

Because the above-listed fluoropolymer backbone are nonreactive and chemically inert, various techniques such as radiation-induced grafting, followed by functionalization using chemical reagents for grafting, composites membrane, etc. are reported in the literature for intruding the appropriate ionic group on the neat polymer chain (Prakash et al. 2020; Balanzat et al. 1995). In this chapter, the details of the preparation of functionalized membrane of polymer electrolytes using different polymeric materials and various techniques used for the functionalization followed by fabrication of single fuel cell setup and to measure the cell performance of the functionalized membrane have been discussed.

18.2 Fundamentals of Fuel Cell Technology

Fuel cell is an electrochemical device. In electrochemical reaction, chemical energy is transformed into electrical energy and heat energy is produced with high efficiencies by the oxidation of different class of fuel in presence of air with the help of redox couple reaction. Electrochemical-based devices are able technologies for the renewable energy, stationary power management, energy storage, pollution control, and greenhouse gas reduction. These devices optimize the cost and size of the electronic devices. For all the above technologies, fuel cell is one of the capable electrochemical devices that produces power in few mW to MW and is being utilized in various applications (Zakaria et al. 2020). Fuel cell produces energy only if there is supply of fuel, and hence, continuous fuel supply is the prime need. The electrochemical process in the fuel cell is not governed by the thermodynamic law like Carnot's cycle; hence, their operation is simple as compared to the internal combustion (IC) process. High efficiency makes them an alternative option of the future power source for a wide range of applications such as transportation, stationary and portable electronic power banks such as computers, laptops, mobiles, watches, video cameras (Hallinan and Balsara 2013). Fuel cells consist of electrode, fuel, and electrolytes. When fuel pass through electrodes (anode/cathode) it convert form of the ions and electrons after reacting with catalyst and the ions pass through the electrolytes which highly resist the flow of electron through the electrolytic membrane alkaline solution (Jana et al. 2017). Further, electrons flow in the outer circuit to balance the chemical reaction. In fuel cells technology, the resultant chemical reaction is similar to the combustion of the fuels but the fuel is separated with an electrolyte, while in combustion there is a direct contact. The fundamental driving force of the migration of the ions through the membrane is its ionic group present in the backbone of the polymer electrolyte membrane or the concentration gradient electrode-electrolytes interface (Jana et al. 2017). The typical open circuit voltage of the polymer electrolytes membrane was reported as ~ 0.7 V. In the 1900s, the development of fuel cells as power sources started but their use was limited like for space research with light weight space and defense applications (Drobny 2012). New attempts were made to develop fuel cells at the end of 1900s or beginning of twenty-first century. In recent years, the fuel cell technologies have been more efficient and environment friendly and act as sustainable energy resources. Presently, the fuel cell technologies are in the verge of commercialization almost in every sector of market, but the overall efficiency is still low and needs improvements. The schematic of the fuel cell setup is shown in Fig. 18.2.

Based on the fuel, electrolytes, and operating conditions the fuel cell is classified into different types. The working principle, used electrolytes, chemical reaction, advantages, disadvantages, and electrical fuel efficiencies are presented in Table 18.1.

The electrical efficiencies of the fuel cell devices depend on the operating temperature. Based on the operational temperature, fuel cell technology is classified broadly into three classes: low temperature (LT), this category includes polymer electrolyte membrane fuel cells whose operating temperature is below 100°C ; solid

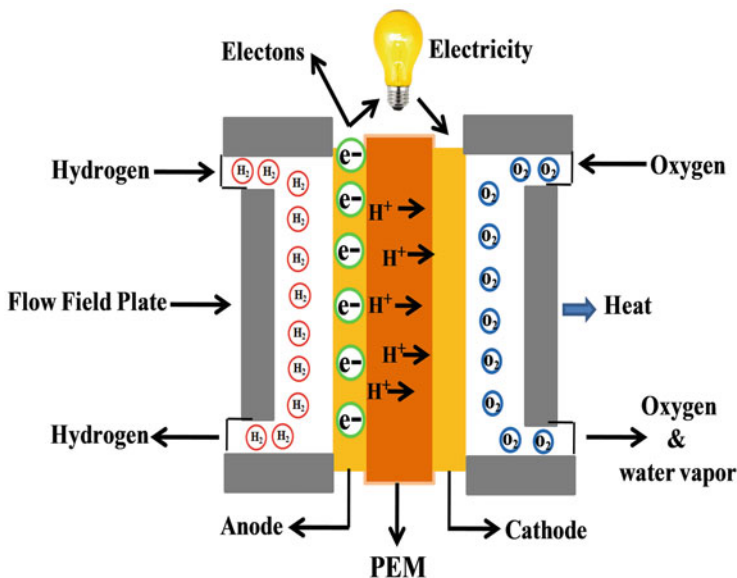


Fig. 18.2 Working principle and fuel cell setup

oxide fuel cells, also known as high temperature (HT) fuel cells, operate at temperatures greater than $800\text{ }^\circ\text{C}$; and moderate temperature (MT) fuel cells are molten carbonate fuel cells whose operating temperature is between 100 and $800\text{ }^\circ\text{C}$ (Badwal et al. 2014). The low temperature operating condition of PEMFCs makes it lower efficiency fuel cell while the SOFCs make them as highest electrical efficiency cells. The electrical efficiency of the cell with equation is dealt in Sect. 18.2.2.

18.2.1 Fuel Cell Requirement and Assembly

Electrochemical device fuel cells have tunable power delivery applied in different fields of life. Presently, most of automobile makers are in succession to lunches the Honda car (Chrysler, GM) buses, boats (Helion), trains, planes scooters, forklifts, even bicycles based on light weight fuel technology such as fuel cell. In 2019, the global fuel cell market capita was ~ 10.5 billion USD, with a registered Compound annual growth rate (CAGR) of 15.5% over the estimated time period (Wang et al. 2011). Continuously increasing order (demand) for unconventional resources of energy is a prime factor driving the development of alternative. The contribution of the shares in market is mainly in stationary, transportation, and portable power sources. The stationary power sources covered approximately 70% market till 2019, and in different types of fuel cell having polymer electrolytes membrane fuel cell (PEMFCs) the contribution was $\sim 67\%$. From the above discussion, it is clear that the polymer membranes as electrolytes are given much attention in fuel cell technologies.

Table 18.1 Classification of the fuel cell devices based on fuel, electrolytes, and operating temperature

Fuel cell	Electrolytes	Operating temperature (°C)	Electrode reactions	Working efficiency (%)	Advantages	Disadvantages	Application	Ref.
PEMFC	Polymer membrane (Nafion117)	≤100	Anode $H_2 = 2H^+ + 2e^-$ Cathode $1/2O_2 + 2H^+ + 2e^- = H_2O$	≤60	LT, quick start up, reduced corrosion due to solid film	Expensive catalyst, highly pure fuel used	Transportation, Stationary, Portable electronic devices	Jana et al. (2017)
DMFC	Polymer membrane	≤70		≤25	LT, quick start up, reduced corrosion due to solid film	Expensive catalyst	Transportation, Stationary, Portable electronic devices	Jana et al. (2015)
AFC	Aqueous solution of KOH/NaOH or anion exchange membrane	≤100	Anode $H_2 + 2OH^- = H_2O + 2e^-$ cathode $H_2O + 2e^- = 2OH^-$	≤60	Low cast and fast electrode reactions in alkaline medium	Sensitive to air and CO_2 , electrolyte management and design of cell	Transportation, Stationary, Portable electronic devices	Lin et al. (2010)
PAFC	Phosphoric acid	≤200	Anode $H_2 = 2H^+ + 2e^-$ Cathode $1/2O_2 + 2H^+ + 2e^- = H_2O$	≤40	Enables CHP due to high temp., increases the turbulence of fuel	Long start up time, Pt catalyst, design of the cell	Military, stationary power generation output in range of 100 kW–400 kW	Sammes et al. (2004)
MCFC	Molten K_2CO_3 and Li_2CO_3	≤650	Anode $H_2 + CO_3^{2-} = H_2O + CO_2 + 2e^-$ Cathode $CO_2 + 2e^- + 1/2O_2 = CO_3^{2-}$	40–45	High efficiency, fuel flexibility, enables CHP, variety of the catalyst	Long start up time, high temperature corrosion of the fuel cell components	Transportation, Distributed power energy	Dicks (2004)

SOFC	Ytria-stabilized zirconia (YSZ), Lanthanum gallate, doped Bi ₂ O ₃ , doped ceramic, etc.	≤800	Anode $H_2 + O^{2-} = H_2O + 2e^-$, Cathode $1/2O_2 + 2e^- = O^{2-}$	≤60	High efficiency, fuel flexibility, High temperature, non-noble catalyst	Long start up time, size and design, high temperature corrosion of the fuel cell components	Distributed power energy, Auxiliary power units in vehicles and stationary power generation	Ormerod (2003)
------	--	------	---	-----	---	---	---	----------------

PEMFC polymer electrolytes membrane fuel cell, DMFC direct methanol fuel cell, AFC alkaline fuel cell, PAFC phosphoric acid fuel cell, MCFC molten carbonates fuel cell, SOFC solid oxide fuel cell

18.2.2 Fuel Cell Efficiency

In electrochemical devices, the transformation of chemical energy to electrical energy is due to temperature and pressure gradients: firstly to transform chemical energy to kinetic energy followed by conversion to electrical energy. The conversion of electricity is classically governed by the Carnot cycle but not limited to the Carnot cycle. The net amount of energy available to produce the electricity during the fuel oxidation reaction is known as the Gibbs free (ΔG) energy. The Gibbs free (ΔG) energy is calculated from the Gibbs-Helmholtz Eq. (18.1) after the fuel oxidation process.

$$\Delta G = \Delta H - T\Delta S \quad (18.1)$$

where ΔH is the heat of enthalpy generated by the oxidation process of the fuel, ΔS is the entropic term and T is the absolute temperature at which the oxidation reaction occurs.

From Eq. (18.1), it is clear that only Gibbs free energy is responsible to convert electrical energy from chemical energy, with the remaining energy to raise the entropy of the system. The open circuit voltage (V_{oc}) of the cell is given by Eq. (18.2).

$$V_{oc} = -\Delta G/nF \quad (18.2)$$

where n is equivalent to the number of electron changes during the oxidation process of the fuel and F is the Faraday constant which is equivalent to the $\sim 96,500$ Coulomb charge or 1 mole electronic charge of atoms. The open circuit voltage of different fuel oxidation reactions are presented in Table 18.2. The maximum thermodynamic

Table 18.2 Thermodynamic parameters such as free Gibbs energy (ΔG), enthalpy (ΔH), open circuit voltages (V_{oc}), thermodynamic efficiencies of fuel cell (η), and oxidation reactions of the cell (Giddey et al. 2012)

Electrochemical (cell reactions)	No. of electrons	$-\Delta H$ (Kcal/mol) Enthalpy	$-\Delta G$ (Kcal/mol) Gibbs free energy	$V_{oc(V)}$ at 25 °C Open circuit voltages	% η_{Th}
$H_2(g) + \frac{1}{2} O_2(g) = H_2O(l)$	2	68.14	56.69	1.23	83
$C(s) + \frac{1}{2} O_2(g) = CO(g)$	2	26.4	32.81	0.71	124
$C(s) + O_2(g) = CO_2(g)$	4	94.04	94.26	1.02	100
$CO(g) + \frac{1}{2} O_2(g) = CO_2(g)$	2	67.62	61.45	1.33	91
$CH_3OH + 3/2 O_2 = CO_2 + 2H_2O(l)$	6	167.9	167.9	1.21	97
$CH_4 + 2O_2 = CO_2 + 2H_2O(l)$	8	195.6	195.6	1.06	92

efficiency (η_{Th}) of the of the fuel cell is defined as the ratio of the Gibbs free energy (ΔG) and heat of enthalpy (ΔH) generated from the cell reaction. The maximum thermodynamic efficiency is given by Eq. (18.3) (Giddey et al. 2012):

$$\begin{aligned}\% \eta_{Th} &= \Delta G / \Delta H \times 100 \\ \% \eta_{Th} &= (1 - T \Delta S / \Delta H) \times 100\end{aligned}\quad (18.3)$$

The thermodynamic efficiency may be increased or decreased depending upon the entropy change during the oxidation process. The thermodynamic parameters, cell reaction, and efficiencies are presented in Table 18.2.

The variation of fuel followed by the cell reaction alters the cell's efficiency, that is, the carbon fuel cell shows the highest cell efficiency approximately 100% while hydrogen, methanol, and methane fuel cells show 83, 97, and 92% thermodynamic theoretical fuel cell efficiencies, respectively. In most of the cases, the entropy values are positive which means that the randomness of the system increases during the oxidation of the fuel and gives the efficiency less than 100%, but in some cases the entropy of the system is negative and the cell efficiency may be more than 100%, which can happen only when the system absorbs heat from surroundings. Maximum cell efficiency is achieved through fuel optimization and temperature. There are no ideal systems operated at maximum as thermodynamics efficiencies. The overall electrical efficiency of cell is different than the thermodynamic efficiency. The factors involved in cell efficiencies are discussed below, for example, fuel utilization and output voltage. When fuel cell stack was operated, the internal losses exist which reduce the open circuit potential (V_{oc}) to operating potential (V_{op}). The losses of the open circuit potential results in the ohmic resistance of the fuel cell parts like electrodes, electrolytes current collector plate, and ionic or gas molecules evolved from the electrode/electrolyte interfaces and electrode over potential losses. Various parameters also alter the operating potentials like concentration gradient, absorption of the impurities, charge transfer, dissociation of the gas molecules on the electrode surface, applied load, etc. The cell V_{op} is given by (Giddey et al. 2012):

$$V_{OP} = V_{OC} - I_d R - \eta_a - \eta_c - I_d r - \eta_{conc} \quad (18.4)$$

where

V_{oc} = open circuit potential.

V_{op} = operating potential.

I_d = current density (normalized with area).

R = internal resistance of air and electrode.

η_a = anodic polarization/overpotential losses at anode/electrolyte interfaces.

η_c = cathodic polarization/overpotential losses at cathode/electrolyte interfaces.

r = internal resistance of air and electrode.

$\eta_{\text{conc.}}$ = concentration polarization related to rate toward electrode surface resulting in the formation of the electrode electrolyte interface, usually noticed at high current density.

The terms $I_d r$ and $I_d R$ refer to the ohmic voltage losses and increase linearly by the increment of load of the system, and nonlinear/nonohmic voltage losses observed with load (current density) are extremely needy in the fuel composition, electrode materials, reaction mechanism, and operating conditions such as temperature, gas supply pressure, and design of the cell stack. The voltage efficiency of the fuel cell is the ratio of the operating potential (V_{op}) and open circuit potential (V_{oc}). The open circuit voltage efficiency decreases with the increase in the load (applied current density), while the maximum power density of the cell is the product of operating voltage (open circuit voltage) and maximum current density. Initially, the power density increases, and then at a certain current density it shows the peak (maximum power density) followed by the decrease of power density. The single cell performance is given in Sect. 18.4.2.

18.2.3 Polymer Electrolyte Membrane and Its Properties for PEMFCs

The polymer membranes are used as electrolytes cum separator of the electrons in fuel cell technology. For the application of polymer membrane in polymer electrolytes membrane fuel cell (PEMFCs), the functionalized membrane should meet the essential properties such as high ionic conductivity (IC), water uptake (WU), ion exchange capacity (IEC), and low permeability of the membrane (Peighamardoust et al. 2010). The functionalized membranes must have excellent mechanical and thermal properties for construction of the membrane electrode assembly (MEA), excellent electrochemical stability in acid/base solution, moderate swelling during the electrochemical reactions, and the most important factor of comparatively low cost and long durability (Golcuk et al. 2013). In addition to the above properties, hydration of the ionic membrane (water content) and thickness of ionic membrane play significant roles and affect the whole performance of fuel cells' assembly. The selection of membrane materials and the processing for the functionalization are more important criteria for efficient membranes.

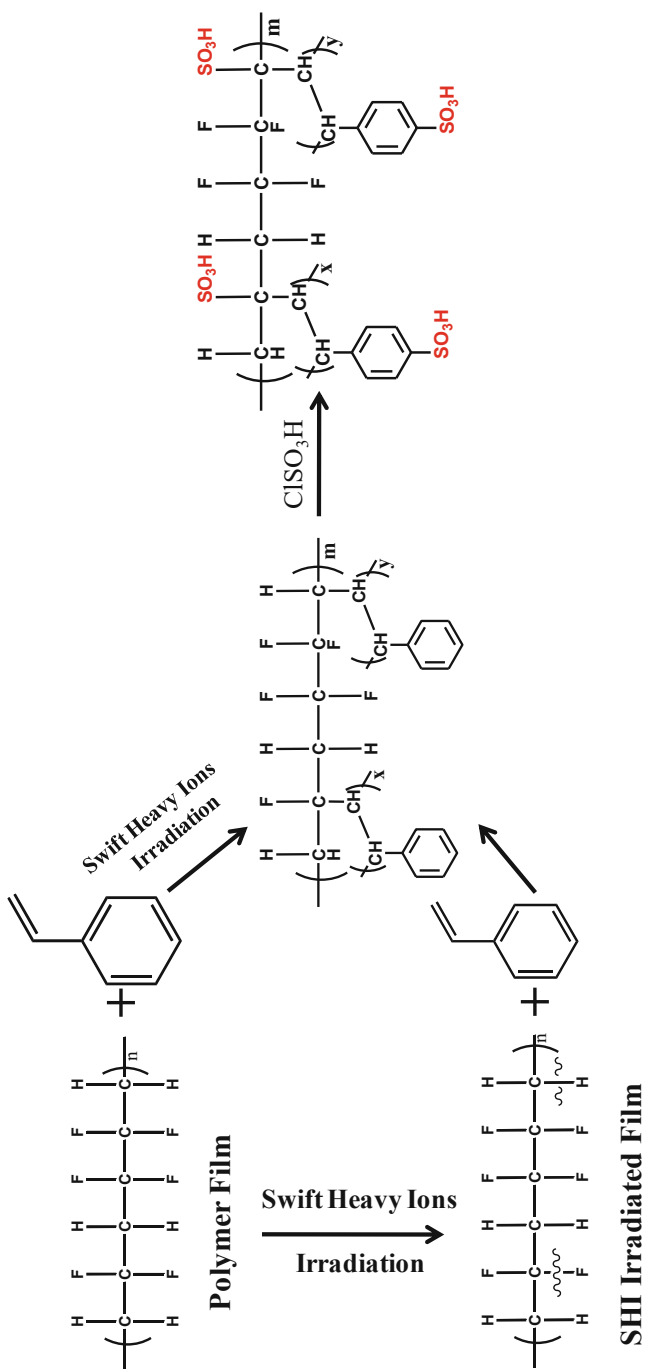
18.3 Fabrication Method of the Polymer Electrolyte Membranes

To achieve the desired properties of the membrane, the grafting and functionalization is of prime importance for tuning the characteristic properties of the membrane for further application as PEMFCs. Based on the nature of materials and functionalization route the polymer electrolyte membranes are classified as follows.

18.3.1 Functionalized Membrane Preparation Via Radiation-Induced Grafting

Radiation-induced graft copolymerization followed by the functionalization is an easiest way to modify the existing polymer with enhanced and imprinting new properties without affecting the intrinsic properties of the polymer. There are particular interests to introduce a variety of functional groups on the backbone of the polymer. In radiation-induced grafting method, the active sites are generated in the chain of base polymer using high energy particle radiation such as γ -radiation, electrons beam radiation, and swift heavy ions (SHI) (Balanzat et al. 1995), and particle radiations. The irradiated polymer is passed through monomer solution, which propagates the side chain polymerization followed by its termination (Jana et al. 2015). Two standard methods are followed for radiation-induced polymerization: first method is preirradiation in an inert atmosphere to trap the radicals followed by copolymerization. In this method, the irradiated polymer is deep in distilled monomer solution under the optimized polymerization condition. If the irradiation experiment is performed in aerobic condition, the free radicals formed by the irradiation react with air to produce peroxide and hydroperoxide species which can be decomposed at elevated temperature, and subsequently they can be used for copolymerization (Gülzow and Schulze 2004). Second method is the simultaneous irradiation and copolymerization, also known as direct method. In this method, the polymer and the monomer solution are kept together before irradiation. Each of the above grafting techniques has its own merits/demerits based on the polymer-monomer recombination condition (Javaid Zaidi and Matsuura 2009). For example, the direct method leads to considerable degree of grafting because of the efficient consumption of radicals formed after the irradiation. While the preirradiation method is effective, mainly when the monomer is more reactive, to obtain the desire level of grafting and optimization of the parameters are required. The chemical processes of these two methods are shown in reaction Scheme 18.1.

The radiation-induced graft copolymerization has several advantages against the other methods for various reasons including simplicity, flexibility of the chemical reaction, and the extent of graft moieties which can be controlled by varying the dose of radiation. This provides an analytical method to develop special design (tuning of properties of the membrane) of membrane for various applications (Ee et al. 2013). For the preparation of the graft copolymerized membrane for various applications present development is related to the radiation induced grafting techniques. The membrane preparation process is cost effective and thereby suitable for industrial process (Jana et al. 2018). Among these radiation techniques, the swift heavy ions (SHI) is one of the most promising techniques for the creation of reactive sites such as free radicals (Saikia et al. 2006). Swift heavy ions are the particle radiation, and the energy, fluence (ions/cm²), and ions alter easily as per the requirement (tailor), that is, the properties of membrane. The fabricated nanochannel/porous membrane prepared through SHI and subsequent sulfonation to convert into conducting nanochannels, which provide the conducting path for the ion (proton) transport through the membrane. Jana et al. used swift heavy ion-irradiated PVDF and its



Scheme 18.1 The chemical reaction of pre- and direct irradiated membrane with subsequent styrene monomer grafting followed by the sulfonation

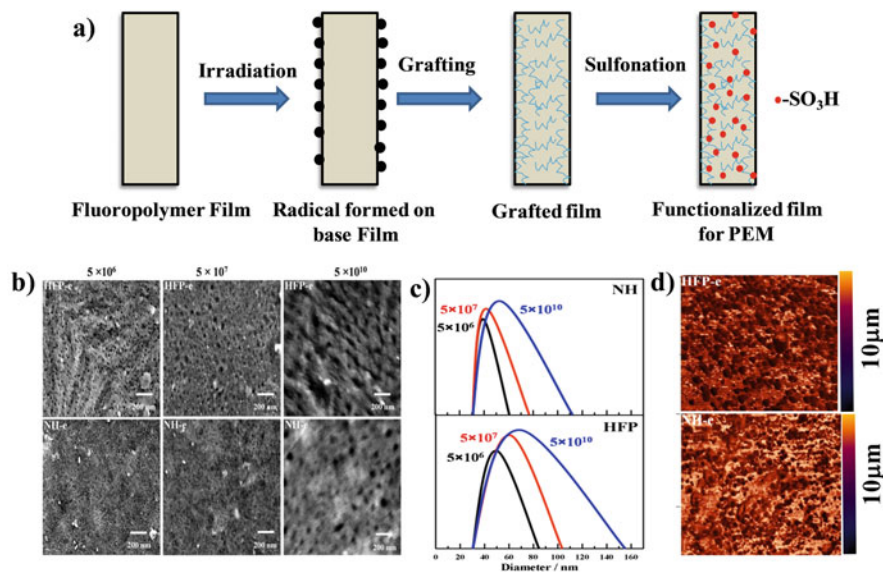


Fig. 18.3 (a) Schematic of the irradiation, grafting followed by the sulfonation; (b) SEM images after the irradiation of SHI followed by chemical treatment; (c) channel distribution through the SEM images; and (d) AFM image of the chemical etched membrane (Jana et al. 2015). Reproduced by permission of The Royal Society of Chemistry (RSC)

copolymers and nanohybrid membrane exclusively for fuel cell applications with better efficiency as compared to commercially available membrane (nafion117) (Jana et al. 2017).

In radiation-induced grafting the irradiation experiment on the membrane matrix mainly follows on three steps such as irradiation of the membrane matrix, grafting of the distilled monomer after sulfonation/ionic group tagging on base matrix as well as grafted specimen. The schematic of radiation process is presented in Fig. 18.3a. High energy swift heavy ion lose their maximum energy when they pass through thin polymer membrane (Prakash et al. 2020), the energy loss is mainly due to the electronic and nuclear collision after polymer SHI interactions. The path of the ions in polymer membrane is generally amorphous, and the amorphous zone of the membrane can be removed with the help of chemical reagent to form through channels of radiated membrane. (Prakash et al. 2019) The dimension of the latent track depends on mass of ions, accelerating energy of the ions, number of ions per unit area (fluence), and time/temperature of the chemical treatment (Balanzat et al. 1995). Further, the generation of the reactive sites is mostly responsible for the radiation-induced grafting after the functionalization process (Balanzat et al. 1995).

SEM (scanning electron microscope) and AFM (atomic force microscope) images of samples before and after SHI bombardment followed by chemical etching indicate a channel distribution as shown in Fig. 18.3b–d. The size of the nanochannel is bigger at higher fluence than that of sample exposed with lower fluence due to

more ion bombardment in the same location. Hence, after the chemical etching, the larger channel dimension found is in accordance with some previous literature (Jana et al. 2013).

At constant fluence nanohybrid membranes exhibit uniform distribution with smaller dimension. Li^+ ion bombarded specimen shows the channel diameter of 30 nm as opposed to 60 nm channel diameter of sample irradiated with Ag^+ ions (Jana et al. 2018). The channel dimension and number density are also influenced due to the variation in etching temperature (Rohani et al. 2009). Rohani et al. reported that the variation of the surface latent track diameter varies by the etching temperature (180 nm at 120 °C, 120 nm at 25 °C, and 100 nm at -84 °C), and from the result it is clear that the pore diameter increases at higher temperature (Rohani et al. 2009). Grasselli and Betz (2005) have prepared etched track membrane by bombarding the heavy ions (Sn) beam on the piezoelectric β -phase PVDF foil and reported the variation of channel dimension by changing the etching time and etchant concentration at constant temperature and fluence (Grasselli and Betz 2005).

The etched membranes have active free radicals inside the nanochannels which are suitable for grafting with olefinic monomers like styrene, thiophene, pyrrole, etc. followed by sulfonation. The evidence of grafting and sulfonation was understood through spectroscopic techniques such as NMR, IR, UV, EDX, and GPSC for the molecular weight and determination of mechanical testing done through universal testing machine. The nanochannel/pores fabricated using accelerator and subsequent grafting followed by the sulfonation is exclusively conduct the ionic species for fuel cell electrolyte application.

18.3.2 Functionalized to Prepare Chemical Modified Membrane

The direct functionalization of polymer matrix using the catalyst and monomer solution followed by different ionic group insertion lead to enhance the ionic properties (ionic conductivity) of the membrane. Fabrication of the membrane is done through compression molding for further applications. There are several literature reports available for direct functionalization followed by the fabrication of fuel cell setup. Prakash et al. reported the direct sulfonation of PVDF-co-HFP and enhanced the pristine properties of the polymer (Prakash et al. 2018). Direct sulfonation of PVDF with various temperature and reaction time generates differentially stable polymer membranes suitable for PEMFCs (Kumar Jana et al. 2015). Aromatic backbone containing polybenzimidazole (PBI) exhibits higher proton conductivity of 114 mS cm^{-1} (Kumar et al. 2020). Coupling of poly (aryene ether) dicarboxylic acid functional group with diamine functional group leads to proton conductivity of 47 mS cm^{-1} and has been applied for proton exchange membrane. The approaches of several research groups have developed sulfonated aromatic copolymers by introducing the sulfonate group on to the main chain. The direct sulfonation is an alternative approach for the preparation of PEM (polymer electrolyte membrane). This method gives a controlled design of molecules and

degree of sulfonation. Major drawback of this method is the location of functionalization and overall mechanical stability of the membrane. To avoid these problems, fluoropolymer without aromatic ring is being considered for membrane design. The chemical modification is one of the important routes to tailor the proton conductivity of functionalized membrane by altering the grafting as well as doping extents for better polymer electrolytes membrane for fuel cell technology.

18.3.3 Blend and Composites Membrane

Several research groups proposed the incorporation of fillers such as acids/ionic group in commercial/conventional polymer electrolyte membranes, such as Nafion/anion exchange resin, by enhancing the water preservation factor, and thereby, provide the additional path for ion transport. These factors give important parameter of proton conductivity enhancement at elevated temperature and relatively low humidity as operating condition required for the functioning of fuel cell. In these aspects, organic/inorganic composite membranes such as Nafion, PFSAs, PBI, SPSF, SPEEK, and PVDF are used (Bébin et al. 2006). Polymer membranes with inorganic nano-fillers, so-called composite membrane, can be produced using different advanced techniques. The water absorbing inorganic oxide (fine powder) impregnation in porous polymeric membrane is one of the conventional routes. Another method is the addition of precursor such as acidic metal alkoxides/ion conducting oxides solution into the pores of the membrane followed by the transfer of precursor for selective ion transportation. In most of the cases, the addition of variety of metal oxides with desired amount of solid commercial membrane Nafion117 leads to improvement of proton conductivity of the membrane at elevated temperature. Hydrophilic inorganic fillers, such as SiO_2 , TiO_2 , ZrO_2 , zeolites etc. (Sahu et al. 2007) to develop composite nafion membranes which enhance the water retention capacity by increasing the binding energy of water and the strength of acids with water molecules, and thereby, alter the ion conduction path in the membrane. These nano-fillers narrow down the hydrophilic channels of nafion matrix (7.9 to 6.5 nm) (Sahu et al. 2009) which leads to inhibit the fuel permeability of the membrane. Some other proton conductor fillers such as $\text{Zr}(\text{HPO}_4)_2$, titanium phosphate (TiP), and $\text{CsO}_4\text{P}^{2-}$, and different heteropolyacids are used in polymer membrane (Sigwadi et al. 2019; Alberti and Casciola 2003). Prakash et al. (2018) incorporated the organically modified nanofiller (30B) in PVDF and its copolymer matrix to alter the proton conductivity and other properties such as barriers, electrical, mechanical, and thermal properties of the functionalized membrane. The functionalization has been done through the accelerator and subsequent chemical modification (Prakash et al. 2019). Some limitations of the polymeric membrane for PEMFCs still exist which require extra attention. Successful membrane for PEMFCs should have sufficient thermal stability, mechanical flexibility, long-term durability, chemical resistance, and easy to membrane electrode fabrication method.

18.4 Fundamental Aspects of Functionalized Membrane for PEMFCs

For polymer electrolytes membrane fuel cell, the functionalized membrane should bear various essential properties like ionic conductivity (k^m), fuel crossover (P —permeability), selective parameter (SP), ionic groups exchange capacity (IEC), percentage water uptake (%WU), and activation energy (E_a). All these properties are key components of the fuel cell membrane for PEMFCs. The details of the explanation and its calculation using different mathematical equation are discussed below.

18.4.1 Proton Conductivity (k_m) and Activation Energy (E_a)

The transport of ions (H^+/OH^-) across the functionalized membrane mainly follows two mechanisms: first is vehicle (electro-osmotic vehicular) mechanism or cooperative mechanism where water molecules combine with the free protons to form hydrated water molecules (H_3O^+) across the membrane through chemical reactions, and second is Grotthuss mechanism, where proton conduction occurs through stepping process/hopping, the movement of proton across the membrane. Grotthuss mechanism favors ion transport, when present in sufficient quantity the exchangeable group is attached with polymer chain. The higher proton conductivity ($k^m/S\text{cm}^{-1}$) of the membrane indicate its suitability for PEMFCs. The activation energy (E_a) is one important thermodynamics physical quantity of the functionalized membrane; lower the E_a , higher will be the proton conductivity value, and in some cases, the higher activation energy indicates high temperature stability of the functionalized membrane. The activation energy (E_a) was calculated using the logarithmic Arrhenius equation Eq. (18.5) (Kumar et al. 2016);

$$\ln \kappa^m = -\frac{E_a}{RT} \quad (18.5)$$

where absolute temperature T in Kelvin and universal gas constant R . The activation energy (E_a) of functionalized membranes was examined using the slope of $\ln(k^m)$ vs. $1000/T \text{ K}^{-1}$.

18.4.2 Methanol and Gas Permeability (P)

Fuel permeability is another important parameter, and lower fuel permeability through the membrane indicates higher fuel cell efficiency. In direct methanol fuel cell (DMFCs), the methanol diffusion across the membrane causes the death of a cell after some days. So, it is significant to lower the methanol cross-over/permeability to enhance electrical efficiency of the fuel cell stack. The methanol permeability is examined through the diaphragm diffusion cell consisting of two components of

cylindrical glass and joined with the help of o-ring and spring clip, where one is filled with distilled water and other is filled with the 50% methanol water mixture. These two cells are separated by a functionalized membrane. Methanol concentration is calculated as a function of time using refractometer instruments and methanol permeability (P) of the membrane is calculated using Eq. (18.6) (Tripathi et al. 2010):

$$P = \frac{1}{A} \frac{C_{B(t)}}{C_A(t - t_0)} V_B L \quad (18.6)$$

In Eq. (18.6), C_A and C_B are the concentration of methanol in both the compartments at time $t - t_0$ and time t , respectively. L is the membrane thickness and A is the cross-section area of membrane and V_B volume of compartment B.

The ratio of proton conductivity (k^m) and methanol permeability (P) provides the selective parameter of a membrane. Prediction of the performance of PEMFCs membrane is estimated through this SP parameter. The gas permeability of hydrogen fuel cell polymer electrolytes membrane is an important parameter for the development of functionalized membrane. The gas permeability through the membrane before and after functionalization was calculated using three-layer parallel gas setup connected with the pressure gauge with constant feed pressure. The circular membrane of $\sim 9 \text{ cm}^2$ area with the thickness of $\sim 30 \mu\text{m}$ is sealed with the aluminum foil and Teflon tape between two circular stainless steels. The soap solution flow meter is generally used for the determination gas permeation rate. The gas permeation rate is calculated using the mathematical Eq. (18.7) (Saxena et al. 2020a):

$$\text{Gas flow rate (Gfr)} = \frac{10 \text{ ml}}{t \times 60} \quad (18.7)$$

where t is time in s and flow rate of gas is cm^3/s . Gas flux is measured from the Gas flow rate per unit area keeping the feed pressure constant ($\sim 80 \text{ psi}$). The normalized gas pressure is measured using Eq. (18.8).

$$\text{Normalized gas Flux} = \frac{\text{Gas flux}}{\text{Guage pressure}} \quad (18.8)$$

where the gauge pressure is the difference of feed and permeates side pressure, gas permeability coefficient (GPS) = $\text{NGF} \times \text{membrane thickness}$, GPS express in barrer ($1 \text{ barrer} = 10^{-10} \text{ cm}^3 [\text{STP}] \text{ cm cm}^{-2} \text{ s}^{-1} \text{ cm Hg}^{-1}$) (Saxena et al. 2020b). Both the methanol permeability and gas permeability are the important parameters of the PEMFCs membrane. Lower the fuel permeability of the membrane, higher will be fuel cell efficiency of the cell. When fuel pass through the membrane the open circuit voltage dropped leading to the damage of the cell. To avoid this effect, the low permeability functionalized membrane is fabricated for the PEMFCs applications.

18.4.3 Water Uptake (WU) and Ion Exchange Capacity (IEC)

Percentage water uptake and ionic group exchange capacity of the membrane directly reflect the number of ionic group present. Higher values of these parameters indicate the greater extent of grafting followed by sulfonation or other ionic group attached with the polymer chain. The comparative study of different functionalized membrane with the characteristic properties against the commercial nafion117 membrane is presented in Table 18.3.

18.5 Fuel Cell Stack and Electrical Efficiency of Membrane: DMFCs

Direct methanol fuel cell (DMFCs) is a type of polymer electrolytes membrane fuel cell, which utilizes the methanol–water ($\text{CH}_3\text{OH} - \text{H}_2\text{O}$) mixture anodic fuel (Oxidation reaction) to generate electricity. The methanol fuel is used directly in fuel cell setup without any reforming unit, when methanol fuel is in contact with catalyst with the help of peristaltic pump and methanol gets oxidized as proton, electron, and carbon monoxide. The protons pass through the membrane electrode assembly and combine with the oxygen to form water as a waste product and heat energy. The membrane separates the electrons and passes through the external circuits and electronic load for storage or instant applications. At anode side Pt-Ru/carbon catalyst is used while at cathode side the Pt/carbon catalyst is used. The basic reason this occurs with ruthenium catalyst at anode side is it forms better complex with carbon monoxide, hazardous gas which needs to be removed during the electrochemical redox reactions. Direct methanol fuel cells are eco-friendly and greener technology. Prakash et al. fabricated the membrane electrode assembly (MEA) of the functionalized membrane such as PVDF and its nanohybrid using radiation induced grafting of the 3-hexyl thiophene monomer (3-HT) on the main chain of the polymer membrane and measured the fuel cell performance of the functionalized membrane with the help of the single cell setup and found power density of 92 mW cm^{-2} corresponding to current density of 300 mAcm^{-2} . This performance is better than the commercial membrane nafion117 (Prakash et al. 2019). The current voltage ($I - V$) polarization curve of the PVDF functionalized membrane and power density vs. current density measurement is presented in Fig. 18.4a, b, respectively, comparing the nafion membrane.

From the literature survey different functionalized membrane with various route of fabrication such as composites membrane, direct functionalized membrane, radiation-induced grafting, nafion–inorganic blend etc. used as PEMFCs and their comparative cell performance is presented in Table 18.4.

The mechanical and thermal stability, durability, and cost of the membrane suggest that the fluoropolymer-based functionalized membrane is suitable for energy applications such as fuel cell technology, and energy harvesting is the future alternative of the renewable energy with stationary as well as portable power sources.

Table 18.3 Characteristic properties of the different membranes against the commercial membrane nafion117

Membrane	Thickness (μm)	(% WU)	IEC (mmol/g)	(% DS)	($k^m/\text{Scm}^{-1} \times 10^{-2}$)	Ref.
Nafion@117	175	38	0.9	27	9.56	Tripathi and Shahi (2009)
PVDF-s	130	22	0.36	27	0.06	Kumar et al. (2015)
PVDF-NH-s	130	27	0.50	32	0.50	Kumar et al. (2015)
HFP-18	80	12	0.78	18	3.72	Prakash et al. (2018)
PVDF-sty-s	30	10	0.22	14	0.05	Prakash et al. (2020)
NH-sty-s	30	14	0.33	16	0.13	Prakash et al. (2020)
PVDF-3HT-s	50	15	–	25	4.59	Prakash et al. (2019)
NH-3HT-s	50	20	–	30	4.21	Prakash et al. (2019)
QAPPESK	50–100		–		0.052	Fang and Shen (2006)
QAPVA	~300		–		0.073	Xiong et al. (2008)
FEP-g PVBtMAOH	~50		1.0		0.011	Herman et al. (2003)
FEP-g PVBtMAOH	~60		0.7		0.021	Danks et al. (2002)
QPPEsn-2	~200		2.12		0.067	Lai et al. (2019)
FPAES-Im-52	–		1.92		0.036	Shen and Pu (2019)

PVDF-s direct sulfonation poly (vinylidene difluoride), *PVDF-NH-s* direct sulfonation of the PVDF nanohybrid membrane, *HFP-18* Direct sulfonation poly (vinylidene fluoride-co-hexafluoro propylene) membrane, *sty* styrene, 3HT 3-hexyl thiophene, *QAPPESK* quaternized poly (phthalazinone ether sulfone ketone), *QAPVA* novel cross-linked quaternized poly (vinyl alcohol) (PVA) membranes, *FEP-g-PVBtMAOH* The radiation-grafting of vinyl benzyl chloride onto poly (hexafluoropropylene-co-tetrafluoroethylene) films with subsequent conversion to alkaline anion-exchange membranes, *QPPEsn* Synthesis of quaternized phenolphthalein based poly (arylene ether sulfone nitrile), *FPAES-Im-52* Synthesis of fluorene-containing poly (arylene ether sulfone)s with imidazolium groups (FPAES-Im-x) and preparation of the membranes

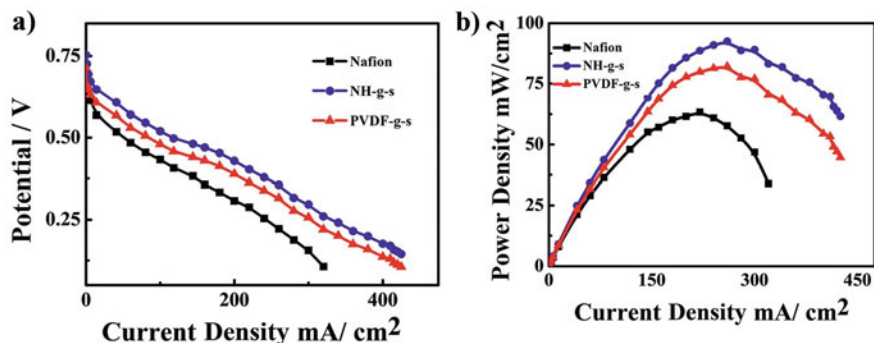


Fig. 18.4 (a) Polarization curve of the functionalized membrane against the commercial membrane; (b) maximum power density (MPD) vs. maximum current density (MCD) plot (Prakash et al. (2019)). (Reproduced by permission of RSC (Royal Society of Chemistry))

18.6 Perspective and Future Scope of Fluoropolymer Membrane

Nafion membrane is being used for the polymer electrolytes membrane fuel cell technology, because of some merits such as high proton conductivity and good mechanical stability. There are some demerits of the commercial membrane like high temperature stability, high fuel permeability, decrease in proton conductivity at higher temperature, and cost of commercial membrane. There is high requirement of an alternative of nafion membrane. Functionalized fluorine-based polymer is the suitable alternative for the polymer electrolytes membrane as they fulfill almost all the demerits of the commercial membrane.

18.7 Conclusion

The aim of this chapter is to focus the functionalized fluoropolymer membrane for the energy applications especially in the field of polymer electrolytes fuel cell membrane. The polymer membrane is key component of PEMFCs. Various techniques such as chemical, composite, and radiation-induced grafting are used for the fabrication of functionalized membranes and among these the radiation-induced grafting technique is promising to introduce desired properties in the functionalized membrane. The swift heavy ions bombardment on polymer membrane creates chemical, physical, and structural alterations. SHI generates free radical, olefinic bonds, and cross-linking among the macromolecules along with the evolution of gases. The path of SHI is amorphous latent track in the membrane. Nanochannels are created by chemical treatment of the membrane and the nanochannels are filled with conducting monomer through in-situ polymerization followed by functionalization of the channels to make them exclusively conducting.

Table 18.4 Comparison table of various membrane materials against Nafion117

Membrane	Activation energy (KJ mol ⁻¹)	P (×10 ⁻⁷ cm ² s ⁻¹)	SP (×10 ⁵ S s cm ⁻³)	Open (V)	Power density (mW/cm ²)	Current density (mA/cm ²)	Reference
Nafion 117	6.52	13.10	0.72	0.73	51.2	140	Tripathi and Shahi (2009)
HFP-g-s (styrene)	6.36	2.91	3.7	0.60	28	140	Jana et al. (2017)
HFP-NH-g-s (styrene)	5.79	1.84	1.8	0.63	31	140	Jana et al. (2017)
CTFE-g-s(styrene)	8.2	4.54	0.56	0.60	30	200	Jana et al. (2018)
CTFE-NH-g-s (styrene)	8.3	4.43	0.78	0.53	44	200	Jana et al. (2018)
HFP-3HT-s	6.09	5.86	1.3	0.66	39	140	Jana et al. (2016)
HFP-NH-3HT-s	4.74	6.76	1.3	0.68	45	140	Jana et al. (2016)
PVDFNF-Nafion	3.0	-	-	0.89	240	470	Li and Liu (2014)
Poly(arylene ethers)	-	-	-	0.71	161	446	Tanaka et al. (2011)
Cross-linked poly (vinyl alcohol)	2.69	1.14	3.00	-	-	-	Saxena et al. (2007)
Nafion/PTFE	-	-	-	0.975	-	1400	Siu et al. (2006)

This conducting channel allowed the transport of proton and reduced the fuel permeability due to dispersion of the nano-dimensional clay. The polymer matrix gives the mechanical as well as thermal stability and controls the channel size and distribution. Ionic conductivity and fuel crossover data of the ionic membrane is appropriate for fuel cell electrolytes membrane. MEA can be constructed out of this functionalized membrane whose efficiency appears to be better than the commercial membrane having low cost. Therefore, PEMFCs with modified polymer membrane is an alternative of the stationary and portable power sources.

Acknowledgments The author O. P. is thankful to UGC for providing fellowship and IUAC (Inter university accelerator center), New Delhi, India, for providing the radiation facilities and financial support provided by the BRNS project No. 37(3)/14/13/2018-BRNS/37133. The authors are thankful to Dr. Saif A. Khan (Scientist materials science div.) of IUAC for his constant support during the beam time and subsequent discussion.

References

- Alberti G, Casciola M (2003) Composite membranes for medium-temperature PEM fuel cells. *Annu Rev Mat Res* 33:129–154
- Badwal SPS, Giddey SS, Munnings C et al (2014) Emerging electrochemical energy conversion and storage technologies. *Front Chem* 2:79
- Balanzat E, Betz N, Bouffard S (1995) Swift heavy ion modification of polymers. *Nucl Instrum Methods Phys Res, Sect B* 105:46–54
- Bébin P, Caravanier M, Galiano H (2006) Nafion®/clay-SO₃H membrane for proton exchange membrane fuel cell application. *J Membr Sci* 278:35–42
- Danks TN, Slade RCT, Varcoe JR (2002) Comparison of PVDF- and FEP-based radiation-grafted alkaline anion-exchange membranes for use in low temperature portable DMFCs. *J Mater Chem* 12:3371–3373
- Dicks AL (2004) Molten carbonate fuel cells. *Curr Opin Solid State Mater Sci* 8:379–383
- Drobny JG (2012) *Polymers for electricity and electronics : materials, properties, and applications*. Wiley, Hoboken, NJ
- Ee A, Mo A, Mm G (2013) Preparation and characterization of commercial polyethyleneterephthalate membrane for fuel cell applications. *J Memb Sci Technol* 3:2
- Fang J, Shen PK (2006) Quaternized poly(phthalazinone ether sulfone ketone) membrane for anion exchange membrane fuel cells. *J Membr Sci* 285:317–322
- Giddey S, Badwal SPS, Kulkarni A, Munnings C (2012) A comprehensive review of direct carbon fuel cell technology. *Prog Energy Combust Sci* 38:360–399
- Golcuk S, Muftuoglu AE, Celik SU, Bozkurt A (2013) Synthesis and characterization of polymer electrolyte membranes based on PVDF and styrene via photoinduced grafting. *J Polym Res* 20
- Grasselli M, Betz N (2005) Making porous membranes by chemical etching of heavy-ion tracks in β -PVDF films. In: *Nuclear instruments and methods in physics research, section B: beam interactions with materials and atoms*. North-Holland, Amsterdam, pp 501–507
- Gülzow E, Schulze M (2004) Long-term operation of AFC electrodes with CO₂ containing gases. *J Power Sources* 127:243–251
- Hallinan DT, Balsara NP (2013) Polymer electrolytes. *Annu Rev Mat Res* 43:503–525
- Herman H, Slade RCT, Varcoe JR (2003) The radiation-grafting of vinylbenzyl chloride onto poly (hexafluoropropylene-co-tetrafluoroethylene) films with subsequent conversion to alkaline anion-exchange membranes: optimisation of the experimental conditions and characterisation. *J Membr Sci* 218:147–163
- Hoogers G (2003) *Fuel cell technology handbook*. CRC, Boca Raton, FL

- Jana KK, Vishwakarma NK, Ray B et al (2013) Nanochannel conduction in piezoelectric polymeric membrane using swift heavy ions and nanoclay. *RSC Adv* 3:6147–6159
- Jana KK, Thakur AK, Shahi VK et al (2015) A poly(vinylidene fluoride-co-hexafluoro propylene) nanohybrid membrane using swift heavy ion irradiation for fuel cell applications. *J Mater Chem A* 3:10413–10424
- Jana KK, Srivastava A, Parkash O et al (2016) Nanoclay and swift heavy ions induced piezoelectric and conducting nanochannel based polymeric membrane for fuel cell. *J Power Sources* 301:338–347
- Jana KK, Tiwari VK, Avasthi DK et al (2017) New generation fuel cell membrane using swift heavy ions. *Chem Select* 2:6413–6437
- Jana KK, Prakash O, Shahi VK et al (2018) Poly(vinylidene fluoride-co-chlorotrifluoro ethylene) nanohybrid membrane for fuel cell. *ACS Omega* 3:917–928
- Javaid Zaidi SM, Matsuura T (2009) *Polymer membranes for fuel cells*. Springer US, Berlin
- Kamcev J, Freeman BD (2016) Charged polymer membranes for environmental/energy applications. *Annu Rev Chem Biomol Eng* 7:111–133
- Kumar Jana K, Charan C, Shahi VK et al (2015) Functionalized poly(vinylidene fluoride) nanohybrid for superior fuel cell membrane. *J Membr Sci* 481. <https://doi.org/10.1016/j.memsci.2015.01.053>
- Kumar K, Charan C, Shahi VK et al (2015) Functionalized poly (vinylidene fluoride) nanohybrid for superior fuel cell membrane. *J Membr Sci* 481:124–136
- Kumar K, Srivastava A, Parkash O et al (2016) Nanoclay and swift heavy ions induced piezoelectric and conducting nanochannel based polymeric membrane for fuel cell. *J Power Sources* 301:338–347
- Kumar BS, Sana B, Unnikrishnan G et al (2020) Polybenzimidazole co-polymers: their synthesis, morphology and high temperature fuel cell membrane properties. *Polym Chem* 11:1043–1054
- Lai AN, Zhuo YZ, Hu PC et al (2019) Enhanced ionic conductivity of anion exchange membranes by grafting flexible ionic strings on multiblock copolymers. *Int J Hydrogen Energy* 45:1998–2008
- Li HY, Liu YL (2014) Nafion-functionalized electrospun poly(vinylidene fluoride) (PVDF) nanofibers for high performance proton exchange membranes in fuel cells. *J Mater Chem A* 2:3783–3793
- Lin B, Qiu L, Lu J, Yan F (2010) Cross-linked alkaline ionic liquid-based polymer electrolytes for alkaline fuel cell applications. *Chem Mater* 22:6718–6725
- Liu FH, Lin CX, Hu EN et al (2018) Anion exchange membranes with well-developed conductive channels: effect of the functional groups. *J Membr Sci* 564:298–307
- Ormerod RM (2003) Solid oxide fuel cells. *Chem Soc Rev* 32:17–28
- Peighambaroust SJ, Rowshanzamir S, Amjadi M (2010) Review of the proton exchange membranes for fuel cell applications. *Int J Hydrogen Energy* 35:9349–9384
- Prakash O, Jana KK, Jain R et al (2018) Functionalized poly(vinylidene fluoride-co-hexafluoro propylene) membrane for fuel cell. *Polymer (Guildf)* 151:261–268
- Prakash O, Jana KK, Manohar M et al (2019) Fabrication of a low-cost functionalized poly (vinylidene fluoride) nanohybrid membrane for superior fuel cells. *Sustain Energy Fuels* 3:1269–1282
- Prakash O, Mhatre AM, Tripathi R et al (2020) Fabrication of conducting Nanochannels using accelerator for fuel cell membrane and removal of radionuclides: role of nanoparticles. *ACS Appl Mater Interfaces* 12:17628–17640
- Rohani R, Yamaki T, Koshikawa H et al (2009) Enhancement of etch rate for preparation of nano-sized ion-track membranes of poly(vinylidene fluoride): effect of pretreatment and high-LET beam irradiation. *Nucl Instruments Methods Phys Res Sect B Beam Interact with Mater Atoms* 267:554–557
- Sahu AK, Selvarani G, Pitchumani S et al (2007) A sol-gel modified alternative Nafion-silica composite membrane for polymer electrolyte fuel cells. *J Electrochem Soc* 154:B123

- Sahu AK, Pitchumani S, Sridhar P, Shukla AK (2009) Nafion and modified-Nafion membranes for polymer electrolyte fuel cells: an overview. *Bull Mater Sci* 32:285–294
- Saikia D, Kumar A, Singh F, Avasthi DK (2006) Study of Li³⁺ ion irradiation effects in P (VDF-HFP) based gel polymer electrolytes for application in Li-ion battery. *J Phys D Appl Phys* 39:4208–4214
- Sammes N, Bove R, Stahl K (2004) Phosphoric acid fuel cells: fundamentals and applications. *Curr Opin Solid State Mater Sci* 8:372–378
- Saxena A, Tripathi BP, Shahi VK (2007) Sulfonated poly(styrene-co-maleic anhydride)—polyethylene glycol—silica nanocomposite polyelectrolyte membranes for fuel cell applications. *J Phys Chem B* 111:12454–12461
- Saxena D, Jana KK, Soundararajan N et al (2020a) Potency of nanolay on structural, mechanical and gas barrier properties of poly(ethylene terephthalate) Nanohybrid. *J Polym Res* 27:1–9
- Saxena D, Soundararajan N, Katiyar V et al (2020b) Structural, mechanical, and gas barrier properties of poly(ethylene terephthalate) nanohybrid using nanotalc. *J Appl Polym Sci* 137:1–12
- Shen B, Pu H (2019) Fluorene-containing poly(arylene ether sulfone)s with imidazolium on flexible side chains for anion exchange membranes. *Int J Hydrogen Energy* 44:11057–11065
- Sigwadi R, Dhlamini MS, Mokrani T et al (2019) The proton conductivity and mechanical properties of Nafion®/ZrP nanocomposite membrane. *Heliyon* 5:e02240
- Siu A, Schmeisser J, Holdcroft S (2006) Effect of water on the low temperature conductivity of polymer electrolytes. *J Phys Chem B* 110:6072–6080
- Smith DW, Iacono ST, Iyer SS (2014) *Handbook of fluoropolymer science and technology*. Wiley, Hoboken, NJ
- Tanaka M, Fukasawa K, Nishino E et al (2011) Anion conductive block poly(arylene ether)s: synthesis, properties, and application in alkaline fuel cells. *J Am Chem Soc* 133:10646–10654
- Thomas A, Kuhn P, Weber J et al (2009) Porous polymers: enabling solutions for energy applications. *Macromol Rapid Commun* 30:221–236
- Tripathi BP, Shahi VK (2009) 3-[[3-(Triethoxysilyl)propyl]amino]propane-1-sulfonic acid–poly(vinyl alcohol) cross-linked Zwitterionic polymer electrolyte membranes for direct methanol fuel cell applications. *ACS Appl Mater Interfaces* 1:1002–1012
- Tripathi BP, Kumar M, Shahi VK (2010) Organic-inorganic hybrid alkaline membranes by epoxide ring opening for direct methanol fuel cell applications. *J Membr Sci* 360:90–101
- Wang Y, Chen KS, Mishler J et al (2011) A review of polymer electrolyte membrane fuel cells: technology, applications, and needs on fundamental research. *Appl Energy* 88:981–1007
- Xiong Y, Fang J, Zeng QH, Liu QL (2008) Preparation and characterization of cross-linked quaternized poly(vinyl alcohol) membranes for anion exchange membrane fuel cells. *J Membr Sci* 311:319–325
- Zakaria Z, Shaari N, Kamarudin SK et al (2020) A review of progressive advanced polymer nanohybrid membrane in fuel cell application. *Int J Energy Res* 44:er.5516

Part IV

Surface Engineering of Ceramic and Composite Biomaterials



Rushikesh Fopase and Lalit M. Pandey

Abstract

Research and applications of biomaterials have been extensively increased in the biomedical field and are proven effective in many clinical needs. Among the popularly used materials for clinical applications, the biocompatible nature of the ceramics makes them suitable for implants, tissue regeneration, and engineering applications. Bioceramics comprising of calcium phosphate and bioglass possess apt tunable characteristics that stimulate the osteocytes and, therefore, are widely used in bone regenerations. Casting ability and controllable mechanical properties of biomaterials are utilized in the scaffold designing for tissue and organ growth for various biomedical requirements. The recent advances in material sciences, especially nanotechnology, have further enabled the design of multifunctional bioceramics by engineering the surface properties and chemical compositions. Certain bioceramic materials such as hydroxyapatite incorporated with iron oxide nanoparticles offer magnetic properties and can be used as multifunctioning biomaterials in magnetic hyperthermia and medical imaging. Scaffolds of such magnetic bioceramics are used in bone cancer therapy with simultaneous imaging for in situ analysis. The porous characteristics of bioceramics are capable of drug loading and controlled release for the prolonged availability required to treat cancer and other diseases. This chapter highlights the characteristics and application of bioceramics for biomedical purposes. The classification and periodic advancements of bioceramics have been discussed in brief. Some recent studies emphasizing the potentials of bioceramics in the biomedical field are described in detail.

R. Fopase · L. M. Pandey (✉)

Bio-Interface and Environmental Engineering Lab, Department of Biosciences and Bioengineering, Indian Institute of Technology Guwahati, Guwahati, Assam, India

e-mail: lalitpandey@iitg.ac.in

Keywords

Bioceramics · Hydroxyapatite · Bioactive glass · Bone tissue engineering · Drug delivery · Hyperthermia · Antifouling

19.1 Introduction

Bioceramics are used in bone implants and tissue regeneration matrices since the beginning of the twentieth century. Over the last few decades, the advancements in material science have widened the scope of bioceramic applications in the biomedical field for the improvement of treatment quality (Hench and Wilson 1993). Increased demand for implants and tissue regeneration therapies with the growing population has boosted the research in the field of bioceramics. Bioceramics offer compatible characteristics similar to the natural tissues, which have resulted in their extended use in the biomedical field.

Bioceramics are biocompatible materials comprising metallic and nonmetallic elements held together by ionic and covalent bonds and processed using thermal energy (Keane 2003). Based on the synthesis process, bioceramics can be in the form of powder or bulk material. Powdered bioceramics are often used as biocompatible coatings over the various biomaterials such as metal implants (Campbell 2003). Interaction ability of bioceramics with the tissue determines the type of bioceramics, namely bioinert (e.g., zirconia, alumina), bioactive (e.g., hydroxyapatite, bioglass), and bioresorbable ceramics (e.g., tricalcium phosphate). The objective of applications and desired characteristics regulate the selection of bioceramics.

Applications of bioceramics range from load-bearing bone and tissue implants, porous scaffold materials, drug delivery vehicles to diagnostics materials. Ca-P bioceramics are popularly used in orthopedic and dental implants because of similar characteristics to natural tissues like bone or teeth (Predoi et al. 2007; Sowmya et al. 2013). Bioceramic scaffolds allow the better integration of cells and stimulate the growth, proliferation, and differentiation for tissue regeneration. Porous and surface-modified bioceramics are useful in the controlled delivery of biomolecules or drug at the implant site (Baino et al. 2015). Incorporation of magnetic materials into the bioceramic matrices allows their use in the hyperthermia cancer treatment and medical imaging (Zhang et al. 2016). Few bioceramics also restrict biofilm formation over the implant and thus act as antifouling agents (Zhang et al. 2017).

This chapter discusses the applications of bioceramics in the biomedical field. Classification of bioceramics with the advancement of technology and science has been described in brief. The properties affecting the selection of bioceramics for various applications are also highlighted. Finally, an emphasis on the recent advancements of bioceramics for various applications has been highlighted to express the potential of bioceramics in the biomedical field.

19.2 Classification and Generations of Bioceramics

Implantation of any foreign material in the body results in the specific cellular responses depending on the types of material. The surface characteristics of the implant govern the interaction between cells and material. Based on the biointerfacial interactions, bioceramic materials can be classified as follows (Pina et al. 2018).

Bioinert Bioceramics These bioceramics are chemically and biologically inert and have no or minimal interaction with the tissues surrounding the implant. Such kinds of materials are used in the implants with the purpose of structural support. Alumina and zirconia are examples of bioinert bioceramics and are used to develop femoral head in the hip implants.

Bioactive Bioceramics These bioceramics are intended to react with the surrounding biological components and integrate with the tissues. Such integration of the bioactive bioceramics with the natural tissues is regulated by changes occurring in the material surface with time. For instance, Ca-P-based bioceramics such as hydroxyapatite (HAp) exchange ions with the biological fluids and form a calcium apatite layer with similar characteristics of mineral phases of natural bone. Other bioactive bioceramics like bioglass and glass-ceramics are being used for treating small bone defects and periodontal problems.

Bioresorbable Bioceramics Certain bioceramic implants get absorbed within the body and are replaced by the natural tissue with the span of time. These bioceramics are bioactive, and their interactions with the biological components lead to the absorption of the implant in the body. Calcium phosphate (Ca-P)-based bioceramics like tricalcium phosphate (TCP) are the mostly used scaffold fabrication materials for tissue regeneration.

Other than the interaction with the tissue, bioceramics can be classified based on the origin, crystallinity, or composition. On the basis of origin, bioceramics are classified as natural and synthetic. For example, calcium carbonate-based shells and bones are natural bioceramics, while alumina and zirconia are synthetically originated bioceramics (Ben-Nissan 2003). In the crystallinity-based classification, lattice structure divides the bioceramics into crystalline and amorphous bioceramics. HAp is one of the most used crystalline bioceramics, while bioglass is an amorphous bioceramic (Naghizadeh et al. 2015; Saxena et al. 2019). Further, composition-based classification is based on the material's principal constituent and is further described in Sect. 19.4.

Based on the applications or the reactivity with the tissues, generations of the bioceramics are defined as shown in Fig. 19.1. With the progress of research in the field of bioceramics, the objective and scope of the applications have been extended. At the beginning of the twentieth century, the sole objective of bioceramics was to obtain nonreactive materials to avoid toxicity to living cells, i.e., biocompatibility (Vallet-Regí and Ruiz-Hernández 2011; Best et al. 2008). These materials aimed to

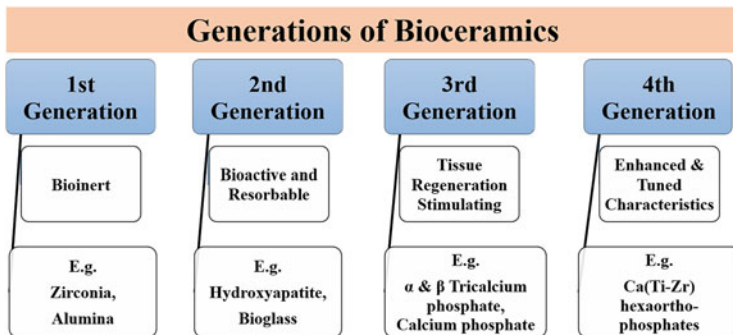


Fig. 19.1 Generations of bioceramics on the basis of biointerfacial interactions

replace natural bone or hard tissues and are called first-generation bioceramics. Ceramics like alumina and zirconia have been used for such purpose as they do not induce any immune responses. These implanted materials get encased with outer acellular collagen coating by the body, and thus no toxic reactions get induced (Castner and Ratner 2002). However, such strategies were not able to solve the problem of the damaged tissues in regards to tissue regeneration.

The regeneration of tissues requires the growth-stimulating conditions and a supporting structure for the development. In the 1970s, researchers have reported the similarities between bone characteristics and some ceramics composed of calcium phosphate (Zapanta-LeGeros 1965). Such materials can interact with the biological components leading to tissue regeneration such as bone. These bioactive bioceramics are referred to as second-generation bioceramics. Ca-P-based and bioglass-like bioceramics possess bioactive characteristics and are capable of inducing osteogenesis (Vallet-Regí 2006). The major drawback of these ceramics is the poor mechanical properties, which limit their use as fillers and coatings. The third generation of bioceramics contributes to the tuned structural and interfacial properties between the bioactive bioceramics and cells. Tunable properties of the bioceramics allow the preparation of different scaffolds, which induce tissue regeneration and support tissue growth. Bioceramics of Ca-P, mesoporous silicas, bioglass, and templated glasses are used in various scaffolds for tissue regeneration (Arcos et al. 2009).

In recent years, researchers have proposed the fourth generation of bioceramics with improved mechanical and surface characteristics to regulate tissue regeneration in a better way (Ning et al. 2016). Various cellular signals are responsible for stimulating tissue generation, and the next-generation bioceramics are proposed based on the bioelectricity system. Such bioceramics like calcium-titanium-zirconium hexaorthophosphates are intended to manipulate cellular signals for stimulation of tissue regeneration. The second aim is to regulate and monitor the communication between host and materials (Ning et al. 2016; Napier and Shimmin 2016).

19.3 Properties of Bioceramics

Biocompatibility is the main criteria for the ceramics intended for biomedical applications. The surface characteristics of the materials define the interaction of the bioceramics with tissues. Therefore, tuning the interface between cells and material is necessary to achieve success in tissue regeneration. In addition, comparable mechanical properties are prerequisite for a given biomedical application.

Mechanical Properties Bioceramics are aimed toward interaction, replacement, and regeneration of the tissues. Therefore, the properties of the applied materials need to match the biological characteristics of targeted tissues. Implants for bone and teeth require to withstand the body's load and, therefore, must have higher mechanical strength. The load experienced by bones varies with the type of physical activity and location where the load is measured. Typically, bones experience a load of about 4 MPa, while that on tendons and ligaments, it is in the range of 40–80 MPa. Hip joints bear the average three times load of the body (3000 N) and around ten times higher load while jumping (Dorozhkin 2018; Currey 2008). Different biological fluids may also have different pH (ionic strengths) from basic to acidic or vice versa in various tissues.

Therefore, an implant needs to possess good mechanical strength and corrosion resistance. Higher mechanical strength and fatigue resistance allow implants to bear and dissipate the load. Thus, higher wear and corrosion resistance of the bioceramics give a long-term stability to implants, eliminating or reducing future surgical requirement (Popa et al. 2004). The mechanical properties of the ceramics are decreased with increasing amorphous phase, microporosity, and grain size. Moreover, highly crystalline, less porous bioceramics have more stiffness and increased tensile and compressive strength. The strength of the bioceramics is inversely proportional to the square of the grain size. However, some of the mechanical properties of bioceramics are not suitable for their use as biomaterials. These properties involve low fracture toughness and elasticity, and high stiffness and brittleness. These limiting properties can be tuned and overcome by using polymer coatings or incorporation of polymers within porous bioceramics (Peroglio et al. 2007).

Scaffolding Ability Scaffolds are designed to guide the new growing tissues in the desired form. Mechanical properties play an essential role in designing and fabrication of the scaffolds for tissue regeneration. The porosity offered by the bioceramic scaffolds is ideal for tissue integration. Interconnected scaffolds with more than 50% pore content of total volume are suitable for tissue integration (Baino et al. 2015). However, the porosity decreases the mechanical properties and should be in balance with the mechanical properties. The scaffold characteristics should also match the surrounding tissue to avoid stress gradient at the biointerface and implant failure (Hench and Wilson 1993). Tuned elasticity, compressive strength, and low brittleness can make bioceramics suitable for scaffolding applications (Yunos et al. 2008; Baino et al. 2015).

Biointerfacial Interactions The biointerfacial interactions between the body and implants are the function of responses from both tissues and implant material. Tissue response depends on the type, health, and age of the host tissue, while the material response is determined by composition, phases, and surface characteristics of the implant. Also, blood flow and the motion between tissue and implant interface play a vital role in the total response of a biomaterial (Dorozhkin 2018). When implanted or administered in the body, the implant bioceramics initially interact with the proteins in the biological fluids. Thus, the adsorbed protein corona layer governs the interaction, proliferation, and migration of cells with the implant surface. The role of adsorbed proteins on the surface for cell adhesion and spreading has been investigated by Hasan et al. (2018). FBS (fetal bovine serum)-treated surface showed higher cell adhesions and spreading compared to surfaces without protein layer absorbed (Hasan et al. 2018). Further, the surface characteristics of the implants majorly affect the cellular interaction of the bioceramics. Surfaces offering higher electronegativity (zeta potential) increase the propensity of cellular attachment on the bioceramic materials, which is the function of the protein corona layer (Smith et al. 2004).

Bioactive and bioresorbable Ca-P-based bioceramics such as HAp and TCP can react with the biological fluids and exchange Ca and P ions. Such ion exchange leads to the formation of the apatite layer over the bioceramic surface by partial dissolution of bioceramics. The apatite layer acts as an attachment site for various growth factors that originate from stem cells and macrophages leading to bone tissue regeneration (Vallet-Regí et al. 2008; Zhou et al. 2019). Cellular differentiation, proliferation, and growth are regulated by cell signaling through specific ions, proteins, and growth factors for specific functions (Rao et al. 2018). Communication and interaction between the cells occur via cell adhesion molecules (CAM) like integrins and cadherins of the extracellular matrix (ECM) (Aplin et al. 1999). Ion- and growth factor-anchored apatite layer formed over the bioactive bioceramics may act as stimulators for such communications for cell growth and proliferation and therefore initiate tissue regeneration. Also, ECM can be influenced by mechanical stimulus from implants, which leads to cellular signaling toward the proliferation and growth of tissues like bone (Sebastine and Williams 2006).

19.4 Few Examples of Bioceramics

Alumina Alumina or aluminum oxide (Al_2O_3) is used as a component of high load-bearing implants like hip prostheses and dental implants since the initial bioceramic era (Boutin 2014). Over a period of time, alumina is used for total replacement therapy as femoral head or coating over the implant material (López 2014). The tensile strength of the Al_2O_3 is tunable by controlling grain size and density. High-density alumina (>99.5% purity) offers excellent wear resistance and high mechanical strength. Also, the stability of the alumina owes to the strong ionic and covalent bonds and thus resistant against strong acidic or alkaline conditions. Hence, good corrosion resistance and biocompatibility make this bioceramic suitable for

long-term implant applications. In the dental implants, fine grain size ($<4\ \mu\text{m}$) $\alpha\text{-Al}_2\text{O}_3$ is prepared by the sintering process with the small amounts ($<0.5\%$) of MgO , SiO_2 , and CaO to avoid grain growth. Such prepared $\alpha\text{-Al}_2\text{O}_3$ offered improved compressive strength allowing higher fatigue and fracture resistance (Hulbert 1993).

Zirconia Zirconia or zirconium oxide (ZrO_2) is a polycrystalline bioceramic and has been used as bioinert bone implants. It exhibits monoclinic phase at room temperature, tetragonal phase above $1170\ ^\circ\text{C}$, and cubic phase above $2370\ ^\circ\text{C}$ before melting (Yoshimura 1988). The phase transformation from tetragonal to monoclinic offers enhanced mechanical properties and is tunable by partial stabilization/substitution of zirconia using yttrium for biomedical implants (Piconi and Maccauro 1999). The grain size of the yttrium-stabilized tetragonal zirconia ranges up to $0.5\ \mu\text{m}$. Yttrium-stabilized zirconia is stabilized at tetragonal or cubic phases providing improved fatigue strength. The desired mechanical properties and good wear performance of the zirconia are comparatively better than alumina (Kumar et al. 2018). However, zirconia may change the phases to monoclinic in the wet environment leading to loss of density and implant strength like femoral head. High density, reduced grain size, and uniform distribution of yttrium between the grains reduce the transformation rate (Piconi et al. 2003; de Almeida et al. 2016).

Alumina-Zirconia Composite Alumina and zirconia offer various advantages of better mechanical properties and inertness. However, these bioceramics may acquire cracking and surface instability due to reaction/interaction with the water molecules. Composites of alumina and zirconia can be used to achieve higher surface stability and mechanical properties for implants (Kumar et al. 2018). Researchers have reported that alumina can stabilize tetragonal and cubic phases of zirconia, and thus, the obtained composites possess improved cracking resistance necessary for load-bearing and long-term applications (Naglieri et al. 2013; Gutknecht et al. 2007).

Ca-P-Based Bioceramics Ca-P-based bioceramics are used since the early twentieth century for bone and dental implants due to their bioactive nature. The ability of Ca-P-based ceramics to interact with the bone and surrounding tissue stimulates the osteogenesis. The load-bearing characteristics of these bioceramics are suitable for application as bone and dental implants. Ca-P-based bioceramics exchange ions with the biological fluid, which initiate the formation of apatite for bone formation (Zhou et al. 2019). The ratio of Ca and P determines the apatite's crystal structure and usually ranges from 1.5 to 1.67, depending on the synthesis conditions. Hydroxyapatite (HAp) $[\text{Ca}_{10}(\text{PO}_4)_6(\text{OH})_2]$ possesses the Ca:P ratio of 1.67, which is similar to natural bone (Vallet-Regi and González-Calbet 2004; Saxena et al. 2019). High crystallinity, stability, controlled degradability, bioactivity, and osteoconductivity make HAp the most suitable candidate for bone tissue engineering applications. The surface activity and biocompatibility of the HAp have been tuned by using many elements such as Fe^{2+} , Zn^{2+} , and Mg^{2+} (Saxena et al. 2018; Tran and Webster 2011; Stipniece et al. 2018). Other than elemental doping, many biological molecules such

as proteins and growth factors have been reportedly incorporated with HAP to improve tissue integration with the implant (Jun et al. 2013).

Another form of apatite, β -TCP [β - $\text{Ca}_3(\text{PO}_4)_2$], contains 1:5 molar ratio of Ca and P and is prepared by a high temperature sintering of apatite (Tampieri et al. 1997). This bioceramic stimulates the osteogenesis and gets resorbed fully with the regeneration of tissues. The mechanical properties of the β -TCP are weak; therefore, some bioactive polymers are used to improve the elastic modulus of material for application in the implants. Sometimes, both phases of HAP and β -TCP can be present in the material offering properties of both constituents, referred to as biphasic calcium phosphate (BCP). Such materials are popularly applied for orthopedic, dental, and as abrasive agent for implant surface modifications (LeGeros et al. 2003).

Silica-Based Bioceramics Silica-based bioceramics are generally amorphous bioceramics. Bioglass is one of the popularly used materials. The composition of the bioglass is silica (45 wt%), CaO (24.5 wt%), Na_2O (24.5 wt%), and P_2O_5 (6 wt %) and coded as 45S5. Bioglass is prepared by the sol-gel method and offers good bioactivity. 45S5, when used in implants, reacts with biological fluids and forms a layer of HAP for better cellular adhesion and osteogenesis (Rahaman et al. 2011; Yadav et al. 2020). Templated glass is the ordered nanostructured mesoporous bioceramic comprising SiO_2 -CaO- P_2O_5 and offers high surface area. The Ca^{2+} ions from CaO control the mesoporosity in the silica structure, while the phosphate group acts as a bioactive component of the material. The high bioactivity of the templated glass results in the quick formation of the apatite layer (8 h as compared to 3 days of bioactive sol-gel glasses) when reacted with simulated body fluid (Izquierdo-Barba and Vallet-Regí 2011). Therefore, templated glass is a new generation of bioceramics with the potential applications in tissue regeneration as well as local drug delivery applications (Vallet-Regi et al. 2012).

19.5 Applications of Bioceramics

19.5.1 Tissue Engineering

Tissue regeneration is one of the most explored research areas, which has widened the scope of bioceramics in medical applications. Regeneration of tissues requires a scaffold structure acting as a support and guiding framework for soft and hard tissues. With technological advancements, the use of bioceramics have escalated from bare supporting materials to tissue replacement, as discussed in the generations of bioceramics. The designed bioceramic materials with tuned mechanical properties are applied for scaffolding purposes (Baino et al. 2015). Such scaffolds can be integrated with growth factors for inducing the osteocytes and with antibiotics/antibacterial agents to avoid bacterial infections. Zhang et al. (2017) reported the modification of 3D-printed β -TCP scaffolds using silver nanoparticle-linked graphene oxide (Ag@GO) by a soaking method. These modified scaffolds were

found to be effective against *Escherichia coli* and accelerated the osteogenic differentiation of bone marrow cells in rabbit bone.

Stem cell stimulation is key to the regeneration of new tissue. The surrounding microenvironment conditions regulate the regeneration capability of stem cells. The required stimulating conditions can be offered or controlled through bioceramic materials. Ca-P-based bioceramics like HAP and TCP exchange ions with the biological fluids in in vivo conditions and regulate proliferation and differentiation of bone cells (Chai et al. 2012; Barradas et al. 2012). Specific growth factors incorporated within the bioceramic scaffolds controlled the release of these growth factors, which in turn induce tissue regeneration. Bakopolou et al. studied the dentin regeneration through Mg-based bioceramics scaffold combined with human treated-dentin matrices (teeth with experimental cavities) and growth factors along with the controlled release of Mg^{2+} , Ca^{2+} , Si^{2+} , and Zn^{2+} (Bakopoulou et al. 2016). The sol-gel prepared scaffolds of bioceramics were shaped for dentin matrix cavities using polyurethane foam to form a porous framework. The scaffolds were adjusted into the cavities and added with human dental pulp stem cells along with growth factors (TGF β -1, DMP-1, and BMP-2) in a complete culture medium. After the observation period (3, 7, and 14 days), the scaffolds were observed for tissue regeneration, and positive results were observed with adequate mesenchymal stem cell markers. The stem cells were observed to undergo odontogenic differentiation inside the scaffolds evidenced by higher expression of several genes, including specific to added growth factors. The released ions from scaffolds acted as a stimulus for the apatite formation. The formation of apatite over the scaffold was confirmed by X-ray diffraction and elemental analysis, which confirmed the potentiality of the scaffold bioceramics for tissue regeneration. Figure 19.2 shows the images of dental tissue regeneration over the scaffolds after 28 days with apatite layers. The formation of bioapatite was confirmed by XRD at 2θ value of 31.8 (Bakopoulou et al. 2016).

Bioceramics have been extensively applied for bone regeneration applications. As bone is the load-bearing framework of the body, bioceramics are modified to possess load-bearing capabilities along with the osteogenic nature (Zhang et al. 2007). Ca-P-based scaffolds are widely used for bone implants. These scaffolds are modified in various ways to tune and improve strength and performance. Polymers like chitosan, alginate, hyaluronic acid, poly(lactic acid), poly(glycolic acid), and silk fibroin are incorporated in the Ca-P-based bioceramics to tackle the brittleness and improve the strength of the bioceramics to fabricate scaffolds (Ramesh et al. 2018; Farokhi et al. 2018). Mondal et al. fabricated poly(lactic acid)-reinforced 3D-printed HAp scaffolds to test their potential in bone tissue engineering (Mondal et al. 2020). Among the different orientations on XY angles used for scaffold printing, the scaffold printed at 90° on the XY plane observed to possess higher compression strength. Further, modification of the scaffold surface with HAp nanoparticles enhanced the compressive strength to ~53 MPa. The HAp nanoparticles also served to improve cell adhesion and proliferation over the scaffolds confirming the applicability of 3D-printing techniques. Other than polymers, several elements are used as dopants in the Ca-P-based bioceramics to modulate the characteristics according to an objective. Researchers have reported the

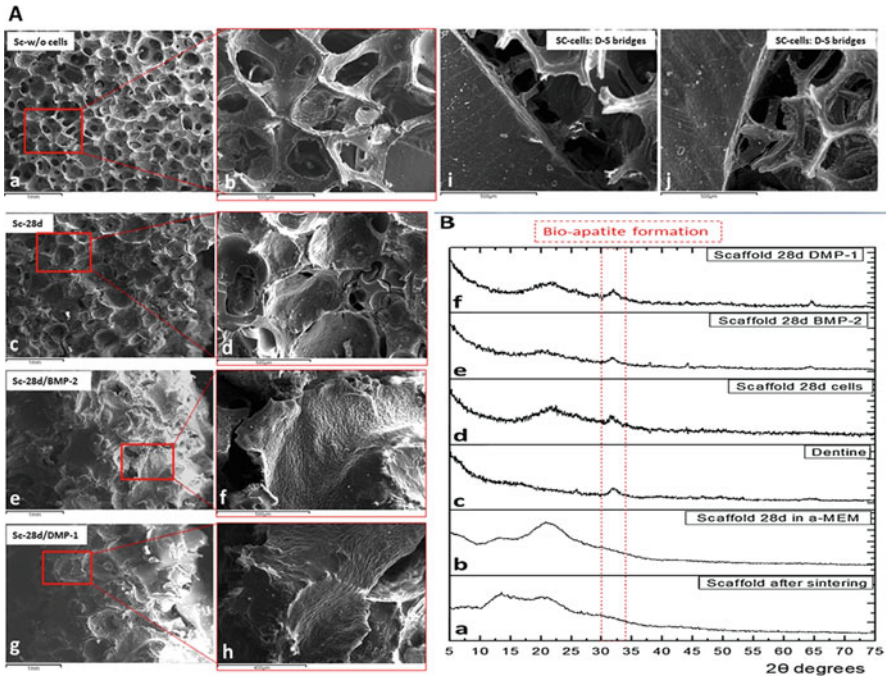


Fig. 19.2 Dental tissue regeneration using bioceramic scaffolds and growth factors. (A) Scanning electron microscope (SEM) micrographs of (a–b): cell-free scaffolds, (c–d): dentin matrix loaded with scaffolds and stem cells construct, (e–f): construct treated with BMP-2, (g–h): construct treated with DMP-1, (i–j): mineralized tissue bridging between the scaffolds and the dentinal cavity walls; (B) XRD pattern of (a): scaffold as control, (b): control scaffold with a phosphate-rich medium for 28 days, (c): control nature dentine, (d): dentin matrix loaded with scaffolds and stem cells construct, (e): construct treated with BMP-2, (f): construct treated with DMP-1. (Adapted with permission from (Bakopoulou et al. 2016))

doping of strontium (Prabha et al. 2020), zinc (Saxena et al. 2018), magnesium (Shao et al. 2016), silver (Dubnika and Zalite 2014), copper (Baino et al. 2018), and graphene oxide (Wu et al. 2015) in Ca-P-based bioceramics for various bone tissue engineering applications.

Likewise, Si-based bioceramics are reported to activate human bone marrow mesenchymal stem cells and osteoblasts via ionic stimulations of signaling pathways to proliferate and differentiate (Zhai et al. 2013; Wu and Chang 2013; Zhai et al. 2012). Recently, Huang et al. reported the capability of silicate bioceramics to modulate the host immune system while stimulating osteogenesis. Two silicate bioceramics, namely akermanite and nagelschmidite, were used to study inflammation responses and osteogenesis. The released Si, Mg, and Ca ions showed the inhibition of inflammatory signaling with simultaneous apoptosis activation of macrophages. Thus, the osteogenic activity of the silicate bioceramics was

confirmed with no interference from the host immune system. Such dual functionalities have eliminated the risk of implant failure with improved tissue regeneration and may guide toward new effective bioceramics for tissue engineering. In another study by Bunpetch et al., Si-based bioceramic scaffolds were used to understand the osteochondral defect repair mechanism in the rabbit model (Bunpetch et al. 2019). The two scaffold variants were prepared as sol-gel products of $\text{Si}_2\text{Ca}_7\text{P}_2\text{O}_{16}$ (Si-Ca-P) and Ca-P, followed by reinforcement using polyvinyl alcohol (PVA). Templates of the porous polyurethane foam were used as a framework for scaffolds and exposed to a high-temperature vacuum to obtain porous Si-Ca-P- and Ca-P-based scaffolds. The animal models were operated to have osteochondral cylindrical cartilage defects on both left and right limbs. Test groups were treated with the prepared scaffolds of Si-Ca-P and Ca-P variants. After the completion of the experimental duration, the sacrificed animal models were analyzed for the growth of the bone tissues at the defect site. Si-Ca-P scaffold-treated models showed rapid and complete repair of the defect compared to untreated and Ca-P scaffold-treated models. Also, a higher ICRS (International Cartilage Repair Society) score and a better ratio of bone volume (BV) to tissue volume (TV) were observed for the Si-Ca-P-based scaffolds. The computed tomography (CT) scan also confirmed the regeneration of tissue at defect sites. Figure 19.3 shows the experimental procedure and observed tissue growth at the defect site. The efficient results of Si-Ca-P scaffolds were dedicated to Si ion released from the scaffolds. The release of Si ions from the Si-Ca-P scaffolds exhibited to promote osteogenesis of bone marrow stem cells and the simultaneous regeneration of cartilage and subchondral bones. The effects of Si ions were confirmed by the transcriptome RNA sequencing performed over cells isolated from experimental sites of the animal model.

19.5.2 Delivery Systems

The success of drug treatment for any disease or injury depends on delivering an adequate amount of active drug at the target site at earliest and for the desired period. When administered in the body, drug molecules have to sustain varying physiological conditions and cross the biological barriers to reach the target site. Also, it is necessary to maintain the concentration of drug molecules for a particular time period. Therefore, a controlled drug delivery system for the desired time is required (Arcos and Vallet-Regí 2013). In hard tissue like bone and teeth, drug delivery is a challenge. In the treatment of bone defects, injury, or bone tumors, implant materials like bioceramics are used as drug delivery systems. Bioceramic scaffolds have porous structures that accommodate biomolecules like enzymes, growth factors, or drug molecules and act as local drug delivery systems (Sarigol-Calamak and Hascicek 2018). Ca-P-based and bioglass bioceramics are proven biocompatible and widely acceptable as drug or biomolecule delivery matrices. These bioceramics can be applied in the form of scaffolds, powders, granules, or coatings depending on the requirement.

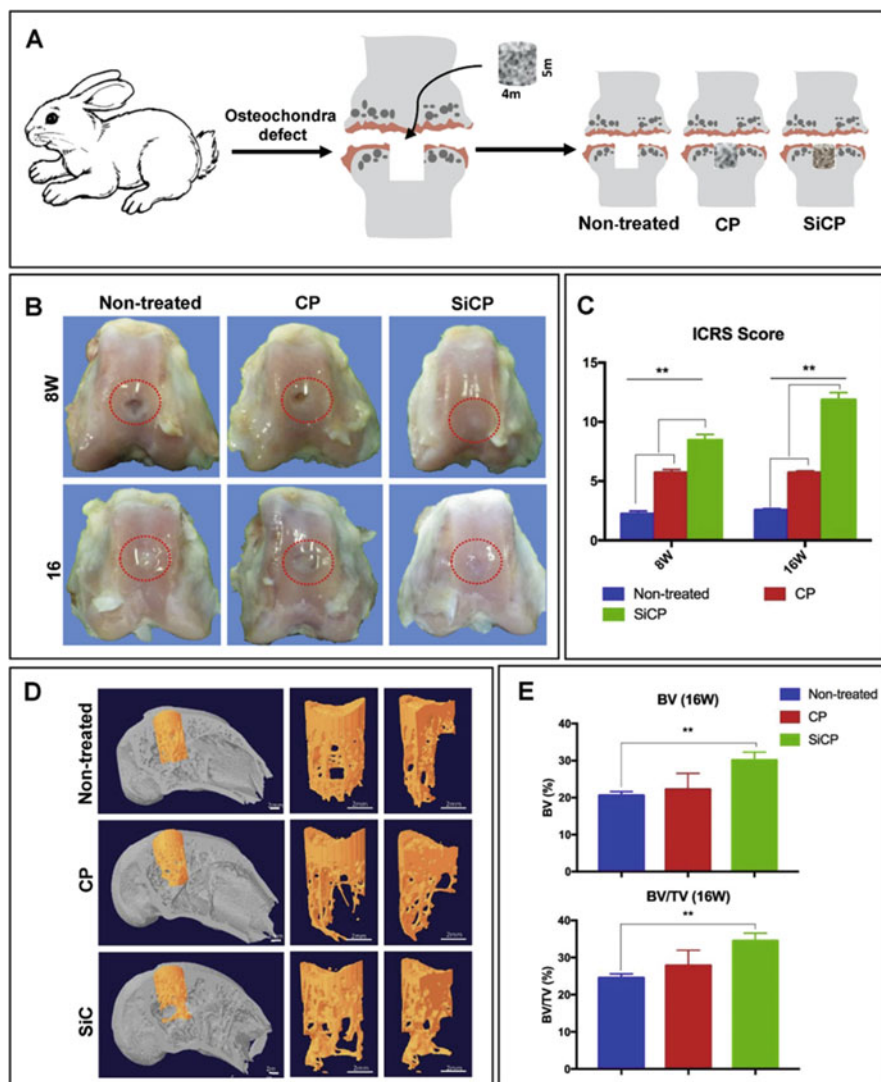


Fig. 19.3 Tissue regeneration for the repair of the osteochondral defect using Si-based scaffolds. (a) Experimental design; (b) Images of defects in the experimental groups; (c) ICRS (International Cartilage Repair Society) score of experimental groups after treatment; (d) 3D micro-CT images for tissue regeneration at defect site; and (e) quantitative analysis of new tissue formation by bone volume (BV) and the ratio of bone volume to tissue volume (BV/TV) after treatment. (Adapted with permission from (Bunpetch et al. 2019))

Loading of drug molecules can be performed during the fabrication of scaffolds or post-fabrication. Most of the drug or biomolecules are susceptible to change in the pH or temperature; hence, the loading of such molecules is avoided during the fabrication of scaffolds (Langer 1998). Post-fabrication loading of target molecules

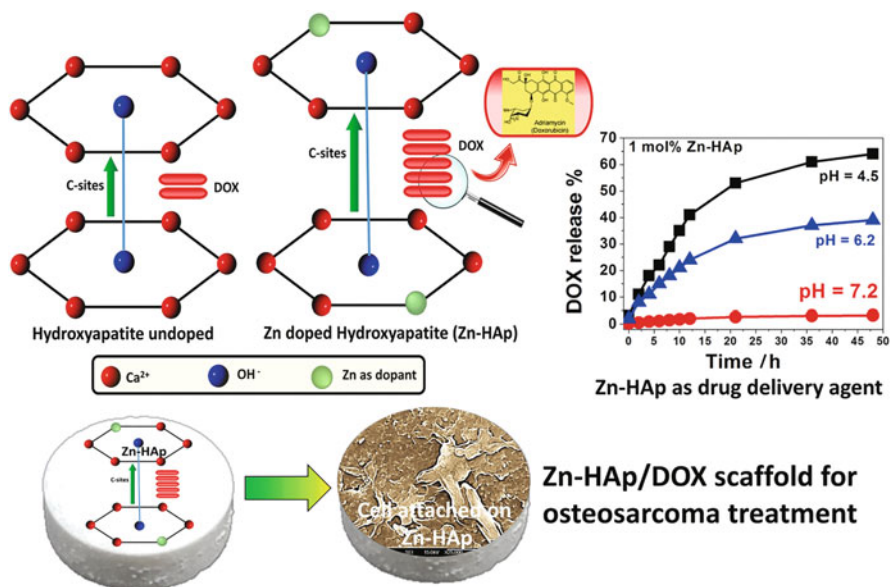


Fig. 19.4 Drug delivery application of Zn-doped HAp bioceramic. (Adapted with permission from (Kim et al. 2018))

is done by simple physical adsorption via van der Waals forces, electrostatic attractions, however offering the less controlled release. In another way, bioceramic scaffolds are modified to have functional groups for the specific interaction of the biomolecules like enzymes and growth factors. Such an approach offers improved binding strength and better-controlled release (Mouriño et al. 2013; Fopase et al. 2020a).

Researchers have reported many studies on the use of HAp for drug delivery applications. Kim et al. have studied the potential of Zn-doped HAp for the doxorubicin delivery and tissue engineering application (Kim et al. 2018). Zn-doped HAp nanoparticles were prepared by the coprecipitation method, and doxorubicin (0.002 M) was loaded by simple physical adsorption. The maximum loading of the drug was observed for 1 mol% of Zn-doped HAp due to increased c-bond length in the crystal structure. The release profile of doxorubicin showed a maximum release of 66% at a pH of 4.5 over 48 h, confirming the suitability for cancer treatment with an acidic pH environment and sustained release of drugs. The scaffolds prepared by these bioceramic materials with the aid of starch as binder showed excellent cellular adhesion and proliferation and proven a potential candidate for drug delivery and tissue regeneration applications. Figure 19.4 shows the schematic for doxorubicin-loaded Zn-doped HAp for drug delivery application.

In another study, Vu et al. reported the application of TCP scaffolds for the controlled release of vitamin D₃ for bone regeneration (Vu and Bose 2020). A sustained supply of vitamin D₃ is required to act as a micronutrient for bone

generation and keeping of bone health. Two types of TCP scaffolds were prepared by traditional fugitive methods and 3D printing methods with random and controlled porosity, respectively. 3D-printed scaffolds showed more surface area and enhanced pore interconnectivity with a pore volume percentage of $48.9 \pm 2.5\%$ than that of the traditionally prepared scaffold of $45.8 \pm 1.5\%$. The loading of the vitamin D₃ (500 µg) was done through a polymer mixture of polycaprolactone (PCL) and polyethylene glycol (PEG) by pouring on scaffolds. The release profile showed the vitamin D₃ release of $37.5 \pm 3.0\%$ from traditional scaffolds while $47.5 \pm 2.8\%$ from 3D-printed scaffolds after 60 days in PBS. The sustained release of the vitamin D₃ because of larger surface area and better interconnectivity also resulted in a higher (up to 50%) human fetal osteoblast adhesion and proliferation on 3D-printed scaffolds compared to traditional scaffolds. Therefore, the use of scaffolds as delivery systems for biomolecules and drugs can be explored for tissue regeneration applications.

Templated glasses are advanced ordered mesoporous bioactive glasses bioceramics used in tissue regeneration and drug delivery systems. The higher surface area to volume ratio allows a higher amount of drug loading and release. The functionalization of the templated glass allows stronger binding affinity and control over the release (Subhpradha et al. 2018). Zhang et al. reported the application of strontium-doped mesoporous bioactive glass (Sr-MBG) scaffolds to deliver dexamethasone for bone regeneration (Zhang et al. 2014). The 3D-printed scaffolds resulted in a higher mechanical strength of 9 MPa and showed stability up to 7 MPa after 7 days of SBF soaking. The maximum drug loading efficiency ($52.5 \pm 1.8\%$) of the scaffold was observed for 5% strontium-doped mesoporous-templated glass. The release profile showed a faster release of 75–85% of the loaded drug in 24 h, followed by a slower release rate. The scaffold showed a good amount of apatite formation over the surface and higher cell adhesion of MC3T3-E1. Therefore, the application of templated glass in the drug delivery model for bone tissue engineering was justified. Figure 19.5 illustrates the application of mesoporous templated glass for drug delivery and bone tissue engineering.

19.5.3 Hyperthermia and Imaging

Magnetic materials are used for targeting and radiotherapy for various types of cancers, including bone cancer. When exposed to alternating frequency, the movement of magnetic moments of the magnetic material elevates surrounding temperature, which is utilized to kill the cancer cells without harming normal cells. Owing to temperature susceptibility, apoptosis is triggered in the cancer cells by elevated temperature, while normal cells dissipate the excess heat through a well-developed vascular system (Fopase et al. 2020b; Fopase and Pandey 2020). Such a treatment strategy is referred to as magnetic hyperthermia, and the range of the hyperthermia temperature is 43–47 °C. Bioceramics incorporated with magnetic materials such as magnetite (Fe₃O₄) and maghemite (γ-Fe₂O₃) are popularly used for this purpose.

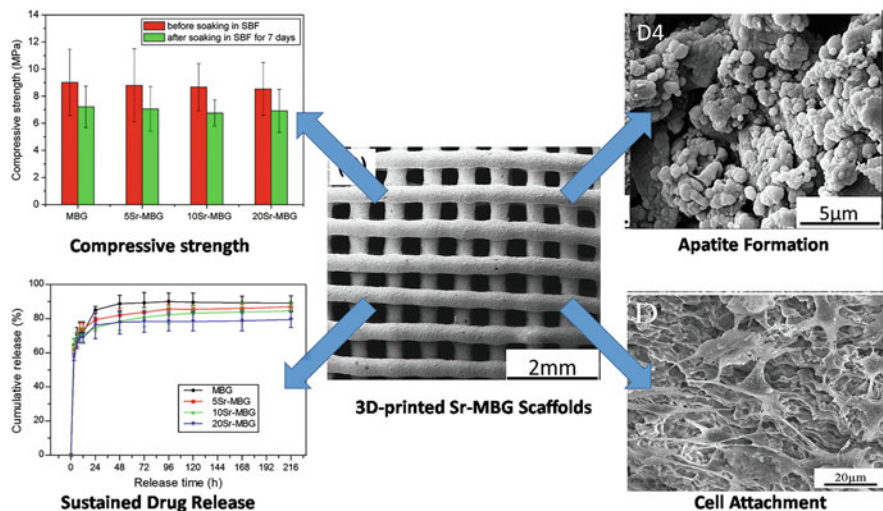


Fig. 19.5 Drug delivery by strontium-doped templated bioactive glass (strontium-doped mesoporous bioactive glass (Sr-MBG)) for bone tissue engineering. (Adapted with permission from (Zhang et al. 2014))

In some cases, doping of Fe^{3+} ions has also been reported by researchers (Farzin et al. 2017; Zhuang et al. 2019). In a study by Farzin et al., multifunctional scaffolds of a bioactive bioceramic hardystonite (HT) were doped with Fe^{3+} for hyperthermia, drug delivery, and tissue engineering applications (Farzin et al. 2017). The sol-gel prepared powders were cast into scaffolds using polyurethane sponge, which showed excellent mechanical properties (1.8–2.5 MPa) due to an increase in Fe^{3+} concentrations and a decrease in porosity. The drug release profile of scaffolds for an anticancer drug cisplatin (cis-dichlorodiammineplatinum(II), CDDP) showed a burst within an initial 3 h followed by a sustained release studied for 240 h with 90% of release. The magnetic studies for the Fe-doped HT showed the magnetic saturation of ~ 1 emu/g with a visible hysteresis loop stating the heat generation due to hysteresis loss. When exposed to an alternating magnetic field of 800 A/m and 750 kHz frequency, the scaffolds powder (15 mg/mL) showed an increase in temperature to 40 °C in 200 s. This rise in the temperature can be utilized to kill the cancer cells, and the loaded anticancer drug can support the treatment for the effective elimination of cancer cells. The Fe-HT scaffolds showed apatite layer formation over the surface when soaked in SBF for 28 days, confirming the bioactivity and suitability for tissue regeneration at bone defects due to cancer tissue. Figure 19.6 depicts a strategic illustration of multifunctional scaffolds for bone cancer treatment.

Other than hyperthermia, magnetic material-doped bioceramics are used for imaging applications such as magnetic resonance imaging (MRI). The magnetic materials in the scaffolds act as the contrast agent and reduce the relaxation time of contrast agents giving higher signal intensity. The relaxation of magnetic moments is

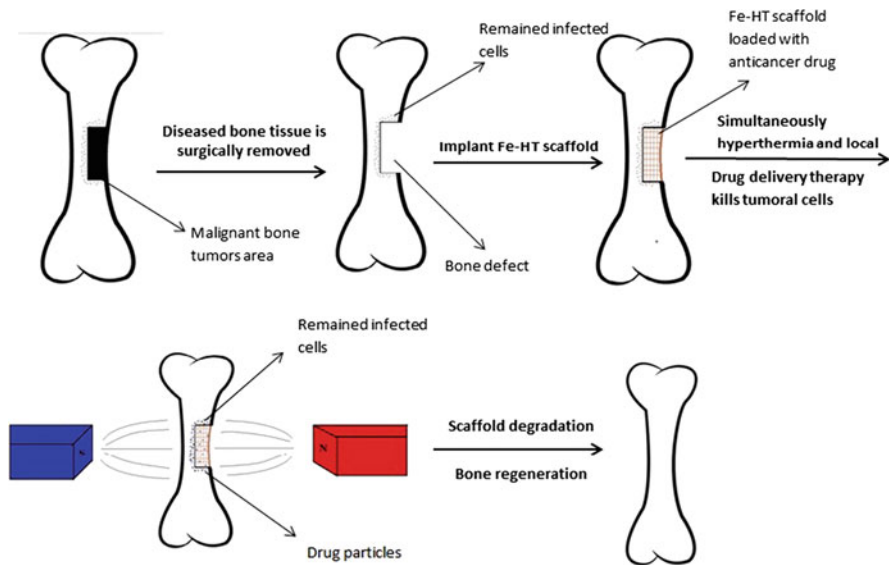


Fig. 19.6 An illustration of multifunctional Fe-HT scaffolds for the treatment for bone tumors by combine therapy of hyperthermia, local drug delivery, and regeneration of tissue. (Adapted with permission from (Farzin et al. 2017))

a function of the type and density of surrounding tissues and can easily differentiate between normal and defected tissues (Grover et al. 2015). Such an approach in tissue engineering helps to analyze the growth and physiological condition of tissues and the state of the implants. The imaging can be used in combination with hyperthermia or drug delivery to see the changes occurring at the target site. Such a multifunctional theranostic approach can improve the efficacy of the tissue regeneration strategy. In a study by Kalidoss et al., the potentials of calcium-deficient hydroxyapatite (CDHA) nanoparticles and Ag, Gd, and Fe ion-substituted calcium-deficient hydroxyapatite (ICDHA) nanoparticles were assessed for multimodal imaging and drug delivery applications (Kalidoss et al. 2019). The nanoparticles were prepared by microwave-accelerated wet chemical methods, and ICDHA showed higher contrast compared to CDHA in X-ray radiography and CT imaging. The magnetic saturation studies showed the diamagnetic behavior of CDHA nanoparticles and the paramagnetic behavior of the ICDHA nanoparticles. T1 and T2 modes of the magnetic resonance imaging showed improved contrast for ICDHA over CDHA using a 4.7 Tesla magnetic resonance system performed in the distilled water. The improved contrast was due to both Gd^{3+} and Fe^{3+} ions in the matrix of HAp. The observed drug-loading efficiencies were 65–70% and 40–55% for CDHA and ICDHA nanoparticles, respectively. Ion substitutions in the HAp reduced the surface area and hence decreased the drug binding. The drug release profiles for CDHA and ICDHA were found to be similar and showed a maximum release of 47–52% in the initial 24 h, followed by slower release up to 120 h. The ICDHA nanoparticles

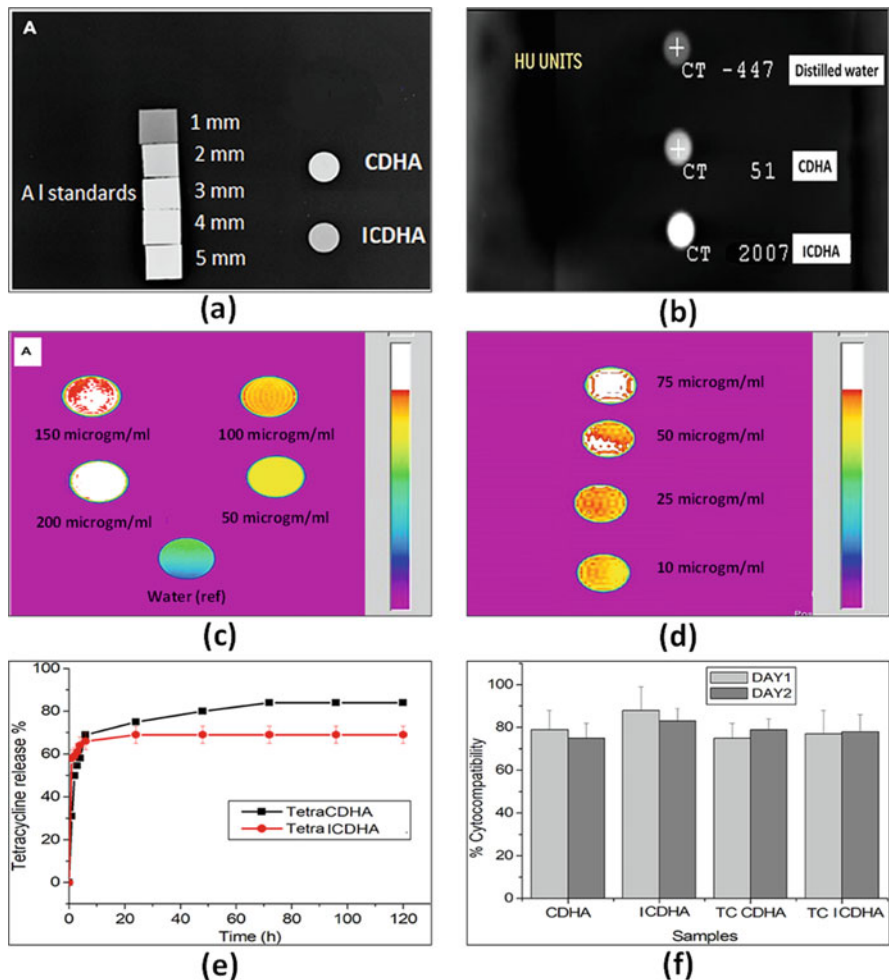


Fig. 19.7 Multifunctional ion-doped calcium-deficient hydroxyapatite for medical imaging and drug delivery application. **(a)** X-ray radiography of ICDHA; **(b)** CT contrast if ICDHA in HU (Hounsfield Units); **(c, d)** T1 and T2 MRI of ICDHA in distilled water; **(e)** release profile for tetracycline loaded on CDHA and ICDHA; and **(f)** cytocompatibility of tetracycline loaded and unloaded CDHA and ICDHA nanoparticles on Swiss 3T3 fibroblast cell line. (Adapted with permission from (Kalidoss et al. 2019))

showed good antibacterial activity due to the presence of Ag ions. The CDHA and ICDHA nanoparticles showed good biocompatibility on Swiss 3T3 fibroblast cells. Figure 19.7 shows the potentiality of multifunctional bioceramics for imaging and drug delivery applications.

19.5.4 Antifouling Property

The surface reactivity of the materials plays a crucial role in the success of the implantation. Nonspecific and unnecessary interactions may result in the toxic or immune response by the host body leading to failure of the implant. Bacterial infections are a significant challenge in medical procedures, and such challenges need major attention while designing the biomaterials. Among the biomaterials, bioceramics have reported a lesser degree of microbial adherence compared to ultra-high molecular weight polyethylene (UHMWPE), stainless steel (SS), and Ti-6Al-4V alloys (Choudhary et al. 2018; Jakubowski et al. 2008). However, a small extent of the infection may cause adverse immune reactions and thus increases the risk of implant failure. Also, biofilm formation over the surface may escape the immune system and generate antibiotic resistance, making it difficult to eliminate or treat (Arciola et al. 2018). Therefore, it is necessary to control the surface reactivity and bacterial adhesion to prevent infection and adverse effects. In this direction, bioceramics are modified to possess antifouling properties to inhibit the random adhesion and interactions.

Zwitterion polymers can be used to modify the surface with a repulsive electrostatic layer over the surface of bioceramic, which repels the bacteria and other contaminants. Colilla et al. showed the dual antibacterial activity of a novel zwitterion SBA-15 bioceramic using alkoxy silane N-(2-aminoethyl)-3-aminopropyl-trimethoxysilane by the co-condensation method having $\text{-NH}_3/\text{-COO}^-$ or $\text{-SiO}^-/\text{-NH}_3$ (Colilla et al. 2014). Thus, modified surface with zwitterion characteristics inhibited adhesion of *S. aureus* compared to bare SBA-15 surface and reduced the risk of infection at the implant site. A similar study by Sanchez-Salcedo et al. modified HAp with the zwitterion pairs of $\text{-NH}_3/\text{-COO}^-$ by 3-aminopropyltriethoxysilane (APTES) and carboxyethylsilanetriol sodium salt (CES) to inhibit the adhesion of *E. coli* (Sánchez-Salcedo et al. 2013). Such antifouling capabilities of bioactive HAp augmented its application in the biomedical field.

Another way to limit the microbial adhesion on the surface is to add antimicrobial agents to the bioceramics constituents. Metal ions such as Ag^+ , Cu^{2+} , Zn^{2+} , and Mg^{2+} are reported to be antimicrobial ions, which can be incorporated into the bioceramics matrices such as HAp and TCP (Veljovic et al. 2019; Saxena et al. 2018). In a study by Choudhary et al., forsterite (Mg_2SiO_4) scaffolds were tested for its antibacterial and mechanical properties for load-bearing applications (Choudhary et al. 2018). The scaffolds showed excellent mechanical properties similar to cortical bone (compressive strength of 201 MPa). The antibacterial activity of the forsterite was observed on both Gram-positive and Gram-negative bacterial strains and found to inhibit more than 75% at a concentration of 2 mg/mL. The bactericidal activity was attributed to the released Mg^{2+} ions from the scaffolds leading to the change of pH into alkaline and killing of bacteria. Thus, such antimicrobial ions containing bioceramics are suitable candidates for biomedical application to reduce the risk of bacterial infections. Figure 19.8 shows the antibacterial potential of the forsterite and thus possible applications.

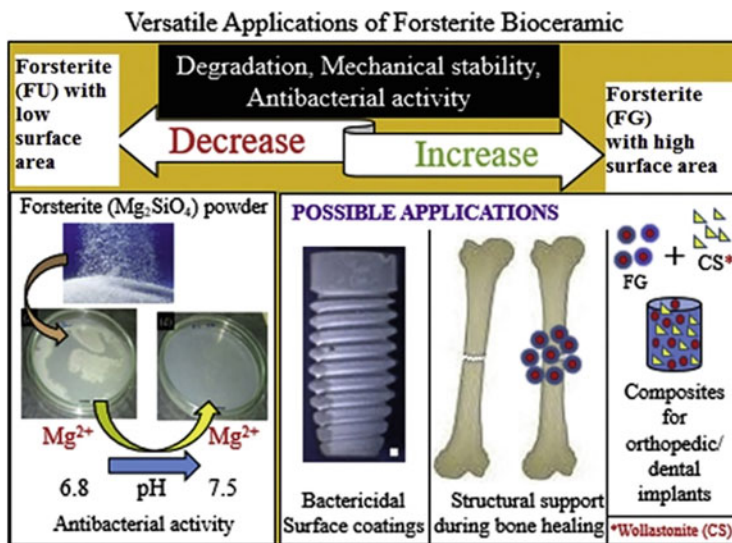


Fig. 19.8 Antifouling of magnesium silicate bioceramic for biomedical applications. (Adapted with permission from (Choudhary et al. 2018))

19.6 Conclusion

Bioceramics are promising biomaterials for various biomedical applications such as orthopedic implants and tissue regeneration since long time. Reactivity of the bioceramics classifies the material into bioinert, bioactive, and bioresorbable. Depending upon the objective of the applications, the type of bioceramics material is selected based on their mechanical and biological properties. Interaction and ability to stimulate tissue regeneration play an important role for the use of the bioceramics in tissue engineering applications. Structural characteristics of bioceramics are useful in bone or dental implants and biocompatible coatings over metallic implants. The recent advances in material science and nanotechnology have enabled to engineer the surface properties and chemical compositions of bioceramics. This in turn has facilitated to design multifunctional bioceramics.

Alumina, zirconia, and titania possess excellent mechanical properties and resistance to corrosion and wear, and thus, they are frequently used in the load-bearing implants and dental applications. Bioceramic-based scaffold provides a temporary framework for the regeneration of the tissues. The porous structure of the bioceramics is also reportedly used for controlled drug delivery applications. In addition, magnetic bioceramics are applied for applications such as magnetic hyperthermia and medical imaging. Antibacterial characteristics of bioceramics do not allow bacterial adhesion over the surfaces of the implant and thus prevent infections owing to antifouling properties. With numerous advantages and ease of tuning, multifunctional bioceramics are proven irreplaceable part of the biomaterials for biomedical applications.

References

- Aplin AE, Howe AK, Juliano R (1999) Cell adhesion molecules, signal transduction and cell growth. *Curr Opin Cell Biol* 11(6):737–744
- Arciola CR, Campoccia D, Montanaro L (2018) Implant infections: adhesion, biofilm formation and immune evasion. *Nat Rev Microbiol* 16(7):397
- Arcos D, Vallet-Regí M (2013) Bioceramics for drug delivery. *Acta Mater* 61(3):890–911
- Arcos D, Izquierdo-Barba I, Vallet-Regí M (2009) Promising trends of bioceramics in the biomaterials field. *J Mater Sci Mater Med* 20(2):447–455
- Baino F, Novajra G, Vitale-Brovarone C (2015) Bioceramics and scaffolds: a winning combination for tissue engineering. *Front Bioeng Biotechnol* 3:202
- Baino F, Potestio I, Vitale-Brovarone C (2018) Production and physicochemical characterization of Cu-doped silicate bioceramic scaffolds. *Materials* 11(9):1524
- Bakopoulou A, Papachristou E, Bousnaki M, Hadjichristou C, Kontonasaki E, Theocharidou A, Papadopoulou L, Kantiranis N, Zachariadis G, Leyhausen G (2016) Human treated dentin matrices combined with Zn-doped, Mg-based bioceramic scaffolds and human dental pulp stem cells towards targeted dentin regeneration. *Dent Mater* 32(8):e159–e175
- Barradas AM, Fernandes HA, Groen N, Chai YC, Schrooten J, Van de Peppel J, Van Leeuwen JP, Van Blitterswijk CA, De Boer J (2012) A calcium-induced signaling cascade leading to osteogenic differentiation of human bone marrow-derived mesenchymal stromal cells. *Biomaterials* 33(11):3205–3215
- Ben-Nissan B (2003) Natural bioceramics: from coral to bone and beyond. *Curr Opin Solid State Mater Sci* 7(4–5):283–288
- Best S, Porter A, Thian E, Huang J (2008) Bioceramics: past, present and for the future. *J Eur Ceram Soc* 28(7):1319–1327
- Boutin P (2014) Total arthroplasty of the hip by fritted alumina prosthesis. Experimental study and 1st clinical applications. *Orthop Traumatol Surg Res* 100(1):15–21
- Bunpetch V, Zhang X, Li T, Lin J, Maswikiti EP, Wu Y, Cai D, Li J, Zhang S, Wu C (2019) Silicate-based bioceramic scaffolds for dual-lineage regeneration of osteochondral defect. *Biomaterials* 192:323–333
- Campbell AA (2003) Bioceramics for implant coatings. *Mater Today* 6(11):26–30
- Castner DG, Ratner BD (2002) Biomedical surface science: foundations to frontiers. *Surf Sci* 500(1–3):28–60
- Chai YC, Carlier A, Bolander J, Roberts SJ, Geris L, Schrooten J, Van Oosterwyck H, Luyten FP (2012) Current views on calcium phosphate osteogenicity and the translation into effective bone regeneration strategies. *Acta Biomater* 8(11):3876–3887
- Choudhary R, Chatterjee A, Venkatraman SK, Koppala S, Abraham J, Swamiappan S (2018) Antibacterial forsterite (Mg₂SiO₄) scaffold: a promising bioceramic for load bearing applications. *Bioact Mater* 3(3):218–224
- Colilla M, Martínez-Carmona M, Sánchez-Salcedo S, Ruiz-González ML, González-Calbet JM, Vallet-Regí M (2014) A novel zwitterionic bioceramic with dual antibacterial capability. *J Mater Chem B* 2(34):5639–5651
- Currey J (2008) The structure and mechanical properties of bone. In: *Bioceramics and their clinical applications*. Elsevier, Amsterdam, pp 3–27
- de Almeida BM, Cardoso KV, Antonio SG, Rizkalla AS, Junior GCS, Arioli Filho JN (2016) Effects of artificial aging conditions on yttria-stabilized zirconia implant abutments. *J Prosthet Dent* 116(2):277–285
- Dorozhkin S (2018) Current state of bioceramics. *J Ceram Sci Technol* 9:353–370
- Dubnika A, Zalite V (2014) Preparation and characterization of porous Ag doped hydroxyapatite bioceramic scaffolds. *Ceram Int* 40(7):9923–9930
- Farokhi M, Mottaghitalab F, Samani S, Shokrgozar MA, Kundu SC, Reis RL, Fatahi Y, Kaplan DL (2018) Silk fibroin/hydroxyapatite composites for bone tissue engineering. *Biotechnol Adv* 36(1):68–91

- Farzin A, Fathi M, Emadi R (2017) Multifunctional magnetic nanostructured hardystonite scaffold for hyperthermia, drug delivery and tissue engineering applications. *Mater Sci Eng C* 70:21–31
- Fopase R, Pandey LM (2020) Iron oxide based magnetic nanomaterials for biomedical applications. In: *Magnetochemistry materials and applications*. Materials Research Foundations, Pennsylvania, pp 276–322
- Fopase R, Paramasivam S, Kale P, Paramasivan B (2020a) Strategies, challenges and opportunities of enzyme immobilization on porous silicon for biosensing applications. *J Environ Chem Eng* 8:104266
- Fopase R, Saxena V, Seal P, Borah J, Pandey LM (2020b) Yttrium iron garnet for hyperthermia applications: synthesis, characterization and in-vitro analysis. *Korean J Couns Psychother* 116:111163
- Grover VP, Tognarelli JM, Crossey MM, Cox IJ, Taylor-Robinson SD, McPhail MJ (2015) Magnetic resonance imaging: principles and techniques: lessons for clinicians. *J Clin Exp Hepatol* 5(3):246–255
- Gutknecht D, Chevalier J, Garnier V, Fantozzi G (2007) Key role of processing to avoid low temperature ageing in alumina zirconia composites for orthopaedic application. *J Eur Ceram Soc* 27(2–3):1547–1552
- Hasan A, Saxena V, Pandey LM (2018) Effect of functional groups of self-assembled monolayers on protein adsorption and initial cell adhesion. *ACS Biomater Sci Eng* 4(9):3224–3233
- Hench LL, Wilson J (1993) Introduction. In: *An introduction to bioceramics*. World Scientific, London (Inglaterra), pp 1–25
- Hulbert S (1993) The use of alumina and zirconia in surgical implants. In: *Advanced series in ceramics*, vol 1, pp 25–40
- Izquierdo-Barba I, Vallet-Regí M (2011) Fascinating properties of bioactive templated glasses: a new generation of nanostructured bioceramics. *Solid State Sci* 13(4):773–783
- Jakubowski W, Ślósarczyk A, Paszkiewicz Z, Szymański W, Walkowiak B (2008) Bacterial colonisation of bioceramic surfaces. *Adv Appl Ceram* 107(4):217–221
- Jun S-H, Lee E-J, Jang T-S, Kim H-E, Jang J-H, Koh Y-H (2013) Bone morphogenic protein-2 (BMP-2) loaded hybrid coating on porous hydroxyapatite scaffolds for bone tissue engineering. *J Mater Sci Mater Med* 24(3):773–782
- Kalidoss M, Yunus Basha R, Doble M, Sampath Kumar T (2019) Theranostic calcium phosphate nanoparticles with potential for multimodal imaging and drug delivery. *Front Bioeng Biotechnol* 7:126
- Keane M (2003) Ceramics for catalysis. *J Mater Sci* 38(23):4661–4675
- Kim H, Mondal S, Bharathiraja S, Manivasagan P, Moorthy MS, Oh J (2018) Optimized Zn-doped hydroxyapatite/doxorubicin bioceramics system for efficient drug delivery and tissue engineering application. *Ceram Int* 44(6):6062–6071
- Kumar P, Dehiya BS, Sindhu A (2018) Bioceramics for hard tissue engineering applications: a review. *Int J Appl Eng Res* 5(13):2744–2752
- Langer R (1998) Drug delivery and targeting. *Nature* 392(6679 Suppl):5–10
- LeGeros R, Lin S, Rohanizadeh R, Mijares D, LeGeros J (2003) Biphasic calcium phosphate bioceramics: preparation, properties and applications. *J Mater Sci Mater Med* 14(3):201–209
- López JP (2014) Alumina, zirconia, and other non-oxide inert bioceramics. In: *Bio-ceramics with clinical applications*, pp 153–173
- Mondal S, Nguyen TP, Hoang G, Manivasagan P, Kim MH, Nam SY, Oh J (2020) Hydroxyapatite nano bioceramics optimized 3D printed poly lactic acid scaffold for bone tissue engineering application. *Ceram Int* 46(3):3443–3455
- Mouriño V, Cattalini JP, Roether JA, Dubey P, Roy I, Boccaccini AR (2013) Composite polymer-bioceramic scaffolds with drug delivery capability for bone tissue engineering. *Expert Opin Drug Deliv* 10(10):1353–1365
- Naghizadeh F, Kadir MRA, Doostmohammadi A, Roozbahani F, Iqbal N, Taheri MM, Naveen SV, Kamarul T (2015) Rice husk derived bioactive glass-ceramic as a functional bioceramic: synthesis, characterization and biological testing. *J Non Cryst Solids* 427:54–61

- Naglieri V, Palmero P, Montanaro L, Chevalier J (2013) Elaboration of alumina-zirconia composites: role of the zirconia content on the microstructure and mechanical properties. *Materials* 6(5):2090–2102
- Napier RJ, Shimmin AJ (2016) Ceramic-on-ceramic bearings in total hip arthroplasty: “The future is now”. *JSES* 27(4):235–238
- Ning C, Zhou L, Tan G (2016) Fourth-generation biomedical materials. *Mater Today* 19(1):2–3
- Peroglio M, Gremillard L, Chevalier J, Chazeau L, Gauthier C, Hamaide T (2007) Toughening of bio-ceramics scaffolds by polymer coating. *J Eur Ceram Soc* 27(7):2679–2685
- Piconi C, Maccauro G (1999) Zirconia as a ceramic biomaterial. *Biomaterials* 20(1):1–25
- Piconi C, Maccauro G, Muratori F, Del Prever EB (2003) Alumina and zirconia ceramics in joint replacements. *J Appl Biomater Biomech* 1(1):19–32
- Pina SCA, Reis RL, Oliveira JM (2018) Ceramic biomaterials for tissue engineering. In: *Fundamentals biomaterials: ceramic*. Elsevier, Amsterdam
- Popa MV, Demetrescu I, Vasilescu E, Drob P, Lopez AS, Mirza-Rosca J, Vasilescu C, Ionita D (2004) Corrosion susceptibility of implant materials Ti–5Al–4V and Ti–6Al–4Fe in artificial extra-cellular fluids. *Electrochim Acta* 49(13):2113–2121
- Prabha R, Ding M, Bollen P, Ditzel N, Varma H, Nair P, Kassem M (2020) Strontium ion reinforced bioceramic scaffold for load bearing bone regeneration. *Mater Sci Eng C* 109:110427
- Predoi D, Barsan M, Andronesu E, Vatasescu-Balcan R, Costache M (2007) Hydroxyapatite-iron oxide bioceramic prepared using nano-size powders. *J Optoelectron Adv Mater* 9(11):3609
- Rahaman MN, Day DE, Bal BS, Fu Q, Jung SB, Bonewald LF, Tomsia AP (2011) Bioactive glass in tissue engineering. *Acta Biomater* 7(6):2355–2373
- Ramesh N, Moratti SC, Dias GJ (2018) Hydroxyapatite–polymer biocomposites for bone regeneration: a review of current trends. *J Biomed Mater Res B Appl Biomater* 106(5):2046–2057
- Rao SH, Harini B, Shadamarshan RPK, Balagandharan K, Selvamurugan N (2018) Natural and synthetic polymers/bioceramics/bioactive compounds-mediated cell signalling in bone tissue engineering. *Int J Biol Macromol* 110:88–96
- Sánchez-Salcedo S, Colilla M, Izquierdo-Barba I, Vallet-Regí M (2013) Design and preparation of biocompatible zwitterionic hydroxyapatite. *J Mater Chem B* 1(11):1595–1606
- Sarigol-Calamak E, Hascicek C (2018) Tissue scaffolds as a local drug delivery system for bone regeneration. In: *Cutting-edge enabling technologies for regenerative medicine*. Springer, Berlin, pp 475–493
- Saxena V, Hasan A, Pandey LM (2018) Effect of Zn/ZnO integration with hydroxyapatite: a review. *Mater Technol* 33(2):79–92. <https://doi.org/10.1080/10667857.2017.1377972>
- Saxena V, Shukla I, Pandey LM (2019) Hydroxyapatite: an inorganic ceramic for biomedical applications. In: *Materials for biomedical engineering*. Elsevier, Amsterdam, pp 205–249
- Sebastine IM, Williams DJ (2006) The role of mechanical stimulation in engineering of extracellular matrix (ECM). In: 2006 International Conference of the IEEE Engineering in Medicine and Biology Society. IEEE, Piscataway, NJ, pp 3648–3651
- Shao H, He Y, Fu J, He D, Yang X, Xie J, Yao C, Ye J, Xu S, Gou Z (2016) 3D printing magnesium-doped wollastonite/ β -TCP bioceramics scaffolds with high strength and adjustable degradation. *J Eur Ceram Soc* 36(6):1495–1503
- Smith I, Baumann M, McCabe L (2004) Electrostatic interactions as a predictor for osteoblast attachment to biomaterials. *J Biomed Mater Res A* 70(3):436–441
- Sowmya S, Bumgardener JD, Chennazhi KP, Nair SV, Jayakumar R (2013) Role of nanostructured biopolymers and bioceramics in enamel, dentin and periodontal tissue regeneration. *Prog Polym Sci* 38(10–11):1748–1772
- Stipnice L, Stepanova V, Narkevica I, Salma-Ancane K, Boyd AR (2018) Comparative study of surface properties of mg-substituted hydroxyapatite bioceramic microspheres. *J Eur Ceram Soc* 38(2):761–768
- Subhadrappa N, Abudhahir M, Aathira A, Srinivasan N, Moorthi A (2018) Polymer coated mesoporous ceramic for drug delivery in bone tissue engineering. *Int J Biol Macromol* 110:65–73

- Tampieri A, Celotti G, Szontagh F, Landi E (1997) Sintering and characterization of HA and TCP bioceramics with control of their strength and phase purity. *J Mater Sci Mater Med* 8(1):29–37
- Tran N, Webster TJ (2011) Increased osteoblast functions in the presence of hydroxyapatite-coated iron oxide nanoparticles. *Acta Biomater* 7(3):1298–1306
- Vallet-Regí M (2006) Revisiting ceramics for medical applications. *Dalton Trans* 44:5211–5220
- Vallet-Regí M, González-Calbet JM (2004) Calcium phosphates as substitution of bone tissues. *Prog Solid State Chem* 32(1–2):1–31
- Vallet-Regí M, Ruiz-Hernández E (2011) Bioceramics: from bone regeneration to cancer nanomedicine. *Adv Mater* 23(44):5177–5218
- Vallet-Regí M, Balas F, Colilla M, Manzano M (2008) Bone-regenerative bioceramic implants with drug and protein controlled delivery capability. *Prog Solid State Chem* 36(3):163–191
- Vallet-Regí M, Izquierdo-Barba I, Colilla M (2012) Structure and functionalization of mesoporous bioceramics for bone tissue regeneration and local drug delivery. *Philos Trans A Math Phys Eng Sci* 370(1963):1400–1421
- Veljovic D, Matic T, Stamenic T, Kojic V, Dimitrijevic-Brankovic S, Lukic MJ, Jevtic S, Radovanovic Z, Petrovic R, Janackovic D (2019) Mg/cu co-substituted hydroxyapatite–biocompatibility, mechanical properties and antimicrobial activity. *Ceram Int* 45(17):22029–22039
- Vu AA, Bose S (2020) Vitamin D 3 release from traditionally and additively manufactured Tricalcium phosphate bone tissue engineering scaffolds. *Ann Biomed Eng* 48(3):1025–1033
- Wu C-T, Chang J (2013) Silicate bioceramics for bone tissue regeneration. *Wuji Cailiao Xuebao (J Inorg Mater)* 28(1):29–39
- Wu C, Xia L, Han P, Xu M, Fang B, Wang J, Chang J, Xiao Y (2015) Graphene-oxide-modified β -tricalcium phosphate bioceramics stimulate in vitro and in vivo osteogenesis. *Carbon* 93:116–129
- Yadav V, Sankar M, Pandey L (2020) Coating of bioactive glass on magnesium alloys to improve its degradation behavior: interfacial aspects. *J Magnesium Alloys* 8:999–1015
- Yoshimura M (1988) Phase stability of zirconia. *Am Ceram Soc Bull* 67(12):1950–1955
- Yunos DM, Bretcanu O, Boccaccini AR (2008) Polymer-bioceramic composites for tissue engineering scaffolds. *J Mater Sci* 43(13):4433–4442
- Zapanta-LeGeros R (1965) Effect of carbonate on the lattice parameters of apatite. *Nature* 206(4982):403–404
- Zhai W, Lu H, Chen L, Lin X, Huang Y, Dai K, Naoki K, Chen G, Chang J (2012) Silicate bioceramics induce angiogenesis during bone regeneration. *Acta Biomater* 8(1):341–349
- Zhai W, Lu H, Wu C, Chen L, Lin X, Naoki K, Chen G, Chang J (2013) Stimulatory effects of the ionic products from Ca–Mg–Si bioceramics on both osteogenesis and angiogenesis in vitro. *Acta Biomater* 9(8):8004–8014
- Zhang F, Chang J, Lu J, Lin K, Ning C (2007) Bioinspired structure of bioceramics for bone regeneration in load-bearing sites. *Acta Biomater* 3(6):896–904
- Zhang J, Zhao S, Zhu Y, Huang Y, Zhu M, Tao C, Zhang C (2014) Three-dimensional printing of strontium-containing mesoporous bioactive glass scaffolds for bone regeneration. *Acta Biomater* 10(5):2269–2281
- Zhang Y, Zhai D, Xu M, Yao Q, Chang J, Wu CJ, Jomc B (2016) 3D-printed bioceramic scaffolds with a Fe₃O₄/graphene oxide nanocomposite interface for hyperthermia therapy of bone tumor cells. *J Mater Chem B* 4(17):2874–2886
- Zhang Y, Zhai D, Xu M, Yao Q, Zhu H, Chang J, Wu C (2017) 3D-printed bioceramic scaffolds with antibacterial and osteogenic activity. *Biofabrication* 9(2):025037
- Zhou Y, Wu C, Chang J (2019) Bioceramics to regulate stem cells and their microenvironment for tissue regeneration. *Mater Today* 24:41–56
- Zhuang H, Lin R, Liu Y, Zhang M, Zhai D, Huan Z, Wu C (2019) Three-dimensional-printed bioceramic scaffolds with osteogenic activity for simultaneous photo/magnetothermal therapy of bone tumors. *ACS Biomater Sci Eng* 5(12):6725–6734



Applications of Nanomaterials in the Textile Industry 20

Satadru Chakrabarty and Kabeer Jasuja

Abstract

The science of nanomaterials has taken giant leaps during the last three decades. Not only has the synthesis of nanomaterials become easier and more accessible, their integration in existing technologies is also becoming more feasible. Nanomaterials present extraordinary opportunities on account of the unique properties packed within their small sizes; this aspect is being used to improve a number of applications. Textile and apparel research too are being benefited by nanotechnology. Nanomaterials such as graphene, carbon nanotubes, metal nanoparticles (Ag/Au, TiO₂, ZnO and CuO) and bio-based nanomaterials have been used in textiles to augment their functionalities. Examples of these functionalities being conductivity, water repellence, microbial control, high strength, anti-static properties, colour blocking, etc. Textile industries have not only been enriched in the products they deliver due to the advent of nanomaterials, they have also benefited from the fact that nanomaterials can be used to degrade pollutants found in textile effluent streams, which have posed serious environmental challenges for a long time. Thus, it seems, the future of textile industry is firmly entrenched in the smart incorporation of nanomaterials. It must also be mentioned that even with the remarkable opportunities that nanomaterials provide to the textile industry, there are some obstacles that need to be addressed such as that of scalability and cost. The lifecycle of nanomaterials and their toxicity in textile products also need to be evaluated and safeguards need to be in place for the safety of the consumer and the environment. In this chapter we will systematically present some perspectives on the foray of nanomaterials

S. Chakrabarty · K. Jasuja (✉)

Discipline of Chemical Engineering, Indian Institute of Technology, Gandhinagar, Palaj,
Gandhinagar, Gujarat, India

e-mail: kabeer@iitgn.ac.in

© The Author(s), under exclusive license to Springer Nature Singapore Pte Ltd. 2022

567

L. M. Pandey, A. Hasan (eds.), *Nanoscale Engineering of Biomaterials: Properties and Applications*, https://doi.org/10.1007/978-981-16-3667-7_20

and the impact they have brought about in the textile industry and where it is headed.

Keywords

Textiles · Apparels · Smart wearables · Nanomaterials · Nanocomposites · Environment

20.1 Introduction

The rapid progress of nanotechnology has also led to the advancement in the science of nanomaterials, which has developed considerably in recent times. Nanomaterials have been in use since Roman times as depicted in the case of the Lycurgus cup (Leonhardt 2007). But it is during the last two decades that we have begun to understand the basic science behind these fascinating materials. This has also led to practical applications where nanomaterials have been used extensively. Areas such as medicine (Fernandez-Fernandez et al. 2011), agriculture (Khot et al. 2012), sensors (Yin and Qin 2013; Li et al. 2009), food (Bradley et al. 2011), environmental remediation (Ghasemzadeh et al. 2014; Daer et al. 2015) have been enriched by the applications of nanomaterials in multitudinous ways. Scientists and industrialists alike are still trying to incorporate nanomaterials in even more areas with the ultimate goal of advancement of technology and to move nanotechnology from lab to real-world consumer products (Thangudu 2020). Because nanomaterials are of extremely small size, their surface chemistry and reactivity are vastly different from their bulk counterparts, this is one of the reasons why gaining deeper insights into the realm of nanomaterials has been challenging. But with the development in powerful microscopic and spectroscopic techniques like transmission, tunnelling and scanning electron microscopy, in conjunction with newer synthesis methods such as molecular beam epitaxy, chemical vapour deposition, etc., these challenges have been overcome (Cao 2004; Xiao et al. 2020; Liu and Hu 2020), thus, paving the way for applications in a wide variety of domains. Nanomaterials can be synthesized via a multitude of procedures, and broadly they can be classified into two main schemes: top-down and bottom-up. The bottom-up route provides the opportunity to synthesize nanomaterials in a wide range of sizes, in turn giving rise to the possibility of using these nanomaterials in various associated applications.

One of the emerging frontiers where nanomaterials are finding an increased prominence is the textile industry, although its footprint is smaller relative to other conventional areas. In spite of that, the textile industry was one of the first to adopt nanomaterials in their products. In some high-performance fields such as that of medical, protective, automotive, and furnishing textiles, nanomaterials are considered to be the next-generation approach for superseding the classical hindrances that these products currently possess (Matsuo 2008; Joshi and Bhattacharyya 2011). Research in the textile field mainly deals with the inclusion of nanoscaled substances (such as nanofibres, nanocomposites, nano-electronics) during the manufacturing or

finishing steps to impart various novel properties (Joshi and Bhattacharyya 2011). It can be conjectured that the potential of nanotechnologies in textile-based applications is immense, and till now, it seems that the community has only scratched the surface. Of late, however, there has been a surge in the endeavour aiming to tap this potential and develop novel nano-based smart and environmentally adaptive textile products (Krifa and Prichard 2020). A stand out aspect of the textile industry is the fact that it provides an easy and ideal interface (the textile itself) for the integration of nanomaterials, electronic components as well as optical devices. This ease of integration leads to the materialization of stimuli receptive products viz. electrical, mechanical, chemical, thermal, magnetic, optical, etc. Some criteria that the nano-engineered materials need to pass include the seamless infusion into fabrics while maintaining breathability and flexibility, providing performance, weight, and appearance. Nanotechnology and, more specifically, nanomaterials can be used to impart permanent functional properties the likes of which have been mentioned earlier without compromising on the intended use of the textile (Yetisen et al. 2016). What makes the current age exciting for the textile industry is that the corporations as well as public figures are embracing wearable technologies which enable them in setting themselves apart in society. Hence, the field is ripe with opportunities for innovations. Figure 20.1 depicts a representative schema of the various applications that nanomaterials are involved within the textile industry. Since textile industry is a relatively low-tech industry, therefore it is primed for newer innovations and the foray of nanotechnology-based materials. A breakdown of the worldwide textile market shows that about 60% of the market is represented by clothing, 35% by furnishing textiles, and the rest is represented by nonconventional and technical textiles such as medical, military, and sports (Ngô and Van de Voorde 2014). It is interesting to note, that at present, most of the manufacturing of textiles has moved from the western hemisphere to the Asian manufacturing hubs. Textile industry has a significant impact on the economy as well as the environment, because with rising population, the demand for wearables has skyrocketed and industries and governments are hard-pressed on that front (Shabbir and Kaushik 2020). As a corollary, it can be said that the involvement of nanomaterials in the textile industrial sphere will provide attractive opportunities for developing Asian economies as it has a high turnover. In Fig. 20.2 the current market shares along with the projected growth of smart textiles in the global market is shown. Even though the opportunities are numerous, there are some challenges that are posed by the applications of nanomaterials in textile industry. The release of nanomaterials such as silver nanoparticles is a source for concern—Ag nanoparticles are documented to be toxic to aquatic organisms (Bianchini and Wood 2002; Wood et al. 1996). Exposure to nanomaterials or particles is also an issue at the workplace, which might cause respiratory issues. Currently, textile industry accounts for about 10% of the carbon emissions globally (Agarwal and Jeffries 2013). Customers today are generally much aware and would therefore want the products be as environmentally friendly as possible. Textile industries would therefore do well if they can ensure climate neutrality and also reduce greenhouse emissions.



Fig. 20.1 Applications of nanotechnology/nanomaterials in textile industry. (Adapted from Yetisen et al. (2016). Copyright 2016 American Chemical Society)

In this chapter, we would systematically present the evolution of the usage of nanomaterials in the textile industry, as well as the current and future direction the industry would take, while also discussing few of the problems associated with widespread use of nanomaterials for textile and apparel-based applications.

20.2 Early Days of Nanomaterials in the Textile Industry

Nanotechnology has found applications in practically all spheres of life, but what led to the foray of this disruptive scientific paradigm into the so-called conventional industry? The answer like in most cases is nature. Scientists found out that a surface structure that mimics the natural world can be developed using nanotechnology and by extension nanomaterials (Barthlott and Ehler 1977). Although nature provided the initial impetus, what has driven the textile industry more and more towards nanoscaled materials was the ever-increasing global competition and rapidly

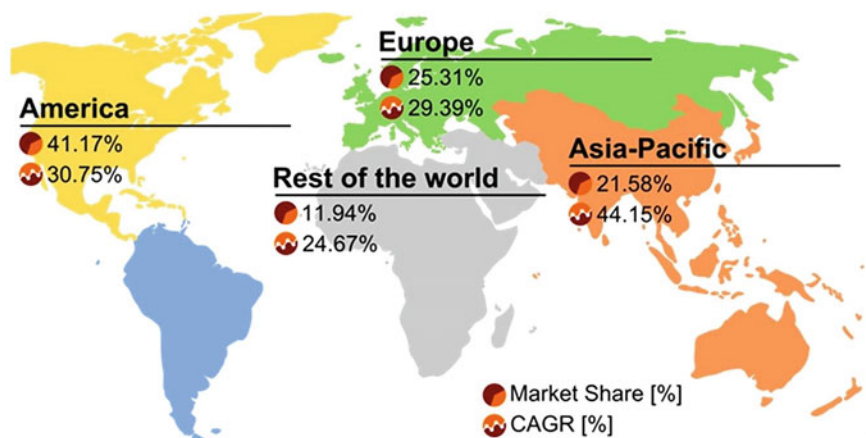


Fig. 20.2 Global share and CAGR by individual regions. (Adapted from Yetisen et al. (2016). Copyright 2016 American Chemical Society)

changing consumer needs. The primary objective of present-day textile industry is to stand out among the competition, achieving this required technological innovation and nanomaterials provided the access to realize this goal (Kaounides et al. 2007). Textiles were among the first industries who adopted the use of nanomaterials, and the first such application came to the fore in the year 1995, the first industrial collaboration taking place with Nano-Tex, LLC being at the helm in the year 2000 (Lo et al. 2007). From there on there was no looking back and various nanomaterials like particles, capsules, tubes, composites, ceramics, sols, fibrillars, and fibres have been commonly applied or integrated in textile substrates (Norberg 2005). This foray of nanomaterials gave rise to what we know today as ‘nanofinishing,’ the technique of *nanofinishing* included various facets such as UV-blocking, anti-microbial, anti-static, water-repellence, and flame retardancy (Mariana 2009; Sawhney et al. 2008).

20.3 Applied Nanomaterials in Textiles

Before delving into the actual applications of nanomaterials, it is also important to understand the entire process of textile manufacturing from the production to their end of use and recycling. It is imperative on the textile manufacturers to ensure that there are no adverse effects on the environment and human health due to the usage of nano-textiles. Figure 20.3 shows the entire life cycle of nano-textiles (Pereira et al. 2020). The central merit of nano-engineered textiles is to achieve various enhanced properties from incorporating nanomaterials. To achieve this, two main forms of nanostructures are used: nanofibres or nanoparticles. In this section we will apprise the reader about the types of nanomaterials that have been researched for their ability to be used in textiles.

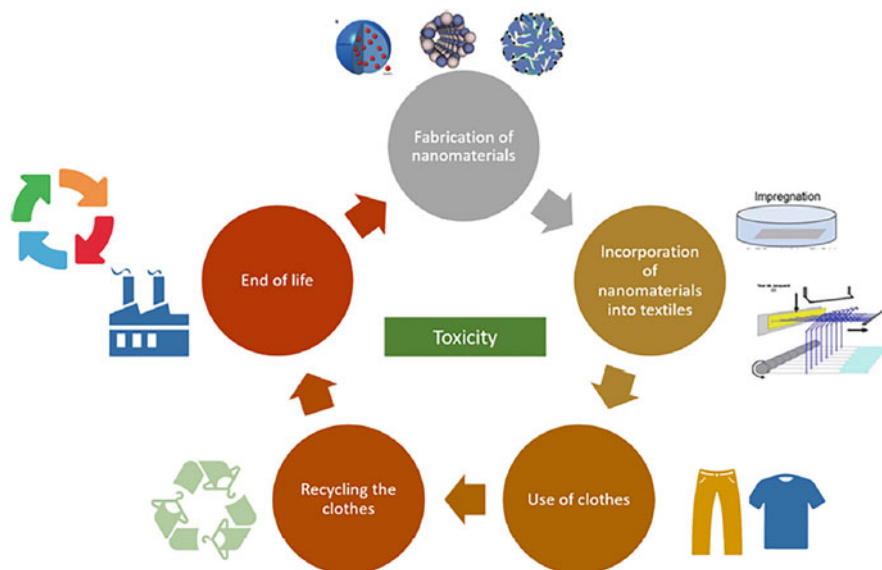


Fig. 20.3 Life cycle of nano-engineered textiles. (Adapted from Pereira et al. (2020) copyright 2020, Elsevier)

20.3.1 Nanotubes

Nanotubes are a class of 1-D nanomaterials where the axial dimension is usually in the micron range and diameter is in nanometres. Of all the nanotubes synthesized, perhaps the most famous of them are carbon nanotubes (CNTs). These nanotubes can again be of two types: single-walled or multi-walled. Since, CNTs are very good conductors of heat and electricity, efforts have been put in to produce conductive fibres by dispersing CNTs into the polymer matrix such as poly-cellulose (Lee et al. 2016). Textiles which can withstand velocity impact have also been investigated by the inclusion of CNTs in epoxy-based textiles (El Moumen et al. 2017). Figure 20.4 shows how the modification of a conventional textile fibre occurs with the addition of CNTs. In addition to that, the flame retardant properties of textiles after addition of CNTs was also investigated along with their thermoelectric textile fabrics (Ryan et al. 2018; Yin et al. 2015). CNTs have also been used as an effective antimicrobial additive in textile fabrics as it was found that these nanotubes could damage the bacterial cell membranes (Lee et al. 2018; Baranwal et al. 2018). Quantum nanorods similar to nanotubes have been immobilized in good amounts on cotton-based fabrics along with metal organic frameworks (MOFs). These immobilizations led to the sensing of toxic gases via conductivity of the rods and the luminescence of the MOFs, paving the way for sensing and electronic textiles. Such nano-chemical sensors show the potential of being used in various textile substrates (Ozer and Hinestroza 2015; Zhukovskiy et al. 2014).

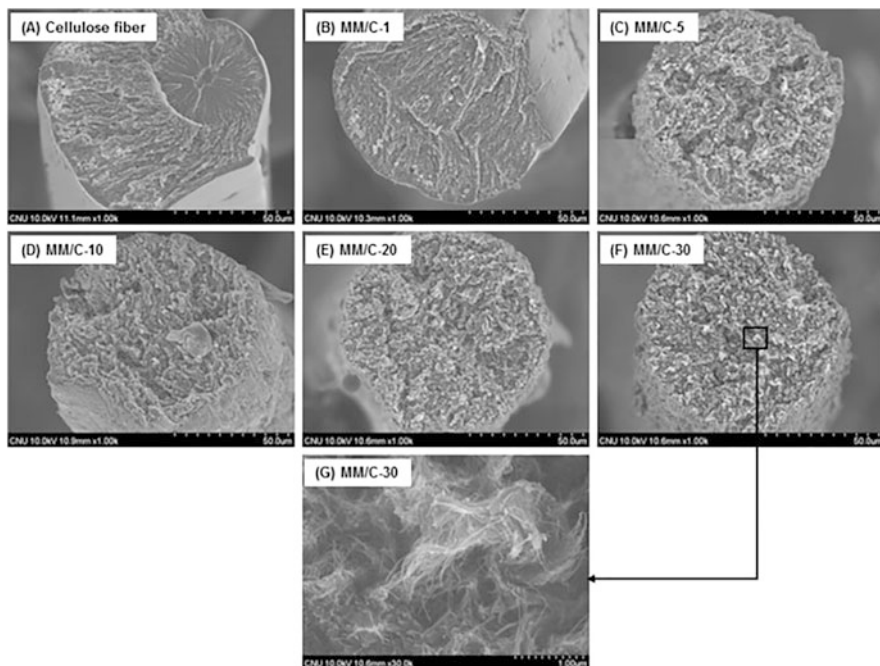


Fig. 20.4 SEM micrograph indicating the modification of cellulose fibre after the addition of CNTs. The numeral indicates the number of hydrogen bonds formed with the cellulose fibre. (Adapted from Lee et al. (2016) copyright 2016 Elsevier)

20.3.2 Nanodiamonds

As the name suggests, these particles are nanoscaled diamond particles, first reported in the 1960s and produced by the mode of detonation (Danilenko 2004). Since then, interest in nanodiamonds (NDs) have increased manifold, owing to their excellent mechanical, chemical, thermal and optical properties (Bradac and Osswald 2018; Mochalin et al. 2012). In a recent report, it was found that coating wool fabrics with NDs led to a great increase in their hydrophilicity (Houshyar et al. 2019b). Not only that the tensile strength and the abrasion resistance of the fabrics were also found to increase. Successful reinforced polyvinyl acrylate (PVA) fibres were obtained by dispersing NDs into PVA matrix in one, while the tensile strength was only moderately enhanced (Indrová et al. 2015). Even cotton fabrics showed greater strength, thermal stability and surface energy when modified with NDs (Houshyar et al. 2019a). It was also found that NDs can enhance a desired property in a polymeric fabric such as polyaniline (PANI), while not adversely affecting its other properties such as conductivity (Tamburri et al. 2012).

20.3.3 Nanoclays and Silica Nanoparticles

Nanoclays are mainly layered mineral silicates categorised into various types such as montmorillonite, bentonite, kaolinite, hectorite and halloysite. They are classified under quasi-2D nanomaterials. Among the various types of clays, montmorillonites (MMTs) have found the most widespread use in materials applications. From the viewpoint of the textile industry too, MMTs have been widely used as filler for fabrics and fibres. Analysis of cotton fabrics which were treated with MMTs during the finishing process to produce functionalised fabrics, showed a marked increase in their flame retardancy and tensile strength. The functionality was also not found to decay after washing (Göcek 2019; Shahidi and Ghoranneviss 2014). In a recent study, nylon fabric modified with bentonite nanoclay showed increase in their hydrophilicity (Abeywardena et al. 2018). It is interesting to note that nanoclays have also been used to produce superhydrophobic textiles (Subasri and Hima 2015). Antibacterial property of nanoclays have also been looked into and established (Maryan and Montazer 2015). An offshoot yet important application of nanoclays is in the area of dye adsorption from textile effluents. Nanoclays have proved to be effective in adsorbing dyes (non-ionic, cationic, anionic), thus also helping in the remediation of the pollution caused by the textile industry (Yang et al. 2005; Stagnaro et al. 2015; Hassani et al. 2015). Similar to nanoclays, silica nanoparticles have also found applications in the textile industry, particularly in enhancing superhydrophobicity of textile fibres such as cotton (Pereira et al. 2011). Recent studies suggest that self-assembly of these nanoparticles impart self-cleaning property to fabrics (Anjum et al. 2020). Since silica nanoparticles have highly ordered structure, they have also been used as colouring agents in textile materials by manipulating the Bragg diffraction of white light with the silica nanoparticles (Gao et al. 2017). Not only does silica nanoparticles impart hydrophobicity, but it also acts as an effective UV blocking agent, thereby making textiles multifunctional (Attia et al. 2017). Figure 20.5 shows the beneficial effect of hydrophobic surfaces on textiles.

20.3.4 Metallic Nanoparticles

A variety of nanoparticles formed from a wide range of metallic precursors has been used in creating functional textiles. Among the various applications probed, antimicrobial properties of metal nanoparticles have been reported in huge numbers throughout the years. Generally, metal ions damage microbial cells owing to their ability to diffuse through the cell membranes and infiltrate to the interior of the bacterial cell and thereby restricting growth and proliferation of the microorganism (Yamanaka et al. 2005). Initially it was believed that metal ions only reside in the cell membranes. Among the common metal nanoparticles, silver nanoparticles have most frequently been used in textiles as antimicrobial agents (Tulve et al. 2015; Ballottin et al. 2017; Ribeiro et al. 2018). The nanoparticles of titanium (Stan et al. 2016), zinc (Kalpana et al. 2018) and copper (Xu et al. 2018) have also been used in antimicrobial textiles. Electrical conductivity can also be enhanced by the usage of

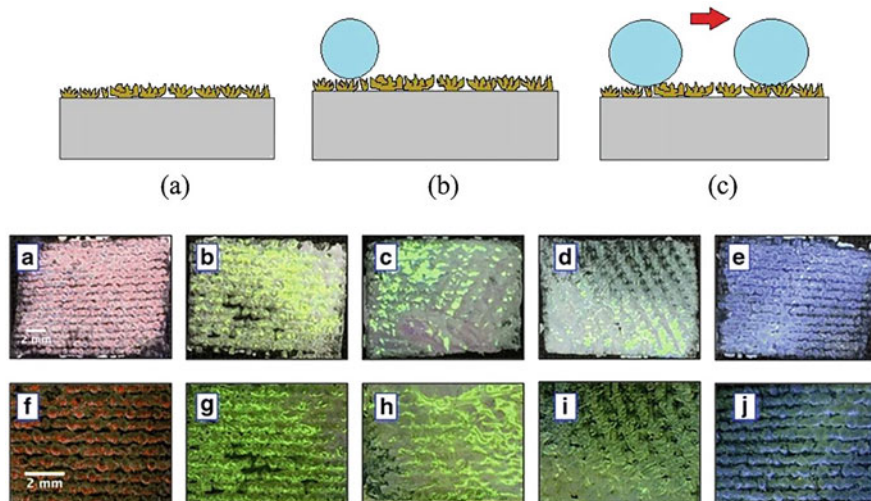


Fig. 20.5 Top panel—Nanoclay on textile substrate, water drop on surface and rolling off due to hydrophobicity. (Adapted from Subasri and Hima (2015) copyright 2015 Elsevier). Bottom panel—(a)–(e) Microscopic images of structurally coloured fabrics with silica nanoparticles. (f)–(j) Corresponding reflectance spectra. (Adapted from Subasri and Hima (2015) copyright 2015 Elsevier)

metallic nanoparticles. For example, gold and silver nanoparticles/nanowires have been used in fabricating e-textiles (Han et al. 2015; Kapoor et al. 2020). Nickel too has been recently favoured as a conductive agent in textile matrices, along with magnetic textiles. Wearable energy storage devices have also been developed using nano-nickel (Bian et al. 2016; Moazzenchi and Montazer 2019; Lu et al. 2018).

20.3.5 Biological Nanomaterials

Bio-based nanomaterials hold an advantage, in that they are mostly environmentally benign and also much less cytotoxic when compared to metallic nanomaterials. Thus these nanomaterials have also gained respectable attention in textile research. Cellulosic and chitosan-derived nanomaterials are presently in the lead in finding applications in the textile industry. Cellulose nanowhiskers have been copolymerised and their candidacy for conductive textiles has been examined (Hebeish et al. 2014). Also, cellulosic nanofibres show improved dyeability and knitting properties while being cost effective and scalable in its manufacture (Jia et al. 2018). Wearable electronics have been gaining traction of late and cellulose nanocrystals are reported to be beneficial in fabricating high-performing supercapacitors and wearable electrodes (Chen et al. 2019). Biodegradability of textiles is an issue that needs to be addressed seriously. Textile fibres derived from cellulosic nanocrystals have demonstrated the ability to be more thermally resistant

as well as being more biodegradable than conventional textiles (Xu et al. 2019). Cellulosic nanofibrils are finding use in 3D printing as well as printing of smart and e-textiles (Cao et al. 2019; Nechyporchuk et al. 2017). Chitosan derived from an abundant biopolymer, namely chitin, is mostly found in the shells of crustaceans. Chitosan has been investigated for its antimicrobial activity, and thus is an attractive candidate as an additive for antimicrobial textiles (Shahid ul and Butola 2019; Morin-Crini et al. 2019; Arshad et al. 2018). In some other applications, nano-chitosan has been used as a strengthening and reinforcing agent for fabrics and also to impart improved washability and hydrophilicity (Shabbir et al. 2017). Truly, chitosan has manifested itself as a versatile substance for the textile industry since it can also be used as a dye adsorbing agent (Qamar et al. 2020; dos Santos et al. 2018) in addition to be used as a textile effluent decolourizer and detoxifier (Bilal et al. 2016). Nanomaterials have also been examined as candidates for drug release in textiles. Although, not strictly a biological nanomaterial, but in one such study Cu benzene tricarboxylic acid MOF-199 was coated and enmeshed in cotton fabrics for controlled release of a known insecticide (permethrin), and the objective was to use the fabric as a preventive measure for malaria (da Silva et al. 2012).

20.3.6 Graphene

No discussion about nanomaterials is complete without invoking graphene. After its discovery in 2004, graphene has taken the world of materials by storm and it shows no signs of subsiding anytime soon. Research focus on graphene and its properties has been intense for years. Scientists and industrialist alike have been proactive to find applications where graphene could be used. It was therefore natural that graphene be probed as a textile additive for achieving augmented functionalities. Primarily, graphene, its derivatives and its composites have been gauged by their candidacy for making textiles conductive (Gu and Zhao 2011; Shateri-Khalilabad and Yazdanshenas 2013; Yu et al. 2011). In one study, where graphene oxide was reduced to rGO, the dispersion could then be applied to the fabric via a pad-dry technique, which could be used as activity monitoring sensor, and at the same time it increases the tensile strength of the fabric, while not compromising the texture and feel of the fabric (Karim et al. 2017). Graphene incorporated e-textiles in their early stages showed poor conductivity and higher power consumption. Steadily enough, this hurdle was surmounted as reported (Afroj et al. 2020) by producing graphene e-textiles with lowest sheet resistance, which have great flexibility and these also do not lose their functionality even after repeated washing cycles. Due to the high conductivity of the fabrics, skin mounted sensors and ultra-flexible supercapacitors can be realised. Besides being used as activity sensors, graphene infused textiles have also been used in cardiac monitoring (Yapici et al. 2015). When compared to conventional electrodes, the graphene-textile composite showed almost the same performance. An important functionality of textiles that is being sought after is that of fire resistance. It was found that when rGO was dry coated onto silk fabrics, they not only showed robust fire resistance but were also conductive (Ji et al. 2017).

20.3.7 Nanomaterials for Textile Waste Treatment

Textile industry is one of the largest producers of wastewater due to its water consumption for various processes. This aspect is also a major impediment to the development of textile industries, as they are one of the biggest water polluters (Holkar et al. 2016). In addition to harmful dyes belonging to azo, anthraquinone, triarylmethyl families being released, the textile wastewater also contains heavy metals like zinc, cadmium, chromium, copper and arsenic in certain cases, which are also an environmental and public health threat (Chowdhury et al. 2017). Thus, removing such waste matter from textile effluents has become of paramount importance. Nanomaterials have a role to play in textile waste remediation as well (Cai et al. 2017). Due to their high surface to volume ratio, nanomaterials act as effective adsorbents. Adsorption is also a widespread technique involved in the removal of heavy metals. In a systematic review by Jawed et al., the types of nanomaterials used as adsorbents have been laid out. Engineered nanomaterials based on carbon, graphene, iron oxide, titanium oxide, silica and bio-nanomaterials were found to be effective in removing heavy metals (Jawed et al. 2020). Processes that brought about surface functionalization, such as cross linking, electrostatic interactions and chelation, were found to augment the adsorption capacity of nanomaterials. Functionalizing nanomaterials with chemical groups which have strong affinity towards specific heavy metals is also a useful method in arresting heavy metal contamination. These modified nanomaterials would in turn also need to be utilised carefully, which would enable effective desorption and reusability for multiple cycles (Pandey 2021). These technological advancements with nanomaterials, if properly implemented, would be beneficial in treating textile-based wastewater. Dyes, which are another major source of contamination in textile wastewater, have also been removed by employing nanomaterials such as zerovalent iron, zinc, Fe_3O_4 , MgO and TiO_2 (Ruan et al. 2019).

20.4 Commercialized Products

Owing to the large research efforts invested in nanomaterials, a good number of products have actually made it to functioning products, which has created a positive feedback loop leading to even greater emphasis on research into nanomaterials-based textile products. In this section we will inform the reader about such products which are currently in use in markets.

1. *Nanosan*: This is a kind of spun polymeric fibre, which is manufactured by integrating microscale particles into the nanofibre structure. These fibres find applications in filter and adsorbent fabrics (AZoNano 2013). These fabrics can also be engineered to perform as high-strength and flexible materials, and Nanosan fibres have been applied to medical, military, filter and even cosmetic products (Smith and Ring 2016; Lademann et al. 2011, 2016; Chun et al. 2014).

Nanosan is marketed by SNS-Nano Fiber Technology (USA), and Schill and Seilacher (Germany).

2. *SmartSilver*: Marketed by Nano-Horizons (USA), this product is an antimicrobial yarn. The company develops silver nanoparticles additives providing antimicrobial resistance to the products where they are integrated (Delattre et al. 2012, 2015).
3. *Wearable Motherboard*: A flagship of medical-textiles, this fabric is marketed by Sarvint Technologies, Inc. (USA). It uses nano-engineered fibres as sensors of bodily indicators such as blood pressure, temperature, heart rate and respiration rate (Esmailzadeh et al. 2015).
4. *NanoSphere*: This is in essence a finishing technology which is touted to impart hydrophobic properties to surfaces mimicking the lotus effect. The company (Schoeller Textiles AG, Switzerland) manufacturing NanoSphere claims that this technique provides better water/oil repellence than conventional textiles and at the same time retaining its breathability as well as comfort, also the marketer claims that textile functionality is maintained even after many washing cycles (Textiles 2020). The company also has several patents for microbicidal and antibacterial nanofibres and polymer finishing with nanoparticles (Greiner and Röcker 2010; Greiner and Hehl 2008) along with substrate finishing applying nanotubes and nanoparticles (Tabellion et al. 2011).
5. *Gore-Tex*: Originally a microporous structure which could be stretched to about 800% of its original length (Gore and Allen 1980), and in addition, also being lightweight and waterproof, owned by W.L. Gore & Associates (USA). In recent times, though the company has been incorporating nanostructures into its products, for example, their engineered jackets (Gore-Tex 2020). Gore-Tex holds patents for burn protective materials (Panse 2013), nanoemulsions, nanofibres for filtration (Gebert 2014; Xu and Hegenbarth 2014), and nanoparticles for electrical conductors (Cotter et al. 1996).

These products/companies represent a miniscule sample of the entire market, most of the companies and products have come out of developed/developing economies. In the near future, focus will shift to the eastern hemisphere with emerging markets in Asia predicted to be in the lead. Table 20.1 (UnderstandingNano 2019) shows an abridged list of companies currently using nanotechnology to improve textile fabrics.

20.5 A Matter of Cost

Industries willing to adopt nanomaterials into their product lines will also have to bear in mind the associated cost with the introduction of such novel materials. Trends show that with evolving technologies, the manufacture of nanomaterials is increasingly becoming commonplace and this in turn is driving the cost down (Rivero et al. 2015). Synthesis of nanomaterials by techniques such as molecular self-assembly, ultrasonication and solution processing have evolved over the years,

Table 20.1 Representative list of companies employing nanotechnology to improve textile fabrics

Company	Product	Advantage
Nano-tex	Fabric enhanced with nanowhiskers	Water/oil, strain resistance
Aspen Aerogel	Fabric enhanced with nanopores	Insulating properties
BASF	Fabric enhanced with nanoparticles (Mincor [®] TX TT)	Better hydrophobicity
NanoHorizons	Fabric enhanced with silver nanoparticles	Microbicidal and odour inhibition
Schoeller Technologies	Fabric enhanced with nanoparticles (NanoSphere [®])	Water and stain resistant
Nanex	Water-repellent coatings	
Nano Group	Nano-treated fabrics	Liquid and stain resistant, UV protection, etc.
Odegon Technologies	Nanoporous materials which act as adsorbents	
Global Photonics	Fabric woven from thread that generates electricity from the sun (FlexPower [™])	Flexible fabric that generates electricity
Konara	Harnessing solar energy (Power Fiber [™])	Electronic wearables

and are now ripe to be introduced in the industrial domain (Wen and Wu 2014; Tulinski and Jurczyk 2017; Lin and Wang 2014; Duan et al. 2020; Charitidis et al. 2014). At present though, insightful research into the exact cost analysis of nanomaterials being used in the textile industry is still lacking in current scientific literature. One reason for that might be that the enhanced textile products, which involve nanomaterials and focus on performance enhancement with cost reduction, mostly fall under the ambit of conventional apparel industry (Cientifica 2012; Yetisen et al. 2016). With the rapid adoption of nanomaterials in textile-based products, this scenario is bound to change. The total value of the global textile industry was estimated to be near \$1 trillion in 2019. The market is expected to grow at a compounded annual growth rate (CAGR) of 4.3% (Grandviewresearch 2020). It was also estimated that the smart textile market (which incorporates nanomaterials in its products as one of its strategies) would have breached the \$5 billion mark by 2020 (Markets 2015). It is also forecasted that the Asia-Pacific region would see the highest CAGR of ~44% in the next 5 years. It is indeed right to state that the textile market will keep steady in its growth trajectory, and developing economies would be at the forefront. With the market pivoting from conventional textile-based products towards more engineered high-functioning wearables, the applications for nanomaterials in the wider market are diverse (Cientifica 2015). One has also to keep in mind that while textile industries are a big generator of wastes, and nanomaterials can also be used in the remediation of textile waste. This we believe would increase the cost of production in the short term for textile industries.

20.6 Issue of Toxicity

As of date, the most commonly used nanomaterial in the textile industry has been nanoparticles, metallic nanoparticles to be precise. Silver nanoparticles have been incorporated in many textile products as functional additives. On investigation it was found that many silver containing products release considerable amount of nanoparticulate matter into liquids used for washing (Quadros et al. 2013; Benn and Westerhoff 2008; Gagnon et al. 2019). It was also seen that some products released particulates at a lower rate than other products, indicating difference in manufacturing processes, which need to be rectified. In another study, it was found that sweat also led to the release of nanoparticles from impregnated fabrics such as shirts and pants. The pH of the sweat determined the amount of release (Kulthong et al. 2010; von Goetz et al. 2013). Besides Ag nanoparticles, some other nanoparticles are also toxic and are released from textiles which are impregnated with these nanoparticles. In a study, the release of TiO₂ nanoparticles in sweat after incubation was ascertained. It was found that in acidic sweat, the release was about 63 $\mu\text{g g}^{-1} \text{L}^{-1}$ when the particle size was lesser than 450 nm and about 725 $\mu\text{g g}^{-1} \text{L}^{-1}$ when size of the particles was greater than 450 nm. In alkaline sweat, the release was 38 and 188 $\mu\text{g g}^{-1} \text{L}^{-1}$, respectively, for the corresponding particle sizes mentioned earlier (von Goetz et al. 2013; Yu et al. 2007). The release of nanomaterials is obviously a source of concern as they are detrimental to aquatic life (Davies et al. 1978; Grosell et al. 2002) and also might disrupt bacterial habitat owing to its antimicrobial properties (Choi et al. 2008). Carbon footprint of textiles will also need to be assessed seriously. In one such study, it was reported that about 2.55–166 kg of CO₂-equivalent was the impact of silver added shirts depending upon the manufacturing process (Walser et al. 2011). In addition to these detriments based on the form of nanomaterial used as well as the method of manufacturing, potential risks to humans can also occur, for example, in the form of inhalation of the nanomaterials (Demou et al. 2009). These investigations are limited in number and scope at present. However, for the boom that is expected in the textile industry, such studies would need to become more prolific in scope to better gauge the adverse effects of nanomaterials from textile products. Nanomaterials have brought about a sea change in the textile industry, but at the same time it has made us—the consumers, aware of the probable damage that these materials can do to the environment and humans alike. Thus, the onus would be on consumer awareness, which would drive the industries to design better life cycle assessments and toxicity analyses at all stages, beginning from the production of nanomaterials to their incorporation into textiles, their usage, washing and eventual disposal and recycle.

20.7 Going Forward

It would not be an unrealistic claim to make that in the near future the customer demand for trendy as well as multi-functional clothing and accessories would keep rising at a brisk pace. The advent of nanomaterials in the textile markets and

industries has to an extent tried to meet this demand; by offering a huge array of materials with varied functionalities to choose from. Nevertheless, scalability, cost effectiveness, ecological impact, time and work hours are a few challenges that stand before the industry. These factors need to be effectively optimised so that commercialization of nanomaterial-based products does not face impediments. Conventional functionalities such as water/oil repellence, antimicrobial, antistatic and colour blocking have been enhanced by incorporating nanomaterials, in addition to these more advanced functionalities such as drug release, electromechanical sensors, photo/thermal/electrical conductivity, and energy harvesting/storing components integrated directly into fabrics are actively gaining the attention of mainstream products and markets. Customers of present day and age are also concerned about the impact that the products they use have on the environment. As such, an avenue for future research is green synthesis of nanomaterials and environmentally benign finishing techniques, as well as stable nano-additives which can withstand repeated washing. A case in point is the development of newer binding mechanics based on covalency, which could better attach nanomaterials to the textile fabrics. Currently, the continued immobilization of nanomaterials within the textile fabrics is a technical challenge. Thus, innovation in the area of surface finishing needs an impetus that would ensure integrity of the textile products in majority of cases. New nano-additives and stabilizers might have to be invented that would prevent the agglomeration of nanomaterials during the formulation and finishing treatments. This would require novel surface-activated polymers or composites that would help in the adhesion of the nanomaterials to a greater degree, without compromising their unique properties. The potential for polluting water and soil looms over these fantastic and innovative products. Commonly used nanomaterials based on silver, titanium, iron, etc. are in certain cases cytotoxic and can disrupt the delicate ecological balance if the release of these nanomaterials goes unchecked. Nano-textile products that have biocidal properties have been found to destroy important soil bacteria upon their release. Also, recycling of these clothing products poses a challenge as mainly they are dumped in landfills further exacerbating soil pollution. Thus, developing analytical tools which can correctly quantify the release of nanomaterials from textile products is becoming the need of the hour. These risks and challenges further warrant that stricter rules be put in place by the regulators and toxicity analysis be done at all stages of usages so that nano-textiles do not become a serious risk to humans, animals and the environment.

References

- Abeywardena SB, Perera S, de Silva KN, Walpalage S, Somaratne M (2018) Bentonite nanoclay assisted hydrophilic nylon fabrics. *Int J Chem Sci*:1–6
- Afroj S, Tan S, Abdelkader AM, Novoselov KS, Karim N (2020) Highly conductive, scalable, and machine washable graphene-based E-Textiles for multifunctional wearable electronic applications. *Adv Funct Mater* 30(23):2000293
- Agarwal B, Jeffries B (2013) Cutting cotton carbon emissions: findings from Warangal, India. World Wildlife Fund, Gland

- Anjum AS, Ali M, Sun KC, Riaz R, Jeong SH (2020) Self-assembled nanomanipulation of silica nanoparticles enable mechanochemically robust super hydrophobic and oleophilic textile. *J Colloid Interface Sci* 563:62–73
- Arshad N, Zia KM, Jabeen F, Anjum MN, Akram N, Zuber M (2018) Synthesis, characterization of novel chitosan based water dispersible polyurethanes and their potential deployment as antibacterial textile finish. *Int J Biol Macromol* 111:485–492
- Attia NF, Moussa M, Sheta AMF, Taha R, Gamal H (2017) Synthesis of effective multifunctional textile based on silica nanoparticles. *Prog Org Coat* 106:41–49
- AZoNano (2013) Nanotechnology in Ohio, USA: market report. <https://www.azonano.com/article.aspx?ArticleID=3240>. Accessed 12 Aug 2020
- Ballottin D, Fulaz S, Cabrini F, Tsukamoto J, Durán N, Alves OL, Tasic L (2017) Antimicrobial textiles: biogenic silver nanoparticles against *Candida* and *Xanthomonas*. *Mater Sci Eng C* 75: 582–589
- Baranwal A, Srivastava A, Kumar P, Bajpai VK, Maurya PK, Chandra P (2018) Prospects of nanostructure materials and their composites as antimicrobial agents. *Front Microbiol* 9:422
- Barthlott W, Ehler N (1977) Raster-Elektronenmikroskopie der Epidermis-Oberflächen von Spermatophyten. In: *Akad d Wiss ud Literatur*
- Benn TM, Westerhoff P (2008) Nanoparticle silver released into water from commercially available sock fabrics. *Environ Sci Technol* 42(11):4133–4139
- Bian X-M, Liu L, Li H-B, Wang C-Y, Xie Q, Zhao Q-L, Bi S, Hou Z-L (2016) Construction of three-dimensional graphene interfaces into carbon fiber textiles for increasing deposition of nickel nanoparticles: flexible hierarchical magnetic textile composites for strong electromagnetic shielding. *Nanotechnology* 28(4):045710
- Bianchini A, Wood CM (2002) Physiological effects of chronic silver exposure in *Daphnia magna*. *Comp Biochem Physiol C Toxicol Pharmacol* 133(1):137–145
- Bilal M, Asgher M, Iqbal M, Hu H, Zhang X (2016) Chitosan beads immobilized manganese peroxidase catalytic potential for detoxification and decolorization of textile effluent. *Int J Biol Macromol* 89:181–189
- Bradac C, Osswald S (2018) Effect of structure and composition of nanodiamond powders on thermal stability and oxidation kinetics. *Carbon* 132:616–622
- Bradley EL, Castle L, Chaudhry Q (2011) Applications of nanomaterials in food packaging with a consideration of opportunities for developing countries. *Trends Food Sci Technol* 22(11):604–610
- Cai Z, Sun Y, Liu W, Pan F, Sun P, Fu J (2017) An overview of nanomaterials applied for removing dyes from wastewater. *Environ Sci Pollut Res* 24(19):15882–15904
- Cao G (2004) Nanostructures and nanomaterials: synthesis, properties and applications. World Scientific, Singapore
- Cao W-T, Ma C, Mao D-S, Zhang J, Ma M-G, Chen F (2019) MXene-reinforced cellulose nanofibril inks for 3D-printed smart fibres and textiles. *Adv Funct Mater* 29(51):1905898
- Charitidis CA, Georgiou P, Koklioti MA, Trompeta A-F, Markakis VJMR (2014) *Manuf Nanomater Res Indus* 1:11
- Chen L-M, Yu H-Y, Wang D-C, Yang T, Yao J-M, Tam KC (2019) Simple synthesis of flower-like manganese dioxide nanostructures on cellulose nanocrystals for high-performance supercapacitors and wearable electrodes. *ACS Sustain Chem Eng* 7(13):11823–11831
- Choi O, Deng KK, Kim N-J, Ross L, Surampalli RY, Hu Z (2008) The inhibitory effects of silver nanoparticles, silver ions, and silver chloride colloids on microbial growth. *Water Res* 42(12):3066–3074
- Chowdhury MAH, Hoque MM, Naher K, Islam M, Tamim U, Alam K, Khan R (2017) Analysis of heavy metals and other elements in textile waste using neutron activation analysis and atomic absorption spectrophotometry. *IOSR J Environ Sci Toxicol Food Technol* 11:14
- Chun I, Frazier LM, Kataphinan W (2014) Three-dimensional structures for cell or tissue culture. US Patent application no. 14/298, 550

- Cientifica Ltd. (2012) Business report: nanotechnologies for the textile market. 18th April 2012. <https://www.innovationintextiles.com/new-report-nanotechnologies-for-textile-markets>. Accessed 18 June 2021
- Cientifica (2015) Smart textiles and nanotechnologies: applications technologies and markets. 2nd July 2012. <https://www.innovationintextiles.com/smart-textiles-and-nanotechnologies-applications-technologies-and-markets/>. Accessed 18 June 2021
- Cotter MA, Zuckerbrod D, Kesler MC, Reynolds JS (1996) Insulated electrical conductor. US Patent No. 5, 580, 654
- da Silva PM, Sierra-Avila CA, Hinestroza JP (2012) In situ synthesis of a Cu-BTC metal-organic framework (MOF 199) onto cellulosic fibrous substrates: cotton. *Cellulose* 19(5):1771–1779
- Daer S, Kharratz J, Giwa A, Hasan SW (2015) Recent applications of nanomaterials in water desalination: a critical review and future opportunities. *Desalination* 367:37–48
- Danilenko VV (2004) On the history of the discovery of nanodiamond synthesis. *Phys Solid State* 46(4):595–599
- Davies PH, Goettl JP, Sinley JR (1978) Toxicity of silver to rainbow trout (*Salmo gairdneri*). *Water Res* 12(2):113–117
- Delattre JL, Hayes DJ, Cuiffi J, Henry M, Kundrat J, Carrigan P (2012) Wash-durable, antimicrobial and antifungal textile substrates. US Patent Application No. 8,183,167.22
- Delattre J, Kundrat J, Henry M, Haupt R (2015). Wash-durable antimicrobial textiles and methods of manufacture. US patent application no. 14/419, 083
- Demou E, Stark WJ, Hellweg S (2009) Particle emission and exposure during nanoparticle synthesis in research laboratories. *Ann Occup Hyg* 53(8):829–838
- dos Santos CC, Mouta R, Junior MCC, Santana SAA, Silva HA, Bezerra CWB (2018) Chitosan-edible oil based materials as upgraded adsorbents for textile dyes. *Carbohydr Polym* 180:182–191
- Duan Z, Zhao Q, Wang S, Huang Q, Yuan Z, Zhang Y, Jiang Y, Tai HJS, Chemical AB (2020) Halloysite nanotubes: natural, environmental-friendly and low-cost nanomaterials for high-performance humidity sensor. *Sens Actuators B* 317:128204
- El Moumen A, Tarfaoui M, Lafdi K, Benyahia H (2017) Dynamic properties of carbon nanotubes reinforced carbon fibers/epoxy textile composites under low velocity impact. *Compos Part B Eng* 125:1–8
- Esmailzadeh H, Rivard M, Arzi E, Légaré F, Hassani A (2015) Smart textile plasmonic fiber dew sensors. *Opt Express* 23(11):14981–14992
- Fernandez-Fernandez A, Manchanda R, McGoron AJ (2011) Theranostic applications of nanomaterials in cancer: drug delivery, image-guided therapy, and multifunctional platforms. *Appl Biochem Biotechnol* 165(7):1628–1651
- Gagnon V, Button M, Boparai HK, Nearing M, O'Carroll DM, Weber KP (2019) Influence of realistic wearing on the morphology and release of silver nanomaterials from textiles. *Environ Sci Nano* 6(2):411–424
- Gao W, Rigout M, Owens H (2017) The structural coloration of textile materials using self-assembled silica nanoparticles. *J Nanopart Res* 19(9):303
- Gebert R (2014) Filter assembly and mounting flange extension for gas turbine filter assembly. US Patent No. 8, 753, 414
- Ghasemzadeh G, Momenpour M, Omidi F, Hosseini MR, Ahani M, Barzegari A (2014) Applications of nanomaterials in water treatment and environmental remediation. *Front Environ Sci Eng* 8(4):471–482
- Göcek İ (2019) Functionalization of textile materials with nanoclay incorporation for improved characteristics. *J Polytech* 22(2):509–522
- Gore RW, Allen Jr SB (1980) Waterproof laminate. US Patent No. 4, 194, 041
- Gore-Tex (2020) Gore-Tex outerwear. <https://www.gore-tex.com/outerwear>. Accessed 12 Aug 2021
- Grandviewresearch (2020) Textile market size, share & trends analysis report by raw material (wool, chemical, silk, cotton), by product (natural fibers, polyester, nylon), by application, by

- region, and segment forecasts, 2020–2027. <https://www.grandviewresearch.com/industry-analysis/textile-market#:~:text=The%20global%20textile%20market%20size,India%2C%20Mexico%2C%20and%20Bangladesh>. Accessed 19 Feb 2021
- Greiner A, Hehl J (2008) Microbical nano- and meso-polymer fibers produced from polymers and honey, for textile applications. Patent Appl. WO2008049251 B. 1
- Greiner A, Röcker T (2010) Polyethylenimine nanoparticle-containing microbical electrospun polymer fibers for textile applications. US patent application no. 12/446, 749
- Grosell M, Brauner CJ, Kelly SP, McGeer JC, Bianchini A, Wood CM (2002) Physiological responses to acute silver exposure in the freshwater crayfish (*Cambarus diogenes diogenes*)—a model invertebrate? *Environ Toxicol Chem* 21(2):369–374
- Gu WL, Zhao YN (2011) Graphene modified cotton textiles. *Adv Mat Res* 331:93–96
- Han JT, Choi S, Jang JI, Seol SK, Woo JS, Jeong HJ, Jeong SY, Baeg K-J, Lee G-W (2015) Rearrangement of 1D conducting nanomaterials towards highly electrically conducting nanocomposite fibres for electronic textiles. *Sci Rep* 5(1):9300
- Hassani A, Khataee A, Karaca S, Karaca M, Kıranşan M (2015) Adsorption of two cationic textile dyes from water with modified nanoclay: a comparative study by using central composite design. *J Environ Chem Eng* 3(4, part A):2738–2749
- Hebeish A, Farag S, Sharaf S, Shaheen TI (2014) Development of cellulose nanowhisker-polyacrylamide copolymer as a highly functional precursor in the synthesis of nanometal particles for conductive textiles. *Cellul* 21(4):3055–3071
- Holkar CR, Jadhav AJ, Pinjari DV, Mahamuni NM, Pandit AB (2016) A critical review on textile wastewater treatments: possible approaches. *J Environ Manage* 182:351–366
- Houshyar S, Nayak R, Padhye R, Shanks RA (2019a) Fabrication and characterization of nanodiamond coated cotton fabric for improved functionality. *Cellul* 26(9):5797–5806
- Houshyar S, Padhye R, Shanks RA, Nayak R (2019b) Nanodiamond fabrication of superhydrophilic wool fabrics. *Langmuir* 35(22):7105–7111
- Indrová K, Prošek Z, Topič J, Ryparová P, Nežerka V, Tesárek PJAP (2015) Mechanical properties of PVA nanofiber textiles with incorporated nanodiamonds, copper and silver ions. *Acta Polytech* 55(1):14–21
- Jawed A, Saxena V, Pandey LM (2020) Engineered nanomaterials and their surface functionalization for the removal of heavy metals: a review. *J Water Process Eng* 33:101009
- Ji Y, Li Y, Chen G, Xing T (2017) Fire-resistant and highly electrically conductive silk fabrics fabricated with reduced graphene oxide via dry-coating. *Mater Des* 133:528–535
- Jia C, Chen C, Kuang Y, Fu K, Wang Y, Yao Y, Kronthal S, Hitz E, Song J, Xu F, Liu B, Hu L (2018) From wood to textiles: top-down assembly of aligned cellulose nanofibers. *Adv Mater* 30(30):1801347
- Joshi M, Bhattacharyya A (2011) Nanotechnology—a new route to high-performance functional textiles. *Text Prog* 43(3):155–233
- Kalpna VN, Kataru BAS, Sravani N, Vigneshwari T, Panneerselvam A, Devi Rajeswari V (2018) Biosynthesis of zinc oxide nanoparticles using culture filtrates of *Aspergillus niger*: antimicrobial textiles and dye degradation studies. *OpenNano* 3:48–55
- Kaounides L, Yu H, Harper T (2007) Nanotechnology innovation and applications in textiles industry: current markets and future growth trends. *Mater Technol* 22(4):209–237
- Kapoor A, Shankar P, Ali W (2020) Green synthesis of metal nanoparticles for electronic textiles. In: *Green nanomaterials*. Springer, Berlin, pp 81–97
- Karim N, Afroj S, Tan S, He P, Fernando A, Carr C, Novoselov KS (2017) Scalable production of graphene-based wearable E-textiles. *ACS Nano* 11(12):12266–12275
- Khot LR, Sankaran S, Maja JM, Ehsani R, Schuster EW (2012) Applications of nanomaterials in agricultural production and crop protection: a review. *Crop Prot* 35:64–70
- Krifa M, Prichard C (2020) Nanotechnology in textile and apparel research—an overview of technologies and processes. *J Text Inst*:1–16

- Kulthong K, Srisung S, Boonpavanitchakul K, Kangwansupamonkon W, Maniratanachote R (2010) Determination of silver nanoparticle release from antibacterial fabrics into artificial sweat. *Part Fibre Toxicol* 7(1):8
- Lademann J, Frazier LM, Kataphinan W (2011) Textile composite material comprising nanofiber nonwoven. US Patent application no. 13/032, 398
- Lademann J, Frazier LM, Kataphinan W (2016) Method for decontaminating the skin with textile composite material. US Patent Application No. 9,345,629
- Lee T-W, Han M, Lee S-E, Jeong YG (2016) Electrically conductive and strong cellulose-based composite fibers reinforced with multiwalled carbon nanotube containing multiple hydrogen bonding moiety. *Compos Sci Technol* 123:57–64
- Lee E-S, Kim Y-O, Ha Y-M, Lim D, Hwang JY, Kim J, Park M, Cho JW, Jung YC (2018) Antimicrobial properties of lignin-decorated thin multi-walled carbon nanotubes in poly(vinyl alcohol) nanocomposites. *Eur Polym J* 105:79–84
- Leonhardt U (2007) Invisibility cup. *Nat Photonics* 1(4):207–208
- Li H, Liu S, Dai Z, Bao J, Yang X (2009) Applications of nanomaterials in electrochemical enzyme biosensors. *Sensors* 9(11):8547–8561
- Lin Z, Wang J (2014) Low-cost nanomaterials: toward greener and more efficient energy applications. Springer, Berlin
- Liu B, Hu X (2020) Chapter 1. Hollow micro- and nanomaterials: synthesis and applications. In: Zhao Q (ed) *Advanced nanomaterials for pollutant sensing and environmental catalysis*. Elsevier, Berlin, pp 1–38
- Lo LY, Li Y, Yeung KW, Yuen CWM (2007) Indicating the development stage of nanotechnology in the textile and clothing industry. *Int J Nanotechnol* 4(6):667–679
- Lu H, Chen J, Tian Q (2018) Wearable high-performance supercapacitors based on Ni-coated cotton textile with low-crystalline Ni-Al layered double hydroxide nanoparticles. *J Colloid Interface Sci* 513:342–348
- Mariana R (2009) Nanotechnology in textile industry. Fascicle of textiles, leatherwork, vol 16. Editura Universității din Oradea, p 83
- Markets Ra (2015) Smart Textiles market by type. In: *Function, Industry, & Geography—Global Forecast to 2020*
- Maryan AS, Montazer M (2015) Natural and organo-montmorillonite as antibacterial nanoclays for cotton garment. *J Ind Eng Chem* 22:164–170
- Matsuo T (2008) Advanced technical textile products. *Text Prog* 40(3):123–181
- Moazzenchi B, Montazer M (2019) Click electroless plating of nickel nanoparticles on polyester fabric: electrical conductivity, magnetic and EMI shielding properties. *Colloids Surf A Physicochem Eng Asp* 571:110–124
- Mochalin VN, Shenderova O, Ho D, Gogotsi Y (2012) The properties and applications of nanodiamonds. *Nat Nanotechnol* 7(1):11–23
- Morin-Crini N, Lichtfouse E, Torri G, Crini G (2019) Applications of chitosan in food, pharmaceuticals, medicine, cosmetics, agriculture, textiles, pulp and paper, biotechnology, and environmental chemistry. *Environ Chem Lett* 17(4):1667–1692
- Nechyporchuk O, Yu J, Nierstrasz VA, Bordes R (2017) Cellulose Nanofibril-based coatings of woven cotton fabrics for improved inkjet printing with a potential in E-textile manufacturing. *ACS Sustain Chem Eng* 5(6):4793–4801
- Ngô C, Van de Voorde MH (2014) Nanotechnology for the textile industry. In: *Nanotechnology in a nutshell: from simple to complex systems*. Atlantis Press, Amsterdam, pp 321–329
- Norberg K (2005) World nanomaterials demand to reach \$90 billion by 2020. *Int Fib J* 20(6):52
- Ozer RR, Hinestroza JP (2015) One-step growth of isorecticular luminescent metal–organic frameworks on cotton fibers. *RSC Adv* 5(20):15198–15204
- Pandey LM (2021) Surface engineering of nano-sorbents for the removal of heavy metals: interfacial aspects. *J Environ Chem Eng* 9(1):104586
- Panse D (2013) Burn protective materials. US Patent No. 8,383,528

- Pereira C, Alves C, Monteiro A, Magén C, Pereira AM, Ibarra A, Ibarra MR, Tavares PB, Araújo JP, Blanco G, Pintado JM, Carvalho AP, Pires J, Pereira MFR, Freire C (2011) Designing novel hybrid materials by one-pot co-condensation: from hydrophobic mesoporous silica nanoparticles to superamphiphobic cotton textiles. *ACS Appl Mater Interfaces* 3(7):2289–2299
- Pereira C, Pereira AM, Freire C, Pinto TV, Costa RS, Teixeira JS (2020) Nanoengineered textiles: from advanced functional nanomaterials to groundbreaking high-performance clothing. In: *Handbook of functionalized nanomaterials for industrial applications*. Elsevier, Amsterdam, pp 611–714
- Qamar SA, Ashiq M, Jahangeer M, Riasat A, Bilal M (2020) Chitosan-based hybrid materials as adsorbents for textile dyes—a review. *Case Stud Chem Environ Eng* 2:100021
- Quadros ME, Pierson R, Tulse NS, Willis R, Rogers K, Thomas TA, Marr LC (2013) Release of silver from nanotechnology-based consumer products for children. *Environ Sci Technol* 47(15):8894–8901
- Ribeiro AI, Senturk D, Silva KS, Modic M, Cvelbar U, Dinescu G, Mitu B, Nikiforov A, Leys C, Kuchakova I, Vanneste M, Heyse P, De Vrieze M, Souto AP, Zille A (2018) Efficient silver nanoparticles deposition method on DBD plasma-treated polyamide 6,6 for antimicrobial textiles. *IOP Conf Ser Mater Sci Eng* 460:012007
- Rivero PJ, Urrutia A, Goicoechea J, Arregui FJ (2015) Nanomaterials for functional textiles and fibers. *Nanoscale Res Lett* 10(1):501
- Ruan W, Hu J, Qi J, Hou Y, Zhou C, Wei XJ (2019) Removal of dyes from wastewater by nanomaterials: a review. *Adv Mater Lett* 10(1):09–20
- Ryan JD, Lund A, Hofmann AI, Kroon R, Sarabia-Riquelme R, Weisenberger MC, Müller C (2018) All-organic textile thermoelectrics with carbon-nanotube-coated n-type yarns. *ACS Appl Energy Mater* 1(6):2934–2941
- Sawhney APS, Condon B, Singh KV, Pang SS, Li G, Hui D (2008) Modern applications of nanotechnology in Textiles. *Text Res J* 78(8):731–739
- Shabbir M, Kaushik M (2020) Engineered nanomaterials: scope in today's textile industry. In: *Handbook of nanomaterials for manufacturing applications*. Elsevier, Amsterdam, pp 249–263
- Shabbir M, Rather LJ, Mohammad F (2017) Chitosan: sustainable and environmental-friendly resource for textile industry. Wiley, Hoboken, NJ, pp 233–252
- Shahid ul I, Butola BS (2019) Recent advances in chitosan polysaccharide and its derivatives in antimicrobial modification of textile materials. *Int J Biol Macromol* 121:905–912
- Shahidi S, Ghoranneviss M (2014) Effect of plasma pretreatment followed by nanoclay loading on flame retardant properties of cotton fabric. *J Fusion Energ* 33(1):88–95
- Shateri-Khalilabad M, Yazdanshenas ME (2013) Fabricating electroconductive cotton textiles using graphene. *Carbohydr Polym* 96(1):190–195
- Smith DJ, Ring H (2016) Absorbent non-woven fibrous mats and process for preparing same. US Patent Application No. 9,457,538
- Stagnaro SM, Volzone C, Huck L (2015) Nanoclay as adsorbent: evaluation for removing dyes used in the textile industry. *Procedia Mater Sci* 8:586–591
- Stan MS, Nica IC, Dinischiotu A, Varzaru E, Iordache OG, Dumitrescu I, Popa M, Chifiriuc MC, Pircalabioru GG, Lazar V, Bezirtzoglou E, Feder M, Diamandescu L (2016) Photocatalytic, antimicrobial and biocompatibility features of cotton knit coated with Fe-N-doped titanium dioxide nanoparticles. *Materials* 9(9):789
- Subasri R, Hima H (2015) Investigations on the use of nanoclay for generation of superhydrophobic coatings. *Surf Coat Technol* 264:121–126
- Tabellion F, Steingröver K, Waeber P, Lottenbach R (2011) Finishing of substrates. US Patent application no. 12/514,279
- Tamburri E, Guglielmotti V, Orlanducci S, Terranova ML, Sordi D, Passeri D, Matassa R, Rossi M (2012) Nanodiamond-mediated crystallization in fibers of PANI nanocomposites produced by template-free polymerization: conductive and thermal properties of the fibrillar networks. *Polymer* 53(19):4045–4053
- Textiles AS (2020). <https://www.schoeller-textiles.com/en/>. Accessed 12 Aug 2020

- Thangudu S (2020) Next generation nanomaterials: smart nanomaterials, significance, and biomedical applications. In: Applications of nanomaterials in human health. Springer, Berlin, pp 287–312
- Tulinski M, Jurczyk MJM (2017) Nanomaterials synthesis methods: protocols and industrial innovations, pp 75–98
- Tulve NS, Stefaniak AB, Vance ME, Rogers K, Mwilu S, LeBouf RF, Schwegler-Berry D, Willis R, Thomas TA, Marr LC (2015) Characterization of silver nanoparticles in selected consumer products and its relevance for predicting children's potential exposures. *Int J Hyg Environ Health* 218(3):345–357
- UnderstandingNano (2019) Nanotechnology fabric companies. <https://www.understandingnano.com/nanotechnology-fabric-companies.html>. Accessed 12 Aug 2020
- von Goetz N, Lorenz C, Windler L, Nowack B, Heuberger M, Hungerbühler K (2013) Migration of Ag- and TiO₂-(nano)particles from textiles into artificial sweat under physical stress: experiments and exposure modeling. *Environ Sci Technol* 47(17):9979–9987
- Walser T, Demou E, Lang DJ, Hellweg S (2011) Prospective environmental life cycle assessment of nanosilver T-shirts. *Environ Sci Technol* 45(10):4570–4578
- Wen W, Wu J-M (2014) Nanomaterials via solution combustion synthesis: a step nearer to controllability. *RSC Adv* 4(101):58090–58100
- Wood CM, Hogstrand C, Galvez F, Munger RJAT (1996) The physiology of waterborne silver toxicity in freshwater rainbow trout (*Oncorhynchus mykiss*) 1. The effects of ionic Ag⁺. *Aquat Toxicol* 35(2):93–109
- Xiao L, An T, Wang L, Xu X, Sun H (2020) Novel properties and applications of chiral inorganic nanostructures. *Nano Today* 30:100824
- Xu P, Hegenbarth J (2014) High purity Perfluoroelastomer composites and a process to produce the same. US Patent No. 8,623,963
- Xu Q, Ke X, Ge N, Shen L, Zhang Y, Fu F, Liu X (2018) Preparation of copper nanoparticles coated cotton fabrics with durable antibacterial properties. *Fibers Polym* 19(5):1004–1013
- Xu X, Song K, Xing B, Hu W, Ke Q, Zhao Y (2019) Thermal-tenacity-enhanced and biodegradable textile sizes from cellulose nanocrystals reinforced soy protein for effective yarn coating. *Ind Crop Prod* 140:111701
- Yamanaka M, Hara K, Kudo J (2005) Bactericidal actions of a silver ion solution on *Escherichia coli*, studied by energy-filtering transmission electron microscopy and proteomic analysis. *Appl Environ Microbiol* 71(11):7589–7593
- Yang Y, Han S, Fan Q, Ugbolue SC (2005) Nanoclay and modified Nanoclay as sorbents for anionic, cationic and nonionic dyes. *Text Res J* 75(8):622–627
- Yapici MK, Alkhidir T, Samad YA, Liao K (2015) Graphene-clad textile electrodes for electrocardiogram monitoring. *Sens Actuators B* 221:1469–1474
- Yetisen AK, Qu H, Manbachi A, Butt H, Dokmeci MR, Hinstroza JP, Skorobogatiy M, Khademhosseini A, Yun SH (2016) Nanotechnology in Textiles. *ACS Nano* 10(3):3042–3068
- Yin T, Qin W (2013) Applications of nanomaterials in potentiometric sensors. *Trends Anal Chem* 51:79–86
- Yin X, Krifa M, Koo JH (2015) Flame-retardant polyamide 6/carbon nanotube nanofibers: processing and characterization. *J Eng Fibers Fabr* 10(3):155892501501000301
- Yu M, Gu G, Meng W-D, Qing F-L (2007) Superhydrophobic cotton fabric coating based on a complex layer of silica nanoparticles and perfluorooctylated quaternary ammonium silane coupling agent. *ApSS* 253(7):3669–3673
- Yu G, Hu L, Vosgueritchian M, Wang H, Xie X, McDonough JR, Cui X, Cui Y, Bao Z (2011) Solution-processed graphene/MnO₂ nanostructured textiles for high-performance electrochemical capacitors. *Nano Lett* 11(7):2905–2911
- Zhukovskiy M, Sanchez-Botero L, McDonald MP, Hinstroza J, Kuno M (2014) Nanowire-functionalized cotton textiles. *ACS Appl Mater Interfaces* 6(4):2262–2269



Properties and Characterization of Advanced Composite Materials

21

Md. Shahruzzaman, Shafiu Hossain, Sumaya F. Kabir,
Tanvir Ahmed, Md. Minhajul Islam, Sabrina Sultana, Abul K. Mallik,
and Mohammed Mizanur Rahman

Abstract

Comparing to the last century, advanced composite materials (ACMs) are currently becoming more important and have perceived significant interest. ACMs are also known as advanced polymer matrix composites and have found broad and recognized applications in the aircraft, aerospace, and sports equipment sectors. The primary advantages of advanced composite materials are their high strength, high stiffness, high modulus, low density, relatively low weight, excellent resistance to fatigue, and corrosion resistance. Materials with such categories are called “advanced” materials. Typical advanced composite materials include reinforced concrete, plywood, fiber-reinforced polymer or fiberglass, ceramic matrix composites, metal matrix composites, etc. However, while advanced composite materials have promised significant benefit, most of them are associated with some undesirable difficulties such as high moisture absorbance capacity, expensive, labor-intensive, less plastic deformation before failure, etc. The unique physical and chemical properties of advanced composite materials are replacing metal components in many uses, particularly in the aerospace industry for aircraft and aerospace structural parts. The focus of this chapter is to point out the characterization techniques of advanced composite materials. In addition,

M. Shahruzzaman (✉) · S. F. Kabir · T. Ahmed · M. M. Islam · A. K. Mallik · M. M. Rahman
Department of Applied Chemistry and Chemical Engineering, University of Dhaka, Dhaka,
Bangladesh
e-mail: shahruzzaman@du.ac.bd

S. Hossain
Department of Chemical Engineering and Polymer Science, Shahjalal University of Science and
Technology, Sylhet, Bangladesh

S. Sultana
Department of Arts and Sciences, Ahsanullah University of Science and Technology, Dhaka,
Bangladesh

various types of advanced composite materials are also presented. It also summarizes what the authors believe are the significant properties and requirements for advanced composite materials.

Keywords

Composite material · Aerospace · Reinforcement · Stiffness · Polymer matrix

21.1 Introduction

Advanced composite material is a great invention in the field of material science, and it performs outstanding characteristics due to its excellent mechanical properties and high strength-to-weight ratio (Carlsson et al. 2014). Generally, composite material consists of a mixture of two or more micro- or macroconstituents resulting in a material that can be designed to have improved properties than the constituents alone. The primary advantages of composite materials are their high strength, high stiffness, high modulus, low density, relatively low weight, excellent resistance to fatigue, and corrosion resistance. The subsequent properties are mainly reliant on the distribution, percentage contents, and geometries of the constituents. Materials with such classes are known as “advanced” materials. In other words, composite material is represented as advanced composites when two or more phased material is combined together in which one of them is stronger and stiffer and serve as the basis of primary load-carrying phase and the other one is a weak link. The story of the advanced composite material has passed a long journey since 1930. Before that people have manufactured different types of laminated composites made of metallic and nonmetallic substances. The development of polymer-based composite materials attracted commercial utilization in numerous fields by 1960. At the beginning, composites are treated as high-class materials which are structured and manufactured for multipurposes such as mechanical and aerospace, automotive, and sporting tools due to their superior features.

Typically, a composite is a combination of two different materials which are termed as continuous phase or matrix or binder and discontinuous phase or reinforcement. On the one hand, the reinforcement material (fibers, whiskers, particulates, or fabrics) delivers the mechanical strength and transfers load in the composite. On the other hand, the matrix protects the reinforcement from abrasion or environment by binding and upholding the alignment or spacing of the reinforcement material with a view to giving it a desirable structure. Depending on the application, the reinforcements can be harder or softer. In case of components that needed excellent wear resistance, harder reinforcements are used, while to attain properties like greasing substances, softer reinforcements having excellent corrosion-resistant properties such as graphite and molybdenum (Mo) are selected. The quality of the composite materials completely relies on the properties of the reinforcements and the matrix. There are several factors that influence the physical characteristics of composite such as the geometrical structure of the discontinuous

phase, size and shape of the reinforcing material, percentage of content, and alignment of reinforcement (Callister and Rethwisch 2011).

Galy et al. (2017) studied the mechanical properties of silicon carbide (SiC)-reinforced aluminum metal matrices (Al-MMCs) and showed that the hardness of the composite decreases after increasing the particle size. In addition, Rao et al. (Rao 2018) experimented the SiC-reinforced Al 7075 and observed that the mechanical properties of the composite was improved by increasing the size of the particle and the ratio of SiC. Pradhan and his coworkers (Pradhan et al. 2017) reported the fabrication of SiC-reinforced aluminum alloy LM6 MMC by stir casting method and studied its tribological properties. The study showed that the minimum friction was obtained in dry sliding condition than moist environment and after that in a basic medium. Moreover, Kandpal et al. (Kandpal and Singh 2017) reviewed the characteristics of Al₂O₃-reinforced Al 6061 composite. The finding of the experiment indicates that the ductility reduced with the increase of reinforcing material (Al₂O₃).

Application of advanced composites can be originated from aerospace, marine, automotive areas to biomedical implants. Nowadays, various composites have been used for strengthening of different structural elements. Fiber-reinforced plastic (FRP) and carbon fiber-reinforced plastic (CFRP) systems become very popular that offer a higher strength-to-weight ratio and stiffness-to-weight ratio than many structural materials. These lightweight composites aid many applications where the potential energy savings and carbon emissions reduction occur. RC beam usually wrapped with the polymer composites such as glass fiber-reinforced polymer, carbon fiber-reinforced polymer, basalt fiber-reinforced polymer, aramid fiber-reinforced polymer, etc. With the recent advancement of composites and due to their superior properties, metal matrix composites have been used in various arenas of engineering. The structures used in aerospace purposes completely depend on the composite materials. These materials are very significant for the development of different aircraft tools and machineries. Numerous aircraft parts, for example, fairings, spoilers, landing gear doors, flight control surfaces, propellers, turbine engine fan blades, and interior components, were developed for their less weight than aluminum materials. The main body and wing of the modern aircraft are made from the composite materials which demand for the detailed knowledge of composite properties due to the repair of composite structures. This chapter provides a concise summary of properties and characterization of advanced composites and their types with their important aspects. It outlines what the authors accept are the critical prerequisites for advanced composite materials.

21.2 Classification

The classifications of advanced composite materials are commonly based on either the forms of reinforcements or the matrices used.

21.2.1 Based on Matrix Materials

Advanced composites are divided into three types based on the geometry of the matrix as follows: polymer, metal, and ceramic.

21.2.1.1 Polymer Matrix Composites (PMCs)

Among available composites, PMCs are currently the most frequently used advanced composites. However, the matrix of PMCs is usually reinforced with ceramic fibers due to their higher strength than the polymer matrix material. The properties of PMCs are influenced by several factors such as the matrix material, reinforcing agent, process control parameters, microstructure, nanostructure, percentage of content, and the interphase. PMCs are familiar in recent years due to the cost-effective and easy manufacturing method. The producers of PMC can make easily affordable products with numerous manufacturing processes. PMCs are composed of matrix material like thermoplastic or thermosetting plastic and one or more reinforcing agents like carbon, glass (E-glass, S-glass, etc.), steel, and natural fibers. Polymers can be processed very conveniently to produce good components, as they are lightweight in nature. Polymer matrix composites (PMCs) deal with a broad range of properties such as low cost, excellent tensile properties, high chemical and corrosion resistance, and outstanding mechanical features. The PMCs are usually applied in skyrocket, airplane, and sporting tools (Bhargava 2012).

21.2.1.2 Ceramic Matrix Composites (CMCs)

Ceramic matrix composites are a mixture of ceramic matrix like calcium aluminosilicate with ceramic particulates, fibers (e.g., carbon or silicon carbide), and whiskers. CMCs are usually solid materials that exhibit strong chemical bonding like ionic and sometimes covalent too. Though ceramics fail catastrophically under tensile or impact loading, the ceramic matrix composites are having exceptional advantages such as high compressive strength, corrosion resistance, high melting points, chemical inertness, low density, and stability at high temperatures (Akca and Gursel 2015). Ceramic matrices are commonly used in elevated heating region of the machineries such as pistons, blades, casing, and rotors in gas-turbine parts. The metal and polymer matrix composites are not suitable for utilization in this purpose. The CMCs can endure at elevated temperatures, and they can operate very efficiently also in corrosive conditions. It is crystal clear that the principal goals of making CMCs are to improve the toughness of the materials for the reason that monolithic ceramics have high stiffness and strength.

21.2.1.3 Metal Matrix Composites (MMCs)

Due to their enhanced mechanical and thermal properties, metal matrix composites are familiar as advanced materials. MMCs perform more excellent properties compared to the other engineering materials in terms of good wear resistance and exceptional thermal conductivity. The excellent elastic characteristics, extreme heat enduring capability, insensitivity to aqueous condition, good corrosion resistance and better wear, tear, abrasion, flaw, and fatigue resistances have made MMCs

more attractable (Akca and Gursel 2015). MMCs show better characteristics than the monolithic metal such as steel. Currently, different metals such as aluminum, copper, iron, nickel, and titanium are the most commonly used matrix metals for MMCs. Among the matrix metals, aluminum-based MMCs are the mostly used MMCs applied in vehicle and aircraft structures due to their good forming and assembling properties, reduced density, high strength, and corrosion resistance.

21.2.2 Based on Reinforcing Materials

Advanced composites can be also classified according to the geometry of the reinforcement as follows: particulate, flake, fibers, nanocomposites, foamed composites, and biocomposites.

21.2.2.1 Particulate Composites

The particulate composites consist of particles incorporated in matrices like alloys and ceramics. As the particles are immersed randomly, they are usually called isotropic. These composites have provided some benefits like better strength, higher operating temperature, and corrosion resistance. Examples of such kind of composites include aluminum particles in rubber and silicon carbide (SiC) particles in aluminum, etc.

21.2.2.2 Flake Composites

Flake composites consist of flat reinforcements of matrices. These composites are very attractable because of high tensile strength, excellent flexural strength and modulus, and easily affordable cost. However, the difficulty associated with the orientation of the flakes has reduced its applications. Glass, aluminum, and silver are the most commonly used flake materials.

21.2.2.3 Fiber Composites

Fibers are generally anisotropic in nature. The fiber composites consist of matrices reinforced with different length of fibers. The basic units of long fiber-matrix composite may be unidirectional or woven fiber laminas. Examples of such kind of matrices are epoxy, aluminum, and calcium aluminosilicate.

21.2.2.4 Nanocomposites

Nanocomposites have attracted a great interest in the field of material science. At least one of the constituent materials of the nanocomposite is in the scale of nanometers (10^{-9} m). The size of the constituent substances of the advanced composite materials are in the microscale (10^{-6} m) range. The nanocomposites show better properties than the composite resulting from the material of microscale. Nanocomposites have played a great role in versatile fields such as pharmaceutical industries, biomedical field, water purification, packaging purposes, food and cosmetics industries, etc.

21.2.2.5 Foamed Composites

Foamed composites perform excellent features among the recently produced materials. The necessity for the production of lightweight constructional materials and acoustic and thermal insulating materials have expedited the invention of foamed composite. The foamed composites may be composed of fiber and polymeric resin. The durability, excellent mechanical properties, and elastic behavior of the foamed composites have increased their applications in versatile fields. The foamed composites can be utilized as noise absorber, barrier for sound transmission, and vibration inhibitor.

21.2.2.6 Biocomposites

Biocomposites are eco-friendly materials that are composed of two or more components containing at least a naturally derived material. The natural polymers include polysaccharides, such as chitin, chitosan, cellulose, heparin, and chondroitin; proteins, such as gelatin, keratin, fibrin, and soy protein; etc. The synergistic effect of the constituent materials in the biocomposites show more excellent property than the individual constituents. The biodegradability, biocompatibility, antimicrobial activity, excellent mechanical properties, and wear resistance of the biocomposites have augmented their utilization in versatile sectors (Hasan and Pandey 2015).

21.3 Manufacturing Process

21.3.1 Compression Molding

Compression molding is one of the oldest methods used to manufacture advanced composite materials. This method is popular in the industrial and commercial fabrication of plastic materials. It is used to manufacture different types of electrical items such as wall switch plates and circuit breakers; kitchen items such as bowl, cups, and dishware; machinery items such as pump components, gears, brake parts, and vehicle panels; and other items such as bottle caps, buttons, protective helmets, etc.

In this process, a thermoset resin is subjected to heating under severe pressure within a closed mold cavity. Under pressure, the resin liquefies as it is heated to the required temperature, and it flows as a viscous liquid to take the shape of the mold. The heat and pressure induce the resin to cure as a result of a chemical reaction. This reaction causes cross-linking of the long polymeric molecules in the resin, thus hardening into the desired part or product (Guerrero et al. 2019). After cooling it down to an extent where the resin has become strong enough to hold its structural integrity, the mold is removed, and the cycle is complete although the curing reaction continues as it cools down to room temperature (Tatara 2017). Some examples of commonly used resins are phenolic (phenol formaldehyde), urea-formaldehyde, silicone, melamine-formaldehyde, vinyl ester, epoxy, polyester, rubber, alkyds,

diallyl phthalate (allyls) along with various elastomers. This method is used to manufacture items having excellent mechanical performance.

21.3.2 Reaction Injection Molding

Reaction injection molding (RIM) is a versatile method for composite manufacturing. In this method, different liquid materials are regulated separately into a mixing head where they are combined by high-pressure impingement mixing. They, then, polymerize to take the shape of the mold. The required equipment includes material conditioning system, high-pressure metering system, mixing head, and mold carrier. As this process requires the mold to hold a chemical reaction, the liquid starting materials are consistent in every shot. For this reason, the material conditioning system has several tanks to hold the starting materials and agitators to make sure that the material in the tanks has a constant temperature.

Poly(dimethylsiloxane), cyclic olefin polymer (COP), cyclic olefin copolymer (COC), polymethylmethacrylate (PMMA), polycarbonate (PC) and polystyrene (PS), and polyurethane are most commonly used materials in this method (Sandström et al. 2015).

21.3.3 Resin Transfer Molding

Resin transfer molding method has gained attention due to its application in natural fiber-reinforced composite fabrication. Different types of materials can be produced by this method including small supporting tools for buses to big machineries for water purification system (Lee and Wei 2000).

The method uses several layers of fiber mats or even cloths laid inside the mold cavity. The resin is placed into the mold through the injection ports and gradually impregnates the fibers. The resin engulfs the mold as air is expelled through the air vents. As the mold is filled up, it is cured (Zhao et al. 2004). The complexity of resin impregnation is influenced by some factors like the alignment of the fibers, mold temperature, resin thickness, and injection pressure. A special type of cost-effective resin transfer molding technique is vacuum-assisted resin transfer molding which is used to produce glass fiber-reinforced composites. This process uses a vacuum to drive the resin to fill the mold.

21.3.4 Filament Winding

Filament winding, a type of open mold method, is a relatively simple method of composite fabrication. This method uses rovings or monofilaments as continuous reinforcements over a rotating mandrel (Shibley 1982). This method is usually employed to manufacture pressure vessels, rocket motors, natural gas vehicle tanks, power transmission shaft sand roller, sporting goods, and boats.

In this method, filament-, wire-, yarn-, or tape-like continuous reinforcements are kept in a rotating form by either impregnating with a matrix material before or impregnating during winding. The wound form is cured after the application of sufficient amount of layers. Finally, the mandrel can be removed or left as part of the structure to meet certain stress conditions. The most popular fiber for commercial filament winding is fiberglass. Aramid fibers have also been used extensively. They can impart great consistency in making by ensuring a low coefficient of strength variation. Lastly, carbon fibers have taken this mantle to an unprecedented height due to its improvements in fiber modulus, tensile strength, and surface finish. The major advantages of the filament winding method are its low cost and capacity to fabricate composite with high fiber volume. The low cost is due to the reason that expensive fibers can be combined with an inexpensive resin to produce an inexpensive but stronger composite.

21.3.5 Lay-Up Manufacturing

Lay-up process opened the possibility of producing thermoplastic composites in large-scale industrial applications. In this process, thermoplastic prepreg tapes are prepared by laying up fibers and resin mixture in a specified pattern. These prepreg tapes are bonded together by heat and pressure. For this purpose, a hot torch or laser is usually used to heat up and melt the thermoplastic matrix. Pressure is applied using a compaction roller after preparing the tapes and heating it up to the required temperature. While the hand lay-up process requires manually laying down individual layers or prepregs by hand. Fibers are pre-impregnated with resin and bundled into tows. Then, they are arranged either in a single unidirectional ply or woven together (Elkington et al. 2015). This process is cost-effective and easily adjustable with different new parts.

21.3.6 Spray-Up Manufacturing

Spray-up manufacturing is another type of open mold method for composite fabrication. This method is also known as directed fiber preforming process. Here, fiber rovings like glass and carbon are chopped and sprayed onto a mold surface along with low viscosity resin. This method is applicable for both synthetic and natural fiber and can be used to fabricate components of structural fittings (Zin et al. 2019).

This method uses spray guns connected to a robotic arm to deposit chopped strands of the reinforcing fiber. The chopped fiber strands are mixed with resin and catalyst and deposited onto a mold surface. Pressure is applied on the mold surface after the composite layering is complete to remove any unwanted void. The advantage of this method is that it helps to prepare materials having dimensionally accurate parts.

21.4 Properties of Advanced Composite Materials

21.4.1 Physical and Chemical Properties

ACMs encompass advantageous physical and chemical properties that make them a multibillion-dollar industry worldwide. These enviable properties include the light weight combined with the high rigidity and thermal immovability, strength in the path of fiber reinforcement, temperature and chemical stability, high strength fiber with low density, hygroscopic tenderness, electrical and environmental robustness, and resistance to corrosion and erosion (Pilato and Michno 1994). Due to these properties, ACMs are taking the place of metal elements in many applications, in particular in the aerospace manufacturing. This section addresses these properties briefly to comprehend the grounds behind growing significance of ACMs in various engineering applications.

21.4.1.1 Weight and Density

In the stringent significance, lightweight construction, which even surpass the performance and safety requirements, are gaining more importance, and in several structural applications, ACMs have been shown to be efficient although having a lighter weight compared to other available materials.

Density of AMC depends on the reinforcement (particle, whisker, or fiber) and matrix used. With increasing weight percentage of reinforced material, bulk density tends to increase. Carbon fiber-reinforced composites have lower density compared to glass reinforced composites. It is also a function of processing temperature, although different composites behave differently with varying temperature. Selection of high- or low-density AMCs depend on their applications in specific condition (Wu and Kim 2011).

21.4.1.2 Hygroscopic Sensitivity

Hygroscopic behavior of a substance is a route in which water molecules are attracted and retained by either absorption or adsorption from the neighboring environment, which is normally as usual in room temperature. As high-performance composites need advanced understanding of their mechanical performance in diverse surroundings, it is required to predict how ACMs behave when they are often exposed to changing humid environments throughout their lifespan. Biocomposites cooperate with the humid atmosphere due to the hydrophilic nature of natural fiber reinforcements, and their sensitivity to moisture is generally described by their complicated multiscale arrangement and biochemical structure (Hill et al. 2009). Réquillé et al. (2019) used hemp/epoxy unidirectional biocomposites to give an extensive comprehension into sorption of moisture over a widespread range of relative humidity to explain its effect on progression of the tensile behavior. Their measurement of moisture sorption and hygroscopic strain showed that an exponential decay of tensile modulus for increasing moisture content and the observed progression of the hygroscopic characteristics is accountable for the formation of inclusive radial stresses on the fiber/matrix interface, which elevates

the transfer of load and improves the performance of the interface. Several researches on how transient residual stresses in PMCs can be influenced by moisture inclusion and influence of anisotropy has been done (Tounsi et al. 2005). In every case, these residual stresses were highly affected by the hygroscopic behavior of the composites and responsible for the optimal design of composite structures. Zawada et al. (2003) studied the fatigue behavior of different CMCs in moist environment. The study showed that direct contact to moisture fog resulted in rapid deterioration of the fiber coating and radically decreased fatigue endurance.

21.4.1.3 Thermal Stability

In order to use ACMs as insulating and structural materials as well as in aircraft engineering, it is important to have a comprehend knowledge about their thermal properties. Takeno et al. (1986) prepared carbon, silicon carbide, and alumina fiber-reinforced epoxies as ACMs and measured their thermal conductivity and thermal contraction to investigate their use in cryogenic application. The study found that these materials are classified as appropriate for cryogenic structural support members and effectiveness under variable thermal condition depends upon the fiber type. Hancox (1998) summarized the works of numerous researchers on effects of thermal cycling and thermal degradation on different PMCs. Thermal cycling damage, mainly matrix cracking resulting in reduced flexural and transverse properties, has been widely documented. There tends to be a minimum temperature, depending on the material, below which no damage or deterioration occurs, but beyond that, for a given processing time and temperature, degradation is higher in oxidized condition than in inert environment. The frictional portion of the interfacial stress was seen to be virtually insignificant when the thermal expansion of the matrix was smaller than that of the fiber and increased linearly with thermal expansion difference when the thermal expansion of the matrix was higher in a number of CMCs reinforced with silicon carbide fibers. A wide range of CMCs are currently being used in heat exchanger, HVAC systems, and emerging energy technologies for their thermal stability (Sommers et al. 2010). Thermal expansion of fiber- and particle-reinforced MMCs over a wide range of temperature exhibits moderate residual strains.

21.4.1.4 Electrical Conductivity and Resistivity

ACMs are extensively used in modern appliances as resistors, sensors, and transducers, such as thermistors, piezoresistors, and chemical sensors. Electrical conductivity of PMCs such as polymer/graphite composites depends on the configuration of percolation arrangement, while it depends on parameters of filler and matrix (Kausar and Taherian 2018). Electrical resistance of PMCs depends on the tensile strength. It increases at the beginning of tensile test, but falls due to the debonding of the fibers/matrix and then suddenly amplifies before the breakdown of the samples due to the breakup of the fibers (Harizi et al. 2019). In CMCs, use of carbon fibers increases the electrical conductivity, provided the fibers associate each other and the voltage source. But in general, CMCs can be used as an excellent electrical insulator. Effectiveness of resistance to electricity of CMCs can be comprehended by dielectric constant, which is the ratio of the permittivity of the

material to that of vacuum. Due to presence of free electrons, metals are highly electrically conductive, and that is why MMCs provide comparatively higher conductivity compared to other conventional composites (Clyne 2018).

21.4.1.5 Magnetic Permeability

Magnetic permeability of any material is known as the material's characteristic to enable the magnetic force line, which is directly proportional to the conductivity of the material to traverse it. PMC material based on Nd-Fe-B reinforced with epoxy provides exceptional amalgamation of better magnetic and mechanical properties. The magnetic filler material is directly accountable for the magnetic activity of the bonded magnets obtained (Grujić et al. 2010). Glass fiber-reinforced epoxy PMC can be mixed with cobalt or barium ferrite particles to introduce magnetic properties among them, which enables excellent ability for the examination of these materials by means of nondestructive tests (NDT) that are sensitive to changes in magnetic field. It helps to establish magnetic flux leakage (MFL) testing, which is a frequently used NDT to identify rust, pitting, fatigue, and wall failure in steel structures, comprising steel pipelines (Fulco et al. 2016). The nanocomposites of iron-aluminum MMC reinforced with carbon nanotube demonstrated an incessant rise in saturation magnetization with the increase in the aluminum content and with integration of cobalt nanoparticles, the soft magnetic characteristics of the MMC substantially enhanced by dropping coercion and retentivity (Tugirumubano et al. 2020). Incorporation of magnetite (Fe_3O_4) nanoparticles into aluminum-based MMC improves its magnetic properties greatly. An increase in the saturation magnetization and remanence magnetization and a gradual drop in coercive field can be found with increasing magnetite content (Ferreira et al. 2016).

21.4.1.6 Corrosion and Erosion Resistance

AMCs corrosion entails the chemical or physical degradation of its components (comprising the structure of the fiber-matrix and the protective surface coat) when introduced to an aggressive atmosphere. Once exposed to CO and CO₂ vapors, carbon and glass fiber-reinforced PMCs experience corrosion. In presence of oxygen, carbon fibers are more vulnerable to oxidation and glass fibers with higher silica content show greater corrosion resistance. Nearly all matrices of metals form oxides with gaseous oxygen; that is why they have a poor resistance to corrosion. Ceramic matrices, on the other hand, exhibit excellent resistance to oxidation (Hihara and Latanision 1994).

Erosion behavior of AMCs refers to weakening the material surface due to mechanical activity, often due to impingement of liquid, slurry scratch, fast-flowing liquid or gas suspended particles, bubbles or droplets, cavitation, etc. Tilly et al. (Tilly and Sage 1970) studied the sand erosion characteristics of composites made from glass/nylon, carbon/nylon, glass/epoxy, and steel/epoxy and accomplished that composite materials typically have low erosion resistance. Pool et al. researched the erosion activity of composites of graphite/polyimide, aramid/polyimide, aramid/epoxy, and graphite/polyphenylene sulphone (PPS) and found that well-bonded ductile fibers pose the lowest erosion rates in a thermoplastic matrix (Pool et al.

1986). In general, glass and graphite fibers are fragile and quickly break. On the other hand, until breakup, aramid fibers break into fibrils and absorb a significant amount of energy and poses better erosion resistance (Mitramajumdar and Aglan 1992).

21.4.1.7 Environmental Friendliness

The applications of composite materials have dramatically increased in the recent years which has become a matter of great concern in terms of sustainable development. The production of composite materials with reducing the number of nonrecyclable plastic wastes and nullifying the environmental impact is the major target to maintain the environmental friendliness. The biocomposites are the green composites that are composed of natural fibers and have very low adverse effect on environment. These composites are very eco-friendly due to their low carbon dioxide emission, reduced energy consumption, biodegradability, and biocompatibility. Recently, these properties are taken into consideration during the production of any type of composite materials.

21.4.2 Mechanical Properties

ACMs comprehend useful mechanical properties that make them exceptional materials for replacing metal and ceramic components. These desirable mechanical properties include tensile strength, flexural strength and modulus, fracture toughness, impact strength, fatigue endurance, hardness, etc., which are discussed in the following.

21.4.2.1 Tensile Strength

PMCs are highly anisotropic material and have higher tensile strength and stiffness. The strength and stiffness of PMCs are high when measured similar to the fibers but low when measured vertical to the fibers. Their stress versus strain curves are normally linear to failure. The general key characteristics of PMC are such that they are more efficient in uniaxial tensile loads and bending, giving less deflections and more resistant to dynamic loads (Kaur and Singh 2020). The fiber-matrix stress transfer function plays an important role on PMC's mechanical efficiency (Mohammed et al. 2015). For instance, Franco and Gonzalez studied the mechanical behavior of high-density polyethylene (HDPE) reinforced with continuous henequen fibers (Herrera-Franco and Valadez-Gonzalez 2004). They observed a 10% increase in longitudinal tensile strength and a 43% increase in the transverse tensile strength (from 2.75 MPa to 3.95 MPa).

CMCs generally possess excellent compression strengths, and their density is very low compared to the structural metals. Gadow et al. (2005) used not only continuous liquid phase-coated carbon fibers but also uncoated fibers to prepare unidirectionally reinforced CMCs with polysiloxane-based matrix. They observed that fibers coated with carbon and silicon carbonitride have increased the strength of

the composite. Though the coatings created decoupling during processing, it improved the fiber-matrix interface properties.

MMCs show excellent tensile modulus and strength when metal matrices are reinforced with any fiber. The stress versus strain curves of MMCs frequently show substantial nonlinearity brought about from yielding of the matrix. MMCs act as brittle materials though they show nonlinearity in stress-strain curves.

21.4.2.2 Flexural Strength and Modulus

Flexural properties denote the stiffness of the materials, and they measure the strength when materials are subjected to bending (Benkhelladi et al. 2020). Franco and Gonzalez (2004) observed that for the HDPE-henequen fiber composites (Fig. 21.1), fiber-matrix adhesion was promoted by fiber surface modifications using a silane coupling agent. They observed that for longitudinal fiber direction, the flexural strength increased from 95.9 to 130.5 MPa, and for the transverse fiber direction, the flexural strength increased from 6.2 to 15.6 MPa, respectively. Such changes represent flexural strength increases of approximately 36% and 251% in longitudinal and transverse directions with respect to the matrix strength. It is clear from the research findings that the modification of surface has little influence on the fiber-dominated behavior of the materials. However, for the matrix-dominated behavior, such as the transverse fiber direction, the improvement in the fiber-matrix interactions shows a more significant role (Suzuki and Ohsawa 2015).

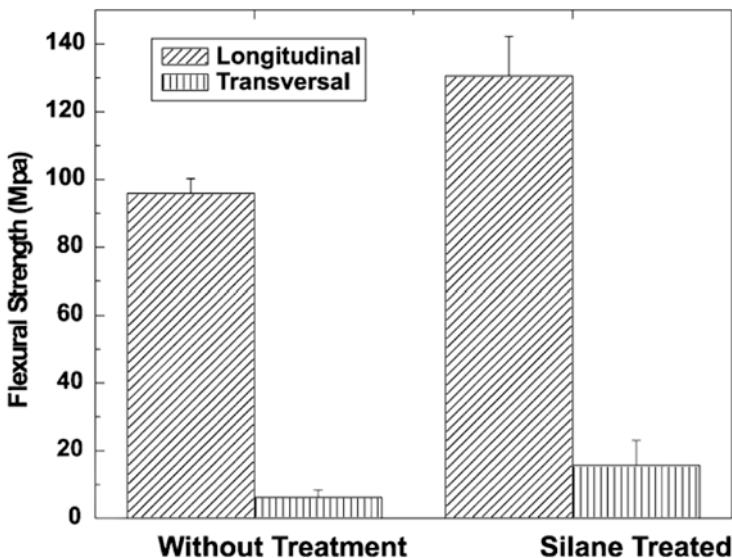


Fig. 21.1 Effect of various fiber surface treatments on the flexural strength of HDPE-henequen composites. (Reprinted from PJ Herrera-Franco and A Valadez-Gonzalez (2004) with permission from Elsevier)

Multidirectional reinforced composites are weaker than unidirectional reinforced composite. Because the number of fibers oriented in any specific directions are very low. The flexural and tensile strengths for a good unidirectional fiber-reinforced CMC was found in the range of 600–1600 MPa. Ochi produced composite materials from kenaf fibers and PLA resin having the unidirectional and biodegradability properties (Ochi 2008). He demonstrated the effect of fiber content on tensile and flexural strengths and found that both properties increase linearly with increasing the amount of fiber up to 50%. Increasing the fiber content up to 70%, the tensile and flexural strengths were found 223 and 254 MPa, respectively. Benkhelladi et al. (2020) prepared composites from three naturally available fibers such as flax, jute, and sisal reinforced with epoxy resin, using a 10–20 wt% volume fraction of fiber. The flexural modulus of flax-, jute-, and sisal-reinforced composites was found 61.87%, 14.80%, and 25.19%, respectively, resulting from the excellent bonding between fibers and matrix. It was concluded that the fiber–matrix interface greatly influences the mechanical properties of composite materials.

The improvements in properties of fiber-reinforced CMCs are dependent upon fiber architecture. Like PMCs, the fiber-reinforced ceramic matrix composites are also anisotropic. Hyde studied the properties of carbon and silicon carbide fiber-reinforced oxide matrix composites, GAKC and GAKS, respectively (Hyde 1993). The ultimate strength of GAKS, determined by four-point flexure, was reported to be of 900 MPa. Fiber-reinforced CMCs possess high modulus, and if the interface is too strong, then matrix cracks form normal to the fibers, propagate in a planar mode through the fibers, and give brittle behavior similar to that in monolithic glasses and ceramics (Grande et al. 1988).

21.4.2.3 Fracture Toughness

Fracture toughness of a fiber-reinforced composite is mainly dependent on the brittleness of the fibers and the interfacial bonding. The efficiency of the interfacial bonding can be characterized by the fiber pull out of a fractured surface. A weak interfacial adhesion causes very extensive fiber pull out, whereas a high interfacial adhesion brings about the breaking of the fibers near the fracture plane of the matrix.

The fracture toughness of the composites is greatly influenced by the alignment of the reinforced fiber to the direction of applied force. The highest strength and fracture toughness of the material is obtained when the reinforcing fibers are aligned parallel to the direction of applied force. Both properties decrease with changing the alignment of the fibers, and it continues to the lowest when the applied force is vertical to the fiber direction. Kepple et al. produced epoxy–carbon composites using carbon fiber (CF) laminas functionalized in situ with carbon nanotubes (CNTs). The CNT as grown on the woven CF was shown to improve the fracture toughness of the cured composite by 46% (Fig. 21.2). This was accompanied by no loss in structural stiffness of the final composite structure. In fact, the flexural modulus was reported to be increased by approximately 5% (Kepple et al. 2008).

A strong interfacial strength is important for better shear properties, whereas poorer interfacial bonding is needed for toughness. The interfacial strength plays a dominant role in determining the shear properties, a higher bond strength give higher

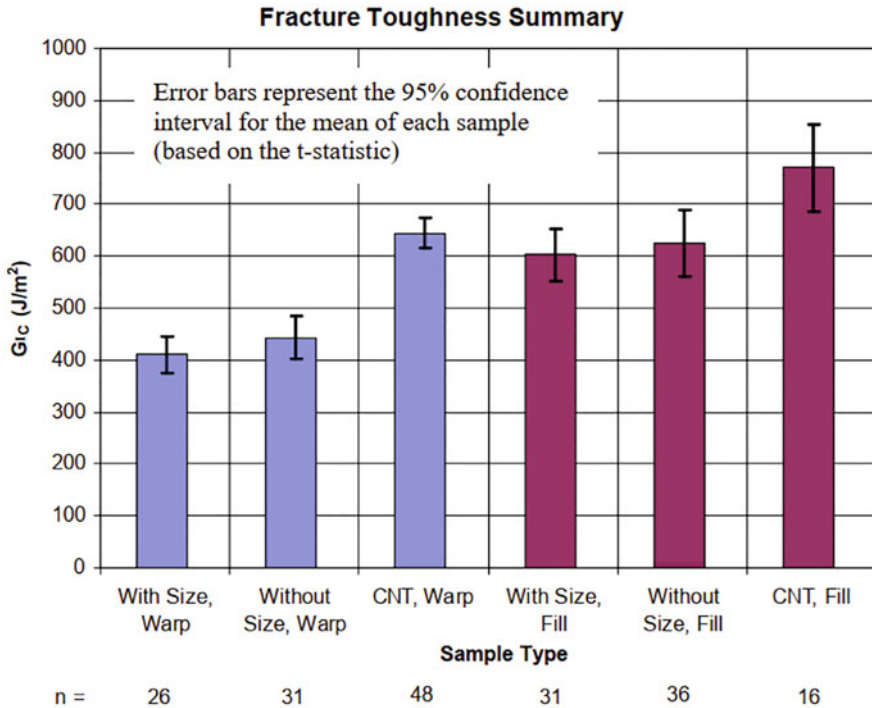


Fig. 21.2 Fracture toughness for carbon epoxy composites. (Reprinted from Kepple et al. (2008) with permission from Elsevier)

composite strength. But weaker longitudinal behavior may occur due to higher bond strength in case of glass and ceramic matrix composites.

A fiber-reinforced CMC is more attractive in comparison to glass and ceramic materials because of its quality to act against catastrophic brittle fracture. The particulate-reinforced CMCs show similar fracture mechanism to the glass and ceramics, while the fiber-reinforced CMCs show different mechanism. So, during using particulate-reinforced CMCs, the manufacturer can plan with greater confidence due to their higher fracture toughness and Weibull moduli.

Furthermore, the deformation and fracture properties of fiber-reinforced MMCs are strictly influenced by several factors such as the ductility of reinforcing fibers, percentage content of fiber, interfacial interaction between reinforcing agent and matrix, distribution of fiber in the matrix, the percentage of strain, and operating temperature. It is reported by Lee et al. (2000) that the flow stress shows positive relation with strain rate but negative with temperature. They found the maximum fracture strain at low-rate testing, although great increase with strain rate and temperature is found in the dynamic range. The fracture toughness of MMCs is invariably lower than that of the base alloy.

21.4.2.4 Impact Strength

Impact is a dynamic event that may involve high contact load acting over a small area for a very short period of time. Composites do not show good impact strength due to the absorption of impact energy by following the fracture mechanics instead of elasticity and plasticity (Kreculj and Rasuo 2018). One of the fundamental quantities in impact dynamic is impact velocity. The fatigue of composites cannot be demonstrated without considering the effect of the damage because of low velocity impacts on the starting of fatigue fracture. In particular, this low energy impact incites delaminations inside the composites, which can spread under cyclic loading. During the prediction of fatigue fracture, the damage initiated by a light impact is considered (Bathias 2006).

Shah et al. (2019) studied the factors upon which the impact resistance and damage tolerance of fiber-reinforced composite depend. The factors are classified into primary and secondary factors. The primary factors include fabric design and resin toughness that greatly influence the impact resistance and damage tolerance of fiber-reinforced composite. Whereas, secondary factors include hygrothermal conditions, stacking sequence, fiber and matrix hybridization, impactor size, shape, and mass. Various methods have been proposed for improving the impact resistance of composites structures such as using tough matrix system, through thickness stitching, woven fabric, and hybrid fibers. The key target of the techniques is to increase the interlaminar fracture toughness and the strength of composites.

For fiber-reinforced composites, Mysamy and Rajendran (2011) found the impact resistance value of 1.53 J for agave fiber epoxy composite with matrix crack growth. They concluded that good chemical bonding between fiber and matrix is important for improved impact strength, flexural strength, and flexural modulus of the composites. Moreover, Hande and Omer (Sezgin and Berkalp 2017) found that by adding high impact resistant fibers in outer layer, and placing high tensile strength fibers at the inner layer, higher impact values and tensile strength of composite materials can be attained simultaneously.

For particle-reinforced composites, for example, PMCs *reinforced* by glass fiber and titania particles, mostly the titania particles, prevents the growing of crack and results in changing the crack and its direction by turning it to a group of minor cracks. This changing in shape and direction of the crack leads to an increase in the material resistance, since there is a bonding between the titania particles and the base material (Marhoon 2018).

21.4.2.5 Fatigue Endurance

The factors that affect the fatigue behavior of brittle composites are matrix cracking, interfacial debonding, and delamination. Fiber-reinforced composites' fatigue failure mechanisms may change with the degree of applied force level. It has been stated that the fatigue strength of a composite is influenced by its constituent fibers and matrix (Papakonstantinou and Balaguru 2007). The composites produced from the same matrix reinforced with different fibers show important differences in fatigue strength.

In PMC, the fatigue damage is not related to plasticity. In case of PMCs reinforced by long fibers, matrix cracks appear first followed by the fracture of the fibers. These microcracks having thickness of one layer cause the starting of damage. Propagation causes multiplication of cracks and bring about delamination, until the rise of ultimate fracture of the fibers. Barkoula et al. (2008) prepared PP-woven composites and observed the possible damage development mechanisms. PP-woven composites was found to have high resistance to fatigue, and their endurance limit was as high as 65% of their UTS. High resistance to fatigue of all-PP composites has good interfacial properties. On the other hand, Pannkoke and Wagner (1991) studied the fatigue behavior of unidirectional (UD) composites with different fibers and matrices and concluded that the fiber-matrix bond probably has little influence on the fatigue resistance of the composite.

The fatigue resistance of PRCs depends on numerous factors such as percentage content of reinforcing agent, particle size, matrix structure, and the presence of defects arising from processing. Different researches have investigated the reason of high fatigue resistance and pointed increased volume fraction and decreased particle size (Chawla et al. 1998; Hall et al. 1994). For an applied stress, the composite undergoes a lower average strain than the unreinforced matrix. Thus, the fatigue lives of particle-reinforced composites are generally longer than those of unreinforced matrix.

21.4.2.6 Hardness

Marhoon (2018) produced polymer matrix composites reinforced with short, random glass fiber and glass fiber with titania particles. He observed that hardness increased with increasing the weight fraction of the titania particles and got better results than for glass fiber alone of same weight fraction. He observed that the type of the added particles to the polymer matrix had a high effect on the hardness of the composites and concluded that since titania has a high hardness, the samples reinforced with glass fibers and titania particles was found to be higher in comparison to sample reinforced with short random glass fiber.

21.4.3 Comparison of Properties of Different Types of Advanced Composite Materials

As we mentioned in the earlier sections, ACMs can be classified in various ways, and most of them are in the PMC and MMC types. Therefore, in this section, the engineering properties like modulus of elasticity, stiffness, tensile strength, etc. have been compared for the MMCs and PMCs. If we consider the composites as AMCs, then PMCs have better properties than MMCs. PMCs are usually anisotropic and have very high tensile strength and stiffness parallel to the reinforcing fiber. Generally, they have linear stress-strain curve. Moreover, PMCs are more effective in uniaxial tensile loads and bending. They have characteristics of resistance to deflections and dynamic loads. PMCs are advanced in the state of art and easy to change design and repair. Furthermore, raw materials for these composites are

Table 21.1 Comparative engineering properties of composite materials

Property	MMC	PMC
Strength axial (Mpa)	620–1240	820–1680
Stiffness (Gpa) axial	130–450	61–224
Specific strength (axial)	250–390	630–670
Specific gravity	2.5–3.2	1.3–2.5
Elastic modulus (Gpa)	419.4	221.7
Transverse strength (Mpa)	30–170	11–56
Transverse stiffness (Gpa)	34–173	3–12
Maximum use temperature (°C)	300	260

cheaper, and they have advanced and low-cost fabrication technology (Keya et al. 2019).

On the other hand, MMCs are also gaining attention in the world of composites due to their good engineering properties of strength for the structural materials. MMCs are usually isotropic material and have better properties like fatigue and wear resistance, strength to density ratios, stiffness to density ratios, etc. than monolithic metals. They also have some advantages than PMCs like better transverse strength and stiffness, more radiation resistance, no moisture absorption, etc. However, they have many limitations of high costs, novel technologies, difficult fabrication processes, inadequate service experience, etc. Comparative engineering properties of MMC and PMCs are shown in Table 21.1 (Kaur and Singh 2020).

21.5 Characterization of Advanced Composite Materials

21.5.1 Tensile Strength Testing

The determination of tensile properties of advanced composite materials is considered very important when the materials are designed for practical application. The test method, sample structure, and application of load significantly influence the result of tensile testing. The sample specimen for tensile testing is prepared according to the American Society of Testing and Standard (ASTM). The shape of the testing sample depends on the orthotropic property of the advanced composite material, which may be defined as the ratio of the axial tensile strength to longitudinal shear strength. Dog-bone-shaped or dumbbell-shaped specimen or ASTM standard D 638 is suitable for low orthotropic, randomly oriented, discontinuous, and moldable composite materials (Rahman and Putra 2019). The difficulty of performing tensile test increases with increasing the orthotropy of the material. The ASTM standard D 638 cannot be utilized for high orthotropic materials because specimen failure may occur at the end of the dog-bone-shaped specimen close to the gripping region of the machine. In this case, the straight sided specimen or ASTM standard D 3039 is designed to eliminate the stress concentration so that the probability of specimen failure can be reduced. The shape of the sample specimens is shown in Fig. 21.3a, b.

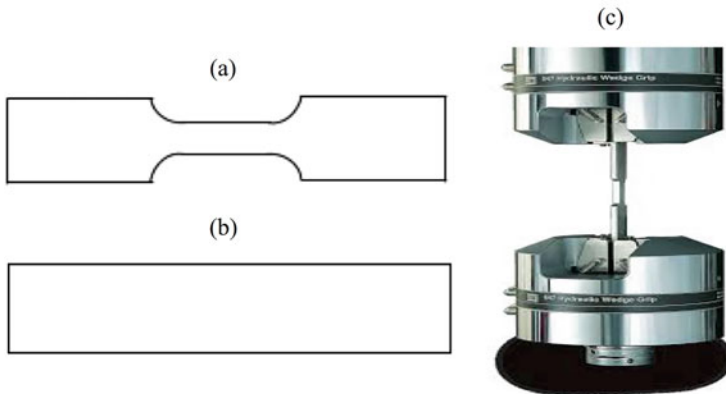


Fig. 21.3 (a) Specimens' shape for tensile testing: (a) dumbbell or dog bone, (b) rectangular bar, and (c) MTS 647 side-loading hydraulic wedge grips. (Reprinted from Rahman and Putra (2019) with permission from Elsevier)

The hydraulic wedge grips have been used for tensile loading of the test specimen, which is shown in Fig. 21.3c. The hydraulic pressure is loaded in the wedge of the hydraulic grips before starting the tensile test by means of external grip supply. The level of hydraulic pressure must be predetermined to make the gripping force adjustable with specimen so that the damage to the specimen can be prevented. Though the hydraulic wedge grip is heavy and expensive, it performs accurate result of the test specimen. The cross-sectional dimensions at various points of the specimen are measured and the strain readings are recorded continuously to produce the stain-stress curve. Furthermore, the important mechanical properties such as poison's ratio, young modulus, and ultimate tensile strength can be determined from the strain-stress curve of tensile testing.

21.5.2 Compression Testing

The suitable compression test method is selected by its ability to produce compression failure without creating global buckling instability of the specimen. During the choice of a testing method, the fixture design, loading technique, and specimen size are considered. There exist several testing machines based on the three different means of load introduction such as shear loading, end loading, and combined loading. The first ASTM standardized compression test method is the shear loaded Celanese compression test fixture, which is developed by Celanese Corporation. The Celanese compression was initially referred to in the ASTM D 3410 standard, but later it was removed because of its misalignment issues. The problem associated with the lack of alignment rods was overcome by the Illinois Institute of Technology Research Institute (IITRI). Then the IITRI compression test method was incorporated into ASTM D 3410 standard. An obvious method was standardized

for end loading compression testing of the plastic materials in ASTM D 695. This testing method was modified by including an L-shaped stand for high-performance composite material, which was commonly termed as Boeing modified ASTM D 695 compression test method. There are merits and demerits of both shear loading and end loading testing method. Combining the favorable features of both loading types, a new compression test method was standardized by ASTM, that is, ASTM D 6641.

21.5.3 Shear Testing

Shear testing is a popular method to determine the shear modulus and shear strength of advanced composite material. There are several shear testing methods that are included in ASTM standard. The commonly used ASTM standard shear testing methods are the Iosipescu shear test (ASTM D 5379), the two- and three-rail shear test (ASTM D 4255), the V-notched rail shear test (ASTM D 7078), the $[\pm 45]_n$ s tension shear test (ASTM D 3518), and the short-beam shear test (ASTM D 2344) (Munro and Lee 1986). The result of shear testing may vary depending on the selection of proper method. The desired shear testing method is carefully chosen based on several factors such as attainable shear properties and applied shear stress. The main difficulty in measurement of quantitative shear properties is the lack of pure and uniform condition of shear stress in the test specimen. The problem associated with the application of uniform shear stress increases with increasing the anisotropy and decreasing the homogeneity of advanced composite material. The accurate evaluation of the shear properties can be attained by reducing the premature failure of the test specimen. This can be achieved by minimizing the extraneous-induced stress such as tensile and compressive stress that are normally combined with shear stress. The data collection procedure and data reproducibility are also very important factor for selecting a suitable testing method. Considering the above-discussed requirements of ideal testing method, the Iosipescu shear testing method is found to be the most prominent technique for determination of shear properties of advanced composite material (Carlsson et al. 2014). The standard specimen for Iosipescu test is prepared by making the flat surface of the top and bottom edge of specimen, which is parallel to each other. In addition, it is processed with 90-degree matching notches cut at specimen mid-length (Janowiak and Pellerin 2007). The Iosipescu shear testing fixture and specimen are shown in Fig. 21.4. A complete shear stress-strain curve can be obtained by embedding a strain gage to one or both face of the test specimen. The shear modulus and shear strength are then calculated from the attained stress-strain curve.

21.5.4 Flexure Testing

Flexure testing is a popular method for analyzing the quality of advanced composite material during the structural fabrication process. The easy preparation of test

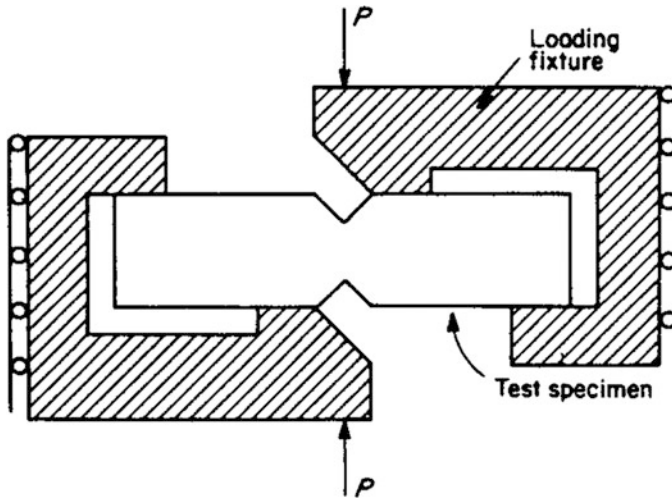


Fig. 21.4 Iosipescu shear testing fixture and specimen. (Reprinted from Lee and Munro (1986) with permission from Elsevier)

specimen and the simple testing procedure have increased the adoptability of flexure testing. The flexure testing is usually performed to determine the flexure modulus and flexure strength of the test specimen (Appusamy et al. 2020). There are two different types of flexure testing standards which are three-point flexure test (ASTM D 790) and four-point flexure test (ASTM D 6272). These flexure testing techniques are included in a new standard (ASTM D XXXX-02) to determine the flexure properties specifically for composite materials which are made by the composite committee of ASTM. Among these flexure testing standards, the ASTM D 790 is most widely used. The flexure test specimen is prepared by maintaining the constant width and thickness of the material. A deflection measuring device or a strain gage is added under the mid-span of the specimen to determine the beam displacement. The strain data are recorded at different load intervals. The set of collected data is arranged to draw the flexure stress-strain curve which is used to calculate the flexure modulus and flexure strength.

21.5.5 Hardness Testing

Hardness testing of advanced composite material is very important to determine the plastic deformation of the material under the influence of external stress. It evaluates the integral property of the surface by determining the material resistance to penetrate at the outer surface. The reinforcing materials of the composite increase the resistance to plastic deformation, which lead to an increase in hardness (Saravanan et al. 2015). The Brinell and Rockwell hardness testing machines are usually used for the determination of hardness which are standardized by ASTM as ASTM E10

and ASTM D 785, respectively. In Rockwell testing, the diameter of the indentation need not be measured which makes it faster than the Brinell testing. In addition, there is no need for surface preparation of the specimen before testing in Rockwell testing machine.

21.5.6 Impact Testing

Impact testing is one of the widely used techniques for determination of the service life of an advanced composite material. It evaluates the capacity of a material to resist fracture under high rate loading or to resist breaking under a shock loading. The impact testing machines measure the amount of energy absorbed by a material during fracture which indicate the toughness of the material. This testing method assesses the brittleness or ductility of the material by thoroughly studying the temperature-dependent brittle-ductile transition. There are two standard types of impact testing methods: Charpy and IZOD (Vieira et al. 2018). The shape of the test specimen, especially the notch, is very important because it can influence the result. Charpy test specimens contain two types of notches: either V-notch (AV shaped notch) or U-notch (key-hole notch), whereas the IZOD test specimens contain only one type of notch. Unlike IZOD test, the Charpy test specimen is placed in horizontal position keeping the notch away from the striker. The application of IZOD test method is limited due to the complicated and inconsistent failure modes. On the other hand, the Charpy test method is more reliable and cost-effective for the determination of impact strength of advanced composite material (Tarpani et al. 2009). Generally, the impact strength is calculated by dividing the impact energy by the thickness of the specimen. The higher impact strength indicates the greater toughness of the material.

21.5.7 Thermo-Elastic Testing

Thermo-elastic response of advanced composite material is determined by measuring the coefficient of thermal expansion (CTE) of material (Dergal et al. 2019). A moisture-free, flat specimen of any dimension is selected for the measurement of CTE of composite. The strain and temperature of the testing materials are monitored by embedding strain gage and thermocouple with the test specimen. These can be performed simultaneously by using a resistance gage circuit. The temperature range of the test is selected by considering the monitoring devices and the composite material. The adhesive used for the bonding of strain gage and specimen is an important factor for determination of CTE. It is selected in such a way that its heat capacity is in the range of designated temperature. Several ASTM standards such as ASTM E228, ASTM D696, and ASTM E831 are used for the measurement of CTE value of composite materials by using vitreous silica dilatometer or thermo-mechanical analysis apparatus.

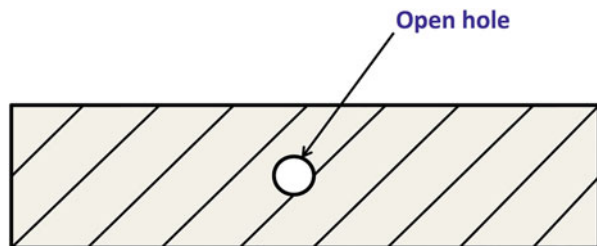
21.5.8 Open-Hole Tension Testing

The open-hole tension testing of advanced composite material is performed to determine the strength of composite material containing a circular hole. The ultimate strength of the material is greatly influenced by the hole-size, reinforcement, and matrix properties of the material and their interfacial bonding. The hole in the material induces brittleness which reduces the strength of the material. The widely accepted models for determination of the tensile strength of these materials are point stress criterion (PSC) and average stress criterion (ASC) (Tinô et al. 2014). The testing material is prepared by selecting the hole in the mid-length of the test specimen. The open-hole test specimen is shown in Fig. 21.5. The applied load versus crosshead displacement is continuously monitored to determine the ultimate load and load displacement behavior.

21.5.9 Microstructural Analysis

Microstructural analysis is very important during the manufacture of advanced composite materials when the materials are designed for any specific application. These analyses are performed to identify the constituent elements, structural shape, size, surface area, porosity, impurities, defects, and crystallinity of numerous composite materials. The microstructural analyses are accomplished with special importance to maintain the desirable structural properties of the nanocomposites. The analyses are carried out by different analytical techniques such as scanning electron microscopy (SEM), transmission electron microscopy (TEM), Fourier-transform infrared spectroscopy (FTIR), nuclear magnetic resonance (NMR), Brunauer-Emmett-Teller (BET), X-ray diffractometer (XRD), etc. The SEM analysis is performed to identify the shape of the reinforcement and matrix materials of the composite. The TEM analysis can measure the size of the nano- and microcomponents used in the composite materials. In a research, a core-shell composite material ($\text{Fe}_2\text{O}_3@$ APFS) using Fe_2O_3 as core and amino phenol formaldehyde resin (APFS) as shell was prepared to get excellent mechanical and thermal characteristics (Sun et al. 2020). The TEM and SEM image shown in Fig. 21.6 represents the core-shell structure and spherical shape of the $\text{Fe}_2\text{O}_3@$ APFS particles, respectively. The FTIR and NMR analyses are carried out to determine the

Fig. 21.5 Open-hole tension test specimen



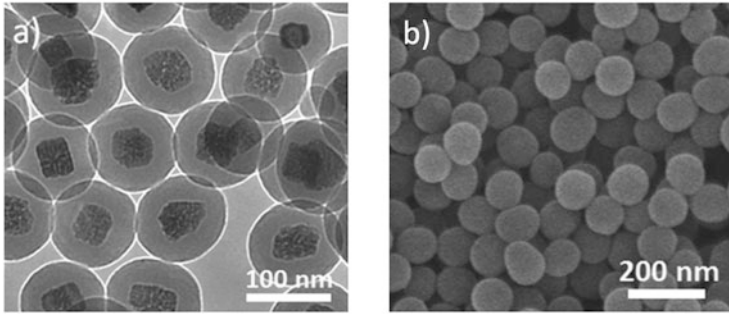


Fig. 21.6 (a) TEM and (b) SEM images of Fe_2O_3 @APFS composite. (Reprinted from Sun et al. (2020) with permission from Elsevier)

functional groups and nuclear spin of the molecules, respectively. The BET analysis can measure the surface area, pore volume, and pore size of the composite materials. The XRD analysis is done to identify the crystalline or amorphous phase of the composite material. These analyses help to make a composite material compatible for targeted utilization.

21.6 Applications

21.6.1 Biomedical Applications

Biocomposites have been successfully used in different biomedical applications such as drug delivery, tissue engineering, body implants, etc. The biocomposites have been utilized properly in targeted and sustained drug delivery which were experimented in different research works. Hasan et al. prepared a nanocomposite from chitosan, polyvinylpyrrolidone, and cellulose nanowhiskers and evaluated its potential as drug carrier for wound healing (Hasan et al. 2017). The result showed that the excellent biocompatibility and high antimicrobial properties of the composite film has made it a suitable material for wound dressing application. Recently, a number of researchers are vigorously working for the fabrication of different composite materials for tissue engineering and body implants applications. In a research, a biocomposite scaffold material was prepared from chitosan, carboxymethyl cellulose, and cellulose nanowhiskers modified with silver nanoparticles for tissue engineering application (Hasan et al. 2018). The excellent antimicrobial, improved mechanical strength, and good biocompatibility properties of the scaffold material have made it capable for bone tissue regeneration and proliferation, and nullifying the bone-related infections. In another research, a composite film of biphasic calcium phosphate with laser textured was prepared to evaluate its suitability for orthopedic applications (Behera et al. 2020). The result showed that the biomaterial performed excellent bioactivity and biocompatibility, enhanced cell spreading and proliferation, and better osteointegration capabilities.

21.6.2 Aerospace

The advanced composite materials have attracted the great interest for the construction of aircraft and spacecraft materials. This is due to meeting all the requirements necessary for the entire aerospace programs. These composite materials perform excellent properties such as light weight, enhanced reliability, corrosion resistance, erosion resistance, durability, etc. Numerous reinforcing agents such as glass, aramid and carbon fibers, etc., and matrix materials such as epoxy, phenolic, polyester, and polyimides are usually selected for the development of composite materials suitable for aircraft tools.

21.6.3 Electronics

The thermoset composite materials are more suitable for electronics applications compared to conventional composite materials. Epoxy, melamine, and phenolic composite materials are used for the production of electronic switch board, electronic sensor, energy storage, circuit board, circuit breakers, insulator, gear, etc. The density, electrical conductivity, and electromagnetic interference properties are strictly maintained to manufacture the desirable composite materials. Wu et al. prepared a composite electrode material from graphene and metal oxide to use as an energy storage, which is shown in Fig. 21.7 (Wu et al. 2012).

21.7 Conclusion

Advanced composite materials (ACMs) have attracted considerable attention over the last few decades. The use of advanced composite materials is inevitable because they provide exceptional mechanical strength. They are unavoidable because they have high stiffness, high modulus, low density, relatively low weight, excellent resistance to fatigue, and corrosion. These unique properties of ACMs make them effective in many uses including aircraft, aerospace, and sports equipment sectors. We expect that the extensive varieties of properties and characterization give rise to

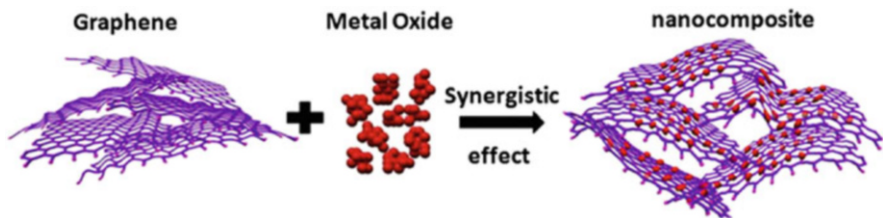


Fig. 21.7 Schematic of the graphene/metal oxide composite. (Reprinted from Wu et al. (2012) with permission from Elsevier)

ACMs as promising materials for future development by emerging products on the market.

References

- Akca E, Gursel A (2015) A review on the matrix toughness of thermoplastic materials. *Period Eng Nat Sci* 3(2):1–8
- Appusamy AM, Eswaran P, Subramanian M, Rajamanickam A, Selvakumar VK, Chandrasekar VP (2020) Invasive Parthenium weed as reinforcement in polymer matrix composite to reduce its environmental impact. *Mater Today Proc.* <https://doi.org/10.1016/j.matpr.2020.03.203>
- Barkoula N-M, Alcock B, Cabrera N, Peijs T (2008) Fatigue properties of highly oriented polypropylene tapes and all-polypropylene composites. *Polym Polym Compos* 16(2):101–113
- Bathias C (2006) An engineering point of view about fatigue of polymer matrix composite materials. *Int J Fatigue* 28(10):1094–1099
- Behera RR, Das A, Hasan A, Pamu D, Pandey LM, Sankar MR (2020) Deposition of biphasic calcium phosphate film on laser surface textured Ti–6Al–4V and its effect on different biological properties for orthopedic applications. *J Alloys Compd* 842:155683
- Benkhelladi A, Laouici H, Bouchoucha A (2020) Tensile and flexural properties of polymer composites reinforced by flax, jute and sisal fibres. *Int J Adv Manuf Technol* 108(2):1–22
- Bhargava AK (2012) *Engineering materials: polymers, ceramics and composites.* PHI Learning Pvt. Ltd, New Delhi, pp 24–440
- Callister WD, Rethwisch DG (2011) *Materials science and engineering: an introduction.* Wiley, New York, pp 1–939
- Carlsson LA, Adams DF, Pipes RB (2014) *Experimental characterization of advanced composite materials.* CRC, Boca Raton, FL, pp 1–243
- Chawla N, Jones J, Andres C, Allison J (1998) Effect of SiC volume fraction and particle size on the fatigue resistance of a 2080 Al/SiC p composite. *Metall Mater Trans A* 29(11):2843–2854
- Clyne TW (2018) Thermal and electrical conduction in metal matrix composites. In: *Comprehensive Composite Materials II*, pp 188–212
- Dergal E, Kudrevatykh O, Quinn N (2019) A dilatometer for the carbon fiber composite tubes, pp 15–26
- El-Galy I, Ahmed M, Bassiouny B (2017) Characterization of functionally graded Al–SiCp metal matrix composites manufactured by centrifugal casting. *Alex Eng J* 56(4):371–381
- Elkington M, Bloom D, Ward C, Chatzimichali A, Potter K (2015) Hand layup: understanding the manual process. *Adv Manuf Polym Comp Sci* 1(3):138–151
- Ferreira L, Bayraktar E, Robert M (2016) Magnetic and electrical properties of aluminium matrix composite reinforced with magnetic nano iron oxide (Fe₃O₄). *Adv Mater Process Technol* 2 (1):165–173
- Fulco APP, Melo JDD, Paskocimas CA, de Medeiros SN, de Araujo Machado FL, Rodrigues AR (2016) Magnetic properties of polymer matrix composites with embedded ferrite particles. *NDT & E Int* 77:42–48
- Gadow R, Kern F, Ulutas H (2005) Mechanical properties of ceramic matrix composites with siloxane matrix and liquid phase coated carbon fiber reinforcement. *J Eur Ceram Soc* 25 (2–3):221–225
- Grande D, Mandell J, Hong K (1988) Fibre-matrix bond strength studies of glass, ceramic, and metal matrix composites. *J Mater Sci* 23(1):311–328
- Grujić A, Talijan NM, Stojanović D, Stajić-Trošić J, Burzić Z, Balanović L, Aleksić R (2010) Mechanical and magnetic properties of composite materials with polymer matrix. *J Min Metall B* 46(1):25–32
- Guerrero P, Muxika A, Zarandona I, De La Caba K (2019) Crosslinking of chitosan films processed by compression molding. *Carbohydr Polym* 206:820–826

- Hall JN, Wayne Jones J, Sachdev AK (1994) Particle size, volume fraction and matrix strength effects on fatigue behavior and particle fracture in 2124 aluminum-SiCp composites. *Mater Sci Eng A* 183(1–2):69–80
- Hancox N (1998) Thermal effects on polymer matrix composites: part 1. Thermal cycling. *Mater Des* 19(3):85–91
- Harizi W, Azzouz R, Martins A, Hamdi K, Aboura Z, Khellil K (2019) Electrical resistance variation during tensile and self-heating tests conducted on thermoplastic polymer-matrix composites. *Compos Struct* 224:111001–111010
- Hasan A, Pandey LM (2015) Review: polymers, surface-modified polymers, and self assembled monolayers as surface-modifying agents for biomaterials. *Polym-Plast Technol Eng* 54(13):1358–1378
- Hasan A, Waibhaw G, Tiwari S, Dharmalingam K, Shukla I, Pandey LM (2017) Fabrication and characterization of chitosan, polyvinylpyrrolidone, and cellulose nanowhiskers nanocomposite films for wound healing drug delivery application. *J Biomed Mater Res A* 105(9):2391–2404
- Hasan A, Waibhaw G, Saxena V, Pandey LM (2018) Nano-biocomposite scaffolds of chitosan, carboxymethyl cellulose and silver nanoparticle modified cellulose nanowhiskers for bone tissue engineering applications. *Int J Biol Macromol* 111:923–934
- Herrera-Franco P, Valadez-Gonzalez A (2004) Mechanical properties of continuous natural fibre-reinforced polymer composites. *Compos Part A Appl Sci Manuf* 35(3):339–345
- Hihara L, Latanision R (1994) Corrosion of metal matrix composites. *Int Mater Rev* 39(6):245–264
- Hill CA, Norton A, Newman G (2009) The water vapor sorption behavior of natural fibers. *J Appl Polym Sci* 112(3):1524–1537
- Hyde AR (1993) Ceramic matrix composites: high-performance materials for space application. *Mater Des* 14(2):97–102
- Janowiak JJ, Pellerin RF (2007) Iosipescu shear test apparatus applied to wood composites. *Wood Fiber Sci* 23(3):410–418
- Kandpal BC, Singh H (2017) Fabrication and characterisation of Al₂O₃/aluminum alloy 6061 composites fabricated by stir casting. *Mater Today Proc* 4(2):2783–2792
- Kaur A, Singh H (2020) A review on comparative study of polymer matrix composites and metal matrix composites. *Int J Res Appl Sci Eng Technol* 8:253–256
- Kausar A, Taherian R (2018) Electrical conductivity in polymer composite filled with carbon microfillers. In: *Electrical conductivity in polymer-based composites: experiments, modelling and applications*, pp 19–40
- Kepple K, Sanborn G, Lacasse P, Gruenberg K, Ready W (2008) Improved fracture toughness of carbon fiber composite functionalized with multi walled carbon nanotubes. *Carbon* 46(15):2026–2033
- Keya KN, Kona NA, Koly FA, Maraz KM, Islam MN, Khan RA (2019) Natural fiber reinforced polymer composites: history, types, advantages and applications. *Mater Eng Res* 1(2):69–85
- Kreculj D, Rasuo B (2018) Impact damage modeling in laminated composite aircraft structures sustainable composites for aerospace applications. Elsevier, Amsterdam, pp 125–153
- Lee S, Munro M (1986) Evaluation of in-plane shear test methods for advanced composite materials by the decision analysis technique. *Composites* 17(1):13–22
- Lee CL, Wei KH (2000) Effect of material and process variables on the performance of resin-transfer-molded epoxy fabric composites. *J Appl Polym Sci* 77(10):2149–2155
- Lee W-S, Sue W-C, Lin C-F (2000) The effects of temperature and strain rate on the properties of carbon-fiber-reinforced 7075 aluminum alloy metal-matrix composite. *Compos Sci Technol* 60(10):1975–1983
- Marhoon II (2018) Mechanical properties of composite materials reinforced with short random glass fibers and ceramics particles. *Int J Sci Technol Res* 7(8):50–53
- Mitramajumdar D, Aglan H (1992) Behaviour of advanced polymer composites in erosive/corrosive environments. *Polymer* 33(9):1855–1859
- Mohammed L, Ansari MN, Pua G, Jawaid M, Islam MS (2015) A review on natural fiber reinforced polymer composite and its applications. *Int J Polym Sci* 2015:1–15

- Munro M, Lee S (1986) Evaluation of in-plane shear test methods for advanced composite materials by the decision analysis technique. *Composites* 17(1):13–22
- Mylsamy K, Rajendran I (2011) The mechanical properties, deformation and thermomechanical properties of alkali treated and untreated agave continuous fibre reinforced epoxy composites. *Mater Des* 32(5):3076–3084
- Ochi S (2008) Mechanical properties of kenaf fibers and kenaf/PLA composites. *Mech Mater* 40(4–5):446–452
- Pannkoke K, Wagner H-J (1991) Fatigue properties of unidirectional carbon fibre composites at cryogenic temperatures. *Cryogenics* 31(4):248–251
- Papakonstantinou CG, Balaguru PN (2007) Fatigue behavior of high temperature inorganic matrix composites. *J Mater Civ Eng* 19(4):321–328
- Pilato L, Michno MJ (1994) *Advanced composite materials*. Springer, Berlin, pp 1–185
- Pool K, Dharan C, Finnie I (1986) Erosive wear of composite materials. *Wear* 107(1):1–12
- Pradhan S, Ghosh S, Barman TK, Sahoo P (2017) Tribological behavior of Al-SiC metal matrix composite under dry, aqueous and alkaline medium. *SILICON* 9(6):923–931
- Rahman R, Putra SZFS (2019) Tensile properties of natural and synthetic fiber-reinforced polymer composites mechanical and physical testing of biocomposites, fibre-reinforced composites and hybrid composites. Elsevier, Amsterdam, pp 81–102
- Rao TB (2018) An experimental investigation on mechanical and wear properties of Al7075/SiCp composites: effect of SiC content and particle size. *J Tribol* 140(3):031601–031608
- Réquilé S, Le Duigou A, Bourmaud A, Baley C (2019) Deeper insights into the moisture-induced hygroscopic and mechanical properties of hemp reinforced biocomposites. *Compos Part A Appl Sci Manuf* 123:278–285
- Sandström N, Shafagh R, Vastesson A, Carlborg C, van der Wijngaart W, Haraldsson T (2015) Reaction injection molding and direct covalent bonding of OSTE+ polymer microfluidic devices. *J Micromech Microeng* 25(7):075002–075013
- Saravanan C, Subramanian K, Krishnan VA, Narayanan RS (2015) Effect of particulate reinforced aluminium metal matrix composite—a review. *Mech Mech Eng* 19(1):23–30
- Sezgin H, Berkalp OB (2017) The effect of hybridization on significant characteristics of jute/glass and jute/carbon-reinforced composites. *J Ind Text* 47(3):283–296
- Shah S, Karuppanan S, Megat-Yusoff P, Sajid Z (2019) Impact resistance and damage tolerance of fiber reinforced composites: a review. *Compos Struct* 217:100–121
- Shibley A (1982) *Filament winding handbook of composites*. Springer, Berlin, pp 449–478
- Sommers A, Wang Q, Han X, T'Joen C, Park Y, Jacobi A (2010) Ceramics and ceramic matrix composites for heat exchangers in advanced thermal systems—a review. *Appl Therm Eng* 30(11–12):1277–1291
- Sun T, Wang Y, Yang Y, Fan H, Liu M, Wu Z (2020) A novel Fe₂O₃@ APFS/epoxy composite with enhanced mechanical and thermal properties. *Compos Sci Technol* 193:108146
- Suzuki K, Ohsawa I (2015) Mechanical properties of Kenaf-PLA composites manufactured by paper-sheet hot press method. *Mech Mater* 40(4):446–452
- Takeo M, Nishijima S, Okada T, Fujioka K, Kuraoka Y (1986) Thermal and mechanical properties of advanced composite materials at low temperatures. *Teion Kogaku (J Cryog Supercond Soc Japan)* 21(3):182–187
- Tarpani JR, Maluf O, Gatti MCA (2009) Charpy impact toughness of conventional and advanced composite laminates for aircraft construction. *Mater Res* 12(4):395–403
- Tatara RA (2017) *Compression molding applied plastics engineering handbook*. Elsevier, Amsterdam, pp 291–320
- Tilly G, Sage W (1970) The interaction of particle and material behaviour in erosion processes. *Wear* 16(6):447–465
- Tinô S, Fontes R, de Aquino E (2014) Theories of failure average stress criterion and point stress criterion in notched fiber-reinforced plastic. *J Compos Mater* 48(21):2669–2676

- Tounsi A, Bouazza M, Meftah S, Adda-Bedia E (2005) On the transient hygroscopic stresses in polymer matrix laminated composites plates with cyclic and unsymmetric environmental conditions. *Polym Polym Compos* 13(5):489–503
- Tugirumubano A, Go SH, Shin HJ, Kwac LK, Kim HG (2020) Magnetic, electrical, and mechanical behavior of Fe-Al-MWCNT and Fe-co-Al-MWCNT magnetic hybrid nanocomposites fabricated by spark plasma sintering. *Nanomaterials* 10(3):436–452
- Vieira JS, Lopes FP, de Moraes YM, Monteiro SN, Margem FM, Margem JI, Souza D (2018) Comparative mechanical analysis of epoxy composite reinforced with malva/jute hybrid fabric by izod and charpy impact test. In: *TMS Annual Meeting & Exhibition*. Springer, Berlin, pp 177–183
- Wu Y, Kim G-Y (2011) Carbon nanotube reinforced aluminum composite fabricated by semi-solid powder processing. *J Mater Process Technol* 211(8):1341–1347
- Wu ZS, Zhou G, Yin LC, Ren W, Li F, Cheng HM (2012) Graphene/metal oxide composite electrode materials for energy storage. *Nano Energy* 1(1):107–131
- Zawada LP, Staehler J, Steel S (2003) Consequence of intermittent exposure to moisture and salt fog on the high-temperature fatigue durability of several ceramic-matrix composites. *J Am Ceram Soc* 86(8):1282–1291
- Zhao J-L, Fu T, Han Y, Xu K-W (2004) Reinforcing hydroxyapatite/thermosetting epoxy composite with 3-D carbon fiber fabric through RTM processing. *Mater Lett* 58(1–2):163–168
- Zin MH, Abdan K, Mazlan N, Zainudin ES, Liew KE, Norizan MN (2019) Automated spray up process for pineapple leaf fibre hybrid biocomposites. *Compos Part B Eng* 177:107306–107314



Insight of Iron Oxide-Chitosan Nanocomposites for Drug Delivery

22

Adib H. Chisty and Mohammed Mizanur Rahman

Abstract

In general, Chitosan (most abundant polymer after cellulose) is a kind of amino polysaccharide derived from chitin in deacetylated form. The primary amine groups of chitosan molecules are accountable to its numerous characteristic responses, for instance, structure which is cationic in nature, regulated drug discharge, mucoadherence, on-site gelation, augmentation of antimicrobials, invasion, etc. The use of nanotechnology in medicine, especially the delivery of drugs, is likely to grow much more swiftly than it has in the past two decades. Many nanoparticles (NPs), including those for cancer therapy, have been found to be assessed more recently for drug distribution. As a result of their 'superparamagnetic' responses, nanoparticles of iron oxide were studied and demonstrated successful use in various applications. Drug-charged iron oxide NPs can accumulate at the site in targeted drug delivery systems, using an external magnetic field. This may result in gradual effectiveness as drugs are released to the site and cells are defeated without destroying healthy cells. This chapter describes recent drug delivery developments using iron oxide core NPs as the carriers of therapeutic agents. In their application as matrices or shells for the fabrication of DDS, both the chitosan and the polymers based on chitosan derivatives are among the maximum scrutinized polymers that occur naturally. It will thus illustrate the characteristic belongings of chitosan or polymers based on chitosan derivatives as a polymer of cationic nature that further results in enhanced bioavailability and greater therapeutic effectiveness of some specific

A. H. Chisty · M. M. Rahman (✉)

Department of Applied Chemistry and Chemical Engineering, Faculty of Engineering, University of Dhaka, Dhaka, Bangladesh

e-mail: mizanur.rahman@du.ac.bd

© The Author(s), under exclusive license to Springer Nature Singapore Pte Ltd. 2022

619

L. M. Pandey, A. Hasan (eds.), *Nanoscale Engineering of Biomaterials: Properties and Applications*, https://doi.org/10.1007/978-981-16-3667-7_22

materials related to drugs on account of their increased bioadherence to dissimilar tissues.

Keywords

Chitosan · Nanoparticles · Nanocomposites · Superparamagnetic

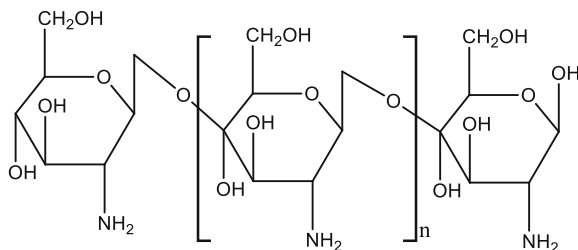
22.1 Introduction

In recent times, nanoparticles that are magnetic in nature have been found to be extensively studied owing to their significant magnetic properties together with technological aspects (Zhou et al. 2009; Zhang et al. 2011a). In literature, the biomedical application of magnetic nanoparticles, for instance, nanoparticles of iron oxide have been described over the past decades (Sharifi et al. 2012; Karimi et al. 2013). Higher saturation magnetization along with higher magnetic susceptibility, non-toxic character, higher chemical strength, non-carcinogenic nature, ability to biodegrade, intrinsic biocompatibility, simplicity of production, comparative easiness in modification, lower reactivity to oxidation and the most responsive surface have been stated to upsurge the application of iron oxide nanoparticles most promisingly in the field of medical science (Fang et al. 2009). Furthermore, such nanoparticles can simply be altered with biocompatible coatings together with targeting, imaging and therapeutic molecules as well (Závišová et al. 2011).

In the meantime, polymers are conventionally well thought as excellent host matrices during the preparation of composite materials. Numerous polymer nanocomposites have been reported to be prepared having a diversity of inclusions, for instance, nanotubes of carbon, materials of semiconductive nature, and magnetic nanoparticles (Wilson et al. 2004). In actual fact, nanocomposites based on polymers have turned out to be a substantial field of current inquiries and improvements because of its probable applications in bioscience and the easiness of engineering nanocomposites having prominent antistatic, magnetic and electric properties. Hence, the materials of composite character consisting of polymer and nanosized iron oxide particles have evoked the substantial consideration of the scientific society as they frequently embrace the required characteristics of the inorganic and organic compounds simultaneously (Sondjaja et al. 2009). In recent times, magnetite nanoparticles were found to be fused into polymers, for example, DNA, polyethylene glycol, polyvinyl alcohol, polyacrylic acid, protein and poly-saccharide mediums to expand its uses in biomedical sector involving the separation of magnetic cell, targeted drug transportation method and resonance of magnetic nature that further results in a successful imaging of clinical diagnosis (Bhatt et al. 2010).

Amongst numerous biopolymers, chitosan has outstanding ability to form films, extended mechanical response, higher bioabsorbability, harmless character, greater water absorbency, proneness to chemical modifications and better cost-effectiveness (Zhang et al. 2010). Chitosan, usually produced from chitin, is considered as one of the major components of crustacean shells and fungal biomass which is easily

Fig. 22.1 Structure of chitosan



obtained while processing the seafood wastes (Yuwei and Jianlong 2011). As shown in Fig. 22.1, chitosan, a polysaccharide which is linear in shape, comprises of arbitrarily dispersed β-(1, 4)-bonding between *N*-acetyl-D-glucosamine and D-glucosamine. Such polymer of biological origin enables the treatment of wound and shows bacteriostatic effect owing to the presence constructive polarities on it at physiological pH while working as a bioadhering agent to upsurge its sustainability at the centre of application. On account of such promising properties, extensive use of chitosan has been found in the sectors associated with biomedical applications compared to other biopolymers (Mahmoudi et al. 2011). On top of biomedical applications, chitosan can be utilized in waste water treatment due to its compatibility with metal ions (Yuwei and Jianlong 2011).

Many attempts have been taken to obtain the synergistic results while combining chitosan with metal oxide nanoparticles (more specially iron oxide nanoparticles). Owing to its supermagnetic nature, iron oxide-based nanocomposites are frequently used for both the magnetically targeted cancer therapy and an improved drug delivery while recovering biomolecules for desired biosensing applications (Gao et al. 2009; Yoo et al. 2012; Fortin et al. 2007). Moreover, the combination of chitosan together with iron oxide nanoparticles (IONPs) in such composites overcomes the clinical limitations associated with IONPs including poor physiological strength, rapid clearance of blood that commences the circulation and particularly the absence of targeted centre in drug delivery systems (Kong et al. 2013; Ma et al. 2013; Lin et al. 2015). The chapter represents an overall discussion on various studies based on chitosan-iron oxide nanocomposites in biomedical applications emphasizing the potential drug delivery system.

22.2 Major Challenges in Drug Delivery

The extent of the successful distribution of drugs has been found to rise and evoke the kind consideration of the scientists and pharmacists as well. Significant improvement of the current drug delivery system can convey and release a drug accurately and securely to the targeted site is becoming the 'holy grail' to the pharmaceutical investigators day by day (Orive et al. 2003c).

Certainly, a significant number of novel delivery systems are reported per annum and practically each and every segment of the body are assessed as a prospective

path for the administration of traditional and innovative medicines. Thus, certain ways of carrying drugs (that are sparingly soluble), peptides and proteins have been developed. Moreover, rigorous assessment of the effective distribution of drugs is still undergoing at the present time.

Therefore, the periphery of drug distribution is altering significantly. Advantages of the innovative preparations are continuously assisting the creation of an innovative marketplace in the boundary of drug distribution. In effect, previous surveys by Business Communications Company Inc. reported the market of the United States with promising investments only for drug delivery systems and are expected to rise by many folds in the upcoming decades (Orive et al. 2003c).

22.2.1 Current Obstacles

Delivery of a drug in a non-toxic and consistent way to the centre of target in a required level is the ultimate goal of medication. However, in case of many drugs, such perfect necessities set up fanfare in spite of expectation. For instance, oral administration is considered as one of the convenient approaches of drug distribution, due to its non-hostile character, sufficient peptide or protein-based drug delivery has not yet been achieved through this track. The phenomenon stated here can be attributed to the presence of acidic conditions prevailing in the stomach and the refusal delivered by the intestine that either modify, terminate or lessen the absorption of approximately all macromolecules along with lessening their bioavailability. Consequently, a huge number of diabetics throughout the world have to go through insulin shots every day that provoke a higher fraction of disregard in this treatment.

Further commonly practiced ways of administering drug molecules are enlisted as the distribution through injection and nasal pathway. In such cases, transportation via nasal track exhibits a deprived accumulation capacity of compounds with polar character, while discomfort and the hesitancy of patients are accompanied by injection to utilize the stated procedure (Illum 2002). Other than nasal drug delivery and injection, administration of drugs throughout the skin is another available alternate. To be successful, drugs must overcome the external sheath known as stratum corneum that inhibits the proper spreading of substances. Other foremost encounters considered are the transmission of drugs in intracellular fluids, tendering drugs into tumour cells and the directed distribution of glycoproteins as well.

The absence of an appropriate drug distribution system is not only responsible for the traditional routes of drug administration and dosage formulas but also a major disadvantage in the advancement of innovative approaches including gene therapy, cell therapy and RNA interference (RNAi) as well (Check 2003). During the therapy related to gene, a virus is allowed to use as a carrier to transport genes that get active inside the cells of a patient. Nonetheless, if the carrier stated here associates with the genes present in a cell, it usually results in uninhibited mutations inducing cancer. Such kind of therapy is not incidental as verified by the disastrous demise of the trial volunteer in the past (Marshall 1999; Check 2002). Correspondingly, if the ability of RNAi approaches is to be understood, scientists should cultivate ingenious methods

Table 22.1 Particular pharmaceutical companies together with their technologies on drug delivery (Orive et al. 2003c)

Firm	Technology	Invention
NanoSpectra Biosciences (Houston, TX)	Nanosized shells	Nanosized particles in ophthalmic treatments
Sontra Medical Corporation (Franklin, MA)	Ultrasound	Sonography in case of transdermal drug distribution
MacroMed Inc. (Sandy, UT)	Poly(D,L-lactide-co-glycolide) microspheres	Drug delivery systems that enable modified administration of difficulty to deliver ratio of reactive molecules
Neurotech SA (Evry, France)	Cells that are encapsulated	Technology related to cell encapsulation in drug delivery to both the eye and the brain
CellMed (Alzenau, Germany)	Cells that are encapsulated	Microencapsulated human cells that are genetically engineered for chronic illnesses

to defend the trivial interfering of RNAs (siRNAs) present in the arteries and to direct those into the correct cells.

Entirely stated downsides have enthused numerous firms related to biotech and pharmaceuticals to improve the approaches of drug distribution, as revealed in Table 22.1, exerting their function in an effective and non-toxic manner. Nonetheless, effective guidelines providing a clear path on the modification of the field of drug delivery were incomplete.

22.2.2 Advances in Drug Delivery

22.2.2.1 Oral Drug Delivery

At present, various research groups are exploring innovative techniques to develop the shield and consumption of peptides after its administration through oral track. For example, the application of biochemicals that are adhesive in nature has been reported to stimulate the permeation of drug molecules via and among the cells of intestine (Orive et al. 2003c). Polymers, for instance, polyanhydrides, bound to both the stomach and across the mucosa of intestine, result in amended bioaccumulation of drugs. Lectins, a second-generation bioadhesives, have been found to be considered due to their non-toxic character and distinct binding characteristics accelerating a ligand-receptor relationship (Kilpatrick et al. 1985; Carreno-Gomez et al. 1999). Scientists are still conducting several research works on blocking protease inhibitors along with cellular pump systems to avoid the potential captivation of firm drug molecules and hence reducing their healing efficacy. In this circumstance, Glytech technology usually intended to provisionally prevent and/or resist the pumping system of p-glycoprotein established by Eurand (Orive et al. 2003c). Outcomes associated with the stated procedure in brute simulations showed improved absorption profiles of various compounds which are therapeutically active.

Drugs, containing peptides, can further get fused to a transferor of macromolecular nature, that is, a polypeptide or polymer (Shen 2003). Presently, polyethylene glycol is considered as one of the most extensively utilized polymers for the alteration of proteins together with therapeutic effectiveness owing to its lower toxic character, cost and commercial accessibility of numerous molecular weight variations as well (Roberts et al. 2002). Applying the parallel technique, Nobex corporation utilized the polymers of lower molecular weight to the active sites of drug molecules resulting in new drug-polymer conjugates (Veronese and Harris 2002). Nobex is utilizing such procedure to establish a formulation of insulin which is able to administrate via oral track. Even, regarding the Phase II medical trial on patients, a prompt dose depending captivation of the insulin together with a lower glucose level prevailing in blood has been attained with no danger.

22.2.2.2 Nasal Drug Delivery

Administration of drugs through nasal routes has evoked much more attention in recent centuries. Various chemical agents as a fascination enhancer have been found to expand the accumulation of drug molecules that are polar in nature. For instance, preparations on the basis of powdered chitosan have been found to be investigated for the proper adenoidal administration of both the morphine and the insulin (Illum et al. 2001). Moreover, the implementation of poly-L-arginine, cyclodextrins along with lipids as effective accumulating agents are correspondingly considered in numerous investigations (Merkus et al. 1999). Numerous communities are working very hard to find an innovative drug distribution technique via nasal track; for instance, Aradigm has established a nozzle-containing element to confirm greater aerosol characteristics every time when a patient breathes in medication. At present, the determination of accuracy of the indicated procedure is in scientific trials for several drugs that include morphine, insulin, testosterone and interferon α -2b as well.

22.2.2.3 Transdermal Drug Delivery

The transdermal application of drugs is directly connected to the circulation of blood. As studied by Langer, two dissimilar mechanisms (i.e. sonograph and iontophoresis) are usually implemented to overcome the resistance of the skin (Langer 2003). By means of iontophoresis, Iomed Inc. has modified Phoresor1 to provide the drug named iontocaine. Other approaches to transdermal drug transportation were found to include the modification of microneedles that build microscale paths through the skin while developing its penetrability (Henry et al. 1998; McAllister et al. 2000).

22.2.2.4 Encapsulation Methods

Incorporation of the molecules that are therapeutically active in microparticulate transportation systems symbolizes a different alternative path to shield and deliver the medication to the targeted site. Microparticles based on polymers, micelles and liposomes are the examples of these systems. Liposomes are considered to be formed from phospholipid bilayers having an internal segment that can be utilized for

encapsulating various drugs (Gabizon 2001; Torchilin and Lukyanov 2003). In a study, Savić et al. stated the micellar growth from two categories of polymers (Savić et al. 2003). In case of administrating the molecular ‘globules’ along with drugs, such nanosized biostable containers were found to cross the barrier of a rogue cell. Even though they could not access the nucleus while being capable of reaching Golgi apparatus and mitochondria constituting the significant objectives for drug delivery. Applying such technique of microencapsulation, academics have now been exploring the opportunity of adding cells working as ‘plants’ discharging healing agents (Orive et al. 2003a). To get success, microcapsules need to be covered with an immunobARRIER of semipermeable nature which can further provide a double-defensive functions called the immunoisolation of the transferred tissue from the providers insusceptible reply that further shield hosts from any kind of biological hazard. Technology regarding the cell encapsulation prevails numerous benefits compared to other encapsulation of peptides comprising the discharge of polypeptidic healing agent and provides the opportunity to control peptide transportation as a role of corporeal necessities (Orive et al. 2003b). Consequently, a varieties of encapsulated cells have been established in numerous uses and to deal numerous infections. These embrace the growth of liver and pancreas, healing of traditional Mendelian disarrays due to the deficiency of gene product and/or in the presence of enzyme, the management of uncontrolled cell dissection and diseases related to nerves (Hortelano et al. 1996; Emerich et al. 1997; De Vos and Marchetti 2002; Strain and Neuberger 2002). Cells, that secrete ciliary factor, have been reported to be enveloped and implemented on puppies affected by a disorder related to the disintegration of photoreceptors. Results revealed that after several weeks of application, an enhanced persistence of the photoreceptor cells was attained with no adverse effects (Tao et al. 2002).

When the particle size, during encapsulation, is minimized to lower than that of 100 nm, the consequence becomes nanotechnology. At present, investment in nanotechnology has been increased throughout the world. As a whole, nanocomposites mostly comprise of nanosized capsules, micelles, fused and nanosized particles. The foremost benefits of such methods are to provide a greater uptake of intracells compared to microsized ones. These have found superior consequences in the distribution of gene, as DNA can easily be undergone encapsulation and sheltered from lysosomal attack and transfected with higher efficacy (Bonadio et al. 1999). In a study, nanodevices comprising of DNA which is connected to the nanoparticles of titanium dioxide have exposed the access to the innovative approaches in the transportation of drugs and nanosurgery (Paunesku et al. 2003). Certain assessments based on nanotechnology deliver additional valuable perceptions for the fascinated readers (Lavan et al. 2002, 2003; Mazzola 2003).

22.3 Chitosan-Based Nanocomposites in Drug Delivery

Most promising results have been obtained with the practices of adding nanosized fillers into the biopolymers derived from natural sources such as chitosan having enhanced biological characteristics mostly aimed at its uses in biomedical sector. The fusion of nanosized backup into the prescribed medium has been performing as a prevailing method to omit the traditional shortcomings related to polymer from biological origin. Nanocomposites based on chitosan are considered too much effective in a number of regions (De Azeredo 2009; Liu et al. 2009). Such nanocomposites show or exhibit prominent improvement in the required characteristics at a very small concentrations of nanosized fillers (5–10 wt%) than that of other composites comprising of 40–50% fillers. Amount of chitosan in various nanocomposites is frequently allowed to remain higher which further consequences superior goods with modified bioactivity and biocompatibility along with enhanced mechanical and thermal stability, and higher transparency (Fernandes et al. 2010). Till now, three kinds of nanofillers have been reported based on their geometry and aspect ratio (Pillai and Ray 2012).

Mechanisms of the novel drug transportation systems usually focus the number of chemotherapeutic agents to the particular site while lessening their systemic circulation. Chitosan-based nanocomposites were found to play the most promising part is the fields that provide a target specific, biostable and biodegradable distribution scheme. In the same way, nanocomposites are continuously evoking massive devotion for the particular diagnostic uses owing to its simplicity of preparation while combining with therapeutic and imaging agents (Lim and Chung 2016). Table 22.2 comprises a list of some effective nanocomposites based on chitosan applied for the distribution of drugs, types of drugs and their implementations as well. Numerous nanosized particles have riveted massive attention nowadays, mostly in imaging of malignant cell, identification and treatment because of their exceptional dimension-dependent characters. Owing to its significant advantages, targeted therapy has become a vital procedure mostly in cancer-related therapy as it expand anticancer therapeutics that are focused on both imaging and therapy. Nanosized composites of numerous categories, founded by chitosan, have been explored as a transporter of drug distribution with particular properties and characteristic applications. In a study by Venkatesan et al. nanocomposite based on hydroxyapatite (Hap) and chitosan (Cs) filled with medicaments called celecoxib was demonstrated as a prospective way of utilizing medicaments in the treatment of malignancy having higher drug accumulation proficiencies together with persistent release profiles (Venkatesan et al. 2011). In vitro studies have been found to exhibit noteworthy antitumour apoptosis together with spell depended acceptance of hydroxyapatite (Hap) and chitosan (Cs) based nanoparticles (filled with celecoxib) in affected cells. In addition, in vivo assessments based on tumour in naked rogue verified extensively superior resistance of tumour development. Such reduction in the volume of tumor (as shown in Fig. 22.2), after the successful treatment with celecoxib and improved nanoparticles, followed the sequence (from minimum to maximum) as: celecoxib-

Table 22.2 Various kinds of nanosized fillers in chitosan matrix, types of drugs used, types of nanocomposites with their prominent applications (Ali and Ahmed 2018)

Types of nanofiller	Drug used	Types of nanocomposites	Applications	Reference
Magnetite, Fe ₃ O ₄	Gemcitabine	Core/shell nanocomposite	Cancer therapy through stimuli-sensitive nanomedicine	Arias et al. (2012)
Magnetite, Fe ₃ O ₄	Bacillus Calmette-Guerin	Hydrogel	Intravesical drug delivery	Zhang et al. (2013)
Hydroxyapatite	Doxorubicin	Hydrogel	Drug delivery	Depan et al. (2009)
Graphene oxide	Camptothecin	Functionalized graphene oxide with chitosan	Distribution of sparingly soluble anticancer drug camptothecin and genes	Harashima et al. (1995)
Montmorillonite (Mnt)	5-fluorouracil	Chitosan-coated alginate-montmorillonite nanocomposite	Drug transporter in persistent release and electrically persuaded drug distribution	Azhar and Olad (2014)
Magnetite, Fe ₃ O ₄	Curcumin	Nanocomposite-coated with Fe ₃ O ₄ nanoparticles	pH-sensitive drug delivery	Prabha and Raj (2016)
Aluminosilicate	Doxorubicin	Chitosan-clay nanocomposite	Controlled and extended release of drug	Yuan et al. (2010b)
Nanosilica	Carvedilol	Spherical nanosilica matrix	Delayed secretion of sparingly soluble drugs	Sun et al. (2013)
Montmorillonite (Mnt)	Oxytetracycline	Nanocomposite	Improved drug permeation	Salcedo et al. (2014)
Fe and Mn magnetic nanocrystals (MNCs)	Doxorubicin	Drug loaded magnetic nanoparticle	Imaging in cancer treatment and pH-sensitive drug distribution	Lim et al. (2013)

filled hydroxyapatite-chitosan particles of nano size > celecoxib in free form > hydroxyapatite-chitosan particles of nano size.

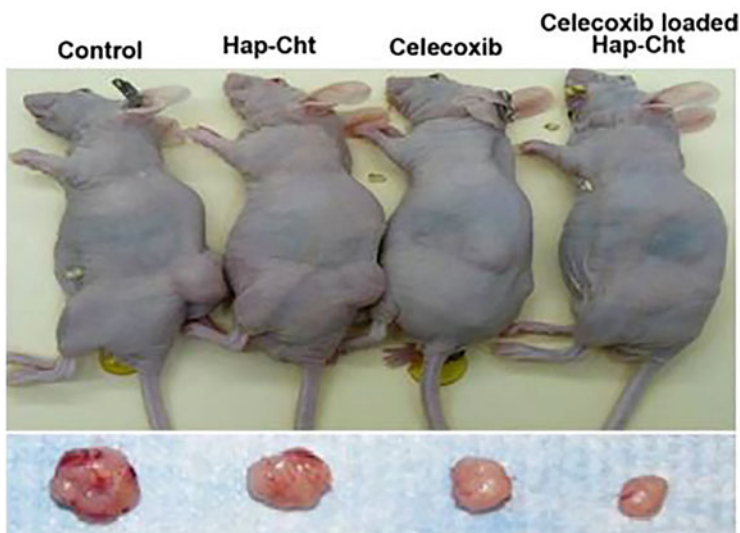


Fig. 22.2 Tumour repressive consequences of control, free celecoxib as medicaments, hydroxyapatite-chitosan and hydroxyapatite-chitosan nanoparticles on both the naked mouse and the size of tumour cell. (Adapted from Ali and Ahmed (2018) with permission from Elsevier)

22.3.1 Nanocomposites Based on Chitosan and Montmorillonite (Clay)

Nanocomposites comprising polymeric substances and clay are among the resources of cumulative consideration due to both of their multifunctional activities. Usually, montmorillonite clay is a constituent of minerals from phyllosilicate groups having an in-layer configuration. It contains silicate sheets of tetrahedral form along with the orthorhombic layers of alumina as inserted amid them (Gutiérrez et al. 2017). Imperfections present in the structure of crystal lattice and isomorphous replacement produce the distribution of negative charge in the plane which is further neutralized by the adherence of metal ions of electropositive nature (Abdeen and Salahuddin 2013). Such imperfection is accountable to its reactivity and interchanging reactions with carbon-based compounds. Moreover, Mnt has an enormous external site that exhibits virtuous ability to interchange cations, adherence capability, clinging skill and drug transportation competence. Various kinds of nanosized clay, differing in opposite ion environment and cation interchanging capability, existed to be implemented in drug release assessments. Nanocomposite having chitosan as a matrix with Cloisite 30B reinforcement revealed promising enhancement in surface roughness and tensile strength (Ali and Ahmed 2018). Similarly, thermal strength and melt activities did not show any drastic alteration during the incorporation of clay (Abdeen and Salahuddin 2013).

In a study, Liu et al. fabricated Cs-Mnt nanocomposite (hydrogel) for the organized discharge of vitamin B₁₂ in the presence of electrostimulation effect

(Liu et al. 2008). The release of vitamin B₁₂ was found to be intensely affected owing to the cross-linked compactness among chitosan and montmorillonite. The extended crosslinking density showed its dependency on the structure of silica sheets acting as a cross-linker in between Cs and Mnt. With the lower amount of Mnt, the kinetics of secretion followed a first-order reaction in pseudo form. In electrostimulation, the discharge profile was altered from diffusion stage to swelling in a precise manner. The electro sensitivity to reproduce 'on' and 'off' actions in higher concentration of Mnt was also minimized though the anti-fatigue response was considerably found to get enhanced. In comparison with pure chitosan, nanosized gel having strength of 2 wt% Mnt provided an essentially required and mechanically reliable pulsatile discharge profile together with exceptional antifatigue behaviour.

Another assessment by Hau et al. explored the successful secretion of ofloxacin by hydrogel consisting of Cs and Mnt where Mnt was incorporated to the beads of chitosan to improve drug entrapment and enlargement behaviour while reducing the rate of release (Hua et al. 2010). In addition, such beads also showed resistance to disintegrate in 10 h of soaking. Therefore, attractions among the opposite charges present in Cs and Mnt were recommended for the improvement of globules strength acting as a potential aspirant as a drug transporter for the prolonged transportation.

In recent times, materials that are mesoporous in nature have also evoked pronounced attention owing to its large surface regions and large holes that mark them suitable host materials in discharging various bioactive chemicals. Shariatinia et al. investigated the sustained discharge of the drug called metformin through a mixture of poly (ethylene glycol)-block-poly (propylene glycol)-block-poly(ethylene) and chitosan polymer-based nanocomposite layers comprising both the mesostructured and aminopropylsilane particles of nanosize (Zhang et al. 2009). The cumulative amount of the nanosized particles present in the films has been found to result in the reduction of extension at break, though the mechanical stability was amplified. The mechanism of drug discharge showed extended release within the first 22–24 h, whereas the rate enhanced slowly in about 15 days. A layer containing 4% aminopropylsilane along with approximately 10% drug exhibited remarkable affinity to water, biostability, drug dissemination character while endeavouring a better distribution method.

Discharge mechanism of paclitaxel, a kind of drug that can fight with malignancy, by polylactide-chitosan composite was explored by Nanda et al. (Houdellier et al. 2012). Here, Mnt was found to act as a matrix and as co-intermixing agent as well. The drug release behaviour was explored to be depended on pH, arrangement of polymer together with the pH of the existing media. Thus, a blend of composites with modified drug-releasing properties appropriate for the basic applications was proposed.

22.3.2 Nanocomposites Based on Chitosan and Magnetic Nanoparticles

Nanocomposites of fusion nature, containing both the organic and inorganic components, have been developing as an innovative and remarkable device in biomedical applications. Hybrid materials show prominently modified characters in comparison with original substance. The usage of nanocomposites with magnetic nature in biomedical, precisely in the treatment of malignancy, is attaining enormous attention progressively. The specific pursuing of anti-proliferative agents to the cancer-affected nerve can be attained following the progressive techniques that result in their discerning way to the particular location via proper stimuli or by a precise acknowledgement method (Arias et al. 2012). In case of incentive moves, the drug transporters are considered to response the exterior stimulations including magnetic gradient, sonography, pH, temperature etc. through facing a change in their characters which lead to the discharge of a biosensitive chemical in exact concentration to the infected region (Yuan et al. 2010a; Meng and Hu 2010). In these processes, efficiency as well as the specificity of the drugs were enhanced along with inferior toxicity. However, the nanocarriers that have magnetic nature need to retain the required characteristics like biostability, lower toxicity and immunogenicity, suitable drug distribution and reactivity to magnetic acclivity. In addition, nanoparticle should encourage the death of malignant tissues utilizing the hyperthermia of magnetic liquids (Ali and Ahmed 2018).

22.3.3 Nanocomposites Based on Chitosan and Carbon Nanotubes

Carbon nanotubes are the most promising arrangements of carbon which were invented in 1991 and consume a cylindrical nanosized configuration comprising of carbon atoms that are sp^2 hybridized in a shape called hexahedron pattern. CNTs show exceptional electrical, mechanical, thermal properties together with ordered pore configuration together with higher specific region (Adewunmi et al. 2016). Such advantages of nanotubes are found to be enhanced by many folds in composites during drug delivery. Biopolymer offers both the biocompatibility and ability to undergo biodegradation when CNTs offer strength, cellular uptake, magnetic and electromagnetic activities (Cirillo et al. 2014). CNTs were completely discovered in drug distribution, mostly in the treatment of malignancy, though the resulted cytotoxicity is a significant anxiety related to it (Zhang and Zhang 2011b). Composite consists of chitosan-CNTs was fabricated through the functionalization of CNTs by Baek et al. and the composite exhibited electrorheological behaviour in the presence of electric fields that can further be advantageous in biomedical use (Baek et al. 2008).

In another study, Bao et al. reported a nanocarrier based on chitosan and functionalized graphene oxide (GO) in the distribution of drugs and genes (Harashima et al. 1995). Amidation process, resulting in amide bond among chitosan and graphene oxide, was utilized to modify graphene oxide with an aggregate of

64 wt% of chitosan imparting better water solubility along with biocompatibility. Camptothecin (CPT), an anti-malignant drug which is water insoluble, was incorporated in the nanosized carrier through lipophilic contact and π - π stacking. The nanosized transporter of the stated composite was found to exhibit almost 20 wt % drug filling and 17.5% releasing at 37 °C within 72 h.

22.3.4 Nanocomposites Based on Derivatized Chitosan

Alteration of chitosan, that is usually brought chemically, plays a very imperative role to expand its prominent characteristics such as lipophilicity, the ability to get dissolved, biostability, biological response etc. (Thomas and Thomas 2013). Modification via the incorporation of different functionalities upsurges its ability to get dissolved in water without influencing its intrinsic oddity (Lu et al. 2007). Revision of chitosan backbone through graft copolymerization and quaternization is considered as the utmost methods that are utilized frequently (Thanou et al. 2001). Yu Li et al. explored the use of modified chitosan nanocomposite by means of γ -ray irradiation polymerization (Yu et al. 2004). Nanosized composites, that were fabricated, revealed enhanced heat strength properties, mechanical response and enhanced water repellency. An incorporation of the folate associated carboxymethyl chitosan-ferroferic oxide together with the nanoparticles of cadmium telluride quantum dot (CFLMNPs) was prepared for the specific drug transportation and imaging of cell via gradual deposition of layers (Sencadas et al. 2012). The resulted composite system showed vigorous magnetic influence together with photoluminescence character even at regular room temperature. Effectiveness of the process and releasing mechanism of anti-malignant drugs can also be implemented for the proper healing of malignancy in human liver with the filling capacity of around 36.6 wt%. The discharge of adriamycin was found to be rely on pH and a particular targeting related to folate receptor was attained.

22.3.5 Nanocomposites Based on Chitosan and Synthetic Polymers

Combination of both the usual and artificial polymers denotes a new type of materials and has evoked much more considerations particularly for biomedical uses. Though the polymers of natural origin reveal superior biostability and biodegradability in such applications in spite of having inferior heat stability and mechanical responses (Goonoo et al. 2013). Hence, the combination of natural and artificial polymer produces new resources that exhibit amalgamations of properties related to both the polymers which could not be attained by single polymers (Sahoo et al. 2010). For instance, mixing of poly(2-hydroxyethylmethacrylate) with gelatin was found to lessen its poor cell adhesion property (Santin et al. 1996). During drug delivery, amalgamation of polymers provides stable and controlled discharge while enhancing their encapsulation and loading capacity as well (Paredes et al. 2014). In addition, doping of nanofillers to the mixture of matrix promotes discharging

behaviour of the medicaments as a dispersion resistor (Liu et al. 2006). Parida et al. explored the sustained delivery of an anti-malignant drug called curcumin from chitosan-polyvinyl alcohol composite (Parida et al. 2011). Furthermore, blending improved both the tensile strength and elasticity of films without any adverse effects on hydrophilicity. The consequence of pH was found prominent on the amount of chitosan than that of polyvinyl alcohol in the prepared layers.

22.3.6 Nanocomposites Based on Chitosan and Other Biopolymers

In order to upsurge the distinctive character of chitosan as a transporter of drugs, chitosan has also been found to use in combination with other biopolymer in drug distribution method. Depending on the nature, biopolymers are usually classified as cationic and anionic that have various biological characters. For instance, alginate was described to be mucoadhesive that reveals exceptional tissue compatibility (Miyazaki et al. 1994). In various studies, dextran showed lower protein binding ability while curdlan exhibited the capability to arrange both the low and high set thermo adjustable ointments at different temperatures and carrageenan revealed very decent gelling property etc. (Massia et al. 2000; Long et al. 2015). Graphene oxide (GO) altered nanocomposite comprising of chitosan and dextran, following the successive deposition of layers, was assessed as a transporter of an anti-malignant drug called Doxorubicin (DOX) (Xie et al. 2016). Successful modification of graphene oxide with both the chitosan and the dextran intensely improved the dispersion ability of anti-malignant doxorubicin and graphene oxide in functional form together with the reduction of regular protein accumulation by the nanosheets of graphene oxide. Such nanocomposite was further found to be absorbed by breast cancer cells representing too much cytotoxicity to cancer cells.

In another study, nanocomposites based on chitosan and alginate derivatives were reported and utilized to estimate the sustained discharge of curcumin (Malesu et al. 2011). The discharge of drug molecules was found more significant in alkaline media in comparison with the acidic environment. Composites based on chitosan and collagen were also utilized in tissue engineering related to cartilage. Collagen, present in the usual matrix of cartilage, is accountable to express the chondrocytes phenotype. Nonetheless, both the lower physical stability and the quick biodegradation speed reduced its implementations in tissue engineering related to cartilage (Doulabi et al. 2014). Amalgamation of scaffolds related to chitosan and collagen generally results in modified physical strength. Addition of cells, assessment of feasibility and proliferation also made such blends more biostable without any cytotoxicity while acting as 3D matrix in tissue engineering associated with cartilage (Yan et al. 2010).

22.4 Iron Oxide-Chitosan Nanocomposites in Drug Delivery

In an assessment, Arias et al. stated the fabrication of a core-shell nanocomposites comprising of chitosan and magnetite laden with an anti-malignant drug molecule named gemcitabine (Arias et al. 2012). Arias along with his group members demonstrated such composites to be operational in the healing of numerous varieties of tumours while overcoming the major drawbacks of gemcitabine. Such drawbacks include a prompt metabolization and an insignificant plasma half-life which generate the necessity of using higher doses that include prominent toxicity (Reddy and Couvreur 2008; Arias et al. 2012). According to the deception technique, both the deception efficacy (%) and the medicament filled (%) with sustained release were prominently improved as well.

Nanosized particles of magnetite (Fe_3O_4 , mean diameter ≈ 10 nm) were selected as an iron oxide nucleus, which is magnetic in nature, owing to their previously explored lower toxicity and biodegradability (Iannone et al. 1991; Müller et al. 1996). Chitosan, a polymer acting as a shell of the nanosized particles of magnetic nature (NPs), was used for designing the nanocomposites owing to biostability, in vivo vulnerability towards lysozymes and non-malignant atmosphere (Pitt 1990). In the proposed study, a co-precipitation technique was applied to formulate a colloids of Fe_3O_4 nanoparticles. Chitosan was synthesized following the coacervation method that involves the accumulation of sodium sulphate and chitosan resulting in reduced solubility of chitosan which further leads its precipitation rapidly. Chitosan- Fe_3O_4 nanocomposites were also prepared following the same technique with a little variation. Finally, gemcitabine was filled following both the surface adsorption and entrapment procedure in the preformed Fe_3O_4 /chitosan nanocomposites (Arias et al. 2012).

In another study, chitosan (CS) was further allowed to get cross-linked by carboxymethyl- β -cyclodextrin (CM- β -CD) polymer altered Fe_3O_4 nanoparticles of magnetic nature and were reported to deliver a hydrophobic anticancer drug, named, 5-fluorouracil (CS-CDpoly-MNPs) (Ding et al. 2015). Carboxymethyl- β -cyclodextrin was allowed to get attached on the surface of Fe_3O_4 nanoparticles (CDpoly-MNPs) attributing to the development of accumulation abilities due to the insertion capacities of its lipophilic hole with anti-malignant drugs of insoluble nature via host to guest relations. Tentative result specified the nanocarriers to exhibit a higher loading efficacy ($44.7 \pm 1.8\%$) through a superior magnetization of 43.8 emu/g. Magnetic nanocomposite of mesoporous nature, mainly composed of magnetite and silica (SiO_2) enfolded with chitosan, was also found to regulate the secretion of doxorubicin in another report (Wu et al. 2017). Chitosan acted as per a hindering species to resist early secretion of the medicaments. The composite showed decent response to pH and released 86.1% of the total medicaments laden in 48 h at a pH value of 4 as well.

Quantum dot and the surface modified magnetic nanoparticles of Fe_3O_4 (CdTe@ZnS) together with chitosan derivative were explored for both the cell marking and secretion of medicaments by Ding et al. (2017). Glutaraldehyde, as cross-linker, was used to modify the strength and chemical assimilation between

different components. The composite showed better magnetic character while using *in vitro* imaging and cell culture as well. Doxorubicin was reported to release from the stated composite depending on the variation of pH.

Prabha and Raj demonstrated a novel preparation and categorization of the drug, curcumin, laden Fe_3O_4 -chitosan-polyethylene glycol (Fe_3O_4 -CS-PEG), Fe_3O_4 -chitosan (Fe_3O_4 -CS) and Fe_3O_4 -chitosan-polyethylene glycol-polyvinylpyrrolidone (Fe_3O_4 -CS-PEG-PVP) particles of nanosize as an efficient carrier of medicaments for the directed drug delivery (Prabha and Raj 2016). In their study, they found curcumin having a modified encapsulation potential and loading capability, however, utilizing the Fe_3O_4 -CS-PEG, Fe_3O_4 -CS and Fe_3O_4 -CS-PEG-PVP particles of nanosize as drug transporters. The *in vitro* secretion analysis of curcumin suggested the Cur-loaded Fe_3O_4 -CS-PEG-PVP, Fe_3O_4 -CS and Fe_3O_4 -CS-PEG particles of nanosize with promising implementations for the treatment of malignancy at different pH as well.

An investigation led by Singh et al. also described an innovative method to formulate chitosan-iron oxide nanocomposite film where hydrothermally fabricated magnetic α - Fe_3O_4 nanoparticles were well distributed in chitosan (Singh et al. 2011). Fabricated composites were found to show prominent applications in biomedical sector as well.

Zhang et al. reported a magnetic and thermosensitive hydrogel in delivering intravesical *Bacillus Calmette-Guérin* (BCG). Hydrogels were fabricated using Fe_3O_4 nanoparticles of magnetic nature (Fe_3O_4 -MNP), chitosan (CS) and *b*-glycerophosphate (GP) (Zhang et al. 2013). In their assessment, the application of a magnetic and thermosensitive hydrogel comprising of chitosan and *b*-glycerophosphate as an appropriate medium for prolonged BCG distribution through intravesical track was firstly described. Thermosensitive gel, which are both injectable and biodegradable, exhibited a quick phase alteration consisting of sol and gel both *in vitro* and *in vivo* at 37 °C with notable magnetic activity. Predominantly, such gel allowed an intravesical uninterrupted discharge of BCG within 48 h with the existence of magnetic region. Continuous distribution of BCG significantly improved the anti-malignant efficiency while inducing a higher resistance in bladder.

Further assessment by Lin et al. explored a multifunctional, biostable and healing nanoparticles (NPs) through the modification of polyethylene glycolated methotrexate (MTX-PEG) and cyanin dye from the near-infrared fluorescent region (Cy5.5) on the exterior of the composite having chitosan and iron oxide particles of nanosize (CS-IONPs) (Lin et al. 2015).

22.5 Characterization of Iron Oxide-Chitosan Nanocomposites

It is considered to be very essential to characterize the synthesized iron oxide-chitosan nanocomposites after its preparation to determine the structural conformation of the newly synthesized composites and to establish their characteristic

properties as well. Several studies have been found to characterize the synthesized products as follows:

22.5.1 SEM/TEM/SAED Analysis of Iron Oxide and Nanocomposite Film

Surface structure of the samples is usually assessed by scanning electron microscopy (SEM) analysis. As revealed in Fig. 22.3, SEM images of chitosan (CS) reveal nonporous and even membranous stages comprising of cupola-shaped cavities, fibrils and crystals of microsize. Furthermore, it indicates the smooth lamellar stages on which a greater quantity of extended fibrils are evidently present. Typical SEM images of nanocomposite film, composed of chitosan and Fe_2O_3 (CS- $\alpha\text{-Fe}_2\text{O}_3$), and

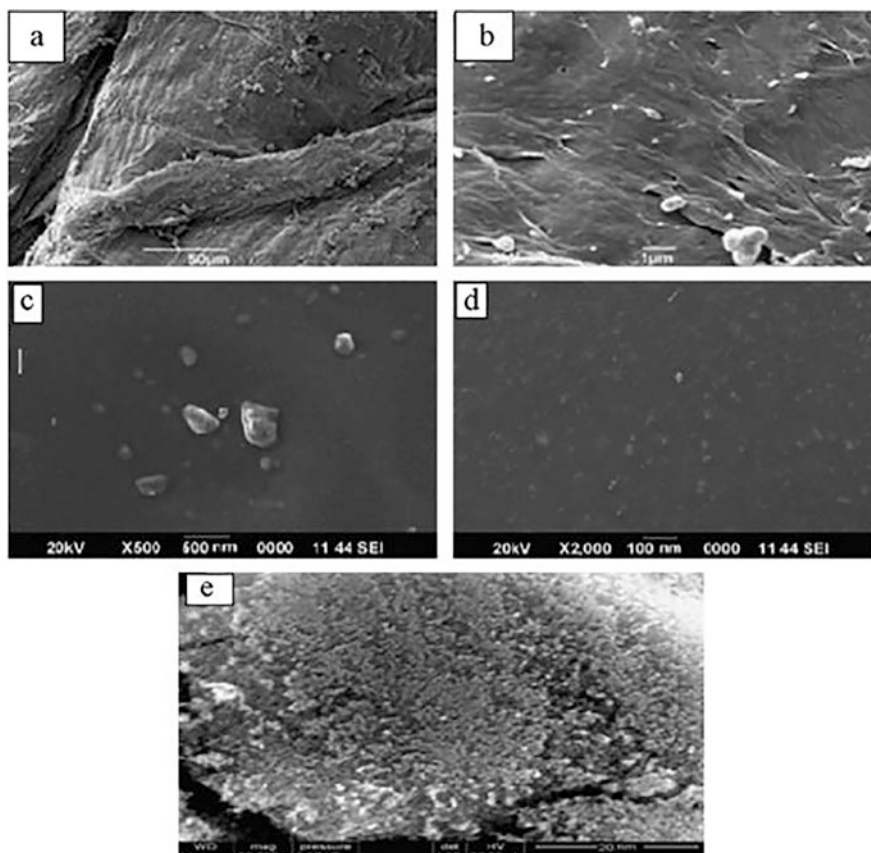


Fig. 22.3 Scanning electron microscopic images of pure chitosan (a, b), nanocomposite film comprising chitosan and iron oxide (c and d) and pure nanoparticles of iron oxide (e) at different magnifications (Singh et al. 2011), Rights (2011), with authorization from Elsevier publisher

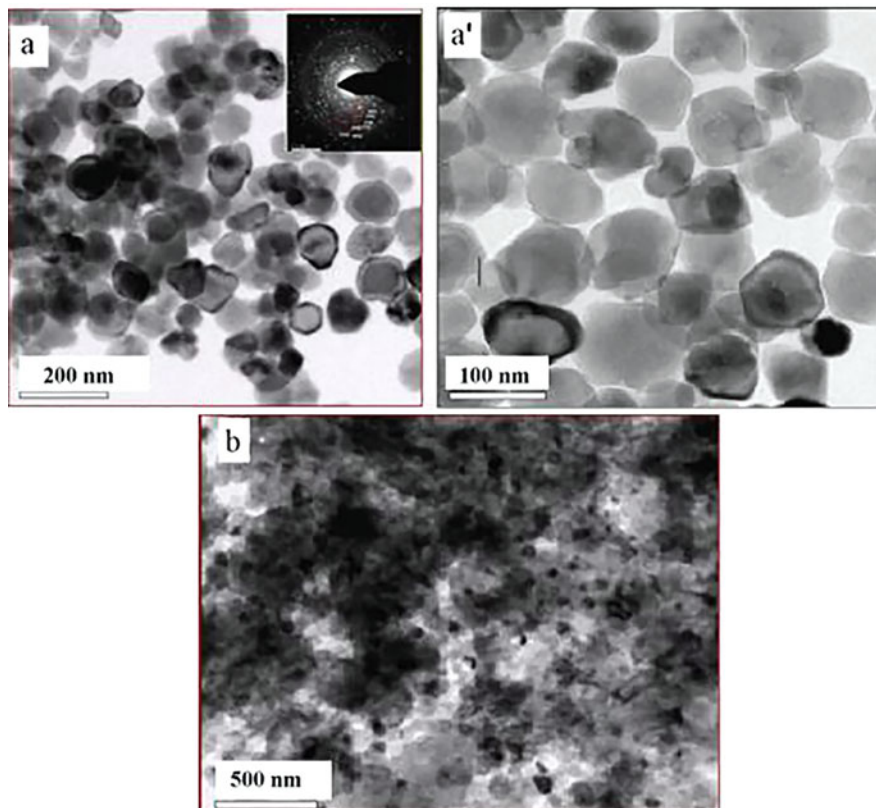


Fig. 22.4 Transmission electron micrograph and (with the insertion of SAED) configuration of iron oxide nanoparticles (a and a' respectively) and nanocomposite film comprising of chitosan and iron oxide (b). (Adapted from Singh et al. (2011), with permission from Elsevier)

hematite nanoparticle are also shown in Fig. 22.3c, d and at different magnifications as well (Fig. 22.3e). According to the figures, the spheroid shape of the CH- α -Fe₂O₃ nanocomposite film is attained when their overall surface is found to be quite granular (as presented in Fig. 22.3c, d) and the diameter of the specimens, particulate in shape, remains in a range of 100–350 nm. The hematite nanoparticles have been found to be uniformly dispersed in the CS matrix indicating the successful entrapment of hematite nanoparticles in chitosan.

Here, Fig. 22.4 demonstrates the transmission electron microscopic (TEM) images of both the naked and coated (with chitosan) hematite nanoparticles. It is found that the free nanoparticles of α -Fe₂O₃ are hexagonal in shape with spherical morphology and average width of about 87 nm. The particular region present in electron diffraction pattern (SAED) (inclusion of Fig. 22.4a), which was collected from the entire area of the nanosized particles, reveals a sequence of deflection patterns along with enlightened marks attributing to the polycrystalline nature of

α -Fe₂O₃ nanoparticles consistent to its crystal planes. Figure 22.4b represents the TEM image of chitosan and Fe₂O₃ nanocomposite. As presented in the figure, the arrangement of CS-coated α -Fe₂O₃ nanoparticles is found looser which also leads to the larger dimension and the average width of such an arrangement (~110 nm).

22.5.2 X-Ray Diffraction (XRD) Analysis

Crystalline structures of chitosan and modified chitosan composites (chitosan, CDpoly-MNPs and CS-CDpolyMNPs) can easily be categorized by XRD configuration in Fig. 22.5a (Ding et al. 2015). No evident diffraction peak is observed and merely a wide crowning situated at about $2\theta = 20.5^\circ$ is identified in the XRD configuration of chitosan which indicate the amorphous structure of raw chitosan. Fundamental distinctive crests of CDpoly-MNPs occurring at the values of about $2\theta = 43.02^\circ, 35.5^\circ, 30.1^\circ, 53.56^\circ, 62.36^\circ$ and 57.18° are correspond to (400), (311), (220), (422), (440) and (511) planes of Fe₃O₄ crystals, correspondingly which further ensure the cubic spinel structure of Fe₃O₄ crystal regarding the regular XRD data. In addition, XRD configuration of CDpoly-MNPs reveals that the successful grafting of CM- β -CD has no impact in the ordered segment alteration of Fe₃O₄. Moreover, the fragile crest (at 2θ) appearing in the range of 18° – 25° in the CDpolyMNPs assigns the covering of macromolecule designated CM- β -CD throughout the centres of magnetic origin (Jiang et al. 2008). The most parallel XRD configurations of CS-CDpoly-MNPs and CDpoly-MNPs also approve the fact that all the magnetic magnetite particles of nanosizes have been effectively incorporated inside the nanosized drug transporters of magnetic nature. Nevertheless, all the characteristic points associated with the marginally descending deflection strength of CDpoly-MNPs coated with chitosan than that of CDpoly-MNPs indicate the relations among chitosan polymer and CDpoly-MNPs. In addition, the

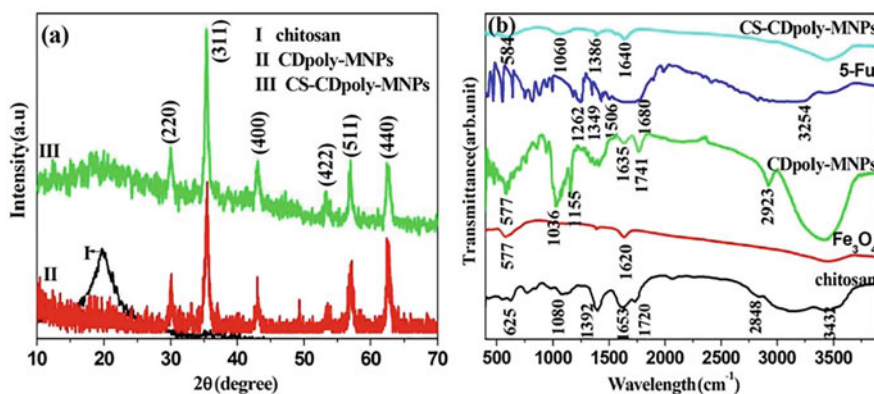


Fig. 22.5 (a) XRD patterns and (b) FT-IR spectra of the nanoparticles of CS-CDpoly-MNP. (Adapted from Ding et al. (2015) with permission from Elsevier)

strength of broad crest at the value of about $2\theta = 20.5^\circ$ is found to be expressively weakened when the unstructured region is comparatively modified. Such phenomena attribute to the presence of cross-linking that destroy both the uniformity and structure of the molecular sequence while decreasing the capability of polysaccharide to get themselves arranged.

22.5.3 Fourier Transform Infrared Spectroscopy (FT-IR) Analysis

Structural changes together with the formation or breaking down of new bonds can be examined by means of FT-IR study. Figure 22.5b illustrates the FT-IR results of Fe_3O_4 , 5-fluorouracil, chitosan and CM- β -CD in CS-CDpoly-MNPs fusion. According to the FT-IR result of chitosan, characteristic bands of adsorption are found at 1080 cm^{-1} , 1653 cm^{-1} and 2848 cm^{-1} that are responsible for vibrational extension of C-O and asymmetric stretching of C-H respectively (Li et al. 2008b). Characteristic band, shown at 3432 cm^{-1} , also assigns the vibrational mode of O-H which is laid over the stretching of N-H and internal hydrogen linkages of the carbohydrates while representing the ability of the residual hydroxyl and amino groups to coordinate with metal (Zhang et al. 2007). The presence of absorption band at 580 cm^{-1} in the FT-IR spectrum of Fe_3O_4 can be attributed to the existence of Fe-O bond (Li et al. 2008a). Entire substantial peaks responsible for CM- β -CD polymer in between 900 and 1200 cm^{-1} are also found to exist in the spectrum of CDpoly-MNPs having a minor change. Furthermore, another distinctive peak at 1635 cm^{-1} (responsible for the presence of metal ion derivatized carboxylic acid group) indicates the reaction between the COOH groups of CM- β -CD polymer and OH groups present on Fe_3O_4 particles ensuring the development of the iron carboxylate (Badruddoza et al. 2011). In the spectrum of antitumour drug 5-fluorouracil, characteristic bands at 506 cm^{-1} , 1349 cm^{-1} and 1680 cm^{-1} can be assigned to the presence of aromatic ring, bending vibration of C-F and C-O bond, respectively, in its structure. In case of the hybrid of CS-CDpoly-MNP, the extension sensations of C-N linkages are found at 1640 cm^{-1} . Such characteristic band clearly depicts the creation of Schiff's base as a consequence of the interaction among the carbonyl groups present in glutaraldehyde and the amine groups existing in chitosan. Moreover, the absorption peak of C-O corresponding to the presence of hydroxyl group has found to become durable and shifted from 1080 cm^{-1} to 1060 cm^{-1} . Lastly, the fascination of Fe-O bond of Fe_3O_4 in the hybrid of CS-CDpoly-MNP additionally proves the successful wrapping of Fe_3O_4 nanoparticles by cross-linked chitosan which is in a virtuous similarity with the inferences of XRD studies.

22.5.4 Surface Thermodynamics with the Development of Polymeric Coating

Assessment of the permitted energy of the surface (designated as, γ_s) of nanomaterials is utilized to evaluate the behaviour of coating using chitosan. The

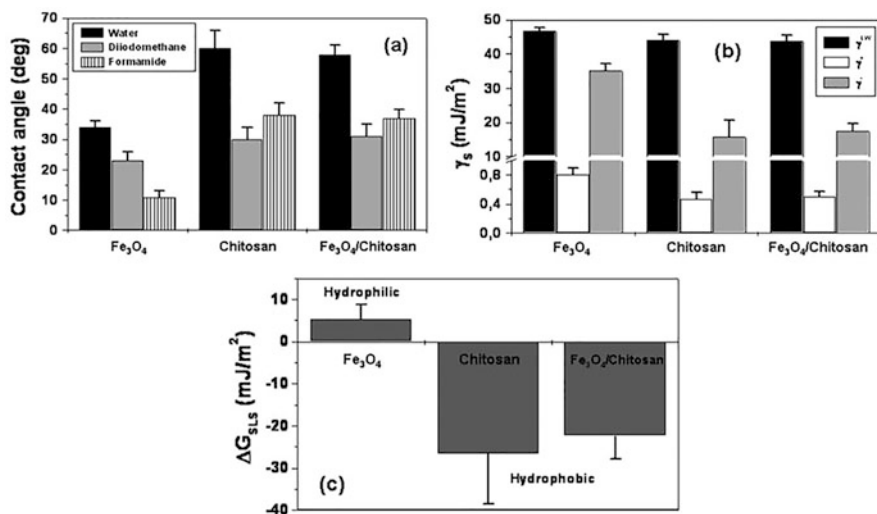


Fig. 22.6 (a) Contact angle, θ (degrees), (b) external free energy constituents (mJ m^{-2}) of chitosan, iron oxide and composite comprising the nanosized particles of iron oxide and chitosan, (c) interfacial energy (mJ m^{-2}) among solid and liquid phases (mJ m^{-2}) along with lipophilic/lipophobic response of the three types of nanoparticles stated above. (Adapted from Arias et al. (2012). Copyright (2012) Royal Society of Chemistry publisher)

angle of contact obtained by three probe liquids on dry particle films suggests the substantial dissimilarities among the three materials (Fig. 22.6a) (Arias et al. 2012). Nonetheless, it is the valuation of the γ_s constituents which delivers the improved categorization of thermodynamics prevailing on the surface (Fig. 22.6b). As given, whatsoever the element being measured, values for the Fe₃O₄/chitosan NPs are found to remain same to those for the bare polymer. For example, electron acceptor components indicate greater values for Fe₃O₄ (a monopolar and electron-donor material) compared to the nanosized particles of chitosan or the nanosized particles following the core and shell configuration. Therefore, the evaluation of thermal behaviour depicts the electrokinetic one with adequate coverage, as the surface free energy constituents (γ_s) of nanocomposites accord nearly with those of pure chitosan NPs.

Changes in the free energy of surface usually remark itself in the lipophilic/water loving character of the nanosized materials. The assessment of the free energy of contact, while avoiding any electrodynamics, among the segments of solid phase dipped in the liquid can be utilized to evaluate hydrophobicity or hydrophilicity of the material (Van Oss 2006).

This quantity of the free energy of interaction remains undesirable for hydrophobic materials whereas interactions, prevailing on the interface, favour fascination between the particles to each other. In contrast, a hydrophilic character correspondingly associates with the constructive values of the free energy of interaction. As

shown in Fig. 22.6c, the hydrophilic character of Fe_3O_4 is found to get modified while providing the core hydrophobic in nature when covered with chitosan.

To conclude, thermodynamic data obtained from the surface also support as well to evaluate the mechanism involving chitosan films placed on the surface of iron oxide particles. Commencing γ_S data, the free energy of interaction between chitosan (C) and magnetite (M) in the liquid atmosphere (A), ΔG_{MAC} can be determined utilizing the following relation by Dupré:

$$\Delta G = \gamma_{\text{MC}} - \gamma_{\text{MA}} - \gamma_{\text{CA}} \quad (22.1)$$

Result of the design (found about $-9.8 \pm 1.1 \text{ mJ m}^{-2}$) reveals the presence of both the acid-base and van der Waals attractions between Fe_3O_4 and the polymer. To conclude, it is thermodynamically preferable for chitosan to stay connected onto Fe_3O_4 NPs than remaining as isolated individuals present in water.

22.5.5 Magnetic Properties

Magnetic sensitivity of the nanosized particles of iron oxide and chitosan composite can be evaluated by studying the hysteresis cycle (as shown in Fig. 22.7a) (Arias et al. 2012). The lenient magnetic properties of the nanosized composite as described above is deceptive in the figure as both the cumulative and diminishing area subdivisions prevailing in hysteresis loop are barely different to the responsiveness of the appliances utilized. The rectilinear segments of the curvature represent original vulnerability (with the proximate value of 1.6 ± 0.1) together with the saturation magnetization (with the proximate value of $167 \pm 2 \text{ kA m}^{-1}$) can be estimated for the nanosized composites with magnetic nature.

The sensitivity of nanosized composites based on core and shell to the applied magnetics can then be assessed by an inspection through the visual microscopy of a hydrous mixture under the coverage of a magnetic slope (1.1 T). Amusingly, initial uniform spreading of the nanosized particles based on core and shell in the magnetofluid has been found to be strongly modified with the development of chainlike masses similar to the outlines (inset in Fig. 22.7a) as the magnetic interaction represents a noteworthy influence in excess of the colloidal attractions between the nanosized particles of composite despite the presence of cover provided by polymers. Figure 22.7b represents heating of magnetofluid (around 10 mg mL^{-1}) based on chitosan and iron oxide in vitro system under the exposure of an oscillating electromagnetic gradient having extended frequency. With the influence of the irregular magnetic slope, fluctuation of magnetic moment in nanocomposite usually generates heat around 45°C . Excitingly, in the presence of such generated heat malignant cells get permanently spoiled (Huber 2005).

According to the figure, temperature was allowed to rise from the existing atmospheric temperature to $\sim 41^\circ\text{C}$ in 15 min roughly. During the exposure of tentative situations, the extreme temperature that can be attained is about 45°C afore stabilization till the culmination of trial. This reveals a valued regulation of

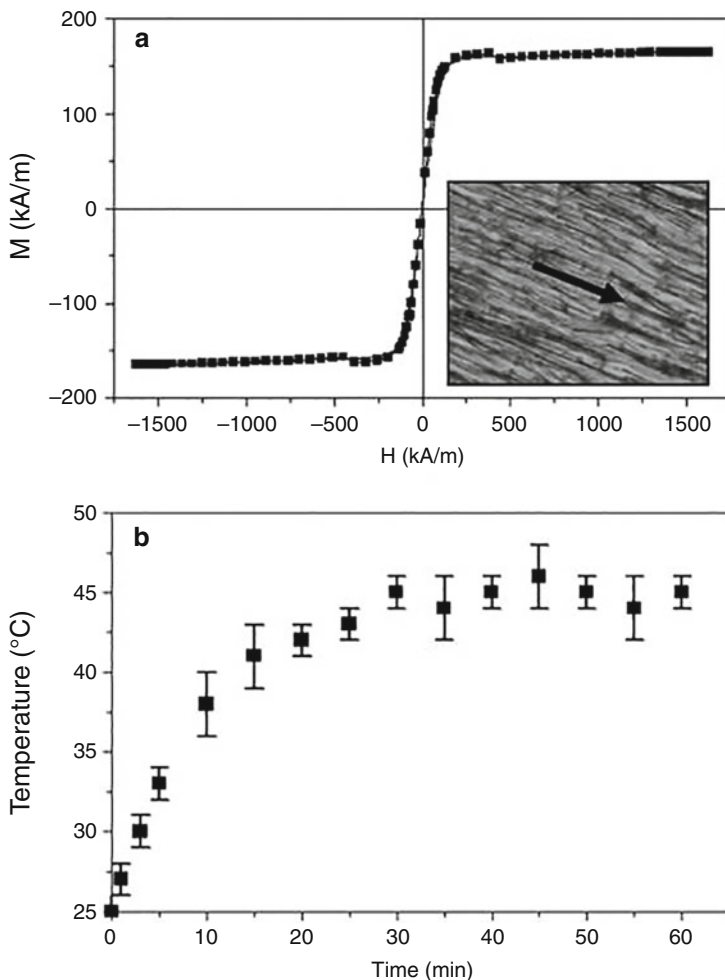


Fig. 22.7 (a) Hysteresis cycle of the nanosized composites comprising of chitosan and iron oxide (inset: optical microscopic image of a core- and shell-based composite in aqueous mixture with the influence of a magnetic slope (1.1 T) parallel to the arrow). (b) Heating curve of a magnetofluid (10 mg mL^{-1}) comprising of chitosan and iron oxide under the exposure of an electromagnetic slope having frequency of 250 kHz and intensity of 4 kA m^{-1} . (Adapted from Arias et al. (2012), Copyright (2012), with permission from Royal Society of Chemistry)

both the heat flux and the temperature acting as elementary requisites to utilize hyperthermia. Moreover, we need to retain in attention while rising the temperature above 48°C as the vigorous tissues adjacent to the tumour site can get scorched and spoiled badly at the elevated temperature (Lao and Ramanujan 2004).

22.5.6 Thermogravimetric (TGA) Analysis

TGA is commonly utilized to evaluate the heat stability of samples under nitrogen atmosphere. Typical thermograms of the film comprising of chitosan and alginate in the deficiency and occurrence of Fe_3O_4 have been shown in Fig. 22.8. The thermograms are almost similar excepting a little transference during the onset of degradation with iron depicting an effective bonding of cores (iron core) to the film. Thorough deterioration of the sheets is obtained at about 1000°C . In case of chitosan alginate film, approximately 4% residue exists at the end of the reaction, demonstrating an almost complete elimination of pattern. With the existence of iron core, the remaining load increases to 6% upon the termination of the reaction.

22.6 Conclusion

Organized and particular drug delivery in biomedical applications have become a remarkable feature with the enhanced availability of highly specific drugs that overcome severe adverse effects. Chitosan, as one of the biocompatible and biodegradable polymer, plays a significant character in such applications. Nanocomposites based on chitosan provide superior properties and incentive matrix for the directed drug transportation. Several studies, associated with the preparations of chitosan and its composites comprising iron oxide nanoparticles, have been discussed here while improving the solubility of insoluble drugs through the formation of complex with enhanced stability and their secured release to the targeted

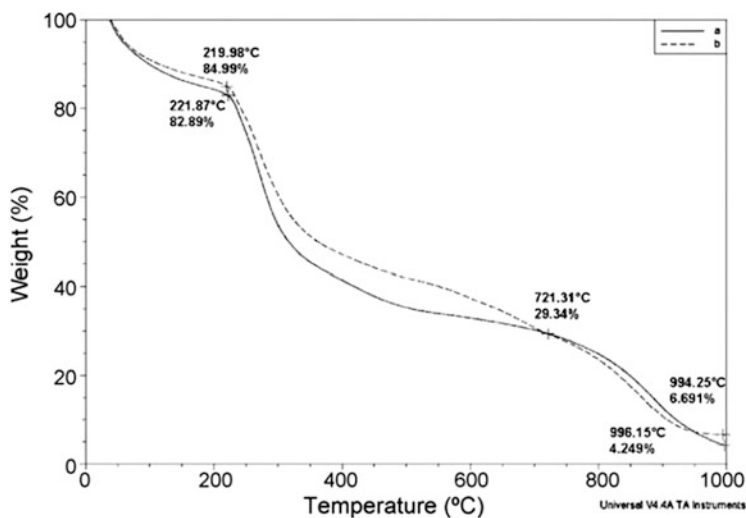


Fig. 22.8 Thermograms of a film comprising of chitosan and alginate with (a) and without (b) iron oxide particles. (Adapted from Sreeram et al. (2009) with permission from Elsevier)

place. Complete characterization of the prepared iron oxide-chitosan nanocomposites supports the stated applications as well.

References

- Abdeen R, Salahuddin N (2013) Modified chitosan-clay nanocomposite as a drug delivery system intercalation and in vitro release of ibuprofen. *J Chem* 2013:576370
- Adewunmi AA, Ismail S, Sultan AS (2016) Carbon nanotubes (CNTs) nanocomposite hydrogels developed for various applications: a critical review. *J Inorg Organomet Polym Mater* 26:717–737
- Ali A, Ahmed S (2018) A review on chitosan and its nanocomposites in drug delivery. *Int J Biol Macromol* 109:273–286
- Arias JL, Reddy LH, Couvreur P (2012) Fe₃O₄/chitosan nanocomposite for magnetic drug targeting to cancer. *J Mater Chem* 22:7622–7632
- Azhar FF, Olad A (2014) A study on sustained release formulations for oral delivery of 5-fluorouracil based on alginate–chitosan/montmorillonite nanocomposite systems. *Appl Clay Sci* 101:288–296
- Badruddoza A, Tay A, Tan P, Hidajat K, Uddin M (2011) Carboxymethyl- β -cyclodextrin conjugated magnetic nanoparticles as nano-adsorbents for removal of copper ions: synthesis and adsorption studies. *J Hazard Mater* 185:1177–1186
- Baek S-H, Kim B, Suh K-D (2008) Chitosan particle/multiwall carbon nanotube composites by electrostatic interactions. *Colloids Surf A Physicochem Eng Asp* 316:292–296
- Bhatt AS, Bhat DK, Santosh M (2010) Electrical and magnetic properties of chitosan-magnetite nanocomposites. *Phys B Condens Matter* 405:2078–2082
- Bonadio J, Smiley E, Patil P, Goldstein S (1999) Localized, direct plasmid gene delivery in vivo: prolonged therapy results in reproducible tissue regeneration. *Nat Med* 5:753–759
- Careno-Gomez B, Woodley J, Florence A (1999) Studies on the uptake of tomato lectin nanoparticles in everted gut sacs. *Int J Pharm* 183:7–11
- Check E (2002) Regulators split on gene therapy as patient shows signs of cancer. Nature Publishing Group
- Check E (2003) RNA to the rescue? Nature Publishing Group
- Cirillo G, Hampel S, Spizzirri UG, Parisi OI, Picci N, Iemma F (2014) Carbon nanotubes hybrid hydrogels in drug delivery: a perspective review. *Biomed Res Int* 2014:825017
- De Azeredo HM (2009) Nanocomposites for food packaging applications. *Food Res Int* 42:1240–1253
- De Vos P, Marchetti P (2002) Encapsulation of pancreatic islets for transplantation in diabetes: the untouchable islets. *Trends Mol Med* 8:363–366
- Depan D, Kumar AP, Singh RP (2009) Cell proliferation and controlled drug release studies of nano hybrids based on chitosan-g-lactic acid and montmorillonite. *Acta Biomater* 5:93–100
- Ding Y, Shen SZ, Sun H, Sun K, Liu F, Qi Y, Yan J (2015) Design and construction of polymerized-chitosan coated Fe₃O₄ magnetic nanoparticles and its application for hydrophobic drug delivery. *Mater Sci Eng C* 48:487–498
- Ding Y, Yin H, Shen S, Sun K, Liu F (2017) Chitosan-based magnetic/fluorescent nanocomposites for cell labelling and controlled drug release. *New J Chem* 41:1736–1743
- Doulabi AH, Mequanint K, Mohammadi H (2014) Blends and nanocomposite biomaterials for articular cartilage tissue engineering. *Materials* 7:5327–5355
- Emerich DF, Winn SR, Hantraye PM, Peschanski M, Chen E-Y, Chu Y, Mcdermott P, Baetge EE, Kordower JH (1997) Protective effect of encapsulated cells producing neurotrophic factor CNTF in a monkey model of Huntington's disease. *Nature* 386:395–399
- Fang C, Bhattarai N, Sun C, Zhang M (2009) Functionalized nanoparticles with long-term stability in biological media. *Small* 5:1637–1641

- Fernandes SC, Freire CS, Silvestre AJ, Neto CP, Gandini A, Berglund LA, Salmén L (2010) Transparent chitosan films reinforced with a high content of nanofibrillated cellulose. *Carbohydr Polym* 81:394–401
- Fortin J-P, Wilhelm C, Servais J, Ménager C, Bacri J-C, Gazeau F (2007) Size-sorted anionic iron oxide nanomagnets as colloidal mediators for magnetic hyperthermia. *J Am Chem Soc* 129:2628–2635
- Gabizon AA (2001) Pegylated liposomal doxorubicin: metamorphosis of an old drug into a new form of chemotherapy. *Cancer Invest* 19:424–436
- Gao J, Gu H, Xu B (2009) Multifunctional magnetic nanoparticles: design, synthesis, and biomedical applications. *Acc Chem Res* 42:1097–1107
- Goonoo N, Bhaw-Luximon A, Bowlin GL, Jhurry D (2013) An assessment of biopolymer-and synthetic polymer-based scaffolds for bone and vascular tissue engineering. *Polym Int* 62:523–533
- Gutiérrez TJ, Ponce AG, Alvarez VA (2017) Nano-clays from natural and modified montmorillonite with and without added blueberry extract for active and intelligent food nanopackaging materials. *Mater Chem Phys* 194:283–292
- Harashima H, Hiraiwa T, Ochi Y, Kiwada H (1995) Size dependent liposome degradation in blood: in vivo/in vitro correlation by kinetic modeling. *J Drug Target* 3:253–261
- Henry S, Mcallister DV, Allen MG, Prausnitz MR (1998) Microfabricated microneedles: a novel approach to transdermal drug delivery. *J Pharm Sci* 87:922–925
- Hortelano G, Al-Hendy A, Ofosu FA, Chang PL (1996) Delivery of human factor IX in mice by encapsulated recombinant myoblasts: a novel approach towards allogeneic gene therapy of hemophilia B. *Blood* 87:5095–5103
- Houdellier F, Masseboeuf A, Monthieux M, Hÿtch MJ (2012) New carbon cone nanotip for use in a highly coherent cold field emission electron microscope. *Carbon* 50:2037–2044
- Hua S, Yang H, Wang W, Wang A (2010) Controlled release of ofloxacin from chitosan-montmorillonite hydrogel. *Appl Clay Sci* 50:112–117
- Huber DL (2005) Synthesis, properties, and applications of iron nanoparticles. *Small* 1:482–501
- Iannone A, Magin R, Walczak T, Federico M, Swartz H, Tomasi A, Vannini V (1991) Blood clearance of dextran magnetite particles determined by a noninvasive in vivo ESR method. *Magn Reson Med* 22:435–442
- Illum L (2002) Nasal drug delivery: new developments and strategies. *Drug Discov Today* 7:1184–1189
- Illum L, Jabbal-Gill I, Hinchcliffe M, Fisher A, Davis S (2001) Chitosan as a novel nasal delivery system for vaccines. *Adv Drug Deliv Rev* 51:81–96
- Jiang Y, Jiang J, Gao Q, Ruan M, Yu H, Qi L (2008) A novel nanoscale catalyst system composed of nanosized Pd catalysts immobilized on Fe₃O₄@ SiO₂-PAMAM. *Nanotechnology* 19:075714
- Karimi Z, Karimi L, Shokrollahi H (2013) Nano-magnetic particles used in biomedicine: core and coating materials. *Mater Sci Eng C* 33:2465–2475
- Kilpatrick DC, Pusztai A, Grant G, Graham C, Ewen SW (1985) Tomato lectin resists digestion in the mammalian alimentary canal and binds to intestinal villi without deleterious effects. *FEBS Lett* 185:299–305
- Kong SD, Sartor M, Hu C-MJ, Zhang W, Zhang L, Jin S (2013) Magnetic field activated lipid-polymer hybrid nanoparticles for stimuli-responsive drug release. *Acta Biomater* 9:5447–5452
- Langer R (2003) Where a pill won't reach. *Sci Am* 288:50–57
- Lao L, Ramanujan R (2004) Magnetic and hydrogel composite materials for hyperthermia applications. *J Mater Sci Mater Med* 15:1061–1064
- Lavan DA, Lynn DM, Langer R (2002) Moving smaller in drug discovery and delivery. *Nat Rev Drug Discov* 1:77–84
- Lavan DA, Mcguire T, Langer R (2003) Small-scale systems for in vivo drug delivery. *Nat Biotechnol* 21:1184–1191

- Li G-Y, Jiang Y-R, Huang K-L, Ding P, Yao L-L (2008a) Kinetics of adsorption of *Saccharomyces cerevisiae* mediated dehydrogenase on magnetic Fe₃O₄-chitosan nanoparticles. *Colloids Surf A Physicochem Eng Asp* 320:11–18
- Li P, Zhu AM, Liu QL, Zhang QG (2008b) Fe₃O₄/poly (N-isopropylacrylamide)/chitosan composite microspheres with multiresponsive properties. *Ind Eng Chem Res* 47:7700–7706
- Lim E-K, Chung BH (2016) Preparation of pyrenyl-based multifunctional nanocomposites for biomedical applications. *Nat Protoc* 11:236–251
- Lim E-K, Sajomsang W, Choi Y, Jang E, Lee H, Kang B, Kim E, Haam S, Suh J-S, Chung SJ (2013) Chitosan-based intelligent theragnosis nanocomposites enable pH-sensitive drug release with MR-guided imaging for cancer therapy. *Nanoscale Res Lett* 8:467
- Lin J, Li Y, Li Y, Wu H, Yu F, Zhou S, Xie L, Luo F, Lin C, Hou Z (2015) Drug/dye-loaded, multifunctional PEG-chitosan-iron oxide nanocomposites for methotrexate synergistically self-targeted cancer therapy and dual modal imaging. *ACS Appl Mater Interfaces* 7:11908–11920
- Liu T-Y, Chen S-Y, Li J-H, Liu D-M (2006) Study on drug release behaviour of CDHA/chitosan nanocomposites—effect of CDHA nanoparticles. *J Control Release* 112:88–95
- Liu K-H, Liu T-Y, Chen S-Y, Liu D-M (2008) Drug release behavior of chitosan-montmorillonite nanocomposite hydrogels following electrostimulation. *Acta Biomater* 4:1038–1045
- Liu X, Hu Q, Fang Z, Zhang X, Zhang B (2009) Magnetic chitosan nanocomposites: a useful recyclable tool for heavy metal ion removal. *Langmuir* 25:3–8
- Long J, Yu X, Xu E, Wu Z, Xu X, Jin Z, Jiao A (2015) In situ synthesis of new magnetite chitosan/carrageenan nanocomposites by electrostatic interactions for protein delivery applications. *Carbohydr Polym* 131:98–107
- Liu G, Kong L, Sheng B, Wang G, Gong Y, Zhang X (2007) Degradation of covalently cross-linked carboxymethyl chitosan and its potential application for peripheral nerve regeneration. *Eur Polym J* 43:3807–3818
- Ma Y, Tong S, Bao G, Gao C, Dai Z (2013) Indocyanine green loaded SPIO nanoparticles with phospholipid-PEG coating for dual-modal imaging and photothermal therapy. *Biomaterials* 34:7706–7714
- Mahmoudi M, Sant S, Wang B, Laurent S, Sen T (2011) Superparamagnetic iron oxide nanoparticles (SPIONs): development, surface modification and applications in chemotherapy. *Adv Drug Deliv Rev* 63:24–46
- Malesu VK, Sahoo D, Nayak P (2011) Chitosan-sodium alginate nanocomposites blended with cloisite 30b as a novel drug delivery system for anticancer drug curcumin. *Int J Appl Biol Pharm* 2(3):402–411
- Marshall E (1999) Gene therapy death prompts review of adenovirus vector. *Science* 286:2244–2245
- Massia SP, Stark J, Letbetter DS (2000) Surface-immobilized dextran limits cell adhesion and spreading. *Biomaterials* 21:2253–2261
- Mazzola L (2003) Commercializing nanotechnology. *Nat Biotechnol* 21:1137–1143
- Mcallister DV, Allen MG, Prausnitz MR (2000) Microfabricated microneedles for gene and drug delivery. *Annu Rev Biomed Eng* 2:289–313
- Meng H, Hu J (2010) A brief review of stimulus-active polymers responsive to thermal, light, magnetic, electric, and water/solvent stimuli. *J Intell Mater Syst Struct* 21:859–885
- Merkus F, Verhoef J, Martin E, Romeijn S, Van Der Kuy P, Hermens W, Schipper N (1999) Cyclodextrins in nasal drug delivery. *Adv Drug Deliv Rev* 36:41–57
- Miyazaki S, Nakayama A, Oda M, Takada M, Attwood D (1994) Chitosan and sodium alginate based bioadhesive tablets for intraoral drug delivery. *Biol Pharm Bull* 17:745–747
- Müller R, Maaßen S, Weyhers H, Specht F, Lucks J (1996) Cytotoxicity of magnetite-loaded polylactide, polylactide/glycolide particles and solid lipid nanoparticles. *Int J Pharm* 138:85–94
- Orive G, Gascón AR, Hernández RM, Igartua M, Pedraz JL (2003a) Cell microencapsulation technology for biomedical purposes: novel insights and challenges. *Trends Pharmacol Sci* 24:207–210

- Orive G, Hernández RM, Gascón AR, Calafiore R, Chang TM, De Vos P, Hortalano G, Hunkeler D, Lacic I, Shapiro AJ (2003b) Cell encapsulation: promise and progress. *Nat Med* 9:104–107
- Orive G, Hernandez RM, Gascón ARG, Dominguez-Gil A, Pedraz JL (2003c) Drug delivery in biotechnology: present and future. *Curr Opin Biotechnol* 14:659–664
- Paredes M, Pulcinelli SH, Peniche C, Gonçalves V, Santilli CV (2014) Chitosan/(ureasil-PEO hybrid) blend for drug delivery. *J Sol Gel Sci Technol* 72:233–238
- Parida UK, Nayak AK, Binhani BK, Nayak P (2011) Synthesis and characterization of chitosan-polyvinyl alcohol blended with cloisite 30B for controlled release of the anticancer drug curcumin. *J Biomater Nanobiotechnol* 2:414
- Paunescu T, Rajh T, Wiederrrecht G, Maser J, Vogt S, Stojićević N, Protić M, Lai B, Oryhon J, Thurnauer M (2003) Biology of TiO₂-oligonucleotide nanocomposites. *Nat Mater* 2:343–346
- Pillai SK, Ray SS (2012) Chitosan-based nanocomposites. *Nat Polym* 2:33–68
- Pitt C (1990) The controlled parenteral delivery of polypeptides and proteins. *Int J Pharm* 59:173–196
- Prabha G, Raj V (2016) Preparation and characterization of polymer nanocomposites coated magnetic nanoparticles for drug delivery applications. *J Magn Magn Mater* 408:26–34
- Reddy LH, Couvreur P (2008) Novel approaches to deliver gemcitabine to cancers. *Curr Pharm Des* 14:1124–1137
- Roberts M, Bentley M, Harris J (2002) Chemistry for peptide and protein PEGylation. *Adv Drug Deliv Rev* 54:459–476
- Sahoo S, Sasmal A, Nanda R, Phani A, Nayak P (2010) Synthesis of chitosan-polycaprolactone blend for control delivery of ofloxacin drug. *Carbohydr Polym* 79:106–113
- Salcedo I, Sandri G, Aguzzi C, Bonferoni C, Cerezo P, Sánchez-Espejo R, Viseras C (2014) Intestinal permeability of oxytetracycline from chitosan-montmorillonite nanocomposites. *Colloids Surf B Biointerfaces* 117:441–448
- Santin M, Huang S, Iannace S, Ambrosio L, Nicolais L, Peluso G (1996) Synthesis and characterization of a new interpenetrated poly (2-hydroxyethylmethacrylate)—gelatin composite polymer. *Biomaterials* 17:1459–1467
- Savić R, Luo L, Eisenberg A, Maysinger D (2003) Micellar nanocontainers distribute to defined cytoplasmic organelles. *Science* 300:615–618
- Sencadas V, Correia DM, Areias A, Botelho G, Fonseca A, Neves I, Ribelles JG, Mendez SL (2012) Determination of the parameters affecting electrospun chitosan fiber size distribution and morphology. *Carbohydr Polym* 87:1295–1301
- Sharifi I, Shokrollahi H, Amiri S (2012) Ferrite-based magnetic nanofluids used in hyperthermia applications. *J Magn Magn Mater* 324:903–915
- Shen W-C (2003) Oral peptide and protein delivery: unfulfilled promises? *Drug Discov Today* 8 (14):607–608
- Singh J, Srivastava M, Dutta J, Dutta P (2011) Preparation and properties of hybrid monodispersed magnetic α -Fe₂O₃ based chitosan nanocomposite film for industrial and biomedical applications. *Int J Biol Macromol* 48:170–176
- Sondjaja R, Hatton TA, Tam MK (2009) Clustering of magnetic nanoparticles using a double hydrophilic block copolymer, poly (ethylene oxide)-b-poly (acrylic acid). *J Magn Magn Mater* 321:2393–2397
- Sreeram KJ, Nidhin M, Nair BU (2009) Synthesis of aligned hematite nanoparticles on chitosan-alginate films. *Colloids Surf B Biointerfaces* 71:260–267
- Strain AJ, Neuberger JM (2002) A bioartificial liver—state of the art. *Science* 295:1005–1009
- Sun L, Wang Y, Jiang T, Zheng X, Zhang J, Sun J, Sun C, Wang S (2013) Novel chitosan-functionalized spherical nanosilica matrix as an oral sustained drug delivery system for poorly water-soluble drug carvedilol. *ACS Appl Mater Interfaces* 5:103–113
- Tao W, Wen R, Goddard MB, Sherman SD, O’rourke PJ, Stabila PF, Bell WJ, Dean BJ, Kauper KA, Budz VA (2002) Encapsulated cell-based delivery of CNTF reduces photoreceptor degeneration in animal models of retinitis pigmentosa. *Invest Ophthalmol Vis Sci* 43:3292–3298

- Thanou M, Verhoef J, Junginger H (2001) Oral drug absorption enhancement by chitosan and its derivatives. *Adv Drug Deliv Rev* 52:117–126
- Thomas D, Thomas S (2013) Chemical modification of chitosan and its biomedical application. In: *Biopolym nanocomposites*. Wiley, Hoboken, NJ, pp 33–51
- Torchilin VP, Lukyanov AN (2003) Peptide and protein drug delivery to and into tumors: challenges and solutions. *Drug Discov Today* 8:259–266
- Van Oss CJ (2006) *Interfacial forces in aqueous media*. CRC, Boca Raton, FL
- Venkatesan P, Puvvada N, Dash R, Kumar BP, Sarkar D, Azab B, Pathak A, Kundu SC, Fisher PB, Mandal M (2011) The potential of celecoxib-loaded hydroxyapatite-chitosan nanocomposite for the treatment of colon cancer. *Biomaterials* 32:3794–3806
- Veronese FM, Harris JM (2002) Peptide and protein PEGylation. *Adv Drug Deliv Rev* 54:453–456
- Wilson J, Poddar P, Frey N, Srikanth H, Mohamed K, Harmon J, Kotha S, Wachsmuth J (2004) Synthesis and magnetic properties of polymer nanocomposites with embedded iron nanoparticles. *J Appl Phys* 95:1439–1443
- Wu J, Jiang W, Shen Y, Tian R (2017) Synthesis and characterization of mesoporous magnetic nanocomposites wrapped with chitosan gatekeepers for pH-sensitive controlled release of doxorubicin. *Mater Sci Eng C* 70:132–140
- Xie M, Lei H, Zhang Y, Xu Y, Shen S, Ge Y, Li H, Xie J (2016) Non-covalent modification of graphene oxide nanocomposites with chitosan/dextran and its application in drug delivery. *RSC Adv* 6:9328–9337
- Yan LP, Wang YJ, Ren L, Wu G, Caridade SG, Fan JB, Wang LY, Ji PH, Oliveira JM, Oliveira JT (2010) Genipin-cross-linked collagen/chitosan biomimetic scaffolds for articular cartilage tissue engineering applications. *J Biomed Mater Res A* 95:465–475
- Yoo M-K, Park I-K, Lim H-T, Lee S-J, Jiang H-L, Kim Y-K, Choi Y-J, Cho M-H, Cho C-S (2012) Folate-PEG-superparamagnetic iron oxide nanoparticles for lung cancer imaging. *Acta Biomater* 8:3005–3013
- Yu L, Li L, Wei'an Z, Yue'e F (2004) A new hybrid nanocomposite prepared by graft copolymerization of butyl acrylate onto chitosan in the presence of organophilic montmorillonite. *Radiat Phys Chem* 69:467–471
- Yuan Q, Hein S, Misra R (2010a) New generation of chitosan-encapsulated ZnO quantum dots loaded with drug: synthesis, characterization and in vitro drug delivery response. *Acta Biomater* 6:2732–2739
- Yuan Q, Shah J, Hein S, Misra R (2010b) Controlled and extended drug release behavior of chitosan-based nanoparticle carrier. *Acta Biomater* 6:1140–1148
- Yuwei C, Jianlong W (2011) Preparation and characterization of magnetic chitosan nanoparticles and its application for Cu (II) removal. *Chem Eng J* 168:286–292
- Závišová V, Koneracká M, Múčková M, Lazová J, Juríková A, Lancz G, Tomašovičová N, Timko M, Kováč J, Vávra I (2011) Magnetic fluid poly (ethylene glycol) with moderate anticancer activity. *J Magn Magn Mater* 323:1408–1412
- Zhang H-F, Zhang L, Cui Y-C (2007) Synthesis of chitosan microsphere-resin supported palladium complex and its catalytic properties for Mizoroki-heck reaction. *React Funct Polym* 67:322–328
- Zhang Q, Song K, Zhao J, Kong X, Sun Y, Liu X, Zhang Y, Zeng Q, Zhang H (2009) Hexanedioic acid mediated surface-ligand-exchange process for transferring NaYF₄: Yb/Er (or Yb/Tm) up-converting nanoparticles from hydrophobic to hydrophilic. *J Colloid Interface Sci* 336:171–175
- Zhang L-Y, Zhu X-J, Sun H-W, Chi G-R, Xu J-X, Sun Y-L (2010) Control synthesis of magnetic Fe₃O₄-chitosan nanoparticles under UV irradiation in aqueous system. *Curr Appl Phys* 10:828–833

- Zhang L, Liu W, Xiao C, Yao J, Fan Z, Sun X, Zhang X, Wang L, Wang X (2011a) Preparation of poly (styrene)-b-poly (acrylic acid)/ γ -Fe₂O₃ composites. *J Magn Magn Mater* 323:3087–3091
- Zhang W, Zhang Z, Zhang Y (2011b) The application of carbon nanotubes in target drug delivery systems for cancer therapies. *Nanoscale Res Lett* 6:555
- Zhang D, Sun P, Li P, Xue A, Zhang X, Zhang H, Jin X (2013) A magnetic chitosan hydrogel for sustained and prolonged delivery of bacillus Calmette–Guérin in the treatment of bladder cancer. *Biomaterials* 34:10258–10266
- Zhou L, Yuan J, Yuan W, Sui X, Wu S, Li Z, Shen D (2009) Synthesis, characterization, and controllable drug release of pH-sensitive hybrid magnetic nanoparticles. *J Magn Magn Mater* 321:2799–2804



Nanocomposites Application in Sewage Treatment and Degradation of Persistent Pesticides Used in Agriculture

23

Nusrat Iqbal, Saurabh Dubey, Manmeet Kaur, Samsul Alam, Amrish Agrawal, Irani Mukherjee, and Jitendra Kumar

Abstract

Globally, nanotechnology is progressively used as wastewater management to remove organic and inorganic impurities. In near future, nanomaterials will play a momentous role in sewage plus industrial wastewater treatment by degrading the toxic compounds. In addition, nanoporous membrane filters have the ability to remove the pathogenic agents from wastewater. Advanced nanocomposites have the capability not only in physical cleanup of wastewater but also in the removal of pathogens/microbes from wastewater. The nanotechnology may be very effectively applied in agricultural sector to mitigate the persistent pesticides by adsorption/degradation with modified nanomaterials. Surface modification or grafting nanomaterials will increase the efficiency and stability of nanomaterials. This chapter presents the utilization of modified and combined form of nanomaterials in effluent treatment and pesticide degradation. Harmful effects of xenobiotics like persistence, toxicity toward non-target organisms, and soil pollution generated by runs of organic pesticides from fields and industrial pollutants can also be removed or degraded into nontoxic form by mineralization. Often useful components like CO_2 , H_2O , ions, and salts form during photocatalysis using metal oxide semiconductor nanostructures. In this chapter, advancements of nanotechnology applications are described along with examples in the sensing, removing, and pollutants degradation for sustainable agriculture and environment.

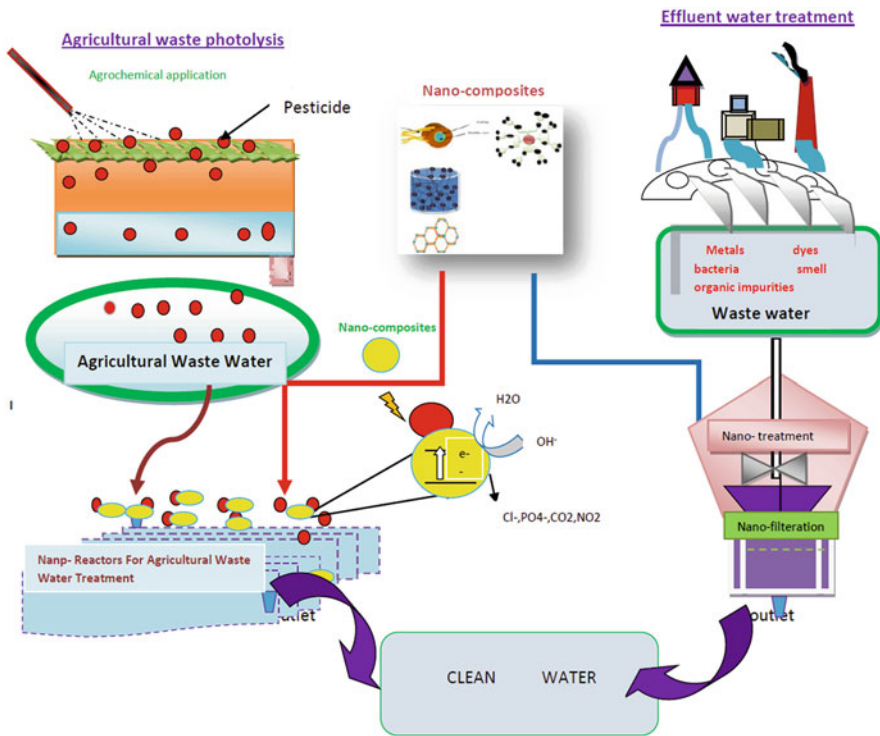
N. Iqbal · S. Dubey (✉) · M. Kaur · S. Alam · A. Agrawal · I. Mukherjee · J. Kumar
Formulation Division, Institute of Pesticide and Formulation Technology, Gurgaon, Haryana, India

© The Author(s), under exclusive license to Springer Nature Singapore Pte Ltd. 2022

649

L. M. Pandey, A. Hasan (eds.), *Nanoscale Engineering of Biomaterials: Properties and Applications*, https://doi.org/10.1007/978-981-16-3667-7_23

Graphical Abstract



Keywords

Nanotechnology · Agriculture · Sewage waste · Nanoparticle · Pollutant · Degradation · Photocatalysis

23.1 Introduction

In developing countries, about one billion population facing the problem of non-availability of potable water resources worldwide and 2.6 billion populations have access to potable water but no techniques to clean up. Consuming the impure and poor quality water results in economic, social, and environmental impact (Moore et al. 2003; Montgomery and Elimelech 2007).

The consumption of contaminated water leads to many impact on health and welfare of people, especially in children and aged. In addition, the environmental and human health impacts can adversely affect the future generations (Keller and Lazareva 2014). Therefore, sufficient, safe, and sustainable water supply is required

for human health and environment safety (Theron and Cloete 2002; Ashbolt 2004; Eshelby 2007).

The major challenges in the availability of potable water caused by droughts, over-rising residents, and contamination of groundwater by different sources which include industrial, municipal, and agricultural runoffs (Moe and Rheitigans 2006; Lee and Schwab 2005; Savage and Diallo 2005; orsmarty et al. 2000). These are the main contaminants which affect the water quality and limit the supply of potable water (Coetser et al. 2007; Kemper 2004; Cong et al. 2005).

The contamination of water bodies is basically originated by agricultural runoffs (like pesticides, fertilizers, irrigated water, etc.) and human wastes (improper drainage, sewage, industrial, etc.) which cause the suitable conditions for algal blooms and lead to the contamination of water bodies (Falconer and Humpage 2005; Rodriguez-Mozaz et al. 2004; Fawell and Nieuwenhuijsen 2003). The potable water is essential for sustaining life in both developing and developed countries. Hence, the feasible and advanced techniques should be considered for removing the scarcity of clean and potable water and fulfill the demand of people all over the world (Weber 2002). So, there is an urgent requirement for the development of pioneering technologies whereby challenges linked with the demand of pure and safe filtered potable water can be addressed.

There are many techniques available to remove the contaminants from water, but nowadays, nanotechnology is playing a pivotal role over conventional techniques in mitigating the contaminants. Nanotechnology provides in situ and field-based miniaturized, rapid, ultrasensitive, and inexpensive method for environmental monitoring and remediation of pollutants and cleanup (Ghasemzadeh et al. 2014; Thatai et al. 2014; Zhang 2003). Various types of nanocomposites have been developed yet as, for example, magnetic nanocomposites for decontamination of water (Kaur et al. 2014), encapsulation of iron oxide nanoparticles *Agrobacterium fabrum strain* nanobiosorbent in alginate polymer for removing metallic impurities (Sharma et al. 2018b; Tiwari et al. 2018). Many other nontoxic polymers have been identified for the encapsulating nanocomposites for the slow and regulated release (Hasan and Pandey 2015). In this chapter, prospects of nanotechnology are critically analyzed in view of sensing the contaminants for effective removal or degradation of the toxic constituents into nontoxic forms. This chapter attempts to bring forth the available developments and advances in nanotechnology applications for safe and clean environment.

23.2 Nanotechnology Application in Water Cleanup

Industries use various metals and chemicals in their process which generate large quality of effluents which contain toxic heavy metals and generate toxic liquids by mineral and mining processing (Foley et al. 2005). Toxic metallic ions include cadmium (Cd), lead (Pb), chromium (Cr), mercury (Hg), nitrate (NO_3^-), perchlorate (ClO_4^-), etc. (Lee et al. 2005; Jarup 2003). These heavy metal and organic contaminants in water bodies impact the public health, environment, and economy.

The high nitrate (NO_3^-) level in water causes detrimental effect to newborn babies and has carcinogenic properties (Kapoor and Iraraghavan 1997; Yang and Lee 2005). High level of perchlorate (ClO_4^-) causes considerable impact on human health and also associated with an induction of hypothyroidism in adults (Cheng et al. 2007; Urbansky and Schock 1999; Balogh et al. 2001). In addition, all chlorinated aromatic contaminants exhibit high toxicity (Xu et al. 2005). The other chlorinated molecule is trichloroethene (TCE), which has remarkably hazardous contaminants present in groundwater and causes hepatic disorders and complications in pregnancies (Nutt et al. 2006). Further, many other halogen-functionalized aromatic compounds are discovered recently which have very long half-life, are chemically stable, and become a very serious environmental contaminant (Keum and Li 2004).

The traditionally available techniques for water cleanup include solvent extraction, carbon adsorption technique, and oxidation processes. These techniques are quite effective in the removal of contaminants, but main limitation is cost and time-consuming process (Patterson 1985; Schwarzenbach et al. 2006). Other processes are biodegradation procedures, which are economical and environment-friendly, but time-consuming (Ahluwalia and Goyal 2007). These drawbacks can be successfully overcome by the use of nanomaterial composites. The characteristic feature of the nanocomposites is the large surface area for improved reactivity in the remediation of drinking water (Urbansky and Schock 1999).

23.3 Nanotechnologies' Advancement

Nanotechnology includes the designing of devices and systems from atomic and molecular level by utilizing in the field of physics, chemistry, biology, and materials science and engineering (Masciangioli and Zhang 2003). Nanocomposites contain nanoscale dimensions within the range of 1–100 nm, and demonstrate novel and advanced chemical, physical, and biological properties. The potential applications of nanotechnology are sensing, detection, and remediation of pollutants in contaminated water (Aseashta et al. 2007; Rickerby and Morrison 2007). Furthermore, nanotechnology facilitates the development of potential monitoring devices in low price and improves the specificity (Riu et al. 2006).

The different nanomaterials which have been used to remove the various impurities are illustrated in Table 23.1. There are many advancements in the application of nanocomposite-oriented cleanup techniques (Ghasemzadeh et al. 2014). Carbon nanotubes (CNTs) which have an exceptional absorption ability play a dual role as biosensor and attract considerable attention for effluent treatment for a wide variety of contaminants (Riu et al. 2006; Scott 2007). Similarly, metallic or bimetallic nanoparticles Ag, Fe, Au, Cu, and Ni/Fe; Cu/Fe; Ag/Fe are successfully used for heavy metal removal and used as biosensor-based monitoring (Zhang et al. 1998; Matheson and Tratnyek 1994). Besides, various other advanced nanocomposites like dendrimers and semiconductor metal oxides have been applied for monitoring and remediation of water, soil, and groundwater (Di et al. 2006;

Botalova et al. 2011). Recently, nanoengineered membranes have been developed by immobilizing with metallic nanoparticles for efficient and fast removal of biological and chemical contaminants (Qu et al. 2013; Wegmann et al. 2008; Whitesides and Grzybowski 2002; Cloete et al. 2010). Recently, self-cleaning nanocomposites are identified which include L-Histidine-doped TiO₂-CdS/PES nanocomposite membranes, polydimethylsiloxane/silica nanocomposite, and bio-cidal oxine/TiO₂ polyvinylidene fluoride membrane nanocomposite (Manoharan et al. 2020; Zangeneh et al. 2020; Gong and He 2020).

23.4 Main ehicles of Nano-Based Effluent Treatment Are Nano-Adsorbent

Nano-adsorbents have wide range of applications because of their extensive range of adsorbing properties. The nano-adsorbent has the potential to remove the contaminants in any form, either in solid, liquid, or gas. In addition to this, nano-adsorbents are equally effective for both organic and inorganic waste removal. Most commonly used nano-adsorbents are (Fig. 23.1):

1. Nanopolymers (dendrimers).
2. Carbon nanotube.
3. Metallic nanoparticles with the modification of outer shell.
4. Zeolites.

23.5 Nano-Adsorbents

23.5.1 Nanopolymers (Dendrimers)

Dendrimers are an efficient nano-adsorbent for wastewater treatment due to high-adsorptive properties and easy to use. Surface modification of dendrimers can enhance the adsorptive capacity for efficient effluent treatment (Yellepeddi et al. 2009) (Table 23.1).

23.5.2 Carbon Nanotubes (CNTs)

Carbon nanotubes are in the shape of cylinder in which macromolecules are arranged in the walls of the tubes in hexagonal lattice of carbon atoms. The side ends of the carbon nanotubes are capped by molecules in the form of fullerene resemblance (Iijima 1991). Large surface area and tubular structure construct the carbon nanotubes a potential adsorber for different applications. The hybridized carbon atomic layers on CNTs are classified as single-walled carbon nanotube (SWCNTs) and multi-walled carbon nanotubes (MWCNTs). Carbon nanotubes have attracted significant consideration since its discovery due to its structural, chemical, and

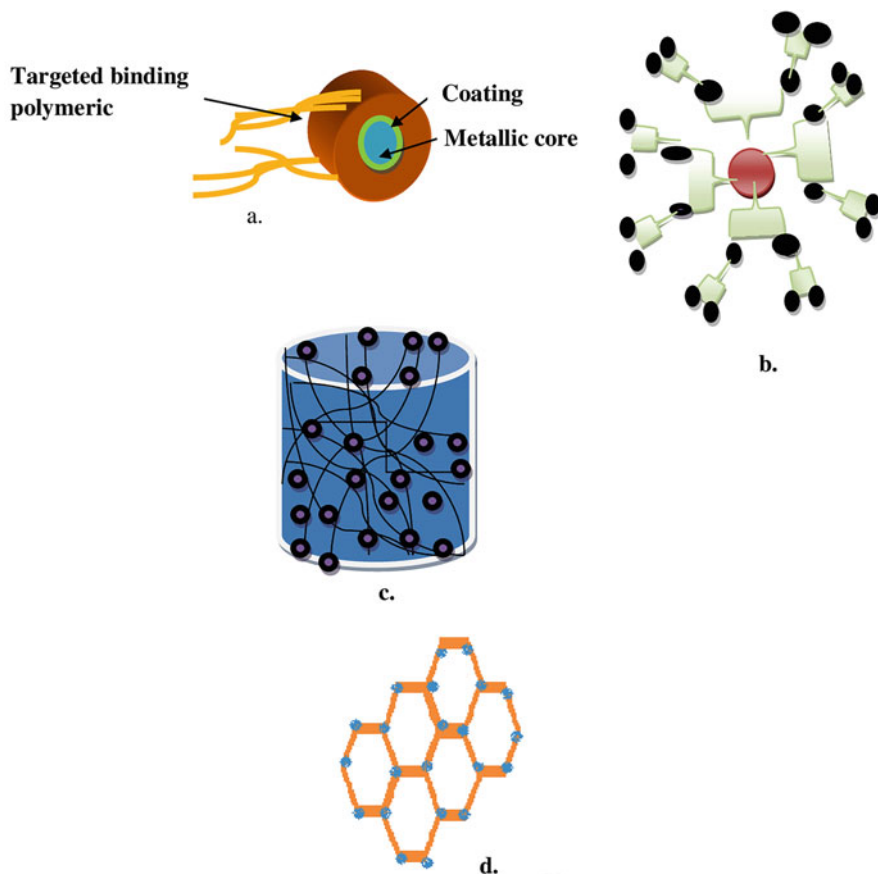


Fig. 23.1 Nano-absorbents for effluent treatment: (a) metallic nanocomposites, (b) nanopolymers (dendrimers), (c) carbon nanotube, (d) zeolites

mechanical properties (Popov 2004; Miyagawa et al. 2005). As a result of their varying properties, they have significant applications in electronics, and chemical and biological composites (Polizu et al. 2006; Balasubramanian and Burghard 2006). Carbon nanotube which has already reported for the adsorption of 1,2-dichlorobenzene (DCB) at pH range of 3–10 CNTs takes 40 min for DCB sorption at the rate of 30.8 mg/g that is calculated as maximum sorption capacity (Peng et al. 2003). Cerium oxide supported high surface area carbon nanotubes (CeO_2 -CNT) has recently discovered as novel sorbent with enhanced capacity, that is, 189 mg/g (Peng et al. 2005). The CeO_2 -CNTs demonstrated induced adsorption efficiency for Cr metal in drinking water in pH range 3–7.4. The adsorption capacity for Cr(I) increased up to 30.2 mg/g in neutral pH which is identified as double in comparison with activated carbon along aluminum oxide (Di et al. 2006).

The novel modification of carbon nanotubes is nanoporous activated carbon fibers (ACFs), made by electrospinning method of CNTs; the surface area is high

Table 23.1 Advanced nanomaterial examples of water cleanup

Nanomaterials	Types	Properties	Potential applications	References
Carbon nanotubes	Single and multiwalled nanotubes of different length and radius	Electrolytic activity, high absorption capacity	Sorbents Chemical and biological sensors	Riu et al. (2006), Scott (2007), Qin et al. (2010) and Hsieh and Ofori (2007)
Metallic nanoparticles	Au, Cu, Fe, Ag in different shape & dimensions	Electrolytic activity; antibacterial activity	Sorbents Chemical and biological sensors	Matheson and Tramnyek (1994) and Zhang et al. (1998)
Magnetic Fe-Oxide	Iron nanoparticles, MeO-Fe ₂ O ₃ where M=Ni, Co, Zn	Superparamagnetic; catalytic sites for H ₂ O ₂	Immunomagnetic separation and concentration	Matheson and Tramnyek (1994) and Zhang et al. (1998)
Dendrimers	Hyperbranched nanostructured with different length and branches	Functionalized end groups	DNA sensors and DNA microarrays	Peng et al. (2003) and Di et al. (2006)
Semiconductor and metal oxides	TiO ₂ , ZnO, ZrO ₂ , CeO ₂	Photocatalytic, electrocatalytic, and antibacterial activity	Photocatalytic damage. Gas sensing probes and biosensing	Falconer and Humpage (2005), Tomalia and Fréchet (2002) and Botalova et al. (2011)
Nanoengineered membranes filtration	Nanofiltration membranes	High selectivity Thermal/mechanical robustness Homogeneous nanopores Higher permeable Efficiency Bactericidal High ionic selectivity	Removal of color, odor Micropollutants Use in ultrafiltration Desalinization	Qu et al. (2013), Wegmann et al. (2008), Whitesides and Grzybowski (2002) and Cloete et al. (2010)
Poly (vinylsulfonic acid)-Ag	Polymer-metal nanocomposites	Multi and microporous	Removal of microorganism from drinking water	Mudassir et al. (2019)

in these nanofibers which is in the range of 171–483 m²/g. Sorption efficiency for organic solvents is increased in comparison to granular-activated carbon (Li et al. 2003).

It has been investigated that multi-walled carbon nanotubes (MWCNTs), after treating with nitric acid, can be efficiently applied for the removal of various heavy metallic ions like Cu (II) (24.49 mg/g), Pb(II) (97.08 mg/g), and Cd(II) (10.86 mg/g) from water. These sorption capacities were higher than in granular form of activated carbon (Lu and Liu 2006). In addition, MWCNTs have shown to good Ni (II) sorption after oxidation with sodium perchlorate. Oxidation reaction further enhanced the CNTs surface properties like total acidic sites and charged carbons atoms, functional groups, thus resulting in them becoming more hydrophilic and therefore able to remove Ni (II) from water samples (Liu et al. 2005a). In addition, SWCNTs and MWCNT have an ability to remove the trihalomethanes from aqueous solution which has been recognized as potential carcinogenic substances which are formed due to the chlorination of drinking water (Bull et al. 1995; Rook 1974; Salipira et al. 2007).

Recently, scientists discovered that cross-linked nanoporous polymers by co-polymerization with functionalized CNTs resulted to form novel polymers which are potentially removed organic contaminants from water bodies (Peng et al. 2005). On the basis of this discovery, functionalized CNTs reported to remove the dioxin more efficiently than the activated carbon from water.

Subsequently, MWCNTs used effectively as adsorber for preconcentration, removal, and isolation of chlorophenols (Zhou et al. 2006a; Cai et al. 2005) and different herbicides and their metabolites from water samples of different water bodies (Zhou et al. 2006b, 2007; Yan et al. 2006; Haider et al. 2003). In addition to the removal of pesticides, these CNTs have been identified as effective tool in adsorption of MCs (cyanobacterial toxins—microcystins) from lake water. These CNTs' outer diameters are in the range of 2–10 nm. These were found higher, potent nanomaterial for the decontamination of drinking water (Lu et al. 2007).

Previous research findings signify that CNTs are efficient and potent adsorbents for the removal of different contaminants/pollutants in drinking water as well as environmental waters. The main limitation associated with this nanomaterial is their high cost, limited water solubility, and difficulty in the collection of these as dispersing medium for cleanup procedures of water. Recently, these limitations have been overcome by the new NaClO-oxidized SWCNTs and MWCNTs, which make it less costly and can be recycled and reused up to ten cycles in water cleanup treatments (Lu and Chiu 2006; Jin et al. 2007).

Furthermore, researchers have been reported an easy method in fabrication of MWCNTs with Fe nanoparticle which displayed superior water solubility and easily recovered from the water by magnetic separation procedures. Carbon nanomaterials (CNTs) are being used potentially in water effluent treatment due to their superior adsorptive properties in removal of different metallic forms. However, due to some drawbacks like low solubility and nonuniform distribution in extracting medium, these are not efficiently used in effluent treatment. Nowadays, to overcome this limitation, research is going on surface modification of carbon nanotubes to enhance

their solubility and efficiency for wastewater treatment. The advanced modifications of carbon nanotubes are discussed in Table 23.1.

23.5.3 Metal Nanoparticles

Metal nanoparticles are easy to synthesize, but the problem of stability and recovery reduces their efficiency for wastewater treatment. Surface modification of nanoparticles not only overcomes these problems but also enhances the efficiency of cleanup of wastewater. Advanced modification so far being done on metal nanoparticles is mentioned in Table 23.2.

23.5.4 Zeolite

Zeolite has wide range of absorptive properties, which allows this to remove all types of contaminants from water efficiently. Zeolites can remove the odor, microbes, and metallic impurities. The current advancement in enhancement of activity of zeolites is presented in Table 23.3.

23.5.5 Nanostructured Membranes

Membrane techniques play a significant role in water purification processes. These membrane-assisted techniques give superior quality over the conventional water purification techniques like sedimentation, flocculation, coagulation, and activated carbon (Strathmann 2001; Iessman and Hammer 1998). Different membrane techniques have been used in water purification and waste treatment which includes ultrafiltration (UF), microfiltration (MF), and nanofiltration (NF) for water purification and wastewater treatment (Peltier et al. 2003; an der Bruggen and andecastele 2003; Ahmad et al. 2004) and reverse osmosis (RO) nanofiltration for removing salt from water (Walha et al. 2007; Mohsen et al. 2003).

Recently, researchers developed carbon nanotube filters in which carbon nanotubes are radially arranged in hollow cylindrical form (Srivastava et al. 2004). Carbon nanotubes (CNTs) could be an efficient filtration device due to certain characteristic features which include controlled geometric shapes, diversified dimensions for definite filtration applications, and density variations (Miller et al. 2001). Besides, nanocarbon filters have many reactive and differently functionalized membrane filters for water filtration applications.

It has been evaluated that the fabrication of aluminum (A-alumoxane) nanoparticles showed the selectivity filtration of synthetic dyes (de Friend et al. 2003). After this, polymeric fabrication of novel nanofiltration membranes has been reported by depositing four to five layers of different polymers like poly(allylamine hydrochloride)/poly(styrene sulfonate) (Stanton et al. 2003). These fabricated novel nanofiltration membranes showed high water influx with the capacity of higher

Table 23.2 Examples of efficient modified nanocomposites

Dendrimer	Grafting membrane	Application	Reference
PAMAM dendrimer	Polytetrafluoroethylene membrane	Enhancing the filtration efficiency	Yoo and Kwak (2013)
PAN nanofibers	Ethylenediamine and Diethylenetriamine (DETA)	Adsorption of heavy metals	Deng and Bai (2004) and Shin et al. (2004)
Poly-(ethylene glycol)	Zero valent iron ($Fe^0 = ZVI$) particles	Removal of hazardous water Pollutants from textile industries	Mohammad et al. (2019)
PAMAM dendrimer	Impregnated on Alginate bead	Removal of cationic and anionic dyes	Yoo and Kwak (2013)
Poly (amidoamine) dendrimer	Sand surface	Removal of nonylphenol from water	Vahid et al. (2019)
Polyamidoamine dendrimer	FO-membrane (forward osmosis)	Domestic wastewater treatment	Xian et al. (2019)
Polyamidoamine dendrimer	Conjugate with magnetic nanoparticles	Heavy metal decontamination of water	Rajesh et al. (2013)
<i>Carbon nanotube</i>			
Carbon nanotube	Magnetic titanium nanotube	Degradation of Biphenyl A from industrial wastewater treatment	Seyyed et al. (2019)
Hydroxylated and carboxylated carbon nanotube	Polyvinylchloride (PVC) hollow fiber membranes (HFMs)	Removal of zinc from waste water	Sharafat et al. (2019)
Multiwalled carbon nanotubes	Metal nanoparticles	Simultaneous removal of pefloxacin and Cu(II) ions from wastewater	Yaoyu et al. (2019)
Carbon nanotubes with PVC membranes	Ar/O ₂ plasma treatment	Enhanced removal of zinc from wastewater	Sharafat et al. (2019)
Magnetic carbon nanotubes	Polyethylenimine cation	Simultaneous capture of methyl orange and chromium (VI) from complex wastewater	Bo et al. (2019)
Carbon nanotube	Iron-loaded microfibers	Removal of m-cresol from effluent wastewater	Yi et al. (2019)
Metal nanoparticle	Grafting agent	Application	References
Ag nanoparticle	Glass bonded by si-o-si	Removal of microbial contaminants	Jahirul et al. (2019)
Fe ₃ O ₄ nanoparticles	Trimellitic acid functionalized	Removal of Pb(II) cations and Cr(VI) anions	Tehreema et al. (2019)
Fe ₃ O ₄ nanoparticles	Amine functionalized surface	Removal of Pb(II) and As (V)	Chairul et al. (2019)
Fe ₃ O ₄ nanoparticles	Starch capped	Remove heavy metals from contaminated water	Prathap et al. (2019)

(continued)

Table 23.2 (continued)

Metal nanoparticle	Grafting agent	Application	References
Ag–TiO ₂ nanoparticles	Polyamide nanofiltration (NF) membrane	Antibacterial activity in water	Habib et al. (2019)
Fe ₃ O ₄ nanoparticles	Zeolitic imidazolate frameworks-67, at eggshell membrane	Removal of heavy metal and dye from wastewater	Niya et al. (2019)
Co-Ferrite nanoparticles	Apocynaceae leaf waste activated carbon	Anti-microbial activity for textile effluent treatment	Bilal and Tahira (2019)
Tg-oxide nanostructures	Carbon nanodots	Dye removal	Srivastava et al. (2004)

Table 23.3 Examples of most recent advancement in zeolite modification

Zeolite	Grafting agent	Application	References
Zeolite with activated carbon	Sodium Alginate	Anti-fouling agent	Stanton et al. (2003)
Zeolite	Ca(OH) ₂ and CaCl ₂	Soft drink wastewater treatment by electro-oxidation	Rosa et al. (2019)
Zeolite	Co(II), Ni(II), and Cu(II) ions	Oxidative degradation of dye	Smita and Bhattacharyya (2019)
Zeolite	Bio-films	Antimicrobial treatment of wastewater	Yingxin et al. (2019)

binding for divalent cations (Ca(II) and Mg(II)) and Cl⁻/SO₂⁴⁻ with selectivity ratios up to 80.

Another advancement in nanofiltration is the functionalization of nanofilters with different polyelectrolytes or polyamines, that constitutes different multifunctional chelating groups (e.g., amines, carboxylic acids, or pyridines), which make strong and steady binding to metallic ions (Rivas et al. 2003). Various researchers have been reported different advanced procedures for the attachment of these chelating groups with nanomembrane internal pore surfaces in metal ions sorption applications (Ritchie et al. 2009; Bhattacharyya et al. 1998).

Amino acids have been identified as an efficient chelating species in which primary amine and carboxylic acid groups are the important sites for metallic ion binding. Hence, amino acid homopolymers can be used for the nanofiltration membrane effectively for metal sorption. Redox-reactive membranes have also synthesized by bimetallic Pt/Fe integrated nanoparticles over cellulose acetate films (Meyer et al. 2004), and Ni/Fe or Pd/Fe particles immobilized over polymeric membrane matrix of polyacrylic acid/polyether sulfone (Xu et al. 2005). The principle application of metallic composites of nanomembranes extensively applied for reductive dechlorination of halogenated organic compounds (HOCs) from water

(Arnold and Roberts 1998; Gotpagar et al. 1997; Matheson and Tratnyek 1994). Several recent findings have exposed that efficiencies of dehalogenation might be improved by iron (Fe) nanoparticles (Zhang 2003; Liu et al. 2005b) or bimetallic nanoparticles (Zhang et al. 2008; Schrick et al. 2002), but the main limitation is the rapid oxidation and hydrolysis reactivity of Fe nanoparticles which will lose the long-term stability of nanoparticles (Giri 2001; Ponder et al. 2000; Wu et al. 2005). Furthermore, some researchers described the modification of alumina and polymeric membranes by immobilization of citrate-stabilized gold nanoparticles by layer by layer adsorption of polyelectrolyte procedure (Dotzauer et al. 2006). The immobilized nanomembranes were found more efficient and discriminating than simple nanomembranes.

The carbon tube cylindrical nanomembrane filters also identified for the removal of bacterial and viral pathogenic species (*Escherichia coli* and *Staphylococcus aureus*) and Poliovirus sabin 1 from contaminated water. Carbon nanotube membrane filters can be reused and cleaned by ultra-sonication or autoclaving. The nanofabrication methods are very useful for developing novel nanocapillary array (NCA) membranes for improved solute retention and decrease the fouling problem (Chatterjee and Shimanti 2005).

23.5.6 Nanoreactive Membrane Filters: Dendrimers

Macromolecular advancements in chemistry have provided many opportunities to synthesize dendritic polymers for the application of effective and superior processes for the purification of contaminated water and the removal of different inorganic anions and organic solutes..

Dendrimers are vastly branched macromolecular structure. These contain central core, for repeating units which composed terminal functional groups (Tully and Frechet 2001; Bosman et al. 1999).

The integral repeating units determine the internal microenvironment and its solubilization properties, and the external terminal functional groups determine the chemical performance of dendrimers in external medium (Klajnert and Bryszewska 2001). These are highly branched polymeric structures sustained many properties of dendrimers, for the synthesis of polydisperse polymers in symmetrical shape (Yates and Hayes 2004; Jikei and Kakimoto 2001; Gao and Yan 2004). Similarly, cyclodextrins are cyclic oligomers of polysaccharide and are of cone shaped that form cylindrical cavity (Del alle 2004; Schneiderman and Stalcup 2000; Tick et al. 2003). The internal cavity of these dendrimers is lipophilic in nature and can encapsulate the organic compounds and form stable inclusion complexes. The external surface contains cyclodextrins with multiple hydroxyl groups for further functionalization. Functionalization leads to diversified molecules for different applications which mainly include the removal of pesticides and other organic contaminants (Sawicki and Mercier 2006; Arkas et al. 2006). These studies are extended for various impregnations with cross-linked dendritic or cyclodextrin polymers (Allabashi et al. 2007).

Table 23.4 Examples of nanostructured and nanoreactive membrane for use in water filtration

Membrane	Pollutant	References
<ul style="list-style-type: none"> Nanomembranes Carbon nanotubes Nanocapillary array membrane (NCA) Nanoreactive membranes 	Bacteria and viruses *NT	Srivastava et al. (2004) and Chatterjee and Shimanti (2005)
<ul style="list-style-type: none"> Alumina membrane Poly styrene functionalized alumina membranes 	Synthetic dyes Divalent cations	de Friend et al. (2003) and Stanton et al. (2003)
<ul style="list-style-type: none"> Amino acid homopolymers functionalized silica and cellulose-based membranes 	Metal ions	Bhattacharyya et al. (1998) and Ritchie et al. (1999)
<ul style="list-style-type: none"> Amino acid homopolymers functionalized polycarbonate track-etched membranes 	Metal ions	Hollman and Bhattacharyya (2004)
<ul style="list-style-type: none"> Pt/Fe laden cellulose acetate film Zero-valent Fe laden cellulose acetate membrane 	Trichloroethylene (TCE) TCE	Meyer et al. (2004)
<ul style="list-style-type: none"> Ni/Fe or Pd/Fe laden polyacrylic acid/polyether sulfone composite membrane 	TCE	Xu et al. (2005)
<ul style="list-style-type: none"> Ni/Fe laden cellulose acetate membrane alumina Polymeric membrane with gold nanoparticles 	TCE 4-Nitrophenol	Wu et al. (2005) and Dotzauer et al. (2006)
<ul style="list-style-type: none"> Poly-impregnated ceramic TiO₂ filters Polymer impregnated ceramic alumina and silicon-carbon filters 	Polycyclic aromatic Hydrocarbons (PAHS) Trihalogen membrane, PAHs, pesticide	Arkas et al. (2005) and Allabashi et al. (2007)

Different studies have recognized that these dendrimers can be modified by highly branched polymers like poly propylene imine, polyamidoamine, polyethylene imine (Diallo et al. 2005; Arkas et al. 2005). These modified dendrimers efficiently take out different organic contaminants from water. Besides, dendritic polymers may also be used effectively as delivery systems for ionic silver (Ag(I)) and quaternary ammonium chlorides for the removal of antimicrobial agents (Balogh et al. 2001; Chen and Cooper 2002). Researchers have been identified that dendrimer-enhanced ultrafiltration (DEUF) process is very useful for removing metal ions from aqueous solutions (Table 23.4).

23.5.7 Biopolymer-Based Nanomaterials

Recent advanced genetics and bio-engineering techniques have been constructed different synthetic gene templates and be controlled at molecular level. These are of different sizes, shapes, compositions, and purposes. At the molecular level, these can

be controlled specifically and which can be used as biopolymers (Hasan and Pandey, 2015). Therefore, protein-based nano-biomaterials properties could be modified by various metal-binding sites (Kostal et al. 2005). The metal-binding proteins may provide superior specificity and affinity in contrast to chemical sorbents (Kostal et al. 2001, 2003). Moreover, the biopolymeric nanocomposites could provide an economical approach, because mass biopolymer production is possible by overexpression of target genes in *E. coli*. ELPs (elastin-like polypeptides) are biopolymers which contain repeating pentapeptide al-Pro-Gly-al-Gly sequence and have similar structural characteristics to mammalian elastin protein. Metal-binding and phase transition properties are the ideal properties of biopolymers for the recovery in different range of temperature, pH, and ionic strength (Urry et al. 1992). In addition, ELPs contain polyhistidine moieties have been reported which possess metal-binding sites which is used to remediate cadmium from contaminated water (Prabhukumar et al. 2004; Lao et al. 2007). In comparison to biosurfactants, ELP biopolymers have 20% higher adsorption which results higher extraction efficiencies in a lower concentration.

23.6 Nanotechnology Application in Agricultural Pesticide Degradation

Nanotechnology has the potential to enhance agricultural productivity as well as in medical treatment. The main applications of nanotechnology are targeted and efficient delivery of agrochemicals and drugs, improved food processing, packaging, and agricultural monitoring, (Scott 2007; Maysinger 2007). In addition, nanotechnology has been delivered many sensor-based techniques for agricultural precision, natural resource management and predetection of pest and pathogens and food contamination (Moraru et al. 2003; Chau et al. 2007). As a result of enhanced surface-to-area ratio, nanomaterials could improve the encapsulation and release efficiency in comparison to traditional encapsulating agents. Remediation of soil for the heavy metals' removal by different conventional and nanocomposites was investigated and the author concluded that applying both methods together will give synergistic effect (Sharma et al. 2018a). The development of liposomes, micelles preparation by nanoemulsions, and cubosomes can improve bioactive compound properties for enhanced delivery systems, food matrix integration, and masking undesired flavors (Chen et al. 2006).

Nanotechnology innovations would be beneficial to consumers, without causing any adverse effect in environment. Various chemical pesticides are being used in crop protection and disease control worldwide. In synthetic pesticides, organochlorine and organophosphorus insecticides have been developed and used extensively. Prolonged usage results persistent residual problem in the environment (Chaudhry et al. 2008). Persistent pesticides also cause hazards to humans and other non-target species and cause health risks like endocrine hormone disorders, increased cancer risk, disturb immune system and reproductive by the persistent pesticides bioaccumulation in food chain. Various abnormalities also occur in other non-target

organisms which include various aquatic and ground organisms. The extensive utilization of pesticides may also cause pest and disease resurgence problem.

Most important section of agricultural nanotechnology research attaining progress in the area of pesticide degradation and converting these into nontoxic and valuable components such as minerals and water is known as photocatalysis mechanism. In this mechanism, semiconducting oxide nanostructures absorb photons and begin redox reactions, which can break the complex organic molecules into simpler component or fragments (Baruah and Dutta 2009). TiO_2 , ZnO , ZnS , Fe_2O_3 , and CdS are the typical examples of semiconductor photocatalysts. These semiconductors have filled valence band and an empty conduction band (Boer 1990).

23.7 Degradation Mechanism of Contaminants by Nanocomposites

Groundwater containing organic contaminants can be degraded and removed totally by photocatalysis (Baruah and Dutta 2009). Titanium dioxide (TiO_2) and zinc oxide (ZnO) are the two efficient photocatalysts which absorb U radiations of electromagnetic spectrum which is 70% of solar spectrum. These metal oxide semiconductors synthesized by using methods like spray pyrolysis, electrophoresis, hydrothermal growth, vapor solid (S) growth, vapor liquid solid (LS) growth, and metal organic chemical vapor deposition (MOCVD) (Baruah and Dutta 2009). It has been investigated that ZnO absorption band shifts toward visible band of electromagnetic spectrum by doping various transitions (Ullah and Dutta 2008; Colis et al. 2006).

Researchers have been reported that DDP degradation by photocatalysis follows Langmuir Hinselwood model of the first-order kinetics (Evgenidou et al. 2005). They have demonstrated that degradation is increased by the addition of some electron acceptors like hydrogen peroxide (H_2O_2) or potassium persulfate ($\text{K}_2\text{S}_2\text{O}_8$) in ZnO nanostructured semiconductors.

In the study, the degradation of highly water soluble pesticides was determined at the pilot plant scale. In the study, solar U light was used in these photosystems: (a) heterogenous photocatalysis (TiO_2) and (b) photo-fenton homogenous photocatalysis (Oller et al. 2006). In heterogenous photocatalysis, three compound parabolic collectors (CPCs) are present, and in homogenous photocatalysis, four CPC units are present under natural illumination. After photolysis process, pesticides mineralized 100% and totally disappear the starting pesticides. Therefore, photocatalysis degradation process has achieved huge attractiveness in wastewater treatment. Peral et al. (1997) have described the applications of decontamination, deodorization, and cleaning of air by photocatalysis mechanism (Mills et al. 1997). Besides, photosynthetic and photocatalytic processes of semiconductor have also been elucidated for the decontamination of organic contaminants, cancer cells' destruction, and the removal of bacteria and viruses from water. There are certain reports explained that like nanoparticles, nanotubes and nanostructured thin films can be used for degrading pesticides. In the recent study, TiO_2 nanotube suspensions were used for degradation of atrazine (2-chloro-4-(ethylamine)-6-(isopropylamine)-

s-triazine), a weedicide (Zhanqi et al. 2007). In a similar study, microwave-assisted photocatalyst was synthesized for the degradation of atrazine. In this study, mineralization efficiency was calculated 98.5% in 20 min. Yu et al. (2007) used TiO_2 thin films for organochlorine pesticides degradation. The study concluded that TiO_2 film can degrade the pesticide within 45 min after illumination by U light. Shankar et al. further fabricated the TiO_2 with thin-film reactor along with zeolites. This coupled photocatalytic device was used in monocrotophos (MCP) and 2,4-dichlorophenoxyacetic acid (DPA) photocatalytic mineralization.

The rate of degradation was observed faster with zeolite- TiO_2 composite in comparison to bare TiO_2 .

23.8 Nanoparticles Role in Pesticide Degradation by Photocatalysts

Nanoparticles have a wide scope of application in different files like from detection to degradation of pollutants in the environment. The nanostructure devices are currently being used for pesticide degradation by photocatalysis where act as nanocatalysts. The nano-photocatalysts oriented degradation of pesticide is fast and efficient than the conventional methods. Pesticide degradation process by the nano-photocatalyst is basically a photo-oxidation process (Ahmed et al. 2016) Many pesticide degradation by nanoparticles are photocatalytic oxidation (metal oxide nanoparticle/U) and photo-fenton and fenton-like system (metallic nanoparticle / H_2O_2 /U).

In photocatalytic oxidation, U irradiation (λ_{max} , 390 nm) is irradiated on metal oxide nanoparticle. Irradiated photons' energy has to be greater than or equal to band gap energy, that is, 3.2 e between electron and hole in covalent band and valence band. In aqueous medium, the valence band holes react with H_2O and form radical OH^\cdot , which will oxidize the pesticide (Fig. 23.2). Similarly, in photo-Fenton and Fenton-like systems, it is also a photocatalytic system in which metal ions form a complex $\text{Fe}(\text{OH})_2^+$ when added to acidic H_2O_2 medium. In U irradiation, $\text{Fe}(\text{OH})_2^+$ decomposes and generates Fe^{2+} ions and OH^\cdot radicals which act as photo-oxidant for pesticide oxidation (Devipriya and Yesodharan 2005) (Figs. 23.2 and 23.3). The nanomaterials are the efficient systems for degradation of persistent pesticides into minerals. The nano-photocatalysts are easy to synthesize and use and economical also.

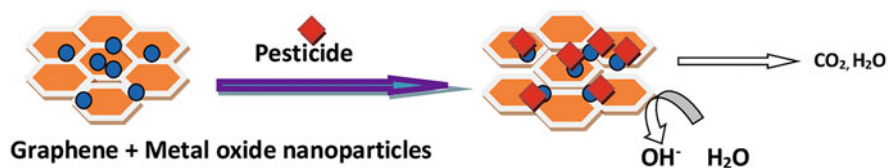


Fig. 23.2 Photocatalytic degradation of persistent pesticides by graphenes and metal nanocomposites

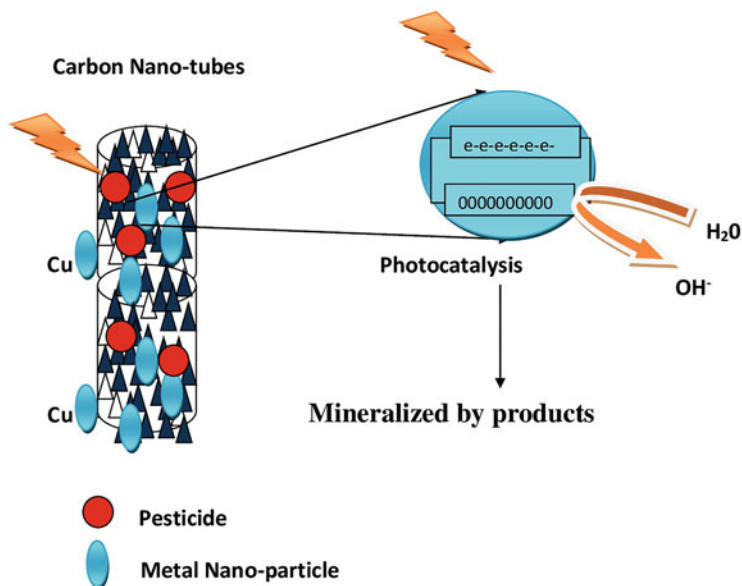


Fig. 23.3 Photocatalytic degradation of persistent pesticides by carbon nanotubes and metal nanocomposites

23.9 Nanomaterials in Photocatalysis

23.9.1 Graphene Oxide (GO)

Graphene combined with metal oxide nanoparticles enhances the efficiency of photo degradation. The fabricated nanoparticles with graphene are widely used in pesticide degradation (El-Shafai et al. 2019). TiO₂GO Nano-composites enhance the photo degradation rate of TiO₂ nanoparticles. In combined form, energy gap between valence and conduction reduced in TiO₂ by which electron transfer is easy for oxidation-reduction reactions (Ali et al. 2018). Hence, cost-effective combination for faster degradation of pesticides under solar radiations evolved.

23.9.2 Carbon Nanotubes

Multiwall carbon nanotubes are two-dimensional adsorbent materials. The adsorption material is considered a promising for degradation of pesticides. It is simple, low cost, and eco-friendly technique. It is very effective in hybrid form with magnetic nanoparticles, silica particles, and porous polymers (Zhan et al. 2014). The MWCNTs in combination with TiO₂ increase the photo-degradation of pesticides (Hui et al. 2009). Earlier studies revealed that activated carbon with multiwall carbon

nanotubes in combined form has efficient activity for remediation of organochlorine pesticides (Shan et al. 2013). The activated carbon increases the porosity as well as surface area for photo-oxidation reactions. Multiwall carbon nanotubes (MWCNTs) can also be used as photocatalyst in ozonolysis reactions for atrazine mineralization (Xiaolei et al. 2018). Recently, scientists have developed a modified multiwalled carbon nanotube with gold nanoparticles in combination with poly (3, 4-ethylene dioxythiophene) for efficient degradation of crop protection agents. For enhancing the degradation of pesticides for longer periods, encapsulation of the metallic nanoparticles by carbon nanotubes has been developed. These have superior catalytical activity and ensure the stability and reusability of carbon nanotubes (Duan et al. 2019). Carbon nanotubes have been modified according to functional entities in the pesticide for complete photolysis.

23.9.3 Metallic Nanocomposites

Nanophotocatalysis is an efficient technology for the mineralization of toxic and persistent pesticides. The nanocomposites are the combination of two components which increase the degradation of pesticides by photocatalytic reaction mechanism (Xiaodan et al. 2006). Heterogeneous nanocomposites are efficient in photodegradation of organic pollutants. Heterogeneous property of nanocomposites enhances the charged surface area for oxidation-reduction reactions and enhances the pesticide degradation rate. A large number of metal oxide composites like magnesium oxide, titanium oxides, copper oxides, zinc oxides, tungsten oxides, and graphene have been developed and utilized for pesticide detection, removal, and degradation. TiO_2 and ZnO nanocomposites are already known for the efficient decomposition of organic pollutants by U-is photons. Another coupled oxide nanocomposite of ZnO/SnO₂ showed good photodegradation of persistent triclopyr pesticide photocatalytical degradation compared to the individual oxide entity. Tantalum isopropoxide and magnesium isopropoxide with silver nanoparticles ($\text{Ag}@\text{Mg}_4\text{Ta}_2\text{O}_9$) have been synthesized for the photo-degradation of atrazine. $\text{Ag}@\text{Mg}_4\text{Ta}_2\text{O}_9$ nanocomposites improve the photocatalytical performance for the degradation of pesticides (Pourya and Hassan 2019). Pd-Au nanoparticles with resin nanocomposites is an advanced approach for the degradation of organophosphorous pesticides. Recently, BiOBr/Fe₃O₄ nanocomposites have been synthesized and can be used for the degradation of organophosphorous pesticides. In composite form, rate of degradation was increased from 85% to 97%. These nanocomposites are easy to prepare, environmentally friendly, and can be recovered without significant change and efficiently reuse.

23.10 Degradation of Organochlorine by Nanoparticles

According to the Stockholm Convention, organochlorines are persistent pesticides, but due to wide range of activity, they are mostly used against agricultural and household pests. The intensive use of these pesticides contaminates the soil and water and because they are not easily degraded in the environment. Different remediation techniques like photochemical degradation, biodegradation, or adsorption are available for degradation of organochlorines, but these techniques are not efficient for complete remediation of organochlorine pesticides. For efficient removal and degradation of persistent organochlorines, an efficient and advanced technology is needed. Nanotechnology-based remediation is a very effective and efficient technology to degrade the organochlorine in a very economical and efficient manner.

Nanoparticle-based degradation pathways based on intermediated formed are:-

- Dehydrochlorination.
- Dichloroelimination.
- Hydrogenolysis.
- Dechlorination.

23.11 Organochlorine Photolysis Mechanism by Nanoparticles

Due to the persistent and bioaccumulative properties, EPA have banned the use of many organochlorines, but their degraded products are sometimes hold long-term detrimental effects than the parent compound (Zaleska et al. 2000). Different degradation methods have been discovered by researchers; among those, the most efficient method basically involves thermal and photo-catalytical processes (Fang et al. 2000). Metallic nanoparticles and surface engineered nanoparticles of Fe_2O_3 , TiO_2 , ZnO , CdS , SiO , etc., have been synthesized for enhancing the rate of photolysis reactions in organochlorine mineralization, where nanoparticles act as nano-photocatalysts. Photocatalysis by nanoparticles requires illumination above 300 nm radiations, these radiations act as energy source for electron transfer by nanoparticles for oxidation reduction reactions in mineralization of organochlorines. The degraded products after complete mineralization of organochlorines are Cl^- , CO_2 , H_2O , NO_3^- , etc. Currently, various workers are involved in advanced research for eco-friendly degradation by surface modification of metallic nanoparticles by natural polymers and bio-organisms (Rahmanifar and Dehaghi 2014; Singh et al. 2013a, b). Examples of photocatalysis of nanoparticles are discussed in Table 23.5.

Table 23.5 Nano-photocatalyst for organochlorine mineralization

S. no.	Nano-photocatalysts	Organochlorine	Process of degradation	Degraded products	Reference
1.	Zero valent iron (FeO) and Magnetite (Fe ₃ O ₄) nanoparticles	DDT, Lindane (-HCH), and Aldrin	Photo-Fenton degradation	Dechlorination	Yuko et al. (2016)
2.	Iron sulfide nanoparticles on biopolymers	Lindane	Biodegradation	1,2,4-Trichlorobenzene	Paknikar et al. (2005)
3.	TiO ₂ nanoparticles Coated films	Hexachlorobenzene (BHC), Dicofof, and Cypermethrin	E photocatalytic degradation	Dechlorination and chloric ions	Binbin et al. (2007)
4.	Pd/Fe ⁰ bimetallic nanoparticles with <i>Sphingomonas</i> sp. Strain NM05	γ-HCH	Photocatalytic and biodegradation	TCB to dichlorobenzene and benzene	Ritu et al. (2013)
5.	Fe ₂ O ₃ nanoparticles	Aldrin, Dieldrin, Endosulfan, Endrin, Heptachlor, Heptachlor Epoxide, Lindane, P-DDT, P, P-DDE, and DDD	Photo-Fenton degradation	Dechlorinated compounds	Ahmed et al. (2016)
6.	Fe/Ni nanoparticles with Carboxymethylcellulose	Hexachlorocyclohexane	Reduction transformations	Benzene and chlorobenzene	Jirui and Hongwen (2015)
7.	TiO ₂ nanoparticles Immobilized on glass beads	Imidachlorpid	Photocatalytic oxidation	NH ₄ ⁺ and NO ₃ ⁻ , Cl ⁻	Akbari and Shokri (2017)
8.	Mixed metal oxides of Bivalent metal ion Mg ²⁺ with Al ³⁺ and Ce ⁴⁺	DDT	Calcination	DDD, DDE (dichlorodiphenyldichloroethylene) and simpler compounds	Manav et al. 2018
9.	Nano-TiO ₂	Alachlor	Photocatalytic degradation	NO ₃ ⁻ + Cl ⁻ + 14CO ₂ + 2H ⁺ + 9H ₂ O	Ashrafui et al. (2018)

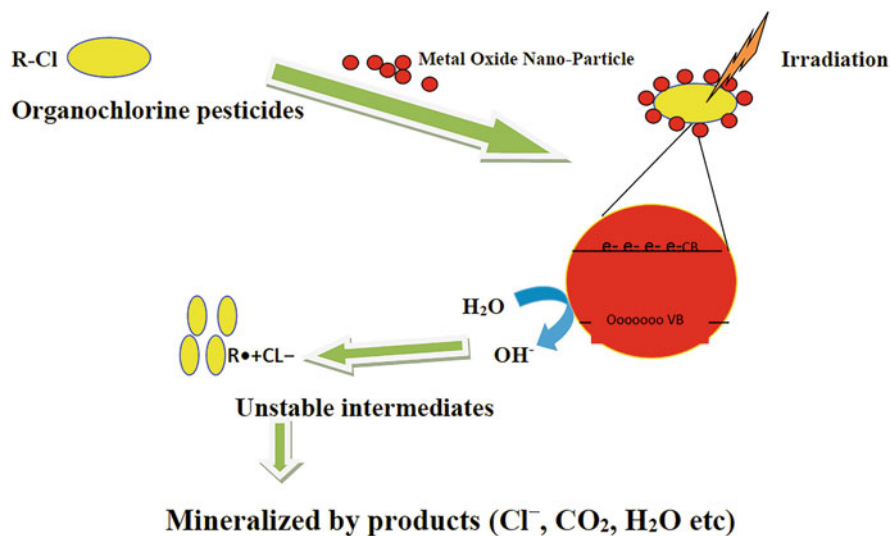


Fig. 23.4 Photocatalytic degradation of organochlorines

23.11.1 Mechanism of Organochlorine Photocatalytic Degradation

See Fig. 23.4 and Table 23.6.

23.11.2 Degradation of Organophosphorous Pesticides by Nanocomposites

Two million tons of organophosphorous pesticides are being used in the world. Due to the excessive use of these pesticides, it leads to persistent problems by partially degraded products in nature. These partially degraded products have long-term persistence property which further leads to bioaccumulation, biomagnifications in bio-organisms. Nanotechnology-based remediation strategies can efficiently degrade the organophosphorous pesticides by dehalogenation, and hydrolytical reactions at room temperature (Nair et al. 2003).

23.11.3 Photocatalytic Degradation Mechanism of Organophosphates by Nanoparticles

Degradation of pesticide by semiconducting nanoparticles is an effective tool for the toxic and persistent pesticides and converts these into eco-friendly mineralized compounds. These nanocatalysts give fast mineralization as compared to conventional ones due to large surface area to volume ratio, which enhances their area of contact toward the pesticides. Photocatalysis by nanoparticles has been widely

Table 23.6 Generalized photocatalytical examples of organochlorines

Pesticide	Use	T (1/2) days	Nanocatalyst	Degradation intermediates	Mineralized product/ stable by products
DDT	Insecticide	1460	TiO ₂ , ZnO, CdS, WO ₃ , α -Fe ₂ O ₃ and TiO ₂ /5 wt% Pt)	Dechlorinated product, e. g., DDD, DDE, ETC	CO ₂ and HCl
Aldrin	Seed and soil	266	TiO ₂	Dieldrin Chlordene 12-hydroxy-dieldrin	CO ₂ and HCl
Alpha (\pm)- BHC	Insecticide	9490	Zero-valent Fe nanoparticles, TiO ₂ is doped with nitrogen	3,4,5,6-tetrachlorocyclohexane 3,4-Dichlorocyclohexadiene	Benzene and chloride ions
Endosulfan	Agricultural pest control	50	Ag, Au, Mg, and Fe nanoparticles Ag doped TiO ₂ nanophotocatalysts	Endosulfane sulfate Endosulfan diol Endosulfan lactone Endosulfane ether	Methylcyclohexane and xylene and chloride ions
Methoxychlor	For crop pest and livestock	180	FeS@hydrotaclites (LHDs) and Fe ₃ O ₄ @LHDs catalysts, silica nanoparticles	1,1-dichloro-2,2-bis(4-methoxyphenyl)ethane (A), 4-hydroxy benzyl alcohol (B), hydroquinone (C), 3,5-dihydroxy-4-methoxybenzyl alcohol (D), Benzoquinone (E) Hexanoic acid (F) and 3-hydroxy-4-methoxy benzoic acid (G)	1. Hexanoic acid 2. 3-hydroxy-4-methoxy benzoic acid 3. Water and dioxide
Imidachlorpid	For soil pest		L-serine capped nickel nanoparticles, mesoporous copper ferrite (meso-CuFe ₂ O ₄)	6-chloro nicotinaldehyde, 6-chloronicotinic acid, 1-(6-chloro-3-pyridinyl) methyl-2-imidazolidinone 6-chloronicotinamide, 1-acetylimidazolidin-2-one, carboxylic acids, N,N-dimethylformamide	NH ₄ ⁺ and NO ₃ ⁻ and Cl ⁻

(continued)

Table 23.6 (continued)

Pesticide	Use	<i>T</i> (1/2) days	Nanocatalyst	Degradation intermediates	Mineralized product/ stable by products
Atrazine	Herbicide	260	TiO ₂ (bulk and immobilized films), Fe-nanoparticles	2-Chloro-4-ethylamino-6-isopropylamino-s-triazine, 2-Hydroxy-4-ethylamino-6-isopropylamino-s-triazine, 2-Hydroxy-4-amino-6-isopropylamino-s-triazine, 2-Hydroxy-4,6-diamino-s-triazine Hydroxy-4,6-dinitro-s-triazine, Trihydroxy-s-triazine	Cl, NO ₃ , CO ₂ and H ₂ O
Dicofol	Miticides	16	TiO ₂ nanoparticles	Bis(4-chlorophenyl) methanone 4-chlorophenyl-4'-hydroxyphenyl, methanone (4-chlorophenyl) phenyl methanone, Diphenyl methanone, and other compounds	CO 4,4'-dichloro- dibenzophenone 2, HCl

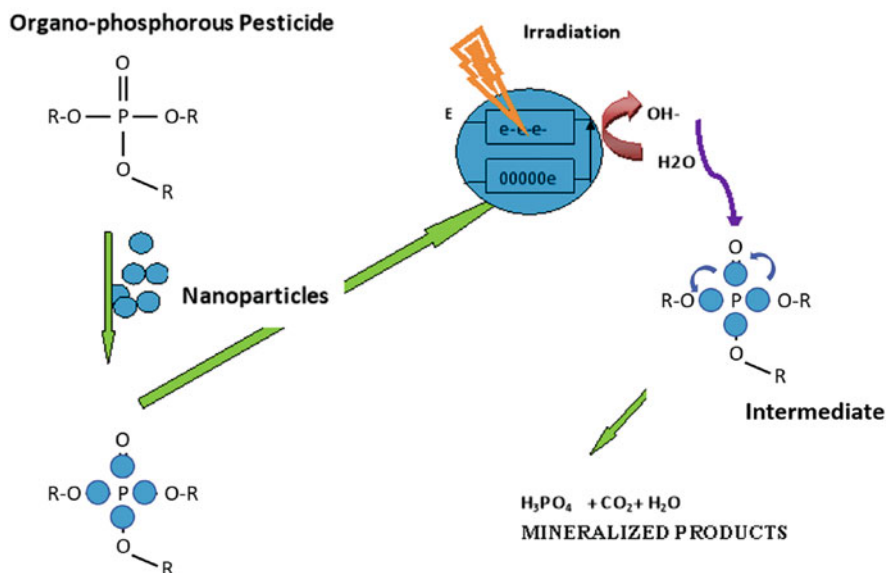


Fig. 23.5 Photocatalytical degradation of organophosphates

studied in organophosphates remediation. Among all the nanoparticle species, TiO_2 is widely used, because of its ability to give continuous supply of oxygen species for oxidation-reduction reactions of organophosphates mineralization (Darjan et al. 2013; Ochiai and Fujishima 2012) (Fig. 23.5 and Table 23.7).

23.12 Conclusion

Till now more attention has been given for the development of potential nanomaterials for the water treatment for the safety of human health and environment. Previous studies indicated that many nanomaterial properties like size, structure, shape, and reactivity make them appropriate for wide range of applications. Moreover, no study has not yet described any toxicity effect on health and environment due to lack of methods and tools. It is very important to develop nanomaterials and investigate their safe usage with full potential. Fresh water and wastewater treatment with advanced nanomaterials plays a significant role to ensure supply of sufficient, safe, and good water quality for human use.

The major contamination sources of water are agricultural wastage which contains pesticides, fertilizers, irrigated water, organic waste, etc. Among these, pesticide residues are the major contamination source and cause many acute and chronic disorders in humans and negatively affect the environment. To combat these hazardous problems, advanced nanocomposites play an important role for degrading the persistent pesticides and other organic contaminants and convert into harmless

Table 23.7 Photocatalytical examples of organophosphates

Pesticide	Use	$T(1/2)$ days	Nanocatalyst	Degradation intermediates	Mineralized product/ stable by products
Chlorpyrifos	Broad-spectrum pesticide	60–120	Au NPs	1. 3,5,6-trichloro-2-pyridinol (TCP) 2. Diethyl thiophosphate	PO_4^{3-} , CO_2 , H_2O , NH_4OH
Profenofos	Herbicide and insecticide	2.2–5.4	Bimetallic catalyst (Fe/Ni)	4-bromo-2-chlorophenol	PO_4^{3-} , CO_2 , H_2O
Malathion	Insecticide for crop pest	2–18	WO_3/TiO_2 , Au-Pd- TiO_2 nanotube film	1. Malaoxon 2. Isomalathion	CO_2 , NO_3^- and PO_4^{3-}
Diazinon	Agriculture and household pest control	21–103	Nano- TiO_2	1. 2-isopropyl-6-methyl-pyrimidin-4-ol (IMP) 2. 2-isopropyl-6-methylpyrimidin-4-yl phosphate (diazoxon) and hydroxydiazinon	Low-chain carboxylic acid
Dimethoate	Insecticide and acaricide	2–4	TiO_2 immobilized on silica gel	1. Phosphonic acid molecule, methylamine 2. Formic acid	CO_2 , NO_3^- , and PO_4^{3-}

components. This process is known as photocatalysis, in this metal oxide nanostructured semiconductor are used. Along with this different nanocomposites have antioxidant and antimicrobial properties for water cleanup. Hence, nanotechnology can give many powerful and efficient tools for the benefit of mankind and healthier nation.

References

- Ahluwalia SS, Goyal D (2007) Microbial and plant derived biomass for removal of heavy metals from waste water. *Bioresour Technol* 98:2243–2257
- Ahmad AL, Ooi BS, Mohammad AW, Choudhury JP (2004) Development of a highly hydrophobic nanofiltration membrane for desalination and water treatment. *Desalination* 168:215–221
- Ahmed S, Saifullah MA, Babu LS, Saiqa I (2016) Green synthesis of silver nanoparticles using *Azadirachta indica* aqueous leaf extract. *J Radiat Res Appl Sci* 9:1–7
- Akbari SA, Shokri M (2017) Photocatalytic degradation of imidacloprid pesticide in aqueous solution by TiO_2 nanoparticles immobilized on the glass plate. *Chem Eng Commun* 204:1061–1069
- Ali MHH, Al-Afify AD, Goher ME (2018) Preparation and characterization of graphene— TiO_2 nanocomposite for enhanced. *Egypt J Aquat Res* 44:263–270

- Allabashi R, Arkas M, Hörmann G, Tsiourvas D. (2007) Removal of some organic pollutants in water employing ceramic membranes impregnated with cross-linked silylated dendritic and cyclodextrin polymers. *Water Res* 41:476–486
- Arkas M, Paleos CM, Eleades L, Tsiourvas D (2005) Alkylated hyperbranched polymers as molecular nanosponges for the purification of water from polycyclic aromatic hydrocarbons. *J Appl Polym Sci* 97:2299–2305
- Arkas M, Allabashi R, Tsiourvas D, Mattausch EM, Perfler R (2006) Organic/inorganic hybrid filters based on dendritic and cyclodextrin “nanosponges” for the removal of organic pollutants from water. *Environ Sci Technol* 40:2771–2777
- Arnold WA, Roberts AL (1998) Pathways of chlorinated ethylene and chlorinated acetylene reaction with Zn (0). *Environ Sci Technol* 32:3017–3025
- Ashbolt NJ (2004) Microbial contamination of drinking water and disease outcomes in developing regions. *Toxicology* 198:229–238
- Ashrafal IM, Mai F, Ikki T, Hideyuki K, Satoshi K (2018) Optimization of alachlor photocatalytic degradation with nano-TiO₂ in water under solar illumination: reaction pathway and mineralization. *Clean Technol* 1:141–153
- Balasubramanian K, Burghard M (2006) Biosensors based on carbon nanotubes. *Anal Bioanal Chem* 385:452–468
- Balogh et al (2001) Dendrimer–silver complexes and nanocomposites as antimicrobial agents. *Nano Lett* 1:32–40
- Baruah S, Dutta J (2009) Hydrothermal growth of ZnO nanostructures. *Sci Technol Adv Mater* 10:1–12
- Bhattacharyya D, Hestekin JA, Brushaber P, Cullen L, Bachas LG, Sikdar SK (1998) Novel polyglutamic acid functionalized microfiltration membranes for sorption of heavy metals at high capacity. *J Membr Sci* 141:121–135
- Bilal SM, Tahira SM (2019) Carbon nanodots and rare metals (RM = La, Gd, Er) doped tungsten oxide nanostructures for photocatalytic dyes degradation and hydrogen production. *Sep Purif Technol* 209:94–102
- Binbin L et al (2007) Structural and magnetic properties of Codoped ZnO based diluted magnetic semiconductors. *Chin Phys Lett* 24:34–73
- Bosman AW, Janssen HM, Meijer EW (1999) About dendrimers: structure, physical properties, and applications. *Chem Rev* 99:1665–1688
- Botalova O, Schwarzbauer J, Sandouk al N. (2011) Identification and chemical characterization of specific organic indicators in the effluents from chemical production sites. *Water Res* 45:3653–3664
- Bo L, Cui Y, Liu X, Li H, Li X (2019) Effect of material composition on nano-adhesive characteristics of styrene-butadiene-styrene copolymer-modified bitumen using atomic force microscope technology. *Int J Adhes Adhes* 89:168–173
- Bull RJ, Brinbaum LS, Cantor KP, Rose JB, Butterworth BE, Pegram R, Tuomisto J (1995) Water chlorination, essential process and cancer hazard. *Fundam Appl Toxicol* 28:155–166
- Cai YQ, Cai Y, Mou SF, Lu YQ (2005) Multi-walled carbon nanotubes as a solid-phase extraction adsorbent for the determination of chlorophenols in environmental water samples. *J Chromatogr A* 1081:245–247
- Chairul II, Fatyasari N, Cheng KL (2019) Removal of Pb(II) and As(III) using magnetic nanoparticles coated montmorillonite via one-pot solvothermal reaction as adsorbent. *J Environ Chem Eng* 7:103000
- Chatterjee D, Shimanti D (2005) Visible light induced photocatalytic degradation of organic pollutants. *J Photochem Photobiol C: Photochem Rev* 6:186–205
- Chau CF, Wu SH, Yen GC (2007) The development of regulations for food nanotechnology. *Trends Food Sci Technol* 18:269–280
- Chaudhry Q, Schroeder P, Werck-Reichhart D, Grajek W, Marecik R (2008) Prospects and limitations of phytoremediation for the removal of persistent pesticides in the environment. *Environ Sci Pollut Res* 9(1):4–17

- Chen CZS, Cooper S (2002) Interactions between dendrimer biocides and bacterial membranes. *Biomaterials* 23:3359–3368
- Chen HD, Weiss JC, Shahidi F (2006) Nanotechnology in nutraceuticals and functional foods. *Food Technol* 60:30–36
- Cheng R, Wang JL, Zhang WX (2007) Comparison of reductive dechlorination of p-chlorophenol using FeO and nano-sized FeO. *J Hazard Mater* 144(1–2):334–339
- Cloete TE, de Kwaadsteniet M, Botes M, Lopez-Romero JM (2010) Nanotechnology in water treatment applications. Caister Academic Press, Norfolk
- Coetser SE, Heath RG, Ndombe N (2007) Diffuse pollution associated with the mining sectors in South Africa: a first-order assessment. *Water Sci Technol* 55:9–16
- Colis S, Bieber H, Bégin Colin S, Schmerber G, Leuvrey C, Dinia A (2006) Magnetic properties of Co-doped ZnO diluted magnetic semiconductors prepared by low-temperature mechanosynthesis. *Chem Phys Lett* 422:529
- Cong CJ, Liao L, Li JC, Fan LX, Zhang KL (2005) Synthesis, structure and ferromagnetic properties of Mn-doped ZnO nanoparticles. *Nanotechnology* 16:981–995
- Darjan A, Camelia D, Dana P, Anca D (2013) Degradation of pesticides by TiO₂ photocatalysis. In: Environmental security assessment and management of obsolete pesticides in Southeast Europe, vol 3, pp 155–163
- De Boer DKG (1990) Calculation of x-ray fluorescence intensities from bulk and multilayer samples. *X-Ray Spectrom* 19:145–154
- de Friend KA, Wiesner MR, Barron AR (2003) Alumina and aluminate ultrafiltration membranes derived from alumina nanoparticles. *J Membr Sci* 224:11–28
- Del alle EMM (2004) Cyclodextrins and their uses, a review. *Process Biochem* 39:1033–1046
- Deng S, Bai R (2004) Removal of trivalent and hexavalent chromium with aminated polyacrylonitrile fibers: performance and mechanisms. *Water Res* 38:2424–2432
- Devipriya S, Yesodharan S (2005) Photocatalytic degradation of pesticide contaminants in water. *Solar Energy Mater Solar Cells* 86:309–315
- Di ZC, Ding J, Peng XJ, Li YH, Luan ZK, Liang J (2006) Chromium adsorption by aligned carbon nanotubes supported ceria nanoparticles. *Chemosphere* 62:861–865
- Diallo MS, Christie S, Swaminathan P, Johnson JH, Goddard WA (2005) Dendrimer-enhanced ultrafiltration. 1. Recovery of Cu(II) from aqueous solutions using Gx–NH₂PAMAM dendrimers with ethylene diamine core. *Environ Sci Technol* 39:1366–1377
- Dotzauer DM, Dai J, Sun L, Bruening ML (2006) Catalytic membranes prepared using layer-by-layer adsorption of polyelectrolyte/metal nanoparticle films in porous supports. *Nano Lett* 6:2268–2272
- Duan P, Ma T, Yue Y, Li Y, Zhang X, Shang Y, Gao B, Zhang Q, Yue Q, Xu X (2019) Fe/Mn nanoparticles encapsulated in nitrogen-doped carbon nanotubes as a peroxymonosulfate activator for acetamiprid degradation. *Environ Sci Nano* 6:1799–1811
- El-Shafai NM, El-Khouly ME, El-Kemary M, Ramadan MS, Derbalah AS, Masoud MS (2019) Fabrication and characterization of graphene oxide–titanium dioxide nanocomposite for degradation of some toxic insecticides. *J Ind Eng Chem* 69:315–323
- Eshelby K (2007) Dying for a drink. *Br Med J* 334:610–612
- Evgenidou E, Fytianos K, Poullos I (2005) Semiconductor-sensitized photodegradation of dichlorvos in water using TiO₂ and ZnO as catalysts. *Appl Catal Environ* 59:81–89
- Falconer IR, Humpage AR (2005) Health risk assessment of cyanobacterial (blue–green algal) toxins in drinking water. *Int J Environ Res Public Health* 2:43–50
- Fang T-H et al (2000) Machining characterization of the nano-lithography process using atomic force microscopy. *Nanotechnology* 11:181–190
- Fawell J, Nieuwenhuijsen MJ (2003) Contaminants in drinking water. *Br Med Bull* 68:99–208
- Foley JA, DeFries R, Asner GP, Barford C, Bonan G, Carpenter SR, Chapin FS, Coe MT, Daily GC, Gibbs HK, Helkowski JH, Holloway T, Howard EA, Kucharik CJ, Monfreda C, Patz JA, Prentice IC, Ramankutty N, Snyder PK (2005) Global consequences of land use. *Science* 309:570–574

- Gao C, Yan D (2004) Hyperbranched polymers: from synthesis to applications. *Prog Polym Sci* 29:183–275
- Ghasemzadeh G, Momenpour M, Omid F, Hosseini MR, Ahani M, Abolfazl B (2014) Applications of nanomaterials in water treatment and environmental remediation. *Front Environ Sci Eng* 4:471–482
- Giri M (2001) Influence of viscoelasticity on the nano-micromechanical behavior of latex films and pigmented coatings. *Electronic Theses and Dissertations*, vol 247, pp 21–32
- Gong X, He S (2020) Highly durable superhydrophobic polydimethylsiloxane/silica nanocomposite surfaces with good self-cleaning ability. *ACS Omega* 8:4100–4108. <https://doi.org/10.1021/acsomega.9b03775>
- Gotpagar JK, Grulke EA, Tsang T, Bhattacharyya D (1997) Reductive dehalogenation of trichloroethylene using zero-valent iron. *Environ Prog* 6:137–143
- Habib Z, Khan SJ, Ahmad NM, Shahzad HMA, Jamal Y, Hashmi I (2019) Antibacterial behaviour of surface modified composite polyamide nanofiltration (NF) membrane by immobilizing Ag-doped TiO₂ nanoparticles. *Environ Technol* 23:1–13
- Haider S, Naithani , iswanathan PN, Kakkur P (2003) Cyanobacterial toxins: a growing environmental concern. *Chemosphere* 52:1–21
- Hasan A, Pandey LM (2015) Review: polymers, surface-modified polymers, and self assembled monolayers as surface-modifying agents for biomaterials. *Polym-Plast Technol Eng* 54:1358–1378(21)
- Hollman AM, Bhattacharyya D (2004) Pore assembled multilayers of charged polypeptides in microporous membranes for ion separation. *Langmuir* 20:5418–5424
- Hsieh Y-H, Ofori J (2007) Innovations in food technology for health. *Asia Pac J Clin Nutr* 16 (1):65–73
- Hui Y-Z et al (2009) Improving gas sensing properties of graphene by introducing dopants and defects: a first-principles study. *Nanotechnology* 20:21–25
- Iijima S (1991) Helical microtubules of graphitic carbon. *Nature* 354:56–58
- Jahirul AM, Mohammad P, Rubia N, Meryam S (2019) Development of sustainable and reusable silver nanoparticle-coated glass for the treatment of contaminated water. *Environ Sci Pollut Res* 26:23070–23081
- Jarup L (2003) Hazards of heavy metal contamination. *Br Med Bull* 68:167–182
- Jikei M, Kakimoto MA (2001) Hyperbranched polymers: a promising new class of materials. *Prog Polym Sci* 26:1233–1285
- Jin J, Li R, Wang H, Chen H, Liang K, Ma J (2007) Magnetic Fe nanoparticle functionalized water-soluble multi-walled carbon nanotubes: towards the preparation of sorbent for aromatic compounds removal. *Chem Commun* 4:386–388
- Jirui Y, Hongwen S (2015) Degradation of γ -hexachlorocyclohexane using carboxymethylcellulose-stabilized Fe/Ni nanoparticles. *Water Air Soil Pollut* 226:280
- Kapoor A, iraghavan T (1997) Nitrate removal from drinking water. *J Environ Eng* 123:371–380
- Kaur R, Hasan A, Iqbal N, Alam S, Saini MK, Raza SK (2014) Synthesis and surface engineering of magnetic nanoparticles for environmental cleanup and pesticide residue analysis: a review. *J Sep Sci* 37:1805–1825
- Keller AA, Lazareva A (2014) Predicted releases of engineered nanomaterials: from global to regional to local. *Environ Sci Technol Lett* 1:65–70
- Kemper KE (2004) Groundwater—from development to management. *J Hydrogeol* 12:3–5
- Keum YS, Li QX (2004) Reduction of nitroaromatic pesticides with zerovalent iron. *Chemosphere* 54:255–263
- Klajnert B, Bryszewska M (2001) Dendrimers. Properties and applications. *Acta Biochim Pol* 48:199–208
- Kostal J, Mulchandani A, Chen W (2001) Tunable biopolymers for heavy metal removal. *Macromolecules* 34:2257–2261
- Kostal J, Mulchandani A, Gropp K, Chen W (2003) A temperature responsive biopolymer for mercury remediation. *Environ Sci Technol* 37:4457–4462

- Kostal J, Prabhukumar G, Lao UL, Chen A, Matsumoto M, Mulchandani A, Chen W (2005) Customizable biopolymers for heavy metal remediation. *J Nanopart Res* 7:517–523
- Lao UL, Chen A, Matsumoto MR, Mulchandani A, Chen W (2007) Cadmium removal from contaminated soil by thermally-responsive elastin (ELPEC20) biopolymers. *Biotechnol Bioeng* 98:349–355
- Lee EJ, Schwab KJ (2005) Deficiencies in drinking water distribution systems in developing countries. *J Water Health* 3:109–127
- Lee JS, Chon HT, Kim KW (2005) Human risk assessment of As, Cd, Cu and Zn in the abandoned metal mine site. *Environ Geochem Health* 27:185–191
- Li YH, Ding J, Luan ZK, Di ZC, Zhu YF, Xu CL, Wu DH, Wei BQ (2003) Competitive adsorption of Pb²⁺, Cu²⁺ and Cd²⁺ ions from aqueous solutions by multi-walled carbon nanotubes. *Carbon* 41:2787–2792
- Liu Y, Chen X, Li J, Burda C (2005a) Photocatalytic degradation of azo dyes by nitrogen-doped TiO₂ nanocatalysts. *Chemosphere* 61:11–18
- Liu Y, Majetich SA, Tilton RD, Sholl DS, Lowry G (2005b) TCE dechlorination rates, pathways, and efficiency of nanoscale iron particles with different properties. *Environ Sci Technol* 39:1338–1345
- Lu C, Chiu H (2006) Adsorption of Zinc (II) from water with purified carbon nanotubes. *Chem Eng Sci* 61:1138–1145
- Lu C, Liu L (2006) Removal of nickel(II) from aqueous solution by carbon nanotubes. *J Chem Technol Biotechnol* 81:1932–1940
- Lu AH, Salabas E, Schüth F (2007) Magnetic nanoparticles: synthesis, protection, functionalization, and application. *Angew Chem Int Ed* 46:1222–1244
- Manav N, Dwivedi , Bhagi AK (2018) Degradation of DDT, a pesticide by mixed metal oxides nanoparticles. *Green Chem Environ Sustain Chem Educ* 3:93–99
- Manoharan RK, Ayyaru S, Ahn Y (2020) Auto-cleaning functionalization of the polyvinylidene fluoride membrane by the biocidal oxine/TiO₂ nanocomposite for anti-biofouling properties. *New J Chem* 44:807–816
- Masciangioli T, Zhang WX (2003) Environmental technologies at the nanoscale. *Environ Sci Technol* 37:102–108
- Matheson LJ, Tratnyek PG (1994) Reductive dehalogenation of chlorinated methanes by iron metal. *Environ Sci Technol* 28:2045–2053
- Maysinger D (2007) Nanoparticles and cells: good companions and doomed partnerships. *Org Biomol Chem* 5:2335–2342
- Meyer DE, Wood K, Bachas LG, Bhattacharyya D (2004) Degradation of chlorinated organic by membrane-immobilized nanosized metals. *Environ Prog* 23:232–242
- Miller SA, Young Y, Martin CR (2001) Electro-osmotic flow in template-prepared carbon nanotube membranes. *J Am Chem Soc* 123:12335–12342
- Mills A, Punte L, Stephan M (1997) An overview of semiconductor photocatalysis. *J Photochem Photobiol A* 108:1–35
- Miyagawa H, Misra M, Mohanty AK (2005) Mechanical properties of carbon nanotubes and their polymer nanocomposites. *J Nanosci Nanotechnol* 5:1593–1615
- Moe CL, Rheingans RD (2006) Global challenges in water, sanitation and health. *J Water Health* 4:41–57
- Mohammad NM, Nabil B, Nemesh WB, Jinping G, Incent N (2019) Stabilization of zero valent iron (Fe⁰) on plasma/dendrimer functionalized polyester fabrics for Fenton-like removal of hazardous water pollutants. *Chem Eng J* 374:658–673
- Mohsen MS, Jaber JO, Afonso MD (2003) Desalination of brackish water by nanofiltration and reverse osmosis. *Desalination* 157:167
- Montgomery MA, Elimelech M (2007) Water and sanitation in developing countries: including health in the equation. *Environ Sci Technol* 41:17–24
- Moore M, Gould P, Keary BS (2003) Global urbanization and impact on health. *Int J Hyg Environ Health* 206:269–278

- Moraru CI, Panchapakesan CP, Huang QR, Takhistov P, Sean L, Kokini JL (2003) Nanotechnology: a new frontier in food science. *Food Technol* 57:24–29
- Mudassir J, Darwis Y, Muhamad S, Khan AA (2019) Self-assembled insulin and nanogels polyelectrolyte complex (Ins/NGs-PEC) for oral insulin delivery: characterization, lyophilization and in-vivo evaluation. *Int J Nanomedicine* 14:4895–4909
- Nair V, Rajesh C, Vinod AU, Bindu S, Sreekanth AR, Mathen JS, Lakshmi B (2003) Suprab strategies for heterocyclic construction via novel multicomponent reactions based on isocyanides and nucleophilic carbenes. *Acc Chem Res* 36:899–907
- Niyaz MM, Mohsen TA, Taghizadeha J, Abdia B, Hayati A, Akbar S (2019) Bio-based magnetic metal-organic framework nanocomposite: ultrasound-assisted synthesis and pollutant (heavy metal and dye) removal from aqueous medium. *Appl Surf Sci* 480:288–299
- Nutt MO, Heck KN, Alvarez P, Wong MS (2006) Improved Pd-on-Au bimetallic nanoparticle catalysts for aqueous-phase trichloroethene hydrodechlorination. *Appl Catal Environ* 69:115–125
- Ochiai T, Fujishima A (2012) Photoelectrochemical properties of TiO₂ photocatalyst and its applications for environmental purification. *J Photochem Photobiol C Photochem Rev* 13:247–262
- Oller I, Gernjak W, Maldonado MI, P'erez Estrada LA, S'anchez P'erez JA, Malato S (2006) Solar photocatalytic degradation of some hazardous water-soluble pesticides at pilot-plant scale. *J Hazard Mater B* 138:507–517
- Paknikar KM, Nagpal , Pethkar A, Rajwade JM (2005) Degradation of lindane from aqueous solutions using iron sulfide nanoparticles stabilized by biopolymers. *Sci Technol Adv Mater* 6:370–374
- Patterson JW (1985) Wastewater treatment technology. Science Publishers, Ann Arbor
- Peltier S, Cotte E, Gatel D, Herremans L, Cavard J (2003) Nanofiltration improvements of water quality in a large distribution system. *Water Suppl* 3:193–200
- Peng XJ, Li YH, Luan ZK, Di ZC, Wang HY, Tian BH, Jia ZP (2003) Adsorption of 1, 2-dichlorobenzene from water to carbon nanotubes. *Chem Phys Lett* 376:154–158
- Peng XJ, Luan ZK, Ding J, Di ZC, Li YH, Tian BH (2005) Ceria nanoparticles supported nanotubes for the removal of arsenate from water. *Mater Lett* 59:399–403
- Peral J, Domenech X, Ollis DF (1997) Heterogeneous photocatalysis for purification, decontamination, and deodorization of air. *J Chem Technol Biotechnol* 70:117–140
- Polizu S, Savadogo O, Poulin P, Yahia L (2006) Applications of carbon nanotubes-based biomaterials in biomedical nanotechnology. *J Nanosci Nanotechnol* 6:1883–1904
- Popov N (2004) Carbon nanotubes: properties and application. *Mater Sci Eng A* 43:61–102
- Pourya M, Hassan S (2019) Evaluation, of the bimetallic photocatalytic performance of Resin–Au–Pd nanocomposite for degradation of parathion pesticide under visible light. *Polyhedron* 170:132–137
- Ponder SM, John GD, Thomas EM (2000) Remediation of Cr(VI) and Pb(II) aqueous solutions using supported, nanoscale zero-valent iron. *Environ Sci Technol* 34:2564–2569
- Prabhukumar G, Matsumoto M, Mulchandani A, Chen W (2004) Cadmium removal from contaminated soil by tunable biopolymers. *Environ Sci Technol* 38:3148–3152
- Prathap S, Uma K, Subhankar P (2019) Biomolecule. Functionalized magnetite nanoparticles efficiently adsorb and remove heavy metals from contaminated water. *J Chem Technol Biotechnol* 94:2009–2022
- Qin Y, Ji X, Jing J, Liu H, Wu H, Yang W (2010) Size control over spherical silver nanoparticles by ascorbic acid reduction. *Colloids Surf A Physicochem Eng Asp* 372:172–176
- Qu X, Alvarez PJ, Li Q (2013) Applications of nanotechnology in water and wastewater treatment. *Water Res* 47:3931–3946
- Rahmanifar B, Dehaghi SM (2014) Removal of organochlorine pesticides by chitosan loaded with silver oxide nanoparticles from water. *Clean Technol Environ Policy* 16:1781–1786
- Rajesh P, Selvamani P, Gomathi E (2013) Waste water treatment through dendrimer—conjugated magnetic nanoparticles. *Int J Chem Technol Res* 5:1239–1245

- Rickerby DG, Morrison M (2007) Nanotechnology and the environment: a European perspective. *STAM* 8:19–24
- Ritchie SMC, Bachas LG, Olin T, Sikdar SK, Bhattacharyya D (1999) Surface modification of silica- and cellulose-based microfiltration membranes with functional polyamino acids for heavy metal sorption. *Langmuir* 15:6346–6357
- Ritchie TK, Grinkova YV, Bayburt TH, Denisov IG, Zolnerciks JK, Atkins WM, Sligar SG (2009) Chapter eleven – reconstitution of membrane proteins in phospholipid bilayer nanodiscs. *Methods Enzymol* 464:211–231
- Riu J, Maroto A, Rius FX (2006) Nanosensors in environmental analysis. *Talanta* 69:288–301
- Ritu A (2013) Simple and effective method of the synthesis of nanosized Fe₂O₃ particles. *J Appl Chem (IOSR-JAC)* 4:41–46
- Rivas BL, Pereira ED, Moreno-illoslada I (2003) Water soluble polymer–metal ion interactions. *Prog Polym Sci* 28:173–208
- Rodriguez-Mozaz S, L’opez de Alda MJ, Barcel’o D (2004) Monitoring of estrogens, pesticides and bisphenol A in natural waters and drinking water treatment plants by solid–phase extraction–liquid chromatography–mass spectrometry. *J Chromatogr* 1045:85–92
- Rook JJ (1974) Formation of haloforms during chlorination of natural waters. *Water Treat Exam* 23:234–243
- Rosa ES, erónica MM, Ivonne LSH, Guadalupe M, Monserrat CJ, Perla TAS (2019) Pre-treatment of soft drink wastewater with a calcium-modified zeolite to improve electrooxidation of organic matter. *J Environ Sci Health Pt A Toxic Hazard Subst Environ Eng* 54:617–627
- Salipira KL, Mamba BB, Krause RW, Malefetse TJ, Durbach SH (2007) Carbon nanotubes and cyclodextrin polymers for removing organic pollutants from water. *Environ Chem Lett* 5:13–17
- Savage N, Diallo MS (2005) Nanomaterials and water purification: opportunities and challenges. *J Nanopart Res* 7:331–342
- Sawicki R, Mercier L (2006) Evaluation of mesoporous cyclodextrin-silica nanocomposites for the removal of pesticides from aqueous media. *Environ Sci Technol* 40:1978–1983
- Schneiderman E, Stalcup AM (2000) Cyclodextrins: a versatile tool in separation science. *J Chromatogr B* 745:83–102
- Schwarzenbach RP, Escher BI, Fenner K, Hofstetter TB, Johnson CA, on Gunten U, Wehrli B (2006) The challenge of micro-pollutants in aquatic systems. *Science* 313:1072–1077
- Schrick B, Blough JL, Jones AD, Mallouk TE (2002) Hydrodechlorination of trichloroethylene to hydrocarbons using bimetallic nickel–iron nanoparticles. *Chem Mater* 14:5140–5147
- Scott NR (2007) Nanoscience in veterinary medicine. *et Res Commun (Suppl)* 31:139–144
- Seyyed AM, Jaafarzadeh N, Gomes HT, Jorfi S, Ahmadi M (2019) Magnetic titanium/carbon nanotube nanocomposite catalyst for oxidative degradation of Bisphenol A from high saline polycarbonate plant effluent using catalytic wet peroxide oxidation. *Chem Eng J* 15:372–386
- Shan C, Zhao W, Lucas X, Lu Daniel J, O’Brien L, Zeyuan C, Ana LE, Rodolfo C-S, Mauricio T, Bingqing W, Jonghwan S (2013) Three-dimensional nitrogen-doped multiwall carbon nanotube sponges with tunable properties. *Nano Lett* 13:5514–5520
- Sharafat A, Syed AUR, Izaz AS, Haiou H (2019) Efficient removal of zinc from water and wastewater effluents by hydroxylated and carboxylated carbon nanotube membranes: behaviors and mechanisms of dynamic filtration. *J Hazard Mater* 365:64–73
- Sharma S, Tiwari S, Hasan A, Saxena , Pandey LM (2018a) Recent advances in conventional and contemporary methods for remediation of heavy metal-contaminated soils. *3 Biotech* 8:216–230
- Sharma S, Hasan A, Kumar N, Pandey LM (2018b) Removal of methylene blue dye from aqueous solution using immobilized *Agrobacterium fabrum* biomass along with iron oxide nanoparticles as biosorbent. *Environ Sci Pollut Res* 25:21605–21615
- Shin DH, Ko YG, Choi US, Kim WN (2004) Design of high efficiency chelate fibers with an amine group to remove heavy metal ions and pH-related FT-IR analysis. *Ind Eng Chem Res* 43:2060–2066

- Singh M, Kalaivani R, Manikandan S, Sangeetha N, Kumaraguru AK (2013a) Facile green synthesis of variable metallic gold nanoparticle using *Padina gymnospora*, a brown marine macroalga. *Appl Nanosci* 3:145–151
- Singh R, Manickam N, Krishna M, Mudiam R, Chandra R, Murthy Misra (2013b) An integrated (nano-bio) technique for degradation of γ -HCH contaminated soil. *J Hazard Mater* 15:258–259
- Smita C, Bhattacharyya KG (2019) Oxidative degradation of Congo red using zeolite Y as a support for Co(II), Ni(II) and Cu(II) ions. *SN Appl Sci* 1:1224
- Srivastava A, Srivastava ON, Talapatra S, Ajtai R, Ajayan PM (2004) Carbon nanotube filters. *Nat Mater* 3:610–614
- Stanton BW, Harris JJ, Miller MD, Bruening ML, Ultrathin (2003) Multilayered polyelectrolyte films as nanofiltration membranes. *Langmuir* 19:7038–7042
- Strathmann H (2001) Membrane separation processes: current relevance and future opportunities. *AIChE J* 47:1077–1087
- Sunandan B, Dutta J (2009) Hydrothermal growth of ZnO nanostructures. *Sci Technol Adv Mater* 10:1–12
- Tehreema N, Mudassir I, Sonia Z, Muhammad IS (2019) Trimellitic acid functionalized magnetite nanoparticles for the efficient removal of Pb(II) and Cr(I) from wastewater streams. *Kor J Chem Eng* 36:860–868
- Thatai et al (2014) Nanoparticles and core-shell nanocomposite based new generation water remediation materials and analytical techniques: a review. *Microchem J* 116:62–76
- Theron J, Cloete TE (2002) Emerging water borne infections: contributing factors, agents, and detection tools. *Crit Rev Microbiol* 28:1–26
- Tick GR, Lourenso F, Wood AL, Brusseau ML (2003) Pilot-scale demonstration of cyclodextrin as a solubility-enhancement agent for remediation of a tetrachloroethene-contaminated aquifer. *Environ Sci Technol* 37:5829–5834
- Tiwari V, Mishra N, Gadani K, Solanki PS, Shah NA (2018) Mechanism of anti-bacterial activity of zinc oxide nanoparticle against carbapenem-resistant *Acinetobacter baumannii*. *Front Microbiol* 9:12–18
- Tomalia DA, Fréchet JM (2002) Discovery of dendrimers and dendritic polymers: a brief historical perspective. *J Polym Sci A Polym Chem* 40:2719–2728
- Tully DC, Frechet J (2001) Dendrimers at surfaces and interfaces: chemistry and applications. *Chem Commun* 6:1229–1239
- Ullah R, Dutta J (2008) Photocatalytic degradation of organic dyes with manganese-doped ZnO nanoparticles. *J Hazard Mater* 156:194
- Urbansky ET, Schock MR (1999) Issues in managing the risks associated with per chlorate in drinking water. *J Environ Manage* 56:79–95
- Urry DW, Gowda DC, Parker TM, Luan CH (1992) Hydrophobicity scale for protein based on inverse temperature transitions. *Biopolymers* 32:1243–1250
- ahid K, Kamala A, Torabiana HA (2019) Stabilizing of poly(amidoamine) dendrimer on the surface of sand for the removal of nonylphenol from water: batch and column studies. *J Hazard Mater* 367:357–364
- an der Bruggen B, andcasteele C (2003) Removal of pollutants from surface water and groundwater by nanofiltration: overview of possible applications in the drinking water industry. *Environ Pollut* 122:435–445
- aseashta A, aclavikova M, aseashta S, Gallios G, Roy P, Pummakarnchana O (2007) Nanostructures in environmental pollution detection, monitoring and remediation. *STAM* 8:47–59
- ieessman W, Hammer MJ (1998) Water supply and pollution control. Addison-Wesley Longman, Menlo Park
- rosmary CJ, Green P, Salisbury J, Lammers RB (2000) Global water resources: vulnerability from climate change and population growth. *Science* 289:284–288
- Walha K, Amar BR, Firdaus L, Quémeuneur F, Jaouen P (2007) Brackish groundwater treatment by nanofiltration, reverse osmosis and electrodialysis in Tunisia: performance and cost comparison. *Desalination* 207:95–106

- Weber WJ (2002) Distributed optimal technology networks: a concept and strategy for potable water sustainability. *Water Sci Technol* 46:241–246
- Wegmann M, Michen B, Graule T (2008) Nanostructured surface modification of microporous ceramics for efficient virus filtration. *J Eur Ceram Soc* 28:1603–1612
- Whitesides GM, Grzybowski B (2002) Self-assembly at all scales. *Science* 295:2418–2421
- Wu L, Shamsuzzoha M, Ritchie SMC (2005) Preparation of cellulose acetate supported zero-valent iron nanoparticles for the dechlorination of trichloroethylene in water. *J Nanopart Res* 7:469–476
- Xian BQ, Wua WS, Wei WH, Yua Z, Zhua X, Zhanga Z, Zhanga RZ, Fuyi C (2019) Polyamidoamine dendrimer grafted forward osmosis membrane with superior ammonia selectivity and robust antifouling capacity for domestic wastewater concentration. *Water Res* 153:1–10
- Xiaodan Y, Wu Q, Shicheng J, Yihang G (2006) Nanoscale ZnS/TiO₂ composites: preparation, characterization, and visible-light photocatalytic activity. *Mater Charact* 57:333–341
- Xiaolei W, Qing L, Minghao L, Yu L (2018) Interference adsorption mechanisms of dimethoate, metalaxyl, atrazine, malathion and prometryn in a sediment system containing coexisting pesticides/heavy metals based on fractional factor design (Resolution) assisted by 2D-QSAR. *Chem Res Chin Univ* 34:397–407
- Xu X, Zhou M, He P, Hao Z (2005) Catalytic reduction of chlorinated and recalcitrant compounds in contaminated water. *J Hazard Mater* 123:89–93
- Yan H, Gong A, He H, Zhou J, Wei Y, Lu L (2006) Adsorption of microcystins by carbon nanotubes. *Chemosphere* 62:142–148
- Yang GCC, Lee HL (2005) Chemical reduction of nitrate by nano-sized iron, Kinetics and pathways. *Water Res* 39:884–894
- Yaoyu C, Xie F, Zhang P et al (2019) Dual-beam super-resolution direct laser writing nanofabrication technology [J]. *Opto-Electronic Eng* 44:1133–1145
- Yates CR, Hayes W (2004) Synthesis and applications of hyperbranched polymers. *Eur Polym J* 40:1257–1281
- Yellepeddi VK, Kumar A, Palakurthi S (2009) Biotinylated poly(amido)amine (PAMAM) dendrimers as carriers for drug delivery to ovarian cancer cells in vitro. *Anticancer Res* 8:2933–2943
- Yi Y, Zhang H, Yan Y (2019) Preparation of novel iron-loaded microfibers entrapped carbon-nanotube composites for catalytic wet peroxide oxidation of m-cresol in a fixed bed reactor. *Sep Purif Technol* 212:405–415
- Yingxin Z, Duo LW, Huang YY, Min JL, Duc NQ, Thang TN, Han T (2019) Insights into biofilm carriers for biological wastewater treatment processes: current state-of-the-of-the-art, challenges, and opportunities. *Bioresour Technol* 288:121619
- Yoo H, Kwak SY (2013) Surface functionalization of PTFE membranes with hyperbranched poly (amidoamine) for the removal of Cu²⁺ ions from aqueous solution. *J Memb Sci* 448:125–134
- Yu B, Zeng J, Gong L, Zhang M, Zhang L, Chen X (2007) Investigation of the photocatalytic degradation of organochlorine pesticides on a nano-TiO₂ coated film. *Talanta* 72:1667–1674
- Yuko N, Ai M, Peter LC, Hisataka K (2016) Nanodrug delivery: is the enhanced permeability and retention effect sufficient for curing cancer? *Bioconjug Chem* 27:2225–2238
- Zaleska A, Hupka J, Wiergowsky M, Biziuk M (2000) Photocatalytic degradation of lindane, p, p'-DDT and methoxychlor in an aqueous environment. *J Photochem Photobiol A Chem* 135:213–220
- Zhang J, Xufang W, Tongwen X (2008) Elemental selenium at nano size (Nano-Se) as a potential chemopreventive agent with reduced risk of selenium toxicity: Com101: parison with S-methylselenocysteine in mice. *Toxicol Sci* 101:22–31
- Zangeneh H, Zinatizadeh AA, Zinadini S (2020) Self-cleaning properties of L-Histidine doped TiO₂-CdS/PES nanocomposite membrane: fabrication, characterization and performance. *Sep Purif Technol* 240:123–234

- Zhan HF, Zhang G, Bell JM (2014) Thermal conductivity of configurable two-dimensional carbon nanotube architecture and strain modulation. *Appl Phys Lett* 105:153105
- Zhang WX (2003) Nanoscale iron particles for environmental remediation: an overview. *J Nanopart Res* 5:323–332
- Zhang WX, Wang CB, Lien HL (1998) Treatment of chlorinated organic contaminants with nanoscale bimetallic particles. *Catal Today* 40:387–395
- Zhanqi G, Shaogui Y, Na T, Cheng S (2007) Microwave-assisted rapid and complete degradation of atrazine using TiO₂ nanotube photocatalyst suspensions. *J Hazard Mater* 145:424–430
- Zhou Q, Xiao J, Wang W, Li G, Shi Q, Wang J (2006a) Determination of atrazine and simazine in environmental water samples using multi-walled carbon nanotubes as the adsorbents for preconcentration prior to high performance liquid chromatography with diode array detector. *Talanta* 68:1309–1315
- Zhou Q, Xiao J, Wang W (2006b) Using multi-walled carbon nanotubes as solid phase extraction adsorbents to determine dichlorodiphenyltrichloroethane and its metabolites at trace level in water samples by high performance liquid chromatography with U detection. *J Chromatogr A* 1125:152–158
- Zhou Q, Xiao J, Wang W (2007) Comparison of multi-walled carbon nanotubes and a conventional adsorbent on the enrichment of sulfonylurea herbicides in water samples. *Anal Sci* 23:189–192



Biomimetic Mineralization of Electrospun PCL-Based Composite Nanofibrous Scaffold for Hard Tissue Engineering 24

Arjun Prasad Tiwari, Shiva Pandeya, Deval Prasad Bhattarai, and Mahesh Kumar Joshi

Abstract

Developing electrospun nanofibrous scaffolds has been expanded as a promising strategy in the field of bone tissue engineering owing to its resemblance to the extracellular matrix in tissues. Polycaprolactone (PCL), a synthetic polymer, is being extensively investigated over the last few decades, especially for its use in the fields of biomedicine and tissue engineering due to its superior properties like good biodegradability, nontoxicity, and remarkable processability. Despite these advantages, electrospun PCL scaffold has a low wettability which affects negatively on the biocompatibility and the process of biomineralization. Therefore, improving wettability of the PCL scaffolds is critical concern for biomedical applications. Various modifications of PCL scaffolds have been reported to improve their ability for biomimetic mineralization and to achieve a conducive interface for living cells. Incorporation of various bioactive nanoparticles/molecules/biopolymers into the PCL nanofibrous scaffolds has attracted a great deal of attention in the field of bone tissue engineering due to their ability to direct biomimetic mineralization. Loose packing of the electrospun PCL nanofibers into

A. P. Tiwari

Department of Mechanical Engineering and Engineering Science, University of North Carolina at Charlotte, Charlotte, USA

S. Pandeya

Department of Pharmacy, Maharajgunj Medical Campus, Tribhuvan University, Kirtipur, Nepal

Central Department of Chemistry, Tribhuvan University, Kirtipur, Kathmandu, Nepal

D. P. Bhattarai

Present Address: Department of Chemistry, Amrit Campus, Tribhuvan University, Kirtipur, Nepal

M. K. Joshi (✉)

Central Department of Chemistry, Tribhuvan University, Kirtipur, Kathmandu, Nepal

e-mail: mahesh.joshi@trc.edu.np

three-dimensional network is the next choice for improved mineralization. Expanding tightly packed nanofibrous scaffold into a three-dimensional form by modified gas-foamed technique results into increased porosity and surface wettability due to reaction-induced changes. The purpose of this chapter is to discuss the recent developments on modification and biomimetic mineralization of PCL-based nanofibrous scaffolds for hard tissue engineering along with to focus on the material characterization as well as cellular behavior of different cell types on the scaffolds.

Keywords

Biomimetic mineralization · Polycaprolactone · Tissue engineering · Electrospun nanofibers · Wettability

24.1 Introduction

Polycaprolactone (PCL) is a semisynthetic biodegradable, bioresorbable, and biocompatible aliphatic polyester (Hajiali et al. 2018). The IUPAC name of PCL is (1, 7)-Polyoxepan-2-one and is commonly called as 6-caprolactone polymer. PCL having wide range of molecular mass (530 Da to 630 kDa, number average molecular weight, M_n) is available. However, PCL having molecular mass in the range of 25–90 kDa is workable polymer with significant mechanical properties (Eshraghi and Das 2010; Labet and Thielemans 2009). As a semisynthetic polymer, PCL can be synthesized via various routes including polycondensation method (e.g., 6-hydroxyhexanoic acid), ring opening polymerization of a lactone (e.g., ϵ -caprolactone), and so on (Castro-Osma et al. 2013; Labet and Thielemans 2009). The PCL synthesized by ring opening of ϵ -caprolactone is specially called poly (ϵ -caprolactone). Presence of ester linkage in PCL makes it hydrolysable in physiological environment which is often triggered by enzymatic, oxidative, and pH-related catalysis (Bartnikowski et al. 2019). Initial and subsequent hydrolysis of PCL leads to macroscopic structural breakdown into small polymer fragments which is further metabolized in cellular level. Furthermore, all the by-products of PCL are excreted by the end of its degradation process. Slow polymer degradation kinetics of PCL over polylactides makes it a choice for biomaterial application. Furthermore, biocompatibility and interesting tailorable properties of PCL increase its usability in the realm of biomedical world. Blending of hydrophobic polymers such as PCL with other natural or synthetic polymer or ceramic materials can introduce some important properties relevant to tissue engineering applications (Hasan et al. 2017; Siddiqui et al. 2018). Relatively low melting point (60 °C), low glass transition temperature, miscibility with large number of polymers, and stability over melt processing offer the application of PCL in the field of regenerative medicine and tissue engineering.

PCL is soluble in common solvents such as chloroform, carbon tetrachloride, tetrahydrofuran (THF), dichloromethane (DCM), and dioxane at room temperature

(Bhattarai et al. 2018, 2019). PCL finds its widespread range of applications for implantable biomaterials, tissue engineering, and drug release application. Regarding the tissue engineering applications, PCL bears some inherent limitations such as its slow degradation rate, feeble mechanical strength, and sparse cell adhesion. Furthermore, PCL exhibits low wettability which limits the biomineralization process as well as cell culture basement where initial interaction of scaffolds with biomolecules begins. Various attempts have been made to address these limitations of PCL so as to effectuate the biomedical applications of PCL-based scaffold. Chitosan/PCL nanofibrous scaffolds are prepared by electrospinning method where the presence of chitosan moieties increases a significant hydrophilicity. The improvement in hydrophilicity was assessed by a decrease in contact angle. The increased hydrophilicity not only enhanced the bioactivity but also enhanced the protein adsorption (Shalumon et al. 2011). Miscibility with some other polymers assists in the preparation of composite or hybrid materials of PCL. Blending of PCL with some other polymers, surface functionalization, pretreatment and posttreatment of the scaffold, etc. are some notable endeavors performed to enhance the properties of PCL-based scaffolds for biomedical applications. To supplement it, PCL hybrid materials with remarkably improved properties can be prepared by incorporating some other materials like calcium phosphate-based ceramics and bioactive glasses and so on.

Tissue engineering and regenerative medicine has been becoming a major stream of study since the past few decades. The discipline of tissue engineering involves cells–scaffold interaction for natural tissue regeneration. Due to ever-increasing accidents as a result of rapid industrialization, urbanization, automatization and traffics, infections, tumors, and so on, the demands of the bone grafts and financial burden are increasing. A major challenge in this area is to develop hierarchical, three-dimensional, appropriate scaffolds capable of integrating and optimizing various properties from nano- to macro-domain in relation to biophysical and biochemical signals for tissue regeneration. Most importantly, bone tissue regeneration or replacements are the major tasks in clinical applications. The autograft is considered as the clinical gold standard to treat the defects and bone injuries (Blokhuys et al. 2013) though it has also many disadvantages. Autografting leads the surgical burdens to the patients, the risk of infection, and developing immunogenicity (Arrington et al. 1996). Bone regeneration is a complex biological process. New bone formation starts from recruiting the osteoblasts to the defect sites through variety of factors like transforming growth factor- β and bone morphogenetic proteins (BMPs) (Santin and Phillips 2012). The osteoblasts accumulate Ca^{2+} and PO_4^{3-} within polarized matrix vesicles promoted by phosphatases, calcium-binding proteins, and potential mitochondria vesicles (Anderson 2003). Collagen framework provides a platform for the spatial arrangement of the precipitated amorphous calcium phosphate into the local environment. This process is referred to mineralization or bone formation. The healing and bone formation themselves are complex processes and take a longer time (Dimitriou et al. 2011). Therefore, the focused on alternative ways of regenerating bone tissues or replacement of diseased or damaged bone is a major research trend in tissue regeneration. The osteoconductive materials

with tunable porosity, mechanical properties, and so on can be a valid alternative to autogenous bone grafts. Application of the biomaterials fulfills that gap at some extent by providing the suitable platform for bone regeneration (Gao et al. 2017; Hasan et al. 2018). The biomaterials promote the osteogenesis, a bone formation process without leaving any toxicity to health. The opted characteristics of the biomaterials for bone tissue engineering are as follows: has an ability to bond with biological macromolecules (bioactive), having the capacity to promote new bone formation from the surrounding established bone (osteoconductive), and having the ability to induce osteoblastic differentiation (osteoinductive) (Hasan et al. 2018; Wang and Yeung 2017). The uses of desired biomaterial would avoid the clinicians' need of harvesting bone from the other sites, and importantly, it would eliminate the patient's pain and discomfort associated to these procedures. The bone itself is the complex chemistry of many entities in which calcium phosphate, shares a major component, is akin to bone apatite. It has been reported that calcium phosphates as a filler component are supporting for osteogenesis and enhanced biomineralization (Shih et al. 2014). Biological products such as hydroxyapatite (HAp), demineralized bone matrix, or synthetic biomaterials such as calcium sulfate, calcium lactate, tri-calcium phosphate, bioactive glasses, or polymer-based substitutes alone or in combined form have been practicing as the bone substitute (Campana et al. 2014; Schlickewei and Schlickewei 2007). The spatially controlled deposition of calcium phosphate minerals into the collagen fibrils is the bone formation process. Bone apatites like calcium-based minerals are brittle by themselves, therefore limiting in solo application in defects for regeneration or as a bone substitute material. A basic tenet of scaffold preparation for bone regeneration is that the scaffold should feature the mechanical properties and architecture of the designed construct.

24.2 Mineralization of PCL-Based Scaffolds

There is a huge interest in the development of suitable scaffolds using a multitude of materials, including natural products, synthetic polymers, and metals, that offer ideal properties for bone regeneration or filling the bone defect. PCL has been emerged as a polymer of huge scope for bone tissue engineering applications due to its good processability, biocompatibility, and solubility in common organic solvent and capability of forming blends solution with different polymers. PCL offers longer degradation period, which benefits for its uses in hard tissue substitution. The electrospun nanofibers can mimic an extracellular matrix (ECM) that is composed of collagen fibrils within the ranges 100–200 nm (Ma et al. 2013). It has been reported that collagens serve as organic templates for bone mineralization; therefore, guidance for the growth of bone-like structures on the PCL fibers considers a rational biomimetic design. Therefore, growing the apatite-like particles toward the PCL nanofibers can be biomimetic to the natural bone. Herein, the grafting of the mineralized matrix into the bone defect is the alternative, easy, and less risky approach for filling the bone defects. Moreover, the mineralized calcium phosphate provides the additional bioactivity and osteoconductivity; therefore, the whole

osteogenesis process can be fastened. In the early 1980s, Bonfield developed the hydroxyapatite reinforced polyethylene, a mechanically compatible implant material for bone replacement, just by mixing the different weight ratio of both components (Bonfield et al. 1981). Various types of PCL scaffolds such as electrospun nanofibers, films, etc. have been prepared for biomedical applications since decades. Among different types of scaffolds, electrospun polymeric scaffolds are being widely investigated as scaffolding materials for bone tissue engineering. However, some inherent properties of PCL such as low tensile strength, stiffness, and hydrophilicity limit its harmonization for natural bone substitute (Xie et al. 2013). Blending with bioactive materials or postmodification of PCL scaffolds contributes to overcome the drawback of the as-spun electrospun PCL membranes to some extent. Table 24.1 presents the surface modification of PCL-based scaffolds reported in the various reports. Polydopamine/PCL composite finds its good application in biomineralization where dopamine, chemical moieties with catechol group, is believed to regulate mineralization of electrospun PCL fibers (Gao et al. 2016; Ghorbani et al. 2019). Minerals coating over electrospun PCL fibers render some important physicochemical properties, such as high stiffness, ultimate tensile strength, and toughness, to match closure to the mechanical properties of native bone (Xie et al. 2013). Besides these, behavior of osteoblasts in the formation of bone nodules on biopolymers/HA can be enhanced. All in all, presence of HA on semisynthetic polymers such as PCL can enhance various supporting properties. Hydroxyapatite plays an important role in the biomechanical properties of bone, including biocompatibility, osteoconductivity, nonimmunogenicity, and so on. Electrospun fibers of PCL can be immersed in supersaturated calcification solution for bio mineralization (Xia and Shi 2016). This offers the possibility of fabricating a biomaterial mimicking the bones with appropriate mechanical strength and load-bearing capacity.

Titanium metal implants were first reported to coat by calcium phosphate in the early 1980s so as to enhance the bonding ability of the implant to the bone. Later, plasma-sprayed technique which was first described by de Groot in the late 1980s (De Groot et al. 1987) was generally used to deposit the HAp particles into the metal implants. HAp particles are added into a plasma tail flame with a high temperature (up to 15,000 °C) in plasma spraying method. The HA particles undergo with a high velocity (nearly with the speed of sound, 300 ms⁻¹) when injected in the plasma flame and are driven against the surface of the substrate. During the process, the HA particles partially melt in the plasma flame and solidify later against the metal substrate, thereby, finally, forming a layer of particles. Since then, several methods have been used in coating of calcium phosphate minerals in order to increase the bioactivity/suitability of the implant for bone regeneration. Thermal spraying, sputter coating, sol-gel deposition, and dip coating are the common approach for calcium phosphate coating on the titanium implant (Arcos and Vallet-Regí 2020; Dehghanhadikolaei and Fotovvati 2019). However, the coating techniques are various depending on the substrate. The titanium implants are considered for the replacement of large bone defects. However, they are nonbiodegradable and nonresorbable. Importantly, long-term placement of the titanium implant faced the biocorrosion and the particles or ions into surrounding tissues, resulting into bone

Table 24.1 Modification of PCL-based composite reported in literature

S. no.	Sample name	Modified with	Treatment methods	Applications	References
1	Electrospun PCL nanofibers	HAp	Plasma treatment	Evaluation for bioactivity	Stastna et al. (2020)
2	Electrospun PCL/gelatin nanofibers	HAp	Electrospray	Mineralization of osteoblasts	Gupta et al. (2009)
3	Electrospun PCL nanofibers	Calcium carbonate	Single electrospinning step	Guided bone regeneration	Fujihara et al. (2005)
4	Electrospun PCL/essential oil	Cinnamon essential	Single electrospinning step	Evaluation for biocompatibility	Phajju et al. (2020)
5	Electrospun PCL/zein nanofibers	Calcium lactate	Single electrospinning step	Evaluation for biocompatibility	Liao et al. (2016)
6	PCL/cellulose nanofibers	Calcium hydroxide	Gas foaming	In vitro osteogenesis	Kim and Tiwari (2020b)
7	Electrospun PCL/drug nanofibers	Single electrospinning step	Single electrospinning step	Evaluation of antibacterial properties	Hassan and Sultana (2017)
8	Electrospun PCL/gelatin nanofibers	nHAp	Single electrospinning step/SBF treatment	Osteogenic differentiation of stem cells	Behere et al. (2020)
9	Electrospun PCL nanofibers	HAp/hardystonite	Single electrospinning step	Evaluation of biocompatibility	Jaiswal et al. (2013)
10	Electrospun 3D PCL nanofiber	Calcium lactate	Electrospinning/posttreatment	Bone regeneration	Hwang et al. (2020)
11	Electrospun PCL nanofibers	Bioglass	Melt electrospinning	Bone regeneration	Ren et al. (2014)
12	Electrospun PCL nanofibers	n/a	Plasma treatment	Increment of the –OH and –C=O functionalities	Martins et al. (2009)
13	PCL/cellulose nanofibers	HAp	SBF treatment	Osteogenesis	Joshi et al. (2015b)

14	Electrospun PCL/cellulose nanofiber	Calcium carbonate	Electrospinning/posttreatment	Bone regeneration	Hwang et al. (2019)
15	PCL film	Calcium carbonate	Solvent casting/gas foaming	Guided bone regeneration	Tiwari et al. (2016)
16	PCL/polydopamine nanofibers	nHAp	Single electrospinning step	Bone regeneration	Gao et al. (2016)

loss as a result of inflammatory reactions (Mombelli et al. 2018). Besides, implant failure and allergic reactions are likely to be occurred due to hypersensitivity reactions (Kim et al. 2019; Safioti et al. 2017). Several works put forward to develop electrospun-based composite scaffolds for filling the gap of small bone defects or bone regeneration even these as its original form may not be appropriate for large bone defects. The suitability of the electrospun nanofibers is enhanced by the simultaneous spinning the filler components such as calcium phosphate with major polymeric solution and/or postelectrospinning process. Postelectrospinning approaches cover an immersion of the as-spun polymeric scaffolds into mineralizing solutions which slowly generates an inorganic coating onto the fiber surface thereby creating the biomimetic surface.

24.3 Synthesis of Mineralized PCL-Based Scaffolds Via Electrospinning

Simultaneous electrospinning is the process of electrospinning of the polymeric solution combined with the inorganic particles in order to make the functional fibrous mats. Simple electrospinning of the polymeric solution produces pure polymeric nanofibers. Since the pure polymeric fibrous membranes are, in general, poorly bioactive and are hardly useful for inducing bone regeneration, introducing bioactive compounds, such as growth factors, bioglasses, and calcium phosphates, are essential. The HA-enriched nanofibers can better provide the adsorption sites due to having more chemical clues, thus enhancing the bioactivity, cell compatibility, and osteogenesis process in overall. On the other hand, the polymeric fibers have low stiffness; therefore, many researchers incorporated the HA, and thus organic–inorganic nanocomposites provide significant mechanical hardness to the scaffold and increase the suitability (Shao et al. 2016; Xu et al. 2020; Yang et al. 2008). Several researches mentioned fibers coated with various forms of apatite, which mimic the natural bone thus providing an ideal environment for osteogenesis and increase the structural stability of the scaffold. Shao et al. (2016) electrospun silk fibroin together with apatite-like particles and used in bone regeneration. However, in simultaneous electrospinning after particles exceeding of certain concentration (maximum loading 10 wt%) limits the electrospinning process. The filler solution can either be precipitated into the polymeric solution during long-time electrospinning process or the inorganic particles can dissolve under the organic solvents. Beading on the fibers and mass aggregation of particles onto the fibers are commonly observed (Lee et al. 2016). Due to the heterogeneous property of the resulting fibrous mat, the wettability and mechanical properties can be varied upon the position of mat. These in turn affect the biocompatibility, mineralization, and eventual osteogenesis process.

Erisken et al. developed functionally graded PCL incorporated nonwoven meshes with tri-calcium phosphate nanoparticles using a new hybrid twin-screw extrusion/electrospinning (TSEE) process (Erisken et al. 2008). This process allowed the time-dependent feeding of various solid and liquid ingredients and their melting,

deairation, dispersion, and pressurization together with electrospinning within the confines of a single process. Park et al. fabricated the beta-tri-calcium phosphate (β -TCP) particles incorporated lactic acid/PCL (LA/PCL) micro/nanofibers via single-step electrospinning process for hard tissue engineering. Incorporation of β -TCP not only enhanced the bioactivity but also enhanced the hydrophilicity and biodegradation of PCL scaffold (Park et al. 2014). Nano-magnesium phosphate (nMP) and nano-hydroxyapatite (nHA) -incorporated PCL composite membranes showed a good attachment and proliferation of bone-forming osteoblasts compared to pure PCL and PCL/nHA (Perumal et al. 2020). Wang et al. developed octacalcium phosphate (OCP)-embedded poly (lactic-co-glycolic acid) (PLGA)/PCL nanofibers via electrospinning and tested the ability of the membranes osteogenesis of bone marrow mesenchymal stem cells (MSCs) (Wang et al. 2019). OCP incorporation supports for the enhanced osteoinductive capacity, as confirmed by activation of alkaline phosphatase (ALP), increased gene expression of bone specific markers, and mineral nodules formation compared to PLGA/PCL. Liu et al. fabricated a highly bioactive PCL/tricalcium phosphate sol, a composite mat as an artificial periosteum covering the surface of the bone defect, to enhance bone regeneration (Liu et al. 2020a). The biomineralization on the composite membranes was found significantly improved compared to the pristine PCL. Furthermore, the mats significantly upregulated the rat bone marrow mesenchymal stem cells' (rBMSCs) activities in terms of proliferation and osteogenic differentiation.

24.4 Postelectrospinning Approach to Synthesize Mineralized PCL-Based Scaffolds

The postelectrospinning approach requires an additional step for biomineralization by introducing the electrospun scaffold into the inorganic phase. This approach allows the homogeneous attachment of particles on the surface of the fibers and contributes to the enhancement of mechanical properties of the matrix and the osteoconductivity (Joshi et al. 2015b; Tiwari et al. 2017, 2018b). A promising approach of coating by apatite-like structure is using simulated body fluids (SBFs). Over the past three decades, SBF has been widely used and developed for the following purposes: (1) bioactivity assessment for biomaterials and (2) surface coating of biomaterials to improve osteoconductivity (Joshi et al. 2015b; Nijssure et al. 2017; Song et al. 2003; Tiwari et al. 2017). SBFs is composed of ions at similar concentrations to those found in body fluid (Gkioni et al. 2010; Kokubo et al. 1990). Therefore, immersing a substrate by adjusting other biological conditions, such as temperature, pressure, and pH, is akin to body physiological condition. The degree of coating and organization of coated particles are governed by the composition of the SBF, ionic strength, pH, temperature, and immersion time. Kokubo (Kokubo et al. 1990) announced the concept of biomimetic mineralization using SBFs in 1990. After that, it is becoming a major tool to study mineralization. The coverage and degree of deposition of calcium phosphate particles are increased with increasing time of immersion mats in SBF solution. SBF contains the high concentration of

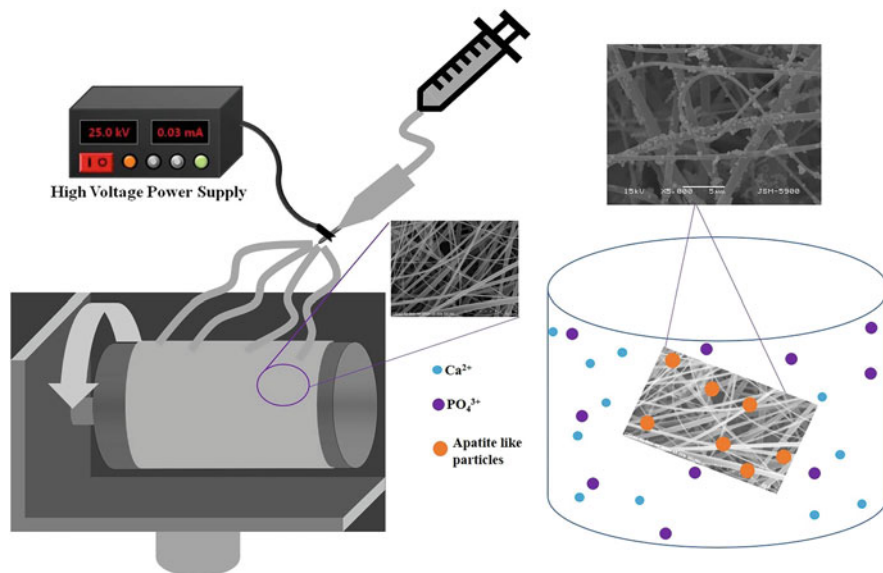


Fig. 24.1 Schematic illustration of fabrication of membranes by electrospinning and SBF treatment

calcium and phosphate ions which later condensates into the hierarchical fashion in response to ECM mimetic electrospun fibers. Being chemically inert, biocompatible, and low-cost bio absorbable synthetic polymer, PCL has been widely applied in a plethora of bone tissue regeneration (Siddiqui et al. 2018; Tiwari et al. 2018a). However, the major limitation of PCL fiber is its hydrophobic nature, which limits the contact with the precursor solution containing calcium phosphate ions thereby low degree of coating take place. To overcome this drawback, composite formation with other bioactive and hydrophilic compounds has been commonly applied. Lee et al. (2014) modified the surface of PCL-gelatin electrospun nanofibers by SBF-mediated coating to produce a bone-like calcium phosphate particles. The functional coating activates the surface and facilitates for cells–biomaterials interaction and osteogenic potential activities when using in in vivo study in a rat model. Xie et al. (2013) demonstrated a novel composite nanofiber scaffold by calcium phosphate attachment to PCL nanofibers. They modulated the mineralization process of composite mat by the coating of mussel-inspired protein, polydopamine, which served as a nucleation center of particles deposition. In one study, apatite-like structures were found attached on the fiber surface homogeneously in the PCL/albumin or PCL/polyethylene glycol (PCL/PEG) mat at a week of immersion under SBF. Further, the fiber junctions were also observed filled with the apatite layer following another week of treatment (Tiwari et al. 2017, 2018b). The production of the bone-like materials in collaboration with polymeric fibers and subsequent implantation can avoid the uses of other harsh techniques of grafting or metal

implants in many cases. This finally can ease the quality of life to patient and prevents from the extra financial burden (Fig. 24.1).

24.4.1 Preparation of Simulated Body Fluid (SBF)

In 1980, Hench (Ogino et al. 1980) observed a silicon oxide-rich layer and calcium phosphate layer strongly bonded to bioglass when implanted in the body environment. This inferred that the *in vivo* synthesis of calcium phosphate film can be reproduced in a buffer solution containing Tris hydroxymethylaminomethane and hydrochloric acid (Tris buffer solution) at physiological condition. Later, Kokubo group identified the layer of calcium phosphate is similar to the bone mineral, crystalline apatite by using micro X-ray diffraction (Kokubo et al. 1990). Subsequently, Kokubo established the SBF-mediated mineralization first at 1990 (Kokubo et al. 1990). But the proposed SBF did not contain sulfate (SO_4^{2-}) ions that are contained in human body fluid. Several modifications have come forward after that. In 1991, he revised the recipe based on the ions present in blood plasma which named as corrected SBF (c-SBF). Comparison of Ion concentrations of SBF with blood plasma is shown in Table 24.2. Since then, the c-SBF has been used widely as SBF for mineralization purposes. The formulae of preparation of SBF are given in Table 24.3.

Kokubo explained the preparation of SBF in following ways (Kokubo and Takadama 2006). Accordingly, initially, take 700 mL of ion-exchanged distilled

Table 24.2 Comparison of ion concentrations of SBF with blood plasma

	Ion concentration (mM)							
	Na^+	K^+	Mg^{2+}	Ca^{2+}	Cl^-	HCO_3^{3-}	HPO_4^{2-}	SO_4^{2-}
Human plasma (blood)	142.0	5.0	1.5	2.5	103.0	27.0	1.0	0.5
Original SBF	142.0	5.0	1.5	2.5	148.8	4.2	1.0	0
Corrected SBF (c-SBF)	142.0	5.0	1.5	2.5	103.0	4.2	1.0	0.5

Table 24.3 Required chemicals for SBF (Tadashi Kokubo 1991)

Order	Reagent	Amount	Purity (%)
1	NaCl	8.035 g	99.5
2	NaHCO ₃	0.355 g	99.5
3	KCl	0.225 g	99.5
4	K ₂ HPO ₄ ·3H ₂ O	0.231 g	99.5
5	MgCl ₂ ·6H ₂ O	0.311 g	99.0
6	1.0 mL HCl	39 mL	98.0
7	CaCl ₂	0.292 g	95.0
8	Na ₂ SO ₄	0.072 g	99.0
9	Tris	6.118 g	99.0
10	1.0 m HCl	0–5 mL	

water with a stirring bar into 1000 mL plastic beaker. Dissolve the reagents of first to eighth orders provided in Table 24.3 into the solution one by one. The chemicals of 9th (Tris) and tenth orders are dissolved in the following process of pH adjustment. Final volume makes up to 1000 mL by adding additional ion-exchanged distilled water.

24.4.2 Techniques to Assess Mineralization

24.4.2.1 Electron Microscopy

Electron microscopy allows studying the morphology and composition of mineralized matrix. Scanning electron microscopy enables the evaluation of surface morphology, while transmission electron microscopy offers the internal structure of the minerals. Tiwari et al. studied the electrospun PCL/PEG and pure PCL membrane for their ability to produce calcium phosphate particles by dipping mats into SBF solution for 7 and 14 days (Tiwari et al. 2017). Seven-day SBF-treated PCL mat (Fig. 24.2) showed few particles hardly found on the nanofiber surface, while the nanofibers beneath the surface layer remained untouched. In contrary, bone appetite-like mineral layers covered with a number of microparticles were found throughout surfaces of the composite scaffold (Fig. 24.2). Nano-nets were also observed to be completely concealed by the particles. Similarly, in the 14-day mineralized mats, more HAp particles were deposited on nanonets-covered PCL/PEG mats compared to PCL or PCL/PEG scaffold not having nanonets (Fig. 24.2). Moreover, large sheet-

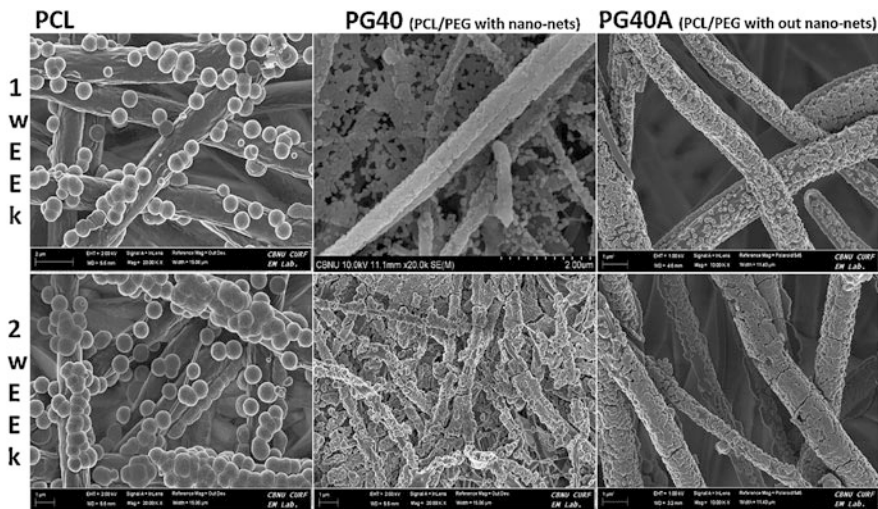


Fig. 24.2 SEM photographs of mineralized PCL, representative heterogeneous PCL/PEG (PG40), and representative PCL/PEG mats without nano-nets (PG40A). The mats were immersed in SBF solution at 37 °C for different period. (Figure adapted from Tiwari et al. (2017) with permission from Elsevier)

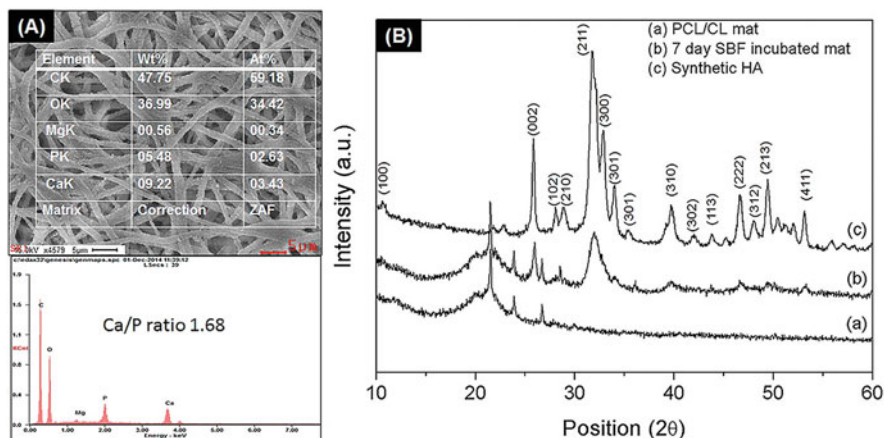


Fig. 24.3 (a) EDX analysis of PCL/cellulose membrane exposed to SBF for 1 week. (b) XRD patterns different samples. (Figure adapted from Joshi et al. (2015b). Copyright (2015) American Chemical Society)

like apatite mineral layers were observed throughout on the composite scaffold. They concluded that the enhanced mineralization on nanonets containing PCL/PEG mats compared to PCL could be affected by a number of factors, such as wettability, surface area, and surface morphology. The elemental composition and mapping can be obtained by energy-dispersive X-ray (EDX) analysis combined with the electron microscopy (Fig. 24.3a). The analysis of X-rays with energies corresponding to the atoms in the specimen emitted when an incident electron hits the specimen surface. Analysis of these X-rays can provide elemental maps of the distribution of elements such as Ca, P, C, O, and N within the sample. From the EDX analysis, the ratio of Ca/P which gives the quality of bone-like mineral formation as suggested (since recommended range of 1:1–2:1 (wt./wt.) by the European Society of Pediatric Gastroenterology Hepatology and Nutrition to confirm optimal bone health and development) (Koletzko et al. 2005) tentative can also be calculated.

24.4.2.2 Fourier Transform Infrared Spectroscopy (FTIR) Analysis

An FTIR analysis is commonly used technique to access the biomineralization of PCL-based scaffolds. FTIR of bioceramics especially HAp exhibits typical bands at 468 cm^{-1} and 605 cm^{-1} corresponding for ν_2 and ν_4 bending, respectively, of O-P-O linkage in phosphate in HA. The peaks located in the range $1150\text{--}990\text{ cm}^{-1}$ is attributed to the symmetric P-O stretching (ν_3) of the phosphate groups, while a peak at 964 belongs to symmetric P-O stretching (ν_1) of phosphate. Stretching and vibrational modes of OH^- groups can be observed at 3570 cm^{-1} and 628 cm^{-1} , respectively (Milovac et al. 2014). There are two possibilities of the carbonate substitution in HAp which generates three structural types, that is, A type, B type, and AB type. Hydroxyl sites are substituted A type HAp, while phosphate tetrahedral sites are takeover in B type. Carbonated HAp is resemblance to the chemistry of

natural human bone than pure HAp and has been proved experimentally to have better biocompatibility. The presence of the peaks at 1456 cm^{-1} and 874 cm^{-1} with high intensity predicts the B-type substitution occurred during HAp synthesis. A close look at spectra hints the presence of small amount of the A-type substituted HAp as indicated by $\nu_2\text{ CO}_3^{2-}$ peak at 879 cm^{-1} and the very weak $\nu_3\text{ CO}_3^{2-}$ peaks at 1549 cm^{-1} . AB-type substitutions are common in case of biological apatites.

24.4.2.3 XRD Patterns

XRD patterns can be recorded to investigate the chemical structure of the PCL-based composite mat exposed to SBF solution. The mineralized PCL mats show the XRD peaks at 2θ values = 25.8° , 31.7° , 32.9° , 34.0° , 39.7° , 46.6° , 49.4° , and 53.2° ascribed to HAp (Fig. 24.3b) (Joshi et al. 2015b). These 2θ values are consistent with the synthetic HAp. However, the peaks centered between 25° and 35° were slightly broadened. This result has been found similar to the XRD of extracted bone mineral from zebrafish fin rays which had smaller sized and a lower degree of mineralization, relative to synthetic HAp. Hence, mineralized electrospun scaffolds share similar properties to the native bone matrix. Another difference found in the XRD data for the mineralized scaffolds relative to the synthetic HAp (Fig. 24.3b) (Joshi et al. 2015b) is the broadening of the peak at 29° with increased intensity. This can be due to the embedding of the amorphous Ca/P in the SBF-treated scaffold. However, the limited differences are found within the diffractograms depending on the mineralization procedures and substrate polymeric material (Rodríguez et al. 2011). Therefore, a number of possibilities to achieve a mineralized scaffold with slightly altered structures cannot be ruled out. The polymer matrix acts as Ca/P base reservoirs for integration into platelets within the collagenous network. Ca/P clusters remain on the surface should enhance mineralization for the successful integration of scaffold into the tissue.

24.4.2.4 Alizarin Red S Staining (ARS Staining)

The ARS staining is used to study the calcium deposition in mineralized matrix. Calcium is a major constituent of matrix. For the ARS staining, SBF-treated scaffolds are immersed in 4% paraformaldehyde for the fixation and later immersed within the ARS solution (50 mM, pH 4.1–4.3) for 30 min at room temperature. ARS staining has ability to bond specifically to calcium. Later the degree of calcium deposition can be imaged by the digital camera as indicated by the pink pale red color staining. Moreover, the extraction of the dye that stained calcium can be quantitatively estimated by spectrophotometer at 492 nm with the help of standard curve made by known calcium concentration. The dyes extraction occurs into the mixture solution of distilled water and 50% acetic acid (1:4 V/V). The acidic solution dissolves the calcium that binding with the dyes. The intensity of pink red color is proportional to the calcium present in the matrix. Cell-induced mineralized matrix can be identified by quantitative measurement of the alkaline phosphatase and collagenase activity or staining by alkaline phosphatase and or collagenase or ARS staining. The collagenase stains the collagen matrix produced during the osteogenesis process. Similarly, the osteogenesis process can be accurately predicting by the

quantitative measurement of the specific genes associated with osteoblastic activities such as Runx, alkaline phosphatase, and Osterix by polymerase chain reaction. Mesenchymal stem cells or osteoblast cells produced the bone matrix typically after at least ~14 days, and the size and shape of the matrix can be varied up on the source of osteoblast in terms of rat, human, rabbit, and mouse (Orriss et al. 2014).

24.5 Recent Advances on Electrospun PCL-Based Structure for Mineralization

Although electrospun PCL membrane has many unique characteristics including large surface-to-volume ratio, interconnected pores, and high porosity, meantime, it has few limitations too for being used directly in tissue engineering. Mainly, it is hydrophobic in nature, which shows slow progression of cell attachment, proliferation, and differentiation or mineralization. Another limitation of the PCL scaffolds alone has slower degradation. The degradation lasts for 2–3 years, mainly attributed to the low contact with the physiological surrounding due to increased hydrophobicity (Engelberg and Kohn 1991). This brings slowing the neo-tissue formation in case of in vivo implantation. Therefore, the surface modification of PCL fibers is the prime concerns. Many reports increase the wettability by introducing water loving functionalities or by blending with other bioactive hydrophilic compounds. Importantly, the resulting as-spun composite membranes are always in two-dimensional (2D), consisting of packed layers of nanofibers that can only allow accessibility of modification limited to the surface of membrane while remaining internally located fibers of the membrane remain untouched. The biomimetic SBF mediated mineralization and cells growth restrict on the surface of sheet-like electrospun membranes. The use of thin layer of the electrospun scaffolds is not sufficient for deep bone defects. This problem can be addressed by replacement of the 2D membranes by three-dimensional multilayer structured scaffolds. In these consequences, several modifications have been put forth to address such limitations while improving additional functionalities.

Designing electrospun-based three-dimensional (3D) scaffolds for the tissue regeneration application evokes much interest due to their several advantages over their corresponding 2D mat. There have been looking for the possibility of the developing the scaffolds that are richer and smarter in the composition as well as structure than electrospun 2D itself. Many groups worked on the developing the 2D mats into 3D sponge in order to make fit for the tissue regeneration. Joshi and co-workers developed 3D multilayer structured electrospun scaffold from the 2D sheet by sodium borohydride mediated gas-foaming process (Joshi et al. 2015a). Similarly, Jiang and co-workers developed the 3D scaffold from the CO₂-foaming technique by simple treatment of as-spun membranes at dry ice/ethanol bath and subsequent freeze drying process (Jiang et al. 2018). Notably, 3D scaffolds showed clear cellular infiltration. As-obtained 3D scaffolds showed high efficiency in bone regeneration in animal study. Tiwari and co-workers successfully modified the as-spun PCL/cellulose membrane with additional functionality by using a modified

gas-foamed technique. They embedded the calcium hydroxide nanoparticles into the 3D PCL/cellulose mesh (Kim and Tiwari 2020a). The resulting 3D composite showed higher cellular infiltration and biomimetic mineralization efficiency than the corresponding 2D mats or noncalcium particles embedded 3D mesh. The gas-foaming method overcome the main drawback of the as-spun PCL mat, that is, hydrophobicity as it progressed to form 3D. The significantly increased porosity of the 2D membrane enhances the water adsorption of the mats via the capillary action which is not feasible in PCL 2D mat due to tightly arranged fibers network. Moreover, the fiber roughness also increases due to the exposure reaction solution in the case of using gas-foaming approach, which also results in increasing the wettability of the hydrophobic mat. The SEM images and fiber size distribution were observed changed slightly following the gas-foaming process (S. E. Kim and Tiwari 2020a). This finally helps the biomineralization and bone formation process.

Remarkably, even more unique structures with intriguing features can also be synthesized by combining electrospinning with hydrogels. Generally, hydrogels are more favored for allowing biomineralization of cellular activities three dimensionally; however, mostly potential hydrogels are poor in mechanical integrity (Feng et al. 2016). Several reports now focused integrating the electrospun mesh with hydrogels, thereby forming the fiber reinforced hydrogels (Chen et al. 2020; Joshi et al. 2020; Maharjan et al. 2021). Multichannel gels which have the ECM mimicking fiber can better support the cell-related activities (Jordan et al. 2017). Integration of as-spun electrospun nanofibers with hydrogel can enhance the synergistic properties to the scaffolds. The smashing of the long and tightly packed fibers of membrane by homogenization into the medium and later assembled into the hydrogel precursor is a commonly used approach (Liu et al. 2020b; Maharjan et al. 2021; Mohan et al. 2015). Moreover, increasing the porosity and loosening the fiber network by gas-foaming and subsequent assembling into hydrogels could also formed the macroporous scaffold with channel-like pores and ECM-like fibers. Such architecture can guide cellular activities. The fiber-assembled hydrogels showed to improve biomimetic mineralization and osteogenesis process than that of the hydrogel alone or three-dimensional structured mesh (Joshi et al. 2020). In another study, the chitosan and bioglass incorporated PCL fiber mats were assembled in an agarose-gelatin hydrogel to generate a 3D hybrid scaffold (Mohan et al. 2015). Accordingly, it can be postulated that the advancement of the electrospun membrane can bring the following advantages over as-spun 2D mats.

1. Increases the physicochemical properties such as hydrophilicity, porosity, surface area, etc.
2. Improves the biomimetic mineralization.
3. Increases the cellular activities. The modification of as-spun 2D membrane increases the suitability of the scaffold by allowing three-dimensional biomineralization and cellular growth.

24.6 Limitation and Future Perspective

Even though the electrospun-based mats bring several benefits, it has also some limitations. The electrospun mat with all requirements for bone regeneration cannot be expected. Generally, 2D sheets have low stiffness which hindered the uses as a bone replacement. Several groups have modified as-spun 2D mats into 3D scaffold materials; still there is the chance of collapsing the 3D structure at some extent when immersed into the liquid media. The 3D scaffolds developed by gas-modifying technique retained the 3D structure by the entrapment of the gases; therefore, the structure can be disturbed once the escaping of the gases for the time being. Despite that the increased porosity, multilayer structure remains exists. In this background, entangling the labile spongy nanofibers into the hydrogels has gained increasing attention to develop new type of hybrid scaffold. Further making composite by printing together with the 3D-printed scaffolds can be a future work in order to overcome the limitations of electrospun-based scaffolds. The 3D-printed scaffolds with tunable mechanical properties along with ECM mimicking labile fibers can show the higher biomineralization and cellular activities. This strategy can be advantageous to develop a scaffold that can directly implant into the targeted site as a bone replacement after the SBF-mediated mineralization. In other hand, it can facilitate the bone regeneration by increasing the biocompatibility, osteoconductivity, and osteoinductivity. Further, the relevant drugs or proteins as a growth factors can be incorporated to further enhance osteogenesis process for rapid bone regeneration in real applications.

24.7 Conclusions

Cell-mediated biomineralization process is the real bone formation process which is a complex mechanism and takes much time to accomplish in a natural way. Herein, electrospun-based PCL fibrous scaffolds have been an attractive substrate facilitating for bone regeneration in a defect sites due to having unique properties such as nontoxic, good mechanical properties. Electrospinning offers the fiber production at a range of nanometer to microscale that mimics the ECM. However, the low hydrophilicity and having less active functional moieties on the PCL fiber surface, actual mineralization process takes much longer time. In this scenario, a modified PCL mat and subsequent *in vitro* mineralization became a significant advancement in tissue regeneration. *In vitro* mineralization study by SBF treatment not only reduces the bone formation process by time but also facilitates the osteogenesis. Several *in vitro* and *in vivo* studies have demonstrated the promising effects of the surface-mineralized fiber scaffolds on initial cell attachment, proliferation, migration, and differentiation. Still, the as-mineralized PCL mats are two dimensional which hinder the uses in large bone defect site. More recently, 3D scaffolds from the as-spun 2D mats have been becoming a promising approach to overcome the limitations of the as-spun PCL-based mats. Further functionalization of 3D mats and assembling together with hydrogels are recently catching a tremendous interest.

Incorporation of biomolecules and suitable drugs into advanced structured scaffolds such as 3D printed, cell laden gels, etc. can be highly beneficial in improvement in the development of the substitutes of bone defects while fastening the bone formation process meantime. This would be the perspective for the future study in the line of development of ready to implant mineralized matrix as the bone substitutes.

Acknowledgments This work was not supported by any funding agencies.

References

- Anderson HC (2003) Matrix vesicles and calcification. *Curr Rheumatol Rep* 5(3):222–226
- Arcos D, Vallet-Regí M (2020) Substituted hydroxyapatite coatings of bone implants. *J Mater Chem B* 8(9):1781–1800
- Arrington ED, Smith WJ, Chambers HG, Bucknell AL, Davino NA (1996) Complications of iliac crest bone graft harvesting. *Clin Orthop Relat Res* 329:300–309
- Bartnikowski M, Dargaville TR, Ivanovski S, Huttmacher DW (2019) Degradation mechanisms of polycaprolactone in the context of chemistry, geometry and environment. *Prog Polym Sci* 96:1–20
- Behere I, Pardawala Z, Vaidya A, Kale V, Ingavle G (2020) Osteogenic differentiation of an osteoblast precursor cell line using composite PCL-gelatin-nHAp electrospun nanofiber mesh. *Int J Polym Mater Polym Biomater*:1–15
- Bhattarai DP, Aguilar LE, Park CH, Kim CS (2018) A review on properties of natural and synthetic based electrospun fibrous materials for bone tissue engineering. *Membranes* 8(3):62
- Bhattarai DP, Tiwari AP, Maharjan B, Tumurbaatar B, Park CH, Kim CS (2019) Sacrificial template-based synthetic approach of polypyrrole hollow fibers for photothermal therapy. *J Colloid Interface Sci* 534:447–458
- Blokhuis TJ, Calori GM, Schmidmaier G (2013) Autograft versus BMPs for the treatment of non-unions: what is the evidence? *Injury* 44:S40–S42
- Bonfield W, Grynblas MD, Tully AE, Bowman J, Abram J (1981) Hydroxyapatite reinforced polyethylene—a mechanically compatible implant material for bone replacement. *Biomaterials* 2(3):185–186
- Campana V, Milano G, Pagano E, Barba M, Cicione C, Salonna G et al (2014) Bone substitutes in orthopaedic surgery: from basic science to clinical practice. *J Mater Sci Mater Med* 25(10):2445–2461
- Castro-Osma JA, Alonso-Moreno C, García-Martínez JC, Fernández-Baeza J, Sánchez-Barba LF, Lara-Sánchez A, Otero A (2013) Ring-opening (ROP) versus ring-expansion (REP) polymerization of ϵ -Caprolactone to give linear or cyclic Polycaprolactones. *Macromolecules* 46(16):6388–6394
- Chen M, Kimpton L, Whiteley J, Castilho M, Malda J, Please C et al (2020) Multiscale modelling and homogenisation of fibre-reinforced hydrogels for tissue engineering. *Eur J Appl Math* 31(1):143–171
- De Groot K, Geesink R, Klein CPAT, Serekian P (1987) Plasma sprayed coatings of hydroxylapatite. *J Biomed Mater Res* 21(12):1375–1381
- Dehghanghadikolaei A, Fotovvati B (2019) Coating techniques for functional enhancement of metal implants for bone replacement: a review. *Materials (Basel, Switzerland)* 12(11):1795
- Dimitriou R, Jones E, McGonagle D, Giannoudis PV (2011) Bone regeneration: current concepts and future directions. *BMC Med* 9(1):66
- Engelberg I, Kohn J (1991) Physico-mechanical properties of degradable polymers used in medical applications: a comparative study. *Biomaterials* 12(3):292–304

- Erisken C, Kalyon DM, Wang H (2008) Functionally graded electrospun polycaprolactone and β -tricalcium phosphate nanocomposites for tissue engineering applications. *Biomaterials* 29(30):4065–4073
- Eshraghi S, Das S (2010) Mechanical and microstructural properties of polycaprolactone scaffolds with one-dimensional, two-dimensional, and three-dimensional orthogonally oriented porous architectures produced by selective laser sintering. *Acta Biomater* 6(7):2467–2476
- Feng Q, Wei K, Lin S, Xu Z, Sun Y, Shi P, Bian L et al (2016) Mechanically resilient, injectable, and bioadhesive supramolecular gelatin hydrogels crosslinked by weak host-guest interactions assist cell infiltration and in situ tissue regeneration. *Biomaterials* 101:217–228
- Fujihara K, Kotaki M, Ramakrishna S (2005) Guided bone regeneration membrane made of polycaprolactone/calcium carbonate composite nano-fibers. *Biomaterials* 26(19):4139–4147
- Gao X, Song J, Ji P, Zhang X, Li X, Xu X, Wei S et al (2016) Polydopamine-templated hydroxyapatite reinforced polycaprolactone composite nanofibers with enhanced cytocompatibility and osteogenesis for bone tissue engineering. *ACS Appl Mater Interfaces* 8(5):3499–3515
- Gao C, Peng S, Feng P, Shuai C (2017) Bone biomaterials and interactions with stem cells. *Bone Res* 5(1):17059
- Ghorbani F, Zamanian A, Aidun A (2019) Bioinspired polydopamine coating-assisted electrospun polyurethane-graphene oxide nanofibers for bone tissue engineering application. *J Appl Polym Sci* 136(24):47656
- Gkioni K, Leeuwenburgh SC, Douglas TE, Mikos AG, Jansen JA (2010) Mineralization of hydrogels for bone regeneration. *Tissue Eng Part B Rev* 16(6):577–585
- Gupta D, Venugopal J, Mitra S, Giri Dev VR, Ramakrishna S (2009) Nanostructured biocomposite substrates by electrospinning and electrospraying for the mineralization of osteoblasts. *Biomaterials* 30(11):2085–2094
- Hajiali F, Tajbaksh S, Shojaei A (2018) Fabrication and properties of Polycaprolactone composites containing calcium phosphate-based ceramics and bioactive glasses in bone tissue engineering: a review. *Polym Rev* 58(1):164–207
- Hasan A, Waibhaw G, Tiwari S, Dharmalingam K, Shukla I, Pandey LM (2017) Fabrication and characterization of chitosan, polyvinylpyrrolidone, and cellulose nanowhiskers nanocomposite films for wound healing drug delivery application. *J Biomed Mater Res A* 105(9):2391–2404
- Hasan A, Waibhaw G, Saxena V, Pandey LM (2018) Nano-biocomposite scaffolds of chitosan, carboxymethyl cellulose and silver nanoparticle modified cellulose nanowhiskers for bone tissue engineering applications. *Int J Biol Macromol* 111:923–934
- Hassan MI, Sultana N (2017) Characterization, drug loading and antibacterial activity of nanohydroxyapatite/polycaprolactone (nHA/PCL) electrospun membrane. *3 Biotech* 7(4):249
- Hwang TI, Kim JI, Joshi MK, Park CH, Kim CS (2019) Simultaneous regeneration of calcium lactate and cellulose into PCL nanofiber for biomedical application. *Carbohydr Polym* 212:21–29
- Hwang TI, Kim JI, Lee J, Moon JY, Lee JC, Joshi MK et al (2020) In situ biological transmutation of catalytic lactic acid waste into calcium lactate in a readily processable three-dimensional fibrillar structure for bone tissue engineering. *ACS Appl Mater Interfaces* 12(16):18197–18210
- Jaiswal AK, Chhabra H, Kadam SS, Londhe K, Soni VP, Bellare JR (2013) Hardystonite improves biocompatibility and strength of electrospun polycaprolactone nanofibers over hydroxyapatite: a comparative study. *Mater Sci Eng C* 33(5):2926–2936
- Jiang J, Chen S, Wang H, Carlson MA, Gombart AF, Xie J (2018) CO₂-expanded nanofiber scaffolds maintain activity of encapsulated bioactive materials and promote cellular infiltration and positive host response. *Acta Biomater* 68:237–248
- Jordan AM, Kim S-E, Van de Voorde K, Pokorski JK, Korley LT (2017) In situ fabrication of fiber reinforced three-dimensional hydrogel tissue engineering scaffolds. *ACS Biomater Sci Eng* 3(8):1869–1879

- Joshi MK, Pant HR, Tiwari AP, Kim HJ, Park CH, Kim CS (2015a) Multi-layered macroporous three-dimensional nanofibrous scaffold via a novel gas foaming technique. *Chem Eng J* 275:79–88
- Joshi MK, Tiwari AP, Pant HR, Shrestha BK, Kim HJ, Park CH, Kim CS (2015b) In situ generation of cellulose nanocrystals in Polycaprolactone nanofibers: effects on crystallinity, mechanical strength, biocompatibility, and biomimetic mineralization. *ACS Appl Mater Interfaces* 7(35):19672–19683
- Joshi MK, Lee S, Tiwari AP, Maharjan B, Poudel SB, Park CH, Kim CS (2020) Integrated design and fabrication strategies for biomechanically and biologically functional PLA/ β -TCP nanofiber reinforced GelMA scaffold for tissue engineering applications. *Int J Biol Macromol* 164:976–985
- Kim SE, Tiwari AP (2020a) Three dimensional polycaprolactone/cellulose scaffold containing calcium-based particles: a new platform for bone regeneration. *Carbohydr Polym* 250:116880
- Kim SE, Tiwari AP (2020b) Three dimensional polycaprolactone/cellulose scaffold containing calcium-based particles: a new platform for bone regeneration. *Carbohydr Polym* 250:116880
- Kim KT, Eo MY, Nguyen TTH, Kim SM (2019) General review of titanium toxicity. *Int J Implant Dent* 5(1):10–10
- Kokubo T (1991) Bioactive glass ceramics: properties and applications. *Biomaterials* 12(2):155–163
- Kokubo T, Takadama H (2006) How useful is SBF in predicting in vivo bone bioactivity? *Biomaterials* 27(15):2907–2915
- Kokubo T, Ito S, Huang ZT, Hayashi T, Sakka S, Kitsugi T, Yamamuro T (1990) Ca, P-rich layer formed on high-strength bioactive glass-ceramic A-W. *J Biomed Mater Res* 24(3):331–343
- Koletzko B, Baker S, Cleghorn G, Neto UF, Gopalan S, Hernell O et al (2005) Global standard for the composition of infant formula: recommendations of an ESPGHAN coordinated international expert group. *J Pediatr Gastroenterol Nutr* 41(5):584–599
- Labet M, Thielemans W (2009) Synthesis of polycaprolactone: a review. *Chem Soc Rev* 38(12):3484–3504
- Lee JH, Park J-H, El-Fiqi A, Kim J-H, Yun Y-R, Jang J-H et al (2014) Biointerface control of electrospun fiber scaffolds for bone regeneration: engineered protein link to mineralized surface. *Acta Biomater* 10(6):2750–2761
- Lee E-J, An AK, He T, Woo YC, Shon HK (2016) Electrospun nanofiber membranes incorporating fluorosilane-coated TiO₂ nanocomposite for direct contact membrane distillation. *J Membr Sci* 520:145–154
- Liao N, Joshi MK, Tiwari AP, Park C-H, Kim CS (2016) Fabrication, characterization and biomedical application of two-nozzle electrospun polycaprolactone/zein-calcium lactate composite nonwoven mat. *J Mech Behav Biomed Mater* 60:312–323
- Liu L, Li C, Liu X, Jiao Y, Wang F, Jiang G, Wang L (2020a) Tricalcium phosphate sol-incorporated poly(ϵ -caprolactone) membrane with improved mechanical and Osteoinductive activity as an artificial periosteum. *ACS Biomater Sci Eng* 6(8):4631–4643
- Liu Y-T, Zhang M, Wang Y, Zhang Y, Song J, Si Y, Ding B et al (2020b) Conductive and elastic TiO₂ Nanofibrous aerogels: a new concept toward self-supported Electrocatalysts with superior activity and durability. *Angew Chem Int Ed* 59:23252–23260
- Ma B, Xie J, Jiang J, Shuler FD, Bartlett DE (2013) Rational design of nanofiber scaffolds for orthopedic tissue repair and regeneration. *Nanomedicine (Lond)* 8(9):1459–1481
- Maharjan B, Park J, Kaliannagounder VK, Awasthi GP, Joshi MK, Park CH, Kim CS (2021) Regenerated cellulose nanofiber reinforced chitosan hydrogel scaffolds for bone tissue engineering. *Carbohydr Polym* 251:117023
- Martins A, Pinho ED, Faria S, Pashkuleva I, Marques AP, Reis RL, Neves NM (2009) Surface modification of electrospun polycaprolactone nanofiber meshes by plasma treatment to enhance biological performance. *Small* 5(10):1195–1206

- Milovac D, Gallego Ferrer G, Ivankovic M, Ivankovic H (2014) PCL-coated hydroxyapatite scaffold derived from cuttlefish bone: morphology, mechanical properties and bioactivity. *Mater Sci Eng C* 34:437–445
- Mohan N, Wilson J, Joseph D, Vaikkath D, Nair PD (2015) Biomimetic fiber assembled gradient hydrogel to engineer glycosaminoglycan enriched and mineralized cartilage: An in vitro study. *J Biomed Mater Res A* 103(12):3896–3906
- Mombelli A, Hashim D, Cionca N (2018) What is the impact of titanium particles and biocorrosion on implant survival and complications? A critical review. *Clin Oral Implants Res* 29(S18): 37–53
- Nijssure MP, Pastakia M, Spano J, Fenn MB, Kishore V (2017) Bioglass incorporation improves mechanical properties and enhances cell-mediated mineralization on electrochemically aligned collagen threads. *J Biomed Mater Res A* 105(9):2429–2440
- Ogino M, Ohuchi F, Hench LL (1980) Compositional dependence of the formation of calcium phosphate films on bioglass. *J Biomed Mater Res* 14(1):55–64
- Orriss IR, Hajjawi MO, Huesa C, MacRae VE, Arnett TR (2014) Optimisation of the differing conditions required for bone formation in vitro by primary osteoblasts from mice and rats. *Int J Mol Med* 34(5):1201–1208
- Park C-H, Kim EK, Tijing LD, Amarjargal A, Pant HR, Kim CS, Shon HK (2014) Preparation and characterization of LA/PCL composite fibers containing beta tricalcium phosphate (β -TCP) particles. *Ceram Int* 40(3):5049–5054
- Perumal G, Sivakumar PM, Nandkumar AM, Doble M (2020) Synthesis of magnesium phosphate nanoflakes and its PCL composite electrospun nanofiber scaffolds for bone tissue regeneration. *Mater Sci Eng C* 109:110527
- Phaiju S, Mulmi P, Shahi DK, Hwang TI, Tiwari AP, Joshi R et al (2020) Antibacterial cinnamon essential oil incorporated poly (ϵ -Caprolactone) Nanofibrous Mats: new platform for biomedical application. *J Inst Sci Technol* 25(2):9–16
- Ren J, Blackwood KA, Doustgani A, Poh PP, Steck R, Stevens MM, Woodruff MA (2014) Melt-electrospun polycaprolactone strontium-substituted bioactive glass scaffolds for bone regeneration. *J Biomed Mater Res A* 102(9):3140–3153
- Rodríguez K, Rennecker S, Gatenholm P (2011) Biomimetic calcium phosphate crystal mineralization on electrospun cellulose-based scaffolds. *ACS Appl Mater Interfaces* 3(3):681–689
- Safioti LM, Kotsakis GA, Pozhitkov AE, Chung WO, Daubert DM (2017) Increased levels of dissolved titanium are associated with Peri-Implantitis—a cross-sectional study. *J Periodontol* 88(5):436–442
- Santin M, Phillips GJ (2012) Biomimetic, bioresponsive, and bioactive materials: An introduction to integrating materials with tissues. Wiley, Hoboken, NJ
- Schlickewei W, Schlickewei C (2007) The use of bone substitutes in the treatment of bone defects—the clinical view and history. In: *Macromolecular symposia*, vol 253. Wiley Online Library, pp 10–23
- Shalumon KT, Anulekha KH, Chennazhi KP, Tamura H, Nair SV, Jayakumar R (2011) Fabrication of chitosan/poly(caprolactone) nanofibrous scaffold for bone and skin tissue engineering. *Int J Biol Macromol* 48(4):571–576
- Shao W, He J, Sang F, Ding B, Chen L, Cui S et al (2016) Coaxial electrospun aligned tussah silk fibroin nanostructured fiber scaffolds embedded with hydroxyapatite–tussah silk fibroin nanoparticles for bone tissue engineering. *Mater Sci Eng C* 58:342–351
- Shih Y-RV, Hwang Y, Phadke A, Kang H, Hwang NS, Caro EJ et al (2014) Calcium phosphate-bearing matrices induce osteogenic differentiation of stem cells through adenosine signaling. *Proc Natl Acad Sci* 111(3):990–995
- Siddiqui N, Asawa S, Birru B, Baadhe R, Rao S (2018) PCL-based composite scaffold matrices for tissue engineering applications. *Mol Biotechnol* 60(7):506–532
- Song J, Saiz E, Bertozzi CR (2003) A new approach to mineralization of biocompatible hydrogel scaffolds: an efficient process toward 3-dimensional bonelike composites. *J Am Chem Soc* 125(5):1236–1243

- Stastna E, Castkova K, Rahel J (2020) Influence of hydroxyapatite nanoparticles and surface plasma treatment on bioactivity of Polycaprolactone nanofibers. *Polymers* 12(9):1877
- Tiwari AP, Joshi MK, Maharjan B, Ko SW, Kim JI, Park CH, Kim CS (2016) Engineering a novel bilayer membrane for bone defects regeneration. *Mater Lett* 180:268–272
- Tiwari AP, Joshi MK, Lee J, Maharjan B, Ko SW, Park CH, Kim CS (2017) Heterogeneous electrospun polycaprolactone/polyethylene glycol membranes with improved wettability, biocompatibility, and mineralization. *Colloids Surf A Physicochem Eng Asp* 520:105–113
- Tiwari AP, Hwang TI, Oh J-M, Maharjan B, Chun S, Kim BS et al (2018a) pH/NIR-responsive Polypyrrole-functionalized fibrous localized drug-delivery platform for synergistic cancer therapy. *ACS Appl Mater Interfaces* 10(24):20256–20270
- Tiwari AP, Joshi MK, Park CH, Kim CS (2018b) Nano-nets covered composite nanofibers with enhanced biocompatibility and mechanical properties for bone tissue engineering. *J Nanosci Nanotechnol* 18(1):529–537
- Wang W, Yeung KWK (2017) Bone grafts and biomaterials substitutes for bone defect repair: a review. *Bioact Mater* 2(4):224–247
- Wang Z, Liang R, Jiang X, Xie J, Cai P, Chen H, Zheng L et al (2019) Electrospun PLGA/PCL/OCP nanofiber membranes promote osteogenic differentiation of mesenchymal stem cells (MSCs). *Mater Sci Eng C* 104:109796
- Xia D, Shi B (2016) Biom mineralization of electrospun polycaprolactone-guided bone regeneration membrane. *Hua Xi Kou Qiang Yi Xue Za Zhi* 34(6):570–574
- Xie J, Zhong S, Ma B, Shuler FD, Lim CT (2013) Controlled biomineralization of electrospun poly (ϵ -caprolactone) fibers to enhance their mechanical properties. *Acta Biomater* 9(3):5698–5707
- Xu T, Sheng L, He L, Weng J, Duan K (2020) Enhanced osteogenesis of hydroxyapatite scaffolds by coating with BMP-2-loaded short polylactide nanofiber: a new drug loading method for porous scaffolds. *Regener Biomater* 7(1):91–98
- Yang F, Wolke J, Jansen J (2008) Biomimetic calcium phosphate coating on electrospun poly (ϵ -caprolactone) scaffolds for bone tissue engineering. *Chem Eng J* 137(1):154–161